NBS SPECIAL PUBLICATION 300

VOLUME 8

Precision Measurement and Calibration

Mechanics

Precision Measurement and Calibration

Volumes available or to be published in the NBS Special Publication 300 series

SP300, Vol. 1, Statistical Concepts and Procedures, H. H. Ku, Editor, Feb. 1969, 436 pages, (SD Catalog No. C 13.10:300/v.1)* Price $5.50

SP300, Vol. 2, Temperature, J. F. Swindells, Editor, Aug. 1968, 520 pages, (SD Catalog No. C 13.10:300/v.2)* Price $4.75

SP300, Vol. 3, Electricity—Low Frequency, F. L. Hermach and R. F. Dziuba, Editors, Dec. 1968, 498 pages, (SD Catalog No. C 13.10:300/v.3)* Price $4.50

SP300, Vol. 4, Electricity—Radio Frequency, A. J. Estin, Editor, June 1970, 450 pages, (SD Catalog No. C 13.10:300/v.4)* Price $5.50

SP300, Vol. 5, Frequency and Time, B. E. Blair and A. H. Morgan, Editors, May 1971, 565 pages, (C 13.10:300/v.5)* Price $6.00

SP300, Vol. 6, Heat, D. C. Ginnings, Editor, Feb. 1970, 400 pages, (SD Catalog No. C 13.10:300/v.6)* Price $5.00

SP300, Vol. 7, Radiometry and Photometry, H. K. Hammond, III, and H. L. Mason, Editors, Nov. 1971, 690 pages, (SD Catalog No. C 13.10:300/v.7)* Price $ 7.00

SP300, Vol. 8, Mechanics, R. L. Bloss and Mary J. Orloski, Editors. 590 pages, (SD Catalog No. C 13.10:300/v.8)* Price $6.25

Volumes in Press**

SP300, Vol. 9, Colorimetry, I. Nimeroff, Editor.

SP300, Vol. 10, Ionizing Radiation, Elmer H. Eisenhower, Editor.

SP300, Vol. 11, Image Optics, Calvin S. McCamy, Editor.

---

* Available by purchase from the Superintendent of Documents, Government Printing Office, Washington, D. C. 20402. Order by the Supt. of Documents Catalog number as given for each volume.

** For announcements of new volumes as issued, complete the form (Notification key N-353) in the back of this volume and mail it to the Superintendent of Documents office.

UNITED STATES DEPARTMENT OF COMMERCE • MAURICE H. STANS, Secretary
U.S. NATIONAL BUREAU OF STANDARDS • LEWIS M. BRANSCOMB, Director

Precision Measurement and Calibration

Selected NBS Papers on

Mechanics

Roscoe L. Bloss and
Mary J. Orloski, Editors

Institute for Basic Standards
National Bureau of Standards
Washington, D.C. 20234

A compilation of previously published papers by the staff of the National Bureau of Standards, including selected abstracts by NBS and non-NBS authors. Issued in several volumes, see page IV.

NBS Special Publication 300 — Volume 8

Coden Nat. Bur. Stand. (U.S.), Spec. Publ. 300, Vol. 8, 590 pages

Issued January 1972

For sale by the Superintendent of Documents, U.S. Government Printing Office, Washington, D.C. 20402
(Order by SD Catalog No. C 13.10 : 300/v.8). Price $6.25
Stock Number 0303-0923

Abstract

This volume is one of an extended series which brings together the previously published papers, monographs, abstracts, and bibliographies by NBS authors dealing with the precision measurement of specific physical quantities and the calibration of the related metrology equipment. The contents have been selected as being useful to the standards laboratories of the United States in tracing to NBS standards the accuracies of measurement needed for research work, factory production, or field evaluation.

Volume 8 consists primarily of published works of the staff of the Mechanics Division of NBS. It includes papers in the fields of acoustics, fluid mechanics, force, gravity, humidity, pressure, strain, vacuum, vibration, and viscosity. Although most of the papers had been previously published, original papers in the fields of "gravity" and "viscosity" are included.

Key words: Acoustics; fluid mechanics; force; gravity; humidity; pressure; strain; vacuum; vibration; viscosity.

Library of Congress Catalog Card Number: 68-60042

Foreword

In the 1950's the tremendous increase in industrial activity, particularly in the missile and satellite fields, led to an unprecedented demand for precision measurement, which, in turn, brought about the establishment of hundreds of new standards laboratories. To aid these laboratories in transmitting the accuracies of the national standards to the shops of industry, NBS in 1959 gathered together and reprinted a number of technical papers by members of its staff describing methods of precision measurement and the design and calibration of standards and instruments. These reprints, representing papers written over a period of several decades, were published as NBS Handbook 77, Precision Measurement and Calibration, in three volumes: Electricty and Electronics; Heat and Mechanics; Optics, Metrology, and Radiation.

Some of the papers in Handbook 77 are still useful, but new theoretical knowledge, improved materials, and increasingly complex experimental techniques have so advanced the art and science of measurement that a new compilation has become necessary. The present volume is part of a new reprint collection, designated NBS Special Publication 300, which has been planned to fill this need. Besides previously published papers by the NBS staff, the collection includes selected abstracts by both NBS and non-NBS authors. It is hoped that SP 300 will serve both as a textbook and as a reference source for the many scientists and engineers who fill responsible positions in standards laboratories.

LEWIS M. BRANSCOMB, *Director.*

Preface

The general plan for this compilation has been reviewed by the Information Committee of the National Conference of Standards Laboratories. The plan calls for Special Publication 300 to be published in 11 volumes as presented on the inside of the front cover.

This division of subject matter has been chosen to assure knowledgeable selection of context rather than to attain uniform size. It is believed, however, that the larger volumes, of approximately 500 pages, will still be small enough for convenient handling in the laboratory.

The compilation consists primarily of original papers by NBS authors which have been reprinted by photoreproduction, with occasional updating of graphs or numerical data when this has appeared desirable. In addition, some important publications by non-NBS authors that are too long to be included are represented by abstracts or references; the abstracts are signed by the individuals who wrote them, unless written by the author.

Each volume has a subject index and author index, and within each volume, contents are grouped by subtopics to facilitate browsing. Many entries follow the recent Bureau practice of assigning several key words or phrases to each document; these may be collated with titles in the index. Pagination is continuous within the volume, the page numbers in the original publications also being retained and combined with the volume page numbers, for example 100–10. The index notation 8–133 refers to volume 8, page 133 of this volume. A convenient list of SI (Système International) physical units and a conversion table are to be found inside the back cover.

The publications listed herein for which a price is indicated are available from the Superintendent of Documents, U.S. Government Printing Office, Washington, D.C. 20402 (foreign postage, one-fourth additional) . Many documents in the various NBS non-periodical series are also available from the National Technical Information Service, Springfield, Va. 22151. Reprints from the NBS Journal of Research or from non-NBS journals may sometimes be obtained directly from an author.

Suggestions as to the selection of papers which should be included in future editions will be welcome. Current developments in measurement technology at NBS are covered in annual seminars held at either the Gaithersburg (Maryland) or the Boulder (Colorado) laboratories. These developments are summarized, along with a running list of publications by NBS authors, in the monthly NBS Technical News Bulletin.

H. L. Mason,
Office of Measurement Services,
NBS Institute for Basic Standards.

Editor's Note

This volume is intended to contain the works of the staff members of the Mechanics Division of the National Bureau of Standards that are currently most pertinent to laboratories engaged in standards or calibration work. In some cases longer papers that are still readily available in their original form have been presented in abstract form only. This was necessary due to space limitations.

The field covered by this volume is diverse, and it would have been presumptuous for the editors to attempt to select the most useful papers in all areas. We therefore gratefully acknowledge the assistance of many senior staff members in reviewing and selecting papers for possible inclusion. Special acknowledgement is extended to Dr. R. S. Marvin and D. R. Tate for preparing special papers on viscosity and gravity where appropriate publications did not exist.

R. L. Bloss and
Mary J. Orloski, *Editors.*

Contents

1. Acoustics

Papers

1. Acoustics — Continued

Papers

Abstracts

2. Fluid Mechanics

2. Fluid Mechanics — Continued

3. Force

4. Gravity

5. Humidity

5. Humidity — Continued

Papers

Abstracts

6. Pressure

7. Strain

8. Vacuum

9. Vibration

Papers Page

10. Viscosity

1. Acoustics

Papers

1. Acoustics—Continued

1. Acoustics—Continued

Acoustic Impedance of a Right Circular Cylindrical Enclosure

FERNANDO BIAGI AND RICHARD K. COOK
National Bureau of Standards, Washington, D. C.
(Received April 12, 1954)

At low frequencies, the acoustic impedance of a right circular cylindrical enclosure (containing air, or other gases) is affected by the cooling effects of the walls. Analytical expressions for the temperature distribution have been obtained, and computations of the effect on the impedance are given in the form of plotted correction factors. These corrections are used in making absolute pressure calibrations of condenser microphones at low frequencies.

The solution presented for the average temperature distribution applies also to the heat-conductivity problem of a uniform volume distribution of sinusoidal heat sources, which are considered to be in phase, inside a cylindrical enclosure having isothermal walls.

IN the past decade the reciprocity technique has been widely used for measuring the pressure response of condenser microphones to be used as sound pressure standards in air. The technique, which has been fully described in various places, makes use of a small enclosure, usually a right circular cylinder. The enclosure (called a coupler) contains air, or other gases, in which sound pressure is produced. The volume V of the enclosure (usually of the order of 10 cc) is chosen so that the pressure fluctuations occur adiabatically at audio frequencies. The acoustic impedance of the enclosure is made use of in the calculations. If B is the ambient barometric pressure, γ the ratio of specific heats of the enclosed gas, and ω the pulsatance of the sinusoidal adiabatic pressure fluctuations, then the impedance is $j\gamma B/\omega V$ ($j^2=-1$).

At infrasonic frequencies the acoustic impedance of the coupler is affected by the cooling effects of the walls. At sufficiently low frequencies, the sound pressure fluctuations occur isothermally, and the impedance is $jB/\omega V$. When the frequency is varied from the adiabatic to the isothermal region, the acoustic impedance can be regarded as a complex number which varies continuously from its adiabatic value to its isothermal value. The problem is to determine quantitatively what happens to the impedance at intermediate frequencies. As has been shown by F. B. Daniels[1] and others, the problem reduces to a determination of the space average of the temperature distribution within the coupler.

Expressions for the acoustic impedance of two parallel plates, a spherical enclosure, and an infinite cylinder have been obtained by Daniels.[1] Nomograms for them have been obtained by M. J. E. Golay.[2] Two infinite series solutions to the problem of the temperature distribution in a right circular cylindrical enclosure will be described in what follows.

SINGLY-INFINITE SERIES SOLUTION

If we apply the first law of thermodynamics and assume that the time variations of the quantities involved are like $\exp(j\omega t)$, then it is possible to reduce the equation for the temperature distribution[3] to

$$\nabla^2 T=\beta^2(T-\alpha) \tag{1}$$

[1] F. B. Daniels, J. Acoust. Soc. Am. **19**, 569 (1947).
[2] M. J. E. Golay, Rev. Sci. Instr. **18**, 347 (1947).
[3] E. C. Wente, Phys. Rev. **19**, 333 (1922).

where

$$\beta^2 = j\omega\rho C_p/K, \quad \alpha = p/\rho C_p,$$

if the radiation term is neglected. In the above equations: C_p = specific heat at constant pressure; ρ = density of the medium; K = coefficient of thermal conductivity; p = amplitude of the sinusoidal sound pressure in the gas, constant throughout the coupler; T = variational temperature of the gas, which is a function of position in the coupler, and whose time-averaged value is zero; α = variational temperature (associated with the sound pressure) which would prevail throughout the gas if the walls had no cooling effect.

The boundary condition at the walls of an enclosure containing air is that the temperature is practically constant. Mathematically, if a = radius of the cylinder and l = its length (see Fig. 1), then

$$T=0 \text{ at } r=a, \text{ and } T=0 \text{ at } z=\pm l/2.$$

Substituting $\tau = (T-\alpha)/\alpha$, we have from Eq. (1)

$$\nabla^2\tau = \beta^2\tau.$$

Consider a cylindrical enclosure having isothermal walls, and containing a gas which is heated periodically by the absorption of thermal radiation, for example. The heat energy added is a sinusoidal function of time, and all parts of the gas receive heat at the same rate and in phase. Then the above differential equations apply, and the solution which we shall present for the temperature distribution in the acoustical problem, will be valid also for the heat conductivity problem.

Since the enclosure is axially symmetric the temperature will not depend on the angular parameter. We seek to construct a solution $\tau(r,z)$ by superposing solutions of the form $R(r)Z(z)$. We find that R and Z must satisfy

$$\frac{d}{dr}\left(r\frac{dR}{dr}\right)+\mu^2 rR=0,$$

$$\frac{d^2Z}{dz^2}+k^2Z=0, \quad k^2+\mu^2=-\beta^2.$$

Solutions to these equations are

$$R=CJ_0(\mu r)+DY_0(\mu r),$$
$$Z=A\cos(kz)+B\sin(kz).$$

The solution must be finite at $r=0$, therefore $D=0$. From the symmetry it is obvious that $B=0$. Thus choosing $C=1$, a general solution can be written as

$$\tau=\sum A\cos(kz)J_0(\mu r). \tag{2}$$

At the walls of the enclosure where $T=0$, $\tau=-1$ which can be substituted into Eq. (2). When $r=a$, τ becomes a function of z, which is equated to -1. When $z=\pm l/2$, τ is a function of r and this also must equal -1. In order to meet both conditions, we can use two series, each of which is zero when one variable

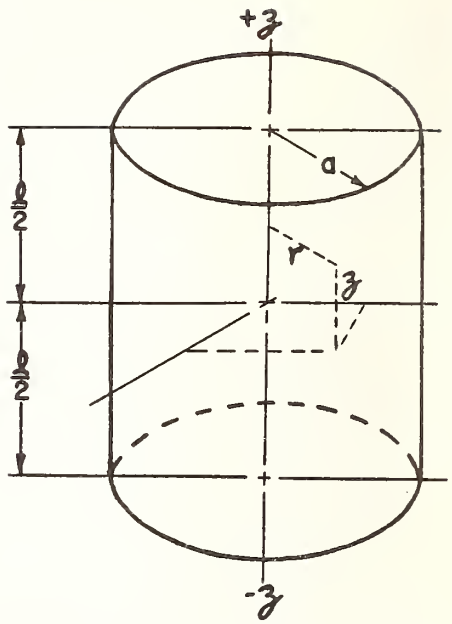

FIG. 1. Coordinates for a right circular cylindrical enclosure.

has the boundary value, and each of which has the value -1 when the other is zero. We will therefore divide the sum (2) into two sums over the indices n and ν. Thus

$$\tau=\sum_n A_n\cos(k_nz)J_0(\mu_nr)+\sum_\nu A_\nu\cos(k_\nu z)J_0(\mu_\nu r). \tag{3}$$

For $r=a$,

$$-1=\sum_n A_n\cos(k_nz)J_0(\mu_na)+\sum_\nu A_\nu\cos(k_\nu z)J_0(\mu_\nu a). \tag{4}$$

If we take $J_0(\mu_n a)=0$, we shall be left with a sum over the index ν. We select A_ν and k_ν so that the sum is a Fourier series of cosine terms equal to the constant -1, each term being zero at $z=\pm l/2$. This gives us

$$A_\nu = 4(-1)^{\nu+1}/lk_\nu J_0(\mu_\nu a), \quad k_\nu=(2\nu+1)\pi/l,$$
$$\mu_\nu^2=-(k_\nu^2+\beta^2), \quad \nu=0,\ 1,\ 2,\ 3,\cdots\infty.$$

We repeat this procedure at $z=\pm l/2$, where $r\neq a$. The sum over the index ν is zero, and we are left with the sum, over the index n, of Bessel's functions equal to -1. The μ_n and A_n are chosen so that the sum is a Fourier-Bessel series equal to -1. Hence

$$A_n=-2/\mu_n aJ_1(\mu_n a)\cos(k_nl/2), \quad J_0(\mu_n a)=0,$$
$$k_n^2=-(\mu_n^2+\beta^2), \quad n=1,\ 2,\ 3,\cdots\infty.$$

Our solution for the spatial distribution of temperature in the coupler is

$$T/\alpha = 1-\sum_{n=1}^{\infty} 2\cos(k_nz)J_0(\mu_nr)/\mu_naJ_1(\mu_na)\cos(k_nl/2)$$
$$+\sum_{\nu=0}^{\infty} 4(-1)^{\nu+1}\times\cos(k_\nu z)J_0(\mu_\nu r)/k_\nu lJ_0(\mu_\nu a). \tag{5}$$

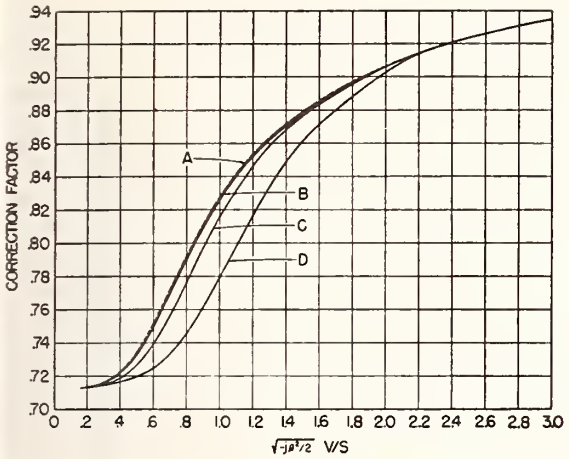

FIG. 2. Correction factors, for the cooling effects of the walls, to the acoustic impedance of various enclosures. V=enclosure volume, and S=surface area. A is for a right circular cylinder having $a/l=1.185$. B is for a sphere. C is for an infinitely long circular cylinder. D is for two infinite parallel planes.

The average temperature within the enclosure is

$$\bar{T}=(2/a^2l)\int_{-l/2}^{l/2}\int_0^a Trdrdz. \tag{6}$$

It can be shown that the integration of the infinite series (5) for T can be carried out term by term. The result is

$$\bar{T}/\alpha=1-8\sum_{n=1}^{\infty}\tan(k_nl/2)/k_nl(\mu_na)^2 - 16\sum_{\nu=0}^{\infty}J_1(\mu_\nu a)/\mu_\nu a k_\nu^2 l^2 J_0(\mu_\nu a). \tag{7}$$

DOUBLY INFINITE SERIES SOLUTION

The sum of a doubly infinite series of Fourier-Bessel functions can also be obtained as a solution for the temperature distribution. Consider the functions $\cos(\pi\mu z/l)\times J_0(\lambda r/a)$, where $\mu=1, 2, 3,\cdots$, and $\lambda=$the positive roots of $J_0(\lambda)=0$, arranged in ascending order of magnitude. These functions form a complete orthogonal set within the right circular cylindrical enclosure for functions $T(r,z)$ which are even in z. We write

$$T/\alpha=\sum_{\mu}^{\infty}\sum_{\lambda}^{\infty}A(\mu,\lambda)\cos(\pi\mu z/l)J_0(\lambda r/a). \tag{8}$$

On substitution of this expression into the differential equation (1), and making use of the expansion for unity, which is

$$1=\frac{8}{\pi}\sum_{\mu=1,3,\cdots}^{\infty}\sum_{\lambda=1}^{\infty}\frac{(-)^{(\mu-1)/2}\cos(\pi\mu z/l)J_0(\lambda r/a)}{\mu\lambda J_1(\lambda)}, \tag{9}$$

we find that μ takes on odd values only. The solution is

$$T/\alpha=\frac{8}{\pi}\sum_{\mu=1,3,\cdots}^{\infty}\sum_{\lambda=1}^{\infty}\frac{(-)^{(\mu-1)/2}\beta^2\cos(\pi\mu z/l)J_0(\lambda r/a)}{\mu\lambda J_1(\lambda)(\pi^2\mu^2/l^2+\lambda^2/a^2+\beta^2)}. \tag{10}$$

The average temperature $\bar{T}$ in the enclosure is

$$\bar{T}/\alpha=(32/\pi^2)\sum_{\mu=1,3,\cdots}^{\infty}\sum_{\lambda=1}^{\infty}\beta^2/\mu^2\lambda^2\times(\pi^2\mu^2/l^2+\lambda^2/a^2+\beta^2). \tag{11}$$

The doubly infinite series (10) for $T(r,z)$ is uniformly convergent in the cylinder, $0\leqq r\leqq a$, $-l/2\leqq z\leqq l/2$. Its derivatives through the second order are all uniformly convergent within any closed region interior to the cylinder. Therefore they can be substituted into the differential equation (1). When this is done, it is found that the series (10) satisfies (1). It is evident that (10) satisfies the boundary conditions, and so it is a solution to the problem at hand.

If $l\to\infty$, so that the enclosure becomes an infinitely long cylinder, we find that both (5) and (10) reduce to the solution given by Daniels for such a cylinder. If $a\to\infty$, they also reduce to the solution for an enclosure formed of two infinite parallel plates.

CALCULATIONS

Expressions (5) and (10) are superficially different, but (5) can be readily transformed into (10) and vice versa. A similar remark applies to the two expressions for $\bar{T}$. Formula (7) can be directly transformed into (11) and vice versa. However it appears that Eq. (11) is more convenient for computation with SEAC (the National Bureau of Standards Eastern Automatic Computer). Equation (11) has the additional advantage over (7) that it does not require the use of transcendental functions with complex arguments.

Computations of the average temperature, for $a=2.15$ cm and $l=1.814$ cm, were made as a function of $-j\beta^2$. Pressure calibrations of condenser microphones are made at the Bureau of Standards in a coupler having these dimensions. The average temperatures were used to compute a correction factor to the acoustic impedance (see Daniels[1]). In Fig. 2 are plotted values

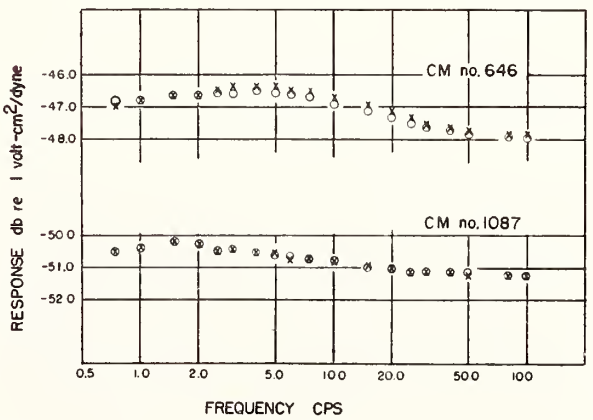

FIG. 3. Responses of Western Electric type 640AA condenser microphones Nos. 646 and 1087 at very low frequencies. ○=calibration with a 3.18 cc coupler. ×=calibration with a 20.1 cc coupler.

of the magnitude of the correction factor (for $\gamma = 1.403$) *vs* the nondimensional parameter $(-j\beta^2/2)^{\frac{1}{2}}V/S$, where V is the volume and S the surface area of the enclosure, as curve A. All cylinders having the same ratio $a/l = 1.185$ will have the same curve A. Curves B, C, and D are, respectively, those for a sphere, infinite cylinder, and parallel plates as obtained by Daniels. Curve A shows that the correction factor for this finite cylindrical enclosure approximates more closely that of a sphere rather than that of an infinite cylinder or that of parallel plates. Curve A is substantially different from the approximate curve given in Fig. 2 of the American Standard Method for the Pressure Calibration of Laboratory Standard Pressure Microphones, Z24.4-1949.

Curves for $a/l = 0.2500$, 0.4138, and 0.7754 were also computed. In each of these cases, the curves were very close to curve A and curve B (for the sphere). The coding of Eq. (10) for numerical evaluation by SEAC will be kept available for some time to come.

APPLICATION TO CALIBRATION OF MICROPHONES

The pressure responses of two condenser microphones were measured utilizing the correction factor of Fig. 2 to the acoustical impedance. Two enclosures having different volumes were used, and the responses obtained are plotted in Fig. 3. The crosses represent calibration in the 20.1 cc coupler, and the open circles the calibration using the 3.18 cc coupler. A correction for the finite diaphragm impedance (0.1 cc equivalent added volume) was used for the calculations made with the 3.18 cc coupler. The results of these measurements and computations indicate that the correction for the temperature effect is small at these frequencies, but useful in that it permits calibration with either coupler with agreement within 2 percent.

Reprinted from The Journal of the Acoustical Society of America, Vol. 26, No. 4, 506–509, July, 1954

Pressure Calibration of Condenser Microphones above 10 000 cps

Bernard D. Simmons and Fernando Biagi
National Bureau of Standards, Washington, D. C.
(Received April 24, 1954)

A "plane wave" acoustic coupler and an electrical admittance method are described for the pressure calibration of condenser microphones in the ultrasonic frequency range. Calibration results are given for frequencies to 40 kc.

INTRODUCTION

THE standard method[1] for the pressure calibration of microphones utilizes an acoustic coupling cavity through which pressure is applied to the diaphragm of the microphone. Figure 1 is a diagram of the NBS 20-cc cavity, designed for use with the Western Electric 640AA condenser microphone, a "type L" standard.[2] Reciprocity calibrations using this cavity are made, with a precision of 1.0 percent and without correction for wave motion or diaphragm impedance, to a frequency of 3000 cps when the cavity is air filled and to 12 000 cps using hydrogen.

The frequency range is limited by the assumption that the ratio of the volume current produced by the driving transducer to the pressure over the microphone diaphragm, the "reciprocity parameter," is the lumped admittance ($\omega V/\rho c^2$) of the volume V of gas enclosed. At low frequencies the pressure in the cavity is uniform and this assumption is valid provided the impedances of the transducer diaphragms are large compared to the cavity impedance. At higher frequencies, for which the wavelength is comparable to the cavity dimensions, wave motion complicates the pressure distribution. The result of departure from the lumped impedance assumption due to wave motion is shown by curve A of Fig. 2.

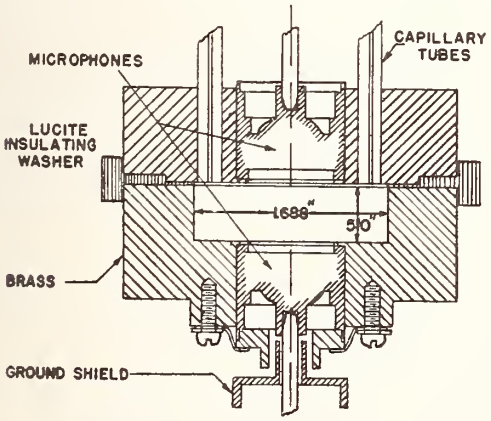

FIG. 1.

The "pattern factor" A is the experimentally determined response in the air-filled cavity relative to the response obtained in the hydrogen-filled cavity.

Considerations in the design of cavities for optimum performance without correction for wave motion are discussed in detail by Beranek,[3] with reference to the experimental work of DiMattia and Wiener. Cook[4] has discussed theoretically the relative influence of the length and radial modes, indicating an optimum ratio of diameter to length, which, for the 20-cc cavity, was experimentally determined to be 3.4/1. Reducing the size of the cavity with the same ratio of diameter to length leads to a slight improvement in frequency range. By a further reduction in size DiMattia and Wiener produced a design which, with a correction for diaphragm impedance, is intended for work in air to 6000 cps. This is probably the limit of what can be

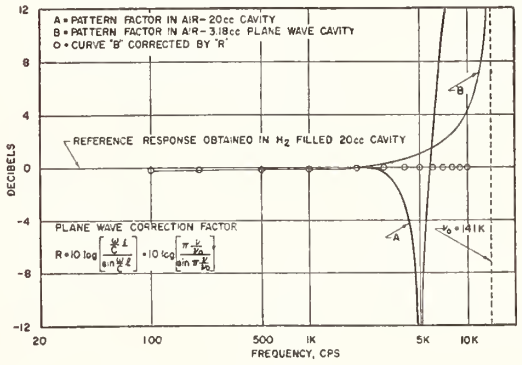

FIG. 2.

achieved with these microphones in the direction of maintaining uniform pressure in a cavity.

Plane Wave Cavity

A correction for wave motion in a cylindrical tube which takes into account both radial and longitudinal variation in pressure is complicated by interaction between the pressure and the modes of vibration of the diaphragms, and involves a knowledge of the diaphragm structures. A considerable simplification is obtained if the frequency of the first radial mode of the cavity is

[1] American Standard Z24.4–1949, American Standard Method for the Pressure Calibration of Laboratory Standard Pressure Microphones, American Standards Association, 70 East 45th Street, New York 17, New York.
[2] American Standard Z24.8–1949, American Standard Specification for Laboratory Standard Pressure Microphones.
[3] L. L. Beranek, *Acoustic Measurements* (John Wiley and Sons, Inc, New York), p. 140 ff.
[4] R. K. Cook, J. Acoust. Soc. Am. **16**, 102 (1944).

Reprinted from The Journal of the Acoustical Society of America, Vol. 26, No. 5, 693–695, September, 1954

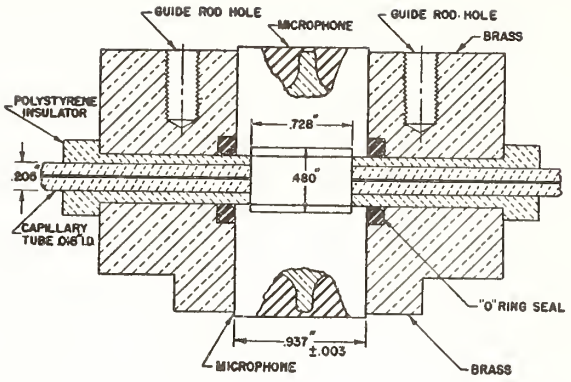

FIG. 3.

substantially above that of the first longitudinal mode. Then, if the impedance of the microphone diaphragm is sufficiently high, the pressure is uniform over the diaphragm surface, and, as is true at low frequencies, is still proportional to the volume velocity of the source.

The wave correction is the increase in pressure at the microphone diaphragm. The pressure and particle velocity in a plane wave are[5]

$$p(x)=Ae^{ikx}+Be^{-ikx}$$

$$u(x)=\frac{1}{\rho c}(Ae^{ikx}-Be^{-ikx}).$$

ρ is the density of the undisturbed medium. $k=2\pi\nu/c$ where ν is the frequency and c the sound velocity. Using the boundary conditions $u(l)=0$, corresponding to an effectively rigid diaphragm, and $u(0)=u$, the pressure at the microphone diaphragm ($x=l$) is

$$p(l)=2\rho cu/(e^{ikl}+e^{-ikl})=\rho cu/\sin kl.$$

At low frequencies as k approaches zero, $\sin kl$ approaches kl and the increase in pressure at higher frequencies is $kl/\sin kl$. In decibels, the correction to the response is

$$R=10\log_{10}\left[\frac{2\pi\nu l}{c}\Big/\sin\frac{(2\pi\nu)l}{c}\right].$$

With these considerations in mind the cavity shown in Fig. 3 was constructed for use with the W. E. 640AA microphone. The two cylindrical sections of the cavity are separated by a polystyrene insulator through which capillary tubes, shown in the cross section, lead into the cavity. The capillaries serve to introduce hydrogen into the cavity. The length l includes the microphone recesses, which vary slightly in depth from one microphone to another. The effective length can be accurately determined from the frequency ν_0 of the first (longitudinal) resonance ($l=\lambda/2$). For this purpose the foregoing expression may be put in the form

$$R=10\log_{10}\left[\frac{\pi\nu/\nu_0}{\sin(\pi\nu/\nu_0)}\right].$$

Using air ν_0 is about 14 kc and the frequency of the first radial mode is 22.7 kc. The volume of the cavity is 3.21 cc.

Response data up to 10 kc using the plane wave cavity are shown on Fig. 2. The zero reference level is the response obtained from the 20-cc hydrogen-filled cavity. Curve B is the uncorrected response obtained from the plane wave cavity when air filled. The circles are corrected values of B using the wave correction factor R. The agreement above 500 cps is close to 1.0 percent. Below 500 cps values diverge slightly (0.3 db) because of the finite impedance of the diaphragm.

The excellent results obtained to 10 kc/sec with the plane wave cavity using air, as compared with the usual results obtained with the 20-cc hydrogen-filled cavity, create a strong presumption that satisfactory calibration data can be obtained using hydrogen in the plane wave cavity at frequencies beyond 10 kc, where difficulties are encountered with the 20-cc cavity.

In order to check the cavity data above 10 kc, an alternate procedure was developed using electrical impedance data. This method will now be described.

Electrical Impedance Method

The performance of the condenser microphone is assumed to be described by the following pair of linear relations between the voltage e and current i on the electrical side and the pressure p and volume current u on the mechanical side.

$$e=\frac{1}{j\omega C_0}i+\frac{-\varphi}{j\omega C_0}u,$$

$$p=\frac{-\varphi}{j\omega C_0}i+Z_m u.$$

The parameter C_0 is the electrical capacitance with the diaphragm restrained from motion, and Z_m is the

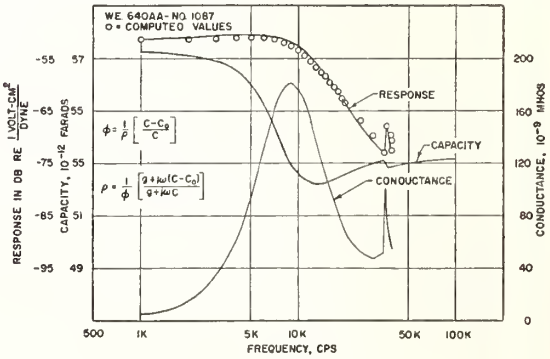

FIG. 4.

[5] P. M. Morse, *Vibration and Sound* (McGraw-Hill Book Company, Inc., New York, 1948), p. 238.

impedance on the mechanical side with the electrical side open circuited.

The parameter φ, which depends on the polarizing voltage and the geometry of the condenser plates, is considered in the following treatment to be independent of frequency.

The microphone response ρ, defined as the ratio of open-circuit voltage to pressure, is

$$\rho = -(e/p)_{i=0} = +\varphi/j\omega C_0 Z_m.$$

If the mechanical load impedance is small compared to Z_m, so that $p=0$, which experimentally was assured by using a quarter-wavelength coupling tube, the electrical admittance is

$$Y = (j\omega C_0) + \varphi^2 \Big/ \left(Z_m - \frac{\phi^2}{j\omega C_0} \right).$$

Solving for Z_m and substituting in the above expression for the response, we obtain

$$\rho = (Y - j\omega C_0) \Big/ \varphi Y = \frac{1}{\varphi} \left[\frac{g + j\omega(C - C_0)}{g + j\omega C} \right],$$

where $Y = g + j\omega C$.

The parameters C_0 and φ are determined experimentally in the following manner. At high frequencies, where the mass reactance of the diaphragm becomes large, the electrical capacitance approaches the blocked value C_0. The value of C_0 was measured at 100 kc. At low frequencies the conductance becomes small and the response is

$$\rho = C - C_0/\varphi\omega C.$$

φ can thus be determined from a value of response at low frequencies. Both φ and C_0 can be determined from values of response at low frequencies.

Figure 4 shows measured values of capacitance, conductance, and response and calculated values of response using the above method.

Figure 5 shows on an expanded scale data from three microphones. The zero reference value is the value of

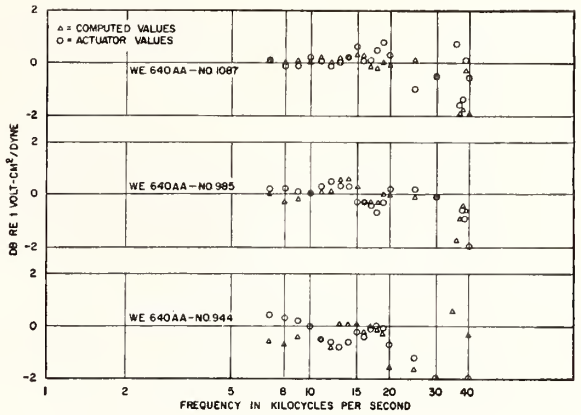

FIG. 5.

the response as measured by reciprocity using the plane wave cavity. The triangular points are the calculated values using the measured capacitance and conductance. The circular points are points which were determined by using an electrostatic actuator.[6] These results indicate a fair agreement between calculated and measured values of response up to about 40 kc.

CONCLUSION

With microphones having the diameter of the W. E. 640AA, a cylindrical enclosure permits calibration, within the usual accuracy (2 percent), up to about 10 kc in air using a correction based on plane wave transmission. With hydrogen in the cavity, results of about the same accuracy can be obtained up to 25 kc and with less accuracy up to 40 kc. Above 40 kc the radial mode of the coupler causes difficulties. However, values of response above 40 kc can still be calculated using impedance data with the assumption the microphone follows the simple four-terminal network theory on which the electrical impedance method is based.

The authors wish to express their appreciation to Dr. R. K. Cook for his interest and helpful suggestion in this work.

[6] Reference 3, p. 173.

Method for Measurement of $|E'/I'|$ in the Reciprocity Calibration of Condenser Microphones

WALTER KOIDAN
National Bureau of Standards, Washington 25, D. C.
(Received February 19, 1960)

A simple method is described for accurately measuring the ratio of the driving current through a capacitor-type sound source to the open-circuit voltage of a microphone used as the sound receptor. Determination of this ratio in a reciprocity calibration procedure eliminates the need for measurement of the capacitance of the reversible microphone.

A SIMPLE technique has been developed for accurately measuring the ratio $|E'/I'|$ in the reciprocity calibration of condenser microphones,[1] where I' is the driving current through the reversible microphone used as a sound source, and E' is the open-circuit voltage of the receptor microphone.

Nielsen's method[2] for performing this measurement makes use of an auxiliary calibrated capacitor through which the microphone driving current flows. The voltage across this capacitor is then observed with the aid of a cathode-follower preamplifier.

The method described below and illustrated schematically in Fig. 1 uses a resistance standard. No preamplifier, other than one for the receptor, is required.

The shell of the reversible microphone is not connected to ground, but rather to one side of a calibrated decade resistance box, R. An insulating ring and shielded calibrating line[3] is used to make this connection. The microphone is driven from a signal generator through a single-conductor shielded cable; stray capacitance across the microphone terminals is controlled by means of a ground shield.[3]

Switches 1 and 2 can be ganged for convenience, connections being made to points A and A' in one position and points B and B' in the other position. At each frequency two adjustments are required:

(1) First, the attenuator is adjusted so that voltmeter V_1 reads the same in both positions of switch 1. The position of switch 2 does not affect this measurement. The voltage which appears across the output of the attenuator is then equal in magnitude to the open-circuit voltage E' of the receptor microphone.

(2) Secondly, resistance R is adjusted so that voltmeter V_2 reads the same in both positions of both switches. The voltage across R is then equal to $|E'|$. The ground shields ensure that the current through R is the same as that through the sound source.

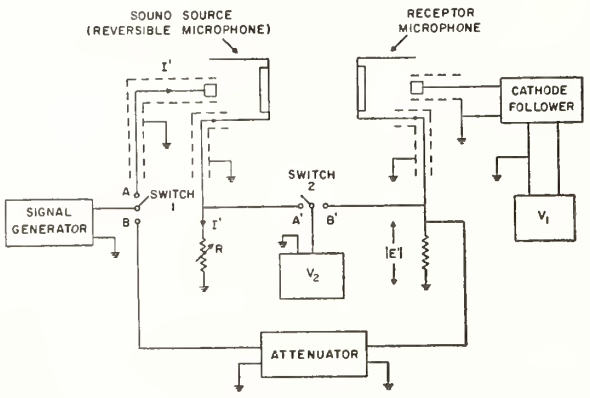

FIG. 1. Schematic diagram of the method for measuring the ratio $|E'/I'|$. Polarizing-voltage supplies and blocking capacitors were omitted from the diagram for clarity.

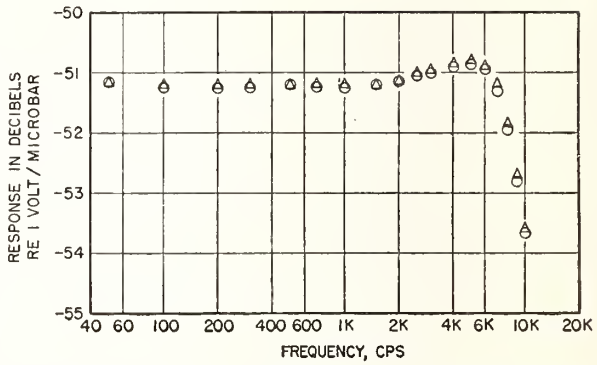

FIG. 2. Pressure response of a Western Electric Company type 640 AA condenser microphone measured by two variations of the reciprocity technique. The circles represent the response calculated from measurements of $|E'/I'|$; the triangles were obtained from measurements of capacitance and voltage-to-voltage ratios.

The desired voltage-to-current ratio is therefore

$$|E'/I'| = R. \tag{1}$$

This result is independent of the attenuator reading; in fact, the signal generator output can be a function of switch positions without affecting the value of R.

The method is adaptable to both pressure (coupler) and free-field calibrations. In a typical pressure calibration of a Western Electric Company type 640 AA condenser microphone, the resistance R varied from 24 350 ohms at 50 cps to 57.5 ohms at 10 kc. The variation of resistance with frequency is in the proper direction to minimize the effect of stray capacitance across R, which can be as large as about 1000 $\mu\mu$farad.

When attenuator readings are also taken, byproducts are the voltage-to-voltage ratio appearing in Cook's formula[4] and the magnitude of the electrical driving-point impedance of the reversible microphone. If the ratio $|E'/E| = A$, where E is the driving voltage, then from Eq. (1), the electrical impedance is $|R/A|$.

A pressure response curve for a type 640 AA microphone obtained by measuring the voltage-to-current ratio is shown in Fig. 2. For comparison, the response curve obtained by capacitance measurements with a Schering bridge and the voltage-to-voltage ratio is also plotted.

Miss June O. Magruder assisted in the laboratory measurements.

[1] W. R. MacLean, J. Acoust. Soc. Am. 12, 140 (1940).
[2] A. K. Nielsen, Acustica 2, 112 (1952).
[3] American Standards Association Standard Z24.4-1949, Fig. 6.
[4] R. K. Cook, J. Acoust. Soc. Am. 12, 415 (1941).

Hydrogen Retention System for Pressure Calibration of Microphones in Small Couplers

WALTER KOIDAN
National Bureau of Standards, Washington 25, D. C.
(Received 16 January 1963)

The pressure calibration of microphones using small hydrogen-filled couplers can be facilitated by connecting relatively large containers of hydrogen to the capillary tubes of the coupler and using additional capillary tubes to vent the large containers to the atmosphere.

IN the usual procedure for performing microphone pressure calibrations in a hydrogen-filled coupler, the coupler is filled with hydrogen through one of its two capillary tubes, and the air is ejected through the other. The concentration of hydrogen is determined by measuring the resonance frequency of a particular mode of the hydrogen-filled cavity and comparing this frequency with that obtained for the same mode when the coupler is filled with air. In order to make measurements at barometric pressure, the hydrogen supply line is detached. This causes the hydrogen in the coupler to be replaced by air at a rate determined by the volume of the coupler and the resistance of the capillary tubes. Readings are taken in order of decreasing frequency, so that the concentration of hydrogen is greatest at the highest frequencies.

In small couplers ($\approx$3 cc or less), loss of hydrogen is too rapid to perform a calibration in this way. In particular, in a plane-wave coupler,[1] one must know the frequency of the first longitudinal mode to be able to calculate a plane-wave correction. This becomes difficult if the resonance frequency is changing quickly.

One way of overcoming the difficulty is to maintain a very small flow of hydrogen to keep the resonance frequency from falling. But this flow produces a static pressure in the cavity which exceeds the ambient barometric pressure, and errors in the measured response can result.

A method for retaining hydrogen adequately at barometric pressure is shown schematically in Fig. 1. Stopcocks B, D, and F are first adjusted so that the hydrogen follows the path ABCDEFG, filling the 100-cc containers in a few minutes. Next, stopcocks F and D are turned to permit the coupler to be filled with hydrogen by the path ABCHIEFK. (The figure shows the stopcock positions while the coupler is being filled.) Then B is turned so that the 100-cc container on the right vents to the atmosphere through capillary J. Finally, the hydrogen supply line is removed.

A precaution to be observed in the second step of the above process is the following: When F and D are adjusted for filling the coupler, the pressure in the hydrogen supply line will rise due to the resistance of the capillary tubes. The resulting pressure in the coupler may be enough to damage the microphones. Therefore, just before stopcocks F and D are turned, the supply pressure should be reduced to a very low value. As the coupler is being filled, the supply pressure should be kept below about 1 in. of water.

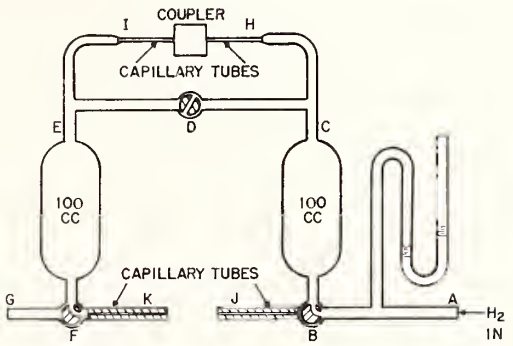

FIG. 1. Hydrogen-retention system for calibration of microphones in small couplers.

During a typical run using a 3.3-cc plane-wave coupler, the first longitudinal mode dropped from 49.0 to 48.5 kc in one-half hour. With another coupler[2] (3.8 cc), the second radial mode changed from 44.4 to 44.0 kc in the same period of time.

Such hydrogen-retention characteristics depend, of course, on obtaining a good seal where the microphones rest on the shelves of the coupler. A thin film of vacuum grease on these contact surfaces is required to obtain a good seal.

Marshall A. Pickett assisted in the construction of the apparatus.

[1] B. D. Simmons and F. Biagi, J. Acoust. Soc. Am. **26**, 693 (1954).
[2] L. L. Beranek, *Acoustic Measurements* (John Wiley & Sons, Inc., New York, 1949), p. 146.

Reprinted from THE JOURNAL OF THE ACOUSTICAL SOCIETY OF AMERICA, Vol. 35, No. 4, 614, April, 1963

Free-Field Correction for Condenser Microphones

WALTER KOIDAN AND DAVID S. SIEGEL

National Bureau of Standards, Washington, D. C.

(Received 1 September 1964)

Differences in the free-field corrections of 1-in. condenser microphones, caused by their different acoustic driving-point impedances, were found to be of sufficient magnitude to warrant a cautious approach to the determination of the free-field response level from measurements of the pressure response level and the addition of a "standard" free-field correction.

THE FREE-FIELD RESPONSE LEVEL MINUS THE PRESSURE RESPONSE level (free-field correction) of a group of type-L condenser microphones[1] having the same external dimensions was recently measured at the National Bureau of Standards. Seven Western Electric Company microphones type 640AA and two Electrical Communication Laboratory microphones type MR103 were included in the tests. Free-field reciprocity measurements were made for sound propagated perpendicular to the diaphragms and pressure reciprocity measurements were made in closed couplers.

The measured differences in the free-field corrections between microphones were larger than could be attributed to experimental errors. As an example, the results for two 640AA microphones, representing extreme cases, are plotted in Fig. 1. The maximum difference is 0.9 dB at 10 kHz.

The differences appear to be caused by the pressure drop that occurs at the diaphragm of a microphone when placed in a free sound field. The net sound pressure on the diaphragm can be represented as the sum of three terms: the free-field pressure, the diffraction pressure for a transducer with a rigid diaphragm, and the pressure drop caused by the motion of the diaphragm. The situation is expressed analytically by Eq. (30) in a paper by Foldy and Primakoff.[2]

The motion of the diaphragm, and, hence, the free-field correction, depends upon the acoustic driving-point impedance and radiation impedance of the microphone for plane waves incident on the diaphragm. This dependence could not be determined accurately because of the difficulty in calculating the impedances for plane-wave excitation. However, a correlation (shown in Fig. 2) was observed between the free-field corrections and the single-degree-of-freedom stiffness parameters. The parameters were measured with the aid of a carrier-frequency circuit[3] under conditions of uniform pressure distribution over the diaphragm. The two 640AA microphones with free-field corrections greater than 10 dB have unusually high stiffness and resistance and are not typical units. Their pressure-response level at low frequencies is about -55 dB *re* 1 V dyn^{-1}·cm^2, which is unusually low.

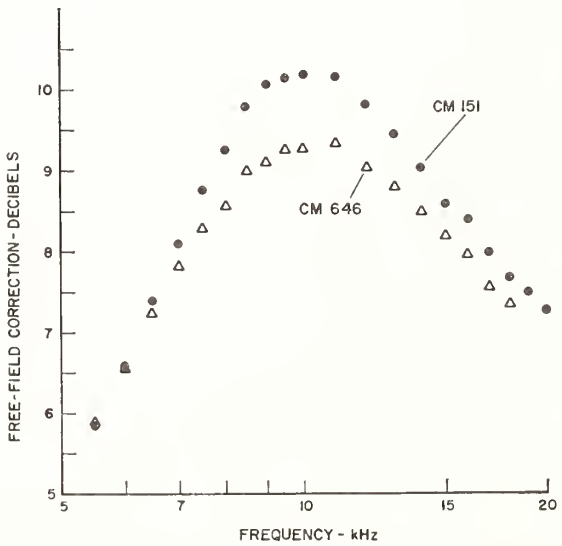

FIG. 1. Free-field corrections for two Western Electric Company type 640AA condenser microphones, representing extreme cases.

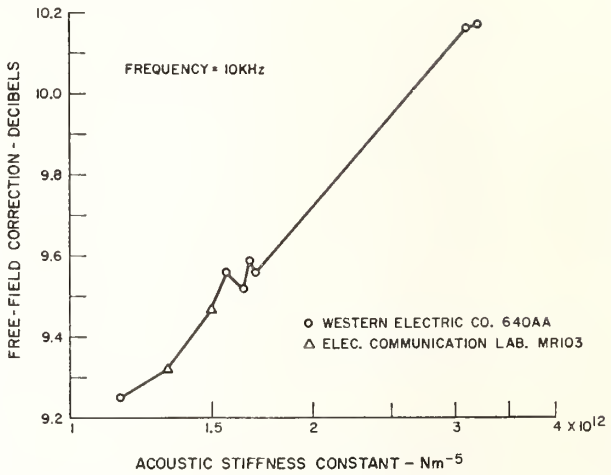

FIG. 2. Free-field correction vs acoustic stiffness constant for 9 type-L condenser microphones at a frequency of 10 kHz.

Most 1-in. condenser microphones of the stretched-membrane type have a resonance frequency (for minimum acoustic impedance) of approximately 10 kHz, at which frequency the resistive component of the radiation impedance becomes appreciable. The resistive component of the acoustic driving-point impedance in this frequency region is not large relative to the radiation impedance, and the pressure-drop term is sizeable. However, the two microphones with stiff diaphragms have resonance frequencies in the neighborhood of 15 kHz, so that their acoustic impedances at 10 kHz are high enough to allow only a relatively small pressure drop at the diaphragms. The net effect is a larger free-field correction than for an average microphone.

The results of these experiments indicate that the free-field response of a type-L microphone may be in error above about 6 kHz if evaluated from measurements of the pressure response and the addition of a "standard" free-field correction, such as that given in American Standards Association Standard Z24.4-1949, "Pressure Calibration of Laboratory Standard Pressure Microphones." However, the use of a standard free-field correction seems justified for microphones manufactured to tolerances sufficiently close to keep their acoustic impedances approximately equal.

[1] American Standards Association Standard Z24.8-1949, "Laboratory Standard Pressure Microphones" (1949).
[2] L. L. Foldy and H. Primakoff, J. Acoust. Soc. Am. 17, 109–120 (1945).
[3] M. D. Burkhard, E. L. R. Corliss, W. Koidan, and F. Biagi, J. Acoust. Soc. Am. 32, 501–504 (1960).

Reprinted from THE JOURNAL OF THE ACOUSTICAL SOCIETY OF AMERICA, Vol. 36, No. 11, 2233–2234, November 1964

Calibration of Standard Condenser Microphones: Coupler versus Electrostatic Actuator

WALTER KOIDAN

Institute for Basic Standards, National Bureau of Standards, Washington, D. C. 20234

The response-frequency characteristic of a "1-in." condenser microphone measured by an electrostatic actuator is likely to be significantly different from that measured by reciprocity in an acoustic coupler because of the radiation impedance of the microphone diaphragm with the actuator in place. It cannot be assumed, except at low frequencies, that the radiation impedance is negligible and that the actuator calibration yields the pressure response. Such an assumption also is apt to lead to errors in the determination of the free-field response when calculated with the aid of the free-field correction.

I. Pressure Calibration

SIGNIFICANT DIFFERENCES ARE OBSERVED IN THE RESPONSE-frequency characteristics of 1-in. condenser microphones, depending on whether the calibration is performed by reciprocity in an acoustic coupler[1] or by an electrostatic actuator.[2] A discussion of this discrepancy is pertinent to the proper use of response data provided by the National Bureau of Standards in test calibrations.

It is important to keep in mind the accepted definition of pressure response[3] to be able to decide whether a particular calibration method really yields the pressure response. In S1.10, the pressure response is defined as e/p, where e is the open-circuit voltage of the microphone and p is the sound pressure on, and uniform over, the exposed surface of the diaphragm due to the application of a sound pressure from an external source. The point to be emphasized here is that p is the *net* sound pressure on the diaphragm. The Standard describes methods for obtaining closely the ideal conditions given in the definition.

In current practice, electrostatic actuators sometimes are used to estimate the variation in pressure response with frequency. First, an absolute measurement of the pressure response is made at a single frequency by reciprocity, or with a pistonphone; then the actuator is used to extend the frequency range under the assumption that the net pressure on the diaphragm is independent of frequency. It turns out that this is rather a poor assumption for typical 1-in. condenser microphones. In general, the net pressure on the diaphragm is equal to the applied electrostatic pressure minus the pressure drop across the diaphragm radiation impedance in the presence of the actuator. The pressure drop is caused by the motion of the diaphragm. (The radiation impedance in the presence of the actuator is referred to below as the "modified radiation impedance.")

The error in a pressure response measurement that results from an actuator calibration depends on the value of the acoustic driving-point impedance of a microphone relative to its modified radiation impedance. At low frequencies (stiffness-controlled region), the driving-point impedance is very high and the error is negligible. However, a large error shows up in the neighborhood of the resistance-controlled region of the microphone, where the driving-point impedance is not very high compared to the modified radiation impedance.

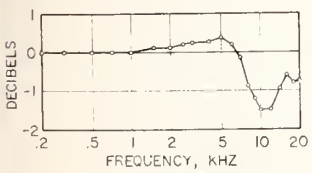

FIG. 1. Actuator-determined response level minus pressure (coupler) response level for a type L laboratory standard microphone without a recess, with an equivalent volume at low frequencies of 0.12 cm³, a resonance frequency of 8.6 kHz, and a Q factor of 0.93.

Figure 1 shows the difference between an actuator calibration and a coupler reciprocity calibration for a typical type L ("1-in.") laboratory standard condenser micriphone[4] whose diaphragm protrudes slightly beyond the shell. Similar results are obtained up to about 15 kHz for type L microphones with a 0.077-in. recess in front of the diaphragm (actuator positioned within the recess).

The possibility of reducing the modified radiation impedance by terminating the microphone–actuator combination in a quarter-wavelength tube was suggested in 1948 by Madella.[5] Measurements with such an arrangement were carried out in 1961 at the National Bureau of Standards[6] using an actuator 0.021 in. thick (Fig. 2). The agreement between coupler calibration and actuator–quarter-wavelength-tube calibration was better than 0.15 dB up to 15 kHz, indicating that the differences plotted in Fig. 1 are, indeed, due mainly to the modified radiation impedance.

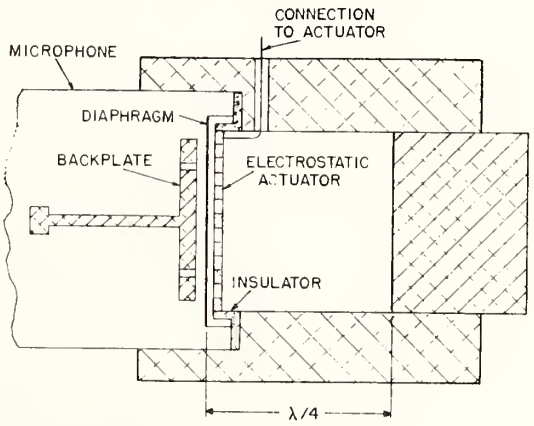

FIG. 2. Arrangement for microphone calibration by an electrostatic actuator terminated in a quarter-wavelength tube.

Further evidence that the radiation impedance is not negligible can be obtained by driving the microphone at its electrical terminals and, simultaneously, measuring the magnitude of the diaphragm motion into different acoustic loads. This experiment can be performed with the aid of a suitable carrier-frequency circuit.[7] In Fig. 3, each of the graphs represents diaphragm motion relative to that observed with the microphone terminated in a quarter wavelength tube—i.e., in a zero acoustic impedance. Thus, the dots represent motion into free space, the dashed lines motion into a modified radiation impedance, and the solid lines motion into a grid–quarter-wavelength-tube combination, all relative to motion into a zero acoustic impedance. Note that the 0.021 in. grid with a λ/4 tube has only a small effect on the diaphragm motion.

II. Free-Field Calibration

The free-field response level minus the pressure response level, referred to in S1.10 as the "plane-wave free-field correction," is tabulated up to 20 kHz in Table A1 of that Standard. The values apply to 1-in. microphones with a recess and with the dimensions shown in Fig. 12 of the Standard. The purpose of the tabulation is to permit calculation of the free-field response from the pressure response.

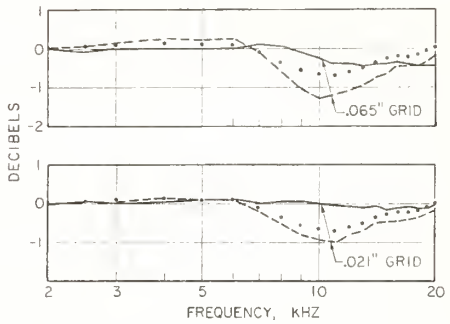

FIG. 3. Effect of acoustic loading on diaphragm motion relative to motion into a quarter wavelength tube: (a) effect of radiation impedance (dots), (b) effect of modified radiation impedance (dashed line), (c) effect of grid and $\lambda/4$ tube (solid line). Type L laboratory standard condenser microphone with a 0.077-in recess, an equivalent volume at low frequencies of 0.084 cm^3, a resonance frequency of 9.2 kHz, and a Q factor of 0.81.

Obviously, the values tabulated in S1.10 cannot be added to the actuator-determined response level to predict the free-field response level without incurring an error similar to that shown in Fig. 1. Users of microphones are less likely to make such a mistake if calibrations performed with electrostatic actuators are not referred to as "pressure calibrations," and if the term *free-field correction* is reserved for the difference between free-field response level and pressure response level as defined in S1.10.

III. Small Microphones

Actuator-determined calibrations on smaller condenser microphones—e.g., with diameters of $\frac{1}{2}$, $\frac{1}{4}$, or $\frac{1}{8}$ in.—will provide a more accurate measure of pressure response variation with frequency than on one inch microphones, since the acoustic driving-point impedance of the smaller units is considerably greater than that of the 1-in. units, and the modified radiation impedance relatively less important.

[1] *USA Standard S1.10-1966, Calibration of Microphones* (U. S. A. Standards Institute, New York, 1966).
[2] H. F. Olson and F. Massa, *Applied Acoustics* (P. Blakiston's Son and Co., Philadelphia, Pa., 1939), 2nd ed., pp. 273–279.
[3] Ref. 1, Paragraph 2.2.
[4] *USA Standard S1.12-1967, Specifications for Laboratory Standard Microphones* (U. S. A. Standards Institute, New York, 1967).
[5] G. B. Madella, J. Acoust. Soc. Amer. **20**, 550–551 (1948).
[6] W. Koidan, J. Acoust. Soc. Amer. **33**, 853 (1961).
[7] W. Koidan, J. Acoust. Soc. Amer. **29**, 813–816 (1957).

Reprinted from THE JOURNAL OF THE ACOUSTICAL SOCIETY OF AMERICA, Vol. 44, No. 5, 1451–1453, November 1968

USA STANDARD FOR THE CALIBRATION OF MICROPHONES, S1.10 - 1966[1]

BACKGROUND AND SUMMARY[2]

By Walter Koidan

I. Background

Three types of microphone calibrations are described in this standard: pressure, free-field, and random-incidence. For those unacquainted with the distinguishing features, a brief description follows.

The pressure response is the term used for the ratio of the open-circuit voltage of a microphone to the applied sound pressure when the sound is incident only on the exposed (front) surface of a microphone diaphragm. The sound pressure is that which exists at the surface of diaphragm, and the pressure response is defined only when the sound pressure is uniform over the surface. The problem of how to obtain a uniform pressure has been investigated rather thoroughly since 1940, and these efforts have culminated in certain "standard" practices, which are described in detail in USA Standard S1.10-1966. The methods involve the use of small, closed cavities of such shapes and dimensions that make it possible to establish a uniform sound field at a microphone diaphragm.

Accurate pressure response measurements are usually made only on a limited but important class of laboratory-type microphones (Type L) which are described in USA Standard S1.12-1967, Specifications for Laboratory Standard Microphones.[3]

---

[1]Available from American National Standards Institute, Inc., 1430 Broadway, New York, New York 10018, price $6.50.

[2]A condensed version of "A New Standard for the Calibration of Microphones", by Walter Koidan, Magazine of Standards 37, No.5, 141-144 (May 1966).

[3]Available as in footnote 1. Price $3.00.

On the other hand, free-field or random-incidence calibrations can be performed on a microphone of almost any shape or size. The free-field response of a microphone is also described in terms of a voltage-to-sound pressure ratio; however, the sound pressure is that which exists in a plane, progressive wave when the microphone is absent. The voltage is that which results when the microphone is immersed in the sound field at a specified orientation with respect to the direction of sound propagation.

For a given microphone, there is a useful relation between the free-field and pressure responses known as the "free-field correction." This relation is determined by separate absolute measurements of the two types of responses. Such experimental work has been carefully performed on Type-L laboratory standard microphones and the results tabulated in an appendix to the standard. There are distinct advantages to using the free-field correction. Free-field measurements require an anechoic chamber, elaborate mechanical devices, and large, stable sound sources. Accurate pressure calibrations of laboratory standard microphones require less equipment and can be performed more economically than free-field calibrations in most laboratories. To determine the free-field response of a standard microphone at a given frequency, it is necessary only to measure the pressure response at that frequency and add the appropriate free-field correction listed in USA Standard S1.10-1966. Thus, the accurate free-field absolute calibrations already made can be used to advantage by other laboratories. Commercially available microphones to which the tabulated free-field corrections apply are listed in an appendix.

Random-incidence response is defined similarly to free-field response, the main difference being that the sound pressure is that in a diffuse sound field when the microphone is absent from the field.

II. Summary of Recommendations

Since about 1940 the accepted basis for the absolute calibration of microphones in the audio frequency range has been the electroacoustic reciprocity theorem. The fundamental techniques were developed between 1940 and 1950; since then progress has been primarily in the form of added refinements, such as extension of the frequency range, increased accuracy, development of auxiliary measurement techniques, and improved theoretical corrections. These developments have been integrated in the standard with the basic theory and methods.

Pressure and free-field calibration methods have been combined in one publication since many definitions, requirements, and techniques are common to both methods. Furthermore, the combination provides a suitable setting for the presentation of a unified treatment of the theory of calibration by reciprocity. The approach was to develop a general expression for the response of a microphone based on the electroacoustical reciprocity theorem, and then to branch off, separately, to the specific conditions applicable to pressure and free-field measurements.

Following the theoretical development, calibration methods and experimental techniques are discussed in detail. A section is devoted to absolute pressure calibration in which formulas are given for the calculation of the pressure response of a microphone measured in a small, closed cavity.

In line with recent trends, the International System of Units (SI) was adopted. (This is advantageous here, since calculations in electroacoustics using MKSA units are very straightforward.) Response levels are expressed in decibels using a reference response of 1 $V/(N/m^2)$. Since the previous reference was 1 $V/(dyn/cm^2)$, the numbers representing response levels will now be larger, the conversion factor being 20 decibels.

The formulas given include only those quantities that are measured in the basic experiments described. These are often accurate enough for most laboratories. For those who need a higher degree of accuracy, correction factors are described individually. They include corrections for capillary-tube effects, heat-conduction losses at the walls of the cavity, wave pattern corrections, and the effect of the acoustic driving-point impedance (equivalent air volume) of a microphone on the effective volume of a cavity.

For pressure calibration in the frequency range below 10 kHz, a 20 cm^3 cavity is recommended. However, because of the onset of wave patterns, this cavity is limited to frequencies below 3 kHz unless it is filled with a gas lighter than air to increase the wave length at a given frequency. Hydrogen, for example, makes the cavity useful as high as 10 kHz. The techniques for using hydrogen are described in some detail, since they are an integral part of the calibration procedure. Incorrect methods can lead to errors or damage to the microphones.

Relatively recently, two smaller cavities have been developed which permit calibrations to be made as high as 20 kHz with good precision. The dimensions of these cavities and suitable experimental techniques for their use are described in a section called "High-Frequency Calibration." However, the volumes of the smaller cavities are only between 3 and 4 cm^3, so that measurements of the volumes are not as accurate as for the 20 cm^3 cavity. A good procedure is to use the 20 cm^3 cavity up to 10 kHz and a smaller one from 10 to 20 kHz.

The section on absolute pressure calibration is followed by one on absolute free-field calibration. The environmental requirements for free-field reciprocity are discussed first, with emphasis on the factors which affect the choice of surface treatment for an anechoic (echo-free) chamber, the distances between transducers, and the distances from the transducers to the walls. Recommendations take into account the relation between these parameters.

To determine if these parameters have been properly chosen for the degree of accuracy required, the standard recommends measurements to verify the inverse square law, i.e., exploration of the sound field along a line in the chamber emanating from the sound sources used in a calibration. The experimental procedure for measuring free-field response by reciprocity is described and formulas are presented for calculating the responses. Many miscellaneous factors, which can easily be overlooked by those not very familiar with the art of free-field work, are discussed.

Descriptions of practical methods for comparison free-field calibration and diffuse-field calibration are included at the end of the standard. These methods can be applied to a wider variety of microphones than absolute methods and are useful for evaluating microphones to be used outside of the laboratory.

A bibliography of seventy-nine references is often referred to in the text of the standard to draw attention to additional information and details available in the literature. Of the references dated 1932 and later, two-thirds appear in the Journal of the Acoustical Society of America, and are readily available.

Key Words: Acoustic coupler, Anechoic chamber, Microphone calibration, Standard.

Calibration of Audiometers

E. L. R. Corliss and W. F. Snyder*
National Bureau of Standards Washington, D. C.
(Received May 19, 1950)

A general description is given of the procedure developed at the National Bureau of Standards for calibrating audiometers. The sources of calibration standards are presented, and there is a discussion of the physics underlying the present technique. Limitations on the validity of the threshold data are pointed out. A method for determining the calibration of audiometer earphones is described. Data on earphone response can be used to gain some insight into the malfunctioning of an audiometer, and the way in which this can be done is indicated.

INTRODUCTION

An audiometer is used to measure auditory threshold. The most widely used type of audiometer is an electronic instrument which generates pure tones of controllable intensity and frequency in an earphone (receiver). The setting of the intensity control when the tone is just audible to the person being tested is a measure of that person's hearing threshold. Whether the threshold is normal or not, however, can be decided only if the audiometer is calibrated in terms of the sound pressure at auditory threshold for people with normal, unimpaired hearing. The hearing loss of a person's ear is the ratio (expressed in decibels) of the sound pressure

* Formerly of the Sound Section, now with the Microwave Standards Section of the National Bureau of Standards.

Reprinted from The Journal of the Acoustical Society of America, Vol. 22, No. 6, 837–842, November, 1950

at the threshold of audibility for that ear to the normal threshold pressure.

The following account is intended to describe a technique for calibrating audiometers, developed in large part at the National Bureau of Standards for the use of persons who manufacture or test these instruments. The procedure is embodied in the provisions of a proposed American Standard Specification,[1] developed by the American Standards Association and the National Bureau of Standards in a joint program.

THRESHOLD STANDARDS

Calibration of an audiometer is fundamentally the determination of the sound pressure produced by the earphone of the audiometer when it is placed on a standard coupler. The coupler consists of a heavy brass shell, enclosing a specified volume of air in an enclosure of simple geometric design. The earphone is placed over an opening in the coupler, and the sound pressures which it produces in the air volume are measured by means of a pressure-sensitive microphone. A diagram of Coupler No. 9A, designed at the National Bureau of Standards, is shown in Fig. 1. The volume of air within the coupler is about 5.7 cc, or approximately the volume within an average ear canal when an earphone is placed over the ear. The sound pressure in the coupler is measured with a calibrated condenser microphone. As shown, the coupler accommodates a Western Electric Type 640A or 640AA microphone; other condenser microphones may be used if they are of the same or smaller size and the coupler is modified so that it still encloses the same air volume.

The threshold voltage of an earphone at any frequency is the voltage which must be applied across its terminals to produce a sound pressure that is the threshold value for normal hearing at that particular frequency. The values in most common use in this country were determined by loudness-balancing from the data obtained during the National Health Survey of 1935–36.[2] From these data, the threshold voltages were determined for certain earphones (Western Electric Type 705A) kept at the Bureau. Because aging of the earphones might change the threshold voltages, the pressures produced in Coupler No. 9A by the audiometer earphones when threshold voltages were applied at their terminals were determined soon after completion of the survey. These pressures became the threshold standard for that particular type of receiver. They are independent of changes in response of the receivers.

The standard coupler pressures are not equal to the threshold pressures in the ear canal because the coupler does not present to the earphone an acoustic load

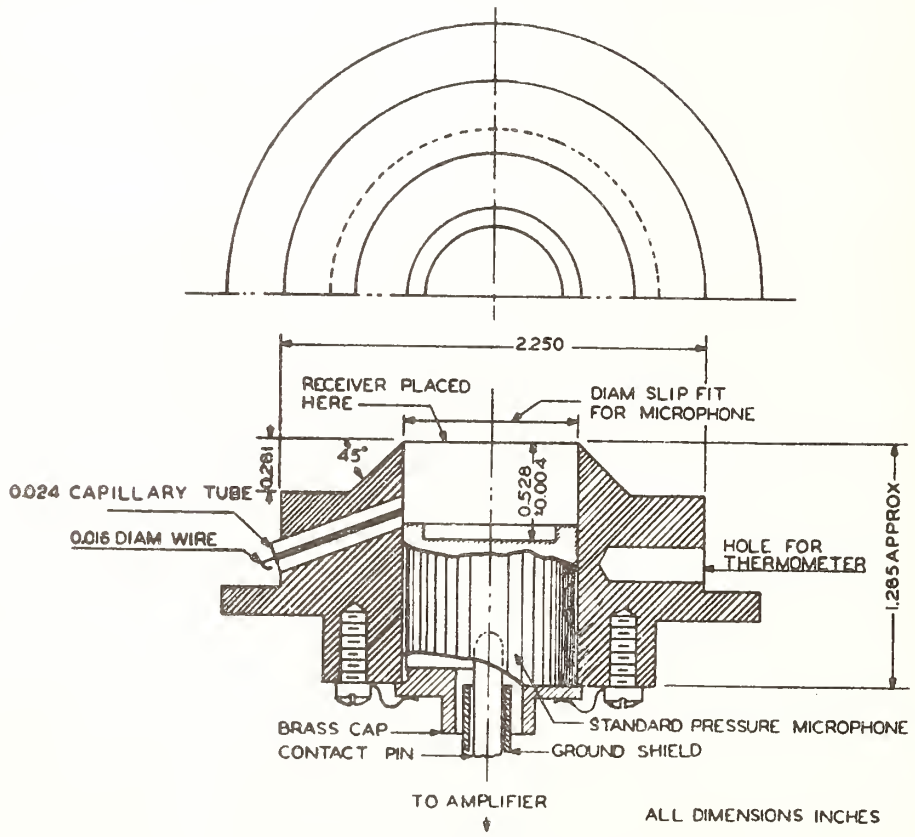

FIG. 1. N. B. S. Coupler No. 9A for calibration of audiometer receivers by means of Western Electric Types 640A or 640AA condenser microphones. The face of the receiver being calibrated rests on the upper edge with a coupling force equal to the weight of the receiver plus 400 g. The diaphragm of the microphone is located 0.528 in. (1.34 cm) below the upper edge of the cavity. The entire assembly is designed for use with a condenser microphone amplifier. (Volume = 5.7 cc.)

[1] American Standard Specification for Audiometers for General Diagnostic Purposes. Copies may be obtained from the American Standards Association, 70 East 45th Street, New York 17, New York.

[2] Reports of the National Health Survey, Hearing Study Series, Bulletin No. 5 (1935–36).

identical with that of the ear canal. Consequently, although the threshold pressures in the ear canal are presumably the same for all earphones, there is no reason to expect the standard coupler pressures to be identical for all types of earphones. A comparison is shown in Fig. 2. It was, of course, known from the beginning that the coupler did not duplicate the acoustic impedance of the ear. The ear presents additional loading due to compliance of flesh, and leakage of sound between the ear and the cap of the earphone, which are not provided by the coupler. It is this fact that makes it necessary to undertake the task of loudness-balancing to establish threshold coupler pressures for each new type of receiver. Until a coupler can be developed which presents a better replica of the ear's impedance over a wide frequency range, the alternative to loudness balancing is to make a complete threshold determination for each new type. If the acoustic load with which a human ear terminates the earphone were duplicated by the coupler, the standard threshold pressures would be identical with those in the average ear canal at threshold, and would be the same for all earphones designed to cover the ear.

Loudness balancing to establish standard threshold rests upon the premise that coupler standard threshold pressures are the same for all earphones of the same type. To determine standard coupler pressures for earphones of a new type, at least six subjects (12 ears) having approximately normal hearing make measurements of the voltages applied at the terminals of the new earphone and the standard earphone which will produce equally loud sounds at sound levels about 20 db above threshold. By combining these data with the measurement of the responses of the earphones when placed on Coupler No. 9A, the standard coupler threshold pressures at various frequencies for the new earphone may be found.

Standard threshold coupler pressures have now been determined for a number of different commercially available audiometer earphones. These values may be obtained from the Bureau by written request if they are needed by a testing laboratory. The threshold figures were originally determined for the octaves of 128 c/sec. Recently a change has been suggested in frequency standards for audiometer tests, from octaves of 128 c/sec. to octaves of 125 c/sec. This change is incorporated in the new American Medical Association and American Standards Association specifications. However, the National Health Survey measurements were made at octaves of 128 c/sec. The threshold pressures for 128 c/sec. octaves have been extrapolated to the new 125 c/sec. base by use of the minimum audible sound pressure curve determined by L. J. Sivian and S. D. White of Bell Laboratories.[3] At the present time, a project is under way at one of the sound laboratories in this country which will result in a direct determination

[3] L. J. Sivian and S. D. White, J. Acous. Soc. Am. 4, 288–321 (1933).

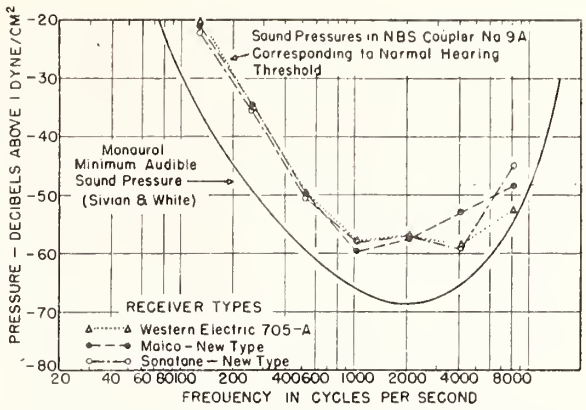

FIG. 2. Comparison of coupler pressures, corresponding to normal threshold for several types of commercial earphones, and the minimum audible pressure determination by Sivian and White. The form of the coupler pressure curve, derived from National Health Survey data, is in general agreement with the minimum audible pressure curve. Even if the coupler were to be a better replica of the ear, a difference of at least 5 db from the Sivian and White data is to be expected. The Sivian and White measurements were made with trained observers, and represent minimum rather than normal threshold.

of the auditory threshold pressures for 125 c/sec. octaves. Pending completion of that work, the extrapolated data are being used.

In Table I, standard threshold pressures in Coupler No. 9A are given for the Western Electric Type 705A earphone. Data for other types of earphones may be obtained by loudness-balancing against a Type 705A earphone or against other types for which standard threshold data are available. However, it might be well to consider that standard threshold data for receiver types other than the WE Type 705A were determined by a loudness-balance technique, and their use as comparison standards for loudness-balance implies an increase in the experimental uncertainty.

SOUND PRESSURE MEASUREMENT

To check the sound pressure output of the audiometer against standard threshold pressures, the sound pressure produced in Coupler No. 9A by the audiometer is measured at one hearing loss dial setting—usually 60 db—for each frequency. The audiometer is operated at the rated voltage stated by the manufacturer. Voltage regulation in the audiometer may be checked by making output pressure measurements at the extremes of line voltage likely to be encountered. The earphone is coupled to the condenser microphone through Coupler 9A. The microphone is connected to a preamplifier of the cathode follower type. An amplifier of fairly high gain is needed to bring the output of the cathode follower up to a level sufficient to actuate an output meter. If the same amplifier is to be used throughout the calibration procedure, gains of 80 to 120 db should be available.

A substituted voltage is used to determine the voltage output of the microphone. The arrangement for inser-

TABLE I. Standard threshold pressures in Coupler No. 9A. Western Electric Type 705A Receiver for octaves of 125 c/sec. and 128 c/sec. (Corresponding to the application of threshold voltages at the earphone terminals.)

Frequency (c/sec.)	Pressure (db above 1 dyne/cm²)	Frequency (c/sec.)	Pressure (db above 1 dyne/cm²)
125	−19.5	128	−20.1
250	−34.4	256	−34.9
500	−49.2	512	−49.5
1000	−57.3	1024	−57.5
2000	−57.0	2048	−57.0
4000	−58.9	4096	−58.5
8000	−53.1	8192	−52.3

tion of the voltage is shown in Fig. 3. With the hearing loss dial set at 60 db, the output meter is read. The hearing loss dial is then turned back to attenuate to a maximum the signal from the audiometer, and a calibrating voltage of the same frequency as that of the audiometer signal is inserted in series with the condenser microphone. The voltage is adjusted by means of a calibrated attenuator until the output meter reads the same as it did when the audiometer tone was being applied. From the amplitude of the calibrating voltage and the voltage response of the condenser microphone the sound pressure in the coupler can be computed. An attenuator of high quality should be used; the resistor across which the voltage is applied should terminate the attenuator with its characteristic impedance. A thermal voltmeter makes a good instrument for measuring the voltage at the input of the attenuator because it gives true R.M.S. readings.

ATTENUATOR DIAL

The pressure produced in the coupler at hearing loss dial settings other than 60 db can be derived from a calibration of the audiometer attenuator (hearing loss dial). For this measurement, the earphone is connected to the audiometer and placed on the coupler, so that the audiometer is loaded with the proper output impedance. A 500-ohm calibrated attenuator is placed in parallel with the earphone. (This impedance is suitable for many audiometer earphones, most of which have impedances of about 10 ohms.) The attenuator is connected to an amplifier and thence to a wave analyzer, which serves as a tuned amplifier and output meter. It is necessary to use a tuned amplifier in order to filter out electrical noise introduced by the high amplification required in the frequency range corresponding to maximum hearing acuity, since at those frequencies the signal voltages will be very low.

The hearing loss dial is checked against the calibrated attenuator by starting at the lowest hearing loss dial setting, with the parallel attenuator at a minimum setting. The difference between the dial steps and the attenuator steps is determined by adjusting the external calibrated attenuator to maintain the output meter readings at about the same point as the hearing loss dial is turned toward higher output settings.

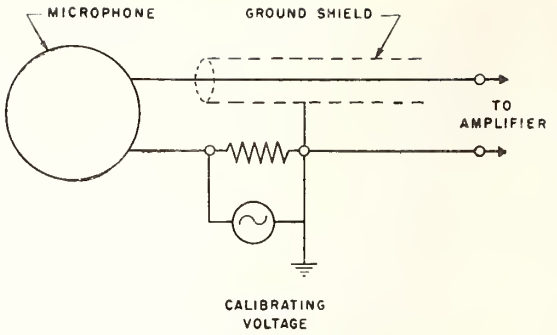

FIG. 3. Technique of introduction of calibrating voltage.

HARMONIC ANALYSIS AND FREQUENCY MEASUREMENT

It is usual for specifications to require that the fundamental of the pure tone signal from the audiometer be at least 25 db above the sound pressure of any harmonic. A harmonic analysis of the audiometer signal is performed with a modification of the assembly described above. The earphone is placed on the coupler, and its acoustic output is picked up by the condenser microphone, which is connected to an amplifier and a wave analyzer. The amplitudes of the various harmonics are measured by means of the wave analyzer.

The frequencies of the audiometer tones can be checked in various ways. They may be checked by audible beats against calibrated tuning forks, or against a calibrated beat frequency oscillator, using audible beats or Lissajous' figures on an oscilloscope. They may be compared with a standard timing frequency by means of electronic counters. The oscillator calibration can be determined by making use of the frequency broadcast from the National Bureau of Standards radio station WWV at Beltsville, Maryland. The standard frequency broadcast can also be used to provide the timing signal for the counters. Audio frequencies of 440 c/sec. and 600 c/sec. are broadcast on several radio carrier frequencies, including 2.5, 5, 10 and 15 Mc. Information on the broadcast schedule and means of making use of the standard frequencies may be secured by writing to the Central Radio Propagation Laboratory, National Bureau of Standards, Washington 25, D. C.

BACKGROUND NOISE LEVEL

The background noise level in the receiver output is evaluated by a weighted measurement of the sound level produced by the audiometer receiver in Coupler No. 9A when the audiometer is on, but the signal tone is interrupted. The relative weighting is that of the zero loudness level curve of intensity level *vs.* frequency. This curve is shown in Fig. 4. The measurement is made for all settings of the hearing loss dial and at all settings of the frequency control, since it has been found that the general noise level varies somewhat with these settings. The characteristics of the power supply influence the

background noise in the audiometer. The noise background introduced by the power supply depends upon the voltage characteristics of the power line, which are described in terms of *TIF* (telephone influence factor).

The *TIF* of a power line is a numerical rating which describes the loudness of noise which it is likely to induce in telephone circuits. Methods for measuring *TIF* are described by Barstow, Blye and Kent.[4] The characteristics of a frequency weighting network for *TIF* measurements are shown in Fig. 5. An average for the *TIF* of power lines throughout the country has been found to be about 15 to 25 for a.c. lines and 80 to 120 for d.c. lines. Of course, if the *TIF* for the particular power lines on which the instrument is to be operated is known, the noise level should be measured when the instrument is operating on a line with that *TIF*, even though the *TIF* values may fall outside the limits of the average values given above.

EARPHONE RESPONSE

If an audiometer in service is suspected of giving incorrect readings, the source of trouble may often be located by making a measurement of the earphone's response. Audiometers are adjusted as a unit, for a particular earphone. If difficulty develops, and spurious threshold measurements are being made, it may be that the earphone has shifted in response, or that the output voltage of the audiometer has changed.

By combining the measured response of the earphone with the standard threshold pressures specified for that type of earphone, the voltages which should be applied to the terminals of the earphone to produce a given sound level may be found, and compared with the actual output voltages which the audiometer supplies across the earphone terminals. A level of 60 db above threshold might be chosen with advantage, so that the voltage to be measured is in a convenient range for accurate measurement. If the voltages put out by the audiometer depart systematically from the requisite values at all frequencies, or are low or high at only one particular frequency, the difficulty is probably in the audiometer circuit. Deviations due to drift in the earphone response usually show a dependence upon frequency.

The earphone response may be measured without a direct measurement of voltage, and this may prove to be a convenience when only part of a calibration is to be carried out on an audiometer. The method depends upon the use of a substitution voltage in the microphone circuit. The voltage is introduced across a resistor which is in series between the microphone shell and ground. Usually this is the terminal impedance of a low impedance attenuator (500 ohms or less), since stray pickup may give trouble if higher impedances are used. The reading of the output meter when the microphone is used as a sound detector is matched by applying a voltage across the terminal resistor which will give the same reading, and noting the attenuation which must be applied to the initial voltage. Since both the signal from

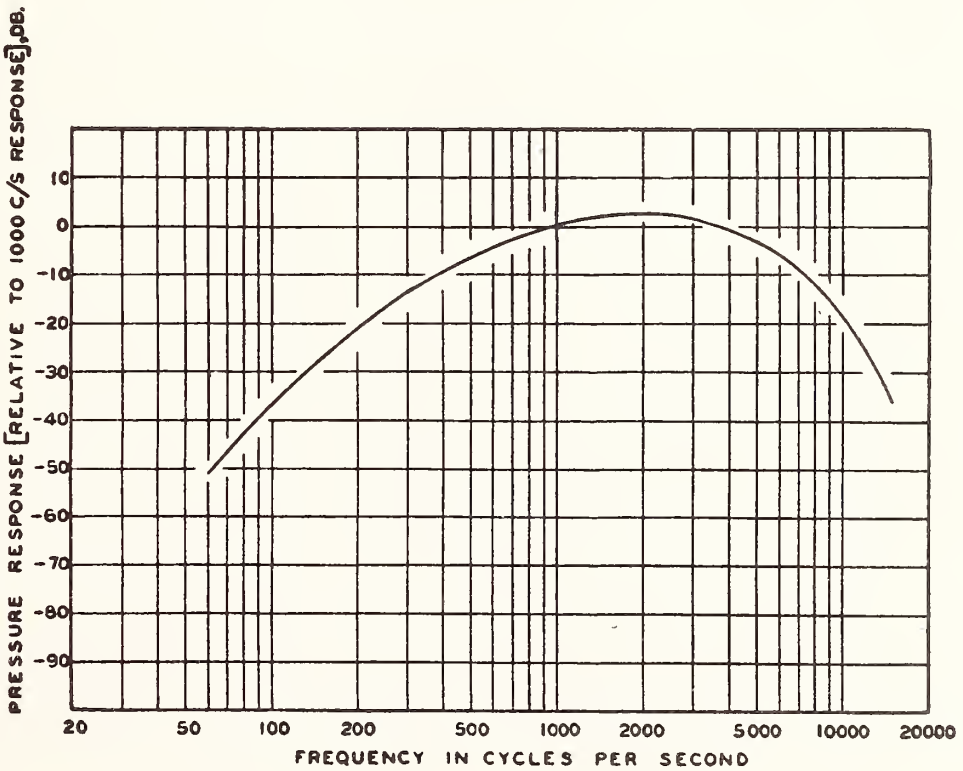

FIG. 4. Pressure response-frequency characteristic of equipment for measurement of noise in air-conduction receiver. (This curve is taken from that published in the article by L. J. Sivian and S. D. White), J. Acous. Soc. Am. 4, 313 (1933), and on page 124 of *Hearing* by S. S. Stevens and H. Davis (John Wiley and Sons, Inc. New York, 1938).

[4] Barstow, Blye, and Kent, Trans. A. I. E. E. 54, 1307 (1935).

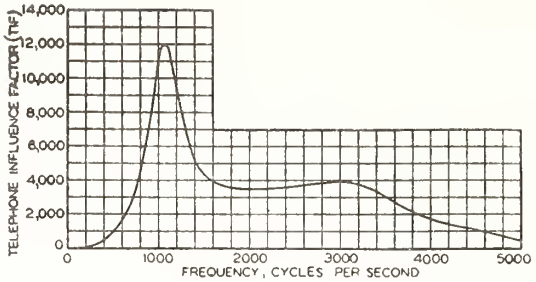

FIG. 5. Frequency weighting network for *TIF* measurements.

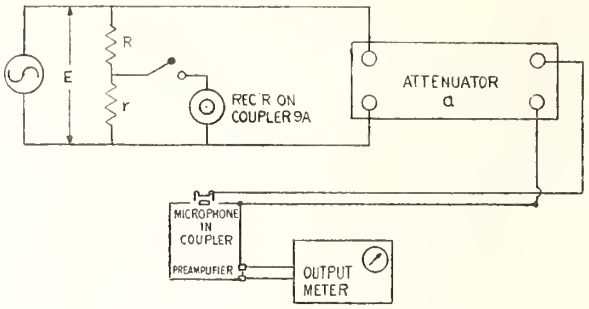

FIG. 6. Arrangement for earphone calibration.

the microphone and the signal from the attenuator are amplified via the same channel, the voltage output of the attenuator will be equal to the output voltage of the microphone. The network for this arrangement is shown in Fig. 4.

The value of resistor "r" (Fig. 4) should be made small so that the voltage across it is not changed appreciably when the earphone is shunted across it. A correction may be made if the impedance of the earphone is known. The value of "R" is chosen so that the attenuator readings are of convenient size. For low impedance earphones a convenient set of values is $R=10$ ohms and $r=0.1$ ohm.

The attenuator is set at a high value so that it contributes no signal when the earphone is serving as a source of sound, and the reading of the output meter is observed. The earphone circuit is then opened, and the attenuator is adjusted to give the same output meter reading.

Let the voltage applied to the input of the attenuator be "E." If the impedance of the earphone can be neglected, the voltage across the earphone is $(E\times r/R+r)$. Expressed in decibels, the voltage level across the earphone is then

$$20 \log_{10}E+20 \log_{10}r/(R+r).$$

Calling the observed attenuator reading "A," the substitute voltage is $20 \log_{10}E-A$, which is the e.m.f. output of the microphone. The sound pressure level in the coupler is $20 \log_{10}E-A-p$, where p is the response of the microphone in decibels relative to 1 volt-cm^2/dyne.

The response of the earphone in decibels relative to 1 dyne/cm^2-volt is the difference between the pressure level in the coupler and the voltage level across the earphone, when the levels are expressed in decibels. The response of the earphone represented by "P" is thus given by

$$P=20 \log_{10}E-A-p-20 \log_{10}E-20 \log_{10}r/(R+r)$$

or,

$$P=-20 \log_{10}r/(R+r)-A-p.$$

The computation of the threshold voltages from the standard threshold pressures in Coupler No. 9A and the earphone response is a simple subtraction. P, the earphone response, is given in decibels above 1 dyne/cm^2-volt. S, the standard threshold pressure, is given in decibels above 1 dyne/cm^2. The threshold voltage level, T, of the earphone is then given, in decibels above 1 volt, by the relation:

$$T=S-P.$$

The threshold voltage in volts can then be looked up as the antilogarithm of $T/20$ in a table of logarithms.

ACKNOWLEDGMENT

The procedure described in this paper has been evolved by the work of a large number of individuals. Auditory thresholds were determined on about 10,000 normal ears in the National Health Survey of 1935–36, under the supervision of Dr. Willis C. Beasley of the U. S. Public Health Service. An objective method for maintaining the threshold standards, and an earphone coupler for use in calibrating audiometer earphones were developed in the Sound Section of the National Bureau of Standards. Various improvements in technique have been contributed by several staff members during the course of their work on audiometry.

A Probe Tube Method for the Transfer of Threshold Standards between Audiometer Earphones*

EDITH L. R. CORLISS AND MAHLON D. BURKHARD
National Bureau of Standards, Washington, D. C.
(Received June 3, 1953)

To establish threshold standards for various types of earphones, from a set of threshold standards that has been determined for one particular type of earphone by a hearing survey, an empirical relationship must be found giving the sound pressures in the calibrating coupler corresponding to equal sound pressures in the ear. This has previously been accomplished by means of loudness balancing between earphones. The method described in this paper makes use of a direct probe measurement of the sound pressure developed by an earphone at the entrance to the ear canal. The experimental process is described and the results of tests to establish the equivalence of the probe method and loudness-balancing are given. In addition, several of the conditions under which loudness-balancing is carried out were investigated by the probe method. Equal loudness sensation was found to correspond to equal sound pressures at the ear, within the limits of experimental error.

INTRODUCTION

THE observed response of an earphone as a sound source is a function of the acoustic load with which it is terminated. Thus, if they differ in internal impedance, earphones that produce the same sound pressure in a human ear usually will not produce equal sound pressure in an ordinary calibrating coupler.† Our present difficulties with the standards for auditory threshold stem from the fact that we do not yet have earphone calibrating equipment that duplicates the physical conditions of measurements on the human ear.

The threshold voltage of an earphone at any frequency is the voltage which must be applied across its terminals to produce a sound pressure that is the threshold value for normal hearing at that particular frequency. Because earphones are calibrated on an "artificial ear" coupler, threshold standards for audiometric purposes are maintained in terms of the sound pressures produced by certain types of audiometer earphones in N.B.S. Coupler No. 9A.

The sound pressure produced by an earphone on the calibrating coupler is not in general the same as that which it would produce on an average human ear, because the coupler does not reproduce the acoustic load presented to the earphone by the ear. Since earphones of various types differ in their internal impedances, each type of earphone will have a different set of coupler pressures corresponding to the development of normal auditory threshold sound pressures in the ear. Therefore, once an auditory threshold survey has been made with a particular type of earphone, the results of this measurement cannot be applied directly to establish standards of normal threshold for earphones of any other type.

To obtain a set of threshold standards for a new type of audiometer earphone, either a complete new auditory threshold determination must be undertaken, or the threshold standards must be derived from existing threshold determinations on a standard type of earphone. This is achieved by determining what relationship of sound pressures in the calibrating coupler corresponds to the generation of equal sound pressures in the ear by both the new and the standard earphone. With present methods, it is not practical to establish for all types of earphones a relationship other than empirical between the response data obtained with a calibrating coupler and the actual response on the ear. As newer designs of earphones are developed, we have the problem of establishing normal threshold standards for them, so that they may be used in audiometry.

The method at present most generally used for the transfer of auditory threshold standards between earphones is a subjective technique, called "loudness balancing." In this process, the subject performing the "loudness-balancing" measurement is located in a sound-isolated room. He has at hand a signal generator, serving two calibrated voltage-dividing networks, each terminating in an earphone. The two earphones are attached to a single handset. One earphone is the standard earphone, for which threshold standards are known. The other earphone is the earphone for which threshold standards are to be determined by transfer from the known values for the standard earphone. The subject adjusts the signal applied to the standard earphone to a voltage level ascertained (from the known threshold standards and the calibration of the earphone) to produce a sound pressure corresponding to 20 db

* This work supported in part by the Office of the Surgeon General of the United States Army.

† A calibrating coupler, or "artificial ear," is a heavy-walled chamber of appropriate dimensions such that when an earphone is placed on it, the total enclosed volume is approximately the same as would be enclosed by the earphone on a human ear. The sound pressure in the coupler is measured with a pressure-sensitive microphone which forms part of the enclosure. See American Standard Z24.9–1949, American Standard Method for the Coupler Calibration of Earphones and American Standard Z24.5–1951, American Standard Specifications for Pure-Tone Audiometers for Hearing Diagnostic Purposes, available from the American Standards Association, 70 East 45 Street, New York, New York. An abridged version of Z24.9–1949 appeared in J. Acoust. Soc. Am. 22, 609 (1950).

See also E. L. R. Corliss and W. F. Snyder, J. Acoust. Soc. Am. 22, 837–842 (1950).

above normal auditory threshold. He then listens, in rapid alternation, to each of the earphones in turn, moving the handset rapidly back and forth so that first one earphone and then the other is presented to the same ear. While doing this, the subject adjusts the electrical signal applied to the second earphone until the sound it generates is equal in loudness to the sound he hears from the standard earphone. He then records the reading of the voltage divider on the second earphone. From this information, and from the calibration of this earphone on the calibrating coupler (NBS No. 9A or equivalent) the sound pressure in the coupler corresponding to normal auditory threshold for the secondary earphone can be computed. This determination usually is performed for at least six subjects having normal auditory acuity. It has been customary to make measurements for both ears of each subject.

It is possible, however, to use a probe inserted through the earphone cap to measure the actual sound pressures generated at the entrance to the ear canal,[1] and thus to determine the relative terminal voltages which must be applied to two earphones to produce equal sound pressures at the entrance to the canal. This objective method has the advantage of being simpler to carry out than loudness balancing, and it is much more rapid. By experiment, we have been able to show that this method gives substantially the same results as luodness-balancing. The probe method also makes it possible to investigate several of the assumptions upon which the entire idea of transferring threshold standards from one type of earphone to another is based.

ORIGIN OF PRESENT STANDARDS

The sound pressure standards for normal auditory threshold maintained by the National Bureau of Standards are derived from the National Health Survey of 1935–1936. The original measurements were determinations of voltages applied at the terminals of the audiometer earphones used in the survey. These voltages were averaged from the values that corresponded to threshold sensation for the 5000 persons whose auditory thresholds were being measured. The primary determination was thus given in terms of mean voltages applied to a specific group of earphones of particular design.

After completion of the survey, the threshold data were transferred to a group of standard earphones designed especially for stability in calibration. "Loudness balancing," as described above, was used to effect the transfer. The fixed voltages applied to the survey earphones were chosen to produce levels of 0 db, 20 db, and 40 db above average normal threshold. Although all three comparison levels yielded essentially the same results for the relative voltages to be applied to the new standard earphones, the data obtained by comparison at the 20-db level showed the least scatter. Hence the transfer process usually has been carried out at the 20 db level.

The loudness-balance measurement gave normal threshold values in the form of voltages applied at the terminals of standard earphones. Immediately after a loudness balance, the earphones were placed on a calibrating coupler and their response was measured. From the loudness-balance data and the earphone response, the sound pressures in the coupler that corresponded to normal auditory threshold were computed for the audiometric frequencies (octaves of 128 cps up to 8196 cps). These sound pressures constitute the normal threshold standard. They are independent of any subsequent aging of the earphone.

PHYSICAL FACTORS IN THE THRESHOLD STANDARDS

The usual calibrating coupler is a hard-walled cylindrical cavity closed at one end by a condenser microphone. When it is closed off by an audiometer earphone, the enclosed volume is approximately the same as the volume enclosed by an earphone held against a human ear. Comparison of the response of earphones on the ear and on the calibrating coupler shows that the coupler does not duplicate the acoustic load presented to the earphone by the ear.[2] For a given voltage applied to the earphone the sound pressures generated in the ear at low frequencies are significantly lower than the sound pressures generated in the coupler. Without phase measurements, it is not possible to decide whether this is due to leakage or to additional compliance.

At high frequencies there are sound patterns in both the ear and the coupler. At any single frequency, however, there is a fixed relationship between the sound pressure measured at the microphone in the coupler and the sound pressure present at the eardrum for each individual ear. The standard coupler 9A was designed so as to minimize pattern effects at particular fixed audiometric frequencies.

A set of threshold standards in terms of sound pressures in a coupler is valid for all earphones of a standard type provided that the high-frequency patterns in both ear and coupler remain constant for all earphones of the type. To maintain the pattern, all earphones of a given type must produce like geometric enclosures, although of course the enclosure on the coupler will differ from that on the ear. Constancy of pattern requires that all earphone cushions for a particular type of earphone be of controlled profile, thickness, and compliance; and that the distance from the front face of the moving diaphragm to the plane of the cushion be held constant.

If, in addition to maintaining the geometry of the

[1] F. M. Wiener and D. A. Ross, J. Acoust. Soc. Am. 18, 401–408 (1946).

[2] See, for example, M. D. Burkhard and E.L.R. Corliss, "The sound pressures developed by earphones in ears and couplers," National Bureau of Standards Report No. 1470 (Februrary 29, 1952).

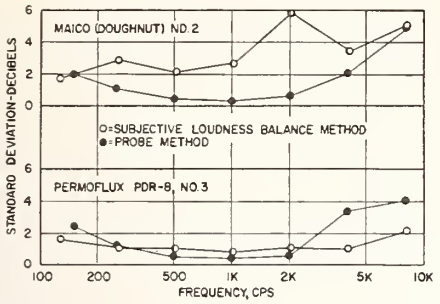

FIG. 1. Comparison of the standard deviations of the measurements on individual persons, arising from physical differences among individuals taking part in the measurements by each method. Six persons performed the loudness balance. Fourteen subjects were used in the probe method.

enclosure, the earphone is held against the ear with a constant coupling force, the acoustic leak at low frequencies for any individual ear will be approximately the same for all earphones of a particular type. However, it is in general not easy to meet this condition when subjective loudness balancing is being carried out, because the comparison and standard earphones must be interchanged rapidly. When threshold standards are transferred by means of the probe technique to be described here, the coupling force can be maintained constant.

So far as we know now, it can be assumed that auditory sensation for any normal individual is a function of the sound pressure presented at the eardrum. As we shall see later, our experimental measurements confirm this assumption. On this basis, the process of loudness balance is justified as a method for establishing a threshold standard for a new type of earphone. When a number of subjects, having hearing adequate for the task, determine what voltages applied to the earphone terminals give the same loudness sensation for both earphones, the sound pressures produced at the eardrum by the earphones are presumed to be equal.

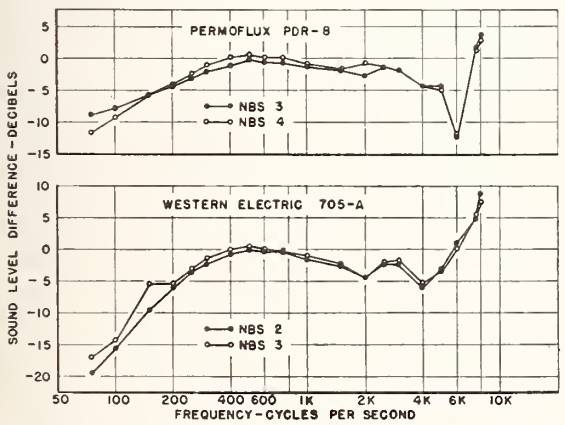

FIG. 2. A check on the basic assumption for transfer of coupler pressure standards for threshold. Difference between average sound level produced in ears and sound level produced in N.B.S. Coupler 9A, with the voltage applied to the earphone held constant. Each pair of curves was obtained with two earphones of the same type.

The loudness-balancing process is slow and unpleasant. It is practical only if it is done at relatively few frequencies and if the number of subjects in a jury is small, although the jury must be kept large enough to insure representative conditions. Because the determination is made at a rather low sound level, each subject must concentrate his attention on the sound, and can work only in especially quiet surroundings.

OBJECTIVE PRESSURE MEASUREMENT

Sound pressures developed by an earphone at the entrance to the ear canal can be observed by means of a probe microphone inserted through the earphone cap. These observations can be used to determine when two earphones, the comparison standard and the earphone for which threshold standards are to be determined, produce the same sound pressure at the entrance to the ear canal.

The transfer of threshold is carried out as follows: The response of each earphone is measured on the calibrating coupler. By probe techniques, the response is measured for each earphone when mounted on the ears of a number of human subjects.

TABLE I. Threshold transfer data. Sound pressures in N.B.S. Coupler No. 9A corresponding to normal auditory threshold.

	(Db re 1 dyne/cm²)			
	Permoflux type PDR-1 Maico "doughnut" cushion		Permoflux type PDR-8 MX41/AR cushion	
Frequency cps	Subjective	Probe	Subjective	Probe
125	−20.4 db	−25.2 db	−21.6 db	−25.4 db
250	−34.2	−34.5	−35.2	−34.7
500	−49.5	−48.7	−49.5	−49.0
1000	−59.4	−58.0	−57.5	−57.4
2000	−57.3	−56.4	−56.9	−58.8
4000	−53.0	−57.7	−59.5	−60.5
8000	−49.2	−52.4	−45.7	−48.1

Let us denote the response, expressed in decibels, of the standard earphone as measured on the coupler by C_s. Let the mean response of the standard earphone as measured on the group of human subjects be H_s. Designate the corresponding quantities for the new earphone by C_x and H_x, respectively. The coupler sound pressures in decibels corresponding to the standards of normal threshold for the new earphone are simply obtained by adding the quantity D to the standard pressures for the standard earphone corresponding to normal threshold, where

$$D=(C_x-H_x)-(C_s-H_s).$$

D is the ratio of the sound pressures developed by each of the earphones in the calibrating coupler for voltages at which they produce equal sound pressures in the ear.

EQUIVALENCE OF RESULTS

If the probe method is equivalent to loudness balancing, the results of the transfer of threshold by both methods should be substantially the same. For

two types of earphones on which the process of threshold transfer had been carried out by loudness balancing, the transfer of threshold was repeated by the probe technique. The responses of the test earphones were measured on both ears of 14 human subjects. The differences between these responses and those measured on the calibrating coupler (Coupler No. 9A) were computed. The same measurements were made for the comparison standard earphone (W. E. Type 705-A). Table I shows the threshold values for the two earphones as determined by both the loudness-balancing and probe techniques.

The group of persons used for the probe method was essentially different from the group used for loudness balancing. Only one person was common to both groups. The threshold values obtained by loudness-balancing are those determined originally when the transfer of threshold standards to these particular types of earphones was performed in our laboratory. From a study of the statistical variations involved, we conclude that the physical differences among individuals cause a major part of the differences shown here between the threshold transfer data determined by each of the methods.

The standard deviations for the two methods are plotted in Fig. 1. The deviation is that arising primarily from physical differences among individuals. The standard deviation for the loudness-balancing method also inevitably includes variations in judgment. That part of the deviation caused by variations among repeated measurements, on a single individual was found to be very small.

A measure for judging the difference between the results of threshold transfer by the two methods is is given by the factor $1/\sqrt{n}$ times the standard deviation, where n is the number of persons involved in the transfer measurements. This corresponds to a confidence level of 0.68. The differences appearing in Table I are significant in comparison to the uncertainties of the measurement only at 125 cps. This difference can be traced to the fact that the earphone is applied to the ear with controlled force when the probe method is used for transfer of threshold. In loudness balancing, the coupling force is not controlled. The force coupling the earphone to the ear has a strong influence upon the effective response of the earphone at low frequencies.[3]

The rather close agreement between the results of threshold transfer by the two methods indicates that the sensation of equal loudness corresponds directly to equal sound pressures at the entrance to the ear canal. This is a fundamental assumption upon which threshold transfer by loudness balancing is based.

Although the uncertainties of measurements are comparable for the two techniques, the probe method makes less demands on the subjects. In the probe technique, the subject is passive, and merely provides a suitable acoustic enclosure. Because no subjective judgment is involved, measurements can be made at convenient sound pressure levels. While the earphone is in place, there is a fairly good seal to the ear, and external noise is excluded to some extent. Measurements by the probe technique can be made quickly, and can be made at a much larger number of fixed frequencies than is feasible when subjective comparison must be relied upon. (Until further threshold determinations are made, however, threshold transfers are limited to the particular fixed frequencies at which the present standards were determined.) A large number of subjects can be used. Since immediate interchange of earphones to determine instantaneous equality is not required, the coupling force holding the earphone to the ear can be controlled.

EXPERIMENTAL BASIS FOR TRANSFER OF THRESHOLD STANDARDS

The idea that threshold standards are applicable to all earphones of a given type implies that all earphones of the given type will show the same consistent difference between their performance on the calibrating coupler and their actual performance on the ear. This assumption can be checked easily by the probe technique. Several pairs of audiometer earphones were compared for this purpose. The results of the check are shown in Fig. 2.

Within the limits of experimental uncertainty, earphones of like type show the same ratio in response between their performance on the coupler and on the ear. This shows that the principle of establishing threshold standards in terms of sound pressure developed in a calibrating coupler is experimentally valid.

The same group of fourteen individuals was used throughout. It should be noted that the uncertainty of measurement sets a lower limit to the tolerance on sound-pressure outputs specified in audiometer adjustment. If the tolerance limits are set substantially closer than the experimental uncertainty in relating ear measurements to coupler measurements, the result does not contribute to the validity of audiometer readings.

Although the probe method for transfer of threshold standards is easier to carry out than loudness balancing, it is necessary with either method to make a transfer for each new type of earphone. Thus each time the design of earphones is changed, a number of human subjects must be assembled and a transfer of standards must be made. If a coupler that terminates earphones with the appropriate acoustic load can be made, it will be possible to make direct comparisons of earphones.

[3] See reference 2, p. 14.

The Response of Earphones in Ears and Couplers*

Mahlon D. Burkhard and Edith L. R. Corliss
National Bureau of Standards, Washington 25, D. C.

Applied voltage responses of seven earphones on both ears of fourteen people were obtained with the aid of a probe tube microphone inserted into the volume enclosed by the earphone. Treatment of the response data by the method of analysis of variance allowed separation of variance effects due to error in repeated measurement, dissimilarity between a given person's ears, and differences among individuals. The latter are found to be the most important effects to contend with in audiometric practice. Effects of application force on sound pressure output of an earphone are examined. Comparisons between the average response on ears and on three superficially different couplers are presented. Responses on ears were substantially different from responses on couplers over parts of the frequency range. Recommendations are given for improving the reliability of audiometric measurements by instrumental refinements.

I. INTRODUCTION

THE work reported in this paper results from a program being carried out at the National Bureau of Standards to improve the methods by which standards of auditory threshold are maintained. For audiometric purposes the threshold of hearing is defined as the minimum sound pressure at the entrance to the ear canal which produces a pitch sensation. A person's threshold of hearing by air conduction is usually measured with a pure-tone audiometer which introduces sounds at specific frequencies and controlled levels into the patient's ear by means of an earphone held over his ear.

The response of an earphone, i.e., its acoustic output as a function of electrical signal, depends upon the acoustic load with which it is terminated. The electrical signal required to produce arbitrary sound pressure levels is usually determined by means of an "artificial ear" coupler. The coupler connects the earphone acoustically to a microphone through a volume approximately the same as that enclosed by the earphone on an average human ear.

Artificial-ear calibrating couplers used in this country for calibration of audiometer earphones are of the hard-walled cylindrical volume type. It is well known that these couplers load an earphone with only volume reactance. As far as can be judged from response measurements, they simulate the ear's impedance over only a small portion of the audio-frequency range. The most satisfactory type of calibrating coupler for audiometry would be one which duplicates closely the termination presented by the average ear at all audiometric frequencies. This would obviate the procedures of making transfers of standard threshold pressure,[1] now needed when new earphone types are developed for audiometric use.

Other investigators have found much variation in the sound pressure under an earphone on an ear, both in regard to the uncertainty of repeated measurement on a person's ear and on the extreme range of pressures occurring in measurements on a number of individuals.[2,3] Thus it had seemed that development of calibrating couplers simulating the ear would not appreciably improve the precision of clinical audiometry. In the work described here the possible sources of the large variations were investigated by observing earphone responses under various conditions of application. One particularly useful result of this study was the finding that by controlling the force of application of the earphone to the ear, the uncertainty of repeated measurements on an ear could be materially reduced. Control of this factor also facilitated study of the other sources of variation.

Applied voltage[4] responses of earphones were studied on ears by means of a capillary probe tube microphone. These measurements and their significance are discussed in part II. In part III comparisons of earphone responses on three superficially different couplers are made.

In the following discussion we shall frequently refer to the sound pressure developed by an earphone in various circumstances. The applied voltage response of an earphone depends primarily on the conditions of earphone use or measurement. Thus, when observed responses differ, it is the result of production of different sound pressures for the same voltage at the earphone terminals.

* Supported in part by the Office of the Surgeon General, U. S. Army.

[1] For background see E. L. R. Corliss and M. D. Burkhard, J. Acoust. Soc. Am. **25**, 990 (1953), and E. L. R. Corliss and W. Snyder, J. Acoust. Soc. Am. **22**, 837 (1950); also, L. L. Beranek, *Acoustic Measurements* (John Wiley and Sons, Inc., New York, 1949), p. 367.

[2] OSRD Report No. 3105, Response characteristics of interphone equipment (Electro Acoustic Laboratory, Harvard University, Cambridge) (1944).

[3] F. M. Wiener and D. A. Ross, J. Acoust. Soc. Am. **18**, 401 (1946).

[4] The applied voltage response of an earphone is defined as 20 times the logarithm to the base 10 of the absolute value of the ratio of the rms sound pressure generated to the rms voltage applied at the terminals of the earphone. This calibration procedure is outlined in the *American Standard Method for the Coupler Calibration of Earphones Z24.9–1949* (American Standards Association Inc., 70 East Forty-fifth St., New York 17, New York). Published in part in J. Acoust. Soc. Am. **22**, 602 (1950).

II. EFFECT OF LOAD IMPEDANCE ON AN EARPHONE

Basically the system for which the response of an earphone is defined and the system by which the response is measured are similar in the measurements under discussion. Let us represent the earphone as a lossless generator of volume velocity shunted by an internal impedance Z_i. The ear or coupler is then treated as a load impedance Z_e in parallel with Z_i. In audiometric determinations it is desirable to produce the same ratio of sound pressure to applied voltage with a given earphone on all ears and in an appropriate calibrating coupler. To maintain the generator pressure output essentially independent of changes in its load Z_e, the internal impedance Z_i must be small relative to Z_e. The types of earphones we have tested do not appear to have internal impedances small enough over all the frequency range to keep the pressure response of the earphone the same for all ears.

III. EARPHONE RESPONSE ON EARS

(A) Experimental Procedure

For measurements on ears, a special head mounting was built to support an earphone and a probe microphone with its preamplifier. This mounting incorporated a calibrated sylphon bellows so that the force of the earphone against the ear could be controlled. It is shown in Fig. 1.

The probe microphone consisted of a capillary steel tube connected to a face-plate that screwed onto the front of a Western Electric 640AA condenser microphone. A small air volume was enclosed between the face-plate and the microphone diaphragm. Sound pressures at the far end of the probe were transmitted to the air volume and picked up by the microphone. The probe was calibrated both in free field and in a cavity against a standard condenser microphone. By inserting the probe into the space between the earphone cap and the ear, sound pressures there could be measured on each of a number of individuals over the frequency range from 75 to 8000 cycles per second.

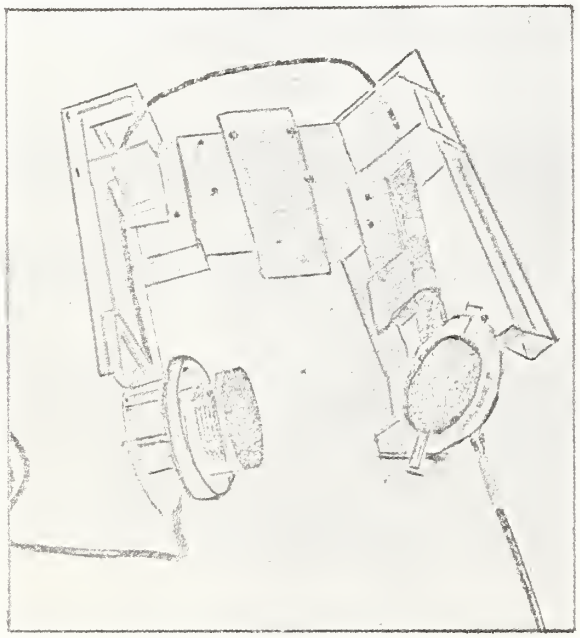

FIG. 1. Equipment for applying earphone to ear. Force is controlled by compression of sylphon bellows a known amount. The 640AA microphone and probe that detect the sound pressure are kept rigidly fixed relative to the earphone.

(B) Average Response of Earphones

Let us now discuss in detail the results of earphone response determinations on couplers and ears. Applied voltage responses were measured for seven standard earphones of four different types on the National Bureau of Standards calibrating coupler No. 9A and on both ears of fourteen individuals. The measurement for all seven earphones was performed twice on three of these subjects to evaluate the error of repeated meas-

TABLE I. Example of applied voltage response of earphones on ears. Data at three frequencies are given for a Permoflux Type PDR-8 earphone. Sequence of presentation has been arranged so that responses observed at 100 cps descend in magnitude. Application force on earphone is 1.5 kg.

Person	Ear	Earphone response, db re 1 dyne/cm²/volt Frequency—100 cps	1000 cps	5000 cps
EJ	L	39.2	40.7	32.8
BS	L	38.7	40.7	41.2
FB	R	38.5	40.7	32.8
AO	L	37.3	40.3	37.5
SE	L	37.0	40.5	35.6
RFB	L	36.9	39.0	28.1
FB	L	36.7	40.5	36.3
EC	L	36.6	39.3	31.9
JW	R	36.4	40.2	36.0
AO	R	36.1	39.6	40.3
RFB	R	35.7	37.4	24.6
EJ	R	35.4	38.9	36.2
EC	R	34.6	39.8	35.7
HL	L	34.2	37.0	39.1
SE	R	33.8	39.6	33.2
JW	L	33.7	40.3	35.3
BS	R	33.0	39.4	38.4
PB	R	32.6	40.7	37.4
MB	L	31.1	39.8	36.4
RDB	R	24.9	40.2	33.1
PB	L	24.5	40.4	38.0
HL	R	24.4	37.9	34.5
MB	R	23.6	40.6	36.3
WK	R	21.2	40.7	32.8
CR	L	20.1	39.9	40.2
RDB	L	19.7	41.7	35.8
WK	L	12.9	39.5	40.6
CR	R	11.7	42.7	29.1
Average response		30.7	39.9	35.4
Minimum response		11.7	37.0	24.6
Maximum response		39.2	42.7	41.2
Spread of observations		27.5	5.7	16.6

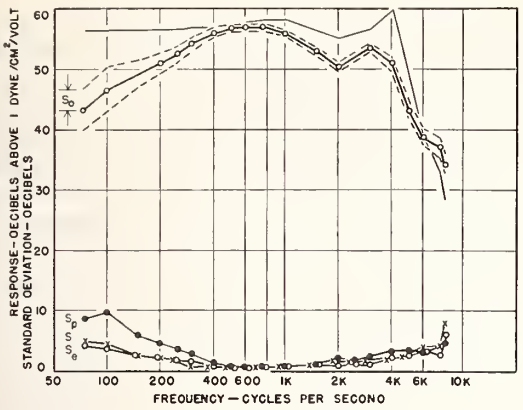

(a) Permoflux Type PDR-1 (MX41/AR cushion)

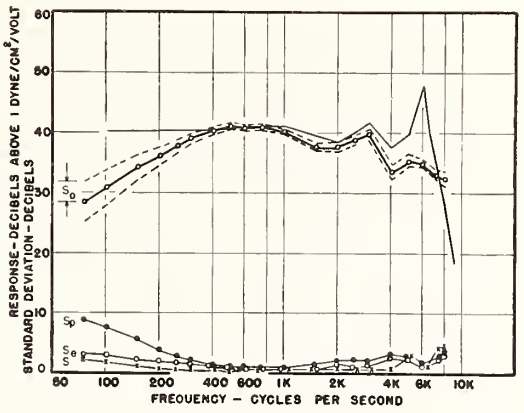

(b) Permoflux Type PDR-8 (MX41/AR cushion)

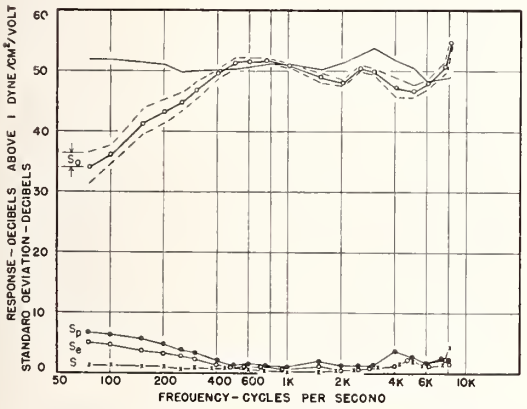

(c) Permoflux Type PDR-10 (MX41/AR cushion)

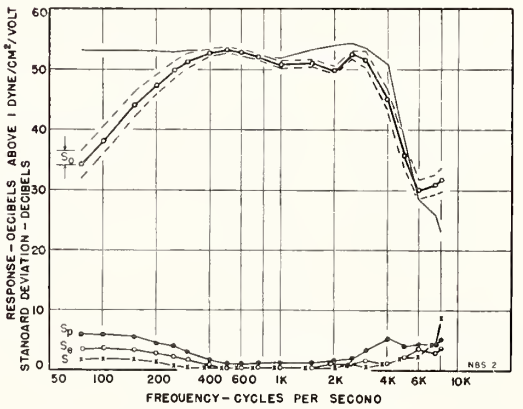

(d) Western Electric Type 705-A. Applied voltage response and precision indices. Heavy line is average of response on both ears of 14 individuals. Light line is response of earphone on coupler No. 9-A, included for reference. s_p, s_e, s, and s_o are statistical indices indicating the variation among responses due to individual physical differences among people, difference between a person's two ears, variation in repeated response determinations, and estimated standard deviation of the mean, respectively.

FIG. 2.

urement. No effort was made to establish clinical control of the people used but their ears were examined by Dr. Glorig of Walter Reed Hospital with an otoscope to note the absence of physical irregularities such as perforated drum membranes, and ear volumes were measured.

To illustrate the range of variation of sound pressures encountered when applying a constant voltage to an earphone on an ear, Table I presents typical applied voltage response determinations. Data at three frequencies are given for a Permoflux Type PDR–8 earphone for both ears of the fourteen individuals used. Noting that the sound pressures developed vary from person to person, we consider that each individual possesses his own particular value which can be found as the average of the earphone response for left and right ears. Also, there will be an average value of the sound pressure response of a particular earphone for a group of people. If an individual is chosen from the group and a measurement made on one ear, the values obtained, excluding measurement errors, differ in general from the population average because: (1) identical results may not be obtained on both ears of the same individual, and (2) the individual's average differs from the population average.

The variability of individual values about the average for our fourteen subjects, and of the discrepancy between the two ears and the individuals' average may be estimated. These estimates have been designated s_p^2, the variance due to the variability of individual averages including measurement errors, and s_e^2, the variance representing the variation between the ears of the same person, also including measurement errors. The positive square roots of these parameters have been plotted for a number of frequencies in Fig. 2 along with that of the estimate of the measurement error variance s^2.

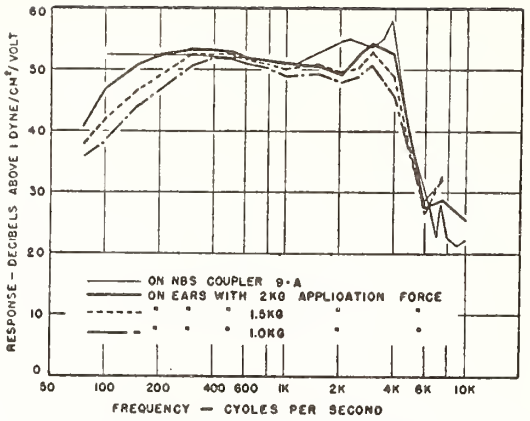

FIG. 3. Applied voltage response of a Western Electric Type 705-A earphone. Force used to hold the earphone on the ear is the parameter yielding the separate curves. Response on National Bureau of Standards Coupler No. 9-A is given for comparison.

Application of the F test[5] to the parameter s_e indicates that it is not significantly different from s, and hence shows that ears tend to occur in "matched pairs" with respect to the sound pressures produced in them by earphones. Using the same criteron, s_p has been found to be significant with few exceptions. The points which show no significance have not been considered important to the overall effect. Thus the dissimilarity noted between both ears of an individual probably results from the random measurement error of this type of measurement, but the variations among subjects result from individual differences which affect the acoustic load of the earphone. The high degree of repeatability of any observation, indicated by low values of the index s, is attributable to the fact that the earphone application force is closely controlled in all cases.

The estimated standard deviation of the average responses of these earphones is given by s_o computed from analysis of variance results. On the basis of the Student distribution[6] and a significance level of one in twenty, it is estimated that the true average response of the earphone for the whole population has a value within $\pm 0.6\ s_o$ of the average shown.

Over the small mid-frequency range of 500 to 1000 cps, the responses of the earphones we used are nearly the same on ears as they are when measured in Coupler No. 9A. Precision of measurement is best in this region, thus precluding the occurrence of this agreement by chance. At lower frequencies uncertainties of measurement become much greater while the average response on ears falls off. At higher frequencies the dissimilar geometries of the ear and coupler undoubtedly contribute much to the differences between the coupler and the ear. The same applies to the increase in uncertainty, because the length of the ear canal and the general shape and size of the external ear are peculiar to each individual. This personal characteristic determines the impedance encountered by an earphone when it is applied to the ear.

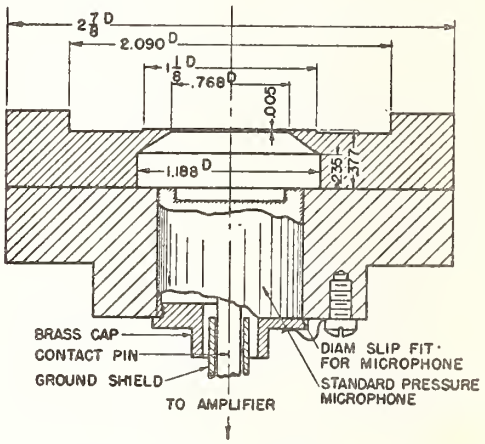

FIG. 5. Joint Radio Board (JRB) calibrating coupler. Earphone was calibrated with cushion removed. Volume=6.0 cc. This differs only slightly in dimensions from the ASA Type I coupler.

We have obtained similar applied voltage response and uncertainty index characteristics for all of the earphones tested on ears by this method.

(C) Earphone Application Force Effect on Earphone Response

It is reasonable to expect that the force with which the earphone is applied to the ear affects the sound pressure developed by it in the ear. Because of the yielding properties of both the flesh and the rubber earphone cap, an increase of application force tends to reduce the volume enclosed under the earphone and at the same time probably tends to close off any acoustic leaks. Effects of earphone application force on earphone response are indicated in Fig. 3 where we show the average of some applied voltage earphone response measurements made on ears at forces of 1.0, 1.5, and 2.0 kg, and on the National Bureau of Standards 9-A calibrating coupler. Although the averages shown result

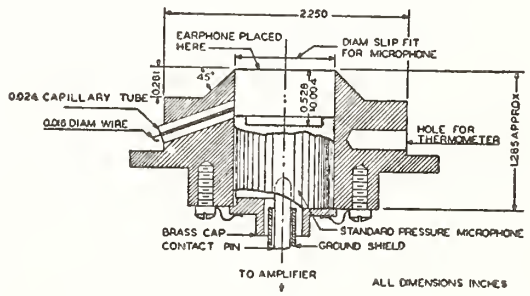

FIG. 4. National Bureau of Standards Calibrating Coupler No. 9-A. Standard threshold pressures for audiometer calibration are maintained in terms of sound pressures generated in this coupler. Volume=5.7 cc.

[5] See any text on statistics, e.g., D. C. Villars, *Statistical Design and Analysis of Experiments for Development Research* (William C. Brown Company, Dubuque, Iowa, 1951).

[6] See e.g., D. C. Villars (reference 5).

from comparatively few observations (3 persons with two repeats for 1.0 kg, 14 persons for 1.5 kg, 4 persons for 2.0 kg), differences to be noted in the average response curves shown are large enough to be statistically significant by the Student t test in most cases.

Apparently the acoustic termination to the earphone tends toward a volume reactance approximating a hard-walled calibrating coupler as the application force is increased. It still would not be practical to extrapolate to the conclusion that the difficulty of relating coupler pressures to ear pressures in calibration procedures can be avoided in this way. We have found that forces in excess of 2.0 kg become unbearably painful and that even a 2.0-kg force can be tolerated only for short periods.

IV. EARPHONE RESPONSE ON COUPLERS

Figures 4, 5, and 6 give cross-sectional drawings of the three artificial ear calibrating couplers investigated. National Bureau of Standards Coupler No. 9–A,[7,8] Fig. 4, is the one for which auditory threshold standards maintained by the Bureau of Standards are specified. It has a volume of 5.7 cc and presents nearly pure volume reactive acoustic load. The original Joint Radio Board 6 cc coupler,[2] Fig. 5, is essentially the same as the Type I coupler specified for Coupler Calibration of Earphones.[4] It, too, presents a load which is nearly pure volume reactance. The design of this coupler is such that the front cushion of the earphone must be removed while it is being calibrated. These couplers are intended to have an air volume approximating that enclosed by an earphone on an ear.

The third coupler is a copy of one used at the National Physical Laboratory, Teddington, England.[9] This coupler, designated B–1, is shown in Fig. 6 as modified to accommodate the type 640AA microphone. It is made up of a cylinder with volume of 5.17 cc having two tubes $14\frac{1}{2}$ feet long let into its side walls. Graduated lengths of wool yarn were drawn into the tubes in an attempt to make the tubes appear infinite in length. The design in theory is intended to produce impedance in accord with data reported by West,[10] and by Inglis, Gray, and Jenkins[11] for the acoustic impedance of ears.

Although the couplers differ somewhat in physical structure, an earphone's applied voltage response measured on each is substantially the same. The response of a 705–A type earphone, given in Fig. 7, showed greater dependence on the coupler structure than both the Type PDR–1 and Type PDR–8 earphones. Morrical *et al.*[12] found much similarity between the responses of an earphone measured on the 9–A and JRB couplers. It is interesting to note that addition of the acoustic leak in the B–1 coupler has not made it significantly different from the 9–A and JRB couplers.

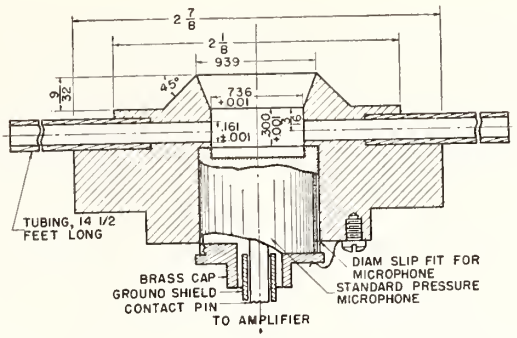

FIG. 6. B-1 Coupler. An adaptation of a coupler employed at the National Physical Laboratory, Teddington, England by R. S. Dadson. It has been modified for use with Type 640AA condenser microphone. Tubes at sides are partially filled with graduated lengths of wool yarn. Volume of cylinder = 5.17 cc.

Comparing responses for the same earphone applied to ears and these couplers, e.g., the data of Figs. 3 and 7, it is evident that the sound pressures produced in ears differ significantly from those in the coupler below 500 cps and above 1000 cps. At higher frequencies differences arise through wave motion effects. This comes about in part because on the ear the pressure was measured directly in front of the earphone but the coupler pressure is measured with a microphone at the coupler bottom. Differences between responses on ears

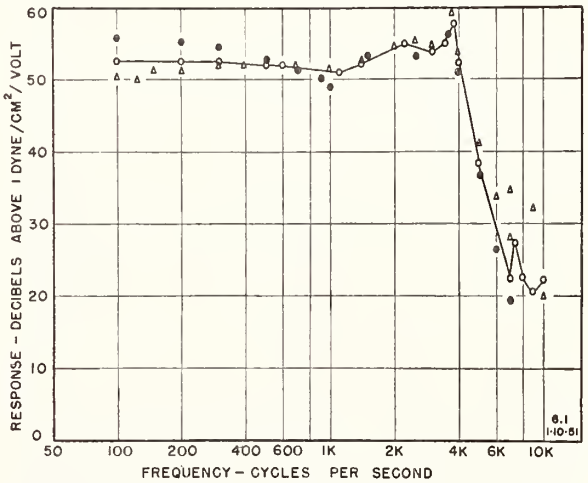

FIG. 7. Applied voltage response of a Western Electric Type 705-A earphone on three superficially different calibrating couplers: o—o on NBS coupler No. 9-A; △ on B-1 coupler; ● on JRB coupler.

[7] American Standard Specification for Audiometers for General Diagnostic Purposes, Specification Z24.5—1951. Available from American Standards Association, Inc., 70 East 45th St., New York 17, New York. Price $.50.

[8] American Standard Specification for Pure-tone Audiometers for Screening Purposes, Specification Z24.12—1952. Available from American Standards Association, Inc., 70 East 45th St., New York 17, New York. Price $.50.

[9] Hearing Aids and Audiometers, Special Report 261, Medical Research Council, His Majesty's Stationery Office, London, England (1947).

[10] W. West, British P. O. Elect. Engrs. J. **21**, 293 (1929).

[11] Inglis, Gray, and Jenkins, Bell System Tech. J. **11**, 293 (1932).

[12] Morrical, Glaser, and Benson, J. Acoust. Soc. Am. **21**, 183 (1949).

and couplers at lower frequencies cannot arise from wave effects. The average of the volumes enclosed under an earphone cap with contour typical of audiometer earphones on ears of 12 of our 14 subjects is 5.3 cc. Reducing coupler volumes to this amount would serve to make the sound pressure in the coupler even higher at low frequencies than it is on the ears.

One obvious source of difference is the mounting of the earphone on the ears and couplers. The coupler terminates in a circular aperture which forms a uniform seal either with the earphone cap or with the front face of the earphone mechanism. Irregularities in the contour of the side of the face prevent a uniform seal by the earphone on the ear. Simple computations show that there is at least one additional component in the acoustic load presented by the ear that is not provided in hard wall volume couplers. Although the acoustic leak in the *B*–1 coupler is designed to introduce a resistive element in the load, the output of the earphones at low frequencies is considerably lower on the ear than on this coupler. The agreement in the range 500 to 1000 cps suggests either that both ear and coupler impedance magnitudes are sufficiently larger than the mechanical impedance of the earphone so that they render the measured response independent of the load used, or that the effective impedances are alike. The former mechanism seems more likely since it would allow for the deviations between responses on the ear and on the coupler observed at frequencies outside this range.

The results indicate that the mechanical impedance of audiometer earphones may be too high relative to the load impedances which are encountered in practice. Because audiometric measurements require that the sound pressure at any frequency be maintained constant for all ears, it is evidently preferable to avoid impedance matching. Instead, earphones chosen for audiometry should exhibit low internal impedance.

VI. CONCLUSIONS

Normal threshold of audibility at a given frequency is the minimum sound pressure at the entrance to the external auditory canal which at that frequency produces an auditory sensation in ears. It is necessary therefore that an audiometer earphone produce the same sound pressure in all of the ears to which it may be applied, otherwise considerable inaccuracy in the threshold measurement may result.

Earphone calibration under prescribed and representative conditions is basic to the maintenance of the standards of auditory threshold. The calibrating coupler now specified for earphone calibrations does not duplicate the acoustic load of the human ear as closely as desired for audiometric work. As a result, the standards of auditory threshold apply only for the earphone with which the threshold determination was made. If a different earphone type is to be used for audiometry, either new threshold determinations must be made for this type of earphone or transfer of the threshold must be made from one earphone to the other. This may be accomplished either by loudness balancing between the earphones or by measuring the pressure under each earphone when it is held on an ear. If, however, the couplers were more representative of the average ear, all of the necessary information about any earphone which was proposed for audiometric measurements could immediately be obtained from the coupler calibration of the earphone. Therefore, a new artificial ear calibrating coupler that will more nearly duplicate the measured impedance of ears is needed. It is evident from sound pressure observations that there are resistive and reactive components in the impedance of an average human ear. At present the standard calibrating couplers in this country are of the hard-wall type, presenting chiefly volume reactive impedances.

Considerable reduction in the variability in sound pressure generated by an earphone on a particular ear has been made by controlling the application force of the earphone. The precision of all audiometric practices could be improved by control of the headband force so that it is the same for all subjects. A force of 1.5 kg has been found advantageous in this investigation. Most headbands now in use give a smaller variable force that depends on head size.

Variations in earphone response on the ears of a group of people will not be eliminated by specifying the application force, however, since the differences are due almost wholly to the physical characteristic of the particular ear on which the measurements were made. Because of this, for a given acuity of the ears of several individuals, observed thresholds will appear to be different to the extent that the responses of the earphone on these ears differ. Thus hearing losses apparently observed audiometrically may not actually exist. It follows directly from the measurements described here, that some cases of hearing loss of the order of 20 db to 30 db may only be due to a decrease in sound pressure at the entrance to the ear because of the acoustical termination which that particular ear presents to the earphone.

Earphones are usually designed empirically for maximum sound energy transfer, thus probably the magnitude of the impedance of the earphone matches the impedance of the ear. For audiometry, however, an earphone should be chosen or designed that has an acoustic pressure output substantially unaffected by acoustic load over the range of impedances encountered on ears. This requires an impedance mismatch, i.e., an earphone with a low driving impedance acting effectively as a constant pressure source.

VII. ACKNOWLEDGMENT

The statistical evaluation of the large quantity of data was carried out at the suggestion and with the

help of Mr. Joseph Cameron of the Statistical Engineering Section, National Bureau of Standards. Dr. Aram Glorig, otologist, of Walter Reed Hospital, Forest Glen Annex, made examinations of the ears of our subjects and was consulted on problems of medical and clinical interest in this work. Mr. R. F. Brown, Jr., and Mr. K. T. Lemmon performed some of the measurements reported here, and Mr. R. P. Thompson carried out some of the statistical computations. The authors greatly appreciate the cooperation of a number of their associates in the Sound Section who furnished their ears for observation.

Reprinted from The Journal of the Acoustical Society of America, Vol. 26, No. 5, 679–685, September, 1954

International Standard Reference Zero for Audiometers

Pearl G. Weissler

National Bureau of Standards, Washington, D. C. 20234

This is a detailed report on the technical activities of ISO's Technical Committee on Acoustics No. 43, Working Group on Threshold of Hearing, which led to the ISO Recommendation R389, "Standard Reference Zero for the Calibration of Pure-Tone Audiometers," November 1964. The activities described are the determinations of the transfer factors from loudness balancing experiments between the five earphone-coupler combinations in R389, the incorporation of the transfer data into the computation of the reference equivalent threshold sound-pressure levels (RETSPL) in R389, and the details of the weighting of the original threshold determinations. A statistical analysis estimates the average standard deviation of the RETSPL in R389 to be 2 dB due in large part to the variance in the transfer factors. The present USASI standards are definitely outside the ISO uncertainty limits at all frequencies. The standard deviation of the differences between adjacent columns in R389 (or the equivalence of the RETSPL for the different earphone-coupler combinations) was estimated to be 2.5 dB. To improve accuracy in audiometry, it is suggested that the variance due to the transfer factors be eliminated by agreement on one standard earphone type.

Foreword

The working Group No. 1 on Threshold of Hearing, of ISO/TC43 on Acoustics, constituted itself as a body of technical experts in 1955 to arrive at a best value for an international threshold reference level for the measurement of hearing. The six members, all associated with laboratories carrying on researches into audiometry and the measurement of hearing threshold, were from Europe and the United States of America. They agreed early in their deliberations (1) to examine carefully all available published data from various laboratories on threshold levels expressed in physical terms, (2) to make additional threshold measurements to resolve any outstanding differences between laboratories, and (3) to carry on any measurements needed to place all the data on a common basis, such measurements to be made in the members' respective laboratories. Completion of these monumental tasks culminated in ISO Recommendation R389.

The details of their efforts are recorded in Mrs. Weissler's paper. Each of the several members, some now retired, had an opportunity to comment on the paper in draft form. Chairman Lüscher aptly remarked: "Es geht daraus die grosse Gründlichkeit der ISO-Untersuchung hervor, so dass an der Richtigkeit des vorgeschlagenen Standards nicht zu zweifeln ist."

Richard K. Cook, *Member*
ISO/TC43-WG1
December 1967

INTRODUCTION

In the United States, we are in the awkard position of being on a double standard in audiometry. One standard is based on the pioneer work of the U. S. Public Health Service in the National Health Survey (1935–1936). It is embodied in the United States of America Standards Institute (USASI) "Specification for Audiometers for General Diagnostic Purposes, *Z*24.5—1951."[1] The other, newer, standard is based on 15 determinations of threshold of hearing by air-conduction performed in five countries from 1952 to 1960 and is embodied in the International Organization for Standardization (ISO) Recommendation R389, "Standard

[1] Available from the U. S. American Standards Institute, 10 E. 40 St., New York, N. Y. 10016.

"Reference Zero for the Calibration of Pure-Tone Audiometers," November 1964.[1]

The latter standard has been approved by the American Academy of Ophthalmology and Otolaryngology and the American Speech and Hearing Association. In the United States of America Standards Institute, a draft of a revision of the audiometer specifications was proposed by a writing group. In this draft (not yet approved), the zero reference level conforms to ISO R389. However, adoption of the proposed comprehensive audiometer specification has been delayed mainly because of dissatisfaction with the ISO zero reference level. Thus both USASI 1951 and ISO R389 zero reference levels for audiometers are in effect at the present time in the United States.

R389 was prepared by a working group of ISO's Technical Committee No. 43 on Acoustics. Its Working Group No. 1 on the Threshold of Hearing consisted of six members, and was chaired by Professor E. Lüscher. The Working Group began its efforts about 1955, and by 1962 had arrived at a first draft. As finally drafted, the main part of the Recommendation consists of a Table that gives the recommended reference equivalent threshold sound-pressure levels (RETSPL) for five earphone coupler combinations, standard equipment in five different countries. It is pointed out in its Appendix A that the reference levels shown in the various columns of the Table all refer to the same auditory threshold levels, an average of 15 determinations, and that the relations between the values in the various columns of the Table have been determined by a cooperative investigation. At one point, it was suggested that some discussion of the derivation of the reference levels could be added as an appendix to the draft. However, it was decided that it would be better for a full report to appear separately in one or more of the audiological journals as a permanent record of the working group's achievement.

Since the publication of ISO R389 in November 1964, there have been a number of articles published (Davis and Kranz, 1964 a, b; Davis, 1965, a, b, c, 1966; Hirschorn, 1967; Weissler, 1965) that describe the ISO Recommendation R389, giving attention to the history of the Recommendation and its significance in the measurement of hearing. In view of this historical background, publication of a full report on ISO R389, including a statistical analysis of the final result was felt to be of interest.

We therefore describe the evaluation of the relations between the columns of the Table, or of the "transfer factors" between the five standard earphone–coupler combinations, and the details of the computation of the common auditory reference levels from the original determinations. The statistical uncertainty of the results is discussed.

I. DETERMINATION OF TRANSFER FACTORS

The Reference Zero published in ISO R389 is based on 15 determinations of threshold of hearing performed in five countries from 1952 to 1960. The results of these studies were expressed in terms of the sound pressure produced by an earphone in an artificial ear or coupler. The general procedure followed was to place an earphone with a pure-tone signal on a person's ear. The intensity of the signal was varied until the sensation of threshold of hearing was reached, and the voltage exciting the earphone was noted. The threshold information was stored by placing the earphone on an artificial ear or coupler with the voltage corresponding to threshold applied to the earphone terminals and noting the sound-pressure level (SPL) produced. This coupler SPL is called the equivalent threshold SPL. It is dependent upon the electroacoustical properties of the earphone type and the acoustic load the coupler presents to the earphone. Thus, two different earphone types will generally produce different equivalent threshold SPL's in the same coupler. Also, the same earphone will produce different equivalent threshold SPL's in two different couplers.

Each of the five countries had its own national standard earphone–coupler combination, and (with some exceptions) each of these threshold studies utilized one of the five standard earphone–coupler combinations. Thus, it was necessary to determine factors among these earphone–coupler combinations so that a threshold determined in terms of one earphone–coupler combination could be expressed in terms of any one of the other combinations. This would have to be done before all the different threshold studies could be combined into a common average.

Thus, under the sponsorship of the Working Group on Threshold of Hearing, five countries undertook to exchange earphones and perform loudness balancing experiments for transfer of threshold. The laboratories in these countries were: (1) the Centre National d'Études des Télécommunications in France, (2) the Physikalisch-Technische Bundesanstalt in West Germany, (3) the National Physical Laboratory in the United Kingdom, (4) the National Bureau of Standards in the United States of America, and (5) the All Union Scientific Research Institute of Metrology in the USSR. For convenience, the five countries and their standard earphone–coupler combinations, hereinafter referred to as "equipments," are described in Table I.

In effect, these five countries formed a sort of measurements ring, and transfers were performed in steps around the ring. Each country exchanged earphones with each of its neighbors and performed a transfer of threshold between its own standard earphone and each of its two neighbors' earphones. For example, Country (1) (France) exchanged earphones with Country (5) (USSR) and Country (2) (West Germany); Country (2) exchanged earphones with Country (1)

TABLE I. National standard earphone–coupler combinations for storing reference equivalent threshold SPL's.

Pattern of earphone	Audio 15	Beyer DT 48 with flat cushion	STC 4026-A	WE 705A	TD 6
Type of artificial ear or coupler	CNET artificial ear	NBS type 9-A coupler (with PTB adapter)	BS 2042 [Fig. 1(a), 2(b)] artificial ear	NBS type 9-A coupler	IEC-3 type artificial ear
Country	France	West Germany	United Kingdom	USA	USSR
Earphone–coupler combination designation	(1)	(2)	(3)	(4)	(5)

and Country (3) (the United Kingdom), etc. Thus there were two transfers performed between the equipments of each adjacent pair of countries. There was one deviation from this plan. Transfer between earphones for (3) and (4) was determined at NPL in England and at two different places in the USA. One USA determination was performed at the Audiology and Speech Center of the Walter Reed Army Medical Center, and the other was done by the Subcommittee on Noise of the American Academy of Ophthalmology and Otolaryngology. The results of these experiments are contained in about 14 committee reports and eight private communications between laboratories from 1952 to 1961.

Each laboratory devised its own experimental procedure, but the basic principles were the same. In each case but one, a subjective loudness balance, or threshold comparison of two earphones was combined with the objective measurements of the response of each earphone on its own coupler. One exception to this procedure was the transfer between the Russian T.D. 6 earphone and the W. E. type 705A earphone. Instead of a subjective measurement, a probe-tube transfer was performed at the National Bureau of Standards following the procedure described by Corliss and Burkhard (1953).

The subjective comparison or loudness balancing consisted in adjusting the voltages on the two earphones at the same frequency until the sound coming from both earphones appeared to be equally loud as judged by a jury of people with normal hearing. By then placing the earphones on their respective couplers, SPL's for the two earphone–coupler combinations that corresponded to equal loudness in the ear at the SPL of the measurements could be determined. Assuming linearity in the equipment and the ear from the acoustical levels of the loudness balancing down to threshold, the same relative SPL's in the earphone–coupler combinations would have been obtained if the loudness balancing had been performed at a lower SPL or at threshold.

Another assumption made is that the juries in different laboratories would make the same equal-loudness judgments. However, a necessary condition for this assumption to be strictly true is that each jury be a random sample of the normal population, which was not the case.

For the probe-tube transfer, similar assumptions of linearity of equipment and that the jury be a random sample are necessary conditions for measurements made in two different laboratories to be strictly comparable. Some systematic differences between the measurements made in two different laboratories can be expected owing to differences in the juries.

The results of loudness balancing, that is, the relative SPL's produced by the two earphone–coupler combinations, are the required transfer factors. By means of these factors, an equivalent threshold SPL found for one earphone–coupler combination can be expressed in terms of another combination. Mathematical details are discussed in the next Section.

In the various transfers, the number of subjects ranged from eight to 25, all with normal hearing. No static coupling force was reported by the CNET. A force of 0.5 kg was used by the United Kingdom, Germany, and WRAMC. The Subcommittee on Noise used 1 kg force, and NBS used 1.5 kg force. At the CNET, the subjective measurement was done at about 60 dB above threshold, with the loudness of the two earphones matched to each other on the same ear. At the PTB, the transfers were accomplished at about 40 dB above threshold with a signal duration of 1 sec and with a 1-sec interval between signals. The loudness of the signal from each of the test earphones placed in turn on the same ear, was matched to the signal from an intermediary earphone placed on the opposite ear. At NPL, three methods of loudness balancing were employed: (1) a "reversal method," in which loudness balance was achieved first with the two earphones under test placed one on the left ear and the other on the right ear, and second with the positions of the earphones

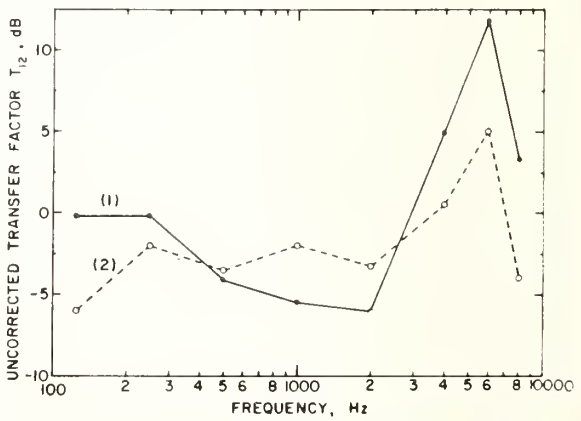

FIG. 1. Uncorrected transfer factor T_{12}. (1) Transfer performed at the CNET, France. (2) Transfer performed at the PTB, Germany.

reversed; (2) a "transfer method" that employed an intermediary earphone and was the same as used at the PTB; and (3) a threshold balance was obtained. Methods (1) and (2) were performed at a loudness of about 50 phons with a signal duration of 1.2 sec on and 0.5 sec off. The three methods appeared to be statistically equivalent. In the US at NBS and the WRAMC, the transfer from the W.E. 705A earphone to the STC 4026A was performed at threshold, while at NBS the transfer to the Russian T.D. 6 earphone was a probe transfer (as mentioned above). At the Subcommittee on Noise, the transfer was at threshold. In the USSR, loudness balancing was achieved at threshold and at some level above threshold. Signal duration was 0.8 sec with a 0.2-sec interval.

Figures 1–5 show the uncorrected transfer factors as a function of frequency. The data points are arbitrarily connected by straight lines. It is quite evident for all transfer factors but T_{12} that there are systematic differences between the laboratories. Also, at 1500 and 3000 Hz, no data had been reported for some of the transfer factors. Interpolated values were used in the computations as described below.

II. INCORPORATION OF THE TRANSFER DATA INTO ISO RECOMMENDATION R389

The following procedure, devised by R. K. Cook, then at the National Bureau of Standards and a member of the Working Group, incorporated the accumulated transfer data into the computation of the final values for ISO Recommendation R389.

The data compiled by the Working Group were of two types, original-threshold determinations and transfer-of-threshold determinations. In the original-threshold studies, voltage on an earphone that produces threshold sensation in the ear was determined. Then the SPL's produced in the associated coupler when the earphone is excited with the threshold voltage was measured. This can be called a "primary determination,"

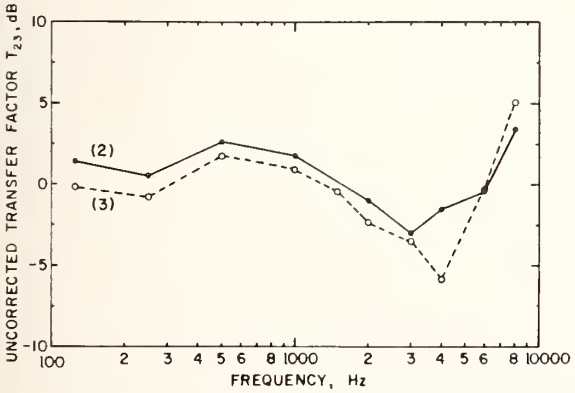

FIG. 2. Uncorrected transfer factor T_{23}. (2) Transfer performed at the PTB, Germany. (3) Transfer performed at the NPL, United Kingdom.

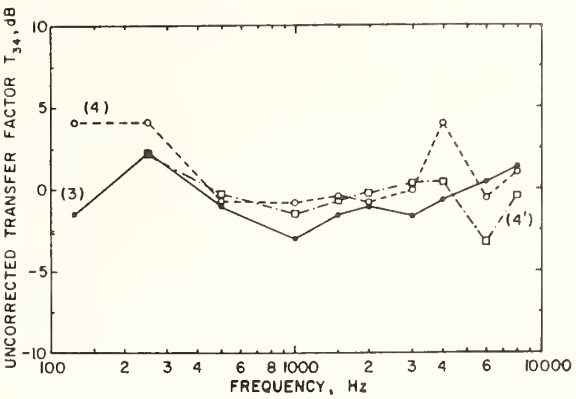

FIG. 3. Uncorrected transfer factor T_{34}. (3) Transfer performed at the NPL, United Kingdom. (4) Transfer performed at WRAMC, USA. (4) Transfer performed at Subcommittee on Noise, USA.

and the SPL's denoted by θ. Primary threshold pressure levels determined on the five earphone–coupler combinations are denoted by θ_1 for earphone–coupler Combination No. 1, θ_2 for Combination No. 2, etc.

In addition, loudness-balancing and probe-tube measurements are available for pairs of earphone couplers. These data can be represented by the pertinent pressure level differences T_{ij}, where

T_{12} = (PRESSURE LEVEL FOR EARPHONE COUPLER NO. 1) − (PRESSURE LEVEL FOR EARPHONE-COUPLER NO. 2),

both earphones being excited by voltages that produce the same loudness in the ear. Assuming linearity from threshold to the level of measurement $\theta_1-\theta_2$ should be $=T_{12}$, $\theta_2-\theta_3$ should be $=T_{23}$, etc., but might not experimentally. There were five T's determined for five pairs of earphone–coupler combinations, T_{12}, T_{23}, T_{34}, T_{45},

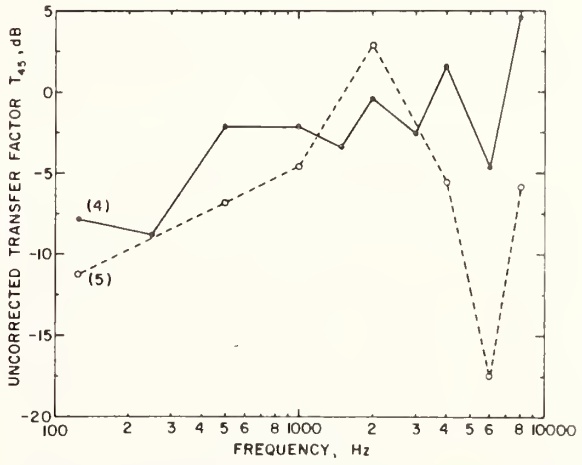

FIG. 4. Uncorrected transfer factor T_{45}. (4) Transfer performed at NBS, USA. (5) Transfer performed at the All Union Scientific Research Institute of Metrology in the USSR.

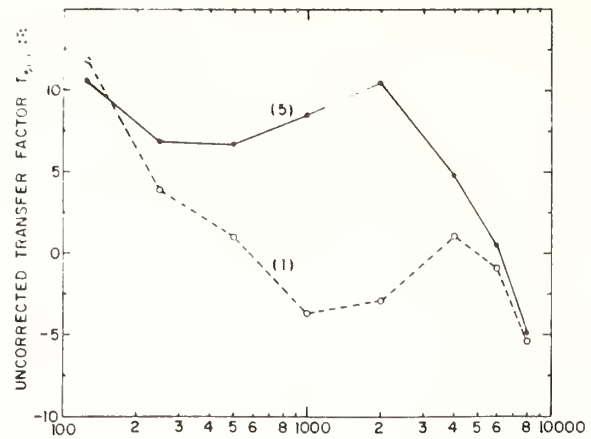

FIG. 5. Uncorrected transfer factor T_{51}. (5) Transfer performed at the All Union Scientific Research Institute of Metrology in the USSR. (1) Transfer performed at the CNET, France.

and T_{51}, where each T_{ij} is the mean of at least two independent determinations. First of all, $T_{12}+T_{23}+T_{34}+T_{45}+T_{51}$ should be zero, if all determinations were accurate.

Let the sum of the measured T's be

$$T_{12}+T_{23}+T_{34}+T_{45}+T_{51}=\Delta. \qquad (1)$$

Δ represents the cumulative errors of measurement. This is distributed by making uniform adjustments of each of the five T values. Replace each T by

$$T-\Delta/5=T',$$

thus

$$T_{12}'=T_{12}-\Delta/5, \quad T_{23}'=T_{23}-\Delta/5, \text{ etc.} \qquad (2)$$

Each T' is called a corrected transfer factor. Primary threshold data obtained in terms of one earphone–coupler combination can be expressed in terms of another earphone–coupler combination by means of the corrected transfer factors. For example, if θ_1 is the SPL determined for earphone–coupler Combination No. 1 corresponding to a primary determination of the threshold voltage for Earphone No. 1, then θ_1-T_{12}' is the SPL for earphone–coupler Combination No. 2 corresponding to threshold voltage exciting Earphone No. 1, and $\theta_1-(T_{12}'+T_{23}')$ is the SPL for Combination No. 3 corresponding to threshold voltage exciting Earphone No. 1. Also,

$$T_{12}'+T_{23}'+T_{34}'+T_{45}'+T_{51}'=0. \qquad (3)$$

Thus, the reference SPL obtained by transferring threshold data from one earphone–coupler combination to another is independent of the direction taken around the ring. Table II shows the corrected transfer factors T'.

TABLE II. Corrected transfer factors.

Frequency (Hz)	T_{12}' (dB)	T_{23}' (dB)	T_{34}' (dB)	T_{45}' (dB)	T_{51}' (dB)
125	−3.0	+0.5	+1.5	− 9.5	+10.5
250	−1.0	+0.5	+3.5	− 8.5	+ 5.5
500	−3.0	+3.0	+0.5	− 3.5	+ 3.0
1000	−2.5	+2.5	−1.0	− 2.0	+ 3.0
1500	−3.0	+1.0	0.0	− 2.0	+ 4.0
2000	−3.5	−1.0	+0.5	− 0.5	+ 4.5
3000	0.0	−2.0	+0.5	− 3.0	+ 4.5
4000	+2.5	−4.0	+0.5	− 2.5	+ 3.5
6000	+9.0	0.0	0.0	−10.5	+ 1.5
8000	0.0	+4.5	+0.5	0.0	− 5.0

III. COMPUTATION OF REFERENCE EQUIVALENT THRESHOLD SOUND-PRESSURE LEVELS

Upon the completion of the threshold determinations used in ISO R389, the task of computing the mean value confronted the Working Group. As stated above, there were 15 threshold determinations performed with either (a) one of the five standard earphone–coupler combinations or (b) with an earphone whose transfer characteristics to one of these standard equipments had been measured. With the known T' transfer factors between the five standard equipments, all the threshold determinations could be put on the same basis, or expressed in terms of any one of the standard earphone–coupler combinations. Once that was done, how would one weight the various determinations? It seemed to the Working Group that a system of weighting based on a statistical analysis of the individual determinations (i.e., according to the number of subjects) might well be incorrect. It was felt that the differences between the determinations appeared to be due more to "equipment" or "experimenter" error than to variance in the population. That is, if the error was due only to instrumentation, the five equipments should be weighted equally; while if the error was due only to the experimenter, all the investigations should be weighted equally. Accordingly at a meeting in Helsinki in 1961, the Working Group decided upon a "square-root" method of weighting, designed to balance these two major types of bias.

The details of the weighting procedure were devised by R. S. Dadson of The National Physical Laboratory. He was then Secretary of the Working Group. The monumental and painstaking task of assembling all the relevant data, the computations, and actual writing of the Recommendation were his responsibility. The following is the procedure he used for computation.

First, the corrected transfer factors were computed as described above. Then all the original data were tabulated as in Table III. In most of these threshold determinations, data were obtained directly with one of the five standard equipments. In some cases, threshold was measured with other earphone types necessitating transferring the data to one of the standard earphones using known transfer factors. These factors, of course, are different from those included in Table II. It was decided to consider the determinations in the latter

TABLE III. Original data with references and preliminary weighting. Where the original data were not obtained with one of the five standard earphone–coupler combinations, the reported values were adjusted by known transfer factors.

Earphone-coupler combination Frequency (Hz)	(1)	(2)	(3)	(3)	(3)	(3)	(3)	(3)	(4)	(4)	(4)	(4)	(4)	(5)
	Equivalent threshold SPL's from original data dB *re* 2×10^{-5} N/m²													
125	41.5	43.0	44.5	48.0	43.0	···	44.0	···	45.3	···	45.5	49.2	···	67.0
250	21.5	21.0	29.5	29.5	22.5	26.0	31.5	29.0	24.3	23.5	25.1	26.3	24.4	49.0
500	8.0	10.0	12.0	12.6	7.5	9.5	11.0	13.0	11.1	10.0	15.2	7.4	9.7	25.5
1000	3.5	5.0	6.0	6.3	3.0	5.0	6.5	5.0	6.9	6.5	8.3	7.2	6.2	14.0
1500	3.0	4.5	7.5	8.2	···	5.0	···	···	5.6	5.5	···	···	7.2	14.5
2000	2.5	6.0	9.0	9.5	9.5	7.5	8.5	10.0	7.9	8.5	10.6	8.6	7.2	14.0
3000	1.5	4.0	6.0	12.5	···	14.0	7.5	6.5	11.5	13.0	···	8.5	6.4	13.0
4000	2.0	5.0	9.0	13.5	10.0	12.5	10.0	10.5	12.4	12.0	12.9	9.0	9.0	14.5
6000	5.0	11.0	9.0	15.5	12.5	9.5	···	14.0	12.9	12.5	···	10.7	18.3	···
8000	8.0	14.5	9.0	16.0	12.5	12.5	···	6.5	12.7	13.5	14.3	10.6	14.8	···
Determination designation	a	b	c	d	e	f	g	h	i	j	k	l	m	n
Preliminary weighting	2.5	1	2 or 1	1	0.5	0.5	0.5	0.5	1	0.5	0.5	0.5	0.5	1

[a] Chavasse and Lehmann (1957) and CNET (1960).
[b] Mrass and Diestel (1959).
[c] Dadson and King (1952) Wheeler and Dickson (1952).
[d] Albrite *et al.* (1958).
[e] P.T.B. (1958) N.P.L. (1959).
[f] Glorig (1959).
[g] Hinchcliffe (1959).
[h] Knight and Coles (1960).
[i] Albrite *et al.* (1958) and Weissler *et al.* (1960).
[j] Glorig (1959).
[k] Harris (1954).
[l] Glorig *et al.* (1956).
[m] Corso (1958).
[n] Sheuviekhman *et al.* (1955).

group as equivalent to one-half a determination each, while the determinations in the group using the standard equipment were considered whole determinations. In addition, two minor determinations using standard equipment but involving only a small number of subjects were also considered equivalent to one-half a determination.

The succeeding steps in the calculations were as follows:

1. For each equipment, (1)–(5), the average threshold levels for the whole group of determinations relating to the particular combination were calculated. These results, together with the total number of determinations used for each equipment, are shown in Table IV.

2. A final weighing factor was allocated to each of the five equipments at the Helsinki meeting in 1961. It had been decided that an equipment credited with "n" determinations should be allocated a weighting factor equal to $n^{\frac{1}{2}}$.

3. The average of the original threshold levels for Equipments (1), (2), (4), and (5) in Table IV were each transferred to equipment (3) by application of the corrected transfer factors in Table II. These are shown in Table V.

4. The weighted average of the threshold levels for the five equipments all transferred to Equipment (3) was evaluated. This is shown in the last column of Table V.

5. The evaluation of the weighted averages for the remaining four equipments was then carried out by direct application of the transfer factors of Table II to the last column of Table V. The final results appear in Table VI, which is the same as the ISO Recommendation R389. Note that the values in Table VI are independent of the particular equipment chosen in Step 3 for evaluation of the final average.

TABLE IV. Average of original threshold levels for each earphone coupler combination. The number of investigations following the preliminary weighting in Table III is shown in parentheses.

Earphone-coupler combination Frequency (Hz)	(1)	(2)	(3)	(4)	(5)
	Equivalent threshold SPL's dB *re* 2×10^{-5} N/m²				
125	41.5(2.5)	43.0(1)	45.3(3)	46.3(2)	67.0(1)
250	21.5(2.5)	21.0(1)	28.6(5)	24.6(3)	49.0(1)
500	8.0(2.5)	10.0(1)	11.4(5)	10.8(3)	25.5(1)
1000	3.5(2.5)	5.0(1)	5.6(5)	7.0(3)	14.0(1)
1500	3.0(2.5)	4.5(1)	7.3(2.5)	6.0(2)	14.5(1)
2000	2.5(2.5)	6.0(1)	9.0(5)	8.5(3)	14.0(1)
3000	1.5(2.5)	4.0(1)	8.6(4.5)	10.2(2.5)	13.0(1)
4000	2.0(2.5)	5.0(1)	10.6(5)	11.3(3)	14.5(1)
6000	5.0(2.5)	11.0(1)	12.1(3.5)	13.5(2.5)	
8000	8.0(2.5)	14.5(1)	11.1(4.5)	13.1(3)	

IV. COMPARISON WITH OTHER WEIGHTING PROCEDURES

It is interesting to speculate about how the final value for the reference equivalent threshold would be affected if different weighting procedures were used. Accordingly, the final average was recomputed giving each determination a weight of 1. It was also recomputed by finding five equipment averages, weighting determinations made with the same equipment equally. Then each of the five equipments were weighted once and a final average taken. Table VII compares these results. All of the computations were performed in terms of the standard equipment for the USA or Country (4). The

TABLE V. Evaluation of final average for earphone-coupler Combination 3. Weighting factors are shown in parentheses.

Earphone-coupler combination	(1)	(2)	(3)	(4)	(5)	
Frequency (Hz)	Equivalent threshold SPL's for Combinations 1–5 referred to Combination 3 by application of the corrected transfer factors (Table II) dB re 2×10^{-5} N/m²					Final weighted average for earphone-coupler Combination 3
125	44.0(1.58)	42.5(1)	45.3(1.73)	47.8(1.41)	59.0(1)	47.1
250	22.0(1.58)	20.5(1)	28.6(2.24)	28.1(1.73)	44.0(1)	28.1
500	8.0(1.58)	7.0(1)	11.4(2.24)	11.3(1.73)	22.5(1)	11.5
1000	3.5(1.58)	2.5(1)	5.6(2.24)	6.0(1.73)	11.0(1)	5.6
1500	5.0(1.58)	3.5(1)	7.3(1.58)	6.0(1.41)	12.5(1)	6.7
2000	7.0(1.58)	7.0(1)	9.0(2.24)	9.0(1.73)	13.8(1)	9.0
3000	3.5(1.58)	6.0(1)	8.6(2.12)	10.7(1.58)	10.5(1)	7.8
4000	3.5(1.58)	9.0(1)	10.6(2.24)	11.8(1.73)	12.5(1)	9.4
6000	−4.0(1.58)	11.0(1)	12.1(1.87)	13.5(1.58)		8.1
8000	3.5(1.58)	10.0(1)	11.0(2.12)	13.6(1.73)		9.8

final averages obtained by using each of these three weighting procedures agree within 1 dB at nearly all frequencies. The exceptions are at 6000 Hz, where the average threshold computed by giving equal weight to each determination is greater than threshold computed by the other two weighting procedures by 3 dB; and at 8000 Hz, the threshold computed giving equal weights to each determination is 1.5–2.0 dB greater than the threshold computed by using the other weighting procedures.

TABLE VI. Recommended reference equivalent threshold SPL's from ISO Recommendation R389.

Earphone-coupler combination[a] Frequency (Hz)	(1)	(2)	(3)	(4)	(5)
	Reference equivalent threshold SPL's dB re 2×10^{-5} N/m				
125	44.5	47.5	47	45.5	55
250	27.5	28.5	28	24.5	33
500	11.5	14.5	11.5	11	14.5
1000	5.5	8	5.5	6.5	8.5
1500	4.5	7.5	6.5	6.5	8.5
2000	4.5	8	9	8.5	9
3000	6	6	8	7.5	10.5
4000	8	5.5	9.5	9	11.5
6000	17	8	8	8	18.5
8000	14.5	14.5	10	9.5	9.5
Country	France	Germany	United Kingdom	USA	USSR

[a] See Table I.

V. STATISTICAL ANALYSIS[2]

If this entire set of threshold and transfer determinations were to be repeated, how closely would the new set of reference threshold values agree with the present set? The final values of the recommended reference equivalent threshold SPL's in Table VI are a function of both the original threshold determination and the transfer factors. Thus, the uncertainty of the reference threshold sound pressures is a function of the uncertainty of both the original threshold determinations and the transfer factors.

Let us look at the details of the threshold computation analytically. Let Z_c denote the value for earphone-coupler Combination (c) that appears in Table IV (for each frequency). This was obtained from Table III using the weights given at the bottom of that Table. Therefore

$$Z_c = \sum_{j=1}^{m} V_{cj} Z_{cj} \sum_{j=1}^{m} V_{cj}, \tag{4}$$

where Z_{cj} is the original threshold determination by the jth laboratory using equipment Combination (c) and V_{cj} is the weight for that laboratory.

From Table V, let W denote the final weighted average for earphone-coupler Combination 3 (for each frequency). Then

$$W = \sum_{c=1}^{5} w_c (Z_c - T_{c3}') \sum w_c, \tag{5}$$

where the weights w_c are shown in parentheses in Table V and T_{c3}' is the corrected transfer factor

TABLE VII. Comparison of different weighting procedures for calculating the reference equivalent threshold SPL.

Frequency (Hz)	RETSPL in terms of Country (4) equipment dB re 2×10^{-5} N/m² ISO R389	Equal weight to each determination	Equal weight to each country's equipment
125	45.5	45.4	46.3
250	24.5	25.0	25.2
500	11.0	11.1	11.5
1000	6.5	6.8	6.8
1500	6.5	6.8	6.8
2000	8.5	8.7	8.8
3000	7.5	8.3	7.4
4000	9.0	10.1	9.0
6000	8.0	10.9	8.0
8000	9.5	11.0	9.1

[2] This Section is based on work done in collaboration with J. Rosenblatt, Statist. Eng. Sec., Natl. Bur. Std., Washington, D. C. 20234.

TABLE VIII. Standard deviation of the ensemble of measurements for each original threshold determination.

Earphone-coupler combination Frequency (Hz)	(2)	(3)	(3)	(3)	(3)	(4)	(4)	(4)	(4)	(5)	Mean
	Standard deviation of threshold determinations (dB)										
125	4.2	6.8	4.2	7.0	···	4.0	7.4	5.3	···	9.75	6.1
250	3.8	7.3	4.2	6.2	4.9	3.6	5.5	6.1	4.5	8.25	5.4
500	3.9	6.5	4.4	5.4	4.9	5.5	4.8	6.0	5.4	6.75	5.3
1000	3.8	5.7	4.4	5.9	3.7	5.4	5.9	6.2	4.15	3.00	4.8
1500	4.6	6.1	5.7	···	···	5.5	···	···	4.8	3.75	5.0
2000	4.7	6.1	3.8	5.8	4.1	5.9	7.4	5.5	4.95	5.25	5.3
3000	5.5	5.9	6.6	6.4	4.6	7.2	···	6.5	4.85	4.50	5.8
4000	5.7	6.9	6.3	6.2	5.6	6.4	10.9	7.2	5.7	7.5	6.8
6000	6.2	9.1	7.9	9.2	8.0	7.0	···	8.3	6.75	···	7.8
8000	7.3	8.7	8.3	13.3	7.8	7.6	16.4	8.4	7.15	···	9.4
Determination designation[a]	b	c	d	g	h	i	k	l	m	n	
No. of people	70	99	25	75	15	33	50	122	75	2000	

[a] See Table III.

for putting Z_c on the Country (3) basis. Also, Eqs. 1–3 express T_{c3}' in terms of the original transfer determinations.

Thus with standard statistical techniques (Ku, 1966) and Eqs. 1–5, the variance of H' can be computed as a function of the variances of the original threshold determinations and the variance of the uncorrected transfer factors.

Let Y_c denote the value given in Table VI for Country (c):

$$Y_c = H' + T_{c3}'. \tag{6}$$

The variance of Y_c can similarly be shown to be a function of the variance of H' and the variance of a transfer determination.

Estimates of the variance of Z_{cj} and T_{ij} were made in the following manner.

In order to estimate the uncertainty in the original threshold determinations their standard deviations were tabulated (Table VIII). From the 14 determinations, 10 sets of standard deviations were obtained; eight from published papers and two computed at NBS from the WRAMC–NBS data.

The mean standard deviation computed at each frequency was considered as typical of a threshold determination.

The standard deviations given in Table VIII reflect within-laboratory variability, presumably for individual threshold determinations. However, each of the numbers given in Table III is affected by not only within-laboratory variability, but in addition, by systematic or other between-laboratories differences. In order to make an estimate of the between-laboratories variability, the original data in Table III were examined. There are six determinations whose results are expressed in terms of earphone–coupler Combination 3 and five determinations in terms of Combination 4. Assuming all the determinations to be equally precise, the standard deviations of the tabulated entries (assumed to be equally weighted elements of a measurements population) for Nos. 3 and 4 were each computed and the results pooled. See Table IX.

TABLE IX. Estimated standard deviation of the reported threshold values for an original threshold determination.

Frequency (Hz)	Standard deviation (dB)
125	2.2
250	2.4
500	2.4
1000	1.1
1500	1.4
2000	1.0
3000	3.3
4000	1.8
6000	3.0
8000	2.7
	Average = 2.1

The average of the pooled standard deviations for all frequencies is 2.1 dB. The average within-laboratory standard deviation for all frequencies is 6.2 dB. The pooled value of 2.1 dB is what whould be expected from within-laboratory variability alone if each laboratory had reported the average of only nine individual determinations ($6.2/9^{\frac{1}{2}} = 2.1$). Since the number of subjects was larger than that in most cases, we may conclude that there is some between-laboratories variability in addition to the within-laboratory variability. Accordingly, the standard deviations in Table IX were considered to be reasonable estimates of the over-all uncertainty of the reported threshold values incorporating both within- and between-laboratories variability, but still within one country's standard equipment. These values were assumed to be typical of a threshold determination and were applied to each original determina-

TABLE X. Uncertainty of transfer factors.

Frequency (Hz)	Average of reported standard errors (dB)	Estimated standard error of a transfer factor determination (dB)	Estimated standard error of a corrected transfer factor $T_{i,i+1}'$[a] (dB)	Estimated standard error of a corrected transfer factor $T_{i,i+2}'$[b] (dB)
125	1.2	2.4	1.5	1.9
250	0.8	1.2	0.8	0.9
500	0.8	2.3	1.5	1.8
1000	0.7	3.9	2.5	3.0
1500		4.1[c]	2.6[c]	3.2[c]
2000	0.9	4.2	2.7	3.3
3000		3.9[c]	2.5[c]	3.0[c]
4000	1.1	3.0	1.9	2.3
6000	1.6	4.3	2.7	3.3
8000	1.7	3.7	2.3	2.9

[a] Estimated standard error of the difference between two adjacent columns in Table VI.
[b] Estimated standard error of the difference between nonadjacent columns, or columns that are two apart in Table VI.
[c] Interpolated values.

tion in Table III in the computations of the uncertainty of the final recommended reference values. It is interesting to note at this point that most of the determinations were made with well over nine people, from 25 to 2000 people. It appears as though it would be more profitable to investigate and reduce systematic differences between measurements made in different laboratories rather than devote time and energy making measurements on huge numbers of people. These data also support the validity of Dadson's weighting procedure compared with a statistical weighting procedure based solely on the number of subjects in each determination.

The uncertainty in the transfer factors was estimated as follows: Data on the standard errors (standard deviations of the reported mean transfer factors) were included in the committee documents for seven of the 11 transfer factor determinations. The second column of Table X shows the average of standard errors reported for the transfer factor determinations at each frequency.

Since each of the five transfer factors was determined by two countries, the pairs of determinations provide additional evidence on the standard errors of the reported values. Since the sum of all the transfer factors should equal zero, the difference between their sum and zero should also provide additional evidence on the standard errors of the reported values. An analysis based on these factors yielded an estimate of the standard error of a transfer factor determination summarized in the third column of Table X. Since the differences between determinations in two countries may also involve a systematic error component, it is not surprising that the estimated standard errors in Column 3 should be larger than in Column 2. The value of the standard errors in Column 3 at each frequency was considered to be the same for each country and each transfer-factor determination and used in the computation of the uncertainty of the final recommended reference equivalent threshold SPL's. It was also used in the calculation of the standard error of the corrected transfer factors. The values at 1000 and 2000 Hz are due in large part to the difference between the two determinations of T_{51}. Since at two frequencies, 1500 and 3000 Hz, data for the transfer factors were incomplete the values of the estimated variances were supplied by interpolation.

Next, the standard deviation of the recommended reference equivalent threshold SPL's were computed. The results are contained in Table XI.

From Table XI, it is apparent that the standard deviation varies somewhat from equipment to equipment. This is due to the weighting procedure and the transfer factors. If each country's equipment had been weighted equally, there would have been no difference in the variances of their reference SPL's. In the calculations for Table XI, it was evident that, in general, the uncertainty of the transfer factors makes a larger contribution to the final variance than does the uncertainty of the threshold determinations. If we assume the variance in the transfer factors to be zero, that is, a perfect measurement, the standard deviation of the final RETSPL would be the same for each country and would be smaller than those in Table XI. Such a calculation was made yielding an estimated standard deviation of 0.7 dB averaged over the frequency range. Somewhat unexpectedly, the values in Table XI in the middle frequencies are higher than in the low frequencies. This may be ascribed to the fortuitous good agreement between countries for T_{51} at low frequencies, as shown in Fig. 5.

From the average of the standard deviations for 1000 8000 Hz for all five equipments, the over-all average standard deviation of the RETSPL in ISO R389 is 2 dB.

TABLE XI. Estimated standard deviation of the recommended reference equivalent threshold SPL's tabulated in ISO Recommendation R389.

Earphone-coupler combination / Frequency (Hz)	(1)	(2)	(3)	(4)	(5)
	Estimated standard deviation (dB)				
125	1.3	1.4	1.3	1.3	1.4
250	1.0	1.0	0.9	1.0	1.0
500	1.3	1.3	1.2	1.3	1.4
1000	1.9	1.9	1.6	1.7	1.9
1500	1.9	1.9	1.8	1.9	2.0
2000	2.0	2.0	1.7	1.8	2.1
3000	2.2	2.2	1.9	2.0	2.2
4000	1.6	1.6	1.3	1.4	1.6
6000	2.4	2.3	2.0	2.2	2.7
8000	2.0	1.9	1.6	1.8	2.3
1000–8000-Hz average	2.0	2.0	1.7	1.8	2.1

Another important question is whether the RETSPL for the different equipments are truly equivalent. Or, in quantitative terms, what are the variances of the differences between the columns of R389? These differences are the corrected transfer factors T_{ij}', and their variances are functions of the variances of the original transfer-factor determinations. Thus, the estimated standard errors of $T_{i,i+1}'$ (the corrected transfer factor between adjacent columns) and $T_{i,i+2}'$ (the corrected transfer factor between two nonadjacent columns, found by taking the sum of two adjacent transfer factors), were computed and the results tabulated in Columns 4 and 5 of Table X.

The "over-all uncertainty" of the difference between determinations by two equipments, defined as three times the average standard deviation of the difference for 1000–8000 Hz (not including interpolated values) was calculated. It is ± 7.4 and ± 9.0 dB for adjacent and nonadjacent equipments respectively. Statistically the over-all uncertainty corresponds approximately to a 98% confidence level. In other words, if a person's hearing is measured by two equipments, the resulting measurements could differ by as much as 9 dB (or more if one includes the uncertainties of the hearing measurements).

In their recent paper, Delany and Whittle (1967) have experimentally measured the equivalence of equipments (2), (3), and (4) by measuring the hearing level of the same group of people with the three equipments. They found statistically significant differences at most frequencies. These differences are all within the over-all uncertainty of ± 7.4 bB for $T_{i,i+1}'$, except at 8000 Hz. From Fig. 1 in their paper, the difference between Equipments (2) and (3), at 8000 Hz, appears to be 9.4 dB, which is considerably larger than 7.4 dB. The uncertainty of Delany and Whittle's measurements would have to be combined with the uncertainty for $T_{i,i+1}'$ in order to make a proper comparison.

Let X_1, X_2, X_3 denote the three mean thresholds shown in their Fig. 1 at various frequencies. The Figure also gives 95% confidence limits, presumably for the means. Now each X_i was derived from an experimentally determined mean U_i corrected by subtraction of the appropriate RETSPL Y_i,

$$X_i = U_i - Y_i.$$

The confidence limits shown refer to the uncertainty in U_i. Consider

$$(X_i - X_j) = (U_i - Y_i) - (U_j - Y_j),$$
$$(X_i - X_j) = (U_i - U_j) - (T_{ij}'). \qquad (7)$$

Thus, from Eq. 7 and standard statistical techniques (Ku, 1966), the uncertainty in $(X_i - X_j)$ can be calculated from the uncertainty in $(U_i - U_j)$ and the uncertainty in (T_{ij}').

Accordingly, at 8000 Hz, the difference between hearing levels measured with Equipments (2) and (3) by Delany and Whittle is 9.4 dB with over-all uncertainty limits of approximately ± 9.1 dB at the 98% confidence level. The difference of 9.4 dB is then slightly larger than one would expect considering both the uncertainty in the hearing-level measurements made by Delany and Whittle and the estimated uncertainty in the difference between equipments in ISO R389.

VI. DISCUSSION OF RESULTS

Considering the variety of conditions under which the threshold determinations were made, the results show surprisingly good agreement. Although most of the threshold determinations have already been published (see footnotes to Table III), it is interesting to summarize briefly some of the conditions under which these measurements have been made. In most of the studies, the age ranged from 18–25 yr, although in one it was as low as 17 and another as high as 40. People tested were from five different countries. They were students, sophisticated laboratory personnel, naval recruits, volunteers at a State Fair, and inhabitants of a rural area. Ten different earphone types were used. In a number of determinations, threshold was considered the lowest level for which two out of three signals were heard, while for two of the determinations, three out of three signals had to be heard. The means of ascending and descending thresholds were used in many studies, while in one, only the decreasing threshold was used. Testing time ranged from several different sittings for one subject to about 30 min per person. Although background noise was carefully measured in some cases, in others the test was reported to have been made in a "quiet" environment. With all these variations, the average standard deviation of 2 dB seems reasonable—especially when one considers that a large part of the uncertainty is due not to the threshold measurements themselves but to the transfer factors.

Figure 6 shows the deviations of the original threshold determinations from ISO R389. There appears to be a systematic difference between Russia's original threshold determination and the others, particularly at frequencies below 1000 Hz where their values fall well above the uncertainty limit of the 6 dB corresponding approximately to a 98% confidence level. The earcaps on the T.D. 6 earphones are large and soft, making it very difficult to position an earphone on an ear without leakage. Earphone output at 125 Hz can vary by as much as 20 dB with a small change in position. Leakage due to incorrect positioning of the earphone on the ear could cause higher values for threshold voltage than if the earphones had been carefully positioned. This, in turn, results in correspondingly higher values of sound pressure in the coupler.

There also appears to be a systematic difference between the present USASI reference values and the

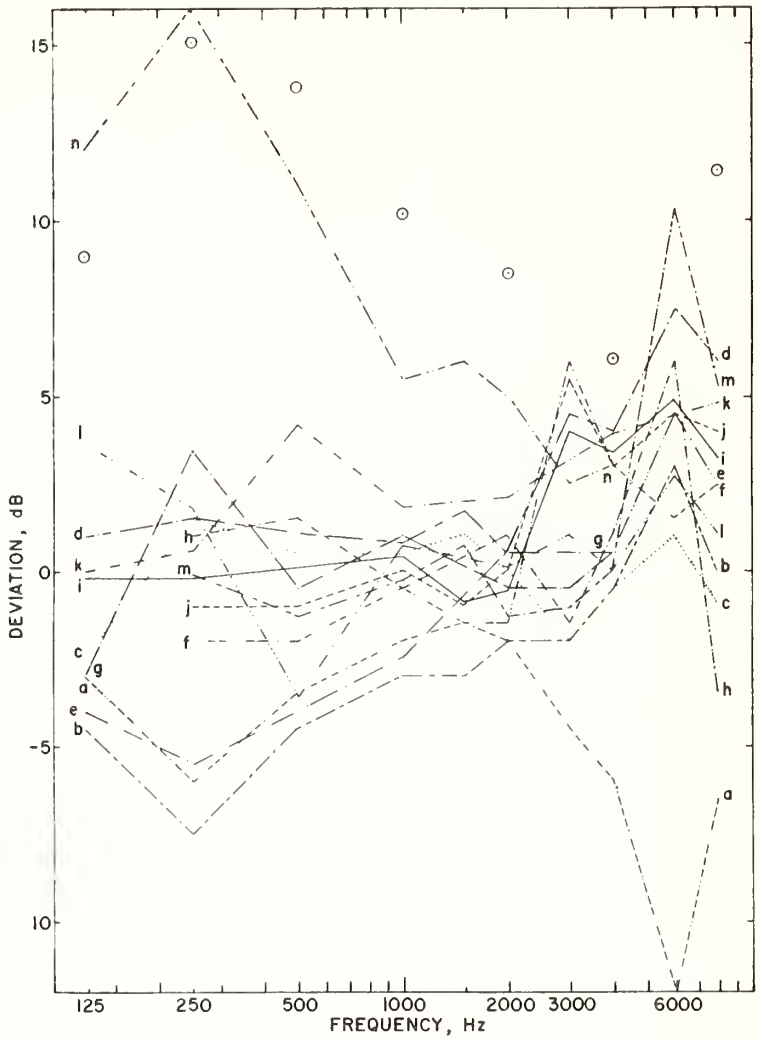

FIG. 6. Deviation of the original data from ISOR 389. Letters on the Figure refer to the determination designation in Table III. The circles are the deviations of USAI 1951 from ISOR 389.

ISO R389. As shown in Fig. 6, the difference is appreciably larger than the average standard deviation of 2 dB at all frequencies.

The uncertainty of the transfer factors obtained by loudness-balancing experiments, between different earphone types, contributes substantially to the uncertainty of the final RETSPL and to the uncertainty of the equivalence of the different equipments. One way to improve the accuracy of our threshold standards would be to agree upon one standard earphone. This could be specified by an earcap with a prescribed size and shape and by a standard acoustic impedance looking into the grille. Unfortunately, it is not possible to eliminate all transfers of threshold between different earphone types by agreeing upon one standard coupler designed to approximate the ear very closely without also agreeing upon a standard earphone. The geometry of a new earphone type may preclude its calibration on any existing coupler. For example, none of the standard artificial ears nor the one described by Delany, Whittle, Cook, and Scott (1967) are suitable for the calibration of circumaural earphones sometimes used in audiometry.

It should be pointed out that in the Table in ISO R389 the designation, "Country of origin of data" is somewhat misleading. It should be clear from this paper that each figure in the Table is a weighted average of data obtained in each of the five countries listed. The figures in each column pertain to the corresponding earphone-coupler combination used as national standards in the designated countries.

ACKNOWLEDGMENTS

The author would like to thank Dr. Richard K. Cook who encouraged the writing of this paper and who made his files on ISO/TC 43 WG1 available. She would also like to thank Robert S. Dadson for his detailed and informative correspondence during the time of the compilation of ISO R389 and Martin Greenspan for much helpful advice on the preparation of this manuscript.

REFERENCES

Cook, J. P., Shutts, R. E., Whitlock, M. B., Cook, R. K., Corliss, E. L. R., and Burkhard, M. D. (1958). "Research in Normal Threshold of Hearing," Arch. Otolaryngol. *68*, 194–198.

Centre Nationale d'Études des Télécommunications (1960). Unpublished Working Group document.

Chavasse, P., and Lehmann, R. (1957). "Contribution a l'Étude Zéro Absolu des Audiometers," Acustica *7*, 132–136.

Corliss, E. L. R., and Burkhard, M. D. (1953). "A Probe Tube Method for the Transfer of Threshold Standards Between Audiometer Earphones," J. Acoust. Soc. Am. *25*, 990–993.

Corso, J. F. (1958). "Proposed Laboratory Standard of Normal Hearing," J. Acoust. Soc. Am. *30*, 14–23.

Dadson, R. S., and King, J. H. (1952). "A Determination of the Normal Threshold of Hearing and its Relation to the Standardization of Audiometers," J. Laryngol. and Otol. *46*, 366–378.

Davis, H., and Kranz, F. W. (1964a). "The International Standard Reference Zero for Pure Tone Audiometers and its Relation to the Evaluation of Impairment of Hearing," J. Speech Hearing Res. *7*, 7–16. Also Trans. Am. Acad. Opthalmol. Otolaryngol. *68*, 484–492.

Davis, H., and Kranz, F. (1964b). "The International Audiometric Zero," J. Acoust. Soc. Am. *36*, 1450–1454. Also Am. Ind. Hyg. Assoc. J. *25*, 354–358 and Ann. Otol. *73*, 807–815.

Davis, H. (1965a). "International Standard Reference Zero for Pure Tone Audiometry," Trans. Am. Acad. Opthalmol. Otolaryngol. *69*, 112–118.

Davis, H. (1965b). "Guide for the Classification and Evaluation of Hearing Handicap in Relation to the International Audiometric Zero," Trans. Am Acad. Opthalmol. Otolaryngol. *69*, 74–751.

Davis, H. (1965c). "The ISO Zero Reference Level for Audiometers," Arch. Otolaryngol. *81*, 145–149.

Davis, H. (1966). Reference Levels and Hearing Levels in Otology, "Ann. Otol. Rhinol. Laryngol. *75*, 808.

Delany, M. E., and Whittle, L. S. (1967). "Reference Equivalent Threshold Sound Pressure Levels for Audiometry," Acustica *18*, 227–231.

Delany, M. E., Whittle, L. S., Cook, J. P., and Scott, V. (1967). "Performance of a New Artificial Ear," Acustica *18*, 231–237.

Glorig, A., Quiggle, R., Wheeler, D. E., and Grings, W. J. (1956). "Determination of the Normal Hearing Reference Zero," J. Acoust. Soc. Am. *28*, 1110–1113.

Glorig, A. (1959). Unpublished committee document.

Harris, J. D. (1954). "Normal Hearing and its Relation to Audiometry," Laryngoscope *64*, 928–957.

Hinchcliffe, R. (1959). "The Threshold of Hearing of a Random Sample Rural Population," Acta Oto-Laryngol. *50*, 411–422.

Hirschorn, M. (1967). "Acoustical Environment for Industrial Audiometric Programs," Sound and Vibration *1*, 8–15.

Knight, J. J., and Coles, R. R. A. (1960). "Determination of the Hearing Thresholds of Naval Recruits in Terms of British and American Standards," J. Acoust. Soc. Am. *32*, 800–804.

Ku, H. H. (1966). "Notes on the Use of Propagation of Error Formulas," J. Res. Natl. Bur. Std. *70 C*, 263–273.

Mrass, H., and Diestel, H. G. (1959). "Bestimmung der Normalhörschwelle für Reine Töne bei Einohrigem Hören mit Hilfe eines Kopfhörers," Acustica *9*, 61–64.

National Health Survey (1935–1936). *Preliminary Reports, Hearing Study Series*, Bulletins *1–7*, U. S. Public Health Service, Washington, D. C.

National Physical Laboratory (1959). Unpublished committee document.

Physikalisch-Technische Bundesanstalt (1958). Unpublished Working Group 1 document.

Sheuviekhman, B. E., Babkin, V. P., and Glekin, G. V. (1955). "Determination of the Value of the Average Threshold Intensity of Sound Perceptible to Mature People," Probl. Physiol. Acoust. *3*, 75–80 (in Russian).

Weissler, P. G., Smith, E. L., Corliss, E. L. R., and Bowman, H. S. (1960). Unpublished data on threshold of hearing of eight normal people reported by NBS to Working Group 1.

Weissler, P. G. (1965). "The New International Standard Reference Zero and its Relation to the Calibration of Audiometers," *Guidlines for Hearing Screening Programs: Calibration of Audiometers*, U. S. Dept. of HEW Welfare Admin., Childrens Bureau.

Wheeler, L. J., and Dickson, E. D. D. (1952). "The Determination of the Threshold of Hearing," J. Laryngol. Otol. *46*, 379–395.

Reprinted from
Journal of the Acoustical Society of America
Volume 44 Number 1 1968

The Determination of Reverberant Sound Absorption Coefficients from Acoustic Impedance Measurements

ALBERT LONDON
National Bureau of Standards, Washington, D. C.
(Received November 1, 1949)

A method is described for utilizing normal absorption coefficient or acoustic impedance measurements to predict reverberant sound absorption coefficients. The average of coefficients for the six standard frequencies determined from acoustic impedance measurements agrees closely with the average reverberant coefficient, for cases where the material may be said to obey the normal impedance assumption. The normal absorption coefficients of some 26 different acoustic materials were measured at 512 c.p.s. Using the method given in the paper, the predicted reverberant coefficient deviated from the measured reverberant coefficient by 0.05 or less for 18 materials, while in only 3 cases were the deviations greater than 0.10. The method should be particularly applicable to the problem of acceptance testing of installed acoustic materials.

In the theoretical development, best agreement with experiment was obtained by introducing a new kind of reverberant statistics which associates with each wave packet in a random field a scalar quantity equal to the square of the absolute value of the sound pressure in each packet, instead of the customary energy flow treatment. Also, it was found necessary to carry out the analysis using a concept of equivalent real impedance to replace the usual complex impedance.

I. INTRODUCTION

IT would be of considerable technological importance if it were possible to determine from laboratory measurements on small samples the sound absorption coefficient one might expect to measure on large samples placed in a reverberant test chamber. A similar problem is that of the field measurement of an acoustic material already applied to the walls of a room. In particular, difficulty is often experienced with acoustic plasters whose acoustic properties may be ruined by improper application. In this case it is of prime importance to be able to measure the coefficient in the field in order to check compliance with purchase specifications which are based on reverberation room coefficients.

In large rooms or auditoriums it may be possible to obtain an approximate idea of the field absorption coefficient by measuring the reverberation time. However, in small rooms, corridors, or other open spaces, it is not possible to use the reverberation time technique. Measurement of the acoustical impedance of the material using tube methods, or short tube methods as developed by Cook[1] and Mawardi[2] seems to be a practical procedure readily applicable to use in the field on those materials for which the absorption is due to the surface and not to mounting effects.

In any acoustic impedance tube measurement, what is in reality measured is the absorption coefficient for normal incidence. Accordingly, the problem reduces to one of relating the reverberant, or random incidence absorption coefficient to the normal incidence coefficient. In the following, we deduce such a relationship which apparently agrees on the average with data obtained for a considerable number of materials. There are certain difficulties associated with the treatment which will be discussed in detail.

[1] R. K. Cook, J. Acous. Soc. Am. **19**, 922 (1947).
[2] O. K. Mawardi, J. Acous. Soc. Am. **21**, 84 (1949).

II. RELATION BETWEEN ACOUSTIC IMPEDANCE AND NORMAL AND RANDOM INCIDENCE COEFFICIENTS

Paris[3] first derived an expression (Eq. (1)) for the sound absorption coefficient, α_θ, for a wave incident at angle θ on an acoustic material which has an acoustic impedance Z:

$$\alpha_\theta = 1 - \left| \frac{(Z/\rho c)\cos\theta - 1}{(Z/\rho c)\cos\theta + 1} \right|^2, \tag{1}$$

where ρc is the acoustic impedance of air.

Let

$$Z/\rho c = z = r + jx. \tag{2}$$

Then Eq. (1) may be written

$$\alpha_\theta = \frac{4r\cos\theta}{(r\cos\theta+1)^2 + x^2\cos^2\theta}. \tag{3}$$

From (3) the normal incidence coefficient α_0, is

$$\alpha_0 = \frac{4r}{(r+1)^2 + x^2}. \tag{4}$$

Using the customary reverberant sound field statistics, the random incidence coefficient $\bar{\alpha}$, is defined by

$$\bar{\alpha} = 2\int_0^{\pi/2} \alpha_\theta \cos\theta \sin\theta d\theta \tag{5}$$

and substituting (3) into (5) results in

$$\bar{\alpha}_P = \frac{8r}{x^2+r^2}\left\{1 + \frac{r^2-x^2}{x(x^2+r^2)}\tan^{-1}\left(\frac{x}{1+r}\right) - \frac{r}{x^2+r^2}\ln[(1+r)^2+x^2]\right\}. \tag{6}$$

[3] E. T. Paris, Proc. Roy. Soc. **115**, 407 (1927).

Equation (6) was first derived by Paris[4] in terms of the acoustic admittance while similar formulations are given by Morse, Bolt, and Brown[5] and by Morse.[6]

In the paper by Morse, Bolt, and Brown,[5] $\bar{\alpha}_P$ was compared with the reverberant sound absorption coefficient $\alpha_{A.M.A.}$ given by the Acoustic Materials Association for four different commercial acoustic materials. The acoustic impedance measurements were those of Beranek.[7] Their conclusions were:

(1) Above 2000 c.p.s., $\alpha_{A.M.A.}$ corresponds to $\bar{\alpha}_P$, indicating adequate diffusion in the sound chamber such that the conditions of random incidence and uniform energy distribution are satisfied.

(2) Below about 500 c.p.s., $\alpha_{A.M.A.}$ usually approximates what Morse, Bolt, and Brown call α_n, the normal absorption coefficient, which is the coefficient for normal incidence for a large number of normal modes and which has the approximate value of

$$\alpha_n \simeq 8r/(r^2+x^2). \tag{7}$$

In the cases where $\alpha_{A.M.A.}$ is larger than α_n at low frequencies, they attribute this discrepancy to mounting conditions and sample size. At low frequencies, then, there is presumed to be incomplete diffusion in the reverberant chamber.

(3) The region between 500 to 2000 c.p.s. is intermediate in the diffusion between that corresponding to α_n and that corresponding to the completely random coefficient $\bar{\alpha}_P$.

FIG. 1. View showing vanes in the reverberation room of the National Bureau of Standards.

(4) For low frequencies the decay curve will be a broken line, the slope of the initial straight portion, covering approximately the first 30 db of decay, corresponding to α_n.

In discussing the above conclusions relative to the experimental technique utilized in the reverberant test chamber of the National Bureau of Standards, one must raise the following points:

(1) It is difficult to see how a very close approximation to complete diffusion cannot help but be assured by the use of two vanes some 8 feet by 8 feet in size (Fig. 1).

(2) Even at low frequencies linear decay curves are obtained over a range of at least 50 db at 128 c.p.s. and up to 70 db at 256 c.p.s.

(3) Linear decay curves can be obtained by restricting the amount of material introduced into the chamber to 72 sq. ft. in accordance with the results obtained by Chrisler.[8] This material is placed on the floor which has a total area of 750 sq. ft.

In what follows, we shall consider a somewhat different method of deriving a reverberant sound absorption coefficient, one which on the average is in better agreement with experiment than $\bar{\alpha}_P$. In addition a somewhat simplified and hence semi-empirical method will be described which enables one to predict the reverberant coefficient from a measurement of r and x, to within an accuracy of 0.05 in the average absorption coefficient for the range of 128 to 4096 c.p.s.

It will be convenient to discuss the latter method first.

Davis[9] in his book *Modern Acoustics* discusses the relationship between the reverberant coefficient and the coefficient obtained from a tube measurement which he calls the stationary-wave coefficient but which in reality corresponds to the coefficient α_0. Figure 2 is a reproduction of Fig. 80 in his book in which is shown a graph of the relationship between the ratio of reverberant to stationary-wave coefficient as a function of stationary-wave coefficient at a frequency of about 500 c.p.s. The best smooth curve was drawn through 11 experimental values. It should be noted that the experimental points were deduced from published values of reverberation coefficients obtained at different times and in different countries while α_0 was measured by Davis and Evans.[10]

The curve of Fig. 2 can be almost fitted exactly by the following procedure:

(1) It is assumed that for a given value of α_0, determined from r and x by Eq. (4), one can define an equivalent impedance z_e, which is real, and which

[4] E. T. Paris, Phil. Mag. **5**, 489 (1928).
[5] Morse, Bolt, and Brown, J. Acous. Soc. Am. **12**, 217 (1940).
[6] P. M. Morse, *Vibration and Sound* (McGraw-Hill Book Company, Inc., New York, 1948), 2nd edition, p. 388.
[7] L. L. Beranek, J. Acous. Soc. Am. **12**, 14 (1940).
[8] V. L. Chrisler, J. Research Nat. Bur. of Stand. **13**, 169 (1934), RP 700.
[9] A. H. Davis, *Modern Acoustics* (G. Bell and Sons, London, 1934), p. 216.
[10] A. H. Davis and E. J. Evans, Proc. Roy. Soc. **117**, 89 (1930).

therefore may be obtained from Eq. (1) by writing

$$\alpha_0 = 1 - \left(\frac{z_e - 1}{z_e + 1}\right)^2 = \frac{4z_e}{(z_e+1)^2}. \tag{8}$$

Equation (8) thus results in two solutions for z_e. However only the solution,

$$z_e = \frac{1+(1-\alpha_0)^{\frac{1}{2}}}{1-(1-\alpha_0)^{\frac{1}{2}}} \tag{9}$$

is compatible with experimental results.

(2) The random incidence coefficient, $\alpha_e{}^*$, corresponding to α_0 is then defined by

$$\alpha_e{}^* = \frac{\int_0^{\pi/2} \{1 - [(z_e\cos\theta - 1)/(z_e\cos\theta + 1)]^2\} \sin\theta d\theta}{\int_0^{\pi/2} \sin\theta d\theta}. \tag{10}$$

Here we note two departures from the definition of random incidence coefficient $\bar{\alpha}$ as given in Eq. (5). First, we make use of a different type of reverberant statistics, or averaging with respect to θ, as evidenced by the fact that the $\cos\theta$-factor does not appear in the integral. A discussion of this type of statistics appears below. The * superscript will be used to refer to this type of averaging. Second, in α_θ, Eq. (1), we have introduced the equivalent impedance z_e and use the resulting expression in Eq. (10). The subscript e will be used to indicate the introduction of z_e.

Carrying out the integration (10) results in the following equation:

$$\alpha_e{}^* = \frac{4}{z_e}\left[\ln(1+z_e) - \frac{z_e}{1+z_e}\right] \tag{11}$$

or substituting (9) into (11), we have

$$\alpha_e{}^* = 4\left[\frac{1-(1-\alpha_0)^{\frac{1}{2}}}{1+(1-\alpha_0)^{\frac{1}{2}}}\right] \times \left\{\ln 2 - \tfrac{1}{2} - \ln[1-(1-\alpha_0)^{\frac{1}{2}}] - \frac{(1-\alpha_0)^{\frac{1}{2}}}{2}\right\}. \tag{12}$$

It will also be of interest to evaluate

$$\bar{\alpha}_e = \frac{\int_0^{\pi/2} \left\{1 - \left[\frac{(z_e\cos\theta - 1)}{(z_e\cos\theta + 1)}\right]^2\right\} \cos\theta \sin\theta d\theta}{\int_0^{\pi/2} \cos\theta \sin\theta d\theta}, \tag{13}$$

which turns out to be

$$\bar{\alpha}_e = \frac{8}{z_e{}^2}\left[1 + z_e - \frac{1}{1+z_e} - 2\ln(1+z_e)\right] \tag{14}$$

or substituting (9) into (14), we have

$$\bar{\alpha}_e = 8\left[\frac{1-(1-\alpha_0)^{\frac{1}{2}}}{1+(1-\alpha_0)^{\frac{1}{2}}}\right]^2 \left\{\frac{2}{1-(1-\alpha_0)^{\frac{1}{2}}} - \frac{1-(1-\alpha_0)^{\frac{1}{2}}}{2} - 2\ln\left[\frac{1-(1-\alpha_0)^{\frac{1}{2}}}{2}\right]\right\}. \tag{15}$$

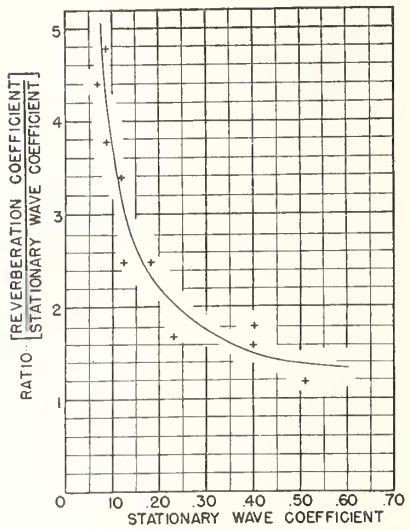

FIG. 2. Plot showing the relationship between the ratio of reverberant to stationary-wave coefficient as a function of stationary wave coefficient at a frequency of about 500 c.p.s. as given by Davis and Evans.

Figure 3 is a comparison between $\alpha_e{}^*/\alpha_0$ *vs.* α_0 as computed from Eq. (12), $\bar{\alpha}_e/\alpha_0$ *vs.* α_0 as computed from Eq. (15) and α_{rev}/α_0 *vs.* α_0 as given by Davis where α_{rev} is the absorption coefficient measured in a reverberant test chamber. It will be seen, that for α_0 below 0.40, the $\alpha_e{}^*/\alpha_0$ curve is in much better agreement with the experimental values than the $\bar{\alpha}_e/\alpha_0$ curve. For $\alpha_0 > 0.40$, both $\alpha_e{}^*/\alpha_0$ and $\bar{\alpha}_e/\alpha_0$ are in close agreement. Experimental values of α_0, however, do not exceed 0.60 so that it is not possible to check the extent to which $\alpha_e{}^*$ or $\bar{\alpha}_e$ agrees with experiment for the larger values of α_0.

Figure 4 is a plot which gives directly $\alpha_e{}^*$ and $\bar{\alpha}_e$ as a function of α_0.

We are thus led to the tentative conclusion that the star-type statistics as defined by Eq. (10) appears to be in better agreement with experiment than the bar-type statistics, as defined by Eq. (14). Further corroboration of this tentative conclusion will be given below in connection with the four commercial materials previously mentioned, for which we will compare α_{rev}, $\alpha_e{}^*$, $\bar{\alpha}_e$, α^*, and $\bar{\alpha}_P$, where in the latter two coefficients we drop the equivalent treatment and work directly with the real and imaginary component of the impedance. That is, α^* is defined by analogy with

Eq. (10) as

$$\alpha^*=\frac{\int_0^{\pi/2}\{1-|(z\cos\theta-1)/(z\cos\theta+1)|^2\}\sin\theta d\theta}{\int_0^{\pi/2}\sin\theta d\theta} \quad (16)$$

or

$$\alpha^*=\frac{4r}{x^2+r^2}\left\{\frac{1}{2}\ln[x^2+(r+1)^2]-\frac{r}{x}\tan^{-1}\left(\frac{x}{1+r}\right)\right\}. \quad (17)$$

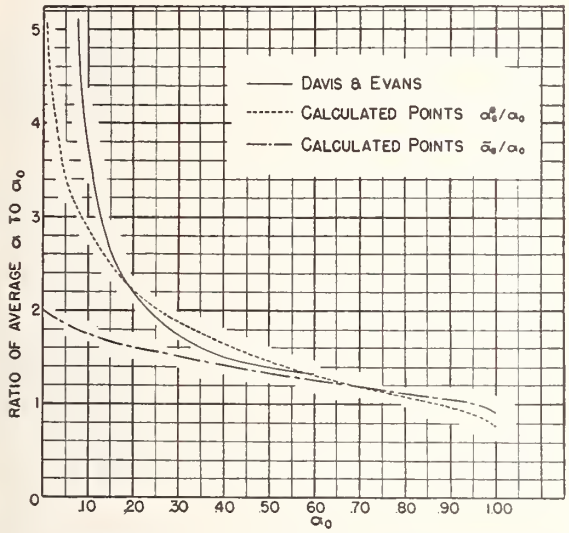

FIG. 3. Comparison between the Davis and Evans curve (Fig. 2), $\alpha_\epsilon^*/\alpha_0$ *vs.* α_0, and $\bar{\alpha}_\epsilon/\alpha_0$. See text.

It is advantageous at this point to discuss the assumptions inherent in the star-type statistics. We consider (Fig. 5) a point 0 of the elementary area dS located at the origin of a spherical coordinate system. We assume that wave packets strike point 0 uniformly from all directions. The number of packets striking 0 from a solid angle $d\Omega$ will thus be proportional to $d\Omega$. We assume that each wave packet carries with it a scalar quantity $|p_i|^2$ which does not vary with angle of incidence and which is the square of the acoustic pressure in the wave. Thus, if P_i^2 is the sum of the individual $|p_i|^2$ wave packets incident at 0, then

$$P_i^2=B|p_i(\theta)|^2\int_0^{2\pi}d\phi\int_0^{\pi/2}\sin\theta d\theta, \quad (18)$$

where B is a constant of proportionality, while the total amount which is absorbed is given by

$$P_{abs}^2=B\int_0^{2\pi}d\phi\int_0^{\pi/2}\alpha_\theta|p_i(\theta)|^2\sin\theta d\theta \quad (19)$$

since α_θ is in reality given by[11]

$$\alpha_\theta=1-\left|\frac{p_r(\theta)}{p_i(\theta)}\right|^2 \quad (20)$$

[11] See reference 6, p. 367.

where $p_r(\theta)$ is the reflected pressure amplitude of a wave incident at angle θ while $p_i(\theta)$ is similarly the incident pressure amplitude. Thus

$$\alpha^*=\frac{P_{abs}^2}{P_i^2}=\frac{\int_0^{\pi/2}\alpha_\theta\sin\theta d\theta}{\int_0^{\pi/2}\sin\theta d\theta}, \quad (21)$$

since $|p_i(\theta)|^2=|p_i|^2$, independent of angle of incidence.

It is to be noted that had we used energy as the scalar quantity associated with each wave packet, it would have been necessary to define the intensity as the amount of energy transmitted through unit area per unit time. This would immediately have required the amount of energy striking dS to be proportional to $dS\cos\theta$ and to the solid angle $d\Omega$, thus giving rise to the usual bar-type statistics. It seems more reasonable to associate the quantity $|p|^2$ with each wave packet for two reasons:

(1) The absorption coefficient as a function of angle of incidence, α_θ, is given by Eq. (20) directly in terms of the ratio of squares of the absolute values of pressures.

(2) In any reverberant test chamber setup, it is customary to use pressure microphones, so that the quantity $|P|^2$ is what is actually measured.

While it is still necessary that the sound field be completely random in phase in order to sum the $|p|^2$ of the individual packets, it is not necessary to assume that $|p|^2$ is proportional to total energy. In many cases, especially at the lower frequencies, this may not be true at all.

The extent to which the star-type statistics is superior to the bar-type statistics is indicated in Table I. Here we list the four commercial materials discussed by

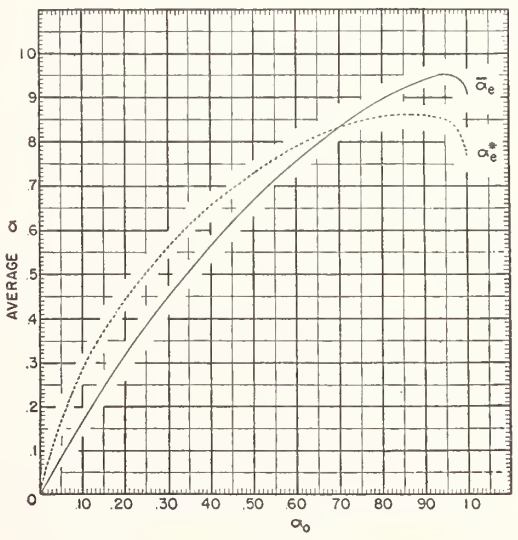

FIG. 4. Plot of $\bar{\alpha}_\epsilon$ and α_ϵ^* *vs.* α_0. See text.

Morse, Bolt, and Brown.[5] The impedance terms r and x were read directly from the curves given by Beranek.[7] The coefficients α_{rev} are the A.M.A. coefficients as read from the graphs,[5] while $\bar{\alpha}_P$, the reverberant coefficient of Paris, Eq. (6), were also read from the graphs. The coefficients α_e^*, $\bar{\alpha}_e$, α^* have been previously defined.

In Table II, the difference in average coefficient (average for all frequencies) relative to the experimental α_{rev} is listed.

In practically every case the star-type coefficient is equal to or better than the corresponding bar-type coefficient. Whereas, $\bar{\alpha}_e$ is usually a close approximation to $\bar{\alpha}_P$, α_e^* is usually much closer to α_{rev} than α^*. The coefficient α_e^* in each case gives the closest approximation to α_{rev}, and with the exception of Acoustex is within 0.05 of α_{rev}. In the case of Acoustex, there is some indication that the reverberant coefficient is too high at the three lowest frequencies relative to other results obtained on the same material. The results on α_{rev} given in Table I were apparently obtained from Bulletin VII of the Acoustic Material Association published in April, 1940. Bulletin No. VIII published June, 1941 lists Acoustex mounted on 1×2 furring strips, which customarily gives higher results at the lowest frequencies than the rigid mounting coefficients reported in Table I, with coefficients of 0.09 and 0.25 at 128 and 256 c.p.s. respectively, while some data obtained and published in Letter Circular LC-506, October, 1937, at the National Bureau of Standards, lists coefficients of 0.19 and 0.41 at 256, and 512 c.p.s., which are in close agreement with α_e^*. It is not known to what extent the acoustic impedance samples were selected from the same batch or samples which were used in the reverberation tests. In fact, it would appear that this was not done, the reverberant coefficients apparently being taken from published data of the A.M.A. The only reliable procedure would be to carry out the acoustic impedance measurements and reverberation measurements on the same batch. In any event, it still appears that, technologically speaking, α_e^* is a close approximation on the average to α_{rev} and hence may be a useful tool in field measurements.

It will be of interest to apply this type of analysis to an absorbent material which, on the basis of previous experiments, apparently does not have a normal acoustic impedance; that is, the ratio of pressure to normal component of velocity is not independent of angle of incidence. In this event, α_θ is not given by Eq. (1) and the variation of α with θ must be determined if an integration of α over θ is to be carried out. Cook and Chrzanowski,[12] in an investigation at the National Bureau of Standards of the absorption of sound by spheres having a hair-felt surface, concluded that the normal impedance assumption apparently was not valid for hair-felt. Inasmuch as they give both acoustic impedance measurements and reverberation room coefficients made on the same bath of hair-felt, uncertainty on this score will be eliminated.

[12] R. K. Cook and P. Chrzanowski, J. Acous. Soc. Am. 21, 167 (1949).

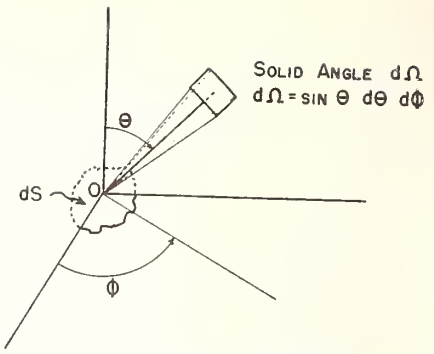

FIG. 5. Representation of solid angle used in star-type statistics.

In Figs. 6 and 7 we compare α_{rev}, α_e^*, and $\bar{\alpha}_P$ for

TABLE I.

f(c.p.s.)	r	x	α_0	α_{rev}	α_e^*	$\bar{\alpha}_e$	α^*	$\bar{\alpha}_P$
			Acoustex, ⅞″					
128	2.6	−21.0	0.023	0.24	0.09	0.04	0.07	0.09
256	1.9	−11.2	0.057	0.29	0.19	0.10	0.13	0.12
512	1.5	− 5.2	0.180	0.60	0.42	0.30	0.28	0.27
1024	1.5	− 1.6	0.681	0.95	0.83	0.82	0.69	0.74
2048	2.2	+ 1.3	0.738	0.83	0.85	0.86	0.79	0.85
4096	4.3	− 0.6	0.605	0.75	0.79	0.76	0.79	0.77
Av. (128–4096)				0.61	0.53	0.48	0.46	0.47
			Celotex C-4, 1¼″					
128	2.6	−12.0	0.066	0.27	0.22	0.12	0.16	0.13
256	2.5	− 6.2	0.197	0.46	0.44	0.32	0.34	0.32
512	2.6	− 1.8	0.642	0.98	0.81	0.79	0.75	0.86
1024	2.8	+ 2.0	0.607	0.79	0.79	0.76	0.74	0.72
2048	5.4	+ 5.0	0.327	0.55	0.59	0.48	0.55	0.48
4096	10.0	+ 0.5	0.330	0.51	0.60	0.49	0.60	0.48
Av. (128–4096)				0.60	0.58	0.49	0.52	0.50
			Permacoustic, 1″					
128	3.2	−13.7	0.062	0.21	0.20	0.10	0.15	0.14
256	3.6	− 6.6	0.222	0.48	0.48	0.36	0.40	0.36
512	4.0	− 3.3	0.446	0.76	0.69	0.62	0.64	0.58
1024	5.0	− 1.8	0.510	0.72	0.74	0.68	0.73	0.68
2048	4.0	− 1.6	0.580	0.75	0.78	0.74	0.76	0.73
4096	3.0	− 1.6	0.646	0.74	0.81	0.80	0.78	0.78
Av. (128–4096)				0.61	0.62	0.55	0.58	0.55
			Temcoustic, ½″					
128	13.5	−30.4	0.048	0.16	0.16	0.08	0.15	0.11
256	14.5	−17.0	0.110	0.28	0.31	0.18	0.28	0.16
512	13.5	−11.0	0.163	0.43	0.39	0.27	0.37	0.28
1024	12.0	− 6.5	0.227	0.49	0.48	0.36	0.47	0.38
2048	12.2	0	0.280	0.44	0.54	0.43	0.54	0.44
4096	9.8	+ 2.5	0.318		0.58			
Av. (128–2048)				0.36	0.37	0.30	0.36	0.27

TABLE II. Difference in average coefficient relative to α_{rev}.

	α_e^*	$\bar{\alpha}_e$	α^*	$\bar{\alpha}_P$
Acoustex ⅞″	−0.08	−0.13	−0.15	−0.14
Celotex C-4, 1¼″	−0.02	−0.11	−0.08	−0.10
Permacoustic, 1″	+0.01	−0.06	−0.03	−0.06
Temcoustic, ½″	+0.01	−0.06	+0.00	−0.09

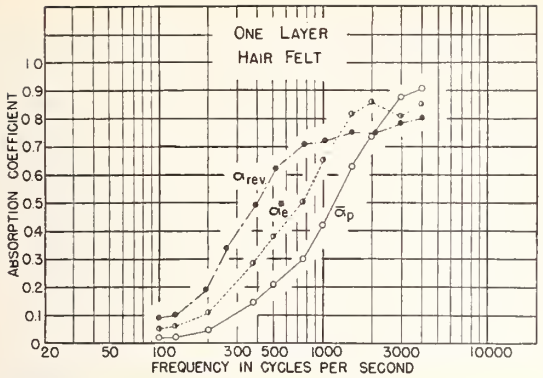

FIG. 6. Comparison between measured reverberant coefficient and predicted reverberant coefficient α_e^* for a single layer of hair-felt. $\bar{\alpha}_P$ is the reverberant coefficient first derived by Paris. Hair-felt is presumed to violate the normal impedance assumption.

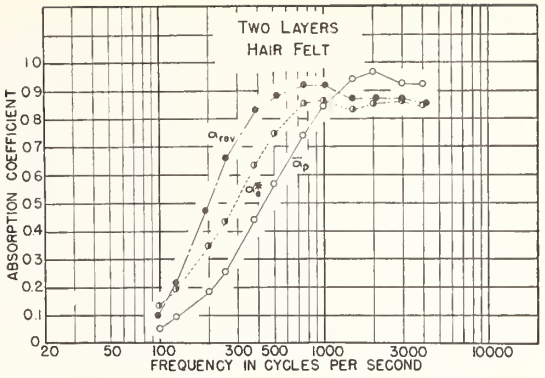

FIG. 7. Comparison between measured reverberant coefficient and predicted reverberant-coefficient α_e^* for two layers of hair-felt. $\bar{\alpha}_P$ is the reverberant coefficient first derived by Paris Hair-felt is presumed to violate the normal impedance assumption.

TABLE III. Hair felt coefficients.

Frequency c.p.s.	Single layer α_{rev}	Single layer α_e^*	Single layer $\bar{\alpha}_P$	Double layer α_{rev}	Double layer α_e^*	Double layer $\bar{\alpha}_P$
128	0.10	0.06	0.02	0.20	0.19	0.10
256	0.34	0.17	0.08	0.66	0.44	0.26
512	0.62	0.38	0.21	0.88	0.75	0.57
1024	0.72	0.66	0.43	0.92	0.86	0.86
2048	0.75	0.86	0.75	0.87	0.85	0.96
4096	0.80	0.86	0.91	0.85	0.85	0.92
Av. (128–4096)	0.55	0.50	0.40	0.73	0.66	0.61

a single and double layer of hair-felt. It will be seen that in each case α_e^* is a much closer approximation to α_{rev} than $\bar{\alpha}_P$. In Table III we consider the average values of the various coefficients for the six standard frequencies.

The lack of very close agreement between α_e^* and α_{rev} may in part be attributed to the failure of the normal impedance assumption.

A further test of the extent of agreement between α_e^* and α_{rev} was made in our laboratory at 512 c.p.s. by measuring[13] the α_0 of samples which had been measured in the reverberation room. A tube having a $9\frac{3}{4}$ inch diameter was used and α_0 was obtained directly by measuring the ratio, ρ, of a pressure maximum to the adjacent pressure minimum. The absorption coefficient, α_0, is given by[9]

$$\alpha_0 = 4\rho/(1+\rho)^2. \qquad (22)$$

Table IV lists the results obtained on twenty-six different materials. Measurements were made on several different pieces of tile (usually 3) of the 72 sq. ft. used in the reverberation room test. In most cases, α_e^* as measured had a maximum deviation of about 0.04 for different pieces of the same material. The coefficient listed in the table is the average for the several pieces used in the measurements. In cases where α_e^* varied excessively between different tiles, the individual measurements are listed.

Of the 26 materials listed in Table IV, 18 values of α_e^* deviate from α_{rev} by 0.05 or less, 5 deviations fall in the range of 0.06 to 0.10, while only three have deviations greater than 0.10. It is interesting to observe that entries 1, 2, and 5, which are Acousti-Celotex tiles, all deviate by 0.10 or more, indicating that possibly the mechanism of sound absorption is such as to violate the normal impedance assumption. Inasmuch as it is impossible to get an α_e^* greater than 0.86, one would expect 1 and 2 to deviate. In the case of 1, the α_0 which

TABLE IV. Tabulation of $\alpha_e^* - \alpha_{rev}$ *vs.* α_{rev} at 512 c.p.s.

Material	α_{rev}		$\alpha_e^* - \alpha_{rev}$
1. $1\frac{1}{4}''$ C-4 Celotex R.I. finish	0.97		−0.11
2. $1\frac{1}{4}''$ C-4 Celotex slow burning	0.94		−0.10
3. $1''$ Certile	0.83		−0.07
4. $1''$ Fiberglas tile perforated	0.79		−0.05
5. $\frac{3}{4}''$ C-9 Celotex	0.78		−0.10
6. $\frac{13}{16}''$ Travacoustic fissured	0.78		−0.05
7. $\frac{3}{4}''$ Certile	0.75		−0.03
8. $\frac{3}{4}''$ Travacoustic fissured	0.72		−0.04
9. $\frac{3}{4}''$ Fiberglas tile perforated	0.71		+0.04
10. $\frac{3}{4}''$ Firtex, perforated	0.71		−0.01
11. $\frac{13}{16}''$ Kelly Island tile, perforated	0.69		−0.02
12. $\frac{3}{4}''$ Fiberglas tile fissured	0.68		+0.03
13. $1''$ Quietone, perforated	0.68		+0.04
14. $1''$ Firtex, perforated	0.68		−0.04
15. $\frac{11}{16}''$ Insulite acoustilite	0.66	−0.16[a] −0.06 −0.15	−0.12
16. $\frac{13}{16}''$ Dantore fissured	0.66		−0.02
17. $\frac{3}{4}''$ Fiberglas tile plain	0.65		+0.07
18. $\frac{13}{16}''$ Dantore fissured	0.65		−0.03
19. $\frac{1}{2}''$ Hansonite perforated	0.62		−0.05
20. $\frac{5}{8}''$ Travacoustic fissured	0.62		−0.01
21. $\frac{1}{2}''$ Firtex perforated	0.55		−0.02
22. $1''$ Softone	0.53	−0.04[b] −0.15	−0.10
23. Sabinite No. 1 Plaster	0.48		+0.03
24. Sabinite No. 2 Plaster	0.48		+0.04
25. $\frac{3}{4}''$ Softone	0.41		−0.05
26. $\frac{3}{4}''$ Acoustex, type 40 R	0.37		+0.19

[a] Individual differences for 3 pieces of tile.
[b] Individual differences for 2 pieces of tile.

[13] These measurements were made by Seymour Edelman and Earle Jones.

TABLE V. $\alpha_e^* - \alpha_{rev}$ *vs.* α_{rev}.

Material	α_{rev}	$\alpha_e^* - \alpha_{rev}$ 12″×12″ tile flush	$\alpha_e^* - \alpha_{rev}$ $9\frac{1}{4}$″ diameter sample in tube
5. $\frac{3}{4}$″ C-9 Celotex	0.78	−0.12	−0.14
9. $\frac{3}{4}$″ Fiberglas perforated	0.71	+0.01	−0.24
14. 1″ Firtex, perforated	0.68	−0.07	−0.09
26. $\frac{3}{4}$″ Acoustex, type 40 R	0.37	+0.19	−0.01

was observed gave exactly the maximum value of α_e^*, i.e., 0.86.

One other feature of these tube measurements should be clarified. All of the measurements listed in Table IV were made using a 12 in.×12 in. tile which was placed in flush contact with a rubber gasket mounted on the end of the tube. In the case of acoustic plasters, a sample having the approximate dimensions of 30 in.×30 in. was used. The reasons for not cutting the samples to fit inside the tube were twofold. First, in any field measurement using the tube, it would not be possible to deface the surface of the installed material, and second, the materials were not expendable, since only at most three pieces had been saved from the reverberation room tests, for identification purposes.

However, some of the materials were cut to fit inside of the tube. The results are listed in Table V for an individual tile before and after cutting to fit inside of the tube.

The results in the table show that Celotex and Firtex have no appreciable absorption due to propagation of the sound wave in the material outside of the geometrical area intercepted by the tube, whereas, both the Fiberglas and Acoustex materials do.

In summary, then, it would appear that the proper procedure for utilizing α_e^* to check field coefficients for agreement with laboratory coefficients is as follows:

(1) Determine α_0 or the acoustic impedance and α_{rev} in the laboratory.

(2) Compute α_e^* from α_0 or from the acoustic impedance measurements.

(3) If the average α_e^* agrees closely with the average α_{rev}, then a field measurement of α_0 or of the acoustic impedance should be sufficient to determine the extent of compliance with the reverberation coefficient.

(4) If the average α_e^* as determined in the laboratory does not agree with the average α_{rev}, it would still be possible, however, to find an average α_e^* in the field from the α_0 or acoustic impedance measurements and the extent of compliance of the field α_e^* with the laboratory α_e^* could then be used as a criterion for acceptability.

III. CONCLUSIONS

A procedure has been outlined whereby normal absorption coefficient or acoustic impedance measurements may be utilized to predict reverberant sound absorption coefficients. The average of coefficients for the six standard frequencies determined from acoustic impedance measurements agrees closely with the average reverberant coefficient, for cases where the material may be said to obey the normal impedance assumption. In the case of normal absorption coefficient measurements, for a large number of materials, good agreement was obtained between the predicted and measured reverberant coefficient. A method of utilizing field measurements of the normal absorption coefficient or of the acoustic impedance for acceptance testing has been indicated which should be applicable even in cases where the normal impedance assumption is violated.

On the theoretical side, we have found best agreement with experiment by utilizing a new kind of statistics which associates with each wave packet in a random field a scalar quantity equal to the square of the absolute value of the sound pressure in each packet, instead of the customary energy flow treatment. On the other hand, it has been necessary to utilize a semi-empirical concept of equivalent impedance as distinguished from the usual complex impedance treatment. The best which can be said for the introduction of this bit of empiricism is that it works, although no reasons for its success are deduced here.

Reprinted from THE JOURNAL OF THE ACOUSTICAL SOCIETY OF AMERICA, Vol. 22, No. 2, 263–269, March, 1950

AMERICAN SOCIETY FOR TESTING AND MATERIALS

1916 Race St., Philadelphia, Pa. 19103

Reprinted from the Annual Book of ASTM Standards, Copyright ASTM

Tentative Recommended Practice for

LABORATORY MEASUREMENT OF AIRBORNE SOUND TRANSMISSION LOSS OF BUILDING PARTITIONS[1]

ASTM Designation: E 90 – 66 T

This Tentative Recommended Practice has been approved by the sponsoring committee and accepted by the Society in accordance with established procedures, for use pending adoption. Suggestions for revisions should be addressed to the Society at 1916 Race St., Philadelphia, Pa. 19103.

In accordance with the Society's policy that tentatives should not be continued indefinitely, this tentative will be discontinued in November, 1970 unless the sponsoring committee takes action to adopt it as standard or the Committee on Standards grants a continuance for an additional year.

Introduction

This recommended practice is one of a series for evaluating the sound insulating properties of building elements. It is designed to measure the performance of an isolated partition element, in a controlled laboratory environment. Others in the series will deal with airborne sound transmission loss of partitions installed in buildings, and the laboratory and field measurement of impact sound transmission through floors.

1. Scope

1.1 This recommended practice covers the laboratory measurement of airborne sound transmission loss of building partitions such as walls of all kinds, floor–ceiling assemblies, doors, and other space-dividing elements.

Note 1—The values stated in U.S. customary units are to be regarded as the standard. The metric equivalents of U.S. customary units given in the body of the standard and in the appendix may be approximate.

2. Significance

2.1 The sound transmission loss is defined in terms of a diffuse incident sound field, and this is intrinsic to the test procedure. The results are most directly applicable to similar sound fields, but provide a useful general measure of performance for the variety of sound fields to which a partition may typically be exposed.

2.2 This procedure is not appropriate for determining the sound insulation performance of a partition exposed to a sound field that contains only a small range of angles of incidence nor is it applicable to sounds produced by direct mechanical contact or impact with the partition.

3. Summary of Method

3.1 The sound insulating property of a partition element is expressed in terms of the sound transmission loss (Note 2). The procedure for determining this quantity

[1] Under the standardization procedure of the Society, this recommended practice is under the joint jurisdiction of ASTM Committee E-6 on Performance of Building Constructions and Committee C-20 on Acoustical Materials. A list of members may be found in the ASTM Yearbook.

Current edition accepted Sept. 8, 1966. Originally issued 1950. Replaces E 90 – 61 T.

(1,2)[2] is to mount the test specimen as a partition between two reverberation rooms, one of which, the source room (Room 1), contains one or more sound sources. The rooms are so arranged and constructed that (apart from the limitations discussed in 5.1 and 6.3) the only significant sound transmission between them is through the test specimen. Then the transmission loss is given by:

$$TL = NR + 10 \log S - 10 \log A_2 \quad (1)$$

where:

log = logarithm to the base 10,
TL = transmission loss,
NR = noise reduction between the two reverberation rooms,
S = area of sound transmitting surface of the test specimen, and
A_2 = total absorption of the receiving room (Room 2), expressed in units consistent with S.

Since 10 log S is easily determined, the problems of measurement are associated with the noise reduction and 10 log A_2.

NOTE 2—In general, the transmission loss is a function of frequency, and measurements are made in a series of frequency bands.

4. Definitions

4.1 The acoustical terminology used in this standard is consistent with Ref. 3 and 4. A few definitions of special relevance are repeated here and interpreted with reference to this recommended practice.

4.2 *Airborne Sound Transmission Loss* (TL) *of a Partition*—The ratio, expressed in decibels, of sound power incident on the partition to the sound power transmitted through and radiated by the partition. The unqualified term denotes that the incident field is diffuse.

NOTE 3—The sound transmission coefficient and sound transmission loss are related through the equation,

$$TL = 10 \log (1/\tau) \quad (2)$$

4.3 *Sound Transmission Coefficient* (τ) *of a Partition*—The fraction of incident sound power transmitted through and radiated by the partition. The unqualified term denotes that the incident sound field is diffuse (Note 3).

4.4 *Noise Reduction* (NR) (*Between Two Rooms*)—The difference between the rms time-space-average sound pressure levels produced in the two rooms by a sound source in one of them.

4.5 *Diffuse Sound Field*—A sound field composed of many randomly oriented waves, with equal probability of energy flow in every direction. It follows that there is no correlation between instantaneous sound pressures at widely separated points.

4.6 *Reverberation Room*—A reverberant room specially designed to facilitate the production therein of a diffuse sound field (see 5.2, 5.3, 5.4).

4.7 *Sound Absorption of an Enclosure* (A)—A measure of the property of an enclosure of absorbing sound power from the sound field it contains. For purposes of this recommended practice, the absorption of the receiving room is determined by means of the Sabine formula for the decay of sound in a room (Note 4). If, following the discontinuance of a sound source in the room, the rate of decay of sound is d (db/sec) in a room of volume V, then the absorption of the room may be determined from the Sabine equation:

$$A = \frac{0.9210\ Vd}{c} \quad (3)$$

where c is the speed of sound in the medium. If V is in cubic feet and c is in ft/sec, then A is given in sabins; if V is in cubic meters and c is in m/sec, then A is in metric sabins (Note 5). This relation is derived on the assumption that the sound field is reverberant and diffuse, as in a reverberation room.

[2] The boldface numbers in parentheses refer to the references listed at the end of this recommended practice.

NOTE 4—This is the only method currently available for the absolute determination of room absorption. It should be noted that this derivation of room absorption is different from that which leads to the absorption term in Eq 1; the latter arises from the relation between steady-state sound power level and sound pressure level in a room. It is believed, however, that, in circumstances for which Eq 1 is valid, the reverberation method yields appropriate values of 10 log A_2.

A more detailed discussion of the relation between the two derivations of room absorption appears in "Steady State Method of Determining Changes in Sound Absorption of a Room (RM 14-3)"[3] and in Ref. 8. A complete description of the reverberation method appears in ASTM Method C 423, Sound Absorption of Acoustical Materials in Reverberation Rooms.[4]

NOTE 5—In some contexts the room absorption in metric sabins is defined as the "equivalent absorption area in square meters."

4.8 *Sound Transmission Class*—The sound transmission class is a single-figure rating derived in a prescribed manner from sound transmission loss values. The rating provides an estimate of the performance of a partition in certain common sound insulation problems. Its scope and the method of derivation are described in "Determination of Sound Transmission Class (RM 14-2)." [3]

5. Test Rooms

5.1 *Flanking Transmission*—The test rooms shall be so constructed and arranged that the test specimen constitutes the only important sound transmission path between them. The sound power transmitted through the test structure shall be at least 10 db greater than the power transmitted into the receiving room by all other paths. The extent to which the above condition is met can be ascertained as follows:

5.1.1 Build into the test opening a wall with a substantially higher transmission loss than any that will normally be tested. The apparent transmission loss measured on such a wall, which may be affected by flanking transmission or other extraneous noise, is a guide to the upper limit of the measuring facility. Measurements may be made to within about 10 db of the values obtained on such a wall.

5.1.2 If the specimen is rigidly connected to the source-room structure there is the possibility that, in addition to the incident airborne sound, extra energy may be imparted to the specimen at the edges because of vibration in the source-room structure. A discontinuity is therefore recommended between the source-room walls and the structure in which the test specimen is mounted.

5.2 *Size and Shape*—The achievement of an adequate approximation to a diffuse sound field in a frequency band requires that there be a sufficient number of room resonances (normal modes) within the test band, that these modes be distributed as uniformly as possible over the band, and that the directions of propagation corresponding to these modes be distributed as uniformly as possible. The extent to which the requirement is met is dependent on the size and shape of the rooms and also on the bandwidth of the test signal and on the nature of diffusing surfaces in the room.

5.2.1 It is recommended that there be at least 20 room modes in the lowest frequency band. To achieve this under the conditions of this recommended practice the room volume should be no less than

$$V = 4\lambda^3 \quad \text{.....(4)}$$

where λ is the wavelength corresponding to the middle frequency of the lowest band, and V and λ^3 are in the same units. Thus, for a band centered on 125 Hz (cycles per second) the recommended minimum volume is 2900 ft^3 (83 m^3); for 100 Hz the recommended volume is 5800 ft^3 (163 m^3). Room volumes down to half the value given by Eq 4 will be acceptable, but are not recommended for new installations.

[3] Appears in Related Material section of the *1969 Book of ASTM Standards*, Part 14.

[4] *1969 Book of ASTM Standards*, Part 14.

5.2.2 To ensure a uniform distribution of modes, with respect to frequency and to angle, no two dimensions of either room should be equal or in the ratio of small integers. The ratio of largest to smallest dimensions of either room shall be less than two. One of the recommended proportions is 1:1.3:1.6.

5.3 *Diffusion*

5.3.1 *Diffusing Means*—In a bare rectangular room the sound field tends to take the form of orthogonal sets of modes, with little coupling between them. To approach a diffuse distribution of sound, it is desirable to modify the system so that there is substantial interchange of energy between modes. This objective may be met by introducing a random arrangement of obliquely oriented diffusing surfaces, either on the boundaries of the room or suspended in the room space. To be effective, the width of a diffusor should be at least a quarter wavelength at the lowest test band (about 3 ft (1 m) for bands centered on 100 or 125 Hz). The total area (one side) of a stationary diffusing system should be about three quarters of the area of the largest single boundary surface.

5.3.2 A particularly effective device is a rotating reflector, set at an oblique angle, which continuously varies the coupling between room modes during the determination of the average sound pressure level. If one or more rotating reflectors are used, an area equivalent to one third to one half the area of the smallest boundary surface appears to be appropriate; stationary diffusors may be used to supplement a smaller rotating vane. Both source and receiving rooms should be fitted with diffusors in accordance with the above recommendations.

5.4 The interior surfaces of the rooms should have at each test frequency an average sound absorption coefficient less than 0.06 (for example, each of the terms A_1/S_1 and A_2/S_2 where S_1 and S_2 are the sums of areas of all exposed surfaces, including diffusors, in Rooms 1 and 2, should be less than 0.06), except that in the lowest test band a maximum of 0.15 is permissible if the absorptive surfaces are well distributed in the room (4).

NOTE 6—An exception is permitted when substantial absorption is introduced by the test specimen itself. The exceptional circumstance should be reported.

5.5 *Ambient Noise Level*—Ambient noise in the receiving room must be substantially lower than the level produced by transmission of the test signal through the test specimen (see 8.5).

5.6 *Construction*—The requirements of 5.1, 5.4 and 5.5 may readily be met if the rooms are constructed of heavy masonry or concrete with the minimum of structural connection to the main building, to the ground and to each other.

6. Test Specimens

6.1 *Size and Mounting*—The test specimen that is to typify a wall or floor shall be large enough to include all the essential constructional elements in their normal size, and in a proportion typical of actual use. The smallest dimension (excluding thickness) should preferably be not less than 8 ft, and shall in any case be not less than 6 ft, except that specimens of doors and other smaller building elements shall be their customary size. Preformed panel structures should include at least two complete modules (panels plus edge mounting elements). In all cases the test specimen shall be installed in a manner as similar as possible to actual construction, with a careful simulation of normal constraint and sealing conditions at the perimeter and at joints within the specimen. Detailed procedures for particular types of building separation elements are recommended in Appendix A1.

6.2 *Aging of Specimens*—Test speci-

mens that incorporate materials for which there is a curing process (for example, adhesives, plasters, concrete, mortar, damping compound) should age for a sufficient interval before testing. Aging periods for certain common materials are recommended in Appendix A1.

In the case of materials whose aging characteristics are not known, repeat tests over a reasonable time shall be made on at least one specimen to determine an appropriate aging period.

NOTE 7—A suggested procedure is to make tests at intervals in the series 1, 2, 4, 7, 14, and 28 days from date of construction, until no change is observed, to the precision of the measurement, between successive tests. A sufficient number of measurements should be made to achieve somewhat greater precision than is otherwise specified in this recommended practice. The minimum aging period should be the interval beyond which no change greater than the precision values of 8.7 is observed.

6.3 *Testing of Specimens Smaller than Test Opening*—When the test opening is reduced by means of a filler wall to accommodate a small test specimen, it is necessary to consider whether a significant portion of the sound is transmitted by way of the filler wall. Frequently it will be necessary to measure the transmission loss of the filler wall (filling the entire test opening with a wall construction similar to the filler wall). The following derivation may be made when the transmission losses of the complete filler wall and of the composite wall formed by the test specimen and filler wall are known.

6.3.1 The transmission coefficients τ_c and τ_f, for composite and filler walls, respectively, can be calculated from the corresponding transmission losses by means of Eq 2. These may be substituted in the following expression for the sound transmission through the composite wall:

$$\tau_c S_c = \tau_s S_s + \tau_f S_f \quad \ldots\ldots\ldots (5)$$

or

$$\tau_s = \frac{\tau_c S_c - \tau_f S_f}{S_s} \quad \ldots\ldots\ldots (6)$$

where:

S_c, S_s and S_f = areas of the composite wall, test specimen, and filler wall, respectively, and

τ_s = transmission coefficient of the test specimen.

Then the transmission loss of the test specimen may be calculated from Eq 2.

6.3.2 It is assumed in the above derivation that the two parts of the composite wall react to the sound field independently of each other, and that the transmission coefficient of a complete filler wall is the same as that of the portion surrounding the test specimen. These simplifications are acceptable as long as $\tau_f S_f$ is small compared to $\tau_c S_c$. Another obvious limitation of the accuracy of the calculation is the accuracy of the measurements from which the difference $(\tau_c S_c - \tau_f S_f)$ is derived; again the calculation is most reliable if $\tau_f S_f$ is much smaller than $\tau_c S_c$.

7. Test Signal

7.1 *Signal Spectrum*—The sound signals used for these tests shall form a series of bands of random (Gaussian) noise containing an essentially continuous distribution of frequencies over each test band. "Pink" noise, comprising random noise of equal power per fractional bandwidth, is recommended.

7.2 *Bandwidth*—The bandwidth of each test signal shall be one-third octave. Specifically, the overall frequency response of the electrical system, including the filter or filters in the source and microphone sections, shall for each test band conform to the specifications given in Ref. 6 for a Class II filter or better.

7.2.1 Filtering may be done in the

source or microphone system or partly in both, provided that the required overall characteristic is achieved. Apart from defining the third-octave bands of test signals, a filter in the microphone system serves to filter out extraneous noise lying outside the test band, including possible distortion products in the source system; a filter in the source system serves to concentrate the available power in the test band.

7.3 *Standard Test Frequencies*—The minimum range of measurements shall be a series of contiguous third-octave bands with center frequencies from 125 to 4000 Hz. If desired, the range may be extended in further third-octave steps downward or upward. Note that extending to lower frequencies will require larger room volumes (see 5.2.2).

7.4 *Continuous Frequency Sweeps*—A continuous frequency sweep may be used if the signal spectrum and bandwidth meet the requirements of 7.1 and 7.2 throughout the frequency range, and if the sweeping speed is slow enough that the same results are observed at the standard frequencies as are obtained with a fixed-band system. If a rotating-vane diffusor is used (5.3.2), the sweeping speed should be slow enough that a full rotation of the vane is completed during a third-octave traverse.

7.5 *Sound Sources*—Preferably more than one sound source should be used in order to achieve an energy distribution as uniform as possible throughout the room. Corner locations are usually desirable since this provides best excitation of the greatest number of room modes. It is recommended that optimum positions be determined by experiment, having in mind the requirements of 8.4. No source shall be closer than 5 ft to the test specimen.

7.5.1 *Sound Power of Sources*—The sound power requirement is dependent on the room absorptions, the nature of the test specimen, and the background noise in the receiving room; the power must be sufficient to meet the requirements of 8.5.

8. Measurement of Noise Reduction (NR)

8.1 The objective is to measure the difference between the time-space-average sound pressure levels in source and receiving rooms. Since only a level difference is required, it is necessary only to determine levels relative to a common reference pressure whose value need not be known. The term "level" is used in this sense throughout this section.

8.2 *Averaging Time*—For each sampling position, the averaging time shall be sufficient to permit an accurate estimate, from observations of a level meter or a level record, of the time-average level. If a rotating vane is used, the average level shall be determined over a sufficient time to take account of variations with vane position.

8.3 *Location of Microphones*—Microphones shall be located so as to sample adequately the sound field in each room space, subject to the following restrictions:

8.3.1 No microphone shall be closer than a half-wavelength (for the center frequency of the lowest band) to an extended boundary or diffusing surface in either room (5).

8.3.2 In the source room no microphone shall be in the direct field of the source.

8.3.3 In the receiving room no microphone shall be closer to the test specimen than a half-wavelength (for the center frequency of the lowest band).

8.3.4 For rooms and test signals that conform to this recommended practice it will generally be found that the sound pressure level tends to be the same at all positions within the restricted space delineated above. The number and location

of microphone positions required to obtain a space average to a given precision (see 8.7) should be determined initially by a detailed survey of the spaces, especially at the lower test frequencies. From such a survey a reduced number of locations, which yield the same average result, may be selected for day-to-day measurements.

8.4 *Combining of Level Measurements*—Following the procedures of 8.2 and 8.3, two sets of sound pressure levels, corresponding to the sampling positions in the two rooms, will be obtained. If the spread in a set of readings is no more than 6 db, the rms space-average sound pressure level for the room will be given to adequate precision by taking the arithmetic mean of the set of levels. For greater spreads, it is necessary to convert the levels to pressures-squared, take the square root of the mean of the pressures-squared, and convert this back to sound pressure level. If the averaging is done by combining microphone outputs electrically, the following precaution must be taken: squared outputs, rather than linear outputs, must be combined; the microphones must be matched in sensitivity within 1 db over the frequency range of interest.

8.5 *Background Noise*—Measurements of background noise should regularly be made to ensure that the observations are not affected by noise due to flanking transmission or other extraneous sound or to electrical noise in the receiving system. The background level must be at least 5 db below the total level due to signal plus background, and corrections must be made unless the background level is more than 10 db below the total level.

8.6 *Microphone Systems and Measuring Procedures*—Measurements at the selected positions in each room may be made with one or more microphone systems (Note 8). When several microphone systems are used, it is necessary to take account of possible differences in system sensitivity. Four possible procedures are given in 8.6.1 to 8.6.4.

NOTE 8—If several microphones are used, the term "microphone system" denotes an individual microphone plus any amplifier and coupling system associated with it, up to the common point at which microphone signals are combined or compared.

8.6.1 Use a single microphone system to make measurements at each position in turn; then the principal problem is to maintain the same source level during both sets of measurements. The observations may be processed directly as specified in 8.4 and 8.7.

8.6.2 Use calibrated microphone systems in the two rooms and correct each observed level according to the individual calibration. In this case, it is desirable to check the relative calibrations of the microphone systems frequently enough to ensure reliable performance. The calibration should occasionally be done at all test frequencies.

8.6.3 A procedure that guards against small errors in system sensitivity is to repeat the measurement procedure of 8.6.2 with microphone systems interchanged between rooms (Note 9). The two level readings thus obtained for each position are averaged; these average values (for each position) form the basic data for processing as specified in 8.4 and 8.7.

NOTE 9—It is still necessary that microphone system sensitivities match closely (within approximately 1 db) in order that the 6-db criterion of 8.4 may be applied; however, the interchanging process tends to cancel out small errors and also reveals the presence of large errors such as might result from faulty equipment.

8.6.4 A further modification of 8.6.3 is to interchange the functions of source and receiving rooms, leaving the microphones in the same rooms. This elimi-

nates the shifting of microphones required in 8.6.3, but requires a knowledge of the absorptions of both rooms since each is in turn the receiving room. In addition, it may be necessary to modify the source-room absorption for one or both directions of measurement in order to obtain meaningful measurements of receiving-room absorptions (see 9.1.2).

Each pair may be averaged and added to 10 log S to yield TL.

8.7 *Number and Precision of Measurements*—A sufficient number of measurements shall be taken to ensure that the mean value of the Noise Reduction (NR) is known to within ±1 db (90 per cent confidence) except for the lowest band, for which the limit shall be ±2 db.

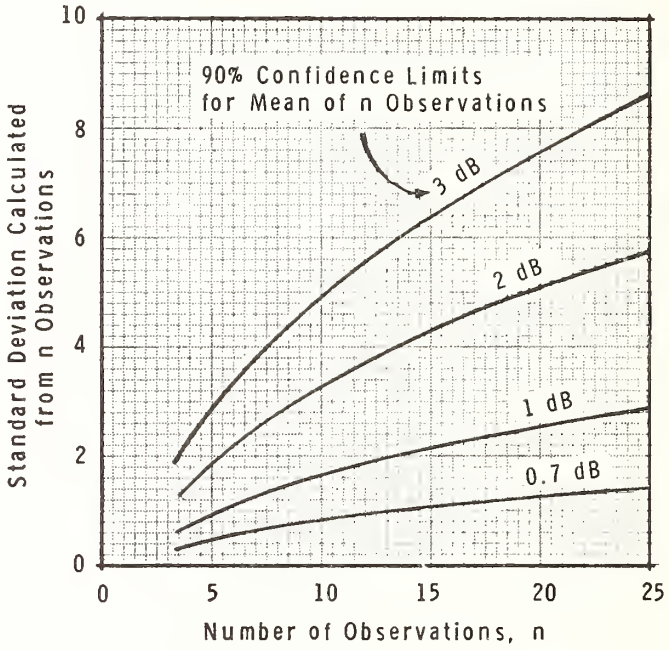

NOTE—Standard deviation $= \left[\sum_{i=1}^{n} (x_i - \bar{x})^2/n\right]^{1/2}$

where x_i are the n observations and $\bar{x}$ is their mean value.

FIG. 1—Number and Precision of Measurements.

For each direction of test, the levels for each room are combined (as specified in 8.4) and the level difference may be determined. The two level differences thus obtained may differ because of differences between sets of microphones or differences in the two receiving-room absorptions. By subtracting the appropriate value of 10 log A_2 in each case, a pair of "normalized" level differences is obtained that should agree apart from variations in system sensitivity.

NOTE 10—For a small number of observations, Fig. 1 derived from Table II, p. 43 of *ASTM Manual on Quality Control of Materials* (STP 15-C, 1951) gives the standard deviations required to achieve 90 per cent confidence limits in the range 0.7 to 3 db. If the basic data are average levels for the two rooms, the standard deviation for the noise reduction will be $(\delta_1^2 + \delta_2^2)^{\frac{1}{2}}$, where δ_1 and δ_2 are standard deviations associated with the two sets of level measurements. Note that variations in microphone sensitivity should be substantially eliminated from the observations before the precision calculation is made. The procedure of 8.6.4 does not conveniently permit this.

9. Determination of 10 log A_2

9.1 The value of 10 log A_2 is obtained by measuring the rate of decay of sound (see 4.7) in Room 2, the receiving room, employing a sound source in Room 2; then A_2 is determined by means of Eq 3 (Note 11).

9.1.1 *Room Condition*—The determination of 10 log A_2 shall be made with Room 2 in the same condition and microphones in the same positions as for the measurement of noise reduction (8. Microphone Systems and Measuring Procedures). Specifically: the transmitting specimen shall remain in place so that its effective absorption (which includes transmission back to Room 1) is included; the loud speakers needed for measuring A_2 shall be present during the measurement of noise reduction, so that their absorption is included.

NOTE 11—This is the only absolute method for determining 10 log A_2. For determining *changes* in 10 log A_2 an alternative method, based on steady-state sound power considerations, is presented in "Steady-State Method of Measuring Changes in Sound Absorption of a Room (RM 14-3)." [3]

9.1.2 *Room Coupling*—Because Room 2 is coupled by the test panel to Room 1, it is possible that the reverberation measurements in Room 2 will be influenced by energy transmitted into Room 1 and then back again during the decay process (7). The importance of this feedback process will vary with the ratio of instantaneous sound levels in the two rooms. The effect will be small if τS is small compared to A_1 and A_2, or if T_1/T_2, the ratio of reverberation times in Rooms 1 and 2, is sufficiently small. A simple test is to determine whether adding more absorption to Room 1 affects the values of T_2; if not, then the error is negligible.

9.2 *Number and Precision of Measurements*—A sufficient number of determinations of 10 log A_2 shall be taken to ensure that the mean value is known to the same precision as specified in 8.7, for level difference measurements.

10. Report

10.1 The report shall include the following:

10.1.1 A statement, if true in every respect, that the tests were conducted in accordance with the provisions of this ASTM recommended practice. Conformance with the relevant sections of Appendix A1 shall also be reported when applicable.

10.1.2 A description of the test specimen; it is desirable that the description be sufficiently detailed to identify the specimen, at least in terms of the elements that may affect its sound insulation performance. The specimen size, including thickness, and the average weight per square foot shall always be reported. Wherever possible, the testing laboratory should observe and report the materials, dimensions, weight, and other relevant physical properties of the major components and the manner in which they are combined, including a description of fastening elements. A designation and description furnished by the sponsor of the test may be included in the report provided that they are attributed to the sponsor. The curing period, if any, and the final condition of the sample, (shrinkage cracks, etc.) shall be reported.

10.1.3 The method of installation of the specimen in the test opening, including the location of framing or stud members relative to the edges, and the treatment of the junction with the test opening. The use of caulking, gaskets, tape, or other sealant on perimeter or interior joints shall be carefully described. Clearances around movable elements such as doors shall be reported.

10.1.4 Sound transmission losses to the nearest decibel for the individual test bands as detailed in 7.3. In addition, if a

frequency sweep is used, a plot of the continuous *TL* curve so obtained shall be included.

NOTE 12—If results are presented in graphical form, it is recommended that the ordinate scale be 2 mm/db and the abscissa scale be 50 mm/decade. If it is necessary to use a larger or smaller scale, the same aspect ratio as above should be used. Whenever possible, the ordinate scale should start at 0 db.

10.1.5 Temperature and relative humidity in the test rooms at time of test.

10.1.6 A statement regarding the precision of the *TL* data, as inferred from the precisions of the two main measurements.

NOTE 13—Assuming that the precisions given in 8.6 and 9.2 are just met, and assuming randomly distributed errors, the 90 per cent confidence limits for *TL* determination would be 1.4 *db* (2.8 *db* for the lowest test band).

10.1.7 If a single-figure rating is given, it shall be the sound transmission class, as described in "Determination of Sound Transmission Class (RM 14-2)." [3]

REFERENCES

(1) E. Buckingham, "Theory and Interpretation of Experiments on the Transmission of Sound Through Partition Walls," Scientific Papers, Nat. Bureau Standards, Vol. 20, p. 193 (1925), (s506).

(2) V. L. Chrisler and W. F. Snyder, "Recent Sound-Transmission Measurements at the National Bureau of Standards," *Journal of Research*, Nat. Bureau of Standards, Vol. 14, p. 749 (1935) (RP800).

(3) American Standard Acoustical Terminology, S1.1, American Standards Association.

(4) American Standard, S1.2, for the Physical Measurement of Sound, American Standards Association.

(5) R. V. Waterhouse, "Interference Patterns in Reverberant Sound Fields," *Journal*, Acoustical Soc. America, Vol. 27, p. 247 (1955).

(6) American Standard, S1.11, for Octave, Half-Octave and Third-Octave Filters.

(7) Thomas Mariner, "Critique of the Reverberant Room Method of Measuring Air-Borne Sound Transmission Loss," *Journal*, Acoustical Soc. America, Vol. 33, p. 1131 (1961).

(8) R. W. Young, "Sabine Reverberation Equation and Sound Power Calculations," *Journal*, Acoustical Soc. America, Vol. 31, pp. 912–921 (1959).

APPENDIX

A1. Preparation and Description of Test Specimens

A1.1 Scope

A1.1.1 This appendix constitutes an interpretation and elaboration, for certain generic types of construction, of the general requirements given in 6.1, 6.2, 10.1.2, and 10.1.3. The types of construction are dealt with in separate sections, largely independent of each other but not independent of the main recommended practice; thus the appropriate sections should be considered as a supplement to the main recommended practice. Special details are spelled out relating to the preparation, installation and aging of test specimens and the reporting of such matters.

A1.1.2 The following generic types of partition are considered:

Masonry Walls (A.1.3),
Plaster Partitions (A.1.4),
Wall-Board Partitions (A.1.5),
Demountable Modular Wall Panel Systems (A.1.6),
Operable (Folding or Sliding) Walls and Doors (A.1.7), and
Swinging Doors (A.1.8).

A1.2 Composite Construction—If a partition includes components corresponding to more than one of the listed types, the appropriate requirements of each type shall apply. For example, a block wall to which plaster is applied shall meet the relevant requirements of Masonry Walls for the basic wall and Plaster Partitions for the plaster layer.

A1.3 Masonry Walls

A1.3.1 *Materials*—The material, dimensions and average weight of an individual masonry unit, and the material, thickness and average area of coverage of mortar shall be determined and reported. The weight per square foot of the completed wall shall be determined by weighing a representative portion of the wall after test.

A1.3.2 *Construction*—The wall shall be built in accordance with usual construction practice except that extra control procedures may be desirable to ensure maintenance of the specified dimensions. The construction procedures should be reported in detail (see also 10.1.2 and 10.1.3).

A1.3.3 *Aging*—Following construction the specimen shall be allowed to age a minimum of 28 days before testing. A temperature of 65 to 75 F and 30 to 55 per cent relative humidity are recommended. For 24 hr immediately prior to a test, the specimen should be conditioned at a temperature of 70 to 75 F. and 45 to 55 per cent relative humidity.

A1.4 Plaster Partitions

A1.4.1 *Materials*—The following information shall be reported:

A1.4.1.1 *Studs*—Material (state species, grade and moisture content if wood), true dimensions, spacing in test opening, end fastening conditions, and weight per lineal foot,

A1.4.1.2 *Fillers*—Materials, weight per square foot of wall, location and method of fastening, and

A1.4.1.3 *Lathing*—Material, dimensions of individual sections and orientation in test specimen, weight per unit area of wall, number and location of fasteners (Note A1), and treatment of edges of specimen.

Note A1—If a resilient fastening device is used, an accurate description of its dimensions and material, preferably in the form of a drawing, shall be reported.

A1.4.1.4 *Plaster*—Materials, thickness of each layer, and the method of application. The weight per square foot of the completed wall (including studs, other framing members and filler materials) should be determined by weighing representative sections after test.

A1.4.2 *Construction*—The test specimen may either be built into a suitable frame, which is then inserted in the test opening, or built into the opening itself. The type of installation and the steps in constructing the specimen (for example, plastering techniques) should be reported in detail. The actual thickness of plaster layers should be determined, for example, by inspection of representative sections after test (see also 10.1.2 and 10.1.3).

A1.4.3 *Aging*—Thick coats (greater than $\frac{1}{8}$ in.) of gypsum plaster shall age at least 28 days before testing; superficial coats ($\frac{1}{8}$ in. thick or less) shall age at least three days. A temperature of 65 to 75 F and a relative humidity of 30 to 55 per cent are recommended.

A1.5 Wall-Board Partitions

A1.5.1 *Materials:*

A1.5.1.1 *Studs*—Material (state species, grade and moisture content if wood), true dimen-

sions, spacing in test opening, end fastening conditions, and weight per lineal foot,

A1.5.1.2 *Fillers*—Materials, weight per square foot of wall location, and method of fastening,

A1.5.1.3 *Wallboard*—Materials, weight per square foot of material, number of layers and thickness of each, orientation of individual panels in test specimen, location and treatment of joints, and number and type of fasteners (Note A1), and

A1.5.1.4 *Laminating Adhesives*—Method of application and thickness.

A1.5.2 *Construction*—See 10.1.2 and 10.1.3.

A1.5.3 *Aging*—If laminating adhesives are used the specimen shall age before testing a minimum of 14 days for water-base adhesives, and three days for non-water-base adhesives. If no laminating adhesives are used, but joints are finished with typical joint and finishing compounds, the minimum aging period shall be 12 hr.

A1.6 *Demountable Modular Wall Panel Systems*

A1.6.1 *Materials and Construction*—The testing laboratory shall report as much physical information as can be determined about the materials and method of assembly of all components of the partition including weights and dimensions of the component parts and the average weight per square foot of the completed partition (see 10.1.2).

A1.6.2 *Installation*—Installation of the test specimen shall be carried out or observed by the testing laboratory and reported in detail (see also 10.1.3).

A1.6.3 *Aging*—If significant quantities of caulking or adhesive materials are required, appropriate aging procedures shall be used (see, for example, 6.2, A1.5.3).

A1.7 *Operable (Folding or Sliding) Walls and Doors*

A1.7.1 *Materials and Construction*—The testing laboratory shall report as much physical information as can be determined about the materials and method of assembly of all components of the partition including weights and dimensions of the component parts and the average weight per square foot of the completed partition. If the specimen consists of an assembly of panels, the number and dimensions of panels comprising the specimen shall be reported. If the specimen is an accordion-type partition, the number of volutes, their spacing and width when extended, shall be reported. Header construction and dimensions shall be reported. Weights of header and the hanging portion of the door shall be given. Latching and sealing devices shall be fully described.

A1.7.2 *Installation*—Installation of the test specimen shall be carried out or observed by the testing laboratory and reported in detail (see also 10.1.3). Clearances at the perimeter between nondeformable portions of door and frame shall be measured and reported. In particular, any features of the installation that require dimensional control closer than $\frac{1}{4}$ in. on height or width of test specimen shall be reported.

A1.7.3 *Operation*—The specimen shall not be designated an operable wall unless it opens and closes in a normal manner. It shall be fully opened and closed at least ten times after installation is completed, and tested without further adjustments.

A1.7.4 *Aging*—If significant quantities of caulking or cementing materials are required, appropriate aging procedures shall be used (see for example 6.2, A1.5.3).

A1.7.5 The specimen area should include the header and other framing elements if these constitute a portion of the separating partition in a typical installation.

A1.8 Swinging Doors

A1.8.1 *Materials and Construction*—The testing laboratory shall report as much physical information as can be determined about the materials and method of assembly of all components of the partition including weights and dimensions of the component parts and the average weight per square foot of the completed partition. Latching and sealing devices shall be fully described. The standard size for a single door specimen shall be 3 ft by 7 ft (inside frame); departures from this, and the reasons, shall be noted.

A1.8.2 *Installation*—Installation of the test specimen shall be carried out or observed by the testing laboratory and reported in detail (see also 10.1.3). Clearances at the perimeter between non-deformable portions of door and frame shall be measured and reported. Less than $\frac{1}{4}$-in. clearance on over-all height and $\frac{1}{8}$ in. on over-all width shall be regarded as special.

A1.8.3 *Operation*—The specimen shall not be designated a door unless it opens and closes in a normal manner. It shall be fully opened and closed at least 10 times after installation is completed, and tested without further adjustments.

Output of a Sound Source in a Reverberation Chamber and Other Reflecting Environments*

RICHARD V. WATERHOUSE
National Bureau of Standards, Washington, D. C.
(Received October 21, 1957)

It is important to know the output of a source as a function of position in a reverberation chamber. Expressions are given for the sound power output of simple monopole and dipole sources as functions of source position in various reflecting environments. They are obtained by the use of the method of images and a general formula due to Rayleigh for the output of a number of simple sources. The cases of a dipole source near a reflecting plane and a simple source near a reflecting edge and corner are treated, and the effect of the band width of the source is considered. The results apply when the reflectors enclose the source, as in a reverberation chamber, unless the distance in wavelengths between parallel walls is small and the absorption in the enclosure is low. Some experimental data are given, and the reverberation chamber method of measuring the power output of sources is discussed. In the general case of an extended source emitting nonspherical waves near reflecting surfaces, it may be more convenient to find the variation of power output with position by experiment than by calculation.

INTRODUCTION

AN important property of sound sources is that their sound power output and directional patterns in general vary when they are placed in different positions near reflecting surfaces.

The effect is caused by the sound reflected from the reflectors reacting back on the source. This reaction can be considered as an impedance reflected onto the source. The reflected impedance varies with the environment, and thus in general the sound power output of the source varies with the environment.

The effect is discussed in the literature,[1–3] and Fischer[4] has given expressions for the dependence on source-reflector separation for a simple source near a plane. In this paper expressions are given for various source-reflector systems that are of interest in architectural acoustics, including the case of a dipole source near a reflecting plane, and a simple source near a reflecting edge and corner.

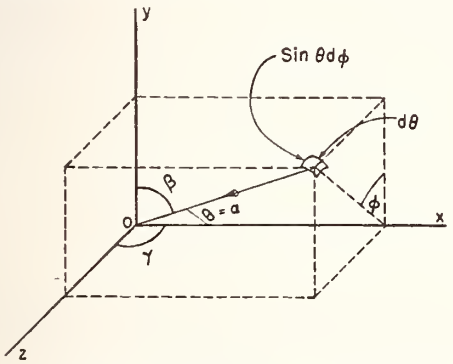

FIG. 1. Coordinate axes used in derivations in text. $\cos\alpha=\cos\theta$, $\cos\beta=\sin\theta\cos\phi$, and $\cos\gamma=\sin\theta\sin\phi$. Element of area on a sphere of radius d with center 0 is $d^2\sin\theta d\theta d\phi$.

These expressions follow from the use of the method of images and a formula due to Rayleigh for the output of a number of simple sources. It is shown that, in general, the power output of the source differs significantly from the free-field value if the distance of the source from the reflector is less than the wavelength of the sound emitted.

These results are of practical importance in several ways. For example, they show where a source must be located in a reverberation chamber if the free-field value of the power output of the source is to be measured. They also enable one to estimate to what extent noise can be reduced or increased by manipulating reflectors near a source. Such manipulation of reflectors could also be used to match a source into a medium.

We first obtain expressions for the power output variations of some simple types of source and reflector, and then consider their application to the more complicated source-reflector systems met in practice.

OUTPUT OF SOURCE NEAR PLANE REFLECTOR

Rayleigh's formula[5–8] for the directional pattern DP of a number of simple sound sources of uniform strength and frequency, placed at arbitrary positions in space, can be written

$$DP \propto \sum_m \sum_n \cos(kd_{mn}+\epsilon_{mn}), \qquad (1)$$

where $k=\omega/c_0$, $\omega=2\pi f$, c_0 is the sound velocity, and f is the frequency of the sound sources.

* A lecture on this topic was given at a meeting of the Acoustical Society of America on December 15, 1955.

[1] Lord Rayleigh, *Theory of Sound* (Dover Publications, New York, 1945), Vol. 2, pp. 108–112.

[2] H. Lamb, *Dynamical Theory of Sound* (Edward Arnold and Company, London, 1931), second edition, pp. 229 and 233.

[3] L. L. Beranek, *Acoustics* (McGraw-Hill Book Company, Inc., 1954), pp. 319–320.

[4] F. A. Fischer, Elek. Nachr.-Tech. **10**, 19 (1933).

[5] Rayligh, *Collected Papers* (Cambridge University Press, London, 1912), Vol. 5, p. 137.

[6] H. Stenzel, Elek. Nachr.-Tech. **6**, 165 (1929).

[7] H. Stenzel, *Leitfaden zur Berechnung von Schallvorgaengen* (Berlin, 1939) (English translation by A. R. Stickley, published by Naval Research Laboratory, Washington, D. C.).

[8] E. Rhian, J. Acoust. Soc. Am. **26**, 704 (1954).

The path difference of rays from sources m and n in the direction with direction cosines $\cos\alpha$, $\cos\beta$, $\cos\gamma$ (see Fig. 1) is d_{mn}, i.e.,

$$d_{mn}=(x_m-x_n)\cos\alpha+(y_m-y_n)\cos\beta+(z_m-z_n)\cos\gamma, \quad (2)$$

where (x_m,y_m,z_m) are the position coordinates of the mth source. ϵ_{mn} is the phase difference between sources m and n. The term "directional pattern" is defined here as the part varying with direction in the expression for the mean squared pressure in the far field of a source.

The sound output W of all the N sources is obtainable by integrating (1) over a sphere, and can be written

$$W/W_f=N+2\sum(\cos\epsilon_{mn})j_0(r_{mn}'), \quad (3)$$

where the sum is taken over every pair of sources. If only one source is real, the rhs of (3) is divided by N. $W_f=2\pi k^2\rho_0 c_0$ is the free-field power output of one source. The spherical Bessel function is $j_0(r_{mn}')=(\sin r_{mn}')/r_{mn}'$, and $r_{mn}'=4\pi r_{mn}/\lambda$, i.e., 4π times the distance in wavelengths between sources m and n.

$$r_{mn}=[(x_m-x_n)^2+(y_m-y_n)^2+(z_m-z_n)^2]^{\frac{1}{2}}. \quad (4)$$

From these formulas we can obtain comparable expressions for the output of a single source near certain reflecting surfaces, by the use of the method of images.[2,9] In this method, sound reflected by the reflector is considered to emanate from one or more image sources. These image sources are placed so that their radiation combines with that of the object source to satisfy the boundary conditions of the problem.

We consider that the reflectors are rigid and 100% reflecting, so the boundary condition is that on the reflecting plane the normal component of particle velocity is zero. The strength, i.e., peak volume velocity, of the source is fixed, and independent of the environment of the source.

For the case of a simple source near a plane reflecting surface, as shown in Fig. 2(a), one image source is enough to satisfy this boundary condition, the image source being equal in strength and phase to the object source.

The directional pattern of the source plus reflector is then, from (1)

$$DP\propto\cos^2 a, \quad (5)$$

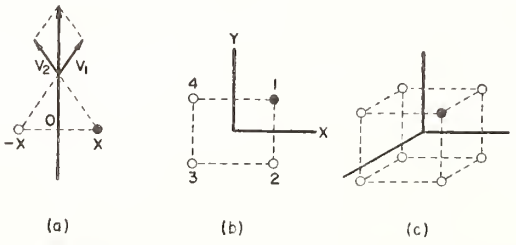

FIG. 2. ● Point source. ○ Image source. Acoustic images at one-wall, two-wall, and three-wall reflectors when one point source is present. The black lines represent the profiles of the reflectors.

[9] H. Lamb, *Hydrodynamics* (Dover Publications, New York, 1945), p. 129.

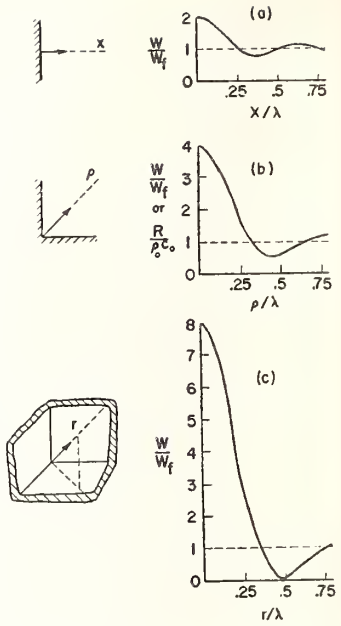

FIG. 3. Theoretical curves for the relative power output W/W_f of a simple source as a function of position near one-, two- and three-plane reflectors at right angles. ρ and r are the distances of the source from the origin along the lines of symmetry, and $k=\omega/c_0$ is the wave number. When the source is many wavelengths away from the reflectors, its power output W approaches the free field value W_f asymptotically. The dashed lines are the asymptotes. See Table II for the expressions plotted here.

where $a=kx\cos\alpha$; the reflecting plane is the yz plane of Fig. 1, and the source is a distance x from it.

The power output W of the source plus reflector[4] is found from (3) to be

$$W/W_f=1+j_0(x'). \quad (6)$$

W_f is the output of the source in a free field, for example, suspended on a string in an anechoic chamber. The spherical Bessel function $j_0(x')=(\sin x')/(x')$, and $x'=4\pi x/\lambda$, i.e., 4π times the distance in wavelengths from source to reflector.

The power output of the source-reflector combination can also be obtained by calculating the impedance seen by the source, as shown in Appendix II.

Expression (6) is plotted in Fig. 3(a). It can be written in terms of the other variables f, the frequency, or k, the wave number, as

$$W/W_f=1+j_0(2kx) \quad (7)$$

$$=1+j_0(4\pi fx/c_0). \quad (8)$$

The form (6) is used here since it is compact and helps to underline the fact that the position in space of the source, measured in wavelengths, is the important variable here.

SOURCE OF ARBITRARY DIRECTIONAL PATTERN

For a sound source of arbitrary directional pattern $A_1=A(\theta,\phi)$, the method of images can still be used, but the image sources must now have particular directional patterns. If the source is distant x from an infinite rigid reflecting plane, an image source with directional pattern $A_2=A(\pi-\theta,\phi)$ is needed to satisfy the boundary condition.

From (1) we then obtain for the directional pattern DP of source and reflector

$$DP \propto A_1^2+A_2^2+2A_1A_2\cos 2a. \quad (9)$$

The power output of the combination is then proportional to

$$\int_0^{\pi/2}\int_0^{\pi}(A_1^2+A_2^2+2A_1A_2\cos 2a)\sin\theta d\theta d\phi, \quad (10)$$

using the coordinate system of Fig. 1. The constant of proportionality is determined by normalization. This expression can be calculated if the functions $A_1=A(\theta,\phi)$ and $A_2=A(\pi-\theta,\phi)$ are given.

As an example, we take $A_1=\cos\theta$, using the coordinate system of Fig. 1, yz being the reflecting plane. This gives the source a figure-of-eight directional pattern like that of a dipole source in a free field with the dipole axis parallel to the x axis. When the source is distant x from the plane reflector, the directional pattern of the combination is found from (9) to be

$$DP \propto \cos^2\alpha \sin^2 a, \quad (11)$$

and the power output from (10) is given by

$$W/W_f=1-j_0(x')+2j_2(x'), \quad (12)$$

where W_f is the free-field value of the power output of the source, $x'=4\pi x/\lambda$, $j_0(x')=(\sin x')/x'$, $j_1(x')=[j_0(x')-\cos x']/x'$, and $j_2(x')=(3/x')j_1(x')-j_0(x')$.

Equation (12), which is the same as Eq. (21) given later in this paper, is plotted in Fig. 4.

EFFECT OF BAND WIDTH

The foregoing results apply to sources emitting sound at one frequency only. For sources emitting sound at a few discrete frequencies, i.e., a line spectrum, the resultant effects are obtained by summing arithmetically the effects at the various single frequencies. For sources emitting continuous bands of noise, analogous results can be found by an integration, as follows.

For a point source emitting noise with a continuous band width f_1 to f_2, (5) becomes

$$DP \propto [1/(f_2-f_1)]\int_{f_1}^{f_2}\cos^2 a\, df, \quad (13)$$

$$\propto 1+[(\sin Bf_2-\sin Bf_1)/B(f_2-f_1)], \quad (14)$$

where $B=(4\pi x\cos\theta)/c_0$.

The relative power output of the source, from (6) and (8) is

$$W/W_f=1+[1/(f_2-f_1)]\int_{f_2}^{f_1} j_0(4\pi fx/c_0)df. \quad (15)$$

The integral is the sine integral, which is tabulated. Graphs of (15) for band widths of $\pm 10\%$, one octave, and 5 octaves are given in Fig. 5. It is apparent that even with the wide band of 5 octaves the main feature of the curve remains.

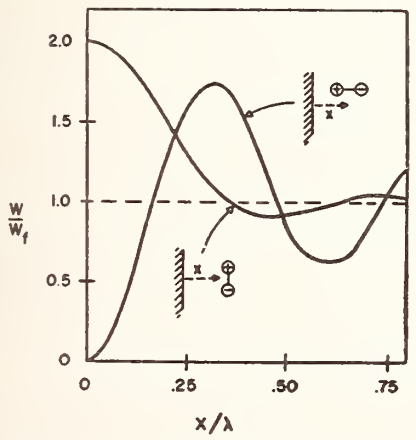

FIG. 4. Theoretical curves for the relative power output W/W_f of a dipole source *versus* distance x/λ in wavelengths from a plane reflector. Two cases are shown, with the dipole axis normal and parallel to the reflector. See Eqs. (21) and (19). The dashed line is the asymptote.

Dipole Source

Expressions for the directional pattern and power output of a dipole source as functions of distance from a plane rigid reflector are obtainable from the general formulas (1) and (3).

When the dipole is in the xy plane of Fig. 1, and its axis makes an angle η with the reflector (yz plane), its directional pattern is

$$DP \propto \sin^2\eta\cos^2\alpha\sin^2 a+\cos^2\eta\cos^2\beta\cos^2 a, \quad (16)$$

and its power output W in terms of W_f, the free-field output of the dipole, is

$$(W/W_f)=1+(3/x')j_1(x') +3\sin^2\eta[(1/x')j_1(x')-j_0(x')], \quad (17)$$

where $j_1(x')=[j_0(x')-\cos x']/x'$.

When the dipole axis is parallel to the plane, $\eta=0$ and

$$DP \propto \cos^2\beta\cos^2 a \quad (18)$$

$$(W/W_f)=1+j_0(x')+j_2(x'), \quad (19)$$

where $j_2(x')=(3/x')j_1(x')-j_0(x')$.

When the dipole axis is normal to the plane reflector, $\eta=90°$ and

$$DP \propto \cos^2\alpha\sin^2 a \quad (20)$$

$$(W/W_f)=1-j_0(x')+2j_2(x'). \quad (21)$$

The foregoing expressions† are tabulated in Table I, and graphs of (19) and (21) are given in Fig. 4.

These results are of some practical interest. For

† Results (18) to (21) were given in a lecture on this topic to the Acoustical Society of America on December 15, 1955. More recently, they were given by U. Ingard and G. L. Lamb, Jr., J. Acoust. Soc. Am. **29**, 743 (1957).

TABLE I. Expressions for the directional pattern and relative power output of a dipole source as functions of distance x from a plane reflecting wall.[a]

	Dipole makes angle η with wall	Dipole axis parallel to wall	Dipole axis normal to wall
Directional pattern, DP	$\sin^2\eta\cos^2\alpha\sin^2 a+\cos^2\eta\cos^2\beta\cos^2 a$	$\cos^2\beta\cos^2 a$	$\cos^2\alpha\sin^2 a$
Relative power output W/W_f	$1+(3/x')j_1(x')+3\sin^2\eta[(1/x')j_1(x')-j_0(x')]$	$1+j_0(x')+j_2(x')$	$1-j_0(x')+2j_2(x')$

[a] $a=kx\cos\alpha$; $x'=4\pi x/\lambda$; $j_0(x')=(\sin x')/x'$; $j_1(x')=[j_0(x')-\cos x']/x'$; $j_2(x')=(3/x')j_1(x')-j_0(x')$. In Fig. 1, the yz plane is reflecting, and the dipole is in the xy plane. See Fig. 4 for graphs of some of the expressions here for the relative power output.

example, at low frequencies a loudspeaker with no cabinet radiates like a dipole, as experimental results given later show.

OUTPUT OF SOURCE NEAR REFLECTING EDGE AND CORNER

When a point source is near 2 reflectors at right angles, 3 image sources are needed to satisfy the boundary conditions, as shown in Fig. 2(b).

The normal velocity components of the sound from sources 1 and 2, 3 and 4, cancel on the xz plane, and similarly for sources 1 and 4, 2 and 3, on the yz plane. Analogous arguments hold for the case of 3 reflectors at right angles, Fig. 2(c), where 7 image sources are needed.

Thus when the source is at (x,y,z) the images in the three reflector case lie at the points $(-x,y,z)$, $(x,-y,z)$, $(x,y,-z)$, $(-x,-y,z)$, $(x,-y,-z)$, $(-x,y,-z)$, $(-x,-y,-z)$, and analogously for the two-plane case.

Inserting these image positions in (1) and (3) we obtain the directional pattern and power output of a simple source near two-, and three-plane reflectors.

The directional pattern for a simple source at position xy near a reflecting edge [xz and yz planes reflecting, see Figs. 1 and 2(b)] is

$$DP\propto(\cos a\cos b)^2, \tag{22}$$

where $a=kx\cos\alpha$, $b=ky\cos\beta$, and the coordinate system and symbols of Fig. 1 are used.

The relative power output is

$$W/W_f=1+j_0(x')+j_0(y')+j_0(\rho'), \tag{23}$$

where $x'=4\pi x/\lambda$, $y'=4\pi y/\lambda$, and $\rho'=4\pi(x^2+y^2)^{\frac{1}{2}}/\lambda$.

If the source is confined to the line of symmetry from the origin, bisecting the angle xoy, its relative power output is

$$W/W_f=1+2j_0(\rho'/\sqrt{2})+j_0(\rho') \tag{24}$$

[see Figs. 3(b) and 9].

When the source is at position (x,y,z) near a reflecting corner the directional pattern is

$$DP\propto(\cos a\cos b\cos c)^2, \tag{25}$$

where a and b are as in (22) and $c=kz\cos\gamma$, (see Fig. 1).

The relative power output of the source is

$$W/W_f=1+j_0(x')+j_0(y')+j_0(z')+j_0(\rho_1')+j_0(\rho_2')+j_0(\rho_3')+j_0(r'), \tag{26}$$

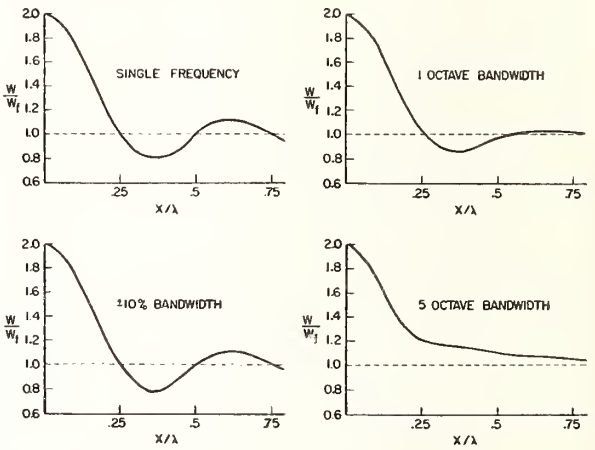

FIG. 5. Theoretical curves for the relative power output W/W_f of a simple source as a function of distance x/λ in wavelengths from a plane reflector, when the source vibrates with various band widths. In the abcissae $\lambda=(\lambda_1+\lambda_2)/2$ where λ_1 and λ_2 are the wavelengths at the extremes of the bands. The dashed lines are asymptotes.

where $\rho_1'=2k(x^2+y^2)^{\frac{1}{2}}$, etc., and $r'=2k(x^2+y^2+z^2)^{\frac{1}{2}}$.

When the source is confined to the line of symmetry from the corner, its relative power output is

$$W/W_f=1+3j_0(r'/\sqrt{3})+3j_0(r'\sqrt{\tfrac{2}{3}})+j_0(r'), \tag{27}$$

[see Fig. 3(c)].

The above results are tabulated in Table II, and some graphs are given in Figs. 3 and 6. The results were obtained by a different technique in a previous paper.[10] Contour maps of Eqs. (17) and (20) are being prepared with the aid of an electronic computer, and it is hoped to publish them in a later paper.

The curves in Fig. 3 are caused by interference, and depend only on the distance in wavelengths between source and reflector.

The power output variation can be considered to result from the source seeing a different radiation resistance R at different positions near the reflector, while the strength or volume velocity of the source remains the same. The ordinates in Fig. 3 can all be labeled R/ρ_0c_0, as in Fig. 3(b).

The curves can also be considered from the standpoint of the method of images. For example in Fig. 2(a), when the source touches the reflector, it concides with its image; its strength is thus doubled, and its power

[10] R. V. Waterhouse, J. Acoust. Soc. Am. 27, 247, 256 (1950).

TABLE II. Expressions for the directional pattern and relative power output of a simple source as functions of position (x,y,z) near 1-plane, 2-plane, and 3-plane reflectors at right angles.[a]

	1-plane reflector (yz plane)	2-plane reflector (xz, yz planes)	3-plane reflector (xy, xz, yz planes)
Directional pattern, DP	$\cos^2 a$	$(\cos a \cos b)^2$	$(\cos a \cos b \cos c)^2$
Relative power output, W/W_f	$1+j_0(x')$	$1+j_0(x')+j_0(y')+j_0(\rho')$	$1+j_0(x')+j_0(y')+j_0(z')+j_0(\rho_1')+j_0(\rho_2')+j_0(\rho_3')+j_0(r')$
	Along line of symmetry	$1+2j_0(\rho'/\sqrt{2})+j_0(\rho')$	$1+3j_0(r'/\sqrt{3})+3j_0(r'\sqrt{\frac{2}{3}})+j_0(r')$

[a] $a=kx\cos\alpha$, $b=ky\cos\beta$, $c=kz\cos\gamma$. $\cos\alpha=\cos\theta$, $\cos\beta=\sin\theta\cos\phi$, and $\cos\gamma=\sin\theta\sin\phi$. $\rho_1'=2k(x^2+y^2)^{\frac{1}{2}}$ etc. $r'=2k(x^2+y^2+z^2)^{\frac{1}{2}}$. $j_0(x')=(\sin x')/x'$. See Fig. 1 and Fig. 3 for graphs of the relative power-output functions above.

output integrated over a whole sphere would be quadrupled. However, only the radiation over $\frac{1}{2}$ a sphere can exist, i.e., in front of the plane wall, and the power output is thus double, not quadruple, the free-field value.‡

For similar reasons, the power output of a simple source goes up to 4 times the free-field value when the source is near a reflecting edge and up to 8 times near a reflecting corner.[11]

Figure 7 shows the interference of the sound-pressure waves from two point sources. The lower part of the figure shows the mean pressure distribution for each source along the line joining the two sources.

When the distance between the sources is less than one wavelength, the high intensity parts of the fields interact, and the total energy present is strongly dependent on the source separation. When the distance between the sources is a few wavelengths, the high-intensity central part of the field of each source is little affected by the interference of the weak outer field of the other source. As the separation of the sources increases, the effect of interference becomes negligible, and the power output of each source approaches the free-field value, as shown in Fig. 3(a).

One feature of the curves in Fig. 3 is that for certain source positions the power output is less than the free-field value. This occurs in all the regions of the graphs in Fig. 3 where the curve is below the dashed lines. In such regions the interference is predominantly destructive, and the power output of the simple source is not increased but diminished.

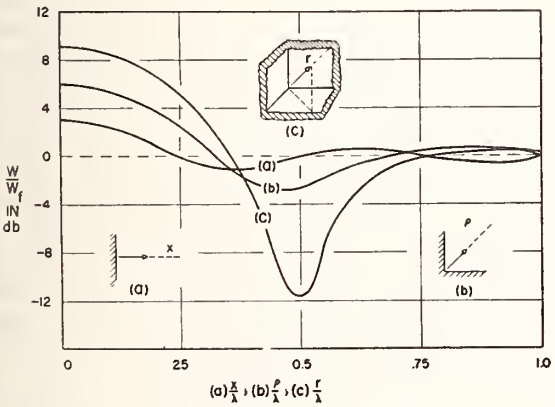

FIG. 6. Decibel plot of curves in Fig. 3.

For example, in Fig. 2(c) the output is less than the free-field output when the source distance r from the corner is in the region $0.36\lambda<r<0.78\lambda$. If the source is fixed at a distance $r=1$ ft from the corner, the corresponding frequency range over which the output is diminished is approximately the octave 400–800 cps.

Figure 3(c) shows the interesting fact that the destructive interference of spherical waves near a reflecting corner can be almost complete. This is perhaps surprising at first sight, in view of the different geometry of the systems formed by the spherical waves and the rectangular reflectors.

When the simple source is moved out from the apex of the corner along the line of symmetry with respect to the three walls forming the corner, the power output reaches a minimum of about 7% of the free-field value at $r=0.49\lambda$. Thus the destructive interference is about 93% complete.

As this source is moved out from the corner, its output starts at 9 db above the free-field value, and then falls to 11.5 db below it in a distance of about $\lambda/2$. Thus at this point the drop in sound power output is 20 db from the initial value, a considerable reduction.

APPLICATION TO ENCLOSURES

The above results for the power output of a source as a function of position near reflectors were derived under the assumption that the reflecting surfaces were of infinite extent, and the question arises as to whether the results are valid when the surfaces form part of an enclosure, such as a reverberation chamber or an ordinary room. When a source radiates in an enclosure, the sound can be reflected back and forth repeatedly, and evidently the impedance reflected back onto the source may differ substantially from the amounts computed above for nonenclosing reflectors.

In the next section of this paper, experimental evidence is given which shows that the results are valid in a large reverberation chamber. Here we will mention physical considerations which indicate that the results

‡ See reference 2. Lamb's *Hydrodynamics* contains an error on this point (see reference 9, p. 498, lines 5 and 6).

[11] H. F. Olson, *Elements of Acoustical Engineering* (D. Van Nostrand Company, Inc., Princeton, 1947), p. 28.

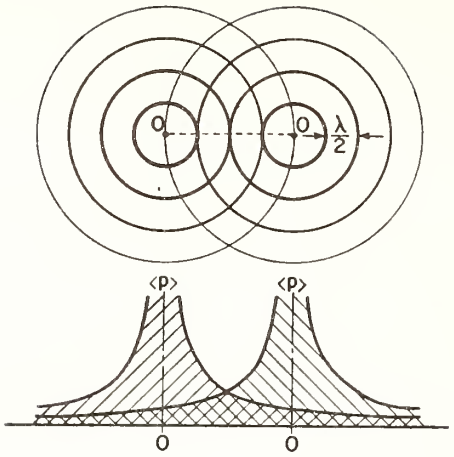

FIG. 7. Interference between the wave systems of two point sources. In the lower part of the figure the rms pressure $\langle p \rangle$ for each source is plotted along the line joining the two sources. Along this line $\langle p \rangle$ falls off according to an inverse first power law. λ is the wavelength.

are approximately true for any enclosure under two restrictions.

These restrictions are (a) that the surfaces of the enclosure other than those being considered as the reflectors must be distant at least a wavelength from the source, and (b) that the absorption in the enclosure must not be too small. Of course, the original limitations imposed on the reflecting surfaces associated with the source still hold, i.e., that these surfaces (c) must be rigid, and perfect or nearly perfect reflectors, and (d) must be large compared to the wavelength.

Under conditions (a) and (b), the reflected energy from the far walls of the enclosure (i.e., those walls not already considered to be associated with the source) will contribute little reflected impedance to the source.

As an example of the effect of a partial enclosure, we can consider the case of a simple point source equidistant from two plane parallel walls. The walls have a pressure reflection coefficient $R \leq 1$ which is independent of the angle of incidence of plane waves.

An analysis of this case is given in Appendix I. The power output of the source depends on the absorption of the walls, and the distance in wavelength separating the walls, as shown in Fig. 8. When the distance between the source and each wall exceeds the wavelength, the power output of the source differs from the free-field value by less than 1 db even when the wall absorption is low.

The image theory of the action of a reflecting environment on a source can be applied to a rectangular reverberation chamber, where the impedance reflected onto the source by the environment will vary with the distance of the source from the reflecting surfaces and the dissipation present. From physical considerations one would expect this to be the case whether the dissipation occurs at the walls or in the medium, and to be independent of room shape.

The next question to consider is whether quantitative criteria can be given for conditions (a) and (b) above. If the absorption of the enclosure is given, how many wavelengths away must reflecting surfaces be for the impedance they reflect on the source to be within given bounds?

Unfortunately, simple answers are possible only in simple cases, e.g., for a simple source near a corner, etc. It should be noticed that the directional pattern of the source is important here. The impedance reflected from a reflector onto a source with a pencil-shaped directional pattern is generally different from that reflected onto a source emitting spherical waves. For in the former case nearly all the sound radiated can be reflected back onto the source by a plane reflector several wavelengths away, while in the latter case only a small fraction can be so reflected.

The curves in Figs. 3, 5, and 8, and the experimental evidence in the next section indicate that for constant velocity sources of spherical waves, reflectors at distances greater than λ from the source will have small (less than 1 db or 25%) effect on the power output, even though the enclosure is very reverberant (e.g., average surface absorption coefficient about 3%).

For directional sources, the corresponding distance will depend on the orientation of the source, and may exceed λ. In such cases, and where the configuration of the reflecting surfaces is not simple, it may be easier to measure the variation of power output with position than to compute it.

EXPERIMENTAL RESULTS

Figure 9 gives some experimental evidence for these effects. The solid curve is a plot of Eq. (24), and gives the theoretical variation of the power output of a simple point source as it is moved away from two reflectors at right angles.

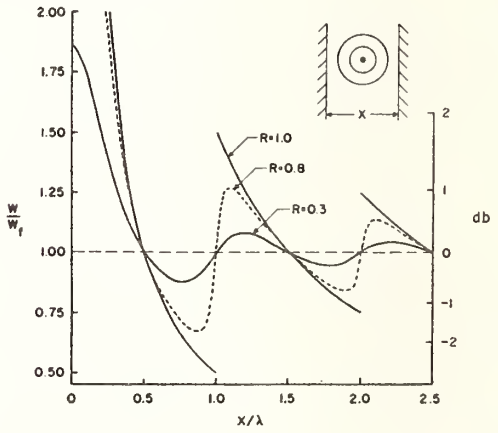

FIG. 8. Theoretical curve for the relative power output W/W_f of a simple point source equidistant from two plane parallel walls. x/λ is the distance in wavelengths between the walls. The walls have a pressure reflection coefficient $R \leq 1$ which is independent of angle of incidence for plane waves. The curve is a plot of Eq. (31).

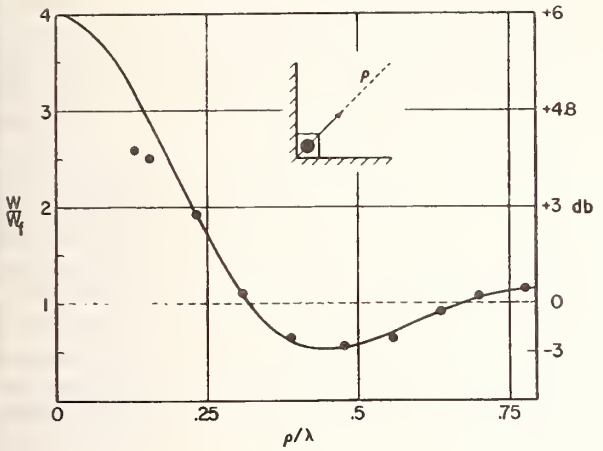

FIG. 9. Relative power output W/W_f of a simple source as a function of distance ρ along the line of symmetry from the origin at the vertex of a two-plane reflector. The solid line is the theoretical curve for a single frequency given by Eq. (24). The curve for a warbled frequency would be little different, see Fig. 5. The points are experimental data for a warbled signal 350±50 cps. The dashed line is the asymptote.

The black dots are experimental points, measured in the National Bureau of Standards reverberation chamber, two walls being used as the two reflectors.

Loudspeakers 4 in. in diam, mounted in small boxes filled with mineral wool, were used to simulate simple sources. They were driven with a warbled signal of frequency 350±50 cps, which gave a wavelength of about 3 ft, i.e., about 6 times the box diameter.

The voltage across each loudspeaker voice coil was kept constant throughout the experiment, in an attempt to make the loudspeaker cones vibrate with constant amplitude, as the theory required. The reasonable agreement obtained between theory and experiment (see the following, and Fig. 9) indicated that the loudspeakers used this way did resemble simple sources of constant strength, except for the near-field region.

One loudspeaker was put in each of the 4 lower corners of the reverberation chamber. The sound level in the chamber was measured by fixed microphones as the sources were moved along the floor away from the corners of the chamber. The measured sound levels gave the sound power output of the sources as functions of position; a uniform reverberant sound field in the central part of the chamber was assumed. Four sources were used instead of one to make the sound field more uniform. The walls of the reverberation chamber were brick, plastered and painted, giving a sound absorption coefficient of about 2% at this frequency.

Experimental points could not be obtained very near the corner owing to the physical dimensions of the loudspeaker box. The two experimental points shown nearest the corner are appreciably off the theoretical curve; this was probably caused by the departure of the loudspeaker field from the spherically symmetric field required by the theory. However, the rest of the data agree quite well with the theoretical curve.

In another experiment, one 4 in. diam loudspeaker was taken out of its box and used to simulate a dipole source. It turned out to be unnecessary to use 4 loudspeakers. A warbled frequency of 300±50 cps was used.

Figure 10 shows the results when the axis of the "dipole" was normal to a reflecting wall. The experimental curve is of the same type as that given by the theory for a dipole, and although there are significant differences between the 2 curves these can reasonably be attributed to the loudspeaker source differing from the ideal dipole source.

Similar experiments were made using 8 in. and 12 in. diam loudspeakers, and in all cases the main features of the theoretical curve were confirmed, but the details varied. It is quite entertaining to perform this experiment in a qualitative way, by moving a loudspeaker away from the wall of a reverberant room, the loudspeaker axis being normal to the wall. The increase in level from the minimum, obtained with the loudspeaker touching the wall, to the first maximum at a distance of about 0.3λ is quite striking.

Experiments with the axis of the loudspeaker dipole parallel to the wall were also performed, and give results which agreed with the theory in a similar way.

Additional confirmation that the theoretical results apply in a reverberation chamber is given by the experimental results already published[10] for the interference patterns that exist at the boundaries of a reverberant sound field.

In that case the source was fixed, and the microphone signal was measured as the microphone was moved along a certain path near the reflecting wall. If the chamber is kept constant, it follows from the theory of reciprocity that if the source and microphone are interchanged, and the source is now moved along the same path near the reflector, the microphone must record the same variation as it did before. This means the output of the source must vary with its position.

Thus the foregoing results for the source follow by reciprocity theory from the existence of the interference patterns in the reverberation chamber, subject to the restrictions that usually apply in reciprocity theory, for example that the source, microphone, and any absorbers present are linear.

An interesting example of reciprocity is that the variation in signal picked up by a velocity microphone when moved normal to a reflecting wall is the same as the variation in output of a dipole source moved along the same path, excluding the very-near-field region. This can be seen by comparing Fig. 4 and Eq. (21) of this paper with Fig. 9 and Eq. (6) on p. 253 of reference 10. Both the velocity microphone and the dipole source have the same figure-of-eight directional pattern, the first as a receiver and the second as an emitter. The orientation of this directional pattern with respect to the wall was the same in both cases, of course.

MEASUREMENT OF THE POWER OUTPUT OF A SOUND SOURCE

In considering some practical consequences of these effects, we first inquire how far one assumption used in deriving the above results will hold in practice. The assumption was that the volume velocity or vibration of the source was independent of changes in the impedance it worked into.

Apparently this is true for most sound sources met in practice, such as transformers, jet engines, appliances, and loudspeakers, although it is hard to find published evidence on this point. Such sources are not matched into the medium, and are little affected by impedance changes within the limits we are considering here.

The internal impedance of such sources is much higher than the radiation impedance of the air they work into. Thus they act analogously to constant current sources in electricity and deliver power proportional to the load resistance.

A related fact is that such sources are inefficient sound generators. A transformer whose whole mass is vibrating, dissipates much more energy in internal friction than in sound radiation, and its motion is evidently largely independent of the latter.

At the present time there is some interest in the measurement of the sound power output of sources; an American Standards Association standard on this topic is in preparation. In this paper we have shown that such measurements may be affected by the presence of a reflector in four ways. A reflector can change the power output, the directional pattern, the extent of the near field, and the radiation impedance of a sound source.

It is clear then that the position of the source relative to reflectors must be carefully considered in measuring its sound power output. One can measure the free-field value, or some other value near a reflector, or perhaps both. As an example, if a transformer is always used mounted on a concrete slab it is probably most useful to measure its power output in that position, and not bother with its free-field output.

In measuring the power output of a simple source by the reverberation chamber method, the source can in principle be placed anywhere in the reverberation chamber, and the results corrected to the free-field value (or the value corresponding to any other position near plane reflectors at right angles) by using the equations in Table II. However, the correction varies with frequency, and the composite correction for the power output of a broad-band source might be laborious to compute. Also the results would be restricted to simple sources.

Thus in practice if the free-field output of a source is required, it is probably most convenient to place the source and microphone(s) far enough away from all reflecting surfaces (walls, floors, ceilings, vanes, etc.) in the chamber for these interference effects to be negligible. For simple sources, the errors from these effects will in general be less than 1 db, if the source and microphones are placed at least $\lambda/2$ from the nearest boundaries, and at least 2λ, say, from the other boundaries of the chamber. See reference 10, p. 254.

For a source with a nonspherical-directional pattern of sound radiation, the corresponding distances will depend on the orientation of the source, and may exceed these. In such cases it may be more convenient to find the variation of power output with position by experiment than by calculation.

ACKNOWLEDGMENT

The author wishes to thank the members of the National Bureau of Standards, particularly Dr. R. K. Cook, for helpful discussions of various points in this paper.

APPENDIX I. OUTPUT OF A SIMPLE SOURCE BETWEEN TWO PARALLEL WALLS

A simple source is equidistant from two-plane parallel walls whose separation is x, and whose pressure reflection coefficient $R \leq 1$ is independent of the angle of incidence of plane sound waves.

At a point a small distance r from the source, on a line making an angle θ with the normal from the source to the reflectors, $r \ll x$ and $r \ll \lambda$, the potential caused by the direct and reflected waves is

$$\psi = (1/r)\cos(\omega t - kr) + (R/x)[\cos(\omega t - kx + kr\cos\theta) + \cos(\omega t - kx - kr\cos\theta)] + (R^2/2x)[\cos(\omega t - 2kx + kr\cos\theta) + \cos(\omega t - 2kx - kr\cos\theta)] + \cdots \quad (28)$$

$$= (1/r)\cos(\omega t - kr) + 2(A\cos\omega t + B\sin\omega t)\cos(kr\cos\theta) \quad (29)$$

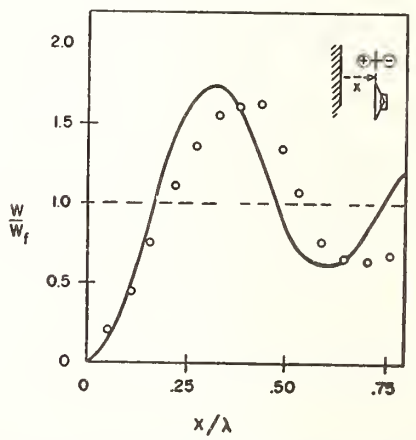

FIG. 10. The curve is taken from Fig. 4. The circles are experimental points measured in a reverberation chamber, for the relative power output W/W_f of a dipole source (axis normal to reflector) *vs* distance x/λ in wavelengths from a plane reflector. See text.

where

$$A=\sum_{n=1}^{\infty}(R^n/nx)\cos nkx$$

and

$$B=\sum_{n=1}^{\infty}(R^n/nx)\sin nkx. \tag{30}$$

From (29) we obtain the pressure $p=-\rho_0(\partial\psi/\partial t)$ and the radial particle velocity $v=\partial\psi/\partial r$. Next the mean value of pv, i.e. $\langle pv\rangle$, is taken, and this expression is integrated over the surface of the sphere of radius r. Then the power output of the source is

$$W=\lim_{r\to 0}4\pi r^2\int_0^{\pi/2}\langle pv\rangle\sin\theta d\theta$$

$$=2\pi\rho_0\omega k(1+2B/k)$$

i.e.,

$$W/W_f=1+(2/kx)\tan^{-1}[(R\sin kx)/(1-R\cos kx)],\qquad R<1, \tag{31}$$

where W_f is the output of the source in a free field.

For $R=1$,

$$W/W_f=1+(\pi/kx),\qquad 0<kx<2\pi$$
$$=1+(3\pi/kx),\quad 2\pi<kx<4\pi,\quad \text{etc.}$$

The solution is finite for all nonzero values of kx; the energy escapes between the walls. For $R=1$, the value of W/W_f jumps discontinuously from $\frac{1}{2}$ to $\frac{3}{2}$ at $kx=2\pi$, and jumps from $\frac{3}{4}$ to 5/4 at $kx=4\pi$, etc.

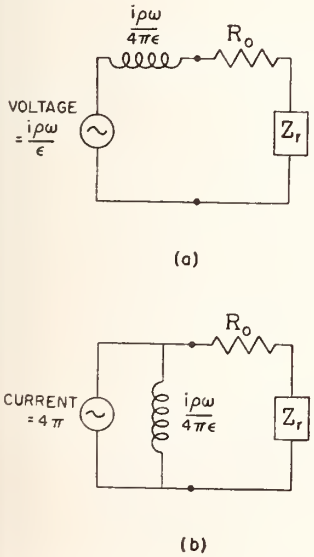

FIG. 11. Equivalent circuits for a sound source consisting of a small pulsating sphere of radius $\epsilon\ll\lambda$. Z_r is the reflected impedance caused by a plane reflector. In the $\lim_{\epsilon\to 0}$ the source becomes a simple point source.

Equation (31) is plotted in Fig. 8. Stenzel[12] gives expressions in the form of infinite series for the velocity potential in some more general cases of this type.

APPENDIX II. IMPEDANCE REFLECTED ONTO SIMPLE SOURCE BY PLANE REFLECTOR

The output of two point sources was calculated by Rayleigh[5] by finding the mean-squared pressure at a point in the far field, and integrating this over a spherical surface. A different method, based on the fact that the reaction of a source (or a reflector) on another source can be considered as a reflected impedance, is as follows.

We consider first a source similar to a simple point source, but with a small finite radius ϵ; the source is thus a pulsating sphere, with volume velocity independent of ϵ. The center of this sphere is distant x from a plane rigid reflector, $\epsilon\ll x$, $\epsilon\ll\lambda$.

The potential ψ at a distance r from the source center, $\epsilon<r\ll x$, λ, can then be written

$$\psi=(1/r)\exp i(\omega t-kr)$$
$$+(1/2x)\exp i(\omega t-2kx+kr\cos\theta). \tag{32}$$

The corresponding pressure and velocity are given by $p=-\rho(\partial\psi/\partial t)$, $v=(\partial\psi/\partial r)$, and the impedance seen by the source is

$$Z=p/4\pi r^2 v\quad\text{at}\quad r=\epsilon \tag{33}$$

$$=(\rho\omega k/4\pi)[1+(\sin 2kx/2kx)$$
$$+i(1/k\epsilon+\cos 2kx/2kx)], \tag{34}$$

dropping second-order terms. Thus $Z=Z_0+Z_r$, where Z_0 is the free-field value of the impedance, and Z_r is the reflected impedance. We then have

$$Z_0=\lim_{x\to\infty}Z \tag{35}$$

$$=(\rho\omega k/4\pi)(1+i/k\epsilon) \tag{36}$$

$$=R_0+iX_0. \tag{37}$$

Equation (34) is equivalent to the electrical circuit shown in Fig. 11(a) which can be transformed to that shown in Fig. 11(b). In the latter, the mass reactance proportional to $1/k\epsilon$ is shunted across the source and becomes infinite as the source approaches a point source of the same volume velocity, i.e., as $\epsilon\to 0$; the source then works into the free-field radiation resistance R_0, due to the medium, in series with the reflected impedance Z_r.

From (36), $R_0=\rho\omega k/4\pi$, and the free-field power output of the source is $\langle I^2\rangle R_0$, where $\langle I^2\rangle$ is the mean-

[12] H. Stenzel, Ann. Physik 43, 1–31 (1943).

squared volume velocity. The reflected impedance, due to the presence of the reflector, is

$$Z_r = R_r + iX_r \tag{38}$$

$$= (\rho ck^2/4\pi)[j_0(x') + in_0(x')] \tag{39}$$

$$= (\rho ck^2/4\pi)h_0(x'), \tag{40}$$

where $j_0(x')$ and $n_0(x')$ are spherical Bessel function of the first and second kind, and $x' = 2kx$; $h_0(x')$ is the spherical Hankel function. A plot of R_r *vs* X_r gives the usual impedance spiral, see Fig. 12. If the reflecting wall is not rigid, but gives a "pressure release" boundary condition ($p = 0$), the corresponding reflected impedance is the same as (40) but negative.

It is emphasized that these impedances[13] apply only to a simple point source. The same reflector will in general reflect a different impedance onto a different type of source, for example, a line source.

The power output of the point source in the presence of the reflector can be calculated in three different ways. (1) By integrating $\langle p^2 \rangle$, the mean-squared pressure, over a surface in the far field which encloses the source. (2) By integrating $\langle pv_{\text{normal}} \rangle$ over any convenient surface enclosing the source, as was done in Appendix I.

[13] G. Laville and T. Vogel, Acustica **7**, 101 (1957).

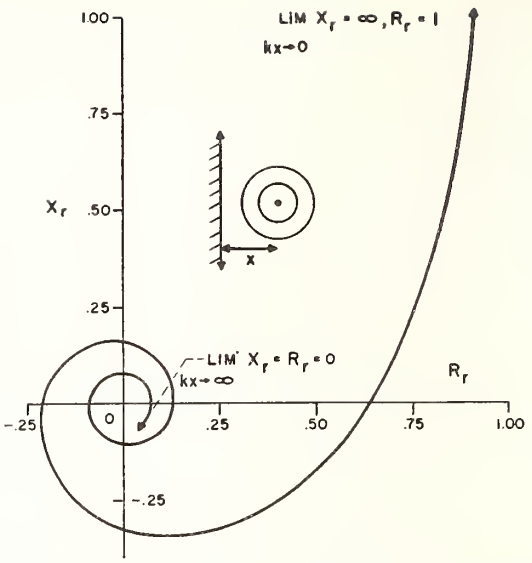

FIG. 12. Impedance diagram showing how the impedance $Z_r = R_r + iX_r$, reflected from a plane reflector onto a simple source, varies with kx.

(3) By taking the product $\langle I^2 \rangle \mathrm{Re}[\lim_{r\to 0}(p/4\pi r^2 v)]$ as above. From (34) this gives

$$\langle I^2 \rangle (\rho\omega k/4\pi)[1 + (\sin 2kx/2kx)] = W_f[1 + j_0(x')]$$

the same as (6).

Reprinted from THE JOURNAL OF THE ACOUSTICAL SOCIETY OF AMERICA, Vol. 30, No. 1, 4–13, January, 1958

AMERICAN SOCIETY FOR TESTING AND MATERIALS
1916 Race St., Philadelphia 3, Pa.

Reprinted from Copyrighted 1966 Book of ASTM Standards, Part 14.

Standard Method of Test for

IMPEDANCE AND ABSORPTION OF ACOUSTICAL MATERIALS BY THE TUBE METHOD[1]

ASTM Designation: C 384 – 58

ADOPTED, 1958

This Standard of the American Society for Testing and Materials is issued under the fixed designation C 384; the final number indicates the year of original adoption as standard or, in the case of revision, the year of last revision.

Scope

1. (*a*) This method of test is limited to the use of apparatus consisting of a tube of uniform cross-section and fixed length, excited by a single tone of selectable frequency, in which the standing wave pattern in front of a specimen upon which plane waves impinge at normal incidence is explored by means of a moving probe tube or microphone.

NOTE.—The most generally accepted method employed for determining the sound absorption coefficients of acoustical materials, used as surface treatment in rooms, is the reverberation chamber method. Its acceptance is based on the fact that field conditions can be closely simulated as regards the incidence of sound waves at random angles and the method of mounting the test specimen. Its disadvantages are that it is relatively expensive and time-consuming, requires a large specimen, and involves elaborate test facilities. The tube method however, is a comparatively simple and rapid technique requiring a specimen of only 1 sq ft or less.

(*b*) This tube method provides absolute measurement of the normal incidence sound absorption coefficient and the specific normal acoustic impedance of a material. Normal incidence coefficients, as measured by this method, are considerably lower than random incidence values, which more closely represent the performance of the material in a room; and there is no simple, unique relation between the two values. Means of estimating random incidence values from the measured normal incidence data are given in Appendix I.

Range of Application

2. (*a*) The lower limit of the frequency range over which measurements may be made is determined by the length of the tube, and the upper limit by its diameter, as explained in Section 6. In tubes of practical design, accurate measurements can be obtained over a continuous frequency range of 10 to 1, and rough indications are possible over a 20 to 1 range.

(*b*) Normal incidence absorption coefficients may be measured from a

[1] Under the standardization procedure of the Society, this method is under the jurisdiction of the ASTM Committee C-20 on Acoustical Materials.

maximum value of 1.00 to a minimum value determined by the largest standing wave ratio obtainable with the highly reflective, rigid plate in place of the sample. With the use of reasonable care in the construction of the apparatus and in the selection of equipment, a minimum value of normal incidence coefficient of 0.04 ± 0.01 can be measured at most frequencies.

(*c*) The range of acoustic impedance values which is of interest in connection with acoustical materials, and to which this method is applicable, corresponds to an acoustic resistance of 0 to 10, expressed in ρc units (see Section 4 (*a*)), and an acoustic reactance of −20 to +20.

Significance of Test

3. (*a*) Acoustical materials have the property of absorbing a considerable portion of the energy of sound waves which strike their surface. They are used chiefly as interior finish for the walls or ceilings, or both, of rooms for the purpose of reducing excessive room reflection and reverberation and thus controlling noise and improving hearing conditions. The acoustical effectiveness of a material is stated in terms of its *sound absorption coefficient*, which is defined as the fraction of the energy of incident sound waves absorbed by the material. Measurement of this quantity is of value both for predicting the results of the installation of a material in a given room, and for rating materials on a comparative basis. The absorption coefficient of a material in general varies with the frequency of the sound, the angle of incidence of the sound waves, and the method of mounting the material.

(*b*) The acoustic impedance of a material is a quantity which is related mathematically to its absorption coefficient, but which can be correlated more readily with physical properties of the material than can the absorption coefficient alone. Impedance measurements are therefore useful in basic research and product development of acoustical materials.

Symbols and Definitions

4. (*a*) *Symbols.*—The symbols used in this method are defined as follows; other symbols will be introduced and defined more conveniently in the detailed description of the procedure:

α_n = normal incidence sound absorption coefficient,
z = specific normal acoustic impedance = $r + jx$,
r = specific normal acoustic resistance,
j = $\sqrt{-1}$,
x = specific normal acoustic reactance,
ρc = characteristic acoustic impedance of free air = 41.5 cgs units (z, r, and x are customarily expressed in terms of their ratio to ρc),
L = corrected or "true" value of the difference in decibels between the maximum and minimum sound pressure levels in the standing wave pattern in the tube,
D_1 = distance from face of specimen to nearest minimum in standing wave pattern, measured in any convenient unit, and
D_2 = distance from first to second minimum in standing wave pattern, measured in same unit as D_1.

(*b*) *Normal Incidence Sound Absorption Coefficient.*—The normal incidence sound absorption coefficient, α_n, of a material, assumed to have a surface of infinite extent, is the fraction of normally incident sound energy absorbed by the material. The absorption coefficient will in general depend both on the

characteristics of the material and on its method of mounting.

(*c*) *Specific Normal Acoustic Impedance.*—The specific normal acoustic impedance, z, of the surface of a material is the complex ratio of sound pressure to the component of particle velocity normal to the surface. This quantity will be hereafter referred to simply as acoustic impedance. The real and imaginary components of the impedance are termed the specific acoustic resistance, r, and the specific acoustic reactance, x, respectively. The relation of acoustic impedance to the normal incidence sound absorption coefficient,[2] is as follows:

$$\alpha_n = 1 - \left[\frac{z/\rho c - 1}{z/\rho c + 1}\right]^2$$

Outline of Method

5. (*a*) The equipment used, an impedance tube of the moving microphone type, consists essentially of a long tube, usually round or square, of fixed length and uniform cross-section, with rigid walls which transmit or absorb negligible sound energy, at one end of which is a source of sinusoidal plane waves and at the other end of which the specimen is mounted. The required test equipment is shown schematically in the block diagram of Fig. 1. An audio signal generator drives a loudspeaker which transmits plane waves longitudinally along the tube. Waves of reduced amplitude are reflected by the specimen and combine with the incident waves to form a standing wave pattern along the tube. This pattern is explored by the movable microphone or probe on the axis of the tube, whose output is fed through an electrical filter to an output-indicating device which indicates the relative pressure amplitudes at the maximums and minimums in the standing wave pattern. An additional requirement for determination of acoustic impedance is a calibrated scale indicating the position of the microphone or probe in the standing wave pattern with respect to the face of the specimen.

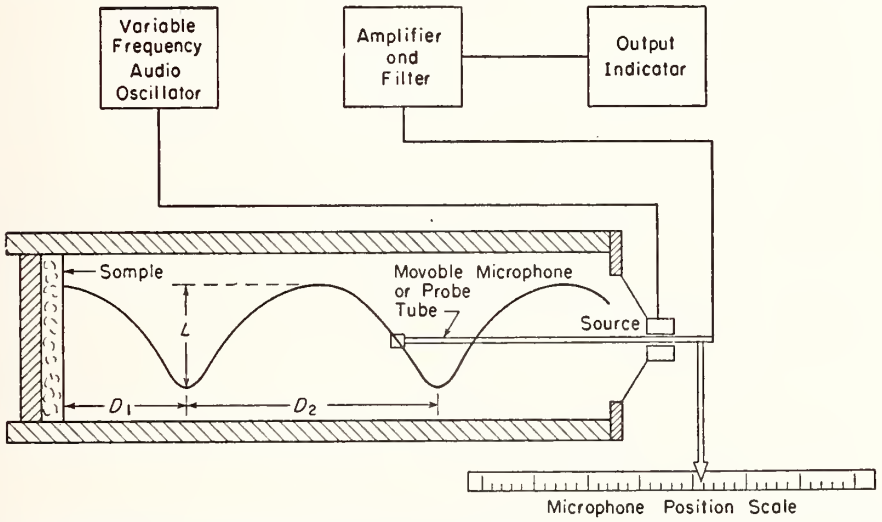

FIG. 1.—Schematic Diagram of Basic Requirements for an Acoustic Impedance Tube.

(*b*) The normal incidence coefficient, α_n, is determined by measuring the difference in decibels, L, between the maximum and minimum pressure amplitude in the standing wave pattern

[2] E. T. Paris, "On the Reflection of Sound from a Porous Surface," *Proceedings*, Royal Society, Vol. 115, p. 407 (1927).

(standing wave ratio), and inserting this value in the formula.[3, 4]

$$\alpha_n = 1 - \left[\frac{(\log_{10}^{-1}(L/20)) - 1}{(\log_{10}^{-1}(L/20)) + 1}\right]^2$$

The relation of α_n to L is shown graphically in Fig. 2.

(*c*) In order to determine the acoustic impedance $z = r + jx$ from tube measurements, it is necessary to determine L, the standing wave ratio in decibels, D_1, the distance from the face of the specimen to the first minimum, and D_2, the distance between two successive minimums, which is equal to the half wavelength for the particular test frequency being used. These values are inserted in the following formula:[5]

$$z/\rho c = \coth (A + jB)$$

where:

$A = \coth^{-1} [\log_{10}^{-1} (L/20)]$

$B = \pi(\frac{1}{2} - D_1/D_2)$

Computational charts of the above equation are shown in Figs. 3 and 4, from which $r/\rho c$ and $x/\rho c$ may be read directly from the measured values of L and D_1/D_2. Formulas for plotting these charts are given in Appendix II, together with information on the "Smith Chart" which is available in published form.

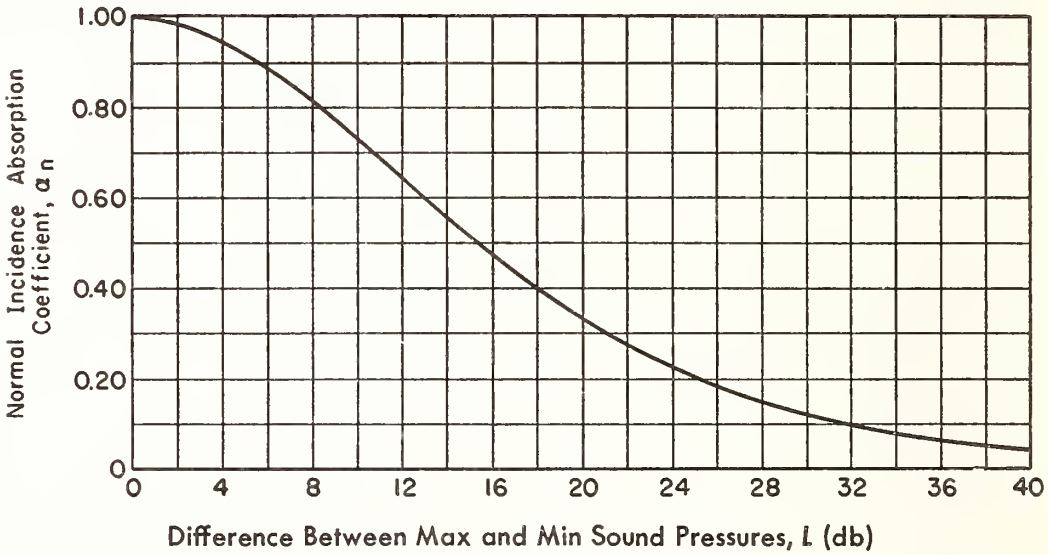

FIG. 2.—Curve Showing Relation of Normal Incidence Absorption Coefficient α_n to the Difference in Decibels L Between the Maximum and Minimum Sound Pressures.

Apparatus[6]

6. (*a*) *Impedance Tube:*

(*1*) When measurements are made of two successive minimums, as is recommended for best accuracy, the length, l, of the tube, in feet, shall be not less than the value given by the following relation:

$$l = \frac{1000}{f_{min}}$$

where f_{min} is the lowest frequency for which measurements are desired.

(*2*) Under certain conditions, as explained in Section 9 (*d*), Item (*1*), measurements may be made with satisfactory accuracy using only the first

[3] H. O. Taylor, "A Direct Method of Finding the Value of Materials as Sound Absorbers," *Phys. Rev.*, Vol. 2, p. 270 (1913).

[4] H. J. Sabine, "Notes on Acoustic Impedance Measurement," *Journal Acoustical Soc. Am.*, Vol. 14, No. 2, p. 143 (1942).

[5] L. L. Beranek, "Acoustic Measurements," John Wiley & Sons, Inc., New York, N. Y., pp. 309–325 (1949).

[6] Manufactured equipment and instrumentation meeting the requirements of this method are available from B & K Instruments, Inc., 3044 West 106th St., Cleveland 11, Ohio.

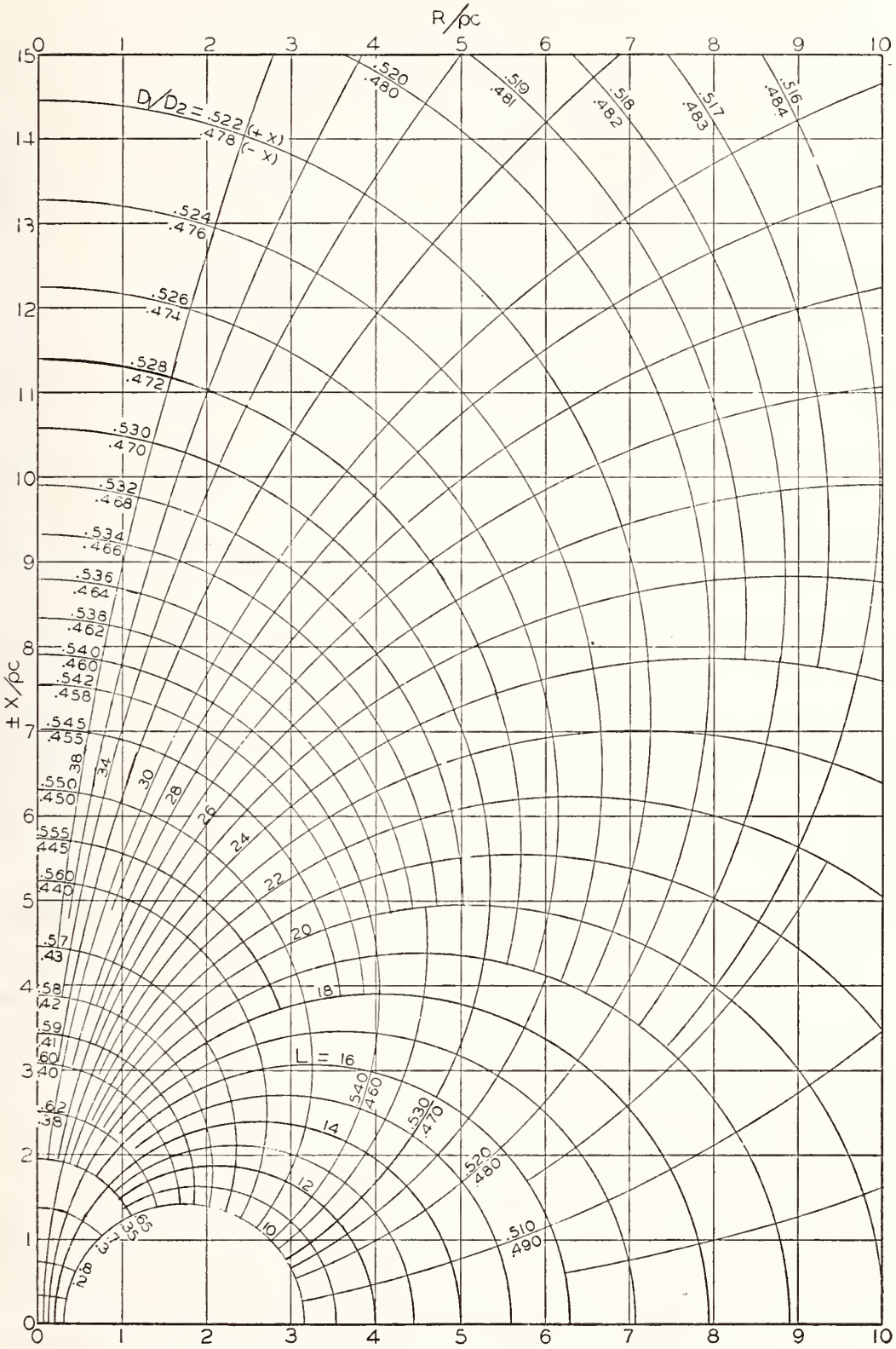

FIG. 3.—Relation of $r/\rho c$ and $x/\rho c$ to L and D_1/D_2. $L = 10$ to 40.

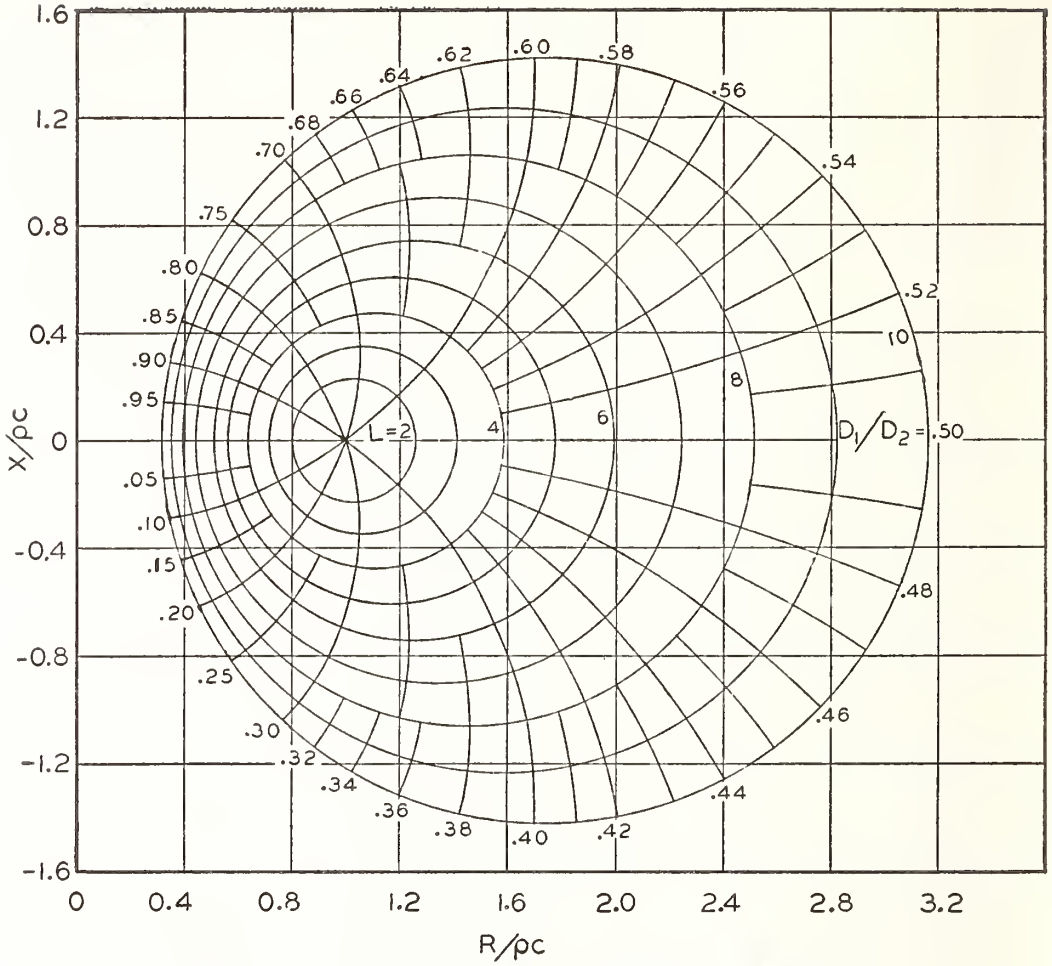

FIG. 4.—Relation of $r/\rho c$ and $x/\rho c$ to L and D_1/D_2. $L = 0$ to 10.

minimum. In this case the length of the tube in feet shall be not less than the value given by the following relation:

$$l = \frac{330}{f_{min}}$$

(*3*) In either case, readings of pressure minimums shall not be taken at any point closer to the source end of the tube than one tube diameter.

(*4*) The inside diameter, d, of a cylindrical tube, in inches, shall be not greater than the value given by the following relation:

$$d = \frac{8000}{f_{max}}$$

For a tube of square cross-section, the inside dimension, d_s, of a side, in inches, shall be not greater than the value given by the following relation:

$$d_s = \frac{7000}{f_{max}}$$

where f_{max} is the highest frequency for which measurements are desired.

(*5*) The interior cross-sectional area of the tube shall be uniform from end to end within 0.2 per cent.

(*6*) The tube walls shall be massive and rigid enough so that dissipation of sound energy through them by vibration is negligible. For an inside diameter of about 3 in., steel or brass tubing of

not less than $\frac{1}{4}$-in. wall thickness is satisfactory, with proportionately thinner walls for smaller diameters. For larger tubes it is advisable to use thicker walls as far as possible, and to provide further damping of vibration by a sand-jacket of at least 1-in. thickness.

(*b*) *Requirements for Measurement of Low Values of Absorption Coefficient.*—The standing wave ratio, L, in the empty tube with a reflective termination shall be at least 5 db greater than the standing wave ratio corresponding to the lowest absorption coefficient it is desired to measure. For example, a standing wave ratio of 40 db represents α_n of 0.04, so that a standing wave ratio for the empty tube of at least 45 db is required to permit measurements as low as this value to a precision of one significant figure. Factors which tend to reduce the standing wave ratio in the empty tube are: the presence of harmonics in the test signal, dissipation of sound energy by the tube walls or the reflective termination, presence of measurable ambient noise at the microphone, electrical noise in the microphone amplifier including 60 cycles and its harmonics, lack of sufficient filtering in the microphone circuit, and, in the case of a probe tube, by-passing of the signal to the microphone by paths other than through the end of the probe tube. In general, 50 db is about as high a standing wave ratio as can be obtained by reasonable precautions, and is adequate for all practical work with typical acoustical materials. Since the value of L enters into the determination of the components of the acoustic impedance, the same requirement on empty-tube standing wave ratio applies for making measurements on materials having high values of acoustic impedance.

(*c*) *Microphone or Probe Tube.*—The microphone or probe tube, together with any supporting fixture inside the tube, shall have a cross-sectional area not greater than 5 per cent of the cross-sectional area of the impedance tube. The wall thickness of the probe tube shall be not less than approximately one eighth of its outside diameter. The position of the microphone or end of the probe shall be maintained within one tenth tube diameter from the central axis of the tube. Any supporting assembly required to do this shall be effectively vibration-isolated from any part of the tube or sound source.

(*d*) *Microphone Output Measuring Equipment.*—The microphone amplifier and indicating meter shall be capable of measuring standing wave ratios up to 50 db to a precision of 0.2 db at all frequencies used. The microphone and all associated output measuring equipment shall have deviations from stability and amplitude linearity of not more than 0.2 db at all measuring levels and frequencies. The stability shall apply to a time interval of 10 min and a range of ambient temperature of 70 to 90 F. At all measuring frequencies there shall be sufficient filtering in the microphone circuit that the harmonic content of the signal with the microphone or probe at a pressure maximum is at least 50 db below the fundamental.

(*e*) *Sound Source.*—The sound source may be a direct radiator loudspeaker or a horn-driver unit and may be secured directly to the end of the tube or to a 45 or 90-deg elbow. Precautions shall be taken to avoid direct transmission of vibration from the sound source to the microphone probe where it enters the tube. If a horn-driver is used, it shall be coupled to the tube through a short exponential horn section; or if it is set into a flat plate covering the end of the tube, this plate shall be completely covered with a 1 to 2-in. thickness of loose felt or mineral wool.

(*f*) *Sound Generating Equipment.*—The oscillator and loudspeaker shall be capable of generating tones of sufficient purity that the harmonic content of the signal after the filter in the microphone circuit will not exceed the value specified in Paragraph (*d*). The amplitude stability of the signal generator and loudspeaker shall be the same as that required for the microphone and its associated equipment, as stated in Paragraph (*d*). The frequency stability of the signal generator shall be such that sudden fluctuations are no greater than 0.1 per cent, and drifts between the measurement of two minimums at the same nominal frequency are no greater than 0.3 per cent. The frequency calibration of the signal generator shall be accurate to ±2 per cent.

(*g*) *Microphone Position Measurement.*—The device for measuring distances D_1 and D_2 shall be accurate to ±0.2 mm. The scale may be in arbitrary units, since only the ratio of D_1 to D_2 is needed.

Sampling

7. Measurements shall be made when possible on a sufficient number of specimens from the available sample to provide a clear indication of the variability of the material.

Mounting of Specimen

8. (*a*) Tubes for measuring specimens of commercial acoustical materials are commonly designed either to accommodate a 12 by 12-in. tile, which is nondestructively tested in a tube of square cross-section, or to receive a disk-shaped specimen cut from a sample for testing in a cylindrical tube of the same diameter. In any case, the shape and area of the specimen shall match closely that of the tube cross-section. This can be assured by having the specimen holder, whether detachable or not, form a direct extension of the tube cross-section.

(*b*) Specimens normally are tested with a rigid backing, which is either brought up in contact with the back of the specimen, or is spaced away a specified distance. The backing shall be a solid steel or brass plate of at least ½-in. thickness for cylindrical tubes up to 4-in. in diameter, and increasing to 1-in. thickness for 12-in. square tubes. The backer shall fit snugly in the specimen holder with as nearly airtight a seal as possible, consistent with free movement. The backer may be provided with a lead screw and crank, or with a sliding rod and set screw, by which it may be anchored rigidly in the desired position.

(*c*) The impedance and absorption coefficient of a material can be affected quite strongly by mounting conditions, and these must be carefully controlled and specified in order to obtain consistent results. The general requirements are that the specimen fit snugly in the holder, so that errors are not introduced by motion of the specimen as a whole under vibratory sound pressure or by absorption in the crack around the edge. In the case of the disk-shaped specimens cut from tiles or other comparatively rigid materials, the specimen shall be cut closely enough for a snug, but not a forcing fit, and the crack after mounting in the holder shall be sealed thoroughly with heavy grease (such as water-pump grease) or Plasticene. The specimen can be held more firmly, if necessary, by greasing the entire edge.

(*d*) In cutting disks of perforated material, the position of the cut shall be chosen so that the number of perforations per unit area of the disk is as close as possible to the number per unit area in an extended field of the perforation pattern. An alternate method is to

cut several disks at random positioning and record the spread and average of the data.

(*e*) In testing 12 by 12-in. tile in a square specimen holder, it is generally not practical nor necessary to seal the edges, first because the joints between tile as laid up on the job normally contribute to their absorption, and second because absorption around the edges in proportion to the total absorption by the face is much less in a 12-in. square specimen than in the 2 to 6-in. diameter specimens generally tested in cylindrical tubes. There is, however, much greater likelihood of errors due to motion of the specimen as a whole, particularly with thin, rigid, light-weight materials. This motion may occur either integrally if the specimen is not firmly held, or diaphragmatically if it is clamped so as to create flexural tension, or if the specimen is warped. In some instances, it may be desired to simulate field mounting conditions and the degree of sample motion characteristic of them, such as nailing to wood furring, or spot-cementing to a solid backing. In any case, the intermediate mounting structure used shall be solidly anchored to the rigid backing of the specimen holder, and the movement of the specimen shall not be restricted in any manner other than by the simulated mounting. At the same time, when impedance measurements are wanted, means shall be provided to position the specimen accurately with respect to the distance scale of the microphone.

Procedure

9. (*a*) *Test Frequencies.*—Test frequencies shall be chosen from the series 125, 250, 500, 1000, 2000, and 4000 cycles, with additional intermediate or extended frequencies if desired.

(*b*) *Measurement of Microphone Distance* (required for impedance measurement only).—In order to measure the distance, D_1, from the face of the specimen to the first pressure minimum, it is necessary to know the position of the acoustic center of the microphone or probe with respect to the external scale on which the microphone position is measured. The acoustic center of the microphone is the point in space with respect to its physical geometry at which the sound pressure is registered by the microphone. For example, a probe tube connected to a microphone responds to the sound pressure which exists a short distance out from the end of the probe instead of exactly at its physical end. The distance, D_1, therefore is the distance from the specimen face

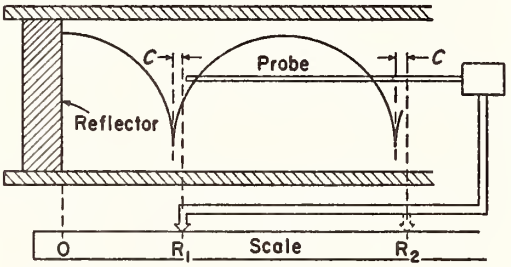

FIG. 5.—Correction for Acoustic Center of Microphone.

to the acoustic center of the microphone when it indicates the first pressure minimum. Since the acoustic center is not readily apparent from the geometry of the microphone, and in general varies with frequency, it is necessary to determine it experimentally. This shall be done as follows:

Place a massive, rigid, highly reflective surface, such as the backing plate of the specimen holder, exactly in the position established for the specimen face, taking precautions to provide an airtight seal around its edges. Move the microphone or probe so that it makes firm and fixed physical contact with the plate. Establish this position as zero on the microphone distance scale (see Fig. 5). Move the microphone until the first

pressure minimum is indicated, and record the scale reading as R_1. Locate the second pressure minimum and record the scale reading as R_2. As shown in Fig. 5,

$$R_1 = D_1 + c$$
$$R_2 = D_1 + D_2 + c$$

where c is the difference between the acoustic center of the microphone and its point of physical contact with the reflective plate. For a highly reflective termination it may be assumed that $D_1 = 0.5\ D_2$. Therefore,

$$c = R_1 - 0.5\ (R_2 - R_1)$$
$$= R_1 - 0.5\ D_2$$

The correction, c, shall be determined in the above manner for each measuring frequency and applied to all scale readings for the first pressure minimum for the measurement of D_1. In determining D_2, the correction may be applied to both scale readings R_1 and R_2, or to neither, whichever may be more convenient.

(*c*) *Measurement of Specimen Location.*—In mounting specimens for impedance measurement, their faces shall coincide as closely as possible with the fixed plane which has been established as the face position. In the case of very soft or rough materials there may be considerable uncertainty as to how closely the actual face is lined up with the face position. This may be partly resolved in interpreting the measurements by recording accurately the distance from the face position to the solid backing behind the specimen.

(*d*) *Variation of Minimums Due to Tube Attenuation.*—Both the incident and reflected waves undergo slight attenuation along the length of the tube which, if the tube walls are suitably massive or highly damped, is due essentially to the viscosity of the air at the inner surfaces of the tube. The net effect on the standing wave is an increase in the values of the successsive pressure minimums with respect to distance from the specimen, with negligible change in the values of the maximums. For frequencies above which two minimums can be measured, the true value, L, of the standing wave ratio shall be determined experimentally for each measuring frequency and each specimen by extrapolating the observed

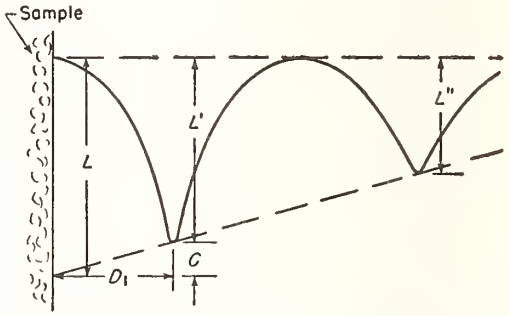

FIG. 6.—Variation of Pressure Minima with Distance from Sample, Due to Attenuation Along Tube.

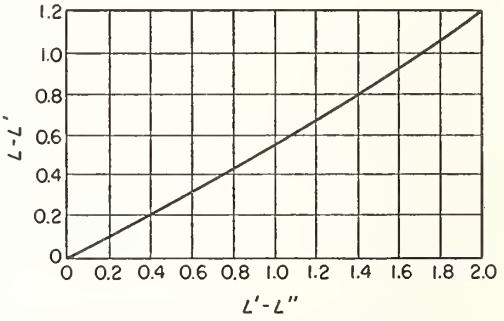

FIG. 7.—Chart for Determining L from Observed Values L' and L'', for $D_1/D_2 = 0.5$.

values, L' and L'', to the face of the specimen (see Fig. 6). If L' and L'' do not differ by more than 2 db, and if D_1/D_2 lies between 0.4 and 0.6, the extrapolation may be performed within ± 0.2 db, which corresponds to the specified accuracy of this method, by use of the chart in Fig. 7. Outside these limits, the value of L shall be determined by the following relations:

$$L = 20 \log_{10} (1/\psi), \text{ and}$$

$$\psi = \psi' - (D_1/D_2)(\psi'' - \psi')$$

where:

$$\psi' = \frac{1}{\log_{10}^{-1} (L'/20)}, \quad \text{and}$$

$$\psi'' = \frac{1}{\log_{10}^{-1} (L''/20)}.$$

(*e*) *Measurements Using One Minimum.*—As mentioned in Section 6 (*a*), Item (*2*), measurements of absorption coefficient and impedance may be made within the specified accuracy of this method under certain conditions at frequencies so low that only one minimum can be obtained in the available tube length. The first of these conditions is that the tube walls be sufficiently free from vibration that attenuation along the tube length will be due essentially to air viscosity. The true value, L, of the standing wave ratio shall be determined from the following relations:

$$L = L' + C,$$

$$C = 20 \log_{10} \frac{\psi'}{\psi' - \alpha D_1}, \text{ and}$$

α = attenuation constant for cylindrical tube

$$= \frac{2.96 \sqrt{f} \times 10^{-5}}{R} \ldots \text{(Kirchoff formula)}^7$$

where:

D_1 = distance from specimen face to first minimum,
R = tube radius,[8]
f = frequency, and
R and D_1 must be in the same units.

If the tube is long enough so that a maximum can be found between the first minimum and a point one tube diameter away from the source end, the value of L' shall be taken as the difference between this maximum and the first minimum. If this maximum does not occur within the available tube length, the highest value of sound pressure obtainable immediately in front of the specimen face shall be taken as a maximum for determining L', provided that this value does not decrease by more than 0.2 db as the microphone or probe is moved away from the specimen face over a distance of 0.01 wavelength.

(*f*) The requirements and procedures in Paragraphs (*a*) to (*e*) apply to absorption coefficient measurements. If impedance measurements are to be made using one minimum, the following additional conditions and steps are required: Since in determining the ratio D_1/D_2 only D_1 can be measured directly at the frequency, f, it is necessary to determine D_2 from the value D_2' measured at a higher frequency, f', for which two minimums are obtained. The value of D_2 is determined by the following relation:

$$D_2 = \frac{f' D_2'}{f}$$

In employing this procedure, the frequency stability of the signal generator shall be within 0.3 per cent during the time required to make readings at the two frequencies, and the ratio of the frequencies, f and f', shall agree with the calibration of the generator within 0.3 per cent. The temperature of the air in the tube shall not vary more than 3 F during the time required to make the two readings.

Report

10. (*a*) Absorption coefficients shall be specifically stated to be normal incidence values, and shall be reported at each test frequency to the nearest multiple of 0.01. If estimated random

[7] L. L. Beranek, "Acoustic Measurements," John Wiley & Sons, Inc., New York, N. Y., p. 72 (1949).

[8] The formula as given applies only to tubes of circular cross section. Although there is no simple expression for tubes of square cross section, it is sufficiently accurate to substitute $d/2$ for R in the above formula, where d is the inside dimension of one side of the cross section of a square tube.

incidence values are included, the method of making the estimate shall be clearly stated.

(*b*) Acoustic impedance values shall be reported at each test frequency as the ratio to ρc of the acoustic resistance, r, and the acoustic reactance, x. For example, $r/\rho c = 3.25$, $x/\rho c = 5.60$. Values of the ratios shall be recorded to the nearest multiple of 0.05.

(*c*) When several specimens of a sample are tested, the individual values shall be recorded and their average shown. If a single specimen is tested, this fact shall be noted.

Precision

11. Tests by this method should enable absorption coefficients to be determined to an incremental precision of ± 0.01 over a range from 0.04 to 1.00. It is difficult to state the corresponding precision of impedance measurements in simple terms, but it will vary approximately between 0.05 and 0.2 ρc units.

APPENDIX I

Relation of Normal Incidence to Random Incidence Absorption Coefficients

A1. (*a*) If plane waves of sound fall on a material at an angle, θ, the sound absorption coefficient, α_θ, depends on θ. When a material is placed in a reverberant sound field, that is, a sound field in which equal sound energy falls on the material from all directions over a hemisphere, the corresponding sound absorption coefficient is sometimes called the statistical absorption coefficient, α_{stat}. This parameter, α_{stat}, is much more useful than α_n, the normal absorption coefficient, since in practice acoustic materials are exposed to sounds from all angles. α_{stat} generally exceeds α_n by a significant amount.

(*b*) The conditions necessary for measuring α_{stat} are closely approximated in well-designed reverberation chambers. The measured values thus obtained are termed α_{rev}. Measurements of α_{rev} are, however, expensive and time-consuming, and it is often desirable to obtain an estimate of α_{stat} from α_n or z, since α_n or z can be measured with reasonable ease on an impedance tube. α_{stat} could be exactly deduced from α_n if the variation of α_θ with θ were known. However, this relationship is hard to measure experimentally, and for most practical materials cannot be deduced theoretically in terms of basic physical properties such as porosity and density. Furthermore, for different materials different relations exist between α_θ and θ. This is not surprising, since materials differ widely in properties such as surface structure, which have a controlling influence on sound absorption.

For these reasons, a guess is usually made for the relation between α_θ or z and θ, allowing α_{stat} to be computed. The results are then compared with existing measurements of α_{rev} to see how good the guess was. Various guesses have been made,[2, 9 to 13] the oldest being the normal impedance assumption of Rayleigh. Unfortunately, none of these assumptions gives results that can be relied on for all materials, and any results so obtained must be considered tentative rather than absolute.

(*c*) Where possible, it is probably better to adopt a direct empirical approach. For several materials, figures for α_n and α_{rev} have been measured. It is found that relations between these two parameters can be established for materials similar as regards certain physical properties, such as air-porosity, perforation, etc., which control acoustic absorption. Then an estimate of α_{stat} can be obtained from α_n or z for a new material if its physical properties are similar to those of a group for which a relationship has been established.

[9] E. T. Paris, "On the Coefficient of Sound-Absorption Measured by the Reverberation Method," *Phil. Mag.*, Vol. 5, p. 489 (1928).

[10] P. M. Morse, "Vibration and Sound," 1st Ed., p. 304 (1936).

[11] F. J. Willig, "Comparison of Sound Absorption Coefficients Obtained by Different Methods." *Journal Acoustical Soc. Am.*, Vol. 10, Apr., 1939, p. 293.

[12] P. E. Sabine, "Specific Normal Impedances and Sound Absorption Coefficients of Materials." *Journal Acoustical Am., Soc.* Vol. 12, Jan., 1941, p. 317

[13] A. London, "The Determination of Reverberant Sound Absorption Coefficients from Acoustic Impedance Measurements," *Journal Acoustical Soc. Am.*, Vol. 22, March, 1950, p. 263.

(*d*) To give a rough idea of the relative values of α_n and α_{stat}, α_n is about one half of α_{stat} for very low values, and approaches equality with it at very high values. The maximum numerical difference occurs at intermediate values and is of the order of 0.25 to 0.35.

APPENDIX II

Charts for Computing Impedance from Tube Data

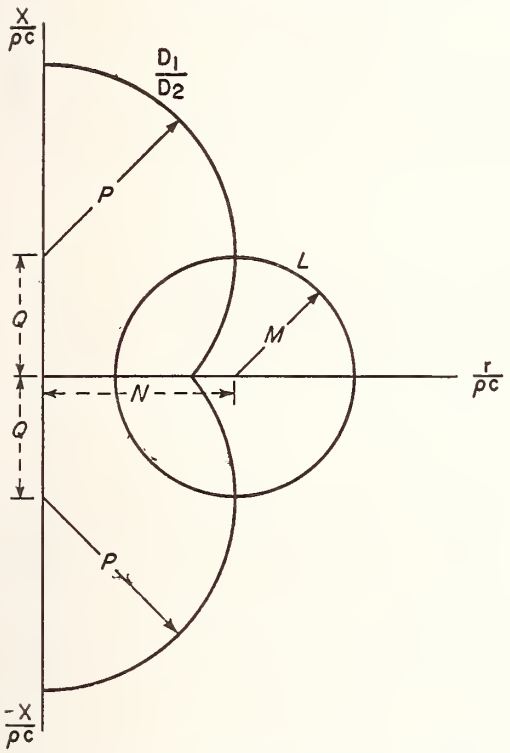

L Contours:

$$M = \frac{K^2 - 1}{2K}$$

$$N = \frac{K^2 + 1}{2K}$$

$$K = \log_{10}^{-1}(L/20)$$

D_1/D_2 Contours:

$$P = \sqrt{1 + \cot^2 (1 - 2D_1/D_2)\ 180 \text{ deg}}$$

$$Q = -\cot(1 - 2D_1/D_2)\ 180 \text{ deg}$$

Fig. 8.—Construction for Plotting Contours of Constant Values of L and D_1/D_2 on the $r/\rho c$, $x/\rho c$ Plane.

A2. (*a*) The computational charts shown in Figs. 3 and 4 cover the range of impedance values which is generally of interest in the study of acoustical materials. In using the chart in Fig. 3, positive values of $x/\rho c$ are given by values of D_1/D_2 greater than 0.5. The contours in Figs. 3 and 4 are circular arcs, whose radii and centers are given in terms of L and D_1/D_2 by the construction shown in Fig. 8.

(*b*) Another type of computational chart which has been found convenient is the "Smith Chart," which was developed by Phillip H. Smith for the original purpose of making rapid calculations of the impedance and standing-wave characteristics of electrical transmission lines. The calculator[14, 15] consists of two discs pivoted concentrically, and a radial arm with a slider, also pivoted at the center. In adapting the calculator to impedance-tube data, the value of L is set by the slider on the radial arm on the scale marked "DB." The two disks should be set with respect to each other so that the $R = 0$, $X = 0$ point on the inner disk coincides with zero "Wavelengths Toward Load" (or Generator) on the outer disk. The rotating arm is then set so that its index line falls on the value of "Wavelengths Toward Load" which is equal to one half D_1/D_2. The intersection of the index line of the radial arm and the cross-hair of the slider on the arm will then locate a pair of $r/\rho c$, $x/\rho c$ values given by the contours on the inner disk.

[14] Fully described in *Electronics*, January, 1944.

[15] These calculators may be obtained from the Emeloid Company, Inc., 1239 Central Ave., Hillside 5, N. J.

A Portable Impedance Tube

Raymond D. Berendt and Henry A. Schmidt, Jr.

National Bureau of Standards, Washington 25, D. C.
(Received 19 March 1963)

A lightweight impedance tube has been developed primarily as an instrument for practical research. It can be used also for precision measurements of acoustical-impedance and sound-absorption coefficients in both laboratory and field installations, over the frequency range 400 to 900 cps. It is useful for the development and manufacturing control of acoustical materials, acceptance testing of acoustical installations in the field, and determination of aging, staining, and redecoration effects on the absorptivity of acoustical materials. Experimental results are presented.

INTRODUCTION

An acoustical-material manufacturer concerned with the development and quality control of his product needs an impedance tube capable of performing accurate, expedient, acoustical measurements on unit specimens of reasonably large area, over a limited but useful range of frequencies. Other measurements such as acceptance testing of acoustical plasters in field installations for conformance with specifications based on laboratory tests must be performed without marring or defacing the surface of the material. Similarly, investigations concerned with the effects of aging, soiling, and redecorating on the absorptive qualities of acoustical materials are best performed in the field, since it is extremely difficult to reproduce such conditions in the laboratory.

Thus, an impedance tube designed specifically for practical research purposes should be capable of performing nondestructive acoustical measurements with ease and precision on large unit specimens of absorptive materials under both field and laboratory conditions. The "portable impedance tube" described here meets these performance criteria. Its advanced design distinguishes it from the prototype "long-tube" model described by E. Jones *et al.*[1]

DESCRIPTION OF THE APPARATUS

Figure 1 is a block diagram of the impedance tube and accessory equipment as used in measurements of normal incidence sound-absorption coefficients of acoustical materials. The impedance tube consists essentially of an aluminum-alloy tube with an 8-in. inside diameter, 24-in. length, and $\frac{3}{16}$-in. wall thickness. Figure 2 shows the detailed construction of the tube assembly. The sound source is a 6-in. PM loudspeaker that is resiliently mounted on an internal baffle plate approximately 6 in. from the closed end of the tube. A miniature magnetic-type microphone is resiliently mounted on a supporting member of the microphone carriage, which is propelled by a motor-driven lead screw, as shown in Fig. 3. The carriage is equipped with two spring-type cantilevered arms bearing small rollers that stabilize the lateral motion of the microphone during traverse. The lead screw is connected with a flexible coupler to the shaft of a slow-speed reversible motor, which is resiliently mounted on the back plate of the impedance tube. A combined manual-control and position-indicating device is coupled to the motor shaft for fine adjustment and positioning of the microphone, as shown in Fig. 4. Mi-

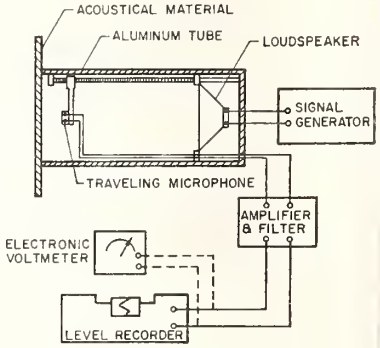

Fig. 1. Block diagram of impedance tube and accessory equipment for measurement of acoustical-impedance and sound-absorption coefficients.

[1] E. Jones, S. Edelman, and A. London, "Long-Tube Method for Field Determination of Sound Absorption Coefficients," J. Res. Natl. Bur. Std. (U. S.) RP, No. 1, 49, 2339 (1952).

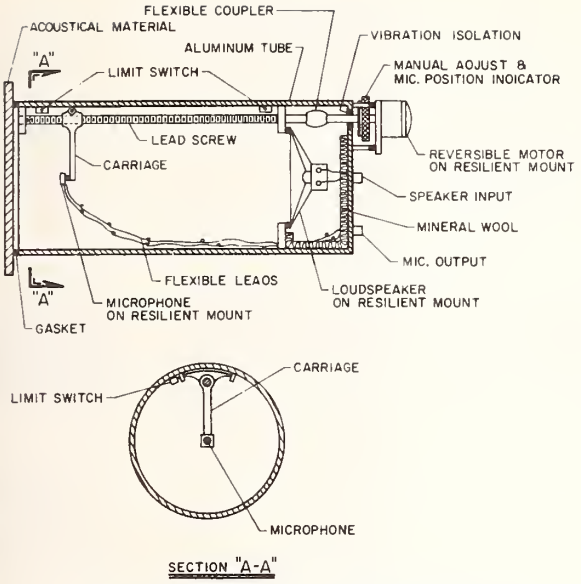

FIG. 2. Schematic drawing of detailed construction of impedance-tube assembly.

croswitches mounted at both ends of the lead screw limit the travel of the microphone carriage during automatic operation.

The tube, lead screw, and microphone carriage were precision-machined and the component assembly carefully aligned for smooth and precise motion. Spring stabilizing and antibacklash elements were embodied in the over-all assembly. Vibration-isolating techniques were used in the mounting of microphone, loudspeaker, lead screw, and motor to avoid vibratory transmission from component elements and outside sources. The open end of the impedance tube is terminated with an annular gasket of soft neoprene rubber to provide an airtight seal against and prevent marring of the acoustical material under test. The material might be on a ceiling or wall.

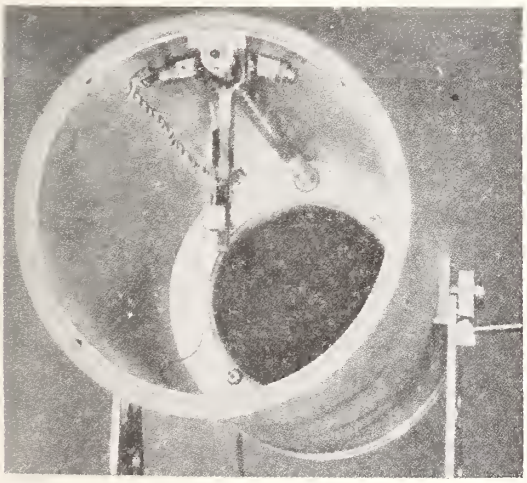

FIG. 3. Open-end view of tube, showing gasket, microphone-carriage assembly, microswitches, and lead screw. The loudspeaker is mounted on the ring plate toward rear of tube.

As shown in Fig. 5, the impedance tube is mounted on a floating-action tripod by which one can apply a uniform and controlled pressure against the acoustical ceiling. The mounting is pivoted so that the tube can be used at any angle between vertical and horizontal. A maximum ceiling height of approximately 10 ft can be reached with the tube mounted vertically and tripod fully extended. The combined weight of tube and tripod assembly is approximately 39 lb, which facilitates operation on scaffolds for measurements on ceilings of greater height. The two clamps mounted on the center column of the tripod were designed for attachment to tubular-type scaffolds.

The consideration of all factors, such as sample area, frequency range, accuracy of measurement, tube resonances, weight, and ease of handling, etc., involved in the construction of the impedance tube resulted in compromising on conventional design[2] to achieve the greatest instrument utility. Thus, for example, the operational frequency range of the tube was chosen to be 400 to 900 cps, a somewhat limited but important midsegment of the frequency range as used in reverberation-room measurements of sound-absorption coefficients. Owing to the design limitations of length and diameter, the lower and upper cutoff frequencies of the impedance tube are approximately 350 and 1000 cps, respectively. The lower limit represents the lowest frequency at which maximum and minimum sound-pressure measurements can be made in the tube, at a distance greater than one tube diameter from the speaker source. Measurements at somewhat lower frequencies run the risk of being made too close to the source, where near-field distortion and lack of planeness in the direct wave occur. The upper limit represents the frequency at which the first transverse mode is likely to appear. The variation of sound pressure, in a plane perpendicular to the tube axis, produced by such modes precludes measurements at higher frequencies.

Whereas in most impedance-tube methods used in laboratories the tile sample is inserted in the tube, here the sample rigidly backed with a steel plate overlaps the end of the tube. The latter arrangement is very convenient experimentally. Further, it more closely simulates the manner in which the tube is used with materials applied to a ceiling or wall, as in field installations, wherein the sample likewise overlaps the end of the tube. In routine laboratory tests, there is no need to seal or enclose the edges of the acoustical tile, since the voids between tiles in a field installation normally contribute to their absorption. We presume that the amount of sound energy that escapes through the exposed edges of the acoustical tile under test in the laboratory is com-

[2] "Tentative Method of Test for Impedance and Absorption of Acoustical Materials by the Tube Method," ASTM, C384 (1958).

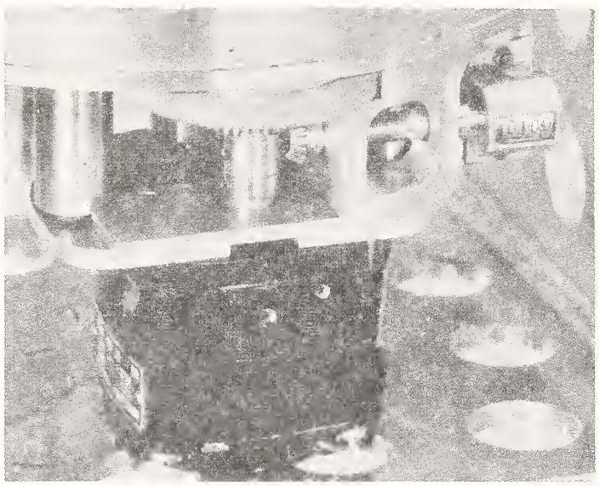

FIG. 4. Base-end view of tube, showing detailed construction of combined microphone-position indicator and manual-control device.

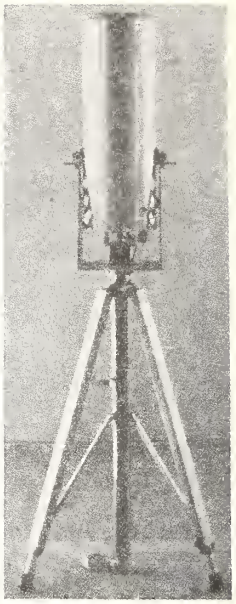

FIG. 5. Impedance tube mounted on floating-action tripod. The two clamps mounted on center column of tripod facilitate attachment to tubular-type scaffold.

parable to that which flows into adjacent tiles or spaces between tiles, as normally installed in the field.

For an acoustical material whose absorptivity is due primarily to porosity rather than to diaphragmatic or flexural motion, the absorption around the edges of a tile in proportion to the total absorption by the face is slight, since the diameter of the tube is large relative to the thickness of the material tested. London[3] showed that the difference between measured absorption coefficients of such materials that overlapped the end of the tube vs the same materials inserted in the tube was about 0.02. In any event, the impedance tube could be easily equipped with a sample holder if desired, for more-sophisticated or accurate measurements of acoustic impedance or absorption. Generally speaking, the design and performance features of the instrument, aside from the above limitations, meet the requirements specified in a proposed standard.[2]

The standard[2] further describes the basic procedure for measurement of absorption and impedance coefficients of acoustical materials. The method consists essentially of setting up a standing wave in the tube terminated with an acoustical sample and traversing the wave pattern with a movable microphone to determine both the maximum–minimum sound-pressure ratio and the distance from the face of the sample to the first minimum pressure point. The computational charts and tables given in this standard[2] relate the various parameters that facilitate direct determination of the normal incidence absorption and impedance coefficients. Other charts based on semiempirical considerations may be used to determine the random-incidence absorption coefficient. Explanations of such determinations are given in various papers,[3–5] and a summary discussion can be found in Appendix I of Ref. 2.

In tests on acoustic materials with a high degree of absorptivity, measurements of the maximum and minimum sound pressures and distance of the latter point from the face of the sample may be made automatically with the instrumentation shown in the schematic drawing. The procedure consists simply of automatically driving the microphone from a maximum pressure-level point near the face of the sample through the standing-wave pattern to a minimum pressure-level point. The level recorder automatically traces on chart paper the sound-pressure-level curve as a function of microphone distance from which the absorption and impedance coefficients can be determined. In the absence of a level recorder, an electronic voltmeter with a decibel scale and the microphone position indicator may be used to determine the maximum–minimum sound-pressure ratio and distance of the minimum pressure point, respectively. Special scales calibrated in percentage may be used on either recorder chart paper or voltmeter for direct determination of the absorption coefficients. In tests with a highly reflective termination or on materials with low absorptivity that result in high maximum–minimum sound-pressure ratios, the manual microphone adjustment is used to locate the extremely sharp minimum-pressure points.

Owing to the presence of second-harmonic distortion in some signal generators and the loudspeaker, and ex-

[3] A. London, "Determination of Reverberation Sound Absorption Coefficients from Acoustic Impedance Measurements," J. Acoust. Soc. Am. 22, 263 (1950).

[4] P. E. Sabine, "Specific Normal Impedances and Sound Absorption Coefficients of Materials," J. Acoust. Soc. Am. 12, 317 (1941).

[5] F. J. Willig, "Comparison of Sound Absorption Coefficients Obtained by Different Methods," J. Acoust. Soc. Am. 10, 293 (1939).

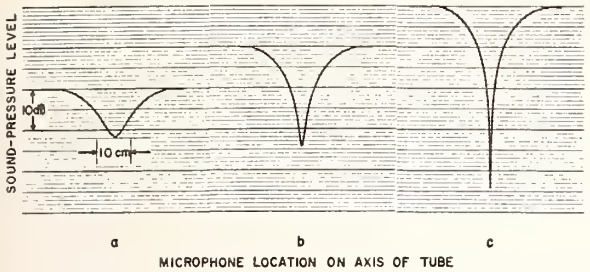

FIG. 6. Sound-pressure level recorded as a function of microphone distance for different terminations. Acoustical tiles were backed with $\frac{1}{2}$-in. steel plate. Test frequency = 500 cps. α = sound-absorption coefficient. (a) $1\frac{1}{4}$-in. perforated cellulose-fiber tile; $\alpha = 0.66$, (b) $\frac{1}{2}$-in. plain surface cellulose-fiber tile; $\alpha = 0.21$, (c) $\frac{1}{2}$-in. steel-plate termination; $\alpha = 0.02$.

traneous noise from other sources, selective amplifiers or filters are used for measurement of the maximum–minimum sound-pressure ratio.

DISCUSSION OF RESULTS

Figures 6 and 7 show experimental results obtained with the apparatus near the cutoff frequencies. The figures show sound-pressure level recorded as a function of microphone position for different sample terminations. The sawtooth or step-type tracings of the maximum pressure portions of the curves were due to the inability of the recorder to respond to incremental pressure changes of less than $\frac{1}{3}$ dB. Instruments of greater resolving power, such as oscilloscopes or electronic voltmeters, produced smooth tracings of the whole curves. The curves were automatically recorded as the microphone traveled from the face of the test-sample termination on the left toward the speaker source at the right. The minimum-pressure points shown were in excess of one tube diameter from the speaker source. The ambient noise level in the tube during automatic operation was more than 10 dB below the signal level at the lowest minimum-pressure point shown.

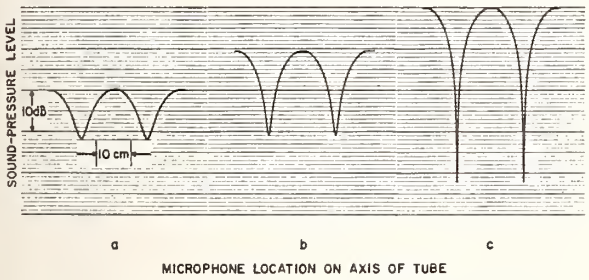

FIG. 7. Same as Fig. 6, except test frequency = 900 cps. (a) $\alpha = 0.64$, (b) $\alpha = 0.32$, (c) $\alpha = 0.03$.

PRECISION

Owing to the precise construction of the microphone traverse assembly, the distance between two minimum-pressure points can be measured with an estimated accuracy of ± 0.002 in. This was confirmed indirectly by repeated measurements of sound-pressure-level minima, during which critical observations of min-point locations or distances between such points were made. The position of the microphone from the axial line of the tube can be maintained within ± 0.004 in. during automatic traverse.

Measurements of the maximum–minimum sound-pressure ratio for a given sample are repeatable within ± 0.10 dB, provided that readout instruments or indicating devices of high resolution are used and the frequency stability of the signal generator is within ± 0.1 cps. This corresponds to a measurement of absorption coefficients within an incremental precision of 0.005 over a range from 0.04 to 1.00.

ACKNOWLEDGMENTS

The authors wish to express their thanks to E. M. King for suggesting the use of the floating action tripod, and to E. H. Eisenhower and G. E. Winzer for their performance testing of the instrument.

Reprinted from THE JOURNAL OF THE ACOUSTICAL SOCIETY OF AMERICA, Vol. 35, No. 7, 1049–1052, July, 1963

AMERICAN SOCIETY FOR TESTING AND MATERIALS
1916 Race St., Philadelphia, Pa. 19103
Reprinted from the Annual Book of ASTM Standards

Standard Method of Test for

SOUND ABSORPTION OF ACOUSTICAL MATERIALS IN REVERBERATION ROOMS[1]

ASTM Designation: C 423 – 66

This Standard of the American Society for Testing and Materials is issued under the fixed designation C 423; the number immediately following the designation indicates the year of original adoption or, in the case of revision, the year of last revision. A number in parentheses indicates the year of last reapproval.

NOTE—Editorial changes were made throughout in December, 1967 and in April, 1969.

1. Scope

1.1 This method covers the measurement of the sound absorption of acoustical materials in a diffuse sound field. When a material is in the form of an extended plane surface, such as an acoustical ceiling or wall treatment, the results shall be given as sound absorption coefficients. When the materials are separate objects, such as theater chairs or unit sound absorbers, the results shall be given in sabins per unit with a description of the number and spacing of the units.

1.2 This method may also be used in measuring the sound absorption of a room which is a necessary part of the measurement technique for sound transmission loss of partitions, sound power of noise sources, and impact sound transmission of floor-ceiling assemblies.

2. Summary of Method

2.1 The absorption coefficient of a test specimen is determined by measuring the change in the decay rate of sound in a reverberation room when the test specimen is brought into it. The test signal is turned on long enough for the sound pressure level in the reverberation room to reach a steady state. When the signal is turned off, the sound pressure level will decrease and the rate of decay, d, may be determined from measurements of the average time, T, for the sound pressure level to decay through a certain range. The absorption, A, of the room and its contents is calculated from the Sabine equation:

$$A = \frac{0.9210\ Vd}{c} \quad \ldots\ldots\ldots\ldots (1)$$

2.1.1 If the volume, V, of the room is in cubic feet and the speed of sound, c, is in feet per second, the absorption will be in sabins. If, however, the volume of the room is in cubic meters and the speed of sound in meters per second, the absorption will be in metric sabins.

2.1.2 Inasmuch as the equation is based on the assumption that the sound field is diffuse before and during decay,

[1] Under the standardization procedure of the Society, this method is under the jurisdiction of the ASTM Committee C-20 on Acoustical Materials. A list of members may be found in the ASTM Year Book.

Current edition accepted Nov. 16, 1966. Originally issued 1958. Replaces C 423 – 65 T.

these conditions must be fulfilled if the measurement is to have meaning (see 5.4).

2.2 Let the subscripts 1 and 2 in the following equations denote, respectively, measurements in the empty room and in the room containing the test specimen. The absorption in sabins added to the room by the test specimen is the difference:

$$A_2 - A_1 = \frac{0.9210\ V\ (d_2 - d_1)}{c} \quad \ldots\ldots (2)$$

2.2.1 When the specimen covers part of a boundary surface of the room which has an absorption coefficient α_1, the sound absorption coefficient of the specimen of area S in sabins per square foot is given by:

$$\alpha = \frac{A_2 - A_1}{S} + \alpha_1 \quad \ldots\ldots\ldots (3)$$

2.2.2 If the absorption coefficient, α_1, of the boundary surface of the room is small enough to be neglected, the absorption coefficient in sabins per square foot of the specimen is given more simply by:

$$\alpha = \frac{A_2 - A_1}{S} \quad \ldots\ldots\ldots\ldots (4)$$

2.2.3 In general, absorption will vary with frequency and measurements are made at a series of six standard frequencies.

2.3 When the test specimen consists of n isolated identical objects, such as unit sound absorbers, the absorption in sabins per unit is given by:

$$\frac{A_2 - A_1}{n} \quad \ldots\ldots\ldots\ldots (5)$$

2.3.1 The measured result will depend on the spacing of the units relative to each other and to any surface within one-half wavelength.

3. Significance

3.1 The sound absorption coefficient of a surface is a property of the material composing the surface. It is ideally defined as the fraction of the randomly incident sound power absorbed by the surface, but in this method the four Eqs 1 to 4 constitute an operational definition of the absorption coefficient.

3.2 Diffraction effects[2] usually cause the area of a specimen material to be effectively greater than its geometrical area, thereby increasing the measured coefficient. When the coefficients are large the measured values may exceed unity. Since the effects of diffraction are less when the area is greater, laboratories are urged, if at all possible, to use a specimen size of at least 72 ft² (6.7 m²) and those planning new laboratories should prepare for larger areas.

3.3 Coefficients measured by this method should be used with caution, for not only are the areas encountered in practical usage usually larger than the test specimen, but the sound is rarely diffuse. In the laboratory, measurements must be made under reproducible conditions, but in practical usage the conditions which determine the effective absorption coefficient are often unpredictable. Nevertheless, regardless of the differences and the necessity for judgment, coefficients measured by this method have been used successfully by architects and consultants in the acoustical design of architectural spaces.

4. Symbols

4.1 The symbols used in the method

[2] V. Chrisler, "Dependence of Sound Absorption Upon the Area and Distribution of the Absorbent Material," *Journal of Research of the National Bureau of Standards*, Vol. 13, 1934, p. 169; T. D. Northwood, M. T. Grisaru, and M. A. Medcof, "Absorption of Sound by a Strip of Absorptive Material in a Diffuse Sound Field," *Journal of the Acoustical Society of America*, Vol. 31, 1959, p. 595; and T. D. Northwood, "Absorption of Diffuse Sound by a Strip or Rectangular Patch of Absorptive Material," *Journal of the Acoustical Society of America*, Vol. 35, 1963, p. 1173.

are defined as follows:

A = sound absorption, in sabins

V = volume of reverberation room, in cubic feet

c = speed of sound, in feet per second

N = range of decay measured, in decibels

T = average time for N decibels decay, in seconds

d = N/T = average rate of decay, in decibels per second

S = area of test specimen, in square feet

α = absorption coefficient, in sabins per square foot, and

NRC = noise reduction coefficient — the average of the coefficients at 250, 500, 1000, and 2000 Hz (hertz or cycles per second), expressed to the nearest integral multiple of 0.05.

5. Reverberation Room

5.1 *Construction*—The reverberation room shall be constructed of massive masonry or concrete materials. The average absorption coefficient of the room surfaces, as determined by empty room measurements, and after allowance has been made for atmospheric absorption, shall be less than 0.06 at all measuring frequencies.

5.1.1 The room surfaces are all the areas from which sound reflects. They include the floor, walls, and ceiling, the sides of a recess as for a door, the sides of a protuberance as a pilaster, and both sides of diffusing panels or moving vanes. The room shall be isolated sufficiently to keep outside noises and structural vibrations from interfering with the measurements.

5.2 *Size and Shape*—The smallest dimension of the room shall be more than one wavelength, λ, and preferably more than two wavelengths of the center frequency of the lowest one-third octave band at which measurements are made. No two room dimensions shall be equal nor in the ratio of small whole numbers. The ratio of the largest to the smallest dimension shall be less than 2:1. The volume (see Note 1) shall be not less than that given by the expression:

$$V = 4\lambda^3 \quad \ldots\ldots\ldots\ldots\ldots (6)$$

NOTE 1—It is recommended that, for laboratories to be built in the future, the smallest dimension be more than two wavelengths and the volume be larger than that required by the expression above. There are two reasons for the trend to larger rooms. With larger rooms the precision of measurement at low frequencies is increased and larger test specimens can be accommodated without violating the restriction of 8.3.1. ISO R354-1963, Measurements of Absorption Coefficients in a Reverberation Room, recommends a room volume larger than 180 m^3 (6357 ft^3) and further recommends, in the case of new construction, that the volume be as close to 200 m^3 (7063 ft^3) as possible. The recommended specimen size is between 10 and 12 m^2.

5.3 *Sound Diffusion*—Means shall be taken to ensure an approximation of a diffuse sound field both before and during decay. Experience has shown the following modifications of room geometry to be more or less helpful: irregularities such as bumps, pillars, or convexities of the order of one wavelength in size, absorbent patches, and nonparallel room boundaries. Experience has also shown that a satisfactory approximation can be achieved with a number of sound-reflecting panels hung or distributed at random angles about the volume of the room, some of them mounted on a rotating shaft, or otherwise kept moving, presenting, in effect, a room which continually changes its shape.

5.3.1 The aim is to achieve a rapid and continuous interchange of energy between the directions of sound propagation and thereby increase the probability that each surface area of the room contributes proportionally to the absorption.

5.4 *Tests for Sound Diffusion*—It is

recommended that the diffuseness of the sound field be investigated in the three following ways. When test signals of one-third octave bands of white or pink noise (see 7.1) centered on the test frequencies are used, the sound field can be considered satisfactorily diffuse if:

5.4.1 At each frequency the decay time is independent of microphone position. The average decay times measured at different microphone positions should be random samples of the same population of average decay times to the precision required in 12.1.

5.4.2 At each frequency the decay time is independent of the test specimen position whether on the floor, wall, or ceiling. The average decay times measured with different test specimen positions should be random samples of the same population of average decay times to the precision required in 12.1.

5.4.3 At each frequency the decay rate does not change during the course of a decay. If, for instance, 30 decibels is the range of decay measured, the average decay times for the first 15 decibels of decay and those for the second 15 decibels should be random samples of the same population of decay times to the precision required in 12.1.

5.5 *Background Noise*—The level of the background noise, which includes both the ambient acoustical noise in the reverberation room and the electrical noise in the measuring instruments, shall be at least 15 decibels below the lowest level at which measurements are made.

6. Sound Source

6.1 The sound source shall be one or more loudspeakers preferably in the trihedral corners of the room.

7. Test Signal

7.1 The test signals shall be one-third octave bands of random noise with a continuous frequency spectrum and with either equal energy per constant bandwidth, called white noise, or equal energy per constant proportional bandwidth, called pink noise (Note 2). The center frequencies shall be selected from the series: 125, 250, 500, 1000, 2000, and 4000 Hz. If intermediate frequencies or frequencies outside this range are desired, they shall be chosen from the USA Standard S1.6-1967 Preferred Frequencies for Acoustical Measurements.

NOTE 2—The use of an integrated sound pulse method of measuring decay rates has been proposed in recent papers.[3] This method is being studied for its possible application to reverberation room procedures but does not yet form a part of this standard.

7.2 A test signal can be limited to a bandwidth of one-third octave in two ways. If the pass-band of the circuit to the loudspeaker is exactly one-third octave wide, the pass band of the microphone circuit, centered on the same frequency, should be wider than one-third octave but no wider than one full octave. If the pass-band of the circuit to the loudspeaker is more than one-third octave wide, the width of the pass-band of the microphone circuit should be exactly one-third octave. The second method is preferred.

8. Test Specimen

8.1 When the specimen is in the form of an extended plane surface, it shall be in one piece, bearing in mind the requirement of 8.3.1. An area of 72 ft² (6.7 m²) is recommended in a shape 8 by 9 ft (2.44 by 2.74 m). However, where the size of the room permits, larger areas may be used to reduce the effects of diffraction, for example:

[3] M. R. Schroeder, "New Method of Measuring Reverberation Time," *Journal of the Acoustical Society of America*, Vol. 37, 1965, pp. 409–412, and M. R. Schroeder, "Response to Comments on New Method of Measuring Reverberation Time," *Journal of the Acoustical Society of America*, Vol. 38, 1965, pp. 359–361.

108 ft² (10 m²) in a shape 9 by 12 ft (2.74 by 3.66 m), and

120 ft² (11.4 m²) in a shape 10 by 12 ft (3.05 by 3.66 m).

An area less than 48 ft² (4.46 m²) shall not be used, and extreme aspect ratios, such as long narrow strips, shall be avoided.

8.2 *Mounting*—Insofar as its acoustical properties are concerned, the specimen shall be mounted in a way to simulate actual installation. When the specimen presents an extended plane surface, care shall be taken to cover tightly the sides of the specimen so that only the front surface area is exposed to the sound field.

8.3 *Placement*—The specimen may be placed on the floor of the reverberation room for convenience of measurement, but when the orientation of the specimen may affect its acoustical properties, provision shall be made for wall or ceiling mounting.

8.3.1 No part of the specimen shall be closer than one-half wavelength from a reflecting surface other than the one backing it. In the smaller reverberation rooms this requirement may make it necessary for the specimen area to be less than 72 ft² (6.7 m²).

8.4 *Volume*—If the volume of the specimen, including its mounting, is so large as to subtract more than 1 per cent from the volume of the room, allowance shall be made in the absorption computation.

9. Procedure

9.1 *Measurement of Decay Rate*—Except for the filters, which shall meet the requirements for Class II or III of the USA Standard Specification S1.11-1966, Octave, Half-octave, and Third-octave Band Filter Sets, the instruments to measure the decay rate are not specified. The time for a given range of decay may be measured, or the decay in a given time, or the slope of the decay curve. The purpose of the measurement is to determine $d = N/T$, the average rate of decay of the sound pressure level in decibels per second. At each frequency make a group of measurements large enough that the average meets the precision requirements of 12.1 (Note 2).

9.2 *Range*—Make the measurements over a range of at least 30 decibels, starting at least 5 decibels down from the beginning of the decay.

9.3 *Microphone Position*—Place the microphone, or microphones, a half wavelength or more from any reflecting surface including the test specimen and outside the direct field of the sound source. Other microphone positions, such as in the trihedral corners of the room, may be used if it is demonstrated that, to the precision required, the same results are obtained.

9.4 *Nonlinear Decays*—Do not use decays which deviate substantially from a straight line over the measuring range. Make periodic checks of linearity, for curved or broken line decays indicate conditions that should be avoided. The conditions often may be a sound field which is not diffuse during the decay, feedback of energy from an adjacent room with a longer reverberation time, or working too close to the background noise level.

Adjustments

10.1 When the absorption coefficient has been calculated by substituting into the expression:

$$\alpha = \frac{A_2 - A_1}{S} \quad \ldots\ldots\ldots\ldots (4)$$

it has been the practice in some laboratories to make one or more adjustments in the measured results.

10.1.1 Since diffraction effects make the measured results greater than the

ideal to a degree not yet completely understood, it is recommended that no adjustment be made for this cause.

10.1.2 Since small changes in temperature and relative humidity during the course of a measurement make large changes in the absorption of the atmosphere at 2000 and especially at 4000 Hz, and since the magnitude of these changes has not yet been agreed upon, it is recommended that measurements in the empty room and in the room containing the test specimen be made under conditions of temperature and relative humidity so nearly the same that no adjustment need be made.

10.1.3 The absorption coefficient, α_1, of the room surface covered by the test specimen should be added. But the absorption coefficients of a smooth, hard, rigid surface, such as a reverberation room floor, are so small that they can be neglected. It is recommended that no adjustment be made for the floor area covered by the specimen.

11. Report

11.1 The report shall include the following:

11.1.1 A statement, if true in every respect, that the test was conducted in accordance with the provisions of this ASTM method of test.

11.1.2 A description of the test specimen, its size and mounting. The description shall be adequate to identify another sample of the same material.

11.1.3 A listing of any numerical adjustments that have been made in the measured results because of diffraction effects, changes in temperature or relative humidity during the test, or allowance for the absorption coefficient of the room surface covered by the test specimen.

11.1.4 A statement of the estimated precision of measurement at each frequency.

11.1.5 *Results of Measurement:*

11.1.5.1 When the specimen is in the form of an extended plane surface, the sound absorption coefficients at the six measuring frequencies to the nearest multiple of 0.01, and the noise reduction coefficient, *NRC*, to the nearest integral multiple of 0.05, with the provision that exact mid-points be reported to the next higher multiple. For example, 0.625 and 0.675 would be reported as 0.65 and 0.70 respectively. When adjusted coefficients are listed in the report, the noise reduction coefficient shall be computed from the adjusted coefficients only.

11.1.5.2 When the specimen consists of isolated objects, the sound absorption at the six measuring frequencies in terms of sabins per unit to the nearest 0.1, if such precision is warranted, and a description of the number and the spacing of the units relative to each other and to any surface within one-half wavelength.

11.1.6 Also, to be considered part of the report but if not included to be made easily available to those who want it, a description of the laboratory and the measurement technique. The description should contain at least the following items:

11.1.6.1 Description of the reverberation room, its construction and dimensions.

11.1.6.2 Customary test specimen size and shape.

11.1.6.3 Instruments used.

11.1.6.4 Temperature and humidity control, if any.

11.1.6.5 Time, temperature, and relative humidity used in uniform preconditioning of specimens, if such procedure is employed.

11.1.6.6 Means of obtaining diffusion and the results of tests of diffusion.

11.1.6.7 Method used to determine the precision of measurement.

11.1.6.8 Detailed description of how

the adjustments of 10. Adjustments are made.

11.1.6.9 General description of the test procedure.

11.1.6.10 Calibration period, reference sources, how often the correct operation of the equipment is checked.

12. Precision

12.1 Repeated measurements of the decay time, or the decay rate, under the same conditions will be expected to show some scatter. At each frequency use the average of a group of measurements and choose the size of the group to give an absorption coefficient to a precision of ± 0.04 at 125 and 4000 Hz and ± 0.02 at all intermediate frequencies with confidence limits of 90 per cent.

AMERICAN SOCIETY FOR TESTING AND MATERIALS

1916 Race St., Philadelphia, Pa. 19103

Reprinted from Copyrighted 1968 Book of ASTM Standards, Part 14.

Tentative Recommended Practice for

MEASUREMENT OF AIRBORNE SOUND INSULATION IN BUILDINGS[1]

ASTM Designation: E 336 – 67 T

This Tentative Recommended Practice has been approved by the sponsoring committee and accepted by the Society in accordance with established procedures, for use pending adoption. Suggestions for revisions should be addressed to the Society at 1916 Race St., Philadelphia, Pa. 19103.

Introduction

This recommended practice is one of a series for evaluating the sound insulating properties of building elements. It is designed to measure the performance of a partition element installed as a part of a building, whatever the configuration. Others in the series deal with the airborne sound transmission loss of an isolated partition element in a controlled laboratory environment, and with the laboratory measurement of impact sound transmission through floors.

The text has been prepared as an integrated whole. For the convenience of the reader it has been organized into eight sections and four appendixes. There is, in addition, a list of reference standards and papers.

1. Scope

1.1 *Measures of Acoustical Insulation*—This recommended practice establishes uniform procedures for the determination of *field transmission loss* (see 4.3, 4.4, and 4.5), that is, the airborne sound insulation provided by a partition (see Note 1) already installed in a building. It also establishes, in Appendix A1 a standard method for the measurement of the *noise reduction* between two rooms in a building, that is, the difference in average sound pressure levels in the rooms on opposite sides of the test partition. Where the test structure is a complete enclosure out-of-doors, neither the field transmission loss nor the noise reduction is appropriate; instead, a method is established for determining the *insertion loss*, also in Appendix A1.

Note 1—The word partition includes in its meaning partitions, walls of all kinds, floors, or any other boundaries separating two spaces, not necessarily enclosed. The boundaries may be permanent, operable, or movable. A ceiling-plenum-ceiling path (7)[2] is also included, though

[1] Under the standardization procedure of the Society, this recommended practice is under the jurisdiction of the ASTM Committee E-6 on Methods of Testing Building Constructions. It was prepared with the cooperation of ASTM Committee C-20 on Acoustical Materials. A list of members may be found in the ASTM Year Book.

Accepted Aug. 29, 1967.

[2] The boldface numbers in parentheses refer to the references at the end of this recommended practice.

special efforts will be necessary, to eliminate flanking transmission through the common wall (see Appendix A4). In this case, the results are comparable to noise reduction rather than to transmission loss.

Note that the noise reduction evaluates the effective acoustical isolation between a pair of adjacent rooms, whereas the field transmission loss refers only to the insulation which a partition interposes in the sound path through it.

1.2 *Types of Field Situation*—The conditions specified (2)[2] for laboratory measurement of the transmission loss for airborne sound, in which the sound fields on opposite sides of the test partition are highly diffuse, very nearly conform to the mathematical model upon which the best available theory is based. Moreover, the greatest body of practical experience deals with transmission loss measurements under such conditions.

1.2.1 Unfortunately highly diffuse fields are not always found in the field; and, the special efforts which would be required to simulate laboratory conditions in the field are often impractical; in any case, they would violate the present meaning of a field test.

1.2.2 Instead, this recommended practice gives measurement procedures for determining the field transmission loss in nearly all cases that may be encountered in the field; no limitation to room-to-room transmission is intended. Thus, several different test procedures are given, each suited to a specific *type* of measurement situation; the appropriate measurement procedure must be selected for each field test according to the *type* of situation which that particular case most closely resembles.

1.2.3 Because it is well-known, the laboratory diffuse-field measurement procedure is described first in this recommended practice, an adaptation of the laboratory test method for use in the field being given in detail in the main body of the text (see Section 6). The alternative test procedures which will be required in field situations where diffuse sound fields do not exist on both sides of the test partition are given in Appendix A2, along with criteria for determining which alternative procedure is appropriate.

1.2.4 These alternative procedures are not interchangeable. In particular, it must not be expected that the alternative procedures will yield the same test values of field transmission loss. For example, the application of the different procedures to evaluate a given wall in place is likely to lead to results that do not agree, because only one of the procedures will be appropriate to that situation. On the other hand, if the same kind of partition is installed in two different locations and the appropriate test procedure is used for each case, the test results may not agree because the wall exhibits different attenuation characteristics depending on the incident sound field (see 3.3, 3.4, and 3.5).

1.2.5 Field transmission loss data should not be reported as conforming to this recommended practice for any field situation that does not conform to a type for which a measurement procedure is given in Section 6 or Appendix A2 (see 1.3 however).

1.3 *Intermediate Configurations*—Field configurations may be encountered which resemble but do not correspond exactly to one of the typical situations described in Section 6 or Appendix A2. For example, the receiving room absorption may be too great for the procedure of 6.1.3 (see 6.3) and too small for the procedure of A2.3 (see A2.3.3.2). In this case, measurements should be made using the procedures of both 6.1.3 and A2.3. If the results of the two test procedures differ by no more than 3 dB in any frequency band, the two sets of results may be averaged and reported as the field

transmission loss, just as though the configuration had corresponded exactly to one of the types described above. In any case, the results of both measurement procedures must be reported. If the results of the two test procedures do not agree within the limits specified above, the test situation does not correspond to a type for which this recommended practice provides measurement procedures (see 5.1.3). The test data are likely to be unreliable and are not to be reported as the field transmission loss.

2. Summary of Method

2.1 The sound insulating property of a partition element is usually expressed in terms of the airborne sound transmission loss, which is the ratio, expressed in decibels, of the sound power incident upon the partition to the sound power transmitted through and radiated by the partition.

2.1.1 In the laboratory test procedure, this ratio is determined by mounting the partition between two reverberation rooms, one of which, the source room, contains one or more sound sources. The rooms are so arranged that the only significant sound transmission between them is through the test specimen. Under these conditions, the transmission loss is related, by a simple equation (2), to the space-time-average sound pressure levels in the two rooms, the area of the test partition, and the total absorption in the receiving room. When these quantities are measured in appropriate frequency bands, the transmission loss as a function of frequency is found.

2.1.2 The simplicity of that recommended practice depends on the provision of diffuse sound fields in both source and receiving rooms. When this situation is encountered in the field the procedure of Section 6 is to be used.

2.1.3 When one or the other (or both) of the test rooms is such that a diffuse sound field does not exist there, different approaches must be used, as specified in Appendix A2.

2.1.4 In all cases, it is the goal of the recommended practice to determine the existing ratio of the power directly incident upon the test specimen to the power radiated directly from it.

2.1.5 Once the primary measurement of field transmission loss is complete, a supplementary test *must* be made to demonstrate that no significant flanking transmission is present. Details of suitable tests for flanking transmission are given in A4.5.

3. Significance

3.1 The problems of making reliable sound insulation measurements in the field are much more difficult than those met in the laboratory. In ordinary buildings, a great variety of test room shapes and sizes will be encountered; the amount of energy exchange at the nominal boundaries of the test specimen will vary widely; and there is often a problem of flanking transmission, that is, of sound arriving in the space on the receiving side of the test partition by paths other than the one directly through the partition. These variations influence the test results to a degree which is not predictable.

3.2 In principle, these same problems exist in laboratory measurements, but their influence is minimized by deliberately restricting the measurements to conditions with random sound fields on both sides of the partition, by the adoption of appropriate dimensions for the test chambers and for the test specimen, and by using special laboratory wall constructions to reduce the effects of flanking transmission (which may, in any case, be measured and evaluated once for all subsequent tests in each facility using the same specimen mounting (2, 3).

3.3 In the field, on the contrary, the effect of the environment must be assessed for each measurement, and the difficulty of determining the field transmission loss will vary correspondingly. Indeed, it is possible that problems raised by flanking transmission or by an unusual field-test situation will make the measurement so difficult as to be impractical. If this is so, it is preferable to acknowledge the fact outright, instead of attempting to apply an inappropriate measurement procedure.

3.4 Evidently, there may be substantial differences between data obtained from similar structures in the laboratory and in a building, even when leaks and flanking transmission have been successfully eliminated. Since it is the purpose of the Field Transmission Loss Test to describe the performance of the partition in relation to the other elements of the building, no effort should be made to adjust the field data to laboratory values. Each field measurement will yield *a* field transmission loss, not *the* field transmission loss, of a partition type.

3.5 As more field measurements are made according to a standard procedure, the range of field transmission loss that may be expected for each partition type in various buildings will become clear. Indeed, it is likely that eventually a partition will be characterized as to its acoustical performance by two ratings: one dealing with the sound insulation which it provides, the other evaluating its expected variability under different conditions of field installation.

4. Definitions

4.1 *General*—This recommended practice follows the definitions and symbols of USA Standard Acoustical Terminology (USAS S1.1-1960) (1) and of USA Standard Method for the Physical Measurement of Sound (USAS S1.2-1962) (20). Some definitions of special relevance are repeated and certain usages are explained here:

4.1.1 *average sound pressure level* ($\bar{L}$) *in a room*—ten times the common logarithm of the ratio of the space-average mean-square sound pressure to the square of the reference sound pressure, the space-average being taken over the entire room volume with the exception of those regions where the direct radiation of the sound source or the near field of the boundaries (walls, furniture, etc.) is of significant influence (see 6.4, A2.2.8, and A2.3.4):

$$\bar{L} = 10 \log \frac{p_1^2 + p_2^2 + \cdots p_n^2}{N p_o^2} \quad \ldots (1)$$

where:

p_o = the reference sound pressure, usually 20 μN/m^2 (0.0002 microbar); the reference pressure should always be stated;

N = the number of measurement positions (see A4.4.2), and

$p_1, p_2 \ldots p_n$ = the rms sound pressure at the N different measurement positions in the room; each p_n^2 should represent the energy in approximately the same fraction of the total room volume.

The average sound pressure level $\bar{L}$ is expressed in decibels. Detailed procedures for determining $\bar{L}$ are given in A4.4, 6.4, and 6.6.1.

4.2 *noise reduction* (NR)—the difference between the average sound pressure level in a room containing one or more sources of sound and that in another (usually adjacent) room. It is calculated as follows:

$$\mathrm{NR} = \bar{L}_1 - \bar{L}_2 \quad \ldots (2)$$

where:

$\bar{L}_1$ = average sound pressure level in the source room, and

$\bar{L}_2$ = average sound pressure level in the receiving room, both as defined in 4.1.1.

The noise reduction is expressed in decibels (see A1.1.2 and A1.1.3).

4.3 *field transmission coefficient* (τ_f)—the fraction of the airborne sound power incident upon the source side of a partition installed in a building to the sound power which is transmitted and radiated into the receiving space. It is calculated as follows:

$$\tau_f = \frac{W_2}{W_1} \quad \ldots\ldots\ldots\ldots\ldots (3)$$

where:

W_1 = sound power (sound energy per second) incident directly upon the partition on the source side, and

W_2 = sound power radiated directly from the quiet side of the partition into the receiving space.

It is explicitly required that the symbols W_1 and W_2 represent steady-state, rather than transient, quantities.

4.3.1 In contrast to laboratory usage, where τ is defined only for diffuse sound fields, no restriction is made here as to the kind of sound field existing on either side of the partition. The field transmission coefficient will depend upon the kind of sound field incident on the specimen. It is the purpose of this recommended practice to identify the sound fields as well as possible in each case and to specify the corresponding appropriate procedure from which to determine the field transmission coefficient (and hence the field transmission loss) for this field situation.

4.3.2 For the purposes of this recommended practice, the power W_2 radiated from the quiet side of the partition may be less than the incident power W_1 because of (*1*) impedance mismatch (reflection of a portion of W_1 back to the source room due to either the mass or the stiffness of the partition); (*2*) energy losses due to damping within the partition or at the boundary; and (*3*) sound energy originally incident on the partition (and thus included in W_1) but leaving at the boundaries of the partition as flexural vibration (and thus not part of W_2). W_2 does *not* include energy flow from the other walls of the source room into the test partition and radiating from it into the receiving space; special efforts may be required to avoid this condition.

4.4 *flanking transmission*—transmission refering both to this last-mentioned component of power as well as to power traveling to the receiving space by paths in no way involving the test partition. Whether flanking transmission includes possible leaks around the partition depends upon the purpose of the test. A decision must be made as to whether the "leaks" are, or are not, a part of the partition (see 5.1.1, 5.1.2, and A4.5.5.3).

4.5 *field transmission loss* (*FTL*)—the acoustical isolation against airborne sound provided by a partition installed in a building; it is ten times the common logarithm of the reciprocal of the existing field transmission coefficient. It may be expressed as follows:

$$FTL = 10 \log \left(\frac{1}{\tau_f}\right) = 10 \log \left(\frac{W_1}{W_2}\right) \ldots (4)$$

The field transmission loss is expressed in decibels.

4.6 *diffuse sound field*—a region containing many randomly oriented sound waves, with equal probability of energy flow in every direction; it follows that there is no correlation between instantaneous sound pressures at widely separated points.

4.7 *sound absorption of an enclosure* (*A*)—a measure of the property of an enclosure of absorbing sound power from the sound field it contains. The absorption of the receiving room may be determined (4) by means of the Sabine equation for the decay of sound in a room: if following the discontinuance of a sound source in the room, one determines the

rate of decay of sound, then the absorption of the room, A, may be determined from the Sabine equation as follows:

$$A = \frac{0.9210\ Vd}{c} \quad \ldots\ldots\ldots\ldots (5)$$

where:

c = speed of sound in air,
V = volume of room, and
d = rate of decay of sound following discontinuance of a sound source in the room, dB/sec.

If V is in cubic feet and c is in feet per second, then A is given in sabins; if V is in cubic meters and c is in meters per second, then A is in metric sabins. This relation is derived on the assumption that the sound field is reverberant and diffuse, as in a reverberation room.

4.7.1 An alternative procedure is permitted, which depends on the relation between the sound power output of a source sounding in the room, the average sound pressure level, and the total absorption in the room (see 6.5.2).

4.8 *field sound transmission class* (*FSTC*)—a single-number rating derived in a prescribed manner from one-third-octave band values of sound transmission loss measured in the field. The rating provides an evaluation of the performance of a partition in certain common sound insulation problems. For its scope and the prescribed method of assignment see Ref (21).

4.9 *noise isolation class* (NIC) — a single-number rating derived in a prescribed manner from measured values of Noise Reduction. The rating provides an evaluation of the sound isolation between two enclosed spaces which are acoustically connected by one or more paths (see A1.1.3).

4.10 *field insertion loss* (FIL) — a measure of the sound isolation between two locations for which, because one of them is not enclosed, neither the transmission loss nor the noise reduction can be determined unambiguously. It is calculated as the difference formed by subtracting the sound pressure level at a location, shielded from a noise source by a barrier or enclosure, from the sound pressure level that would exist at the same location in the absence of the barrier.

5. Test Specimen

5.1 In this recommended practice, the special significance of a field test is that the test partition is to be measured just as it is found in the field. Nevertheless, some judgment must be used to ensure that the field conditions, as found, are consistent with the purposes of the test.

5.1.1 *Noise Reduction Test*—If the purpose of the test is to determine how much isolation the occupants of a certain pair of neighboring spaces are enjoying, then any peculiarities of the situation must be accepted as part of the existing isolation and no preparation of the test specimen is either needed or permitted. In this case, only the noise reduction is required; A1.1.2 specifies appropriate procedures for the measurement of noise reduction.

5.1.2 *Transmission Loss Measurement*—On the other hand, if the test is intended to demonstrate that the performance of the test partition complies with a specification, or if the test data are intended to determine the field transmission loss of a given field installation of the test partition (which data, taken together with other field data on nominally identical test specimens, will serve to typify the field performance of that partition type), then care should be taken to see that all conditions are "typical," and that the hazards of measurement are minimized, as specified in 5.1.3 below.

5.1.3 *Test Location*—Find a test specimen of the desired type in surroundings

most suitable for the test, especially in cases involving acceptance testing of structures for conformance with sound insulation specifications. The two spaces which the test specimen separates should be selected on the basis of suitable size and shape, of absorption conforming to types described in this recommended practice (including Appendix A2), of freedom from structural irregularities near the test partition, of freedom from flanking, etc.

5.1.3.1 *Source Room or Receiving Room Very Small*—A serious difficulty arises in defining transmission loss in situations where either the source room or the receiving room is small compared to the wavelength of sound. In these cases, there is, strictly speaking, no radiation of the sound energy, but only a pulsating, quasi-static pressure throughout the room; hence, one cannot speak of "incident" or "radiated" sound power, and the transmission loss cannot be defined in the usual way. This situation will occur in any closed space if the frequency is low enough. A criterion is given (see 6.2.1 and Fig. 1) for determining the frequency below which the concept of transmission loss loses meaning. For frequencies below this limit, no attempt is to be made to determine field transmission loss, though the noise reduction may be measured and reported at these frequencies.

5.2 *Size and Mounting*—The size of the test specimen should be typical of the type of partition under study. Very small partitions sometimes yield different transmission loss values from similar large ones, and should not be used for test purposes unless the small size is characteristic of the construction being investigated; such an exceptional feature shall be made clear in reporting the results. Partitions 8 by 9 ft or larger may be considered large enough that dimensional effects are not critical.

5.2.1 The mounting conditions of the test specimen should be representative of an ordinary and typical installation. Any unusual feature should be avoided unless this peculiarity is characteristic of the structure under investigation, in which case this fact must be stated clearly in all reports of the data.

5.3 *Flanking Transmission*—In many installations in the field, sound can arrive in the receiving space by paths other than that directly through the partition under test.

5.3.1 If the test is intended to determine the isolation actually existing between the spaces adjacent to the partition, no effort should be made to reduce the flanking transmission, since it is an intrinsic element of the existing isolation. If, however, the field transmission loss of the partition is to be determined, all significant flanking *must* be eliminated. A4.5.5 describes a mandatory procedure for ensuring that no substantial flanking is present.

5.4 *Drying and Curing Period*—Test specimens that incorporate materials for which there is a curing or drying process (for example, adhesives, plasters, concrete, mortar, damping compound) should age for a sufficient interval before testing. Aging periods for certain common materials are recommended in Section A1 of Ref (2).

6. Diffuse Sound Field Test Procedure

6.1 *Theory For Sound Transmission Loss:*

6.1.1 The theory for transmission loss in a diffuse-field was first developed by E. Buckingham (5, 8, 9). An ideal diffuse sound field is characterized by equal sound energy density at every point in the field and also by the condition that any small element of volume may be considered as a non-directional sound source radiating sound energy uniformly in all directions. Thus, in a

diffuse sound field the individual wave packets of sound energy striking the test partition arrive with equal probability from all angles of incidence.

diffuse condition, as determined by the application of the criteria described in 6.2 and 6.3, test methods similar to the laboratory procedures may be applied.

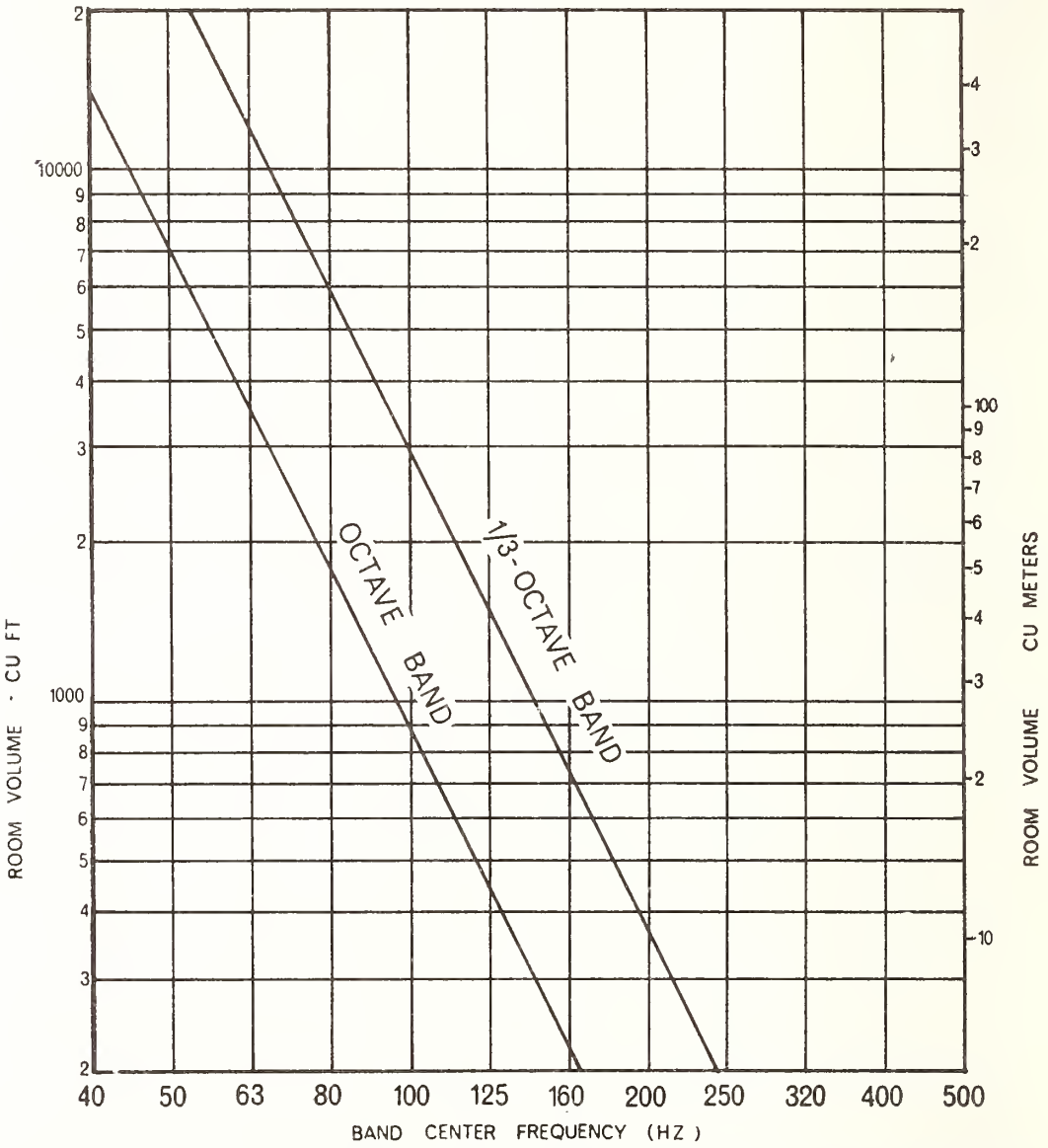

FIG. 1—Room Volume for Which There Will Be Ten or More Normal Modes per Measurement Bandwidth, Shown as a Function of Band Center Frequency, for Octave and One-Third Octave Bands.

6.1.2 This treatment has been taken as the basis of ASTM Recommended Practice E 90, for Laboratory Measurement of Airborne Sound Transmission Loss of Building Partitions (2). If a field situation is found to conform to the General requirements concerning instrumentation and test procedures are given in Appendixes A3 and A4.

6.1.3 If the test partition separates two rooms, each of which lends itself to the establishment of a diffuse sound

field, the source room may be insonified by random noise from one or more loudspeakers to produce a diffuse sound field there. Some of this noise will be transmitted through the test partition to produce a diffuse field in the receiving room. The sound transmission loss of the test partition may then be derived from measurements in the two rooms according to the following equation:

$$\text{FTL} = \bar{L}_1 - \bar{L}_2 + 10 \log S - 10 \log A_2 \quad (6)$$

where:

FTL = transmission loss in dB of the test partition; the prefix *F* is added to signify field measurement,

$\bar{L}_1$ = average sound pressure level in Room 1, the source room (see 4.1.1),

$\bar{L}_2$ = average sound pressure level in Room 2, the receiving room,

S = area of the test partition (in square feet or square meters), and

A_2 = total sound absorption in Room 2; if S is in square feet, A_2 should be expressed in sabins; if S is in square meters, A_2 should be expressed in metric sabins (see 6.5). Note that A_2 is the absorption with the test partition in place; sound transmitted back into Room 1 through the test partition constitutes part of the sound absorbed from Room 2.

In general, the acoustical properties of the partition and of the rooms are functions of frequency; tests are to be made in a series of contiguous one-third octave bands of frequency between 100 and 5000 Hz (subject to the criterion for room diffusion of 6.2.1).

6.2 *Test Environment Defined*—The test procedures of Section 6 shall be used in the field if the environment conforms to the requirements of 6.2.1 and 6.3 below.

6.2.1 *Room Size:*

6.2.1.1 The measurement method of Section 6 requires diffuse sound fields on both sides of the test partition. The sizes of the source room and receiving room determine to a large extent (for a given measurement bandwidth) the lowest frequency at which the sound fields will be adequately diffuse: the larger the room, the lower the limiting frequency.

6.2.1.2 In laboratories, the test rooms are usually made large enough and are so treated that adequate diffusion is obtained at the lowest frequency of interest. In the field, however, where the room size must be accepted as given and may be small, the frequency below which a diffuse field will not exist (and below which the procedures of this section are, therefore, not valid) may limit the low-frequency range of measurement.

6.2.1.3 For suitable accuracy in determining the average sound pressure levels in the source and receiving rooms (see Eq 6), there shall be at least 10 modes per measurement bandwidth. The lower limit of frequency for which this will occur, using one-third-octave bands, may be determined from the volume of the smaller of the two test rooms by reference to Fig. 1 (16).[3]

6.3 *Absorption of the Rooms*—The rooms will be suitable for the application of the test procedure of Section 6 if (in addition to complying with 6.2.1) the average (over all room surfaces) absorption coefficient is no greater than 0.25 at each test frequency for either room (see 1.3 (17)).

6.4 *Selection of Measurement Positions in Source and Receiving Rooms*—The sound pressure close to the walls of a room will be greater than that cor-

[3] A curve is also given for octave-band measurements, for use with the test procedures of Appendix A2.

responding to the average energy density in the room (18). Therefore, for the measurement of the space-average sound pressure levels, $\bar{L}_1$ and $\bar{L}_2$ (see 4.1.1), the microphones shall be located preferably more than one half and certainly no less than one-third wavelength from room boundaries or any other large reflecting surfaces, including the test partition. In addition, no microphone in the source room shall be in the direct field of a sound source. Directions for the manipulation of microphone systems are given in Section 8.6 of Ref (2)

6.5 *Measuring the Absorption of the Receiving Room*—An adjustment involving the total sound absorption A_2 of the receiving room is to be applied (see Eq 6) to the measured noise reduction between the source and receiving rooms in order to determine the field transmission loss of the partition. This absorption shall be measured either by the decay rate method (4), or with the aid of a reference sound source.[4] The determination of receiving room absorption shall be made with the receiving room in the same condition (except perhaps for the addition of a single sound source), and using similar microphone positions as the measurement of noise reduction.

6.5.1 *Decay Rate Method*—If the absorption of the receiving room is to be determined from the decay rate, the measurement procedure (4) summarized in 4.7 shall be followed. The test signal shall be the same, particularly with respect to bandwidth, as that used for the sound pressure level measurements.

6.5.2 *Reference Sound Source Method*—If a sound source is available whose power output L_w is known, the value of 10 log A_2 in the receiving room can be calculated from a measurement of the average sound pressure level $\bar{L}_p$ established there by the operation of the reference sound source (10,11,12, and 22). In a diffuse sound field, the sound power level L_w of a source, the average sound pressure level $\bar{L}_p$ in the room, and the total sound absorption A_2 of the room are related (11) as follows:

$$10 \log A_2 = L_w - \bar{L}_p + 16.5 \ldots . (7)$$

or

$$A_2 = \text{antilog} \left(\frac{L_w - \bar{L}_p + 16.5}{10} \right) \ldots (8)$$

where:
reference power for $L_w = 10^{-12}$w; and
reference sound pressure for $L_p = 20\ \mu N/m^2$ (0.0002 dynes/cm^2).

6.5.2.1 The reference source may be a loudspeaker whose power output has been previously determined for a given electrical power input in each frequency band.

6.5.2.2 Alternately, another sound source whose sound power output is constant enough for usable accuracy is a modified centrifugal fan (11). For its power output level see Table A1.

6.5.2.3 The determination of absorption as a function of frequency shall be carried out in bandwidths the same as are used to measure sound pressure level differences.

6.6 *Interpreting the Data to Determine the Field Transmission Loss:*

6.6.1 *Level Readings:*

6.6.1.1 From the sound pressure level readings at several microphone positions in both the source and receiving rooms, determine the average sound pressure levels in the respective rooms in accordance with 4.1.1.

6.6.1.2 If the range of levels in each room is less than 6 dB, the level readings

[4] The method of determining room absorption described by A. London (6)—which depends on measuring the sound pressure level as a function of distance from the test partition to determine the point at which the transition occurs from the (diminishing) direct field of the partition to the (uniform) reverberant field of the receiving room—is likely to be impossible or misleading in rooms having absorptive ceilings or floors, or both.

in decibels may be averaged directly. If the range for either room exceeds 6 dB, it is necessary to convert each observed level in that room to pressure-squared, to average the several pressure-squared values, and to reconvert the average pressure-squared to average sound pressure level.

6.6.1.3 The difference between the space-average sound pressure levels $\bar{L}_1$ and $\bar{L}_2$ so obtained in the source and receiving rooms is the noise reduction defined in 4.2.

6.6.2 The radiating surface area of the test partition in the receiving room is determined with careful attention to the decision (see A4.5.5.3), as to what elements constitute the test specimen. This value of S is used, along with A_2, measured in consistent units as determined in 6.5, to correct the sound pressure level differences of 6.6.1.3 to field transmission loss as indicated in Eq 6.

7. Reporting of Data

7.1 In contrast to the laboratory standard, this recommended practice standardizes the measurement procedures, but not the physical configuration for the test. Because the physical configuration cannot be standardized, careful reporting of the exact test conditions is necessary to permit a meaningful evaluation of the field test results.

7.1.1 *Statement of Conformation to Standard*—A statement is required, if it is true in every respect, that the tests were conducted in accordance with the provisions of this ASTM recommended practice. No data may be published as complying with this recommended practice, without indicating which procedure under Section 6 or Appendixes A1 or A2 was used. The criteria for choosing that procedure should be stated, as well as the method by which they were established.

7.1.2 *Description of Test Configuration*—A complete description shall be given of the surroundings of the area in which the test is conducted.

7.1.2.1 *Description of Test Environment*—A sketch of the source and receiving spaces and their environs shall be given, showing both the plan of the test area and a section through the test partition. A description shall be given of the structures bounding the test partitions, including floor, ceiling, and wall structures of the source and receiving spaces.

7.1.2.2 *Furnishing of Source and Receiving Rooms*—A complete description shall be given of the furnishings of the test rooms adjacent to the test partition, noting the position with respect to the test partition of any bulky objects.

7.1.3 *Description of Test Specimen*—A complete description of the test specimen shall be given, including all of the essential constructional elements, the size, thickness,[5] and the average weight per unit area of the specimen.

7.1.3.1 The description of the test specimen should as far as practicable be based upon measurement and examination of the specimen itself, rather than upon the building plans or information received from the builder or others.

7.1.3.2 The composition of plaster mixes or plastic masonary applications shall be stated, if possible, and also the surface finish and method of application. The drying or curing period, if any, and the final condition of the sample (shrinkage cracks, etc.) shall be reported. In the case of preformed panels, such as doors and office partitions, operable or not, the edge conditions shall be specified in as much detail as possible. Clearances around movable elements shall be re-

[5] If there are no access panels, outlet boxes, etc., which would permit a direct measurement of wall thickness, one can often deduce the wall thickness by measurement between windows separated by the test wall.

ported. If the construction or installation of the test specimen is, for some reason, such that the results do not represent normal performance of the specimen, this fact shall be stated explicitly.

7.1.4 *Nature of Test Signals*—A description shall be given of the type of test signals used in the measurements, both for absorption measurement and determination of level differences between source and receiving rooms, stating the bandwidth of measurement and the frequencies at which tests were made.

7.1.5 *Description of Test Procedure:*

7.1.5.1 A complete listing of the instruments used for the measurement shall be made. This should include the name, make, and type number of the instruments.

7.1.5.2 The lower frequency limit of the test rooms shall be stated as determined in 6.2.1. Field transmission loss shall not be reported for lower frequencies, though the noise reduction may be stated.

7.1.5.3 A complete description of the method of measurement shall be given by reference to appropriate paragraphs in this recommended practice, noting any exceptions (see A4.1.2).

7.1.5.4 If a reference sound source is used to measure room absorption, a description and identification of this source shall be given, including the calibration for sound power level output.

7.1.6 *Background Noise Level*—The background noise levels in the receiving room shall be given in graphic form, in comparison with the actual average sound pressure levels observed during the transmission loss tests on both sides of the test partition. These three curves shall be given on standard graph paper to the same scale as that on which the field transmission loss results are reported as described in 7.1.7 below.

7.1.7 *Statement of Test Results of Field Transmission Loss Measurement*—The test results shall be stated to the nearest 1 dB at the specified frequencies in tabular form and also shall be shown in graphic form on standard graph paper. The measured total absorption in the receiving space, at each of the test frequencies shall be stated (see Eq 8). The temperature and relative humidity in both test rooms shall be given.

NOTE 3—If results are presented in graphical form, it is recommended that the ordinate scale be 50 mm/decade. If it is necessary to use a larger or smaller scale, the same aspect ratio as above should be used. Whenever practicable, the ordinate scale should start at 0 dB.

7.1.8 *Statement of Qualifications to Accuracy of Test Results*—Taking into account all the available information about the field test, a statement should be made about the probable accuracy and reliability of the test results, and the extent to which the results of this test are representative of the partition type. Special mention shall be made of unusual size of test partitions, unusual size or shape of the test rooms, or other irregularity which may be expected to make the measured results differ significantly from other field tests on the same type of partition.

7.1.9 *Comparison with Existing Laboratory Data*—A comparison may be made between the measured field data and any available laboratory data for nominally identical partitions. An explanation may be offered, if appropriate, of significant differences between the laboratory and field data (see A4.5.4).

7.1.10 *Field Sound Transmission Class (FSTC)*—For test partitions whose field transmission loss has been measured in one-third octave bands and for which, by applying the methods of A4.5, no significant flanking has been found to exist, a field sound transmission class (FSTC) may be assigned (21).

APPENDIXES

A1. Measuring Noise Reduction or Field Insertion Loss

A1.1 Isolation Between Rooms

A1.1.1 When the field transmission loss of the test partition is not at issue but one wants to know only how much isolation the occupants of the pair of rooms enjoy, the noise reduction should be measured. The test procedure for this quantity is identical to that given in Section 6 for determining the field transmission loss, except that no measurement is required of the receiving room absorption. Note that the noise reduction is associated with the two test rooms, not with the dividing partition alone, and it may or may not involve flanking transmission.

Note A1—The general recommendations of Appendixes A3 and A4 shall be followed here, as applicable.

A1.1.2 *Noise Reduction*—Noise reduction is a measure of the isolation between two *enclosed* spaces, within each of which it is possible to determine the space-average sound pressure level. The difference between these average sound pressure levels is determined as described under 6.6.1.3 and is reported, with no further correction, as the noise reduction between the two rooms.

A1.1.3 *Noise Isolation Class (NIC)*—If a single-number rating of noise reduction is desired, it shall be the noise isolation class (NIC), determined as follows. For field situations where the noise reduction between a pair of rooms has been measured in one-third octave bands, a single-number rating may be assigned to evaluate the acoustical isolation existing between these two rooms (**21**). No other single-number evaluation of noise reduction is sanctioned.

A1.2 Field Insertion Loss (FIL)

A1.2.1 *General*—When the test structure is a complete enclosure out-of-doors, surrounding either the source or receiver, it will be impossible to establish unambiguously an average sound pressure level in the outside space, and hence neither noise reduction nor field transmission loss has unambiguous meaning. In this case an appropriate measure of the isolation provided by the enclosure is the field insertion loss, measured either from outside the enclosure to inside or vice versa, as described below. The choice as to which is the appropriate procedure should be based on the intended purpose of the enclosure.

A1.2.2 *Outside-to-Inside*—For an external noise source, the field insertion loss is the difference formed by subtracting the average sound pressure level within the enclosure from the sound pressure level which would have existed there in the absence of the test enclosure. In measuring the field insertion loss from outside to inside the enclosure, the noise source should be located so as to simulate the sound field against which the enclosure is supposed to provide acoustical insulation. The sound pressure level which would have existed in the protected spot without the enclosure may be approximated by measuring the sound pressure level at the same distance, but in a different direction, from the source. (If the source is directional, it should be turned to face the microphone.) Care should be taken to avoid unwanted reflections from large near-by objects. The average sound pressure level within the enclosure should be measured as in 6.4 and 4.1.1. The Field Insertion Loss (FIL) is found from the following equation:

$$\text{FIL} = L_d - \bar{L}_2 \quad \text{(A1)}$$

where:

L_d = sound pressure level measured at the same distance, d, from the source as the center of the enclosure, and

$\bar{L}_2$ = average sound pressure level within the enclosure.

A1.2.3 *Inside-to-Outside*—On the other hand, if the enclosure is designed to confine the sound energy from some noisy source, the test procedure is similar in principle to that described in A2.3; but, since it is impractical to assign an effective radiating area for the test specimen (that is, the entire enclosure), the procedure of that section cannot be followed. To determine the field insertion loss, one can measure on the

outside, at some arbitrary distance, the sound pressure level of the test source as attenuated by the enclosure; but, one must compute the sound pressure level that would have existed at the same point in the absence of the enclosure. This is done by determining the power output of the test source from a measurement of the absorption A_1 of the enclosure and the average sound pressure level within the enclosure; from this one can allow for spherical divergence (assuming small source dimensions) to calculate what the sound pressure level would have been at the outside measurement position if the enclosure were not there. The insertion loss is thus found as follows:

$$\text{FIL} = \bar{L}_1 - L_d + 10 \log \frac{A_1}{16\pi d^2} \quad \text{(A2)}$$

where:

$\bar{L}_1$ = average sound pressure level inside the enclosure,

L_d = sound pressure level measured at a point outside the enclosure a distance, d, from the center of the enclosure, determined by either of the procedures explained in 6.5, and

A_1 = total absorption within the enclosure.

If d is in feet A_1 should be expressed in sabins; and, if d is in meters A_1 should be expressed in metric sabins.

A2. Test Procedures for Non-Laboratory-Like Configurations

A2.1 General

A2.1.1 For certain field test configurations that do not conform to the requirements of Section 6, alternative test procedures are given in this appendix. For these procedures, as contrasted with that in Section 6, measurements in octave bands of frequency are permitted. The general recommendations of Appendixes A3 and A4 shall be followed as applicable, for the test procedures given here.

Note A2—None of these methods is exactly as described by A. London (6), whose equations depend to some extent on the equipment he used.

A2.1.2 In each case it is the goal of the test procedure to determine the existing ratio of the sound power directly incident upon the test specimen and the power radiated directly from it. A supplementary test, as described in A4.5 must be performed in each case to demonstrate the absence of any significant flanking transmission.

A2.2 Source Outdoors or in Highly Absorptive Space, and Reverberant Receiving Room

A2.2.1 When the source of sound is out-of-doors or in a highly absorptive space, sound power travels outward from the source as in a free field. Under these conditions the acoustical power incident on the test partition can be calculated from a knowledge of the sound pressure in the incident, nearly plane, wave.

A2.2.2 This test situation differs from that of Section 6 in that the sound is incident upon the test partition from only one direction for each sound source. In order to determine the field transmission loss unambiguously, therefore, the test procedure must utilize only a single sound source for excitation of the test panel. The transmission loss will usually be different for each angle of incidence of sound upon the partition; therefore, it is necessary to measure (by moving the source) and report the field transmission loss for several angles of incidence between the normal (0 deg) and 75 deg away from the normal. Measurements for angles of incidence greater than 75 deg away from the normal are unreliable and are not recommended.

A2.2.3 To determine the sound pressure level L_1 associated with the incident wave, it will usually be most convenient to measure the average pressure $\bar{L}_{1o}$ at the face of the partition at several positions near the center and to subtract 6 dB to correct for the pressure doubling which will occur at this surface (unless the surface is acoustically absorbent, in which case see A2.2.8.3).

A2.2.4 On the receiving side of the test partition, the power radiated from the test specimen into the reverberant space is determined from a measurement of the average sound pressure level in the receiving room as in the procedure of Section 6.

A2.2.5 Under these conditions the field transmission loss is given as follows:

$$\text{FTL} = \bar{L}_{1o} - \bar{L}_2 + 10 \log \left(\frac{1}{4} + \frac{S \cos \theta}{A_2} \right) \quad \text{(A3)}$$

where:

$\bar{L}_{1o}$ = average sound pressure level measured at the face of the partition on the source side, = $L_1 + 6$; and

θ = angle which the incident sound makes with the normal to the partition.

The other symbols are as described in Section 6.

A2.2.6 If the test structure is a complete enclosure out-of-doors, neither the transmission loss nor the noise reduction is appropriate; in

this case refer to A1.2 for a procedure for determining the insertion loss.

A2.2.7 *Test Environment Defined:*

A2.2.7.1 *Receiving Room Size* and *Absorption of the Receiving Room*—The requirements for room absorption and for the lower limiting frequency for which diffuse conditions can be assumed to exist are the same, in the receiving room, as for the diffuse field procedures described in Section 6. Therefore, the restrictions of 6.2.1 and 6.3 apply here, with respect to the receiving room.

A2.2.7.2 *Absorption of the Source Room*—For the test procedure of this section to be valid, it is necessary that the pressure incident on the source side of the test partition be free of reverberant energy. Therefore, the average absorption coefficients of all the source room surfaces (except the test partition) shall be at least 0.75 (see 1.3).

A2.2.7.3 *Source Position*—It is also desirable that the sound wave be as nearly plane-progressive as possible. To this end, the (single) source of sound should be placed as far from the test partition as is consistent with keeping the entire partition within the direct field of the source and achieving the desired angles of incidence upon the test partition.

A2.2.8 *Measurement Positions:*

A2.2.8.1 *Receiving Room Side*—In the receiving room, measurements are to be made in the reverberant field. The procedure of 6.4 should be followed.

A2.2.8.2 *Source Side*—On the source side, measurements may be made at the face of the partition, if the source room side of the partition is highly reflective. For measurement of the average sound pressure level $\bar{L}_{1_o}$ at the face of the partition, the microphone should be placed as near the partition as possible without actually touching the surface and without interfering with the sound field being measured. The diaphragm of the microphone should be oriented perpendicular to the surface of the partition. A single microphone on a long stick may be moved around over the face of the partition to determine an average level; or, the average may be calculated from several measurements at fixed positions.

NOTE A3—At frequencies between 2000 and 5000 Hz, only microphones of $\frac{1}{2}$ in. in diameter, or less, will give accurate indications of the sound pressure level at the surface.

2.2.8.3 A*lternative Method*—An alternative, indirect method of evaluating the sound wave incident on the surface of the test partition is useful when the surface is absorptive. The sound pressure level $\bar{L}_1$, corresponding to the incident wave alone, is measured out-of-doors or in an otherwise free field at the same distance from the source as the test partition (if the source is directional it should be turned to face the microphone); this level plus 6 dB is then used in place of $\bar{L}_{1_o}$ in Eq A3.

A2.2.9 *Measuring the Absorption of Receiving Room:*

A2.2.9.1 The absorption of the receiving room may be measured by either of the methods described in 6.5.

A2.2.10 *Interpreting the Data to Determine Field Transmission Loss:*

A2.2.10.1 The average sound pressure levels on the source side and in the reverberant field on the receiving side, and their difference are to be determined by the averaging procedure of 6.6.1.2.

A2.2.10.2 The correction term involving the area of the partition and the absorption of the receiving room, is determined as in 6.6.2. The angle θ between the normal to the partition and the direction of the incident sound must also be measured and included in the correction term of Eq A3. A simple protractor will give a sufficiently accurate reading of the angle θ.

A2.3 Reverberant Source Room, Receiving Space Highly Absorptive or Outdoors:

A2.3.1 In this case the sound power W_1 incident on the test partition is related, as in Section 6, to the space-average sound pressure level in the source room. The procedure of Section 6 cannot be used, however, for on the receiving side of the partition there is no reverberant field and hence no unique meaning to the space-average sound pressure level. For example, if the receiving space is outdoors, one could, by extending the distance of the measurement position indefinitely, find as low a sound pressure level as desired.

A2.3.2 Instead, the sound power radiated from the partition is assessed by measurements at close-in positions and the field transmission loss is determined as follows:

$$\text{FTL} = \bar{L}_1 - \bar{L}_2' - 6 \quad \text{.....(A4)}$$

where:

$\bar{L}_1$ = average sound pressure level in the source room, and

$\bar{L}_2$ = space-average sound pressure level taken throughout a region near the test surface (but not closer than a quarter wavelength) in the receiving space (**8,9**).

A2.3.3 *Test Environment Defined:*

A2.3.3.1 *Source Room Size and Absorption of the Source Room*—The requirements for room absorption and for the lower limiting frequency

for which diffuse conditions can be assumed to exist are the same, in the source room, as for the diffuse field procedures described in Section 6. Therefore, the restrictions of 6.2.1 and 6.3 apply here.

A2.3.3.2 *Absorption of the Receiving Room*—The average absorption coefficient of the surfaces of the receiving space shall be at least 0.75 (see 1.3).

A2.3.4 *Measurement Positions:*

A2.3.4.1 *Source Side*—On the source side of the partition, the measurements should be made throughout the reverberant space to determine $\bar{L}_1$, following the procedures of 6.4.

A2.3.4.2 *Receiving Side*—The measurements on the receiving side should be made in a region near the surface to determine $\bar{L}_2'$ following the procedure of 6.4, except that no measurement position should be farther from the partition than half a typical partition dimension, nor closer than a quarter wavelength.

A2.3.5 *Measuring the Absorption of the Receiving Space*—In order for the procedure of this section to apply, the absorption in the receiving space must be high enough that the reverberant component of the sound field is effectively suppressed. Hence, it is not strictly correct to use methods for the measurement of absorption whose validity depends on the predominance of a diffuse field; this would eliminate both methods of 6.5. However, one needs to know only the *approximate* absorption in the receiving space to determine whether the environment qualifies for the test procedure described in this section; for this purpose the methods of 6.5 are suitable.

A2.3.6 *Interpreting the Data to Determine Field Transmission Loss:*

A2.3.6.1 The average sound pressure levels in the source and receiving spaces, and their corresponding difference, are to be determined as in 6.6.1. No correction for test partition area nor receiving room absorption is required; Eq A4 is used to determine the Field Transmission Loss.

A2.4 Both Source and Receiving Spaces Highly Absorptive: Plane Wave Both Sides

A2.4.1 In this situation, provided the source is far enough away, a plane progressive wave exists on both sides of the test partition. Where the source room is too small for this to be the case, judgment must be used to decide whether the maximum obtainable radius of curvature of the incident wave is such that the entire surface of the test partition is irradiated by a substantially plane wave, as required by the procedure of this section.When a plane wave is incident upon the test panel, an approximately plane wave may be assumed to radiate away from the panel on the receiving side. In terms of the sound pressure levels L_1 and L_2 in the incident and transmitted waves the field transmission loss is expressed as follows:

$$\text{FTL} = L_1 - L_2 \quad \text{(A5)}$$

However, it will usually be difficult to determine L_1 directly, because of reflections from the insonified face of the panel; therefore, it is preferable (unless the panel face is absorptive) to measure the average sound pressure level $\bar{L}_{1_o}$ at the face of the panel on the source side and to subtract 6 dB to correct for pressure doubling as follows:

$$\text{FTL} = \bar{L}_{1_o} - L_2 - 6 \quad \text{(A6)}$$

Alternatively, the method of A2.2.3 may be used to determine L_1 for use in Eq A5; or, $L_1 + 6$ may be used in place of $\bar{L}_o$ in Eq A6. Again as in A2.2 the field transmission loss should be determined as a function of the angle of incidence, θ.

A2.4.5 *Test Environment Defined*—The average absorption coefficients of all the surfaces of both source and receiving rooms (except the test partition) shall be at least 0.75 (see 1.3). The sound source should be located according to the recommendations of A2.2.7.3.

A2.4.6 *Measurement Positions:*

A2.4.6.1 *Source Side*—On the source side, the measurements should be made at the face of the partition, following the procedure of A2.2.8.2 or the alternative (free field) measurement of A2.2.8.3.

A2.4.6.2 *Receiving Side*—On the receiving side, the measurements should be made near the face of the partition, following the procedure given in A2.3.4.2 for $\bar{L}_2'$.

A2.4.7 *Measuring the Absorption of the Test Rooms*—The procedures of A2.3.5 should be followed to determine whether or not the field situation qualifies for use of the procedures of this section.

A2.4.8 *Interpreting the Data to Determine Field Transmission Loss*—The average sound pressure levels on both sides are to be determined for various angles of incidence (θ = 0 to 75 deg). No correction for partition area is required. The field transmission loss is determined from Eq A5 or A6 using $\bar{L}_2'$ as found in A2.4.6.2 for L_2, and $\bar{L}_{1_o}$ as found in A2.4.6.1.

A3. Instrumentation

A3.1 Microphones

A3.1.1 *General:*

A3.1.1.1 Microphones shall be stable and substantially omnidirectional in the frequency range of measurement. A condenser microphone with an associated cathode-follower as impedance transformer is preferred (because of its accuracy, stability and flat frequency response). Crystal or ceramic microphones are subject to a cable correction but may be used when the temperature is stabilized, or when the microphone system itself is temperature-stable. A stable wide-range dynamic microphone is also suitable. The microphone should be calibrated periodically throughout the test frequency range by a qualified laboratory technique (**13**).

A3.2 Microphone Amplifier

A3.2.1 For amplifying the microphone signal, either a stable microphone amplifier shall be used, or a sound level meter (**14**).

NOTE A4—In using USA Specification S1.4-1961, General-Purpose Sound Level Meter (**14**), to meet the requirements of amplifying the microphone signal, omit reference to paragraphs pertaining to the "A" and "B" networks.

A3.3 Frequency Analyzers

A3.3.1 For the test procedure of Section 6, frequency analyses shall be made in one-third octave bands, particularly if it is expected that a field sound transmission class will be assigned. For very informal tests and for the procedures of Appendixes A1 and A2, full octave bands may be used. (There is an advantage in the use of octave-band filters when a diffuse field is required in either of the test rooms, since the wider bandwidth allows measurement to lower frequencies in rooms where the diffusion is limited by their small size (see 6.2.1)).

NOTE A5—All filters used for frequency analyses in the procedures of this standard shall comply with the requirements of Specification for Octave, Half-Octave and Third-Octave and Filter Sets (S1.11-1966), for a Class II or BIII filter (**15**).

A3.4 Graphic Level Recorder

A3.4.1 A graphic level recorder may be used to record the sound pressure levels in the source and receiving spaces, provided that it complies with the requirements of Ref (**14**) for accuracy of rms readings. A calibration signal shall be recorded at the beginning and the end of each set of readings and all gain settings shall be noted on the graphic record.

A3.4.2 A graphic level recorder may also be used to record the decay of sound energy for the determination of absorption in the receiving room. At least 30 dB of the sound decay should be recorded, if possible. If this is not possible, the effective relation of signal to noise (in decibels) should be stated.

A3.4.3 The inherent decay rate of the recorder should be checked by rapidly shorting the recorder input while it is registering a near-full-scale input signal. The graphic record of this check should be retained. The inherent decay rate of the recorder (in decibels per second) shall be at least twice the decay rate of the sound in the test room.

A3.5 Reference Sound Source for Absorption Measurements:

A3.5.1 A reference (that is, constant output) sound source may be used to establish the total absorption in the receiving room. The reference source shall meet the following requirements:

A3.5.1.1 The sound from the reference source shall be broadband in character and without significant single-frequency components; the maximum sound pressure level of any single frequency component should be at least 10 dB below the octave-band sound pressure level.

A3.5.1.2 The sound power output of the source shall be great enough to comply with the requirements of A4.6 of this recommended practice..

A3.5.1.3 The mean square sound power output of the source shall remain constant (within ± 1 dB) over an extended period of time.

A3.5.1.4 The source shall have a resilient mounting or shall be placed on a soft pad suitably designed to prevent transmission of noise and vibration to the structure on which it is mounted.

A3.5.1.5 The source shall be essentially nondirective.

A3.5.1.6 The source shall have a maximum short-term time-variation of sound pressure level for any octave band not greater than 2 dB (measured on the slow scale of a sound level meter).

A3.5.1.7 The source shall be physically small, of the order of 1 to 2 ft maximum dimension.

A3.5.1.8 The reference source may be a loudspeaker; if so, it should be driven by (bands of) random noise and its total sound power output for a given electrical input shall be constant within the limits prescribed in A3.5.1.3 and in A3.5.1.6.

A3.5.1.9 Another acceptable form of reference sound source is a modified centrifugal fan, direct-connected to an induction motor with

TABLE A1—POWER OUTPUT OF AN AVERAGE ILG SOURCE IN A REVERBERATION ROOM

NOTE—The ILG source must rest on the bare floor, at least a half-wavelength away from other reflecting or absorptive surfaces. No cover, grille, or shroud should be attached to the fan.

Band Mid-Frequency, Hz	Sound Power Level (Diffuse Field)[a] dBre 10^{-12} w	
	One-Third Octave Band	Octave Band
40	69.0	
50	70.0	
63	70.5	75.5
80	71.0	
100	71.0	
125	72.5	77.5
160	74.0	
200	74.0	
250	75.0	79.5
315	75.0	
400	75.0	
500	75.5	80.0
630	75.0	
800	75.0	
1000	75.5	80.5
1250	76.0	
1600	76.0	
2000	76.0	80.5
2500	75.5	
3200	75.0	
4000	74.0	79.0
5000	74.0	
6300	74.0	
8000	73.0	77.5

[a] The values which appear in this table represent the average of several measurements of the ILG source in reverberant rooms. Measurements in a free-field, however, yield results which exceed the tabulated values by as much as 8 dB at frequencies below 200 Hz. These differences are attributed to a reaction of the room upon the source.

Attention is called to these differences because the (higher) free-field values may be cited in other standard test procedures. For the purpose of this document, the reverberation room data are appropriate, since the aim is to determine the total absorption in a quasi-reverberant space. On the other hand, if the aim is to determine, by means of a reverberation room comparison of an unknown with a reference sound source, the total sound power which would be emitted out-of-doors, the free-field ILG data would be used.

TABLE A1—*Continued*

stable speed characteristics (11,12). The sound power output level of this source as a function of frequency, when operated on the floor well away from walls and other large reflecting surfaces, is fairly constant; approximate average values are given in Table A1.

NOTE A6—Such a sound source is available from the ILG Electric Ventilating Co., 2850 N. Pulaski Rd., Chicago, Ill. The model number is ILG DSN 10910.

A3.5.1.10 The reference sound source shall be calibrated by a laboratory that is adequately equipped for the accurate measurement of sound power level on an absolute basis. A reverberant room method of test shall be used. See Section 3.5 of Ref (20). The sound power level calibration of the reference sound source shall be made in whatever frequency bandwidth is to be used for the analysis of sound in the measurement of field transmission loss; if the reference source is mechanical, any pertinent corrections for speed (line-voltage), temperature, barometer, etc., should be included.

A3.6 Sound Source(s) for Transmission Loss Measurements:

A3.6.1 One or more electro-acoustical sound sources shall be used to obtain the average sound pressure level difference for determination of transmission loss (or noise reduction or insertion loss). These sources may generate broadband or filtered random noise.

A3.6.1.1 The source(s) shall provide sufficient sound power at all frequencies to meet the requirements of A4.6 and A4.1.3.

A3.6.1.2 Directional loudspeakers should be avoided so as to minimize the danger of non-uniform incidence of sound on the test partition. The use of more than one loudspeaker may be necessary to generate a sound pressure level great enough to measure constructions with high transmission loss. High efficiency is more important than high fidelity in a loudspeaker for this application, though a smooth, flat (±5 dB, 100 Hz to 5000 Hz) frequency response is highly desirable.

Note A7—Some of the instructions given in the procedures (such as those concerning the placement of loudspeakers and microphones) do not necessarily contribute to increased accuracy of measurement, but are prescribed arbitrarily so that independent investigators will be more likely to arrive at the same numerical results.

A4.1 Generation of Sound Field on Source Side

A4.1.1 *Sound Source(s)*—The sound source shall be one or more loudspeakers, driven with adequate electrical power to satisfy the requirements of A4.1.3 and A4.6 and with any type of signal dscribed in A4.2 below.

A4.1.2 *Sound Source Position(s)*—Each loudspeaker should be placed in or near a trihedral corner of the room in order to excite as many room modes as possible. (This recommendation holds for most procedures; exceptions may be necessary in certain situations.) The room corners in which the loudspeakers are to be placed should be selected as follows: if one stands with his back to the test partition in the source room, the first loudspeaker shall be placed on the floor in the far right-hand corner; the second on the floor in the far left-hand corner; additional loudspeakers, if used, should be evenly spaced on the floor between the first two. If, for some reason, this convention cannot be followed, this fact should be noted and the position of the loudspeakers should be described in the test report.

A4.1.3 *Source Room Level*—The sound pressure level in the source room should be great enough to provide a signal level in the receiving room at least 10 dB above the background noise level in the measurement band at all test frequencies (background noise means here the combination of acoustical and electrical noise, see Section 1.26 of Ref (1)). Since this condition will usually be most difficult to achieve at low frequencies, the speaker should be capable of radiating the lowest test frequency efficiently.

A4.2 Test Signals

A4.2.1 *Signal Spectrum*—The source-room sound signals used for these tests shall form a series of bands of random (Gaussian) noise containing an essentially continuous distribution of frequencies throughout each test band. "Pink" noise, comprising random noise of equal power per fractional bandwidth (throughout the frequency range and also within each band) is recommended. These signals may be generated in the field with a random noise source and filter set (separate from the analyzer filter) or may be prerecorded on magnetic tape for reproduction in the field.

A4.2.2 *Test Frequencies*—The nominal test frequencies shall be selected (subject to the criterion for room diffusion of 6.2.1) from the following series: 100, 125, 160, 200, 250, 315, 400, 500, 630, 800, 1000, 1250, 1600, 2000, 2500. 3150, 4000, and 5000 Hz. Contiguous test bands shall be used, so that data are obtained for all frequencies within the chosen range. Pure tones shall not be used, since they give rise to large fluctuations in the sound field which are strongly dependent on freqnency and position.

A4.2.3 *Bandwidth*—The bandwidth of each test signal except for informal tests, shall be one-third octave for the procedure of Section 6. For the procedures of Appendixes A1 and A2, either octave or one-third octave bands may be used. The over-all frequency response of the electrical system, including the filter or filters in the source and microphone circuits, shall for each test band conform to specification for Octave, Half-Octave and Third-Octave Band Filter Sets (S1.11-1966), for a Class II or III filter (15).

A4.2.4 Filtering may be done either in the source or microphone system or partly in each, provided that the required over-all characteristic is achieved. Apart from defining the bands of test signals, a filter in the microphone system serves to filter out extraneous noise lying outside the test band, including possible distortion products in the source system; a filter in the source system serves to concentrate the available power in the test band.

A4.3 Sensitivity Check

A4.3.1 All instruments shall be carefully checked at the time of the tests. This is particularly important in field measurements where the hazards of transportation increase the likelihood that the equipment will be found out of adjustment at the test site.

A4.3.2 When source room levels and receiving room levels are to be measured with the same instruments, sensitivity checks shall be performed before beginning the measurements in each room and at intervals during the test, to assure drift of not more than 0.5 dB.

A4.3.3 When two sets of sound level measuring equipment are used for measurement of sound levels in the source and receiving rooms, the sensitivity of both sets shall be checked before field tests are begun and at intervals of not more than 30 min thereafter. The same calibration equipment shall be used for all calibrations. The microphones must all be of the same make and model.

A4.3.4 The sensitivity check of the microphone(s) shall be made using an acoustic or electrostatic calibrator which has electronic drift of not more than 0.5 dB in a day. The sensitivity check shall usually consist of impressing a known sound pressure upon the microphone and noting the unfiltered electrical output of the entire microphone system, keeping account of all variable gain settings in the equipment. This establishes a sensitivity in terms of which all subsequent electrical outputs, filtered or not, can be converted back to sound pressure levels at the microphone, taking account of the filter response and any changes of gain in the system.

NOTE A8—A nominal sine wave having less than 10 per cent distortion and unvarying amplitude to within 0.1 dB is recommended.

A4.3.4.1 If only relative levels are required (for example, if the same system is used in both source and receiving rooms, and the absorption of the receiving room is determined from the decay rate, rather than from the absolute levels established by a reference source), a check is needed only to assure that the over-all sensitivity remains constant throughout the test. The checking procedure should be carried out in such a way as to eliminate errors caused by variations in response between microphones when used in reverberant sound fields.

A4.3.5 The sensitivity check in the field need be made at only one frequency within the range from 200 to 1250 Hz.

A4.3.6 The entire measuring set-up (including the microphone, all cables, and instruments) shall be included in the check for sensitivity. The entire set-up must be rechecked after any changes, adjustments, or substitutions of cables or equipment.

A4.4 Sound Pressure Level Measurements

A4.4.1 *Averaging Time*—For each sampling position, the averaging time shall be sufficient to permit an accurate estimate, from observations of a sound level meter or a graphic level record, of the time-average sound pressure level.

A4.4.2 *Number and Precision of Measurements*—One or more microphones, or a single moving microphone may be used to determine the average sound pressure level in the test rooms. If only one or two microphones are used, the average may be obtained by moving them to several different stations in the rooms. If a large number of microphones are used at different stations in the rooms, their outputs may be observed consecutively by switching between microphones.

A4.4.3 It is not recommended that the electrical outputs of two or more microphones be combined. However, if the averaging is done by combining outputs electrically, the following precaution must be taken: squared outputs, rather than linear outputs, must be combined; the microphones must be matched in sensitivity within 1 dB over the frequency range of interest.

A4.4.4 A minimum of five measurement positions shall be used (see 6.4), but measurements shall be made at enough positions that the standard deviation of the mean of the N readings in each frequency band is less than 2.0 dB, defined as follows:

$$\text{Standard deviation} = \sqrt{\frac{\Sigma_n (L_n - \bar{L}_n)^2}{N (N - 1)}} \quad ..(11)$$

For convenience in making this calculation, $\bar{L}$ may be computed from $(\Sigma_n L_n)/N$. However, the average $\bar{L}$ to be used in calculating field transmission loss must conform with the definition in 4.1.1.

A4.4.5 *Measurement Filters*—Where the bandwidth of the sound source is greater than the desired analysis bandwidth, or where it is necessary in order to meet the requirements of A4.1.3, analyzing filters must be used in the measuring equipment. These filters must conform to the requirements of A3.3. The same filters should be used to measure both the absorption in the receiving room and the average sound pressure levels in the test spaces.

A4.5 Checks for Flanking Transmission

A4.5.1 In measurements where the field transmission loss of the test panel is required, rather than just the noise reduction, flanking transmission must be reduced to a negligible amount so that the measured levels in the receiving room correspond to only that sound which is transmitted through the partition under test. The following procedures may be used to determine whether or not significant flanking exists. Note that the flanking test of A4.5.5 is mandatory.

A4.5.2 The first and simplest check is to walk around the receiving room and, listening either with a stethoscope or with the unaided ear, try to detect obvious leaks, where sound is entering the space by way of unintended paths.

NOTE A9—A word of caution is in order concerning the use of a stethoscope to detect leaks: ordinarily the diaphragm head of the instrument is removed and one probes with the open end of the tube into corners and along edges where leaks are suspected. As the tip of the tube is

moved into a corner, one usually hears an increase in sound level at high frequencies due to "pressure doubling" near boundaries and corners; this effect should not be mistaken for a sound leak.

A4.5.3 One may also investigate whether the surfaces of the receiving room other than the test partition are vibrating significantly at the frequency of the sound source; an accelerometer may be used to compare the vibration of the test partition with that of other surfaces. The average vibration level of each of the other room surfaces should be at least 10 dB below that of the test partition.

A4.5.4 After the transmission loss calculations have been made, the resulting field data may be compared with laboratory transmission loss data for a similar type of partition. One should not necessarily expect close agreement, but widely divergent trends may indicate the existence of flanking paths, of leaks, or of deviations from the nominal construction of the test specimen.

A4.5.5 The following test shall be performed, for all field transmission loss measurements according to the procedures of Section 6 and Appendix A2, to demonstrate the absence of significant flanking transmission:

TABLE A2—CORRECTIONS FOR AMBIENT SOUND PRESSURE LEVELS

	dB						
Difference between sound pressure level measured with sound source operating and ambient sound pressure level alone.	4	5	6	7	8	9	10
Correction to be subtracted from sound pressure level measured with sound source operating to obtain sound pressure level due to sound source alone....	2.2	1.7	1.3	1.0	0.8	0.6	0.4

A4.5.5.1 After the ordinary measurements have been made to determine the field transmission loss, a special temporary shield (see below) shall be added to the test partition to increase its effective transmission loss. The measurements are then repeated. If the measured values of transmission loss change as a result of the added skin by at least 3 dB, it can be assumed that no significant flanking exists. If this is not the case, then the flanking paths must be located and corrected.

NOTE A10—An alternative procedure (which is more difficult but may help eliminate existing flanking paths in addition to detecting their presence) is to add a second skin to all four boundaries (the side walls, floor and ceiling) adjacent to the test specimen and remeasure the average sound levels. In this case, any change in measured results is usually an indication that flanking transmission present in the original test has been reduced.

A4.5.5.2 All data for which the flanking transmission cannot be effectively eliminated must be clearly identified in the report, but it may be stated that the field transmission loss is at least as great as the flanked data indicate.

A4.5.5.3 A convenient means of adding the supplementary skin is to support pieces of $\frac{1}{2}$-in. gypsum board or plywood in front of the test panel at a distance of about 6 in.

NOTE 11—It may be convenient to arrange the panels in a splayed, zig-zag configuration so that, when the edges are taped, the array is free-standing, like a decorative screen.

A4.5.5.4 The total projected surface area of the added skin should be slightly smaller than that of the test panel itself. All internal joints of the skin should be sealed by taping. A substantial amount of sound absorbing material should be distributed evenly throughout the airspace between the skin and the test panel. To form a seal around the edges of the skin, strips of heavy ($\frac{1}{2}$ lb/ft^2) flexible sheeting (such as lead-filled vinyl plastic or sheet neoprene) should be taped to the edges of the skin and also the walls bounding the test partition.

A4.5.5.5 Care must be taken that the area thus shielded comprises all of, but no more than, the structural elements making up the specimen under test. For example, in the case of an operable or demountable partition, it is usually understood that the manufacturer has the responsibility of providing an adequate seal to the surrounding structure; this seal, therefore, is part of the specimen under test. In this case, the supplementary skin should be taped just *outside* the seal, so that the seal is covered (as part of the specimen) for the second measurement.

A4.5.5.6 The supplementary skin may be added on either side of the test partition, but if

it is applied on the source side, there is no need to remeasure the absorption in the receiving space.

A4.6 Check for Background Noise

A4.6.1 At the beginning and end of each test a check shall be made for electrical and acoustical background noise by measuring the sound pressure level in the receiving room in each frequency band used for the transmission loss tests. This measurement shall be made with no modification of the test setup or test room, except that the sound source shall be turned off. If the sound pressure level measured with the source operating is at least 10 dB greater in each frequency band than with the source silent, the error in the test measurement due to background noise will be less than $\frac{1}{2}$ dB.

A4.6.1.1 *Correction for Ambient Sound Pressure Level*—If, in any frequency band, the average sound pressure level in the receiving room with the sound source operating exceeds the ambient sound pressure level by only 4 to 10 dB, the observed receiving room levels are likely to be in error. The true sound pressure level due to the sound source alone may be approximated by applying to the measured levels the corrections listed in Table A2. These corrections are based on the assumption that the indicating meter responds to root-mean-square (rms) sound pressure, but they are approximately applicable to the indicating instruments used in standard sound-level meters. It is further assumed that the ambient sound pressure and the sound pressure due to the sound source are incoherent and can, therefore, be added on a "pressure-squared" basis. If the contributions from the sound source and the ambient noise are coherent, phase relations are important and corrections in general terms cannot be stated.

A4.7 Measuring the Damping of the Partition

A4.7.1 For some types of partition there is a strong influence of partition damping on the observed transmission loss. Although this exact relation is not yet well understood, it is desirable that data on in-place partition damping be collected for later reference and study. Accordingly, this recommended practice encourages, but does not require, for each test specimen whose transmission loss is measured in the field, a measurement of the damping (loss-tangent) as a function of frequency (19).

A4.8 Temperature and Relative Humidity

A4.8.1 Wet- and dry-bulb temperature readings should be made in both source and receiving rooms. The relative humidity should be calculated and reported for both rooms.

References

(1) USA Standard Acoustical Terminology (USAS S1.1-1960).

(2) ASTM Recommended Practice E 90, for Laboratory Measurement of Airborne Sound Transmission Loss of Building Partitions, *1967 Book of ASTM Standards*, Part 14.

(3) ISO Recommendation R 140, "Field and Laboratory Measurements of Airborne and Impact Sound Transmission," (1960).

(4) ASTM Method C 423, Test for Sound Absorption of Acoustical Materials in Reverberation Rooms, *1967 Book of ASTM Standards*, Part 14.

(5) Buckingham, Edgar, "Theory and Interpretation of Experiments on the Transmission of Sound Through Partition Walls," *Scientific Papers of the Bureau of Standards*, No. S-506, Vol 20 (1925).

(6) London, A., "Methods for Determining Sound Transmission Loss in the Field," *National Bureau of Standards Research Paper*, p. 1388 (1941). (See cautionary note in Appendix A2.)

(7) "Standard Specification for Ceiling Sound Transmission Test by Two-Room Method," *Acoustical Materials Association Method of Test AMA-1-II* (1967).

(8) Beranek, L. L., *Acoustics*, McGraw-Hill Inc., New York, N. Y., pp. 324–327 (1954).

(9) Beranek, L. L., "Noise Reduction," "Some Practical Acoustical Measurements," eq. 7.3, and Chapter 13, "The Transmission and Radiation of Acoustic Waves by Solid Structures," McGraw-Hill Inc., New York, N. Y. (1960).

(10) Measurement of Sound Power Radiated from Heating, Refrigerating, and Air Conditioning Equipment (ASHRAE Standard 36-62).

(11) Wells, R. J., and Wiener, F. M., "On the Determination of the Acoustic Power of a Source of Sound in Semi-Reverberant Spaces," *Noise Control*, Vol 7, January 1961, pp. 21–29.

(12) Hardy, Howard, "Standard Mechanical Noise Sources," *Noise Control*, Vol 5, pp. 22–25 (1959).

(13) Method for Pressure Calibration of Laboratory Standard Pressure Microphones (USAS S1.10-1966).

(14) Specification for General-Purpose Sound Level Meters (USAS S1.4-1961).

(15) USA Standard Specification for Octave, Half-Octave and Third-Octave Band Filter Sets (USAS S1.11-1966).

(16) Sepmeyer L. W., "Computed Frequency and Angular Distribution of the Normal Modes of Vibration in Rectangular Rooms," *Journal of the Acoustical Society of America*, Vol 37, 1965, p. 413–423.

(17) Benson, R. W., and Huntley, R., "The Effect of Room Characteristics on Sound Power Measurements," *Noise Control*, Vol. 5, 1959, pp. 59–77.

(18) Waterhouse, R. V., "Interference Patterns in Reverberant Sound Fields," *Journal of the Acoustical Society of America*, Vol 27, 1955, p.247.

(19) Watters,B. G., "Transmission Loss of Some Masonry Walls," *Journal of the Acoustical Society of America*, Vol 31, 1959, pp. 898–911.

(20) USA Standard Method for the Physical Measurement of Sound (USAS S1.2-1962).

(21) Proposed Classification for Determination of Sound Transmission Class (ASTM RM 14-2) (1966).

(22) Proposed Method of Steady-State Determination of Changes in Sound Absorption of a Room (ASTM RM 14-3) (1966).

ISO RECOMMENDATION R 140 - 1960

FIELD AND LABORATORY MEASUREMENTS OF AIRBORNE AND IMPACT SOUND TRANSMISSION[1]

Abstract by R. L. Bloss

This recommendation provides definition of terms (average sound pressure level, average sound pressure level difference, normalized level difference, sound reduction index or transmission loss, and normalized impact sound level) and describes methods for field and laboratory measurements of airborne sound transmission and impact sound transmission. Generation of the sound field, measurement of the appropriate parameter, and presentation of the results are discussed.

This recommendation was accepted by the ISO Council in January 1960 following approval by twenty member bodies and with the opposition of one member body. While the techniques outlined may be in some respects inadequate, the present recommendation describes uniform methods of testing and presentation of data which permit direct comparison of results obtained by different workers.

Key Words: Airborne sound, Impact sound, Measurement, Sound insulation, Sound transmission.

---

[1] Available from American National Standards Institute, Inc., 1430 Broadway, New York, New York 10018, price $2.40.

AMERICAN STANDARD METHOD FOR THE PHYSICAL MEASUREMENT OF SOUND ANS S1.2 - 1962[1]

Abstract by R. D. Berendt

This standard is concerned with the measurement of sound produced by any source, device, machine or apparatus under specified conditions of use in various types of acoustical environments ranging from highly diffuse and reverberant enclosures to free field, outdoor situations or anechoic chambers.

The standard establishes methods for measuring and reporting the sound pressure levels and sound powers radiated by a source of sound as a function of frequency. Instrumentation, microphone locations, acoustical properties of the enclosures, measurement of the appropriate parameters, and presentation of results are discussed.

This standard was approved on August 20, 1962 by the American Standards Association, Inc., presently the American National Standards Institute.

Key Words: Diffuse field, Free field, Reflecting plane, Semireverberant field, Sound power, Sound pressure level.

---

[1] Available from American National Standards Institute, Inc., 1430 Broadway, New York, New York 10018, price $2.50.

2. Fluid Mechanics

U. S. Department of Commerce National Bureau of Standards

RESEARCH PAPER RP850

Part of Journal of Research of the National Bureau of Standards, Volume 15, December 1935

EFFECT OF HUMIDITY IN HOT-WIRE ANEMOMETRY

By Galen B. Schubauer

ABSTRACT

The possibility of a humidity effect on the heat loss from a heated wire in an air stream has long been recognized, but only recently was the effect found experimentally by Paeschke. The effect is to increase the heat loss at the higher humidities. The present paper describes an experiment conducted to verify the existence of the effect. The results show an increase of heat loss per degree rise in wire temperature of about 2 percent for a change in the partial pressure of water vapor from 0.007 to 0.023, or a change in relative humidity from 25 to 70 percent in the neighborhood of 25° C. The effect may be explained by an effect of humidity on the thermal conductivity of air.

A hot-wire anemometer consists essentially of a small electrically heated wire, usually of platinum, which may be exposed to an air stream in which the speed is to be measured. Associated apparatus is required for controlling the heating current and measuring the rate of heat loss from the wire. The theoretical relation between the rate of heat loss and the air speed is given by the following formula due to King: [1]

$$\frac{H}{\Delta T}=4.18\, l\, (k+2\sqrt{\pi k\rho c r V}), \qquad (1)$$

where

H=heat loss from the wire to the surrounding air in watts.
ΔT=temperature elevation of the wire above the temperature of the surrounding air in degrees C.
l=length of the wire in centimeters.
k=thermal conductivity of air in cgs units.
ρ=density of air in cgs units.
c=specific heat of air at constant volume in cgs units.
r=radius of wire in centimeters.
V=air speed in centimeters per sec.

Since the heat lost from the wire by radiation is neglected in equation 1 and also since k, near the wire, and r may not be known with sufficient accuracy, the hot-wire anemometer cannot be used as an absolute instrument, but must be calibrated by measuring $H/\Delta T$, or some related quantity, in a stream of known speed. It is the universal experience of those working with hot-wire anemometers that the calibration cannot be relied upon over long periods of time. Aside from such changes as may occur due to damaging of the wire in handling, other changes of a seemingly erratic nature take place which are difficult to account for, and which have done much to discourage the use of hot-wire anemometers in precise work.

[1] L. V. King, *On the convection of heat from small cylinders in a stream of fluid: Determination of the convection constants for small platinum wires with application to hot-wire anemometry.* Phil. Trans. Roy. Soc. 214, 373, (1914).

It has long been suspected that changes in the heat loss from the wire may occur through the effect of humidity on such quantities as k, ρ, and c in equation 1. It is known that the presence of water vapor in the air increases the thermal conductivity for small partial pressures of the vapor,[2] and for this reason an increase of heat loss with increasing humidity is to be expected. The effect of humidity on the product of density and specific heat is exceedingly small and as a contributing factor can probably be neglected. While it is possible to predict the direction of the effect from equation 1, it is difficult to estimate its magnitude due to the neglected radiation loss. Furthermore the value of k for air containing small amounts of water vapor is not definitely known at temperatures below 80° C.

An increase in the heat loss from a wire as the result of increasing the humidity was recently found experimentally by W. Paeschke.[3] An earlier attempt to find an effect of humidity, made by Kennelly and Sanborn[4] in connection with the effect of air density on the heat loss from a wire, led to the conclusion that the effect, if present, was too small to be detected. However, in the latter tests, no humidity measurements were made.

The effect was investigated at the National Bureau of Standards in a small return-circuit wind tunnel in which the relative humidity could be varied between 25 and 70 percent. The wire, which was of platinum 0.05 mm in diameter and 27.0 mm long, was placed in the working section about 10 cm from a standard pitot-static tube by which the speed was measured. The direction of the air flow was upward and normal to the wire. All accompanying apparatus, such as current controls and potentiometer, were located outside the tunnel where the humidity remained essentially constant.

The relative humidity in the tunnel could be raised from about 25 to near 70 percent in 2 or 3 hours by placing water in troughs along the tunnel walls and allowing a large area of cloth, inside the tunnel on the return-duct walls, to become wet by capillary attraction. The removal of the water and the circulation of outside air through the tunnel lowered the relative humidity to within a few percent of the outside value in about 4 hours. It was possible therefore to change rather quickly from one condition to another without the necessity of changing the temperature or disturbing the experimental setup. The relative humidity was measured by a hair hygrometer, which had previously been calibrated.

Since the air temperature changed but little, varying only between 23 and 27° C, and the barometric pressure remained essentially constant at 756 mm of mercury, the humidity changes were really changes in the absolute humidity. By taking into account the temperature changes, the readings of the hygrometer were converted into absolute numidities. These are expressed here in terms of the partial pressure of water vapor, denoted by p_2.

The experimental procedure consisted in measuring the potential drop across the wire at various wind speeds for a constant heating current. The wire temperature was allowed to vary with the speed. Using these data together with the temperature resistance curve for

[2] H. A. Daynes, Gas Analysis by Measurement of Thermal Conductivity. Cambridge University Press, p. 23 (1933).
[3] W. Paeschke, *Feuchtigkeitseffekt bei Hitzdrahtmessungen*, Physik Z. 36, 564 (1935).
[4] A. E. Kennelly and H. S. Sanborn, *The influence of atmospheric pressure upon the forced thermal convection from small electrically heated platinum wires*, Proc. Am. Phil. Soc. 52, 55 (1914).

the wire, which was obtained by measurements of the wire resistance at the temperature of the surrounding air, $H/\Delta T$, the heat loss per degree rise in temperature, was calculated. From a number of such determina-

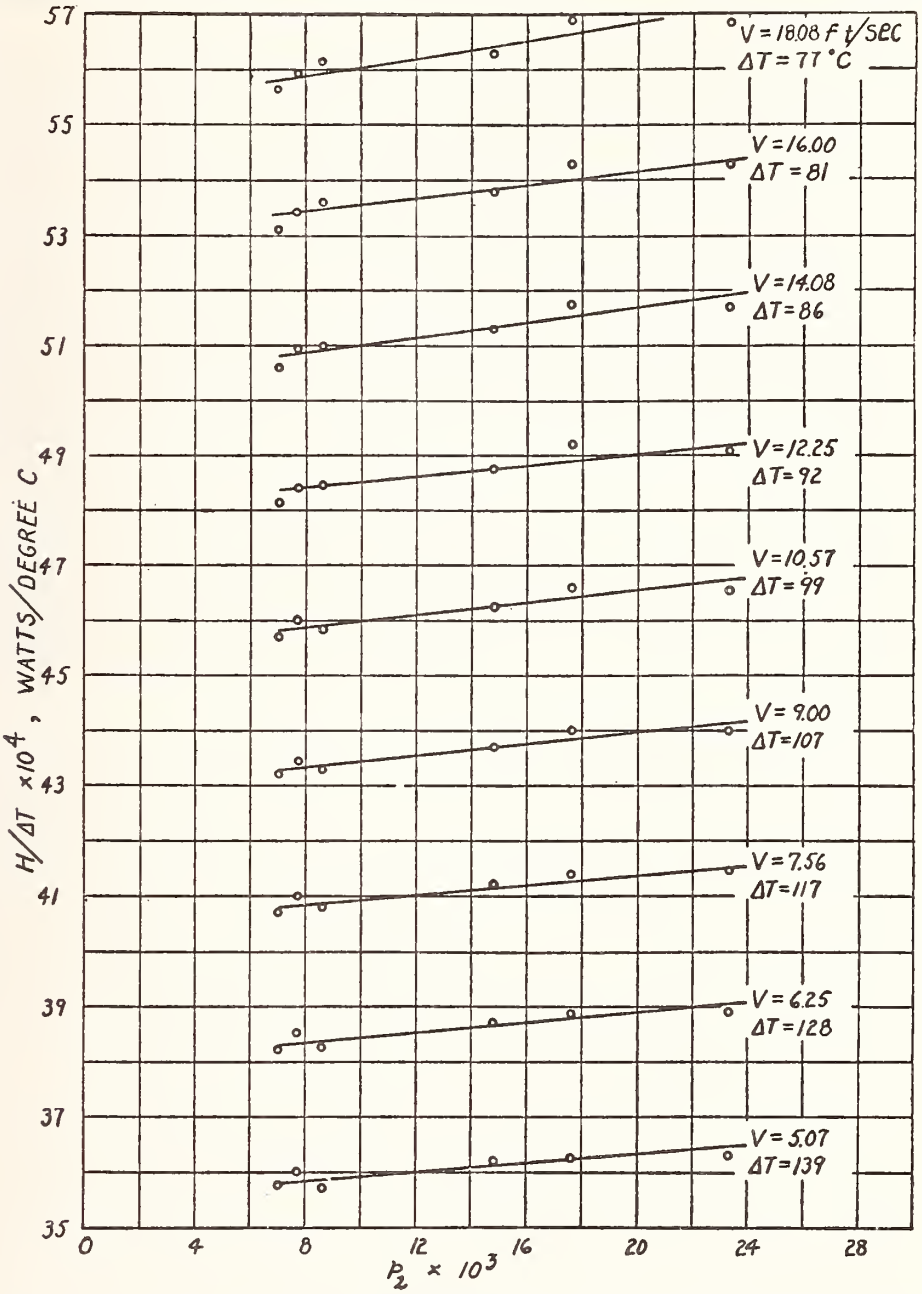

FIGURE 1.—*Variation of heat loss per degree rise in wire temperature with variation in humidity.*

(p_2=partial pressure of water vapor.)

tions corresponding to several relative humidities ranging from 25 to 70 percent, the variation in $H/\Delta T$ with humidity was determined.

The results obtained with a heating current of 0.464 ampere are summarized in figure 1. The spacing between curves in this figure

is determined by the change in $H/\Delta T$ in going from one speed to the next. The approximate temperature elevation ΔT of the wire corresponding to the various speeds is also shown. Considering a change in p_2 from 0.007 to 0.023, figure 1 shows an average increase in $H/\Delta T$ of about 1.8 percent.

An effort was made to determine the effect of wire temperature by obtaining a similar set of curves in the same speed range using a lower heating current (ΔT ranging from 42 to 70° C). In the latter determination the accuracy was lower, but the same general change in $H/\Delta T$ with humidity was found as in figure 1. In these determinations the average change in $H/\Delta T$ corresponding to a change in p_2 from 0.007 to 0.023 was 2.0 percent. There is therefore no conclusive evidence of a dependence of the effect on wire temperatures. These results agree well with those obtained by Paeschke, where a 2-percent increase in heat loss was found for a change in the relative humidity from 30 to 80 percent.

The precision of the present work does not warrant a more definite conclusion than that approximately a 2 percent change in heat loss per degree rise in temperature may be expected for a change in p_2 between the above limits (0.007 to 0.023), corresponding to a change in relative humidity from 25 to 70 percent in the neighborhood of 25° C. For practical purposes the effect may be regarded as linear. Under the present conditions, a change in heat loss of this magnitude was equivalent to a change in air speed of about 6 percent. Hence, if errors of this order are to be avoided, it is essential that the humidity be taken into account both in calibration of the wire and in its subsequent use.

Washington, September 7, 1935.

U. S. Department of Commerce National Bureau of Standards

RESEARCH PAPER RP1056

Part of Journal of Research of the National Bureau of Standards, Volume 19, December 1937

EFFECT OF YAW ON VANE ANEMOMETERS

By Roy H. Heald and Paul S. Ballif

ABSTRACT

The effect of yaw on the performance of three vane-type anemometers was determined in the wind tunnel. Observations were made for angles of yaw within a range of 35 degrees on either side of the zero position. Maximum positive errors of 1, 4, and 5.5 percent were found for the three instruments when the angle of yaw was approximately 15 degrees. The magnitude of the error depends on the design.

CONTENTS

I. INTRODUCTION

The customary practice in using a vane anemometer is to mount the instrument so that the axis of rotation of the vane wheel is parallel to the axis of the fan or duct for which measurements are to be made. Usually no attempt is made to determine whether or not the air flow is parallel to the duct or fan axis, it being assumed that no appreciable error is introduced on this account. Ower [1] states, for a particular instrument, that the directional effects due to yaw may introduce errors of the order of 1 percent for angles of inclination less than about 20 degrees, but points out the uncertainties involved in drawing conclusions from the performance of a single instrument. Differences in design of anemometers constructed by different manufacturers are often encountered in practice. Hence differences in response to directional effects are to be expected, especially when the direction of air flow makes a large angle with the reference axis.

Recently, in determining the air deliveries of electric fans, the direction of air flow was found to be inclined 20 degrees or more to any plane containing the fan axis. In such cases, accurate results can be obtained with an anemometer mounted with its axis parallel to the fan axis only if the correction factor for airstream inclination is known and applied. For this reason an investigation was undertaken

[1] E. Ower. Measurement of Air Flow, 2d ed., p. 119. (Chapman and Hall, London, 1933.)

37172—38

to determine the effect of airstream inclination, in yaw,[2] on the performance of the three vane anemometers used in the fan tests. The information may be of interest to other investigators who have occasion to use vane anemometers under unfavorable conditions of air flow.

II. DESCRIPTION OF THE ANEMOMETERS

The anemometers used in these experiments are shown in the halftone figure 1, and in the detail drawings, figure 2. The length/diameter ratios of the cylindrical housings are 0.43 for anemometer *A*; 0.32 for anemometer *B*; and 0.59 for anemometer *C*. Anemometers

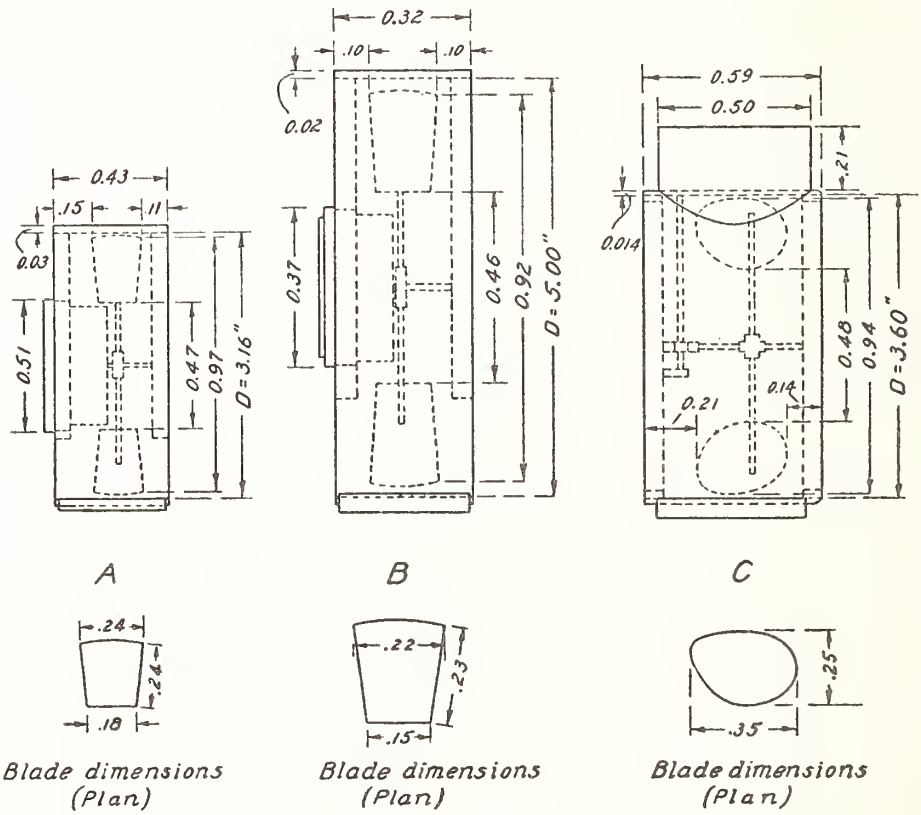

FIGURE 2.—*Line drawings of the anemometers.*

The dimensions are given as decimals of the inside diameter of the housing.

A and *B* are dial indicating. Anemometer *C* transmits signals electrically.

The plane of rotation of the upstream tips of the rotor vanes is 0.11 diameter within the housing for anemometer *A*; 0.10 diameter for anemometer *B*; and 0.14 diameter for anemometer *C*, the inside diameter of each housing being used as a reference. The rotor vanes have plane surfaces.

[2] The yaw angle is defined as the angle in a horizontal plane between the axis of the instrument and the direction of air flow. Since the anemometer is nearly a symmetrical instrument the effects of pitch, i. e., of inclination in a plane normal to the yaw plane, are not expected to differ greatly from the effects of yaw.

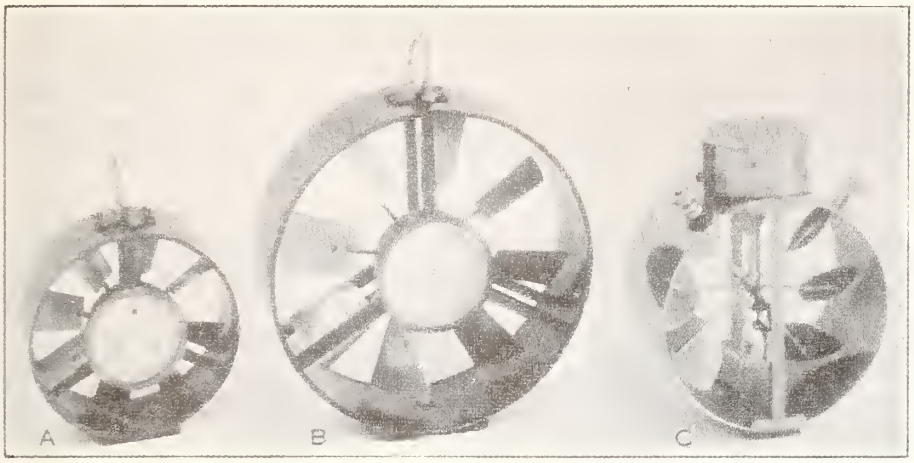

FIGURE 1.—*Three vane-type anemometers (A, B, and C) used in the experiments.*

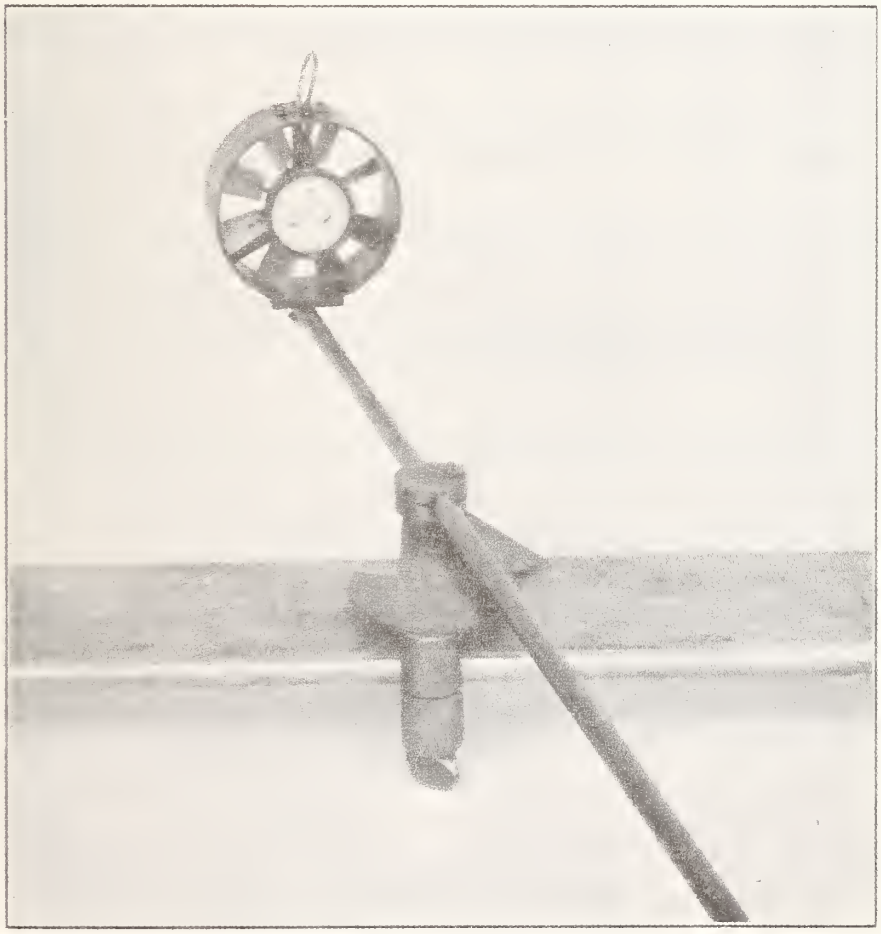

FIGURE 3.—*Anemometer support.*

III. METHOD OF TEST

The anemometers were tested in the 54-inch wind tunnel of the National Bureau of Standards. The instrument under test was attached to a cylindrical mounting rod ⅜ inch in diameter and 3 feet long. The mounting rod was clamped to a faired strut (fig. 3) fixed to the tunnel walls. The effect of the presence of the strut and clamping device was determined for each anemometer by observing the indicated velocity when the instrument was mounted various distances ahead of the strut. As may be seen in figure 4, the effect of the strut and clamp was found to be small for positions more than 6 inches ahead of the strut.

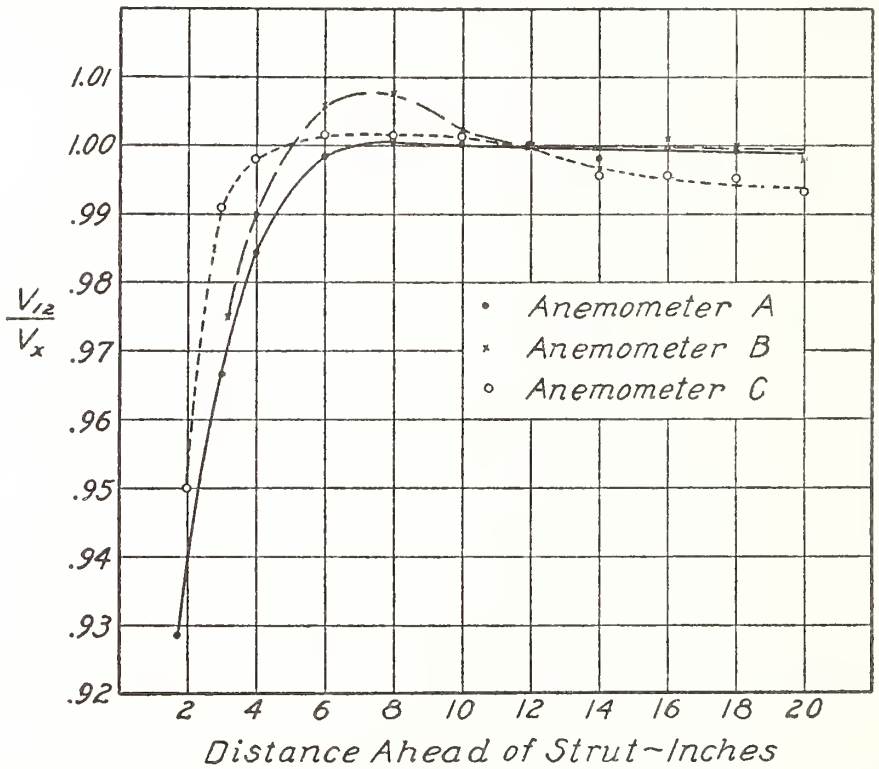

FIGURE 4.—*Effect of support interference on the velocity indications for zero yaw.*

V_{12}=indicated velocity at point 12 inches ahead of the strut.
V_x=indicated velocity at point x inches ahead of the strut.

The method of mounting the anemometers, illustrated in figure 3, permitted yawing of the mounting rod through an angle of about 45 degrees on either side of the center position. Yaw settings were read on a graduated scale mounted on the clamp. The mounting screw in the base of the anemometer was maintained at a point 12 inches ahead of the strut and midway between opposite walls of the wind tunnel for all angle settings by adjusting the clamp and mounting rod. Thus the effect of the small velocity gradient in the wind tunnel was eliminated.

The velocity indicated by each anemometer was observed for angles of yaw in intervals of 5 degrees through a range of −35 to +35 degrees. At least two observations of indicated velocity were made

for each yaw setting and for each of two air velocities, approximately 800 feet per minute and approximately 1,500 feet per minute. The constancy of the air velocity through the tunnel during the tests was of the order of 1 percent. The time interval for each observation was about 2 minutes.

IV. RESULTS

The ratio of the true air velocity in the wind tunnel to the velocity indicated by the anemometer was computed for each observation. The results for anemometer *B* are plotted in figure 5. The curves are similar to those obtained for instruments *A* and *C*. The difference in the value of the ratio, true velocity/indicated velocity, for air velocities of 800 feet per minute and 1,500 feet per minute is characteristic of the three anemometers tested and results from the non-

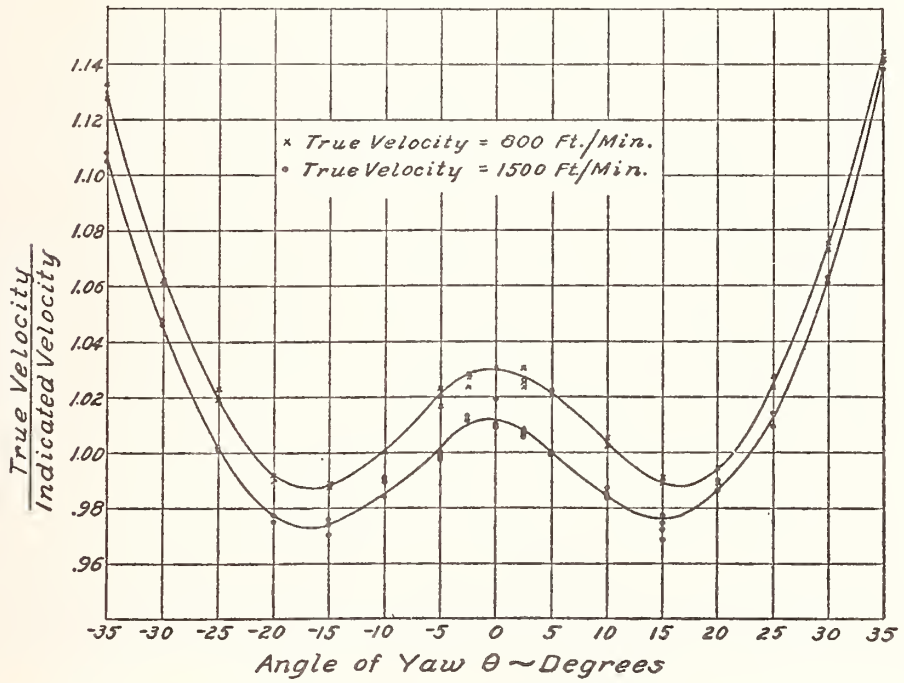

FIGURE 5.—*Values of true velocity/indicated velocity for positive and negative angles of yaw, anemometer B.*

linear relationship between the friction of the bearings and indicating-mechanism load and the torque applied to the vanes by the air stream. Ordinarily, corrections for this difference are made by using the calibration curve for the instrument.

The ratio of the indicated velocity V_0 for zero yaw, to the indicated velocity V_θ for angle of yaw θ, was computed for each observation. The curves in figure 6 show the mean values of V_0/V_θ, all of the observations obtained for a given angle of yaw for each instrument being used. In general, the indicated velocity increased as the angle of yaw was increased, reaching a maximum when the angle of yaw was about 15 degrees. Further increase in the angle of yaw resulted in a decrease in indicated velocity. The indicated velocity for 15 degrees of yaw, for anemometers *A*, *B*, and *C*, was about 5.5, 4, and

1 percent, respectively, greater than the indicated velocity at zero yaw; for approximately 30, 27, and 18 degrees of yaw, respectively, the indicated velocity was the same as for zero yaw and for greater angles of yaw the indicated velocity was less than for zero yaw.

It will be noted from figures 1 and 2 that anemometer *A* which showed a maximum positive error of 5.5 percent, is substantially different in design from anemometer *C*, which showed a maximum positive error of about 1 percent. For example, there is a decided difference in the shape of the vanes. Also, the dial of anemometer *A* exerts a blocking effect over about 25 percent of the area of the housing, while the housing of anemometer *C* is comparatively free from obstruction. Further, the length/diameter ratios of the housings are

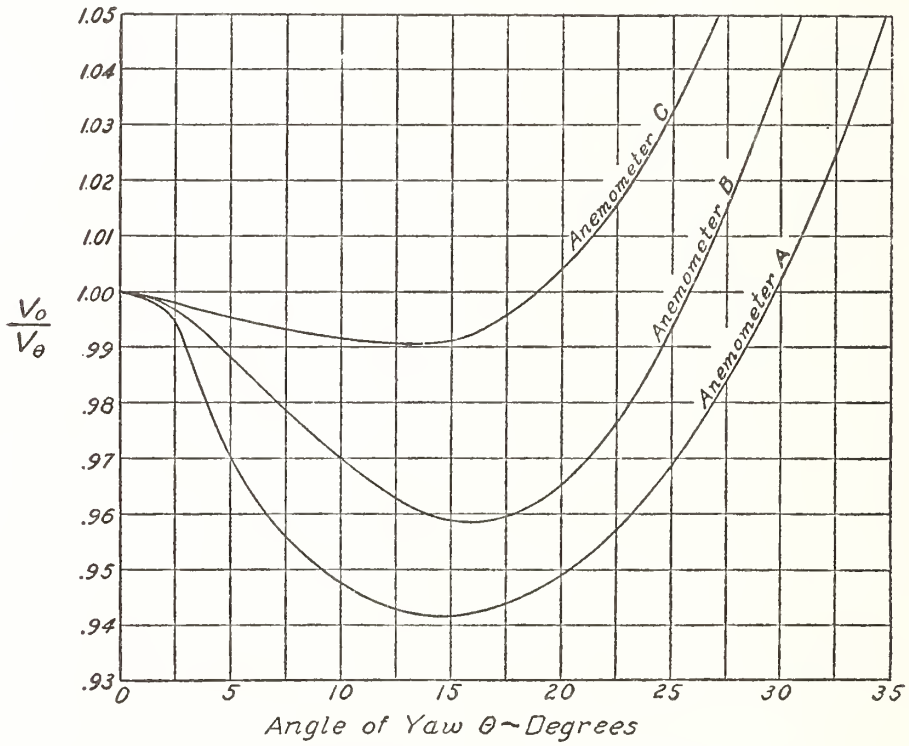

FIGURE 6.—*Effect of angle of yaw on the velocity indications.*
The curves give mean values of V_0/V_θ.

different. Other dissimilarities are to be found, such as differences in wall thickness and external fittings.

A few experiments were made wherein the length/diameter ratio of anemometer *A* was increased about one-third by adding a cylindrical extension to the housing. The results showed a decrease of a small amount in the directional error. Hence it appears that the magnitude of the error due to inclination of the airstream depends on the design of the anemometer, and it is not possible to ascribe the differences in directional sensitivity of the instruments used to any one design characteristic.

The use of the curves in figure 6 is shown by the following example. Suppose the reading of anemometer *A*, corrected for the calibration error at zero yaw, to be 1,240 feet per minute. Also suppose the

direction of air flow with respect to the anemometer axis to be 20 degrees. This angle corresponds to the angle Θ and usually may be determined with sufficient accuracy by means of a light thread and a protractor. Referring to figure 6, the correction factor for anemometer *A* when Θ is 20 degrees is 0.949. Hence the true velocity, in a direction making an angle of 20 degrees with the anemometer axis, is 1,240 × 0.949=1,176 feet per minute.

In most cases it is desired to know the component of the airstream velocity parallel to the axis of the fan or duct. This component is determined by resolving the true velocity, obtained as above, in the direction of the anemometer axis. In the example the value is 1,176× cos 20°=1,105 feet per minute. It will be noted that the component of airstream velocity parallel to the axis of the fan is 10.8 percent less

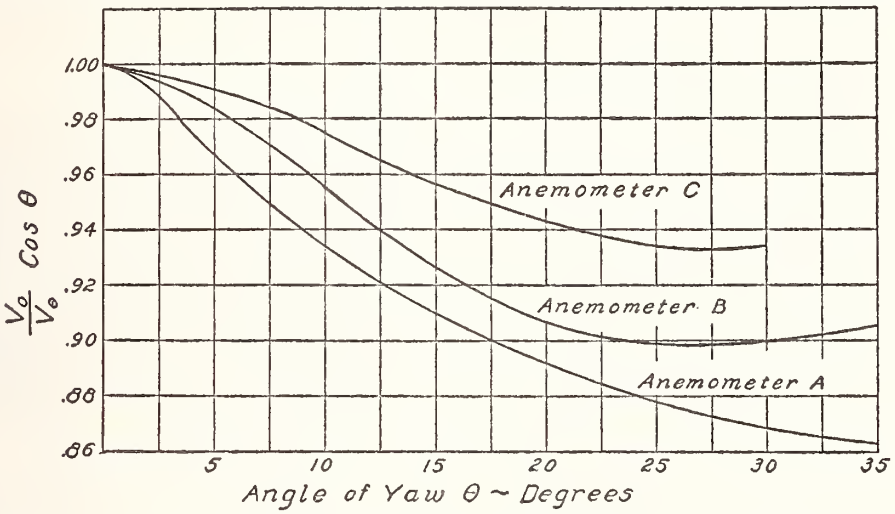

FIGURE 7.—*Correction curves for the anemometers to facilitate computation of the axial component of the velocity.*

than the velocity indicated by the anemometer. To facilitate computation in similar cases, the ordinates of the curves in figure 6 may be multiplied by cosine Θ and be plotted as shown in figure 7.

V. CONCLUSIONS

The effect of airstream inclination on the performance of three vane anemometers was determined in the wind tunnel. The results show the presence of substantial directional errors within the 0- to 35-degree range of yaw angles. A maximum directional error of about 5.5 percent occurred when one of the instruments was displaced about 15 degrees from alignment with the air stream of the wind tunnel. An error of about 1 percent was observed when an anemometer of substantially the same diameter but of different design was displaced the same amount. The experiments indicate that the magnitude of the error due to inclination of the air stream depends on the design of the anemometer.

WASHINGTON, September 25, 1937.

U. S. Department of Commerce
National Bureau of Standards

Research Paper RP1872
Volume 40, April 1948

Part of the Journal of Research of the National Bureau of Standards

Effect of Support on the Performance of Vane Anemometers

By Galen B. Schubauer and Gerald H. Adams

One of the more important factors affecting the accuracy of a measurement of air speed with a vane anemometer is the manner in which the instrument is supported. An awareness of this fact is important, because the user must devise his own support. It is shown that seemingly minor changes in the support may change the indicated speed by 5 percent, and that holding an anemometer in the hand may increase the indicated speed by as much as 17 percent. In order to insure the reliability of a speed measurement, an interference-free type of support is recommended.

I. Introduction

The accurate measurement of air speed with a vane anemometer depends on an accurate calibration and on conforming strictly to the conditions for which the calibration will be valid. These conditions involve primarily the manner in which the anemometer is supported.

For many years calibrations were conducted at the National Bureau of Standards by means of a whirling arm, a device that moves the instrument along a circular path through the air at constant speed. The instrument was simply fastened to a flat plate at the end of the arm as shown in figure 1, and the arm was rotated at a series of known rates. The accuracy of a calibration by this method was limited by the so-called swirl correction, a necessary but rather uncertain correction applied to the peripheral speed of the arm to take account of the rotation of the air in the room produced by the rotating arm.

In June 1947, it was decided to conduct all calibrations of vane anemometers in the wind tunnel where absolute speed measurements could be based entirely on the standard pitot-static tube. In making the change to the wind tunnel, the question of the proper means of supporting an anemometer was brought to the fore. It was already known that the support could affect the rate of an instrument and that the best way to avoid possible error was to use the same type of support at all times. The flat plate, formerly used with the whirling arm, could be defended only on the grounds that manufacturers in failing to supply a supporting member of any sort presumably left the user free to adopt any support that suited his convenience—even to holding the anemometer in his hand. To throw some light on the importance of this question, it was decided to investigate the performance of several sizes of vane anemometers of the type shown in figures 1 to 5 on the various types of support shown in the figures. The investigation was conducted in the Bureau's 4½-foot wind tunnel.

II. Interference-Free Mounting

If an anemometer is suspended in a wind stream on wires so fine that they are incapable of producing interference, a performance free from support interference may be obtained. By comparing the performance obtained in this way with that obtained on the rod type of support shown in figure 2, it has been found that a rod no greater than ½ in. in diameter produces no measurable interference when it extends directly downstream. Effects from members supporting the rod itself may be made negligible by placing them at a sufficient distance downstream. This requires a minimum distance of the order of 16 times the diameter or cross-stream width of such members. In the mounting shown in figure 2 ample margin has been allowed, and the mounting is interference free. The portion of the rod directly under the anemometer is flattened to about ⅛ in. in thickness. In the investigation of the interference produced

FIGURE 1. *Anemometer supported on flat plate.*

FIGURE 2. *Anemometer supported on rod.*

by other types of support, the performance on the support in question was compared with that on the rod.

III. Other Supports Investigated

1. Whirling-Arm Mounting

The flat plate on which anemometers were mounted in the past for a whirling-arm test is shown in figure 1. A wooden member simulating the end of the arm is shown to the right. The plate is ⅛ in. thick and 3 in. wide. The distance from the end of the arm to the end of the plate is 12½ in. The wind moves normal to the face opposite the dial and parallel to the flat side of the plate.

2. Hand Support

The types of hand support shown in figures 3, 4, and 5 were chosen not as recommended methods of support, but rather as manners in which an observer might be inclined to hold an anemometer in making a measurement of air speed. The models are intended to respresent approximately an adult hand and arm. The arm length is not intended to be correct, and the body is not represented. This would correspond to the case where the observer's body is completely outside the wind stream. Figures 1 to 5 all show a 4-in. anemometer, the size referring to the inside diameter of the cylindrical housing.

Figure 3, hand 1, shows one finger through the ring of the anemometer and two fingers supporting the housing. The arm extends to the side and is at right angles to the wind.

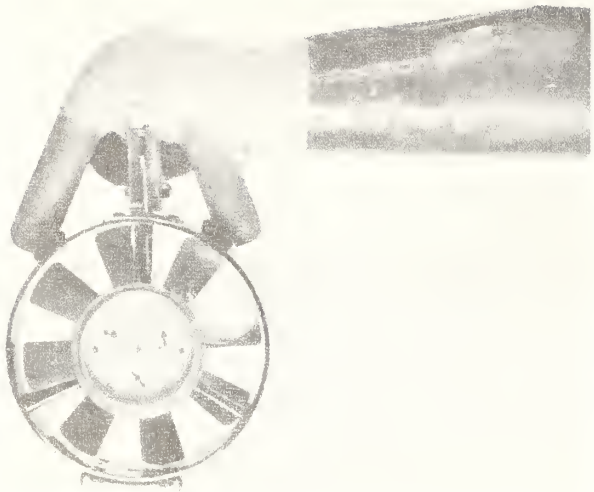

FIGURE 3. *Hand 1 supporting anemometer.*

Figure 4, hand 2, shows one finger through the ring allowing the anemometer to hang down freely. The arm is at right angles to the wind. The thumb is on the downstream side.

Hand 3 in figure 5 shows an anemometer being held by means of a short handle. The arm is directly downstream inclined at an angle of 45 degrees to the wind.

III. Results

Curves showing the performance of a 3-, 4-, and 6-in. anemometer are given in figures 6, 7, and 8, respectively.

The speed indicated by an anemometer depends on the rate of rotation of the vane wheel, which in turn depends on the setting of the vanes, the diameter of the wheel, the speed and direction of the air through the wheel, and the friction of the instrument. The true speed is the speed of a uniform parallel flow of air that would exist if the anemometer and its supports were absent. The indicated speed may be less than, equal to, or greater than the true speed depending on the factors that control the rate of rotation of the vane wheel.

The performance given in figures 6, 7, and 8 is in terms of the ratio of the indicated speed to the true speed plotted against the true speed. Displacement of the various curves from that marked "rod" shows the altered performance due to the

FIGURE 4. *Hand 2 supporting anemometer.*

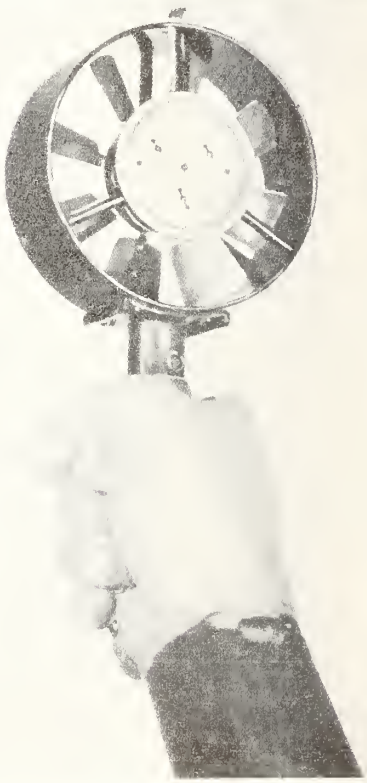

FIGURE 5. *Hand 3 supporting anemometer by short handle.*

interference of the support. It will be noted that the ratio of indicated to true speed is increased in every case. The reason for this is that the air speed through the instrument increases locally due to the fact that the air must flow around the support.

The changes in indicated speed due to interference are given in table 1 as percentages of the true speed at several values of the true speed. There is an indication that the percentages decrease slightly with increasing speed, but the change is scarcely outside the experimental error. The column of averages may therefore be used as a reliable index of the various interference effects. It will be seen that the interference effects are about the same on the 3- and 4-in. anemometers but somewhat less on the 6-in. anemometer. A decrease with increasing size is to be expected, because the anemometer becomes larger relative to its support. As hands 1 and 2 produced roughly the same effect, hand 1 was used only with the 4-in. anemometer.

TABLE 1. *Change in indicated speed due to interference, expressed as percentage of true speed*

Support	True air speed, fpm					Average
	400	600	800	1,200	1,600	
3-IN. ANEMOMETER						
	Percent	*Percent*	*Percent*	*Percent*	*Percent*	*Percent*
Rod	0	0	0	0	----	0
Plate	5.6	5.6	5.4	5.0	----	5.4
Hand 1	----	----	----	----	----	----
Hand 2	15.6	16.1	15.4	14.4	----	15.4
Hand 3	14.6	14.5	14.1	13.4	----	14.2
4-IN. ANEMOMETER						
Rod	0	0	0	0	0	0
Plate	5.5	5.3	5.4	5.1	4.7	5.2
Hand 1	18.1	17.1	16.8	16.2	15.9	16.8
Hand 2	18.1	16.9	16.5	16.5	16.8	17.0
Hand 3	11.5	11.8	11.9	11.7	----	11.7
6-IN. ANEMOMETER						
Rod	0	0	0	0	0	0
Plate	5.6	4.3	3.7	3.3	----	4.2
Hand 1	----	----	----	----	----	----
Hand 2	12.7	11.8	11.9	11.9	12.0	12.1
Hand 3	10.7	10.3	10.1	9.7	9.6	10.1

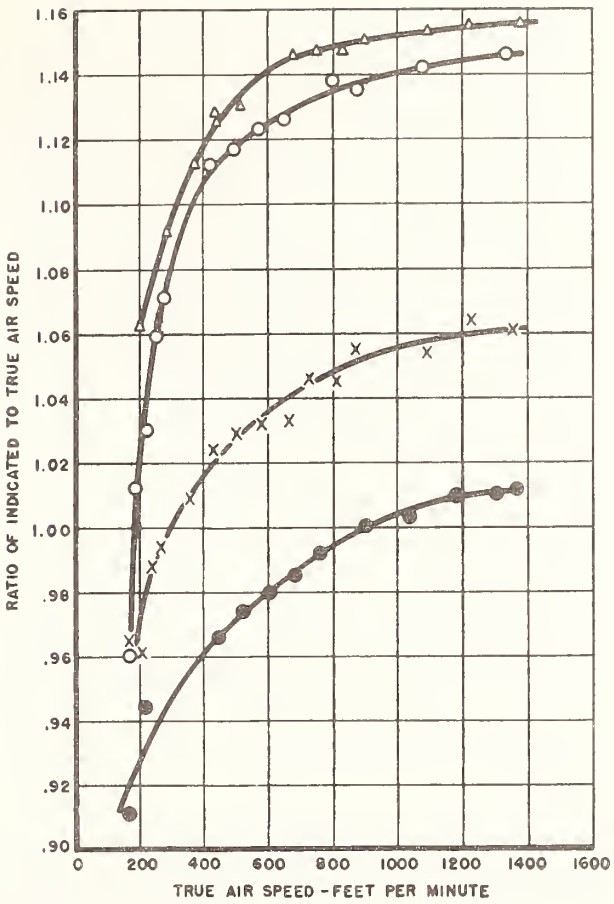

FIGURE 6. *Performance of 3-inch, eight-vane anemometer.* △, Hand 2; ○, hand 3; ×, plate; ●, rod.

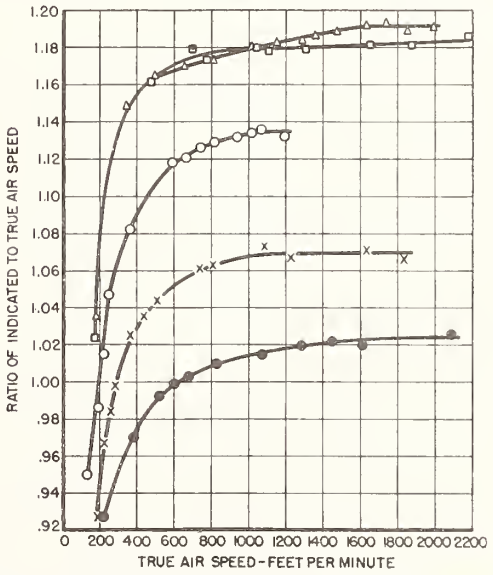

FIGURE 7. *Performance of 4-inch, eight-vane anemometer* △, Hand 2; □, hand 1; ○, hand 3; ×, plate; ●, rod.

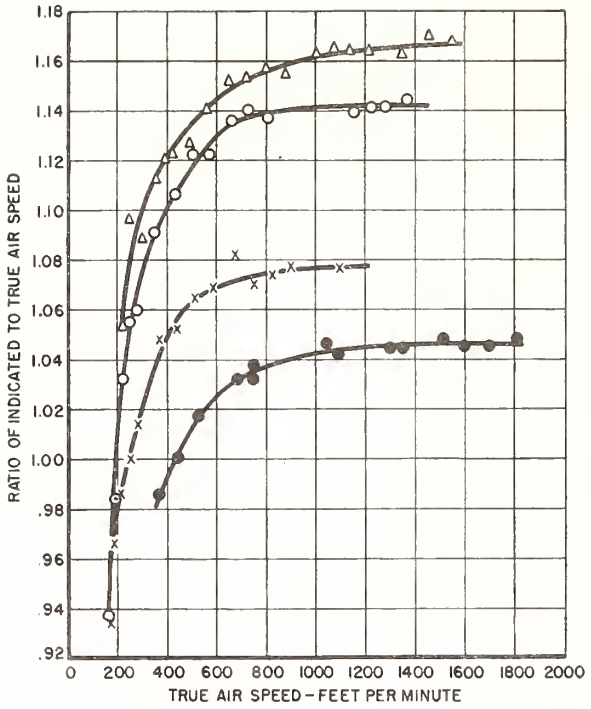

FIGURE 8. *Performance of 6-inch, 10-vane anemometer.*

△, Hand 2; ○, hand 3; ×, plate; ●, rod.

All of the effects demonstrated here are large compared to the inherent accuracy of a calibration curve. The scatter of the points about any one mean curve in figures 6, 7, and 8 shows that a calibration curve is defined to an accuracy of better than 1 percent. However, there may be systematic errors in the measurement of speeds below 400 feet per minute amounting to several percent, so that the scatter of observations is not a reliable indication of the absolute accuracy at the lower speeds. Nevertheless, interference effects are likely to be the major source of error unless the same support system is used at all times. The support, therefore, becomes in effect part of the instrument and changing it amounts to changing the instrument.

Not all interference effects will be as large as those shown here, for the effect depends entirely on the size, position, and shape of the support. If the bulk of the support is to the rear of the anemometer, the effect may be in the opposite direction. It is entirely possible that some disposition of the support may be made such that effects from the side and effects from the rear just

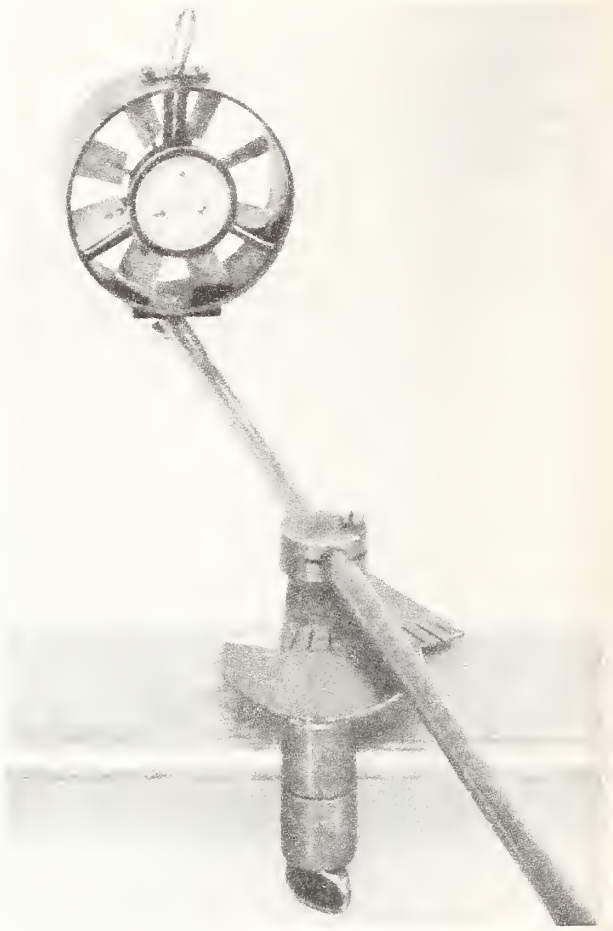

FIGURE 9. *Anemometer on rod clamped to strut.*

cancel. However, proper balance might be difficult to obtain over the entire speed range of an instrument and also would be affected by wind direction. Directional effects on anemometers without support interference have been treated in a previous paper.[1]

IV. Adoption of a Standard Mounting for Calibration Purposes

In considering the question of a standard mounting, it is helpful to keep in mind the fact that any mounting must be regarded as part of the instrument. As an anemometer supplied by a manufacturer should be regarded as a complete instrument, it is assumed that nothing should be added to it. Therefore, as the rod support is equivalent aerodynamically to adding nothing,

[1] Roy H. Heald and Paul S. Ballif, Effect of yaw on vane anemometers, J. Research NBS **19,** 685 (1937) RP1056.

the rod support of figure 2 has been adopted for the purpose of calibration.

Experience with vane anemometers at the National Bureau of Standards has shown that it is possible to employ the rod support under nearly all conditions of use. Even when it is necessary to use a short rod, the interference from the member holding the rod is likely to be small. According to Heald and Ballif (see footnote 1), for example, the clamping device and strut shown in figure 9 had a negligible effect at distances downstream of 1 foot or more. Even at 4 in., the interference effect was only of the order of 1 or 2 percent. The strut in this case was 1¼ in. thick and 3 in. wide and extended completely across the tunnel.

WASHINGTON, November 4, 1947.

Liquid-Flowmeter Calibration Techniques

By M. R. SHAFER[1] and F. W. RUEGG,[2] WASHINGTON, D. C.

Calibration techniques for liquid flowmeters are discussed with emphasis on problems which are known to influence the accuracy of calibration procedures. Also, reference methods which have been used to evaluate the comparative accuracy of different calibrators are described. The results of comparative accuracy tests on four calibrators of different designs are presented and it is shown that the agreement between these is within ±0.15 per cent in the test range of 10,000 to 100,000 lb per hr. The many precautions necessary to approach this precision from the traditionally accepted "plus and minus one per cent" are given in detail.

Introduction

In the course of a continuing program of research and development at the National Bureau of Standards on aircraft fuel-metering-accessory test equipment, conducted under the sponsorship of the Bureau of Aeronautics, the performance of various liquid flowmeters has been investigated as well as equipment and techniques for their calibration. Experience has demonstrated that absolute accuracies better than ±0.3 per cent are possible in the calibration of direct-indicating flow-rate meters. It is believed that the calibration techniques used to attain such accuracies are of sufficient general interest to warrant presentation here. Thus the objectives of this paper are to present a discussion on flowmeter-calibration techniques; to present data obtained at the National Bureau of Standards and elsewhere; to demonstrate the present state of the flowmeter-calibration art; and to describe some of the limitations of existing calibration equipment and procedures.

The techniques discussed herein are applicable to totalizing meters for which calibration procedures are established and defined (1).[3] However, our primary interest and experience have been restricted to direct-reading liquid flowmeters operating under steady-flow conditions in the range 5 to 100,000 lb per hr.

A meter calibration may be considered accurate only for the conditions existing at the time the calibration data were taken. Thus those quantities which can influence the performance of the meter must be known, measured, and controlled during precise calibration work. Factors influencing the performance of the different type meters have been investigated and reported in numerous papers, among which are (2 to 7). These factors are the density, viscosity, and temperature of the liquid; upstream, and to a lesser extent, downstream flow disturbances; the vapor pressure and absolute pressure level; and the orientation and scale sensitivity of the meter. Of course, the influence of these varies widely among the different type meters.

Summarizing the possible influences on meter performance, it may be noted that the influence of density usually can be predicted through analysis. The erratic effects of viscosity are most pronounced with the smaller sized meters and can be established only through calibration tests. Temperature exerts its influence through its effects upon the configuration of the meter and upon the physical properties of the test liquid. Vapor pressure and pressure level should have no appreciable influence provided compressibility of the liquid is not significant and the pressure level is sufficient to prohibit vapor formation. Finally, meters are sensitive to external flow disturbances, and this effect generally increases with meter size and flow rate. In fact, inadequate control of flow disturbances is one of the greatest sources of error in precise work.

Although meter characteristics may seem a separate problem from that of calibration, it must be stressed that precise calibration work cannot be performed unless these are given ample consideration in specifying and controlling the conditions of calibration.

Selection and Calibration of Instrumentation

Extreme accuracy is now possible in the measurement of mass, time, and those other quantities required for the flowmeter calibration. Perhaps some thoughts regarding the selection and calibration of the separate instrumentation items may be of value before discussing representative calibration systems. The calibrator will require a timer, scales for the measurement of mass or prover tanks for volumetric determinations, thermometers, density-measuring instruments, and perhaps a viscometer. Each of these must have sufficient sensitivity and accuracy to serve its intended purpose.

Electronic-counter timers are preferred for measuring the time interval. Many different makes are now available which operate on the principle of counting the pulses from a tuning fork or quartz-crystal oscillator. These usually indicate in units of 0.001 sec and have provisions for electronic actuation. They are considered to be better suited for this application as compared to synchronous clocks and stop watches which are dependent upon the frequency of the power supply, have minimum scale divisions of 0.1 sec, and utilize mechanical methods of actuation. Standards of time and frequency are broadcast by the National Bureau of Standards over station WWV in Maryland and WWVH in Hawaii (8). These precise signals, accurate 2 parts in 100 million, are adequate and convenient references for the calibration of timers.

Volumetric calibrating systems will require prover tanks. Specifications and calibration procedures for these are given in (1). Accuracies better than 0.1 per cent of the nominal tank volume can be attained with prover tanks provided adequate and proper temperature corrections are applied.

For the gravimetric-type calibrator a scale of conventional design, equipped with weighbeam and counterpoise is recommended. The addition of quick-weighing or automatic indication devices is not considered necessary and possibly might prove detrimental to over-all accuracy as compared to the free-swinging lever system. For smaller capacities, a straight lever system or even the equal-arm balance should be used. Balances of the torsion-tape and/or flexure-plate type also will prove suitable because of their inherent stability. Features influencing their selection and use will include capacity, smallest weighbeam graduations, and sensitivity which can be adjusted by the manufacturer as required.

Before placing the scale in service, two tests extending over the

---

[1] Research Engineer, National Bureau of Standards.

[2] Physicist, National Bureau of Standards.

[3] Numbers in parentheses refer to the Bibliography at the end of the paper.

Contributed by the Research Committee on Fluid Meters and presented at the Annual Meeting, New York, N. Y., December 1–6, 1957, of The American Society of Mechanical Engineers.

Note: Statements and opinions advanced in papers are to be understood as individual expressions of their authors and not those of the Society. Manuscript received at ASME Headquarters, July 24, 1957. Paper No. 57—A-70.

load range at which it will be used should be conducted. The first should be made before, the other after installation of the weigh tank and its connections. If the two are not in agreement, connections are likely interfering with proper functioning of the scale and the conditions should be corrected. This calibration should be done with test weights that meet C tolerances (9 and 10) and not by the comparison of one scale with another. Test weights may be secured from state or city Weights and Measures Departments, or if these are not available, the services of the scale manufacturer should be secured. The National Bureau of Standards will certify test weights in Washington, D. C., or at the National Bureau of Standards Master Scale Depot located in the Clearing Industrial District of Chicago, Ill. A self-contained or built-in type scale is desired to prevent damage to which portable type scales are subject during moving and handling. Also, the scale must be protected from wind and air currents while in use, since even light air currents produce weighing errors of appreciable magnitude.

Temperatures should be indicated preferably with mercury-in-glass thermometers usually of the range 0 to 120 F graduated in single degrees and accurate to one degree or better. Standards, specifications, and methods of testing liquid-in-glass thermometers are reported in (11) for the range −110 to +750 F. This reference lists the range, subdivisions, maximum permissible scale error, and installation instructions for the numerous types of thermometers used in test work.

In those calibration applications requiring a conversion between volumetric and gravimetric units, the measurement of liquid density is of extreme importance. Instruments for determination of liquid gravity or density include the hydrometer, pycnometer, and Westphal balance. The hydrometer is the simplest of these and it yields fairly accurate results. Specifications, tolerances, and methods of certification for hydrometers are described (12). If the test liquid is a petroleum product, any necessary conversion from specific-gravity units to density and corrections for temperature differentials can be made conveniently on the basis of Petroleum Measurement Tables (13) which contain conversion and thermal-expansion factors for all liquid-petroleum products within the specific gravity range 0.46 to 1.10.

A Static Weighing Calibration System

Calibration of a liquid flowmeter involves a determination of the time interval required for a measured mass or volume of fluid to pass through the meter, at a constant indicated rate, under the specified conditions of calibration. As extreme accuracy is possible in the measurement of mass and time, the limiting factors in the procedure are the technique, the sensitivity of the meter, the constancy of the indicated flow rate, the mechanics of collection of the fluid, and the method of timer actuation.

In presenting this discussion of a representative flowmeter-calibrating system, an apparatus which was designed and constructed at the National Bureau of Standards will be described. This was developed to obtain a precision of about 0.1 per cent with two basic features in mind: (*a*) A way was sought to collect the fluid with a minimum disturbance to the steady state of flow through the meter; and (*b*) a method was desired whereby the mass of the liquid collected could be measured under a "static" condition of no flow into the collection tank. In this way the problem of accurate measurement of mass and time could be reduced to a minimum as nearly all dynamic considerations were eliminated. A schematic diagram of the apparatus is presented in Fig. 1. This particular system was used for the evaluation of flow rates in the range 5000 to 100,000 lb/hr,

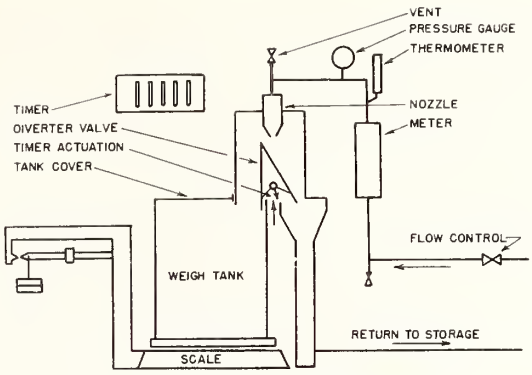

Fig. 1 NBS static weighing calibrator

which can be extended through the techniques described herein. Essential components are the flow-rate supply and control, the meter under calibration, a flow-diverter valve, an electronic timer, and a platform scale and tank.

The function of the flow-rate supply-and-control system is to deliver filtered liquid, of known physical properties, at a closely controlled temperature to the meter under test. Additional functions are to eliminate surges and pulsations within the fluid and to provide a convenient, sensitive method of control whereby all desired flow rates may be set and maintained to within 0.1 per cent of the desired value. Also, this system must contain provisions to assure positive elimination of all gas and vapor from the liquid before entering the meter with special consideration being given to the possibility of vapor formation during the throttling action of the flow-control valve.

Quantities influencing the performance of the meter under test have been discussed briefly. Of these, the upstream flow disturbances are the most difficult to detect and control when working to tolerances of a few tenths of one per cent. Such disturbances include flow distribution, pulsations, and rotational flow which originate within the pumps and fuel-supply components. They cannot be conveniently eliminated completely by placing a straight length of pipe upstream of the meter.

Some success has been obtained with a flow straightener consisting of bundles of small tubing and screens placed within a larger tube installed at or near the entrance of the meter under test. This helps in defining the calibration conditions. Also, the flow straightener in conjunction with master meters provides a more stable secondary reference for evaluating the comparative accuracy of different calibrators. As a final remark on this subject of upstream disturbances, the throttling valve should never be installed at the entrance to the meter as erratic disturbances may be introduced which will impair the precision of calibration. Rather, this valve should be located on the downstream side if possible.

The function of the diverter valve is to direct the flow as desired to storage or to the weigh tank without disturbing the rate of flow through the meter. Leak detectors should be provided to assure that none of the metered flow can bypass the weigh tank during the weigh-time interval. Also, in the static test method, the diverter valve should actuate the timer during its traverse and divert the flow quickly.

The particular diverter used in our apparatus was made of 0.035-in. cold-rolled steel in the form of an inverted V, each side being 15 in. long and 12 in. wide, with an included angle of 30 deg. The center of rotation was $2^1/_2$ in. above the base. Angular displacement was performed by a pneumatic-piston device having equal speeds in both directions with pneumatic cushions provided

at the end of the stroke. Time of positioning of the diverter was such that about 30 millisecond were required to cut through the liquid stream.

The counter-type timer should be actuated by electronic means, and in our apparatus actuation was accomplished by the diverter valve at the mid-point of its travel. This timer indicated in units of 0.001 sec and was calibrated against the standard reference time signal.

The platform scale used in this work was purchased on the open market. The scale is a self-contained, straight-lever type equipped with suspension main load-bearing assemblies and a single bar weighbeam graduated to 100 lb in $^1/_2$-lb divisions. A complement of counterpoise weights provided a total capacity of 5000 lb. Modifications performed at the National Bureau of Standards included the installation of a vernier scale on the main sliding poise to give readings to 0.05 lb. Also, concrete supports were provided for all main-lever-fulcrum bearings and for the weighbeam assembly to give a "built-in" scale. Thus the possibility of damage to which portable scales are subject during transit was eliminated.

The balance-ball elevation was adjusted to give a sensibility reciprocal of 0.1 lb at a load of 1000 lb. Sensibility reciprocal is defined as the amount of weight required to shift the weighbeam from an equilibrium position at the middle, to equilibrium at either extremity of the trig loop. Immediately prior to the flowmeter-calibration work, a scale calibration was made using 50-lb test weights known to be accurate within Class C maintenance tolerances of ±40 grains. Both ascending and descending loads were used in the range of loads to be encountered and no hysteresis was observed. Considering the sensitivity, precision of calibration, and constancy of the scale as determined by the tests, it was practicable to determine minimum net weights of 400 lb to an absolute accuracy of better than 0.05 per cent.

The weigh tank had a capacity of 64 cu ft. No connection of any kind was attached to the tank when weigh determinations were being made, and the tank was emptied by inserting the inlet hose of a transfer pump. However, a drain valve would be adequate if the tank has sufficient elevation with reference to the liquid reservoir. In installations requiring permanent, flexible tank connections, tests must be conducted to assure that these are not interfering with the proper operation of the scale.

Calibration of a meter at a selected rate of flow was performed by first determining the tare weight while the diverter valve directed the flow to "return to storage." The diverter was then operated to direct the liquid into the weigh tank and this operation automatically started the timer. After collection of an appropriate amount of liquid, the diverter was repositioned to return to storage, automatically stopping the timer. The gross weight was then measured and the net determined for the indicated time interval. It should be noted that weight determinations were not made while liquid was entering the scale tank. Weights determined by this method require a correction for air buoyancy (1) magnitude 0.1 to 0.2 per cent, to obtain the true weight.

Another important consideration in precise calibration techniques is the piping between the meter and the weigh system. This must be such as to assure that all of the flow and only that flow indicated by the meter is collected in the weigh tank during the calibration run. Aside from the obvious requirement of no leakage or bypass from these connections, complete elimination of gas and vapor must be assured so gas compression or expansion cannot occur. Always remember, one of the greatest sources of measurement inaccuracy is improper gas elimination. Thus the meter-discharge lines should be as short and small as possible with vents provided at high points for gas elimination. As a general rule, the volume of the discharge piping should not exceed 5 or at most 10 per cent of the flow collected during a calibration run.

Discharge connections of small volume also reduce the effects of thermal expansion and contraction of the liquid if an appreciable change in temperature is encountered during a run. For instance, the coefficient of cubical expansion of petroleum products is about 0.06 per cent per deg F, and 10 deg F change in temperature during the test could introduce an error of 0.06 per cent if the volume of piping is only 10 per cent of the volume of fluid collected.

Volatility of the liquid is an important consideration because of loss by evaporation. Our weigh tanks and diverter valves were provided with covers to reduce loss of vapor and the test liquid was a naphtha having a Reid vapor pressure of less than 0.1 psi. No measurable evaporation loss was detected. However, for high vapor-pressure liquids, such as gasoline, considerable refinement of the techniques described herein is required to eliminate both loss by evaporation and vapor formation in the meter-discharge lines. The ideal solution appears to be a pressurized weigh system, but this will introduce many additional complications.

Examples of Dynamic Weighing Calibrators

The static weighing method of flowmeter calibration is time-consuming and thus not well suited for those applications in which convenience of operation is important. Thus dynamic weighing is utilized frequently. This determines the time interval required to collect a preselected weight of liquid, the weighing being performed while the liquid is entering the scale tank or other weight-determining collector. Although experience has demonstrated that the accuracy of dynamic calibrators can be just as good as the static method described, additional dynamic factors must be considered.

Three different dynamic calibrators will be considered briefly. Method 1, shown schematically in Fig. 2, utilizes a free-swinging lever scale. With this arrangement, the weight of the fuel in the tank increases until it overcomes the resistance of the counterpoise weights on the end of the weighbeam which then rises and actuates the timer. At this time an additional weight is added to the pan depressing the weighbeam. When it rises again the timer is stopped. This procedure requires acceleration of the scale just prior to both the start and stop actuation of the timer.

Three important dynamic phenomena take place during this weigh cycle. They are: The change in the impact force of the falling liquid between the initial and final weigh points; the collection of an extra amount of fluid from the falling column by the rising level in the tank; and the change in inertia of the scale and weigh tank with the resultant change in time required to accelerate the weighbeam past the timer trip point.

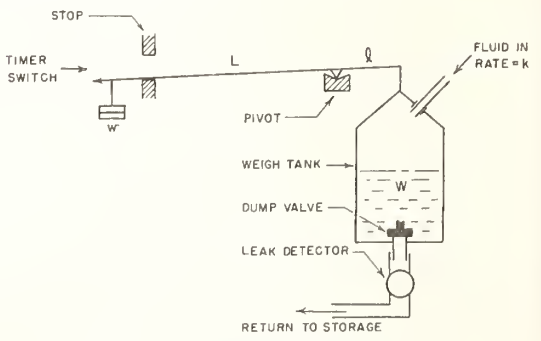

Fig. 2 Dynamic weighing calibrator 1

It can be demonstrated that the decrease in impact force is essentially equal and opposite to the additional weight collected from the falling column. Thus, even though each of these may be appreciable, they cancel each other. The effect of change in inertia between the initial and final weigh points can become appreciable and should be considered whenever the weight of liquid collected contributes significantly to the inertia of a scale system requiring a relatively large travel of its weighbeam to the point of timer actuation. This method of weighing is used frequently in other situations, and an explanation of the inertia errors involved may be of interest.

Consider a scale consisting of a single, massless lever, as illustrated in Fig. 2, having arms of length l and L. When fluid is added to a tank at a mass rate k, the collected weight W eventually will balance the counterpoise weights w. A further collection of liquid will then deflect the lever past the point of timer actuation as a result of the unbalance kt and its corresponding torque $ktgl$, where t is time measured from the instant of balance and g is the acceleration of gravity.

As a first approximation, this torque is equal to the product of the moment of inertia of the fluid and counterpoise weight and the angular acceleration $d^2\theta/dt^2$. If the scale ratio L/l is large, the moment of inertia is essentially that of the counterpoise weights, and the equation of motion of the scale may be written

$$ktgl \simeq wL^2 \frac{d^2\theta}{dt^2} \quad \ldots\ldots [1]$$

which reduces to

$$ktg \simeq WL \frac{d^2\theta}{dt^2} \quad \ldots\ldots [2]$$

as w is approximately equal to Wl/L.

Integrating twice, using constants of integration equal to zero, and rearranging, gives the time required for deflection through an angular displacement θ

$$t \simeq \left(\frac{6L\theta W}{kg}\right)^{1/3} \quad \ldots\ldots [3]$$

Thus for a constant deflection and flow rate, the time required for deflection should be approximately proportional to $W^{1/3}$. This was tested on one dynamic weighing calibrator having a scale ratio of 50:1 and constant values of $\theta = 0.007$ radian and $k = 6.4$ lb per sec. The results, plotted in Fig. 3, give a least-squares curve of

$$t = 0.031W^{0.43} \quad \ldots\ldots [4]$$

This value of 0.43 for the exponent of W is in reasonable agreement with the derived value of 1/3 considering the precision of the experimental work and the approximations used in deriving Equation [3].

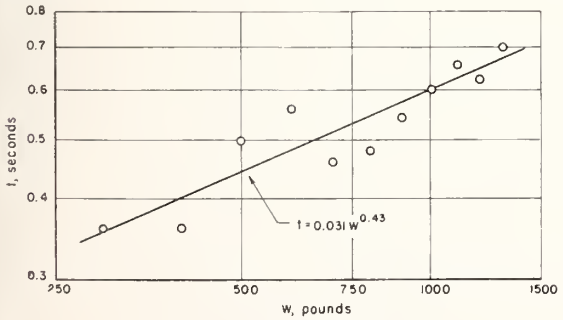

Fig. 3 Scale deflection time

The error of interest in dynamic weighing is the difference Δt between the time required for the deflection of the weighbeam at the final weight W_2 and at the tare weight W_1. Referring to Equation [3] this is derived as

$$\Delta t = t_2 - t_1 \simeq \left(\frac{6L\theta}{g}\right)^{1/3} \frac{(W_2^{1/3} - W_1^{1/3})}{k^{1/3}} \quad \ldots\ldots [5]$$

which is the inertia error in the measured time interval $T = (W_2 - W_1)/k$ required to collect the net weight of liquid. Dividing by T the percentage error is

$$\text{Per cent error} = \left(\frac{\Delta t}{T}\right) 100 \simeq 100 \left(\frac{6L\theta}{g}\right)^{1/3} k^{2/3} \left(\frac{W_2^{1/3} - W_1^{1/3}}{W_2 - W_1}\right) \quad \ldots\ldots [6]$$

The relation expressed in Equation [6] was checked by comparing dynamic calibrator 1 with the NBS static calibrator using a method to be described later. The results are plotted in Fig. 4, in which different symbols are used to designate the various flow rates. Values obtained from Equation [6], with $L = 2.2$ ft and $\theta = 0.007$ radian, are shown by the solid line. Equation [4], transposed to the co-ordinates of the figure, is shown as a dashed line.

The data of Fig. 4 are in reasonable agreement with Equations [6] and [4]. Thus it is believed that these are a measure of the inertia errors involved in this form of dynamic weighing. When the deflection of the weighbeam was reduced from 0.007 to about 0.0004 radian, the inertia effects became indistinguishable from the other small errors of the system.

At the time the tests were conducted to obtain the data of Figs. 3 and 4, we were not attempting an evaluation of the inertia error, but only demonstrating its presence. W_1 was not determined and it was necessary to estimate its value in these analyses. Thus the data should not be considered precise. However, it is believed these data are sufficient for the purpose of demonstrating that significant inertia errors may result from this method of dynamic weighing.

Dynamic calibration method 2, shown in Fig. 5, collects the liquid in a tube or cylinder of known cross-sectional area and uses the pressure existing at the bottom as a measure of the weight of liquid collected. The vertical rise in liquid between the initial or tare and the final weigh positions is usually in the range 2 to 20 ft. Thus it is necessary to measure and/or indi-

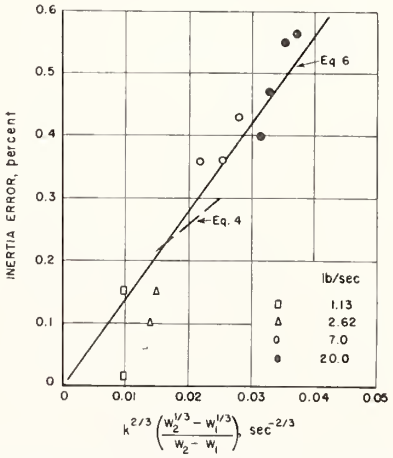

Fig. 4 Inertia error of dynamic method 1 for $(L\theta)^{1/3} = 0.249$

cate this pressure difference of 1.5 to 15 in. of mercury to a precision better than 0.1 per cent. The majority of installations use mercury manometers as the pressure-measuring device with electrodes, corresponding to different collected weights, spaced at accurately determined intervals. Contact between these and the mercury, in conjunction with electronic circuitry, provides the impulse for actuation of the timer. The contact spacing in these manometers must remain constant and any dirt or oil film which may effect the contact closure must be eliminated.

Important considerations for method 2 are: Effects of thermal expansion on the standpipe cross-sectional area and on the density of the manometer fluid; incomplete drainage of the cylinder walls before commencing the weigh-time determination, a significant factor in working with high-viscosity liquids; and changes in air pressure within either the cylinder or manometer column during the timing interval. The line between the cylinder and manometer well must never contain air or vapor. Also, the difference in elevation between its connections to the cylinder and manometer should be small so changes in the density of liquid within this line will have no influence on the height of the mercury. This is especially important when test-liquid temperatures differ from either that of the room or the mercury.

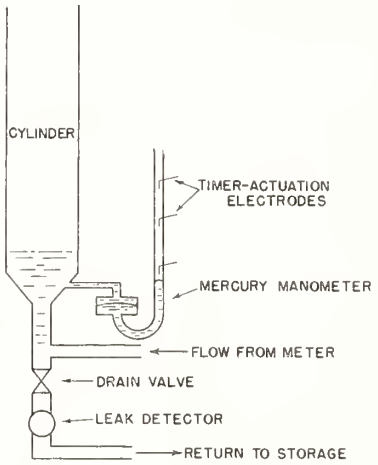

Fig. 5 Dynamic weighing calibrator 2

Dynamic considerations applicable to method 2 are first to ascertain that the pressure-measuring device has completed its acceleration and attained a constant velocity before the weigh-time interval is commenced. Also, oscillations resulting from the natural frequency of the pressure indicator must not exist. The other dynamic consideration is that of air compression in the collection vessel, especially at higher flow rates, resulting from restrictions such as flame arresters placed in the vent. It is readily seen that appreciable errors indicating higher than actual flows can result when such restrictions exist.

Dynamic calibration method 3, Fig. 6, employs bench dial scales for the measurement and indication of the weight of liquid. Nine light-beam intercepting paddles were added to the indicating dial, each corresponding to a predetermined weight. In operation, when sufficient liquid has entered the weigh tank to overcome the selected tare, the indicating mechanism of the scale commences to move around the dial. The first interruption of the light beam, occurring when the tare weight is balanced, starts the timer. An adjustable time-delay relay is provided whereby the phototrip circuit will not stop the weigh cycle until a selected time interval has been exceeded. Thereafter, when the next paddle intercepts the light beam the timer is stopped, the

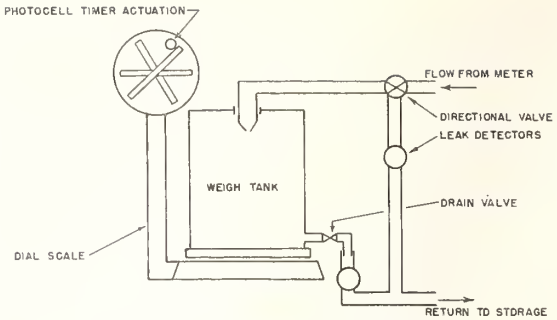

Fig. 6 Dynamic weighing calibrator 3

weight corresponding to that paddle is recorded, and the time is observed and recorded.

Dynamic considerations of method 3 are impact force and decrease in height of the falling liquid column as explained for method 1. Another consideration is the acceleration of the scale and its indicating mechanism to a constant velocity prior to the starting of the timer and maintenance of this velocity until the end of the weigh-time interval. Also, bench dial scales usually have constant sensitivity which, even when adequate at full scale, leads to larger percentage errors at the smaller weights. Thus good precision cannot be expected when the lower portion of the dial or range of the scale is used.

No attempt has been made to reveal all possible sources of dynamic errors in this discussion. These, of course, vary considerably with the different methods utilized. However, an attempt has been made to demonstrate that a static check and calibration of the instrumentation are not sufficient to prove the absolute accuracy of a dynamic-weighing method of calibration, as the response of the instrumentation used under transient conditions is a very important consideration.

Evaluation of Calibration Procedure and Equipment

The evaluation of calibration procedures and equipment includes a consideration of the ease and convenience of operation. Features which may be considered here are: The sensitivity and stability of the flow control; the temperature control; the time required to perform a weigh-time determination; and the time interval required to empty the weigh system between successive runs. All of these are of interest to the engineer in deciding whether a particular unit meets the general requirements of its intended purpose. These are not always the same for different applications, as more emphasis upon calibration time is necessary in a stand designed for production tests as compared to one used occasionally for high-accuracy tests of reference meters.

However, after these general performance characteristics are deemed satisfactory for the intended application, there still remains the all-important questions as to the precision of the measurement procedure and the absolute accuracy. The term precision as used in this paper refers to the variations or differences between repeat measurements. In the construction and operation of any calibrating unit, considerable attention will be directed towards refining the measurement procedure to reduce the variation so that it becomes insignificant. Unfortunately, this state is not always achieved and it may be necessary to evaluate the magnitude of the variations obtained.

The methods of statistics (14) define many units of variation by which the precision of a measurement procedure may be expressed. Among these are the "standard deviation," the "standard deviation of the average," the "confidence interval," and the "difference between duplicates." These are extremely useful to the engineer concerned with measurements and should

be used more extensively in flowmeter-calibration work. The ISO/TC-30 Committee of Fluid Measurements has recommended the use of twice the standard deviation as the tolerance limit in fluid-metering. An application of this tolerance is discussed by Jorissen (15).

It is beyond the scope of this paper to explain and demonstrate the application of statistics to precision of flow measured. However, the precision of the calibration procedure must be evaluated and the standard deviation provides a useful comparative unit for this purpose. A few representative statistical values will be presented to demonstrate the precision of flowmeter-calibration procedures attained in our laboratory. When data for ten successive runs are compared, using nominal timing intervals of 60 sec, the following representative values of precision result:

Standard deviation = 0.08 per cent
Standard deviation of the average = 0.03 per cent
Ninety-five per cent confidence interval = 0.06 per cent
Difference between duplicates does not exceed 0.12 per cent 80 per cent of the time

These data were obtained during calibration of sensitive float-type flowmeters. Naturally, they are dependent upon the sensitivity of the meter under calibration and meters with low-scale sensitivity will reduce this precision considerably.

Large differences between duplicate runs will be encountered occasionally. These are caused by insufficient time in bringing the meter and the liquid to operating temperature and incomplete purging of the system of gases. This happens frequently when small meters are calibrated on large-capacity stands. Other causes of large differences are insufficient tare time, with dynamic calibrators, and continuous readjustment of flow when such is necessary to provide a steady flow indication. In fact, experience generally demonstrates that minimum variability results when the flow-control valve can be left at a constant setting during the calibration time-interval.

After the calibration procedure and equipment have been adjusted to give satisfactory precision of measurement, a check of the absolute accuracy is desirable to detect the presence of constant errors. The best method for such a check is to use two or more different experimental procedures to measure the same quantity. Errors are then noted when averages disagree by an amount larger than is to be expected from the precision of the measurements. Perhaps our experience will be of help to others concerned with this problem.

In 1954 the National Bureau of Standards was requested to evaluate three dynamic weighing calibrators, one each of the designs of Figs. 2, 5, and 6, to determine whether their absolute accuracies were within the tolerance of ±0.25 per cent. Two of these stands, A and B, were in our laboratory. It was decided that the best method of detecting constant errors in these would be through the use of a different experimental procedure to measure the same flow rate. A static weighing stand, NBS, similar to that of Fig. 1, was constructed for this purpose. The third calibrator, C, is installed at another facility and some other technique was required as moving the NBS stand was not convenient. Thus it was decided to use direct-reading flowmeters as secondary references.

The following procedure was used for the determination of the accuracy of calibrators A and B at our laboratory. The calibrating stand under evaluation provided storage of liquid, pumps, filter, and flow and temperature control. In operation, the unknown flow rate was maintained constant as indicated by a sensitive float-type flowmeter operating at a constant temperature with a liquid of constant physical properties. This constant flow rate was evaluated alternately by the calibration stand under test and by the NBS static weighing method, the flow being

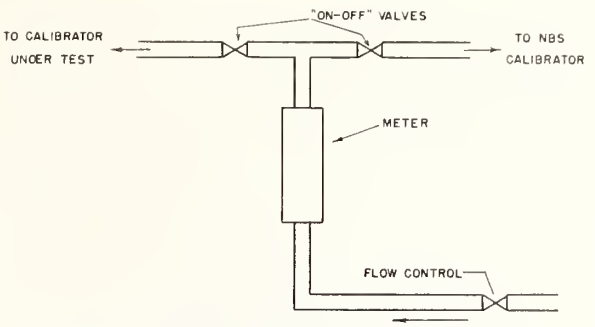

Fig. 7 Comparative accuracy-evaluation procedure

directed as desired by "on-off" valves placed downstream from the meter as shown in Fig. 7. The averages of four or five flow determinations made by each apparatus were then compared to obtain the difference between the calibrator under test and the NBS apparatus for the particular flow rate. This method has two important advantages: (*a*) The same quantity was being measured by two different procedures; and (*b*) upstream connections to the meter and downstream connections for a reasonable distance are never disturbed in directing the flow as desired to one of the two calibrating methods. Thus the conditions of calibration at the meter are identical.

For the evaluation of calibrator C, two secondary reference meters were selected. The first, range 7000 to 27,000 lb per hr, is of the float-type design having a logarithmic taper, a constant scale sensitivity of about 4 mm per per cent of indicated flow, and a stainless-steel float. All liquid passes through the metering tube. The larger meter is an experimental prototype design, range 35,000 to 100,000 lb per hr, and consists of the foregoing meter in parallel with a fixed orifice. As will be demonstrated later, this was not suitable as a secondary reference and a third meter was used. The third meter has a range 30,000 to 100,000 lb per hr, is a float-type having a 500-mm scale, and all of the flow passes through the glass metering tube. This served as an adequate secondary reference in the determination of the accuracy of calibrator C with a single exception.

Prior to the initial calibration of the three reference meters, the inlet and outlet connections were standardized. This included a 2-in. orifice upstream discharging into about 6 ft of 4-in. tubing connected to the meter inlet. The orifice was used in an attempt to obtain identical entrance flow conditions on the different calibrators. The meters were calibrated first at a few selected test points with the NBS apparatus and were then taken to calibrator C where the tests were repeated again by the same operator. Test fluids having a Reid vapor pressure of 0.1 psi and a kinematic viscosity of 1.10 centistokes were used at each location. Corrections were computed and applied for the different specific gravities of 0.783 and 0.779.

The final results of the tests are given in Fig. 8 which shows the per cent deviation of the individual calibrators from the average results for all four. Different symbols are used to designate the calibrators and each plotted point is the average of four to six separate determinations of rates of flow. Since some of these data may be considered proprietary information, we are not attempting to present the specific performance of any particular method other than the NBS static weighing apparatus represented by the open circles. Rather, the primary purpose is to show the extent of agreement obtained between four different methods of determination of flow rate. Where two identical symbols are plotted for the same flow rate, they represent the use of two different weights with corresponding timing intervals of about 30 and 60 sec. The average from which the deviations

were computed was obtained from the data within the ±0.15 per cent band with each calibrator assigned an equal weight.

As can be seen, the great majority of points are within ±0.15 per cent and the exceptions will now be discussed. Three deviations of about 1 per cent were obtained in the range 40,000 to 70,000 lb per hr with calibrator C. It must be understood that these are not an indication of the accuracy of this calibrator. Rather, they have been included to demonstrate difficulties encountered with the secondary reference meter of the orifice-bypass type. These deviations represent a change in the performance of this meter as a result of different upstream flow disturbances between the two calibrators, NBS and C. It has been concluded that a significant swirl or rotational flow difference existed between the two stands which was sufficient to affect the performance of the orifice-bypass meter by about 1 per cent.

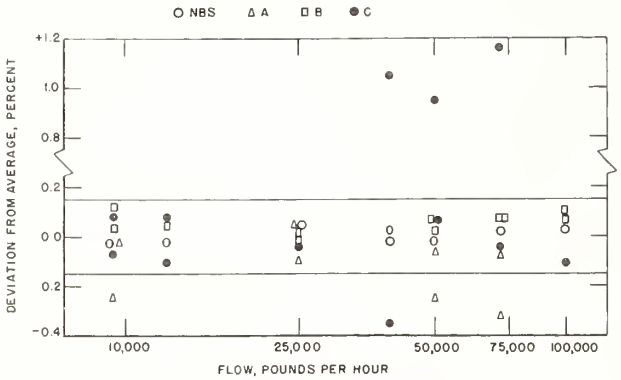

Fig 8 **Comparison of four calibrators**

Still referring to Fig. 8, good results were obtained on calibrator C in the range 50,000 to 100,000 lb per hr with the third reference meter. A low reading of −0.35 per cent was obtained at 40,000 lb per hr, the lowest float position where sensitivity of this meter to upstream disturbances is a maximum. Thus it is demonstrated that two different calibrators can both be accurate and yet give different calibration results because of the influence of different upstream flow disturbances on the meter under test.

The other three low points of Fig. 8 were obtained using small test weights on a weighing mechanism of insufficient sensitivity. It is also possible that some unevaluated dynamic effects were present here.

Excluding the extreme points of Fig. 8, the resulting agreement between the four different methods of flow-rate determination may be considered quite good as it is within ±0.15 per cent. The program also enabled the detection of inertia errors of about 0.5 per cent and influences of disturbances upstream from the meter of about 1.0 per cent in one case and 0.4 per cent in another. Thus, through the procedures described herein, it has been possible to detect and correct errors in calibration equipment and procedures having magnitudes of less than 1 per cent.

Conclusions

Precise calibration of flow-rate meters requires a knowledge and control of each parameter which may influence the performance of the meter under test. Among these are the physical properties and temperature of the test liquid, at times the absolute pressure level, and the influence of upstream flow disturbances. The latter is perhaps the most difficult to specify and control when working to accuracies better than 1 per cent and is one of the primary reasons for apparent discrepancies in results between different calibrators.

Extreme accuracy is now possible and certified standards are available for the measurement of mass, time, temperature, and density which a calibrator is required to control or indicate. However, in designing a specific calibrator, an intelligent selection of the instrumentation for range and sensitivity is necessary if adequate precision and accuracy are to result. Also, provisions must be included to insure that all of the liquid and only that liquid which passes through the meter will be collected in the calibrator.

Examples of both static and dynamic weighing calibrators have been presented. For the particular calibrators and flow ranges investigated, there is not a significant difference in the absolute accuracies. However, dynamic weighing methods are subject to errors which are not exposed by a static calibration of the instrumentation. Thus it seems desirable that dynamic weighing calibrators of new designs should be evaluated for accuracy by comparisons with other calibration methods.

Acknowledgments

The suggestions and assistance of H. H. Russell of the Mass and Scale Section and H. S. Bean of the Fluid Meters Section, in advising on problems related to this work, are gratefully acknowledged. Also, we freely admit that many of the techniques and possible sources of errors described herein have been pointed out by others who have been more than liberal in advising us of their experiences. Among these are V. P. Head of Fischer and Porter Company, and A. W. Brueckner of G. L. Nankervis Company.

Bibliography

1 "ASME-API Code for Installation, Proving, and Operation of Positive Displacement Meters in Liquid Hydrocarbon Service," American Petroleum Institute Code No. 1101, Revised January, 1952, American Petroleum Institute, New York, N. Y.

2 "Discharge Coefficients of Square-Edged Orifices for Measuring the Flow of Air," by H. Bean, E. Buckingham, and P. Murphy, *National Bureau of Standards Journal of Research*, vol. 2, March, 1929, Research Paper No. 49.

3 "The Laws of Similarity for Orifice and Nozzle Flow," by J. L. Hodgson, TRANS. ASME, vol. 51, 1929, part 1, FSP-51-42, pp. 303–332.

4 "Fluid Meters, Their Theory and Application," fifth edition, 1957, in press, prepared by ASME Research Committee on Fluid Meters, ASME, New York, N. Y.

5 "Coefficients of Float-Type Variable-Area Flowmeters," by V. P. Head, TRANS. ASME, vol. 76, 1954, pp. 851–862.

6 "Correcting for Density and Viscosity of Incompressible Fluids in Float-Type Flowmeters," by M. R. Shafer, et al., *National Bureau of Standards Journal of Research*, vol. 47, no. 4, 1951, Research Paper No. 2247, pp. 227–238.

7 "Survey of Mass-Rate Flow-Measuring Principles," by Y. T. Li and S. Y. Lee, ASME Paper No. 55—SA-72, unpublished.

8 "Standard Frequencies and Time Signals WWV and WWVH," Letter Circular LC-1023, June, 1956, National Bureau of Standards Boulder Laboratories, Boulder, Colo.

9 "Precision Laboratory Standards of Mass and Laboratory Weights," National Bureau of Standards Circular 547, August, 1954, available from Superintendent of Documents, U. S. Government Printing Office, Washington, D. C.

10 "Specifications, Tolerances, and Regulations for Commercial Weighing and Measuring Devices," National Bureau of Standards Handbook H44, September, 1949, available from Superintendent of Documents, Washington, D. C.

11 "ASTM Standard on Thermometers," by T. W. Lashof and L. B. Macurdy, prepared by ASTM Committee E-1, American Society for Testing Materials, Philadelphia, Pa., December, 1953.

12 "Testing of Hydrometers," by J. C. Hughes, National Bureau of Standards Circular 555, October, 1954, available from Superintendent of Documents, Washington, D. C.

13 "ASTM-IP Petroleum Measurement Tables," ASTM Designation D1250, American edition, American Society for Testing Materials, Philadelphia, Pa.

14 "Statistical Methods for Chemists," by W. J. Youden, John Wiley & Sons, Inc., New York, N. Y., second printing, 1955.

15 "On the Evaluation of the Accuracy of the Coefficient of Discharge in the Basic Flow-Measurement Equation," by A. L. Jorissen, TRANS. ASME, vol. 75, 1953, p. 1323.

Discussion

R. L. Galley.[4] A most interesting and thorough exposition of the pitfalls awaiting the novice in calibrating flowrate-measuring devices, this paper is one of the most practical treatments of a long-neglected subject that has come to the writer's attention. The authors are to be commended on their work and on this paper. It deserves wide circulation.

As one engineer who has devoted over a quarter of a century to the measurement of flow, the writer has seen the pitiful results of many amateur calibrators who did not know of all the precautions that should be observed, as the authors point out. The following comments are offered:

1 One assumes that the work deals only with volumetric and not with the so-called "mass" or gravimetric flowmeters. Of course, the same techniques would apply with either.

2 The problem of vapor pressure in testing hydrocarbon fuels is well explained, but the user is well advised that in calibrating certain turbine-type flow sensors in the same fuels, even a satisfactory line pressure does not always preclude the possibility of local cavitation in the region of the turbine blades. This can throw results way off, and one would never suspect the reason by the vapor-pressure criterion alone.

3 The authors do not mention Reynolds numbers, and the reader is left to assume that flow conditions at the test meter are sufficiently turbulent.

4 Gravity flow through the test rig is much safer than pumped flow, as this provides a better test condition.

S. R. Grotta.[5] A flow-correlation program similar to that described in the paper was carried out by the writer's company. A different approach was made, however, in the type of meter used as a reference.

It was felt that a reference meter should feature portability and ease of installation. Since the turbine meter fills this requirement in the higher flow ranges (above 250 lb per hr) better than the variable-orifice meter, an investigation was conducted to evaluate its suitability for this application. The program involved tests of flowmeter repeatability under various conditions which probably would affect all types of volumetric flowmeters.

Most of the tests were conducted with matched pairs (same make and size) of turbine meters installed in a recirculating flow system. The output signal of each flowmeter was fed into a separate electronic pulse counter. Since the output pulse is a measure of volumetric flow, permitting the counter to totalize these pulses for a sufficient period of time a direct indication of the total volume of fluid passed through the meter was produced. When the two turbine meters were placed in series and the counting sequence started and stopped simultaneously, the total counts from the two were nearly equal, with a slight difference being due to manufacturing tolerances. The ratio of the total counts (meter A divided by meter B) was found to remain constant over a wide range of flow. The standard deviation for 15 observations was 0.02 per cent. The maximum deviation from the mean was 0.03 per cent. By interchanging the meter positions in the pipeline and repeating tests we found that the effect of the initial plumbing configuration was less than 0.05 per cent.

The effect of flow-system-plumbing configuration on meter performance was investigated using this test procedure. Valves and elbows were placed in the pipe at the locations shown in Fig. 9. An elbow immediately upstream of a 1-in. meter produced an error as great as 0.9 per cent. The addition of a straight pipe 6 diameters in length ahead of the meter reduced this error to less than 0.2 per cent. The different makes of turbine meters tested were all affected by the flow pattern set up by the elbow. The degree of effect, however, varied from make to make.

After the selection of turbine meters suitable for reference use was made, a correlation program was carried on between the NBS calibrator and the Pratt & Whitney flow-calibrating standpipes. These standpipes, as company standards, are used to perform several hundred calibrations per year. Fig. 10 shows a portion of the correlation data. These data are plotted as pulses per gallon versus frequency (cps). As can be seen, the results of the correlation were very encouraging. A distinct advantage of the turbine flowmeter for correlation studies is that the accuracy of the data

[4] Consulting Engineer, Flowmeter Specialist, Woodland Hills, Calif.

[5] Experimental Engineer, Pratt & Whitney Aircraft, East Hartford, Conn.

PLUMBING CONFIGURATION FLOW DIRECTION →	1" DIAMETER TURBINE FLOWMETERS		
	MAKE I	MAKE II	MAKE III
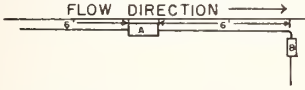	.91	.69	.84
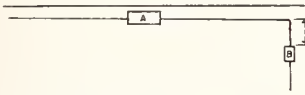	.21	.23	00
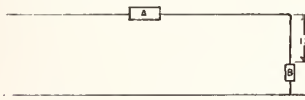	.15	.06	.00
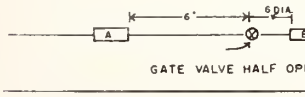 GATE VALVE HALF OPEN	.10	METER ERRATIC	.15
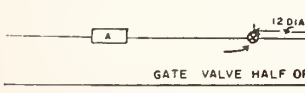 GATE VALVE HALF OPEN	.02	METER ERRATIC	.14

FIGURES ARE AVERAGE OF THREE OBSERVATIONS

Fig. 9 Per cent error in flow measurement caused by close proximity of elbow or valve to turbine flowmeter

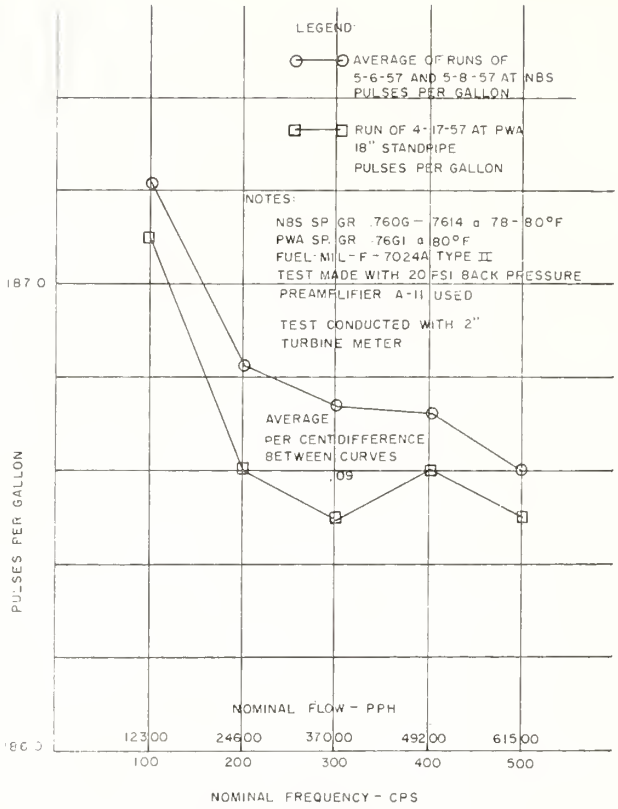

Fig. 10 National Bureau of Standards flowmeter correlation with Pratt & Whitney Aircraft

is not affected by small flowrate variations during the run. The flowrate is, in effect, averaged by the totalizing counter and timer the same as it is averaged by the weigh tank or standpipe used for calibration.

Turbine meters are not immune to all problems, however. Great care must be taken to keep the turbine rotor free of lint or other foreign material and protected from being nicked or scratched by hard objects. The observations made by the authors, emphasizing the importance of specific gravity and temperature measurements for the float-type meters, are even more important for turbine-meter applications. We also have found, as has been stated with regard to float-type meters, that air or vapor in the system causes serious error. Cavitation at the turbine-meter outlet also has been a source of trouble. This difficulty was eliminated by the application of back pressure.

It is apparent that many pitfalls have to be avoided both in calibrating turbine flowmeters and employing them for correlation studies. We feel that a document setting forth recommended procedures in the installation and use of turbine flowmeters would be very useful to those industries requiring a high degree of accuracy in flow measurements.

Finally, consideration should be given to means for conducting calibrations and correlations at elevated temperatures, up to 500 F and at pressures to 1000 psi.

V. P. Head.[6] Every fluid-mechanics laboratory should profit from the authors' treatment of inertia error. Beam travel from rest to timer operation is often $^1/_4$ or $^1/_2$ in. Note in Equation [6] that $L\theta$ is the displacement, y, of the counterweight end of the beam. Neglecting tare weight, and noting that W/k is the duration of the run T, and denoting per cent error by e, Equation [6] becomes

$$y = \frac{g}{6} T^2 \left(\frac{e}{100}\right)^3 \quad \ldots\ldots\ldots\ldots\ldots\ldots [7]$$

Using $g = 386$ in./sec^2, an average 60 sec time run requires y to be less than 0.00023 in. for 0.1 per cent, or 0.028 in. for 0.5 per cent, or $^1/_2$ in. for 1.3 per cent inertial error. Diverse beam scale dynamic rigs prevalent in university and aircraft test laboratories in past years are at best 1 per cent devices, and increasing use of the diverter, authors' Fig. 1, is to be encouraged, especially with water at low temperature where evaporation rates are negligible.

After a year of dynamic weighing experience at General Electric's A G T Division, we were using two scales and timers with pump and flowmeter between, and with 50 to 200 lb actual weights moved from receiver scale to supply scale after timers were started. Flexible hoses were hopeless. Small vertical pipes of outside diameter d extended almost to the bottom of both cylindrical liquid tanks of inside diameter D. Buoyancy of the volume of pipe plus its contained liquid was corrected by

$$W_{\text{actual}} = W_{\text{indicated}} \left(1 - \frac{d^2}{D^2}\right) \quad \ldots\ldots\ldots\ldots [8]$$

This system served only to detect gross errors in damaged meters and provide meter corrections, accurate within about 0.5 per cent, for the effects of large viscosity variations. Otherwise, meters were probably more accurate without the supposed corrections.

The writer then undertook the development of a new primary standard for liquid-mass measurement, and a number of other aircraft laboratories contributed to its perfection. Known as the standpipe liquid weigher, and illustrated in the authors' Fig. 5, this new primary standard is not proprietary, and educational as well as industrial laboratories are encouraged to construct their own. While dynamic weighing is almost always used, static weighing by means of a single micrometer-actuated contact also could be employed, with a synchronized diverter-timer switch as in the authors' Fig. 1. When regarded as primary, with the mass per inch of mercury W/H calculated from Equation [9] (which follows), performance has consistently been ± 0.15 per cent. Attempts to determine W/H by weighing withdrawn fluid on conventional scales has led to errors as large as 0.6 per cent and proved that conventional scales are secondary devices in need of constant restandardization.

Let ρ_{hg} = mercury density at 70 F, ρ_l and ρ_a = average liquid and atmospheric densities, grams per cc. Let A_l = standpipe area, A_W = manometer well area, and A_t = manometer tube area, all in square inches at 70 F. The constant including atmospheric-buoyancy correction is

$$W/H = 0.0361276 \frac{\rho_l A_l}{\rho_l - \rho_a} \left[\rho_{hg}\left(1 + \frac{A_t}{A_W}\right) - \rho_a\left(1 + \frac{A_t}{A_l}\right) - \rho_l\left(\frac{A_t}{A_W} - \frac{A_t}{A_l}\right)\right] \quad \ldots\ldots [9]$$

Small thermal corrections, Fig. 11, are used when necessary. Variations of ρ_l and ρ_a from assumed average values have trivial effects. In the writer's opinion, this primary liquid-weight standard is as reliable as any in the world, though, of course, the many factors affecting flowmeters as well as those producing difference between flow at the meter and flow into the standard, so capably emphasized by the authors, always must be kept in mind.

[6] Director of Hydraulic Research, Fischer & Porter Co., Hatboro, Pa. Mem. ASME.

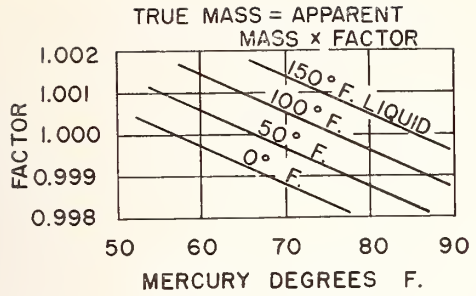

Fig. 11 Thermal-expansion corrections for standpipe liquid weigher

T. M. Morrow.[7] The authors are to be commended on the clear, concise presentation of the problems encountered in the calibration of flowmeters with dynamic weighing calibrators. They also are to be complimented on the conservative evaluation of the effect of these problems on the state-of-the-art of liquid-flow measurement.

Obviously, it is impossible to discuss in detail each source of measurement error noted in the paper. This discussion, therefore, will be limited to the presentation of an over-all picture of the effect which the results of this study can produce in the art of liquid-flow measurement.

The techniques used in the comparisons are obviously the result of careful study and planning to achieve more accurate flowmeter calibrations. Each problem is discussed with clarity noting the effects produced not only in the flow range tested, but also in the higher ranges of flow.

The careful planning and execution of the tests should be noted. Only through closely controlled and monitored test conditions could such significant results be obtained. Such tests are necessary to detect errors which many manufacturers of flowmeter-calibrating equipment consider insignificant.

To evaluate fully the extent of these errors it is necessary to have very accurate information concerning all the factors influencing the test. Only when each of these tests can be repeated a sufficient number of times to determine the existence and extent of the error, can a true evaluation be made of total error effect. By repeated tests and quantitative analysis the authors have determined that these errors are significant and their effects should be considered in precise flowmeter calibrations.

The Naval Bureau of Ordnance calibration program is confronted with accuracy requirements increasing from the nominal 1 or $^1/_2$ per cent at industrial level to a primary standard level of better than 0.1 per cent. This accuracy is not only required at the flowrates at which the National Bureau of Standards tests were conducted, but over the range of flows from 15 lb per hr to more than 2,500,000 lb per hr. This paper, therefore, represents a step toward the achievement of the required accuracy over this range. The limiting factor, until now, has been an inability to determine the rate of increase of these potential errors at higher flowrates in dynamic weighing calibration systems.

The tests and results presented in this paper are being studied carefully by the Naval Bureau of Ordnance to find a means of applying the equipment and techniques found therein to the area of high-flow, high-accuracy, liquid-flow measurement. Before further progress can be made in adapting present, or developing new, flow-measuring devices to newly developed fuels, hydraulic fluids, and liquid oxidizing agents, the characteristics peculiar to these liquids must be determined and evaluated.

These evaluations and the errors discussed in this paper should be considered for their effect on higher accuracy requirements.

[7] Measurement Standards Division, U. S. Naval Inspector of Ordnance, Pomona, Calif.

It is suggested, indeed urged, that the authors continue their program of research and evaluation of the errors of liquid-flowmeter calibrators and that it be expanded to meet existing and future requirements of increased accuracy and higher flow ranges.

E. A. Spencer.[8] It is interesting to compare the equipment developed by the authors with that used to test flowmeters at the Government's Mechanical Engineering Research Laboratory at East Kilbride, Glasgow.

This laboratory, which is one of the research stations of the Department of Scientific and Industrial Research, has a number of circuits, using water as the working fluid to cover a wide range of sizes and flowrates, the maximum capacity being 6,000,000 lb/per hr (30 cu ft per sec). A smaller version of the main rig is comparable with the NBS static calibrator and was designed for flowrates up to 180,000 lb per hr through 6-in. piping. Early experiments indicated that very high accuracies could be obtained more easily with a static weighing technique than with volumetric tanks[9] and in fact direct weighing has been adopted in all the flow-calibration systems of the laboratories. In the main rig a weighbridge capable of weighing 30 tons of water was installed while for the smaller version a 2000-lb platform machine having a sensitivity of $^1/_4$ oz has been found adequate, the minimum period for diversion into the measuring tanks being 30 sec. Like the NBS system the movement of the diverter past its mid-travel position actuates an electronic counter and the diversion time can be measured in milliseconds.

One of the major differences between the authors' system and MERL is in the siting of the flow-control valve. In the latter a spear valve similar to that used for a Pelton wheel is situated at the end of the calibration line and the round jet issuing from this is changed to a thin rectangular stream by a fishtail nozzle attached to the valve. High-speed cine films have shown that the diverter moves across this stream in about 40 millisec. Experience with this method of flow control which ensures a safe positive pressure at the meter position has been very satisfactory and is considered preferable to the upstream position selected by the authors. In view of their remarks on the dangers of upstream throttling the reason for not siting the valve between the meter and the tee-junction to the calibrators is not apparent.

Although as the authors point out a calibration is only absolutely true for the actual conditions at the time of the test, the value of such a test on a flowmeter is that it should provide data which can be applied to the subsequent use of the meter in its final installation. The introduction of flow straighteners at or near the upstream entry to the meter may produce artificial conditions which will differ substantially from those experienced in practice and give rise to significant errors. Are the authors recommending that in effect a flow straightener should become part of the meter? Even with this arrangement it is desirable that the laboratory installation should be free from rotational disturbances such as those indicated by the extreme test points in the comparison of the four calibrators. Were the authors able to measure the amount of the swirl upstream from the reference meters?

The authors are to be congratulated on the very high standards of precision achieved with the equipment in calibrating flowmeters. These figures which are dependent on the sensitivity of the meter could usefully be supplemented by results on the steadiness of the rate of flow by comparing the successive measurements of the actual flowrate determined by the NBS calibrator. At MERL it has been found that the standard deviation of such repeated determinations with the control valve at a set position is

[8] Principal Scientific Officer, Fluid Mechanics Division, Mechanical Engineering Research Laboratory, Glasgow, Scotland.

[9] "The Accurate Calibration of Flowmeters With Water," by E. A. Spencer and A. T. J. Haward, *Trans. Society of Instrument Technology*, vol. 9, 1957, p. 1.

0.1 per cent. It should, however, be noted that the supply to the calibration lines is from a constant-head tank and not direct through a pump.

Authors' Closure

The authors wish to express their appreciation for the encouraging comments of the discussers. Regarding the comments by Mr. Galley, it is correct to state that the techniques are equally applicable to either volumetric or gravimetric flowmeters. His observations on cavitation in turbine sensors are important as the high velocity at the turbine blades, with its corresponding reduction in static pressure, frequently is a cause of vapor formation especially with hydrocarbon liquids. The authors are also in agreement that the flow must be uniformly turbulent at the test meter, and that gravity flow provides a better test condition for precision work.

Mr. Grotta brings out an important characteristic to be considered in the selection of reference meters; namely, much greater precision can be obtained with reference meters of the totalizing type having a calibration constant essentially independent of flow rate. The newer electronic methods of digital readout can be employed with these and the absence of an exact flow setting will not influence the results significantly. This eliminates the human error associated with the observation and setting of flow rate and greatly increases the precision of the calibration procedure.

The treatment of inertia error by Mr. Head is correct for the assumption of zero tare weight and a massless scale and weigh tank. As they are never attained actually, his dynamic errors are the maximum to be expected. However, even if these are given due consideration, the possibility of a significant inertia influence should be considered when dynamic weighing is used.

Mr. Morrow has effectively presented the fact that the old industrial tolerances of one per cent are no longer adequate, at least in the field of national defense, and has discussed a requirement for standards approaching the accuracy level of 0.1 per cent. Although the various individual components and instruments required for this precision are available, Spencer[9] has demonstrated the considerable work involved in attempts to attain such accuracy. The problem becomes even more complicated when one realizes that new hazardous liquids at both high and low temperatures and throughout wide pressure ranges are involved.

With reference to Dr. Spencer's very constructive comments it should be mentioned that a fundamental difference in objectives exists. Dr. Spencer is attempting to establish a flow rate laboratory having the highest possible accuracy, whereas the apparatus described in this paper was constructed for the single purpose of evaluating the performance and accuracy of three dynamic type calibrators of commercial manufacture. These had been designed for installation in industrial facilities for the calibration of flowmeters used in the aircraft industry. Thus in this particular work it was necessary to use the pumps, heat exchangers, and flow control valves supplied with the calibrators as part of the evaluation procedure. This is the reason the flow control valve was located upstream from the meter. The authors are in complete agreement that throttling should be accomplished downstream from the meter whenever possible.

Regarding the subject of flow straighteners, every type of flow rate indicating meter is influenced by the upstream flow conditions. The authors still recommend that flow straighteners should be considered part of the meter in applications requiring accuracies of a fraction of one per cent. This is especially true in the aircraft field where meter installation conditions deviate considerably from the ideal. Sprenkle and Courtright[10] have recently discussed a few types of straighteners and have demonstrated their effect upon the precision of flow measurement with orifice-type metering elements.

No attempt was made to measure the swirl upstream from the reference meters, it being deemed sufficient for our purposes merely to demonstrate that its presence contributed a significant influence. The authors are in agreement that laboratory calibrators should be free from rotational disturbances and pulsations. Naturally, such is best accomplished by utilizing a gravity supply. However, this is not always feasible in industrial installations especially those using hazardous liquid-hydrocarbons as the working fluid.

[10] "Straightening Vanes for Flow Measurement," by R. E Sprenkle and N. S. Courtright, *Mechanical Engineering*, vol. 80, February, 1958, p. 71.

(*Reprinted from the Transactions of the ASME for October, 1958*

CALIBRATION OF BELL PROVERS BY DIMENSIONAL ANALYSIS AND BY CUBIC FOOT STANDARDS

Comparison of "Strapping" and "Bottling"

by Charles T. Collett*

INTRODUCTION

The calibration of bell-type provers is a very worthy subject for a course in gas measurement because provers are standards and standards are the very foundation on which all measurements are based. After a manufacturer produces a bell designed to receive or discharge 2, 5, 100, or some other nominal number of cubic feet of gas, it must be calibrated to determine its true volume and must be recalibrated at intervals during its life, if it is to serve as an adequate standard.

As a background for studying the calibration of a bell prover, let us examine some of the characteristics of a good standard for a volume of gas. First of all and most obviously it must become larger or smaller with a minimum of pressure change as gas enters or leaves it. It must have a minimum of friction involved in the operation of its moving parts, because friction will introduce objectionable back pressures in the gas stream or raise the pressure in the volume which we are attempting to measure. For strength and rigidity it will have a circular cross-section. Preferably it will contain no liquid becuase liquids have properties sensitive to temperature, will change position under pressure, and will adhere more or less to any surface with which they come in contact. The material of which the standard is made will have a small coefficient of thermal expansion so that it will change its size as little as possible when temperature variations occur. So, the idealized standard for gas volume would perhaps be a piston, moving with a minimum of friction, and gas tight in a true cylinder.

In reality, all existing standards for gas measurement must in some way make a compromise between desirable and undesirable characteristics. For instance, we accept the use of liquids to secure the advantages of perfectly gas-tight seals with a minimum of friction between moving parts. For higher accuracy we may sacrifice large capacity, and vice versa. One standard now available consists of a plastic piston with a mercury-ring seal, moving in a precision-bore glass cylinder. The travel of the piston and the mean diameter of the cylinder can be measured to within a few thousandths of an inch. These are coming into general use for volumes up to about one-half cubic foot. Above this size the cost of the precision-bore glass tube and the difficulty of maintaining the mercury seal eliminate this type of construction from consideration at present.

---

*Physicist, National Bureau of Standards
Presented at Appalachian Gas Measurement Short Course, Morgantown, W. Va., August 26, 1964 and American Gas Association Operating Section Distribution Conference, Minneapolis, Minn., May 4, 1965.

Bell-type provers are a special form of piston-cylinder combination in which the cylinder (bell) moves and the piston (sealing liquid) would ideally remain stationary. In this case the volume of gas discharged would be very simply the internal volume of a section of the cylinder.

However, the level of sealing liquid does change for several reasons. As the bell descends the immersion of additional metal displaces liquid and raises the surface. The internal gas pressure is usually higher than atmospheric, and this depresses the liquid level between the inside of the bell and the inner wall of the tank, with a corresponding rise in the level between the outer surface of the bell and the outer wall of the tank. As the bell rises, liquid adheres to both inner and outer surfaces, lowering the level in the tank. The adhering liquid flows down the surfaces and raises the level in the tank gradually and at a decreasing rate for hours and even days. The level also changes slightly because of temperature variations.

Each of these changes has some effect on the calibration and use of a prover. Although it would be a pleasing circumstance if they were not encountered, fortunately none of them seriously impair the value of the device as a standard. The variations can either be shown to be insignificant, or can be taken into account by the application of suitable corrections.

For several decades, indeed about as long as meters have been checked against provers, it has been almost a universal practice to calibrate a bell-type prover by "bottling" it; that is, to transfer a cubic foot of air between a standard bottle and the prover. This procedure, which was described as early as 1926 in a publication of the National Bureau of Standards [1], had apparently become so traditional that for a long time not much attention was given to the possibility of finding other and perhaps better methods. However, several years ago, Mr. Hilding V. Beck and some of his associates in the American Meter Company developed an entirely different method of calibration in which the physical dimensions of the bell and the tank and the levels of the sealing liquid are measured, and the capacity is then computed. Because a steel tape is passed around the circumference of the bell, the procedure has become known as "strapping" [2].

It is the purpose of this paper to compare the methods of calibration by bottling and strapping, including some of the advantages and disadvantages of each, and to point out the sources and effects of the measurement uncertainties involved in each method.

1. CALIBRATION BY CUBIC-FOOT BOTTLE

The immersion type cubic-foot bottle now in general use is well known in the gas industry. The nickel or chromium-plated copper bottle is open at the end of the lower neck and may be lowered into a tank of sealing liquid, usually a light oil of low vapor pressure. As the liquid enters at the

bottom and fills the interior up to a graduation mark on the gage glass in the upper neck, one cubic foot of air is displaced and flows through a connecting tube to the prover bell, which rises.

The transfer of air can be from the descending bottle to the rising bell of the prover, or from the descending bell to the rising bottle. In either case the results should be approximately the same, except for slight differences in the behavior of the sealing liquid. A residual amount will remain on the walls of the instrument that has been standing in a raised position before it descends, while the rising surfaces of the other will carry adhering liquid upward. Because the total involved surface area of the bell will not be the same as that of the bottle, a perfect duplication of performance between the two cases cannot be expected.

Transfers can be made with the system under normal prover pressure, or with the counterweights adjusted to balance the bell at atmospheric pressure. The first method produces the slight difficulty of setting the liquid level in the gage glass of the bottle while it is slightly below the level of the surface in the tank; also it involves the necessity of raising the bottle at the end of the transfer until one or two small bubbles of air are seen to escape.

For each cubic foot of air to be passed into or out of a prover, the bell is first placed in a position, by manipulating the rotary slide valve, so that the trial begins with a cubic-foot mark on the scale opposite the pointer. If the scale, the standard, and the procedure were all perfect, the next cubic-foot mark would be exactly opposite the pointer at the end of the test. The difference between one cubic foot and the volume indicated by the scale is the error determined by the calibration. This procedure is repeated to measure successive cubic-foot increments until the entire range of the prover has been tested.

Frequently the bottle has been replaced by another device called a "Stillman cubic-foot standard" after its inventor, the late Mr. M. H. Stillman of the National Bureau of Standards [3]. A movable bell rises and descends in an annular tank very similar to that of a prover. The bell is guided by a central vertical column sliding in a close-fitting cylinder, and upward travel is limited by an adjustable stop. This standard is about as accurate as a cubic-foot bottle, is used in a similar procedure, and offers the additional advantage that it is easily portable. By draining the sealing oil from it, and placing it in its carrying case, a task which can be accomplished quite readily, the user can easily transport it from place to place, say by automobile. It is as easily set up and placed in service, except that a period of several hours is sometimes required for the temperature of the standard to stabilize and become equal to that of the prover to be tested. Because of its portability and its relatively small size

compared to a bottle in an immersion tank, it has found wide-spread acceptance by State public utility commissions and offices of weights and measures. Like the bottle, it can be sent to NBS for calibration.

The foregoing brief description of calibration by bottling is considered sufficient for the purposes of this article; the reader is referred to publications [1] and [2] in the list of references for complete detailed instructions on this traditional and widely used procedure.

2. CALIBRATION BY STRAPPING

The procedure of strapping a prover is well described in an article by Mr. Beck [4] and he has kindly given the writer his permission to draw freely from the material therein. The following discussion is illustrated by figures 1 and 2, which show diagrammatically the cross section of a typical bell-type prover. The capacity of the bell, i.e., its internal volume, plus the volume of the metal in the bell, is designated as the "outside volume." Each term applies only to the volume above the liquid surface, or "seal."

The validity of the method is based on this relationship: When a prover bell is lowered from any position to any other position, the volume of gas discharged will be equal to the outside volume above the seal at the first position, minus the outside volume above the seal at the second position, plus the volume of the metal in the scale that becomes immersed, and minus the volume of the fluid that rises between the outside of the bell and the main tank. The truth of this statement is not immediately obvious, but will be made clear by a simple analysis.

Figure 1 illustrates the bell position at 0 on the scale, with an internal pressure represented by the difference in levels of the sealing liquid inside and outside of the bell, designated by H. As the bell descends to position 100, as shown in figure 2, if there were no change in the level of the sealing liquid, the volume of gas, Q, discharged would be equal just to the change of interior volume of the bell, B, above the liquid surface. However, the level of the surface in the annular space between the main tank and the outside of the bell, and the level between the inside of the bell and the center tank, rise because some liquid is displaced by the metal in the bell and the scale. The volume of liquid which rises between the inner tank and the interior surface of the bell, W, displaces gas and therefore adds to the volume of gas, Q, which is discharged. The interior volume change, B, is equal to the outside volume change, V, minus the volume of the metal that becomes immersed, M. The volume of the immersed metal of the bell, M, plus the volume of the immersed metal of the scale, S, is equal to the volume of the liquid which rises between the inside surface of the bell and inner tank, W, plus the volume of the liquid which rises between the outside surface of the bell and the main

tank, T. Stating these facts by symbols and rearranging:

$$Q = B + W \qquad B = V - M \qquad M + S = T + W$$

$$Q = V - M + W \qquad M = T + W - S$$

$$Q = V - T - W + S + W$$

$$Q = V + S - T$$

The last equation shows that the statement of principle, upon which the method is based, is indeed true.

The outside volume of the bell is obtained by measuring the circumference, or "girth", with a calibrated steel tape, determining the vertical distance through which the bell travels by measuring the distance between graduation marks on the scale, and then calculating the volume. The tape has thickness and is read on the outer surface, therefore a correction is necessary. On the assumption that the extension and compression of the layers of the tape outside and inside the center are approximately equal, the thickness multiplied by π is deducted from the circumference reading. However, there is a commercially available steel tape reading directly in diameter of a cylindrical object, with the tape thickness taken into account.

Manufacturers state that prover bells are usually quite cylindrical, with circumferences which do not deviate more than about plus or minus 0.03 inch from the average circumference. If the bell is found to be as cylindrical as this figure indicates, an adequate calibration could be based on the average girth, and the scale would have equal divisions throughout its length. However, some bells will be found which deviate more than this amount from a perfect cylinder, and the decision as to how many increments should be individually calibrated will be based on the pattern and amount of deviation. In laying out a plan for a calibration, the scale point at the middle of the increments being tested should be selected, and the corresponding plane of intersection of the liquid with the bell should be observed. The circumference of the bell should be measured in this plane.

The volume of liquid which rises in the tank is computed from the change in surface level and the bell and tank dimensions. Liquid-level readings should be carefully made by means of a micrometer depth gage firmly held and unmoving on a flat upper surface of the tank.

For the relationship $Q = V + S - T$ to be rigorously true, two requirements must be satisfied. First, the prover and counterweights must be adjusted to insure that the pressure within the bell is the same at any position as well as those seen in Figs. 1 and 2. This may be checked by connecting a

good draft gage or inclined manometer to indicate the internal pressure. Another procedure is to open the interior to atmosphere by means of the prover rotary valve, adjust the counterweights until the bell remains stationary at any position, and perform the calibration under these conditions. Second, and again speaking in the most rigorous sense, there should be no liquid adhering to or draining down the walls, a condition which is theoretically never achieved. The practical effect of this will be discussed in a subsequent section.

A typical set of measured values and the simple calculations required are shown below. Not all of the recorded figures given can be justified by the accuracy of the measurements, but they are retained for clarity in the illustration.

Average observed circumference of prover bell	66.047 in.
Length of scale, 0 to 5 ft^3	25.031 in.
Average thickness of prover scale	0.117 in.
Average width of prover scale	1.125 in.
Average distance between outer surface of bell and inner surface of outer prover tank	1.942 in.
Oil rise in tank for bell travel 0 to 5 ft^3	0.345 in.
Thickness of strapping scale	0.006 in.
Corrected average circumference of prover bell, $66.047 - (3.14 \times 0.006) =$	66.028 in.
Bell diameter, $D = 66.028 \div 3.1416 =$	21.017 in.
Outside volume of bell, $V = \frac{3.1416 \times (21.017)^2}{4 \times 144} \times \frac{25.031}{12} =$	5.0254 ft^3
Volume of immersed portion of scale, $S = \frac{25.031 \times 1.125 \times 0.117}{1728} =$	0.0019 ft^3
Tank diameter at sealant level, $D_2 = 21.017 + 2(1.942) =$	24.901 in.
Volume of oil rise, $T = \frac{3.1416\ (24.901^2 - 21.017^2)}{4 \times 144} \times \frac{0.345}{12} =$	0.0280 ft^3
Volume of air discharged, $V + S - T =$	4.9993 ft^3
Scale too short by $\frac{5.000 - 4.9993}{5.000} \times 100 =$	0.014%

3. COMPARISON OF GENERAL CHARACTERISTICS AND SOURCES OF UNCERTAINTIES

Bottling

Most cubic-foot bottles are calibrated at the National Bureau of Standards by weighing them while filled with water. The reported volume is estimated to be accurate to within 1 part in 25,000 or 0.004%. However, the only link between this standard and the prover being tested is the air that fills the system during the test, and the accuracy of the final results can be only as good as this connecting link will permit. Air will change in volume by about 1 part in 500 per degree F of temperature change, therefore if bottle and prover temperatures differ by 1 °F an error of about 0.2% will result. It is recognized that the bottle should stand close to the prover in a room with stable temperature until the temperatures of the instruments are nearly the same, and an overnight period is desirable.

The value within which successive bottling calibrations should agree was stated as 0.3% in 1926 [1] and 0.2% in 1965 [2]. Careful observers working in rooms with stable temperatures can readily repeat their results within 0.1%.

Sealing liquids, whether oil or water, adhere more or less to the walls of bottles and bells as they are raised, and drain back into the tanks rapidly at first and then more slowly. Some oil may be retained on the walls for many hours, but a 3-minute draining period in advance of a test run is thought to eliminate any significant errors from this cause [5].

With the exception of preliminary waiting periods, the process of bottling is accomplished within a few minutes of actual work, and the amount of data recorded is small compared to that required in strapping. Dents and any other significant deformations of a prover bell are automatically included in the results of a bottling calibration, and the procedure may also call attention to friction or unbalance in the chain, pulley, and counterweights.

Immerson-type bottles are suitable only for semi-permanent installation in laboratory-type rooms, but the Stillman cubic-foot standard offers about the same inherent accuracy combined with complete portability.

Strapping

One of the outstanding characteristics of the strapping method is its insensitivity to changes in ambient temperature. In contrast with air, the steels and coppers used in bells and in measuring tapes have a linear expansion of only a few parts per million per °F. A tape is in firm contact with a bell during the measurement of its circumference; their temperatures thus tend to be nearly equal. About the only other requirement as to temperature is that it should not be changing rapidly enough during the calibration to affect the level of the sealing liquid, a very unlikely circumstance.

The steel scales, verniers, and micrometers used in strapping should be of high quality; the bias or error inherent in the instruments should be relatively insignificant compared to the uncertainties associated with making the measurements.

If reasonable care is used in calibrating, say, a 5 ft^3 prover, the maximum variations between measurements by different observers and at different times should be not more than: 0.01 inch for the length of the scale; 0.001 inch for the average thickness and width of the scale; 0.001 inch for the change in fluid surface level; and 0.003 inch for the bell diameter and the distance from bell to tank.

A variation of 0.01 inch in measuring the scale length, for instance, will produce a change in the computed scale error of 0.05%. In contrast, a variation of 0.01 inch in the measurement of the width of the scale will not affect the computed scale error within the limits of significant figures retained. In the improbable event that all the values of a set of measurements were larger, or all were smaller, than the values of another set by the maximum amounts estimated above, the total variation in the computed values for scale length error would not exceed 0.07%.

When a bell is first raised, for a few seconds the adhering sealing liquid drains downward so rapidly that waves are visible as they descend. If the liquid is oil, the surface level during this brief period will be abnormally low, by as much as 0.05 inch in a 5 ft^3 prover tank, equivalent to a computed scale error of 0.05%. Actually this drainage can be detected for several hours, but its effect on the surface level becomes negligible after just a few minutes. A careful observer should make a few readings with the micrometer depth gage while the bell remains stationary at its uppermost position, and thus determine when the effect of drainage is small enough to be disregarded.

Since the calculations depend upon the relationships between the circumferences and diameters of circles and the diameters and altitudes of cylinders, the bell must have a cross section close to a true circle. If this requirement were not satisfied it could not be claimed that the calculations were rigorously true. Actually this does not cause any real difficulty. Manufacturers say that the production of a prover bell with a truly round cross section is not difficult by modern methods. Strapping has no tendency to distort the shape of the bell; on the contrary it has a theoretical, but insignificant tendency to make the shape of the bell approach a cylinder. Even if a circular cross section should be distorted into an ellipse by decreasing one diameter 1 percent and increasing the diameter at right angles also by 1 percent, the total change in area would be only about 0.01 percent.

Appreciation is extended to the Rockwell Manufacturing Company and the American Meter Company for supplying information and assistance.

REFERENCES

1. Gas Measuring Instruments, Circular 309, National Bureau of Standards, 1926.

2. Displacement Gas Meters, Handbook E-4, American Meter Company, 1965.

3. A Portable Cubic-Foot Standard for Gas, M. H. Stillman, Technologic Paper T114, National Bureau of Standards.

4. Calibration of Bell Provers, H. V. Beck, American Gas Association Monthly, September 1964.

5. Gas Meter Specification OP58-2, American Gas Association.

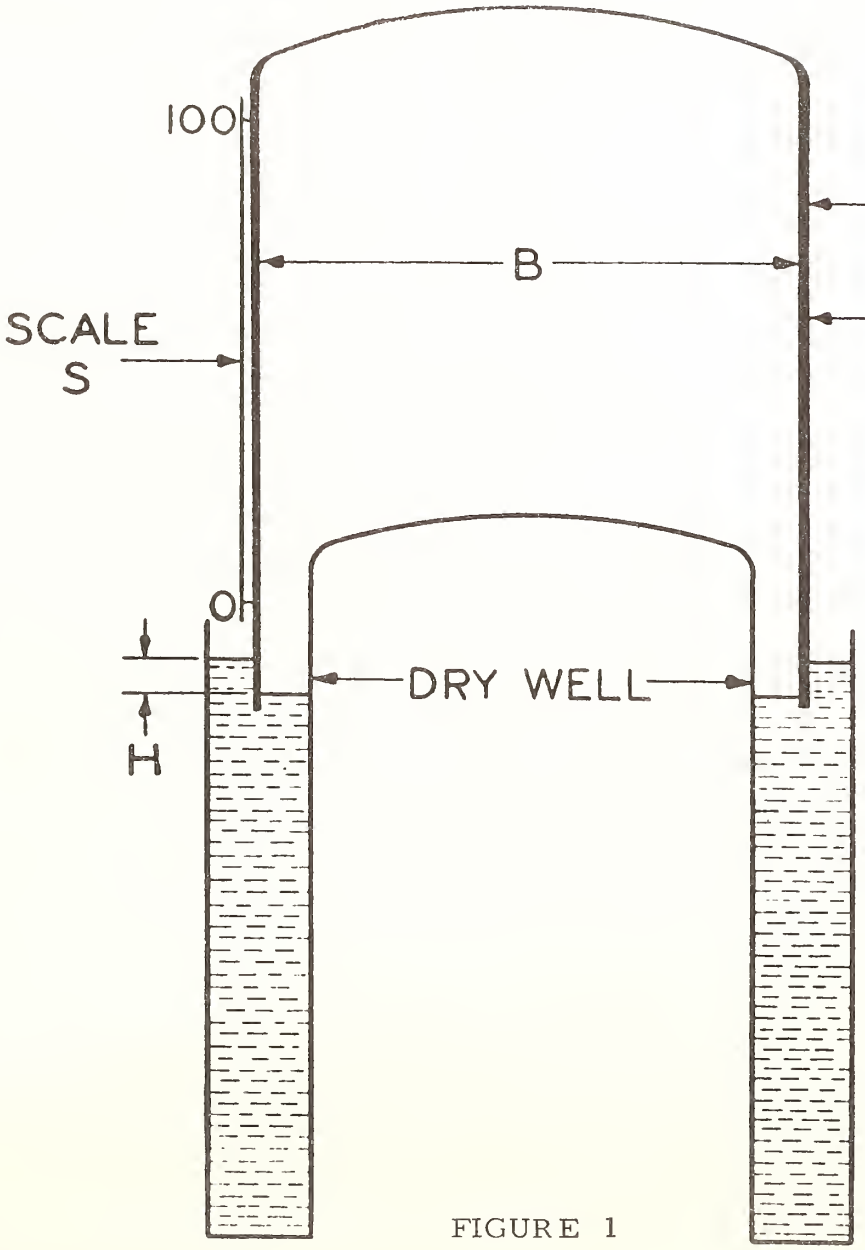

FIGURE 1

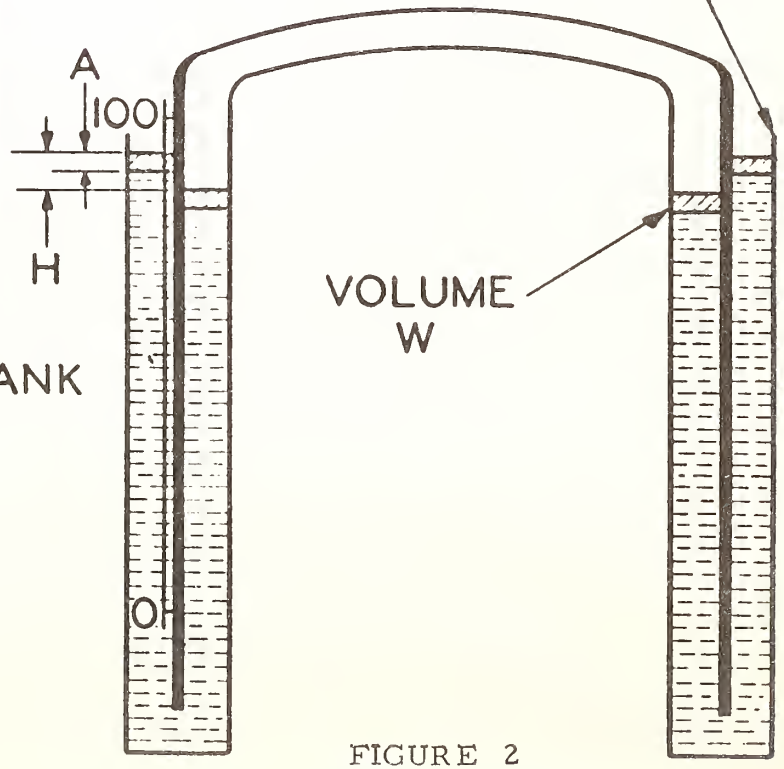

FIGURE 2

An Examination of the Effects of Heat Transfer and Compressible Flow on the Performance of Laminar Flowmeters

By F. W. Ruegg and H. H. Allion

National Bureau of Standards
Washington, D. C. 20234

Presented at:

Fluid Meters Golden Anniversary
Flow Measurement Conference
Pittsburgh, Pennsylvania
September 26-28, 1966

THE AMERICAN SOCIETY OF MECHANICAL ENGINEERS
United Engineering Center
345 East 47th Street
New York, New York
10017

I. ABSTRACT

Laminar meters are now widely used for measurement of gas flow, and high accuracy can be achieved with proper calibration and use. It has been found necessary to modify Poiseuille's law for laminar flow to explain the performance of meters over the wide range of flow conditions encountered. A one-dimensional flow analysis is used to derive the effects of meter shape, heat transfer, and compressibility of the gas on meter performance. A relationship between the meter flow coefficient and the similarity parameters of Reynolds number, Prandtl number, Mach number, and Knudsen number is given in a form that is convenient for both the calibrator and user of the meter. The small but significant effects predicted are compared with experimental results.

II. INTRODUCTION

The laminar flowmeter is finding acceptance as a convenient instrument for measurement of gas flow, and a variety of sizes and designs are in use. Both accurate measurement and flexibility of use should be promoted through an improved, more complete understanding of the phenomena encountered in a practical meter operating over a wide range of conditions. The design of commercial meters is the result of compromises between requirements of size, multiplicity of channels, cost, flow theory, and other requirements. Although the discussion is mainly about flow theory and its application, some aspects of commercial or "practical" meters are also discussed.

In this paper, using information in the literature, flow through a model which simulates some features of a practical meter is analyzed to derive the effects on meter performance of (a) gas properties including compressibility, (b) meter design, (c) heat transfer, and (d) the effect of "slight" rarefaction and slip flow of the gas if encountered. Some approximations are necessary to derive a useable meter equation that describes the influence of the effects mentioned. The description of the flow given by Hagen and Poiseuille, with volume rate proportional to pressure differential, is corrected by factors containing the appropriate similarity parameters. The resulting meter equation is given in a form that utilizes measured quantitites directly to determine the flow coefficient and the corresponding rate of flow. Results of experiments over a wide range of conditions with two gases and two meters are treated as required by the meter equation.

It is hoped that calibrating, reporting and use techniques will be improved. Meter designs, which are not yet standardized, may benefit

through this attempt to derive the effect of some of the practical aspects of meter construction.

III. THE METER

The model chosen for the meter is illustrated in Figure 1 and consists of n identical slots of length L from stations 1 to 3, with ends of the slots connected to common plenum chambers of cross-sectional area $A_o = 2aS$. Half-height of each slot is called b, depth normal to the plane of the figure is S, and A_1 is the total cross-sectional area of the n slots assumed much smaller than A_o. Flow separation in the region of length ℓ between the abrupt contraction and station 1 is possible with unknown effects therein. A constant velocity is assumed across station 1 where the velocity profile starts to develop towards a fully developed, parabolic profile at station 2. Laminar flow with a parabolic velocity profile exists between stations 2 and 3, and is assumed not to be distorted significantly by heat transferred to or from the meter body. At station 3 the ends of the slots connect to a plenum chamber which also has cross-sectional area A_o. Pressure taps in the side walls are used to measure static pressures P_o and P_4 in each plenum chamber.

Although laminar flow is assumed to exist in the slots, the possibility of turbulent flow in the plenum chambers should be considered. Flow in a slot with one side 2b much smaller than the other side S can be characterized by a Reynolds number R_b as given by

$$R_b = \frac{2w}{\mu Sn} \tag{1}$$

using μ and w as the fluid viscosity and total mass flow, respectively, and the assumption that each slot receives an equal share of the flow. The Reynolds number in the plenum of hydraulic mean depth $m = 2aS/(4a+2S)$

is given by

$$R_a = \frac{4w}{\mu(4a+2S)} \tag{2}$$

and the ratio R_a/R_b is

$$\frac{R_a}{R_b} = \frac{Sn}{(2a+S)} \quad . \tag{3}$$

In the case of a meter with a single slot, n = 1, the length of side 2a is usually approximately equal to S and R_a is smaller than R_b. However, for a meter with many slots and with $2a \ll S$, R_a will approach nR_b, giving the possibility of turbulent flow in the plenum chambers. A similar analysis for a meter with concentric, annular slots also gives $R_a \simeq R_b n$, and also a possibility of turbulent flow in the plenum chambers.

IV. FLOW ANALYSIS

The fall in pressure $(P_o - P_4)$ from stations 0 to 4 is given by the sum

$$P_o - P_4 = (P_o - P_1) + (P_1 - P_2) + (P_2 - P_3) + (P_3 - P_4) \tag{4}$$

and information in the literature is used to derive the part that each term plays in the sum. The influence of compressible flow and heat transfer on $(P_1 - P_2) + (P_2 - P_3)$ is derived using a one-dimensional analysis of the flow of a perfect gas. Both heat transfer and compressibility are assumed to play a small, but significant, role in the result. Coefficients are used in the one-dimensional alaysis to make the results applicable to the actual flow pattern which is, for all practical purposes, two-dimensional between stations 1 and 3. The results are given as a functional relationship

$$f(\psi, \psi R_b, M, \sigma, A) = 0 \tag{5}$$

for a flow coefficient for the meter, ψ, and the similarity parameters R_b, M, σ and A. These parameters are the Reynolds number, Mach number,

Prandtl number and a shape factor for the meter, respectively. ψ is a ratio of $(P_o-P_4)/\mu Q$ to the value given by Poiseuille, $[(P_o-P_4)/\mu Q]_o$, with μ and Q the fluid viscosity and total volume rate of flow, respectively. A second shape factor for the meter, L/b^2A_1, is implicitly included in $[(P_o-P_4)/\mu Q]_o$. Equation (5) may be used as a basis for a calibration curve for the meter.

A. (P_o-P_2). Referring to Figure 1, effects of the sudden contraction between stations 0 and 1, and development of laminar flow between stations 1 and 2 are treated as corrections to a fully developed flow starting at x = 0. Measurements reported by S. T. McComas and E. R. G. Eckert [1][1] in a developing laminar flow along a circular tube downstream from an abrupt entrance indicated the possibility of flow separation at the entrance, but no measurable irreversible pressure loss therefrom. In their experiment the velocity across the plenum chamber was presumably a constant or possibly similar to a fully developed, turbulent flow. The pressure measured in the fully developed laminar flow at station 2 was essentially equal to that predicted for a flow which started with a constant velocity across the tube. Distance ℓ between the abrupt entrance and station 1 is assigned as a reminder that a pressure tap located in a region of possible flow separation may indicate an abnormally low pressure, and with the reservation that the question of the length of the separated flow region and its effects is not definitely resolved. E..M. Sparrow, T. S. Lundgren and S. H. Lin [2] derived the pressure drop for a developing laminar flow between parallel planes and reported it as a correction P_c over and above that for a fully developed flow. For a continuum (or non-slip) flow

[1] Numbers in [ ] refer to the literature references.

regime, P_c approached a limit value of about 0.85 q_2. The term q is defined as $\frac{1}{2}\rho V^2$, with ρ and V the fluid density and bulk velocity, respectively. The distance between stations 1 and 2, x_1-x_2, or the distance in which P_c approached 98 percent of 0.85 q_2 is given in [2] as

$$x_1-x_2 = 0.04bR_b \ . \tag{6}$$

Corresponding values given by S. Goldstein [3] are $0.6q_2$ for P_c and about $0.04bR_b$ for x_1-x_2. Considering the results presented in [1] and [2], x_2 is also taken as $0.04bR_b$, and if the meter length L is longer than x_2, P_c is considered as 0.85 q_2. For a meter shorter than 0.04 bR_b, P_c depends on the length. The results of [2] are approximated here by the relation

$$1 - \frac{P_c(x)}{0.85\ q_2} \simeq \exp(-100x/bR_b),\ L < 0.04bR_b \ . \tag{7}$$

If turbulent flow exists at station 0, Bernouilli's equation between stations 0 and 2 may be written, with subscript t to represent the turbulent case, as follows:

$$(P_o-P_2)_t = q_1 - q_o + P_c,\ L > 0.04bR_b \ . \tag{8}$$

At this point it is desirable to write the q's in equation (8) in terms of a $\bar{q}$ based on average conditions of temperature $\bar{T}$ between stations 1 and 3, and pressure $\bar{P}$ between stations 0 and 4. A relation between q_1 and $\bar{q}$ can be shown to be as follows:

$$q_1 = \bar{q}\ \frac{\bar{P}}{P_1}\ \frac{T_1}{\bar{T}}\ \frac{(\bar{A})^2}{A_1^2} \ . \tag{9}$$

For incompressible flow between stations 0 and 1, equation (9) transforms equation (8) to

$$(P_o-P_2)_t = \bar{q}\ \frac{\bar{P}}{P_1}\ \frac{T_1}{\bar{T}}\left(1 - A^2 + \frac{P_c}{q_1}\right) \tag{10}$$

using A_1 for $\bar{A}$ and A_2, and A as the ratio A_1/A_o. Equation (10) can also be written in the form

$$P_o - P_2 = \bar{q}\, C_{i,t} \tag{11}$$

with $C_{i,t}$ derivable from Equation (10).

If laminar flow exists at station 0, Bernouilli's equation may be applied to the flow between station 0 and 2 as

$$(P_o - P_2)_L = (q_1 - \frac{54}{35} q_o + P_c) \tag{12}$$

using 54/35 as a factor to derive the kinetic energy per unit mass from the bulk velocity in the laminar region. Velocity across a thin duct ($a \ll S$) with laminar flow therein was derived from the equation

$$V(y) = V_c\ (1 - \frac{y^2}{b^2}),\ 0 \leq y \leq b \tag{13}$$

with y as the variable distance from the center of the duct. Equation (13) can also be used to show that V is $\frac{2}{3}V_c$, with V_c the velocity at the center. Equation (12) for $(P_o - P_2)_L$ is transformed with the aid of an equation similar to Equation (9) to:

$$P_o - P_2 = \bar{q}\, C_{i,L} = \bar{q}\, \frac{\bar{P}T_1}{P_1\bar{T}}(1 - \frac{54}{35} A^2 + \frac{P_c}{q_1}) \ . \tag{14}$$

Use of the pressure correction procedure outlined above requires that equation (4) be modified as follows:

$$P_o - P_4 = (P_o - P_1) + (P_1 - P_2)_c + (P_1 - P_3) + (P_3 - P_4) \ . \tag{15}$$

In this form subscript c identifies the pressure correction between stations 1 and 2, and $(P_1 - P_3)$ will be calculated below for a fully developed flow.

B. $(P_1 - P_3)$. The influence of friction, gas compressibility, and heat transfer on the pressure drop $(P_1 - P_3)$ is derived starting with a

generalized, one-dimensional flow equation as given by A. H. Shapiro [4]. In terms of the Mach number M the equation is

$$\frac{dM^2}{M^2} = \frac{kM^2 f(M)}{1-M^2}\,\frac{4f\,dx}{4b} + \frac{(1+kM^2)f(M)}{1-M^2}\,\frac{dT^\circ}{T^\circ} \tag{16}$$

in which k is the ratio of specific heats, T° is the stagnation temperature which changes as heat is transferred, and f(M) is $1 + \frac{1}{2}(k-1)M^2$. A proper choice for the friction factor f in Equation (16) gives the correct results for a flow that is actually two-dimensional from a one-dimensional analysis. Use of the Mach number M implies that the fluid is compressible and therefore a choice of f based on incompressible flow theory should be justified. R. A. Noftzger and J. R. Moszynski [5] demonstrate that the velocity profile is little changed by the compressibility from the parabolic profile and conclude that the distortion has a small effect compared to the acceleration of the fluid along the duct. With little distortion of the profile an "incompressible f" is a reasonable choice. A multiplication of both sides of Equation (16) by $(1-M^2)/(kM^2 f(M))$ gives

$$\frac{1-M^2}{kM^2 f(M)}\,\frac{dM^2}{M^2} = \frac{4f\,dx}{4b} + \frac{1+kM^2}{kM^2}\,\frac{dT^\circ}{T^\circ} \tag{17}$$

Integration of this will require some approximations.

Integration of the left side of Equation (17), assuming k constant, gives

$$\int \frac{(1-M^2)}{kM^2 f(M)}\,\frac{dM^2}{M^2} = \frac{-1}{kM^2} + \frac{k+1}{2k}\,\ell n\,\frac{f(M)}{M^2}\,. \tag{18}$$

Some relations as given by [4] and used to transform Equation (18) to a more useful form are listed below:

(a) $M^2 = V^2 C^{-2}$, C = velocity of sound

(b) $C = (kR\,T/W)^{\frac{1}{2}}$, R = universal gas constant

W = molecular weight

(c) $T^\circ = Tf(M)$, T = static temperature (19)

(d) $w = PA_1M(Wk/RT)^{\frac{1}{2}}$, w = mass flow

(e) $w = \rho Q = \rho A_1 V = \frac{PW}{RT} A_1 V$

(f) $\bar{q} = \frac{1}{2}\bar{\rho}\bar{Q}^2/A_1^2$

Equation (18) is transformed, using relations (a), (b), (c) of Equation (19), to get

$$\int \frac{(1-M^2)dM^2}{kM^2 f(M)M^2} = \frac{-1}{kM^2} - \frac{k+1}{2k} \ell n \frac{V^2 W}{kR\, T^\circ} . \tag{20}$$

Insertion of the limits of integration in the logarithmic term is performed (approximately) with aid of the differential calculus (as $d\ell nx = dx/x$) and with the aid of Equation (19e). The differential calculus (to find $d(P^2T^{-1})$) and Equation (19d) are used to expand $k^{-1}M^{-2}$, and Equation (20) becomes:

$$\int_1^3 \frac{(1-M^2)dM^2}{kM^2 f(M)M^2} = \frac{2A_1^2 W}{w^2 R} \frac{P_{1,3}}{\bar{T}} (P_1-P_3) \left(1 + \frac{P_{1,3}}{2(P_1-P_3)} \frac{T_3-T_1}{\bar{T}}\right) - \frac{k+1}{2k}\left(\frac{2(T_3-T_1)}{\bar{T}} + \frac{2(P_1-P_3)}{P_{1,3}} - \frac{T^\circ_3-T^\circ_1}{\bar{T}^\circ}\right) \tag{21}$$

The technique of inserting the integration limits assumes that change of all quantities is small compared to their absolute value. The influence of small, second order quantities ignored ordinarily will not be detectable.

The first term on the right side of Equation (17) may be integrated after replacing f with K/R_b as given by [3]. Thus, we have

$$\int \frac{f\,dx}{b} = \frac{KA_1}{4bw} \int \frac{\mu\, dx}{b} = \frac{\mu_o K A_1}{4bw} \int \left(\frac{T}{T_o}\right)^r \frac{dx}{b} \tag{22}$$

with the viscosity expressed as dependent on temperature with exponent r. R. H. Norris and D. D. Streid [6] numerically integrated the energy equation for a two dimensional, laminar flow field assumed not distorted

by the heat transfer from boundaries at temperature T_w. Their results are reported in the form of a table of Nusselt numbers (Nu) vs. values of the parameter $\varphi(x) = \alpha R4b/x$. It can be shown that the mean or "mixing cup" temperature T at any point x along the meter is given by the relation

$$\frac{T(x) - T_w}{T_1 - T_w} = \theta(x) = 1 - 4\frac{Nu}{\varphi(x)} \tag{23}$$

when Nu is based on the temperature difference at the inlet. Their results transformed in this manner yield an approximate relation for θ, to be used herein, in the form:

$$\theta(x) \simeq \exp[-(32/\varphi(x)]. \tag{24}$$

From Equation (24) values of θ for small distances from the inlet are not more than about 8 percent greater than those given in [6].

Equation (24) is based on a fully developed flow field, but here it is to be applied to the developing field with justification as follows. E. R. G. Eckert and R. M. Drake, Jr. [7] report on local values of Nu in the developing region inside a circular tube. In the last 90 percent of the length of the developing field the values of Nu are, on the average, about 15 percent larger than for the fully developed flow. For flow between parallel planes, the difference is expected to be about the same, and the error in using equation (24) will not be large. Thus the eight percent error in equation (24) may be partially compensated when it is used in the developing flow field.

Assuming that the meter responds to viscosity μ as determined from T(x) given by θ, equations (22) and (23) yield, using the first term of a series expansion of T^r,

$$\int \frac{f\,dx}{b} = \frac{\mu_o K A_1}{4bw} \int \left(\frac{T_w}{T_o^\circ}\right)^r \left[1 + r\theta \frac{T_1 - T_w}{T_w} + \text{------}\right] \frac{dx}{b}. \tag{25}$$

An integration, using θ as given by equation (24), and the assumption that σ and R in $\varphi(x)$ are constants, produces

$$\int_1^3 \frac{f\,dx}{b} = \frac{KA_1}{4bw}\frac{L}{b}\mu_w f(\varphi) \quad . \tag{26}$$

This contains the viscosity $\mu_w = \mu_o\,(T_w/T_o)^r$ modified by a correction factor $f(\varphi)$ given below:

$$f(\varphi) = \left(1 - \frac{T_1 - T_w}{T_w}\varphi(L)\right)\left[\exp\left(-32/\varphi(L)\right)-1\right])^r \quad . \tag{27}$$

In considering the final term of equation (17), the second on the right, it is noted this also involves the effect of heat transfer on the meter performance. In this integration M is assumed a constant and equal to $M_{1,3}$ the average between stations 1 and 3. Little error is introduced by this assumption as we are interested in small values of dT°/T° only. With the aid of equation (19d) and the above assumption, the integral can be written

$$\int \frac{1+kM^2}{kM^2}\frac{dT^\circ}{T^\circ} = \left(1 + \frac{WA_1^2P_{1,3}^2}{w^2R\bar{T}}\right) \ell n\ T^\circ \quad . \tag{28}$$

Again, using $d\,\ell n\,x = dx/x$ for inserting the integration limits we have:

$$\int \frac{1+kM^2}{kM^2}\frac{dT^\circ}{T^\circ} = \left(1 + \frac{WA_1^2P_{1,3}^2}{w^2R\bar{T}}\right)\frac{T_3^\circ - T_1^\circ}{\bar{T}^\circ} \quad . \tag{29}$$

All terms of equation (17) are now in forms useful to find (P_1-P_3), and the equation is now written, using equations (21), (26), and (29) as

$$\frac{2A_1^2W\,P_{1,3}(P_1-P_3)}{w^2R\bar{T}}\left(1 + \frac{P_{1,3}}{2\Delta P}\frac{\Delta T}{\bar{T}}\right) - \frac{k+1}{2k}\left(\frac{2\Delta T}{\bar{T}} + \frac{2\Delta P}{P_{1,3}} - \frac{\Delta T^\circ}{\bar{T}^\circ}\right) =$$

$$\frac{KA_1L\mu_w f(\varphi)}{4wb^2} + \left(1 + \frac{WA_1^2P_{1,3}^2}{w^2R\bar{T}}\right)\frac{\Delta T^\circ}{\bar{T}^\circ} \tag{30}$$

with ΔP taken as (P_1-P_3), ΔT taken as (T_3-T_1), and $\bar{T}^\circ$ as $\frac{1}{2}(T^\circ_1 + T^\circ_3)$.

The equation above can be simplified by combining like terms after $\Delta T/T$ is expressed in terms of $\Delta T^\circ/T^\circ$. Using equations (19a), (19c) and (19e) we have

$$\frac{\Delta T}{T} \simeq \frac{\Delta T^\circ}{T^\circ}\left(1 - (k-1)M^2_{1,3}\left[\frac{\Delta P T^\circ}{P \Delta T^\circ} + \frac{1}{2}\right]\right) . \tag{31}$$

Equation (31) is an approximate relation because terms containing M^4 have been omitted. Use of equation (31), and a multiplication of both sides of equation (30) by $2\bar{q}$ (see (19e) and (19f)), transforms it to

$$(P_1-P_3)\frac{P_{1,3}}{\bar{P}}\left(1 - \frac{2\bar{q}}{\bar{P}}\frac{(\bar{P})^2}{P^2_{1,3}}\left[1 + \frac{P_{1,3}\Delta T^\circ}{\Delta P \bar{T}^\circ}\right]\right) = \frac{K l \mu_w \bar{Q} f(\Phi)}{8 b^2 A_1} , \tag{32}$$

a form which illustrates the effect of heat transfer and compressibility on the pressure drop (P_1-P_3). The influence of compressibility appears in the term $2\bar{q}/\bar{P}$ which can also be written as $k\bar{M}^2$.

C. (P_3-P_4). The conservation of momentum theorem as given by [4] is used to derive the pressure change across the abrupt enlargement at station 3. No skin friction is assumed at the walls of the plenum chamber and therefore the theorem gives:

$$A_4(P_3-P_4) = A_o(P_3-P_4) = \rho\int V_4^2 dA_o - \rho\int V_3^2 dA_o . \tag{33}$$

As before, we consider the flow laminar at station 3, and include both turbulent and laminar flow cases at station 4.

In the turbulent case, V_4 is essentially constant across station 4, and equation (13) is used for the velocity profile at station 3 (inside the slot). Equation (33) is now written in the form

$$A_o(P_3-P_4) = \rho_4 V_4^2 A_o - 2\rho_3 V_c^2 \int_o^b \left(1 - \frac{y^2}{b^2}\right)^2 S \, dy . \tag{34}$$

An integration, substitution of $\frac{3}{2}V_3$ for V_c, use of a relation for the q's as in equation (9) and an assumption that $\rho_3 = \rho_4$ transforms equation (34) to that below:

$$(P_3-P_4)_t = q_3(2A^2 - \frac{72}{15}A) = \bar{q}\,\frac{\bar{P}}{P_3}\,\frac{T_3}{\bar{T}}(2A^2 - \frac{72}{15}A) = \bar{q}\,C_{e,t}\,. \qquad (35)$$

A similar analysis for the case of laminar flow at stations 3 and 4 yields

$$(P_3-P_4)_L = q_3\,\frac{72}{15}(A^2 - A) = \bar{q}\,\frac{\bar{P}}{P_3}\,\frac{T_3}{\bar{T}}\,\frac{72}{15}(A^2 - A) = \bar{q}\,C_{e,L}\,. \qquad (36)$$

The term $P_{1,3}/\bar{P}$ in equation (32) can now be evaluated using equation (10) (with $P_c = 0$ to derive P_1) and equation (35) for turbulent flow, and equations (14) (with $P_c = 0$ to derive P_1) and (36) for laminar flow in the plenum chambers. Pressures P_1 and P_3 are derived from these equations. One half of their sum, taken as $P_{1,3}$, when divided by one-half the sum of P_o and P_4, or $\bar{P}$, gives the ratio $P_{1,3}/\bar{P}$ in the turbulent case as

$$(\frac{P_{1,3}}{\bar{P}})_t = 1 + \frac{\bar{q}}{2\bar{P}}(C_{e,t} - C_{i,t} + \frac{P_c}{q_1}) \qquad (37)$$

and as

$$(\frac{P_{1,3}}{\bar{P}})_L = 1 + \frac{\bar{q}}{2\bar{P}}(C_{e,L} - C_{i,L} + \frac{P_c}{q_1}) \qquad (38)$$

in the laminar flow case. In both equations above, P_c/q_1, is assumed to adequately represent the term $(P_c\bar{P}T_1/q_1\bar{T}P_1)$. Both of the above equations are essentially functions of A, a shape factor for the meter, with pressure and temperature correction factors applied to A to derive $\frac{P_{1,3}}{\bar{P}}$.

D. $\underline{(P_o-P_4)}$. Before summing the individual terms of equations (4) or (15)to find (P_o-P_4), each of which has been expanded in the previous sections, equation (32) is first modified for the term $P_{1,3}/\bar{P}$. This

expression appears in equations (37) and (38), and when inserted into equation (32) the latter becomes,

$$(P_1-P_3)\left(1-\frac{2\bar{q}}{\bar{P}}\left[1+\frac{P_{1,3}\Delta T^\circ}{\Delta P\bar{T}^\circ}-\frac{C_e-C_i}{4}-\frac{P_c}{4q_1}\right]\right)=\frac{KL\mu_w\bar{Q}f(\varphi)}{8b^2A_1}. \qquad (39)$$

A sum of the individual terms of equation (4) can now be written, using equations (11) or (14), equations (35) or (36), and equation (39), as follows:

$$P_o-P_4=\bar{q}(C_i+C_e)+\frac{KL\mu_w\bar{Q}f(\varphi)}{8b^2A_1F(M)}. \qquad (40)$$

A correction factor F(M) therein is taken from equation (39) as

$$F(M)=1-\frac{2\bar{q}}{\bar{P}}\left(1+\frac{P_{1,3}\Delta T^\circ}{\Delta P\bar{T}^\circ}-\frac{C_e-C_i}{4}-\frac{P_c}{4q_1}\right) \qquad (41)$$

to account for the effects of heat transfer and compressibility. Equation (40) is the sum of the pressure drops associated with the end effects and with the region of viscous flow. The latter is that given by Poiseuille modified by the correction factors $f(\varphi)$ and F(M) for heat transfer and compressibility. Without these factors equation (40) is the same as commonly used and reported on by H. H. Allion [8]. It should be noted that the end effect coefficients also appear in F(M) as a result of basing $\bar{Q}$ on $\bar{P}$ and $\bar{T}$.

The correction factor F(M) for the effects of compressibility and heat transfer, as stated in equation (41), is based on a one-dimensional analysis and use of bulk properties in the equations of motion and energy. R. A. Naftzger and J. R. Moszynski [5] used the classical momentum equation (for two-dimensional flow) and reduced it, for an assumed isothermal flow, to the boundary layer equation for a compressible fluid. This was solved subject to the assumption of similarity of velocity profiles at all points in the channel. One of the results of the solution was a correction factor for the compressibility effect. The compressibility correction factor given by equation (41) is in agreement with the results of [5] to a value of 0.5 for M. The results of the present experiments (to be described) are not carried beyond a value of M of about 0.3. Therefore it is suggested, pending results of further analysis and data, that use of F(M) be restricted to those cases in which M is less than 0.3.

E. The Laminar Meter Equation. Equation (40) is now rearranged to measure the meter performance in terms of the Poiseuille prediction, as the viscous flow effect is expected to be dominant. This leads to a coefficient which permits a sensitive as well as convenient means of describing the meter's performance. It is also desirable to be able to derive $\bar{Q}$, usually the unknown quantity, directly from measurements made

at the meter. This requires either an explicit solution of the equation for $\bar{Q}$, or optionally, an arrangement in which $\bar{Q}$ appears in only one side of the equation. It will be noted by examining equation (40) that as $\bar{Q}$ approaches zero, the ratio $(P_o-P_4)/\mu_w\bar{Q}$ approaches the value $KL/8b^2A_1$, which is now labeled as $[(P_o-P_4)/\mu\ Q]_o$. This may be called Poiseuille's flow coefficient for incompressible, laminar flow in a duct without end effects. We also use Ψ as the quantity

$$\Psi = \frac{(P_o-P_4)/\mu_w\bar{Q}}{[(P_o-P_4)/\mu\ Q]_o} \tag{42}$$

which may be considered a flow coefficient for the meter. If both sides of equation (40) are divided by $\mu_w\bar{Q}[(P_o-P_4)/\mu\ \bar{Q}]_o$ and multiplied by Ψ, the equation takes the form, using $\bar{q} = \frac{1}{2}\bar{\rho}\bar{Q}^2/A_1^2$, as written below:

$$\Psi^2\left(1 - \frac{f(\Phi)}{\Psi F(M)}\right) = \frac{1}{2}\ \frac{\bar{\rho}(P_o-P_4)}{\mu_w{}^2A_1{}^2}\ \frac{C_i + C_e}{[(P_o-P_4)/\mu\ Q]_o{}^2}\ . \tag{43}$$

Some comments regarding the laminar meter equation (43) are now appropriate and are listed below:

(1) F(M) as given in equation (41) contains some quantities not easily measured, such as ΔP, P_1, P_3, q_1, q_2, instead of (P_o-P_4), $\bar{P}$, and $\bar{q}$ which ordinarily are measured or derived from the measurements. In principle the procedure outlined herein can be used to derive them from the measured quantities for use in F(M). However, it is expected that the coefficients C_i, C_e and the end effects will not be known with sufficient accuracy to warrant such a procedure. The error caused by use of (P_o-P_4), $\bar{P}$ and $\bar{q}$ in their place in F(M) probably will not be significant.

(2) The term on the right side of equation (43) can be written as

$$\frac{1}{2}\frac{\bar{\rho}(P_o-P_4)}{\mu_w^2 A_1^2}\frac{C_i + C_e}{[(P_o-P_4)/\mu_w Q]_o^2} = \psi R_b \frac{b(C_i + C_e)}{KL} \qquad (44)$$

which demonstrates that equation (43) contains ψR_b as specified by equation (5). Further, all of the similarity parameters of equation (5) are implicitly included in equation (43).

(3) It is unlikely that practical, commercial meters can be made with (a) all slots identical and (b) with slots and plenum chamber arranged for the same flow in each slot as used in the derivation of equation (43). Disregarding the latter problem, and considering n non-identical slots, equation (40) should be applied to each by labeling all terms therein except (P_o-P_4), K, L, $\bar{\rho}$, and μ_w with subscript i (i = 1 to n). Use of the procedure leading to equation (43) gives n equations which when summed become

$$\psi^2\left(\sum_1^n \frac{\bar{Q}^2}{Q_i^2} - \frac{1}{\psi}\sum_1^n\left[\frac{\bar{b}^2}{b_i^2}\frac{A_1}{A_i}\frac{f_i(\Phi)}{F_i(M)}\frac{\bar{Q}}{Q_i}\right]\right) = \left(\frac{\bar{\rho}(P_o-P_4)}{2\mu_w^2 A_1^2}\frac{1}{[(P_o-P_4)/\mu Q]_o^2}\right) \times \left(\sum_1^n (C_i + C_e)_i \frac{A_1^2}{A_i^2}\right) \qquad (45)$$

using an average half-height $\bar{b}$ in $[(P_o-P_4)/\mu Q]_o$. The sums involving quantities $\bar{Q}/Q_i$ probably cannot be determined explicitly from equation (40), at least for a practical meter. More importantly, equation (40) can be used to demonstrate that both sums in the left side of equation (45) are variables dependent on $\bar{\rho}(P_o-P_4)/\mu_w^2$ as well as on the construction of the slots. Therefore equation (43) is not entirely valid for practical meters which are built with non-identical slots. For this case it appears that calibration must be employed to determine the relationship between the quantity on the left side in terms of that on the right side of equation (43).

(3) Under conditions of low pressure inducing "slight" rarefaction, the molecular mean free path λ for the gas in the meter becomes comparable to b, and the effects of slip-flow should be detectable. An approximate correction for slip may be incorporated into equation (43) by multiplying F(M) therein by (1 + 3Kn), as used by [2], with the Knudsen number Kn defined for use here as λ/b. In more familiar terms Kn is approximately $1.5M/R_b$ as given in [7], and the slip-flow effect is estimated as less than one-half percent when $M/R_b < 10^{-3}$. When $M/R_b > 0.07$ as possible under condition of still lower pressure, a transition to free molecule flow begins, and a modification of the correction for slip should be necessary.

V. EXPERIMENTAL DATA ANALYSIS

Two meters were calibrated with air over a range of pressure levels to determine if the preceeding analysis correctly describes the meter performance and the magnitude of the compressibility effect. Data has not yet been obtained to determine if the analysis correctly describes the effect of heat transfer. One of the two meters was similarly calibrated with helium to determine if the laminar meter equation (43) correctly predicts the effect of change of gas properties. Evaluation of the constants in equation (43) may be performed by a "complete" calibration of a meter over a range of pressure and temperature levels, and once determined the constants should be applicable to all "perfect" gases. However, a "limited" calibration, defined as a determination of ψ vs $\bar{\rho}(P_o-P_4)/\mu_w^2$, may be sufficient for many uses of the meter. Transfer of a "limited" calibration from one gas to another also would be desirable for maximum utility of calibrations, as will be discussed.

A. Meters. Two commercial meters tested are identified by the numbers 93 and 96, each containing a single slot sized for a nominal capacity of 1 and 30 liters per minute, respectively. The slot for meter 93 probably was formed by milling a groove into a flat plate, which was then soldered to another flat plate to provide the fourth side of the slot. Meter 96 contained a slot between two concentric tubes, with distance between the tubes small compared to their diameters. Dimensions for the meters are tabulated below, using other quantitites expressed in the foot, slug, second system of units to derive the values given for $[(P_2-P_4)/\mu Q]_o$:

	(x_3-x_2), ft	S, ft	$bx10^4$, ft		A_1, ft^2	A	$[(P_2-P_4)/\mu Q]_o$, ft^{-3}
			Mfg.	Derived	Derived		
Meter 93	0.225	0.0156	4.6	4.84	$1.51x10^{-5}$	0.006	$1.905x10^{11}$
Meter 96	0.271	0.205	5.2	6.6	$2.7x10^{-4}$	0.08	$6.86x10^{9}$

It will be noted that two values of the half-height b for the slots are listed, and that length of the metering elements is given as that between stations 2 and 3. The latter is given because the upstream pressure tap is not located in the plenum chamber, but about 0.04 ft downstream from the beginning of the slot for both meters. Disregarding the uncertainty about entrance effects and distance ℓ, equation (6) specifies that the laminar flow field would be more than 98 percent developed at the tap location with values of R_b up to 2000 and 1500 for meters 93 and 96, respectively. With the restriction that values of R_b are less than 1500, both C_1 and P_c/q_2 in equation (43) should be zero for its use with these two meters, and P_o should be replaced with P_2.

One of the values of b given for each meter is derived from values of $[(P_2-P_4)/\mu\ Q]_o$, also tabulated, using 24 for K and the values of

x_3-x_2 (for L) and the values of S. A curve of observed values of $(P_2-P_4)/\mu_w\bar{Q}$ vs $\bar{\rho}(P_2-P_4)/\mu_w{}^2$ was extrapolated to zero for the latter coordinate to find the Poiseuille flow coefficient tabulated for meter 96. For meter 93, the plots showed a pronounced knee in the curves for both gases, and a value of the Poiseuille flow coefficient $[(P_2-P_4)/\mu\ Q]_o$ approximately two percent larger than the intercept value is taken as the reference value for the derivation of ψ. This choice permits the data (for $\psi \geq 1$) to be fitted to equation (43) as will be described. The "knee" at the fast change of slope of the "limited" calibration curves ψ vs $\bar{\rho}(P_2-P_4)/\mu_w{}^2$ is illustrated in figure 2 as in the neighborhood of $R_b = 100$. As ψ is not based on the intercept value of $[(P_2-P_4)/\mu_w Q]$, ψ becomes less than 1 as the flow approaches zero. Returning to the derived values of b, the value for meter 93 is in reasonable agreement with that specified by the manufacturer, but for meter 96 it is about 25 percent larger than specified.

B. Transfer of a "Limited" Calibration ψ. Equation (43) requires, for transfer, that $2\bar{q}/\bar{P}$ in F(M) be equal for both gases, as well as equality of the two values of ψ and of the two values of $\bar{\rho}(P_o-P_4)/\mu_w{}^2$. Values of the viscosity correction factor $f(\varphi)$ should also be equal, but this will not be considered in the following analysis for the case of no heat transfer. With subscripts δ and β used to identify two gases and by use of the gas law ($P = \rho RT/W$), the three equalities mentioned can be stated as follows:

$$\text{(a)} \quad \bar{Q}_\delta = \bar{Q}_\beta \left(\frac{W_\beta\ T_\delta}{W_\delta\ T_\beta}\right)^{1/2}$$

$$\text{(b)} \quad (P_o-P_4)_\delta = (P_o-P_4)_\beta \frac{(\mu_w\ \bar{Q})_\delta}{(\mu_w\ \bar{Q})_\beta} \qquad (46)$$

$$(c) \quad \frac{\bar{P}_\delta}{(\bar{T}_\delta)^{1/2}} = \frac{\bar{P}_\beta}{(\bar{T}_\beta)^{1/2}} \frac{\mu_{w,\delta}}{\mu_{w,\beta}} \left(\frac{W_\beta}{W_\delta}\right)^{1/2}$$

Equation (46c) is the most useful of the three equations. It was derived by substitution of the gas law and equations (46a) and (46b) into the required equality of the two values of $\bar{\rho}(P_o-P_4)/\mu_w^2$. As it contains all three requirements for transfer, a "limited" calibration curve of ψ vs $\bar{\rho}(P_o-P_4)/\mu_w^2$ obtained at constant levels of $\bar{P}_\beta$ and $\bar{T}_\beta$ can be used for gas δ at levels $\bar{P}_\delta$ and $\bar{T}_\delta$ as given by equation (46c).

Three separate "limited" calibration curves are plotted in figure 2. for meter 93, each derived from calibration data for both helium and air to test the validity of the transfer equation (46c). This equation requires, for the same temperature (near ambient), that the pressure level for helium be about 2.9 times that for air. Data points for helium at the pressure levels of 15.2, 30.5 and 43.5 psia define the same curves as those for air at corresponding pressure levels of 5.25, 10.5 and 15 psia, but a few of the data points do differ from their respective curves by almost 1/2 percent. We infer that equation (46c) provides a basis for transferring "limited" calibration curves from one gas to another. The accuracy of transfer depends, of course, on the accuracy to which the gas viscosities involved in the transfer are known.

Figure 2 demonstrates that if only a single "limited" calibration curve is available for a meter, the meter should be used near the condition existing during calibration. Thus the user should maintain $\bar{P}$ and $\bar{T}$ in the meter as in the calibration (or as derived with equation (46c) if deviation is necessary), observe differential pressure $\Delta P_{obs.}$, and enter the graph with the calculated value of $\bar{\rho}\Delta P_{obs}/\mu_w^2$ to find the corresponding value of ψ. Volume rate Q at conditions $\bar{P}$, $\bar{T}$ is then given by the equation below:

$$Q = \frac{1}{\Psi_{curve}} \frac{\Delta P_{obs}}{\mu_w} \frac{1}{[(P_2-P_4)/\mu Q]_o} . \qquad (47)$$

If several "limited" calibration curves are available, the user could deviate from the meter calibration conditions, either by using equation (46c) to find suitable use conditions, or by interpolating between the calibration curves for the desired use conditions. These techniques would avoid errors (possibly up to 5 percent for meter 93) caused by using a "limited" calibration over an extended range of conditions.

C. Complete Calibration. The laminar meter equation (43) cannot be evaluated directly unless the coefficient $(C_i-C_e)/4$ in F(M) is accepted as derived from coefficients C_i and C_e which are given by equations (14) and (36), respectively. It seemed advisable to use the data to determine $(C_i-C_e)/4$, as well as the other coefficient (C_i+C_e), and then from these determine C_i and C_e individually for comparison with the values given by equations (14) and (36). Use of two terms of a binominal series expansion of the reciprocal of F(M) permits equation (43) to be written as

$$D\Psi^2 - E\Psi - F\Psi \frac{\bar{\rho}\,\bar{Q}^{-2}}{\bar{P}A_1^{\,2}} = \frac{1}{2} \frac{\bar{\rho}(P_2-P_4)}{\mu_w^{\,2} A_1^{\,2}} \frac{1}{[(P_2-P_4)/\mu Q]_o^{\,2}} . \qquad (48)$$

Coefficient D is presumably equal to E, (C_i+C_e) is given by D^{-1}, and $(C_i-C_e)/4$ is derivable from coefficients F and D as follows:

$$\frac{C_i-C_e}{4} = \frac{F}{D} - 1 . \qquad (49)$$

For meter 93, a least squares fit of the data (for $\Psi \geq 1$) with a standard deviation of the fit of 0.4 percent based on Ψ, determined coefficients D, E(= 0.998D) and F in equation (48) with standard deviations of 6, 6 and 18 percent, respectively. It did not seem likely that equation (48) could account for the "knee" displayed by the curves of

figure 2, without making the standard deviation of the fit much larger than 0.4 percent, and data for $\psi \leq 1$ was therefore excluded. Coefficients $(C_i + C_e)$ and $(C_i - C_e)/4$, for both meter 93 and 96, together with values of C_i and C_e derived from both the data and from equations (14) and (36) are listed below:

	Meter 93	Meter 96
$(C_i - C_e)$	-0.48 ± 0.60	-0.37
$(C_i + C_e)$	0.46 ± 0.03	1.9
C_i, data	-0.01 ± 0.3	0.2
C_i, analysis	0	0
C_e, data	0.47 ± 0.3	1.7
C_e, Eq (35)	-0.03	-0.4

Coefficient C_i is nearly zero as expected from the location of pressure tap for P_2, with the rather large uncertainty deriving from the factor of four in equation (49) and the 18 percent standard deviation for coefficient F. The value of C_e is not negative as expected, and only with the negative uncertainty included is it in reasonable agreement with the value given by equation (35).

Figure 3 shows the data of figure 2 for meter 93 together with additional data for air plotted according to the form suggested by equation (48). Values for R_b and M/R_b are also included to illustrate in another way the range of the calibration data. There is some evidence that the data points for helium are generally below the line in figure 3. The possibility of a systematic error, perhaps arising from the particular choice of a viscosity for helium, is suggested. However, the error is less than 0.4 percent in terms of ψ.

Meter 96 was calibrated with air over a range of pressures from 3 to 30 psia, with $\bar{T}$ near ambient, to provide additional information on performance of laminar meters. Figure 4 contains a plot of the data in terms of the quantities in equation (43), using coefficient $(C_i - C_e)/4$ selected by trial until all data points reasonably define a single calibration curve. For the conditions of test, the compressibility correction was as large as about 3 percent based on values of ψ. Coefficients for this meter are listed in the previous table, with the value $(C_i + C_e)$ equal to 1.9 as derived from the slope of the curve in the lower 40 percent of the flow range. Based on values of ψ, the data departs from the straight line used to define the slope by about 3 percent at the largest flowrate. Coefficients C_i and C_e are not in good agreement with those given by the theory herein, presumably because equation (43) does not account for the "practical" aspects of the meter construction.

It is probable that meter 96 is similar to one with non-identical slots as previously discussed. Eccentricity or nonparallel alignment of the tubes forming the flow passage could cause the annular distribution of the flow to change with rate. Although the data does not define a straight line, as would be desirable, it does appear that the function of ψ in equation (43) is adequate to correlate the data within the calibration range. Values of R_b and M/R_b are included in figure 4 to illustrate the range of the data, and the symbols used there indicate the values of $\bar{P}$.

The "complete" calibrations of the types described by equation (48) for meter 93 or by figure 4 for meter 96 probably will not be directly

involved in routine use of the laminar meter. Rather, they should find use in generating curves for routine use in measuring the flow of the desired (perfect) gas at selected levels of $\bar{\rho}$, or if more convenient, at selected levels of ρ_o or ρ_4. For a chosen density level, each assumed value of (P_o-P_4) gives a value of $\bar{\rho}(P_o-P_4)/\mu_w^2$. This value is then used to find the corresponding value of $(\psi^2 - \psi F^{-1})$ by analytical or graphical techniques, depending on the meter and its calibration. To find $\bar{Q}$, the quadratic equation for ψ is solved (with $\bar{Q}$ assumed zero) for a first trial value of ψ_1, which in turn gives a first trial value of $\bar{Q}_1$ by using equation (47). Ordinarily a second and final trial value of ψ_2 can be determined with sufficient accuracy by including the compressibility term, based on $\bar{Q}_1$, in $(\psi^2-\psi F^{-1})$, and the final $\bar{Q}_2$ is derived from ψ_2 with equation (47). Values of $\bar{Q}_2$ so determined can be plotted vs the assumed values of (P_o-P_4) to define an operating calibration curve for the chosen density level.

VI. CONCLUSION

An equation for a laminar gas meter has been derived with correction factors to be applied to a flow coefficient derived from the Hagen-Poiseuille relationship. The equation derived has been tested with air and helium in a single slot meter over a wide range of flow and pressure levels. Presentation or use of the data may involve a "limited" calibration concept, or a "complete" calibration concept. A "limited" calibration results in one or more performance curves at selected levels of pressure and temperature. The curve(s) were usable with both gases and transferable to other conditions derived as described. A "complete" calibration should be generally useful and involves a determination of

the meter coefficients for use in the analytic equation (43) given or for use in a graphical display of the functional relationship between the pertinent similarity parameters. It is probable that the graphical method will be required for use with practical, multi-channel meters.

VII. NOMENCLATURE

a	half height of plenum chamber
A	A_1/A_o
A_o	plenum chamber area
A_1	total area of slots, 2bSn
b	half-height of slots
c	half-height of metal between slots
c_p	specific heat
C	velocity of sound
C_i	inlet end effect coefficient, Eqs (11) and (14)
C_e	outlet end effect coefficient, Eqs (35) and (36)
D,E,F	coefficients in Eq (48)
f( )	indicates function of the quantity in ( )
f (φ)	viscosity correction factor, see Eq (27)
f	friction factor
f(M)	$1 + \frac{1}{2}(k-1)M^2$
F(M)	compressibility and heat transfer correction factor, Eq (41)
k	specific heat ratio
K	constant in Poiseuille's incompressible laminar flow equation
Kn	Knudsen number
ℓ	unknown flow separation length ℓ
L	slot length beyond ℓ
m	mean hydraulic depth, area ÷ perimeter.
M]	Mach number
Nu	Nusselt number based on (T_1-T_w)
n	number of slots
P	pressure

P_c	flow development pressure correction
q	$\frac{1}{2}\rho V^2$
Q	total volume rate of flow
ΔP	$= P_1 - P_3$
ΔT	$= T_3 - T_1$
R_a, R_b	Reynolds numbers
R	gas constant
S	depth of slot normal to plane of Fig. 1
T_w	meter body temperature
$T^\bullet$	stagnation temperature
T	static temperature
V	bulk velocity
w	total mass flow
W	molecular weight
x	distance from station 1
y	distance from midpoint of slot normal to flow direction
$\bar{P}$	$= \frac{1}{2}(P_o + P_4)$
$\bar{T}$	$= \frac{1}{2}(T_1 + T_3)$
$[(P_o - P_4)/\mu Q]_o$	$= KL/8b^2A_1$
θ	dimensionless temperature, Eq (24)
μ	absolute viscosity
ρ	density
σ	Prandtl number, μc_p/(thermal conductivity)
$\varphi(x)$	$\sigma R4b/x$
Ψ	ratio of flow coefficient to the flow coefficient at zero flow, see Eq (42)
λ	molecular mean free path

Subscripts

0,1,2,3,4	stations in the meter
c	center of slot, or correction term
w	meter temperature
a,b	Reynolds number basis
i	slot number
0	reference condition of temperature
L	laminar flow
t	turbulent flow
δ	gas identity
β	gas identity

Superscript

-	average condition
o	stagnation temperature

VIII. REFERENCES

[1] S. T. McComas, E. R. G. Eckert. Laminar pressure drop associated with the continuum entrance region and for slip flow in a circular tube. Trans. ASME, J. App. Mech., Paper No. 65-WA/APM-5.

[2] E. M. Sparrow, T. S. Lundgren and S. H. Lin. Slip flow in the entrance region of a parallel plate channel. Proceedings of the 1962 Heat Transfer and Fluid Mechanics Institute. Stanford University Press.

[3] S. Goldstein, Editor. Modern developments in fluid dynamics. Oxford University Press, Amen House, London E.C.4. 1957.

[4] A. H. Shapiro. The dynamics and thermodynamics of compressible fluid flow. The Ronald Press Co., New York, 1953.

[5] R. H. Naftzger, J. R. Moszynski. The viscometric flow of a gas near its critical point. Case Institute of Technology, June 1965.

[6] R. H. Norris, D. D. Streid. Laminar-flow heat-transfer coefficients for ducts. Trans. ASME 62 (1940) 525.

[7] E. R. G. Eckert, R. M. Drake, Jr., Heat and mass transfer. McGraw Hill Book Co., New York, 1959

[8] H. H. Allion, Calibration and use of laminar flowmeters. Proceedings of the 1965 Appalachian Gas Measurement Short Course. University of West Virginia, Morgantown, West Virginia.

IX. LIST OF FIGURES

1. The laminar meter

2. Three "limited" calibration curves for meter 93 with air and helium: $\overline{T}$ = 534 °R, and $\overline{P}$ as indicated by symbols below.

Air	□ 5.25	△ 10.5	○ 15 psia
Helium	■ 15.2	▲ 30.5	● 43.5 psia
Curve No	1	2	3

3. "Complete" calibration for meter 93 with air and helium: $\overline{T}$ = 534 °R, $M/R_b < 3 \times 10^{-4}$, pressure $\overline{P}$ as indicated by symbols below. Dashed lines represent the standard deviation of the fit of 0.4 percent based on Y.

Air	× 25	+ 20	○ 15	◇ 12.5	△ 10.5	* 7.5	□ 5.25 psia
Helium			● 43.5		▲ 30.5		■ 15.2 psia

4. "Complete" calibration for meter 96 with air: $\overline{T}$ = 534 °R, $M/R_b < 3 \times 10^{-4}$, pressure $\overline{P}$ as indicated by symobls below.

Symbol	×	○	△	□
psia	30	15	7	3

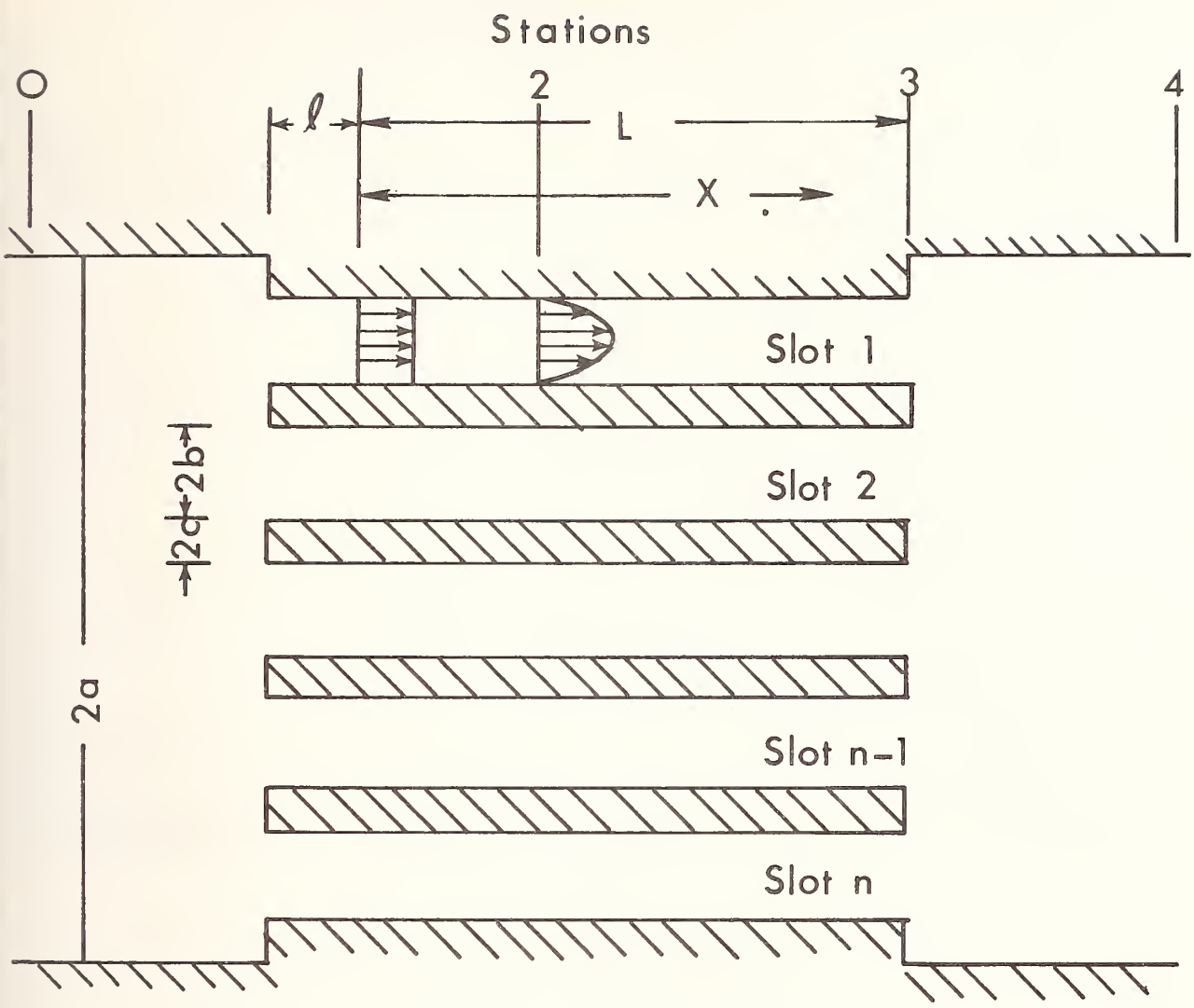

Figure 1. The laminar meter

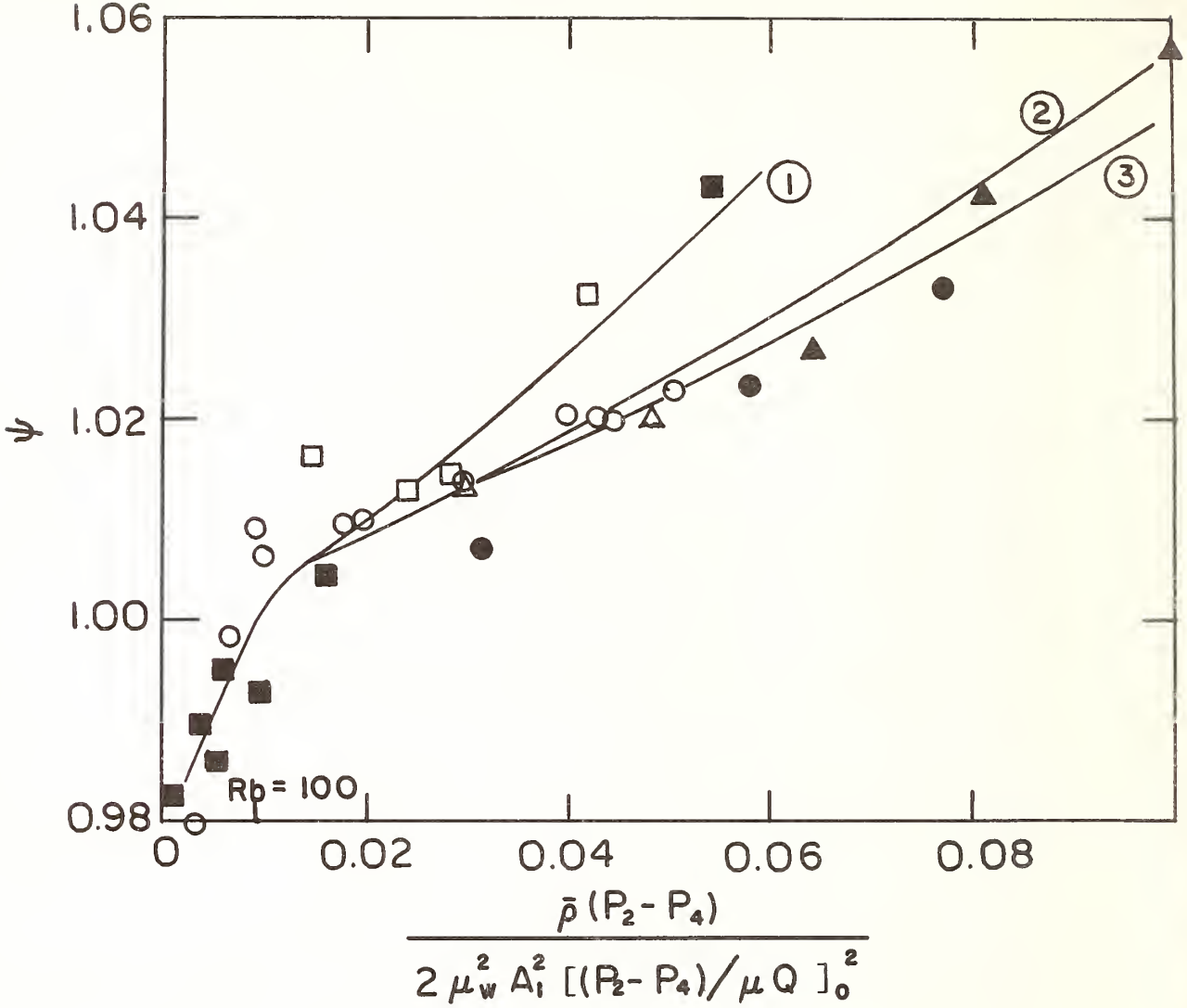

Figure 2. Three "limited" calibration curves for meter 93 with air and helium: $\bar{T}$ = 534 °R, and $\bar{P}$ as indicated by symbols below.

Air	□ 5.25	△ 10.5	○ 15 psia
Helium	■ 15.2	▲ 30.5	● 43.5 psia
Curve No.	1	2	3

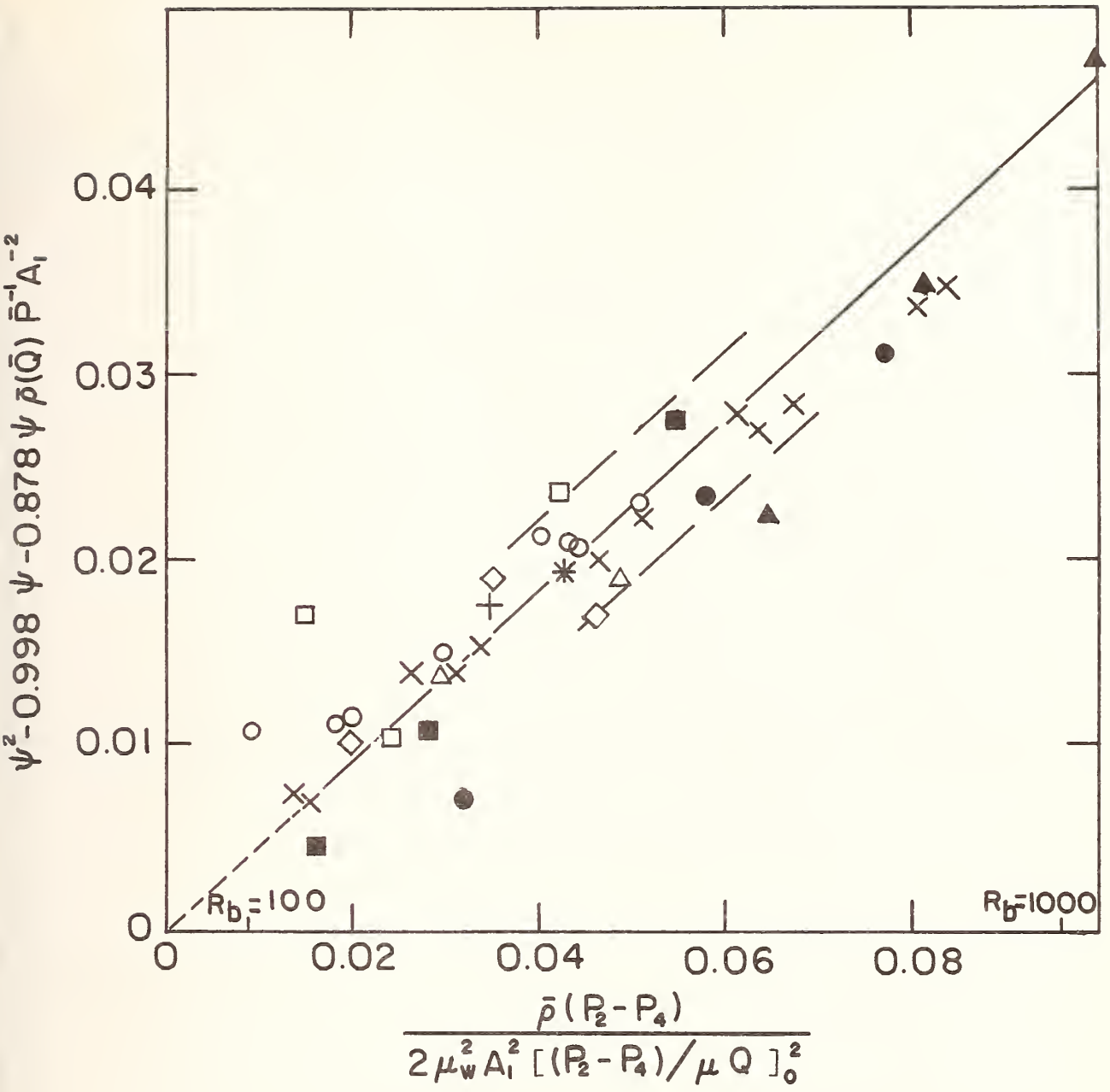

Figure 3. "Complete" calibration for meter 93 with air and helium: $\overline{T}$ = 534 °R, $M/R_b < 3 \times 10^{-4}$, pressure $\overline{P}$ as indicated by symbols below. Dashed lines represent the standard deviation of the fit of 0.4 percent based on ψ.

Air	×	+	○	◇	△	✳	□
	25	20	15	12.5	10.5	7.5	5.25 psia
Helium			○		▲		■
			43.5		30.5		15.2 psia

203-33

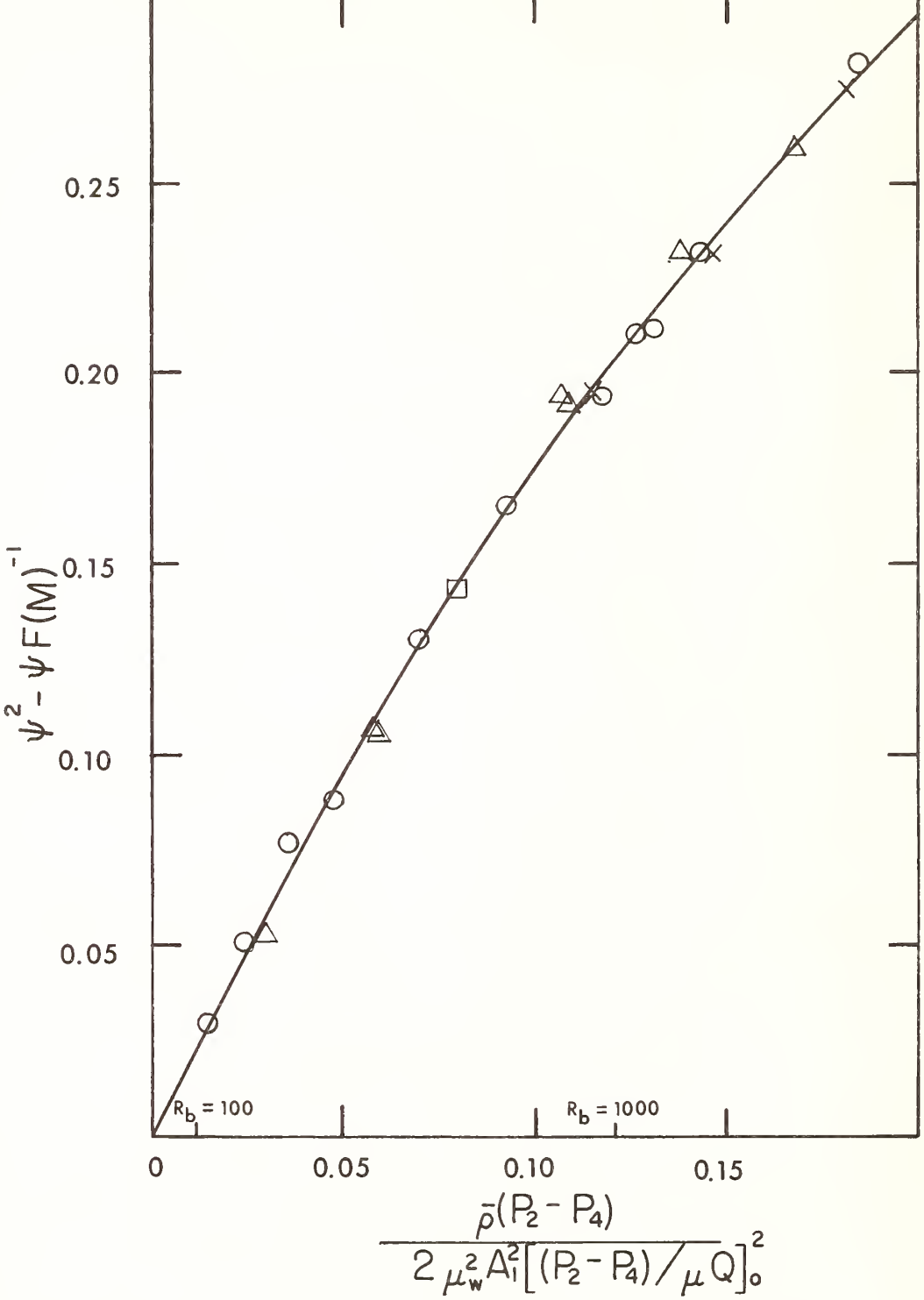

Figure 4. "Complete" calibration for meter 96 with air: $\overline{T}$ = 534 °R, $M/R_b < 3 \times 10^{-4}$, pressure $\overline{P}$ as indicated by symbols below.

Symbol	×	○	△	□
psia	30	15	7	3

3. Force

U. S. Department of Commerce
National Bureau of Standards

Research Paper RP1726
Volume 37, July 1946

Part of Journal of Research of the National Bureau of Standards

Temperature Coefficients for Proving Rings

By Bruce L. Wilson, Douglas R. Tate, and George Borkowski

Proving rings for calibrating testing machines are not compensated for change in elastic properties and dimensions with temperature. For this reason, temperature-correction factors must be used in computing ring loads from deflections obtained at temperatures that differ from the temperature of calibration. Temperature coefficients for 14 representative rings were computed from calibration results obtained at temperatures of 70° and 100° F. The temperature coefficient of one ring for the range +70° to −93° F was determined from measurements of the natural frequencies at these temperatures. The temperature coefficient of a proving ring is shown to be equal to the temperature coefficient of Young's modulus of elasticity plus twice the coefficient of thermal expansion of the material of the ring.

I. Introduction

The proving ring is the most widely used elastic calibration device [1][1] for calibrating testing machines that apply forces to engineering materials and structures. About four-fifths of such devices submitted to the National Bureau of Standards for calibration during the past year were proving rings. The rings are not compensated for the change in elastic properties and dimensions with temperature, therefore, a knowledge of the temperature coefficient is required for use in computing ring loads from deflections obtained at temperatures that differ from the temperature during the calibration of the ring.

The tests described were undertaken (a) to determine experimentally the temperature coefficients of a number of representative proving rings for the usual range of room temperatures, (b) to determine the coefficient of a representative

[1] Figures in brackets indicate the literature references given at the end of this paper.

Contents

ring at a temperature near −100° F, and (c) to determine whether the temperature coefficient may be calculated with sufficient accuracy from measured values of the temperature coefficient of Young's modulus of elasticity and the coefficient of thermal expansion for the material of a ring.

II. Description of Proving Ring

The proving ring has been described in a previous paper [2]. Briefly, it is an elastic ring in which the deflection of the ring, when loaded along a diameter, is measured by means of a micrometer screw and a vibrating reed mounted diametrically in the ring. One of the rings used in the tests reported is shown in figure 1. This ring, which was used for the tests at −93° F, was made of steel having the following chemical composition: C, 0.50 percent; Cr, 1.00 percent; and Ni, 1.75 percent. It was heat treated to show a Vickers number of about 475 (diamond indenter, load=120 kg). It is believed that each of the proving rings tested had a total alloying content not exceeding 5 percent.

Proving rings are usually calibrated in deadweight machines [3], in which their deflections are determined for 10 uniformly spaced loads. The calibration factor, the ratio of the load to the deflection of the ring, is calculated, and the results are shown graphically as in figure 2. When a ring is used to measure loads, the observed deflection is multiplied by the product of the calibration factor read from the calibration graph and a temperature correction factor.

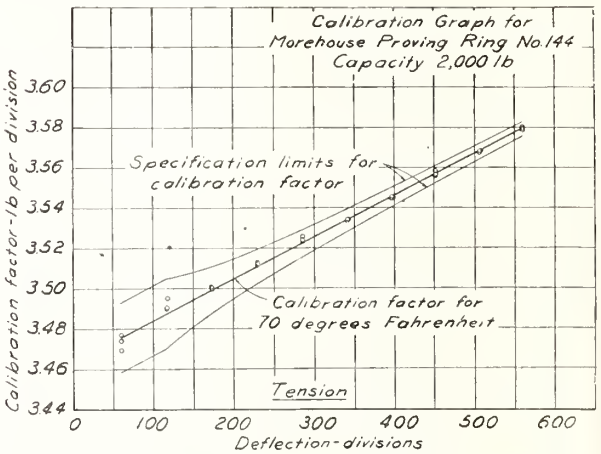

FIGURE 2.—*Calibration graph for Morehouse proving ring No. 144.*

III. Theory of Thermal Effects

1. Relationship Between Temperature Coefficient and Deflection for Proving Rings

The temperature coefficient, k, of a proving ring is defined by the equation

$$k=(1/F_c)(dF/dt), \tag{1}$$

in which F_c is the calibration factor for the ring at the standard temperature of calibration.

The calibration factor F_t for any temperature, t, becomes

$$F_t=F_c[1+k(t-t_c)], \tag{2}$$

where

F_t=calibration factor for a temperature of t degrees

t_c=standard temperature of calibration.

Equation 2 may be written in terms of deflections measured in dial divisions as

$$d_c=d_t[1+k(t-t_c)], \tag{3}$$

in which

d_c=deflection of the ring at a temperature of t_c degrees

d_t=deflection of the ring at a temperature of t degrees.

Solving equation 3 for the temperature coefficient

$$k=\frac{d_c-d_t}{d_t(t-t_c)}. \tag{4}$$

By means of equation 4 the temperature coefficient for a ring may be computed from deflections for the same load obtained at different temperatures.

2. Relationship Between Temperature Coefficient of Proving Ring and Temperature Coefficient of Young's Modulus of Elasticity and Coefficient of Thermal Expansion

The deflection in the direction of the load of a closed circular ring of rectangular cross section

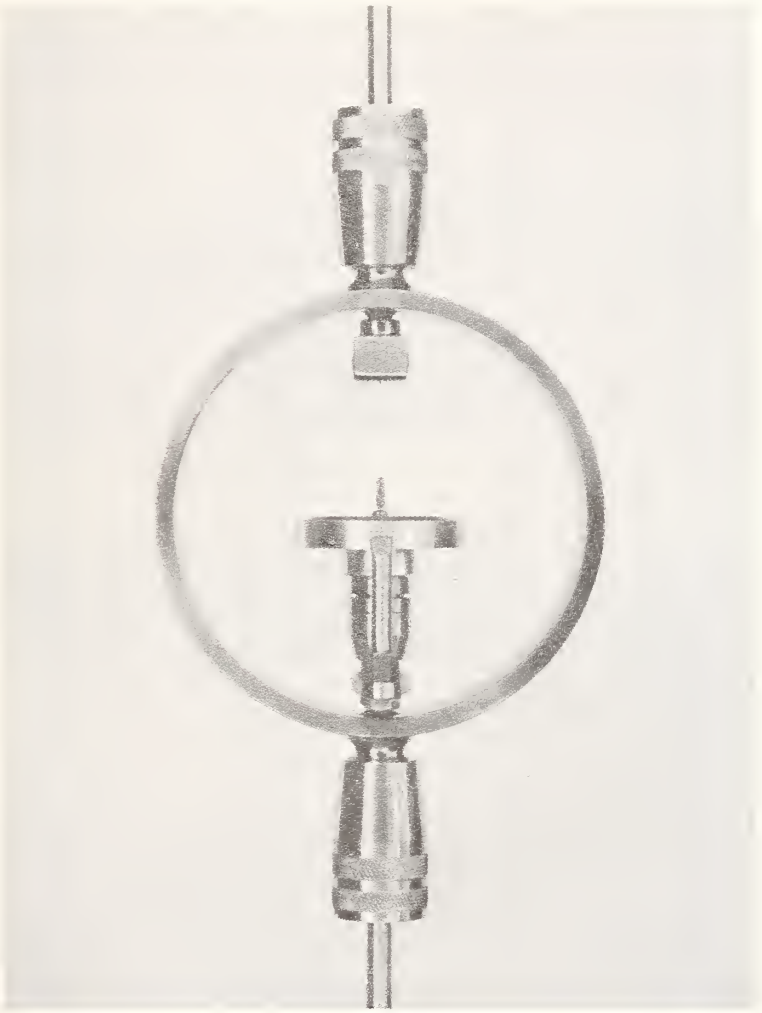

FIGURE 1.—*Morehouse proving ring No. 144, capacity 2,000 lb, with tension fittings attached to external bosses.*

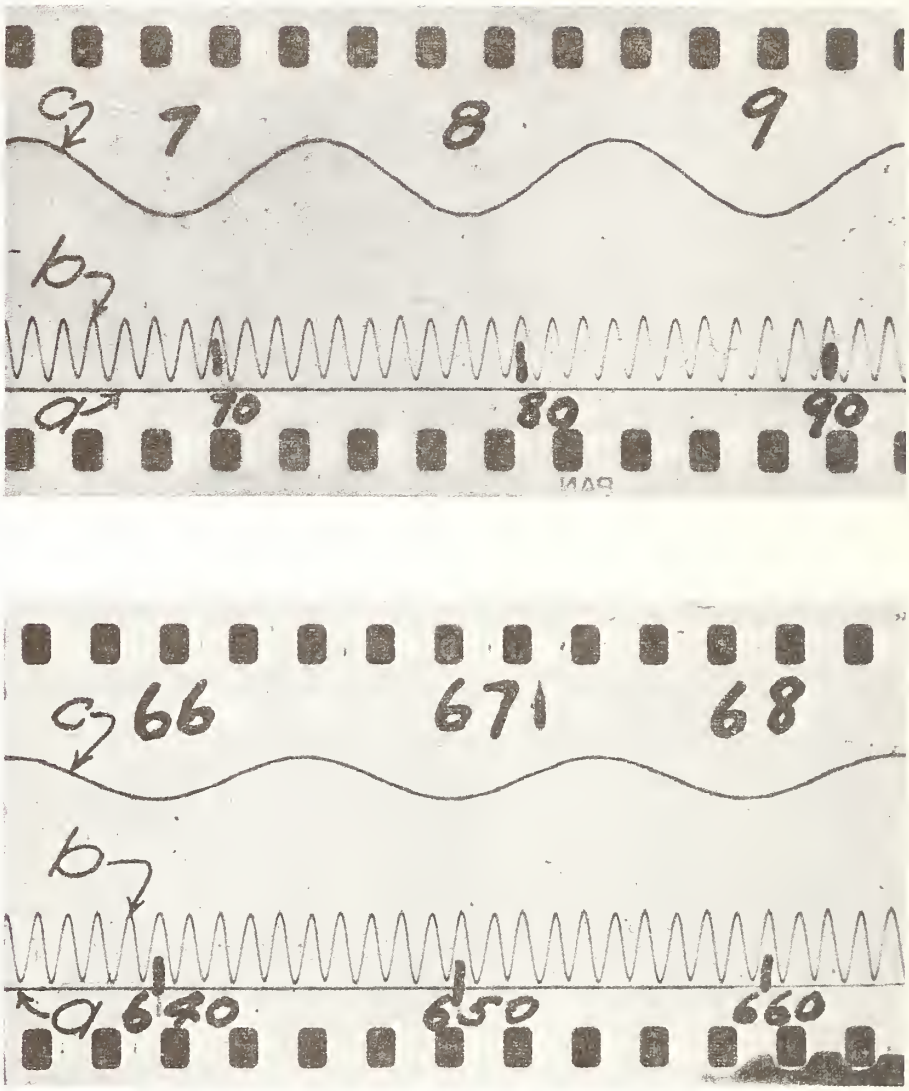

FIGURE 4.—*Reproductions from film exposed in the autographic autocollimator; (a) reference line, (b) time scale, (c) ring vibration as indicated by Tuckerman strain gage.*

loaded at opposite ends of a diameter is given approximately by the expression eq 4
where

$$d=APr^3/Elh^3, \tag{5}$$

d=deflection of the ring in the direction of the forces
A=a numerical constant
P=load on the ring
r=initial radius of curvature of the neutral surface
E=Youth's modulus of elasticity of the material of the ring
l=width of the cross section of the ring
h=thickness of the cross section of the ring.

The deflection of a proving ring is not exactly proportional to the load as indicated in equation 5. The calibration factor increases slightly with increasing tensile load as shown in figure 2. Usually the calibration factor for 10-percent capacity load differs from the calibration factor for capacity load by less than 3 percent.

As the calibration factor of a proving ring is, by definition, the ratio of the load to the deflection of the ring measured in dial divisions, the effect of changing temperature on the micrometer screw should be included in the expression for the calibration factor. Usually the micrometer screw is made of steel and has about the same coefficient of thermal expansion as the ring. If the axial travel of the micrometer screw per unit dial division is denoted by N, the calibration factor F may be written as

$$F=(PN/d). \tag{6}$$

After combining equations 5 and 6 the result may be expressed as

$$F=BEL^2, \tag{7}$$

in which

B=a numerical quantity, constant for a given ring
E=Young's modulus of elasticity, lb/in.^{2}
L=a quantity having the dimensions of length, in.

Differentiating equation 7 with respect to temperature and then dividing by equation 7,

$$\frac{1}{F}\frac{dF}{dt}=\frac{1}{E}\frac{dE}{dt}+\frac{2}{L}\frac{dL}{dt}. \tag{8}$$

Since the value of F changes by less than 1 percent over the temperature range in which proving rings are ordinarily used, it is permissible to write

$$\frac{1}{F}\frac{dF}{dt}=\frac{1}{F_c}\frac{dF}{dt}=k,$$

the temperature coefficient of the ring.
Since

$$\frac{1}{E}\frac{dE}{dt}=e.$$

the temperature coefficient of Young's modulus of elasticity

$$\frac{1dL}{Ldt}=\alpha,$$

the coefficient of linear thermal expansion.
Equation 8 may be written

$$k=e+2\alpha. \tag{9}$$

By means of equation 9 the temperature coefficient of a proving ring may be calculated from the temperature coefficient of Young's modulus of elasticity and the coefficient of thermal expansion.

3. Relationship Between Temperature Coefficient and Spring Constant for Proving Rings

The temperature coefficient of a proving ring may be computed from measurements at two temperatures of the natural frequency of the elastic system consisting of the ring and its load of dead

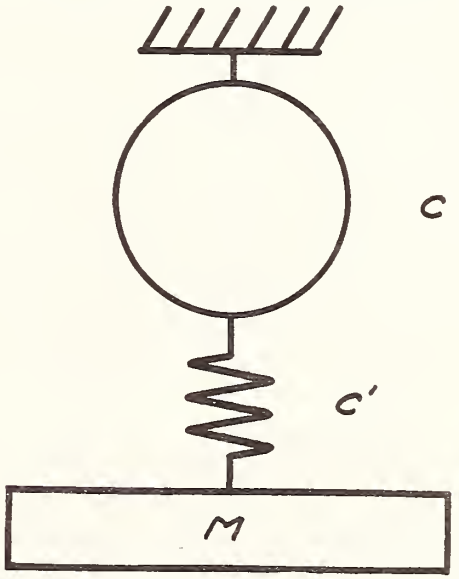

FIGURE 3.—*Elastic system used in the vibration tests.*

The load applied to the ring is represented by M, the spring constant of the ring by c, and the spring constant of the loading fixtures by c'.

weights shown in figure 3. The natural frequency of the system may be written [5]

$$f=\frac{1}{2\pi}\sqrt{\frac{cc'}{(c+c')m}}, \tag{10}$$

in which

f=natural frequency of the system
c=spring constant, load per unit deflection, for the proving ring
c'=spring constant for the loading fixtures
m=mass suspended from the ring.

From equation 10 the spring constant for the ring at any temperature, t, is

$$c_t=\frac{mc'(2\pi f)^2}{c'-m(2\pi f)^2}. \tag{11}$$

An expression for the temperature coefficient in terms of the spring constants of the ring may be derived from equation 4, which gives the relationship between the temperature coefficient and the deflections of the ring. It may be shown that

$$k=\frac{c_t-c_c}{c_c(t-t_c)}+\alpha, \tag{12}$$

in which

c_t=the spring constant of the ring for the temperature t degrees
c_c=the spring constant of the ring for the temperature t_c degrees
α=the coefficient of linear thermal expansion.

The last term in equation 12 is due to the change in pitch of the micrometer screw with temperature. By means of equation 12 the temperature coefficient of a proving ring may be calculated from the spring constants of the ring for two different temperatures and the thermal coefficient of linear expansion of the material of the ring.

IV. Experimental Procedure

1. Temperature Range 70° to 100° F

The tests were made in dead-weight testing machines [3], the loading frames of which are inclosed in a temperature controlled room. The air temperature of the room could be maintained near 70° or 100° F and held constant to within one-half degree Fahrenheit.

During the calibrations a steel block having a section approximately equal to the section of the ring being calibrated and long enough to reduce thermal end effects was placed near the ring. The bulb of a sensitive calibrated thermometer was sealed into a hole bored to the center of the block. The calibrations of the rings were made with both the block temperature and the air temperature maintained within one-half degree Fahrenheit of the desired temperature. The average temperature of the block during the interval of calibration was taken as the average temperature of the ring.

2. Temperature Range +70° to −93° F

For tests at −93° F the ring was inclosed in a wire-mesh cage, which in turn was inclosed in a box supported by the upper pulling rod. For the low-temperature tests the space between the wire-mesh cage and the box was packed with solid carbon dioxide. The box and cage were so designed that, although the ring was almost completely surrounded by solid carbon dioxide, sufficient clearance was provided for the ring to vibrate without damping effects produced by friction with the cage or the walls of the box. Vibration tests at 70° were made with the box in place.

The temperature of the ring was measured by means of five calibrated chromel P-alumel thermocouples in contact with the surface of the ring. It is believed that the errors of the temperature measurements did not exceed 1 degree Fahrenheit. During the low-temperature tests, the temperature of the ring differed from point to point due to conduction of heat along the pulling rods, but in no case did the temperature measured at any point differ from the average temperature by more than 5 percent of the total temperature range.

Vibration of the ring was produced by a single impact of a small hammer swung from a constant height about a fixed axis. The hammer swung freely, struck a rubber pad, and was caught on the first rebound. Therefore, the initial amplitude of the ring vibration was very nearly constant.

The natural frequency of the vibration of the 2,000-lb-capacity ring loaded to about 60-percent-capacity load was measured by means of a Tucker-

man strain gage attached to projections on the pulling rods of the ring. The images from the gage, a reference mirror, and a vibrating mirror controlled by the standard 60-cycle-frequency signal from the Bureau's Radio Section were photographed in an autographic autocollimator. The film was moved continuously by a synchronous motor at a speed of approximately 10 inches per second. The length of film exposed during each run was sufficient to photograph at least 60 complete wavelengths of the ring vibration. Typical records are shown in figure 4.

The frequency was determined from measurements of the number of time waves corresponding to a fixed number of wavelengths of the ring vibration. By projection, the number of time wavelengths was determined to within 0.1 time wavelength. In no case, it is believed, did the error in the measurement of the frequency exceed 0.02 percent.

The effect of damping on the frequency was calculated from measurements of the amplitudes on each film. In no case was the calculated error due to damping greater than 0.001 percent.

Under ordinary conditions of use sufficient time elapses after the application or removal of load to a proving ring to permit almost complete temperature equalization before readings are observed, and the action may, therefore, be considered isothermal [6]. During the vibration tests the frequency was about 12 cycles per second, and the action was nearly adiabatic. As the difference between temperature coefficients for steel rings determined under isothermal and adiabatic conditions can be shown to be less than 1 percent [7], no correction was considered necessary.

The spring constant of the loading fixtures (c', equation 10) was nearly independent of the temperature of the ring as the temperature of the air surrounding the rods and frame of the deadweight machine was constant. The constant c' was evaluated by substituting in equation 11 a value of c_t derived from the calibration graph of the ring for 70° F and the measured natural frequency of the system for a ring temperature of 70° F.

V. Results

1. Temperature Range 70° to 100°F

The temperature coefficients were determined for 14 proving rings for the range of temperatures from 70° to 100° F. In preliminary tests it was observed that the result obtained by computing the coefficient for the three highest of the 10, uniformly spaced test loads applied to the ring, e. g., 80, 90, and 100 percent of capacity, did not differ significantly from the result computed for 10 uniformly spaced test loads. Therefore, the temperature coefficients were determined for the three highest test loads. The temperature coefficient, k (equation 4) was computed for each ring by the method of least squares.

Typical average deflections for a 100,000-lb-capacity compression proving ring are as follows:

	Applied load—		
	80,000 lb	90,000 lb	100,000 lb
Deflection, for 101.6° F, divisions	484.21	545.33	606.67
Deflection, for 70.2° F, divisions	482.07	542.82	603.82
Difference, divisions	2.14	2.51	2.85

TABLE 1.—*Temperature coefficients for proving rings for the temperature range 70° to 100° F*

Capacity	Temperature coefficient, k	
	Compression per ° F	Tension per ° F
MOREHOUSE MACHINE CO. PROVING RINGS		
Pounds		
2,000	−0.000144	−0.000134
10,000	−.000148	----------
10,000	−.000143	----------
10,000	−.000152	----------
10,000	−.000146	----------
20,000	−.000155	−.000147
50,000	−.000155	----------
100,000	−.000160	−.000149
100,000	−.000146	----------
100,000	−.000150	----------
100,000	−.000158	----------
TINIUS OLSEN TESTING MACHINE CO. PROVING RINGS		
2,000	−0.000123	----------
20,000	−.000155	----------
100,000	−.000151	----------

Average value of the temperature coefficient for proving rings, $k = -0.000148$/° F

The temperature coefficient calculated from these data by the method of least squares is

$$k = -0.000146 \text{ per degree Fahrenheit}$$

Temperature coefficients for the 14 proving rings are given in table 1.

The temperature coefficients for proving rings varied from −0.000123 to −0.000160, the mean value being −0.000148 per degree Fahrenheit. This value corresponds to the value −0.000149 per degree Fahrenheit calculated by means of equation 9 from values for the coefficients of Young's modulus of elasticity and thermal expansion reported by Dadourian [8]. Keulegan and Houseman [9] reported results from which computed values were obtained ranging from −0.000132 to −0.000146 per degree Fahrenheit for steels of less than 5 percent total alloying content.

The temperature coefficient of one of the rings differed from the average value for all of the rings by 0.000025 per degree Fahrenheit. For this ring, correction by means of the average value for a temperature difference of 30° F, a considerably greater temperature difference than is ordinarily encountered, would result in an error of 0.075 percent. This is less than the tolerance (0.1 percent) for proving rings [2].

2. Temperature Range +70° to −93° F

Low-temperature measurements were made on the proving ring shown in figure 1. The calibration graph for this ring for a temperature of 70° F is shown in figure 2.

The temperature-correction coefficient was calculated from measurements of the natural frequency of vibration recorded on six films. The following results were obtained.

Temperature	Frequency	Spring constant of ring	Temperature coefficient per °F
°F	c/s	lb/in.	
69.4	12.391	23,050	−0.00023
−93.2	12.585	23,940	----------

The value −0.00023 obtained for the temperature range +70° to −93° F differs considerably from the average value of −0.00015 obtained for the temperature range 70° to 100° F. Benton [10] also reported a considerable increase in the temperature coefficient of Young's modulus at low temperatures. The greatest source of error in the low-temperature tests was the nonuniformity of the temperatures of different portions of the ring. Nevertheless, it is believed that the value reported is not in error by more than 1 part in 23.

As a check on the method used in the low-temperature tests, the temperature coefficient of a ring was measured by the same method over a temperature range of 70° to 178° F by means of heaters mounted in the box used for the low-temperature tests. A value $k = -0.000153$ per degree Fahrenheit was obtained, which agrees with values obtained in the dead-weight machines.

VI. Conclusions

The temperature coefficients of a group of 14 proving rings were measured for the temperature range 70° to 100° F and found to average −0.00015 per degree Fahrenheit. This value is in agreement with values calculated from the results of other observers for this temperature range.

The work of Keulegan and Houseman [9] has indicated that the temperature coefficient of Young's modulus changes very slowly in the range of temperatures ordinarily encountered in the operation of testing machines. It is believed, therefore, that for rings made of steel having a total alloying content not exceeding 5 percent, the temperature coefficient will not vary more than 10 percent from 30° to 120° F. An error of 10 percent in the temperature coefficient will introduce less than 0.05-percent error in the calculated ring load for a temperature difference of 30° F, a greater difference than is usually encountered.

The temperature coefficient of a proving ring was also measured for the temperature range +70° to −93° F and found to be −0.00023 per degree Fahrenheit.

The temperature coefficients of rings made of steels having a total alloying content exceeding 5 percent may be expected to differ significantly from the values reported.

VII. References

[1] Am. Soc. Testing Materials Standards 1944, part I, Metals, p. 954.

[2] B. L. Wilson, D. R. Tate, and G. Borkowski, Proving rings for calibrating testing machines, Circular NBS C454 (1946).

[3] B. L. Wilson, D. R. Tate, and G. Borkowski, Dead-weight machines of 111,000- and 10,100-pound capacities, Circular NBS C446 (1943).

[4] S. Timoshenko, Strength of materials, part II, ch. 2 (D. Van Nostrand Co., Inc., New York, N. Y. 1930).

[5] Den Hartog, Mechanical vibrations, second edition, p. 41–49 (McGraw-Hill Book Co., Inc., New York, N. Y., 1940).

[6] L. B. Tuckerman, discussion, Proc. Am. Soc. Testing Materials, part II, **32,** 594 (1932).

[7] J. H. Poynting and J. J. Thomson, A text-book of physics-heat, ninth edition, pp. 284–304 (Charles Griffin & Co. Ltd., London, 1928).

[8] H. M. Dadourian, Phys. Rev. [II], **XIII,** 337 (1919).

[9] G. H. Keulegan and M. R. Houseman, BS J. Research **10,** 289 (1933) RP531.

[10] J. R. Benton, Phys. Rev. **16,** 17 (1903).

Washington, April 16, 1946.

U. S. DEPARTMENT OF COMMERCE
HENRY A. WALLACE, Secretary
NATIONAL BUREAU OF STANDARDS
E. U. CONDON, Director

Circular of the National Bureau of Standards C454

PROVING RINGS FOR CALIBRATING TESTING MACHINES

By
BRUCE L. WILSON, DOUGLAS R. TATE,
and GEORGE BORKOWSKI

[Issued August 14, 1946]

UNITED STATES
GOVERNMENT PRINTING OFFICE
WASHINGTON : 1946

PREFACE

The trend in present-day engineering design is toward the use of efficient, lightweight structural elements and machine parts. Such elements have of necessity been utilized by aircraft and ordnance engineers, and their application is now being given increased attention by engineers in all fields. In the development of efficient designs it is necessary that materials be tested before being used as structural elements and machine parts to insure that they will have the required mechanical properties. Structures and subassemblies must also be tested to verify the soundness of design and point the way to still more efficient designs. This testing requires the use of accurate load-indicating testing machines. To insure the reliability of the test results obtained with load-indicating testing machines, frequent periodic calibration is recognized as being essential. A study of methods of calibrating testing machines, initiated at the Bureau some 25 years ago, showed the equipment then available to be inadequate and led to the development of the proving ring by H. L. Whittemore and S. N. Petrenko. The proving ring, because of its accuracy, constancy, and convenience, is now the most widely used device for the calibration of testing machines. Several hundred of these devices are now in service in commercial and government laboratories in this country and abroad. This Circular summarizes the Bureau's experience in the calibration and use of proving rings and makes recommendations for their proper use.

E. U. CONDON, *Director.*

PROVING RINGS FOR CALIBRATING TESTING MACHINES

By Bruce L. Wilson, Douglas R. Tate, and George Borkowski

ABSTRACT

A description is given of the proving ring, which was developed at the National Bureau of Standards to provide an accurate portable load-measuring device for calibrating testing machines. Methods are described for calibrating proving rings by dead weights for loads up to 111,000 lb and by means of other calibrated proving rings for higher loads. Rings which complied with the specification included in the paper were subjected to tests to determine the errors introduced by variations of the conditions of use. Provided reasonable care is exercised in using proving rings, the errors are shown to be small compared to ±1 percent, the generally recognized tolerance for testing machines.

CONTENTS

I. INTRODUCTION

Experience at the National Bureau of Standards and in other laboratories in using testing machines that apply forces to engineering materials and structures has indicated the advisability of frequent periodic calibration of such machines, if reliable test results are to be obtained. To insure the accuracy of the results obtained with a machine, it is necessary that the calibration include loads up to the capacity load of the machine. Some types of low-capacity machines may be calibrated to capacity by means of standard weights or by means of standard weights and proving

levers. Because these methods of calibration were not adequate for calibrating all types of small machines, and particularly, because they were inadequate for calibrating large testing machines, experiments were undertaken more than 20 years ago with portable elastic devices which could be calibrated under accurately known forces and then transported to the testing machine and used to measure the forces applied by the testing machine. These experiments led to the development of the proving ring [1, 2, 3][1] by H. L. Whittemore and S. N. Petrenko. The development and commercial production of the proving ring led to a greatly increased use of elastic calibration devices and made it necessary to provide facilities for the calibration of these devices. For calibrating devices up to 111,000 lb two dead-weight testing machines [4] have been installed at the Bureau. Methods of calibrating elastic devices for loads up to 300,000 lb by means of several 100,000-lb-capacity rings have been developed. The purpose of this paper is to describe the proving ring, its calibration, and performance under various conditions of use.

II. DESCRIPTION OF PROVING RINGS

1. DEFINITION

A proving ring is an elastic ring, suitable for calibrating a testing machine, in which the deflection of the ring when loaded along a diameter is measured by means of a micrometer screw and a vibrating reed mounted diametrically in the ring.

2. DESIGN

(a) SHAPE

A compression proving ring is shown in figure 1. Forces are applied to

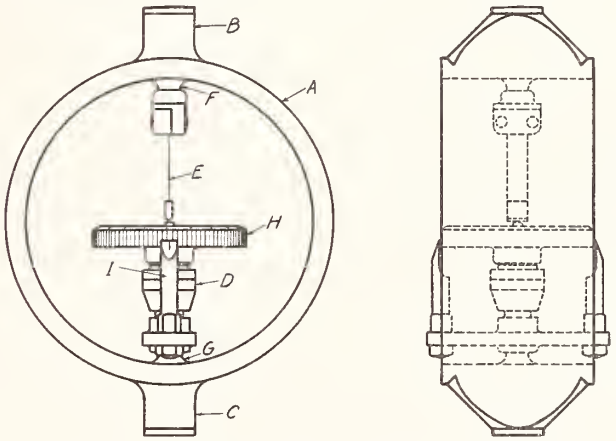

FIGURE 1.—*Proving ring for measuring compressive forces.*

the ring, A, through the integral external bosses, B and C. The resulting deflection of the ring is measured with a micrometer screw, D, and a vibrating reed, E, which are attached to integral internal bosses, F and G. By means of a graduated dial, H, and an index pointer, I, the deflection of the ring may be measured in divisions of the micrometer dial. A proving ring for measuring both tensile and compressive forces is shown in figure 2 with the tension fittings attached.

[1] Figures in brackets indicate the references given at the end of this paper.

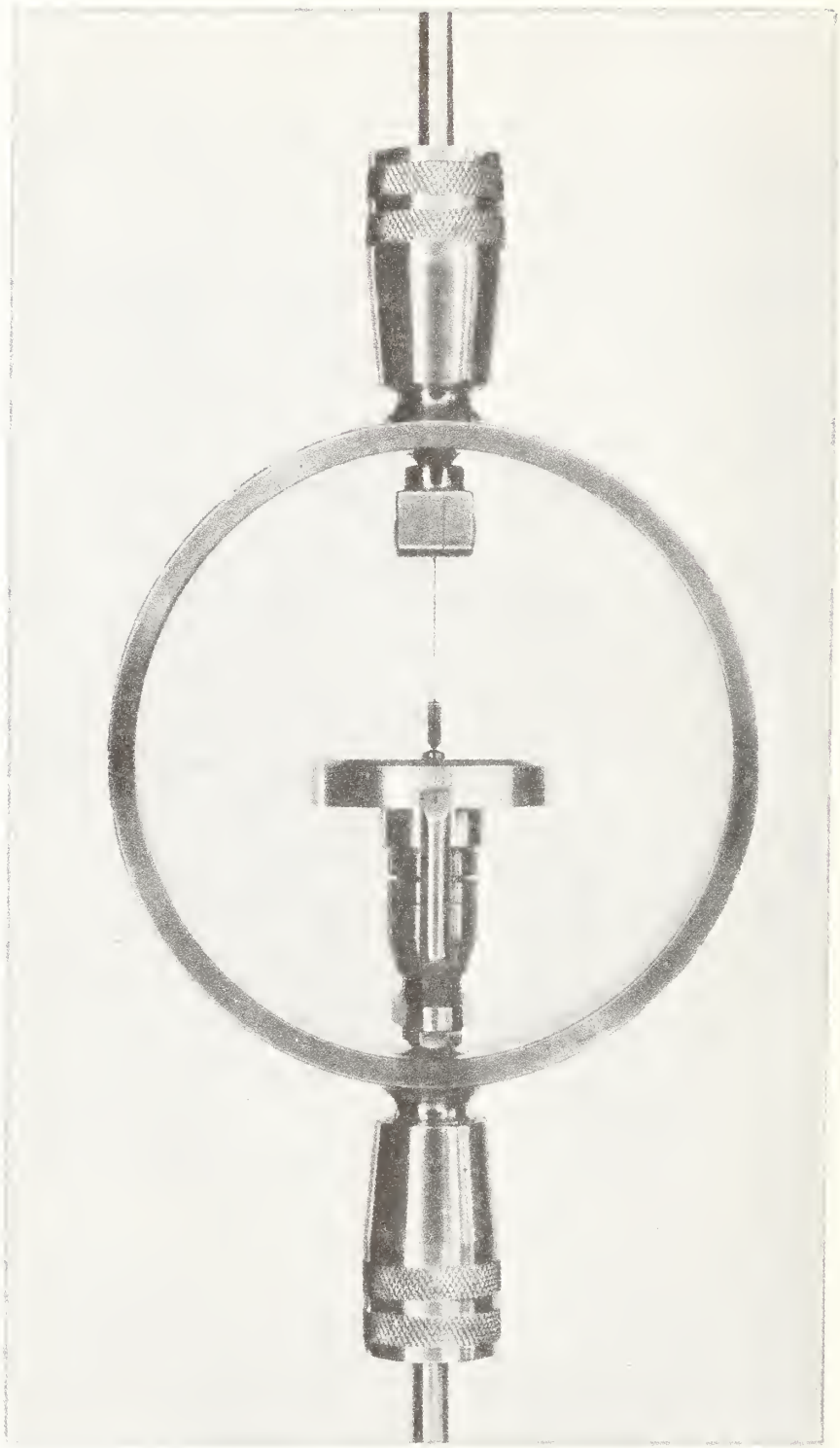

FIGURE 2.—*Proving ring for measuring both tensile and compressive forces, with tension fittings attached.*

The end of the lower external boss of a compression proving ring usually is plane and perpendicular to the axis of the bosses. The end of the upper external boss is usually convex. It is frequently made a portion of a sphere having as center the center of the end of the lower external boss and a radius equal to the over-all height of the ring. The external bosses of rings for measuring tensile forces are provided with tension fittings for applying forces to the ring. The fittings usually include spherical bearings to minimize eccentric loading of the ring.

(b) CAPACITIES

Compression rings having capacities from 300 lb to 300,000 lb, and tension rings having capacities as great as 100,000 lb have been submitted for calibration. The over-all heights of compression rings vary from about 6 in. for 2,000-lb rings to 19 in. for 300,000-lb rings. The weights of compression rings vary from about 2 lb for 2,000-lb rings to 150 lb for 300,000-lb rings.

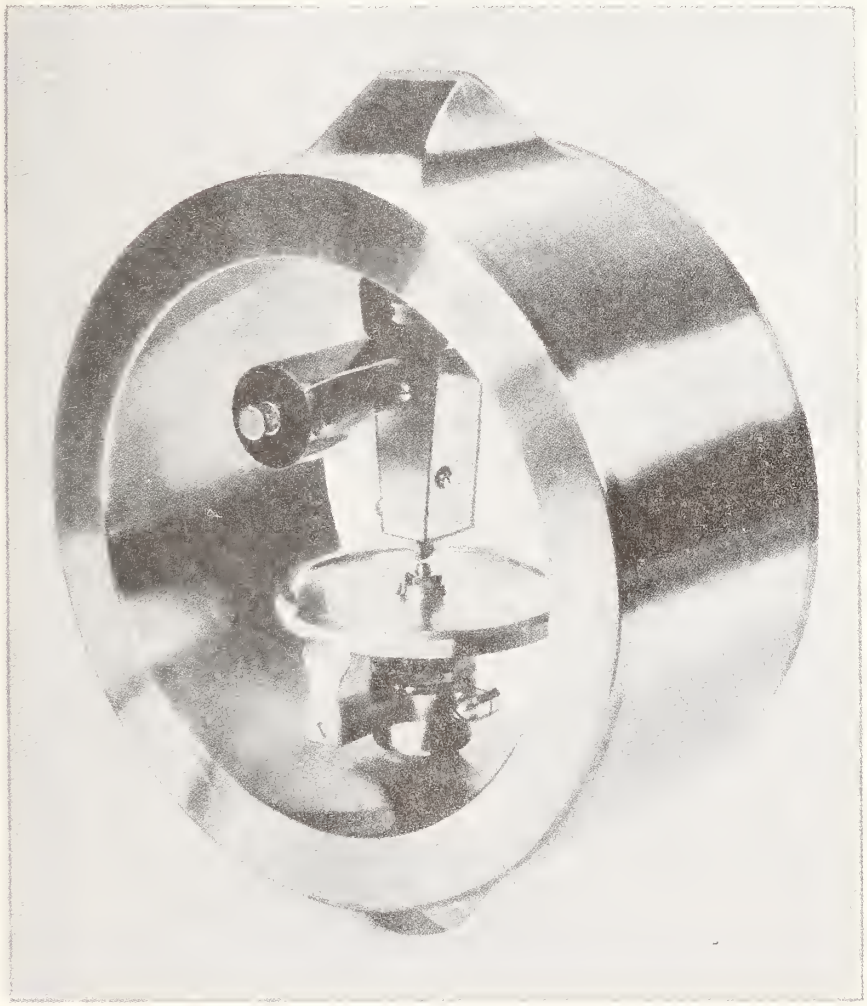

FIGURE 3.—*Proving ring equipped with electrically operated vibrating reed.*

The weights and heights of tension rings without tension fittings are a little greater than for compression rings of corresponding capacities.

(c) DEFLECTION-MEASURING APPARATUS

The vibrating reed and micrometer screw provide a sensitive and reliable means for measuring the change in diameter of the ring under load. When the reed is vibrating and the micrometer screw is adjusted so that the button on the spindle contacts the vibrating reed, a sensitive indication is produced, which varies rapidly as the button is advanced. Experience indicates that with micrometer screws having pitches varying from 40 to 64 threads per inch, as commonly supplied on most proving rings, readings may be made with a sensitivity of about one or two hundred thousandths of an inch.

Two types of vibrating reeds are used on proving rings; one type is operated manually and the other is driven electrically [5]. Figures 2 and 3 show proving rings having the two types of vibrating reeds. When reading a ring equipped with a manually operated vibrating reed, the lower end of the reed is pushed aside about ½ inch with the end of a pencil or other suitable object and released. Use of the finger is not recommended because changes in length of the reed with temperature change the reading of the ring. While the reed is vibrating, the dial is rotated, advancing the button into the path of the reed until a characteristic buzzing sound is produced, and the time required to reduce the amplitude from about ½ in. to zero amplitude is 2 or 3 seconds. Either or both of these effects may be used by the operator in setting the dial. With no contact between the reed and button, the vibration will continue from 10 to 15 seconds. An operator usually has no difficulty in obtaining reproducible readings to about ±0.1 dial division at zero load. Different operators will obtain zero-load readings that differ by more than this amount, as will a single operator if he uses different sound intensities and different lengths of time for stopping the motion of the reed. As deflections of the ring are the differences between zero-load readings and load readings, it is important that the operator adjust the dial in the same way in making each reading. Different operators will obtain comparable deflections even though their methods of adjusting the dial differ.

With the electrically driven reed the best results are obtained by turning the dial to advance the button just far enough to interfere with the vibration of the reed. This condition can be detected better by watching the change in amplitude of the reed than by listening for the change in intensity or frequency of the sound. Readings taken by advancing the button until a large change in amplitude is produced or until the motion is nearly stopped have been found much less reliable than readings taken in the manner described above.

Experience indicates that the combination of a well-made micrometer screw and vibrating reed is about equal in sensitivity and superior in ruggedness and accuracy to dial micrometers for measuring the deflections of elastic devices. The best dial micrometers commercially available have errors several times the errors of well-made micrometer screws. For this reason, the American Society for Testing Materials [6] permits the use of devices having dial micrometers only at the test loads for which they have been calibrated.

(d) DEFLECTION

Proving rings are usually designed to have a deflection of 0.05 to 0.10 in. under capacity load. The dimensions of a ring that will have approximately a desired deflection may be computed by means of equations given in engineering textbooks. Equations for computing the deflection of plain rings loaded at opposite ends of a diameter have been published by Timoshenko, Bach and Baumann, and Larard [7, 8, 9, 10]. For a plain ring having a rectangular cross section, the equation given by Timoshenko reduces to the following:

$$d = \frac{Pr^2}{eElt}\left\{\frac{\pi}{4} - \frac{2}{\pi}\left(1 - \frac{e^2}{r^2}\right) + \frac{2e}{r}\left[\frac{2}{\pi}\left(1 - \frac{e}{r}\right) + 0.265\pi\right]\right\},$$

where

d = deflection of the ring in the direction of the loaded diameter, in.

P = applied load, lb
r = radius of the centerline of the ring, in.
E = Young's modulus of elasticity for the material of the ring, lb/in.^{2}
l = width of the cross section of the ring, in.
t = thickness of the cross section of the ring, in.

$$e = r - \frac{t}{\log_n \dfrac{1 + \frac{1}{2}\frac{t}{r}}{1 - \frac{1}{2}\frac{t}{r}}}.$$

Actually, the measured deflections of proving rings are about 25 percent less than the deflections computed by means of equations derived for plain rings because of the stiffening effect of the integral bosses. As the relationship between the deflection of a proving ring and the applied load is determined by applying accurately known forces to the ring, the derivation of an equation which would take into account the stiffening effect of the bosses is unnecessary.

(e) STRESS

To obtain satisfactory elastic behavior of a ring, the maximum stress must be less than the stress required to produce an appreciable permanent set in the material. Equations for computing the maximum bending moment in a plain ring loaded at opposite ends of a diameter are given by Timoshenko, Bach and Baumann, and Larard [7, 8, 9, 10]. The following equation derived from Timoshenko's results gives the maximum stress for a ring having a rectangular cross section:

$$\sigma_{max} = \frac{Pr}{elt\pi}\left(1 - \frac{e}{r}\right)\frac{\left(\frac{t}{2} - e\right)}{\left(r - \frac{t}{2}\right)},$$

where

σ_{max} = maximum fiber stress across the inner cylindrical elements passing through the load line, lb/in.^{2}
P = applied load, lb
r = radius of the centerline of the ring, in.

l = width of the cross section of the ring, in.
t = thickness of the cross section of the ring, in.

$$e = r - \frac{t}{\log_n \dfrac{1 + \frac{1}{2}\frac{t}{r}}{1 - \frac{1}{2}\frac{t}{r}}}.$$

This equation for plain rings does not apply accurately to proving rings having integral bosses (fig. 1) because the bosses influence the stress distribution in the plane containing the maximum bending moment. Experience has demonstrated that stress values calculated by the above equation are satisfactory for design purposes, provided there are adequate fillets where the bosses join the ring and no "stress raisers" are present. Breakage of some rings through holes and stamped numbers has indicated the desirability of avoiding holes, stamped numbers, tool marks, cracks, etc.

Except for rings having deflection-measuring apparatus attached by means of plugs or screws, computed working stresses as high as 150,000 to 165,000 lb/in.^{2} have been found satisfactory.

(f) MATERIAL AND FINISH

Proving rings are usually made of alloy steel, rough-machined from annealed forgings, heat treated, and then ground to size. Probably rings unpolished after heat treatment or finished by some other method would be satisfactory. One chromium-plated ring has given satisfactory service for several years at the Bureau.

Satisfactory proving rings designed along the lines indicated in the preceding sections have been made from a steel having the following chemical composition: Carbon, 0.50 percent; chromium, 1.00 percent; and nickel, 1.75 percent. This steel is heat treated to give about the following properties in tensile tests:

Yield strength (offset=0.05 percent)	210,000 lb/in.^{2}
Tensile strength	230,000 lb/in.^{2}
Elongation in 2 inches	8 percent.

III. CALIBRATION

1. GENERAL

All proving rings submitted for calibration at the National Bureau of Standards are calibrated for compliance with the performance specification given in the appendix, section VIII. This specification does not give detailed requirements for the design of proving rings, but it does include performance requirements that have been found necessary to insure that rings will maintain their calibrations satisfactorily with ordinary use and with the handling to which rings shipped by commercial carriers are subjected.

Proving rings are calibrated by determining the relationship between accurately known forces and the corresponding deflections.

2. LOADS NOT EXCEEDING 111,000 LB

Two dead-weight testing machines [4] have been installed at the National Bureau of Standards for calibrating elastic calibration devices.

With the larger machine, compressive and tensile loads from 2,000 lb to 111,000 lb by 1,000-lb increments may be applied. With the smaller machine, loads from 200 lb to 10,100 lb by 100-lb increments may be applied. The errors of the weights do not exceed about 0.01 percent.

3. LOADS EXCEEDING 111,000 LB

Calibration loads exceeding 111,000 lb are applied to large proving rings by means of three calibrated 100,000-lb-capacity proving rings as shown in figure 4. The three nearly identical calibrated rings are placed

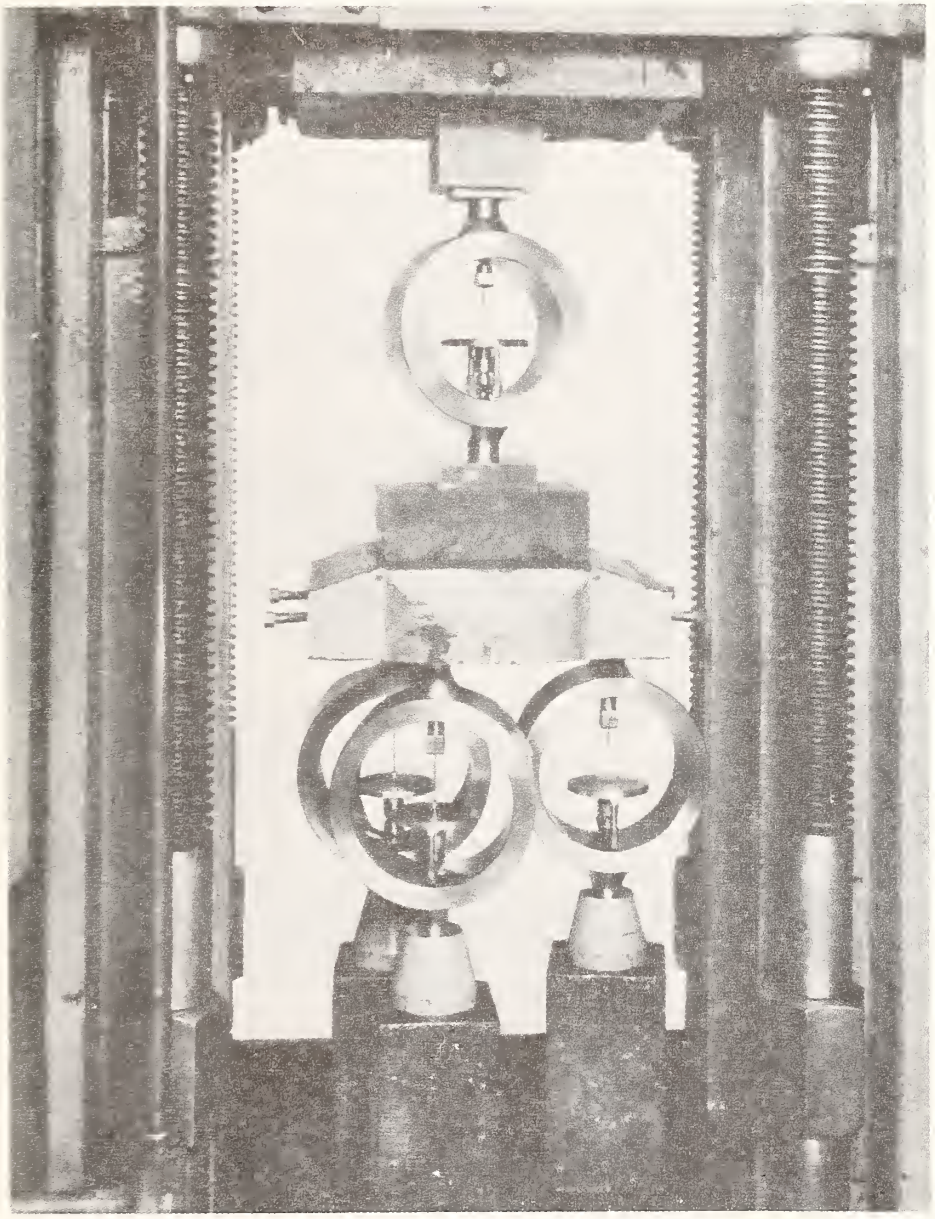

FIGURE 4.—*Calibration of a proving ring for loads exceeding 111,000 lb by means of three calibrated 100,000-lb-capacity proving rings.*

in a vertical testing machine at the corners of a triangle so oriented that the centroid of the triangle lies on the axis of the machine. A thick steel plate is placed over the upper bosses of the three rings. The ring to be calibrated is placed on a hardened block on the plate above the three rings and so located that when forces are applied to the rings by means of the testing machine, the deflections of the three lower rings are equalized to within about 1 percent.

During the calibration the load indicated by the testing machine is disregarded. The four proving rings are read simultaneously while the load is held constant or increased very slowly. The force applied to the ring being calibrated is the sum of the forces measured by the three previously calibrated rings.

This method of calibration has been used for loads up to 300,000 lb, the capacity load of the largest compression ring submitted for calibration. The errors of measuring the load applied to the ring being calibrated do not exceed 0.1 percent. Calibration factors (see below) computed from results obtained in the dead-weight machine and from results obtained on the same rings by the method described fit smooth curves about equally well. The relatively smaller observational error in determining the deflection of the ring for the higher loads compensates for the greater errors of the loads measured with the three rings so that the departure of individual calibration factors is little greater for a given ring for loads exceeding 111,000 lb than for loads applied by dead weights.

4. LOADING PROCEDURE

Proving rings are calibrated by increasing the loads to the test loads. Compressive loads, except those on concave and convex bearing blocks [appendix, paragraph II-5(d)], are applied to the lower boss of a ring through a plane, hardened steel bearing block and to the upper boss either through a ball or a soft-steel block. Tensile loads are applied to a ring through pulling rods provided with the ring. The tension fittings usually include two or more spherical bearings so that the ring will not be loaded eccentrically.

Proving rings are usually calibrated for 10 approximately equally spaced loads from 10-percent-capacity load to capacity load. A preliminary preload to capacity is desirable to stabilize the no-load reading of the ring. Before and after each load reading, a no-load reading of the ring is observed. The deflection of the ring is computed as the difference between the load reading and the average of the no-load readings observed immediately before and after the application of the load. For each deflection the calibration factor, which is the ratio of the load to the corresponding deflection, is computed.

5. CALIBRATION GRAPH

The calibration factors are plotted on the calibration graph as a function of the deflection, as shown in figure 5. Well-made rings in good condition exhibit a nearly linear relationship between the calibration factors and the deflection. The calibration factor for compression rings decreases with increasing ring deflection, as shown in figure 5. The calibration factor for tension rings increases with increasing ring deflection.

In using the ring the load is computed from the ring readings by multiplying the ring deflection by the calibration factor read from the calibration graph.

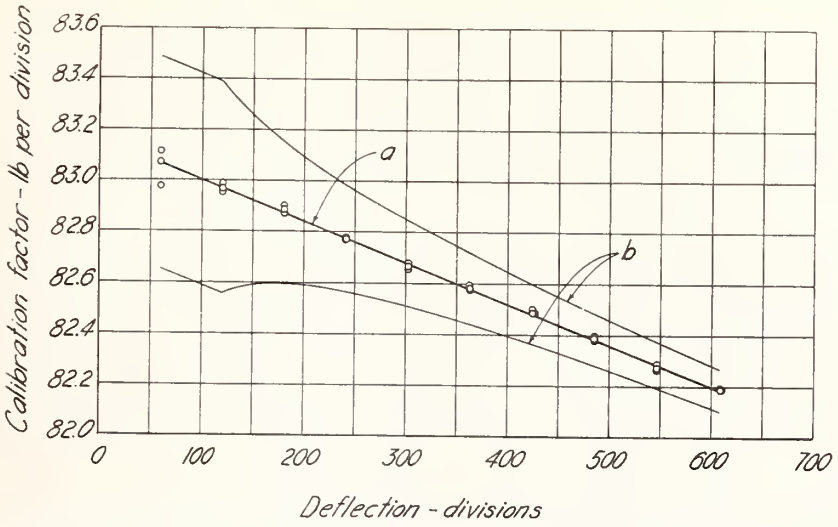

FIGURE 5.—*Calibration graph for 50,000-lb-capacity compression proving ring.*
Line "a" represents the calibration line for 70° F; line "b" represents the specification limits.

6. TEMPERATURE COEFFICIENT

Because the dimensions and the elastic properties of a ring change with temperature, the deflection of a ring for a given load varies with the temperature. The variation is not large for small temperature changes; usually it is less than 0.02 percent per degree Fahrenheit. Calibration results for proving rings are given for a temperature of 70° F. When the rings are used to calibrate testing machines and the ring temperature is different from 70° F, the results may be corrected for temperature by the formula

$$d_{70} = d_t \, [1 + K \, (t - 70)],$$

where

d_{70} = deflection of ring at a temperature of 70° F
d_t = deflection of ring at a temperature of t degrees Fahrenheit
K = temperature coefficient of the ring
t = temperature, degrees Fahrenheit, during test.

The temperature coefficient, K, depends primarily upon the temperature coefficient of Young's modulus for the material of the ring. The temperature coefficient of Young's modulus for steels depends upon the chemical composition of the steel and its heat treatment. For rings made of steels having a total alloying content not exceeding 5 percent, the value $K = -0.00015$ per degree Fahrenheit has been found sufficiently accurate. For some other steels, values of the temperature coefficient of Young's modulus of elasticity, that would result in values of K ranging from -0.00011 to -0.00024 have been observed. Most of the proving rings submitted for calibration are made of steel having a total alloying content not exceeding 5 percent.

Calibrations of proving rings in the dead-weight machines at the National Bureau of Standards are made at 70° F, whereas calibrations at loads beyond the capacity of these machines are made at room temperature, usually in the range 65° to 90° F, and then corrected to 70° F.

IV. USE

1. CALIBRATION OF TESTING MACHINES

Proving rings are used primarily for calibrating testing machines, the purpose for which they were developed. In figure 6, a 100,000-lb-capacity compression proving ring is shown in a vertical hydraulic testing ma-

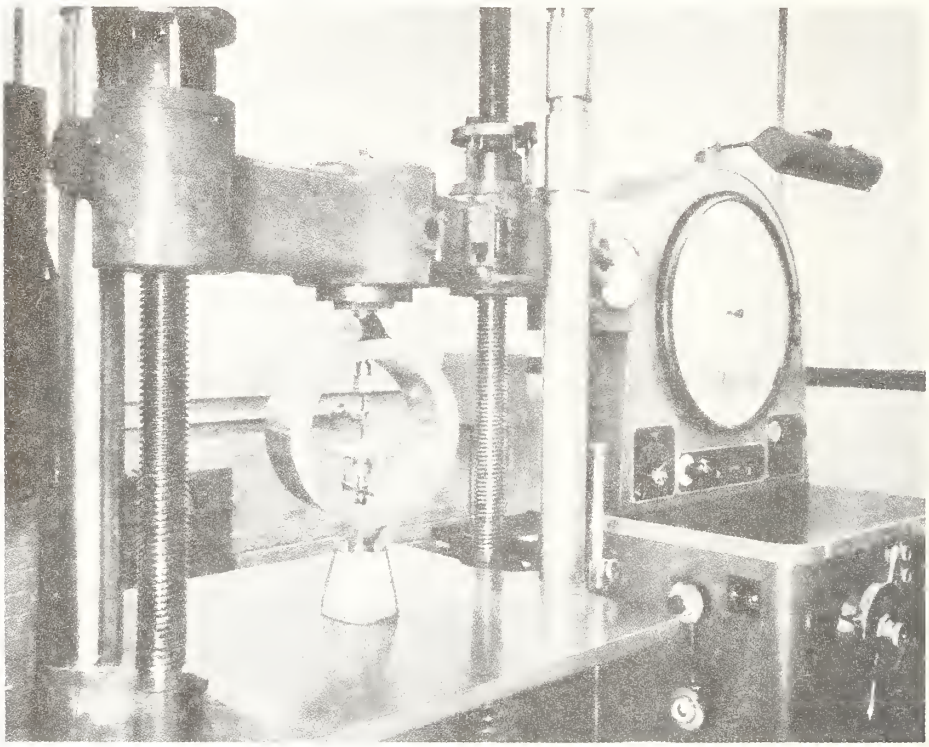

FIGURE 6.—*Proving ring in testing machine ready for the calibration of the testing machine in compression.*

chine. The ring, together with bearing blocks through which the loads are applied to the external bosses, takes the place of the specimen in the machine. When rings are used for calibrating horizontal testing machines, the no-load ring readings are taken with the rings supported by their external bosses.

In carrying out a calibration, two operators are required to read the indicated load of the testing machine and the ring simultaneously. The temperature of the air near the ring is recorded so that the proper temperature corrections may be applied.

A sample data sheet for the partial calibration of one scale range of a testing machine is given in table 1.

The results in the first three columns of table 1 were observed during the calibration. The results in the fourth column were obtained by subtracting from each load reading the average of the no-load readings taken before and after the load reading. The ring load was computed by multiplying the ring deflection for 70° F by the corresponding calibration factor. The error in pounds was computed by subtracting the ring load from the machine reading.

TABLE 1.—*Data sheet for the partial calibration of 200,000-lb scale range of hydraulic testing machine with a 100,000-lb-capacity proving ring*

Machine reading	Temperature	Ring reading	Ring deflection	Ring[a] deflection for 70° F	Calibration[b] factor	Ring load	Error of testing machine	Percentage error of testing machine
lb	*° F*	*div.*	*div.*	*div.*	*lb/div.*	*lb*	*lb*	
0	79	32.1						
60,000		442.7	410.6	410.05	145.85	59,806	+194	+0.32
0		32.1						
80,000		581.2	549.05	548.31	145.58	79,823	+177	+ .22
0		32.2						
100,000		719.6	687.4	686.47	145.31	99,751	+249	+ .25
0		32.2						
60,000		442.8	410.6	410.05	145.85	59,806	+194	+ .32
0		32.2						
80,000		580.8	548.6	547.86	145.58	79,757	+243	+ .30
0		32.2						
100,000		719.4	687.4	686.47	145.31	99,751	+249	+ .25
0	79	31.8						

[a] Ring deflection for 70° F = Ring deflection for 79° F $(1 - 9 \times 0.00015)$
[b] Read from the calibration curve or calculated from the equation:
Calibration factor = 146.66 − 0.00197 × deflection for 70° F.

To obtain information concerning the reproducibility of the readings of a testing machine the errors are frequently determined for two or more

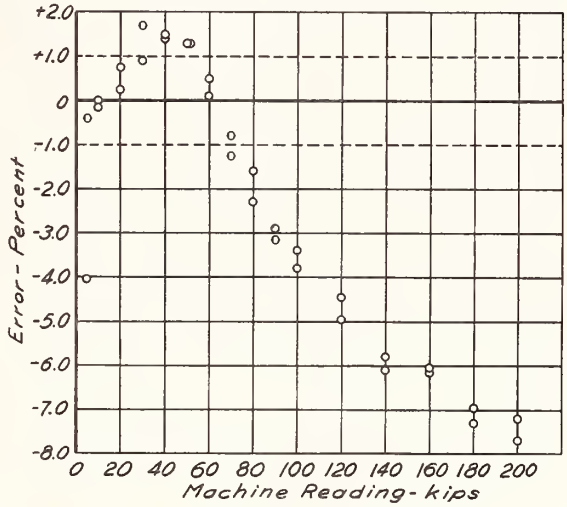

FIGURE 7.—*Calibration results obtained on a 200,000-lb-capacity testing machine in need of repairs.*

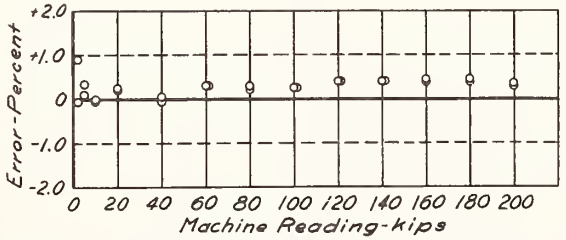

FIGURE 8.—*Calibration results obtained on a 200,000-lb-capacity testing machine in good condition.*

applications of the same indicated testing-machine loads. The results of complete calibrations of two testing machines are given in figures 7 and 8 to illustrate results for machines in unsatisfactory and satisfactory conditions. The American Society for Testing Materials [6] tolerance lines of ± 1 percent are shown by the dashed lines. The machine found to be unsatisfactory (fig. 7) had been in regular use prior to its calibration.

Several rings may be used together, as shown in figure 9, to calibrate machines having capacities exceeding the capacity of a single ring. The

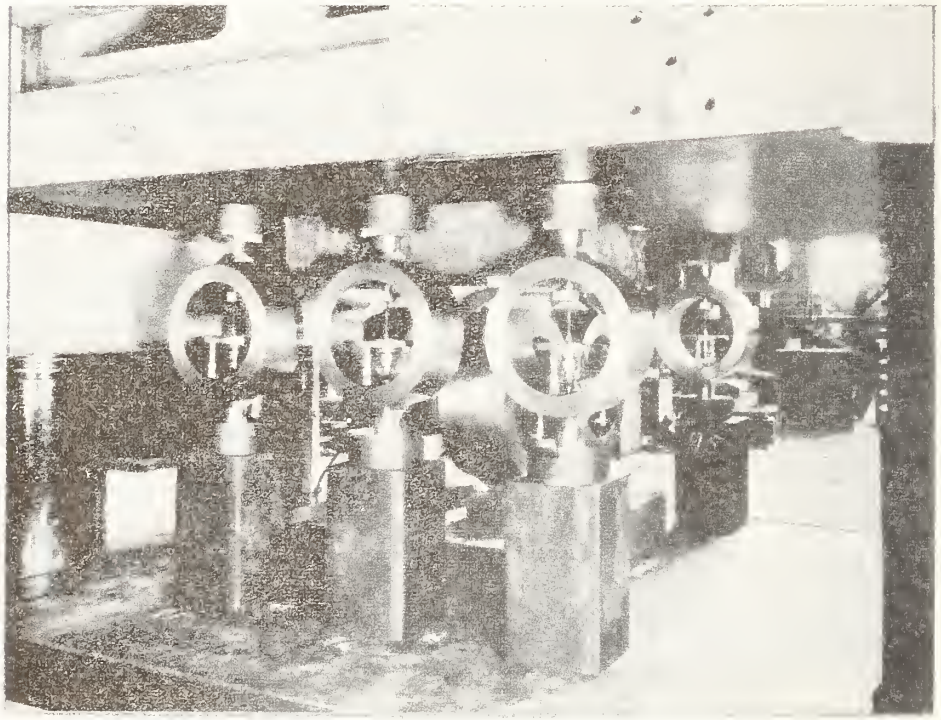

FIGURE 9.—*Eight compression proving rings arranged to be loaded in parallel to obtain test loads equal to the sum of the forces applied to the individual rings.*

indicated load of the testing machine and the rings are read simultaneously, and the ring load is computed as the sum of the loads carried by the individual rings. By this method, calibrations have been made with proving rings for loads up to about 2 million pounds.

2. OTHER USES

Proving rings have also been used as dynamometers, for weighing elevator cars, and for weighing bridge reactions [11].

V. ERRORS

1. ERRORS DUE TO VARIATIONS IN LOADING SCHEDULE

During calibration proving rings are read within a few seconds after the load is applied or removed and a no-load reading is observed before and after each load reading. It is not always possible to follow such a time schedule in using proving rings, and it is sometimes necessary to use them for measuring decreasing as well as increasing loads. To de-

termine the errors that might result from such variations in the conditions of use, dead-weight tests at 70° F were made on three rings having capacities of 3,000 kg, 20,000 lb, and 100,000 lb. Each of the rings had been calibrated and found to comply with the requirements of the specification given in the appendix.

After having been unloaded for more than 24 hours, each ring was loaded to capacity and kept under capacity load for 3 hours. Ring readings were observed as soon as possible after the load was fully applied and again after intervals from ½ minute to 3 hours after application. The maximum observed creep under capacity load for the 3-hour period was 0.05 division, or 0.01 percent of the capacity load.

After each ring had remained under capacity load for 3 hours, the load was completely removed. The no-load reading of the ring was observed as soon as possible and again after intervals from ½ minute to 3 hours after removal of the load. In every case the no-load reading changed during the first half-hour of the 3-hour period. The maximum observed zero shift was 0.4 division, or 0.06 percent of the capacity deflection. Within 32 minutes for the 3,000-kg and 20,000-lb rings and within 64 minutes for the 100,000-lb ring, the no-load readings equalled the no-load reading observed before the application of the capacity load.

The hysteresis at half-capacity load was determined for each ring by computing the difference between the ring readings at half-capacity load observed before and after the application of capacity load. The results indicated a hysteresis of 0.10 percent for the 3,000-kg and 100,000-lb rings and 0.15 percent for the 20,000-lb ring.

2. ERRORS DUE TO INSTANTANEOUS TEMPERATURE EFFECT

When a proving ring is loaded, both tensile and compressive stresses are set up in the material of the ring. An increase in temperature occurs in the material subjected to compressive stresses, and a decrease in temperature occurs in the material subjected to tensile stresses [12, 13]. Consequently, the reading of a suddenly loaded (or unloaded) proving ring changes as the temperature throughout the material of the ring becomes equalized. This equalization occurs so rapidly that it may be ignored without significant error in rings not exceeding 100,000-lb capacity. For larger rings, errors due to this cause become negligible if readings are taken no sooner than 30 seconds after removal of load. No delay in taking readings under load is necessary because with ordinary testing machines the time required to apply and adjust the test load and read the ring is great enough to permit nearly complete temperature equalization.

3. ERRORS DUE TO ANGLE OF LOAD LINE

If a proving ring is loaded through suitable bearing blocks or tension fittings in a testing machine whose platens are plane and parallel, the load line will be very nearly coincident with the axis of the bosses of the ring. For compression rings a lack of parallelism of the heads of the testing machine may result in an inclination of the load line with respect to the axis of the bosses of the ring.

To determine the magnitude of the error introduced by an inclination of the load line, a 100,000-lb-capacity compression proving ring was loaded in the 111,000-lb-capacity dead-weight machine through 2- and 4-degree wedges, as shown in figure 10. The errors resulting from these

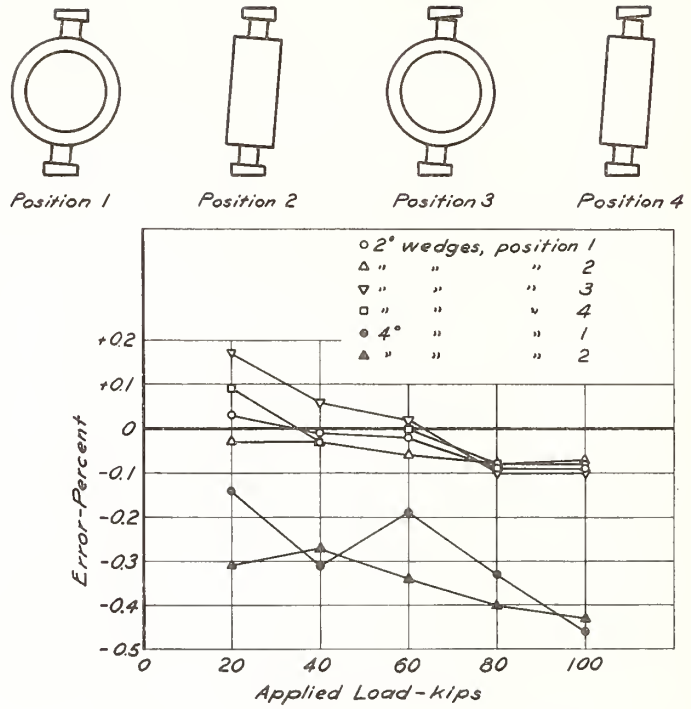

FIGURE 10.—*Effect of the angle of the load line on the calibration of a 100,000-lb-capacity proving ring.*

conditions of loading are plotted in percent as a function of the applied load. The maximum errors introduced by the 2-degree wedges were about 0.17 percent at 20-percent-capacity load and 0.1 percent at capacity load, values which do not exceed the tolerances of 0.5 percent and 0.1 percent, respectively, given in the Bureau specification for proving rings. The maximum error introduced by the 4-degree wedges was about 0.46 percent at capacity load.

As an angle of less than 2 degrees can easily be detected by inspection, there is no reason for the occurrence of appreciable errors due to inclination of the load line.

4. ERRORS DUE TO CHANGE OF CALIBRATION WITH TIME

The relationship between the deflection of a proving ring and the applied load depends not only upon the dimensions of the ring but also upon the elastic constants of the material of the ring. Provided the dimensions are not altered by removing material or by plating the surface, and provided a ring has not been overloaded or subjected to sufficient wear to introduce errors from these causes, a study of the constancy of the calibration with time may be expected to indicate the magnitude of any change in elastic constants with time.

Experience indicates that there is no appreciable aging effect for rings made of the steel described on page 7. The results of a study of the calibrations of three 300,000-lb-capacity rings for a 12-year period are given in figure 11. Each ring was calibrated seven times during this

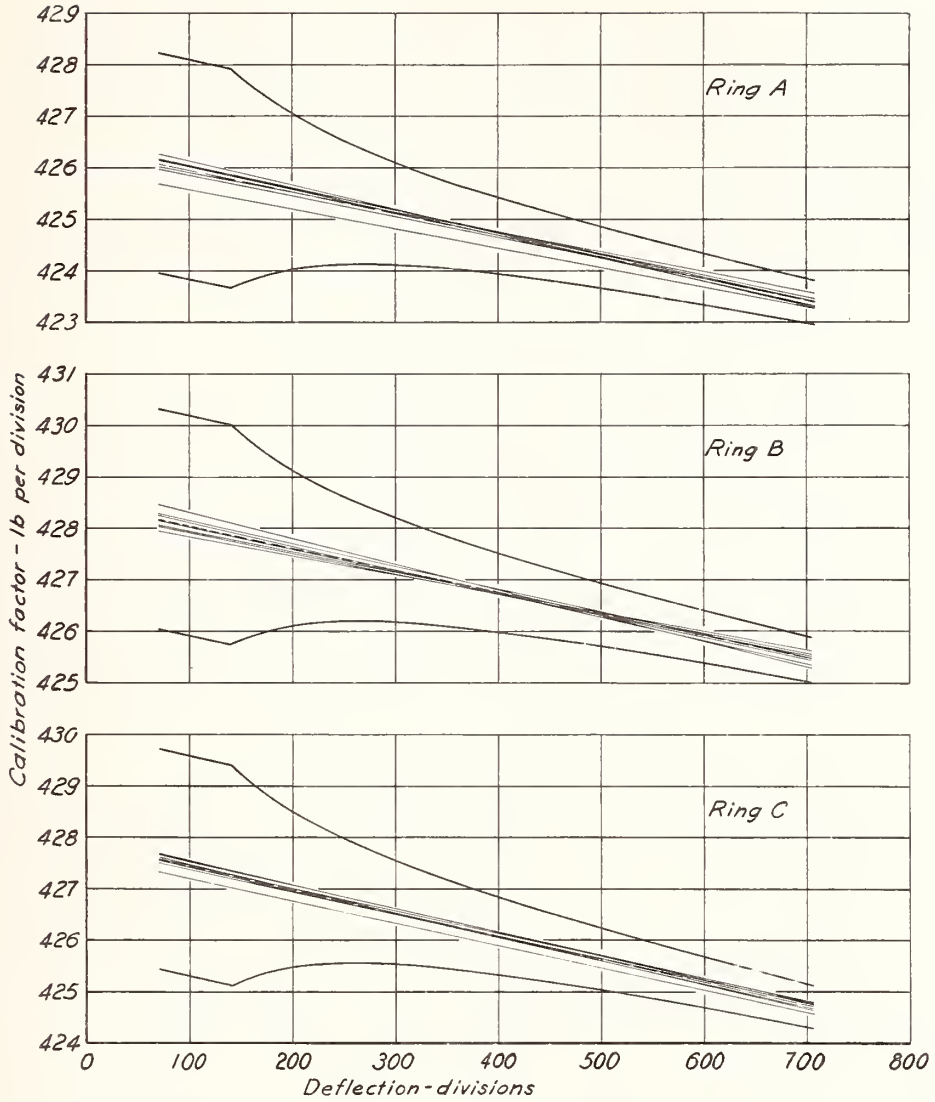

FIGURE 11.—*Effect of time and use on the calibrations of three proving rings for calibrations spaced over a period of years.*

The dashed line represents the average of the individual calibration lines indicated by the light lines which were drawn to represent experimental points not shown. The curved lines are the specification limits corresponding to the average calibration line.

period. The individual lines drawn to represent each calibration are shown as solid lines. An "average" calibration line for each ring is shown by a dashed line. Specification limits corresponding to the dashed line, computed as defined in the appendix, are shown for each ring. It is evident that the changes in calibration with time are small compared to the tolerances for constancy. Furthermore, the small changes observed indicated no progressive trend but were apparently random changes of a magnitude about equal to the experimental error of determining a given calibration line. Experience with other capacities of rings is in accord with the results given for the 300,000-lb rings.

5. ERRORS DUE TO WEAR

Each time the reading of a proving ring is observed, the end of the vibrating reed repeatedly strikes the button on the spindle of the micrometer screw, tending to wear the contacting surfaces. Although the rate at which metal is worn away varies with the operator and frequency of use, ultimately the alteration in the shapes of the surfaces leads to errors in the measured deflections of the ring.

Errors of this type generally may be observed as a cyclic departure of the calibration points from the straight line of the calibration curve,

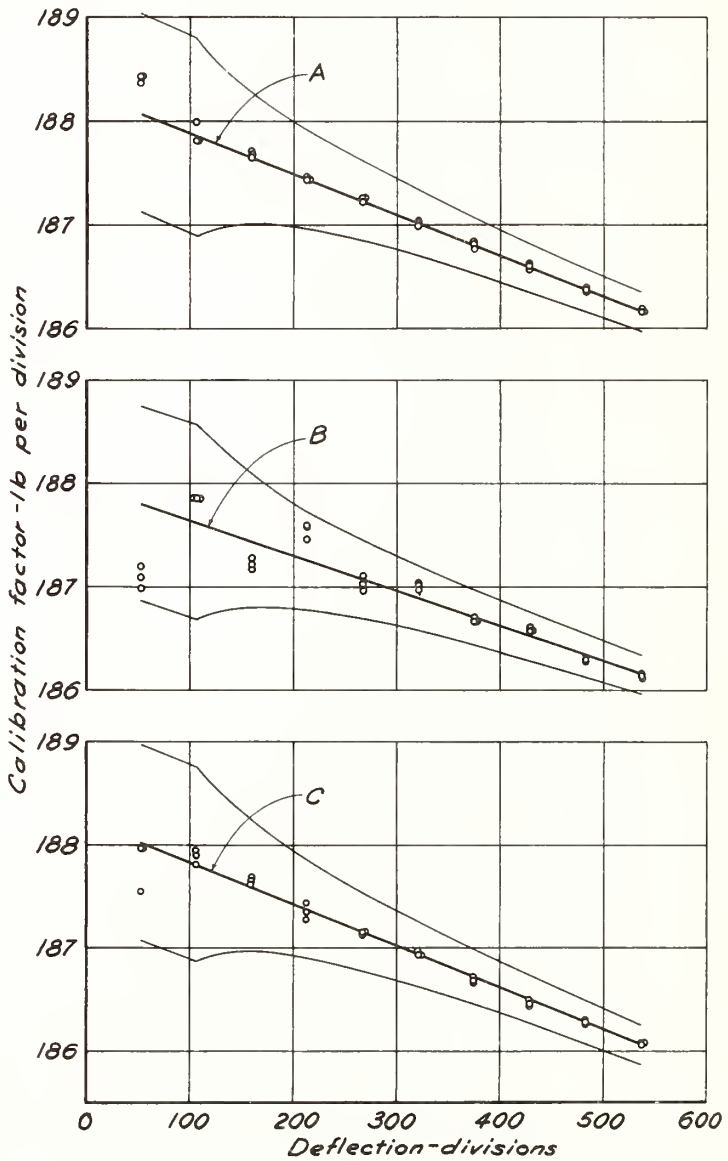

FIGURE 12.—*Effect of wear on the calibration results.*
A, Original calibration of a new ring; *B*, calibration of the same ring after considerable use; and *C*, calibration of the same ring after reconditioning of the worn surfaces of the deflection-measuring apparatus after the calibration marked *B*.

as shown in figure 12. In this figure, *A* shows the original calibration of a 100,000-lb-capacity ring, *B* shows the calibration made after considerable use, and *C* shows the calibration made after the worn surfaces of the deflection-measuring apparatus had been refinished. Experience indicates that for rings used frequently the worn surfaces should be refinished at intervals of 2 or 3 years.

The calibration of a ring that has been overloaded sufficiently to produce a set is permanently changed, and the ring should be recalibrated after any necessary repairs. A considerable number of rings have been recalibrated after having been overloaded and reconditioned and have shown satisfactory performance.

VI. CONCLUSIONS

Proving rings that comply with the specification included in the appendix are suitable for determining the errors of the indicated loads of testing machines. Such rings, provided they are not overloaded, subjected to excessive wear or otherwise damaged, maintain their calibrations without significant change over periods as long as 12 years. However, it is recommended that rings be recalibrated after intervals of from 1 to 2 years. Even under unusual conditions of use the errors of proving rings certified to comply with the specification given in the appendix are small compared to the generally recognized tolerance of ± 1 percent for testing machines.

VII. REFERENCES

[1] Proving ring. U.S. Patent 1,648,375 issued to H. L. Whittemore and S. N. Petrenko.

[2] Proving ring. U.S. Patent 1,927,478 issued to H. L. Whittemore and S. N. Petrenko.

[3] S. N. Petrenko, Elastic ring for verification of Brinell hardness testing machines, Trans. Am. Soc. Steel Treating C.22, 420 (1926).

[4] B. L. Wilson, D. R. Tate, and G. Borkowski, Dead-weight machines of 111,000- and 10,100-pound capacities, Circular of the NBS C446 (1943).

[5] Testing instrument. U.S. Patent 1,694,187 issued to R. B. Lewis.

[6] ASTM Standards, 1944, part I, Metals, p. 953–961.

[7] S. Timoshenko, Strength of materials, part II, second edition, ch. 2 (D. Van Nostrand Co. Inc., New York, N. Y., 1941).

[8] C. Bach and R. Baumann, Elastizitat und Festigkeit, 9th edition, p. 502 (Julius Springer, 1924).

[9] C. E. Larard, The elastic ring acted upon by equal radial forces, Phil. Mag. [7] C.22, 129–143 (1931).

[10] C. E. Larard, The elastic ring. A comparison of strains determined experimentally with the strains calculated from the elastic ring theory, Phil. Mag. [7] C.22, 1183–1188 (1931).

[11] C. M. Spofford and C. H. Gibbons, Weighing bridge reactions with proving rings, Eng. News Rec. C.22, 446–449 (1935).

[12] M. F. Sayre, Thermal effects in elastic and plastic deformation, Proc. ASTM, part II, C.22, 584 (1932).

[13] L. B. Tuckerman, discussion, Proc. ASTM, part II, C.22, 594 (1932).

VIII. APPENDIX

NATIONAL BUREAU OF STANDARDS SPECIFICATION FOR PROVING RINGS FOR CALIBRATING TESTING MACHINES

(Letter Circular LC 822, April 15, 1946)

INTRODUCTION

The National Bureau of Standards has had more than twenty-five years of experience in calibrating testing machines which apply forces to engineering materials. This experience has indicated the advisability of frequent periodic calibration of such machines, if reliable test results are to be obtained. It also indicated the need for a calibrating device which would be sufficiently accurate for the purpose and at the same time more readily portable and convenient in use than the devices previously available. Proving rings were developed at the National Bureau of Standards to meet this need.

This specification is the result of over 20 years' experience in the development of proving rings and in calibrating them periodically in dead-weight calibrating machines. It contains requirements which have been found necessary to insure that proving rings complying with them will be satisfactory, reliable instruments for calibrating testing machines.

These technical requirements are identical with those in Letter Circular 657, which this specification supersedes. The simplified procedure for the recalibration of rings previously certified is justified by the experience of the past 7 years.

I. DEFINITIONS

1. PROVING RING

A proving ring is an elastic ring, suitable for calibrating a testing machine, in which the deflection of the ring when loaded along a diameter is measured by means of a micrometer screw and a vibrating reed mounted diametrically in the ring.

2. READING

A reading is the value indicated by the micrometer dial when it has been adjusted to contact the vibrating reed.

3. DEFLECTION

The deflection of the ring for any load is the difference between the reading for that load and the reading for no load.

4. CALIBRATION FACTOR

The calibration factor for a given deflection is the ratio of the corresponding load to the deflection.

II. COMPLETE CALIBRATION

1. MARKING

The maker's name, the capacity load, and the serial number of the ring shall be legibly marked upon some part of the instrument.

2. MICROMETER DIAL

(a) The dial of the micrometer shall be of the uniformly graduated type. When successive graduation lines on the dial are set to one fixed index line, the positions of successive graduation lines nearly diametrically opposite referred to another fixed index shall differ from each other by not more than 1/20 of the smallest division of the dial.

(b) The smallest division of the dial shall be not less than 0.05 inch and not more than 0.10 inch.

(c) The width of any graduation line on the dial shall not exceed one-tenth of the average distance between adjacent graduation lines.

(d) The width of any index line shall be not less than 0.75 and not more than 1.25 times the average width of the graduation lines on the dial.

3. OVERLOAD

The ring shall be overloaded repeatedly to a load of not less than 9 percent nor more than 10 percent in excess of the capacity load. The difference between the

no-load reading after the first overload and the no-load reading after any subsequent overload shall not exceed one-tenth of one percent of the deflection of the ring under capacity load.

4. STIFFNESS

Under the capacity load the ring shall deflect not less than 0.040 inch.

5. CONSTANCY

(a) *Range 1/10 to 2/10-Capacity Load.*—The observed deflection of the ring, for an applied load of not less than one-tenth nor more than two-tenths of the capacity load, shall differ from the average of at least three successive observations for the same applied load by not more than one-half of one percent of the deflection for the applied load.

(b) *Range 2/10 to Capacity Load.*—The observed deflection of the ring, for any applied load not less than two-tenths nor more than the capacity load, shall differ from the average of at least three successive observations for the same applied load by not more than one-tenth of one percent of the deflection for the capacity load.

(c) *Disassembling.*—The difference between the deflections of the ring, observed before and after the deflection-measuring apparatus is removed and then replaced, shall be not greater than the maxima specified in paragraphs II-5(a) and II-5(b) of this specification, under the loads there specified.

(d) *Bearing Blocks.*—A compression proving ring shall be loaded through plane, concave, and convex bearing blocks. The deflections of the proving ring for the minimum load and for the maximum load applied by dead weights during the calibration shall be determined when the load is applied to the lower boss of the ring through concave and convex bearing blocks. The difference between the average deflections observed using the concave bearing block and the average deflections observed using a plane bearing block for the same loads shall not exceed the maxima specified in paragraphs II-5(a) and II-5(b) of this specification. The differences between the average deflections observed using the convex bearing block and the average deflections observed using a plane bearing block for the same loads shall not exceed the maxima specified in paragraphs II-5(a) and II-5(b) of this specification. The concave and convex bearing blocks shall comply with the following requirements:

(1) They shall be steel.

(2) The Brinell numbers shall be not less than 400 and not more than 600.

(3) The radii of curvature of the spherical surfaces shall be not less than 9 feet and not more than 10 feet.

III. RECALIBRATION

1. CONSTANCY

(a) *Range 1/10 to 2/10-Capacity Load.*—The observed deflection of the ring, for an applied load of not less than one-tenth nor more than two-tenths of the capacity load, shall differ from the average of at least three successive observations for the same applied load by not more than one-half of one percent of the deflection for the applied load.

(b) *Range 2/10 to Capacity Load.*—The observed deflection of the ring, for any applied load not less than two-tenths nor more than the capacity load, shall differ from the average of at least three successive observations for the same applied load by not more than one-tenth of one percent of the deflection for the capacity load.

(c) *Comparison with Last Calibration.*—The observed deflections of the ring during recalibration shall differ from the deflections observed at the time of the last calibration by not more than the maxima specified in paragraphs III-1(a) and III-1(b) of this specification, under the loads there specified.

(d) *Alternative Procedure.*—If the ring fails to comply with the requirements of paragraph III-1(c) of this specification, the deflection-measuring apparatus shall be removed and then replaced. The difference between the deflections observed before and after this is done shall be not greater than the maxima specified in paragraphs III-1(a) and III-1(b) of this specification, under the loads there specified.

IV. METHOD OF CALIBRATION

1. COMPLETE CALIBRATION

The proving ring shall be calibrated in accordance with the requirements given in section II, Complete Calibration:

(a) If the ring has not been calibrated by the National Bureau of Standards since the revision of this specification on April 4, 1934.

(b) If the ring was not certified when last calibrated by the National Bureau of Standards.
(c) If the ring has been repaired or modified since its last calibration by the National Bureau of Standards.

2. RECALIBRATION

Except as provided in paragraphs IV-1(a), IV-1(b), and IV-1(c), Complete Calibration, a ring shall be recalibrated in accordance with the requirements given in section III, Recalibration.

3. LOADS NOT EXCEEDING 110,000 LB

For loads not exceeding 110,000 lb the proving ring shall be calibrated by applying dead weights known to within 0.02 percent.

4. LOADS EXCEEDING 110,000 LB

For loads exceeding 110,000 lb the applied load shall be known to within 0.1 percent.

5. LOADING PROCEDURE

The proving ring shall be calibrated under increasing loads. Compressive loads, except as provided in paragraph II-5(d), shall be applied to the lower boss of the ring through a plane, hardened-steel bearing block and to the upper boss either through a ball or a soft-steel block. Tensile loads shall be applied to the ring through the pulling rods provided with the ring.

6. TEMPERATURE CORRECTION

To compensate for temperature changes which occur during calibration, the deflections of the proving ring shall be corrected for temperature using the formula

$$d_{70} = d_t [1 + K (t - 70)],$$

where

d_{70} = deflection of ring at a temperature of 70° Fahrenheit

d_t = deflection of ring at a temperature of t degrees Fahrenheit

K = temperature coefficient

t = temperature, degrees Fahrenheit, during test.

The coefficient K depends upon the chemical composition of the steel of which the ring is made and its heat treatment. For steels having a total alloying content not exceeding five percent, the value $K = -0.00015$ per degree Fahrenheit is sufficiently accurate. For some other steels, values of K have been found ranging from -0.00011 to -0.00024. When the proving ring is submitted for calibration, the value of K shall be furnished this Bureau by the person submitting the ring or by the manufacturer of the ring.

V. METHOD OF REPORTING RESULTS

1. CERTIFICATES OF CALIBRATION

For a ring which complies with the requirements of this specification, a certificate of calibration will be issued including a calibration graph showing the calibration factor as a function of the ring deflection.

2. REPORTS

For a ring which does not comply with the requirements of this specification, a report will be issued giving the results in the form of a table and stating wherein the ring fails to comply.

WASHINGTON, March 25, 1946.

PREPRINT INSTRUMENT SOCIETY of AMERICA
19th Annual ISA Conference and Exhibit • October 12-15, 1964, New York
Preprint Number 12.3-2-64

UNCERTAINTIES ASSOCIATED WITH PROVING RING CALIBRATION

by Thomas E. Hockersmith
Mechanical Engineer
Harry H. Ku
Mathematical Statistician
National Bureau of Standards
Washington, D. C.

ABSTRACT

A method of error analysis is presented using data obtained from dead-weight calibration of various capacity proving rings. A breakdown of the errors into components by statistical methods and their combination into a final uncertainty statement is discussed in detail. Graphical representations are used in several places to help in the exposition.

Extension of the analysis and method of handling calibration data for multiple proving ring setups is discussed in an effort to show that the same general method of analysis should be adequate.

INTRODUCTION

A proving ring is a compact and dependable force measurement device developed at the National Bureau of Standards by H. L. Whittemore and S. N. Petrenko for the original purpose of calibrating testing machines. A typical proving ring is shown in Figure 1. It consists basically of the following components; an elastic steel ring with diametrically opposed integral loading bosses, a vibrating reed, and a micrometer dial and screw assembly. The reed and micrometer screw assembly are mounted along the diameter concentric with the bosses. When a load is applied to the ring a deflection is measured by turning the micrometer screw until positive contact is made with the vibrating reed. This deflection value is read in terms of the arbitrary scale inscribed in the face of the micrometer dial. For details on the design, use, and calibration of proving rings, see Circular of the National Bureau of Standards C 454 [1]*.

In recent years a significant increase in the use of the proving ring as a secondary transfer standard, in the field of force measurement, has precipitated the need for information dealing with accuracy of the calibration process. The purpose of this paper is to discuss methods of extracting such information from the calibration data and to present the results in a useable form.

UNCERTAINTY

Calibration may be generally thought of as the process of comparing an unknown with a standard and determining the value of the unknown from the accepted value of the standard. The accuracy of the reported values are usually given in terms of bounds to inaccuracy, or limits of uncertainty.

In any calibration process there are three possibilities available in dealing with the uncertainties. These are:

1. Report only the values obtained and make no statement about their uncertainty.
2. Make some statement of the uncertainties affecting the calibration process based on personal judgement and general experience.
3. Through the use of error analysis form an objective estimate of the uncertainties affecting the reported values.

The uncertainty of a measurement process may be characterized by giving (1) the imprecision, and (2) limits to the overall systematic error. Imprecision means the degree of mutual disagreement, characteristic of independent measurements of a single quantity, yielded by repeated applications of the process under specified conditions. The accepted unit for the imprecision of a calibration process is the standard deviation, σ, which provides a measure of how close a particular calibration result in hand is likely to agree with the results that might have been (or might be) obtained by the same calibration process in this (or other) instance(s). The larger the value of σ, the more imprecise the method of measurement, and the greater the disagreement to be anticipated between strictly comparable calibrations.

The systematic error of a calibration process refers to the more or less consistent deviations of the values observed, from the standard, or from the value intended to be measured. If the direction and the magnitude of systematic error were known with sufficient accuracy, a correction could be applied to render the reported values free from bias. Usually only limits of systematic error can be given, e.g., resulting from the uncertainty in the deter-

*The numbers in brackets refer to similarly-numbered references at the end of this paper.

mination of the mass of weights in a dead-weight load calibrating machine. Limits of systematic error are generally based on knowledge and experience with similiar measurements, information available from special studies, and judgement. In calibration the sources of systematic errors are usually studied carefully, and their effect on the final results minimized or eliminated if possible.

The total uncertainty of a calibration process places limits on its probable inaccuracy. It includes both the imprecision and the systematic error. Accuracy requires precision but precision does not necessarily imply accuracy. For example, a calibration process may be highly precise and yet when applied to a standard yield values consistently greater, or consistently less, than the accepted value of the standard.

The present method of reporting proving ring calibration employed by the NBS does not give explicitly a single expression of the overall uncertainty involved, but instead, gives estimates of the imprecision and systematic error from which the total uncertainty can be derived. This practice is in keeping with the recommendations on "Expression on the Uncertainties of Final Results" in Chapter 23 of NBS Handbook 91 [2]. The estimate of imprecision of the calibration process is given by the standard errors of the tabulated load values, which measure the combined performance of the calibration process and the particular ring. Bounds for the systematic errors are given in percent error of applied load for both dead-weight loads, and loads measured by means of a multiple ring setup.

DEAD-WEIGHT CALIBRATION

A dead-weight calibration of a proving ring consists of ten nearly equally spaced loads applied in either the 10,100-lb or the 111,000-lb capacity testing machines presently in use at the National Bureau of Standards.

Three runs of ten loads are taken on each ring to make up a calibration. Before and after each load reading a no-load reading is taken and recorded. The average of the two no-load readings is subtracted from the load reading to yield a deflection value of the ring under that load. This yields a total of thirty deflection values, three values for each load point from ten-percent of capacity to capacity load. These thirty deflections are punched on computer data cards with their corresponding load values and are fed into an electronic digital computer. A second degree equation of the form

$$D = a + bL + c(L)^2$$

is fitted to the averages of the three deflection values for each load, where

D = average deflection value
L = load in pounds

and a, b, c, are coefficients. The computer program performs the task of statistically analyzing the data, fitting the data by the method of least squares, and printing out a load versus deflection table as well as the various statistical quantities included in the report. The thirty deflection values obtained during the calibration of a 100,000-lb capacity proving ring are given in Table 1. A sample of the load versus deflection table printed out as a result of the computer fit of these data is found in Table 2.

The selection of a second degree equation in terms of load was decided upon as a result of preliminary investigation, both theoretical and experimental, to determine the proper degree of the calibration curve to represent the characteristics of the proving ring as evidenced by the raw data. At the same time it was necessary to keep in mind the many problems associated with applying an error analysis to such data.

Figure 2 shows the three deflection values at each of the ten load points for proving ring A, with most of the linear trend removed from the deflection values. The smooth curve represents the plot of the computed deflection values derived from the second degree fit with the same linear trend removed. This figure shows how well the second degree curve fits the observed deflections.

Several interesting and useful comparisons resulting from the error analysis and fitting techniques employed are as follows. From the dispersion of the three deflection values at each load point about their average, the standard deviation of a deflection value can be computed with two degrees of freedom. Since these standard deviations computed over the range of loads are comparable in magnitude, the ten values may be pooled together. This pooled value of the standard deviation, denoted as s_w, can be compared to its long run average value over many previous calibrations to determine if the calibration process is under control, i.e., stable with respect to precision.

A standard deviation s associated with the calibration of this particular ring can be computed from the residuals of the ten average deflection values about the second degree curve. This value of the standard deviation, s, can be compared with the pooled standard deviation of an average deflection value, $s_w/\sqrt{3}$, obtained from the ten sets of triplicate deflection values (i.e., the pooled estimate of the standard deviation of an individual deflection divided by $\sqrt{3}$). If the two standard deviations s and $s_w/\sqrt{3}$ are of

nearly the same magnitude then the ring is in good condition and the scatter of the points is due mainly to the inability of the calibration process as a whole to repeat. Conversely, if the standard deviation s computed from the deviations of the ten average deflection values from the curve is considerably larger than $s_w/\sqrt{3}$, the estimated standard deviation of an average deflection value, then the condition of the ring is not good and reconditioning by the manufacturer is indicated. An example of this can be seen in figure 2. This ring is apparently not in good condition since the broken curve connecting the averages of the three deflection values at each load point does not follow the fitted curve closely. For rings in good condition, the two curves are practically indistinguishable on a graph to this scale. In the future this type of reasoning may be used as a basis for acceptance or rejection of a particular device.

Previously a calibration graph was included with the calibration certificate as shown in figure 3. This graph was a plot of the calibration factor for the ring in pounds per division versus the deflection in divisions. The straight line through the points was drawn for "best fit". Because the calibration factors were computed by dividing each deflection into its corresponding load, the points of the plot near the lower end of the load range, of the device, show considerably more dispersion than the points near the upper end. Therefore the upper points were considered to be better indicators for the drawing of the "best fit" line through the plotted points. In the case of the second degree fit of deflection versus load by the method of least squares, the individual points are treated with equal weight, a more accurate fit of the calibration data is obtained, and no possibility of personal bias is introduced.

The above can be illustrated as the by-products of a simple test designed and suggested by W. J. Youden of NBS. This test consisted of several operators taking readings with a proving ring under various known dead-weight loads. These loads were then computed as if they were unknown using first the table of load values from the second degree fit and second the load values derived from the "best fit" curve. Comparison showed that over the range of the ring, the load values computed from the second degree fit were closer to the actual known loads applied to the ring. Therefore, if the ring is to be used over its entire calibrated range the second degree fit gives more accurate load values. The same data were also used to check the computed limits of uncertainty for the particular ring and in no case did the difference between the actual and computed load value exceed these limits. A sample of the values determined during this experiment can be found in Table 3.

In order to arrive at some measure of dependability of the values given in the load table the corresponding confidence interval is needed. To determine such an interval, the standard error of a deflection value for a given load is computed and some multiple of this value is used as limits of uncertainty on the imprecision.

To predict a deflection value D_i for a particular given load L_i, the deflection value can be expressed as $D_i = a + bL_i + cL_i^2$. Thus D_i is a linear combination of the coefficients estimated, and its standard error s_i can be expressed in terms of the standard deviation s (estimated from the residuals of the fit, with seven degrees of freedom), and the load L_i, and the variance-covariance matrix $[C_{ij}]$ of the estimated coefficients a, b, and c, as follows:

$$s_i^2 = \underline{L}'[C_{ij}]\,\underline{L}\,s^2$$

where the vector $\underline{L}' = (1, L_i, L_i^2)$.
(For details of the method of polynomial fitting used and the calculation of the standard error s_i the reader is referred to sections 6-3 and 6-5 of Chapter 6 of NBS Handbook 91 "Experimental Statistics" [2].)

The dependence of s_i on the value of L_i indicates that D_i values corresponding to L_i values at the two ends of the range of L have larger prediction errors than do D_i values corresponding to L_i in the center portion. For convenience, the largest value of the standard error s_i computed from the above expression is used for all values of L_i in a proving ring report, and for ten equal increments of equally spaced loads L_i, the value of the largest standard error, s_i, is approximately equal to 0.79s. This is converted into load in pounds by multiplying 0.79s by the maximum calibration factor, in pounds per division, for the particular ring.

Using the t statistic and the computed standard error a confidence interval for the deflection value on the curve for a single given load can be calculated. In calibration work, however, we require not merely the calculation of a confidence interval for the deflection value corresponding to a single load, but the calculation of a confidence band for the whole calibration curve. Therefore, a wider interval will be required for the same level of confidence. The confidence band for a line as a whole is discussed on pages 5-15 to 5-17 of reference [2] and for entire curves, in Chapter 28 of [3], where it is shown that in the general case, the half width at $L = L_i$ of the confidence band for the curve as a whole is:

$$\sqrt{k\,F_{.05}(k,\nu)} \times s_i ,$$

where k is the number of coefficients estimated, ν is the number of degrees of freedom in estimating s_i, and F is an appropriate upper percentage point of the distribution of the F statistic (as an illustration we are using the upper 5%

point). Thus for $k = 3$, $\nu = 7$, and ten equal increments of loads the half width of the 95% confidence interval is $\sqrt{3 \times 4.35} \times 0.79s = 2.86s$. (Since the largest value of the computed standard error is used, the confidence level is at least 95%.) Therefore the over-all limits of uncertainty for the calibration by this procedure could be expressed as $2.86 \times s$, (s is the standard deviation given in the report), plus the systematic error.

It may appear that the above procedure for determining the limits of uncertainty in the calibration of a proving ring by basing it on the prediction of a deflection value for a given load is a reverse procedure. However, for the method of calibration described this seemingly reverse procedure is the proper one. Figure 4 is a schematic diagram of the deflection - load curve obtained from a calibration with the corresponding confidence band sketched about it. For any given load, the true deflection value is expected to be situated within the band. Conversely, if a deflection value d is given, a horizontal line parallel to the load axis will intercept the curve at the corresponding load value $\hat{L}$; in addition this line will also intercept the band at two points L_i and L_u which give the corresponding lower and upper confidence limits for the load. This is true provided that the deflection value is known without error. If the uncertainty of the deflection value can be represented by D_i and D_u, then the corresponding confidence interval for the load will be wider, as given by L'_i and L'_u. In other words, the accuracy with which the deflection readings are obtained in using the ring must be taken into account by the user of the ring.

Each load value given in the table of load versus deflection is therefore the predicted value of the load, given a deflection value, and is expected to be within the uncertainty limits given for the calibration.

CALIBRATION OF RINGS USING MULTIPLE RING SETUPS

The present practice for calibrating proving rings with nominal capacities in excess of 110,000 lb is as follows:

1. to divide the nominal capacity into ten approximately equal increments,
2. to calibrate the ring by dead weights for the increments of load less than 110,000 lb, and
3. to calibrate the ring by either a 3, 4, or 5 proving ring setup for the remaining increments of load.

For a calibration using this procedure there are a number of problems relating to the analysis of data and interpretation of results. Some of these problems cannot be solved without considerable changes in the procedure of calibration. Since such changes are impractical, and in the near future dead-weight calibration capacity will be extended to 1,000,000 lb, one solution is to fit multiple ring calibrations by the same method as that for the dead-weight calibrations. The following discussion is based on the results of calibrations of rings fitted by this method.

Examination of these results showed no evidence of bias in the sense that residuals of the fit at the two adjoining increments of load, i.e. the last dead-weight and the first multiple ring load, are not unusually large or consistently of opposite sign. For this to remain true it is necessary that the calibrations of the rings used to determine the load in a multiple ring setup be unbiased. To insure that this condition is maintained the rings owned by the Bureau are usually reconditioned yearly and are calibrated frequently.

For dead-weight calibration the errors of the applied loads were assumed to be negligible in fitting the data; for multiple ring calibration, errors are introduced in the determination of the loads applied. Thus a non-linear functional relationship is to be estimated between deflection and load where the measurements of both are subject to error. There is no simple solution to this problem except that experience in this laboratory has shown that the least square fitting procedure still gives satisfactory estimates provided the errors are small compared with the range covered. This requirement is satisfied since each increment of load is more than 700 times the magnitude of the error involved.

Considering the above, and from a study of numerous past calibrations, it was decided the deflection should be fitted as a function of load since the former is believed to have larger errors than the latter.

Since the dead-weight calibration is presumably more precise than the multiple ring calibration, the question of weighting the observations prior to least square fitting was considered. Results of the rings studied indicated that the standard deviation of an average deflection obtained from multiple ring calibrations was not significantly larger than that for the dead weights. Thus the inflation of this deviation due to the errors in the loads does not increase the total imprecision by any appreciable amount. The use of weighting factors is therefore not of practical importance.

Examination of the plot of residuals resulting from fitting deflections to the loads, both in dead weights and in multiple ring setups, indicates that the deviations of the data points

from the fitted curve contribute a large part of the total error. In view of this it appears reasonable that the averages of the deflection readings should be used for fitting, similar to the procedure used for dead-weight calibration. Thus, the standard error includes the imprecision components of the calibration error for both the ring being calibrated and the rings being used to measure the applied load.

Bounds for systematic error of a multiple ring setup can be estimated by summing (1) the systematic error due to the dead weights (2) the systematic difference due to change with time in the calibrated values of the load measuring devices, and (3) other sources of error due to the inherent difficulties in using and reading the devices simultaneously. For example, such an estimate can be given an percent error of applied load for loads in excess of the dead weights.

CONCLUSION

In the above we have presented a procedure for the determination of limits of uncertainty for the calibration of proving rings. The method of analysis includes; the fitting of this type of data to an appropriate curve by the method of least squares, the use of confidence intervals and bands as limits of imprecision, and the estimate of bounds for systematic error.

Since many types of devices and instruments are calibrated similiarly at selected points along their ranges, it is believed that the procedures outlined above may be useful, when properly modified, in yielding a realistic evaluation of the uncertainties associated with their calibration.

ACKNOWLEDGMENT

Acknowledgment is made to Churchill Eisenhart of the National Bureau of Standards for the many helpful discussions and suggestions.

REFERENCES

(1) B. L. Wilson, D. R. Tate, and G. Borkowski, "Proving Rings for Calibrating Testing Machines", NBS Circular C 454, U. S. Government Printing Office, Washington 25, D. C.
(2) M. G. Natrella, "Experimental Statistics," NBS Handbook 91, U. S. Government Printing Office, Washington 25, D. C.
(3) M. G. Kendall and Alan Stuart, Advanced Theories of Statistics, Hafner Publishing Co., New York, 1961.

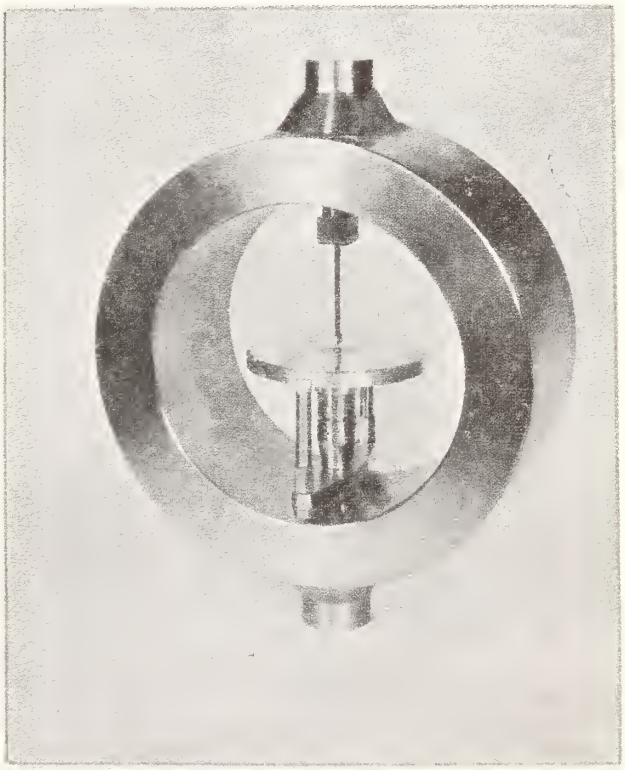

Figure 1 Proving Ring

Table 1 A Calibration of Proving Ring A

Applied load lb	Deflection Run 1 div	Run 2 div	Run 3 div
10,000	68.32	68.35	68.30
20,000	136.78	136.68	136.80
30,000	204.98	205.02	204.98
40,000	273.85	273.85	273.80
50,000	342.70	342.63	342.63
60,000	411.30	411.35	411.28
70,000	480.65	480.60	480.63
80,000	549.85	549.85	549.83
90,000	619.00	619.02	619.10
100,000	688.70	688.62	688.58

Table 2 - Computed Load Table in lb for 70 Degrees F for Proving Ring A

Deflection Div	0	1	2	3	4	5	6	7	8	9
60.	-	-	-	-	-	-	-	-	9952.	10099.
70.	10245.	10392.	10538.	10685.	10831.	10978.	11124.	11270.	11417.	11564.
80.	11710.	11856.	12003.	12149.	12295.	12442.	12588.	12735.	12881.	13027.
90.	13174.	13320.	13467.	13613.	13759.	13906.	14052.	14199.	14345.	14491.
100.	14638.	14784.	14930.	15077.	15223.	15369.	15516.	15662.	15808.	15954.
-	-	-	-	-	-	-	-	-	-	-
-	-	-	-	-	-	-	-	-	-	-
-	-	-	-	-	-	-	-	-	-	-
-	-	-	-	-	-	-	-	-	-	-
-	-	-	-	-	-	-	-	-	-	-
640.	93007.	93151.	93295.	93439.	93582.	93727.	93871.	94014.	94158.	94302.
650.	94446.	94590.	94734.	94878.	95021.	95165.	95309.	95453.	95597.	95741.
660.	95885.	96029.	96173.	96316.	96460.	96604.	96748.	96892.	97035.	97179.
670.	97323.	97467.	97611.	97754.	97898.	98042.	98186.	98330.	98473.	98617.
680.	98761.	98905.	99048.	99192.	99336.	99480.	99623.	99767.	99911.	100054.

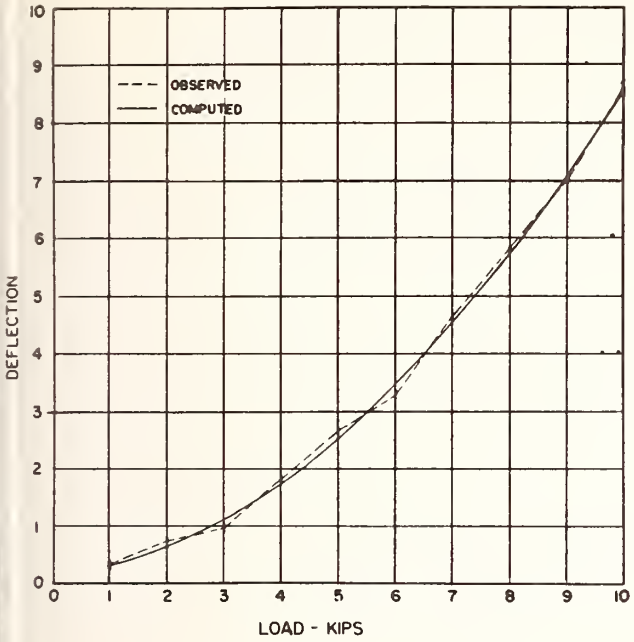

Figure 2 Observed and Fitted Calibration Curves for Proving Ring A

Note: Deflection = Deflection value minus 68.00 x (the number of the load increment)

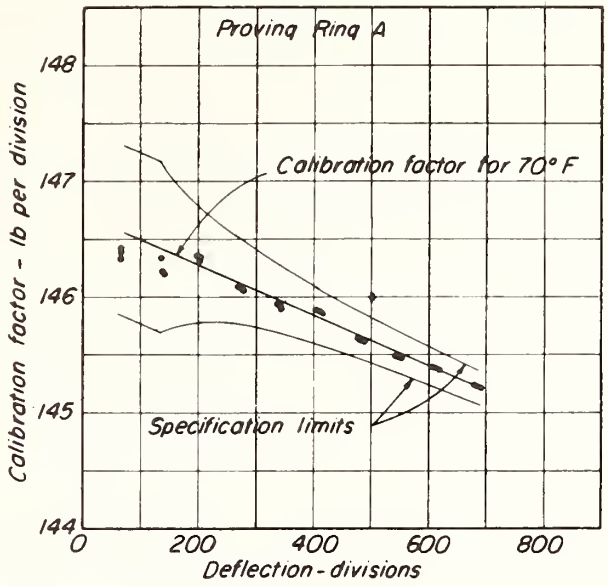

Figure 3 Calibration Graph for Proving Ring A

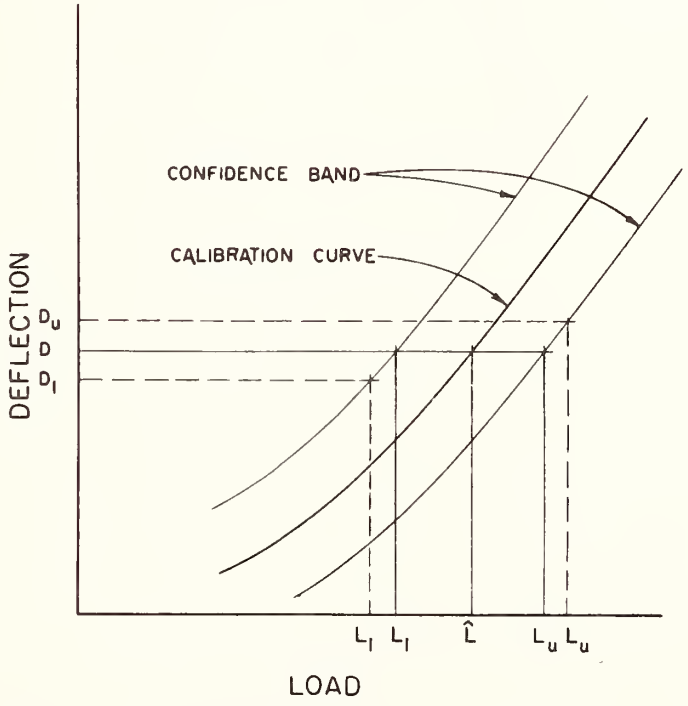

Figure 4 Determination of Confidence Limits for a Load given a Deflection Value

Table 3 - Sample Results of Experiment Designed by W. J. Youden of NBS for Proving Ring A

A	B		C		
Load applied to ring	Computed load using second degree fitting method	Column A minus Column B	Computed load using "best fit" method	Column A minus Column C	Ring reader
lb	lb	lb	lb	lb	
10,070	10,077	- 7	10,090	-20	1
30,000	29,987	+13	29,994	+ 6	1
40,050	40,059	- 9	40,064	-14	1
80,020	80,032	-12	80,036	-16	1
10,020	10,033	-13	10,046	-26	2
30,050	30,047	+ 3	30,053	- 3	2
40,000	40,011	-11	40,016	-16	2
80,070	80,081	-11	80,082	-12	2
10,000	9,993	+ 7	10,007	- 7	3
30,070	30,063	+ 7	30,069	+ 1	3
40,020	40,029	- 9	40,034	-14	3
80,050	80,061	-11	80,062	-12	3
10,050	10,058	- 8	10,068	-18	4
30,020	30,010	+10	30,013	+ 7	4
40,070	40,087	-17	40,096	-26	4
80,000	80,025	-25	80,030	-30	4

4. Gravity

JOURNAL OF RESEARCH of the National Bureau of Standards—C. Engineering and Instrumentation
Vol. 70C, No. 2, April–June 1966

Absolute Value of g at the National Bureau of Standards

D. R. Tate

Institute for Basic Standards, National Bureau of Standards, Washington, D.C.

(April 6, 1966)

A determination of the absolute value of the acceleration due to gravity has been completed at the National Bureau of Standards near Gaithersburg, Maryland. The value, reduced to a gravity meter station on the floor of the site is 9.801018 m/s² with a standard deviation of 0.3×10^{-5} m/s². The absolute value, which is 13.2×10^{-5} m/s² (13.2 milligals) less than the corresponding Potsdam value, is in general agreement with other recent absolute determinations.

Key words: Absolute gravity, acceleration, free-fall, g, geodesy, gravity, Potsdam system.

The National Bureau of Standards has recently completed a determination of the acceleration due to gravity at its new facility near Gaithersburg, Md. The measurements were made in the Engineering Mechanics Building during the months of April, May, and June of 1965.

The determination was derived from observations of the increase in speed of a one-meter fused silica tube falling freely within a vacuum chamber which was itself falling with approximately the acceleration due to gravity. The measurements included data from four different fused silica tubes yielding a total of 36 sets of observations. Each set was normally composed of 16 independent free-fall observations. There were no statistically significant differences among the results for the four tubes, the observed variations being well within that expected on the basis of the standard deviation of 1.4×10^{-5} m/s² found for individual sets of observations.

The determination was made in Room 129 of Building 202 at the National Bureau of Standards. The site is illustrated in figure 1, taken from the 1965 report of D. A. Rice of the U.S. Coast and Geodetic Survey to Special Study Group No. 5 of the International Association of Geodesy, for their compilation of excenters [1] for World First Order Gravity Stations. The absolute determination was made 30 cm east and 26.3 cm above the point marked NBS–1. The absolute value was reduced to the reference point NBS–2 on the floor of the room by gravity meter connections made by the U.S. Coast and Geodetic Survey during October 1965. These connections are included in the report to Special Study Group No. 5.[2]

The determination resulted in an absolute value of gravity for NBS–2 of:

$$g = 9.801018 \text{ meters/second}^2.$$

The standard deviation of this value based on statistical variation but not including systematic error was less than 0.3×10^{-5} m/s.²

The point NBS–2 has a value of 9.801150 m/s² obtained by gravity meter connections based on a Potsdam value of 9.80118 m/s² for the national gravity base in the Department of Commerce Building in Washington, D.C. The absolute value is therefore 13.2×10^{-5} m/s² (13.2 milligals) less than the Potsdam value for NBS–2.

A complete description of the experimental procedure will be given in a forthcoming publication.

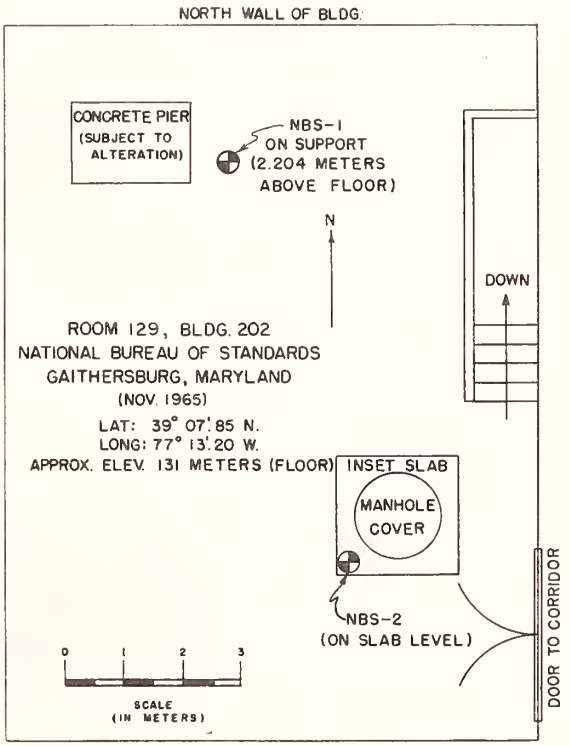

FIGURE 1. *Gravity stations at the National Bureau of Standards.*

[1] Excenters are gravity stations located in the vicinity of a primary station and connected to it by accurate gravity measurements. A connection to an excenter is equivalent in accuracy to a connection to the primary station.

[2] These data are available from the files of the U.S. Coast and Geodetic Survey.

(Paper 70C2–225)

UNITED STATES DEPARTMENT OF COMMERCE
Maurice H. Stans, Secretary
NATIONAL BUREAU OF STANDARDS • A. V. Astin, Director

TECHNICAL NOTE 491

ISSUED AUGUST 1969
Nat. Bur. Stand. (U.S.), Tech. Note 491, 10 pages (Aug. 1969)
CODEN: NBTNA

Gravity Measurements and the Standards Laboratory

D. R. Tate

Mechanics Division
Institute for Basic Standards
National Bureau of Standards
Washington, D.C. 20234

For sale by the Superintendent of Documents, Government Printing Office
Washington, D.C., 20402 - Price 25 cents

Contents

Gravity Measurements and the Standards Laboratory

D. R. Tate

The local value of the acceleration due to gravity is a fundamental datum for almost every standards laboratory as it, together with accurate standards of mass, is the basis for the standards involving force. Instruments used as standards in this area include precise deadweight piston gages, deadweight calibrators for force transducers, liquid manometers, and earth field accelerometer calibrators. The practical realization of the absolute ampere and the absolute volt require a knowledge of force. This paper presents the basic information about how gravity measurements are made and outlines procedures for obtaining a suitable value for a given location. It also gives a brief discussion of the background and meaning of the term "standard gravity", and its application in the computation of forces in units of the pound-force and the kilogram-force.

Key words: Absolute gravity, deadweight, force, geodetic pendulum, gravity, gravity meter, Potsdam system, standard gravity, units of force.

1. Introduction

The local value of the acceleration due to gravity is a matter of considerable importance to almost every standards laboratory as it, together with accurate standards of mass, is the basis of all force measurements. Instruments for the measurement of acceleration, accelerometers, have also reached a stage where, for earth field calibrations, the acceleration due to gravity must be known quite accurately. It is the purpose of this paper to present the basic information about how gravity measurements are made and to outline the procedures for obtaining a suitable value for a given location.

2. Gravity Networks

Gravity measurements have been made by geodesists for many years and a well developed science, with instrumentation and technique, has grown up in the field. Primarily the interest of the geodesist is to gain a better knowledge of the shape and structure of the earth, and the work that has been done has resulted in a network of gravity values

covering the greater portion of the habitable parts of the world. This network, with its excellent coverage in Europe and the Americas, affords a ready-made basis for obtaining satisfactory values in most laboratories.

It is helpful to understand the methods by which gravity networks have been established. The direct measurement of the acceleration due to gravity through the observation of time and distance is a difficult undertaking and not well adapted to survey methods. Consequently the principle has been to establish an absolute value at some one point and to make the survey measurements with instruments that measure the difference in gravity between two points, starting at the absolute site and moving out in the closed-loop technique commonly employed in other types of surveys. The network values in existence today are derived from an absolute measurement made in Potsdam, Germany.

3. Absolute Measurements

Absolute determinations of the acceleration due to gravity, in addition to being difficult and time consuming, have in the past been subject to serious systematic errors which were large when compared to the accuracy of differential measurements made with survey type instruments. Consequently it has been desirable to make additional absolute measurements at various points in the world network, even though only one such determination is theoretically necessary. Up to quite recently, absolute measurements were restricted by practical considerations to locations in the national standards laboratories of some of the larger nations.

The classic absolute measurement was made at Potsdam by Kühnen and Furtwängler and published in 1906[1]*. It was made by the use of reversible pendulums of the Kater type and resulted in a value of 9.81274 m/s^2 for that station. Subsequent absolute determinations made in Washington by Heyl and Cook[2] and at Teddington, England by Clark[3], gave values 15 to 20 parts per million less than the Potsdam result after consideration of the gravity differences between the sites. In recent times absolute measurements have been made from observations on freely falling objects in vacuum by several workers[4,5,6,7,8,9]. A discussion of absolute determinations is given by A. H. Cook[10].

The conclusion has been reached that the original Potsdam value is in error by about 14 parts per million, and in October of 1968 the International Committee on Weights and Measures adopted a resolution that, for the needs of metrology, the value at Potsdam should be regarded as 9.81260 m/s^2.

---

*Figures in brackets refer to references at the end of this paper.

Currently the development of stabilized gas laser systems has made it possible to make absolute determinations in which the falling object is one reflector of a Michelson interferometer. This technique improves the accuracy over the older methods by about an order of magnitude. Measurements by this method are under way by Faller[11] and Sakuma[12]. Faller's apparatus is sufficiently portable that it can be transported from one laboratory to another and it is expected to prove most useful in giving precise values for a number of points in the pattern of the world gravity network.

4. Survey Measurements

As indicated previously, the values of gravity at most points of interest are determined from the cumulated differences between a series of stations starting at a point where the absolute value is known or assumed. Usually, values for well known intermediate points have been established through a number of redundant measurements made over a period of years. An interesting example of this is the well established gravity tie made between Potsdam and Bad Harzburg. Since Potsdam lies in East Germany, it was not accessable to geodesists from nations outside of the Soviet Bloc for many years and Bad Harzburg in Western Germany became the reference point for the western nations.

Instruments used for gravity surveys fall into two basic categories. Originally, all such measurements were made with instruments of the pendulum type, known as geodetic pendulums. These pendulums have, in essence, an unknown but constant length, and the difference in gravity between two stations is deduced from the changes in period of the pendulum when it is swung at the two sites. Successful measurements with pendulums of this type require highly developed techniques, painstaking care, and considerable time for each determination[13].

In more recent years, a different type of instrument has been used for gravity survey work. These instruments, known as gravity meters, operate on the principle that a mass suspended by a spring will change its equilibrium position with changes in gravity. Since gravity differences are small, such instruments are examples of ingenious design[14] and construction. Usually the mass is attached to an arm pivoted at the other end with the torque due to the mass being opposed by a non-linear spring and moment arm arrangement. The arrangement is usually such that the system is very near to unstable equilibrium so that a small change in the force on the mass tends to produce a large displacement of the arm. The actual motion is limited by stops and the arm is brought back to its initial position by a fine spring actuated by a micrometer screw adjustment. These instruments must be calibrated by measuring gravity differences between points having known differences, such as stations with geodetic pendulum gravity values.

5. Local Values of Gravity

The principal agency of the United States Government for the determination of gravity values is the Coast and Geodetic Survey, a part of the Environmental Science Services Administration of the U. S. Department of Commerce. The Coast and Geodetic Survey has on file values of gravity measured in many parts of the country and new measurements are constantly being added to the list.

In cases where a standards laboratory is working at an exceptionally high level of accuracy, it may be desirable to have a direct gravity tie made by means of a gravity meter from the nearest network site to the point of interest in the laboratory. For many laboratories, a value of ample accuracy can be obtained by computation from the nearest established network station. The Coast and Geodetic Survey can provide assistance with such a computation if they are given the latitude, longitude, and elevation of the laboratory point where the value is needed. The latitude and longitude should be furnished to the nearest 0.1 minute of arc, and the elevation above sea level within about five feet. At most locations of standards laboratories, this type of information will enable the computation of gravity with a standard error not exceeding $\pm$ 0.00004 m/s^2. Values furnished by the Coast and Geodetic Survey are accompanied by an estimate of standard error.

In general, repeat gravity measurements for a particular location are unnecessary. Diurnal variations, following the luni-solar tidal cycle, do not exceed ± 0.000003 m/s^2, and secular changes of the order of 0.00001 m/s^2 have not been confirmed since the advent of precise gravity measurements.

6. Standard Gravity

The term "standard gravity" is so widely encountered and so much misunderstood that some explanation is desirable. Standard gravity bears no relationship to any system of gravity measurements, absolute or otherwise. It is simply an acceleration that has been adopted by agreement among the nations of the world as the definition of the engineering units of force. These units of force, taken as the weight of a unit mass, were objectionable in their original form because they varied with the location of the mass on the surface of the earth. By common consent it was agreed that such a definition must be tied to some specific location on the globe, and a value at 45 degrees latitude and sea level seemed a reasonable compromise. Any other location would have been equally valid providing everyone agreed to it. In 1901, five years before the publication of the Potsdam absolute determination, the International Conference on Weights and Measures adopted a value of 9.80665 m/s^2 as the definitive value[15]. This value had been obtained by reducing an absolute measurement made at the International Bureau of Weights and Measures by Monsieur Defforges to 45 degrees and sea level. Later it was pointed out that, because of the existence of

gravitational anomalies, there was no unique value for that latitude and elevation. In 1913, the International Conference reviewed the situation and reaffirmed that the conventional value should be represented by the number 9.80665 m/s^2. In essence, this meant that the definition of the practical units of force was not to be based on the weight at 45 degrees and sea level, but on the arbitrarily adopted acceleration value.

It may be seen from this that the value of 9.80665 m/s^2 is an arbitrary value of acceleration and not the value of gravity at a specific location. It is not expected that this value will be changed in the future.

7. The Computation of Forces

In the standards laboratory it is frequently necessary to calculate the force exerted by a given mass in air as, for example, in the operation of a deadweight piston gage pressure standard. The force, F, is calculated from the relationship

$$F = Kmg\left(1 - \frac{\alpha}{\rho}\right)$$

where m is the mass, g is the local value of the acceleration due to gravity, α is the density of air, and ρ is the density of the mass. If m is given in terms of "apparent mass versus brass standards in normal air", α should be assigned the value 1.2 kg/m^3, the adopted value for the density of normal air, and ρ should be assigned the value 8400 kg/m^3, the adopted value for the density of brass.

The quantity K is a numerical factor, the value of which depends upon the units of F, m, and g. In the SI system of units,

$K = 1$, for F in newtons, m in kilograms, and g in meters per second squared.

Other relationships are as follows:

$K = 1$, for F in dynes, m in grams, and g in centimeters per second squared,

$K = 1$, for F in poundals, m in pounds mass, and g in feet per second squared,

$K = 1/32.17405$ for F in pounds force, m in pounds mass, and g in feet per second squared,

K = 1/980.665 for F in pounds force, m in pounds mass, and g in centimeters per second squared,

K = 1/9.80665 for F in kilograms force (kiloponds), m in kilograms mass, and g in meters per second squared.

8. Summary

Most laboratories that carry out calibration functions involving force measurements, such as various forms of pressure measuring instruments, force transducers, and certain types of accelerometer calibrations using the earth's field as a reference, need a suitable value of gravity established within the laboratory. The value need not be determined by actual gravity measurement except in exceptional cases. A value within 0.0001 m/s^2 (10 milligals) gives force values within one part in 100,000 which is adequate for most purposes. For most locations of standards laboratories, a value well within this limit can be obtained from the Coast and Geodetic Survey. In any case, it is advisable to write to them to ascertain if it is available.

The term "standard gravity", e.g. 9.80665 m/s^2, is in reality an arbitrarily defined acceleration adopted to define units such as the pound-force and kilogram-force. It is not the value of gravity at any specific location and is not affected by any corrections to the Potsdam system.

9. References

1. F. Kühnen and P. Furtwängler, Bestimmnung der absoluten Grösze der Schwerkraft zu Potsdam (Veröffentlichung des K. Preuszichen geodatischen Institutes, N. F. no. 27) Berlin: P. Stankiewicz 1906.

2. P. R. Heyl and G. S. Cook, The value of gravity at Washington, J. Res. NBS 17, 805-39(1936)RP946.

3. J. S. Clark, An absolute determination of the acceleration due to gravity, Phil. Trans. Roy. Soc. London, Ser. A., 238, 65-123(1939).

4. P. N. Agaletskii and K. N. Egorov, Rezul' taty absoliutnykh opredelenii uskoreniia sily tiazhesti v punkte VNIIM (Leningrad), Izmeritel Tekhn., Vol for 1956, no. 6, 29-34.

5. A. I. Martsiniak, Opredelenie absoliutnoi velichiny uskoreniia sily tiazhesti po padeniiu zhezla v vakuume, Izmeritel Tekhn. Vol for 1956, no. 5, 11-15.

6. H. Preston, Thomas and others, An absolute measurement of the acceleration due to gravity at Ottawa, Can. J. Phys 38, 824-52 (1960).

7. A Thulin, Une détermination absolue de g au pavillon de Breteuil, par la methode de la chute d'une règle divisée, Ann. Géophys, 16, 105-27 (1969).

8. A. H. Cook, A new absolute determination of the acceleration due to gravity at the National Physical Laboratory, England, Phil. Trans. Roy. Soc. London, Ser. A., 261, 211-252 (1967).

9. D. R. Tate, Acceleration due to gravity at the National Bureau of Standards, J. Res. NBS, 72C (Engineering and Instrumentation) No. 1, 1-20 (1968).

10. A. H. Cook, The absolute determination of the acceleration due to gravity, Metrologia, 1, no. 3, 84-114 (July 1965).

11. J. A. Hammond and J. E. Faller, Laser interferometer system for the determination of the acceleration of gravity, IEEE J. Quantum Electronics, QE-3, no. 11, 597-602 (1967).

12. A. Sakuma, Etat actuel de la nouvelle determination absolue de la pesanteur au Bureau International des Poids et Mesures, International Association of Geodesy, Bulletin Géodésique, n.s., no. 69, 249-260 (1 Sept. 1963).

13. C. H. Swick, Pendulum gravity measurements and isostatic reductions, Coast and Geodetic Survey Special Publication No. 232 (1942).

14. Gravitation, Encyclopaedia Britannica, 1959 edition, 10, 663-682.

15. Comité International des Poids et Mesures, Comptes rendus de la troisième conférence générale des poids et mesures, Quatrième Séance, 66-70, (22 Octobre 1901).

16. Comité International des Poids et Mesures, Comptes rendus de la cinquième conférence générale des poids et mesures, Troisième Séance, 42-44, (14 Octobre 1913).

5. Humidity

5. Humidity—Continued

UNITED STATES DEPARTMENT OF COMMERCE • Charles Sawyer, *Secretary*
NATIONAL BUREAU OF STANDARDS • E. U. Condon, *Director*

Methods of Measuring Humidity and Testing Hygrometers

Arnold Wexler and W. G. Brombacher

National Bureau of Standards Circular 512

Issued September 28, 1951

261-1

Contents

Methods of Measuring Humidity and Testing Hygrometers

A Review and Bibliography

Arnold Wexler and W. G. Brombacher

This paper is a review of methods for the measurement of the water-vapor content of air and other gases and for the production and control of atmospheres of known humidity for hygrometer testing and calibration and for general research. Among the hygrometric techniques discussed are psychrometry, mechanical hygrometry, dewpoint measurement, electric hygrometry, gravimetric hygrometry, thermal conductivity, index of refraction, pressure and volume measurements, and dielectric constant. Descriptions are given of suitable equipment for establishing desired humidities over a wide range of temperature. A list of 157 selected references pertaining to hygrometry is included.

1. Introduction

The conditions under which the relative or absolute humidity of gases are measured, recorded, or controlled vary greatly, and as a result, many methods of humidity measurement have been developed or proposed. However, for some applications there is at present no satisfactory method available for such measurements, and the available information on methods and instruments for measuring humidity is quite scattered. This Circular, with the appended references, is intended to answer inquiries on humidity measurement in a more comprehensive manner than may be done by correspondence.

Knowledge of the moisture content of solid materials, particularly paper, wood, and grain, is often required during some stage of processing or storage. The equipment, known as moisture meters, used for this purpose is not discussed in this Circular.

In many cases a substantial gaseous equilibrium exists between the solid and the surrounding atmosphere. A satisfactory determination of the moisture content of the solid can be made by the relatively easy measurement of the humidity of the atmosphere, once the relation between the two has been established. The same is true, of course, for liquids of definite composition, except that the water content may vary.

2. Definitions

Relative humidity is the ratio, usually expressed in percent, of the pressure of water vapor in the gas to saturation pressure of water vapor at the temperature of the gas. In engineering, relative humidity is sometimes defined as the ratio of the weights per unit volume of the water vapor in the gas mixture and the saturated vapor at the temperature of the gas mixture. The two definitions are equivalent for all practical purposes.

Absolute humidity of a gas mixture may be defined as the pressure of water vapor, or as the weight per unit volume of water vapor.

Specific humidity, a term of use in air conditioning, is the weight of water vapor in air per unit weight of the dry air.

Dewpoint is the temperature to which water vapor must be reduced in order to obtain a relative humidity of 100 percent that is, to obtain saturation vapor pressure.

Instruments from which the relative humidity is determined are called either psychrometers or hygrometers. Generally, the dry- and wet-bulb instrument (described later) is called a psychrometer, and direct indicators of relative humidity are called hygrometers.

Hygrographs are recorders of relative humidity.

3. Classification of Instruments

Humidity-measuring instruments and methods may be divided into the following classes for convenience. No exhaustive search of the literature was made to insure a complete listing of all proposed instruments, so that it is anticipated that some omissions exist.

Dry- and wet-bulb. Measurements depending on the change in temperature due to rate of evaporation from wet surfaces, an example of which is the dry- and wet-bulb or sling psychrometer.

Mechanical hygrometers. Measurement of a change in a dimension of an absorbing material, such as human hair or goldbeater's skin.

Dewpoint indicators and recorders. Instruments which indicate or record the temperature at which dew from the gas (air and water vapor) mixture under test will just form. A common type employs a mirror for observing the formation of the dew.

Electrical hygrometer. Measurement of the electrical resistance of a film of moisture absorbing material exposed to the gas under test.

Gravimetric hygrometer. Measurement of weight of moisture absorbed by a moisture absorbing material.

(a) Increase in weight of a drying agent as gas with a constant moisture content is passed through it.

(b) Change in weight of an absorbing material with change in moisture content of the gas under test.

Thermal conductivity method. Measurement of the variation in thermal conductivity of a gas sample with water vapor.

Spectroscopic method. Measurement of the change in intensity of selected absorbing spectral lines with change in humidity of the gas under test.

Index of refraction. Measurement of change in index of refraction of a moisture absorbing liquid with change in ambient humidity.

Pressure or volume. Measurement of the pressure or volume of the water vapor in a gas sample.

Thermal rise. Measurement of the temperature rise of a material exposed to water vapor.

Mobility of ions. Measurement of the change in mobility of ions due to the presence of water vapor.

Dielectric constant. Measurement of the dielectric constant of a gas with change in water-vapor content.

Critical flow. Measurement of the variation of pressure drop across two combinations of nozzles, operating at critical flow, with a desiccant between one pair of nozzles.

Diffusion hygrometer. Measurement of effects due to diffusion of gases with and without water vapor.

Chemical methods. Procedures involving chemical reactions or phenomena.

For sources of supply for the instruments indicated as commercially available, consult *Thomas Register of American Manufacturers* or *The Instruments Index.*

4. Description of Instruments

4.1. Dry- and Wet-Bulb Psychrometer

The psychrometric method of determining humidity is of importance in the fields of meteorology, air conditioning, refrigeration, and the drying of foods, lumber, etc. Its basic simplicity and fundamental calibration have made it the dominant means for measuring the moisture content of air. The elemental form of the psychrometer comprises two thermometers. The bulb of one thermometer is covered with a moistened cotton or linen wick and is called the wet-bulb, whereas the bulb of the other thermometer is left bare and is referred to as the dry-bulb. The evaporation of water from the moistened wick of the wet-bulb thermometer produces a lowering in temperature and from the readings of the two thermometers and the air or gas pressure, the humidity, absolute or relative, may be determined. It is current standard practice to ventilate the thermometers by slinging, whirling, or forced-air circulation.

To obtain the relative or absolute humidity, the relation between the wet- and dry-bulb readings and the actual pressure of the water vapor must be known. This correlation was obtained by Ferrel (26)[1] in 1886, based on the data of Marvin and Hazen, who made numerous observations of wet- and dry-bulb readings with sling and whirled psychrometers and simultaneous determinations of dewpoints with Regnault and Alluard dewpoint apparatus. Ferrel, after reducing these data, fitted them into the expression

$$e = e' - AP(t - t')$$

where, in metric units,

$A = 6.60 \times 10^{-4}\ (1 + 0.00115t')$

e = partial pressure of water vapor in mm Hg at the dry-bulb temperature t°C

e' = saturation pressure of water vapor in mm Hg at the wet-bulb temperature t'°C

P = total pressure (which, in the case of meteorological observations, is atmospheric pressure) in mm Hg

[1] Figures in parentheses indicate the literature references at the end of this paper.

and where, in English units,

$A = 3.67 \times 10^{-4} [1 + 0.00064 (t' - 32)]$

e = partial pressure of water vapor in in. Hg at the dry-bulb temperature t°F

e' = saturation pressure of water vapor in in. Hg at the wet-bulb temperature t'°F

P = total pressure in in. Hg.

Starting from fundamental concepts, several theories have been developed that attempt to explain the phenomena that occur at the wet-bulb and which, at the same time, yield expressions of the form used by Ferrel. The first equations for use in psychrometry were developed by Ivory (21) in 1822 and extended by August (22) in 1825 and Apjohn (23) in 1837. The so-called convection theory is the result of their work. In 1911, Carrier (28, 42) and in 1922, Lewis (40) reestablished the basis of this theory and renamed it the adiabatic saturation theory. This theory, which depends on a heat balance at the wet-bulb, found wide acceptance in the air-conditioning and refrigerating industries and has been used extensively in the construction of phychrometric charts. The agreement between theory and experimental data was investigated by Carrier (28) and Dropkin (87). Their results indicate that for most work of engineering accuracy, the adiabatic saturation theory is adequate for predicting the vapor pressure of water vapor from wet- and dry-bulb readings. Maxwell (11) in 1877 deduced an equation based on the diffusion of heat and vapor through a surface gas film on the wet-bulb. In recent years, further work has been done experimentally (71) and theoretically (73) on psychometric theory, and in reviewing the subject (93).

As the psychrometric formula gives the partial pressure of the water vapor of the gas under test, a computation is necessary to convert to humidity in other terms. The relative humidity, for example, is obtained from the equation

$$RH = \frac{e}{e_s} \times 100,$$

where

e = the partial pressure of water vapor as determined by the psychrometric formula

e_s = the saturation pressure of water vapor at the dry-bulb temperature

RH = the relative humidity, in percent.

In practice, calculations directly involving the use of the psychrometric formula are rarely made. The customary procedure is to employ tables (1, 4, 5, 7, 13, 14, 15, 16, 18, 44, 67, 81, and 96) or charts or curves (1, 9, 18, 77, 82, 100, 107, 115) that conveniently and rapidly yield the relative humidity, vapor pressure, or dewpoint from the dry- and wet-bulb thermometer readings and the air pressure.

The sling psychrometer (1, 8, 12, 15, 60), using two mercury thermometers, is the common form of this instrument. It is relied upon principally by meteorologists and is widely used by other scientists and by engineers for measuring relative humidity. Ventilation is obtained by swinging the thermometers to produce a minimum air velocity of 900 ft/min at sea level (higher at altitude). It is supplied by firms manufacturing meteorological instruments and by many laboratory apparatus supply houses. Stationary thermometers, with ventilation produced by a motor-driven fan or blower integral with the instrument, are known as Assmann or aspiration psychrometers (1, 8, 12, 60). These are also commercially available from a smaller number of firms. Unventilated psychrometers are unreliable and hence rarely used.

In addition to the mercury-in-glass thermometer, other temperature measuring devices may be adapted for psychrometric use. Resistance thermometers (47, 64, 70) thermocouples (68, 69, 72, 89, 90, 108), and bimetal thermometers (148) can be used for both indicating, recording, and control. Thermocouples are of special interest where low lag is important, where there is little or no ventilation (72, 89, 90) or where very low relative humidities (91) are to be measured.

Instead of direct temperature measurements, the temperature of the thermometers may be equalized (140). In this method the temperature of the wet-bulb is raised to that of the dry-bulb and the heat measured which is required to maintain equilibrium. This is accomplished by winding a manganin wire heater around the wet-bulb and under the wick and measuring the current when the wet- and dry-bulb thermometers read alike. A convenient arrangement utilizes a differential thermocouple psychrometer whose output is read on a galvanometer. The current to the wet-bulb heater is adjusted until the galvanometer no longer deflects.

The psychrometric method often may be applied in specialized or unconventional conditions. At temperatures below freezing, the psychrometer continues to function, but the magnitude of the depression is greatly reduced and proper precautions must be taken to obtain reliable data (121). At elevated temperatures or low relative humidities, special instruments (56), tables (67) and techniques (74) must be used. Most tables and charts are designed for use at atmospheric pressures. When low or high pressures are encountered, either special tables (15, 44) or charts (82) must be used or the relative humidity must be computed.

Where the moisture content of gases other than air is to be determined, the psychrometric constant A must be modified, to account for the physical properties of the particular gas. Values of A for several mono-, di- and triatomic gases are given by Brauckhoff (143).

Among the factors influencing the performance and accuracy of the psychrometric method are (a) the sensitivity, accuracy and agreement in reading of the thermometers, (b) the speed of air past the

wet-bulb thermometer, (c) radiation, (d), the size, shape, material and wetting of the wick, (e) the relative position of the dry- and wet-bulb thermometers, and (f) the temperature and purity of the water used to wet the wick. A discussion of these factors will be found in (1, 8, 12, 15, 35, 37, 46, 60, 74, 78, 90, 98, 121, 151).

The thermometers used in psychrometry should be high-grade matched instruments, else appreciable error may be introduced. While a calibration of the thermometers is desirable, an intercomparison at several temperatures to determine whether they read alike usually suffices. In addition, when high accuracy is desired and low relative humidities are measured, corrections for the emergent stem of the wet-bulb thermometer should be applied.

Thermometer errors may combine in several ways to influence the accuracy of the relative humidity. Thus either the dry-bulb thermometer or the wet-bulb thermometer or both may be in error. The magnitude of the error in relative humidity will depend not only on the magnitude of the thermometer errors, but also on their particular combination, since both the dry-bulb temperature and the wet-bulb depression are required for a determination. Occasionally, in psychrometric work, instead of measuring both the dry- and wet-bulb temperatures separately, the dry-bulb temperature and the wet-bulb depression are measured, from which the wet-bulb temperature can be computed for use in entering commonly available tables. The latter is obtained by measuring the temperature difference with, say, a differential thermocouple, one end of which is maintained dry and the other wet. Here the errors may occur either in the dry-bulb measurement or in the depression measurement or in both. Errors in the depression, however, may be considered as equivalent to errors in the wet-bulb reading, so that essentially the combinations of errors are the same as those first listed.

In order to obtain an estimate of the errors in relative humidity arising from thermometer errors, it will be assumed that psychrometric measurements are made at atmospheric pressure (29.92 in. Hg), at dry-bulb temperatures of 150°, 100°, 75°, 50°, and 32° F, and at wet-bulb depressions of 0.1, 1.0, and 10° F. For these given conditions, the errors in relative humidity, due to (a) a negative error of 1° F in wet-bulb temperature with the dry-bulb temperature correct, (b) a positive error of 1° F in dry-bulb temperature with the wet-bulb temperature correct, (c) an error of 1° F in dry-bulb temperature and an error of 1° F in wet-bulb temperature, both errors being negative, and (d) a positive error of 1° F in dry-bulb temperature and a negative error of 1° F in wet-bulb temperature, have been determined and are given, correspondingly, in table 1. It is seen in (c), table 1, that the errors are greatly reduced if the thermometers are matched.

TABLE 1. *Error in relative humidity due to uncorrected errors in the thermometers*

(a) Dry-bulb thermometer reads correctly; wet bulb thermometer reads 1 deg F low

Dry bulb temperature	Error in relative humidity at a wet bulb depression of—		
	0.1 deg F	1.0 deg F	10 deg F
°F	%	%	%
150	2.6	2.6	2.1
100	3.6	3.5	2.9
75	4.6	4.5	3.7
50	6.7	6.6	5.6
32	10.5	10.3	----------

(b) Dry bulb thermometer reads 1 deg F high; wet bulb thermometer reads correctly

Dry bulo temperature	Error in relative humidity at a wet bulb depression of—		
	0.1 deg F	1.0 deg F	10 deg F
°F	%	%	%
150	2.6	2.5	2.0
100	3.5	3.4	2.6
75	4.5	4.4	3.1
50	6.6	6.4	4.3
32	9.8	9.4	----------

(c) Dry bulb thermometer reads 1 deg F low; wet bulb thermometer reads 1 deg F low

Dry bulb temperature	Error in relative humidity at a wet bulb depression of—		
	0.1 deg F	1.0 deg F	10 deg F
°F	%	%	%
150	0.00	0.02	0.11
100	.00	.03	.32
75	.00	.05	.51
50	.00	.11	1.24
32	.02	.26	----------

(d) Dry bulb thermometer reads 1 deg F high; wet bulb thermometer reads 1 deg F low

Dry bulb temperature	Error in relative humidity at a wet bulb depression of—		
	0.1 deg F	1.0 deg F	10 deg F
°F	%	%	%
150	5.1	5.0	4.1
100	7.0	6.8	5.4
75	8.9	8.7	6.7
50	13.0	12.7	9.8
32	19.8	19.3	----------

The psychrometric constant, A, in the Ferrel formula is not invariant but is a function of the velocity of ventilation across the wet-bulb thermometer, and reaches a minimum value as the velocity is increased. This is reflected as a maximum wet-bulb depression. Any further increase in velocity will have negligible effect. When the velocity is sufficiently high so that A, is constant, then the magnitude of the velocity need not be measured or estimated. For most mercury-in-glass thermometers with bulbs ¼-inch diameter or less, the acceptable minimum rate of ventilation is

900 ft/min. If this velocity is not achieved, then the measured wet-bulb depression will not be a maximum, and the use of the psychrometric formula, tables or charts will yield values of relative humidity that are too high.

The heat absorbed by the wet-bulb due principally to radiation tends to raise the wet-bulb temperature so that a true depression is not attained. To minimize this effect, radiation shielding is commonly employed. One method of such shielding, successfully used in some ventilated psychrometers, is to surround the wet-bulb with an external primary metal shield and to insert an auxiliary shield between the primary external shield and the wet-bulb, this auxiliary shield being covered with a wick so that, upon moistening, the auxiliary shield may be brought close to the wet-bulb temperature thereby practically eliminating the source of radiation and conduction due to the difference between the dry- and wet-bulb temperatures.

The function of the wick is to retain a thin film of water on the wet-bulb so that evaporation may continue until the true wet-bulb temperature is reached. Cotton or linen tubing of a soft mesh weave serves well for this purpose because of its excellent water-absorbent properties. Sizing in the wick material, encrustations forming after use and lack of a snug fit interfere with the maintenance of a continuous film of water. Substances in solution in the wick water, due either to impurities on the wick or in the water used for moistening will change the saturation vapor pressure of water and hence affect the results. Wicks should therefore be cleaned and replaced frequently, and distilled water should be used for moistening. The wick should extend beyond the bulb and onto the stem of the thermometer, for an inch or so, in order to reduce heat conduction along the stem to the bulb.

Although the temperature of the water used to moisten the wick is often at dry-bulb temperature, it should be preferably that of the wet-bulb or slightly higher. The use of water that has been brought to the wet-bulb temperature is especially important when the ambient temperature is high and when the relative humidity is low.

If the temperature of the water used to wet the bulb is too high, it may take a long time for the bulb to cool to wet-bulb temperature, and before this point is reached the water may have evaporated sufficiently so that the thermometer never reaches the wet-bulb temperature. If the moistening water temperature is appreciably lower than the wet-bulb temperature, the thermometer temperature will climb throughout the period of ventilation, remaining constant at the wet-bulb temperature only as long as there is sufficient water to keep the bulb surrounded with a film of water. If the temperature of the water used for moistening is at, or slightly above or below, the wet-bulb temperature, then the wet-bulb will remain or quickly attain the wet-bulb temperature and remain at this value for an appreciable length of time so that it can be read easily and accurately.

A separation of the dry- and wet-bulbs is necessary in order to prevent the air that passes the wet-bulb, and is thereby cooled by the evaporating water, from contacting the dry-bulb and giving rise to an erroneous dry-bulb reading. To avoid this, the thermometers may be arranged so that the air flows across the dry-bulb before it reaches the wet-bulb or the air sample may be divided so that one part flows across the wet-bulb and the other part across the dry-bulb.

4.2. Mechanical Hygrometer

In hygrometers of this type, human hair is commonly used as the sensing element. In indicators the midpoint of a bundle of hairs under tension is connected by the simplest possible lever system to a pointer. In recorders a pen arm, which is substituted for the pointer, traces an ink record on a clock-driven drum.

The hair hygrometer indicates relative humidity directly over a wide range of temperature, but its reliability rapidly decreases as the ambient temperature decreases below freezing (0° C).

At temperatures below freezing (0° C) the hair hygrometers indicate relative humidity in terms of the vapor pressure of supercooled water, not that of ice (117).

The chief defect is the lack of stability of the calibration under usual conditions of use. However, tests recently completed at this Bureau on two good quality recorders indicated little average shift in calibration over a period of almost 1 year; the hysteresis (difference in indication, humidity increasing and decreasing) was of the order of 3-percent relative humidity. See (1, 8, 12, 38, 45, 83, 88, 117) for performance data.

Reliable data on the lag of the hair hygrometer are lacking, particularly at low temperatures. Suddenly subjecting hygrometers at about 25° C to a change in relative humidity requires of the order of 5 minutes to indicate 90 percent of the change in relative humidity; this time interval increases with decrease in temperature of the hairs, and is of the order of 10 times greater at −10° C. The effect of temperature on the calibration of hygrometers commercially available is not well established for temperatures below 0° C.

At the best, indications of the hair hygrometer have a reliability of about 3 percent in relative humidity at room temperature when exposed to a constant relative humidity long enough to obtain equilibrium. The large time lag of the hair hygrometer is a serious barrier to accuracy if changing humidity is being measured.

The hair hygrometer is made by a large number of industrial instrument companies, including meteorological instrument firms; the hair hygro-

graph (recorder) is made by a smaller but still large number of these firms.

The hair element with suitable accessories is widely used as a humidity controller in air-conditioning and other applications. The zero shift so evident in instruments measuring ambient humidity is less troublesome when the relative humidity about the element is maintained nearly constant (50, 62, 129). Controllers are available from a sizable number of industrial instrument firms.

A recent development in this country has been the use of goldbeater's skin in disk form by Serdex (139). It is claimed, but not yet generally accepted, that the performance is essential better than that of the human-hair type. See (134) for performance data at low temperatures; as for the hair hygrometer, the indication at temperatures below freezing of instruments reading correctly above freezing, is in terms of relative humidity of the vapor pressure of supercooled water.

Many organic materials are hygroscopic. Thus wood fibers have been used as a sensing element. Also plastics (152) in a form similar to bimetal have some application and perhaps are the most open to exploration. A cotton filament as a torsion element (53) has been tried. None of these seem to give essentially better, if as good performance as human hair and thus far have had only limited application.

4.3. Dewpoint Indicators and Recorders

When water vapor is cooled, a temperature is reached at which the phase changes to liquid or solid. At this temperature, condensation continues until an equilibrium between the vapor and liquid or solid phase is established. The temperature at which the vapor and liquid or vapor and solid phases are in equilibrium uniquely fixes the pressure of the vapor phase (saturation vapor pressure) and therefore determines the absolute humidity.

If the temperature at which water vapor must be cooled for it to be in equilibrium with its liquid or ice state is measured, then the humidity is obtained directly from it. The dewpoint method provides a convenient technique for ascertaining this temperature. Basically, the procedure is to reduce the temperature of a mirror until dew or frost just condenses from the surrounding air or gas sample. The temperature at the surface of the mirror at the instant dew or frost appears is defined as the dewpoint. If the temperature of the air or gas sample is measured and the initial humidity of the sample surrounding the mirror is kept unaltered, the initial relative humidity can be computed from a knowledge of the saturation vapor pressures at the two temperatures.

It should be noted that the formation of frost is not always positive because of the lack of a crystal nucleus, so that supersaturation may occur. Supersaturation is less likely to occur with respect to the liquid phase than with the ice phase. At a given saturation pressure, if ice does not form on the mirror, dew will form as the mirror temperature is lowered, hence there is always a little uncertainty whether the first clouding of the mirror represents the dewpoint (with condensed water) or the frost point.

Values of the saturation vapor pressure of water, at temperature above and below freezing, are readily available in various handbooks and compilations (1, 2, 4, 6, 15, 16, 17, 18, 128). There is some discordance in the values given in the listed references. However, for most applications in the field of humidity measurement or control, there is little to be gained in the use of any one table in preference to the others. The values given in table 2 are reproduced from the Smithsonian Meteorological Tables (16). At temperatures below 0° C, the saturation vapor pressures refer to water vapor in equilibrium over ice. Saturation vapor pressures of water vapor below 0° C in equilibrium over supercooled water are given in table 3 and are reproduced from the International Critical Tables (17).

The dewpoint instrument serves as a useful research tool for the determination of humidity in meteorology as well as for the determination of water vapor content in flue gases, gasoline vapors, furnace gases, compressed gages, and closed chambers. While the dewpoint instrument has been under considerable development in the past decade, principally along the line of improving the temperature control, means of indication, and automatic recording, it has been used in elemental form as far back as the early part of the last century. Dalton and Daniells used simple dewpoint hygrometers. Regnault (24) developed an instrument that has been used as a prototype and standard for many years in the measurement of atmospheric humidity. Essentially, it consisted of a thin polished silver thimble containing ether. Air was aspirated through the ether to cause evaporation and hence cooling of the thimble. The temperature of the ether at the appearance and disappearance of dew was observed and the mean taken as the dewpoint. A thermometer in a second thimble, near the first, gave the ambient temperature and, by comparison, the second thimble helped in the recognition of the appearance and disappearance of dew on the first thimble. Improvements and variations of the Regnault design were made by Alluard (25), and others (32, 41, 45, 55, 57).

The early models used ether for cooling and mercury-in-glass thermometers for temperature and measurement. Recent models have employed such cooling schemes as compressed carbon dioxide, dry ice, liquid air (for very low dewpoints) and mechanical refrigeration. In addition, metal mirrors are now commonly used, the

TABLE 2. *Saturation vapor pressure of water vapor in millimeters of mercury with respect to water above 0°C and with respect to ice below 0°C*

(Reproduced from the Smithsonian Meteorological Tables)

Temp, °C	0	1	2	3	4	5	6	7	8	9
−70	0.0019	----------	----------	----------	----------	----------	----------	----------	----------	----------
−60	.0080	0.0070	0.0061	0.0053	0.0046	0.0040	0.0035	0.0030	0.0026	0.0022
−50	.0294	.0260	.0229	.0202	.0178	.0156	.0137	.0120	.0105	.0092
−40	.0964	.0859	.0765	.0680	.0605	.0537	.0476	.0421	.0373	.0329
−30	2878	.2591	.2331	.2094	.1880	.1686	.1511	.1352	.1209	.1080
−20	.7834	.7115	.6456	.5854	.5303	.4800	.4341	.3923	.3541	.3194
−10	1.9643	1.7979	1.6444	1.5029	1.3726	1.2525	1.1421	1.0406	.9474	.8618
−0	4.5802	4.2199	3.8868	3.5775	3.2907	3.0248	2.7785	2.5505	2.3395	2.1445
0	4.5802	4.924	5.291	5.682	6.098	6.541	7.012	7.513	8.045	8.610
10	9.210	9.846	10.521	11.235	11.992	12.794	13.642	14.539	15.487	16.489
20	17.548	18.665	19.844	21.087	22.398	23.780	25.235	26.767	28.380	30.076
30	31.860	33.735	35.705	37.775	39.947	42.227	44.619	47.127	49.756	52.510
40	55.396	58.417	61.580	64.889	68.350	71.968	75.751	79.703	83.820	88.140
50	92.639	97.33	102.23	107.33	112.66	118.20	123.98	130.00	136.26	142.78
60	149.57	156.62	163.96	171.59	179.52	187.75	196.31	205.19	214.41	223.98
70	233.91	244.21	254.88	265.96	277.43	289.32	301.63	314.38	327.59	341.25
80	355.40	370.03	385.16	400.81	416.99	433.71	540.99	468.84	487.28	506.32
90	525.97	546.26	567.20	588.80	611.08	634.06	657.75	682.18	707.35	733.28
100	760.00	----------	----------	----------	----------	----------	----------	----------	----------	----------

TABLE 3. *Saturation vapor pressure of water vapor in mm mercury with respect to supercooled water*

(Reproduced from the International Critical Tables)

Temp, °C	0	1	2	3	4	5	6	7	8	9
−0	4.579	4.258	3.956	3.673	3.410	3.163	2.931	2.715	2.514	2.326
−10	2.149	1.987	1.834	1.691	1.560	1.436	---------	---------	---------	---------

warming of which by heat from the ambient atmosphere has been augmented by electric resistance or induction heating. The temperature of the mirror surface is frequently measured by thermocouples affixed several hundredths of an inch below the surface or actually on the surface of the mirror. While mercury-in-glass thermometers are still used, their high lag introduces an uncertainty in the temperature reading. In one instrument, the temperature is measured by a carbon dioxide vapor pressure thermometer in which the mirror is integral with the bulb (19). Visual observation of dew or frost has often been replaced by photoelectric detection of reflected or scattered light from the mirror and is indicated on an electrical meter, or automatically recorded. The output of the photoelectric circuit has been used also to control the heat input to the mirror and thereby to maintain the mirror temperature at the dewpoint. Photoelectric observation below the frost point has several advantages. Electronic circuits may be employed that automatically maintain a constant film thickness on the mirror. There can then be little question of whether the liquid or solid phase is involved, for supercooled liquid will not long exist under such conditions without changing to ice. There will be no supersaturation for lack of a crystal nucleus.

For information on these later forms of dewpoint indicators and recorders operating at atmospheric pressure, see (79, 95, 97, 102, 104, 110, 127, 135, 142, 144, 145, 146). Dewpoint indicators requiring visual observation and manual operating of the cooling system are available from dealers in scientific laboratory equipment. Dewpoint indicators and recorders employing photoelectric detection are made by a limited number of manufacturers.

Several dewpoint indicators have been developed that are of novel form or of specialized use. An instrument for use at high pressures is described in (133). In another instrument the sample of gas under test is pumped into a closed chamber and is then cooled by adiabatic expansion to a lower pressure. By repeated trials a pressure ratio can be secured so that a cloud or fog is just formed when the pressure is suddenly released. The dewpoint is computed from the ratio of the initial to final pressure and the measurement of the initial temperature. One version of this instrument (45) employs a vacuum pump for exhausting a reservoir into which the gas sample eventually is expanded. A commercial version (130) uses a small hand pump for compressing the gas sample and then expands the gas into the atmosphere. No adequate data on performance limits are available.

A polished rod or tube of high thermal conductivity, heated at one end and cooled at the other end so that dew forms on part of the rod (43) has been used to obtain the dewpoint. The temperature of the rod measured at the dew boundary is the dewpoint. There has been no commercial development of this device. Unpublished data indicate that it is unreliable at dewpoints below the ice point (0° C) because no satisfactory ice—no ice boundary is obtainable.

Use has been made of the change in conductivity

between electrodes on a glass thimble for detecting the dewpoint (45, 59).

The dewpoint method may be considered a fundamental technique for determining vapor pressure or humidity. However, the certainty of the dewpoint measurement is influenced by several factors, some of which are of such indeterminate nature as to make an estimate of the accuracy difficult. It is not always possible to measure the temperature of the mirror at the surface or to assure that no gradients exist across the surface. The visual detection of the inception of condensation cannot be made with complete assurance nor is it probable that two different observers would detect the dew or frost at the same instant. It is usual practice for the dewpoint to be taken as the average of the temperature at which dew or frost is first detected, on cooling of the mirror, and the temperature at which the dew or frost vanishes, on warming of the mirror. This procedure does not assure a correct answer since care must be taken to locate the thermometer, so that no temperature gradient exists from the cold source to the mirror face or to the gas as a whole. The photoelectric detection of the dewpoint usually depends upon achieving an equilibrium condition on the mirror surface during which the amount of dew or frost remains constant. It has been reported (146) that the dewpoint so measured, down to −35° C, agrees on the average to 0.1 deg C with the dewpoint measured visually with a Regnault instrument.

The uncertainty of measuring the dewpoint decreases with decrease in temperature. Below low 0° C uncertainty definitely exists if the eye is used for detecting the first sign of condensation, for it cannot distinguish or differentiate between the liquid and ice phase with the minute trace of water involved. With a photoelectric system in which the mirror alternately cools and then warms so that condensation forms and evaporates, the photocell is likewise incapable of determining whether the condensate is liquid or solid. With a photoelectric system in which a constant film thickness is automatically maintained on the mirror, ice will form on the mirror, for, as previously explained, supercooled water cannot long exist on a free and exposed surface.

Dewpoint instruments have been built with reported sensitivities of 0.1° C (27) and 0.01° C (97) and with reported accuracies of ±1 percent of the vapor pressure (27) at temperatures above freezing and ±1° C at −70° C (127).

4.4. Electrical Hygrometers

Dunmore. These hygrometers commonly depend upon the change in electric resistance of a hygroscopic material with change in humidity. In one design, largely developed by Dunmore (94, 99, 103), two parallel wires of a noble metal are wound upon a polystyerene cylinder or strip. A hygroscopic coating of polyvinyl acetate or polyvinyl alcohol and dilute lithium chloride solution is placed between the wires. At constant temperature the logarithm of the electrical resistance between the parallel wires varies approximately linearly with the logarithm of the relative humidity and is measured by a suitable Wheatstone bridge, preferably using alternating current, or other suitable electric circuits. The electric resistance at constant relative humidity is highly dependent upon temperature, especially at temperatures below 0° C.

The hygrometer was primarily developed for use in radiosondes in which the output is fed to a radio transmitter and controls an audio frequency. It is widely used for this purpose and is manufactured by a number of firms. An indicator and a controller for industrial use is now available commercially.

An elementary theory of the electric hygrometer has been proposed by Schaffer (132).

Similarly, as for the hair hygrometer, the chief defect has been in stability of calibration, which seems to have been overcome in the model for industrial use. The continuous application of direct current causes polarization with a resultant shift in calibration and ultimate deterioration. At temperatures above freezing, the response to humidity changes is rapid, but at lower temperatures, time lags are appreciable. Some data on the performance at low temperatures are given in (134 and 150). One of the advantages of this design is that it is remote indicating an adaptable for control. See also (113 and 114).

Dewcel. Another form of the electric hygrometer is the "dewcel", which is remote indicating and can be used for control (136, 154). Essentially it indicates the dewpoint temperature. The sensing element, similarly as the Dunmore element, has a parallel wire winding with the material between the wires kept wet with a wick impregnated with a saturated solution of lithium chloride. The element is heated by an electric current passed between the parallel wires until its temperature is such that the element neither loses nor gains moisture from the surrounding atmosphere. The electric resistance of the element increases if the temperature is above the equilibrium temperature, since the solution concentration increases by evaporation, and vice versa, and thus the vapor pressure of the solution on the element is automatically brought to and maintained in equilibrium with the surrounding vapor pressure. The temperature of the element, which is measured either by a resistance or liquid filled thermometer, determines the vapor pressure of the lithium chloride solution which in turn equals the pressure of the water vapor in the surrounding atmosphere. The scale can be graduated in terms of dewpoint insofar as the vapor pressures for saturated lithium chloride are accurately known. It is approximately 15 percent of that of water

down to temperatures of about 0° C. With certain restrictions the dewpoint is measurable in the range −16 to +160° F. Stability of calibration under service conditions is claimed.

This instrument can be used for remote indicating, recording and control. It functions best in still air, and when the ventilation of the sensitive element becomes excessive (greater than 50 ft/min), suitable means must be used to reduce the ventilation, if accuracy is to be maintained.

Weaver. Weaver and Riley (147) have developed a type of electric hygrometer which has application in routine checking of water vapor content of gases, particularly those in high pressure cylinders.

The sensitive element is a film of electrolyte, usually phosphoric and sulfuric acid, with suitable electrodes for use in measuring the electric resistance of the film, all mounted in a small case, as an aviation engine spark plug, suitably modified. Since the electric resistance of the film is unstable, a comparison procedure is resorted to, in which the resistance of the film in equilibrium with the atmosphere to be measured is immediately matched by exposing to an atmosphere, the moisture content of which can be controlled in a known way.

In the primary use of the instrument, in measuring the dryness of aviator's oxygen, pressure control was found to be most convenient and is described here only in its most elemental form. Gas, usually nitrogen, is humidified 100 percent while at high pressure. A sample of this nitrogen, at atmospheric pressure, is passed through the cell and the resistance noted, usually as the reading of a galvanometer in an unbalanced alternating-current Wheatstone bridge. Then a sample from the compressed gas under test is passed through the cell, at a pressure which is reduced until the same reading is obtained. From the measured pressures and the known water content of the saturated sample, either the weight of water vapor per unit volume, vapor pressure, or relative humidity of the test sample can be computed.

The instrument is characterized by speed, the use of a small sample and greater sensitivity than is possessed by other instruments or methods comparable in these respects. It is available commercially.

Lichtgarn. The variation in electric resistance with relative humidity of selected underfired clays has been investigated by Lichtgarn. The performance data are incomplete as yet, and no elements appear to be commercially available (137).

Gregory humidiometer. Gregory (120) has utilized the electric resistance of cotton impregnated with LiCl or $CaCl_2$ solution to measure humidity. This method has been applied to the measurement of humidity on the skin and clothes of a human subject (131).

Burbidge and Alexander. The variation in electric resistance of cotton wool and human hair has been investigated by Burbidge and Alexander (51). The logarithm of the resistancy of these materials is proportional to relative humidity.

4.5. Gravimetric Hygrometry

a. Change in Weight of Drying Agent

The well-known gravimetric method is accepted as the most accurate for determining the amount of water vapor in a gas. The gas mixture of measured volume and known pressure and temperature is passed over a moisture absorbing chemical, usually phosphorous pentoxide for results of the highest accuracy, and its increase in weight determined. For the data, the weight of water vapor per unit volume and the relative humidity of the gas sample can be computed. Considerable care is required to obtain reliable data (3, 27, 66, 149). This method is employed only in fundamental calibration of instruments or exact determinations of water vapor content.

b. Change in Weight of Absorbing Material

In this type of hygrometer a moisture absorbing material such as human hair, or a chemical, or combinations of both to obtain a structure convenient to handle, is continuously weighed by a delicate balance with an indicator and calibrated humidity scale. The weight of the material must change only with change in the relative humidity of the ambient air (109, 118, 119). Instruments of this type are not known to be available commercially.

4.6. Thermal Conductivity

The difference in thermal conductivity between air (or other gases) and water vapor is utilized so that the temperature, and thus the electric resistance of a hot wire in a small cell varies with change in humidity of the air sample. Two hot wires, one in a reference cell exposed to dry air, are in a bridge circuit, the output of which is a function of the vapor pressure of water in the sample. The theory has been developed by Daynes (31) and Shakespear (34). A model was built by Leeds & Northrup (61, 76). This hygrometer is limited in sensitivity at low temperatures owing to the low vapor pressure of water vapor existing at these temperatures. It has considerable promise as a recorder of humidity in a closed space and in meteorology. It is limited by the fact that it is not specific for water vapor but indicates any change of composition of the gas entering the instrument.

Schwarz (138) has called attention to the possibility of subjecting the water-vapor sample to an inhomogeneous electric field in a thermal conductivity apparatus. Since the water molecule is a dipole, an additional circulation of the water

vapor, in contrast to that obtained with air, is secured. This effect can be expected to add to the effect of differences in the heat conduction of air and water vapor. No development work appears to have been done on this possibility.

4.7. Spectroscopic Method

Instruments have been developed in which infrared bands which are absorbed by water vapor are compared in intensity with another band not so absorbed. The sample of air under analysis may be in a tube (116, 125) with the spectral bands obtained from a lamp or may be the entire atmosphere with the sun furnishing the spectral bands (124). The effect of water vapor upon the energy of the received radiation may be measured by phototubes or thermocouples. The instrument is not made commercially.

4.8. Index of Refraction

Some experimental work has been done on the variation of the index of refraction of a thin film of glycerine with water vapor content of the ambient air (29 and 48). The method, even if successfully developed, appears to have only limited application.

4.9. Measurement of Pressure or Volume

The volume of water vapor in a gas sample can be measured if its change in volume is measured at constant pressure before and after the water vapor is absorbed. Conversely, if the volume is held constant, the change in pressure gives the pressure of the water vapor. These methods are useful only in laboratory investigations. The difficulty of obtaining accurate determinations increases rapidly with decrease in temperature of the gas sample. See (1 and 8) for descriptions of a number of instruments of this type.

In one form of constant pressure apparatus a manometer and also a graduated tube containing an absorbing liquid, such as sulfuric acid, are connected to a gas container. In operation sulfuric acid is slowly admitted to the container to absorb the water vapor in the sample and at the same time in sufficient volume to maintain constant the absolute pressure of the gas, as indicated by the manometer and a barometer. The volume of acid admitted is the volume of water vapor in the sample, subject to corrections for lack of constancy of temperature or of the reference pressure.

If the apparatus just described is modified so that the sulfuric acid forms part of the original volume, a constant volume apparatus results. In this case the change in pressure as the water vapor is absorbed is the water-vapor pressure.

The tilting form of absorption hygrometer described by Mayo and Tyndall (33) is essentially a constant volume instrument. Here the absorbing material is installed in a piston which moves from one end of the cylinder containing the gas sample to the other as the cylinder is oscillated, thus forcing the gas through the absorbing chemical. This piston action reduces the time required for complete absorption of the water vapor. The fall in gas pressure which is measured is the water vapor pressure. The device is proposed as a working standard in calibration of hygrometers. It is not available commercially.

One version of constant-volume hygrometer (105) completely dispenses with an absorbing chemical and, instead, uses low temperatures to condense part of the water vapor content of a gas sample, and from a measurement of the temperature and reduction in pressure, permits the determination of the initial vapor pressure. In this instrument, two identical vessels, one containing dry gas and the other the gas sample of unknown water vapor content, are sealed and connected through a differential manometer. The vessels are then immersed in a liquid bath and gradually cooled until the differential manometer registers a pressure difference, indicating that condensation of water vapor has taken place in the gas sample. At this point the temperature and pressure difference are read. From the saturation pressure at the observed temperature and from the pressure difference, the initial water vapor content is then computed.

By employing a liquid-air trap, the moisture in a large volume of gas can be condensed and then suitably measured. The known volume of gas is passed through the trap and, while the low temperature is maintained, the trap is evacuated. The apparatus is then allowed to warm up, preferably in a thermostatted bath, and the vapor pressure measured. Experience with this method at this Bureau indicates that for frost points below $-20°$ C, it is better than the direct determination of the frost point. When using this method with gases containing carbon dioxide, the temperature of the air trap is raised above $-78°$ C before evacuation. This permits any condensed carbon dioxide to be vaporized and removed from the trap.

For additional information on absorption hygrometers, see (30, 85, 86, 101, 111).

4.10. Thermal Rise

The rise in temperature accompanying the exposure of dry cotton wool to moist air has been employed as a means of indicating humidity (see (36 and 45) for details).

4.11. Mobility of Ions

The change in the mobility of ions, produced by α-rays and γ-rays, due to the presence of water

vapor has been investigated (45, 51). While a small effect has been observed, no practical hygrometer has been developed.

4.12. Dielectric Constant

Birnbaum has developed a recording microwave refractometer (153) of high sensitivity that can continuously sample and record the dielectric constant of a stream of air or gas. Since the dielectric constant of air varies with water-vapor content, this instrument may be employed as a recording hygrometer. The refractometer operates by comparing two identical cavity resonators. Into one of these cavities, the test sample is introduced. The resulting differences in resonance frequency between the two cavities is then a measure of the dielectric constant of the test sample. In addition to its high sensitivity, the refractometer has a time response, limited by the response of the recording milliammeter, of about one-half second to discrete changes in dielectric constant. A similar instrument has been reported by Crain (157).

4.13. Critical Flow

Wildhack (156) has proposed a means of measuring relative humidity which utilizes sonic, or critical, flow through small nozzles. Two sets of two nozzles in series are arranged in parallel, with critical flow maintained through all nozzles. At critical flow the mass flow through each nozzle is independent of the downstream pressure, and is directly proportional to the entrance pressure. An absorber of water vapor is placed between one series pair of nozzles, which reduces the mass flow and hence the gas pressure at the entrance to the downstream nozzle. Measurement of the difference in entrance pressures between the two downstream nozzles, of the absolute pressure of the gas at the entrance to the referenced downstream nozzle, and of the gas temperature, will serve to determine the relative humidity of the gas.

4.14. Diffusion Hygrometer

The difference in density of completely and partially saturated air, at the same temperature, has been employed to measure air humidity (49). Esentially, a column of atmospheric air is balanced against a column of saturated air. The difference in density of the two columns causes the lighter saturated air to diffuse upward into the atmosphere and the atmospheric air, because of its greater density to diffuse downward into a saturation chamber where it, in turn, becomes fully humidified. The rate of diffusion is then directly related to the vapor pressure of the atmospheric air and is detected and measured by means of the deflection produced in a suspended vane. It is claimed that this water vapor diffusion method can operate over a wide temperature range, is continuously indicating or recording, is easy to operate and is portable.

A different approach was used in the hygrometer described by Greinacher (122). His instrument is based on the difference in diffusion of water vapor and air through a semipermeable membrance. A porous clay plate cemented to an opening in the wall of an enclosed vessel containing a desiccant preferentially permits air diffusion and prevents water vapor diffusion. A differential manometer, communicating with the enclosed vessel and the ambient atmosphere (whose humidity is being measured), registers a pressure drop Δp_1 that is directly proportional to the partial pressure e of the water vapor in the ambient atmosphere. In order to avoid consideration of the constant of proportionality of the apparatus a similar vessel with an identical porours clay plate and manometer, but containing water instead of the dessicant, is employed. The pressure drop Δp_2 indicated by the latter arrangement is directly proportional to the difference between the saturation vapor pressure e_s and the ambient partial pressure e at the ambient temperature. The relative humidity is given by the relation.

$$RH = 100 \times \frac{e}{e_s} = 100 \times \frac{\Delta p_1}{\Delta p_1 + \Delta p_2}$$

Further theoretical consideration of this hygrometer are presented by Spencer-Gregory and Rourke (141). The instrument is reported to be extremely sensitive to rapid temperature changes which may give rise to erroneous readings.

4.15. Chemical Methods

Several methods are available for the determination of the moisture content in gases by chemical means. A very simple and qualitative indicator may be made based on the change in color, from blue to pink, of cloth or paper impregnated with cobaltous chloride, as the humidity increases. When a color comparison scale is employed with this indicator, a rough estimate of the relative humidity is obtained (75). Cobaltous bromide may similarly be used, with a threefold increase in sensitivity. The colors of these cobalt salts are affected by temperature as well as humidity. The quantitative measurement of water vapor has been successfully made by using cobaltous bromide as an indicator in a visual (112) and in a photoelectric (123) colorimetric method.

There is a series of compounds of ketones and Grignard reagents which can form internal ions accompanied by the development of intense color, induced by the presence of water. Some useful compounds are the complexes of Michler's ketone (tetramethyl-diaminobenzophenone) and Grignard reagent (ethyl magnesium bromide, methyl

magnesium iodide, or phenyl magnesium iodide). An apparatus, employing the color change of these compounds, has been developed, primarily for detecting moisture in compressed oxygen (19). The apparatus and method involves sealing a measured amount of compound with dry sand in a glass ampule. Then, under a controlled and uniform rate of gas flow, the ampule is broken and the time for the movement of the resultant color front along a specified distance is measured. This time, for a given batch of ampules identically made, is a function of the moisture content, the temperature and rate of flow.

A method for the analytical determination of the water content in a wide range of materials was proposed by Karl Fischer in 1935 (84). His reagent, a solution of iodine, sulfur dioxide and pyridine in methanol, is the basis of titrimetric procedures that have been applied to moisture determinations in gases (20).

5. Test Methods

The testing and calibration of hygrometers involve the production and control of atmospheres of known relative humidity over a wide range of temperatures. While the methods of humidity production are varied, they may be classified, conveniently, into several categories. The equipment for producing the known relative humidity must be designed so that hygrometers to be tested can be conveniently exposed to the controlled atmosphere.

The sections below are restricted largely to the description of methods of producing a constant humidity of known amount useful for calibration of hygrometers.

5.1. Basic Methods

Relative humidity is related, through the fundamental gas laws, to such parameters as temperature, pressure, and water-vapor content. Several convenient and practical methods are available of directly establishing atmospheres of known relative humidity with sufficient precision and accuracy by the measurement and control of these parameters, without requiring auxiliary humidity measuring and sensing instruments.

The principle of divided flow may be employed, when flow is permissible, to produce any desired humidity. Apparatus, based on this principle, has been described in (76) for use at temperatures above freezing and in (134 and 149), for use at temperatures below 0° C (32° F). A stream of dry air is divided accurately, usually by means of a proportioning valve, into two parts. One part is saturated, with respect to water or ice; the other part is maintained dry. The two parts are then recombined in a test chamber and exhausted into the air. The relative humidity is given by the ratio of the division. A simplified schematic diagram of this method is shown in figure 1.

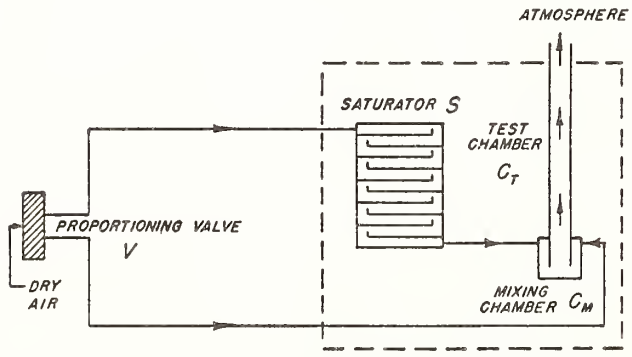

FIGURE 1. *Simplified schematic diagram of the principle of operation of the divided-flow humidity apparatus.*

In the recirculation or two-temperatures method, a stream of air is saturated at a controlled temperature and then the temperature of the mixture is elevated, without loss or gain in moisture. A measurement of the two temperatures serves to determine the relative humidity. To insure complete saturation at the lower temperature, the air stream is recirculated in a closed system from the saturator (at the lower temperature) to a test chamber (at the higher temperature) and back to the saturator. The temperatures must be accurately measured and controlled; for example, at 20° C (68° F) an error of 0.2° C (0.3° F) in either temperature measurement represents 1 percent error in relative humidity, which error increases at lower temperatures. Laboratory equipment of this type has been built (106, 155), but none is commercially available. The method is illustrated in figure 2.

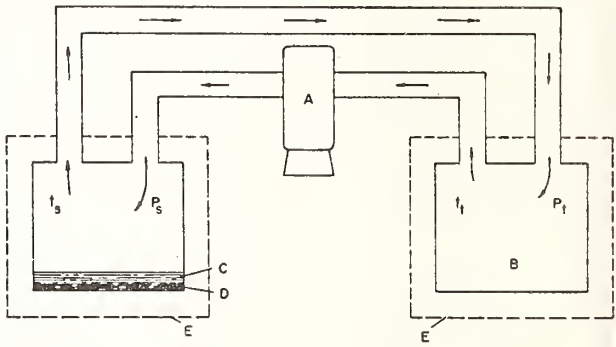

FIGURE 2. *Simplified schematic diagram of the two-temperature recirculating method of relative-humidity production.*

A, gas pump; B, test chamber; C, water; D, saturator; E, thermostatted bath.

In the two-pressure method (147) a stream of air (or some other gas) at an elevated pressure is saturated and the pressure of the saturated air is reduced as required to obtain any desired humidity. Since the desired relative humidity is required, usually, at atmospheric pressure, the elevated pressure is so adjusted that the air, upon expansion to atmospheric pressure, will be at the proper relative humidity. The pressure of the air and water vapor mixture is measured at both the elevated and reduced pressures, and so are the temperatures, if they differ. To insure that the saturator and test chamber temperatures remain the same, and also to provide a means of controlling and establishing any desired temperature, the saturator and test chamber are immersed in a thermostatted bath. To prevent condensation the saturated air temperature must not fall below the dewpoint, which may require heating the mixture at or before it flows through the pressure-reducing valve. Even at room temperature, control of the saturator temperature will be necessary if the air flow is appreciable. At constant temperature, the relative humidity is roughly the ratio of the two pressures, assuming ideal gas laws. More accurate computation of the relative humidity takes into account deviations from the ideal gas laws (147).

One type of saturator employed in this method consists of a cylinder filled with clean sand and water through which the air passes. Another type similarly consists of a cylinder into which water has been added, but the air in this type enters the cylinder tangentially to and above the water (or ice) surface and, after swirling around many times over the water, emerges through a central port at the top. A sketch of this method is shown in figure 3.

In the water or steam injection method for the precise control of relative humidity, moisture and dry air are mixed in desired proportions, using nozzles, orifices or other metering elements in conjunction with pressure reducers. See (67) for one application.

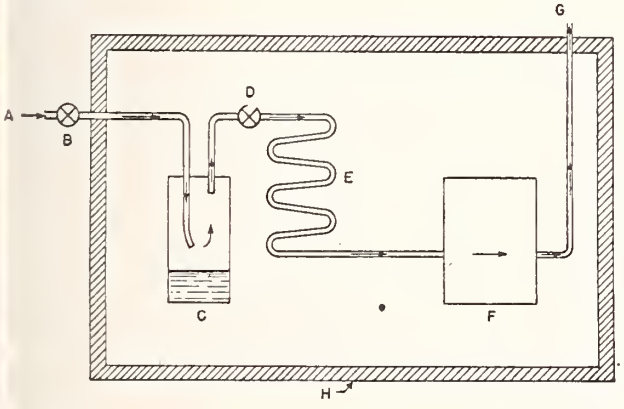

FIGURE 3. *Simplified schematic diagram of the two-pressure method of relative-humidity production.*

A, High-pressure source; B, pressure reducer; C, saturator (water or ice); D, valve; E, heat exchanger; F, test chamber; G, to atmosphere; H, thermostatted bath.

5.2. Secondary Methods

Very convenient methods exist for establishing atmospheres of known relative humidity which depend upon the equilibrium vapor pressure of water when a chemical is dissolved in it. These methods are ideally suited for controlling the relative humidity of a small closed space. Equilibrium conditions are more rapidly established when air circulation or stirring, as by means of a fan or blower, is employed. In all these methods, the test chamber should be kept free of hygroscopic materials, such as wood.

The saturated salt solution method is inexpensive and simple and produces constant relative humidities that are roughly independent of temperature. This method is used frequently for calibrating mechanical type hygrometers. A sealed chamber is required, for which a large glass jar or bell jar is often suitable. The salt solution is made up as a slushy mixture in a glass or enameled tray or in the glass jar, if used, with the solution spreading over as large an area as practicable. Distilled water and chemically pure salts must be used. The salts listed in table 4 have been found useful; for a list of others see (4). The data in table 4 are based partly on the vapor pressure data given in the International Critical Tables (17) and partly on dewpoint measurements made at this Bureau.

TABLE 4.—*Saturated salt solutions suitable for use in humidity control*

KNO_3=potassium nitrate
NaCl=sodium chloride
$Mg(NO_3)_2.6H_2O$=magnesium nitrate
$MgCl_2.6H_2O$=magnesium chloride
LiCl=lithium chloride

Temperature		Relative humidity of saturated salt solution				
		KNO_3	NaCl	$Mg(NO_3)_2.6H_2O$	$MgCl_2.6H_2O$	LiCl
°C	°F	%	%	%	%	%
0	32	97	76	54	34	19
5	41	96	76	54	33	16
10	50	95	75	53	33	14
15	59	95	75	53	33	13
20	68	94	75	53	33	12
25	77	93	75	52	33	11
30	86	92	75	52	32	11
35	95	90	75	51	32	11
40	104	89	75	51	31	11

Water-sulfuric-acid mixtures (39, 52, 63) produce atmospheres of relative humidity that depend on composition and temperature. Two techniques may be employed. The liquid may be exposed in a suitable tray in a sealed chamber to give the equilibrium vapor pressure of the mixture, or air may be bubbled or otherwise brought into intimate contact with the liquid. Wilson's data (39) are reproduced in table 5.

TABLE 5. *Relative humidity obtained from water-sulfuric acid solutions*

Relative humidity	Percentage of H_2SO_4 (by weight) at—			
	0° C	25° C	50° C	75° C
%				
10	63.1	64.8	66.6	68.3
25	54.3	55.9	57.5	59.0
35	49.4	50.9	52.5	54.0
50	42.1	43.4	44.8	46.2
65	34.8	36.0	37.1	38.3
75	29.4	30.4	31.4	32.4
90	17.8	18.5	19.2	20.0

Water-glycerine mixtures (63) will similarly produce atmospheres of known relative humidity. The techniques employed with water-sulfuric acid mixtures work equally well with water-glycerine mixtures. The relative humidity obtainable at 25° C from various water-glycerine solutions are given in table 6.

TABLE 6. *Relative humidity obtained from water-glycerine mixtures at 25° C*

Relative humidity	Glycerine (by weight)	Specific gravity
%	%	
10	95	1.245
20	92	1.237
30	89	1.229
40	84	1.216
50	79	1.203
60	72	1.184
70	64	1.162
80	51	1.127
90	33	1.079

5.3. Control Methods

In response to a sensing element, such as a mechanical hygrometer, electrical hygrometer, or psychrometer, the humidity of a closed space may be raised by water, spray or steam injection, by exposure to a water surface or wet wicks, or by the introduction of saturated or high humidity air (or gas), or the humidity may be lowered by chemical absorption, or the introduction of dry air (or gas). The controls that are used may be manual or automatic.

One type of controlled-humidity chamber design (32, 45) consists, essentially, of a sealed chamber, such as a bell jar, in which air circulation is obtained by means of a fan. Two trays, each with a tight cover that can be raised and lowered externally, are placed in the chamber. One tray contains a chemical absorbent, such as sulphuric acid, silica gel or Drierite, while the other contains distilled water, preferably with exposed cotton or linen wicks. The cover of the appropriate tray is raised until a hygrometer indicates that the desired relative humidity has been attained. The cover is then dropped and, since the chamber is sealed, the humidity remains constant. This chamber may be made automatic by using the output of a sensing element, through an appropriate circuit, to raise or lower the required cover.

See (8, 10, 12, 50, 54, 58, 62, 65, 92, 114, and 129), for additional suggestions and details.

5.4. Comparisons with Standards

While it is preferable to use atmospheres of known relative humidity for testing or calibration, it is often desirable to make spot checks of mechanical hygrometers and hygrographs under prevailing atmospheric conditions or even, in some cases, to test or calibrate hygrometers in chambers where the humidity is not known or only known approximately. Under these conditions, the readings of the instrument under test may be compared with those of a standard instrument.

It is generally considered that the primary standard in hygrometry is the gravimetric method of water vapor measurement. However, except for work of the highest order of accuracy, this method is seldom used as a working standard. On the other hand, proved designs of dewpoint indicators and recorders are frequently employed as working standards where accuracy is desired. Many models are in the nature of laboratory instruments, especially those depending on visual observation and manual temperature control, requiring skilled personnel for successful operation so that they are not usually used in routine calibrations. The dry- and wet-bulb psychrometer is particularly suited for rapid routine work. It should be used with caution in small enclosures, for evaporation from the wet-bulb may increase the relative humidity of the space being measured. If adequate ventilation is secured and proper precautions are observed, the psychrometer is calibrated merely by having its thermometers calibrated.

6. Selected References

6.1. Books and Pamphlets

(1) Feuchtigskeitmessung. H. Bongards. R. Oldenburg, Berlin. 322 p (1926). (Excellent general treatise)

(2) Properties of ordinary water substance. N. Ernest Dorsey. Reinhold Publ. Co. (1940).

(3) Dictionary of applied physics. Section on humidity by Skinner (1923). Glazebrook.
(Deseribes psychrometrie, dewpoint and gravimetrie methods of humidity measurement.)

(4) Handbook of chemistry and physics. p. 1925, 30th ed. (1946). Chemical Publ. Co., 26 Court St., Brooklyn 2, N. Y. $6.00.

(5) Heating, ventilating and air conditioning guide. American Society Heating & Ventilating Engrs., New York (1944).

(6) Wärmetabellen der Phys. Tech. Reich. L. Holborn, K. Scheel, and F. Henning. Friedr. Vieweg & Sohn, Braunschweig (1919).

(7) Psychrometertafeln. Jelineks. VII Aufl., Leipzig (1929).
(8) Handbuch der Meteorologischen Instrumente. E. Kleinschmidt. Julius Springer, Berlin (1935). (Section on measurement of atmospheric humidity and evaporation.)
(9) Mechanical engineers handbook. Lionel S. Marks. McGraw-Hill (1941).
(10) Controlled humidity in industry. M. C. Marsh. Charles Griffin & Co., Ltd. (London) (1935).
(11) Diffusion. C. Maxwell. Encyl. Brit. 9th ed., 7, 218 (1877).
(12) Meteorological instruments. W. E. K. Middleton. University of Toronto Press (1941). (Chapter on measurement of atmospheric humidity.)
(13) Chemical engineers handbook. J. H. Perry. McGraw-Hill Book Co., New York, 2d ed. (1941).
(14) Aspirations-Psychrometertafeln des Prens. Met. Inst. III Aufl. Preuss. Met. Inst. Braunschweig (1927).
(15) Psychrometric tables. U. S. Weather Bureau WB No. 235 (1912). (Supt. of Documents, Washington 25, D. C.) 15¢.
(16) Smithsonian meteorological tables. Smithsonian Institution (1939).
(17) International critical tables, III, 211. E. W. Washburn. McGraw-Hill Book Co., New York.
(18) Psychrometric tables and charts. O. T. Zimmerman and I. Lavine. Industrial Research Service, Dover, N. H. (1945) $7.50.
(19) Oxygen research. Summary technical report of Division 11, NDRC, 1 (1946) chap. 14. Instruments for testing oxygen. S. S. Prentiss. p. 320.
(20) Aquametry. Applications of the Karl Fischer reagent to quantitative analysis involving water. John Mitchell, Jr. and Donald Milton Smith. p. 168 Interscience Publishers, Inc., New York (1948).

6.2. Articles

(21) On the hygrometer by evaporation. J. Ivory. The Philosophical Magazine and Journal 60, 81 (1822).
(22) Über die Verdunstungskalte under deren Anwendung auf Hygrometrie. E. F. August. Annalen der Physik und Chemie 335, 69 (1825).
(23) On the theory of the moist bulb hygrometer. Apjohn. Trans. Roy. Irish Acad. 17, 275 (1837).
(24) Etudes sur l'Hygrométrie. V. Regnault. Ann. Chim. Phys. (3) 15, 129 (1845).
(25) Kondensationhygrometer. Alluard. Symons Month. Met. Mag. 13, 55 (1877).
(26) Annual Report, Chief, U. S. Signal Officer. Ferrel. Appendix 24, pp 233–259 (1886).
(27) Report on hygrometric methods; first part, including the saturation method and the chemical method, and dewpoint instruments. W. N. Shaw. Phil. Trans. Royal Soc. 179, 73 (1888).
(28) Rational psychrometric formulae. W. H. Carrier. Trans. ASME 33, 1005 (1911).
(29) Determination of relative humidity of the air by refractometry. Giraud. J. Physique 3, 900 (1913). (Used change of index of refraction of glycerine with humidity.)
(30) Improved methods of hygrometry. A. N. Shaw. Trans. Roy. Soc. Can., Ser. 3, 10, 85 (1916). (Absorption hygrometers.)
(31) The theory of the katharometer. H. A. Daynes. Proc. Roy. Soc. London A97, 273 (1920). (Thermal conductivity method.)
(32) Some modified forms of hygrometers. E. Griffiths. Trans. Phys. Soc. London 35, VIII (1921–2). (Description of psychrometer, dewpoint apparatus and humidity chamber.)
(33) The tilting hygrometer; a new form of absorption hygrometer. H. G. Mayo and A. M. Tyndall. Proc. Phys. Soc. London 34, lxvii (1921–22). (Moisture abstracted from air sample by P_2O_5 and change of pressure measured.)
(34) The katharometer. G. A. Shakespear. Proc. Phys. Soc. London 33, 163 (1921). (Thermal conductivity method of humidity measurement.)
(35) The wet and dry bulb hygrometer. P. S. Skinner. Trans. Phys. Soc. London 34, lx (1921–22). (Some experimental work on psychrometric formula.)
(36) A thermal hygrometer. A. M. Tyndall and A. P. Chattock. Proc. Phys. Soc. London 34, lxxii (1921–22). (Method depends on exposing dry cotton wool to damp air and measuring temperature rise.)
(37) Note on psychrometry in a wind tunnel. R. A. Watson Watt, Proc. Phys. Soc. London 34, lxiv (1921–22). (Effect of ventilation on psychrometric constant.)
(38) The theory of the hair hygrometer. F. J. W. Whipple. Trans. Phys. Soc. London 34, 1 (1921–22). (Mathematical treatment.)
(39) Humidity control by means of sulphuric acid solutions with critical compilation of vapor pressure data. R. E. Wilson. J. Ind. & Eng. Chem. 13, 326 (1921). (Data percent sulfuric acid solution against relative humidity at 0°, 25°, 50° and 75° C.)
(40) The evaporation of a liquid into a gas. W. K. Lewis. Mech. Eng. 44, 325 (1922) and 55, 567 (1935).
(41) Direct determination of gasoline-air mixtures. W. A, Gruse. Ind. Eng. Chem. 15, 796 (1923).
(42) The temperatures of evaporation of water into air. W. H. Carrier and D. C. Lindsay. Trans. ASME 46, 36 (1924).
(43) A new method for determining the temperature of the dewpoint. M. Holtzmann. Phys. Zeitschrift 25, 443 (1924). In German. (Polished rod type dewpoint indicator.)
(44) Hygrometry in deep mines. R. S. Jones. Colliery Guardian (England) 128, 1437–38, 1499–1500 (1924).
(45) The measurement of humidity in closed spaces. Ewing and Glazebrook. Spec. Report No. 8, Food Investigation Board, Dept. of Scientific and Ind. Research (London) (1925). Revised ed., E. Griffiths (1933).
(46) Energy transformations in air currents and applications in the measurement of atmospheric humidity. Paine. Proc. Nat. Acad. Sci. 11, 555 (1925).
(47) A new relative humidity recorder. L. Behr. J. Opt. Soc. Am. 12, 623 (1926). (A circuit and recorder for automatically giving relative humidity by the phychrometric method using resistance thermometers.)
(48) A hygrometer employing glycerine. E. Griffiths and J. H. Awbery. Proc. Phys. Soc. London 39, 79 (1926). (Used change of index of refraction of glycerine with humidity.)
(49) Continuous indicating hygrometer. Romberg and Blau. J. Opt. Soc. Am. 13, 717 (1926).
(50) An automatic humidity control. W. H. Apthorpe and J. J. Hedges. J. Sci. Inst. 4, 480 (1927). (Hair element controls a circuit which controls supplies of moist and dry air to the chamber.)
(51) Electrical methods of hygrometry. P. W. Burbidge and N. S. Alexander. Trans. Phys. Soc. London 40, 149 (1927–28). (Used resistance of cotton wool and human hair; also measured change in mobility of ions due to water vapor.)
(52) The vapor pressure of water over sulfuric-acid-water mixtures at 25° C and its measurement by an improved dewpoint apparatus. J. R. I. Hepburn. Proc. Phys. Soc. London 40, 249 (1927). (Revision of Wilson's data, ref. 37.)
(53) Influence of humidity on the elastic properties of cotton. Mann. Shirley Inst. Memoirs 6, 53

(1927). Also J. Text. Inst. 18, T253 (1927). (Torsion hygrometer from cotton filament.)
(54) Notes on temperature and humidity control cabinets. Circ. No. 310 Paint & Varnish Manufacturers Assoc. (May 1927).
(55) Determination of volatility of gasoline. R. Stevenson and J. A. Babor. Ind. End. Chem. 19, 1361 (1927). (An apparatus for determining the dewpoints of air-gasoline mixtures. Visual observation of optical change of a platinum black mirror.)
(56) A hygrometer for use in timberseasoning kilns. E. Griffiths. Trans. Phys. Soc. London 41, 426 (1928).
(57) Dehumidification of air. C. S. Keevil and W. K. Lewis. Ind. & Eng. Chem. 20, 1058 (1928). Dewpoint apparatus.)
(58) Humidity test equipment. E. B. Wood. Instruments 1, 135 (1928). (Describe air-conditioned test room, controlled by sprays and radiators, chambers controlled by sulfuric acid-water mixtures, and chambers controlled by saturated salt solutions.)
(59) An electrical method for the determination of the dewpoint of flue gases. H. F. Johnstone. U. Ill. Eng. Exp. Station. Cir. 20. (1929). (Automatic method for recording dewpoint depending upon conductivity between platinum electrodes on glass thimble.)
(60) Industrial humidity instruments. M. F. Behar. Instruments 3, 549, 605, 659 (1930).
(61) A high-sensitivity absolute-humidity recorder. C. Z. Rosecrans. Ind. & Eng. Chem. Anal. Ed. 2, 129 (1930). (Thermal conductivity apparatus.)
(62) A simplified humidity control. W. H. Apthorpe and M. C. Marsh. J. Scientific Insts. 8, 152 (1931). (Hair element equipped with contacts.)
(63) Control of relative humidity in a small enclosed space. F. T. Carson. Paper Trade Journal (Oct. 1931). (Describes water-sulfuric acid and water-glycerine mixture method of humidity control.)
(64) Resistance thermometers for the measurement of relative humidity or small temperature differences. D. C. Rose, Can. J. Research 5, 156 (1931).
(65) An improved method of maintaining constant humidity in closed chambers. R. H. Stoughton. J. Sci. Inst. 8, 164 (1931). (Hygrotstat controls air circulation past a wet muslin surface.)
(66) The water content of saturated air at temperatures up to 100° C. J. H. Awbery. Proc. Phys. Soc. London 44, 143 (1932). (Determined by gravimetric method.)
(67) The basic law of the wet- and dry-bulb hygrometer at temperatures from 40 to 100° C. J. H. Awbery and E. Griffiths. Proc. Phys. Soc. London 44, 132 (1932). (Description of experimental determination of psychrometric chart at elevated temperatures based on gravimetric and dewpoint measurements. Data presented.)
(68) Über thermoelektrische Feuchtigkeitsmessung. L. Kettenacker. Z. für Instrumentenkunde 52, 319 (1932).
(69) Determination of relative humidities by means of thermocouples. J. H. Lanning. Ind. Eng. Chem. Anal. Ed. 4, 286 (1932).
(70) Apparatus for the measurement of relative humidity. J. H. Orchard. Trans. Phys. Soc. London 44, 224 (1932). (Description of a platinum resistance thermometer psychrometer).
(71) An experimental study of the wet-bulb hygrometer. T. K. Sherwood and E. W. Comings. Trans. Am. Insti. Chem. Eng. 28, 88 (1932).
(72) Ein Psychrometer ohne künstliche Belüftung. H. Wald, Z für d. ges Kalte-Ind. 39, 111 (1932).
(73) The theory of the psychrometer. J. H. Arnold. Physics 4, 255 (1933).
(74) Some improvements in psychrometry. D. B. Brooks and H. H. Allen. J. Wash. Acad. Sci. 23, 121 (1933).
(75) Color changes in hygroscopic salts and their use for humidity measurements. Alfred Swartz. Messtechnik 9, 87 (1933).
(76) Supplying atmospheres of known humidity. A. C. Walker. Bell. Lab. Record VII, 169 (1933). (Dry and saturated air mixed to produce desired relative humidities. Method used to test L&N thermal conductivity humidity recorder.)
(77) The Mollier Psychrometric Chart. F. Keppler Refrig. Eng. 27, 136 (1934).
(78) The present state of psychrometric data. Keyes and Smith. Refrig. Eng. 27, 127 (1934).
(79) An apparatus for the determination of the dewpoint. E. B. Moss. Proc. Phys. Soc. 46, 450 (1934).
(80) A formula and tables for the pressure of saturated water vapor in the range 0 to 374°C. N. S. Osborne and C. H. Meyers. J. Research NBS 13, 1 (1934) RP691.
(81) An investigation of the wet- and dry-bulb hygrometers at low temperature. J. H. Awbery and E. Griffiths. Proc. Phys. Soc. of London 47, 684 (1935).
(82) Psychrometric charts for high and low pressures. D. B. Brooks. NBS Pub. M146 (1935) (out of print).
(83) The transient condition of the human hair hygrometer element. A. F. Spilhaus. Mass. Inst. Tech. Meteoro. Course (Cambridge, Mass.). Professional Notes No. 8 (1935).
(84) A new method for the analytical determination of the water content of liquids and solids. Karl Fischer. Angew. Chem. 48, 394 (1935).
(85) A sulfuric acid hygrometer. A. Blackie. J. Sci. Inst. 13, 6 (1936). (Absorption hygrometer that gives vapor pressure of water directly.)
(86) A vapor pressure hygrometer. J. J. Dowling. J. Sci. Inst. 13, 214 (1936). (Moisture content of air determined by reduction in pressure of a fixed volume due to absorption by a chemical drying agent.)
(87) The deviation of the actual wet-bulb temperature from the temperature of adiabatic saturation. D. Dropkin. Cornell U. Eng. Exp. Stat. Bul. No. 23 (1936).
(88) The behavior of a single-hair hygrometer under varying conditions of temperature and humidity. W. G. Iles and K. Worsnop. Trans. Phys. Soc London 48, 358 (1936).
(89) Messung der Luftfeuchtigkeit mit Thermoelementen ohne künstliche Beluftung. Von We. Koch. Gesundheits-Ingenieur 59, 504 (1936).
(90) The use of thermocouples for psychrometric purposes. R. W. Powell. Trans. Phys. Soc. London 48, 406 (1936).
(91) The measurement of very low relative humidities. A. Simons. Proc. Phys. Soc. London 48, 135 (1936).
(92) A humidity control device for ovens. C. T. Webster. J. Sci. Inst. 13, 412 (1936). (Psychrometer controls steam injection and excess moisture condensation.)
(93) A review of existing psychrometric data in relation to practical engineering problems. W. H. Carrier and C. O. Mackey. ASME Trans. 59, 32 and 528 (1937).
(94) An electrical hygrometer and its application of radio meteorography. F. W. Dunmore. J. Research NBS 20, 723 (1938) RP1102.
(95) Determination of low humidity with dewpoint potentiometer. A. K. Frank. G. E. Rev. 41, 435 (1938).
(96) New tables of the psychrometric properties of air-vapor mixtures. W. Goodman. Heating, Piping

and Air Cond. 10, 1, 119 (1938). (Based on Keenan and Keyes steam tables.)
(97) Accurate determination of dewpoint. A. W. Hixson and G. E. White. Ind. & Eng. Chem. Anal. Ed. 10, 235 (1938).
(98) The effect of radiation on psychrometic reading. D. Dropken. Cornell U. Exp. Stat. Bul. 26 (Oct. 1939).
(99) An improved electrical hygrometer. F. D. Dunmore. J. Research NBS 23, 701 (1939) RP1265.
(100) The psychrometric chart, its application and theory. W. Goodman. Heating, Piping and Air Cond. 11, 357, 421, 485, 549, 613, 671, 749 (1939); 12, 6, 107, 171, 239, 303, 367, 431, 486 (1940).
(101) Study of Rideal absorption hygrometer. H. W. Harkness. Rev. Sci. Inst. 10, 237 (1939).
(102) Dewpoint hygrometer for use at low temperature. C. A. Winkler. Canadian J. of Research 17, Sec. D, 35 (1939).
(103) An improved radiosonde and its performance. H. Diamond, W. S. Hinman, F. W. Dunmore, and E. G. Lapham. J. Research NBS 25, 327 (1940) RP1329. (Electric hygrometer.)
(104) A dewpoint recorder for measuring atmospheric moisture. C. W. Thornthwaite and J. C. Owen. Monthly Weather Review 68, 315 (1940).
(105) Studies with the condensation hygrometer. T. Okada and M. Tamura. Proc. Imp. Acad. (Tokyo) 16, 141 and 208 (1940).
(106) Equipment for conditioning materials at constant humidities and at elevated temperature. J. G. Wiegerink. J. Research NBS 24, 639 (1940) RP1303.
(107) A new psychrometric chart for low temperatures and humidities. C. W. Deverall. Heating and Ventilating 38, 51 (June 1941). (Expanded scale at low temperature.)
(108) The construction and use of a thermoelectric psychrometer. C. Lorenzen, Jr. Temperature—Its measurement and control in science and industry. American Institute of Physics, p. 660 (1941).
(109) The optical hygrometer and its working. L. D. Mahajan. Indian J. Physics 15, 425 (1941).
(110) Electric dewpoint recorder. R. H. Reed. In symposium on Temperature—Its measurement and control in science and industry. American Institute of Physics, p. 655 (1941).
(111) Chemical absorption hygrometer as meteorological instrument. C. W. Thornthwaite. Trans. Am. Geophys. Union, pt II, 417 (August 1941).
(112) On the measurement of water vapor in gases. F. C. Todd and A. W. Gauger. Proc. Amer. Soc. Test. Mat. 41, 1134 (1941). (Colorimetric method described using cobaltous bromide in n-butyl alcohol as an indicator).
(113) Study of electric hygrometer. R. N. Evans and J. E. Davenport. Ind. & Eng. Chem. (Anal. ed.) 14, 507 (1942).
(114) Bridge controlled relay circuit for Dunmore relative humidity elements. R. L. Andrews. Rev. Sci. Inst. 14, 276 (1943).
(115) Two nomographs for low and high wet-bulb range solve psychrometric problems. E. Berl and G. A. Sterbutzel. Chem. & Met. Eng. 50, 142 (Dec. 1943). (Alignment charts for obtaining relative humidity from dry- and wet-bulb readings.)
(116) A spectroscopic hygrometer. L. W. Foskett and N. B. Foster. Bul. Am. Meteoro. Soc. 24, 146 (1943). Abstract, Aero. Eng. Rev. 2 (April 1943).
(117) Calculation of the relative humidity from hair hygrometer readings during balloon ascents. E. Glückauf. Qtr. J. Royal Meteoro. Soc. 70, 293 (1944). (Theoretrical investigation of low temperature lag of hair hygrometers and method of correcting radiosonde data.)
(118) Humid hysteresis of Mahajan's optical hygrometer and others. L. D. Mahajan. Indian J. Physics 18, 216 (1944).
(119) Time lag and humid fatigue of hygrometers. L. D. Mahajan. Indian J. Physics 18, 293 (1944).
(120) Meteorological investigations at Ikye, Part I. Instruments Branch (British) Air Ministry, JMRP No. 17 (May 1944). (Gregory humidiometer; relative humidity measured as a function electrical resistance of Egyptian cloth soaked in LiCl or $CaCl_2$ solution.)
(121) Psychrometry in the frost zone. D. D. Wile. Refrig. Eng 48, 291 (1944).
(122) Ein neuer Feuchigkeitsmesser; das Diffusionshygrometer. H. Greinacher. Hel. Phys. Act. 17, 437 (1944).
(123) A colorimetric method for determining the water vapor content in fuel gases utilizing the Evelyn colorimeter. R. J. Pfister and D. J. Kirley. Amer. Soc. T .st. Mat. Bul. 127, 17 (1944).
(124) Spectrophotometer for determination of water vapor in vertical column of atmosphere. N. B. Foster and L. W. Foskett. J. Optical Soc. Am. 35, 601 (1945). (Use phototube to measure changes in absorption of sun's spectral band, 9340 angstroms, due to water in path.)
(125) A photoelectric hygrometer. B. Hamermesh, F. Reines, S. Korff. Nat. Adv. Com. Aero. Tech. Note 980 (1945). (Absorption of spectral band measured by photoelectric means.)
(126) Hitemp psychrometric chart. O. T. Zimmerman and I. Lavine. Industrial Research Service, Dover, N. H. (1945). $12.50.
(127) Meteorology of the lower stratosphere. G. M. B. Dobson. Proc. Roy. Soc. A185, 144 (1946).
(128) Low-pressure properties of water from —160 to +212°F. J. A. Goff and S. Gratch. Heating, Piping and Air Conditioning, (1946).
(129) Recorder and controller for temperature and humidity. V. D. Hauck, R. E. Strum and R. B. Colt. Electronics 19, 96 (1946). (Human hair element periodically controls an electrical resistance.)
(130) Illinois Testing Laboratories dewpoint indicator. Instruments 19, 278 (1946).
(131) A method of measuring temperature on the skin and clothing of a human subject. L. W. Ogden and W. H. Rees. Shirley Institute Memoirs XX, 163 (1946). (Description of electric hygrometer made by boiling cotton fabric in LiCl solution. Relative humidity is a function of resistance and temperature.)
(132) A simple theory of the electric hygrometer. W. Schaffer. Bul. Am. Meteoro. Soc. 27, 147 (1946).
(133) Hygrometer for high pressure gases. W. W. Beuchner and L. R. McIntosh. Rev. Sci. Inst. 18, 586 (1947).
(134) Investigation on absorption hygrometers at low temperatures. E. Glückauf. Proc. Phys. Soc. London 59, 344 (1947). (Description of divided flow type of test apparatus, performance of goldbeater's skin elements, and the electric hygrometer as a function of temperature.)
(135) An improved continuous indicating dewpoint meter. F. A. Friswold, R. D. Lewis and R. C. Wheeler, Jr. NACA Tech. Note No. 1215. Washington, D. C. (Feb. 1947).
(136) Humidity measurement by a new ssytem: Dewcel. W. F. Hicks. Refrig. Eng. 54, 351 (1947). Also Instruments 20, 1128 (1947). (Foxboro electric hygrometer.)
(137) New method of measuring relative humidity. F. Lichtgarn. Instruments 20, 336 (1947). (Preliminary results on the use of ceramic materials as electrical resistance elements.)

(138) Analysis of gas mixtures containing a para-electric component. N. Schwarz. Physica (Holland) A1, 47 (1947). (Thermal conductivity effect increased by an electric field imposed on gas sample.)

(139) Serdex hygrometer. Rev. Sci. Inst. 18, 591 (1947). (Goldbeater's skin hygrometer.)

(140) The measurement of humidity. H. S. Gregory. Instrument Practice 1, 367, 447 (1947).

(141) A theoretical basis for the diffusion hygrometer. H. Spencer Gregory and E. Rourke. Phil. Mag. 38, 573 (1947).

(142) Surface Combustion Corp. furnace-atmosphere humidity recorder. Instruments 20, 730 (1947).

(143) Psychrometric moisture determination in gases. H. Bruckhoff. Arch. Tech. Messen. *Issue No. 152*, T17 (1947).

(144) A method for the continuous measurement of dewpoint temperatures. D. N. Bussman. Report of Dept. of Meteorology, U. of Chicago.

(145) An automatic dewpoint meter for the determination of condensable vapors. T. T. Puck. Rev. Sci. Inst. 19, 16 (1948).

(146) Moisture measurement with an electronic dewpoint indicator. V. E. Suomi. Instruments 21, 178 (1948).

(147) Measurement of water in gases by electrical conduction in a film of hygroscopic material and the use of pressure changes in calibration. E. R. Weaver and R. Riley. J. Research NBS 40, 169–214 (1948) RP1865. (For a description of of commercial model see Instruments 20, 160 (1947). (Electric hygrometer). (Supt. of Documents, Washington 25, D. C.). 25¢.

(148) Weston all-metal humidity indicator. Rev. Sci. Inst. 19, 123 (1948).

(149) Divided flow type, low temperature humidity test apparatus. Arnold Wexler. J. Research NBS 40, 479 (1948) RP1894. (Supt. of Documents, Washington 25, D. C.). 10¢. (Describes method of combining dry and saturated air to produce desired relative humidities.)

(150) Low temperature performance of radiosonde electric hygrometer elements. Arnold Wexler. J. Research NBS 43, 49 (1949) RP2003. (Supt. of Documents, Washington 25, D. C.). 10¢

(151) Some possible sources of error in operating the Assmann psychrometer. M. E. Woolcock. Instrument Practice 4, no. 1, 13 (1949).

(152) Biplastic strip hygrometer. Mod. Plastics 26, 73 (March 1949).

(153) A recording microwave refractometer. George Birnbaum. Rev. Sci. Inst. 21, 169 (1950).

(154) Test and adaptation of the Foxboro dewpoint recorder for weather observatory use. J. H. Conover. Bul. Am. Meteoro. Soc. 31, no. 1, 13 (Jan. 1950). (Tests on Dewcel for accuracy, lag and utility for meteorological use.)

(155) Recirculating apparatus for testing hygrometers. Arnold Wexler. J. Research NBS 45, 357 (1950) RP2145.

(156) Versatile pneumatic instrument based on critical flow. W. A. Wildhack. Rev. Sci. Inst. 21, 25 (1950).

(157) Apparatus for recording fluctuations in the refractive index of the atmosphere at 3.2 centimeters wavelength. C. M. Crain. Rev. Sci. Inst. 21, 456 (1950).

Pressure-Humidity Apparatus[1]

Arnold Wexler and Raymond D. Daniels, Jr.

An apparatus for producing atmospheres of known relative humidity, based on the "two-pressure principle", is described. It has a working space (test chamber) of 1 cubic foot, in which the relative humidity may be varied and controlled from 10 to 98 percent, the temperature from −40° to +40° C, the air flow up to 150 liters per minute, and the test-chamber pressure from ½ to 2 atmospheres. The humidity in the test chamber may be set and maintained to an accuracy of at least ½ of 1-percent relative humidity.

1. Introduction

The pressure-humidity equipment is a laboratory apparatus for producing atmospheres of known relative humidity by control of the pressure in the test chamber of air saturated at a higher pressure. As this apparatus was developed primarily for hygrometer research and calibration, especially on electric hygrometer elements, which, during use, are subjected to a wide temperature range, it was essential that the temperature of the working space should be adequately controlled and maintained at any desired value from −40° to +40° C. Futhermore, it was desirable that any relative humidity, from 10 to 98 percent, should be conveniently produced and that a change could be made rapidly from any one value of relative humidity to any other value. Finally, it was also desirable to have a means of varying the rate of air flow through the working space, selected to have a volume of about 1 ft³.

An apparatus has been developed that successfully meets the above requirements. It operates on what may be called the "two-pressure principle." Basically, the method, shown in elemental schematic form in figure 1, involves saturating air, or any gas, with water vapor at a high pressure and then expanding the gas to a lower pressure. If the temperature is held constant during saturation and upon expansion, and the perfect gas laws are assumed to be obeyed, then the relative humidity, RH, at the lower pressure, P_t, will be the ratio of the absolute values of the lower pressure, P_t, to the higher pressure, P_s, that is, $RH=100\times P_t/P_s$.

Water vapor-air mixtures depart from ideal gas behavior, so that the simple pressure ratio does not strickly define the relative humidity. Weaver [2] [3] has shown that an empirical equation of the form

$$RH=100\times\frac{P_t}{P_s}\frac{(1-KP_t)}{(1-KP_s)},$$

where the constant K has a value of 0.00017 when the pressure is expressed in pounds per square inch, more closely yields the true relative humidity. The magnitude of the correction introduced by the term $(1-KP_t)/(1-KP_s)$ is shown in table 1 for the applicable range of test-chamber pressures (½ to 2 atm) and relative humidities (10 to 100%). With atmospheric pressure in the test chamber the maximum error does not exceed ¼ of 1-percent relative humidity and hence, for most work, may be neglected. Even at a test-chamber pressure of 2 atm, the maximum error is less than 0.5-percent relative humidity. For very precise work, it is preferable to use the empirical equation.

TABLE 1. *Error due to nonideal behavior of water-vapor–air mixtures*

Test-chamber pressure	Relative humidity, percent					
	100	80	60	40	20	10
	Error in relative humidity, percent					
abs atm						
½	0	0.02	0.05	0.08	0.10	0.11
1	0	.05	.10	.15	.20	.23
2	0	.10	.20	.30	.41	.47

The pressure method was developed by Weaver and Riley (see footnote 2) for the calibration of electrically conducting hygroscopic films used in the measurement of water vapor in gases. Their equipment was designed for low rates of gas flow and was used under ambient room-temperature conditions.

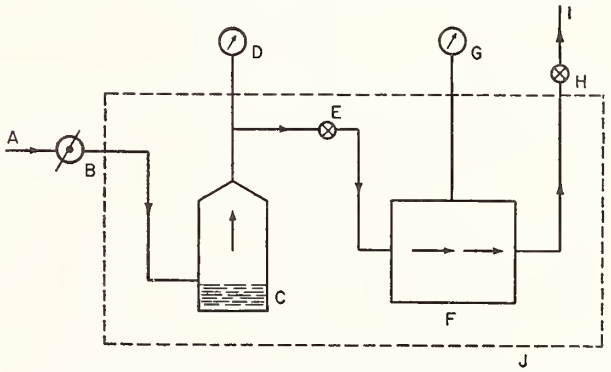

FIGURE 1. *Simplified schematic drawing of the principle of operation of the pressure-humidity apparatus.*

A, high-pressure air source; B, pressure regulator; C, saturator; D, pressure gage; E, expansion valve; F, test chamber; G, pressure gage; H, exhaust valve; I, atmosphere or vacuum source; J, constant-temperature bath.

[1] The development of this apparatus was sponsored by the Aerology Branch of the Bureau of Aeronautics.
[2] E. R. Weaver, and R. Riley, J. Research NBS 40, 169 (1948) RP1865.
[3] E. R. Weaver, Anal. Chem. 23, 1076 (1951).

Their saturator was a small cylinder, containing water and filled with fragments of pumice or stream-washed gravel through which the gas could be bubbled under pressure.

2. Description of Apparatus

The apparatus is shown in block diagram in figure 2 and schematically in figure 3. It consists, essentially, of the following functional components, through which air flows continuously: A high-pressure air source, a low-temperature drying system, a filtering system, a warm-up unit, a pressure regulator, a humidifying system, an expansion valve, a test chamber, and an exhaust control system.

Air is supplied from a 250-psig reciprocating compressor, *A1*, figure 3, capable of delivering 5 ft^3/min of free air at room temperature. This air is filtered (*A2*) to remove pipe scale, dirt, dust, or other solid material, and is then introduced into the drying system (fig. 4).

Water from the air at the supply pressure is removed by freezing in a train of four drying units immersed in a bath, *D*, containing a mixture of dry ice and Stoddard solvent. The first two units, *A4* and *A5*, are large-capacity centrifugal water separators. These are followed by a copper coil, *A6*, and a baffle dryer, *A7*. Particles of snow or ice and droplets of oil (from the compressor) are caught by a filter, *A8*, which is maintained immersed in the same low-temperature bath, *D*.

The air emerges from the dryer at about −78° C. It is then heated in the warm-up unit to a temperature somewhat greater than that being maintained in the thermostatted liquid bath, *B*. The warm-up unit consists of an electric heater, *A9*, that is controlled by a thermoregulator, *A10*. Two pressure regulators, *A13*, and *A14*, in series reduce the pressure and maintain it constant in the hymidifying system.

Saturation is accomplished in four stages. The air is first passed through the external gross saturator, *A15*, which is kept at a higher temperature than the bath, *B*, and then through the three bath saturators, *A18*, *A20*, and *A22*. The gross saturator, because of its higher temperature, introduces water vapor in excess of that required for complete saturation at bath temperature. The combination of heat exchangers *A17*, *A19*, and *A21* and centrigfugal saturators *A18*, *A20*, and *A22* precipitates this excess water vapor so that just complete saturation is obtained in the final saturator, *A22*. The bath saturators and heat exchangers are shown in figure 5.

The saturators are simple in design and function equally well below as well as above the freezing point of water. They are similar to a type previously used [4] with considerable success. Each saturator consists of a cylinder to which water is added to a convenient depth. Air is discharged through a nozzle into the chamber above the water surface and tangential to the vertical walls and is exhausted through a central port in the top. The centrifugal force creates a whirlpool action that thoroughly mixes the water vapor with air. Spray and liquid water are forced to the walls by centrifugal force, so there is little tendency for liquid water

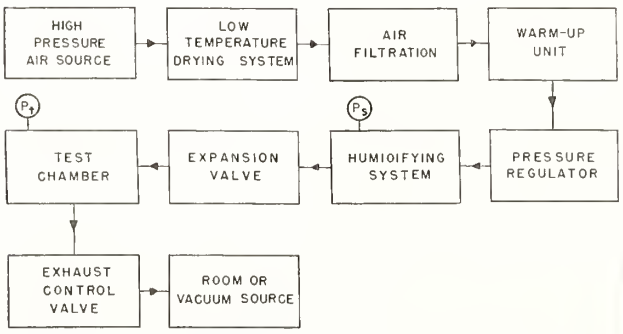

FIGURE 2. *Block diagram of the pressure-humidity apparatus.*

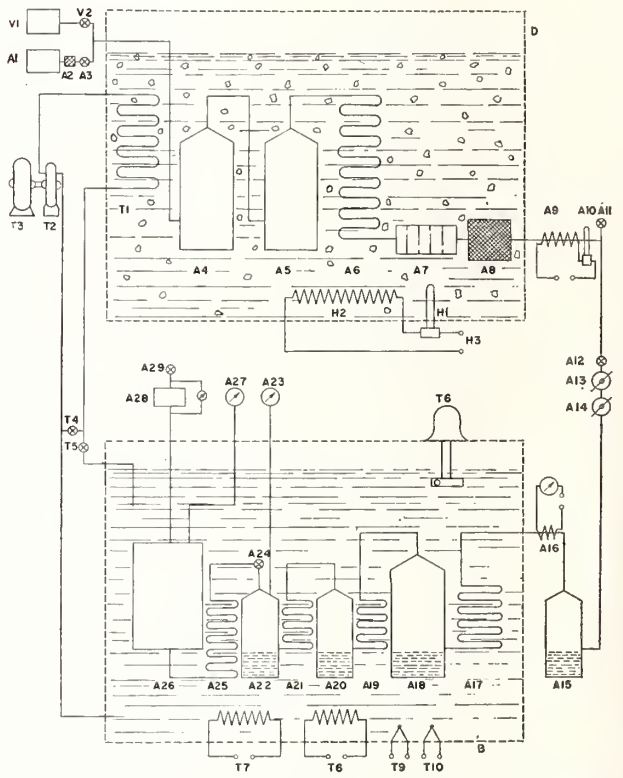

FIGURE 3. *Schematic flow diagram of the pressure-humidity apparatus.*

A1, high-pressure source; A2, filter; A3, valve; A4, centrifugal water separator; A5, centrifugal water separator; A6, copper cooling coil; A7, fin air dryer; A8, low-temperature filter; A9, electric heater; A10, bimetal thermoregulator; A11, air reversal valve; A12, shut-off valve; A13, pressure regulator; A14, pressure regulator; A15, external gross saturator; A16, resistance thermometer and indicator; A17, 19, 21, 25, copper coil heat exchangers; A18, 20, 22, centrifugal saturators; A23, 27, pressure gages; A24, expansion valve; A26, test chamber; A28, linear flowmeter; A29, exhaust control valve; B, insulated liquid (Stoddard solvent, constant-temperature bath; D, insulated dry-ice batb; H1, bimetal thermoregulator; H2, electric heater; H3, input voltage; T1, Stoddard solvent cooling coil; T2, positive rotary displacement pump; T3, motor; T4, Stoddard solvent bypass valve; T5, Stoddard solvent control valve; T6, centrifugal stirrer; T7, constant electric heater; T8, intermittent electric heater; T9, 10, thermistors; V1, vacuum source; V2, vacuum shut-off valve.

[4] Arnold Wexler, J. Research NBS 45, 357 (1950) RP2145.

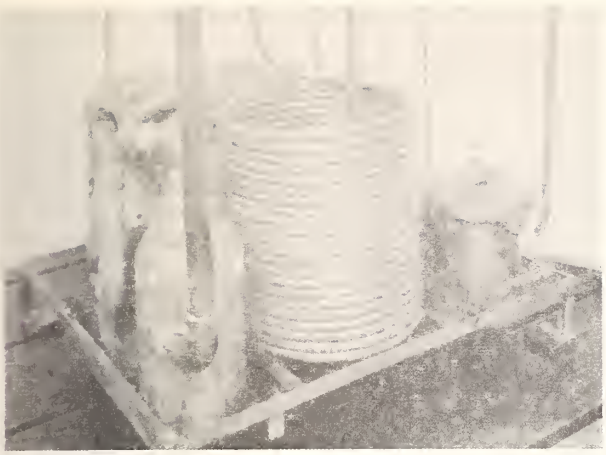

FIGURE 4. *Drying system and Stoddard solvent cooling coil.*

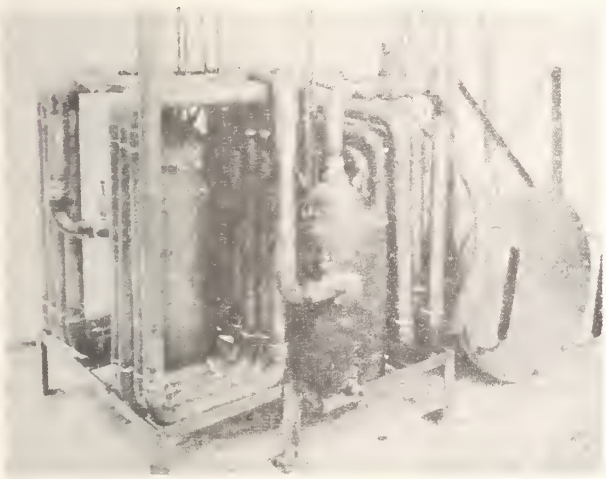

FIGURE 5. *Bath saturators, heat exchangers, and test chamber.*

to emerge through the exit port. A multilayer fine-wire screen baffle is used at the exit as a further guard against the escape of liquid water. As air does not bubble through the water but only passes over its exposed surface, the water may be frozen without impairing the functioning of the saturator.

Upon emerging from the final saturator, *A22*, the pressure of the air is reduced by expansion valve *A24*. Because a temperature drop may occur in the air at the expansion valve, a final heat exchanger, *A25*, is provided for bringing the air to bath temperature before it enters the test chamber, *A26*.

The working space, *A26*, is a cylindrical chamber having a nominal volume of 1 ft^3. It is shown with the cover removed in figure 6. Tubular outlets extend from the chamber to allow electric leads to be brought in and out of the working space. The air discharges from the chamber into a linear flowmeter, *A28*, and then through an exhaust control valve, *A29*, into a vacuum source or simply into

FIGURE 6. *Test chamber with cover removed.*

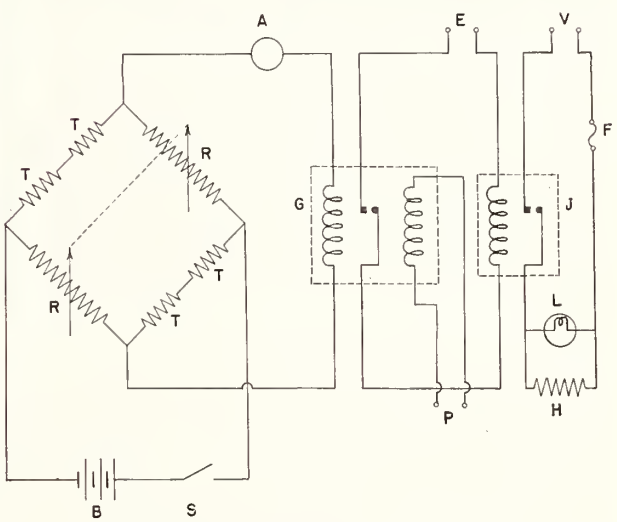

FIGURE 7. *Temperature control circuit.*

T, Thermistor; R, precision helical rheostat; B, 22½-v battery; S, battery switch; A, microammeter; G, ½ a galvanometer relay; P, input from pulsing circuit; F, fuse; J, power relay; E, input voltage for power relay coil; H, intermittent bath heater; V, input voltage for intermittent heater; L, pilot lamp.

the room air. The chamber is suspended from a counterweight system so that it can be easily raised above or immersed into the liquid bath, *B*. A length of flexible metal hose, between the test chamber, *A26*, and the final heat exchanger, *A25*, permits the test chamber to have the required motion.

The saturation pressure, P_s, is measured in the final saturator, *A22*, by gage *A23*, and the test pressure is measured in the test chamber by gage *A27*. These measurements are made with high-precision

laboratory test gages that have been calibrated against the National Bureau of Standards pressure standards. For atmospheric or reduced pressures, a high-quality calibrated aneroid barometer is used. From atmospheric pressure up to 2 atm, a mercurial manometer is employed. The higher pressures are determined with either a 0- to 50-psig or a 0- to 200-psig Bourdon tube gage.

The temperature of the liquid bath, *B*, can be adjusted to and closely regulated at any temperature from −40° to +40° C by a simple on-off thermostatting system. Stoddard solvent, which is used as the bath liquid so that low temperatures may be attained, is actively agitated by a centrifugal stirrer, *T6*, and is circulated from the bath, *B*, by a positive rotary displacement pump, *T2*, through a copper coil, *T1*, immersed in a mixture of dry ice and Stoddard solvent in bath *D* and back into bath *B*. By proper manual setting of a bypass valve, *T4*, and a control valve, *T5*, the rate of Stoddard solvent flow is adjusted so that the bath *B* tends to cool slightly. The desired bath temperature is established by resistances (coupled helical precision rheostats), *R*, in a Wheatstone bridge circuit, figure 7. Thermistors, *T*, with temperature coefficients of 4 percent/deg C, are employed as the temperature-sensitive elements. Any cooling disturbs the bridge balance, which is sensed by a galvanometer relay, *G*. A current of ½μa deflects the galvanometer pointer against a magnetic contact, actuating a power relay, *P*, and, in turn, intermittent bath heater, *H*. The operation of an electromagnetic plunger returns the pointer to a sensing position. If the bridge is unbalanced, the pointer will deflect and again throw on the heater; if the bridge is in balance, the pointer will remain in a null position. An electronic pulsing circuit, *P*, periodically triggers the plunger so that the pointer may sense the bridge balance.

3. Operation of Apparatus

The method of operation of this equipment is simple. The instrument, material, or device under investigation is inserted into the test chamber, the latter closed and immersed into the liquid bath. Distilled water is added to each saturator to an appropriate depth. Solid carbon dioxide is then added to the dry-ice bath, *D*. The temperature of the liquid bath is brought to and maintained at the desired value. Air from the high-pressure source is allowed to pass through the apparatus and the pressures in the saturators and test chamber adjusted to give any preselected relative humidity. The thermoregulator controlling the temperature of the air passing through the warm-up unit is set to maintain a temperature in the external saturator several degrees higher than in the liquid bath. When thermal equilibrium had been established in the components in the liquid bath, the pressure ratio indicates the correct relative humidity in the test chamber. Changing the relative humidity primarily involves adjusting the pressure regulators so that they will maintain a new pressure in the saturators. To maintain a constant air flow, a minor adjustment of the expansion valve is also made.

When atmospheric pressure is desired in the test chamber, the air emerging from the chamber is allowed to exhaust directly into the room. Elevated pressures in the chamber are obtained by throttling the flow from the chamber by means of the exhaust control valve, *A22*, figure 3. Reduced pressures in the chamber are achieved by attaching a vacuum source to the exhaust control valve and adjusting the valve to give the required reduced pressure.

In operating below freezing, one precaution must be observed. The level of the water in each saturator must be kept below the inlet nozzle, otherwise, on freezing, the opening will be sealed by ice.

The equipment may be operated continuously for 8 to 16 hr, after which the accumulated water in the dryer should be removed. Failure to do so may result in clogging of the dryer by ice and the reduction, or even complete stoppage, of air flow.

The removal of water from the dryer is accomplished in two steps. First the dry ice bath is raised to room temperature by a thermostat, *H1*, and heater, *H2*. Then suction is applied by vacuum source *VI* and room air drawn through the reversal valve, *A11*, and dryer until all the water has been evaporated. Overnight operation usually suffices to remove most of the water.

4. Performance and Accuracy

The psychrometric and dew-point methods of humidity measurement were used independently to evaluate the accuracy of the humidity produced by the equipment. A thermocouple wet-and-dry-bulb hygrometer was employed over a wide range of relative humidities and at temperatures from 0° to 30° C. A dew-point instrument having a thermocouple embedded just below the surface of a small (¼ in. in diameter) mirror for temperature measurement, manually controlled heating and cooling of the mirror, and visual observation through a telescope for dew and frost detection, was constructed and used to measure dew points from room temperature down to −27° C. A series of experiments was made in which the relative humidity measured by the above two methods was compared with the relative humidity given by the ratio of the test-chamber pressure to the saturator pressure. The results are shown in table 2. The average difference in percentage of relative humidity between the psychrometrically determined values and the apparatus values given by the pressure ratio is ±0.4 percent, and the average difference in percentage of relative humidity between the value determined by dew-point measurement, and the apparatus value given by the pressure ratio is ±0.6 percent. Similarly, the algebraic average differences are −0.2 and 0.0 respectively. It may be assumed that as there is no marked tendency for the differences to be either positive or negative, the air passing through the saturators emerges neither supersaturated or undersaturated.

Table 2. *Summary of calibration*

Date of run	Nominal ambient bath temperature	Relative humidity produced by pressure-humidity apparatus	Relative humidity measured by—		Difference in relative humidity between pressure-humidity apparatus and—	
			Dew-point hygrometer	Psychrometer	Dew-point measurement	Psychrometric measurement
	°C	%	%	%	%	%
3-28-51	23.5	96.1	----	96.2	-----	−0.1
		90.1	----	91.1	-----	−1.0
		81.6	----	82.3	-----	−0.7
		74.4	----	75.2	-----	−.8
		59.6	----	59.7	-----	−.1
		50.1	----	50.5	-----	−.4
		38.0	----	38.4	-----	−.4
		25.1	----	25.4	-----	−.3
3-28-51	9.7	92.9	----	92.4	-----	+.5
		79.8	----	79.8	-----	.0
		61.0	----	61.0	-----	.0
		49.5	----	49.3	-----	+.2
		37.2	----	37.0	-----	+.2
		24.6	----	24.2	-----	+.4
3-28-51	30.4	92.6	----	92.9	-----	−.3
		78.3	----	78.6	-----	−.3
		59.6	----	59.7	-----	−.1
		49.2	----	49.4	-----	−.2
		37.0	----	37.2	-----	−.2
		24.9	----	24.8	-----	+.1
4-6-51	24.7	97.9	96.7	----------	+1.2	-----
		88.8	88.7	----------	+0.1	-----
		77.6	75.9	----------	+1.7	-----
		77.4	77.9	----------	−0.5	-----
		54.8	55.4	----------	−.6	-----
		36.9	37.3	----------	−.4	-----
		23.0	23.9	----------	−.9	-----
4-16-51	6.0	96.9	97.0	96.9	−.1	0.0
		90.6	92.1	91.4	−1.5	−.8
		77.9	78.6	78.5	−0.7	−.6
		57.7	58.5	58.2	−.8	−.5
		42.7	42.9	42.6	−.2	+.1
4-18-51	6.0	96.2	96.3	94.7	−.1	+1.5
		53.9	54.7	53.8	−.8	+0.1
		36.6	36.6	36.7	.0	−.1
		28.3	28.4	28.8	−.1	−.5
		23.2	23.1	23.5	+.1	−.3
4-19-51	−4.8	96.8	97.1	----------	−.3	-----
		86.0	86.7	----------	−.7	-----
		74.7	74.7	----------	.0	-----
4-24-51	−9.6	76.4	75.9	----------	+.5	-----
		68.3	68.2	----------	+.1	-----
		54.1	53.5	----------	+ 6	-----
4-25-51	−19.8	96.3	95.6	----------	+ 7	-----
		88.0	89.1	----------	−1.1	-----
		78.7	78.2	----------	+0.5	-----
		66.4	65.0	----------	+1.4	-----
		56.7	55.6	----------	+1.1	-----
				Arithmetic avg.	±0.6	±0.4
				Algebraic avg.	.0	−.2

The relative-humidity range obtainable is limited by the range of ratios of test-chamber pressure to saturator pressure. The maximum saturator pressure that can be employed with this apparatus is about 150 psi. When the test chamber is maintained at its maximum pressure (about 2 atm), the minimum relative humidity is about 20 percent. At atmospheric pressure, a relative humidity as low as 10 percent is readily produced, and at a reduced pressure of ½ atm, the minimum relative humidity decreases to 5 percent.

The temperature range of the equipment extends from −40° to +40° C. The upper end is limited by the flash point of the bath liquid (Stoddard solvent). However, by substituting water for Stoddard solvent as the bath liquid, the upper end of the temperature range may be extended to about 90° C.

The accuracy with which any desired relative humidity may be established is a function of the uniformity of temperature in the apparatus, particularly in the final saturator and the test chamber. The relative humidity in the test chamber will be equal to the pressure ratio of the test chamber to final saturator only if these two units are at the same temperature. The distribution of temperature within the saturators, test chamber, and surrounding liquid bath was explored by means of thermocouples, located at the inlet, outlet, and in the water of each saturator, near the front and rear of the test chamber, and at four separate points within the liquid of the bath. As an indication of the variations in temperature that may exist in the apparatus, data are presented in table 3 of the average temperatures at various locations for three 2-hour runs at different ambient temperatures. It may be seen that the differentials are of minor magnitude, especially between the final bath saturator and the test chamber.

Table 3. *Temperature distribution*

Location	Temperature		
	°C	°C	°C
Initial bath saturator:			
Air inlet	9.55	23.33	30.24
Air outlet	9.57	23.30	30.25
Water	9.66	23.29	30.30
Intermediate bath saturator:			
Air inlet	9.63	23.35	30.45
Air outlet	9.65	23.36	30.44
Water	9.63	23.29	30.39
Final bath saturator:			
Air inlet	9.64	23.39	30.48
Air outlet	9.65	23.40	30.44
Water	9.66	23.36	30.43
Test chamber:			
Front	9.64	23.35	30.40
Rear	9.61	23.35	30.37
Bath:			
Side of test chamber	9.64	23.38	30.40
Expansion valve	9.64	23.39	30.40
Rear of test chamber	9.61	23.39	30.39
Bottom	9.58	23.38	30.39

The constancy of bath temperature is of importance, for quite often materials or hygrometers under investigation are temperature dependent. The control system has effectively regulated the bath at temperatures from −40° to +40° C. For periods of time of 2 to 5 hours, average fluctuations of 0.02 to 0.05 deg. have been observed.

5. Discussion

This equipment has been used successfully for calibration testing and research. The working space of 1 ft^3 is ample for most instruments, materials, and devices that have to be completely immersed in an atmosphere of known relative humidity. There is no theoretical limitation on the size of the test chamber that may be employed with this type of

equipment; a larger sized chamber would simply require a larger surrounding liquid bath. Neither is there any limitation on the geometry of the test chamber. A cylinder was chosen in this case for ease of construction, but any other space configuration can be substituted. Even in the present design, the cylindrical test chamber can be uncoupled from the setup, and, within the limitation of the available bath space, any other size, shape, or design of chamber can be attached.

Occasionally air of known or preestablished dew point is required at a place or instrument remote from the test chamber. The desired dew point can be readily produced by the apparatus, and all or part of the air from the test chamber can be piped wherever needed. The only limiting factor involves the temperature of the ambient air, which must not drop below the dew point of the air flowing through the transmission tubing, because condensation may occur in the lines.

The range of relative humidities obtainable with this type of equipment may be extended to much lower values by using a higher pressure source. A 250-psig compressor, operating between 150 to 200 psig, is used in the present design and provides relative humidities that are sufficiently low for most purposes. Much higher pressures would necessitate components capable of withstanding those high pressures. Similarly, for flows in excess of 5 ft^3/min, a compressor having a larger volume capacity would be required.

The rapidity with which the relative humidity may be changed depends primarily on the time involved in adjusting the pressure regulator, which controls the saturation pressure. Minor adjustments of the expansion valve and the exhaust control valve may be required after the major pressure adjustment has been made. These operations can easily be executed within 30 sec. At low rates of flow, the limiting factor ceases to be the time required for performing the above mechanical operations and becomes, instead, the time involved in purging air of one relative humidity, with air of another relative humidity. The component with the maximum air volume is the test chamber. It has a space of about 1 ft^3, so that the purging time depends upon the rate of air flow through this 1-ft^3 volume.

6. Summary

An apparatus of versatility and convenience for producing atmospheres of known relative humidity has been developed and constructed at the Bureau. It operates on the "two-pressure principle," whereby air is saturated at a high pressure and expanded to a lower pressure, the relative humidity at the lower pressure being the ratio of the lower to higher pressure, provided the operation is performed at constant temperature.

Important parameters can be varied and controlled over wide ranges: relative humidity from 10 to 98 percent; temperature from −40° to +40° C; flow up to 150 liters/min; test-chamber pressure from ½ to 2 atm. The relative humidity can easily be changed from one value to another within 30 sec.

Independent checks on the accuracy of the relative-humidity production with the psychrometric and dew-point methods have yielded average agreements of ±0.4 to ±0.6 percent. As the latter methods of measurement are probably no more accurate than about ±0.5 percent, it is reasonable to assume that the apparatus produces relative humidities that are known to at least ±0.5-percent relative humidity.

Washington, December 12, 1951

Relative Humidity-Temperature Relationships of Some Saturated Salt Solutions in the Temperature Range 0° to 50° C[1]

Arnold Wexler and Saburo Hasegawa

The relative humidity-temperature relationships have been determined in air in equilibrium with saturated salt solutions of lithium chloride, $LiCl \cdot H_2O$; magnesium chloride, $MgCl_2 \cdot 6H_2O$; sodium dichromate, $Na_2Cr_2O_7 \cdot 2H_2O$; magnesium nitrate, $Mg(NO_3)_2 \cdot 6H_2O$; sodium chloride, NaCl; ammonium sulfate, $(NH_4)_2SO_4$; potassium nitrate, KNO_3; and potassium sulfate, K_2SO_4, over a temperature range of 0° to 50° C, using the dewpoint method. The relative humidity is a continuous function of temperature, and, except for sodium chloride, is monotonic. The curve for sodium chloride increases from 74.9-percent relative humidity at 0° C to a maximum of 75.6 percent at 30° C and then gradually decreases to 74.7 percent. The maximum change in relative humidity with temperature, about 15-percent relative humidity as the temperature increases from 0° to 50° C, occurs with saturated salt solutions of sodium dichromate and magnesium nitrate.

1. Introduction

Saturated salt solutions are very useful in producing known relative humidities, principally for testing and calibrating selected hygrometers and hygrographs at temperatures above 0° C. The saturated salt solution is made up as a slushy mixture with distilled water and chemically pure salt in a glass or enameled tray and is enclosed in a sealed metal or glass chamber. When equilibrium conditions, usually hastened by forced air circulation or stirring, are attained, the chamber space is at a constant relative humidity. Some saturated salt solutions produce relative humidities that are roughly independent of temperature.

The equilibrium values of relative humidity of the saturated solutions of several salts used in calibration and testing are listed in NBS Circular 512 [1][2] and are based partly on vapor-pressure data given in the International Critical Tables [2] and partly on dewpoint measurements made at NBS. The relative humidity-temperature relationships of these, as well as several other, saturated salt solutions have been redetermined and are the subject of this paper.

The measurement of vapor pressure or vapor pressure lowering of a salt solution may be made in several ways. The differential methods are based on the determination of the difference in vapor pressure between the solution and solvent, using a sensitive differential manometer. In the dynamic method, the boiling point of the solution is determined under reduced pressure. The transpiration, or gas-saturation, method involves the gravemetric measurement of the water-vapor content of an inert gas saturated by passage over or through the salt solution. The dewpoint method consists in reducing the temperature of a mirror surface until condensation occurs.

The dewpoint method was utilized in this investigation. With this method, measurements could readily be made in the presence of an air atmosphere under conditions similar to those occurring in the use of saturated salt solutions for humidity-control purposes. Furthermore, other than using chemically pure salts of reagent grade and distilled water, no special precautions were taken. Thus the salts contained trace impurities, and the water was air saturated.

2. Description of Apparatus

The experimental setup shown in figure 1 was used to determine the equilibrium vapor pressure of a saturated salt solution. The bottom of a 2-liter Wolff flask, A, was filled to a depth of 2 inches with a saturated solution of a salt, B, made up as a slushy mixture with a pure reagent grade chemical and distilled water. A dewpoint apparatus, C, was inserted through one side neck of the flask; an air stirrer, D, was inserted through the central neck of the flask; and two copper-constantan thermocouples, E and F, were inserted through the other side neck of the flask. The Wolff flask was immersed in a liquid bath, O. Automatic temperature control of the bath was achieved by a system in which thermistors, in a bridge circuit, detected the temperature unbalance and a heater, H, supplied heat in proportion to the unbalance. Below room temperature, a cooling system, I, was used to reduce the bath temperature.

The shaft of the air stirrer, D, was supported in a close-fitted bearing and driven, through a belt and pulley, by an external remotely positioned motor.

Thermocouple, E, measured the air temperature within the Wolff flask, thermocouple, F, measured the temperature of the saturated salt solution, and thermocouple, H, measured the temperature of the liquid bath. These thermocouples were made with cotton-covered Bakelite-insulated wire. To insure that no spurious electromotive force would be

[1] This investigation was financially supported by the Aerology Branch, Bureau of Aeronautics, Department of the Navy.

[2] Figures in brackets indicate the literature references at the end of this paper.

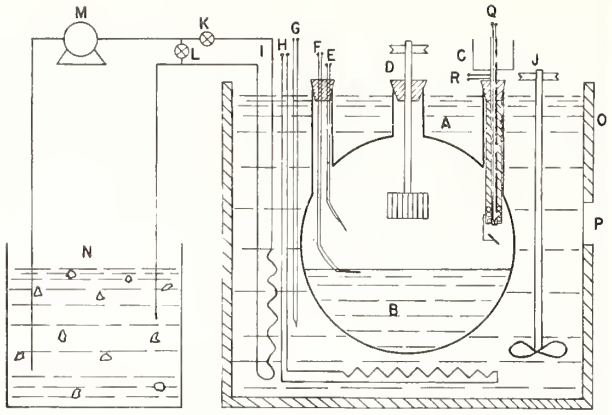

FIGURE 1. *Experimental setup.*

A, 2-liter Wolff flask; B, saturated salt solution; C, dewpoint apparatus; D, air stirrer; E, thermocouple for measuring air temperature; F, thermocouple for measuring temperature of saturated salt solution; G, thermocouple for measuring bath temperature; H, bath heater; I, cooling system; J, liquid bath stirrer; K, cooling system control valve; L, cooling system by-pass valve; M, cooling system pump; N, Stoddard's solvent mixed with dry ice; O, liquid thermostated bath; P, position external to bath from which a light is projected on the dewpoint mirror and from which the dewpoint mirror is observed with a telescope.

introduced because of electrolytic action, each junction was coated and protected with polystyrene cement. The thermocouple leads were covered with grounded equipotential shields. A precision potentiometer was used to measure the thermocouple electromotive force with a precision of better than 1 microvolt.

A light was projected on the dewpoint mirror and the mirror was viewed, through a telescope, from position, P, external to the liquid bath.

Details of the dewpoint apparatus are shown in figure 2. A brass cup, A, 3 inches in diameter and 3 inches deep, was attached to one end of a ¼-inch-outside-diameter copper tube, B, 1/32-inch in wall thickness. A dewpoint mirror, H, was soldered to the other end of the copper tube. This mirror, ¼-inch-outside-diameter and ⅛ inch thick, was machined from copper, with a recess equal to the wall thickness of the copper tube so that it would fit snuggly in the end of the tube. The reflective surface of the mirror was first ground and polished, then plated with chromium, and finally lapped to within one-half fringe of optical flatness. A 1-mm-diameter hole was drilled in the center of the mirror, from the rear, to within about 1/64 inch of the front reflective surface. A copper-constantan thermocouple, C, B&S gage No. 30, was inserted into the hole and soldered to the mirror.

An insulated-wire heater, E, was wound around the copper tube close to the mirror end. This heater was controlled by a variable transformer from a 60-cycle a-c power source. Glass-wool insulation, G, was wrapped around the copper tube and retained in position by a Bakelite tube, F, ¾-inch outside diameter. A galvanometer mirror, I, attached to the Bakelite tube by a metal bracket, J, allowed convenient viewing of the dewpoint mirror.

The addition of dry ice and alcohol to the brass cup, A, figure 2, served as a cold source for cooling

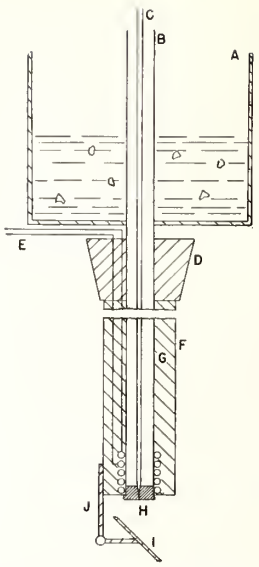

FIGURE 2. *Dewpoint apparatus.*

A, Brass cup; B, copper cooling tube; C, thermocouple; D, rubber stopper; E, heater; F, Bakelite tube; G, glass wool insulation; H, dewpoint mirror; I, viewing mirror; J, support bracket.

the dewpoint mirror, H, through conduction along the copper tube, B. By decreasing the voltage applied to heater, E, the temperature of the dewpoint mirror could be lowered gradually until dew or frost was detected. By increasing the voltage applied to heater, E, the temperature of the mirror could be raised slowly until all dew or frost disappeared. The dewpoint mirror temperature corresponding to the instant of appearance and disappearance was measured by thermocouple, C.

3. Experimental Procedure

The procedure employed in making observations was to adjust the liquid-bath temperature to some desired value and then permit the Wolff flask, with its contents to come to temperature equilibrium. After equilibruim had been established, an observer would manipulate the dewpoint heater control and simultaneously view the dewpoint mirror until he had obtained five successive appearances and disappearances of dew or frost on the dewpoint mirror. A second observer would then repeat the process under the same operating conditions. Occasionally, the two observers would take repeat sets of observations. In this fashion, for any one salt, data were obtained at 10-deg. intervals from 0° to 50° C.

4. Results

For purposes of this investigation, it was assumed that the dewpoint corresponded to the mean of the observed temperature at which dew first appeared and then disappeared. For a given observer, each dewpoint therefore corresponded, usually, to the average of a minimum of 10 temperature observa-

TABLE 1. *Observed temperature-relative humidity data*

Lithium chloride $LiCl \cdot H_2O$						
Temperature °C	0.23	9.56	19.22	29.64	39.64	46.76
Relative humidity %	14.7	13.4	12.4	11.8	11.8	11.4
Magnesium chloride $MgCl_2 \cdot 6H_2O$						
Temperature °C	0.42	9.82	19.53	30.18	39.96	48.09
Relative humidity %	35.2	34.1	33.4	33.2	32.7	31.4
Sodium dichromate $Na_2Cr_2O_7 \cdot 2H_2O$						
Temperature °C	0.60	10.14	19.82	30.04	37.36	47.31
Relative humidity %	60.4	57.8	55.5	52.4	50.4	48.0
Magnesium nitrate $Mg(NO_3)_2 \cdot 6H_2O$						
Temperature °C	0.39	9.85	19.57	30.47	40.15	48.10
Relative humidity %	60.7	57.5	55.8	51.6	49.7	46.2
Sodium chloride NaCl						
Temperature °C	0.92	10.23	20.25	30.25	39.18	48.30
Relative humidity %	75.0	75.3	75.5	75.6	74.6	74.9
Ammonium sulfate $(NH_4)_2SO_4$						
Temperature °C	0.39	10.05	20.04	30.86	39.97	47.96
Relative humidity %	83.7	81.8	80.6	80.0	80.1	79.2
Potassium nitrate KNO_3						
Temperature °C	0.62	10.17	20.01	30.70	40.35	48.12
Relative humidity %	97.0	95.8	93.1	90.6	88.0	85.6
Potassium sulfate K_2SO_4						
Temperature °C	0.54	10.08	19.81	30.44	39.94	48.06
Relative humidity %	99.0	98.0	97.1	96.8	96.1	96.0

tions. The dewpoint, for a salt at a test temperature, was taken as the mean of the dewpoints obtained by each observer.

The ambient temperature was assumed to be the mean of the air temperature and the salt temperature within the Wolff flask. As these temperatures were relatively stable for appreciable periods of time, only one such set of temperature readings was obtained by each observer for his corresponding set of dewpoint observations.

The relative humidity in equilibrium with the saturated salt solution is given by

$$RH = \frac{e_d}{e_a} \times 100,$$

where e_d is the vapor pressure of pure water at the dewpoint temperature, and e_a is the vapor pressure of pure water at the ambient temperature. The vapor pressures given in the Smithsonian Tables [3] were used in this computation.

The mean relative humidity at each observed test temperature is presented in table 1 for eight different saturated salt solutions ranging in relative humidity from about 11 percent to 99 percent. The data for each salt were plotted, and the best smooth curve obtainable by eye was drawn through the plotted points. The faired values from this smooth curve are given in table 2. They represent the best estimates of the relative humidities obtained with these salts at the selected temperatures.

TABLE 2. *Faired values of relative humidity versus temperature*

Temperature	Relative humidity of saturated salt solution							
	$LiCl \cdot H_2O$	$MgCl_2 \cdot 6H_2O$	$Na_2Cr_2O_7 \cdot 2H_2O$	$Mg(NO_3)_2 \cdot 6H_2O$	NaCl	$(NH_4)_2SO_4$	KNO_3	K_2SO_4
°C	%	%	%	%	%	%	%	%
0	14.7	35.0	60.6	60.6	74.9	83.7	97.6	99.1
5	14.0	34.6	59.3	59.2	75.1	82.6	96.6	98.4
10	13.3	34.2	57.9	57.8	75.2	81.7	95.5	97.9
15	12.8	33.9	56.6	56.3	75.3	81.1	94.4	97.5
20	12.4	33.6	55.2	54.9	75.5	80.6	93.2	97.2
25	12.0	33.2	53.8	53.4	75.8	80.3	92.0	96.9
30	11.8	32.8	52.5	52.0	75.6	80.0	90.7	96.6
35	11.7	32.5	51.2	50.6	75.5	79.8	89.3	96.4
40	11.6	32.1	49.8	49.2	75.4	79.6	87.9	96.2
45	11.5	31.8	48.5	47.7	75.1	79.3	86.5	96.0
50	11.4	31.4	47.1	46.3	74.7	79.1	85.0	95.8

TABLE 3. *Scatter of data about smooth curves*

Nominal temperature	Relative-humidity deviation of data from curve of saturated salt solution							
	$LiCl \cdot H_2O$	$MgCl_2 \cdot 6H_2O$	$Na_2Cr_2O_7 \cdot 2H_2O$	$Mg(NO_3)_2 \cdot 6H_2O$	NaCl	$(NH_4)_2SO_4$	KNO_3	K_2SO_4
°C	%	%	%	%	%	%	%	%
0	0	+0.3	0	+0.2	+0.1	0	−0.5	0
10	0	−.3	0	−.3	−.1	0	+.4	+.1
20	0	−.2	+.2	+.8	0	0	−.2	−.1
30	0	+.3	−.1	−.3	0	0	+.1	+.2
40	+.2	+.5	−.1	+.5	−1.0	+.4	+.1	−.1
50	−.1	−.2	+.2	−.6	0	0	0	+.1
Average	0	±0.3	±0.1	±0.6	±0.2	±0.1	±0.2	±0.1

The plots of relative humidity versus temperature yield curves that are continuous and, generally, vary little with temperature over the temperature range of 0° to 50° C. These plots are shown as solid-line curves in figures 3 to 10. The maximum variation of relative humidity with temperature occurs with saturated solutions of sodium dichromate and magnesium nitrate. For these salts there is an absolute decrease in relative humidity of about 15 percent as the temperature increases from 0° to 50° C. The scatter of the mean experimental values above the smooth curves is given in table 3. The greatest scatter of the data occurs with sodium chloride and is ±0.6 percent relative humidity. For the other salts, the scatter is equal to or less than ±0.3 percent relative humidity.

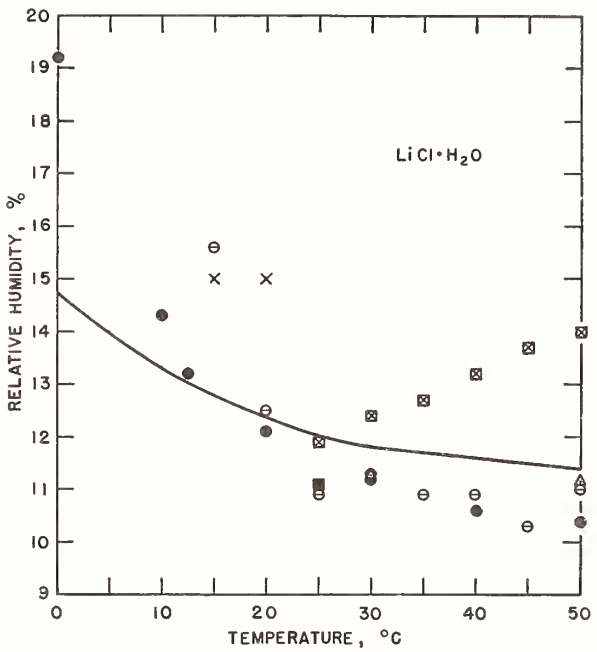

FIGURE 3. *Comparison of the faired NBS results with results of other experimenters.*

Figures 3 to 10, inclusive, show a comparison of the faired NBS results, as solid-line curves, with the results of other experimenters. The following symbol notation is used throughout these figures:

- ● ICT [2]
- ○ Foote, Saxton, and Dixon [4]
- ┼ Leopold and Johnston [5]
- △ Sakai [6]
- □ Adams and Merz [7]
- ◇ Burns [8]
- × O'Brien [9]
- ▲ Speranskii [10, 15]
- ▽ Prideaux [11]
- ◆ Edgar and Swan [12]
- ■ Stokes and Robinson [13]
- ✳ van't Hoff [14]
- ▼ Carr and Harris [16]
- ◑ Lescoeur [17]
- ▭ Derby and Yngve [18]
- ⊙ Konduirev and Berezovskii [19]
- ⊖ Ewing, Klinger, and Brandner [20
- ◬ Johnson and Molstad [21]
- ⊖ Huttig and Reuscher [22]
- ⊠ Gokcen [23]

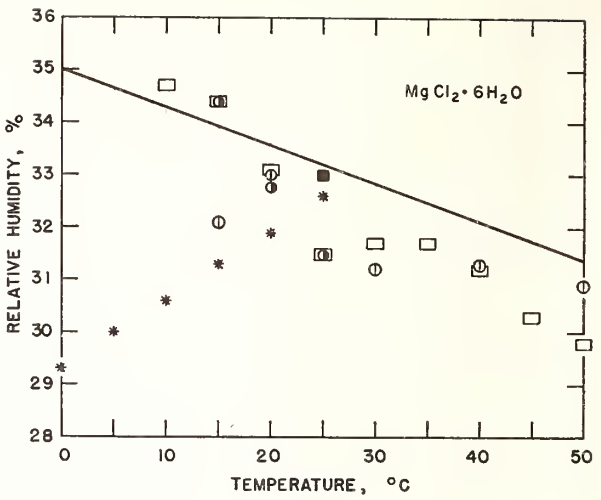

FIGURE 4.
(See fig. 3)

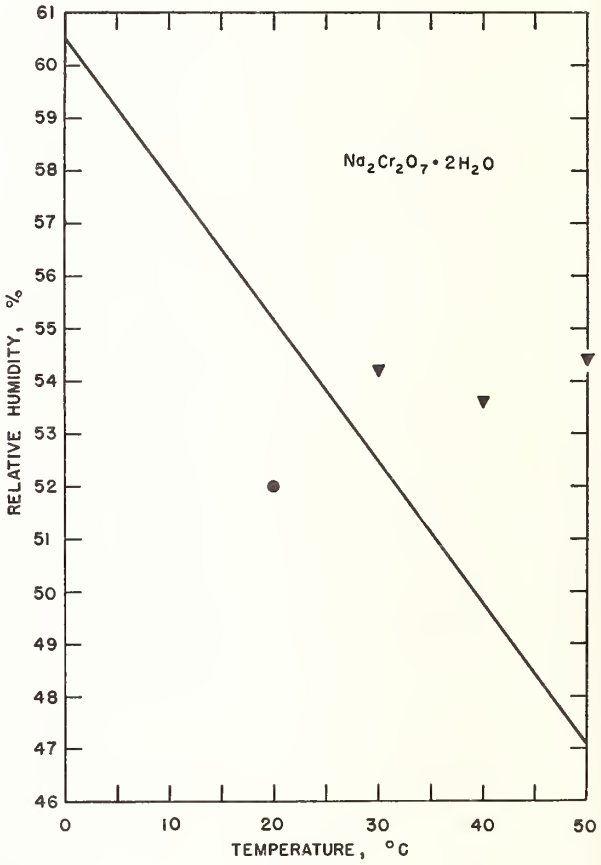

FIGURE 5.
(See fig. 3)

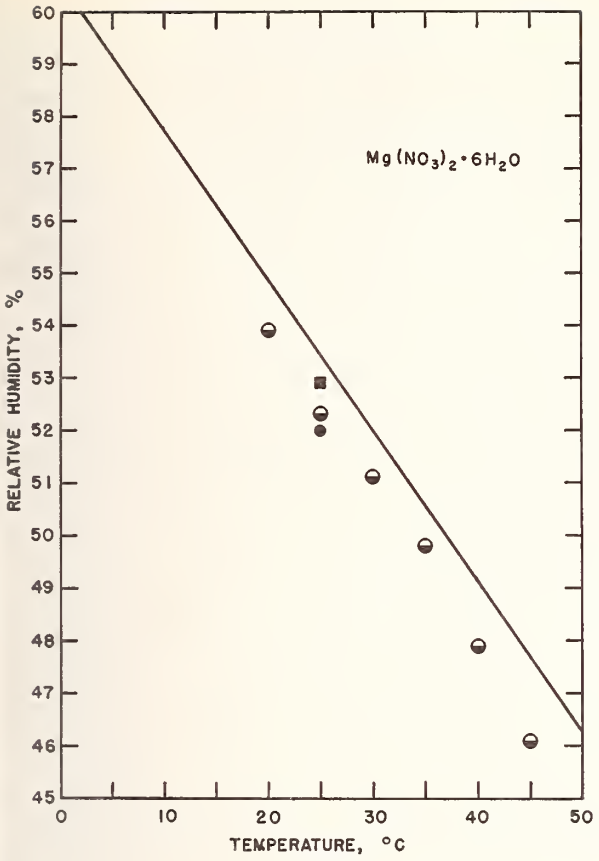

FIGURE 6.
(See fig. 3)

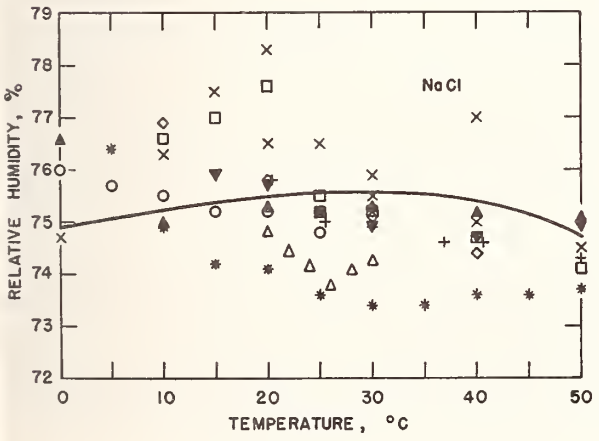

FIGURE 7.
(See fig. 3)

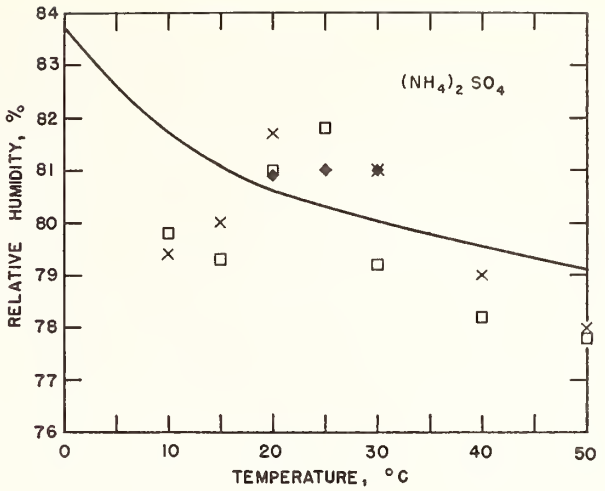

FIGURE 8.
(See fig. 3)

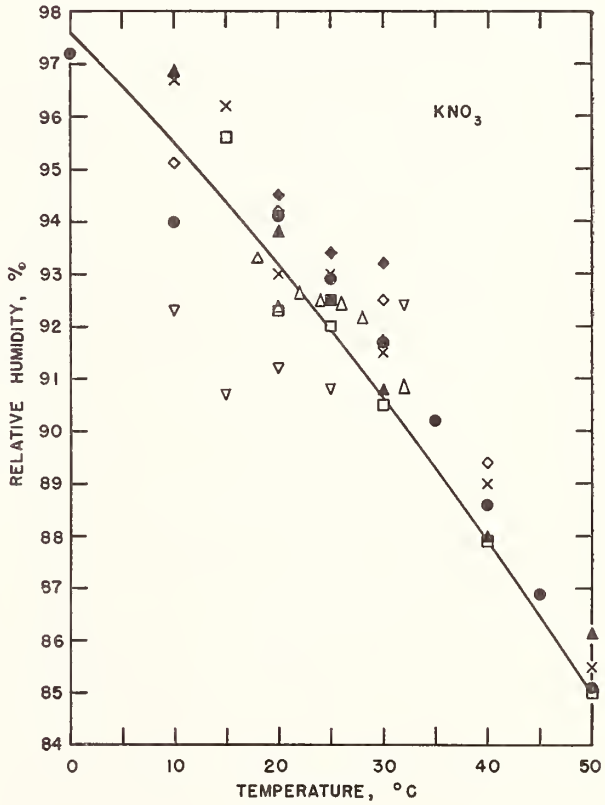

FIGURE 9.
(See fig. 3)

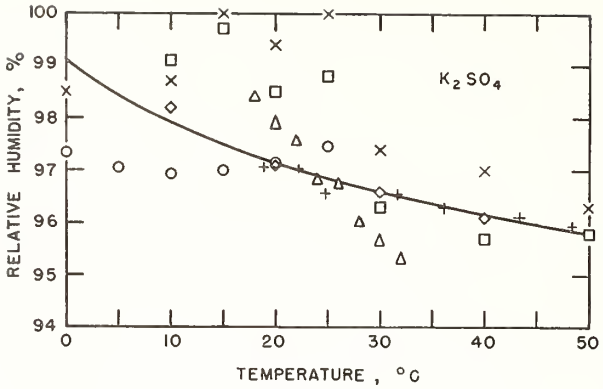

FIGURE 10.
(See fig. 3)

5. Discussion

5.1. General

There are several advantages to the use of the dewpoint method in determining the equilibrium relative humidity over a saturated salt solution. The experimental setup can be relatively simple, requiring only a temperature-controlled liquid bath for maintaining the salt solution and its containing vessel at some fixed temperature and a dewpoint detector. The dewpoint can be measured in the presence of an air (or other noncondensible) atmosphere. Methods that depend on the direct measurement of vapor pressure, either absolute or differential, require careful elimination of all gases and vapors except the water vapor from above the salt solution as well as the elimination of any dissolved gases in the solution because these would produce a serious error in the vapor pressure. The absolute accuracy of the vapor-pressure measurement increases with decreasing dewpoint for a given accuracy in the dewpoint measurement. For example, if the dewpoint is measured with an accuracy of 0.1 deg C, the corresponding accuracy in vapor pressure is 0.008 mm Hg at −20° C, 0.034 mm Hg at 0° C, 0.109 mm Hg at 20° C, and 0.296 mm Hg at 40 °C. The accuracy, in terms of percentage of vapor pressure, is 0.8 percent at −20° C, 0.7 percent at 0° C, 0.6 percent at 20° C, and 0.5 percent at 40° C. Thus, the percentage accuracy in vapor-pressure determination by the dewpoint method, for a given dewpoint accuracy, is roughly independent of dewpoint or vapor pressure. The dewpoint method is an indirect method; it yields a temperature from which the vapor pressure is obtained by recourse to tables. One of the inherent limitations of the method lies in the basic accuracy of the tables. For most work, and particularly for this investigation, the standard tables are considered to have adequate accuracy.

5.2. Errors

In determining relative humidity by the dewpoint method, the principal errors arise in the measurement of the dewpoint temperature and the ambient temperature. The precision of the temperature measurement, using calibrated single-junction copper-constantan thermocouples and a calibrated precision potentiometer, was 0.01 deg C, but the accuracy was probably no better than 0.05 deg C. As (1) the thermocouple for measuring the dewpoint was imbedded only several hundredths of an inch below the surface of the dewpoint mirror, (2) the body of the mirror was copper, and (3) the rates of heating and cooling were uniform and slow, it seems reasonable to assume that any temperature differentials within or across the mirror were negligible, say, no more than 0.01 to 0.02 deg C. Because of the relatively low thermal conductivity of liquid water, the temperature differential across the thickness of a dew film was possibly of greater magnitude. In cooling, the mirror was colder than the exposed dew surface and in heating, it was warmer. Two factors tend to reduce the importance of this. First, by averaging the temperatures at which dew is first observed to appear and then disappear, the errors due to the differentials across the dew, because they are of opposite sign, tend to cancel. Second, by keeping the thickness and quantity of dew small, the differentials can be reduced to a minimum.

The manually operated and visually observed dewpoint hygrometer required a certain degree of skill for successful use. After some experience in its use, it was possible to control the rate of heating and cooling so that the mirror temperature could be followed easily with a potentiometer, the appearance and disappearance of dew could be detected readily, and the thickness of the dew deposit kept as small as desirable. An observer could repeat a series of, say, five dewpoint determinations, at any one time, with an average deviation of a single determination from the mean of 0.04 deg C, with an average deviation of the mean of 0.01 C, and with an average range of 0.13 deg C. The average difference in temperature between the appearance and disappearance of dew was 0.5 deg C, whereas the maximum difference ever observed was 2 deg C. The dewpoint appeared to be independent of the various observed differences in temperature between the appearance and disappearance of dew.

The dewpoint (the average, usually, of five repeat determinations) obtained by any one observer had an average deviation from the mean of two or more observers of 0.07 deg C. The average deviation of the mean dewpoint of all observers for a salt solution at any temperature was 0.04 deg C. The mean range in dewpoint for all of the test conditions for two or more observers was 0.16 deg C.

Because the dew was visually detected, it is likely that different observers used different criteria for defining the appearance or disappearance of dew.

This may account to some extent for the spread in dewpoint from one observer to another.

Below 0° C, either frost or dew (supercooled water) may be deposited on the surface of the dewpoint mirror. In all cases (which included dewpoints as low as −23° C) the deposit first detected was dew. If the mirror temperature was not permitted to fall too far below the dewpoint, then dew remained on the mirror throughout the determination. If the mirror temperature dropped appreciably below the dewpoint, the dew changed to frost.

The ambient temperature was taken as the mean temperature of the salt solution and air. These latter two temperatures differed from each other because of the heat sources and sinks associated with the setup. The fan used for stirring the air within the chamber introduced heat through agitation; conduction along the shaft added or abstracted heat, depending on whether the room temperature was above or below that of the test chamber. The dewpoint hygrometer served as a serious heat sink, for, by the very nature of its operation, it has to be maintained below test-chamber temperature. Although the insulation surrounding the conduction rod aided appreciably in reducing the magnitude of the heat loss, there was still enough loss to produce a temperature differential between the salt solution and air. The test-chamber temperature may therefore have an average uncertainty, because of this differential, of 0.09 deg C.

The root-mean-square uncertainty in the dewpoint determination is 0.07 deg C and in the ambient (test chamber) temperature is 0.10 deg C. The corresponding uncertainty in relative humidity varies from a maximum of 1.2 percent for the high-humidity saturated salt solutions to 0.2 percent for the low-humidity saturated salt solutions.

5.3. Comparison of Results With Those of Other Investigators

The NBS results are compared with those of other investigators in figures 3 to 10, in which the NBS results are shown as solid-line curves. The results of some workers were reported for a limited temperature range or, occasionally, for only one temperature. Wherever necessary, results that were presented in terms of vapor pressure were converted into relative humidity.

It is apparent from these figures that there is a certain degree of scatter among the values reported by other researchers as well as some disagreement between the NBS results and those values. In general, these other results fall within a band of values that is, on an average, roughly within ±1½-percent relative humidity of the NBS results.

5.4. Use of Saturated Salt Solutions

When saturated salt solutions are employed for humidity control, experience has shown that certain precautions must be observed in order that the theoretical values may be used without the need of measurement. It is necessary to enclose the saturated salt solution in a sealed chamber. The chamber and the fixtures therein must be made of nonhygroscopic materials, preferably metal or glass, else the time required for humidity equilibrium to be achieved may be very great, sometimes of the order of days or weeks. The chamber, salt solution, and ambient air should be brought to temperature equilibrium. It is desirable for the salt solution to occupy as large a surface area as possible and for some means of air ventilation or circulation to be provided. In the latter regard, if at all possible, the motor that drives the fan or blower should be external to the chamber. Otherwise, the heat dissipated by the motor will gradually raise the internal chamber temperature and introduce some uncertainty in the equilibrium relative humidity. The time required for humidity equilibrium to be reached with saturated salt solutions depends on several factors: (1) the ratio of free surface area of the solution to chamber volume, (2) the amount of air stirring, and (3) the presence of hygroscopic materials. It is conjectured that agitating the saturated salt solution may increase the rate at which equilibrium is achieved.

As ideal conditions are rarely obtained in practice, it is probable that the theoretical values of relative humidity are seldom reached. In general use, saturated salt solutions should not be expected to control the relative humidity to closer than about 1-percent relative humidity of the theoretical values.

6. References

[1] Arnold Wexler and W. G. Brombacher, Methods of measuring humidity and testing hygrometers, NBS Circular 512 (1951).

[2] International Critical Tables **1,** 68 (McGraw-Hill Book Co., New York, N. Y., 1927).

[3] Smithsonian Meteorological Tables, 6th Revised Edition (1951).

[4] H. W. Foote, Blair Saxton, and J. D. Dixon, The vapor pressures of saturated aqueous solutions of certain salts, J. Am. Chem. Soc. **54,** 563 (1932).

[5] H. Geneva Leopold and John Johnston, The vapor pressure of the saturated aqueous solutions of certain salts, J. Am. Chem. Soc. **49,** 1974 (1927).

[6] W. Sakai, The study of urea, *1.* The hygroscopic properties of (the) double substance. The vapor pressure of saturated solution(s) of salts, J. Soc. Chem. Ind. Japan, **43,** Suppl. binding 104 (1940).

[7] J. R. Adams and A. R. Merz, Hygroscopicity of fertilizer materials and mixtures, J. Ind. Eng. Chem. **21,** 305 (1929).

[8] Robert Burns, Conditioning of insulating materials for test, Bell Telephone System Monograph B–986 (1937). Source of material not given.

[9] F. E. M. O'Brien, J. Sci. Instr., **25,** 73 (1948).

[10] A. Speranskii, The vapor pressure and integral heat of solution of saturated solutions, Z. physik. Chem. **78,** 86 (1912).

[11] E. B. R. Prideaux, The deliquescence and drying of ammonium and alkali nitrates and a theory of the absorption of water vapor by mixed salts, J. Soc. Chem. Ind. **39,** 182–5T (1920).

[12] G. Edgar and W. O. Swan, Factors determining the hygroscopic properties of soluble substances, I. Vapor pressure of saturated solutions, J. Am. Chem. Soc. **44,** 570 (1922).

[13] R. H. Stokes and R. A. Robinson, Ind. Eng. Chem. **41,** 2013 (Sept. 1949).
[14] J. H. van't Hoff, E. F. Armstrong, W. Hinrichsen, F. Weigert, and G. Just, Gips und Anhydrit, Z. physik. Chem. **45,** 257 (1903).
[15] A. Speranskii, Vapor pressure of saturated solutions, Z. physik. Chem. **70,** 519 (1910).
[16] D. S. Carr and B. L. Harris, Ind. Eng. Chem. **41,** 2014 (Sept. 1949).
[17] M. H. Lescoeur, Researches sur la dissociation des hydrates salines et des composés analogues, Ann. Chem. Phys. (7) **2,** 85 (1894).
[18] I. H. Derby and Victor Yngve, Dissociation tensions of certain hydrated chlorides and the vapor pressures of their saturated solutions, J. Am. Chem. Soc. **38,** 1439 (1916).
[19] N. V. Konduirev and G. V. Berezovskii, Vapor pressure of saturated solutions and hydrates of magnesium chloride, J. Gen. Chem. (USSR) **5,** 1246 (1935).
[20] Warren W. Ewing, Ernest Klinger, and John D. Brandner, Vapor pressure-temperature relations and the heats of hydration, solution and dilution of the binary system magnesium nitrate-water, J. Am. Chem. Soc. **56,** 1053 (1934).
[21] Ernest F. Johnson, Jr., and Melvin C. Molstad, Thermodynamic properties of aqueous lithium chloride solutions. An evaluation of the gas-current method for determination of thermodynamic properties of aqueous salt solutions, J. Phys. & Colloid Chem. **55,** 257 (1951).
[22] F. H. Huttig and F. Reuscher, Studien zur Chemie des Lithiums. I. Über die Hydrate des Lithiumchlorids und Lithiumbromids, Z. anorg. Chem. **137,** 155 (1924).
[23] Nevzat A. Gokcen, Vapor pressure of water above saturated lithium chloride solution, J. Am. Chem. Soc. **73,** 3789 (1951).

WASHINGTON, February 19, 1954.

20. A Pneumatic Bridge Hygrometer for Use as a Working Humidity Standard

Lewis Greenspan

National Bureau of Standards, Washington, D.C.

ABSTRACT

A pneumatic bridge, utilizing two sets of critical flow nozzles in series and arranged to form a network analogous to a Wheatstone bridge, is described. By inserting a desiccant between the two nozzles in one arm of the bridge and measuring the ensuing pressure difference across the bridge produced by the absorption of the water from the test gas in one arm of the bridge, a measure of the humidity of the test gas is obtained. The equation expressing the relationship between the bridge pressure ratio, I, and the mixing ratio, r, defined as the mass of water per mass of dry gas, is given by

$$I = 1 - \frac{1 + Kr}{(1+r)^{1/2}\,(1+r/E)^{1/2}}$$

where E is the ratio of the molecular weight of water to that of the dry test gas and K is an empirically determined constant. The bridge pressure ratio is the ratio of a measured pressure difference to the sum of two measured absolute pressures.

This instrument may be calibrated against a suitable reference standard. When calibrated against the NBS gravimetric hygrometer, a value of $K = 20.62 \times 10^{-3}$ was obtained. The largest error measured, over the range of 0.15 to 19.1 mg of water vapor per gram of dry air, was 0.025 mg of water vapor per gram of dry air. The upper limit to the effect of random errors and possible systematic errors in terms of mixing ratio is estimated at 0.050 mg of water vapor per gram of dry air or ¼ per cent of full scale. The instrument was designed for use as a working or transfer standard for humidity measurements.

INTRODUCTION

A need exists for working humidity standards which can be used to calibrate industrial and laboratory type humidity instruments. Such working humidity standards may in turn be calibrated by higher class humidity standards. To be useful as a working standard, an instrument should have a stable response which is predictable by means of a theoretical or empirical formula. The pneumatic bridge hygrometer is such an instrument.

The pneumatic bridge is roughly analogous to a Wheatstone bridge, where nozzles are the analog of the resistors and a differential pressure gauge is the analog of the galvanometer. The bridge is balanced when the ratio of the volumetric flow in the downstream nozzle to that in the upstream nozzle is identical for both arms of the bridge and the pressure difference across the bridge will then be zero. When a specific absorber, which removes one component of the gas mixture flowing through the bridge, is incorporated into one branch of a balanced bridge, between the upstream and downstream nozzles, pressure unbalance. approximately proportional to the partial pressure of the absorbed gas constituent, occurs and is measured by the differential pressure gauge.

The general principle of this instrument was first described by W. A. Wildhack.[1] The author has built a version of this instrument to measure the partial pressure of oxygen.[2] Another instrument along these lines is described by Wildhack, Perls, Kissinger, and Hayes.[3]

The pneumatic bridge hygrometer described below was developed for the purpose of obtaining a highly accurate, stable and dependable humidity standard.

THEORY

The essential element of the pneumatic bridge is the critical flow nozzle. Whenever the ratio of the pressure in the throat of the nozzle to the entrance pressure is less than the critical pressure ratio, the gas flow in the throat is sonic. Under this condition, the flow rate is independent of the downstream pressure and is only a function of upstream parameters. The theory of critical flow through a nozzle is well known. The volumetric rate of flow of an ideal gas through a nozzle under adiabatic, isentropic, critical-flow conditions can be given by[4]

$$F_I = A\left(\frac{2n}{n+1}\right)^{1/2} R_c^{1/n}\left(\frac{P}{\rho}\right)^{1/2} \tag{1}$$

where

F_I = the entrance volumetric flow rate of an ideal gas
A = the nozzle throat area
n = the ratio of the specific heat at constant pressure to the specific heat at constant volume for the entrance gas
P = the entrance pressure
ρ = the density of the entrance gas
R_c = the critical pressure ratio and is equal to $(2/[n+1])^{n/(n-1)}$.

Equation (1) applies whenever the ratio of nozzle throat pressure to entrance pressure is less than R_c.

The volumetric flow rate of a real gas through a nozzle under non-ideal conditions is given by[1, 4]

$$F = DA\left(\frac{2n}{n+1}\right)^{1/2} R_c^{1/n}\left(\frac{P}{\rho}\right)^{1/2} \tag{2}$$

where

F = the volumetric flow rate of a real gas
D = the nozzle discharge coefficient for a particular gas.

The discharge coefficient is intended to account for the deviations from ideal gas behavior of a real gas, the departures from isentropic flow due to friction, contour imperfections, etc.

For dry air at 300°K and 760 mm Hg pressure, R_c in Eq. (2) is equal to 0.53.

For convenience, Eq. (2) will be developed into a form useful to this discussion.

The equation for mass flow, ρF, under these conditions is given by

$$\rho F = DAZ(P\rho)^{1/2} \tag{3}$$

where

$$Z = \left(\frac{2n}{n+1}\right)^{1/2} R_c^{1/n} \tag{4}$$

The density of a gas containing water vapor is given by

$$\rho = \frac{P}{CRT}\,\frac{1+r}{1+r/E} \tag{5}$$

where

C = the compressibility of the gas mixture having a mixing ratio r, pressure P and temperature T
R = the gas constant for 1 gram of the dry gas
T = the absolute temperature of the gas
r = the mixing ratio (grams of water per gram of dry gas)
E = the ratio of molecular weight of water to that of the dry gas.

Substituting Eq. (5) into Eq. (3), we obtain the expression for the mass flow of a moist gas through a nozzle under critical flow conditions:

$$\rho F = \frac{DAZP}{(RTC)^{1/2}}\left(\frac{1+r}{1+r/E}\right)^{1/2} \tag{6}$$

If a fluid flows through two nozzles in series, the mass flow through each will be the same under equilibrium conditions, provided no sources or sinks exist between the two nozzles. If the fluid is a moist gas and if the flow is critical in both nozzles, the equilibrium condition for mass flow through nozzles 1 and 2 in series is given by

$$\rho_1 F_1 = \rho_2 F_2 = \frac{D_1 A_1 Z_1 P_1}{(RT_1 C_1)^{1/2}}\left(\frac{1+r}{1+r/E}\right)^{1/2} = \frac{D_2 A_2 Z_2 P_2}{(RT_2 C_2)^{1/2}}\left(\frac{1+r}{1+r/E}\right)^{1/2} \tag{7}$$

where the subscripts 1 and 2 refer to the upstream and downstream nozzles, respectively.

Solving for the entrance pressure, P_2, to the

second nozzle (downstream nozzle) in Eq. (7), we obtain

$$P_2 = \frac{D_1 A_1 Z_1}{D_2 A_2 Z_2} \left(\frac{T_2 C_2}{T_1 C_1}\right)^{1/2} P_1 \qquad (8)$$

If a sink is interposed between the two nozzles in the form of a desiccant which absorbs all of the water vapor from the moist gas, we have

$$\rho'_2 F'_2 = \rho_1 F_1 - \rho_{w_1} F_1 = \frac{\rho_1 F_1}{1+r} \qquad (9)$$

where the prime refers to the dried state of the gas, $\rho'_2 F'_2$ is the mass flow of dried gas and ρ_{w_1} is the density of water in the entrance gas.

Since $r = 0$ in the dried gas, it follows that

$$\rho' F' = \frac{D_1 A_1 Z_1 P_1}{(R T_1 C_1)^{1/2}} \frac{1}{(1+r)^{1/2}(1+r/E)^{1/2}} = \frac{D'_2 A_2 Z'_2 P'_2}{(R T'_2 C'_2)^{1/2}} \qquad (10)$$

Solving for the entrance pressure at the downstream nozzle, we obtain

$$P'_2 = \frac{D_1 A_1 Z_1}{D'_2 A_2 Z'_2} \left(\frac{T'_2 C'_2}{T_1 C_1}\right)^{1/2} \times \frac{1}{(1+r)^{1/2}(1+r/E)^{1/2}} P_1 \qquad (11)$$

Substituting Eq. (8) into Eq. (11), we have

$$P'_2 = \frac{D_2 Z_2}{D'_2 Z'_2} \left(\frac{T'_2 C'_2}{T_2 C_2}\right)^{1/2} \times \frac{1}{(1+r)^{1/2}(1+r/E)^{1/2}} P_2 \qquad (12)$$

If we arrange four nozzles x_1, x_2, y_1 and y_2 in an array analogous to a Wheatstone Bridge, as shown in Fig. 1, and place a desiccant in one arm of the bridge, say the x arm, the pressure difference across the bridge (the difference in pressure between the entrance to the downstream nozzle x_2 and the entrance to the downstream nozzle y_2) will be given by

$$(\Delta P)_x = P_{y_2} - P'_{x_2} = P_{y_2} - \frac{D_{x_2} Z_{x_2}}{D'_{x_2} Z'_{x_2}} \left(\frac{T'_{x_2} C'_{x_2}}{T_{x_1} C_{x_2}}\right)^{1/2} \times \frac{1}{(1+r)^{1/2}(1+r/E)^{1/2}} P_{x_2} \qquad (13)$$

where $(\Delta P)_x$ is the pressure difference across the bridge when the desiccant is in the x branch.

Equation (13) does not yet provide the means of determining the mixing ratio because P_{x_2} is not a measureable quantity while the desiccant is in the x branch. Of course the desiccant could now be removed from the x branch and P_{x_2} determined, but in this case the operation would be as complicated as operating the bridge in a symmetrical

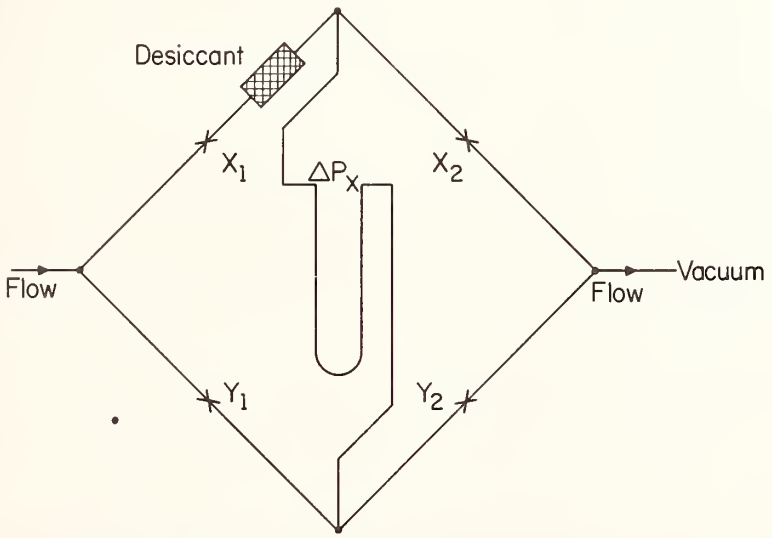

FIG. 1. Simplified schematic of pneumatic bridge hygrometer.

manner, since a manometer reading would also be required with the desiccant out of the x branch in order to obtain a zero value. Rather than this, repeating the original operation in the other branch offers advantages in minimizing sorption and leakage errors, while requiring no greater complication.

If we now switch the desiccant to the y branch, the pressure difference across the bridge is given by

$$(\Delta P)_y = P'_{y_2} - P_{x_2} = \frac{D_{y_2}Z_{y_2}}{D'_{y_2}Z'_{y_2}}\left(\frac{T'_{y_2}C'_{y_2}}{T_{y_2}C_{y_2}}\right)^{1/2} \times \frac{1}{(1+r)^{1/2}(1+r/E)^{1/2}} P_{y_2} - P_{x_2} \quad (14)$$

The difference between the two readings, $P = P_x - P_y$, is given by

$$\Delta P = \left\{P_{y_2}\left[1 - \frac{D_{y_2}Z_{y_2}}{D'_{y_2}Z'_{y_2}}\left(\frac{T'_{y_2}C'_{y_2}}{T_{y_2}C_{y_2}}\right)^{1/2}\right] + P_{x_2}\left[1 - \frac{D_{x_2}Z_{x_2}}{D'_{x_2}Z'_{x_2}}\left(\frac{T'_{x_2}C'_{x_2}}{T_{x_2}C_{x_2}}\right)^{1/2}\right]\right\} \times \frac{1}{(1+r)^{1/2}(1+r/E)^{1/2}} \quad (15)$$

If the nozzles x_2 and y_2 are similar in shape and size and if the entire bridge is immersed in a temperature controlled bath, the following approximations may be made:

$$\frac{T'_{y_2}}{T_{y_2}} = \frac{T'_{x_2}}{T_{x_2}} = \frac{T'_2}{T_2} \quad (16)$$

$$\frac{D_{y_2}}{D'_{y_2}} = \frac{D_{x_2}}{D'_{x_2}} = \frac{D_2}{D'_2} \quad (17)$$

$$\frac{Z_{y_2}}{Z'_{y_2}} = \frac{Z_{x_2}}{Z'_{x_2}} = \frac{Z_2}{Z'_2} \quad (18)$$

$$\frac{C'_{y_2}}{C_{y_2}} = \frac{C'_{x_2}}{C_{x_2}} = \frac{C'_2}{C_2} \quad (19)$$

Substituting these approximations into Eq. (15), we obtain

$$\Delta P = (P_{y_2}+P_{x_2})\left[1 - \frac{D_2Z_2}{D'_2Z'_2}\left(\frac{T'_2C'_2}{T_2C_2}\right)^{1/2} \times \frac{1}{(1+r)^{1/2}(1+r/E)^{1/2}}\right] \quad (20)$$

Equation (20) can be converted into the following expression for the pressure ratio, I.

$$I = \frac{\Delta P}{(P_{x_2}+P_{y_2})} = 1 - \frac{(D_2Z_2/D'_2Z'_2)(T'_2C'_2/T_2C_2)^{1/2}}{(1+r)^{1/2}(1+r/E)^{1/2}} = 1 - \frac{f(r)}{(1+r)^{1/2}(1+r/E)^{1/2}} \quad (21)$$

In order to achieve an accuracy of 0.1 per cent of full scale, $f(r)$ must be known to better than 0.002 per cent. There is some uncertainty as to the exact behaviour of small nozzles and, therefore, of their discharge coefficients. In addition, the ratio of specific heats and the compressibility of moist gases are not known with high accuracy. Even though the nozzles are immersed in a constant-temperature bath, the heat generated by the absorption of water vapor in the desiccant and the cooling due to the gas expansion in the nozzles tend to make T'_2 differ from T_2. The absolute pressure of the dried gas is less than the absolute pressure of the corresponding moist gas, thereby possibly introducing differences in the values of some of the parameters. The function $f(r)$ can be determined empirically with the requisite accuracy.

Since $f(r)$ is the product of certain ratios of gas constants for moist and dry gas, $f(r)$ is a function of the amount of moisture in the moist gas. Although the theoretical form of this function is not known, $f(r)$ may be represented with high accuracy, as indicated by the results, by $1 + Kr$, where K is an empirical constant. Equation (21) then becomes

$$I = 1 - \frac{1 + Kr}{(1+r)^{1/2}(1+r/E)^{1/2}} \quad (22)$$

Another useful form in which to express the instrument response is in terms of the partial pressure of water vapor, e, in the water vapor-gas mixture as defined by the following equation for ideal gases:

$$e = \frac{r}{E + r} P \quad (23)$$

where P is the total pressure. Solving for r, we obtain

$$r = \frac{Ee}{P - e} \quad (24)$$

Substituting Eq. (24) into Eq. (22) and sub-

stituting P_1 for P in order to refer to e in the entrance gas, we obtain

$$I = 1 - \frac{1 + K[Ee/(P_1-e)]}{[1+Ee/(P_1-e)]^{1/2}[1+e/(P_1-e)]^{1/2}} \quad (25)$$

which may be written as

$$I = 1 - \frac{1 - (1-KE)\, e/P_1}{[1-(1-E)\, e/P_1]^{1/2}} \quad (26)$$

Considering a system of water vapor in air, we may substitute the value 0.62197 for E and, using the binomial expansion, the instrument response may be written as

$$I = (0.81099-0.62197\mathrm{K})\frac{e}{P_1} + (0.13542-0.11756\mathrm{K})\left(\frac{e}{P_1}\right)^2 + (0.03671-0.03331\mathrm{K})\left(\frac{e}{P_1}\right)^3 + \cdots \quad (27)$$

which for values of e not exceeding 22 mm Hg at normal atmospheric pressures may be approximated to better than ¼ per cent by

$$I = (0.8130-0.6237K)\frac{e}{P_1} \quad (28)$$

Substituting $\Delta P = (P_{x_2}+P_{y_2})\, I$ into Eq. (28), we obtain

$$\Delta P = (0.8130-0.6237\mathrm{K})\left(\frac{P_{x_2}}{P_1}+\frac{P_{y_2}}{P_1}\right) e \quad (29)$$

The quantities P_{x_2}/P_1 and P_{y_2}/P_1 are bridge constants which may be determined by simple pressure measurements and will be designated by the symbols α_x and α_y respectively. Substituting these constants into Eq. (29) and solving for e, we obtain

$$e = \frac{\Delta P}{(\alpha_x+\alpha_y)\,(0.8130-0.6237\mathrm{K})} = \beta \Delta P \quad (30)$$

where β is an overall constant defined by Eq. (30).

Equation (30) requires only that the pressure difference across the bridge be read to determine vapor pressure.

DESCRIPTION

A schematic representation of the hygrometer is shown in Fig. 2. Test gas enters valve V_1, and passes through heat exchanger E_1, and then enters the bridge block where it splits into two streams, one stream passing through nozzle x_1 and the other through nozzle y_1. The x and y streams then flow through four-way valves V_x and V_y respectively. These valves are set so that the streams either flow through or bypass drying trains D_x and D_y. In normal operation, V_x and V_y are positioned so that one stream traverses its drying train while the other bypasses its drying train. The streams continue on through heat exchangers E_x and E_y and nozzles x_2 and y_2 and finally combine and discharge from the instrument through valve V_0 into a vacuum pump.

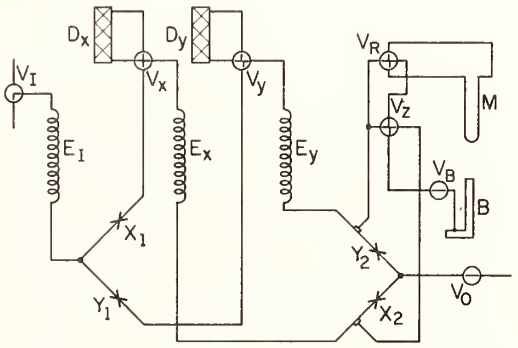

FIG. 2. Schematic diagram of pneumatic bridge hygrometer.

The pneumatic bridge contains pressure taps just upstream of nozzles x_2 and y_2 which are connected to a barometer B and a differential manometer M through shut-off valve V_B and four-way valves V_Z and V_R. Valve V_B allows isolation of the barometer from the instrument, while valve V_Z provides for determination of the manometer zero, and valve V_R reverses the manometer connections to the bridge. In operation, the barometer is connected to the y branch. The heat exchangers and bridge are suspended in a temperature-controlled, stirred oil bath T.

Figure 3 shows an exploded drawing of the bridge which consists of a bridge body, four nozzles and four nozzle sealing caps. The

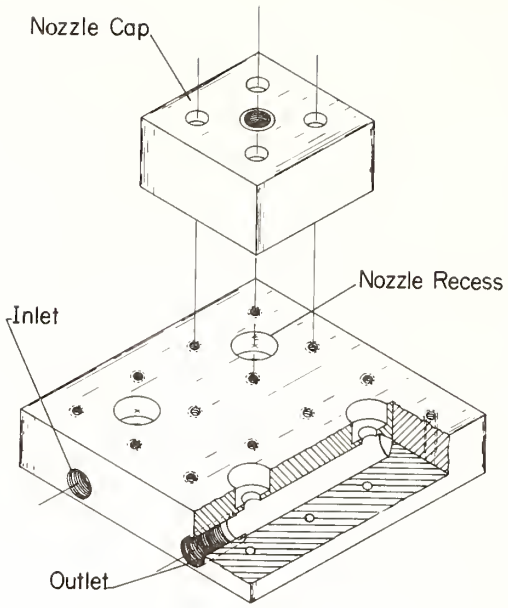

FIG. 3. Nozzle block.

bridge body is made of stainless steel and is $3\frac{1}{8}$-in. long, 3-in. wide and $\frac{3}{4}$-in. thick. It has four recesses to receive the four nozzles, inlet and outlet pipe connections and internal channeling to merge the proper flow streams.

All nozzles are formed in stainless steel discs $\frac{5}{8}$-in. in diameter and $\frac{3}{16}$-in. thick. Nozzles x_1 and y_1 have nominal throat diameters of 0.025 in., and nozzles x_2 and y_2 have nominal throat diameters of 0.042-in. The nozzles were formed by drilling the discs with appropriate sized drills and then flaring the exits with 2-degree tapered reamers. The entrance edge was also flared for a small distance with a reamer. The throat diameters were adjusted by reaming until the desired ratio of nozzle areas was obtained in each arm of the bridge. One of the nozzles was then critically adjusted by reaming, until the differential pressure across the bridge with room air flowing through both arms was very small.

The nozzles are sealed to the bridge body by "Teflon" "O" rings, which are held in place by $1\frac{1}{2}$-in. square by 1-in. thick stainless steel caps, each of which has a through hole and female pipe threads for the connection of tubing. These caps are secured to the body by means of screws.

Figure 4 shows a drawing of a drying train. Each train consists of a large and a small glass absorption tube connected in series. The large tube has an internal volume of about 1.4 liters and is first in the train; the small tube has an internal volume of about 45 cc. Both tubes are sealed with caps having standard taper ground glass joints and lubricated with a silicone high-vacuum grease. Tubing can be attached to glass nipples at the base of the tube and peak of the cap by means of "Teflon" ferrule stainless steel fittings. The two tubes of the drying train are interconnected in such a way that the flow through each travels upward. The large tube is filled with indicating anhydrous calcium sulfate. The smaller tube is filled with glass fiber wool, which has been thoroughly mixed with phosphorous pentoxide. At the exit of each tube there is a "Teflon" felt filter to prevent carryover of the desiccant.

Each pressure tap (piezometer) upstream of x_2 and y_2 consist of eight 0.016 in. diameter holes equally spaced on a circle around a straight section of $\frac{5}{16}$-in. o.d. stainless steel tubing. These holes are contained within a fitting which goes over the $\frac{5}{16}$-in. o.d. tubing and is sealed to the tubing. From this fitting, $\frac{1}{4}$-in. o.d. stainless steel tubing transmits the pressure to valves V_B, V_Z and V_R. The absolute pressure at x_2 and y_2 is read by means of a mercurial barometer with a sensitivity of 0.05 mm Hg pressure, while the differential pressure between these points is read by a moving cistern type manometer, containing high vacuum oil and having a sensitivity of about 0.001 mm Hg pressure.

The bridge and heat exchangers are immersed in an oil bath. A centrifugal stirrer maintains uniform temperature throughout the bath, and a mercury-in-glass thermoregulator controls electric heaters through a sensitive relay to maintain the bath constant at 34°C with a bath fluctuation of ± 0.03°C. The intermittant heat input may be set at 250 watts, 42 watts or $17\frac{1}{2}$ watts by means of switches. The lowest heat value (the usual operating heat) may be adjusted to other values less than 42 watts by selection of proper resistors. These intermittent heat loads are in addition to the steady heat load of the stirrer and the negative heat load of the test gas which is cooled by expansion.

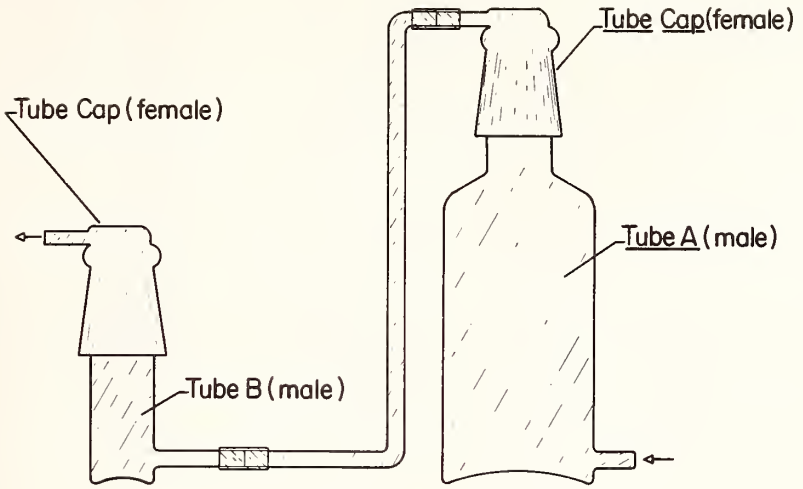

FIG. 4. Absorption train.

Heat exchanger E_I is a six-foot coil of $\frac{3}{8}$-in. o.d. stainless steel tubing. Heat exchangers E_x and E_y are five-foot coils of $\frac{3}{8}$-in. o.d. stainless steel tubing. All flow tubing is $\frac{3}{8}$-in. o.d. stainless steel or "Teflon" with the exception of the pressure tap assembly, which is $\frac{5}{16}$-in. o.d. stainless steel. All pressure signal tubing is $\frac{1}{4}$-in. o.d. stainless steel or "Teflon". The outlet valve, V_o, is a brass plug valve, with an "O" ring on the plug providing the seal. All other valves are plug type valves with stainless steel bodies and "Teflon" plugs. All valves are mounted on the front panel of the instrument along with all of the electrical switches.

All components, with the exception of the oil bath, are attached to a 17 × 13-in. shelf or to a 26 × 19-in. front panel. The oil bath sits on another 17 × 13-in. shelf at the bottom of the instrument. The two shelves are also attached to the same front panel, which in turn is mounted on the front of a cabinet 28 in. high, 22 in. wide and 14 in. deep, which encloses the instrument. The cabinet has top and back access doors. The entire instrument may be removed from the cabinet as a unit when greater access to the components is desired. Two inlet and one outlet connections are provided on the front panel. By means of inlet valve, V_I, either of two test gases may be selected or rapidly switched. A vacuum pump connects to the outlet and insures critical flow through the nozzles, by maintaining an adequately low outlet pressure. In this instrument, the outlet pressure is maintained at less than 74 mm Hg absolute pressure.

OPERATION

When the hygrometer is used as a working standard, the test gas entering the hygrometer is maintained at a constant absolute pressure and constant water vapor content. In addition, since the hygrometer draws approximately ten liters of gas per minute, some form of humidity generator for delivering air with a constant moisture is desirable. With the absorber in the y branch, the differential pressure, $(\Delta P)_y$, is read on the manometer and P'_{y_2} is read on the barometer. The sum of P'_{y_2} and $(\Delta P)_y$ yields P_{x_2}. Valves V_x and V_y are then each reversed, removing the absorber from the y branch and placing an absorber in the x branch. $(\Delta P)_x$ is read on the manometer while P_{y_2} is read on the barometer. The sum of the absolute values of $(\Delta P)_x$ and $(\Delta P)_y$ is obtained by taking the difference between the two manometer readings and is ΔP. No zero readings are necessary, but in order to compensate for drift, from any

cause whatsoever, while the readings are made, readings should again be made with the absorber in the x branch. The two sets of differences thus obtained are averaged. Various other combinations of readings may be used. In the calibration of this instrument, four readings, constituting a set of 3 ΔP determinations, made up the value of each point. The order in which the readings were taken was reversed for successive points. The preferred pattern is determined by the stability of the test sample and the degree of precision required.

When the highest accuracy is not required, the absorber can be left continuously in one branch of the bridge, and the manometer reading, when corrected for zero, will be proportional to the partial pressure of the water vapor. In this type of operation, a periodic determination of the zero should be made by reading the manometer while the absorber is switched out of both branches.

CALIBRATION AND RESULTS

The pneumatic bridge hygrometer was calibrated against the NBS gravimetric hygrometer at 20 points over a range of 0.15 to 19.1 mg of water per gram of dry air. This was accomplished by having the pneumatic bridge hygrometer and the gravimetric hygrometer simultaneously draw samples from the NBS pressure humidity generator. The standard hygrometer gives a mixing ratio which is the average value for the total sample drawn and is accurate to 0.1 per cent of indicated value. The pneumatic bridge hygrometer measures the water vapor content at the moment. In order that both instruments measure the same water vapor content, many readings, spaced at approximately equal time intervals, were made at each point by the pneumatic bridge throughout the entire period of the test. These readings were averaged, and the average values were used in the compilation of results.

The value for K was determined from the 20 calibration points which covered a range of mixing ratios from 0.1 to 19.1 mg of water per gram of dry air. The value of K so determined was 20.62×10^{-3} with a standard error of 0.36×10^{-3}. The standard deviation of a single bridge pressure ratio measurement was determined to be 0.0104×10^{-3}. Using this value for K, mixing ratios were determined from bridge pressure ratios for each of the calibration points. The several values at each level give indication of the presence of systematic errors at most of the levels. Using an upper three standard deviation limit for the largest average (of 3 values) as a limit to the possible systematic errors leads to $0.0116 + 3\,(0.0104/\sqrt{3}) = 0.0296$, which when added to three standard deviations of the bridge pressure ratio leads to an estimate for uncertainty in the bridge pressure ratio of 0.0608×10^{-3} or 0.26 per cent of the highest bridge pressure ratio obtained in the calibration. This is equivalent to an uncertainty in the mixing ratio of 0.050 mg of water per gram of dry air.

An analysis of possible systematic errors based on uncertainty of various bridge parameters and gravimetric hygrometer error gave an estimated maximum systematic error in the bridge pressure ratio of 0.024×10^{-3} which is in reasonable agreement with the above statistical estimate of 0.030×10^{-3}.

Substituting 0.0206 for K in Eq. (30) along with a measured value of 0.4002 for α_x and 0.4090 for α_y, we obtain $e = 1.544\ P$. A comparison of values of e as determined from the standard hygrometer data and the pneumatic bridge hygrometer was made for fourteen calibration points. These are tabulated in Table 2 along with the results of least squares solutions. As might be expected, the least squares linear solution of the calibration data of the pneumatic bridge yields a closer fit. The least squares solution, adjusted so that it passes through the origin of the same data, yields a slightly poorer fit. It is evident that if a linear calibration of the pneumatic bridge hygrometer is desired in terms of partial pressure e, a least squares linear solution of the calibration data yields the best results. The least squares linear solution through the origin yields a slightly less precise but simpler solution.

DISCUSSION AND CONCLUSIONS

The design of this instrument includes many features intended to reduce or eliminate potential sources of error. Sorption and desorption of water vapor from the interior walls of the flow passages were minimized by

Table 1. Pneumatic Bridge Hygrometer Calibration

Mixing Ratio, r, Standard Hygrometer (mg/g)	Bridge Pressure Ratio, I, $\Delta P/(P_{x_2}+P_{y_2}) \times 10^{-3}$	Mixing Ratio, r Pneumatic Bridge (mg/g)	Error, r Pneumatic Bridge (mg/g)	Error, r Pneumatic Bridge (%)	Error, r Pneumatic Bridge (% full scale*)
4.6104	5.8942	4.6215	+0.0111	0.24	0.058
4.6029	5.8806	4.6108	+ .0079	.17	.041
4.5967	5.8764	4.6075	+ .0108	.23	.056
9.9577	12.6263	9.9705	+ .0128	.13	.067
9.9385	12.6017	9.9508	+ .0123	.12	.064
9.9404	12.6007	9.9500	+ .0096	.10	.050
19.1191	23.9261	19.1220	+ .0029	.01	.015
19.1363	23.9421	19.1351	− .0012	− .01	.006
19.1295	23.9052	19.1048	− .0247	− .13	.129
3.7158	4.7380	3.7105	− .0053	− .14	.028
3.7150	4.7345	3.7077	− .0073	− .20	.038
3.7181	4.7244	3.6998	− .0183	− .50	.096
1.9524	2.5152	1.9651	+ .0127	.65	.066
0.89253	1.1568	0.90253	+ .01000	1.11	.052
.61870	0.8047	.62759	+ .00890	1.42	.047
.14762	.1882	.14668	− .00093	−0.64	.005
.62966	.8186	.63844	+ .00878	1.38	.046
.60260	.7828	.61049	+ .00790	1.29	.041
.61579	.7932	.61861	+ .00282	.46	.015
.32728	.4215	.32859	+ .00132	.40	.007

* Full scale defined as 19.1351.

Table 2. Pneumatic Bridge Hygrometer Calibration in Partial Pressure of Water*

e* Standard Hygrometer (mm Hg)	ΔP Pneumatic Bridge Reading (mm Hg)	1.544 ΔP Derived Formula (mm Hg)	1.539 ΔP+0.0134 Least Squares Formula (mm Hg)	1.540 ΔP Least Squares Formula Through Origin (mm Hg)
5.3881	3.4962	5.3981	5.3941	5.3841
5.3821	3.4890	5.3870	5.3830	5.3731
5.3725	3.4850	5.3808	5.3768	5.3669
11.6712	7.5647	11.6799	11.6555	11.6496
11.6439	7.5462	11.6513	11.6270	11.6211
21.8447	14.1967	21.9197	21.8621	21.8629
21.8592	14.2025	21.9286	21.8710	21.8719
21.8356	14.1758	21.8874	21.8341	21.8307
4.3835	2.8322	4.3729	4.3722	4.3616
4.3763	2.8243	4.3607	4.3600	4.3494
4.3745	2.8159	4.3477	4.3471	4.3365
2.2977	1.4939	2.3066	2.3125	2.3006
1.0411	0.6807	1.0510	1.0610	1.0483
0.7296	0.4775	0.7373	0.7483	0.7354

* Partial pressure of water, e, is defined by $e = [r/(0.62197+r)]\ P$.

the exclusive use of stainless steel and "Teflon". Although the drying train was made of glass, sorption and desorption from glass should present no problem, due to the presence of the desiccant. The relative effect of sorption was further reduced by use of a rather large gas flow (10 lpm) and by the technique of switching the absorber from one arm to the other.

Pressure reading errors were reduced by the use of the piezometer as a pressure tap and by the switching of the absorber train from one arm to the other. This switching technique has the further effect of eliminating pressure errors due to any constant leakage in any part of the system with the exception of the drying trains and their associated tubing. Because the drying trains are not continuously in the system, a leakage of 0.1 cc/min. could cause an error of 0.04 per cent of the highest value calibrated. The highest leakage measured on this system was 0.02 cc/min., which could cause a full scale error of 0.008 per cent.

The large tube in the absorber train was filled with indicating anhydrous calcium sulfate to remove the bulk of the water, while the small tube of the train contained phosphorous pentoxide to remove the last vestiges of water from the gas. By this method, only infrequent absorber changes were required. No estimate was made of the quantity of water that might fail to be absorbed nor of the error resulting. General experience indicates that phosphorous pentoxide is capable of virtually complete water absorption.

Another source of error could be introduced if the flow path between the upstream and downstream nozzles offered so great a pressure drop that critical flow was not maintained in the upstream nozzle. This condition would not be present unless the tubing and drying train produced a pressure drop of around 80 mm Hg. Although the design of the instrument makes this possibility unlikely, a precautionary check can be made by comparing the zero readings with both absorbers out of the bridge and with both absorbers in the bridge.

If the temperature of the gas, entering one of the downstream nozzles, differed from the condition assumed in Eq. (16) by 0.01°C, an error of 0.06 per cent of the highest value used in the calibration would ensue.

At maximum reading, the instrument is more than forty times as sensitive to an error in the manometer reading as compared with an error in the barometer reading. Nevertheless, with an estimated error of 0.001 mm Hg pressure in the manometer and an estimated 0.05 mm Hg pressure error in the barometer, the barometer contributes more to the estimated error in mixing ratio at full scale than does the manometer. At lower mixing ratios, the manometer error remains constant, while the barometer error decreases proportionately. It is estimated that at full scale there is an error of 0.016 per cent of full scale due to the errors in the barometer and differential manometer pressure readings. At low mixing ratios, this estimated error decreases to 0.01 per cent of full scale.

It is possible that the fluctuations in the pressure difference across the instrument are related to condensation and freezing that may occur in the nozzle throats due to adiabatic cooling. If so, it may be possible to reduce these fluctuations by raising the bath temperature.

The empirical value for K obtained does not agree with calculations based on the assumption that $D'_2 = D_2$, and $T'_2 = T_2$. It has been suggested that the discharge coefficient of a small nozzle is anomalous in behavior. If this is so, using larger nozzles in the bridge might bring the empirical K closer to the computed value. There is also a possibility that T'_2/T_2 is not equal to 1. If T'_2 exceeded T_2 by 0.12 °C at the highest r values encountered in this work, and if the amount it exceeded was proportional to r, the difference between the computed and empirical K would essentially be explained. Further work may help resolve this question.

When it is desired that the instrument be related to water vapor partial pressure, the data indicate that a least squares solution of e with respect to ΔP provides the best fit. Although calibration has shown that e could be measured with an accuracy approaching the measurement of r, it should be observed that e is not as fundamental a quantity as r for a real gas. Furthermore, if any of the nozzles were to change in contour or area due to wear or dirt accumulation, e would be subject to greater error than r.

As presently constructed, the pneumatic bridge hygrometer is an instrument that can be usefully employed in the calibration of

other humidity indicators or as a direct measuring hygrometer of high accuracy. Due to the size and complication of the present design, its greatest use appears to be as a transfer standard. Simpler and smaller instruments of this general type having less accuracy can be designed for other uses.

With the present state-of-the-art, the pneumatic bridge hygrometer must be calibrated against a reference standard if it is to yield measurements of the highest accuracy.

Acknowledgment. The author wishes to acknowledge the cooperation and assistance given him by Joseph M. Cameron of the Statistical Engineering Section of the National Bureau of Standards in the evaluation of the calibration results.

References

1. Wildhack, W. A., "A Versatile Pneumatic Instrument Based on Critical Flow," *Rev. Sci. Instr.*, **21**, No. 1, 25–30 (January 1950).
2. Greenspan, L., "An Oxygen Partial Pressure Warning Instrument," *J. Res. Natl. Bur. Std.*, **67C**, No. 1 (January to March 1963).
3. Wildhack, W. A., Perls, T. A., Kissinger, C. W., and Hayes, J. W., "Continuous-Absorption Hygrometry with a Pneumatic Bridge Utilizing Critical Flow," in "Humidity and Moisture," Vol. I, p. 552, New York, Reinhold Publishing Corp., 1964.
4. ASME Research Committee on Fluid Meters, "Fluid Meters, Their Theory and Application," 5th ed., The American Society of Mechanical Engineers, 1959.

22. A Comparison between the National Bureau of Standards Two-pressure Humidity Generator and the National Bureau of Standards Standard Hygrometer

S. Hasegawa, R. W. Hyland and S. W. Rhodes

National Bureau of Standards, Washington, D.C.

ABSTRACT

A 3 × 3 Graeco-latin square experiment was used for testing four parameters of the National Bureau of Standards two-pressure humidity generator to determine which parameters influence the accuracy of the generator. The external saturator temperature, the saturation temperature, the saturator pressure, and the air flow were varied and the calculated mixing ratio of the generator was compared against the mixing ratio as measured with the National Bureau of Standards standard gravimetric hygrometer.

The results show that for the highest accuracy, the National Bureau of Standards' pressure humidity apparatus has a maximum flow limitation of under five standard cubic feet per minute (scfm). Tentative values of the correction factor for the saturation pressure of pure water vapor when used to compute the humidity of water-air mixtures were obtained. The correction factor is a function of saturation temperature and pressure. It is estimated that the maximum uncertainty in the mixing ratio produced by the generator is ½ per cent over a range of final saturator temperature of 25 to −20°C and final saturator pressure of 0 to 60 psia.

INTRODUCTION

The National Bureau of Standards pressure humidity generator[1] is an apparatus that produces a continuous flow of air of fixed moisture content. It is used extensively for testing and calibrating hygrometers. The operation of the generator is based on the two-pressure principle. A stream of air is first saturated at an elevated pressure and then isothermally expanded to a lower pressure, usually atmospheric pressure, in a test chamber. In normal operation, the air is presaturated in an external preliminary saturator (located outside the main temperature-controlled bath) at a temperature that is higher than the desired final saturation temperature. The air then is cooled and brought to the final saturation temperature in an internal humidifying system (located in the main temperature-controlled bath) consisting of three saturators interconnected with heat exchangers. Excess water is condensed out and deposited in the internal humidifying system. The humidity of the moist air is computed from the measurements of temperatures and absolute pressures in the final saturator of the internal humidifying system and in the test chamber. For the highest accuracy, a correction is applied to account for the non-ideal gas behavior of moist air.

In the original evaluation of this generator, which was based on a comparison with a thermocouple psychrometer and a dew-point hygrometer, it had been concluded that the accuracy with which the generator would produce a known relative humidity was ½ of 1

per cent in units of relative humidity. Recently the National Bureau of Standards has developed a standard hygrometer,[2] based on a gravimetric method, which can measure the mixing ratio of a gas sample with a maximum uncertainty of about 12 parts in 10^4. Using the standard hygrometer, the reproducibility and accuracy of the generator is now being redetermined.

Among the known parameters that may influence the behavior and performance of the generator, the external saturator temperature, the internal final saturation temperature (i.e., the temperature in the last stage of the internal humidifying system), the final saturator pressure, and the volumetric flow rate were considered the critical ones. A preliminary investigation therefore was made to see which of these parameters significantly affects the accuracy.

EXPERIMENTAL DESIGN

An experiment was designed utilizing a 3×3 Graeco-latin square[3] that permitted the above four parameters to be tested at each of three levels. The parameters were arranged in the following form:

$\Delta t_{15}, P_1, T_{25}, F_5$	$\Delta t_5, P_4, T_0, F_5$	$\Delta t_0, P_2, T_{-20}, F_5$
$\Delta t_{15}, P_2, T_0, F_3$	$\Delta t_5, P_1, T_{-20}, F_3$	$\Delta t_0, P_4, T_{25}, F_3$
$\Delta t_{15}, P_4, T_{-20}, F_1$	$\Delta t_5, P_2, T_{25}, F_1$	$\Delta t_0, P_1, T_0, F_1$

where

Δt = the difference in temperature between the external saturator and the final saturator, the subscript indicating the amount in degrees C that the former exceeds the latter

P = the final saturator pressure, where $P_1 = 15.4$ psia, $P_2 = 29.2$ psia, $P_4 = 63.8$ psia

T = the final saturator temperature, where $T_{25} = 25°C$, $T_0 = 0°C$, $T_{-20} = -20°C$

F = the rate of air flow, where $F_1 = 1$ scfm, $F_3 = 3$ scfm, $F_5 = 5$ scfm (i.e. the cfm under standard conditions of 20°C and 1 atm).

Each box of the square represents a run in which the four parameters were maintained at the designated levels. The humidity produced by the generator during a run was computed and also measured by the gravimetric hygrometer. The difference between the computed and measured humidity for a run constituted the basis for studying the effect of parameter level on performance.

A comparison of the results of the runs between each of the three columns of the Graeco-latin square is used to indicate whether the level of external saturator temperature affects the generator performance. Similarly, a comparison of the results of the runs between each of the three rows is used to indicate whether the level of flow affects the generator performance. From the results of the two sets of diagonal columns the effects of final saturation pressure and final saturation temperature are obtained.

RESULTS AND DISCUSSION

If water vapor and air, separately and in gaseous mixture, are assumed to obey the perfect gas laws and the Gibbs-Dalton law of partial pressure, then the mixing ratio of moist air is given by the equation

$$r = \frac{0.62197\, e}{P - e} \tag{1}$$

where r is the ratio of the mass of water vapor to the mass of associated dry air, e is the partial pressure of the water vapor in the water vapor-air mixture, and P is the total pressure of the water vapor-air mixture. By substituting the saturation vapor pressure e_s of the pure vapor phase of water in equilibrium with a plane surface of its liquid or solid phase for e in the above equation, the ideal saturation mixing ratio r_s is obtained. The saturation mixing ratio is a function of the total pressure and the temperature of the moist air. Equation (1) may be used to compute the ideal mixing ratio produced by the generator by using values of e_s from saturation vapor pressure tables[4] corresponding to the temperature in the final saturator of the internal humidifying system and by substituting values of the absolute pressure in the final saturator for the total pressure P.

Ideal saturation mixing ratios were computed for each of the nine runs comprising the 3×3 Graeco-latin square and compared with

the mixing ratio measured by the National Bureau of Standards standard hygrometer. A percentage difference was obtained by using the equation

$$d = \frac{r_h - r_g}{r_g} \times 100 \qquad (2)$$

where r_h is the computed ideal mixing ratio for the humidity generator and r_g is the measured mixing ratio obtained with the standard (gravimetric) hygrometer. The results are given in Table 1:

Table 1. The Percentage Difference Between r_h and r_g

+0.46% ($\Delta t_{15}, P_1, T_{25}, F_5$)	−1.11% ($\Delta t_5, P_4, T_0, F_5$)	−1.80% ($\Delta t_0, P_2, T_{-20}, F_5$)
−1.01% ($\Delta t_{15}, P_2, T_0, F_3$)	−0.94% ($\Delta t_5, P_1, T_{-20}, F_3$)	−1.40% ($\Delta t_0, P_4, T_{25}, F_3$)
−4.54% ($\Delta t_{15}, P_4, T_{-20}, F_1$)	−0.70% ($\Delta t_5, P_2, T_{25}, F_1$)	−0.73% ($\Delta t_0, P_1, T_0, F_1$)

Consider the three horizontal rows. In the first row, F_5 is common to all three boxes, in the second, F_3, and in the third, F_1. Since all the other parameters are present in each row at the same three levels, it will be assumed that these other parameters have a similar effect on the algebraic averages of the d's of each row, so that the algebraic averages are indicative only of the correlation of F with d. The same type of analysis may be made for the vertical columns to yield values of d for each level of Δt, for one set of diagonals to yield values of d for each level of P, and for the other set of diagonals to yield values of d for each level of T. These results are shown in Table 2.

It is estimated that the errors in the measurement of the total pressure and the temperature in the final saturator may produce a maximum uncertainty of ½ of 1 per cent in the computed mixing ratio r_h of the generator. The difference disclosed by the nine runs of the experiment are in all cases but one larger in magnitude than the estimated maximum uncertainty of the generator, suggesting that each of the parameters investigated is significant to the performance of the generator. It has been well established, however, that water vapor and air, and mixtures thereof, do not behave as ideal gases, nor does the Gibbs-Dalton law of partial pressures hold for moist air. Furthermore, the saturation-vapor density of the water substance in the presence of an inert gas[5-12] is higher than when the pure water substance alone is present. These factors may be accounted for by using a correction factor f[5] in the equation for computing the actual mixing ratio at saturation for moist air:

$$r_s = \frac{0.62197\, fe_s}{P - fe_s} \qquad (3)$$

where f is a function of total pressure and temperature.

Two courses of action are now feasible. Appropriate values of f, obtained from the published results of other workers,[5, 6] may be inserted into Eq. (3) to compute r_s for each of the nine runs, or values of f may be calculated by using r_g in Eq. (3). Since the standard hygrometer yielded measured values of r_g of high accuracy, the latter course was followed. The results are tabulated in Table 3 and plotted in Fig. 1.

Table 3. Values of f Obtained by Using r_g

	Temperature (°C)		
	25	0	−20
Saturator Pressure (psia)	Correction Factor for Moist Air		
15.4	0.995	1.007	1.009
29.2	1.007	1.010	1.018
63.8	1.014	1.011	1.041

Table 2. The Effect of Parameter Levels on the Percentage Difference between r_h and r_g

	d		d		d		d
Δt_0	−1.31%	P_1	−0.40%	T_{25}	−0.55%	F_1	−1.99%
Δt_5	−0.92%	P_2	−1.17%	T_0	−0.95%	F_3	−1.12%
Δt_{15}	−1.70%	P_4	−2.35%	T_{-20}	−2.43%	F_5	−0.82%

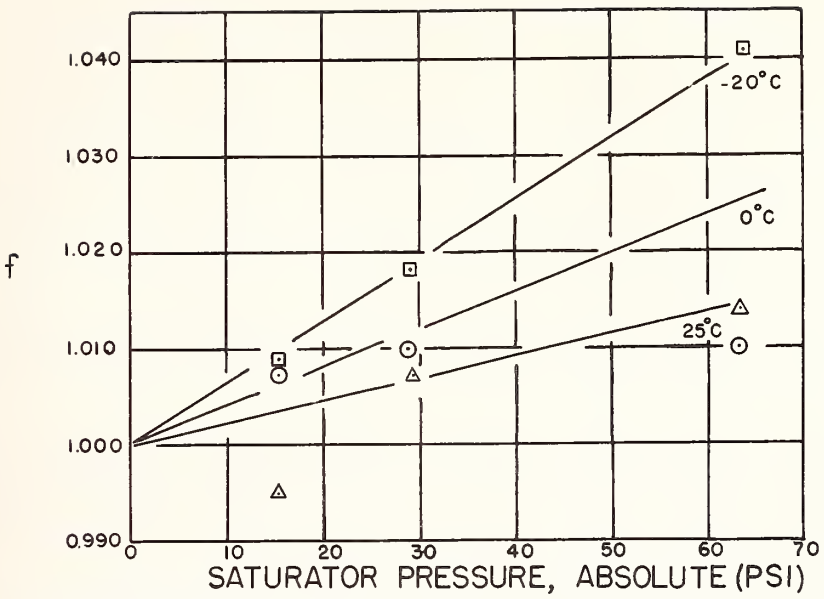

FIG. 1. Estimate of saturation correction factor f as a function of total pressure and constant temperature.

In plotting the curves in Fig. 1, it was assumed that, for absolute pressures up to 64 psia, the correction factor f, for a given temperature, was a linear function of total pressure and that the origin of the curve corresponded to $f = 1$ at $P = e_s$.

It may be noted that the curves fit the data rather well except for two points. From Eq. (3) and the correction factor f from Fig. 1, a mixing ratio r_h can be obtained for each run and, in turn, a new value of d can be computed. The Graeco-latin square, with these new values of d in the appropriate boxes, is shown in Table 4.

TABLE 4. THE PERCENTAGE DIFFERENCE BETWEEN r_s AND r_g

+0.78% ($\Delta t_{15}, P_1, T_{25}, F_5$)	+1.26% ($\Delta t_5, P_4, T_0, F_5$)	−0.04% ($\Delta t_0, P_2, T_{-20}, F_5$)
+0.08% ($\Delta t_{15}, P_2, T_0, F_3$)	+0.05% ($\Delta t_5, P_1, T_{-20}, F_3$)	0.00% ($\Delta t_0, P_4, T_{25}, F_3$)
−0.11% ($\Delta t_{15}, P_4, T_{-20}, F_1$)	−0.12% ($\Delta t_5, P_2, T_{25}, F_1$)	−0.13% ($\Delta t_0, P_1, T_0, F_1$)

The percentage difference d for each level of each of the four parameters is given in Table 5. Only the percentage difference for F_5 now exceeds the estimated maximum uncertainty of ½ per cent inherent in the measurement of the generator's saturation pressures and temperatures. Thus if the correction factor f as given in Fig. 1 is accepted as valid, then it may be concluded that only at a volumetric flow rate of 5 scfm is there a significant error. Further, from the sign of the d for F_5 it may be postulated that at this flow rate there is incomplete saturation of the air stream. The two points which are not close to the best straight lines in Fig. 1 are those obtained in runs with flow rates of 5 scfm.

The question may now be raised as to how well the f values resulting from this experiment

TABLE 5. THE EFFECT OF PARAMETER LEVELS ON THE PERCENTAGE DIFFERENCE BETWEEN r_s AND r_g

	d		d		d		d
Δt_0	−0.06%	P_1	+0.23%	T_{25}	+0.22%	F_1	−0.12%
Δt_5	+0.40%	P_2	−0.03%	T_0	+0.40%	F_3	+0.04%
Δt_{15}	+0.25%	P_4	+0.38%	T_{-20}	−0.03%	F_5	+0.67%

Table 6. Comparison of Some Saturation Vapor Pressure Correction Factors

Saturator Pressure (psia)	Saturator Temperature (°C)	Saturation Vapor Pressure Correction Factor		
		Webster[6]	Goff[5]	NBS
63.9	25	1.015	1.016	1.014
29.4	25	1.007	1.008	1.006
15.3	25	1.004	1.005	1.003
15.4	0	1.005	1.005	1.006
29.1	0	1.010	1.008	1.011
63.8	0	1.022	1.018	1.024
15.4	−20	1.008	1.005	1.010
29.2	−20	1.015	1.010	1.018
63.8	−20	1.034	1.021	1.040

agree with those of other workers. Webster[6] and Goff[5] have investigated the air-water vapor mixture over the temperature and pressure range covered in this investigation. In Table 6, the NBS values of f obtained from Fig. 1 are compared with those given by Webster and Goff. It must be emphasized that the NBS values are based on limited data over a narrow pressure range and are preliminary in nature. There appears to be close agreement among the three sets of values except one point corresponding to a pressure of 64 psia and a temperature of −20°C, where Goff's value is approximately 2 per cent lower than NBS's value, whereas Webster's value is only 0.6 per cent lower than NBS's value.

References

1. Wexler, A., and Daniels, Jr., R. D., "Pressure Humidity Apparatus," *J. Res. Natl. Bur. Std.*, **48**, 269 (1952).
2. Wexler, A., and Hyland, R. W., "The NBS Standard Hygrometer," in "Humidity and Moisture," Vol. III, p. 389, New York, Reinhold Publishing Corp., 1965.
3. Youden, W. J., "Statistical Methods for Chemists," New York, John Wiley & Sons, Inc.
4. "Smithsonian Meterological Tables," 6th revised edition 1951.
5. Goff, J. A., "Final Report for the Working Subcommittee of the International Joint Committee on Psychrometric Data," *ASME Trans.*, **71**, 903 (1949).
6. Webster, T. J., "The Effect on Water Vapour Pressure of Superimposed Air Pressure," *J. Soc. Chem. Ind.*, **69**, 343 (1950).
7. Pollitzer, F., and Strebel, E., "Über den Einfluss indifferenter Gase auf die Sättigungs-Dampfkonzentration von Flüssigkeiten," *Z. Phys. Chem.*, **110**, 768 (1924).
8. Bartlett, E. P., "The Concentration of Water Vapor in Compressed Hydrogen, Nitrogen, and a Mixture of these Gases in the Presence of Condensed Water," *J. Am. Chem. Soc.*, **49**, 65 (1927).
9. Saddington, A. W., and Krase, N. W., "Vapor-Liquid Equilibria in the System Nitrogen-Water," *J. Am. Chem. Soc.*, **56**, 353 (1934).
10. Weaver, E. R., and Riley, R., "Measurement of Water in Gases by Electrical Conduction in a Film of Hygroscopic Material and the Use of Pressure Changes in Calibration," *J. Res. Natl. Bur. Std.*, **40**, 169 (1948).
11. Weaver, E. R., "Electrical Measurement of Water Vapor with a Hygroscopic Film," *Anal. Chem.*, **23**, 1076 (1951).
12. Schuster, F., and Baukrowitz, G., *Gas Wasserfach*, **95**, 198 (1954).

JOURNAL OF RESEARCH of the National Bureau of Standards—C. Engineering and Instrumentation
Vol. 72C, No. 1, January–March 1968

An Adiabatic Saturation Psychrometer

Lewis Greenspan and Arnold Wexler

Institute for Basic Standards, National Bureau of Standards, Washington, D.C. 20234

(November 17, 1967)

An adiabatic saturation psychrometer for measuring the humidity of gases, as well as the vapor content of vapor-gas mixtures, is described. The instrument behaves in accordance with predictions deduced solely from thermodynamic considerations. With water-air, water-hydrogen, carbon tetrachloride-hydrogen, carbon tetrachloride-oxygen and toluene-air systems, at room temperature, atmospheric pressure, and gas flow rates of 1.3 to 5.2 liters per minute, measured wet-bulb temperatures agree with calculated "thermodynamic wet-bulb temperatures" to within the accuracy of the measurements and the uncertainties in the published thermodynamic data used in the computations. For the water-air system, the systematic and random errors due to these sources are estimated at 0.027 deg C and 0.019 deg C respectively. The agreement between the calculated and measured wet-bulb temperature is 0.029 deg C, which at a dry-bulb temperature of 25 °C and an ambient pressure of 1 bar is equivalent to an uncertainty in relative humidity which varies from 1/8 to 1/4 percent. The time constant is a function of the gas flow rate; at flow rates of 3.75 to 5.2 liters per minute, the time constant is of the order of 3/4 minute.

Key Words: Adiabatic saturation, gas mixtures, humidity, hygrometer, mixing ratio, moist gas, psychrometer, psychrometric factor, saturation, thermodynamic wet-bulb temperature, vapor content, wet-bulb.

1. Introduction

The psychrometer is one of the oldest and most common instruments for measuring the humidity of moist air. In its elemental form it consists of two thermometers; the bulb of one is covered with a wick and is moistened; the bulb of the other is left bare and dry. Evaporation of water from the moistened wick lowers its temperature below the ambient or dry-bulb temperature. The wet-bulb temperature attained with the conventional psychrometer is dependent on many factors in addition to the moisture and temperature state of the gas [1–4].[1] Although attempts have been made to develop a theory that would correctly interrelate the parameters affecting the behavior of the conventional psychrometer, there is no theory which completely describes its performance. In the well-known convection or adiabatic saturation theory [5–10], the principles of classical thermodynamics exclusively are used to derive a formula that predicts the humidity of a moist gas from wet- and dry-bulb thermometer measurements. Unfortunately the conventional psychrometer, even under steady-state conditions, is an open system undergoing a nonequilibrium process which cannot be depicted completely by classical thermodynamic theory. It is fortuitous that the formulas so derived yield results that are in nominal agreement with empirical facts for water vapor-air mixtures. When these formulas are applied to other vapor-gas mixtures, they fail to predict the correct vapor content.

The wet-bulb thermometer of a psychrometer in a steady-state condition experiences simultaneous heat and mass transfer. Although theories based on heat and mass transfer laws lead to equations which have a structural similarity to those derived from thermodynamic reasoning as well as to those of empirical origin, they also involve the ratio of thermal to mass diffusivities [3, 11–21]. Even these equations, which yield results in closer agreement with experimental data, do not completely depict all psychrometric behavior. For the water-air system, the ratio of thermal to mass diffusivity is close to one, accounting, in part, for the nominal agreement between the predictions based on the convection theory with those based on heat and mass transfer laws. In general, this ratio is greater than one [11, 22].

It would be advantageous to have an adequate theoretical basis for the behavior of the conventional psychrometer, but lacking a rational theory which accurately and fully describes the operation of the conventional psychrometer, one can invert the problem and inquire whether a psychrometer can be built which will behave in accordance with the postulates of classical thermodynamics. It appears that such a psychrometer can be designed and constructed and

[1] Figures in brackets indicate the literature references at the end of this paper.

that its behavior can be predicted by thermodynamic reasoning and expressed in mathematical form.

2. Theoretical Considerations

Consider a closed system undergoing an isobaric quasi-static process in which compressed liquid (or solid) at pressure P and temperature T_w is introduced into a gas at pressure P, temperature T, and mixing ratio[2] r to bring the gas adiabatically to saturation at pressure P, temperature T_w, and mixing ratio r_w. The term "gas" as used here and elsewhere in this paper is intended to include a gaseous mixture of which one constituent or component is a permanent gas or mixture of permanent gases and the second constitutent or component is the vapor of the compressed liquid involved in the psychrometric process and manifests itself as a product of evaporation. Since the process is adiabatic and isobaric the sum of the enthalpies of the various phases within the system are conserved, thus the initial and final enthalpies are equal, leading to the following equation:

$$h(P, T, r) = h(P, T_w, r_w) - (r_w - r) \cdot h'_w(P, T_w) \qquad (1)$$

where

$h(P, T, r)$ = The enthalpy of $(1+r)$ g of gas mixture at pressure P, temperature T and mixing ratio r, that is, the enthalpy of a mixture consisting on 1 g of the vapor-free gas and r g of the vapor component;

r = the mass of vapor in the original gas mixture per unit mass of vapor-free gas with which the vapor is associated;

$h'_w(P, T_w)$ = the enthalpy of 1 g of pure compressed liquid (or solid) of the vapor component at pressure P and temperature T_w;

$h(P, T_w, r_w)$ = the enthalpy of $(1+r_w)$ g of gas mixture saturated with respect to the second or vapor component at pressure P and saturation temperature T_w, that is, the enthalpy of a gas mixture containing one gram of vapor-free gas and r_w g of the vapor component; and

$r_w = r_w(P, T_w)$ = the mass of vapor component of the gas mixture per unit mass of vapor-free gas of the mixture when it is saturated with respect to the vapor component at pressure P and temperature T_w.

The "thermodynamic wet-bulb temperature" is defined [23] as the solution for T_w in eq (1).

In order to facilitate the mathematical development we introduce the following additional notation:

$\Delta T = (T - T_w)$ = The wet-bulb depression;

$h(P, T_w, r)$ = the enthalpy of $(1+r)$ g of gas mixture at pressure P, temperature T_w (the same as the "thermodynamic wet-bulb temperature" of the original gas mixture), and mixing ratio r (the same as the mixing ratio of the original gas mixture);

$h(P, T, 0) = h(P, T, r=0)$ = the enthalpy of 1 g of the pure first (vapor-free) component of the mixture at pressure P and temperature T; and

$h(P, T_w, 0) = h(P, T_w, r=0)$ = the enthalpy of 1 g of the pure first component of the mixture at pressure P and temperature T_w.

[2] In several of the engineering disciplines r is called the humidity ratio.

Let

$$F = F(P, T, T_w, r) = [h(P, T, r) - h(P, T_w, r)] \qquad (2)$$

and

$$C_{p,m} = \frac{[h(P, T, 0) - h(P, T_w, 0)]}{(T - T_w)} = \frac{1}{(T - T_w)} \int_{T_w}^{T} C_p \, dT \qquad (3)$$

where

C_p = the specific heat at constant pressure of the pure vapor-free component.

Also let

$$C_{pv,m} = \frac{[h(P, T, r) - h(P, T_w, r)] - [h(P, T, 0) - h(P, T_w, 0)]}{r(T - T_w)} \qquad (4)$$

and

$$L_{v,r} = \frac{[h(P, T_w, r_w) - h(P, T_w, r) - (r_w - r)\, h'_w(P, T_w)]}{(r_w - r)} \qquad (5)$$

From the above definition, it will be clear that $C_{p,m}$ represents the mean specific heat at constant pressure of the pure vapor-free first component over the temperature range from T_w to T. The entity $C_{pv,m}$ may be interpreted as the "effective" specific heat at constant pressure P of the vapor component of the mixture taken as a mean over a temperature range from T_w to T and at a mixing ratio of r. Finally, $L_{v,r}$ may be understood as the "effective" latent heat of vaporization (or sublimation) of the vapor component of the mixture at constant pressure P and constant temperature T_w. It will be seen that $L_{v,r}$ is taken as a mean while $(r_w - r)$ gram of vapor component evaporates into the gas mixture from a plane surface of its liquid phase per gram of first component. Both mixture and liquid must be at the same pressure P and temperature T_w, the gas mixture having a mixing ratio r initially and attaining a mixing ratio r_w finally as a result of the process of evaporation.

It should be noted that the "effective" specific heat $C_{pv,m}$ and the "effective" latent heat of vaporization $L_{v,r}$ both differ from their counterparts pertinent to the pure phase of the second (vapor) component owing to the interactions between the molecules of the first and second components of the gas mixture, and due to other small effects [24].

By adding to the function F each of the quantities $h(P, T, 0)$ and $h(P, T_w, 0)$, both with positive and negative signs, respectively, one obtains the useful identity

$$\begin{aligned} F &= [h(P,T,r) - h(P,T_w,r)] \\ &= [h(P,T,r) - h(P,T,0)] - [h(P,T_w,r) - h(P,T_w,0)] \\ &\quad + [h(P,T,0) - h(P,T_w,0)]. \end{aligned} \tag{6}$$

When one subtracts $h(P, T_w, r)$ from both the left-hand and right-hand members of eq (1), it is obvious that the left-hand member transforms to the function F. Therefore, the right-hand member of eq (1) *minus* $h(P, T_w, r)$ is also equal to F, so that we can equate this difference to eq (6) which yields the relationship

$$\begin{aligned} &[h(P,T_w,r_w) - h(P,T_w,r)] - (r_w - r)h'_w(P,T_w) \\ &\quad = [h(P,T,r) - h(P,T,0)] \\ &\quad - [h(P,T_w,r) - h(P,T_w,0)] \\ &\quad + [h(P,T,0) - h(P,T_w,0)]. \end{aligned} \tag{7}$$

Inspection reveals that the product $(r_w - r)L_{v,r}$ is equal to the left-hand member of eq (7), while the sum of the products $(T - T_w)C_{p,m}$ and $r(T - T_w)C_{pv,m}$ is equal to the right-hand member of eq (7). On making these substitutions in eq (7) it transforms to

$$(r_w - r)L_{v,r} = [C_{p,m} + rC_{pv,m}](T - T_w). \tag{8}$$

On introducing the "psychrometric factor" A and the ratio B defined by

$$A = C_{p,m}/L_{v,r} \tag{9}$$

$$B = C_{pv,m}/L_{v,r} \tag{10}$$

substituting these in eq (8), and solving it for r, one finds

$$r = \frac{r_w}{[1 + B\Delta T]} - \frac{A\Delta T}{[1 + B\Delta T]} \tag{11}$$

where $\Delta T = T - T_w$.

Solving eq (11) for A one obtains

$$A = \frac{r_w - r[1 + B\Delta T]}{\Delta T}. \tag{12}$$

The "psychrometric factor" A as defined by eq (9) is identically equal to the "psychrometric factor" A as given by eq (12).

For the case where the initial mixing ratio of the gas is zero, eq (12) reduces to

$$A = \frac{r_w}{\Delta T}. \tag{13}$$

If the vapor and the gas separately and admixed with one another obey the ideal gas laws, eq (11) becomes

$$r = \frac{r_w}{(1 + B'\Delta T)} - \frac{A'\Delta T}{(1 + B'\Delta T)} \tag{14}$$

or, alternately, in terms of vapor pressure,

$$e = \frac{e_w}{(1 + B'\Delta T)} \frac{(P - e)}{(P - e_w)} - \frac{(P - e)A_0\Delta T}{(1 + B'\Delta T)} \tag{15}$$

where

$$A_0 = \frac{M_g}{M_v} \frac{C'_p}{L'_v} \tag{16}$$

$$A' = \frac{C'_p}{L'_v} \tag{17}$$

$$B' = \frac{C'_{pv}}{L'_v} \tag{18}$$

and

e = the partial pressure of the vapor component in the original gas mixture;
e_w = the saturation vapor pressure of the liquid phase of the vapor component at temperature T_w;
P = the total pressure;
C'_{pv} = the pure phase specific heat of the vapor at constant pressure;
L'_v = the pure phase latent heat of vaporization of the vapor;
C'_p = the specific heat of the vapor-free gas at constant pressure;

A_0 = the so-called "psychrometric constant" (which appears in most formulas for the conventional psychrometer [3]);
M_g = the molecular weight of the vapor-free gas component; and
M_v = the molecular weight of the vapor component.

When e and e_w are small compared to P and $B'\Delta T$ is small compared to one, which is the case for the water-air system at dry-bulb temperatures T up to about 45 °C, eq (15) reduces to

$$e = e_w - A_0 P \Delta T \tag{19}$$

which is identical to the classical equation often used to represent the behavior of the conventional psychrometer.

It does not appear feasible to construct a practical psychrometer that is an embodiment of a closed system undergoing the ideal adiabatic isobaric saturation process which serves as the basis of eq (1). On the other hand, an open system undergoing a steady-flow process would appear to be operationally feasible, and such a system was constructed and its performance investigated. The aim was to approach ideal conditions as closely as practical, namely to bring compressed liquid (or solid) to pressure P and temperature T_w, to evaporate it into a gas stream at pressure P, temperature T and mixing ratio r, and to bring the gas adiabatically to saturation at pressure P, temperature T_w, and mixing ratio r_w. This system then becomes an adiabatic saturator operating at constant pressure. If nothing enters to violate the conditions of eq (1), the adiabatic saturator becomes an "adiabatic saturation psychrometer" since measured values of P, T, and T_w can be inserted into eq (11) to obtain the mixing ratio of the entrant gas stream. It was realized that practical and theoretical matters, such as heat exchanges due to radiation and conduction, and pressure drop associated with flow, would be among the factors limiting the possibility of attaining the ideal, especially in view of the desire to keep the apparatus simple for ease of construction. It was left, therefore, to experiment to serve as the indicator of how close the actual psychrometer conformed to theory.

3. Background

In 1922, W. K. Lewis performed several experiments in which a dried gas was bubbled through a volatile liquid in a Dewar flask containing glass beads, the gas being discharged into the liquid through a vacuum-jacketed glass inlet tube. For water-air, water-carbon dioxide, toluol-air and chlorbenzol-air the gas substantially became saturated and the liquid (as well as the effluent gas) eventually reached a steady-state temperature that was essentially the "thermodynamic wet-bulb temperature." The readings of wet-bulb temperature in the experiments using water, toluol and chlorbenzol as the liquid were independent of air velocity and of the amount of air contact with the liquid. This was not the case in the experiments with liquids of higher vapor pressure. The discrepancy probably was due to incomplete saturation and incomplete heat transfer between the gas and liquid rather than lack of constancy of the wet-bulb temperature as Lewis assumed.

Nanda and Kapur [28] performed similar experiments, bubbling dried air into a Dewar containing such liquids as acetone, methyl alcohol, ethyl alcohol, and butyl alcohol. After a considerable length of time, the liquid temperature approached the "thermodynamic wet-bulb temperature."

We also repeated these experiments, and in doing so found it necessary to use a vacuum-jacketed glass inlet tube, such as Lewis had used, for bubbling the gas through the liquid in the Dewar flask. With this inlet tube, which reduced precooling of the inlet gas prior to discharge into the liquid, steady-state temperatures of the liquids were obtained, which were in close agreement with calculated "thermodynamic wet-bulb temperatures," provided the gas flow was very low and only after extended continuous flow, usually hours.

Although "thermodynamic wet-bulb temperatures" could be obtained with the Dewar flask, the low gas flow rates, and the extremely long time necessary to reach steady-state conditions at these flow rates, seemed to preclude its use as a practical instrument for measuring humidity.

Carrier and Lindsay [25], and Dropkin [14] constructed large scale, engineering-type apparatus for obtaining adiabatic saturation. The essential feature of these devices was the provision for passing air over surfaces moistened with water that had been precooled to, or close to, the wet-bulb temperature, within well-insulated ducts. The experiments performed by these investigators were limited to the water-air system.

In 1961, J. D. Wentzel described a psychrometer which apparently measured the "thermodynamic wet-bulb temperature" of water-air with high accuracy [29]. In his instrument, Wentzel attempted to saturate adiabatically a stream of test air (whose humidity was to be measured) with water vapor in a fashion that appeared to approach the idealized steady-flow adiabatic process. Basically his instrument consisted of a vacuum-insulated glass tube, the inner walls of which were silvered to reduce radiation effects. The tube was partially filled with a moistened natural sponge through which the air flowed. Makeup water was added intermittantly, in one design, and continuously in a second design. In the latter version, the continuous flow of makeup water was precooled by an essentially equivalent instrument through which part of the gas stream was channeled. To preclude the possibility of drying of the sponge, excess makeup liquid was used. Wet-bulb temperatures were measured with thermocouples imbedded in the moistened sponge. Wet-bulb temperature measurements for the water-air system corresponded very closely to "thermodynamic wet-bulb temperatures." It is well known, however, that the wet-bulb temperature for moist air as measured with a conventional psychrom-

eter nominally is not very different from the "thermodynamic wet-bulb temperature" so that further demonstration is required to establish that a psychrometer is undergoing a true thermodynamic wet-bulb process. This could have been accomplished by the use of liquid-gas systems other than water-air for which the wet-bulb temperature as indicated by a conventional psychrometer, and the "thermodynamic wet-bulb temperature" differ appreciably.

L. P. Harrison [26] has proposed three psychrometer designs for measuring "thermodynamic wet-bulb temperature," each design involving the employment of three concentric tubes so arranged as to insure intimate contact between gas and liquid and therefore to insure adiabatic saturation.

We first duplicated Wentzel's instrument with some modifications. Whereas Wentzel successfully had employed natural sponges as his saturating element, we were unsuccessful in the use not only of natural but also of artificial sponges because of the tendency for the liquid to be blown out by the gas stream. Only when we finally resorted to cotton cheesecloth did the instrument operate satisfactorily. Various liquid-gas systems were tried and although wet-bulb temperatures approaching "thermodynamic wet-bulb temperatures" were obtained, these were not sufficiently close to one another to form the basis of an accurate measuring system. The best results were achieved with the water-air system. The major defect in the instrument appeared to be the lack of sufficient precooling of the liquid so that it would feed into the saturating element at, or very close to, the "thermodynamic wet-bulb temperature." With the water-air system the operation of an adiabatic saturation psychrometer is less sensitive to the liquid feed temperature than it is with some other liquid-gas systems.

We then developed an instrument utilizing vacuum-jacketed glass tubes, as in the Wentzel instrument, but employing a different saturating element and a novel feed arrangement that precools the liquid very close to the wet-bulb temperature. "Thermodynamic wet-bulb temperatures" were closely approached with various liquid-gas systems, as well as with water-air.

4. Description

The instrument is shown in figures 1 and 2. It consists of a vacuum-jacketed glass saturator tube, A, that is surrounded by a glass Dewar flask, B. Within the saturator tube is a thermocouple, C, for measuring dry-bulb temperature, wicking, D, for saturating the gas stream, and a feed tube, E, through which liquid is introduced for moistening the wicking. A thermocouple, F, for measuring wet-bulb temperature is located beyond the outlet end of the saturator tube. The saturator tube is centered and held in the Dewar flask by a stopper, G. There is a pressure tap, H, at the outlet end of the saturator tube and an exit flow line, I, through which the effluent gas leaves the instrument. The test gas enters at the inlet end of the saturator tube, flows through the saturator tube, emerges at the outlet end of the saturator tube, reverses direction, flows over the exterior surface of the saturator tube and discharges through the exit flow line and micrometer valve, J.

The main component is the saturator tube fabricated with double walls, with the space between the walls evacuated and sealed. The tube is silvered to reduce radiation effects, is 13 in long, and has an o.d. of 1/2 in and an i.d. of 0.15 in. It is within this saturator tube that the "thermodynamic wet-bulb process" occurs.

The liquid feed system comprises a graduated reservoir, K, a preliminary heat exchanger, L, a main heat exchanger, M, and a feed tube, E. Liquid flows from the reservoir, through the heat exchangers, the feed tube, and onto the wicking. The reservoir is mounted on a vertical rod. Its elevation can be adjusted to provide the required head of liquid to maintain the flow necessary for complete and continuous moistening of the wicking. The preliminary heat exchanger is a 12-ft

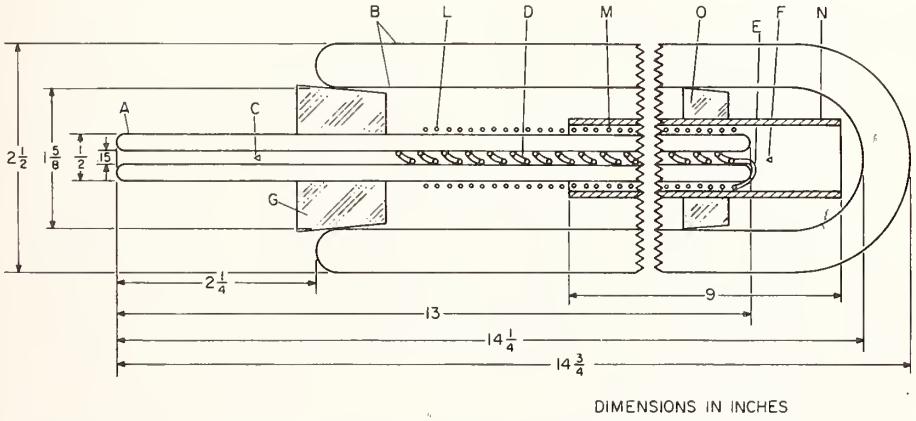

FIGURE 1. *Adiabatic psychrometer—principal section*

A. Vacuum-jacketed glass saturator tube; B. glass Dewar flask; C. Dry-bulb thermocouple; D. Cotton wicking; E. liquid feed tube; F. wet-bulb thermocouple; G. saturator tube rubber stopper; L. preliminary heat exchanger; M. main heat exchanger; N. flow guide; O. flow guide cork stopper.

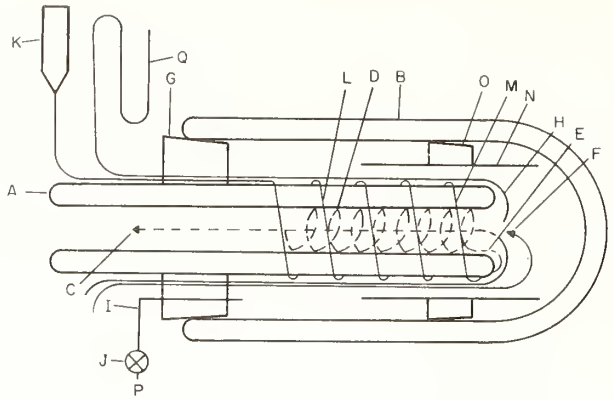

FIGURE 2. *Adiabatic psychrometer—schematic*
A, Vacuum-jacketed glass saturator tube; B, glass Dewar flask; C, dry-bulb thermocouple; D, cotton wicking; E, liquid feed tube; F, wet-bulb thermocouple; G, saturator tube rubber stopper; H, static pressure tap; I, exit flow line; J, micrometer exhaust valve; K, graduated reservoir; L, preliminary heat exchanger; M, main heat exchanger; N, flow guide, O, flow guide cork stopper; P, vacuum source; Q, oil manometer.

length of polytetra fluoroethylene tubing, with an o.d. of about 0.045 in and an i.d. of about 0.021 in, loosely wound for 6 in around the outside of the saturator tube, connected at one end to the reservoir and at the other end to the main heat exchanger. The latter is a 5-ft length of stainless steel tubing, with an o.d. of 0.0355 in and an i.d. of 0.023 in, wound into a 5/8-in diam helix that fits over the outlet end of the saturator tube for a distance of 4 in. The feed tube is fabricated from 2 ft of the same PTFE tubing as used in the preliminary heat exchanger. It is wound into a helix which fits inside the saturator tube and extends inward for 10 in from the outlet end.

The feed tube is covered with a close-fitting sleeve of cotton wicking. One end of the sleeve terminates 1/2 in inside the outlet end of the saturator tube; the other end is tied tightly with cotton thread immediately beyond the discharge port of the feed tube.

The wet- and dry-bulb thermocouples are made from calibrated No. 40 copper and constantan wires encased in PTFE tubing like that described above. The dry-bulb thermocouple junction is located 1 1/2 in inside the inlet end of the saturator tube and upstream of the wicking; the wet-bulb thermocouple junction is located just beyond the outlet end of the saturator tube downstream of the wicking. Both junctions are placed along the axis of the saturator tube.

A silvered glass Dewar flask, 12 in long and with an i.d. of 1 5/8 in, encloses most of the saturator tube. The saturator tube fits tightly within a concentric hole in a No. 9 rubber stopper which, in turn, fits snugly into the mouth of the Dewar flask. The two sets of thermocouple wires, the preliminary heat exhanger, the pressure line, and the exit gas flow line are fed separately through, and tightly fitted in, holes in the stopper.

Within the Dewar flask is a glass tube, N, 9 inches in length, 7/8-in o.d., and 1/16-in thick, that is, in turn, supported by a cork stopper, 0. The saturator tube with its associated components is positioned concentrically inside the glass tube. The latter serves as a flow guide for channeling the gas over the surface of the main heat exchanger. It reduces the size of the annulus through which the gas flows and improves the heat transfer between the liquid in the main heat exchanger and the gas.

The exit flow line is connected to a micrometer valve and then to a vacuum source, *P*. The pressure line is connected to an oil manometer, *Q*, which, in conjunction with a barometer which measures ambient atmospheric pressure, yields the absolute pressure at the outlet end of the saturator tube. A potentiometer and null detector are used to measure the emfs generated by the thermocouples. The saturator assembly is maintained in a horizontal orientation.

The saturator tube is constructed with a vacuum jacket to reduce heat transfer between its interior and its surroundings. The outer Dewar flask serves the purpose of providing additional thermal insulation from the ambient atmosphere for the test gas. The design of the liquid-feed tube and wicking combination is intended to provide a large evaporative area to the flowing gas while reducing as far as practical the pressure drop and total liquid heat capacity. The liquid-feed heat exchanger provides for the automatic precooling of the liquid by the gas which has been brought to the wet-bulb temperature by the moistened wicking. Counter flow of gas and liquid is used to obtain the maximum heat exchange. It was intended that the total heat capacity of the heat exchanger and its contained liquid should be as small as possible. The preliminary liquid-feed heat exhanger is not considered to be part of the thermal capacity of the main heat exchanger and is a slight embellishment for heat exchange purposes. The liquid reservoir height adjustment is used to control the rate of liquid feed. Both thermocouples were located so as to be exposed only to and in contact with the gas stream.

5. Operating Procedure

The instrument is operated by establishing a continuous flow of sample gas and liquid. After steady-state conditions are reached, the wet- and dry-bulb temperatures and the pressure are measured.

The test gas is fed to the saturator tube at atmospheric pressure. Because of the use of glass in the construction of the saturator tube and the Dewar flask and the use of stoppers for assembling and sealing these components, the maximum pressure within the psychrometer is limited to about 1 atm. The outlet port of the micrometer valve is attached to a vacuum source. The micrometer valve is calibrated in terms of air flow over the range 0 to 6.2 liters per minute. By means of a density correction, the equivalent flow is obtained for any other gas. Thus, by an appropriate micrometer setting any desired flow within this range can be established through the psychrometer. Since the valve functions as a variable critical flow orifice, the volumetric flow through the psychrometer, for a given micrometer setting, is essentially constant.

The height of the reservoir is set so as to produce a liquid flow rate that is approximately three times that

required to completely saturate the vapor-free test gas. This liquid flow rate is measured by timing the change in volume of the liquid in the graduated reservoir. If drying occurs in any part of the wicking, a temperature transient is propagated through the saturator that upsets the thermal equilibrium of the instrument and yields an erroneous wet-bulb temperature. Excess liquid insures that the wicking is always completely moistened; the excess is carried through the saturator by the flow of gas and collects in the Dewar flask where it can be drained manually or automatically. Since the liquid enters and emerges from the saturator tube at essentially wet-bulb temperature, the enthalpies of the excess liquid flowing into and out of the saturator are essentially equal and therefore do not contribute to the overall enthalpy balance as given in eq (1).

5.1. Tests

Since eq (1) represents an interrelation among parameters P, T, T_w, and r such that $f(P, T, T_w, r)=0$, then if any three parameters, say P, T, and r are measured and inserted into the equation, the fourth, T_w, can be calculated. If, in addition, a measurement is also made of T_w, the calculated and observed "thermodynamic wet-bulb temperatures" can be compared. Such a comparison offers a measure of the conformance of psychrometer behavior with theory.

Equation (12) may be expressed in the form

$$\frac{C_{p,m}}{l_{v,r}}=\frac{r_w-r[1+B\Delta T]}{\Delta T} \tag{20}$$

in which the right- and left-hand sides are different functions of the same parameters, that is,

$$A_1(P, T, T_w, r)=A_2(P, T, T_w, r). \tag{21}$$

By inserting the same set of measurements of the parameters (P, T, T_w, r) into A_1 and A_2 these two functions can be calculated and compared. Such a comparison offers an alternate method of checking whether the psychrometer performs in accordance with theory. It should be recognized that A_1 and A_2 are alternate expressions of the "psychrometric factor."

A series of experiments was performed with the psychrometer, with various liquid-gas systems, to obtain experimental or observed values of the wet-bulb temperature which is given the notation $(T_w)_{obs}$. With the same values of parameters P, T, and r, the "thermodynamic wet-bulb temperature" was calculated. To differentiate it from the observed value it is given the notation $(T_w)_{calc}$. Because of the difficulty of generating vapor-gas mixtures of known mixing ratios to supply to the psychrometer, only dry, vapor-free gases were used. Thus, in each case the mixing ratio r of the gas was zero. All experiments were performed at room temperature (about 25 °C), except for four test points with water-air which were performed at about 37 °C, and at atmospheric pressure (about 1 bar). The flow rate of the test gas mixture was varied over the range 0.8 to 6.2 liters per minute. The possible implications due to the restriction $r=0$ will be discussed later.

The following systems were selected for the experiments: water-air, water-hydrogen, carbon tetrachloride-oxygen, carbon tetrachloride-hydrogen, and toluene-air. The gases were obtained from a commercial source in steel cylinders compressed to a pressure of about 120 atm. The carbon tetrachloride was of spectro grade, the toluene of reagent grade, and the water of distilled grade purity. These systems encompass a range of thermal to mass diffusivity ratios of 0.9 to 4.5 as shown in table 5.

The experimental setup is shown in figure 3. The gas from a cylinder, R, was passed through a high pressure reducer, S, and a low pressure reducer, T, in series, a drier filled with phosphorous pentoxide, U, and a stainless steel heat exchanger, V, immersed in a temperature-controlled liquid bath, W, and then fed into the psychrometer, X, at a pressure of about 1 atm. The desired gas flow rate was obtained by the appropriate setting of the micrometer on the exhaust valve, J. The reservoir, K, was filled with the test liquid and its elevation adjusted so that the liquid flow rate was approximately three times as great as that calculated as necessary to completely saturate the test gas at the wet-bulb temperature.

Tests were also performed to determine the speed of response of the instrument. Using air as the sample gas, and water as the liquid, the psychrometer was subjected to a nominal step-function change in mixing ratio at a dry-bulb temperature of 25 °C and at an ambient atmospheric pressure of about 1 bar. Dry air was fed to the psychrometer. After steady-state conditions were reached, the connection feeding the dry air to the inlet of the saturator tube was quickly removed and ambient (room) air was drawn in producing an increase in mixing ratio. The procedure was then reversed producing a decrease in mixing ratio. The emf from the wet-bulb thermocouple was fed to a precision potentiometer. The unbalance of the potentiometer was amplified and recorded as a function of time. After nulling the potentiometer for the steady-state initial wet-bulb temperature condition, a trace was obtained of the wet-bulb temperature change produced by the step-function change in mixing ratio.

5.2. Results

A comparison is shown in table 1 between the observed and calculated "thermodynamic wet-bulb temperatures," $(T_w)_{obs}$ and $(T_w)_{calc}$, for the several liquid-gas systems that were investigated. The absolute pressures P in the region of the wet-bulb thermocouple are given in column 1. Column 2 lists the approximate flow rates of the gas at the inlet end of the psychrometer, that is, at temperature T. Columns 3 and 4 list the observed (measured) dry- and wet-bulb temperatures. The calculated wet-bulb temperatures, obtained by solving eq (23) or (24) (see appendix) for T_w, are given in column 5. The differences between the observed and calculated wet-bulb temperatures, $[(T_w)_{obs}-(T_w)_{calc}]$, are tabulated in column 6.

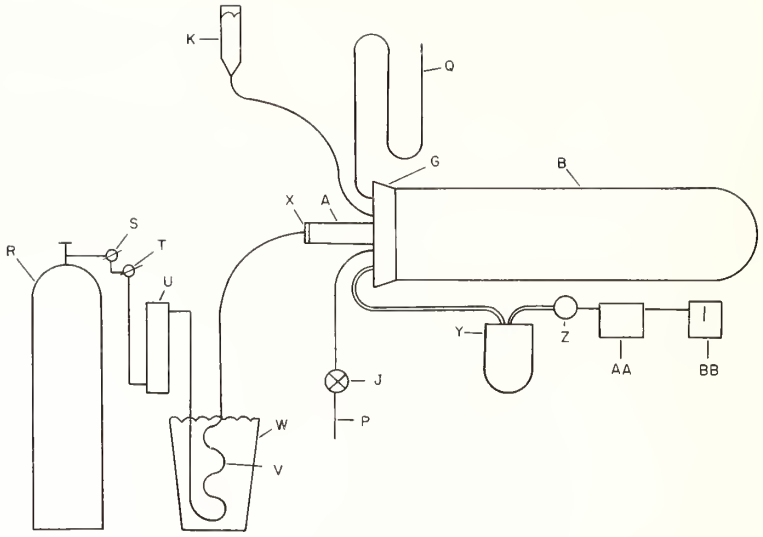

FIGURE 3. *Test setup—schematic*

J. micrometer exhaust valve; K. graduated reservoir; P. vacuum source; Q. oil manometer; R. compressed gas cylinder; S. high pressure reducer; T. low pressure reducer; U. drier; V. heat exchanger; W. temperature-controlled liquid bath; X. psychrometer; Y. reference junction ice bath; Z. thermocouple selector switch; AA. precison laboratory potentiometer; BB. null indicator.

Columns 7 and 8 of table 1 give values of the "psychrometric factor" $A_2=\frac{r_w}{\Delta T}$ and $A_1=\frac{C_{p,m}}{L_{v,r}}$ respectively, for the various liquid-gas systems studied. The differences (A_2-A_1) are given in column 9 while the percentage difference $\frac{(A_2-A_1)}{A_2}$ 100 are given in column 10.

Since in this imperfect world one cannot expect perfect agreement between experimental and theoretical values, it is desirable to have some criteria by which the reasonableness of the agreement can be assessed. An error analysis was therefore made to obtain estimates of the accuracy of the calculated "thermodynamic wet-bulb temperature" using the observed, or measured parameters P, T, and r. It is apparent that an iterative method must be used to solve eq (23) or (24) for T_w. Furthermore, the parameters P, T, T_w, and r must be known or assumed in order to obtain values of the enthalpy functions $h(P, T, r)$, $h(P, T_w, r)$, $h(P, T_w, r_w)$ and $h'_w(P, T_w)$, the latent heat of vaporization function $L'_v(T_w)$ and the saturation mixing ratio function $r_w(P, T_w)$. Not only do the measurement errors in P, T, and r enter into estimation of the error in $(T_w)_{calc}$, but experimental and other systematic uncertainties in the enthalpies, latent heats of vaporization and saturation mixing ratios must be accounted for. A similar analysis was made to obtain estimates of the accuracy of the psychrometric factors A_1 and A_2 using the observed parameters P, T, T_w, and r. Details of the analyses are given in the appendix, along with the sources of the thermodynamic data and physical constants used in the calculations. The results of the analyses are presented in tables 2, 3, and 4.

The parameters used in the computation of $(T_w)_{calc}$, A_1 and A_2 are listed in column 1 of table 2. The nominal magnitudes of the parameters are given in column 2. Estimates of the systematic and random errors in these parameters are given in columns 3 and 4 while the corresponding systematic and random errors in the wet-bulb temperature difference $[(T_w)_{obs}-(T_w)_{calc}]$ and in the psychrometric factor difference (A_2-A_1) produced by the estimated errors in these parameters are given in columns 5, 6, 7, and 8. Thus, for example, an estimated systematic error of 0.01 deg C in T for the water-air system produces a corresponding systematic error or 0.005 deg C in $[(T_w)_{obs}-(T_w)_{calc}]$ in the water-air system. The estimated overall systematic error in $[(T_w)_{obs}-(T_w)_{calc}]$ was obtained by summing the individual systematic errors listed in column 5. Similarly the estimated overall systematic error in (A_2-A_1) was obtained by summing the individual systematic errors in column 7. The estimated overall random error in $[(T_w)_{obs}-(T_w)_{calc}]$ and in (A_2-A_1) was obtained by computing the root-mean-square value of the individual random errors in columns 6 and 8, respectively. The estimated overall errors may be considered as guesses of the differences between $(T_w)_{obs}$ and $(T_w)_{calc}$ and between A_2 and A_1 which may be expected to occur due to systematic and random errors, provided the psychrometer otherwise acted in accordance with eq (1).

Table 3 lists, for each liquid-gas system, the average of $[(T_w)_{obs}-(T_w)_{calc}]$ and an estimate of the standard deviation of the average. Estimates of the overall systematic error and the overall random error, given in table 2, are repeated here for convenience in making comparisons. Table 4 gives similar values for (A_2-A_1).

TABLE 1. *Comparison between wet-bulb temperatures and psychrometric factors*

Pressure P	Flow	Dry-bulb temperature T	Wet-bulb temperature			Psychrometric factor			
			Observed $(T_w)_{obs}$	Calculated $(T_w)_{calc}$	Difference $[(T_w)_{obs}-(T_w)_{calc}]$	$A_2=\frac{r_w}{\Delta T}$	$A_1=\frac{C_{p,m}}{L_{v,r}}$	Difference (A_2-A_1)	Percentage difference $\frac{(A_2-A_1)}{A_2}\times 100$
Bars	Liter per minute	deg C	deg C	deg C	deg C	10^{-5}/deg C	10^{-5}/deg C	10^{-5}/deg C	%
Water—Air									
0.9745	1.4	24.80	7.87	7.86	0.01	40.65	40.57	0.08	0.2
.9737	1.4	24.73	7.81	7.82	−.01	40.54	40.57	−.03	−.1
.9816	1.4	24.62	7.80	7.83	−.03	40.42	40.57	−.15	−.4
.9806	1.4	24.65	7.82	7.84	−.02	40.49	40.57	−.08	−.2
1.0002	1.4	25.11	8.24	8.21	.03	40.76	40.59	.17	.4
0.9943	2.1	37.07	13.25	13.26	−.01	40.71	40.75	−.04	−.1
.9948	2.1	37.01	13.19	13.24	−.05	40.53	40.75	−.22	−.5
.9943	2.1	37.02	13.27	13.24	.03	40.88	40.75	.13	.3
0.9978	2.1	37.02	13.23	13.27	−.04	40.56	40.75	−.19	.5
1.0000	2.1	24.98	8.15	8.14	.01	40.61	40.58	.03	.1
1.0005	2.1	25.02	8.16	8.17	−.01	40.55	40.58	−.03	−.1
1.0008	2.1	25.02	8.18	8.17	.01	40.64	40.59	.05	.1
1.0008	2.1	25.08	8.22	8.20	.02	40.70	40.59	.11	.3
1.0007	2.1	25.17	8.25	8.24	.01	40.65	40.59	.06	.1
0.9818	6.2	24.88	8.07	7.95	.12	41.19	40.58	.61	1.5
.9829	6.2	24.85	8.10	7.95	.15	41.38	40.58	.80	1.9
Water—Hydrogen									
0.9718	5.2	24.40	7.60	7.58	0.02	576.8	575.0	1.8	0.3
.9807	5.2	24.29	7.57	7.60	−.03	573.1	575.0	−1.9	−.3
.9823	5.2	24.25	7.56	7.59	−.03	572.8	575.0	−2.2	−.4
.9851	5.2	24.40	7.63	7.68	−.05	571.2	575.0	−3.8	−.7
Carbon tetrachloride—Oxygen									
0.9929	1.3	24.52	−8.50	−8.52	0.02	416.8	416.1	0.7	0.2
.9714	1.9	24.67	−8.73	−8.72	−.01	415.6	416.0	−.4	−.1
.9876	1.9	24.66	−8.56	−8.53	−.03	415.1	416.1	−1.0	−.2
.9878	1.9	24.45	−8.66	−8.60	−.06	413.8	416.0	−2.2	−.5
.9870	1.9	24.41	−8.69	−8.62	−.07	413.6	416.0	−2.4	−.6
1.0114	0.8	24.26	−8.17	−8.39	.22	424.8	416.3	8.5	2.0
Carbon tetrachloride—Hydrogen									
1.0061	2.1	23.93	−8.71	−8.83	0.12	6.519	6.451	68	1.0
0.9970	2.1	23.82	−8.83	−8.97	.14	6.531	6.450	81	1.2
.9839	2.9	24.18	−8.96	−9.00	.04	6.471	6.449	22	.3
.9843	2.9	24.20	−8.98	−8.99	.01	6.453	6.449	4	.1
.9848	2.9	24.12	−9.01	−9.01	.00	6.447	6.448	−1	−.0
Toluene—Air									
0.9981	1.4	25.47	6.79	6.84	−0.05	236.8	238.2	−1.4	−0.6
.9986	1.4	25.37	6.74	6.80	−.06	236.5	238.2	−1.7	−.7
.9923	1.4	25.15	6.65	6.64	.01	238.4	238.2	0.2	.1
.9930	1.4	25.13	6.65	6.64	.01	238.5	238.2	0.3	.1
.9764	2.1	25.58	6.65	6.70	−.05	236.8	238.2	−1.4	−.6
.9784	2.1	25.54	6.62	6.70	−.08	236.0	238.2	−2.2	−.9
1.0056	0.8	25.09	6.90	6.73	.17	242.9	238.3	4.6	1.9
1.0075	0.8	24.98	6.90	6.70	.20	243.9	238.3	5.6	2.3

If the errors in $(T_w)_{obs}$ and $(T_w)_{calc}$, or in A_2 and A_1, were solely random, then the average of the appropriate difference, for a given liquid-gas system, would tend toward zero. Since the averages are not equal to zero, one would expect that these values are experimental measures of the systematic errors and should therefore have the same magnitudes as the estimates of the overall systematic errors. The standard deviations of the differences about these averages, on the other hand, are indicators of the experimental random errors and so, correspondingly, should have a close relationship to the estimates of the overall random errors.

It can be observed from table 3 that the average values of $[(T_w)_{obs}-(T_w)_{calc}]$ are smaller than the estimates of the overall systematic errors of $[(T_w)_{obs}-(T_w)_{calc}]$. This is also the case for (A_2-A_1) as shown in table 4. This is probably due to an overly conservative estimate of the individual systematic errors of the parameters (especially f_w) and the fact that summing the corresponding individual systematic errors of the appropriate differences gives a maximum.

It can be observed further from tables 3 and 4 that the estimates of the standard deviations are considerably greater than the estimates of the over-

TABLE 2. *Error analysis*

Parameter	Nominal magnitude of parameter	Estimated error of the parameter		Estimated error of $[(T_w)_{obs}-(T_w)_{calc}]$ due to parameter error		Estimated error of (A_2-A_1) due to parameter error	
		Systematic	Random*	Systematic	Random	Systematic	Random
				deg C	deg C	10^{-5}/deg C	10^{-5}/deg C
Water—Air							
$(T_a)_{obs}$ °C	8.	0.01	0.015	0.010	0.015	0.052	0.08
T °C	25.	.01	.024	.005	.011	.024	.06
P bar	1.0		.0002		.002		.01
M_i $\frac{g}{g\ mol}$	18.01534	.00006		.000		.000	
M_g $\frac{g}{g\ mol}$	28.9645	.0009		.000		.060	
f_w	1.004	.0008		.006		.033	
e_a bar	0.0107	.0000043		.003		.016	
C_p $\frac{J}{g\ °C}$	1.0	.00036		.003		.015	
h'_g $\frac{J}{g}$	33.	.025		.000		.000	
h_f $\frac{J}{g}$	2,516	.084		.000		.001	
Estimated overall error				.027	.019	.14	.10
Water—Hydrogen							
T_w °C	8.	0.01	0.015	0.010	0.015	0.74	1.11
T °C	25.	.01	.024	.005	.011	.35	0.83
P bar	1.0	.01	.0002		.002		.12
M_i $\frac{g}{g\ mol}$	18.01534	.00006		.000		.00	
M_g $\frac{g}{g\ mol}$	2.01594	.00001		.000		.010	
f_w	1.	.005		.039		2.91	
e_a bar	0.0104	.0000042		.003		.23	
C_p $\frac{J}{g\ °C}$	14.2	.00042		.000		.02	
L_v $\frac{J}{g}$	2,483	1.76		.005		.40	
Estimated overall error				.062	.020	4.65	1.39
Carbon Tetrachloride—Oxygen							
T_a °C	−9.	0.01	0.015	0.010	0.015	0.37	0.56
T °C	25.	.01	.024	.003	.008	.12	.31
P bar	1.0		.0002		.002		.09
M_i $\frac{g}{g\ mol}$	53.82315	.002		.000		.00	
M_g $\frac{g}{g\ mol}$	31.9988	.0001		.000		.00	
f_a	1.	.005		.057		2.14	
e_a bar	0.027	.000093		.038		1.46	
C_p $\frac{J}{g\ °C}$	.92	.000167		.002		0.9	
L_v $\frac{J}{g}$	214.	1.09		.055		2.14	
Estimated overall error				.165	.017	6.32	.65
Carbon Tetrachloride—Hydrogen							
T_w °C	−9.	0.01	0.015	0.010	0.015	6.0	8.9
T °C	25.	.01	.024	.003	.008	2.0	4.7
P bar	1.0		.0002		.002	.1	1.3
M_i $\frac{g}{g\ mol}$	153.82315	.002		.000		.1	
M_g $\frac{g}{g\ mol}$	2.01594	.00001		.000		.0	
f_w	1.	.005		.056		33.2	
e_a bar	0.027	.000091		.038		22.6	
C_p $\frac{J}{g\ °C}$	13.4	.00406		.000		0.2	
L_v $\frac{J}{g}$	214.	1.09		.054		32.9	
Estimated overall error				.161	.017	97.0	10.1
Toulene—Air							
T_a °C	7.	0.01	0.015	0.010	0.015	0.27	0.40
T °C	25.	.01	.024	.004	.010	.13	.31

TABLE 2. *Error analysis*—Continued

Parameter	Nominal magnitude of parameter	Estimated error of the parameter		Estimated error of $[(T_w)_{obs}-(T_w)_{calc}]$ due to parameter error		Estimated error of (A_2-A_1) due to parameter error	
		Systematic	Random*	Systematic	Random	Systematic	Random
				deg C	deg C	10^{-5}/deg C	10^{-5}/deg C
Toulene-Air—Continued							
P ..... bar	1.0		.0002		.002		.05
M_v ..... $\frac{g}{g\ mol}$	92.14181	.00008		.000		.00	
M_a ..... $\frac{g}{g\ mol}$	28.9645	.0009		.000		.01	
f_w	1.	.005		.049		1.20	
e_w ..... bar	0.014	.000014		.010		.24	
C_p ..... $\frac{J}{g\ °C}$	1.00	.00036		.002		.07	
L_e ..... $\frac{J}{g}$	423.	.88		.021		.40	
Estimated overall error				.096	.018	2.32	.51

*Estimated standard deviation of an observation.

TABLE 3. *Summary of wet-bulb temperature differences* $[(T_w)_{obs}-(T_w)_{calc}]$

System	Average	Standard deviation of the differences about the average	Estimated overall systematic error Δ_s	Estimated overall random error* Δ_r	Estimated total error $(\Delta_s+\Delta_r)$	Rejection criterion $(\Delta_s+3\Delta_r)$
	deg C	deg C	deg C	deg C	deg C	deg C
H_2O-Air	+0.015	0.053	0.027	0.019	0.046	0.084
H_2O-Air (Restricted flow)	−.003	.026	.027	.019	.046	
H_2O-H_2	−.021	.033	.062	.020	.082	.122
CCl_4-O_2	+.013	.108	.165	.017	.182	.216
CCl_4-O_2 (Restricted flow)	−.029	.035	.165	.017	.182	
CCl_4-H_2	+.060	.064	.161	.017	.178	.212
C_7H_8-Air	+.018	.109	.096	.018	.114	.150
C_7H_8-Air (Restricted flow)	−.038	.042	.096	.018	.114	

*Estimated standard deviation of an observation.

TABLE 4. *Summary of psychrometric factor differences* (A_2-A_1)

System	Average	Standard deviation of the differences about the average	Relative average	Estimated overall systematic error Δ_s	Estimated overall random error* Δ_r	Estimated total error $(\Delta_s+\Delta_r)$
	10^{-5}/deg C	10^{-5}/deg C	%	10^{-5}/deg C	10^{-5}/deg C	10^{-5}/deg C
H_2O-Air	+0.08	0.27	.19	0.14	0.10	0.24
H_2O-Air (Restricted flow)	−.01	.12	−.02	.14	.10	.24
H_2O-H_2	−1.6	2.4	−.27	4.65	1.39	6.04
CCl_4-O_2	+0.5	4.0	+.12	6.32	0.65	6.97
CCl_4-O_2 (Restricted flow)	−1.1	1.4	−.26	6.32	.65	6.97
CCl_4-H_2	+35.	37.	+.25	97.	10.	107.
C_7H_8-Air	+0.5	3.0	+.21	2.3	0.5	2.8
C_7H_8-Air (Restricted flow)	−1.0	1.0	−.43	2.3	.5	2.8

*Estimated standard deviation of an observation.

all random errors. The overall random errors were based on estimates of the individual random error to be expected in measurement of each of the parameters in a system in static equilibrium. The measurements were made in a dynamic system under conditions close to steady-state, but with some fluctuation of inlet temperature. Since the thermocouple emfs were not read simultaneously and since the wet-bulb thermocouple does not respond to changes in inlet temperature as rapidly as does the dry-bulb thermocouple, it is likely that the actual random temperature errors were greater than that estimated. That the standard deviation was approximately two- to three-fold the estimated overall (static) random error, does not seem disturbing, but does indicate that some contributory effects were not accounted for.

Examining the data in table 1, one finds that there are several sets of measurements which yielded excessively large individual differences in $[(T_w)_{obs}-(T_w)_{calc}]$.

The criterion was established to reject any difference which exceeded the sum of the estimated overall systematic error plus three times the estimated overall random error in $[(T_w)_{obs}-(T_w)_{calc}]$. It was assumed that such large differences represented anomalous behavior of the psychrometer. The application of this criterion led to the rejection of two sets of data for the water-air system, one set of data for the carbon tetrachloride-oxygen system, and two sets of data for the toluene-air system. These rejected sets of data included all experiments performed at the lowest and highest flow rates, that is, at 0.8 and 6.2 liters per minute, and none within the flow rate range of 1.3 through 5.2 liters per minute.

Average differences and estimates of the standard deviations of the average differences were recomputed excluding the rejected differences, and are given in tables 3 and 4 under the heading "restricted flow." Whereas the average algebraic differences initially were positive in sign for the water-air, carbon tetrachloride-oxygen, and toluene-air systems, after applying the rejection criterion, the sign in each case was negative. The magnitude of the average algebraic difference decreased by a factor of five for the water-air system, but doubled for the carbon tetrachloride-oxygen and toluene-air systems. The new ("restricted flow") estimates of the standard deviations were smaller by a factor of about two to three

and agreed more closely with the estimates of the overall random error.

It appears that the rejection process eliminated both low and high flow-dependent systematic errors. This is to be expected since at very low flows heat losses to the ambient atmosphere become a noticeable fraction of the heat supplied by the test gas. At very high flows, incomplete saturation and incomplete heat exchange apparently occur.

Corrections or error estimates could be made for radiative or conductive heat losses, incomplete saturation, change of kinetic energy of the gas stream, heat supplied by incoming liquid or other factors that might tend to affect the performance of the psychrometer. In designing this instrument, an attempt was made to make these sources of error as negligible as feasible, so that corrections would not need to be applied. Since the purpose of these tests was to determine how well the instrument actually performed its intended function as an adiabatic saturation psychrometer, such corrections were not made in this evaluation.

Though on the average the measured wet-bulb temperatures differ little from the calculated wet-bulb temperatures, there is a prevalence for the measured temperature to be lower than the calculated temperature for the "restricted flow" cases. This probably stems from the fact that the true f_w-factor is greater than unity whereas a value of one was used for all systems except water-air in determining $(T_w)_{calc}$.

For the water-air system, for which the f_w-factor is known and therefore was used, $(T_w)_{calc}$ is much closer to $(T_w)_{obs}$ on the average than for any other system.

The response time traces obtained appeared to have the general shape of exponential functions as one would expect. The time constant τ was obtained by measuring the time required for the wet-bulb temperature to undergo 63 percent of its total change for each test condition. Figure 4 is a plot of these measured time constants against gas flow rate for the two conditions tested. The time constant is a function of gas flow rate. At flow rates of 3.75 to 5.2 liters per minute the time constant is about 3/4 of a minute.

Although the temperature of the liquid at the point where it discharges onto the wicking was not measured, several calculations were made to obtain estimates of how close this temperature approached the "thermodynamic wet-bulb temperature." For example, with water flowing at a rate calculated to be three-fold that required to saturate an air flow of 1 1/2 liters per minute at inlet conditions of zero mixing ratio, 25 °C dry-bulb temperature, and 1 bar pressure, the liquid feed temperature was calculated to be 0.2 °C higher than "thermodynamic wet-bulb temperature." This, it was estimated, would elevate the wet-bulb temperature by approximately 0.008 °C. If the inlet relative humidity of the gas were higher, the other inlet and flow conditions remaining unchanged, the absolute temperature error in the liquid feed would be less, but the percentage error in the experimental psychrometric factor, would be the same.

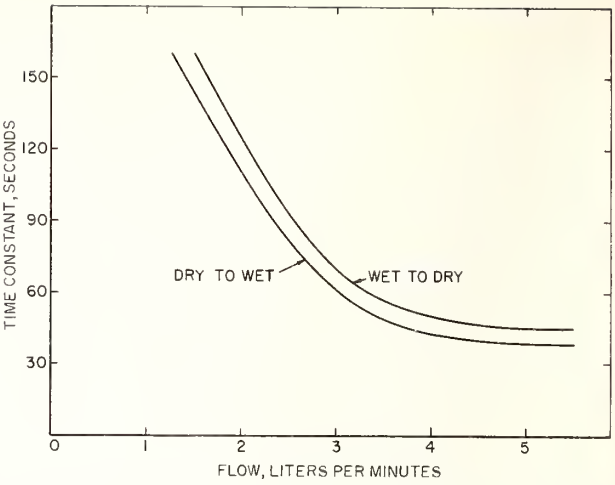

FIGURE 4. *Time constant versus inlet gas flow rate for water-air system.*

It is important to reiterate that the adiabatic saturation psychrometer behaves very differently from conventional types of psychrometers. This is shown in table 5 which compares the psychrometric factor ratios A_2/A_1 at $r=0$ obtained at NBS with the adiabatic saturation psychrometer and with three types of conventional thermocouple psychrometers corrected for radiation losses; it also lists ratios based on results reported by other investigators on conventional psychrometers. The ratio is essentially unity for the adiabatic saturation psychrometer for the five systems listed; it differs significantly from unity for the conventional types of psychrometer, although for the water-air system the magnitude of the difference is smaller than for the other systems.

TABLE 5. *Typical psychrometer performance*

System	Ratio of thermal to mass diffusivities	Ratio of psychrometric factors, A_2/A_1						
		NBS instruments				Other instruments		
		Adiabatic saturation psychrometer[a]	Thermocouple psychrometer A[b]	Thermocouple psychrometer B[b]	Thermocouple psychrometer C[b]	Arnold [11][b]	Sherwood [12]	Lewis [13]
H_2O-Air	0.9	1.000	1.14	1.04		0.95	1.21	
H_2O-H_2	1.7	0.997	1.64	1.47	1.53			
CCl_4-O_2	3.0	.997	2.33		2.23			
CCl_2F_2-H_2	4.5	1.005			2.79			
C_2H_6-Air	2.6	0.996		2.07	1.96	1.77	2.08	2.5

[a] Shielded against radiation.
[b] Corrected for radiation.

6. Discussion and Conclusions

The theoretical basis governing the operation of this instrument has been demonstrated at room temperature, atmospheric pressure, and over the flow range of 1.3 through 5.3 liters per minute, by tests with several liquid-gas systems subject to the re-

striction that the data were limited to the condition $r=0$. Since zero mixing ratio produces the maximum wet-bulb depression for any given dry-bulb temperature, and since such effects as radiative and conductive heat losses tend to have a greater influence with increasing depression, the $r=0$ condition subjects the psychrometer to its severest experimental test. Use of the gas temperature just beyond the outlet end of the saturator tube rather than the temperature of the moistened wicking as the wet-bulb temperature further increases the assurance that this instrument is producing "thermodynamic wet-bulb temperatures." Since essentially all cooling of the incoming gas occurs by heat transfer from the gas to the moistened wicking, the average temperature of the moistened wicking must of necessity be equal to or less than the average temperature of the exit gas. It is possible under some circumstances (for example, where the ratio of thermal to mass diffusivity is less than 1) for the moistened wicking to be cooled below the "thermodynamic wet-bulb temperature," but it is extremely unlikely that the average temperature of the exit gas could be as low as the "thermodynamic wet-bulb temperature" without satisfying the postulates that form the theoretical basis for eq (1).

Although the intended use of this instrument is to measure the water vapor content of gases, it is possible to use it for the determination of other vapors in gases and perhaps for the determination of f_w for particular vapor-gas combinations. The latter might be done by controlling inlet gas temperatures in such a way as to produce wet-bulb temperatures which correspond to those at which the vapor pressure and latent heat of evaporation of the liquid are well known.

Due to the difficulty of producing known vapor concentrations in gases other than zero, this instrument was only tested at the condition $r=0$. Its performance characteristics, therefore, have been demonstrated only at this condition. We believe however, that the characteristics would not be altered significantly were the psychrometer operated at $r>0$. Furthermore, as mentioned above, for any given dry-bulb temperature, $r=0$ produces the minimum wet-bulb temperature and subjects the psychrometer to the maximum radiative and conductive heat losses, and hence is the most severe condition under which to test the behavior of a psychrometer.

It is of interest to predict how well one could measure the water vapor content of air with this psychrometer. Whereas the magnitude of the error in wet-bulb temperature probably is related directly to the difference between wet- and dry-bulb temperatures, we will use for our prediction the error obtained at $r=0$ which is in all likelihood maximum since the wet- and dry-bulb temperature difference is maximum, and handle it as though it were a fixed error although it is likely smaller at higher relative humidities. For our estimate of this error we will use the average value of $[(T_w)_{obs}-(T_w)_{calc}]$ plus one standard deviation of this quantity obtained from the "restricted flow" test points. This should give us a one-sigma error estimate. Assuming a dry-bulb temperature of 25 °C, a total pressure of 1 bar, and using the above error in wet-bulb temperature, it is estimated that the psychrometer can be used to determine the relative humidity to within ¼ percent. Table 6 gives the error estimates in both the mixing ratio and relative humidity determination at various inlet relative humidities.

TABLE 6. *Estimated instrument error for water vapor-air system at 25 °C, 1 bar pressure and various relative humidities*

RH	Δr	ΔRH
%	g vapor/g vapor-free gas	%
0	0.000025	0.13
20	.000029	.15
40	.000034	.17
60	.000038	.19
80	.000043	.21
100	.000049	.23

The suggestions and criticisms of L. P. Harrison, ESSA, Weather Bureau, Silver Spring, Md., are gratefully acknowledged.

7. Appendix. Computations and Sources of Constants

$(T_w)_{calc}$ was computed for each experimental point by solving one of the following equations in an iterative manner, using measured values of P and T:

$$h(P, T, 0)=h(P, T_w, r_w)-r_w h'_w(P, T_w) \quad (22)$$

$$h(P, T, 0)=h(P, T_w, 0)+r_w L'_v. \quad (23)$$

A_2 was computed for each experimental point equating A_2 to A in eq (13) into which the measured values of P, T, and T_w were substituted. A_1 was computed for each experimental point by using one of the following equations into which the measured values of P, T, and T_w were substituted;

$$A_1=\frac{r_w[h(P, T, 0)-h(P, T_w, 0)]}{\Delta T[h(P, T_w, r_w)-h(P, T_w, 0)-r_w h'_w(P, T_w)]} \quad (24)$$

$$A_1=\frac{[h(P, T, 0)-h(P, T_w, 0)]}{\Delta T L'_v} \quad (25)$$

where A_1 is the equivalent of A in eq (9).

Equations (22) and (24) were used for the water-air system and are exact. Equations (23) and (25) are approximations and were used for all other systems because neither the gas mixture enthalpy $h(P, T_w, r_w)$ nor the "effective" latent heat of vaporization $L_{v,r}$ for these systems was known.

In all cases r_w was determined by solution of the following equation:

$$r_w = \frac{M_v}{M_g} \frac{f_w e_w}{(P - f_w e_w)} \quad (26)$$

where f_w = a function of pressure and temperature for a given liquid-gas system.[3]

Each of the individual errors in $(T_w)_{calc}$ is associated with an error in one of the parameters entering into its calculation. The error in $(T_w)_{calc}$ was obtained by solving eq (22) or (23), as appropriate, using the parameter value plus its estimated error in the calculation and subtracting $(T_w)_{calc}$ from the result. The individual errors in $(A_2 - A_1)$ were obtained by solving equations (13) and (24) or (25) as appropriate, using the parameter value plus its estimated error in the calculation along with the values of $(T_w)_{calc}$ obtained from prior computation. The solution of these equations gives the error directly since $A_2 - A_1 = 0$ at $(T_w)_{calc}$ when there are no errors.

The results of the error computations are given in table 2.

Water-Air System. $h(P, T, r)$, $h(P, T_w, r)$ and $h(P, T_w, r_w)$ were obtained by solution of the following equation:

$$h = \frac{7}{2} R [T + \frac{8}{7} r \frac{M_g}{M_v} (T + 1354.74)] + \Delta h$$

$R = 0.068557$ ITcal-K^{-1}(g dry air)$^{-1}$ or 0.28703 J-K^{-1} (g dry air)$^{-1}$.

and Δh was obtained from table 85 of the Smithsonian Meterological Tables [31].

Values of h'_w were linearly interpolated from a table given by Goff [24] and values of f_w were obtained by linear interpolation in both T and P from values given in Table 89 of the Smithsonian Meteorological Tables [31]. The saturation vapor pressure of water was obtained by solution of an equation given by Goff [32]. The estimated errors in these parameters are given in table 2.

Water-Hydrogen System. $h(P, T, 0)$ and $h(P, T_w, 0)$ were obtained for vapor-free hydrogen by linear temperature interpolation of the tabulated values given by Hilsenrath [33]. Values of L'_v were obtained from steam tables [34]. In the absence of data on the factor f_w at the experimental test conditions, a value of unity was assumed for f_w. Values of e_w were obtained in the same manner as with the water-air system. The estimated errors in these parameters are given in table 2.

Carbon Tetrachloride-Oxygen System. $h(P, T, 0)$ and $h(P, T_w\ 0)$ were obtained for vapor-free oxygen by linear temperature interpolation of tabulated values given by Hilsenrath [33]. Values of L'_v were obtained by linear interpolation from the tabulation in the International Critical Table [35]. A value of unity was ascribed to f_w and vapor pressures were calculated from the following equation given by Hildebrand [36]:

$$e_w = \text{Antilog}\,[6.89406 - \frac{1219.58}{227.16 + T_w}] \text{ mm Hg}$$

or

$$e_w = 0.0013332 \text{ Antilog}\,[6.89406 - \frac{1219.58}{227.16 + T_w}] \text{ bars.}$$

The estimated errors in these parameters are given in table 2.

Carbon Tetrachloride-Hydrogen System. Enthalpies were obtained as in the water-hydrogen system and all other parameters were obtained as in the carbon tetrachloride-oxygen system. The estimated errors in these parameters are given in table 2.

Toluene-Air System. $h(P, T, 0)$ and $h(P, T_w, 0)$ were obtained for vapor-free air by linear interpolation of tabulated values given by Hilsenrath [33]. Values of e_w were obtained from the equation of Rossini [37]:

$$e_w = \text{Antilog}\left[6.95464 - \frac{1344.800}{219.482 + T_w}\right] \text{ mm Hg}$$

or

$$e_w = 0.0013332 \text{ Antilog}\left[6.95464 - \frac{1344.800}{219.482 + T_w}\right] \text{ bars.}$$

A value of unity was assigned to f_w and L'_v was computed from the equation given by Scott [38]:

$$L'_v = \frac{11637 - 4.823\ T_w - 1.260 \times 10^{-2} T_w^2}{92.141}$$

where T_w is given in degrees Kelvin. According to Scott, this formula is applicable over the temperature range of 298 to 410 °K. However, since it was used to extrapolate values of L'_v at 280 °K, allowance for this fact was made in estimating the error in L'_v. The estimated errors in these parameters are given in table 2.

8. References

[1] Monteith, J. L., Error and Accuracy in Thermocouple Psychrometry, Proceedings of the Physical Society, B **LXVII**, 217 (1954).

[2] Bindon, H. H., A Critical Review of Tables and Charts Used in Psychrometry, Humidity and Moisture **1**, 3 (Reinhold Publishing Corp., New York, 1965).

[3] Harrison, L. P., Some Fundamental Considerations Regarding Psychrometry, Humidity and Moisture **3**, 71 (Reinhold Publishing Corp., New York, 1965).

[4] Wylie, R. G., Psychrometry, Report PA-4, Commonwealth of Australia, Commonwealth Scientific and Industrial Research Organization, National Standards Laboratory, Division of Physics, University Grounds, Sydney, Australia. July 1949.

[5] Ivory, J., On the hygrometer by evaporation, Philosophical Magazine **60**, 81 (1822).

[6] August, E. F., Uber die Verdunstungskälte und deren Anwendung auf Hygrometrie, Ann. der Physik und Chemie **5**, 69 (1825).

[7] Apjohn, J., Formula for inferring the dewpoint from indications of the wet-bulb hygrometer, Phil. Mag. **6**, 182 (1835).

[8] Apjohn, J., On the theory of the moist bulb hygrometer, Trans. Roy. Irish Acad. **17**, 275 (1837).

[3] The saturation vapor pressure of a liquid substance in the presence of an inert gas differs from that when the pure substance alone is present. The factor f_w accounts for this difference. It is defined as $f_w(P, T_c) = \frac{X_c P'}{e_w}$ where X_c is the mole fraction of the vapor in a vapor-gas mixture under saturation at temperature T_w and total absolute pressure P.

[9] Whipple, F. J. W., The wet and dry bulb hygrometer: The relation to theory of the experimental researches of Awberry and Griffiths, Proc. Phys. Soc. London **45,** 307 (1933).
[10] Carrier, W. H., Rational psychrometric formulae, Am. Soc. Mech. Engrs. Trans. **33,** 1005 (1911).
[11] Arnold, J. H., The theory of the psychrometer. II. The effect of velocity, Physics **4,** 334 (Sept. 1933).
[12] Sherwood, T. K. and Comings, E. W., On experimental study of the wet-bulb hygrometer, Trans. Am. Inst. Chem. Eng. **28,** 88 (1932).
[13] Lewis, W. K., The evaporation of a liquid into a gas—a correction, Mech. Eng. J. **55,** 567 (1933).
[14] Dropkin, D., The Deviation of the Actual Wet-Bulb Temperature from the Temperature of Adiabatic Saturation, Cornell University Engineering Experiment Station, Bulletin No. 23 (July 1936).
[15] Brun, E. and Lions, M., Sur la theorie generale du psychrometrie et sur une methode simple d'etude experimentale des lois de diffusion forcie, C.R.A.S. (Paris) **222,** 1071 (1946).
[16] Kawata, S. and Omori Y., An investigation of thermocouple psychrometer I, J. Phys. Soc. Japan **8,** No. 6, 768 (1953).
[17] Maxwell, J. C., Diffusion, Encyl. Brit. 9th Ed. VII, 218 (1877).
[18] Mieghem, J. Van, La Thermodynamique du Thermometre Mouille, Bull. Classe Sci. Acad. Roy. Belgi. Bruxilles **27,** 85 (1941).
[19] Svennson, A., Verdunstung und Abkühlung oder Erwärmung in dem Laminaren Gasstrom von Konstanter Geschwindigkeit. Anwendung auf Assmansche Aspiration-psychrometer, Arkiv. f. Mat. Astron. och Physik. Stockholm, Hafte 4, **22A,** 23 (1932).
[20] Threlkeld, J. L., Thermal Environmental Engineering, Prentice-Hall, Inc., Englewood Cliffs, N.J. (1962).
[21] Weber, S., Psychrometrets Teori, Dansk Videnskobernes Selsk, Mathem-fys. Medd **3,** No. 19 (1921).
[22] Arnold, J. H., The theory of the psychrometer. I. The mechanism of evaporation, Physics **4,** 255 (July 1933).
[23] Goff, J. A., Standardization of thermodynamic properties of moist air—final report of working subcommittee, International Joint Committee on Psychrometric Data, ASHVE Journal Section, Heating, Piping and Air Conditioning **55,** 118 (1949).
[24] Goff, J. A., and Gratch, S., Thermal properties of moist air, ASHVE Journal Section, Heating, Piping and Air Conditioning **51,** 334 (June 1945).
[25] Carrier, W. H. and Lindsay, D. C., The temperature of evaporation of water into air, Trans. of Am. Soc. Mech. Eng. **46,** 739 (1924).
[26] Harrison, L. P., Proposal for an Experimental Triple-tubed Adiabatic Saturator to Measure Thermodynamic Wet-Bulb Temperature as a Limit Approached During the Saturation Process, Humidity and Moisture **1,** 33 (Reinhold Publishing Corp., New York, 1965).
[27] Lewis, W. K., The Evaporation of a Liquid into a Gas, Trans. Am. Soc. Mech. Engrs. **44,** 325 (1922).
[28] Nanda, V. S. and Kapur, R. K., A note on the thermodynamics of the wet- and dry-bulb hygrometer, Indian J. Phys. **31,** 391 (1948).
[29] Wentzel, J. D., An instrument for the measurement of the humidity of air, American Society of Heating, Refrigeration and Air Conditioning Engineers Journal **66,** 67 (Nov. 1961).
[30] Harrison, L. P., Fundamental Concepts and Definitions, Humidity and Moisture **3,** 3 (Reinhold Publishing Corp., New York, 1965).
[31] Smithsonian Meteorological Tables, Smithsonian Institution, Washington, D.C. (1951).
[32] Goff, J. A., Saturation Pressure of Water on the New Kelvin Scale, Humidity and Moisture **3,** 289 (Reinhold Publishing Corp., New York, 1965).
[33] Hilsenrath, J., et al., Tables of thermal properties of gases, NBS Circ. 564 (1955).
[34] Bain, R. W., Steam Tables, Department of Scientific and Industrial Research, National Engineering Laboratory, East Kilbride, Scotland (1964).
[35] International Critical Tables (McGraw-Hill Book Co., Inc., New York, N.Y., 1928).
[36] Hildenbrand, D. L. and McDonald, R. A. The Heat of vaporization and vapor pressure of carbontetrachloride; the entropy from calorimetric data, J. Phys. Chem. **63,** 1521 (1959).
[37] Rossini, F. D., et al., Values of Physical and Thermodynamic Properties of Hydrocarbons and Related Compounds (Carnegie Press, Pittsburgh, Pa., 1953).
[38] Scott, D. W., et al., Toluene thermodynamic properties, molecular vibrations and internal rotation, J. Phys. Chem. **66,** 911 (1962).

(Paper 72C1–267)

Calibration of Humidity-Measuring Instruments at the National Bureau of Standards*

ARNOLD WEXLER†
National Bureau of Standards
Washington, D.C.

The National Bureau of Standards provides a service to government agencies and to the public for the calibration of humidity-measuring instruments. The equipment and procedures employed in making these calibrations and the available ranges and accuracies are described. Calibrations are performed by subjecting the instrument under test to atmospheres of known moisture content produced by the NBS two-pressure humidity generator. The most accurate calibrations are made with the NBS standard hygrometer, a device based on the gravimetric method. With the latter, a measurement can be made with an estimated uncertainty (estimated bounds to systematic error plus three times the standard deviation) of 13 parts in 10^4.

INTRODUCTION

FOR MANY YEARS, the National Bureau of Standards has provided government agencies a service for the calibration of humidity-measuring instruments. In 1964, this service was extended to the public. Hygrometers suitable for use as laboratory or plant standards and having high accuracy and stability are accepted for calibration. Usually, the calibration is performed by subjecting the test instrument to atmospheres of known humidity produced by the NBS two-pressure humidity generator.[1] If the highest accuracy is required, the test instrument is compared with the NBS standard hygrometer,[2] an apparatus that is based on the gravimetric method of moisture measurement and possessing the highest order of accuracy in the NBS hierarchy of humidity-measuring instruments.

This paper briefly describes the NBS standard hygrometer and the NBS two-pressure humidity generator, discusses the calibration ranges and accuracies obtainable, outlines the procedures employed in making calibrations, and summarizes the humidity-calibration services currently available to the public. Details on NBS measurement services, policies, procedures, and fees are given in NBS Miscellaneous Publication 250.[3]

NBS STANDARD HYGROMETER

The NBS standard hygrometer is based on the well-known gravimetric method of moisture determination. It yields a direct measure of water-vapor content in absolute units of mass of water vapor per unit mass of associated dry gas. In meteorology, this quantity is usually called the mixing ratio; in several of the engineering disciplines, it is referred to as the humidity ratio; and in the chemical field it is often expressed as parts per million by weight (ppm). In theory, the gravimetric

*Contribution of the National Bureau of Standards, not subject to copyright. Presented at the 14th National Symposium, Analysis Instrumentation Division, Instrument Society of America, May 19–22, 1968, Philadelphia, Pennsylvania; revised October 1968.

†Chief, Humidity Measurements Section, Mechanical Measurements Branch, Mechanics Division, Institute of Basic Science; ISA Fellow Member.

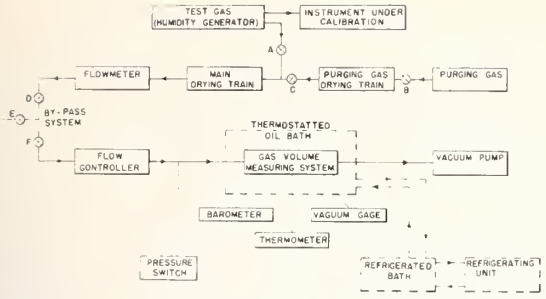

Figure 1. Block diagram of the gravimetric hygrometer. *A–F*: Shut off or control valves.

method has great inherent precision and accuracy. In practice, great care must be exercised in making a determination, and careful attention must be given to a multitude of details.

Figure 1 is a block diagram of the essential components of the NBS standard hygrometer. Figure 2 is a schematic flow diagram of the hygrometer. The apparatus basically comprises a drying train for removing the water vapor from a moist gas and a gas volume measuring system for measuring the volume of the dry gas. Prior to a run, the apparatus is flushed with a dry purging gas. Then a test gas of constant humidity from the NBS two-pressure humidity generator is allowed to flow simultaneously through the NBS standard hygrometer and the instrument under calibration. At the termination of a run, the mass of water vapor removed by the drying train, which consists of three interchangeable glass absorption U-tubes filled with anhydrous magnesium perchlorate and phosphorous pentoxide, is determined by precision weighing. The total volume of dry gas is measured by counting the number of times two calibrated cylinders, each of about 30 liters capacity, are evacuated and filled alternately. By means of a pressure switch, a vacuum pump, and associated automatic controls, each of the two cylinders is evacuated and filled to a preset pressure, producing a continuous flow of test gas. The cylinders are immersed in a thermostatted oil bath. After each filling, the gas collected in the cylinder is allowed to reach equilibrium, and then the gas pressure and temperature are measured. The mass of the dry gas is obtained by multiplying the volume by the appropriate gas density.

The gravimetric hygrometer provides an average value of the moisture content of a test gas for the duration of a run. The test gas is sampled at flow rates of 2 liter/min or less for periods of time long enough to ensure that the mass of water collected by the drying train is sufficient to permit weighing with high accuracy (about 0.6–1.0 gm). Thus, as the humidity decreases, the duration of a run increases. The following practical considerations limit the humidity range over which the hygrometer is used: The highest measurable value is determined by ambient room temperature. Since the latter is controlled nominally at 25 C, to prevent condensation in the lines, the dew-point temperature of the test gas must be kept below 25 C. The highest measurable humidity is limited, therefore to a mixing ratio of about 20 gm water vapor per kg dry air, although this hygrometer may be capable

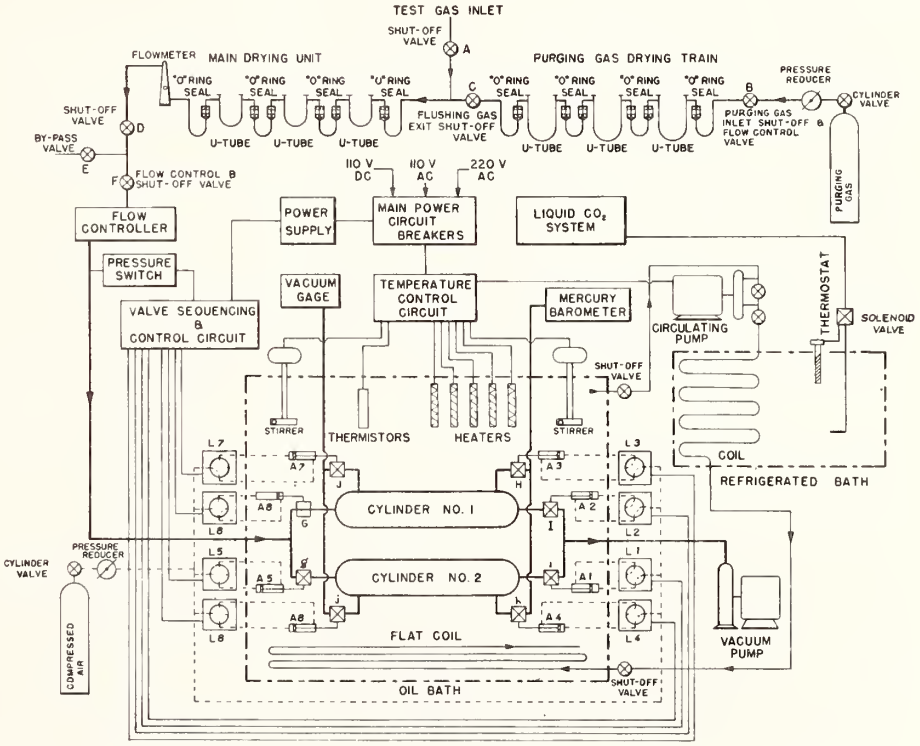

Figure 2. Schematic flow diagram of the gravimetric hygrometer. L1–L8: Solenoid-actuated air valves. A1–A8: Air actuators. *G, g, H, h, I, i, J, j*: On–off vacuum-type ball valves.

of measuring higher values. The lowest measurable value is governed largely by the sampling time, which, in turn, is related to operator endurance and equipment reliability. Mixing ratios as low as 0.2 gm/kg have been measured without any degradation in accuracy, but this is seldom done since it involves continuous sampling for about 30 hr. The duration of a run arbitrarily has been set at 10–12 hr as a reasonable limit. This permits mixing ratio measurements as low as 0.4 gm/kg.

NBS TWO-PRESSURE HUMIDITY GENERATOR

The NBS two-pressure humidity generator is an apparatus which produces atmospheres of known humidity.[1] Figure 3 is a simplified flow diagram which illustrates the principle of operation and shows the basic components. Compressed gas, usually atmospheric air, is cleaned, dried, and passed through an external saturator that is temperature-controlled at 10–15 C above the desired saturation temperature. It picks up water vapor in excess of that necessary for saturation at the desired saturation temperature. It then flows through a series of three saturators with interconnecting heat exchangers that are immersed in a thermostatted liquid bath. Excess water is condensed out. The gas leaves the final saturator completely saturated, with vapor in equilibrium with either the liquid or solid phase of distilled water (depending on the temperature) at an absolute pressure P_s and temperature T_s. It now flows through an expansion valve into a test chamber maintained at some lower absolute pressure P_c and at the same temperature T_s, and finally exhausts into the surrounding atmosphere. Measurements of the temperature and pressure within the final saturator and the test chamber or other test space establish the moisture content of the test gas.

Calibrations are made with the NBS two-pressure humidity generator in terms of various expressions which are measures of the quantity of water vapor in a moist gas: mixing ratio, dew-point temperature, relative humidity, and volume ratio. These expressions are defined on the basis of real-gas behavior and account for the fact that the saturation pressure of pure water in the presence of an inert gas differs from that when pure water alone is present. These expressions have values which differ from those based on properties of an ideal gas.

Figure 3. Simplified flow diagram of the NBS two-pressure humidity generator. *A*: High-pressure air source. *B, C*: Desiccant towers for cleaning and drying air. *D*: Pressure regulator. *E*: External saturator. *F, H, J, M*: Heat exchangers. *G, I, K*: Internal saturators. *L*: Expansion valve. *N*: Test chamber. *O*: Exhaust control valve. *P*: Ambient atmosphere or vacuum. *Q, R*: Pressure gauges. *X, Y*: Thermostated liquid baths.

The saturation mixing ratio r_w of a moist gas at absolute pressure P and temperature T is given by[4]

$$r_w = M_w f e_w / M_g (P - f e_w) \tag{1}$$

where M_w is the molecular weight of water vapor; M_g is the molecular weight of the gas; $e_w = e_w(T)$ is the saturation pressure over a plane surface of the pure phase of liquid or solid water at temperature T; and f is a function of pressure and temperature for a given vapor–gas system. The function f is defined[4] as

$$f = f(P, T) = (x_w)_{P,T} P / e_w \tag{2}$$

where $(x_w)_{P,T}$ is the mole fraction of water vapor in a saturated vapor–gas mixture at absolute pressure P and temperature T.

The mixing ratio r_w^* of the moist gas emerging from the generator is therefore

$$r_w^* = \frac{M_w f(P_s, T_s) e_w(T_s)}{M_g [P_s - f(P_s, T_s) e_w(T)]} \tag{3}$$

If experimental values, formulations, or tabulations of the function f and the saturation vapor pressure e_w are available, then measuring the saturator pressure P_s and saturator temperature T_s permits the computation of r_w^*.

Goff and Gratch[5,9] have computed low-pressure tables of the function f based, primarily, on experiments performed at atmospheric pressure.[7] Webster[8] has measured vapor concentrations of saturated compressed air over a range of pressures and temperatures, and has computed corresponding ratios of the measured concentrations to that of pure water vapor. Experimental determinations are now being made at NBS on the mixing ratios of saturated compressed air, which, it is expected, will yield accurate values of the function f over a wide range of pressures and temperatures. As an indication of the magnitudes involved, at 25 C, the function f has a value of about 1.004 at a pressure of 1 bar[1] and about 1.032 at a pressure of 10 bars. Goff and Gratch[9] also have computed tables of the saturation vapor pressures. These have been published in convenient form by the Smithsonian Institution.[6]

The percentage relative humidity, RH, of a moist gas at absolute pressure P and temperature T is defined as follows[4]:

$$RH = (x/x_w)_{P,T} \times 100 \tag{4}$$

where x is the mole fraction of water vapor in a given volume of moist gas at P and T; and x_w is the mole fraction of water vapor in the same volume of moist gas saturated with respect to a plane surface of clean water at P and T.

Equation (4) can be expressed in the form

$$RH = \frac{f(P, T_d)}{f(P, T)} \frac{e_w(T_d)}{e_w(T)} \times 100 \tag{5}$$

[1] 1 bar = 10^3 N/m^2. 1.01325 bars = 1 atm.

where T_d is the "thermodynamic dew-point temperature" of the moist gas (this will be defined below).

It should be noted that this real-gas definition of relative humidity includes the function f and that only in the case of ideal-gas behavior, or if water vapor is present in a space unadmixed with any other gas, is the relative humidity defined by

$$RH = [e/e_w(T)] \times 100 \tag{6}$$

where e is the actual pressure of water vapor in a space at temperature T, and e_w is the saturation vapor pressure at temperature T.

The relative humidity RH^* in the test chamber of the generator, obtained by substituting equation (2) into equation (4), is

$$RH^* = [f(P_s, T_s)P_c/f(P_c, T_s)P_s] \times 100 \tag{7}$$

The "thermodynamic dew-point (or frost-point) temperature" T_d of a moist gas at absolute total pressure P is defined as that temperature at which the moist gas is saturated with respect to a plane surface of clean liquid (or solid) water.[4] If a moist gas at absolute total pressure P has a mixing ratio r, and if the temperature of this moist gas is reduced until it is saturated at the same pressure P, then the saturation mixing ratio r_w of the moist gas is equal to the initial mixing ratio r, i.e.,

$$r = r_w(P, T_d) \tag{8}$$

Substituting equation (1) into equation (8) yields

$$\frac{rP}{(M_w/M_g) + r} = f(P, T_d)e_w(T_d) \tag{9}$$

an equation which relates the initial mixing ratio r to the "thermodynamic dew-point (or frost-point) temperature" T_d.

If equation (9) is applied to the NBS two-pressure generator, then the "thermodynamic dew-point (or frost-point)" T_d^* of the moist gas flowing from this apparatus is obtained by the iterative solution of

$$\frac{r_w^* P}{(M_w/M_g) + r_w^*} = f(P, T_d^*)e_w(T_d^*) \tag{10}$$

or

$$f(P_s, T_s)e_w(T_s)(P/P_s) = f(P, T_d^*)e_w(T_d^*) \tag{11}$$

where r_w^* is the mixing ratio produced by the generator and is calculated from equation (3); e_w and f are values obtained from suitable tables; and P is the absolute pressure in any space or volume that is filled with the moist gas, e.g., the mirror chamber of a dew-point hygrometer.

The volume ratio of a moist gas is an expression for humidity that is exact only if the ideal gas laws and Amagat's law of partial volumes are obeyed. Under these ideal conditions, the partial volume of a component in the vapor–gas mixture is equal to the product of the mole fraction of that component and the total volume. For a real vapor–gas mixture, it is convenient to define an "effective partial volume" for each component in an analogous way, with the understanding that the "effective partial volume" of each component is not generally equal to that volume that would be present if the component existed alone at the same total pressure as the mixture. Thus

$$v_w' = xV \tag{12}$$

$$v_g' = yV \tag{13}$$

where v_w' is the "effective partial volume" of water vapor in the vapor–gas mixture; v_g' is the "effective partial volume" of gas in the vapor–gas mixture; V is the total volume of the vapor–gas mixture; x is the mole fraction of water vapor in the vapor–gas mixture; and y is the mole fraction of gas in the vapor–gas mixture.

The ratio V of effective partial volumes is therefore

$$V = \frac{v_w'}{v_g'} = \frac{x}{y} = r\frac{M_g}{M_w} \tag{14}$$

where r is the mixing ratio of the vapor–gas mixture; M_g is the molecular weight of the gas component; and M_w is the molecular weight of the water-vapor component.

Here V is identically equal to the mole ratio, i.e., the number of moles of water vapor per mole of associated dry gas. To obtain the volume ratio V^* of the effluent moist gas from the generator, the mixing ratio r_w^* produced by the generator is substituted for r in equation (14). Thus, substituting equation (3) into equation (14) yields

$$V^* = \frac{f(P_s, T_s)e_w(T_s)}{P_s - f(P_s, T_s)e_w(T_s)} \tag{15}$$

The usual procedure in performing a calibration is to select the values of humidity desired in the units appropriate to the instrument under calibration and then to bring the generator to the temperatures and pressures that will yield the required humidities. Establishing a specific temperature, or changing from one temperature to another, is time consuming, for it involves heating or cooling a liquid bath of about 300-liter capacity. Establishing or changing the pressure is accomplished simply and quickly by rotating the handle on a pressure regulator. After the required temperature and pressure have been reached, sufficient time is allowed for the test instrument to reach equilibrium. The criterion for this is that there shall be no significant change in the readings on the test instrument successively repeated at two or more 5- or 10-min time intervals.

ACCURACY

The mixing ratio determined by the NBS standard hygrometer is a computed quantity whose magnitude is the ratio of two measurable quantities—the mass of water vapor in a given moist-gas sample and the associated mass of dry gas. The mass of water is determined directly by weighing, while the mass of gas is determined indirectly through measurement of its volume and a knowledge of its density.

The high accuracy is the result of a complex chain of measurements, corrections, and procedures. Consider,

e.g., the mass of water vapor absorbed by the desiccant in a U-tube. It depends not only on the face values of the weights used in the initial and final weighings on a precision analytical equal-arm balance, but also on such factors as the buoyancy effect on U-tube, tare, and weights, the adsorption of water vapor on the external surfaces of the U-tube, tare, and weights, static charge on U-tube and tare, convective air currents within the balance case, handling and treatment of the U-tube, and efficiency of absorption by the desiccant. Each of these factors, in turn, depends on several others. Thus, the buoyancy correction is affected by the initial and final air density and the external volumes of the U-tube, tare, and weights. Ambient air density is computed from measurements of temperature, pressure, and humidity. If all the links in the chain leading to a mass measurement are accounted for in a suitable fashion, it is estimated that the random uncertainty (standard deviation) in the mass of water vapor collected in the drying train is 0.022 %. From similar analyses for volume and density of the gas, it is estimated that the random uncertainties (standard deviations) in these quantities are 0.0073 % and 0.013 %, respectively, yielding a standard deviation in mixing ratio of 0.027 %. Systematic errors, such as efficiency of desiccant absorption, flow rate effect, and leakage may add up to about 0.046 %. The total uncertainty (estimated bounds to systematic error plus three times the standard deviation) in mixing ratio is therefore 0.13 %.

The humidity produced by the NBS two-pressure humidity generator is a computed quantity whose magnitude is based on one or more measured quantities and, usually, one or more physical constants and functions. The uncertainty in the humidity arises from the random and systematic errors in the measured parameters, the uncertainty in the values of the physical constants and functions, and the deviation in the generator behavior from that postulated by theory.

To determine the uncertainty in the computed value of the humidity, the generator was considered a "black box" and calibrated against the NBS standard hygrometer[10] at each of three saturator temperatures (+25 C, 0 C, and −20 C). Using saturation vapor pressures

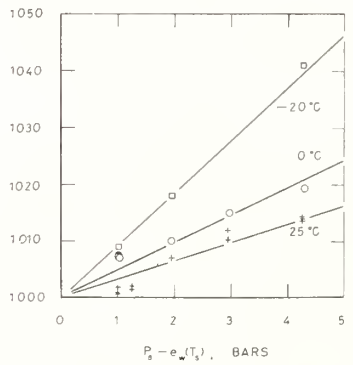

Figure 4. Experimental *f* for NBS two-pressure humidity generator.

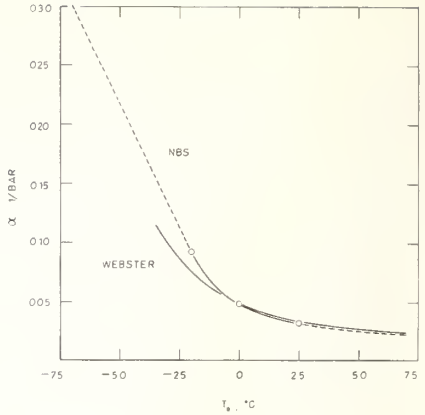

Figure 5. Relation between the slope $\alpha(T_s)$ and the saturation temperature T_s. Dotted sections of NBS curve are extrapolations. Curve based on Webster's data[8] included for comparison.

derived from the Goff–Gratch formulation[6] and mixing ratios measured by the NBS standard hygrometer,[2] values of f were computed from equation (3). These values were fitted to a linear equation of the form

$$f(P_s, T_s) = 1 + \alpha(T_s)[P_s - e_w(T_s)] \qquad (16)$$

where $\alpha(T_s)$, the slope, is a function of saturator temperature T_s. Figure 4 is a plot of the experimentally determined values of $f(P_s, T_s)$ vs $[P_s - e_w(T_s)]$ for each of the three saturator temperatures. The slope for each curve was calculated by the method of least squares. Figure 5 is a plot of $\alpha(T_s)$ vs T_s, the dotted portion of this curve representing an extrapolation. The second curve, included for comparison, is based on Webster's data.[8] The two curves agree reasonably well from +70 C to −10 C. Below −10 C, they diverge, the NBS curve rising more rapidly with decreasing temperature.

The faired values of $f(P_s, T_s)$ obtained by the NBS calibration include any systematic errors in the molecular weights of air and water vapor, in the saturation vapor pressure $e_w(T_s)$ of water, and in the measured parameters P_s and T_s. They also reflect any systematic departures in generator behavior from theory. Although the NBS faired values of $f(P_s, T_s)$ have a theoretical significance, they should be viewed primarily as experimental calibration factors for the generator.

The uncertainty in the measured values of $f(P_s, T_s)$ is due to the errors in the measurement of mixing ratio, saturator pressure, and saturator temperature. The estimated uncertainty in measuring mixing ratio consisted of a systematic error of 0.046 % and a random error (standard deviation) of 0.027 %. Calibration corrections were applied to the measured values of P_s and T_s; it is estimated that the residual systematic errors in these parameters were negligible. It is estimated that the random error (standard deviation) in P_s was 0.05 % and that the random error (standard deviation) in e_s, due to the random error (standard deviation) in T_s, was 0.08 %. Thus the estimated uncertainty in $f(P_s, T_s) = 0.046 + 3[(0.027)^2 + (0.05)^2 + (0.08)^2]^{1/2} = 0.34$ %. The

TABLE I
Slope $\alpha(T_s)$

Saturator temperature T_s (deg C)	Slope $\alpha(T_s)$ (bar^{-1})	Estimated uncertainty in slope (bar^{-1})
70	0.00232	0.0010
60	0.00247	0.0010
50	0.00266	0.0010
40	0.00281	0.0010
30	0.00306	0.0005
20	0.00343	0.0005
10	0.00397	0.0005
0	0.00482	0.0005
−10	0.00624	0.0005
−20	0.00922	0.0005
−30	0.01357	0.0030
−40	0.01776	0.0060
−50	0.02195	0.0100
−60	0.02614	0.0200
−70	0.03033	0.0300

corresponding estimated uncertainty in slope α at the three test temperatures is of the order of 0.0005/bar. At temperatures below −20 C and above 25 C, extrapolated values must be used. Consequently, larger uncertainties have been assigned to α in these regimes. Table I lists the faired values of α for temperatures from +70 C to −70 C, as derived from the NBS curve in Figure 5, and their corresponding estimated uncertainties. If these values of α are used in equation (16) to compute $f(P_s, T_s)$ for substitution into equation (3), it is estimated that for any saturator pressure up to 10 bars in the range +25 C to −25 C, corresponding to mixing ratios of 20 to 0.15 gm water vapor per kilogram dry air, the uncertainty in r_w^* does not exceed 0.5%. For mixing ratios in the range $0.15 > r_w^* \geq 0.007$, the uncertainty is 3%, and for mixing ratios in the range $0.007 > r_w^* \geq 0.002$, the uncertainty is 10%. Similar estimates have been made of the uncertainties in producing known dew-point temperatures, relative humidities, and volume ratios with the generator. Since the equations used in computing these units are different, and since different combinations of parameters are involved, the ranges and accuracies for the various units are not necessarily equivalent to each other.

Table II lists the ranges and accuracies of the NBS standard hygrometer and the NBS two-pressure humidity generator in several different humidity parameters commonly used in reporting calibration results. These accuracies refer only to the NBS standards. In estimating the accuracy attainable with instruments calibrated against these standards, allowance must be made for the inevitable deterioration of accuracy resulting from such factors as the differences in time and environment and the history of use between an NBS calibration and the point at which the calibrated instrument is used, as well as for the errors disclosed by the calibration.

CALIBRATION SERVICES

Acceptance of an instrument for calibration depends upon the type of hygrometer and the nature of the user's requirements. Requests for calibration should be accompanied by technical information on the type of instrument, manufacturer, operating range(s), and number of test points required. Calibrations can be

TABLE II
NBS Humidity Calibration Ranges and Accuracies

Standard	Humidity parameter	Range	Accuracy*
Standard (gravimetric) hygrometer	Mixing ratio r (gm water vapor/kg dry air)	0.19 to 20	0.13% of value
Two-pressure humidity generator	Mixing ratio r_w^* (gm water vapor/kg dry air)	$0.002 \leq r_w^* < 0.007$	10% of value
		$0.007 \leq r_w^* < 0.15$	3% of value
		$0.15 \leq r_w^* \leq 20.0$	0.5% of value
	Dew-point temperature T_d^* (deg C)	$-70 \leq T_d^* < -65$	1.2
		$-65 \leq T_d^* < -55$	0.8
		$-55 \leq T_d^* < -45$	0.5
		$-45 \leq T_d^* < -30$	0.2
		$-30 \leq T_d^* \leq +25$	0.1
	Volume ratio V^* (ppm)	$2 \leq V^* < 12$	10% of value
		$12 \leq V^* \leq 250$	3% of value
		$250 \leq V^* \leq 30{,}000$	0.5% of value
	Relative humidity RH^* (%) at test chamber temperatures T_c of:		
	$-55\text{ C} \leq T_c < -40\text{ C}$	10–98	2.5
	$-40\text{ C} \leq T_c < -30\text{ C}$	10–98	1.0
	$-30\text{ C} \leq T_c \leq +60\text{ C}$	10–98	0.5

*The estimated bounds to systematic error plus three times the standard deviation.

furnished in terms of most humidity parameters, including dew-point temperature, mixing ratio, volume ratio, and relative humidity.

Calibrations with the NBS two-pressure generator are performed in either of two ways: (1) The instrument, or its sensor, is placed inside a test chamber and is subjected to a known humidity, or set of humidity points, at any desired controlled temperature in the range of +40 C to −55 C. Instruments must be remote-indicating or recording, since there is no provision for observing a dial or other indicator within the test chamber. The electric hygrometer is a typical example of an instrument calibrated in this fashion. (2) The instrument is located in the laboratory under ambient conditions, i.e., at atmospheric pressure and 25 C, and a continuous flow of the test gas of known humidity is fed to it at any desired flow rate up to about 80 liters/min. The upper humidity of the test gas is limited to a dew point of 25 C; otherwise condensation may occur. The lowest dew point that can be generated is −70 C.

Calibration of a test instrument against the NBS standard hygrometer is carried out using the NBS two-pressure humidity generator as a source of constant humidity. The test instrument is placed in the test chamber of the generator or located in the laboratory. The NBS standard hygrometer continuously samples the test gas. During a run, readings are repeatedly made on the test instrument, and these are averaged to yield a mean value.

The results of calibration are issued to the customer as formal reports.

REFERENCES

1. Wexler, Arnold, and Raymond D. Daniels, Jr., "Pressure Humidity Apparatus," *J. Res. Natl. Bur. Std. (U.S.)* **48**, 269, 1952.
2. Wexler, Arnold, and Richard W. Hyland, "The NBS Standard Hygrometer," *NBS Monograph* **73**, May 1, 1964; Arnold Wexler (ed.), *Humidity and Moisture, Vol. III*, Reinhold Publishing Corporation, New York, 1965, p. 389.
3. "Calibration and Test Services of the National Bureau of Standards," *NBS Misc. Publ.* **250**, 1965.
4. Harrison, Louis P., "Fundamental Concepts and Definitions Relating to Humidity," *Humidity and Moisture, Vol. III*, Arnold Wexler (ed.), Reinhold Publishing Corporation, New York, 1964, p. 3.
5. Goff, J. A., and S. Gratch, "Thermodynamic Properties of Moist Air," *Trans. ASHVE* **51**, 125, 1945.
6. List, Robert J., *Smithsonian Meteorological Tables*, Smithsonian Institution, Washington, D.C., 1951.
7. Goff, John A., J. R. Anderson, and S. Gratch, "Final Values of the Interaction Constant for Moist Air," *Trans. ASHVE* **49**, 269, 1943.
8. Webster, T. J., "The Effect on Water Vapor Pressure of Superimposed Air Pressure," *J. Soc. Chem. Ind.* **69**, 343,1950.
9. Goff, J. A., and S. Gratch, "Low-Pressure Properties of Water from −160 to 212°F, *Trans. ASHVE* **52**, 95, 1946.
10. Hasegawa, S., R. W. Hyland, and S. W. Rhodes, "A Comparison between the National Bureau of Standards Two-Pressure Humidity Generator and National Bureau of Standards Standard Hygrometer," *Humidity and Moisture, Vol. III*, Arnold Wexler (ed.), Reinhold Publishing Corporation, New York, 1965, p. 455.

UNITED STATES DEPARTMENT OF COMMERCE • Sinclair Weeks, *Secretary*
NATIONAL BUREAU OF STANDARDS • A. V. Astin, *Director*

Electric Hygrometers

Arnold Wexler

This Circular is a review of the art of measuring the moisture content of air by the methods of electric hygrometry. The basis of these methods is the change in electrical resistance of a hygroscopic material with change in humidity.

1. General Introduction

Many, if not most, materials sorb and desorb water vapor as the ambient relative humidity increases or decreases. Associated with this sorption, there is usually a corresponding change in electrical resistance of the material. Materials which display a humidity-dependent change in resistance can be utilized as humidity sensors. However, for a sensor to be of practical use, it should have a reversible and reproducible humidity-resistance characteristic. Such sensors, or elements, when coupled with suitable measuring circuits constitute the electric hygrometer class of instruments. An electric hygrometer, therefore, may be defined as an instrument for determining the moisture content of air (or any gas) by the measurement of the electrical resistance of a hygroscopic material with change in humidity. In line with this definition, instruments that may use electrical meters or recorders or electronic devices in their circuitry, or that may require electric current for their operation, but that do not measure the resistivity or conductivity of a hygroscopic material are not discussed.

It is convenient to classify the sensors, in accordance with their basic principles of operation, into those that depend upon (a) the conductivity of aqueous electrolytic solutions, (b) the surface resistivity of impervious solids, (c) the volume resistivity of porous solids, (d) the resistivity of dimensionally-variable materials, and (e) the temperature of saturated salt solutions. These categories are not necessarily mutually exclusive nor do they include all possible ways in which resistance can be used for humidity sensing. They simply provide a basis for a description and discussion of many of the sensors that are in use or have been proposed.

Key words: Electric hygrometer, humidity, hygrometer.

National Bureau of Standards Circular 586

Issued September 3, 1957

23 pages

The NBS Standard Hygrometer[1]

Arnold Wexler and Richard W. Hyland

Abstract

A gravimetric hygrometer is described that serves as the NBS standard instrument for the measurement of the moisture content of gases on an absolute basis in terms of mixing ratio (mass of water vapor/unit mass of dry gas). The National Bureau of Standards and other laboratory reference and working instruments are compared and calibrated with this instrument. The measuring operation involves the absorption of the water vapor from a water vapor-gas mixture by a solid desiccant and the determination of the mass of this water vapor by precision weighing; it also involves the determination of the volume of the associated gas of known density by counting the fillings of two calibrated stainless steel cylinders. An automatic system permits the sampling of the test gas at any desired flow rate up to 2 l/min. (STP) and for any desired number of fillings. The instrument provides a value of the mixing ratio averaged over the time interval of a test.

The construction and operation of the instrument is described. Discussions of the tests and calibrations of component parts and of the sources of errors also are included. An analysis of the random and systematic errors effecting the overall accuracy in the determination of mixing ratio shows that if 0.60 gram of water vapor is collected from moist air, then the estimated maximum uncertainty expected for mixing ratios between 27 mg/g and 0.19 mg/g is 12.7 parts in 10^4.

Key Words: Gravimetric hygrometer, Humidity standard, Hygrometer, Mixing ratio, Moisture standard, Standard hygrometer.

[1]Available from the Superintendent of Documents, U. S. Government Printing Office, Washington, D. C. 20402. Price: 30 cents, NBS Monograph 73, Issued May 1964,

HUMIDITY AND MOISTURE [1]

Measurement and Control in Science and Industry

Arnold Wexler, Editor in Chief

Abstract by M. J. Orloski

The measurement and control of humidity--water in the vapor phase--and moisture--water in the absorbed or adsorbed phase--play an important role in such scientific disciplines as physics, chemistry, biology and medicine, in many branches of engineering, in meteorlogy and in agriculture, and in such diverse industrial fields as air conditioning, drying refrigeration, cryogenics, storage, food processing, packaging, materials manufacturing and processing, gas transmission, and electronics. Humidity and Moisture presents the expanded proceedings of the First International Symposium on Humidity and Moisture held in Washington, D. C. in 1963. Topics in the four-volume set range from humidity standards and fundamentals, through means of measuring and controlling humidity and moisture, to specific applications.

Volume One, Principles and Methods of Measuring Humidity in Gases, forms a complete reference work on instrumentation for water vapor measurement. There are sixty-eight chapters, divided among six general sections: I Psychrometry; II Dew-Point Hygrometry; III Electric Hygrometry; IV Spectroscopic Hygrometry; V Coulometric Hygrometry; VI Miscellaneous Methods.

Volume Two, Applications, is concerned with the application of humidity and moisture measurement to many fields and disciplines. There are forty-seven chapters divided among four general sections: I Biology and Medicine; II Agriculture; III Environmental Chambers; IV Air Conditioning.

Volume Three, Fundamentals and Standards, contains thirty-four chapters divided between two sections. Section I, Fundamentals, pertains mostly to the basic principles, properties and relationships of water vapor-gas mixtures.

[1] Humidity and Moisture, Arnold Wexler, Editor in Chief, Reinhold Publishing Corporation, New York, 1965.

It contains definitions, nonmenclature and units; thermodynamics and transport properties of water vapor and water vapor-gas mixtures; virial coefficients and interaction constants; deviations and departures of gas laws from ideality for water vapor-gas mixtures. Section II, Standards, is devoted to methods of testing and calibrating hygrometers, humidity generators, test apparatus, test chambers, and saturated salt solutions for humidity control. It also contains important and essential data and information for the testing, evaluation and calibration of humidity measuring instruments.

Volume Four, Principles and Methods of Measuring Moisture in Liquids and Solids, contains thirty six chapters divided into two parts. Part A pertains to principles and methods of measuring moisture in liquids and solids. New improved and more accurate indicators, records and methods of measurement are described; emphasis is given to physical and chemical methods, dielectric resistance and capacitance methods, nuclear magnetic resonance and neutron scattering techniques. Part B is devoted to the interaction of moisture and materials. Special topics of interest and importance to industry are absorption of water vapor by thin materials, dimensional changes in plastic films by moisture, and resistance of textile materials to diffusion of water vapor. These and many more topics make this volume extremely valuable to the packaging, plastics and textile industries.

Key Words: Coulometric hygrometry; Dew point; Electric hygrometer; Environmental chambers; Equation of state of moist gages; Humidity; Humidity generator; Humidity measurement, application of; Humidity standards, Hygrometry; Interaction of moisture and materials; Moist gages; Moisture in materials; Moisture measurement, capacitance method; Moisture measurement, chemical method; Moisture measurement, dielectric method; Moisture measurement, nuclear method; Moisture measurement, physical method; Moisture measurement, resistance method; Pneumatic bridge hygrometer; Psychrometry; Saturated salt solution; Spectroscopic hygrometry.

6. Pressure

6. Pressure—Continued

The Piston Gage as a Precise Pressure-Measuring Instrument

By D. P. JOHNSON[1] and D. H. NEWHALL[2]

The errors which must be considered for accurate measurements of pressure with piston gages are discussed. A new design of piston gage is described which permits the operator to control the clearance between piston and cylinder at any operating pressure. Instrumental errors are thus substantially reduced, particularly those resulting from elastic distortion. A check list of errors inherent to piston gages is presented. These errors are to be considered when instruments are used to accuracies better than ½ of 1 per cent. The need for a check on the long-time variations of the piston gage is supplied by the fixed points, changes of state of some very pure materials which take place at definite pressures. Such are the melting pressure of solid mercury at 0 C, the melting pressure of water at 30 C, the transition between crystalline states of bismuth. As an indication of its possibilities the experimental model of the controlled-clearance piston gage was used to measure the melting point of mercury at 0 C. Results were in satisfactory agreement with Bridgman's value.

Introduction

INDUSTRIAL engineers sometimes ask how they may benefit by the concern of the National Bureau of Standards over a primary standard of pressure with an accuracy of 0.01 per cent or better. An industrial engineer may be concerned with processes which require the control of pressures within, say, ±1 per cent. To be sure of holding the pressures within the required range, he will have on his control panel, pressure gages with an accuracy of, say, 0.3 per cent. The manufacturer of the pressure gages will have in his production line a calibration bench. Here the gages will be checked against standards which should be better than the instruments calibrated by at least a factor of 3, preferably a factor of 10, that is, from 0.1 to 0.03 per cent. The manufacturer should have in his standards room instruments somewhat better than the bench standards, with an accuracy better than 0.03 per cent, preferably about 0.01 per cent.

There are many research laboratories in industry engaged in getting fundamental engineering data with an accuracy of 0.1 per cent or better. Phenomena which are sensitive to pressure may require instrumentation accurate to 0.03 or even 0.01 per cent.

The National Bureau of Standards should have primary standards which are somewhat more accurate than any instrument portable enough to be brought in for calibration. There are pressure-measuring instruments which are capable of an accuracy of 0.01 per cent at pressures up to a few thousand pounds per square inch. The primary standards against which these are calibrated should be definitely better, with an accuracy of 0.003 per cent. The possible accuracy drops off as the pressures increase, and considerable effort is required to develop primary standards adequate to the present requirements in the high-pressure field.

Pressure-Standards Apparatus

In a primary standard the measurement of any physical quantity is referred directly to the standards of mass, length, and time. The device should be so simple in principle that all of the errors inherent in the instrument either can be eliminated or evaluated. Two commonly used primary standards are the mercury column and the dead-weight piston gage. The choice of instrument is not limited by accuracy, but by convenience. Twenty pounds per square inch is approximately equal to the head of a convenient 40-in. column of mercury. To measure 30,000 psi would require a column of mercury about 1 mile high.

The first extensive use of the free-piston gage was by Amagat (1).[3] The basic form and two modifications are in current use. They are illustrated in Figs. 1, 2, and 3.

Simple Piston Gage. The most familiar form of piston gage is shown in Fig. 1. It is a fitted piston-and-cylinder arrangement with means to apply known weights on the piston. The piston is rotated or oscillated to reduce friction. When the pressure applied to the piston develops a force sufficient to support the dead weights, they will be lifted. The weights may be placed on top of the piston or be suspended below it by a yoke. The weights may rotate with the piston or the piston may be rotated or oscillated independently of the weights. It is necessary for some fluid to leak past the piston for lubrication. The leak should be kept small to provide sufficient floating time to establish equilibrium and to make the required observations. This is particularly important at high pressure.

Differential Piston. Professor Michels (2) of Holland has designed a sensitive piston gage for high pressure, Fig. 2. It is a series of two differential-area pistons both carrying dead weights. The first piston (A) is suitable to pressures of 3000 kg/cm² (43,000 psi).

When its output is piped to the upper side of the second piston (B), the force developed is additive to the dead-weight load. The second piston makes the unit suitable to 10,000 kg/cm² (142,000 psi). Leakage is controlled by an interference fit between piston and cylinder. At high pressure the piston becomes free to rotate. The use of similar pistons of various sizes permits measurements over a wide range.

Re-entrant Cylinder. Professor Bridgman (3), early in his work developed a free-piston gage with re-entrant cylinder, Fig. 3. The bottom tip portion of the piston (p) and outside surface of cylinder (C) are subjected to the measured pressure. The bore of the re-entrant cylinder (C) grows smaller as pressure increases, regardless of the wall ratio (W = OD/ID). Since the clearance between the piston and cylinder diminishes with increasing pressure, and the leakage is reasonably small, the upper limit of the range is determined by the initial clearance. The initial clear-

[1] National Bureau of Standards, Washington, D. C.

[2] Harwood Engineering, Inc., Walpole, Mass.; formerly with Foxboro Company, Foxboro, Mass. Jun. ASME.

Contributed by the Industrial Instruments and Regulators Division of The American Society of Mechanical Engineers and presented at the Seventh National Instrument Conference, Cleveland, Ohio, September 9–10, 1952.

Note: Statements and opinions advanced in papers are to be understood as individual expressions of their authors and not those of the Society. Manuscript received at ASME Headquarters June 30, 1952. Paper No. 52—IIRD-2.

[3] Numbers in parentheses refer to the Bibliography at the end of the paper.

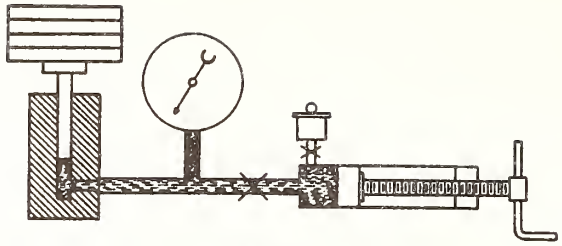

Fig. 1 Simple Piston Gage

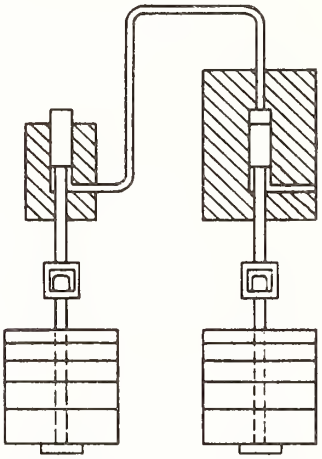

A, Low-pressure section B, High-pressure section

Fig. 2 Differential-Area Piston Gage

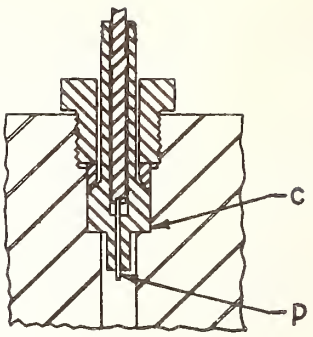

p, Piston
C, Cylinder

Fig. 3 Piston Gage With Re-entrant Cylinder

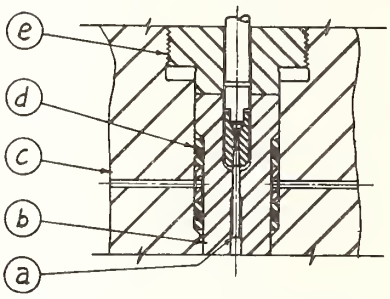

a, Piston
b, Cylinder
c, Jacketing cylinder
d, Packing rings
e, Closing nut

Fig. 4 Controlled-Clearance Piston Gage

ance was chosen so that the crevice closed completely at approximately 210,000 psi, and the instrument was used to approximately 190,000 psi to a precision of approximately 0.1 per cent. The fluid used was a mixture of glucose, glycerin, and water.

The literature abounds with descriptions of instruments which are variations of the basic concept of the simple piston gage. Mostly, they are clever arrangements to allow the operator to handle small weights. It is probably fair to say that uncertainties are built into the devices in proportion to the departure from the simply loaded piston.

Controlled-Clearance Piston Gage

The clearance between the cylinder and piston must be kept small if the piston gage is to be useful on the score of (*a*) knowledge of the effective area, (*b*) high sensitivity, (*c*) manageable leakage of the fluid past the piston. The large elastic distortions, particularly in the cylinder, have set severe limitations on the useful range.

The controlled-clearance piston gage, Fig. 4, permits a size adjustment of the cylinder bore to the desired clearance. The measuring piston (a) is contained in a jacketed cylinder (b). An independent pressure is used between the jacketed and jacketing cylinder (c) to deform the jacketed cylinder to the desired clearance. The pressure in the jacketing cylinder is sealed off by Bridgman unsupported area rings (d) whose initial seal is accomplished by a mechanical load from nut (e).

The relation between the pressure P_J required in the jacketing cylinder and the pressure P_M being measured is expressed approximately by

$$P_J = K + L P_M$$

in which K is the pressure required to close the crevice at zero internal pressure. The value of L depends on the position of the ring of minimum clearance. If the ring is near the top of the cylinder, L will be about 0.7; if away from either end, the preferred condition, L will be about 0.35. Depending on the initial clearance, the jacketing pressure can be either greater or less than the pressure being measured. The jacketed cylinder and piston are disposed in the design so that the seal between them will be accomplished sufficiently far from the ends of the piston to avoid local distortions which result from end effects. To avoid end effect further, the jacket cylinder is "bellmouthed" at both ends of its bore.

The free-falling time is controlled readily by minor adjustments of jacket pressure. If the close clearance is maintained, the effect of the distortion of the cylinder is eliminated. It will be shown later that this is a notable improvement since in other designs the elastic distortion of the cylinder is one order greater than the distortion of the piston. A still further improvement probably will result from the use of carboloy pistons. Otherwise the apparatus is more elaborate than unique. The elaborations take advantage of well-known design points with a view to maintaining accuracy and precision, and to securing ease in manipulation.

The dead-weight system, Fig. 5, is patterned after the 10,100-lb dead-weight system in the Engineering Mechanics Section at the National Bureau of Standards (4). The dead weights themselves (f) are made of austenitic stainless steel for long-time stability and freedom from oxidation, corrosion, and magnetism. The loading system has 1000 lb of dead weight, consisting of nine 100-lb platters held in a chain suspension attached to the yoke (g). The weights are lifted on and off the suspension by the power cylinder (h) on the base. Smaller 10 and 5-lb weights (i)

are provided for hand-loading on the yoke. The piston is rotated either clockwise or counterclockwise by means of a pulley (j) and motor arrangement to eliminate the corkscrew effect. It is patterned after that described by Meyers and Jessup (5). The yoke suspension rods (k) are insulated electrically from the upper cross rail (l). Thus, by electrical sensing, there is assurance that the weights supported by the piston are free of other parts.

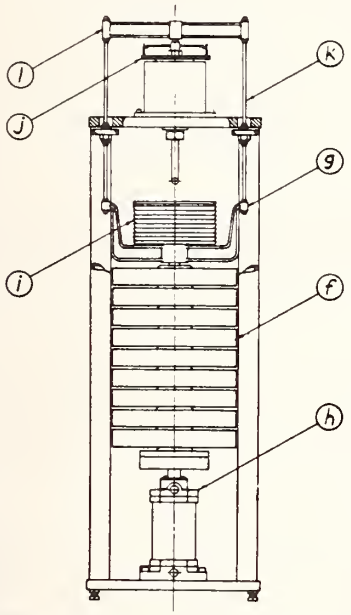

f, Large dead weights of 100 lb each
g, k, l, Yoke suspension
h, Power cylinder to load large dead weights
i, Small dead weights of 5 and 10 lb
j, Pulley for rotating piston

FIG. 5 LOADING MACHINE FOR CONTROLLED-CLEARANCE PISTON GAGE

The measuring piston and cylinder are so arranged that they may be removed readily and interchanged with similar components for other ranges. The cost of the piston assemblies is on the order of 3 per cent of the total cost of the instrument, while the piston itself represents only a fraction of 1 per cent of the total cost of the instrument. The change-over from one piston size to another is done readily with hand tools.

ERRORS OF A PISTON GAGE

Definitions. A pressure is a force per unit area. A force of 1 lb will be defined as that which will accelerate a mass of 1 lb at the normal acceleration of gravity, 980.665 cm/sec^2 or 32.174 ft/sec.^{2} The U. S. pound is defined as the 0.4535924277 part of the international kilogram. The U. S. standard inch is defined as 100/3937 international meters (6).

To obtain the pressures as so defined, the indications of a practical dead-weight piston gage are subject to a number of corrections. The more important of these, which will be of concern to those who hope to measure a pressure to a part in a thousand, will be discussed in some detail. Some of these errors can be evaluated and corrections applied, but in every case there will remain some residual uncertainty which may or may not be important.

Effective Area. The effective area of a piston gage is the mean of the area of the cylinder and that of the piston, provided the piston is concentric with the cylinder and falling at a rate at which the volume displaced by the piston is equal to the leak between it and the cylinder. This is true for any clearance and for fluid of any viscosity. If, because of other volume changes in the system, the piston is falling at any other rate, of the same order of magnitude, the effective area will be changed by an amount of the order of the square of the clearance distance.

Elastic Distortions. The following formulas may be found with the assistance of standard texts on elasticity (7):

The change Δd in the diameter d, in a solid piston subjected to end pressure P and surrounded by pressure P_c (P is the pressure being measured and P_c the pressure in the crevice) is given by

$$\frac{\Delta d}{d} = \frac{\nu P}{E} + \frac{P_c}{E}(\nu - 1) \quad [1]$$

where ν is Poisson's ratio and E is Young's modulus.

The change Δa in the bore radius a of a hollow cylinder of outside radius $b = wa$, where P_o is the pressure on the outside, P_a is the pressure on the inside, and P_z is the pressure on the end face, is

$$\frac{\Delta a}{a} = \frac{P_a}{E}\left[\frac{(1-\nu) + (1+\nu)W^2}{W^2 - 1}\right] - \frac{P_o}{E}\left(\frac{2W^2}{W^2-1}\right) + \frac{\nu P_z}{E} \quad [2]$$

In the piston gage the pressure varies along the length of the crevice between piston and cylinder. At the bottom it equals the pressure being measured; at the top it falls to zero. The fall of pressure probably will be concentrated in a small portion of the length. The effective pressure in the crevice, to be used in calculating the distortion, will depend on the location of the region of falling pressure. If this region is at the bottom of the piston, the effective pressure will be small. If it is at the top, so that the crevice is filled with liquid at high pressure, then the effective pressure may be nearly as high as that being measured.

Small variations in dimensions may have a great effect on the position of the pressure drop. (It is even possible that the position may be a function of pressure.) The variations may occur because of the design, because of irregularities in machining, or because of distortions in use. For example, when a piezoelectric gage is calibrated by a sudden release of pressure, the piston of a gage connected to the system will drop violently. If it is stopped at the blind end of a cylinder it may mushroom slightly, Fig. 6(a). If it is stopped by contact with the open end of the cylinder, the latter may develop a burr, Fig. 6(b). Therefore it can be said with certainty, only that the effective pressure in the crevice is less than the pressure measured. The distortions of the piston and cylinder may be calculated on the basis of an effective pressure in the crevice which is the mean between that at the two ends, provided that the fall of pressure takes place in a region remote from the ends of the piston, and of the bore of the cylinder. "Remote" can be taken as one diameter in the case of the piston, and three bore diameters for the cylinder.

Piston. Case 1: When the pressure in the crevice is one half the pressure being measured, we have the following change ΔA in the area A using Equation [1], a value of 0.28 for Poisson's ratio and 30×10^6 psi for Young's modulus

$$\frac{\Delta A}{A} = \frac{2\Delta d}{d} = -0.53\frac{P}{10^8} \quad [3]$$

At 200,000 psi this amounts to —0.11 per cent.

Case 2: If the fall of pressure is at the top of the piston and occurs over a length which is small compared to the diameter, $P_c = P$

$$\frac{\Delta A}{A} = \frac{2\Delta d}{d} = \frac{-2.9P}{10^8} \quad [4]$$

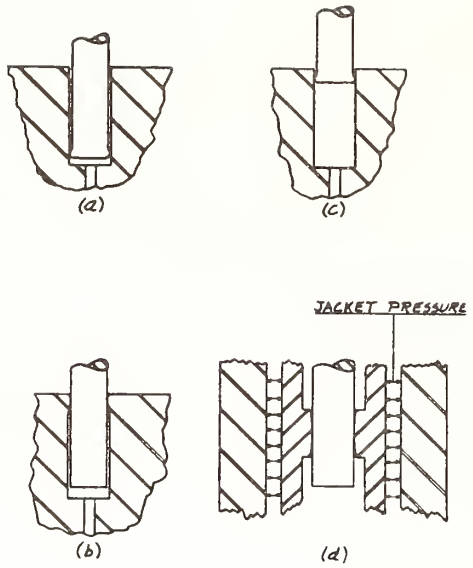

FIG. 6 PRESSURE DISTRIBUTION IN PISTON GAGES

(*a*, Piston and cylinder at low pressure; *b*, piston and cylinder at high pressure; *c*, piston at low pressure, cylinder at high pressure; *d*, top of piston at low pressure, bottom at high pressure. Cylinder controlled to fit piston.)

At 200,000 psi this amounts to —0.58 per cent.

Case 3: If the fall of the pressure is at the bottom of the piston $P_c = 0$

$$\frac{\Delta A}{A} = \frac{2\Delta d}{d} = \frac{+1.9P}{10^8} \quad [5]$$

At 200,000 psi this amounts to +0.38 per cent.

Piston Gage, Simple Cylinder, and Piston. Here the cylinder is subjected only to the pressure in the crevice. Equation [2] is applicable, with the terms

$$P_o = 0,\ P_s = 0,\ \text{and}\ P_a = P_c = \frac{P}{2}$$

For a wall ratio $W = 3$

$$\text{The change in area} = \frac{\Delta A}{A} = \frac{2\Delta a}{a} = \frac{5.1P}{10^8} \quad [6]$$

At 200,000 psi this amounts to +1.02 per cent.

The change in effective area of the gage will be the mean of the changes in the cylinder and piston (Case 1) or

$$\frac{\Delta A_{eff}}{A} = \frac{\Delta d}{d} + \frac{\Delta a}{a} = \frac{2.3P}{10^8} \quad [7]$$

At 200,000 psi this amounts to +0.46 per cent.

If the piston is expanded at the lower tip (Case 3), in a blind cylinder, Fig. 6(*a*), the distortion at 200,000 psi might vary from +0.19 per cent at the bottom of the stroke, to +0.70 per cent when the tip of the piston has risen several bore diameters away from the end of the cylinder, Fig. 6(*c*).

Piston Gage With Re-entrant Cylinder. The end face and outside of the re-entrant cylinder are subjected to the pressure measured so that $P_s = P_o = P$. If $P_a = P/2$ the distortion $\Delta A/A$ of the cylinder of wall ratio 3 is

$$\frac{\Delta A}{A} = \frac{2\Delta a}{a} = \frac{-4.02P}{10^8} \quad [8]$$

At 200,000 psi this amounts to —0.8 per cent.

The change in effective area of the piston gage (piston Case 1) is

$$\frac{\Delta A}{A} = \frac{\Delta d}{d} + \frac{\Delta a}{a} = \frac{-2.28P}{10^8} \quad [9]$$

At 200,000 psi this amounts to —0.46 per cent.

Controlled-Clearance Piston. In this instrument the dimensions of the cylinder change with those of the piston. The piston extends outside the section of close clearance with the cylinder by several diameters, so that the conditions for using the mean value of the pressure in the cylinder are satisfied, Fig. 6(*d*). Therefore the elastic distortion is that of the piston alone. For steel with $\nu = 0.28$ and $E = 30 \times 10^8$ psi, the change in area is

$$\frac{\Delta A}{A} = -\frac{0.53P}{10^8} \quad [10]$$

At 200,000 psi this amounts to —0.11 per cent.

For carboloy, with $\nu = 0.22$ and $E = 88 \times 10^6$ psi

$$\frac{\Delta A}{A} = -\frac{0.39P}{10^8} \quad [11]$$

At 200,000 psi this amounts to —0.08 per cent.

Measurement of Area. In the size range used in pressure gages, the piston diameters can be measured to 10 microinches or a little less. The corresponding uncertainties in the measured error are given in Table 1.

TABLE 1 EFFECT OF A 10-MICROINCH ERROR IN DIAMETER

Nominal area, sq in.	Approximate diameter, in.	Error in area, per cent
1/200	0.0798	0.025
1/100	0.1128	0.018
1/50	0.1596	0.012
1/20	0.2523	0.008
1/10	0.3568	0.006
1/5	0.5046	0.004
1/2	0.7979	0.0025

The gain in accuracy by increasing the size of the piston is somewhat more than that shown in the table since more precise methods of measurement are available for the largest size.

Measurement of Mass. The weights should be of the materials and quality required for the better commercial-scale weights. The material should be nonporous, corrosion and wear resistant, nonmagnetic. Weights usually are adjusted by the manufacturer to about 0.01 per cent. They can be calibrated to 0.001 per cent. In precise work, these corrections should be applied.

Gravity. The readings of Bourdon-tube pressure gages, manganin-wire gages, and such phenomena as elasticities, viscosities, phase changes, and chemical reactions, are functions of the absolute pressure. They are not sensibly affected by the local value of gravity. The pressure measured by a piston gage loaded with a particular set of dead weights is proportional to the local value of gravity. The convention here used is that the readings of elastic and dead-weight pressure gages should correspond when the dead weights are acted upon by gravity at the standard value of 980.665 cm/sec².

In the southern part of the United States, the value of gravity will be more than 0.1 per cent smaller than the standard value. In Canada and the northern part of the United States the local value will be higher.

If the latitude ϕ and the elevation h in feet above sea level are known, the gravity correction C_g will be given approximately by

$$C_g = -R\ (0.00261 \cos 2\phi + 0.000000095\ h + 0.00006)$$

where R is the reading of the piston gage.

This correction usually will compensate for gravitational

variation with an error of less than 0.005 per cent in any part of the United States.

For example: At Boulder, Colo., the reading on a piston gage, before gravity correction, was 101,200 psi. The latitude was 40°01′ ($\cos 80°02' = +0.1730$) the elevation 5350 ft

$$C_g = -101{,}200\,(0.00261 \times 0.1730 + 0.000000095 \times 5350 + 0.00006)$$
$$= -101{,}200\,(0.00102) = -103$$

so that the corrected pressure = 101,200 —103 = 101,097 psi.

In this case had the value observed at this location by the U. S. Coast and Geodetic Survey been used, the corrected pressure would have been 101,091 psi. This difference of 6 psi is reasonable, since the errors in the formula are largest in mountainous country.

Air Buoyancy. The mass of the piston and loading weights is determined on the ordinary commercial basis, i.e., by weighing in air, on an equal-arm balance, against standard brass weights (density 8.4 grams per cc). In precise work, the mass of the load on the piston should be reduced by an amount equal to the mass of the air displaced by the weights.

The density of air at room temperature and sea-level pressure is about 0.0012 gram per cc; and the mass under these conditions will be reduced by 1 part in 7000.

Temperature. The effective area of a carbon-steel piston and cylinder may be expected to increase about 13 ppm per deg F temperature rise; for a stainless-steel piston and cylinder the increase in area will be about 18 ppm per deg F.

The temperature of the piston is somewhat higher than that of the surroundings because of the dissipation of energy in the fluid escaping between the piston and cylinder. The temperature rise in the piston is difficult to estimate because of the uncertainty in the thermal transfer between the piston and the exterior. Since the dissipated energy is proportional to the rate of leak, measurements can be made at various rates, and an extrapolation made to zero leak.

Aging. Over a period of years the dimensions of the piston and cylinder may change by as much as 1 part in 1000 because of aging effects. Wear also will change the dimensions, and is likely to result in irregular performance. Extreme precautions to keep grit out of the fluid are required. The dead weights may lose weight from wear, or may gain weight by oxidation or collection of dirt.

Height and Piston-Buoyancy Corrections. It usually happens that the gage being tested, or the point at which the pressure is to be measured, is not at the same level as the lower end of the piston. Therefore correction should be made for the pressure difference due to the head of oil between these points. The correction is negative when the gage is above the piston. When oil is used in the piston gage, the correction will be approximately 0.03 psi for each inch difference in level.

When the submerged part of the piston is of uniform cross section, the pressure measured is that at the level of the lower end of the piston. In some designs the piston is enlarged to provide a stop for its upward motion or to give increased strength. If these enlargements are submerged in liquid, the weight of the fluid displaced by the enlargement should be subtracted from the dead-weight load.

With some designs it is not possible to observe the liquid level, and therefore not possible to determine the submerged volume. In such a case it is necessary to determine the buoyancy correction by test. It will usually be less than a pound per square inch.

Pressure Drops in Lines. Whenever possible, the piston gage should be connected into a leak-tight system, with tubing of the largest bore consistent with strength and safety, in order to avoid pressure drops in the lines. If this is impossible, the layout of tubing should be such that the piston gage is connected to the test vessel with a line through which the least possible flow of fluid occurs.

Friction. If the piston and cylinder come into contact, or if any part of the dead weight touches the supporting frame, sliding friction will introduce uncertainties. A film of fluid between piston and cylinder is usually maintained by rotation or oscillation. With rotation there is the possibility of a corkscrew effect, an axial thrust produced by helical irregularities on the surface of the piston and cylinder. Observations should be repeated with the piston rotating in the opposite direction. If the hydraulic fluid is a good lubricant and has a suitable viscosity, a film can be maintained with either rotation or oscillation. A lubricating film can be maintained with a fluid of very low viscosity (even air) provided the piston is rotated above a critical speed. This speed depends on the fluid, the symmetry of loading, and the clearances, etc. It must be determined experimentally for each instrument.

Intercomparison Techniques

Since the percentage accuracy of the measurements of the diameter is better for a large piston than for a small one, the intercomparison of piston gages of differing ranges provides an opportunity of improving the accuracy of the latter. In addition, there is the opportunity of averaging out some of the effects of varying properties of the materials of the piston, and of picking up possible mistakes in measurements.

In an intercomparison by cross floating, two piston gages are connected together and to a common pressure generator, such as the intensifier, of suitable range and capacity. Either piston gage can be isolated by means of valves in the connecting tubing. A telescope with an eyepiece scale or the equivalent, is set up to observe the position of one of the pistons in its range of motion. At the selected pressure, the rate of fall of each piston is observed with the gage isolated. The two gages are connected together and one of the loads adjusted by adding small weights until both pistons fall at approximately the same rate as when isolated. An exact balance is usually not obtained, but by observing rates of fall at various loads, an interpolation can be made to the load for which the rates of fall would be the same with the gages connected as when they are isolated.

By having one of the pistons fall repeatedly over the same interval, while the other falls through various parts of its range it is possible to observe small variations in diameter. By this method a commercial piston gage with a simple cylinder was ascertained to have an effective area constant over its length to within 1 part in 50,000. Since the diameter of this piston was about 0.16 in., it must have been uniform to 1.6 microinch or better.

This particular observation happened to have been made at a pressure of about 1000 psi. When the same kind of comparison was attempted at 5000 psi, the rate of fall was so much greater that the comparison was quite unsatisfactory. The enormous change in sensitivity was caused by an increase in the bore of the cylinder estimated to be only about 8 microinches.

Calibration Against a Mercury Column

An alternative primary standard is the mercury column. Readings on it are also subject to a large number of corrections, most of which are counterparts of those for the piston gage. The reader may refer to Glazebrook (8) or Meyers and Jessup (5) for a discussion of them. The latter authors set up a 150-psi mercury column, with an accuracy of 0.01 per cent, compared it with piston gages of 0.01 per cent accuracy, and had agreement within 0.01 per cent at pressures up to 1050 psi. They set up a

pressure on one piston gage, added the pressure measured by the mercury column, and compared the sum with the pressure on a second piston gage. The pressure measured by the mercury column was then added to that on the second gage and compared with a new pressure set up on the first. The process was continued until the glass tubing broke. Keyes (9) has carried a similar procedure up to pressures as high as 15,000 psi.

While this method is quite satisfactory at low pressures, the accuracy falls off rapidly at higher pressures. For example, suppose that a 150-psi mercury column is used to calibrate a pair of 30,000-psi piston gages, which have a sensitivity of 1 ppm of their range or 0.03 psi. Then each 150-psi step in this comparison can be done to 0.03 psi, or 1 part in 5000. But the area of a piston good enough to attain this sensitivity probably can be measured to better than 1 part in 10,000.

The small distortion of the cylinder or piston in the 150-psi step of pressure gives rise to just as large a correction, in relation to the 150 psi, as the larger distortion under 30,000 psi is with respect to the 30,000-psi range of the instrument.

A satisfactory comparison with a mercury column will give the user of the piston gage the valuable assurance that he has not overlooked some large systematic error in the latter. But a calibration of a piston gage against a mercury column cannot be regarded as inherently better than a standardization by direct measurement on piston and weights.

Fixed Points on the Pressure Scale

Primary pressure standards are not portable. In order to attain an over-all accuracy of 1 part in 10,000, attention must be paid to a great many factors. As a result, although the mercury column or piston gage is simple in principle, it will be surrounded by so many auxiliaries that its bulk will be large in the aggregate. To tear it up by the roots and send it to another laboratory for a calibration is a formidable task. Even if all this were done, there would be no assurance that essential parts would endure the hazards of shipment. There is a real need for a means of calibration that can be put in a suitcase, or even better, sent by first-class mail.

One solution to this problem is a set of experiments which can be repeated at any laboratory and will reproduce definite pressures. In some cases a suitable transfer instrument and a set of fixed-pressure points would replace the primary standard. The analogous situation exists in the field of temperature measurement. The platinum-resistance thermometer and four fixed-temperature points define the temperature scale over a range of 600 C to the satisfaction of most users.

The fixed-pressure points may be based on changes of state or polymorphic transformations which should satisfy the following conditions:

1 The substances involved should be obtainable in a pure state.

2 The transition should take place at a sharply defined pressure, with no range of indifference.

3 There should be a large volume change, or other effect, for ready identification.

4 The reaction should run rapidly.

5 The dependence of the pressure on temperature or other possible parameters should be slight.

6 It should be possible to contain the substances so as not to damage the pressure vessel.

Triple points are particularly suitable since they are unique in both temperature and pressure, provided all three phases are present. In a two-phase system a volume change is associated with a thermal change, and time is required to approach equilibrium. At a triple point, adjustments among all the components take care of thermal and volume changes simultaneously.

Bridgman's value of the freezing pressure of mercury at 0 C, 7640 kg/cm² (108,660 psi), has been used by a number of observers. Occasionally a higher temperature has been used when a higher pressure was required. The temperature coefficient of the melting pressure is about 3000 psi per deg C, so that accurate temperature measurements and precise control are required. These are much easier at 0 C, where an ice bath can be used.

In his work at the high pressures Bridgman has used the bismuth I–II transition at about 360,000 psi for the calibration of his manganin-wire pressure cells.

The four triple points between liquid water and various ices appear to be promising. These are L-I-III at about 30,000 psi; L-III-V near 50,000 psi; L-V-VI near 90,000 psi, L-VI-VII near 320,000 psi. Between these points the melting-point pressure at various temperatures can be used. The Geophysical Laboratory of the Carnegie Foundation (10) is reporting its pressure measurements on the basis of a value of 9630 bars (139,670 psi) for the freezing pressure of water at 30 C, with the expectation of adjustment if a better determination should change that value.

Professor Bridgman measured pressures at the phase changes of water and of mercury in 1912. Since then, in so far as is known, there has not been an independent determination. Rather, the value reported by him has been used without question. While the Bridgman values were sufficiently accurate for his pioneering work, a vast amount of data reported with greater accuracy than that claimed by Bridgman are still dependent on his value. This is not as serious as it might seem at first glance. Bridgman's value should stand until an independent determination has been made with the improved tools of the present day. Quantitative work reported prior to the publication of the new value will have to be corrected when correlated to subsequent work—should a correction for Bridgman's value be indicated.

Mercury-Point Determination

In order to test the possibilities of the controlled-clearance piston gage, and to get the "feel" of the experiment, a determination was made of the melting pressure of mercury at 0 C. Use was made of a transfer gage, at first a manganin-wire pressure cell, and for the final runs, a gold-chromium-wire pressure cell. The determination can be broken into three steps as follows:

(*a*) Measurement of melting pressure of mercury in terms of transfer instruments.

(*b*) Calibration of transfer instruments in terms of piston gage.

(*c*) Direct measurement of area of piston and mass of deadweight load.

Mercury-Point Comparisons. The apparatus found to be convenient was arranged as shown schematically in Fig. 7. Two laboratory-type intensifiers were used. The intensifiers were driven and charged by hand-operated 10,000-psi pumps. White gasoline was the high-pressure fluid used. Kerosene had been found unsuitable in an earlier experiment. The upper side of the low-pressure piston of the intensifier A (normally vented to the air), was filled with a liquid and connected to a sight glass to indicate the piston displacement, and hence the changes in volume. With a $^1/_8$-in-bore sight glass, the displacement of the column was 360 times that of the piston.

The mercury bomb was a simple high-pressure vessel with a cavity 1 in. diam and approximately 3 in. long. Freshly distilled mercury was sealed in a polyethylene sack and placed in the bomb cavity.

A gold-chromium resistance element, subjected to the high pressure, was used as a transfer device. The gold-chromium resistance was part of a 120-ohm equal-arm bridge. The other arms were in a bath at room temperature, close to the pressure cell. The bridge was driven by alternating current at 1000 cps,

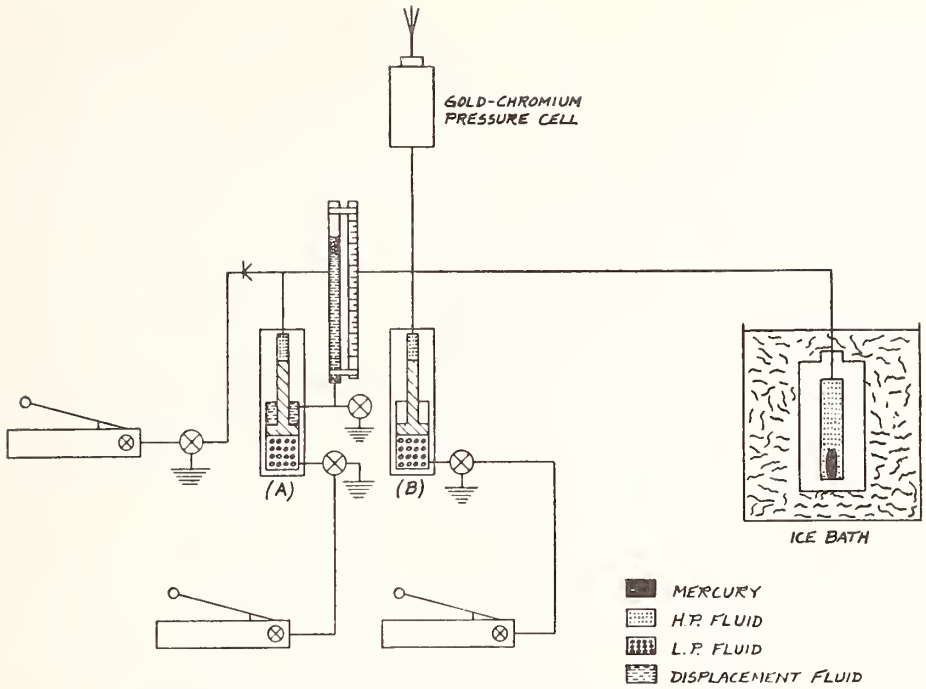

FIG. 7 APPARATUS FOR DETERMINATION OF MERCURY FREEZING PRESSURE

50 milliamp total current. One arm of the bridge was shunted by an adjustable resistance box. An a-c null indicator was used to detect balance. The sensitivity of the indicator was adequate to detect changes in the resistance of the gold-chromium wire of 1 part in 10^7. A duplicate bridge in a temperature-controlled bath was used to correct for drift in the null indicator. The drift during a run was not more than 1 part in 10^6.

The system was charged to about 10,000 psi by a hand pump. This pressure was held in the system by a check valve when the hand pump was removed. The piston of intensifier (B) was then advanced to the end of its stroke raising the pressure to about 90,000 psi. Another check valve held the pressure in the rest of the system after the pressure in intensifier (B) was released. During the rest of the experiment the pressure was raised by advancing the piston of intensifier (A). The movement of the piston of this intensifier was followed in the sight glasses.

If the volume is plotted against pressure, at constant temperature, there is obtained a nearly straight line *A-B*, Fig. 8, representing the compression of the liquid, a horizontal straight line *B-C*, representing the change in volume at constant pressure of the mixture of liquid and solid, and the nearly straight line *C-D* representing the compression of the solid. This is under isothermal conditions, which are never realized by the experimenter. When the specimen is compressed, it is heated, and is therefore at a pressure which is a little high. If only one phase is present, either liquid or solid, the approach to equilibrium is nearly completed after 5 min. With both phases present, the latent heat of the phase change is large, and a relatively long time is required for the system to come to equilibrium as this heat is transferred to the bath.

In these measurements the pressure is increased in steps of about 5000 psi, and the piston held stationary at each step for 5 min. As long as only liquid mercury is present, the pressure drops back slightly and stabilizes during each hold period, *A* to *B*, Fig. 8. When solid mercury makes its appearance, the pressure drops back farther in the 5-min period and the curve drops off,

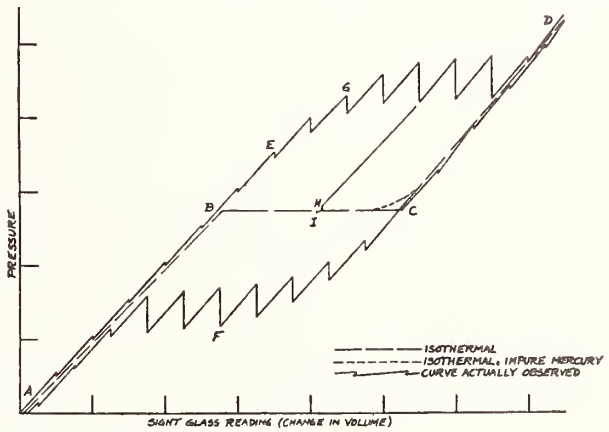

A-B—Liquid phase only
C-D—Solid phase only
B-C—Liquid and solid phases present at 0 C
A-B-E-G-D—Mercury compressed in steps; specimen heated by freezing
D-C-F-A—Mercury expanded in steps; specimen cooled by melting
H, I—Approaches to equilibrium with both phases present

FIG. 8 IDENTIFICATION OF FREEZING PRESSURE OF MERCURY BY VOLUME CHANGE

as at *E*. When the all-solid line *C-D* is reached, there is an abrupt transition to the quick equilibrium condition, and on further compression, the curve resembles *A-B*.

On expansion, a zig-zag line *D-C-F-A* would be described. If at the point *G*, the volume were held constant the pressure would settle out toward the equilibrium point. The time of several hours required for a close approach to equilibrium may exceed the experimenter's patience. A quicker way is to juggle pressures so as to start close to the expected asymptote, as at *H* or *I*. Then the equilibrium pressure can be approached from both sides,

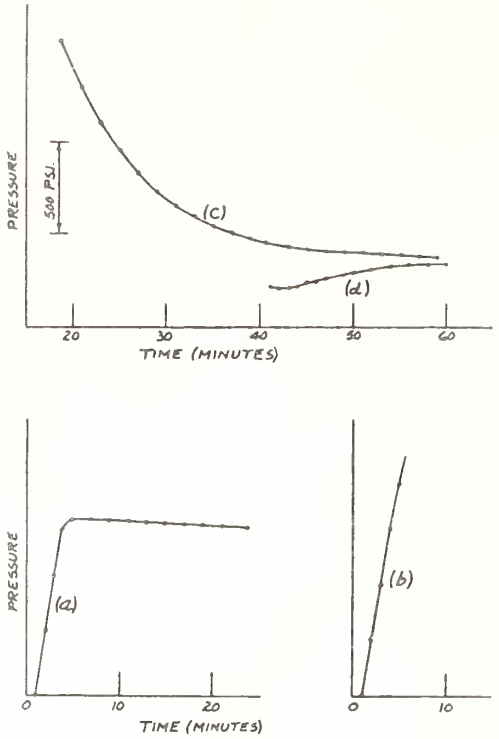

(*a*) Approach to equilibrium after expansion; one phase present
(*b*) Pressure change immediately after expansion; both phases present
(*c*) Approach to equilibrium after compression; both phases present
(*d*) Approach to equilibrium after expansion; both phases present

FIG. 9 DETERMINATION OF MERCURY FREEZING PRESSURE; PRESSURE-TIME RELATIONS

the decay being followed only long enough to predict the position of the asymptote. This should be repeated at several points along the line *B*-*C'*, including one point close to *C*. If the mercury is impure, the corner at *C* will not be sharp, as in the dotted line.

In addition to the plot of pressure (or what is more convenient, readings on the transfer gage) against volume, it is also desirable to plot pressure against time. In Fig. 9 are such curves. In (*a*) only liquid is present, and the decay is rapid. This is a leak check showing a loss of about 3 psi per min after disappearance of the initial transient following an expansion; (*b*) was taken near (F) with both phases present; (*c*) and (*d*) were taken at (H) and (I) and define the melting pressure as their common asymptote.

It is desirable that the system be absolutely tight. If the leak in, say, 30 min cannot be detected by the pressure-measuring means when only one phase is present, its effect may be neglected. If it is perceptible but small, its effect can be estimated and a correction applied.

From a curve such as (*a*), Fig. 9, with only one phase present, the leak in psi per minute may be estimated. The flow through the leak is supplied by the expansion of the fluids, mostly gasoline, and the contraction of the pressure vessel under this pressure change. The fall of pressure with both phases present, as (*c*) Fig. 9, can be divided into two parts, the pressure drop associated with the expansion of the fluid under the leak, and that associated with the change in volume due to the phase change. When the pressure is falling rapidly, as at the beginning of curve (*c*), the mercury is freezing, the sample is warmer than its surroundings and is giving up heat to the pressure vessel. When the pressure is falling very slowly, the fluids are expanding very slowly, and most of the leak is supplied by the expansion which results from melting of the sample. The sample then will be absorbing heat from the pressure vessel and will be a little cooler. At the point of (*c*) where the slope is the same as that of the leak curve, the sample is neither melting nor freezing and its temperature is the same as that of its surroundings. The difference between the pressure at this point and that at the asymptote is approximately the leak correction.

An alternative and equivalent estimate of the effect of leak is obtained by multiplying the rate of leak from curve (*a*) by the time constant of the decay of pressure in curve (*c*) or (*d*).

Calibration of Transfer Instrument. The arrangement of apparatus used in calibrating the gold-chromium pressure cell is shown in Fig. 10. A pressure was generated by intensifier (A), and admitted to the controlled-clearance piston gage (B). This pressure was indicated on the gold-chromium pressure cell (C) with the same bridge and null indicator used in the observations on the mercury point. The jacketing cylinder of the piston gage was subjected to pressures generated by intensifier (D) and measured by a manganin cell (E) which was part of a Wheatstone bridge of the strain-indicator type.

A dead-weight load was set up on the piston gage, the pressure raised until the piston was at the top of its travel. While the piston fell through its range ($^1/_8$-in.) observations were made on the pressure under the piston with the gold-chromium cell, on the jacketing pressure with the manganin cell, and on the time of fall. The jacketing pressure was adjusted until the rate of fall was about 30 sec. Readings were made at the top and the bottom of the travel. The dead-weight load on the piston was increased in 20-lb steps until the pressure used in the mercury-point measurements had been exceeded. The load corresponding to the mercury point was obtained by interpolation between calibration points on the basis of the resistance change in the gold-chromium cell.

Measurement of Piston and Dead Weights. The 20-lb weights

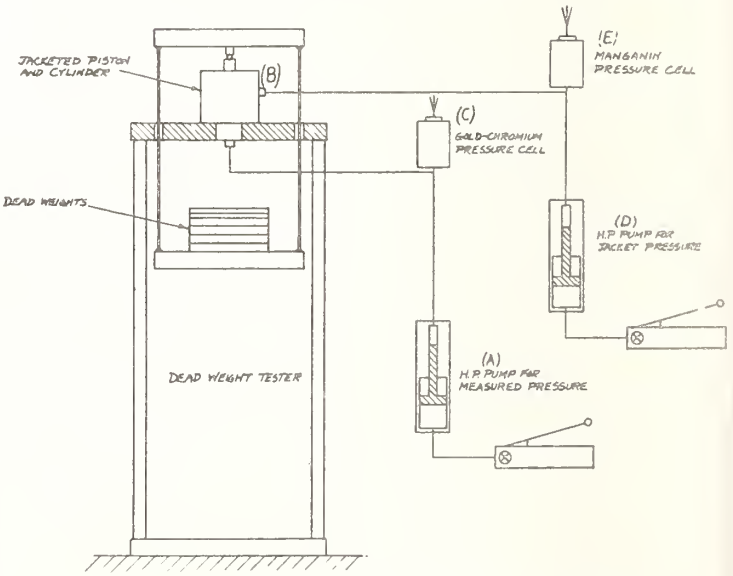

FIG. 10 CALIBRATION OF GOLD-CHROMIUM PRESSURE CELL

had been adjusted by the Massachusetts State Sealer of Weights and Measures to within 0.001 lb of their nominal mass. The yoke, weight hanger, piston, and so on, were weighed to an accuracy of about 0.001 lb.

The piston was measured by the Gage Section of the National Bureau of Standards with an accuracy of about ±0.00002 in.

Results. The results of the measurement and the estimates of the various errors are summarized in Table 2. The errors characteristic of piston gages, in general, have already been discussed at length.

TABLE 2 SUMMARY OF RESULTS

Weights: 268.73 lb
Area: 0.0024446 sq in.
Pressure uncorrected: 109,930 psi

	Correction, psi	Residual error, psi
Zero shifts, in mercury-point runs	...	∓ 65
Zero shifts, in piston-gage runs	...	±215
Correction for leakage	+ 20	± 10
Piston measurement, ±0.00002 in.	...	± 80
Piston taper, 0.00003 in.	...	±120
Residual clearance, 0.000010 to 0.000020 in.	— 30	± 10
Elastic distortion	+ 65	± 10
Temperature of piston	— 25	± 15
Weight measurement	...	± 10
Buoyant effect of air on weights	— 15	
Gravity at Foxboro	— 35	± 5
Temperature of ice bath, ±0.02 C	...	± 60
Conduction down tubing	—150	±150
Total correction	—170	
Corrected pressure	109760	±750

The mass load on the piston gage at the pressure for which the resistance change was the same as that observed in the mercury fixed-point runs was obtained by interpolation between observations in the piston-gage runs. The area was the average in the upper $^1/_4$ in. of the piston, based on direct measurement. The uncorrected pressure is the mass load divided by the area.

There were differences in zero before and after the mercury-point and the piston-gage runs. The two zero readings were averaged, on the assumption of equal changes during increase and decrease.

The system was found to be losing pressure at a rate of about 2 psi per min when only liquid was present. This rate was multiplied by the 10-sec time constant of the approach to equilibrium conditions when both phases were present.

The residual clearance between piston and cylinder was estimated from the leakage rate, including the effect of the expansion of the fluid under the pressure change during the fall of the piston, and assuming that the drop in pressure occurred in $^1/_{10}$ in. of length of the piston.

The elastic distortion of the steel piston was calculated from Equation [10].

The value of gravity was interpolated from Coast and Geodetic Survey data at points within 10 miles of Foxboro, Mass., where the experiment was conducted.

The temperature of an ice bath, using good commercial ice, usually can be expected to be 0.00 ± 0.02 C. Several measurements of samples during these tests fell within this range. The conduction of heat down the pipe to the mercury cell would raise the temperature of the latter by an amount estimated not to exceed 0.1 C.

A difference between pressures at the upper and lower limits of travel of the piston was observed. This was found to be caused by a taper in the piston which developed when the piston had been scored in previous tests. (This taper of 0.00012 in. in $^1/_2$ in. of length was 10 to 100 times that which would be tolerated in a new piston.) The ratio of 0.7 between change of jacket pressure and change of measured pressure indicated that the line of contact between piston and cylinder was near the top. The area of the piston was computed on the diameter of 0.05579 ± 0.00002 in. measured $^1/_8$ in. from the top. An additional uncertainty in area was taken as that corresponding to the taper in $^1/_8$ in. of length.

Additional possible errors, not evaluated, include those resulting from possible changes in the resistance in the gold-chromium wire which were not reflected in the zero shift. This alloy is a new one for pressure measurement, and very little experience has been accumulated. In particular, little or nothing is known as to the proper pressure-seasoning treatment. (This particular element had been subjected to two applications of pressure to 140,000 psi.)

Difficulties Encountered. A number of mechanical difficulties resulted from the escape of mercury from its container in an early experiment. A small quantity got into other parts of the system, and amalgamated with brass packing rings, the heads of pistons, and the like. Numerous failures of these parts resulted. No autofrettaged cylinders failed. It was found that a polyethylene bag was tough and flexible enough to hold the mercury. Wherever possible, the inlets to pressure cells, intensifiers, and the like, should be at the bottom, and the inlet to the mercury bomb at the top, and the tubing arranged so that escaped mercury droplets will drain to the mercury bomb.

In the manganin and gold-chromium cells the packing used for the insulated electrical lead included a plastic which softened in contact with kerosene or gasoline, and was responsible for a progressively increasing electrical leakage. This was serious since one corner of the Wheatstone bridge is grounded, and a leakage through 100 megohms will produce a significant error. Other packing materials are being tried.

Conclusions

The measurements of the melting pressure of mercury were of value in trying out new equipment in the high-pressure field and in pointing out the direction of future improvements in technique and apparatus.

The controlled-clearance piston gage was used at pressures as high as 120,000 psi, with no indication that the limit of its range was being approached. (The pressures to which this instrument was used were limited by fittings rated at 100,000 psi.) Adequate floating times for the measurements were obtained. Indications were that clearances could be held to a few microinches, provided the surfaces of the piston and cylinder were that good. The small clearances make necessary precautions to eliminate abrasive particles in the working fluid. The use of carboloy pistons may be indicated from considerations of wear.

The gold-chromium pressure cell seemed promising. The time required to reach constant readings seemed somewhat shorter than for manganin. The very small temperature coefficient should be valuable. The elastic defects of hysteresis, drift, and after-effect, required further study since they were obscured by the electrical leakages in other parts of the bridge.

These measurements give a value 1 per cent higher than obtained by Bridgman for the melting pressure of mercury. This difference is not serious in view of the rather large experimental error of ±0.7 per cent due to identifiable sources.

The largest errors can be reduced substantially in future work. A better choice of the insulating material in the electrical leads should reduce the troubles with zero shift. An unworn piston would have variations in diameter less than a tenth as great as those in the one used. The temperature of the mercury sample can be measured directly.

Acknowledgments

This work was carried out with the support of the Foxboro Company, Harwood Engineering, Inc., and the National Bureau of Standards. The authors are indebted to numerous people in those organizations for assistance. They particularly wish to

thank Dr. Brombacher of the National Bureau of Standards, and Mr. Howe of the Foxboro Company for their encouragement; Mr. George Champagne for his technical assistance; Mr. Howard Fuller, who designed and operated the a-c null indicator used. The authors have profited from many suggestions made by Professor Bridgman.

BIBLIOGRAPHY

1 "Mémoires sur l'élasticité et la dilatabilité des fluides jusqu'aux très hautes pressions," by E. H. Amagat, *Annales de Chemie et de Physique*, vol. 29, 1893, pp. 68–136 and 505–574.

2 "Einfluss der Rotation auf die Empfindlichkeit einer absoluten Druckwage," by A. Michels, *Annalen der Physik*, vol. 72, 1923, pp. 285–320; vol. 73, 1924, p. 577.

3 "The Measurement of Hydrostatic Pressures Up to 20,000 Kilograms Per Square Centimeter," by P. W. Bridgman, Proceedings of the American Academy of Arts and Sciences, vol. 47, 1912, p. 321.

4 "Dead-Weight Machines of 111,000 and 10,100 Pound Capacities," by B. L. Wilson, D. R. Tate, and George Borkowski, NBS Circular C446, June, 1943.

5 "A Multiple Manometer and Piston Gages for Precision Measurements," by C. H. Meyers and R. H. Jessup, National Bureau of Standards, *Journal of Research*, vol. 6, 1931, p. 1061, RP324.

6 "Units of Weight and Measure, Definitions and Tables of Equivalents," National Bureau of Standards Miscellaneous Publication M121.

7 "Strength of Materials, Part II. Advanced Theory and Problems," by S. Timoshenko, The Macmillan Company, New York, N. Y., 1936.

8 Glazebrook-Dictionary of Applied Physics.

9 "Methods and Procedures Used in the M.I.T. Program of Investigation of the Pressures and Volumes of Water to 460 C," by F. G. Keyes, Proceedings of the American Academy of Arts and Sciences, vol. 68, 1933, p. 505.

10 "Equilibrium in Binary Systems Under Pressure I. An Experimental and Thermodynamic Investigation of the System, NaCl–H_2O, at 25°," by L. H. Adams, *Journal of the American Chemical Society*, vol. 53, October, 1931, p. 3769.

D. P. JOHNSON, J. L. CROSS, J. D. HILL, and H. A. BOWMAN
National Bureau of Standards, Washington 25, D. C.

Elastic Distortion Error in the Dead-Weight Piston Gage

Development of the intermolecular theory depends on high accuracy pressure-volume-temperature measurements which in turn depend on understanding limitations of the piston gage. Error growth from data uncorrected for gage distortion is shown here.

ELASTIC DISTORTION OF the piston and cylinder of a dead weight pressure gage have concerned experimenters for many years. Changes of clearance have limited the range between pressure where the piston seizes and that where the leak is excessive. When a piston is measured in the open (at atmospheric pressure) or calibrated at low pressures and used at higher pressures, extrapolation has required an estimate of the change of effective area with pressure. For pressures above a few thousand atmospheres, this estimate is the largest single uncertainty in measuring pressures.

Even at lower pressures, elastic distortion is significant in work at high precision. In determining the compressibility factor (PV/RT) of a gas, the correction for elastic distortion of the pressure gage can amount to one part in 10,000 at 100 atm. and 1 part in 1000 at 1000 atm. Thermodynamic quantities which depend on the derivative with respect to pressure may be in error by a larger proportion. The elastic distortion error is particularly troublesome because it affects pressure ratios as well as absolute pressures.

Effect on Virial Coefficients

The dead weight, free piston gage is based on the relation,

$$P = W/A_e \qquad (1)$$

where W is weight supported by the piston and A_e is the effective area of the piston. There are other supplementary corrections and measurements with their related uncertainties, but only effect of pressure on effective area will be discussed here.

As a first approximation, the effective area is a linear function of the pressure, so that

$$A_e = A_o(1 + aP) \qquad (2)$$

where A_o is effective area of the piston at low pressure.

Uncorrected pressure, P_1, obtained by adding pressure denominations of the weights, or dividing total weight by the measured area, is then a quadratic function of the true pressure,

$$P_1 = \frac{W}{A_o} = P(1 + aP) \qquad (3)$$

Suppose the results of a PVT (pressure-volume-temperature) determination are worked up in terms of uncorrected pressure to obtain a set of virial coefficients of powers of the molar volume,

$$P_1V = RT\left(1 + \frac{B_1}{V} + \frac{C_1}{V^2} + \frac{D_1}{V^3} + \ldots\right) \qquad (4)$$

The effect of elastic distortion can be seen by solving for pressure and substituting from Equation 3 to obtain

$$P(1 + aP) = \frac{RT}{V} \times \left(1 + \frac{B_1}{V} + \frac{C_1}{V^2} + \frac{D_1}{V^3} + \ldots\right) \qquad (5)$$

This quadratic in P can be solved and developed in Taylor's series to give

$$\frac{PV}{RT} = 1 + \frac{B_1 - aRT}{V} + \frac{C_1 - 2B_1aRT + 2a^2R^2T^2}{V^2} + \frac{D_1 - 2C_1aRT + 6B_1a^2R^2T^2 - 5a^3R^3T^3 - B_1^2aRT}{V^3} + \ldots \qquad (6)$$

The alternative expression for the virial in powers of the pressure may be written

$$P_1V = RT + BP_1 + CP_1^2 + DP_1^3 + \ldots \qquad (7)$$

Substitution from Equation 3 and dividing through by $(1 + aP)$ gives

$$PV = \frac{RT}{1 + aP} + BP + CP^2 \times (1 + aP) + DP^3(1 + aP)^2 + \ldots \qquad (8)$$

When the first term of the right side is developed in series and the third and later terms are multiplied out,

$$PV = RT + (B - aRT)P + (C + a^2RT)P^2 + (D + Ca - a^3RT)P^3 \qquad (9)$$

A value of $a = -10^{-6}$ per atm. has been observed on a piston gage of 1000 atm. range, using a steel piston and thick walled, re-entrant brass cylinder. Nearly as large positive values have been observed with simple, nonre-entrant cylinders. For comparison, compressibility of mercury in an open column introduces a correction corresponding to $a = 2 \times 10^{-6}$ per atmosphere.

A value $a = 10^{-6}$ atm. would change the second virial coefficient for helium by about 0.2% at 300° K. and 0.6% at 800° K.

Mercury Column Calibration

The structure of some piston gages is such that direct measurement of area and computation of elastic distortion cannot be made with the requisite accuracy. Therefore, many experimenters have calibrated the piston gage in terms of a mercury column.

Mercury columns which are open to the atmosphere at the top have been used to measure pressures of a few hundred atmospheres. One in current use, described by Roebuck and others (*14–16*) is a multiple column usable up to 200 atm.

Several experimenters, including Keyes and Dewey (*9*), Michels (*12*), Meyers and Jessup (*11*), Bett, Hayes, and Newett (*4*), have used mercury columns in which pressure can be applied at both ends. These can be used in several ways. One requires a pair of piston gages one of which is balanced against the open mercury column. Without changing the pressure setting of the first piston gage, the pressure developed by the mercury column is added to it, and the second gage is balanced against the combination. Pressure of the mercury column is then added to that of the second gage, and the first gage balanced against the combination. This process can be continued to obtain a calibration of the piston gage in terms of the mercury column or until pressure limit of the apparatus is reached. The design limit of the column of Bett, Hayes, and Newett is 2500 atm.

Because these comparisons were tedious, another procedure was used by Michels (*12*). It requires a stable, reproducible reference pressure P (not known exactly), the mercury column, and the piston gage to be calibrated. The piston gage is balanced against the

Elastic Distortion Error in the Dead-Weight Piston Gage

Change of effective area as a function of pressure limits accuracy of a piston gage at pressures above a few thousand atmospheres and has a significant effect in precision work at a few hundred atmospheres.

If a piston gage is calibrated against a mercury column over a limited range at high pressure, absolute pressure of that calibration cannot be inferred without knowledge of elastic distortion in the piston gage.

For certain designs, effective area can be calculated from elastic theory without detailed knowledge of pressure distribution. This calculation is made for the piston of a controlled-clearance piston gage. Results are shown for a comparison between two piston gages, showing about 0.02% change in area for 300 atm. change of pressure.

D. P. JOHNSON, J. L. CROSS, J. D. HILL, and H. A. BOWMAN
National Bureau of Standards, Washington 25, D. C.

Reprinted from INDUSTRIAL AND ENGINEERING CHEMISTRY

Vol. 49, Page 2046, December 1957

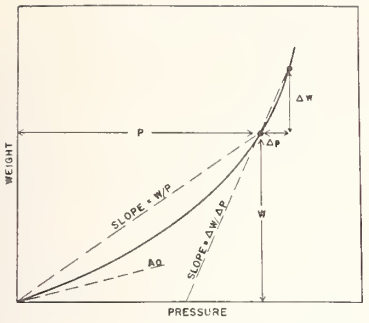

Figure 1. Relation between pressure and weight on the piston in a dead-weight piston gage

reference pressure and the load, W, noted. Pressure ΔP developed by the mercury column is then added to or subtracted from the reference pressure, and the piston gage balanced against the combination. The new load is $W + \Delta W$ and the ratio, $\Delta P/\Delta W$, is the gage constant which, if measured at a single high pressure, cannot be used to determine effective area or absolute pressure of the measurement. To see this, let the curve of Figure 1 be the relation between the weight on the piston and the pressure under it. Buoyancy and head-of-oil corrections are presumed applied correctly so that zero pressure corresponds to zero load. If area of the piston is independent of pressure, the relation of W and P is linear and has the slope A_o.

In general, the relation to the first approximation is the parabola obtained from Equation 3,

$$W = A_oP(1 + aP) \qquad (10)$$

where A_o is the slope of the curve at the origin. Effective area A_e is ratio W/P or the slope of a chord through the point (W, P) and the origin. The change in load for the increment of pressure (the reciprocal of the gage constant) defines the slope $\Delta W/\Delta P$ of the chord across the increment of the curve. If the increment is small, the slope is practically dW/dP, that of the curve at (W, P). By differentiation of Equation 10,

$$\frac{dW}{dP} = A_o(1 + 2aP) \qquad (11)$$

which is not the same as W/P.

To define effective area, comparison with the mercury column should be repeated at other pressures as widely scattered as is practicable. After a few such observations, the shape of the curve can be seen and a value for the effective area determined. The accuracy improves as more observations are made to fill in the gaps; eventually it becomes comparable with that of the full calibrations.

Michels used this method to calibrate a piston gage of 250 atm. range, with a 4.5-meter mercury column. Because of the limited range of the column used at this time (1924), accuracy of comparison with the piston gage, about 1 part in 2400, was not adequate to observe change in area of the gage with pressure. The agreement with subsequent measurements (*13*) reported in 1932 with an open 27.5-meter mercury column was within about 3 parts in 10,000.

Beattie and Edel (*3*) made similar measurements up to 541 atm., using an 8.1-meter mercury column between two piston gages. Within their accuracy, variation of area with pressure was negligible.

One significant correction in the mercury column calibrations is that for compressibility of mercury. Measurements on this quantity ultimately refer to absolute measurements on a solid, such as Bridgman's (*5*) determination for bulk compressibility of pure iron. Because bulk compressibility appears in the expression for area change of the piston, direct computation of such area change and calibration by a mercury column have at least this systematic error in common. Of course, many measurements on the piston gage are quite distinct from those on the mercury column; they have different systematic errors so that comparison between the piston gage and mercury column is a valuable check.

Elastic Deformation of Piston

Detailed calculation of elastic deformation of the piston and cylinder is a formidable problem. Solutions for elastic distortions have not been obtained for many shapes encountered in piston gages—e.g., distortion produced by a pressure gradient close to a change in diameter of a part. In a detailed analysis, it is necessary to consider simultaneously: relation between stresses and strains in the parts; effect of strains on clearance between piston and cylinder; effect of changes in clearance on pressure drop in the fluid, which determines stress distribution in the cylinder; and effect of pressure on properties of the fluid. At a pressure of 1000 atm., all these interactions are large. Deformation may exceed initial clearance, pressure drop at constant flow is inversely proportional to the cube of the clearance, and viscosity of some fluids in common use changes by a factor of 10 in 1000 atm.

Even rough estimates of variation in area with pressure are sometimes useful. For example, suppose a gage having a range of 50 atm. has a reproducibility at full load of 1 part in 10,000. Calculations show that the elastic distortion could not exceed $a = 10^{-6}$ per atm. under any reasonable distribution of pressure. The maximum change of area in a range of 50 atm. would not exceed 1 part in 20,000. There is little value in looking for such a change because it is less than the reproducibility of the gage.

For certain configurations of piston and cylinder, details of pressure distribution need not be known to calculate the effective area. Thus Bridgman (*6*) made the "assumption that the radial displacement at any point is proportional to the normal pressure at that point, and is the same as that in an infinite cylinder subjected to the same pressure over its entire length. This assumption is probably fairly close to the truth where the extent of the cylinder exposed to the pressure is long compared with the radius, and the pressure varies gradually from point to point." The effective area is the mean of the areas at the top and bottom.

The requirement of a "long" region of pressure gradient turns out to be unduly restrictive. An attempt at a detailed study of the pressure distribution led to the conclusion that most of the pressure drop in a high pressure gage occurs in a very short length, perhaps less than the diameter of the piston. Some unsuccessful attempts were made to achieve a design which would satisfy the requirement of a long region of pressure gradient. It was then necessary to accept the reality of a short region of pressure gradient, and to look for less restrictive conditions than those of Bridgman.

Design Considerations. Design of the controlled clearance piston gage incorporates two features which facilitate computation of effective area: First, by adjustment of the pressure, Pj, in the acket surrounding the cylinder, clearance between piston and cylinder can be reduced to a value comparable to the surface irregularities, at any pressure in the crevice. In work of high accuracy, leak rate is measured at various jacket pressures and extrapolated to zero leak rate (zero clearance). The computation of distortions need be made only for the piston since the cylinder is made to fit it. Second, the piston is simple in shape, being a long, solid cylinder ex-

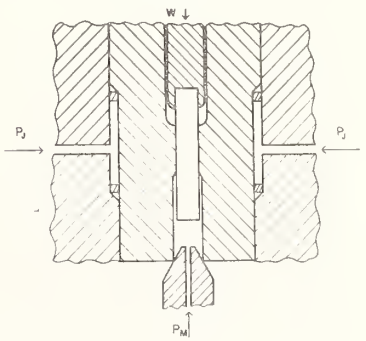

Controlled-clearance gage

tending out of the region of pressure gradient for at least one diameter in each direction.

Basic Assumptions. The following calculation of distortions for such a piston is based on a linear elastic theory with its consequences of symmetry, superposition, and reciprocity.

The problem of distortions in the neighborhood of a pressure step on a long, solid cylinder has been solved, at least for some materials (*7*). It is not necessary to go into the solution in detail, but only to make use of its symmetry, which does not depend on the material. In particular, anistropic materials are admitted. Such might be encountered if the piston were fabricated of hard-drawn rod or wire, or if it were case hardened so that the surface skin had different properties from the interior. The practical requirement that the piston reman round under load would eliminate more unsymmetrical materials, but it would permit such types as hexagonal crystals with the principal axis along the length of the piston. Figure 2,*A*, represents distortion of a long solid cylinder, produced by a unit pressure step, plotted as a function of the axial coordinate. The cylinder is subjected to unit pressure on the end faces, and on all the curved surface to the left of coordinate u. The function $F(z,u)$ represents half the fractional change in cross-sectional area at coordinate z produced by the distribution of unit pressure with a step at u. For $z \ll u$, $F(z,u)$ approaches the value $F(-\infty)$ which represents distortion if the whole cylinder were subjected to unit pressure. To the right for $z \gg u$, $F(z,u)$ approaches the value $F(+\infty)$ which represents the distortion if only the end faces of the cylinder were loaded. If A_o is the measured area under zero load, area $A'(z)$ at z under a unit pressure step at u is

$$A'(z) = A_o[1 + 2F(z, u)] \qquad (12)$$

This corresponds to the general description of strain by Love (*10*) where fractional change in diameter under a unit pressure step is $\frac{\Delta d}{d} = \sqrt{1 + 2F(z,u)} - 1$, or nearly $F(z,u)$ for small strains.

Similarly in Figure 2, B, $F(u,z)$ is half the fractional change in area at point u, caused by a unit pressure step at point z. Shape of the two curves is the same, but one is displaced axially with respect to the other.

Symmetry of the solution is such that the algebraic sum of the two distortions, $F(u,z)$ and $F(z,u)$, is equal to the sum of the distortions at the two asymptotes. That is,

$$F(u, z) + F(z, u) = F(+\infty) + F(-\infty) \qquad (13)$$

As expected from Saint-Venant's principle, decay rate for distortions on either side of a pressure step is so great that small changes in strains occur beyond a distance of one diameter. If a solid cylinder of infinite length were cut off at a distance of one diameter or more from the pressure step, distortion at the cut would change by not more than 1 or 2% of $F(+\infty)$ or $F(-\infty)$. At points removed from the cut by as much as one diameter, the change in distortions would be quite inappreciable. It follows that so far as distortions in the region of the pressure gradient are concerned, the piston of a controlled clearance gage behaves like an infinite solid cylinder.

In addition to the normal pressures, the piston is subject to shearing forces caused by motion of the viscous pressure fluid in the crevice. Axial flow of fluid and consequently the axial component of the shearing force, approaches zero as clearance is reduced to zero. Tangential forces which result from rotation of the piston might produce a change of area in an anisotropic material such as a rod drawn with a twist, but these forces and distortions reverse in sign if direction of rotation is reversed. Therefore, if significant they can be evaluated.

Calculation of Effective Area. It is now possible to show that effective area of the piston is equal to the mean of the areas it would have if subjected all over to the conditions of the two ends, provided that no part of the pressure gradient is close to the ends. "Close" means within a diameter.

At zero pressure, let the piston have a length b and a uniform cross-section area of measured value, A_o. In use, the bottom of the piston and the lower part of its length will be subjected to the pressure P_m to be measured. The axial stress, $Z_z = -P_m$ will be compressive over the whole length. For some distance at the top, the transverse compressive stress will be zero. In the middle portion of the piston, pressure in the crevice is uniform around the circumference and expressible as some undetermined function, $P(z)$, of distance z from the bottom of the piston. Whatever this distribution of pressure may be, it may be represented as the integral of a sequence of elementary pressure steps of magnitude $\frac{dP(z)}{dz}\,dz$ each taking place in an element of length dz, located at coordinate z. If superposition holds, the distortion at a point a distance u from the bottom can be represented as the sum, or integral, of the distortions produced by the several pressure steps. Then the area $A(u)$ at u will be given by

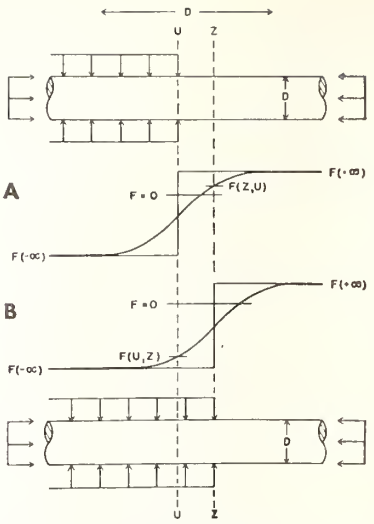

Figure 2. Elastic deformation of long cylinder under unit load on end faces and part of curved face. *A* and *B* are pressure steps at *u* and *z*, respectively. Axial coordinates in graphs are expanded as compared with diameters in load diagrams

$$A(u) = A_o\left[1 + \int_o^b 2F(u, z)\,\frac{dP(z)}{dz}\,dz\right] \qquad (14)$$

Now the piston can be regarded as a stack of elementary pistons of thickness du, and each sustaining a pressure difference $\frac{dP(u)}{du}\,du$. The weight, dW, which each elementary piston supports is $A(u)\,\frac{dP(u)}{du}\,du$, and the total weight W would be given by the integral

$$W = A_e P_m = \int_o^b A(u)\,\frac{dP(u)}{du}\,du \qquad (15)$$

Substituting from Equation 14 gives

$$A_e P_m = A_o \int_o^b \frac{dP(u)}{du}\,du + A_o \int_o^b \int_o^b 2F(u, z)\,\frac{dP(z)}{dz}\,\frac{dP(u)}{du}\,dz\,du \qquad (16)$$

The variables u and z are in fact different labels for the same coordinate, the quantities $P(z)$ and $P(u)$ are both representations of the same pressure distribution, and the operations are definite integrals taken between the same limits. Results of the double integration would be identical if labels u and z were interchanged, replacing $F(u,z)$ by $F(z,u)$, or $2F(u,z)$ by $F(u,z) + F(z,u)$, giving

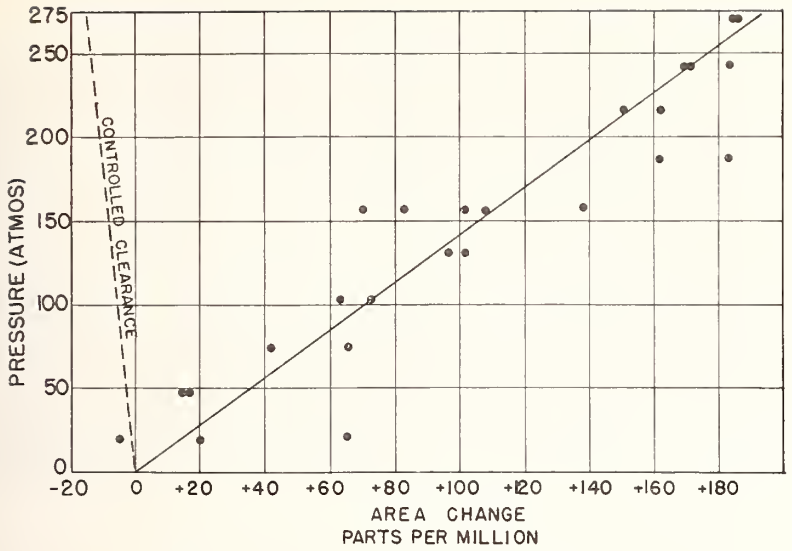

Figure 3. Change in effective area with pressure

● Working standard piston gage
– – – – Calculated for cantralled-clearance piston gage

$$A_e P_m = A_o \int_o^b \frac{dP}{du}\,du + A_o \int_o^b \int_o^b \times$$
$$[F(u, z) + F(z, u)] \frac{dP}{dz}\frac{dP}{du}\,dz\,du \quad (17)$$

At this point the symmetry condition of Equation 13 can be introduced. The two asymptotic values of the distortion are constant and can be taken out of the integrals. Now the integrations of the pressure gradients with respect to z and u are independent of each other and can be performed separately, so that

$$A_e P_m = A_o \int_o^b \frac{dP}{du}\,du + A_o[F(+\infty) +$$
$$F(-\infty)] \int_o^b \frac{dP}{dz}\,dz \int_o^b \frac{dP}{du}\,du \quad (18)$$

Since each integral is equal to the measured pressure, P_m, after integrating and factoring out one P_m,

$$A_e = A_o + A_o[F(+\infty) + F(-\infty)]P_m \quad (19)$$

But $A_o[1 + 2F(+\infty)P_m] = A(\text{top})$, the area which the piston would have if it were all subjected to the conditions at the top, and $A_o[1 + 2F(-\infty)P_m] = A(\text{bottom})$, the area under the conditions at the bottom. Comparing the mean of the two areas with Equation 19 shows that

$$\tfrac{1}{2}[A(\text{top}) + A(\text{bottom})] = A_o + A_o[F(+\infty) + F(-\infty)]P = A_e \quad (20)$$

which was to be proved.

The effective area is not equal to the mean of areas at the two end conditions of the piston if the region of pressure change is too close to one end. Thus, if the pressure change is concentrated at the extreme lower end of the piston, stress conditions of the top prevail over the entire length and the effective area equals that of the top. The case of a step function pressure change at a distance from the end (say the bottom) of 0.1 radius is considered by Tantor and Craggs (*17*). Under these conditions, the effective area is $A_e = 0.38\ A(\text{bottom}) + 0.62\ A(\text{top})$. These data show a rapid approach of the effective area to the mean of areas obtained under uniform stress corresponding to the end conditions.

There remains the problem of expressing distortion in terms of measurable elastic constants. Let rectangular coordinate axes be laid out so that z coordinate is along the axis of the piston, and x and y coordinates are normal to the axis. If e_{xx} and e_{yy} are strains in the two transverse directions, the fractional change in area will be

$$\frac{A_e - A_o}{A_o} = \tfrac{1}{2}(e_{xx} + e_{yy})\,\text{top} + \tfrac{1}{2}(e_{xx} + e_{yy})\,\text{bottom} \quad (21)$$

Using the notation of Love (*10*), these strains can be expressed in terms of stress components such as X_x thus:

$$e_{xx} = C_{11}X_x + C_{12}Y_y + C_{13}Z_z + C_{14}Y_z + C_{15}Z_x + C_{16}X_y \quad (22a)$$

$$e_{yy} = C_{21}X_x + C_{22}Y_y + C_{23}Z_z + C_{24}Y_z + C_{25}Z_x + C_{26}X_y \quad (22b)$$

At the top, under end load, $Z_z = -P_m$ and the other stress components are zero. At the bottom, under hydrostatic pressure, $X_x = Y_y = Z_z = -P_m$ and the other (shear) stress components are zero. Then

$$\frac{A_e}{A_o} = 1 - \frac{P_m}{2}(C_{11} + C_{12} + 2C_{13} + 2C_{23} + C_{21} + C_{22}) \quad (23)$$

This expression can be evaluated in terms of bulk modulus and Young's modulus. The volume compressibility under hydrostatic pressure is defined as

$$\frac{1}{V}\frac{dV}{dP} = \frac{1}{k} = C_{11} + C_{12} + C_{13} + C_{21} + C_{22} + C_{23} + C_{31} + C_{32} + C_{33} \quad (24)$$

and the axial linear compressibility (reciprocal of Young's modulus E_z) under end load is

$$\frac{1}{L}\frac{dL}{dP} = \frac{1}{E_z} = C_{33} \quad (25)$$

Comparison with Equation 23 shows that

$$\frac{A_e}{A_o} = 1 + \frac{P_m}{2}\left(\frac{1}{E_z} - \frac{1}{k}\right) \quad (26)$$

provided that $C_{13} = C_{31}$ and $C_{23} = C_{32}$, as is the case in any linear elastic theory. This result holds, regardless of the elastic asymmetry of the piston.

If the piston is isotropic and has Young's modulus E and Poisson's ratio σ, the bulk compressibility $1/k = \dfrac{3 - 6\sigma}{E}$ so that

$$\frac{A_e}{A_o} = 1 + \frac{P_m(3\sigma - 1)}{E} \quad (27)$$

For a steel, taking $E = 2 \times 10^6$ atm., $\sigma = 0.28$, $A_e = A_o(1 - 8P/10^8$ atm.). For a carboloy, taking $E = 6 \times 10^6$ atm., $\sigma = 0.22$, $A_e = A_o\ (1 - 5.7\ P/10^8$ atm.). If $\sigma = 1/3$ as is nearly the case for copper alloys, there is no change in effective area with pressure.

Nonlinear effects and other uncertainties. These are small but measurable deviations from linearity in the elastic behavior of materials which may be used in pistons. Nonlinearity disturbs the mathematical conveniences of symmetry, superposition, and reciprocity which must be replaced with more complicated relations. Lack of good data on effect of pressure on elastic moduli precludes anything better than a guess. If Bridgman's (*5*) data on iron is a reasonable guide, nonlinear effects would affect the area by 1 or 2 parts in 10,000 at 10,000 atm.

A more important uncertainty is that of the elastic moduli themselves. For example, variation in Young's modulus from one steel to another may be several per cent, and variations of the same order have been observed between samples cut from the same billet. If handbook values for the elastic constants are used, an uncertainty of several parts in 10,000 in the effective area may be expected at 10,000 atm. Uncertainty in the elastic modulus of a particular

specimen, measured on a conventional testing machine, is comparable.

Ultrasonic techniques of measuring elastic constants show promise. A precision of a fraction of a per cent is claimed for small specimens, and measurements can be made under pressure. Of particular value would be observations directly on the piston itself. Some difficulty may be encountered in measuring the elastic constants in the transverse direction. Cook (*7*) has outlined measurements necessary to determine the various elastic constants of an anisotropic material, and their variation with pressure.

Experimental Measurement of Change of Area

Piston gages by most domestic manufacturers have been calibrated at the National Bureau of Standards. If the instrument has a range of more than 150 atm. and is in good order, elastic distortion is observed.

The most extensive series of observations to date (Figure 3) were obtained from comparing two piston gages in use at the National Bureau of Standards. One is the Harwood controlled-clearance piston gage, 20,000 pounds per square inch, currently in use as a primary standard. The other is of common commercial design, 5000 pounds per square inch, with steel piston and a brass cylinder of the simple type. It had been in use for over 20 years as a working standard for calibrating piston gages.

The two gages were connected together, pressure was applied until both pistons floated, and the loads adjusted until there was no flow of fluid in the connecting line. Ratio of the two loads was then equal to the ratio of the two effective areas. The area of the controlled clearance piston gage had been measured directly. Its distortion, calculated in accordance with the theory described previously, is plotted as a dashed line. Effective area of the working standard, determined from the ratio of loads, is plotted as individual points.

Observations, taken on three different days, scatter about a straight line with a standard deviation of about 1 part in 45,000. This line represents an area change of a little more than 2 parts in 10,000 for a 300-atm. change of pressure ($a = +6.8 \times 10^{-7}$ per atm.). The change is within the range of pressure coefficients that can be expected from a gage having a steel piston and thick-walled brass cylinder. If the region of pressure gradient is well below the top of the cylinder, so that effective pressure in the crevice is half the pressure being measured, formulas developed by Johnson and Newhall (*8*) give $+5.2 \times 10^{-7}$ per atm. average change for piston and cylinder. If the pressure gradient is concentrated at the extreme top of the cylinder, the value might be as high as 11.2×10^{-7} per atm.

Parenthetically, effective area of the working standard agrees within 1 part in 10,000 with that obtained by Meyers and Jessup in 1939, using piston gages, described by them (*11*), for which this degree of accuracy was claimed. This agreement indicates that the working standard piston gage was more stable than those used by Beattie and Bridgman (*2*). Since it was several years old at the earlier comparison, it had had time to reach a stable condition.

Problems for Future Studies

In the foregoing discussion, little has been said about elastic distortion in the cylinder. In the controlled-clearance gage this may be justified on the basis that the characteristics of the cylinder presumably drop out when it is made to fit the piston. But most instruments do not include the controlled-clearance feature. Therefore, effect of the distortion of the cylinder should be studied, using configurations for which elastic-theory computations can be made.

Phenomena in the hydraulic fluid between the piston and cylinder should be studied. Details in variation of clearance and pressure drop along the length of the piston may be included, taking into account variation of viscosity with pressure. Although these details are not needed to calculate area of some pistons, they will help in understanding behavior of cylinders and other pistons. Certainly the static and dynamic effects of eccentricity between the piston and cylinder should be included.

Some effects should be mentioned which have caused trouble in determining effective area by comparison of piston gages. Although not necessarily related to elastic deformation, they may mask the phenomena under study. Most large errors in dead-weight piston gages have been traced to one or more of these effects.

Buoyancy. The weight of fluid displaced by submerged portions of the piston must be subtracted from the load. In some instruments, submerged volume changes from top to bottom of the stroke, enough to change pressure by 0.02 atm. Structure should be such that surface level of the fluid is nearly constant, and known at all times, so that the submerged volume can be calculated.

Corkscrewing. Occasionally direction of rotation will affect the pressure developed by the piston gage. This has been laid to helical tool marks on the piston, cylinder, or guide bearing. Observations should be taken at least occasionally, reversing the direction of rotation but changing nothing else.

Eccentric loading errors. If weights are stacked off center, the behavior may be erratic. Pressure may fluctuate in synchronism with rotation of piston, or its average value depend on speed but not direction of rotation. These troubles are worst in instruments where weights are stacked in a tall pile on top of the piston. A suspended, nonrotating load may oscillate abnormally when the piston is rotated or oscillated at a particular speed. The difficulties associated with eccentric loading may be more serious at certain speeds of rotation. These effects are entangled with the phenomena in the hydraulic fluid lubricating the piston.

Literature Cited

(1) Barton, M. V., *J. Appl. Mechanics* **8**, 3, A-97 (1941).
(2) Beattie, J. A., Bridgeman, O. C., *Ann. Physik* **12**, No. 5, 827 (1932).
(3) Beattie, J. A., Edel, W. L., *Ibid.*, **11**, No. 5, 633 (1931).
(4) Bett, K. E., Hayes, P. F., Newett, D. M., *Phil. Trans. Roy. Soc. London Ser.* A **247**, No. 923, 59–100 (1954).
(5) Bridgman, P. W., *Proc. Am. Acad. Arts Sci.* **58**, 166–242 (1923).
(6) *Ibid.*, **44**, 8, 200–17 (1909).
(7) Cook, R. K., *J. Acoustical Soc. Am.* **29**, 4, 445–9 (1957).
(8) Johnson, D. P., Newhall, D. H., *Trans. Am. Soc. Mech. Engrs.* **75**, 3, 301–10 (1953).
(9) Keyes, F. G., Dewey, J., *J. Optical Soc. Am.* **14**, 6, 491–504 (1927).
(10) Love, A. E. H., "Mathematical Theory of Elasticity," 4th ed., Articles 24, 66, Cambridge, Univ. Press, Cambridge, Eng., 1934.
(11) Meyers, C. H., Jessup, R. S., *Bur. Standards J. Research* **6**, 1061 (1931). RP324.
(12) Michels, A., *Ann. Physik* **73**, 7–8, 577–623 (1924).
(13) Michels, A., *Proc. Acad. Sci. Amsterdam* **35**, 6–10, 994–1003 (1932).
(14) Roebuck, J. R., Cram, W., *Rev. Sci. Instr.* **8**, 215 (1937).
(15) Roebuck, J. R., Ibser, H. W., *Ibid.*, **25**, 46–51 (1954).
(16) Roebuck, J. R., Miller, E. E., *Ibid.*, **10**, 179–80 (1939).
(17) Tantor, C. J., Craggs, J. W., *Phil. Mag. Ser.* 7, **38**, 214–25 (1947).

Received for review April 8, 1957
Accepted June 19, 1957

Division of Industrial and Engineering Chemistry, High Pressure Symposium, 131st Meeting, ACS, Miami, Fla., April 1957. Development of controlled-clearance piston gage supported in part by the Ordnance Corps, Watertown Arsenal, Contract No. TR3-3002.

Journal of Research of the National Bureau of Standards—C. Engineering and Instrumentation
Vol. 63C, No. 1, July–September 1959

A Tilting Air-Lubricated Piston Gage for Pressures Below One-Half Inch of Mercury [1]

U. O. Hutton

(May 8, 1959)

A description is given of a tilting dead-weight piston gage constructed at the National Bureau of Standards for ranges of differential pressure up to about 0.5 inch of mercury. A resolution of better than 1 part in a hundred thousand of full scale has been obtained by use of the toolmaker's sine bar method of angle measurement. The scale is a linear function of the sine. The instrument can be calibrated from basic measurements of length and weight, is rugged, and may be constructed in almost any laboratory mechanical shop. Sources of possible errors in reading are discussed in detail. Comparative tests with certain other gages or manometers are cited wherein linearity was found to be within 1 part in 10,000 and agreement within 2.5 parts in 10,000. The uses of the gage are briefly discussed.

1. Introduction

A need exists for pressure-measuring or controlling devices for ranges of low pressure, particularly the pressure range corresponding to atmospheric pressure at high altitudes. The need is more acute where measurement and control are both required. For the study of the pressure-deflection characteristics of diaphragms of high sensitivity, no device discussed in available literature [1] seemed conveniently applicable to the problem where constancy of pressure difference from a datum was desired for various lengths of time up to 24 hr. Conventional air-lubricated piston gages are nicely applicable to this problem approaching within about 0.4 in. of mercury of the datum pressure with a resolution of at least 1 part in 10,000. This report describes a piston gage to cover from about 0.5 in. of mercury to the datum pressure with a resolution of 1 part in 100,000 and means of pressure adjustment without resort to weight changing.

In exploring the characteristics of gages suitable for the contemplated tests, several air-lubricated piston gages were made from medical hypodermic syringes of 25- and 100-cm^3 capacity. These syringes had hollow pistons and could be employed to as low a pressure as 0.4 in. of mercury. Schemes for employing such gages with opposed pistons were abandoned because of the loss of resolution as the pressure difference set up by the pistons becomes small. In handling a well-lapped syringe it was observed that air lubrication for a low-density piston was surprisingly adequate even if the piston was not vertical. Brubach's experiments [2] encouraged an attempt to devise a piston gage, the incremental loading of which would be adjusted by changing the angle of tilt instead of the weights as on the conventional dead-weight testers. Distinct advantages of this design are that it reaches high resolution without resort to delicate structures and requires neither optical nor electrical amplification. The extended scale available is gained through the use of a micrometer and end gage block.

2. Description of Piston Gages

In development, two models were constructed that will be referred to as Models I and II. Model II incorporates all the features of Model I so that a discussion of Model I is possibly not of great value; however, its simplicity of construction and the high sensitivity and resolution attained may make it applicable in some cases where the additional complexity of Model II is not warranted. The first model is of such simplicity that it may be constructed and a basic calibration made in a short time in almost any laboratory. The principles of the gage are so elementary that adherence to the details being described is not suggested as being necessary. Dimensions and other specific details as used are included for guidance in understanding the structures on which performance data is presented.

2.1. Description of Gage, Model I

For the piston-cylinder combination, four 100-cm^3 syringes were obtained. Two of these were found to be sufficiently tight for adaptation. They were put through a hand-lapping operation where lapping powder, Linde A (½ μ), was used in a creamy water suspension. From ½ to 2 hr lapping was employed using a combination of rotary and longitudinal motion with the addition of water or lapping compound as required. The lapping operation was considered complete when a piston, washed and dried, would just fall of its own weight in its cylinder oriented in a vertical position with the piston at any radial angle. It does not seem possible to overlap such a combination with this size of lapping particle using water as a lubricant because of the hydrodynamic lubrication furnished by the lapping motion; however, it was always possible to remove the high areas on the

[1] The major part of this work was sponsored by the Flight Control Laboratory, Wright Air Development Center, Wright-Patterson Air Force Base, Ohio.

piston and cylinder so that the freedom-of-fall condition described was obtained. The tighter areas may be recognized while lapping by the degree of dispersion of the lapping compound and after drying by the higher grade finish on the closer surfaces. Extra attention may be given the high areas by localized finger pressure on the cylinder and by choice of the piston orbit to bring them into frequent play. In some of the better lapped areas, white light interference fringes have been visible but this is not necessary for proper performance.

After lapping, the cylinder and piston were cut with a diamond saw as shown in figure 1, then mounted on a sine bar, shown in figure 2 to form a piston gage. The piston is weighted as desired and floats without rotation in the cylinder on an air film as a bob. The cylinder is supported on another portion of the original hypodermic piston employed as an air-lubricated pinion bearing. The micrometer anvil and sine pivot are at such a relative height that the piston is horizontal when the micrometer is fully retracted.

The cylinder must be rotated to keep the piston free. It was originally rotated by an air jet directed against the teeth of a 4-in. diam spur gear concentrically mounted on the cylinder, but later by a 25-w, 2,700-rpm shaded-pole induction motor operated at ⅓ voltage with a rubber band (No. 32) as a belt over the motor shaft and around the cylinder. A slight finger spin is sometimes required for starting, and under the light load conditions prevailing, the rubber band, as a belt, lasts several weeks and vibration or temperature transmissions from motor to cylinder are negligible.

The piston is eccentrically loaded to prevent its rotation as shown in figure 2. One inch of vertical travel of the micrometer corresponds to 40 revolutions of the micrometer screw. The length of the scale on the barrel of the micrometer is 1.5 in., which gives a total scale length for 40 revolutions of 60 in., with a readability of 0.005-in., corresponding to 1 in 10,000.

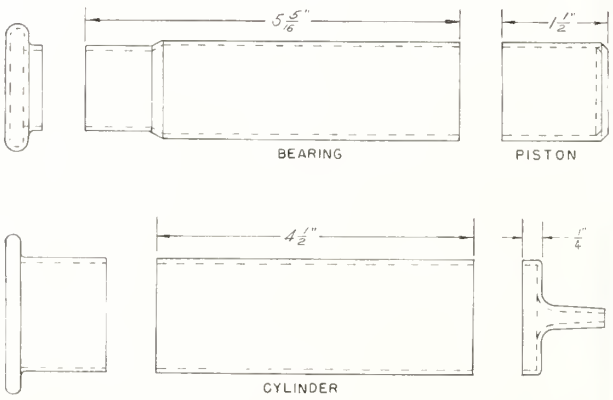

FIGURE 1. *Sawing of hypodermic syringe to obtain parts for piston gage.*

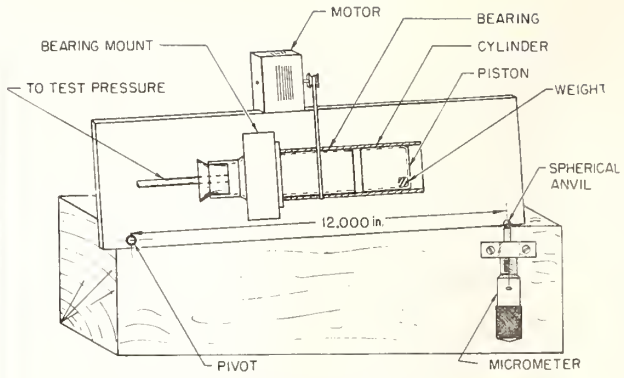

FIGURE 2. *Tilting piston gage, Model I.*

2.2. Description of Gage, Model II

As a result of the experience with Model I, a second gage, Model II, was built. The design was changed so that the tilt can be measured over a 90-deg angle from the horizontal by means of gage end-blocks and 1-in. micrometer caliper. The cylinder on this model was made from 1.250-in. diam precision-bore glass tube. The piston and bearing were prepared, by lapping, from ordinary Pyrex tubing in an attempt to avoid the slight taper that is present in a hypodermic syringe. See figures 3, 4, 5. Instead of the wood base of the original model, a 2×6×12-in. surface plate was used as a base. This provides a satisfactory surface on which to wring the gage blocks used to establish the altitude of the triangle (this being the measure of the tilt). The pivots for the piston support bar and for the micrometer mount are hardened steel cones and spaced 10.000 ±0.002 in. apart.

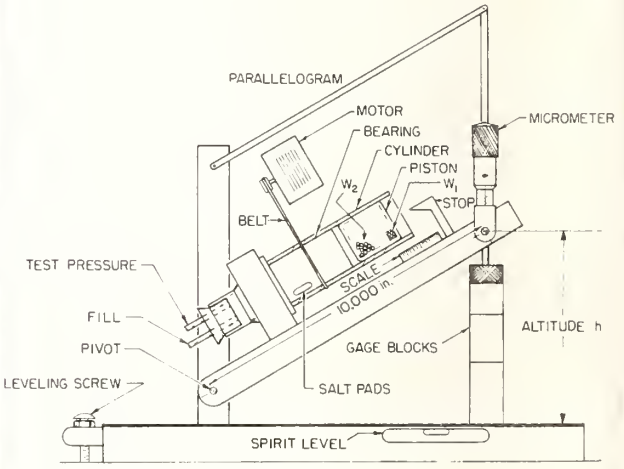

FIGURE 3. *Tilting piston gage, Model II.*

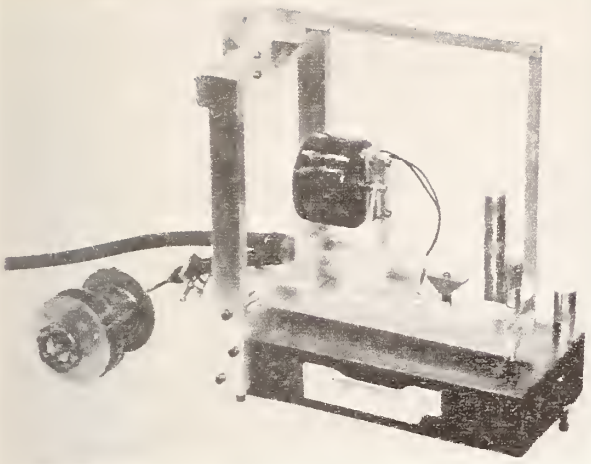

FIGURE 4. *Tilting piston gage, Model II, in zero position.*

The micrometer support mount is positioned by a parallelogram structure so that the micrometer axis is maintained perpendicular to the surface of the base plate. The pressure connection is made through the pivot bearing as shown. A stop is provided to prevent the piston being blown out, and for convenience in observing that the level of the base plate is unaltered, a sensitive spirit level is provided. A small fan motor with a rubber belt provides the rotational movement of the cylinder. The piston is closed with an inside fitted cap and a fixed cast lead weight, W_1, is used and is advantageously located at the upper end of the piston so that its vertical component will be as nearly as possible through the center of the piston supporting area with a tilt of 3–4 in. In addition to the main weight, W_1, the piston is loaded with an auxiliary weight, W_2, composed of lead shot or other such movable weights, the purpose of which will be discussed in section 5.5.

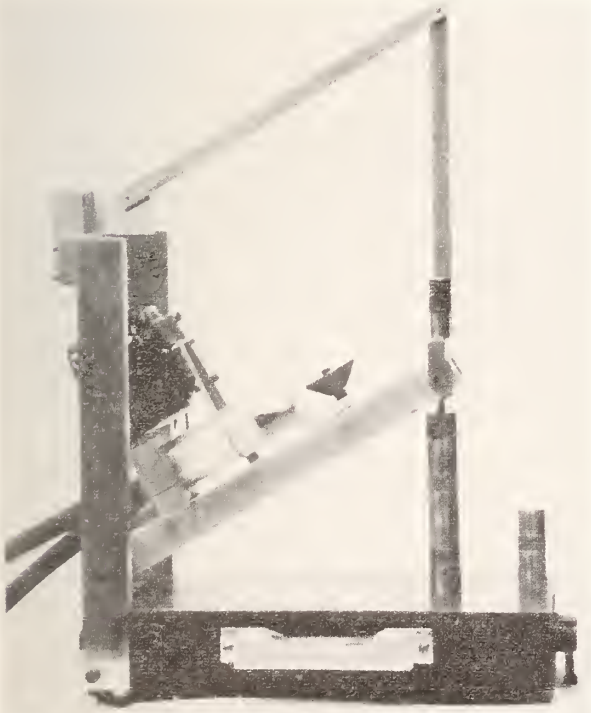

FIGURE 5. *Tilting piston gage, Model II, in tilted position.*

A change in altitude, h of 1 in. is provided by each 1-in. end-block placed under the micrometer and each 1-in. block is equivalent to 10 percent of the piston weight which is carried by the air pocketed under the piston. The pressure developed by the piston in this pocket is in direct proportion to altitude, h. Altitudes up to 8 in. have been employed. For altitudes from 8 to 10 in. the eccentric position of the weights will not always overcome the cylinder drag and prevent rotation.

The scale length of this model using the combination of the micrometer and end blocks is effectively eight times the scale length of Model I, and thus is readable to 1 part in 80,000. Some experiments have been made with a 6-in. diam reading dial such as used on the more precise micrometers. This provides a scale length of 6,000 in. readable to 1/32 of an inch and a zero stability of the same order as the resolution.

Two pressure connections to the lower surface of the piston are provided, one for connection to the chamber or space in which the pressure is to be measured and the other, marked "Fill" in figure 3, to replenish air lost by leakage. A controllable volume shown in figure 4 is connected to the "Fill" opening. The function of the salt pad is discussed in section 5.4.

3. Calibration

The pressure difference p between the two end surfaces of the piston is determined by the relation

$$p=\frac{mg}{a}\sin A=\frac{mgh}{ad}$$

where m is the mass of the weight; g, the acceleration of gravity; h, the altitude of the triangle (fig. 3); a, the effective cross-sectional error of the piston; d, the distance between the pivots of the sine bar and calipers (fig. 3); A, the angle of elevation of the sine bar.

It is seen that mg/ad is a constant for any one design, weight of piston and at any one location. When these constants are known, it is only necessary to measure h to determine the pressure. If the weight mg is in grams and the other quantities in centimeters, p is in units of grams per square centimeter; similarly if mg is in pounds and the other quantities in inches, p is in units of pounds per square inch.

The piston weight is readily determined, if desired, to 1 part in 100,000.

In the investigation, relative readings of high precision and reproducibility were desired, but the basic calibration was of lesser concern. Consequently, the precise determination of effective area was not attempted. The effective area has been assumed to be the mean of the cylinder and the piston areas. The diameter of the piston was measured to approximately 1 part in 10,000 by means of a micrometer caliper. The cylinder diameter which is difficult to measure accurately with mechanics' micrometers had an accuracy of about 1 part in 4,000. Thus the effective area was probably known to an accuracy of about 1 part in 2,000. Higher precision in this determination would require not only more precise measurement but a combination of piston and cylinder without measurable taper or dimensional irregularities. Meyers and Jessup [4] (as well as later workers) suggest effective diameter determination by manometric methods, and with a suitable manometer available this method would be perferred to clearance measurements. Where a basic gage calibration is required, effective area determination to 1 part in 25,000 for a 1-inch piston should not be too difficult.

There is also some change in area possible, due to internal pressure in the cylinder. Correction for this error may be made from empirical data. And, finally, the effective area may be slightly influenced by the change in the eccentricity of the piston for different angles of tilt. No error from this source has been separated, but some allowance for such an error is indicated in the later tabulation. No dimensional changes have as yet (after 1 year) been recognizable due to either wear or secular changes.

The vertical component of the piston weight is proportional to the sine of the angle of tilt which requires a knowledge of both the altitude and hypotenuse of the triangle (see fig. 3). The leg or altitude of the triangle, measured by the micrometer and gage blocks, can be measured to an accuracy of 0.00005 in. For equal absolute accuracy in the value of the sine of the angle, the hypotenuse must be known to the same accuracy as the altitude.

4. Performance

The base of the instrument must be maintained level. Since the resolution is equivalent to the sine of an angle of 2 sec of arc, the axis of the base should be maintained to within at least 1 sec of the horizontal. For highest accuracy, the gage needs to be leveled on a rigid table in a room free from excessive drafts and where the temperature uniformity is such that a thermal expansion error of significance will not exist in either the altitude or area measurements.

The first step is to zero the gage. This is the condition where the pressure connection is open to the room, and the piston in the rotating cylinder is at an equilibrium position touching neither end-stop. Under this condition the axis of the piston is, of course, horizontal. The gage is then connected, to the test pressure, using an independent connection to some type of reservoir to introduce or release air for the repositioning of the piston when desired. When it is desired to provide a definite pressure to a gage to be calibrated, set the altitude h with the micrometer or with micrometer and end-gage blocks to give the pressure desired. This pressure will be maintained at the test connection so long as the piston floats without touching either end-stop. If an unknown pressure is to be determined, connect the apparatus in the same manner but set h, step by step, until all axial motion of the piston is canceled. This can ordinarily be accomplished in less than a minute.

Tests of various sorts have been improvised to determine the performance of this type of piston gage. Certain tests were performed on Model I and not repeated on Model II. Also, some tests were devised after Model II was in operation and were not performed on the earlier model. Test results are included irrespective of their being obtained on the earlier or on the more advanced model where they seemed to provide pertinent information on the gage performance.

The readings of the piston gages were compared with those of several sensitive pressure-measuring instruments in order to obtain information on its performance characteristics. These were: (a) An Ascot-Casella micromanometer [3]; (b) a vertical air-lubricated piston gage adapted from a 100-cm^3 hypodermic syringe; and (c) a sensitive 2-in. mercury manometer having a null indicator based upon a capacitance bridge [5]. The Ascot-Casella instrument has a torsion balance to measure the difference in the product of the pressure and area of two bells floating on kerosene.

4.1. Zero Stability

Particular attention was given to a study of the repeatability of the gage zero since full advantage of the gage resolution is available here, whereas under the loaded condition stability can be determined only to the degree that the load may be held constant. The zero, as referred to, is determined under the condition of both ends of the piston exposed to atmospheric pressure. The altitude h is adjusted by means of the micrometer until the piston floats without axial drift. The repeatability of the zero, determined after altering the former setting by varied amounts, with either intermittent or continuous rotation, has been found to be in the same order as the resolution of the micrometer reading. Six consecutive hourly readings showed variations of $+0.0002$ to -0.0001 in. in altitude. Daily readings with no rotation of the cylinder during the night have repeated within the same limits for at least 5 days. The influence of other factors on the zero were studied and the results of the tests may be summarized as follows:

(a) There was no visible change in zero with an ambient temperature change of 5° C.

(b) A change in the axial position of the piston of ⅛ in. each side of the initial balance point caused a total zero variation of 0.0002 in.

(c) A doubling of the cylinder rotational speed was observed to affect the zero by 0.0002 in.

(d) The piston weight was increased 5-fold without observable change in the zero.

(e) A piston with an end load of 500 g was reversed so that the load was positioned first in an outboard position, then inboard position. The average readings, in each position, were identical with a variation in individual readings of only 0.0002 in.

Some later tests were made with a 6-in. dial on the micrometer. Altitude resolution with this micrometer was 0.00005 in. and zero repeatability in tests over several days was to the same limit. With a 30-g piston weight this corresponds approximately to a pressure of 4×10^{-7} in. of mercury.

4.2. Comparison Tests, Pressure Controlled by Tilting Piston Gage

The first experiments to determine the stability of the reading when the pressure was controlled by maintaining a constant tilt of the piston gage were made with the Ascot-Casella micromanometer as a reference standard. Readings were made on the micromanometer for a period of 20 min while a constant altitude, or tilt, was maintained on the piston gage during which the axial position of the piston varied ¼ in. The micromanometer indications varied approximately 0.2 scale divisions with a full-scale reading of 250 scale divisions. This indicated a repeatability of about one part in 1,000 at a pressure corresponding to about 1 percent of full scale on the piston gage.

Additional comparisons were made in the above pressure range using a hook gage with a resolution of about 0.001 in. of water as the reference standard. The repeatability in readings of the piston gage was about the same as with the Ascot-Casella micromanometer. The stability and reproducibility of the zero position of the tilt gage was considerably better than the readings as obtained with either the Ascot-Casella or hook gage. For this reason it was believed a more reliable reference should be used and subsequent comparison tests were made with the 2-in. mercury manometer or the vertical air-lubricated gage.

Comparison tests were made at three pressure ranges obtained by varying the weight of the piston. For each piston weight the tilt, or altitude, of the piston gage was varied. In all of these tests the tilting piston gage is acting as a pressure regulator. The pressure readings were made on the reference instrument, in this case the 2-in. mercury manometer.

The results of the low-pressure range comparison are given in table 1. The check readings were made 5 min after the first reading. The resolution of the 2-in. manometer is about 0.00005 in. of mercury. It will be seen that the increments for successive increases of 0.2 in. in altitude decrease somewhat as the altitude increases; this increase in sensitivity is not considered significant since the total variation is within the resolution of the 2-in. manometer.

The results of the comparison at an intermediate pressure range are shown in table 2. The test was again made on Model I piston gage but with a greater load on the piston. The pressure given in column 2 of table 2 was calculated from the constants of the piston gage and the altitude following the procedure outlined in section 3. The difference in the pressures calculated for the piston gage and determined from readings on the 2-in. manometer are given in column 4. The difference amounts to about 1 part in 2,000 of the pressure and is compatible with the resolution of the 2-in. manometer and the uncertainty in the determination of the effective area of the piston.

TABLE 1. *Low-pressure range comparison* [a] *tilting piston gage Model I and 2-in. manometer*

Tilting gage	2-in. manometer		Increments
Altitude in.	*Reading in.* Hg	*Average*	*For 0.2 in.*
0.2000	0.00160		
.2000	.00161	0.00160	0.00160
.4000	.00320		
.4000	.00320	.00320	.00160
.6000	.00479		
.6000	.00476	.00478	.00158
.8000	.00633		
.8000	.00635	.00634	.00156

[a] The reference pressure is 1 atm.

TABLE 2. *Intermediate pressure range comparison* [a] *tilting piston gage Model I and 2-in. manometer*

Tilting gage		2-in. manometer	Difference
Altitude in.	*Pressure in.* Hg *calc.*	*Pressure in.* Hg	*Inches* Hg
1.0000	0.03741	0.03745	0.00004
3.0000	.11223	.11227	.00004
5.0000	.18705	.18709	.00004
7.0000	.26187	.26197	.00010
9.0000	.33669	.33684	.00015

[a] The reference pressure is 1 atm.

The results of the comparison at the highest pressures thus far employed are shown in table 3. The test was made on Model II piston gage. Again the pressures calculated from the piston gage altitude and constants are compared with the pressures derived from readings made on the 2-in. manometer. Here the pressures agree within about 3 parts in 10,000, an amount far less than the expected uncertainty in determining the effective area of the piston. The linearity, which is independent of the piston area, is within about 1 part in 10,000.

TABLE 3. *High pressure range comparison* [a] *tilting gage Model II and 2-in. manometer*

Tilting gage		2-in. manometer	Difference
Altitude in.	*Peading in* Hg *calc.*	*In.* Hg	*In.* Hg
0	0	0	0
4.0000	.28700	.28706	.00006
7.0000	.50225	.50242	.00017

[a] The reference pressure is 1 atm.

4.3. Comparison Tests, Pressure Controlled by an Auxiliary Instrument

The experimental model of a vertical piston gage was employed at the lowest pressure of its range in a test where the pressure in the system was set and controlled by the vertical piston gage. The altitude of the tilting piston gage, adjusted to bring both pistons to an approximately steady axial position was read at intervals of time. The same point was observed over several hours and repeated the following morning. The results are shown in table 4.

TABLE 4. *Comparison of tilting air-lubricated* [a] *piston gauge with a vertical air-lubricated piston gauge*

Elapsed time	Tilting gage		Vertical piston gage
hr	*Altitude in.*	*Pressure in. Hg calc.*	*Pressure in. Hg*
0	8.6535		0.32321
½	8.6535		.32321
4	8.6545		.32321
24	8.6537		.32321
Average	8.6538	0.32313	0.32321

[a] The reference pressure is 1 atm.

The maximum departure in the altitude reading of the tilting piston gage from the average was 0.0007 in. or less than 1 part in 10,000. The difference between calculated pressures as determined by the two gages is on the average 0.00008 in. of mercury or 3 parts in 10,000. Again this is less than the expected error in the determinations of the effective areas of the pistons.

This test demonstrated also the ease of balancing the pressures in the two gages by the adjustment of the tilt altitude with the micrometer. The initial balance would be obtained within 4 min and, after an altitude change of smaller magnitude, balance could be restored in less than one minute. With careful attention and with optical magnification of piston drift a balance can often be effected in one quarter of this time.

None of these comparative tests provided data that shows reproducibility of the reading deflection to the precision anticipated from the performance of the instrument at zero. Although the 24-hr test interval in table 4 showed only a change of two parts in 80,000, one intermediate reading in the series showed a departure of five times this. An imperfect regulation of the test pressure could be the cause for such variations. In another test Model I tilting gage set at two arbitrary heights, was used as a pressure regulator and Model II was repeatedly adjusted to this pressure. The data are given in table 5. Here the reproducibility of the setting is 1 part in 25,000.

TABLE 5. *Repeatability test on Model II, Model I performing as a regulator* [a]

Elapsed time	Model I	Model II
Minutes	*Altitude in.*	*Altitude in.*
0	0.900	0.6038
40	.900	.6038
125	.900	.6038
0	4.0	2.5587
5	4.0	2.5588
10	4.0	2.5587
15	4.0	2.5587
30	4.0	2.5588
55	4.0	2.5588

[a] The reference pressure is 1 atm.

4.4. Off-Center Loading of the Piston

The effect on the pressure generated by the tilting piston by off-center piston loading was investigated. The center of gravity of the piston for small angles of tilt may be readily positioned over the approximate center of the load supporting area. However, wide variations are desired in tilt, say up to 75° or 80° from the horizontal, in which case the center of gravity of the piston may not even lie directly above any portion of the bearing support area. To test for this effect the piston was end loaded with lead weights and the tilting piston gage connected to the 2-in. mercury manometer. The altitude of the tilting piston gage was set to 7 in., producing a pressure of approximately 0.225 in. of Hg. The difference in height of the two mercury columns of the manometer was observed, first with the piston inserted into the tilting gage with the piston weight at the elevated end, and then with the piston reversed end-for-end. This procedure was repeated several times.

The difference in the readings of the mercury manometer, for the orientations of the weighted piston in the tilting piston gage, corresponded to 0.000125 in. in altitude in the 7-in. deflection. This is less than 1 part in 50,000 and is about equivalent to the least reading of the null indicator of the mercury column.

5. Other Factors Affecting the Performance

A number of factors are considered which may affect the satisfactory operation of the piston gage and in some measure may contribute to errors in pressure readings.

5.1. Maintenance

The maintenance to keep this gage in excellent calibration and operating condition has been of very minor character. The maintenance so far required has been an occasional cleaning of the piston and cylinder. Cleaning has usually been at intervals of at least 1 month. As there is no wear on the gage itself in use, the precision parts should be expected to have a long life.

5.2. Temperature

The most significant error believed present is that due to the change in effective area of the piston through the thermal expansion of the materials of

which they are made. For Pyrex glass the thermal expansion affects the area less than one part in 100,000/°C, for which an approximate correction is readily applied if necessary. If wide temperature variations are anticipated and the highest accuracy is required, the material in the sine bar configuration should, of course, have the same temperature coefficient as the gage blocks.

5.3. Low-Pressure Limits of Operation

Only exploratory tests have been conducted at reduced absolute pressures. In these tests the entire piston gage was placed in a pressure chamber and usually the piston gage has been at its zero position.

While the results of these tests indicate the possibility of operation of the piston gage at lower absolute pressures than anticipated, greater difficulty has been experienced in the dissipation of electrical charges on the piston. The use of the salt pad to control the humidity was ineffective. A conductive piston and cylinder might be a solution to this problem but fabrication of these elements was not undertaken. In lieu of conducting materials several "antistatic" agents have been employed. For example a very thin film of sulfuric acid on the glass surface has given completely satisfactory operation to a pressure of a few mm of mercury for at least an hour. Also, but with an accumulating electrical charge, the piston gage has operated at zero position for several hours at an absolute pressure of below 0.01 mm of Hg and at 0.0025 mm of Hg for more than an hour. Remarkably there was no indication or suggestion of "lubrication" failure.

The axial motion of the piston at very low pressure becomes very sluggish. The rotational drag on the piston produced by the rotating cylinder first decreases as the pressure is lowered, reaching a minimum at about 2 mm of Hg, then as the pressure is lowered further there is a rapid increase in the drag which remains about constant to the lowest pressures reached. A "coefficient of friction" calculated for this lowest pressure was 0.4 as compared to a value of only 0.025 at the 2 mm abs pressure and 0.1 at atmospheric pressure.

At low pressures the static and kinetic friction appear to be about equal, differing from the case at atmospheric pressure where it is sometimes necessary to start the motor repeatedly to secure cylinder rotation without spinning the piston.

The piston had been in use for many hours, thus wearing off the high spots, before the low-pressure tests were made, and the continued smooth operation at low pressure was only obtained when the film of sulfuric acid was present. Without the acid film it was not ordinarily possible to keep the piston in a floating condition at pressures below 1 mm of Hg. This beneficial behavior of the acid film may be due to its action as a lubricant or to its power to reduce formation of electrical charges or both. The effect of electrical charges on the axial control of the clean piston was estimated to be as much as 20,000 times greater than the effect when the glass surfaces were acid treated.

The air lubrication of the close-fitting bearings of the piston gage particularly at low pressures, warrants further discussion. The horizontal air piston may be regarded as a journal bearing to which the classical hydrodynamical theory of lubrication applies. Computations based on Sommerfeld equations as given by Hersey [6] indicate the load bearing capacity to be at least 10 g/cm^2, more than adequate and the calculated coefficient of friction is a few percent, which is in reasonable agreement with experience.

However, a number of the factors involved in the operation of this instrument are not so easily treated by theory. The Sommerfeld equations assume that the bearing fluid is incompressible and Newtonian, with a definite viscosity. At atmospheric pressure, with a bearing load of the order of 5 g/cm^2 the assumptions of incompressibility would be expected to apply fairly well. At reduced pressures, however, the compressibility of the gas becomes important. To support the bearing load the pressure below the piston must exceed that above the piston by some 3 to 5 mm of Hg. At 1 mm of Hg ambient pressure the gas must, in the crevice below the piston, be compressed by several times and the Sommerfeld theory would be expected to break down. Also when the mean-free path of the gas becomes comparable to the clearance the phenomenon of slip would become important. This will also occur at ambient pressures of the order of a millimeter of Hg. Down to these pressures there is only a slight variation of viscosity with pressure and so there should be very little difference in the coefficient of friction from this source.

At the very low ambient pressures of a few microns of Hg the ratio of load pressure to ambient pressure and also the ratio of mean free path to clearance are of the order of 100 or a thousand to 1 and the classical lubrication theory would not be expected to apply. An attempt was made to setup the theory of lubrication for the case in which the mean-free path was very large in comparison with the clearance. This bogged down because of the geometrical complexity but it was possible to see resemblances to the classical theory.

The direction of eccentricity makes an angle with the direction of the load which is on the order of 90 deg. The rotation of the cylinder sets up a drift which forces gas into the converging wedge, building up a pressure which will support the load. In the classical theory the gas escapes from the wedge by the viscous flow, in the molecular case the escape is by diffusion. Qualitatively the two cases are similar, but with a different dependance on the local clearance. It appears that at least part of the load can be supported by hydrodynamic lubrication even in the range of molecular flow.

Another mechanism might be expected at the lowest pressures. The treatment with sulphuric acid probably leaves the glass with a large content of water which might out-gas for a long time when

first evacuated. Also the surface of the glass may be somewhat more slippery than when it is quite clean.

The preliminary considerations of theory are quite obviously raising more questions than can now be answered and it is clear that there is room for more study.

5.4. Force From Static Charges

In the earlier use of the gage a sluggishness in the response of the piston was occasionally observed. This was connected with the phenomenon reported by Brubach [2] who states "Some of the syringes had a tendency to center themselves, that is, when the plunger was stabilized at a given point and then pushed in or out of the barrel, the plunger would return approximately to the original point of stabilization." It was suggested in his paper that this action is a function of the asymmetry of the cylinder or piston. However, this phenomenon was believed due to the accumulation of static charges on the piston and was soon connected with changes in the room humidity. The sluggishness was usually present when the relative humidity was lower than 50 to 55 percent and always absent at higher humidities. A simple method of elimination of this trouble was through humidity control. This was readily accomplished by inserting in the hollow bearing of the tilting gage a small blotting paper disk soaked in saturated sodium chloride. This maintained the required humidity for several weeks without rewetting. Since the remedy for this trouble was so simple an exhaustive study of the phenomenon was not made.

The entire force from the electrical charges on the piston when at rest axially, seemed radial and no error in the controlled pressure was observed. When piston motion is required to counterbalance any volume change, the restraining force may, for a few seconds, be a substantial proportion of the piston weight but entirely disappears in 20 to 30 sec if a new position is established. In effect it is as though a considerable amount has been added to the inertia of the piston but nothing to its weight. The piston behaves as though it had a frictionless spring control on its axis with the spring support attached to a frictionless dashpot.

5.5. Piston Oscillations

Usually the piston operates with a slight rotational oscillation of several degrees; sometimes the oscillation is entirely absent, but at other times, with some condition critical, such as tilt, piston weight, or rotational speed, the oscillation of the piston increases in amplitude until the piston weight carries over the top. When this occurs the piston continues to rotate at the speed of the cylinder and the gage is inoperable. In the search for some history of this phenomenon a letter of Professor Ott, Ohio State University [7], relative to the failure of the Hackensack bascule bridge which he likened to "a pendulum suspended from a rotating shaft" was unearthed as describing a similar situation. In his discussions, Professor Ott states "for low speeds the friction decreases rapidly with speed, and the relative motion being greater during the back than during the forward stroke, the angular momentum imparted during the forward stroke would be more than that taken away during the back stroke" and consequently the amplitude of the oscillation increases. This analysis was applied to an oil-lubricated bearing in the reference but would appear to similarly explain the encountered oscillation on this air-lubricated device.

It was found that internal damping in the piston could be used to control the oscillation over a wide range, so instead of using only the eccentrically positioned cast lead weight, loose lead "bird shot" were added to approximately 25 percent of the total piston weight. The movement of the shot on small oscillations is sufficient to damp out any progressive increase in their amplitude.

These oscillations limit the highest pressure that can be reached with the tilting gage. With Model II about 0.5 in. of Hg can be developed at a tilt angle of about 60° at 400 rpm of the cylinder with maintenance of good piston stability. Higher pressures should be possible with closer fitting and greater precision in the cylinder surfaces. A recent loading with tungsten carbide granules instead of lead has allowed an angle of tilt of 80° because of higher damping and a lower center of gravity due to the higher density of the material.

5.6. Centrifugal Force

As the cylinder rotates some rotational spin is imparted to the air in the cylinder. This spinning force increases with increase in the rotational speed of the cylinder or with increase, longitudinally, in the distance between the piston and the bearing which would expose more of the cylinder area to the enclosed air. The effect of this centrifugal force was investigated by increasing the space between the piston and the bearing from $\frac{1}{16}$ in. to $\frac{5}{16}$ in., reading any change in altitude with the micrometer. The altitude change was +0.0001 in., which is the least reading of the micrometer. As an additional check the rotational speed of the cylinder was advanced from 200 rpm to 600 rpm. The reading of altitude at the higher speed was within 0.0001 in. of the lower. It was concluded from these tests that any pressure developed by this centrifugal force under normal conditions of operation was without significant effect.

5.7. Pressure Variations Due to Dynamic Sources

The piston gage itself is not sensitive to high-frequency fluctuations in pressure but under certain circumstances the fluctuations created by the piston gage may objectionably affect the connected apparatus. These fluctuations can arise from three sources; first, seismic motions, horizontal or vertical; second, any axial component of symmetrical character imparted by the cylinder rotation; and third, from the mechanism used to make up losses in the

enclosed volume. Such an effect in the order of 2×10^{-5} in. of Hg has been found when following the deflections of a sensitive diaphragm with light fringes. Effects exceeding one light fringe have been observed. These fluctuations have been satisfactorily controlled by connecting the gage to the diaphragm with some damping interposed such as small bore tubing.

5.8. Leakage

Leakage from the enclosed volume back of the piston may take place past the piston and the bearing since both are air-lubricated. The test made on Model I with a very low rotational speed while in a vertical position showed a leakage of air of 0.5 cm³/min at a differential pressure of 0.3 in. of Hg. The leak decreases to zero, of course, when the piston gage axis is horizontal. This leakage is usually obscured by the pumping which occurs.

5.9. Pumping

The volume enclosed by the piston is subject to change due to pumping through the air bearings while the cylinder is rotating and may be either into or from the atmosphere. Usually the rate of volume change exceeds the rate of leakage. In the applications for which this gage is being developed the actual loss or gain of volume by leakage and pumping is not significant. When the piston gage is used either as a manometer or as a pressure regulator, the reading has been proven independent of the piston position over a range of 5/16 in., also little manual manipulation is required to maintain the piston position constant to within even 1/16 in. by venting or admitting air in some manner, such as by the adjustment of the screw compressed bellows illustrated in figure 4. It has been found practical to control an admitting valve by a photocell sensing the piston position. Such a controller may readily be added so the chief concern has been to determine whether any error is introduced in the gage readings by any axial forces acting on the piston produced by the pumping or variation in the pumping.

Various influences on the pumping rate were investigated. The pumping action was generally assayed by closing off the line into the gage, observing the axial motion of the piston over a suitable time, usually 5 min, and converting the linear motion of the piston into an equivalent gain or loss in gas volume in the closed space. The results of some of the tests are given below:

(a) With a 90-g piston at zero altitude the pumping rate was, for instance, 0.4 cm³/min loss in volume. With other conditions of piston loading, belt tension, or altitude, the rate might be up to 1 cm³/min and as frequently a gain in volume as a loss.

(b) The speed of rotation of the cylinder had but slight effect on the pumping rate within the limits tested. Practically identical rates were obtained with a four to one range in the speed of cylinder rotation. Even reversing the direction of rotation by running with a crossed belt, in various trials, gave the same rate of pumping, and in the same direction, as before. This seems to reduce the possibility of the pumping being due here to any screw conveyor action from surface marks or scratches on the cylindrical surfaces.

(c) The weight on the piston had a large influence on the pumping rate. At normal speed and with a piston weight of 30 g a gain of 0.2 cm³/min was noted; and under the same conditions but with a piston weight of 150 g the rate of gain was 2.0 cm³/min.

(d) A test was made in which the belt tension was progressively increased. Since the belt pull was upwards on the cylinder and positioned near the outboard end of the bearing, tightening the belt would decrease the bearing load and would at a certain point approximate an equally distributed loading. Under the conditions where light belt tension gave a pumping rate of 1.0 cm³ loss per minute the gradual increase in tension passed through a condition where there was no pumping and on to where the rate was an 0.4 cm³ gain per minute. The increase in belt tension did not result in an observable tilt of the piston axis.

(e) The piston was allowed to rotate with the cylinder by sealing it to the cylinder with a drop of machine oil. The rate of volume gain was found unchanged, indicating no pumping through the piston-cylinder clearance.

(f) The load in the piston was now arranged as unsymmetrically as possible. A 116-g end load was used, arranged so that the center of gravity was slightly off any portion of the piston area. On making tests with this weight in both the outboard and inboard positions the same rate of pumping was obtained in each case, 0.04 cm³/min loss. Also as noted previously under zero stability the identical zero was obtained with both configurations. The effect of the unbalanced loading of the piston on the readings, as previously noted, was negligible.

(g) With a piston load of 116 g and the pumping in a direction to increase the air volume in the cylinder, the tilt of the gage was increased until the leakage rate and pumping rate were identical. Under this condition the pressure in the gage corresponded to 0.1 in. of mercury.

This series of tests seemed to prove that the pumping is chiefly through the cylinder-bearing clearance. Even if some pumping does occur through the piston-cylinder clearance, the magnitude of this effect is less than the resolution of the gage.

A more refined study may be attempted when opportunity is presented in order to determine if, under any conditions not yet covered, there is a measurable axial component reacting on the piston.

Hints as to the mechanism of the pumping are presented in some references on oil lubrication. McKee and McKee [8] studied the distribution of oil pressure in journal bearings and in their eccentric loading test show that the maximum pressure line in the bearing is askew with respect to the axis of the bearing. Also, considerably later, F. W. Ocvirk [9] reported on axial and twisted misalinement as affecting oil-pressure distribution in a similar bearing and clearly illustrated with three-dimensional graphs the askew maximum pressure area under these load conditions.

Neither author discusses transfer of oil through the bearing, but it does seem obvious that if the maximum pressure line (due to dynamic lubrication forces) is askew to the axis of the cylinder the minimum clearance line is also askew, although possibly not in the identical position, and the combination of an askew pressure line followed by a parallel minimum clearance line creates the condition for an axial flow of the lubricant. It is likely that some bell-mouthing also exists to accentuate the off-axis conditions. The conditions causing this askew pressure line, that is, eccentric loading, axial and twisted misalinement, and bell-mouthing (the latter occurring because of the former three) are all present to a much greater degree in the bearing than on the piston. This seemingly bears out the empirical evidence associating the pumping with the bearing. This analysis also suggests methods for reducing the pumping. One method would be to concentrically load the bearing, possibly by the addition of a second bearing or by arranging the bearing to lie outside of the cylinder. A second method would be to lessen twisting misalinement forces by having the rotational drive placed advantageously. Reduction of these latter forces will decrease the likelihood of bell-mouthing in use.

This pumping action is of limited importance in the piston gage. The considerable discussion presented here arises because of the difficulty encountered in the attempt to discover if any errors in pressure measurement arise from this action. The primary cause of the difficulty is the fact that the gage has a resolution some 10-fold greater than any conveniently available instrument on which an error from this source could be evaluated by comparative testing.

5.10. Gage Volume

In apparatus where a small constant volume system is required or desired the volume of this gage may be excessive, particularly when combined with the gage leaking and pumping that have just been discussed.

The motion of the piston can be observed, if desired, by low-power optical magnifying means and the position change corresponding to the gain or loss of 0.05 cm^3 is reasonably visible, but the volume change of the gage is always significant when there is a movement of the piston. At differential pressures less than 0.1 in. of Hg, the increased volume may be contaminated by "in" pumping from the atmosphere in which the gage is operated.

5.11. Centrifugal Force on the Piston

An axial force on the piston will exist if the cylinder rotates with any eccentricity. If eccentric motion is imparted to the piston, an axial component may result, affecting the apparent mass of the piston. The construction employed, where the same straight bore of the cylinder is used both to position the cylinder on its bearing and to support the piston, is believed to reduce the eccentricity error to a very low value. No error from this source on either of the models has been detected by change in zero with change in cylinder rotational speed.

5.12. Summary of Accuracy Limitations

The limitations upon the accuracy introduced by all factors are collected and summarized in table 6. Where dependent upon deflection, the values listed may be assumed for a tilting gage set at an altitude h of 5 in. and having a medium-weight piston. Many of these listed values are not known to sufficient precision to establish their variation with gage deflection. Values have been assigned in various cases to represent what is, at present, believed to be the maximum error that would be contributed by the listed factor. In many cases the value of 0.0001-in. is assigned because this represents the resolution of the gage reading at the time of the error investigation. Some of these errors may not even be of this significance. A few of the values entered are lower than this since they were studied when higher resolution was available for the reading.

Table 6

Factor	Accuracy limit in inches of altitude	
	Basic	Relative
1. Level	0.0001	0.00005
2. Temperature	.0001	.0001
3. Area	.0005*	.0002
4. Sine	.0001	.00005
5. Static charges	.0001	.0001
6. Piston oscillation	.0001	.0001
7. Centrifugal pressure	.0001	.0001
8. Dynamic pressure	.0001	.0001
9. Leakage	.0001	.0001
10. Pumping	.0001	.0001
11. Gage volume	.0001	.0001
12. Centrifugal force on weight	.0001	.0001
13. Weight determination	.0001*	.00005
14. Zero reproducibility	.00005	.00005
15. Reading reproducibility	.0001	.0001

In the error columns the values under "Basic" are assigned to cover the error of the instrument as a primary standard. In the column under "Relative" the values are based on the ability of the gage to repeat a reading either as a gage or as a pressure regulator. The errors without asterisks are subject to variations dependent on random influences. The errors marked with the asterisk are unidirectional. The 5-in. altitude with the medium-weight piston corresponds to a pressure reading of about 0.4 in. of Hg. The maximum predicted error in the basic measurement is 8×10^{-5} in. of Hg and in the relative measurement is less than 4×10^{-5} in. of Hg.

6. Design Modifications

Although because of its simplicity, an air-lubricated bearing has been employed for the cylinder, this is by no means essential and does have the inconvenience of considerably increasing the exchange between the atmosphere within and without the gage. Oil-lubricated journals or ball bearings

could be employed and the pressure chamber sealed with O-rings.

Where it is desired to work from a pressure datum other than that of the room, this may be accomplished by several means. For instance, identical air-lubricated bearings for the cylinder may be employed at both ends of the piston. This has been done at times, but a very nice mechanical assembly is required to allow disassembly for cleaning or adjusting the piston weight. If self-alinement ball bearings were employed this need not be a difficult reassembly.

Alternately, a particularly compact structure could be made by making the outer surface of the cylinder the bearing face, concentric with and outside the piston support area and fitted with two end pressure taps, as shown in figure 6. Alternatively the whole device may be enclosed by a belljar or to insure ease of access to the micrometer for adjustment, the cylinder section only might be enclosed and driven through a magnetic coupling.

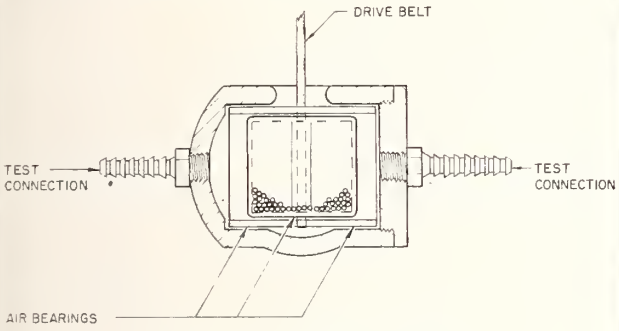

FIGURE 6. *Modified piston gage.*

Symmetrical pressure connections are provided to control the reference pressure also. The bearings are outside of the cylinder.

If the reference pressure is to be a high vacuum, the highest precision would be necessary in the cylinder fitting. Even with the smallest working clearance between the piston and cylinder the approach to the reference pressure would presumably be limited by the leakage past the piston, and the operation would be limited to an average pressure that would allow an air film for lubrication of the piston.

For a reference standard, it is believed that the most desirable piston and cylinder combination would be of fused quartz because of the stability of this material and also because of its nice working qualities. The fitting of the piston to the cylinder and area measurements might be performed to a much higher order of accuracy than with glass. Transparency of the cylinder seems desirable for observation of the piston although for a structure such as figure 6 an end window would suffice, in which case the cylinder and piston could both be metallic. It is desirable for the piston and cylinder to be of identical materials to avoid temperature effects in the close fits required.

To reach the lowest pressures the piston weight should be the least possible. No attempt has been made to determine the optimum diameter of the piston. A diameter on the order of 1 in. is convenient to work with, but smaller diameters might be employed with equal satisfaction if the volume or leakage of the gage is particularly significant. The eccentric weight for the piston may be, on various arrangements, suspended outside of the cylinder in order to provide greater leverage if needed.

The micrometer or height setting means might be driven by a servomotor to maintain a null piston position. Increased resolution is available if the micrometer were provided with a 6-in. reading circle or a digital readout, and provided that the screw has commensurate accuracy.

7. Field of Application

Because of its sensitivity and inherent accuracy it is believed that this gage has application as a calibrating standard in the range of differential pressure up to at least ½-in. of mercury and possibly can be extended to twice this. Its aperiodic motion and low-temperature coefficient (particularly if of quartz) reduces the time for a calibration.

Tests at zero differential pressure but at low absolute pressure indicate that measurements can be made at absolute pressures down to a few millimeters of Hg. With further development, it appears possible to extend the lower pressure limit down below a 0.1 of a millimeter of Hg.

As a manometer to read an unknown pressure in the above range, it has considerable versatility and with its dead-beat characteristics allows readings to be obtained rapidly. As a pressure regulator to reproduce precise settings, it has the unique advantage of the commonly used dead weight tester.

8. References

[1] W. G. Brombacher and T. W. Lashof, Bibliography and index on dynamic pressure measurement, NBS Circ. 558 (1953).

[2] H. F. Brubach, Some laboratory applications of the low friction properties of the dry hypodermic syringe, Rev. Sci. Inst. **18,** 363 (May 1947).

[3] H. R. Hindley, A differential manometer, J. Sci. Inst. **24,** 295 (1947).

[4] C. H. Meyers and R. S. Jessup, A multiple manometer and piston gage for precision measurements, BS J. Research **6,** 1061 (1931) RP 324.

[5] Manometer for calibrating high-altitude pressure devices, NBS Tech. News Bull. **43,** 71 (1959).

[6] M. D. Hersey, A short account of the theory of lubrication, J. Frankl. Inst. **220,** 93 (1935).

[7] P. W. Ott, Letter to Eng. News Rec. **103,** 785 (1929).

[8] S. A. McKee and T. R. McKee, Pressure distribution in oil films of journal bearings, Trans. Am. Soc. Mech. Eng. **APM–51–15,** 161 (Nov. 1931).

[9] F. W. Ocvirk, Measured oil film pressure distribution in misaligned plain bearings, Lub. Eng. **10,** 262 (Oct. 1954).

WASHINGTON, D.C. (Paper 63C1–5)

UNITED STATES DEPARTMENT OF COMMERCE • Frederick H. Mueller, *Secretary*
NATIONAL BUREAU OF STANDARDS • A. V. Astin, *Director*

Mercury Barometers and Manometers

W. G. Brombacher, D. P. Johnson, and J. L. Cross

National Bureau of Standards Monograph 8

Issued May 20, 1960

Reprinted August 1964 with corrections

For sale by the Superintendent of Documents, U.S. Government Printing Office
Washington 25, D.C. Price 40 cents

366-1

Foreword

Preparation of this Monograph on mercury barometers and manometers was undertaken to fill the need of manufacturers and users for information which is now scattered through the literature and in some cases unpublished. This information is primarily on the sources of error and methods for their correction. Moderately extensive tables of corrections for temperature, gravity, capillarity, and other errors are included, mainly for application to portable instruments. The various types of instruments are defined and design features affecting the accuracy discussed in some detail.

The preparation of this monograph is part of the work on pressure standards now in progress in the Mechanics Division, B. L. Wilson, Chief, under the direct supervision of E. C. Lloyd, Chief of the Mechanical Instruments Section.

A. V. Astin, *Director.*

ERRATA SHEET TO ACCOMPANY

NBS MONOGRAPH 8, MERCURY BAROMETERS AND MANOMETERS

Table 1 - Conversion Factors for Various Pressure Units
Equivalent for Unit Value in First Column

Pressure Unit Value		millibars	mm mercury 0°C	in.mercury 0°C	gram/cm^2	lb/in^2	lb/ft^2	cm water 20°C	in water 20°C
1 atmosphere	=	1013.250	760.000	29.9213	1033.227	14.69595	2116.22	1035.08	407.513
1 millibar(mb)	=	1	0.75006	0.029530	1.0197	0.014504	2.0885	1.0215	0.40218
1 mm mercury(mm Hg)	=	1.3332	1	0.03937	1.3595	0.019337	2.7845	1.3619	0.53620
1 in.mercury(in Hg)	=	33.864	25.400	1	34.531	0.49115	70.726	34.573	13.619
1 gram/cm^2(g/cm^2)	=	0.98067	0.73556	0.028959	1	0.014223	2.0482	1.0018	0.39441
1 lb/in^2(psi)	=	68.9476	51.715	2.0360	70.307	1	144	70.433	27.730
1 lb/ft^2	=	0.47880	0.35913	0.014139	0.48824	0.0069444	1	0.48912	0.19257
1 cm water 20°C	=	0.97891	0.73424	0.028907	0.99821	0.014198	2.0444	1	0.3937
1 in. water 20°C	=	2.4864	1.8650	0.73424	2.5354	0.036063	5.1930	2.5400	1

1 atmosphere = 10332.3 = Kg/m^2 = 1.03323 Kg/cm^2

1 bar = 1000 millibars = 10^6 dynes per sq cm

1 inch = 2.54 cm (old value, 2.54000508 cm; 2 parts per million greater)

1 pound = .45359237 Kg (old value, .45359243 Kg; 2 parts per 15 million greater)

Density of water at 20°C = .998207 grams/cm^2

February 7, 1961

Contents

Mercury Barometers and Manometers

W. G. Brombacher, D. P. Johnson, and J. L. Cross

The various designs of mercury barometers and manometers are briefly described, with a more extended discussion of the various design elements which may affect the achievable accuracy. Sources of error in measuring pressures are described in considerable detail, particularly for portable instruments, including scale, temperature, gravity, capillarity, vacuum errors and return gas column. Methods of minimizing those errors and of making the corrections, including extensive tables, are presented. Standard conditions are defined and the pertinent properties of mercury given. The paper contains 65 literature references.

1. Introduction

Mercury barometers and manometers are widely used in aeronautics, meteorology, science, and industry. In aeronautics they are used to calibrate a multitude of pressure measuring instruments, including altimeters, rate-of-climb meters, airspeed indicators, manifold pressure gages and Mach meters, many of these instruments demanding continually increasing accuracy [581].[1] In meteorology, mercury barometers are used to measure the atmospheric pressure. In industry and industrial research laboratories barometers are used principally to measure atmospheric pressure, whereas the mercury manometer has a multitude of applications.

The principal objectives in preparing this Monograph are: (a) To outline the inherent errors of mercury barometers and manometers and to provide information and tables for correcting these errors; (b) to briefly describe the variety of design elements of these instruments which are critical in obtaining precision and accuracy; and (c) in some measure to contribute to national standardization of practices and methods of measuring pressure with mercury columns.

A great deal of the material in this report reflects the experience of the National Bureau of Standards in this field of pressure measurement. However, a number of manufacturers have made substantial contributions to the art.

Present day needs are not only for increased accuracy in pressure measurements, but also for an extension of the range of mercury barometers and manometers. Mercury barometers and manometers up to 10 ft in height are now being required but such instruments are relatively awkward to transport and use. The reading difficulty is in a fair way of being eliminated by the use of the photocell detector coupled with automatic setting of the photocell to the mercury level.

2. Definitions

1. Pressure is the force per unit area exerted by a gas, liquid, or solid.

2. Absolute pressure is the total pressure.

3. Differential pressure is the difference in pressure of a fluid at any two levels or of two fluids at any two levels. The height of a liquid column, corrected to standard conditions, measures the differential pressure existing between the two menisci; when the pressure above one meniscus is zero, the absolute pressure is measured.

4. Gage pressure is differential pressure with respect to atmospheric pressure. Gage pressure plus the atmospheric pressure equals the absolute pressure.

5. Barometers (from *baro*—, weight+*meter*, measure) are instruments for measuring the pressure of the atmosphere. Manometers on the other hand (from *mano*—, thin, rare+*meter*) are instruments for measuring the pressures of gases or vapors. In both instruments the pressure may be balanced against a column of mercury in a tube or against the elastic force of a spring, an elastic diaphragm, or the like, as in an aneroid barometer. Manometers are frequently used with other liquids than mercury and often are used differentially in a U-tube with one end either open to the atmosphere or to a gas under pressure. One authority [231] considers all manometers to be differential manometers and says, "The barometer as generally understood, is a particular case of a manometer in which one of the two pressures is zero."

Thus, all of the instruments considered here are strictly speaking, manometers, whether used to measure absolute or differential pressure.

In course of application of barometers to other purposes than given above, the definition of barometers has been extended by common consent to include many types of portable manometers which measure absolute pressure. This distinction between barometers and manometers will be followed in view of its convenience.

6. Aneroid barometers are barometers, the pressure sensitive element of which is an evacuated corrugated diaphragm capsule, a metal bellows or a Bourdon tube in contrast to mercury barometers in which the height of a column of mercruy is a measure of the pressure.

[1] Figures in brackets indicate the literature references on page 45.

7. U-tube manometers are those which have two tubes the same in bore, commonly having the shape of an elongated U. The U-tube is filled with mercury or other liquid so that two liquid surfaces exist in the tube. The difference in pressure applied to the two liquid surfaces is measured by the difference in height of the two liquid surfaces.

8. U-tube barometers are U-tube manometers in which the pressure on one liquid surface, usually mercury, is maintained at essentially zero pressure, as by evacuating the space above the tube and sealing the tube.

9. Cistern barometers or manometers are those in which the diameter of one mercury column is much larger than the other to provide a reservoir which is usually called a cistern. A single scale mounted along the side of the tube is used to measure the height of the mercury column. There are many forms of cistern barometers, some of which have reasonably well accepted names, as indicated below.

(a) Fortin barometers are cistern barometers in which the height of the mercury surface in the cistern can be adjusted by eye to the level of a fixed index, which insures a fixed zero reference for the scale. These barometers are primarily used to measure atmospheric or ambient absolute pressure.

(b) Fixed cistern barometers usually have a single scale ruled so as to compensate for the change in zero position due to the rise and fall of the mercury in the cistern with change in pressure.

(c) Fixed cistern barometers often are designed to measure only ambient pressure in which case the space above the mercury in the cistern is not gas tight. The Kew barometer, developed in England and the Tonnelot, developed in France, are of this type.

10. Altitude barometers are fixed cistern or U-tube barometers in which the design is such that the absolute pressure in closed systems can be measured. For this purpose the cistern of cistern barometers is entirely sealed except for a connecting nipple. The U-tube barometer needs only a suitable nipple. Altitude barometers of the fixed cistern type, when used to calibrate altimeters, may sometimes have a scale calibrated in altitude units corresponding to the altitude pressure relation of a standard atmosphere, in addition to a pressure scale.

11. Standard, sometimes called normal, barometers strictly speaking are barometers of the highest precision and accuracy. More loosely, they are barometers used to calibrate other barometers, to be suitable for which their errors must be known, and their precision and accuracy should be superior to that of the barometers to be tested.

12. The sign of an error in indication of an instrument is determined by the relation

$$E=R-T$$

and of a correction by

$$C=T-R$$

where E is the error; R, the reading; T, the true value; and C is the correction. It follows that

$$E=-C.$$

13. Scale error is the error in the reading of a barometer or manometer caused by errors in graduation of the scale and vernier. Practically for portable barometers it is the residual error remaining after corrections normally made are applied for other errors.

14. Zero error is the error in reading of a barometer or manometer when the differential pressure applied to the two liquid surfaces is zero.

15. Correction for temperature is the correction required to reduce the reading of the barometer or manometer to a reading corresponding to the density of mercury and the length of the scale at selected standard temperatures. See section 3.2 for the selected standard temperatures.

16. Correction for gravity is the correction required to reduce the reading of the barometer or manometer to a reading corresponding to a selected standard gravity, discussed in section 3.2.

17. Capillary error is the amount that a mercury meniscus is depressed below the height corresponding to the applied differential pressure of which the primary cause is the surface tension of mercury.

3. Principle of Measurement and Standards

3.1. Principle of Measurement

In measuring pressure by the height of a liquid column, the weight (not mass) of a column of unit area numerically equals the pressure difference. For a liquid column in which the upper surface is subjected to a vacuum, the fundamental relation for the pressure it exerts is

$$P=\rho gh \qquad (1)$$

where

P is the absolute pressure in dynes per square centimeter or poundals per square inch at the lower liquid surface, if

ρ is the density of the liquid in g/cm^3 or lb/in.^{3};

g is the acceleration of gravity in cm/sec^2 or in./sec^2; and

h is the height of the liquid column in centimeters or inches.

If the pressure is desired at some other point in the system differing in elevation from the lower liquid surface, correction must be made for the weight of the intervening column of gas or liquid. (See sec. 12). For manometers which measure either the differential or gage pressure, the fundamental relation is similar to eq (1)

$$p=P_2-P_1=\rho gh \qquad (2)$$

where

p=differential or gage pressure in dynes per square centimeter or poundals per square inch.

P_1 and P_2=the absolute pressures at the upper and lower liquid surfaces of the manometer.

The other terms have been defined.

Strictly speaking, the differential pressure defined in eq (2) is the difference between the pressures impressed upon the upper and lower liquid surfaces. At some other elevation or level, correction must be made for the weight of the intervening column of gas or liquid (see sec. 12).

For both eq (1) and (2) $\rho gh/g_s$ is the pressure expressed in grams per square centimeter or in pounds per square inch where g_s is standard gravity, 980.665 cm/sec² or 386.088 in./sec²;

$$P \text{ or } p=\frac{\rho gh}{g_s}. \qquad (1.1)$$

3.2. Standard Conditions

In many cases the height of the liquid column is taken as a measure of the pressure, then

$$h=\frac{P}{\rho g} \text{ or } \frac{p}{\rho g}. \qquad (1)$$

Since both ρ and g are only approximately constant, some ambient condition must be selected as standard so that this pressure unit bears a fixed relation to the metric or English unit pressure.

The density of mercury at any one pressure is fixed by its temperature, hence it is general practice to use the density of mercury at 0° C subjected to a pressure of 1 atm. Since measurements are rarely made at 0° C, readings generally require correction for deviation from 0° C. these are discussed in section 9.

The height of mercury columns as a measure of pressure has been based for many years on a value of the acceleration of gravity of 980.665 cm/sec² (32.1740 ft/sec²) by physicists and engineers [011]. While this value was selected because it was believed to be the value at 45 deg lat, there is little merit in tying a pressure standard to a latitude, and uniform acceptance of a value is of greater importance. Meteorologists have varied in their choice from time to time, using 980.62 cm/sec² up to 1953, when the International Meteorological Organization also adopted 980.665 cm/sec² for this purpose [533, 534, and 556]. Corrections are usually necessary for deviation of ambient gravity from the standard value, which are discussed in section 10.

Mercury manometers and barometers are often calibrated to indicate the height of the mercury column in terms of mercury at 0° C, when the instrument is at another temperature, for example, 20° C, 25° C, 62° F, or 100° F.

3.3. Pressure Units

In cgs units the fundamental pressure unit is the dyne/cm². By definition, 1 bar=10^6 dyne/cm², and accordingly the convenient unit, 1 mb=1,000 dynes/cm².

In English units, the primary pressure unit is the poundal per square foot, but the practical unit is the pound per square inch (psi).

Another unit is the pressure of one atmosphere defined for fixed points on the International Temperature Scale as 1013.250 mb [493]. This definition provides for stability in the definition of the pressure unit in atmospheres. This pressure is equivalent to that exerted by a column of mercury 760 mm high, having a density of 13.5951 g/cm³ and subject to a gravitational acceleration of 980.665 cm/sec.² The value of 13.5951 g/cm³ was taken for the density of mercury at 0°C; it differs only slightly from the value reported in a recent determination at the National Physical Laboratory [571], also table 4.

Note that owing to the slight compressibility of mercury under its own weight, multiples or submultiples of 760 mm of mercury do not precisely correspond to the same multiples or submultiples of 1013.250 mb. Except for very precise pressure measurements, this difference is neglected.

Conversion factors for a number of commonly used pressure units are given in table 1. The conversion factors for centimeters and inches of water are based on a value of the density of water at 20°C of 0.998207 g/cm³. For values of the primary units involved in computing table 1 (see ref. [551]), except for the value of the pound in terms of the kilogram and the inch in terms of the centimeter. Changes in the conversion factors have recently been adopted, retaining as standard the mass of 1 kg and the length of 1 cm. The change is 2 parts per million in the length of the inch (shorter) and 2 parts per 15 million in the pound (smaller). Most of the table is also accurate for the obsolete units.

The units, gram per square centimeter, pound per square inch, etc., involve a force of 1g or of 1 lb. This force is a mass of 1 g or 1 lb. subjected to the standard value of gravity, 980.665 cm/sec² or its equivalent, where required.

Other units often used are: (a) barye=1 dyne/cm² (b) micron=0.001 mm of mercury; (c) tor (or torr)=1/760 of 1 atm, closely, 1 mm of mercury; pieze (French)=10 mb.

4. Properties of Mercury

Only the properties of mercury of importance in manometry will be discussed. The melting point is −38.9°C and the boiling point at 1 atm, about 357°C. For general information on mercury see ref. [421, 522, and 574].

4.1. Density of Mercury

A redetermination of the density of mercury is in progress at the National Physical Laboratory; the density by one method of measurement [571] is 13.5458924 g/cm³ at 20°C under a pressure of 1 atm. This value reduces to 13.5950889 g/cm³ at 0°C, a value not significantly different from that generally accepted, 13.5951 g/cm³.

Based on the value for the density of mercury at 0°C, the density at other temperatures is obtained from the relations:

$$V=V_0\,(1+0.0001818\,t),\ t \text{ in } °C \qquad (4)$$

$$V=V_0\,(1+0.0001010\,(t-32)),\ t \text{ in } °F \qquad (5)$$

$$\rho=\frac{1}{V} \qquad (6)$$

where V, V_0=specific volume at temperature t and at 0°C

ρ=the density.

Equations (4) and (5) apply primarily when mercury is subjected to a pressure of 1 atm. Practically they are useful up to the point where the compression of mercury becomes significant, certainly up to at least 1 atm.

The value of the coefficient of cubical expansion $m=1{,}818\times10^{-7}$ per ° C is a sufficiently accurate approximation which is widely used, and standard for most purposes. More accurate values, based upon the relation,

$$m\times10^8=18144.01+0.7016t+0.0028625t^2+0.000002617t^3$$

are given in ref. [413], where t is the temperature in ° C, from 0° to 350° C. The exact mean values of $m=(V_t-V_0)/V_0t$ are given below for a few temperatures; for a more extended table see table 10 of ref. [413].

The value of the density of mercury at temperatures above 0° C is less than the true value when computed using $m=1{,}818\times10^{-7}$. It is seen that for room temperatures, the approximate value m is sufficiently accurate for use in manometry in all but the most precise work.

The ratio of the density of mercury at t° C to that at 0° C are presented in table 2. These are taken from table 12 of ref. [413] and are based upon the precise value of the coefficient of expansion, not the average value $1{,}818\times10^{-7}$ per ° C.

Temperature	True coefficient	Error in density using eq (4)
° C	$m\times10^8$	*Parts per million*
0	18, 144	0
10	18, 151	2. 9
20	18, 159	4. 2
30	18, 168	3. 6
40	18, 177	1. 2
50	18, 187	3. 5

Values of the density of mercury are given in tables 3 and 4 for various temperatures. These are based upon the ratios given in table 2; in table 3 upon the value of 13.5951 g/cm³ at 20° C, all when the mercury is under a pressure of 1 atm. The density in g/cm³ is given in table 3A, and in lb/in.³ in table 3B. In table 3B the recently adopted values for the inch and the pound given in table 1 were used to obtain the density in lb/in.³; these densities are 5.9 parts per million smaller than those based upon the previous values.

Tables of the specific volume of mercury at various temperatures and of the true temperature coefficient of mercury, dV/V_0dt, are given in ref. [413].

4.2 Vapor Pressure of Mercury

The vapor pressure of mercury is given in table 3A, computed from the equation

$$\log P=11.0372-\frac{3{,}204}{T},$$

where P is the vapor pressure in microns of mercury; and T is the absolute temperature in ° K. This is an empirical equation derived by Ernsberger and Pitman [558] to fit the data of previous investigators and fits their experimental values within 1 percent in the temperature range 12° to 53° C. These values agree closely with the computed values given in ref. [516] and are about 2 percent lower than the computed values in ref. [535]. The vapor pressures given in the International Critical Tables and in ref. [531] are about 10 percent lower, and those in ref. [414], still lower. See ref. [471] for data at temperatures higher than listed in table 3A and for references to earlier original work.

4.3. Surface Tension of Mercury

The best value for the surface tension of mercury [461] and [494] is 484 at 25° C, 479 at 50° C, and 474.5 dynes/cm. at 75° C. This refers to mercury in a vacuum. For mercury in contact with air no valid data appears to exist [494] but is expected

to be somewhat less than for a vacuum. Impurities and particularly oxidation will affect the surface tension of mercury, probably lower it, but the amount of change is speculative. See section 11 for a more detailed discussion.

4.4. Compressibility of Mercury

The decrease in volume, ΔV, per unit volume of mercury with increasing pressure P in bars at 25° C is [121, 542]:

$$\Delta V=4.0391\times10^{-6}\,P-0.7817\times10^{-10}\,P^2 +0.191\times10^{-14}\,P^3. \quad (7)$$

For most manometer applications the approximate relation given below is satisfactory:

$$\Delta V=aP-bP^2 \quad (8)$$

where

$a=4.04\times10^{-6}$, $b=0.78\times10^{-10}$ for P in bars

$a=4.09\times10^{-6}$, $b=0.80\times10^{-10}$ for P in atmospheres

$a=5.38\times10^{-9}$, $b=0.81\times10^{-16}$ for P in millimeters of mercury

$a=137\times10^{-9}$, $b=89\times10^{-15}$ for P in inches of mercury

Computations based on eq (8) follow:

Pressure bars	Decrease in unit volume	Density of mercury
		g/cm^3
0	0	13. 59505
1	4.04×10^{-6}	13. 5951
10	40.4×10^{-6}	13. 59565
100	463×10^{-6}	13. 60058
1,000	$3,960\times10^{-6}$	13. 6478

It follows that for pressures below 10 atm the last term in eq (8) can usually be neglected, and

$$\Delta V=aP \quad (9)$$

or

$$V=(1-aP)V_0 \quad (10)$$

and

$$\rho=\frac{\rho_0}{1-aP}=\rho_0(1+aP), \quad (11)$$

where a is a constant with values given above for various units of pressure: V is the volume at unit pressure P; ρ_0, ρ are respectively the density of mercury at zero pressure and at P.

C. H. Meyers at the National Bureau of Standards, based on Bridgman's data, arrived at the following values for constant a in eq (11), to cover the pressure range up to 1,000 in. of mercury: $a=1.36\times10^{-7}$ for P in in. of mercury, and $a=5.36\times10^{-9}$ for P in mm of mercury. These data are unpublished.

4.5. Purity and Composition

The possible variation of isotopic composition of mercury from various sources and subject to various processes, primarily distillation, affects the density and is therefore important in precise manometry. Estimates based upon some data indicate that the variation in the density of mercury will not exceed one part in 30,000 due to extreme variation in isotopic composition. However, exact data on isotopic composition of mercury secured from different sources or subjected to various procedures in distilling are lacking to a large extent. See ref. [571] for a review of the present situation.

The effect and methods of removal of impurities are of particular interest. All but traces of metals dissolved in mercury can be removed by a procedure of distillation [574]. Methods of testing for purity of mercury are discussed in ref. [571], which indicate that with isotope tracers one part in 10^8 of base metals can be detected. Very small quantities of base metals which form an amalgam with mercury, rise to the surface and are easily detected by the surface contamination.

Air is not absorbed by mercury, as is indicated by the fact that barometers have maintained a good vacuum above the mercury column for years. However, air bubbles may be trapped in the mercury, and should be removed, usually accomplished by subjecting the instrument to several pressure cycles while jarring the instrument sharply.

Water trapped in mercury can only be removed by subjecting the mercury to a temperature above 100° C. Water in a barometer is particularly troublesome since a satisfactory vacuum cannot be obtained above the mercury column.

In general, mercury compounds are formed as a result of contact of air and other gases with the mercury surface, and remain there. Gases containing sulfur are particularly active in forming such compounds. Detection of such compounds, even in small amounts is simple; accurate observations on the mercury surface become difficult or impossible.

On procedures for cleaning mercury, see refs. [531, 561, 571, 574, 591].

Experience indicates that mercury remains free from contamination when stored in bottles of soft glass, at least more so than in containers of other materials on which extended experience is available.

4.6. Electrical Resistance of Mercury

The electrical resistivity K of mercury is:

$$K=\frac{SR}{l} \qquad (12)$$

where R is the resistance, l the length of the column in centimeters and S the area of the cross section in square centimeters.

At 0° C, $K=94.07$ and at 100° C, $K=103.25$ μohm-cm [531]. These values are for a pressure of 1 atm and they decrease measurably as the pressure increases [191].

5. Types of Barometers and Manometers

Barometers and manometers are basically simple instruments where the primary measurement to be made is the height of the mercury column. Other measurements must be made also in order to convert the indicated height of the mercury column to accepted or standard pressure units.

Many factors must be considered in the design of a barometer or manometer such as portability, range, accuracy, convenience and degree of automation in making readings, and usefulness for the application. As a result many designs have been evolved. The principal designs will be only briefly considered, since the emphasis here is on performance rather than design. The descriptions in this section will be augmented in the next section by some design details of the means which are used to meet problems more or less common to all barometers and manometers.

The essential features and components of a first class barometer are indicated in figure 1. Alternatives for detecting the position of the mercury surface and for measuring the column height are indicated; these and the other components will be discussed in this and the succeeding section. When the accuracy required is not high, some of the components or accessories can be and are omitted, but for highest accuracy the function of all is significant and where selection is possible, those producing the greater accuracy must be chosen.

There are a large number of clever schemes for amplifying the indicated height of a mercury column, particularly in measuring small differential pressures. The precision of reading is thereby increased, also the accuracy, but not to the same degree as the precision. Most of the schemes require some extra manipulation. The devices described in ref. [453, 513], are exceptions in that they are automatic in operation. Another device, not automatic but easily made so, is described in ref. [483]. See also ref. [391] for descriptions of a number of designs. These devices all come under the general head of micromanometers, which include mechanical devices also; detailed consideration of these is in general outside of the scope of this report.

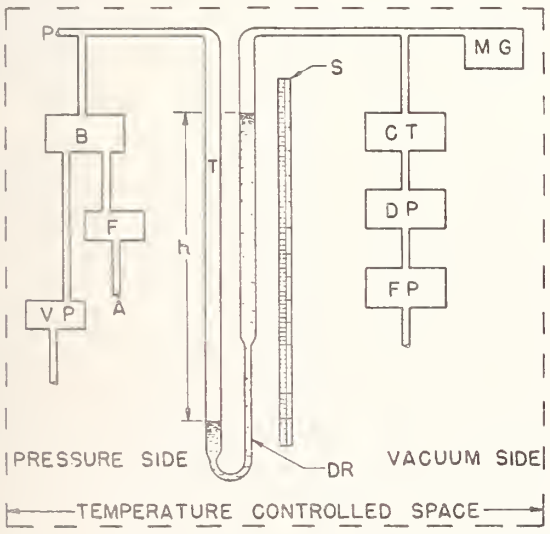

FIGURE 1. *Principal elements of a precise laboratory barometer system.*

T, barometer tube; *DR*, restriction in tube bore for damping; *S*, scale, or precision screw plus controls, or gage blocks; sighting device, not shown, either telescope, photocell or other optical devices; *MG*, McLeod or other vacuum gage; *CT*, liquid air trap; *DP*, diffusion pump; *FP*, forepump; *F*, filter; *B*, barostat; *A*, air supply; *VP*, vacuum pump; and *P*, line to point where pressure is to be measured.

5.1. Fortin Barometers

The Fortin barometer is one of the oldest forms of commercial barometers, having been used for measuring atmospheric pressure by meteorological services for about 100 years [301]. The barometer tube is surrounded, except for reading slits, by metal tubes one fixed to the cistern assembly and another short one, movable up and down within the first. The movable tube carries the vernier and ring used for sighting on the mercury meniscus. The fixed tube has the pressure scale, usually plated brass, adjustably attached to it.

The cistern has an index fixed to its top wall, usually a thin ivory or bone rod, tapering to a point at the lower end. The cistern is essentially a leather bag which can be raised or lowered by a metal plate at the end of a screw, which can be turned by hand at the bottom of the cistern.

To take a reading the mercury in the cistern is brought up until it is just in contact with the index, thus bringing the mercury surface into alinement with the zero of the scale. Valid readings are made only when the mercury level in the cistern is so adjusted. Since the lower end of the scale does not extend to the cistern, the distance from the cistern mercury surface to a point on the graduated scale must be determined, usually by comparing at the same pressure the reading of the Fortin barometer with that of a standard barometer.

The Fortin barometer can be used only to measure ambient pressure and is widely used by meteorological services and in laboratories to measure atmospheric pressure. Pressure equilibrium with the ambient gas is obtained in the cistern by a vent at its top or through the chamois seal above the mercury.

The most common range of the Fortin barometer is 28 to 31 in. of mercury (about 950 to 1,050 mb; about 710 to 790 mm of mercury). For use at stations well above sea level, barometers with ranges extending from 20 to 31 in. of mercury have been built. With no great trouble the range could be from 4 to 5 in. of mercury upward to any value within reason, but in practice it is tailored to the range of pressures expected at its location.

The quality of Fortin barometers is measured practically by the bore of the tubing used, which in large measure also determines the diameter of the cistern. Fortin barometers are commonly made in this country with tubing either 0.25, 0.6 or 0.8 in. bores. For modest accuracy measurements, which is for the most laboratory requirements the irreducible limit, the tubing bore is 0.25 in. (6.35 mm). For the highest accuracy reasonably attainable with Fortin barometers, the tubing bore is about 0.8 in. (20.3 mm). The slight increase in accuracy obtained with the 0.8 in. bore is balanced by the greater degree of portability of the 0.6 in. bore barometer.

The Fortin barometer is designed to be safely portable in the upside down position. Before slowly tipping it over, the cistern mercury level control is operated to force mercury up the tube until the cistern is nearly filled. Thus splashing of the mercury is practically eliminated and the vacuum in the tube preserved. See [591] for detailed instructions.

5.2. U-tube Barometers and Manometers

In its simplest form the U-tube barometer or manometer consists of a U-tube containing mercury and a scale between the legs of the U for reading the position of the two mercury surfaces. If precision bore tubing is used, reading the position of the mercury surface in one leg may be sufficient. In manometers the pressure to be measured is applied to one leg and the other leg left open to the atmosphere if gage pressure is to be measured, or connected to the reference pressure if differential pressure is to be measured. In barometers the space above the mercury surface in one leg is evacuated.

The above described design of U-tube manometer is widely used; of barometers, less so. The described reading means are crude so that both the precision and accuracy are low. A big step in improving the accuracy is to add a vernier and a means for sighting on the mercury surfaces. This and other reading means are discussed more fully in sec. 6.

In order to reduce the error due to the capillary depression in fixed cistern barometers, discussed in a later section, barometers of the highest precision and accuracy are of the U-tube type. Diverse reading means and additional accessories are used as discussed in sec. 6.

U-tube manometers are used conveniently to measure gage pressures up to about 50 psi (about 3 to 3½ atm); for this range the mercury column is about 10 ft (3 m) high. Manometers for measuring differential pressures at high pressures are discussed below in section 5.5. Manometers may be used to measure absolute pressures if the space above one mercury surface is evacuated.

5.3. Fixed Cistern Barometers and Manometers

Mercury barometers in which the mercury level in the cistern cannot be adjusted during the reading process are called fixed cistern barometers. Here the barometer tube extends below the surface of the mercury in a cistern of much larger cross section than the tube so that the rise and fall of mercury level is small, but not negligible, in comparison to that in the tube. The larger the cross section of the cistern, within limits, the less the zero shift due to change in the meniscus height of the cistern mercury.

To compensate for the rise and fall of the mercury level in the cistern with pressure, the scale graduations are foreshortened, that is 1 mm differences in reading on the scale are less than 1 mm apart. Thus

$$D=\frac{AR}{A+a} \tag{13}$$

where

D = the distance between two graduations
R = the indicated interval between two graduations
A = the cross sectional area of the mercury in the cistern
a = the internal cross sectional area of the tube.

In practical designs D/R will vary from about 0.97 to 0.985.

In fixed cistern barometers used to measure only ambient atmospheric pressure, the cistern is vented to the atmosphere. This form of barometer, heavily damped by a restriction in the tube bore, is commonly used on shipboard by the meteorological services of the world, but is being superseded gradually by aneroid barometers because they are less sensitive to acceleration. In Great Britain the fixed cistern barometer of this type is called a Kew pattern barometer and is the type chiefly used by the British Meteorological Office. A French design which has had, and probably still has, some application is known as the Tonnelot barometer. The chief virtue of the Tonnelot barometer is that an adjustment is provided for reducing the cistern volume, as in the Fortin, so that the tube and cistern can both be completely filled with mercury to obtain safe portability.

The fixed cistern barometer lends itself to securing a leak tight cistern so that gas pressures in a closed system can be measured. It has been and is widely used as a working standard for calibrating altimeters and aneroid barometers. For such use the cistern is made airtight except for a nipple, to which a chamber or instruments themselves are connected by tubing. Pressure control means are connected to the system.

In earlier designs the cistern and barometer tube were made coaxial. However, as lower and lower absolute pressures have had to be measured, it has been found necessary to have an offset cistern so that readings can be made down to zero pressure. Obviously, fixed cistern manometers have also necessarily had to have offset cisterns if differential pressures below about 3 in. of mercury were to be measured. Reasonable accuracy is difficult to attain at pressures below about 1 mm of mercury in designs having a range to an atmosphere and above from either the cistern or U-tube instruments. Measurements of absolute pressures below 1 mm of mercury are in the realm of vacuum measurement which is outside of the scope of this report.

Fixed cistern barometers have generally been constructed to measure pressures below about 1 atm. Barometers have been built to have a range up to 2 or 2½ atm, but these instruments are bulky and unwieldy to transport.

The scale is usually graduated in pressure units but often has an added altitude scale based upon the altitude-pressure relation of the standard atmosphere. A vernier sensitivity as low as 0.05 mm of mercury (0.002 in.) is sometimes provided with the idea of realizing this accuracy. However, the accuracy of a fixed cistern barometer is limited by uncertainty in surface tension effects in the cistern to at least 0.1 mm of mercury, as discussed in sec. 11.

5.4. Standard Barometers

A primary or standard barometer may be defined as a barometer which measures absolute pressures with precision, and requires no comparison test with another barometer to determine its errors. Perhaps, and preferably, a standard barometer is an instrument which measures absolute pressure with an accuracy greater than that of the barometer or pressure gage under test. A better term in many cases is working or secondary standard. Under the latter definition a calibrated Fortin barometer with a tube bore of 0.6 in. is a suitable standard for testing Fortin barometers with a tube bore less than about 0.4 in. Also a fixed cistern barometer when used to calibrate altimeters and aneroid barometers is a standard barometer.

Discussion here will be limited to standard barometers the calibration of which is made in terms of the basic standards of mass, length, and time and thus require no calibration by comparison with another barometer. Highly precise and accurate barometers or manometers have been constructed at the National Physical Laboratory [333, 552], Massachusetts Institute of Technology [412], International Bureau of Weights and Measures [592], and the National Bureau of Standards [545, 553]. In these a great deal of attention has been given to the reduction insofar as possible, of all sources of error and uncertainty in order to obtain an accuracy of at least 0.001 mm of mercury. Convenience in making readings, however, has had to be sacrificed to accuracy.

The National Physical Laboratory standard barometer [333] has also been constructed, with some modifications to extend its pressure range, by the South African National Physical Laboratory [557]. The Physikalisch-Technischen Bundesanstalt, Braunschweig, also has constructed a standard barometer with an accuracy of 0.005 mm of mercury [576] (see sec. 6.1.2).

All of the above instruments are of the U-tube type; other design details will be discussed in sec. 6.

A standard barometer constructed at the University of Helsinki [554], has an estimated accuracy of 0.01 mm of mercury.

For calibrating portable barometers the National Bureau of Standards has another standard barometer of the U-tube type which can be read to 0.01 mm of mercury, and has an accuracy of 0.02 to 0.03 mm of mercury. This accuracy is sufficient for most portable barometers submitted, but improvements to increase accuracy are inevitably becoming necessary as requirements for portable barometers become stringent. This barometer is briefly described in reference [491], but many of the design features will be touched upon in sec. 6.

5.5. Recording Mercury Barometers

A number of designs for recording atmospheric pressure based upon the mercury barometer were developed in the period around 1900 [301]. These never came into general use, in view of the greater convenience and portability of the barograph based upon aneroid capsules, particularly since the latter proved adequate in performance for meteorologists. Principally, the primary designs were based upon: (a) The rise and fall of a float in the mercury of the barometer cistern; and (b) the use of a beam balance to weigh either the barometer tube or cistern which varies approximately as the atmospheric pressure.

For relatively rough measurements, the height of a mercury column has been recorded by recording the change in resistance or voltage of a fine wire extending through the mercury column. The resistance or voltage drop varies regularly as the length of wire immersed in the mercury column changes and thus is a measure of the pressure. (See ref [532] and sec. 6.1.9.)

A record can be obtained of the height of a mercury column if the position of a photocell is

governed by a precision screw or other means. Since power is available to drive the screw, its angular deflection can be recorded by various means. One such recorder is described by Haynes [511] for obtaining a record of the calibration of the baroswitches of radiosondes.

5.6. High-Pressure Manometers

Mercury amalgamates with steel at high pressures, causing the failure of steel vessels containing mercury, more likely in the case of hardened than soft steel. Experiments [496] indicate that ultimate failure of steel tubes will occur at pressures in the range 4,000 to 6,000 atm. No data are available on stainless steels.

For practical reasons high pressure mercury manometers have generally been limited to about 60 ft, giving a pressure range of about 24 atm (360 psi). To obtain higher pressures, two designs are available. The first, practically useful only to calibrate piston gages, consists of a single U-tube and requires in addition two piston gages in order to transfer the measurements as the mercury column is subjected to steps of absolute pressure to the ultimate range desired, which may be many times the differential pressure measurable with the U-tube manometer. See the next section for additional details.

The second design is the multiple manometer consisting of a series of U-tube mercury columns, with the low pressure side of one mercury column connected to the high pressure side of the next mercury column. (See sec. 5.6.2.)

For measuring small differential pressures at high pressure a ring balance has had some application. (See sec. 5.6.3.)

5.6.1. Single *U*-tube High Pressure Manometers

Keyes and Dewey [271], Michels [321], and Bett, Hayes, and Hewitt [541] have constructed single U-tube mercury manometers for measuring differential pressures at high pressure. All were primarily used to calibrate piston gages. The essential features of the Bett et al., manometer are typical and will be described.

The manometer is about 30 ft high, with the tubes water jacketed to maintain them at constant temperature. The two mercury surfaces are detected by fixed electrical contacts, requiring adjustment of both the pressure and volume of mercury in the system to obtain a valid reading. Keyes and Dewey also used electrical contacts to detect the mercury surfaces, but made them vertically movable with means to measure the movement. An invar tape is used to measure the differential in height between the electrical contacts, which is necessary since compression effects can be expected to change this distance as the absolute pressure is increased. Elaborate provision is made for transferring the position of the electrical contacts horizontally to the measuring tape.

The manometer can be used to calibrate piston gages at pressure steps equal to its differential pressure range. Two piston gages are required. These, installed at levels between the mercury surfaces, are connected to the manometer, alternately to the lower and higher pressure leg of the manometer at each pressure step. The connecting lines are filled with a petroleum derivative which has relatively good viscosity characteristics at high pressure. Valves are provided to connect the piston gages to either leg of manometer, as desired.

In operation, the pressure difference of each step is determined from a knowledge of the height of the mercury column, of necessity corrected to standard temperature and gravity, and corrected for compressibility of the mercury. This pressure difference must be transferred to the piston of the piston gages, which requires a knowledge of the difference in elevation between the mercury surface and the piston, and of the density and compressibility of the transmitting liquid. To obtain pressure continuity so that the total pressure on the piston gages can be determined, a reference pressure must be established in passing from one pressure step to the next. This is done by a pressure balance on one piston gage when connected to the lower leg of the manometer (high pressure) and then, without changing the weights, connecting it to the upper leg of the manometer (low pressure). The pressure in the low pressure side of the manometer is then adjusted so the reference piston is in balance. Except for some small relatively constant corrections involving the transfer liquid column, the pressure continuity is preserved.

It is obvious that the sum of the differential pressures (plus atmospheric pressure) equals the total pressure. From the weight balancing the pressures acting on the pistons at each step, the effective area of the piston can be computed.

It is of interest to note that Bett and his coworkers plan to calibrate piston gages to 2,000 bars (nearly 2,000 atm, 30,000 psi) involving 175 transfers. Keyes and Dewey had a manometer about 28 ft high and calibrated piston gages to nearly 600 atm (about 9,000 psi). Michels avoided the labor of the continuous step-by-step process and used his manometer to calibrate piston gages against differential pressure only at selected aboslute pressures, known only approximately.

An elaborate discussion of the sources and amounts of the errors in high pressure U-tube manometers is given by Bett et al. [541].

5.6.2. Multiple Tube Manometers

Multiple tube manometers have been extensively developed for use in measuring pressure in physical experiments by Meyers and Jessup [311] and Roebuck and his coworkers Crain, Miller, and Ibser [371, 544]. The manometer of Jessup and Meyers, using glass tubes, had a range of 1,000 psi while that of Roebuck went to 3,000 psi (200 atm).

The Roebuck manometer will be briefly described. The instrument has U-tubes connected in series so as to secure nine mercury columns. The transmitting liquid from the top of one mercury column to the bottom of the next was toluene. The tubes were of steel, 1/16 in. in bore, about 1,746 cm (57 ft) high. Electrical contacts were first used to detect the position of the mercury surfaces, and later advantageously changed to a sighting device by using a section of transparent material in the tubes. Invar measuring tubes were used to measure the column heights. Many accessories were required to meet problems, notably a barostat, for details of which see ref. [544].

The differential pressure between the two terminal mercury surfaces is simply the sum of the heights of the individual mercury columns (here nine) times the difference in the densities of mercury and the transmitting liquid. Obviously the liquid column heights must be individually reduced to standard conditions which involves applying corrections for deviations from standard temperature and for compressibility of the two liquids. Further correction is needed if the pressure is desired at a level differing from that of the lower mercury surface.

5.6.3. Ring Balance

The ring balance has been applied to measuring small pressure differences at high pressure [361]. This is a torus or hollow doughnut of small cross section. At the top, the two sides of the hollow space are sealed from each other; sufficient mercury is placed in the hollow to seal off each side from the other. The gas at a slightly different pressure is fed to each compartment of the ring balance through entrances which will not affect the weighing operation to be described. The entire ring balance is hung from a knife edge placed at a point just above the center of gravity of the torus. A beam mounted on the outside of the torus permits weights to be applied to rotate the torus. When a small differential pressure exists in the ring balance, the mercury is displaced, upward on one side and downward on the high pressure side. This causes the torus and beam unit to rotate about the knife edge to a new equilibrium position. Weights are then added to the beam until the beam is restored to the original equilibrium position. The weights are a function of the differential pressure.

6. Design Elements of Barometers and Manometers

Many new developments in mercury manometry have been produced in the last few years and are still being evolved as a result of needs in various laboratories for greater accuracy and precision in measuring absolute and differential pressures. Such needs as greater speed and ease in measuring and controlling pressures and safer portability have also greatly stimulated development work. The principal directions of development and its status will be briefly discussed.

6.1. Methods of Detecting the Mercury Surface

These methods cannot always be completely separated from the means of measuring the height of the column which however, insofar as feasible, is considered separately in sec. 6.2. Quite a few methods are used to detect the position of the surface of the mercury in barometers and manometers.

6.1.1. Sighting on the Meniscus by Eye

In sighting on the meniscus by unaided eye, if there is any pretense to accuracy, a sighting ring is provided. The lower edge of the sighting ring, in front and behind the meniscus, is used as a reference and is lined up with the top of the meniscus. The sighting ring is usually attached to the vernier and must bear a known relation with the zero of the vernier in order to obtain a valid reading. This relation offers no difficulty in determination if the barometer is calibrated or its zero correction determined. It is obvious that the plane of the sighting ring should be horizontal and not move with respect to the vernier. The final adjustment of the sighting ring and vernier combination is usually made with a control screw of limited travel.

If the meniscus height is to be measured, the sighting ring is also set upon the line of contact of mercury to glass, usually with much less accuracy than on the meniscus, due to the raggedness of this line of contact and the difficulty of securing good illumination. Tapping the tube helps if done before making any settings on the mercury surface.

Illumination of the meniscus so as to sharply define the crown of the meniscus is essential for accuracy. In some situations a miniature electric lamp behind a translucent screen illuminating the mercury surface from behind has been found helpful.

It is estimated that the precision of sighting by eye probably is not better than 0.001 in. (0.025 mm). This estimate assumes optimum viewing conditions as to illumination and sharpness of the meniscus. In portable barometers and manometers the sighting precision is ordinarily not the factor that limits the accuracy.

6.1.2. Sighting on an Index

An index, such as an ivory point, which can be lowered to the mercury surface, or the mercury raised to it, is with proper illumination a very precise detecting means. If the mercury is bright, and parallel lines on paper are reflected from the

surface to viewer's eye, the point of contact can be determined to 0.001 mm (ref. [141]).

The contact is judged to be made when a small dimple in the mercury just disappears as the mercury level is lowered, or the index is raised.

The use of an index has the disadvantage of an extra operation, since it has to be adjusted before making a reading. However, in some designs it is quite feasible to make the setting automatically. The index makes an electrical contact with a small voltage output, which, amplified, can be used to operate a mechanical device which adjusts the mercury level. See ref. [453] for an example.

The index is used in the cistern of Fortin barometers to set the mercury level to a predetermined height. It may be remarked that the cleanliness of the mercury surface is preserved much longer if the index be kept aboye the mercury when readings are not being taken.

In some fixed cistern barometers a fixed index is installed in the cistern and the pressure determined when the index contacts the mercury. If subsequently this pressure is found to change, the change may be incorporated into the scale correction, or the need of other corrective action is indicated; also it is used as an indicator of the amount of mercury required for the barometer, if the barometer is shipped dry and filled with mercury in the field.

In general the use of an adjustable index on a mercury surface subject to a pressure differing from atmospheric pressure requires a stuffing box. One manufacturer, in order to increase the accuracy of a fixed cistern barometer used as a working standard, installed an index in the cistern and adjusted it through a stuffing box with a micrometer head, in this way measuring the rise and fall of the cistern mercury. The cistern was made of glass.

In the Braunschweig standard barometer [576], a fixed index is installed above the mercury surface in the vacuum space and a movable index above the lower mercury surface. Only atmospheric pressure is measured. At any pressure in its range, the mercury is forced up the tubes by a plunger in an auxilliary cistern so the upper index just touches the mercury; the lower index, together with a short scale, is then adjusted to contact with the mercury. Contact is observed with a microscope. The movement of the short scale is measured with reference to a fixed mark on the barometer support, the distance of which to each index had been previously measured.

Another manufacturer, to facilitate calibration at fixed pressures (barometer thermostatted) installed tungsten contacts at selected intervals in a glass barometer tube [495]. These were adjusted to within 0.001 in. of the desired values. By means of a selection switch a selected contact was connected to a low voltage. When the proper pressure was attained by adjustment, an audible buzzing signal was heard in earphones by the operator. Probably visual observation was also needed to make sure the contact did not dip into the mercury. This system could also be made automatic by adaptation of the means described in ref [453].

When sighting by eye on an index the mercury surface can be detected to a precision of at least 0.001 mm. With a fresh mercury surface detection by electrical contact has a precision of about 0.005 mm; this precision falls markedly as the mercury surface fouls.

6.1.3. Mercury Float

A float has been installed in the tube on the mercury by one manufacturer. A horizontal mark on the float is sighted on by eye. The barometer requires comparison with a standard barometer to determine the relation of the mark to the meniscus level.

In another design the same manufacturer mounts a thin steel disk on the float in the barometer tube. The movable sighting and vernier unit carries with it a small magnet on a shaft free to rotate. Proper alinement of the sighting device is indicated when a pointer attached to the shaft rotates to indicate zero on the vernier as a result of the force of attraction between the magnet and disk. When the sighting device is again moved so that the vernier zero is alined with the next scale division of the main scale, the pointer will indicate on the vernier the distance the sighting device has moved. From scale and vernier readings, the pressure can be deduced. Again at least one barometer reading must be compared with that of a standard barometer.

In another design by another manufacturer, the float carries a piece of magnetically permeable material. A differential transformer encircling the tube can be moved up or down to detect the position of the core piece on the float. The signal from the differential transformer is amplified to operate a servomotor to position automatically the differential transformer symmetrically with respect to the core piece. The angular motion of the servomotor is used to secure an indiction of the pressure.

For reproducible capillary error the float should be shaped so that the mercury surface always contacts the float at a fixed level. This can be secured by a sharp corner on the float where contact is made. If the mercury surface is nearly level in the vicinity of the line of contact, the depression of the float due to capillarity will be of the same order as the capillary depression of mercury in a tube having a radius equal to the clearance between the float and the tube wall.

6.1.4. Sighting With a Telescope

As a matter of convenience manometers and barometers are often read by cathetometers. To push the accuracy to the limit requires attention to the details discussed below.

In this method the observer views the mercury surface with a telescope. The telescope is mounted

on a cathetometer so that it can be raised and lowered as needed to view the mercury surface. For convenience two telescopes are best used so that both legs of a U-tube instrument can be observed independently, and with greater simultaneity. If one telescope is used and the inability to measure low pressures is permissible, the two mercury surfaces should be one directly above the other. Preferably the scale should be installed alongside of the barometer of manometer tubes, and read at some optical distance through the telescope; the need for this installation will be discussed in section 6.2. If the scale is so read, the vernier is provided by means of a reticule in the telescopes or a filar eyepiece. The reticule requires that the magnification of the telescope be fixed, so that the distance of the scale from the telescope is fixed. The filar eyepiece with its screw requires an additional reading to transfer the reading to a scale graduation.

To locate the meniscus top accurately and with ease, it must be illuminated. For this purpose it has been found reasonably satisfactory to use miniature electric lamps with a green translucent material between the lamp and mercury column. The lamp units are mounted behind each mercury column and are movable vertically by hand or preferably by small motors to the best position with reference to the mercury surface. The meniscus must be sharply defined and be without highlights. A more elaborate method is described in ref. [412].

The cathetometer must be rigidly built so as not to flex appreciably when small torques are applied which tend to turn it about a horizontal axis. The cathetometer must be free to rotate about a vertical axis and for the angle of turn needed to view the mercury surfaces and scale, must rotate truly vertical. If the axis of rotation is off the vertical one degree of arc, a rotation of 1½ deg may change the height sighted on at 2 m by as much as 0.9 mm. It must therefore be possible to plumb the cathetometer. For essential details on the design of a cathetometer for precision applications see ref. [351, 412]. For details on the alinement errors see sec. 6.6.

When the distances from the mercury meniscus and from the scale to the telescope are the same and the optical axes of the two telescopes are parallel, it is not necessary that the telescope axes be precisely horizontal. In some cases, it may be desirable to set the telescopes at a slight angle off horizontal to gain the maximum illumination. A horizontal indication of the level bubble mounted on the telescope may not necessarily indicate that the optical axis of the telescope is horizontal. To check this, the telescope is sighted on the scale and the scale reading noted; the telescope is reversed in its mounting, the cathetometer rotated 180° and the scale reading again observed. The difference between the two readings is an indication of the deviation of the optical axis of the telescope from horizontal.

Since in telescopic sighting the barometer and sighting device are separated by distances up to 5 ft it is essential, for precision measurements, that there be no relative motion of the parts while readings are in process. If mounted on the concrete or wood floor of a building, walking in the vicinity of the installation may cause measurable changes in readings. Vibrations are also troublesome. In general, for accuracy better than 0.1 mm of mercury it is necessary to install the unit in a basement room, on a foundation separate from that of the building. The working standard at the National Bureau of Standards is so installed on a separate cork-concrete platform. Other installations may be just as satisfactory; the barometer and associated apparatus described in ref. [412] is mounted on structural members of considerable rigidity.

The working standard barometer at the National Bureau of Standards used to calibrate barometers and precision aneroid barometers is of the U-tube type, utilizing two telescopes on a cathetometer for making the readings. The overall accuracy is now estimated at 0.02 to 0.03 mm of mercury (0.0008 to 0.0012 in.) with a precision of reading of 0.01 mm. The limitation, however, is probably not in the sighting means which has a precision of the order of 0.005 mm.

The ultimate in developing the telescopic sighting method is perhaps in the MIT barometer [412], where special attention was given to all sources of error or difficulty. The accuracy aimed for was 0.001 mm of mercury; that attained was estimated at 0.005 mm of mercury.

Two micrometer microscopes are used in the NPL standard barometer [333, 552], sighting on the mercury surfaces through optical flats. The settings are transferred to a line standard to obtain the column height. Only atmospheric pressure is measured, with an estimated uncertainty of 0.01 mb (0.003 in. of mercury).

6.1.5. Photocell Detector

The essential features of detecting the position of a mercury surface, with a photocell are: (a) A light source to silhouette or illuminate the mercury surface; (b) one or more photocells in a circuit to provide an electrical signal dependent on the position of the mercury surface; and (c) an indicator that responds to the electrical signal. The electrical signal is a more or less invariable function of the position of the optical system with respect to the mercury surface. The position indicator thus reads zero when the photocell is at the desired position, goes to the left or right when the photocell position is too high or low. The electrical signal, amplified, may be used to drive a servomotor which keeps the photocell at a position corresponding to the mercury surface. As an aid to detecting malfunctioning, provision is usually made for visual sighting on the mercury surface.

Restricting comments to the mercury surface

detecting system, it is seen that any change in characteristics of the light source, or the photocell, may affect the balancing position of the unit relative to the mercury surface. In a barometer used to calibrate radiosondes, [511] where photocell detection was used, a second photocell was used to compensate for changes in the characteristics of the light source. Light from the light source was permitted to fall upon the compensating photocell, the output of which was fed to one arm of the Wheatstone bridge so as to achieve compensation. This was believed necessary because it was doubtful whether the bright light source remained constant. Fully as important, and probably less easy to eliminate, is the effect of film forming on the inside tube surface. The change in intensity of the light reaching the photocell directly affects the position of the photocell, since it must move to a position admitting more light in order to secure a balanced position. In at least one device, the light passes through the barometer tube before reaching the compensating photocell. If the film is uniform in density, compensation for the effect of the film is thus achieved. If not uniform, the tube must be cleaned or replaced. However, with two photocells, any change in characteristics of either will affect the position of the photocells with reference to the mercury surface at the balance point.

A photocell detector unit has been developed [572] in which no compensation is used for the light source variation. The photocell is primarily sensitive to red and infrared so that the light source is operated at low filament temperatures, and variations in characteristics are less likely to occur. However, changes in the balancing position of the photocell detector with reference to the mercury surface can still occur if a film forms on the tube surface.

Barometers and manometers of both the U-tube and cistern types are being made with photocell detectors. In the U-tube instruments, two photocell detectors each with its own accessories are required.

One advantage, perhaps doubtful, of the power amplification possible with the photocell is that a selected pressure can be maintained. The photocell can be set to the position corresponding to a selected pressure and, instead of positioning the sighting device, the servomotor can operate a valve to maintain the pressure constant. A barostat, independent of the barometer, may be preferable for several reasons, as discussed in the section on Scale Errors.

The accuracy of commercially available barometers and manometers with clean mercury and tubes in setting the photocell detector is of the order of 0.001 in. (0.025 mm). This accuracy or precision is not realized over all. No data are available on the variation expected as the instrument and components age. One manometer [572] is stated to have a repeatability of reading within 0.05 mm (0.002 in.) which includes all sources of error in the mechanical and electronic system.

6.1.6. Capacitance Detector

Stimson [454, 553] used a capacitance type pickup in the U-tube manometer designed to measure gas pressures accurately. A steel plate, 35 mm (1.38 in.) in diameter, electrically insulated was installed above the mercury surface in each of two shallow cells 7.3 mm (2.87 in.) in diameter. A reference capacitance was installed in a shielded chamber above each cell. The electrical capacitance between the steel plate and the mercury surface is a measure of the separation between the plate and the mercury surface. A means for comparing the capacitance of the reference capacitor and the mercury capacitor is provided. One of the two cells is wrung to a pile of Hoke gage blocks (end standards) so its height can be changed.

A description of the measuring procedure will aid in visualizing the design. First the pile of gage blocks under the movable cell is found that will make height of the steel plates in both cells nearly the same. The cells are evacuated and the mercury level is adjusted so that the separation between the mercury meniscus and the steel plates is approximately 0.15 mm. One reference capacitor is then adjusted slightly so that each reference capacitor has a value equal to the capacitance between its steel plate and the mercury surface. The pressure to be measured is applied to the mercury surface in one cell and the other cell (still evacuated) is raised on a higher pile of gage blocks. The quantity of mercury in the system and the pressure are then adjusted so that the capacitance of the mercury to the plate in each cell is equal to its reference capacitance. The change in height of the pile of gage blocks is the measure of the pressure applied.

The precision of detecting the vertical position of the mercury surface in this manner stated to be less than 0.0001 mm (4×10^{-6} in.).

Los and Morrison [513] used the capacitance between an invar plate and a mercury surface to measure differential pressures in the range 0 to 2.5 mm of mercury (0.1 in.). The variation in beat frequency of two oscillators to which the capacitances were singly connected served to measure the pressure. Column heights were not measured directly, so that calibration was necessary, for which an improved design of McLeod gage was used. Data are given to show the nonlinearity of beat frequency with change in height of the invar plates above the mercury surface. In this design a precision of 0.1 to 0.2μ of mercury was claimed for the range 0 to 0.2 mm of mercury, and 0.1 percent or better for the range above 0.2 mm of mercury.

6.1.7. Optical Reflection Dectors

An optical probe which is being applied to a U-tube barometer has been developed by the National Physical Laboratory [573]. The U-tube barometer is vertical while the optical probe is hori-

zontal, a right angle prism being used to transmit reflections from the mercury surface to the probe. Two horizontal tubes movable as a unit on a track have their axes intersect at a selected angle. A light source at the end of one tube passes through a grid to the mercury surface. The light reflected from the mercury surface passes through the second tube and through a grid exactly similar to the first. If the mercury surface is precisely at the intersection of the two tube axes, maximum illumination is received at the exit of the second grid. At any other position the brightness of the light at the exit is less. The accuracy of setting is stated to be about 0.5μ (20×10^{-6} in.).

For detection of brightness a photocell is placed at the exit of the second grid. For reference a second photocell receives some of the reflected light from a lightly aluminized glass plate placed ahead of the second grid. The output of the two photocells is amplified and passed through a Wheatstone bridge, which in the balanced condition indicates the maximum brightness of the reflected light coming through the second grid.

The optical tubes are mounted on precision ways for adjusting their position to that where the light received by the grid exit photocell is a maximum. A fixed line standard, with optical accessories for viewing, serves to measure the position of the tubes on the ways. Alinement of the ways must be held within close tolerances; the errors introduced, and their amounts, are discussed in ref. [573].

The barometer, not discussed in ref. [573], consists of a stainless steel U-tube, 4 in. in diameter. The range is 1 atm or more. Any glass plate between the light and mercury surface should preferably be optically flat.

In order to obtain observations on the two mercury surfaces, the difference in height of which is to be measured, two optical probe systems as described above are used. These can be coordinated by measurements made when both legs of the barometer are subjected to the same pressure.

Another optical probe, described by Moser [555, 575], detects equality in the meniscus curvature. It was used to establish the equality of two pressures and, while possibly applicable in detecting a mercury surface in connection with precise pressure measurement, has not so far as is known been so applied. A brief description of the probe as used may be of interest.

The operation of the probe depends upon the fact that at a hole ending with a sharp edge the mercury meniscus is captured by the sharp edge. Moser desired to obtain an equality of gas pressure in two systems. The gas pressures from the two systems were brought into two vertical chambers about 3 mm in diameter and 15 mm high. The bottom ends of these chambers ended in sharp edges, at the same level, in a manifold filled with mercury. The tops of the chambers were sealed with glass windows. Gas pressures were adjusted in the chambers till the menisci were nearly plane at the sharp edges. Light from point sources above the chambers passed down through 45° semireflecting plates, through the chamber windows to the mercury menisci, whence they were reflected back through the windows to the 45° plates, and out horizontally to telescopes. Small changes of pressure in the chambers changed the curvature of the menisci. When the radii of curvature were equal to half the distance to the point light sources the reflected light beams became parallel and the field was uniformly illuminated. The uncertainty of equality in the pressure settings was said to be ±0.002 mm of mercury.

6.1.8. Interference Fringes

Terrien [592] describes three ways in which interference fringes from two mercury surfaces can be used to detect the relative vertical distance apart of the mercury surfaces. In all cases the length of the significant light paths must be equal. This is secured by a mechanical adjustment of the position of a reflector or reflectors, the amount of which is used as a measure of the column height.

One of the methods originates in Japan, another in Russia, and the third is due to Terrien. Briefly, in the design due to Terrien, a beam of white light is split by a half-silvered surface. One beam passes through a Michaelson interferometer, and is reflected to one of the mercury surfaces. The other beam is reflected to the other mercury surface. Upon reflection the beams reverse their paths and are reunited as they issue from the interferometer. If the optical path lengths are exactly equal, and if the mercury surface has infinitesimal ripples, a condition difficult to prevent, the observed fringes are white, not colored. The fringes are detected by a photocell. To obtain exact equality in the light paths two horizontal prism reflectors are adjusted horizontally as a unit. The amount of the horizontal motion is a measure of the height of the mercury column.

Both the Japanese and Russian interferometer methods require two light sources.

6.1.9. Resistance Wire

One method of transducing a pressure to an electrical quantity which can be easily recorded, or indicated as desired, is to stretch a wire through the mercury column. A voltage is applied to the upper end of the wire and to the mercury. The electrical resistance of the wire must be greater than that of the mercury column; sensitivity increases with difference in resistance per unit length. As the mercury column falls, the resistance of the circuit rises.

Either the resistance of the circuit is measured with a Wheatstone bridge or the drop in potential with a potentiometer. The use of a recording potentiometer is discussed in ref. [532]. A nichrome wire has been used [501, 532]; a carbon

rod [543]; and in tandem, a 9H lead from a lead pencil and a steel wire to complete the electrical circuit [562].

Apparently none of the experimenters with this form of pressure indication required high accuracy, since in most cases rather small bore tubing was used. Variable capillary effects can be expected to affect the accuracy, both at the glass and mercury surface and at the wire and mercury surface. About the latter boundary not much can be done to effect an improvement beyond an uncertainty of several tenths of a millimeter. This limitation seriously limits the method in any application to really precise and accurate measurements. Its convenience merits its use when high accuracy or precision are not required.

6.1.10. Gamma Ray Pickup

This method of detecting a mercury surface is useful in measuring differential pressures at high pressure where a steel tube must be used to secure adequate strength [514]. A narrow beam of gamma rays from a radium source are projected through the tube. On the other side of the tube an ionization chamber is placed. The ionization chamber and radium are mounted as a unit with an indicator of their position on a scale. A discontinuity in the intensity of received gamma radiation received by the ionization chamber is observed when the unit moves vertically by the mercury surface. A precision of $\pm \frac{1}{2}$ mm is claimed.

6.2. Measurement of Mercury Column Height

Methods of measuring the height of a mercury column have been discussed to some extent in previous sections but some elaboration is needed. A simple, widely used, method is to visually estimate the height of the column by comparison with a scale alongside of the mercury column, either with or without a sighting ring.

Refinements in measuring, to which further discussion is limited, are: (a) the use of a scale and vernier; (b) a cathetometer; (c) a precision screw; and (d) gage blocks.

6.2.1. Scale and Vernier

Ordinarily the scale is a separate member, more convenient to calibrate in this form, which is attached to the structure supporting the glass tubes containing the mercury. A sighting ring, free to slide or controlled in position by a rack and pinion arrangement, and a vernier with its zero alined with the sighting ring, form a unit. In taking a reading the bottom of the sighting ring is alined with the top of the mercury meniscus and its position determined on the scale.

Verniers are customarily made with a least reading not below 0.05 mm or 0.002 in., since the overall accuracy achievable does not warrant greater precision.

Scales on portable instruments are commonly made of brass. In one design a plastic scale is used, which is discussed in sec. 6.8.

For precise measurements of pressure the scale must be ruled on a first class ruling engine under controlled conditions of temperature. If the reference temperature for the scale is 0° C, a convenient, but not necessarily essential reference temperature, the ruling engine can be manipulated so that the scale is accurate at 0° C. This practice is commonly followed, theoretically at least, for portable barometers, with one exception. This exception is the Fortin barometer commonly used in meteorology the scale of which when in inches of mercury is graduated to be accurate at 62° F. The scale so graduated is becoming obsolete because meteorologists now use the millibar as the unit of measurement, and transition is well under way to barometers so calibrated. The temperature at which scales may be graduated to be accurate will be discussed in more detail in the section on temperature errors.

Scales attached to the barometer or manometer have to be read by an observer so close to the barometer, that he affects its temperature. Since this affect is normally a transient, some uncertainty is introduced in the accuracy of the measured temperature of the barometer, particularly since in most instrument designs the thermal lag of the thermometer, of the scale, and of the mercury all differ measurably. This uncertainty can be reduced, if the desired accuracy justifies it, by obvious expedients, such as reading the thermometer before initiating the pressure measuring process and by making the thermal lag of the thermometer about the same as that of the mercury in the barometer. This effect is mentioned here, because it is one of the principal reasons for instrument designs in which readings are made by an observer at a distance from the barometer or manometer [563].

6.2.2. Cathetometer and Scale

In the preferred method, used as long ago as 1889 by Professor Morley in determining the density of air, a scale is placed alongside of the mercury tubes and is read through a telescope or telescopes mounted on a cathetometer. The telescopes are from about a foot to six feet away from the scale and tubes in the various designs. The mercury meniscus and scale should be at equal optical distances from the focal plane of the objective lenses of the telescope.

The other method is to locate the mercury mensicus with the telescope mounted on the cathetometer and determine its height by reading the position of the telescope on the scale attached to the cathetometer. This method is not usually used in precise work unless the telescope is quite close to the mercury column, in itself undesirable because of uncertainties introduced in the mercury and scale temperature. The objection to the method is the necessity for maintaining the optical axes of the telescope or telescopes horizontal

within close limits. For example, if the telescope objective is 1 m away from the scale, the telescope axes must be held horizontal within 3½ min of arc in order to avoid errors up to 0.1 mm in measurement. This source of error is practically eliminated in the preferred method.

Returning now to the preferred method, the scales may be either of invar, stainless steel or other reasonably noncorrosive material with a known temperature coefficient of expansion and stable in dimensions. They are graduated in either 0.5 or 1.0 mm divisions. If the barometer or manometer is of the U-tube type and is to be used as a standard, it is only necessary to have the scale calibrated against a standard scale and to establish or know its linear coefficient of expansion in order to apply the correction for temperature. If the scale is calibrated at a temperature close to that of its use, less accurate knowlege of its coefficient of expansion is needed.

To determine subdivisions of the scale divisions, that is fractions of 0.5 or 1.0 mm, two methods have been followed. In the first, a sight is taken on the mercury meniscus, the telescope is rotated about a vertical axis to sight on the scale and the telescope raised or lowered until the sighting cross hair is coincident with a scale division. A micrometer screw is used to raise or lower the telescope and is read to give the fractional scale division. Thus two adjustments of the cross hair position are required. In the other method a reticule is placed in the focal plane of the telescope, and can be used as a vernier when the telescope is at the proper distance from the scale, a distance which can be adjusted when installing the cathetometer. In taking a reading the cross hair in the telescope is brought into coincidence with the mercury meniscus, the telescope rotated to the scale and the reading obtained similarly as on a scale with a vernier.

From experience limited to one arrangement of a reticule it was found that considerable training is required to obtain reliable readings and that some attention must be paid to the illumination in order to distinguish clearly between the divisions of the scale and of the reticule. It does have the advantage that only one adjustment of cross hair position is needed.

6.2.3. Precision Screw

Use of the rotation of a precision screw to measure the height of a mercury column appears to be the logical method if automatic indications are desired; particularly if mechanical means are used. The lead screw, mounted in a vertical position, can be used to raise or lower the sighting mechanism. A counter connected to the screw by means of a gear train may be used to count the revolutions of the screw and so provide a digital indication of the pressure. A photocell detector of the mercury surface position, or other sensing device which provides an electrical signal indicating the position of the mercury surface may be used to drive a servo system connected to the screw to achieve automatic positioning of the sighting mechanism.

There is nothing to preclude the use of the precision screw as a means of manual measurement of the height of the mercury column, though it may not prove practical, except as a check on the automatic reading. It is merely necessary to have a sighting ring adjusted by manually rotating the screw through gearing and read the rotations of the screw on a suitable indicator.

The screw can be made to measure as precisely as desired, possibly to a part in 100,000, for the length required in barometers. The only barrier is the expense in securing the precision, which of course increases as the length of screw increases. Uniformity of pitch is highly desirable. The pitch will vary with temperature for the materials of which the screw would ordinarily be made, but this effect on the accuracy can be eliminated by maintaining the barometer or manometer at constant temperature or by applying corrections. The latter procedure in the present applications of the screw to manometry will prove inconvenient.

6.2.4. Gage Blocks

For high accuracy, Stimson [454, 553], has used gage blocks, calibrated to two parts in a million, to measure the height of the mercury column in a manometer. The manometer is of the U-tube type; it has articulate joints in one leg, and the mercury menisci are in cells of large diameter in order to minimize errors from capillary depressions. The amount of the mercury and the pressure can be adjusted to bring the mercury menisci to reference positions in the cells. These reference positions are determined with the capacitance pickup, described in sec. 6.1.6. The height of the pile of gage blocks for the zero reference is obtained when both cells are evacuated. When gage blocks are subsequently added and the pressure adjusted to bring the mercury to the same reference positions in the cells, the added blocks give the direct measure of the height of the mercury column.

Obviously to realize the accuracy inherent in the use of the gage blocks, many precautions must be taken. Principally, temperature control and temperature equilibrium to about 0.01° C before taking a reading are both necessary. Coupled with the necessity of obtaining a zero reference reading sometime before and after each pressure determinations, it is seen that pressure measurements are a time-consuming operation. In the present state of the development, realizing the accuracy possible from gage blocks is essentially a research operation.

6.3. Illumination of the Mercury Surface

For sighting on the mercury meniscus by eye, guided by a sighting ring, only simple means of illumination are justified. If the installation is such that the mercury meniscus is poorly defined

in daylight, it is only necessary to install a low-wattage (flashlight) lamp behind the mercury meniscus with a ground glass, or better a green translucent paper, in front of the lamp. A similar arrangement helps with setting the index in the cistern of Fortin barometers.

For more precise measurements made by sighting on the meniscus with a telescope, the above described lamp installation is often adequate. The height of the lamp and diffuser assembly can be best adjusted by a small motor operated by the observer. The adjustment of the lamp height may be critical in order to obtain a well-defined meniscus repeatably the same. Highlights on the mercury meniscus from other sources of illumination can be troublesome but can be avoided by shielding or better by eliminating the sources while making a setting.

In order to secure the ultimate in precision in sighting on the meniscus through a telescope, experimenters [333, 412], agree in the necessity of having parallel or nearly parallel light on the meniscus. A further refinement, [412], is to have the illumination nearly parallel in the vertical direction, but diffuse horizontally; this illumination can be secured with a cylindrical lens. In the end, experimentation is necessary to determine the invariant optical configuration associated with the meniscus on which to sight. This may be an outstanding reflection from the meniscus, rather than the outline of the meniscus, which may be indefinite when a precision of the order of 0.001 mm is desired.

6.4. Vacuum Above Mercury Column

This discussion relates only to instruments where a vacuum must be maintained above the mercury column. In fixed cistern and Fortin barmometers used only to measure atmospheric pressure, no provision is made, beyond a careful procedure in filling the barometer tube, for maintaining the vacuum. The design is usually such that, following a precautionary procedure to prevent admitting air into the tube, the barometer can be tipped upside down, or better if the design permits nearly horizontal with the upper end of the tube lower than the cistern, and the air bubble removed by tapping the tube. This procedure in the hands of experienced persons is usually reasonably effective. However, in practically all barometers a small gas bubble will be visible when the barometer is tipped just enough to fill the tube with mercury, in fact will also exist in freshly filled barometers.

The situation is not serious in barometers used solely to measure atmospheric pressure. Such barometers are known to have maintained a satisfactory degree of vacuum for many years without attention.

The procedure of filling a barometer tube may be of interest. First, the tube must be clean. In filling the tube with mercury by any practical procedure it is almost necessary that the mercury be above 100° C in order to eliminate water vapor entirely. In the end the only really satisfactory method is to distill the mercury into the tube in a system which is kept evacuated, preferably with a diffusion pump. The tube being filled should be kept at a temperature somewhat above 100° C and should be outgassed by well known procedures before the filling operation.

The situation is different in fixed cistern barometers which are more or less continuously used to calibrate altimeters and aneroid barometers where large cyclic changes in the pressure in the cistern are required. In a relatively short time of such use, the vacuum seriously deteriorates. If the space above the mercury column is observed in a darkened room while the pressure in the cistern is reduced, luminescence of the mercury vapor in the tube will be seen, probably caused by the discharge of an electrical charge on the walls of the tube resulting from the contact difference of potential between the mercury and glass. This seems to accelerate the formation of gaseous products or promote outgassing of the glass. In any event painting the outside wall of the glass tubing, but not where it would interfere with visibility of the meniscus, with a metallic electrically conducting paint greatly reduces the rate at which the vacuum deteriorates.

To facilitate removal of gas above the mercury column, fixed cistern barometers are designed so that the open end of the glass tube is covered by the mercury in the cistern, independent of its orientation, vertical, horizontal, or upside down. This makes it possible to eliminate much of the gas from the tube by a simple procedure. The cistern is evacuated, the barometer is oriented to an almost horizontal position with the open end of the tube a little above the closed end, thus tremendously increasing the volume of the gas bubble by reducing the pressure. As mercury flowed back into the tube the gas bubble moved up the tube and out. However, for complete removal the bore of the tube at the open end has to exceed 3 mm.

Shipment of fixed cistern barometers has also been a problem. Usually the barometer has been shipped in an upside down position, suspended in a box, but breakage of the tube due to rough handling occurred frequently.

6.4.1. Mercury Sealed Valve

The situation just described led to the development of barometer tubes with a mercury sealed valve at the top. Barometers with these tubes are shipped unfilled with mercury, and thus more safely, and the procedure of maintaining a vacuum is much simplified. The valve is so designed that it opens outward, but is normally kept closed by a force, usually produced by its own weight. A small cup around the seal holds a small amount of mercury for a more positive seal. The gas that accumulates above the mercury column may be

removed by evacuating the space above the seal while the mercury in the tube is forced up by applying pressure to the system until it is forced out through the mercury seal. It is sometimes necessary to manually lift the valve slightly off its seat to permit the gas bubbles to escape. Some idea of the quantity of gas in the tube can be obtained by observing the number of bubbles that come through the mercury seal.

With this valve, a barometer can be shipped free of mercury and the mercury added at the place of installation. Securing a vacuum requires many repetitions of the above described procedure at intervals up to a week, and the procedure can be repeated when there is any doubt about the vacuum.

6.4.2. Pump

The vacuum above the mercury column can be maintained by the use of a vacuum pump, which can produce a vacuum better than the accuracy required for portable barometers. These pumps are operated while the barometer is being used.

For standard barometers and where high precision in absolute pressure measurement is desired, more elaborate pumping systems are used. In its simplest form, the top of the tube is connected to a diffusion pump backed up by a mechanical vacuum pump. To prevent oil vapor from the diffusion pump entering the barometer vacuum system, a liquid air trap can be used. To measure the vacuum a McLeod gage or other type vacuum gage may be connected to the system.

6.5. Tubing

At present for portable barometers, precision bore Pyrex tubing is generally used. There is some evidence that less chemical interaction and less scum develops at the mercury-glass interface with some other kinds of glass, but any definite conclusion is probably debatable in the present state of our knowledge.

Precision bore tubing apparently has satisfactory optical properties in the bore, but its external surface may have irregularities which deviate the light rays as they pass from the glass into the atmosphere. Thus the position of the meniscus as seen may be up or down from its position. This deviation may be called a prismatic error since it is similar to the deviation of rays passing through a prism. The deviation is generally kept within bounds by selection of the tubing and in occasional cases by grinding the outside of the precision bore tubing to uniformity.

Precision bore tubing is exceedingly useful in fixed cistern barometers and manometers and in U-tube instruments where the height of mercury in only one leg is measured. When using precision bore tubing the scale contraction is a constant; if the tubing were irregular in bore, the difference in the two column heights would still be unchanged, but the scale error of the readings on a single scale would fluctuate with the irregularity in the bore.

As will be discussed in detail in sec. 11, the uncertainty in capillary error can only be reduced by increasing the bore of the tubing. Barometers with any pretense to accuracy must have a tubing bore of at least ¼ in.; the uncertainty in pressure measurement for this bore is about 0.01 in. of mercury (0.25 mm). Increasing the bore to 0.6 in. (15 mm) lessens the uncertainty to about 0.004 in. ($\pm$0.10 mm), if no capillary corrections are made to the readings.

In precise measurements, if the mercury meniscus is sighted upon through glass, the tubing is enlarged at the sighting levels and optical flats form part of the mercury container in the line of sighting. (See ref. [333].)

If metal tubing is used in whole or in part, steel or preferably stainless steel must be used. Most other metals amalgamate with mercury. Barometer or manometer cisterns are generally made of stainless steel or glass.

6.6. Alinement of Scales and Sighting Devices

In manometry it is necessary to measure the vertical height of the mercury column. The errors introduced by misalinement of the scale and accessories, may be divided into two types, one the cosine error, the other the sine error.

The cosine error is caused by the scale not being vertical; it, in general, equals the scale reading times 1-cos a, where a is the angle of tilt. An error of one part in 10,000 is produced by the scale tilting 49 min of arc. There is usually no difficulty in reducing this error to practical limits, by adjustments provided in most portable barometers. Most barometers designed to hang from a hook do not hang vertically; their scales are adjusted to be vertical by means of a separately supported ring encircling the cistern, with screws to control its horizontal position. Platform barometers and manometers are provided with leveling screws.

The sine error is some function of the separation of the mercury columns, or the distance of the scale from the mercury columns, or some other distance significant in the measurement; all multiplied by the sine of the angle of misalinement. It usually occurs when a measurement requires transfer from one vertical to another. In general, the sine error is a constant, independent of the height of the mercury column, if the misalinement does not vary in amount. It is often corrected for as part of the zero error, discussed in section 8.1, and indistinguishable from other causes of it.

In general the sine error equals the pertinent distance times the sine of the angle of misalinement; for an error of 0.1 mm, this angle is 34 min of arc for 1 cm of distance, 17 min for 2 cm, or for an error of 0.01 in., 34 min of arc for 1 in. of distance. Several examples of sources of this error are outlined below.

Some barometers, such as the Fortin, are equipped with a zero index in the cistern for setting

the mercury surface in the cistern. If the scale does not hang vertically, both a sine and cosine error are introduced. The sine error equals the product of the distance of the index to the center of the tube times the sine of the deviation angle. To eliminate the sine error, the Fortin barometer is adjusted to hang so that, upon rotating the barometer, the relative vertical position of the index and mercury surface in the cistern is invariant. If the scale is then vertical, the cosine error is also eliminated.

In sighting upon the mercury meniscus with a telescope, with the scale attached to the cathetometer, the sine error is proportional to the distance of the scale to the mercury column. To reduce the error to a reasonable amount, the optical axis of the telescope must be maintained horizontal within excessively close limits; therefore this location of the scale should be avoided, as discussed in section 6.2.2.

In making readings with a telescope, where the scale is in the preferred position along side of the mercury column, a sine error may be introduced if the cathetometer does not rotate about a true vertical axis. If the cathetometer axis is displaced from the vertical at right angles to the vertical plane of sight, the sine error is a maximum; if tilted in the vertical plane of sight the sine error is zero. Assume, for example, that a scale is between the two legs of a U-tube barometer. To transfer the observed level of one meniscus to the scale, assume that the telescope sighting line runs uphill; to the other meniscus it runs downhill. If the maximum rotation of the cathetometer required is over an arc l at the scale, and A is the angle of tilt of cathetometer axis in the vertical plane at right angles to the plane of sight, the rise r of the sighting line of the telescope is to a good approximation $l \sin A$. For the practical case of an arc length of 10 cm a total rise r, or an error, of 0.1 mm is obtained for a tilt of about 4 min. The large effect of small tilts indicates the necessity of reducing the transfer distance l to the minimum and most important, the need for a rugged, rigid cathetometer, since constancy in axial alinement is a primary necessity.

If the ways along which a sighting ring and vernier unit of an instrument slide are not vertical in the vertical plane of sighting, a sine error is introduced. If the scale is not vertical, a cosine error is additionally introduced. The sine error equals the product of the distance of the scale from the center of the tube and the sine of the angle of tilt. For a distance of 2 cm and an error of 0.1 mm the tilt of the ways is 17 min of arc.

Misalinement giving rise to the sine error which varies with the reading can be avoided to the degree needed for the designed accuracy by good design and care in the construction of instrument.

6.7. Instrument Temperature

If the uncertainty in pressure measurement is to be held to 0.01 percent (0.1 mb at 1 atm) the mercury temperature must be known within $\pm 0.6°$ C, and proportionately smaller for better accuracy. The scale temperature, if brass, needs to be known to only approximately ten times this uncertainty (that is 6° C) for the same accuracy limits (0.01%). For precise pressure measurements it is seen that the mercury temperature must be known to very close limits, which involves both the measurement and control of temperature.

6.7.1. Measurement of Temperature

In simple portable barometers the temperature is measured by mercury thermometers, with their bulbs imbedded in a metal shield. Thermal lag is thus introduced in the thermometer which it is hoped will equal that of the mercury in the barometer or manometer, but in the nature of things, can only approximate it. A better arrangement sometimes used in laboratory instruments is to place the thermometer in a tube of mercury, more or less simulating the barometer tube [576]. Since at best the mercury thermometer cannot be depended upon for an accuracy better than 0.01° C, resistance thermometer or thermocouples are preferable when better accuracy is needed.

It is generally assumed, probably without significant error, that the scale and mercury column temperatures are identical. In view of the lower temperature coefficient of the scale, the error is held to a minimum if the effort is directed to obtaining the mercury temperature.

In the absence of continual control of the instrument temperature, special attention must be given to thermal lags if the ambient temperature is varying or has varied. It takes hours for an unventilated barometer or manometer to come to temperature equilibrium with its surroundings after an abrupt shift in the ambient temperature. See ref [563] for some data. The thermal lags of the barometer and attached thermometers in spite of all effort are unlikely to be the same. Within limits the two temperatures, instrument and thermometer, are reasonably identical only if the thermometer reading has not changed appreciably, say a few tenths of a degree, over a period of time, say at least ½ hr.

In portable barometers where the observer performs operations while standing close to the instrument the temperature is influenced if the barometer temperature differs from body temperature. With care to reduce this time to the minimum, and by reading the thermometer first, this uncertainty can be reduced to manageable limits, say of the order to 0.2° C.

6.7.2. Control of the Temperature

Two methods of controlling the temperature of the instruments are in use. In the first, the barometer is enclosed in a cabinet in which air is circulated and thermostatted at a selected temperature above the expected ambient temperature. This temperature should be as low as practical in

order to avoid evaporation of mercury into the cooler lines where amalgamation of metal and mercury may occur. Generally the cabinet is divided vertically into two compartments except for necessary ducts; the barometer or manometer is installed in one and the electrical heater and circulating fan, in the other. The thermostat is in the same compartment as the barometer. The air is forced to flow in a circuit, down the heater compartment and up the barometer compartment. Refinements are incorporated in order to eliminate temperature differences along the length of the barometer, but these cannot be eliminated entirely, since even with no heat exchange the temperature falls nearly 0.01° C/m of elevation, i.e., adiabatic change.

The other method is to install the barometer in a room in which the temperature is maintained constant. Primary standards and others where high precision is required are usually so installed. A subbasement room is desirable because its temperature will have a smaller diurnal variation. Generally such a room will require a source of both heat and cooling, thermostatically controlled. Ventilation will be required, so directed as to eliminate vertical temperature gradients as far as practical. The closeness and stability of the temperature control is determined by the accuracy desired in the pressure measurements.

Controlling the instrument temperature with reasonable accuracy must be continuous night and day because securing thermal equilibrium of the instrument with its surroundings requires many hours.

6.8. Automatic Compensation for Temperature and Gravity Error

Both the corrections for deviation from standard temperature and gravity are directly proportional to the height of the mercury column, as discussed in detail in secs. 9 and 10. Mechanical means have been developed so that readings on fixed cistern barometers may be automatically compensated for these errors.

In one design a long auxiliary rod is hinged at the zero of the scale and is adjustable angularly about a horizontal axis. Actually, the hinge is slightly below the scale zero in cistern barometers in order to include a correction for the change in mercury height in the cistern with temperature. Any change in angular position thus causes a vertical displacement at any point along the rod which is a function of the radius, i.e., the barometer reading. The sighting device and vernier unit is connected to the rod through a lever system and is free to slide up or down the rod as a unit during adjustments needed to make a reading. The arrangement is such that when the auxiliary rod is vertical, the vernier position is unaffected by the lever system. This corresponds to zero temperature and gravity correction. If the auxiliary rod deviates angularly from its vertical position, the vernier is moved up or down relative to the sighting device by the lever system. The amount of motion of the vernier is proportional to the chord defined by the deflection of the auxiliary rod from the vertical. This chord length is approximately proportional to the height of the mercury column. Two additive adjustments of the angular position of the auxiliary rod angle are provided, one for gravity error and one for temperature error compensation. The auxiliary rod can be manually set to the angular position corresponding to local gravity and then to an angular position determined by the measured instrument temperature. A scale graduated in gravity units and one graduated in temperature are provided to indicate the adjustment to be made [515].

The permitted angular motion in one design is about 2 deg, while about 6 deg is needed. This need is taken care of by amplification of the rod motion by the lever system.

Another design of mechanical automatic compensator for temperature and gravity error has been developed. A fixed vertical rack is used instead of the hinged rod. A gear forming part of the vernier and sighting unit of the barometer runs on this vertical rack. A screw on the same shaft as the gear positions a wedge in contact with a lever which controls the vertical position of the sighting device. The rack makes this control proportional to the height of the mercury column and thus to the temperature and gravity correction. The gravity and instrument temperature for which correction is desired can be set into the corrector by manual adjustment of the angle the control lever makes with the horizontal.

A variation of the design just described and developed by the same manufacturer depends upon a vertical wire extending the entire scale length. A pulley attached to the sighting device and vernier unit has the wire looped around it, so that its angular motion, as the sighting device moves up and down, is proportional to the height of the mercury column, and thus to the gravity and temperature correction. Through a system of gears, a rack, and a lever the sighting device and vernier position is controlled as a function of the height of the mercury column. By this design sliding contacts are eliminated. The effective radius of the lever is adjustable, by which the gravity and temperature for which correction is desired can be set into the corrector.

A novel method of automatic compensation for temperature error which is also commercially available is the use of a plastic scale which is stretched between rigid supports to a length determined by the mercury temperature and local gravity. As the scale is stretched the distance between scale graduations is expanded proportional to its length starting at the bottom. This gives readings corrected for temperature as required. A scale graduated in temperature units indicates the degree of stretch necessary.

It is obvious that the extension of the plastic scale between two temperatures is the sum of the

linear expansion of the scale support with increase in temperature and an extension produced by the adjustment of a screw. The total stretch must be repeatable time after time, that is, the scale must be taut when in use. In the design now available this condition is met for temperature variations ordinarily experienced by the instruments.

The accuracy of automatic compensators need be considered practically only for the range of temperatures differing from the temperature at which the instrument is calibrated. At the calibration temperature of the instrument, the error is automatically incorporated into the scale error, or adjustments made on the instrument to correct it. The accuracy on this basis can be held to ± 0.1 mm of mercury (0.004 in.), perhaps even better, an amount which is well within uncertainties in measurement due to other causes.

6.9. Damping and Lag

Mercury column instruments have little application in making dynamic pressure measurements. However some remarks on the dynamic characteristics may be pertinent.

Damping is usually necessary and generally incorporated in the form of a restriction or a short length of capillary tubing between the two legs of a U-tube instrument or in between the tube and cistern of a fixed cistern instrument. This damping reduces the effect of undesired column pulsations or pumping, such as would occur on an undamped barometer on a ship at sea.

Consider a manometer consisting of a U-tube connecting two cisterns of equal area. Assume it filled so that a mercury surface exists in both cisterns. In oscillation the differential equation governing the motion is, assuming laminar flow:

$$\frac{\rho L A_c \ddot{x}}{A_t}+\frac{8\pi\eta L A_c \dot{x}}{A_t^2}+2\rho g x=0. \tag{13}$$

From which it follows that the period T is

$$T=\frac{2\pi}{\left[\frac{2g}{L}\frac{A_t}{A_c}-\frac{16\pi^2\eta^2}{\rho^2 A_t^2}\right]^{1/2}} \tag{14}$$

and the undamped free period T_0

$$T_o=2\pi\left(\frac{A_c L}{2A_t g}\right)^{1/2}. \tag{15}$$

For critically damped motion the two terms in the denominator of eq (14) are equal, achievable by controlling A_t. Separating the variables with which damping may be controlled from the constants, this equality becomes

$$\frac{LA_c}{A_t^3}=\frac{\rho^2 g}{8\pi^2\eta^2}. \tag{16}$$

When the column oscillates at about 0.8 of the critical damping, it will return to rest in a time equal to 67 percent of the free period T_0, which appears to be an optimum value for the damping. On this, eq (16) becomes

$$\frac{LA_c}{A_t^3}=\frac{0.8^2\rho^2 g}{8\pi^2\eta^2}. \tag{17}$$

In the above equations:

L=length of the tubing connecting the cisterns
A_c=area of each cistern
A_t=internal area of the tube
x=displacement or amplitude of the oscillation of the mercury in the cistern from its equilibrium position
$\dot{x}$=velocity of the mercury in the tube
$\ddot{x}$=acceleration of the mercury in the tube
ρ=density of mercury
η=viscosity of mercury
g=acceleration of gravity
T and T_0=period and undamped free period of oscillation of the mercury column, respectively.

Equation (15) shows that the undamped mercury column has a free period depending only upon its length and the ratio of the areas of the cistern and tubing. Ordinarily this period cannot be found experimentally because of the viscous damping of the flowing mercury, and the restriction offered to flow by the finite size of the tubing.

7. Sources of Error

Ordinarily the readings of portable barometers and manometers are corrected only for scale errors and for deviations of the instrument from the standard temperature and gravity. The scale error is determined by a calibration of the portable barometer against a standard instrument. It includes a correction for many other factors, including capillarity and vacuum, which while assumed to be constants, may change with time. For measurements to the limit of accuracy of most portable instruments this assumption is reasonably tolerable.

The situation is quite different for instruments from which a high degree of accuracy is required. More corrections, and to higher accuracy, must be made, and of course, greater care must be exercised in designing the parts significantly affecting the accuracy and in controlling the

environment of the barometer. The following table illustrates the situation for barometers, where corrections and controls are given to secure in one case, an accuracy of 0.1 mm of mercury and in the other, 0.01 mm of mercury in each factor. Obviously to increase the overall accuracy of the measurement, each factor must have a proportionately smaller tolerance.

The overall error can be easily held within 0.1 mm of mercury except for the temperature uncertainty, zero stability and capillary depression. Some care is necessary to be certain that the barometer temperature is known to an accuracy well within 0.8° C. The change in capillary error with time is such that in barometers with tubes less than about 12 mm bore, calibration will be frequently needed. For this a criterion is the degree of fouling of the mercury surface. For fixed cistern barometers, particularly if the cistern is opaque so the surface can not be seen, the zero shift in calibration due to volume changes in the cistern meniscus probably limits the accuracy at best to 0.1 mm of mercury.

The tolerance for each factor is for an error in that factor of either 0.10 or 0.01 mm of mercury.

Accuracy, mm of mercury— / Inch of mercury—	0.10 / 0.004	0.01 / 0.0004
Factor	Tolerance	Tolerance
1. Zero error (stability of zero)—mm	0.10	0.01
2. Scale error (reliability of scale)—mm	.10	.01
3. Sensitivity of vernier or detecting means—mm	.10	.01
4. Temperature uncertainty at 1 atm—° C	.8	.08
at ½ atm—° C	1.6	.16
5. Capillary depression error—mm	0.10	.01
6. Alinement uncertainty (sec. 6.6):		
(a) Cosine error, at 1,000 mm of Hg	0°49′	0°15′
(b) Sine error, in practical cases	4 to 10′	0.4 to 1′
7. Vacuum uncertainty, mm of mercury	0.10	0.01
8. Gravity in cm/sec² must be known at 45° latitude within at 1 atm	.13	.013
at ½ atm	.26	.026
9. Altitude difference in feet between measured and desired point, at 1 atm	3.6	.36

On the other hand no portable barometer has as yet been developed which can meet all of the above tolerances for an accuracy of 0.01 mm of mercury. Items 2, 3, 4, 5, and 7 require special design features in the barometer to secure an accuracy sufficient to hold the overall error within 0.01 mm of mercury. This can be achieved apparently only in a precision type, laboratory instrument, not readily portable.

A number of the errors of barometers for which corrections can be more or less readily made, particularly for portable barometers, are considered in detail in the following sections. Other sources of error and methods and means for their correction for barometers of high precision are discussed in sec. 6.

8. Scale Errors

Strictly speaking, scale errors are the errors in the graduation of the scale at the chosen standard temperature. For standard barometers of high accuracy this definition holds. The scale can be checked against a standard meter bar and corrections are applied to the scale readings as found needed as a result of the calibration.

While many manufacturers take no less care in graduating the scales of portable barometers and manometers, the accuracy required does not ordinarily justify the expense of testing the scale alone. Uniformity in spacing the graduations which is absolutely essential, can be checked adequately by using the vernier as a length standard at various points on the scale.

This practice leads to a more practical definition of scale error. The portable instrument is calibrated against a standard barometer or manometer, and its readings corrected for temperature and gravity errors, zero error if obtainable, and possibly for capillary errors. The difference in the reading so corrected, and the pressure determined by the standard instrument is defined as the scale error.

The scale error thus derived may include errors: (a) Caused by installing the scale so that its zero or zero projected is not at the zero pressure point; (b) caused by overfilling or underfilling the instrument with mercury; (c) due to the effect in fixed cistern instruments of a tube bore different from that for which the scale is graduated (foreshortening constant is in error); (d) due to incorrect alinement of sighting ring and vernier zero; (e) due to capillary error, if not separately corrected for; (f) due to sighting errors introduced by poor optical quality of the tubing; (g) due to the imperfection in the vacuum above the mercury column; and (h) due to temperature error if the installed thermometer is in error. Naturally in barometers and manometers of good design and where care is used in assembly, many of these errors are insignificant. An exception is the capillary error, which will change with time, as discussed in sec. 12. The size, and more important, the uniformity at various readings, of the scale error, together with the precision of reading, is a measure of the quality of the barometer or manometer.

8.1. Zero Error

The difference in reading of a U-tube, and the reading of a cistern, barometer or manometer when both mercury surfaces are subjected to the same pressure is defined as the zero error. The design may be such that the zero error cannot be obtained, notably Fortin and cistern instruments which do not have scales going to zero. It can be obtained on practically all U-tube instruments. Usually the zero error in barometers is determined when both mercury surfaces are subjected to a vacuum, but often when subjected to atmospheric

pressure. The value usually differs slightly in the two procedures, if no correction is made for capillarity, because of variability in the capillarity in the two surfaces, or because of possible flexure of the cistern of a fixed cistern barometer when vacuum is applied. It is usually more convenient to determine the zero error in barometers when both mercury surfaces are subjected to a vacuum; in manometers, when subjected to atmospheric pressure.

The zero error may include any error introduced by: (a) Failure to adjust the zero of the scale so as to indicate the height of the mercury column; (b) misalinement involving a sine error; and (c) capillary errors, to some degree.

If a U-tube barometer is installed; (a) To have no cosine error of misalinement; (b) has an adequate vacuum above the mercury column; (c) has a constant value of the sine error of misalinement; and (d) has a scale known to have adequate accuracy, a determination of the zero error, is all that is theoretically necessary to calibrate it. All of these assumptions can be verified without serious difficulty, and in fact must be met if any calibration is to have validity. Actually, as a check, comparison with a standard barometer at some pressure well above zero is advisable. The error thus found should agree, within the expected accuracy of the barometer, with the zero error.

The foregoing discussion applies also to a U-tube manometer, except of course, vacuum may not be involved.

The accuracy of a barometer is no greater than the accuracy with which its zero error can be determined. The probable error, and the average deviation and maximum deviation of a single observation of a number of independent observations of the zero error are all useful in determining the accuracy.

Knowledge of the zero error is extremely valuable to the ultimate user of the barometer or manometer, when it can be determined at any time with little trouble. If it differs significantly from the originally determined value, the installation can be checked for misalinement, the vacuum adequacy checked and the amount of mercury in cistern instruments corrected, as necessary. If a difference develops with time, capillarity change (dirty mercury) or loss of mercury from fixed cistern barometers is probably the cause, in which case the instrument tubing will need cleaning, or mercury needs to be added. If the change in zero error has some cause which it is not desired to correct, the calibration errors at all readings may be shifted by the amount of the change.

It should be noted that the zero error for U-tube instruments is not affected by normal changes in instrument temperature. The zero error of cistern barometers varies with temperature, in most practical designs, by an amount which does not exceed 0.1 mm for a 10° C (18° F) shift from the temperature at which it was originally determined.

8.2. Method of Test

The test for scale error at a single ambient temperature is often called a calibration test. It, and the zero determination if possible, are usually the only laboratory tests made on portable barometers or manometers. The test essentially consists in comparing the readings of the instrument under test at controlled pressures within its range with those of a standard instrument when both are subjected to the same pressure and to constant environmental conditions, mainly temperature.

Standard barometers or manometers are either primary standards or working standards. The primary standard has its precision and accuracy fixed by the excellence of its design and workmanship and by the application of corrections determined either theoretically or by test of its components against standards of the requisite accuracy. A working standard is one used to calibrate other instruments; in this sense a primary standard may also be a working standard. A working standard should ideally have a precision and accuracy about ten times that of the instrument under calibration; actually this is often of necessity violated in practice. In many cases the working standard of a manufacturer is a barometer or manometer of the same design as the instrument under calibration but is one selected for better quality which has been carefully calibrated.

As indicated in the table in sec. 7, the uncertainty in the temperature of both the working standard and the instrument under test must be much less than 0.8° C at 1 atm of pressure if an accuracy of 0.1 mm of mercury is to be obtained, and less than 0.08° C for an accuracy of 0.01 mm of mercury. These temperature uncertainties are proportional to the pressure, greater if the pressure is greater, and less if the pressure is less. This indicates the necessity of control of the ambient temperature. Due to the large thermal lag of barometers, the safest procedure is to maintain the instrument temperature constant within the necessary limits during the entire period of the test, and obviously during use afterwards also. Practically this requires installation in an air conditioned room, adequately ventilated, except for the short time when the room pressure has to be measured, when the ventilation may introduce undesirable pressure gradients. The scale error test is commonly made at a temperature between 22° and 25° C; at the National Bureau of Standards, 25° C.

In making readings the top of the mercury meniscus is always sighted upon.

In computing the scale error, the reading of the barometer under test is first corrected for zero, temperature and gravity error, which are discussed in other sections. The difference, corrected barometer reading minus the pressure determined from the reading of the standard barometer, is

the scale error. The scale correction is of the opposite algebraic sign.

If a correction is made for the capillary error, (see sec. 12), which is rarely applied to the readings of portable barometers, this correction is also applied to the reading, after applying the corrections for temperature and gravity error. The scale error is then computed as outlined above.

The procedure given above for computing the scale error is strictly speaking in error in that the temperature correction has also been applied to the scale error. This procedure could be corrected as follows: first determine an approximate scale error by the procedure outlined, then apply this scale correction to the reading and correct this reading for temperature and gravity error. The scale error is the original reading minus the last obtained corrected reading.

This refinement is ordinarily unnecessary for portable barometers. For example, assume a scale error of 4 mm of mercury (which is really excessive), and a temperature deviation of 15° C from the test temperature, then the error introduced is 0.01 mm of mercury (0.0004 in.), an insignificant amount. In effect this error is a measure of the undesired dependence of the scale error upon temperature.

8.2.1. Fortin Barometers

The distinguishing feature of barometers which are designed to measure atmospheric pressure only is that the air-space of the cistern is always connected to the ambient air. This class includes Fortin barometers and fixed cistern barometers, such as the Kew-pattern and Tonnelot. The construction of these barometers is such that the zero error can not be determined by direct observation; consequently the zero error is incorporated into the scale error. Normally, the barometers are tested when subjected to ambient atmospheric pressure.

The readings of these barometers are compared with those of a working standard for at least 10 days in order to obtain a valid correction. The thermometer attached to each barometer is also read. The comparison readings should be made when the atmospheric pressure is most free from oscillations, and sudden changes, which can be determined from the trace being made by a microbarograph. These atmospheric pressure oscillations may occur suddenly and be 0.1 and more millimeters of mercury and are most troublesome when there is a high, gusty wind. Under these conditions simultaneity in the readings of the standard and the barometer under test is almost impossible to obtain. In Washington the most quiescent pressure period during normal working hours is from about 4 to 5 p.m.; normally valid comparisons can be made at this time three or four days each week.

The atmospheric pressure variation will almost never cover the pressure range of the barometer, normally about 75 mm of mercury or 100 mb. Actually for this pressure range a single correction suffices, if the graduations of the scale are uniformly spaced, a condition which can be checked independently by readings made with the vernier at a number of positions on the scale.

However, barometers which have to be used at high elevations have a measuring range up to 250 mm of mercury. These are generally Fortin barometers. In these cases it is not entirely safe to assume that the scale error can be represented by a single number obtained in a test at sea level pressure. One way of testing these long-range barometers requires that they be installed in a chamber the internal pressure of which can be controlled and measured, as discussed in sec. 9.4.

Another way of obtaining a calibration of these long-range barometers, if accuracy requirements can be met, is to use as the working standard a fixed cistern barometer with an airtight cistern which has been tested as described in the next section. The scale error test as above described is then made at the high-altitude location of the barometer. This procedure is practical for the meteorological services, since the barometers at the various stations need to be tested from time to time, probably more conveniently done at the barometer station.

In testing atmospheric pressure barometers having a tubing bore of ¼ in. (6.35 mm), a Fortin barometer of known scale error having a tubing bore of 0.6 in. (15 mm) or more is adequate as a working standard. Fixed cistern barometers of the quality used to test aviation altimeters or precision aneroid barometers are equally serviceable as a working standard if their scale errors have been determined.

The average of the scale errors determined by the comparison readings is taken as the scale error of the barometer, if all are considered equally valid and there is no indication that the scale error varies with the scale reading. Maximum deviations from the average and the probable error of a single observation, if at least about ten comparisons are available, are computed, and are indicators of the quality of the barometer.

8.2.2. Altitude Barometers

Testing altitude barometers requires a closed system essentially such as shown schematically in figure 2. Altitude barometers include all those in which the cistern is airtight except for a nipple, and U-tube barometers. In figure 2, S is a standard barometer of the U-tube type with its scale: $B1$, $B2$, and $B3$ are barometers to be tested; VP is a vacuum pump; F is a filter; M is a large volume manifold; B is a barostat; and A is an air supply.

The system must be leaktight in order to avoid pressure gradients in the system which will affect the accuracy of the readings. Insofar as possible metal or glass tubing should be used, using butyl rubber or plastic tubing only to make short length connections. Rubber tubing can be used only if

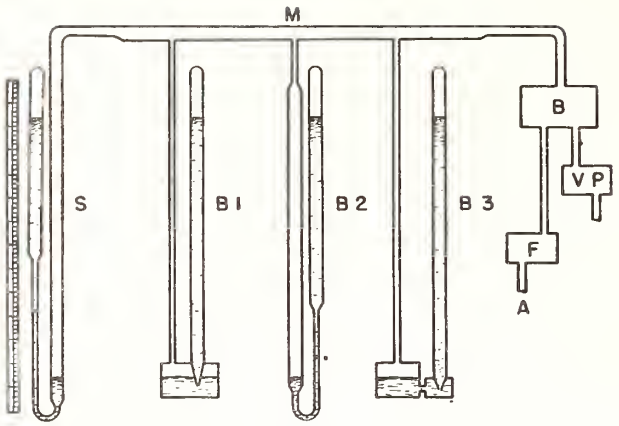

FIGURE 2. *Set up for testing altitude barometers.*

S, standard barometer (see fig. 1); *B1*, fixed cistern barometer; *B2*, U-tube barometer; *B3*, high altitude range fixed cistern barometer; *B*, barostat; *F*, filter; *M*, large volume manifold or plenum chamber; *A*, air supply, *VP*, vacuum pump.

practically free from sulfur. Satisfactory tubing of rubber or plastic is hard to find, since some give up gasses which contaminate the mercury and others are permeable to air or water vapor to an objectionable degree. To test for tightness, the system is subjected to the lowest pressure indicated by the barometers. The barometers are read, and the procedure is repeated again the next day. A rise in pressure of about a centimeter of mercury is considered excessive. To locate leaks, various parts of the system, including individual barometers, can be isolated by pinch clamps after making the initial readings.

The barostat, used to maintain the absolute pressure in the system at constant selected value, is a valuable accessory. It will be described in sec. 8.3.

The test procedure is simple in principle. The absolute pressure in the system is controlled by operating the vacuum pump, control valves and setting the barostat if one is available. At each pressure step, the standard barometer, barometers under test, and the thermometers associated with each barometer are read. It is preferable to make readings on both the down and up side of the pressure cycle. From these readings the pressure is obtained by applying the necessary corrections to readings made on the standard barometer. The readings of the barometers under test are corrected for zero, temperature and gravity errors. The scale errors are then computed. Obviously if the barometer under test has an automatic corrector for temperature and gravity errors, this is set to the correct ambient values of these quantities, and the scale error is the difference, barometer reading minus the pressure. Again, if the barometer under test is maintained at a constant temperature in its own chamber and its scale is graduated to read free from temperature error, only the gravity correction need be applied to its reading.

Usually, due to the labor and expense involved, only two tests on different days are ordinarily made on a given instrument to determine the scale errors. Several independent readings at each test point are a big aid in fixing limits to the accuracy, as well as giving an average value to use as the scale error.

8.2.3. Manometers

The apparatus and procedure for calibrating differential mercury manometers are similar in details to those for altitude barometers shown in figure 2. Since differential (usually gage) pressure is measured, the standard manometer has no evacuated space above the mercury column.

Instead of the barostat, a pressure controller is used. A commercially available diaphragm type pump in combination with a ballast chamber and pressure controller is convenient for the purpose.

Perhaps the most important difference is in the range of the manometers now needed, which now extends to 4 atm and more. Portability becomes a problem, so that testing against a standard at some other laboratory becomes impractical. This means that the scale only can be checked for accuracy and the desired accuracy must be designed into the manometer and its installation.

8.3. Barostat

The barostat designed and used at the National Bureau of Standards is shown in cross section in figure 3. Plates B and H are fixed in relative positions by four rods. Plates F and G are free to move between limit stops. Bellows E is sealed gastight to plates F and H, and is evacuated. Bellows A is sealed by plates B and G and has three connections through plate B, one at P for an air intake, one at S for connection to a vacuum pump, and one at T connecting into the system the absolute pressure of which is to be controlled. The pressure control valve consists of a ball V attached to spring L. Spring controlled plunger D operates the valve. The ball seats into a conical opening. The plates F and G are connected to a scale pan on which weights M can be placed.

In operation weights, corresponding to a pressure approximately the value desired, are placed upon the pan. If chamber A is originally at atmospheric pressure the plates F and G remain against the upper stop and the valve KV is consequently wide open. With air entering tube P and being evacuated through tube S, the pressure in bellows A falls until the pressure therein balances the weights. At this pressure the valve KV closes sufficiently so that the air flowing in through P equals that flowing out through S. Any deviation in flow changes the upward force on FG and either opens or closes valve KV, which changes the airflow through S until the pressure in A again balances the weights.

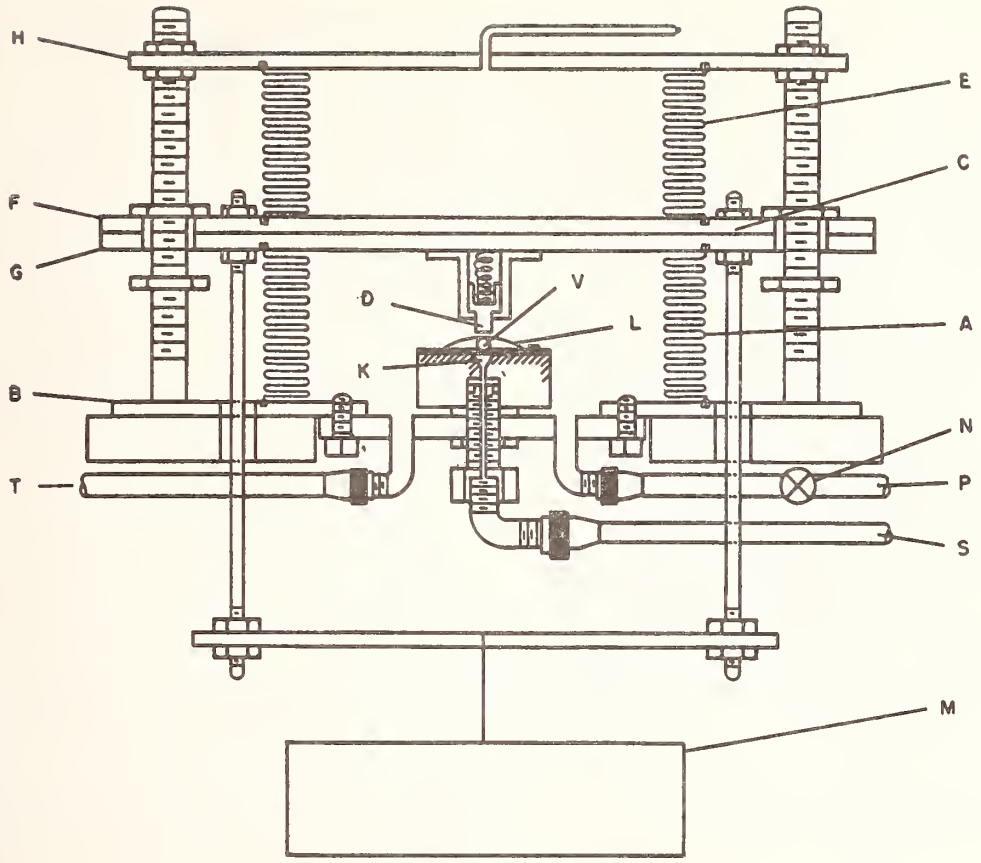

FIGURE 3. *NBS barostat.*

E, evacuated bellows; *A*, bellows maintained at desired pressure; *H* and *B*, fixed mounting plates; *F* and *G*, floating mounting plates; *M*, weights attached to *F* and *G*; *D*, spring controlled plunger; *V*, ball valve attached to spring *L*; *K*, valve seat; *P*, pressure line; *S*, suction or vacuum line; *N*, a valve; *T*, line to system the pressure of which is controlled by the barostat.

The performance is dependent upon the flow of air into bellows *A* through *P*; for optimum pressure control this airflow is about 1 liter/min secured by valve *N* and a suitable rotameter in line *P*, not shown in figure 3.

The bellows are copper plated brass and are about 5¾ in. in diam. The weight required to balance at 1 atm is nominally 330 lbs. These weights are applied manually; a mechanical weight lifter would be a desirable improvement.

The barostat controls the pressure to within 0.01 mm of mercury during the time needed to make readings, about 10 min.

The barostat fails as an absolute pressure gage by a few tenths of a millimeter of mercury, that is the pressure obtained at various times by a given weight does not repeat by this amount. Perfection of the barostat in this respect has not been undertaken.

9. Temperature Errors

It is evident that mercury barometers and manometers can read correctly at only one temperature principally because of the thermal expansion of the mercury and the scale, but also of certain other parts of the instrument. The height of the mercury column in terms of the density of mercury at 0° C (32° F) is desired. Deviations from the selected standard temperature requires the application of corrections to the instrument readings.

Generally the scale is graduated so that the column height is indicated when the scale is at 0° C. Exceptions are that manometers frequently, and barometers more rarely, have scales graduated to indicate the height of the mercury column at 0° C when the instrument temperature is at some selected value, commonly 20° or 25° C (68° or 77° F). Also, an exception are the scales of Fortin barometers still in use in meteorology graduated in inches, which are specified to indicate inches accurately when the scale is at 62° F (16.67° C). The requirement now is that the scale be graduated to be accurate at 0° C (32° F) [564].

The temperature correction for all types of

barometers and manometers is generally computed from formulas derived from the pertinent design constants of the instruments and the coefficients of thermal expansion of the pertinent parts. For any particular design, tests are essential in order to check the validity of the assumptions made in deriving the correction formula; these tests are particularly essential if the barometer or manometer temperature is much different from that at which the zero and scale errors were determined.

The thermometers attached to barometers and manometers may be in error. If no correction is applied for such error, either during calibration or service use of the barometer, and the error has a small constant value at all temperatures experienced, the resultant error in the temperature correction of the barometer will be almost entirely absorbed in the scale error. Variable errors in the attached thermometer over a few tenths of a degree may introduce significant errors in the pressure determination, unless corrected. If there are errors in the thermometer, any correction table which is set up for the barometer should obviously be based upon the reading of the thermometer, not the true temperature.

9.1. Basic Formula

The basic temperature correction formula is applicable to all portable barometers and manometers in which the height of the column is measured with a scale not foreshortened. It is directly applicable to Fortin and U-tube barometers and U-tube manometers, and as will be discussed later, with some modification to fixed cistern instruments.

The following terms are defined:

C_t=temperature correction of barometer reading to secure height of column at t_0

R_s=barometer reading corrected for scale error

R_t=barometer reading corrected for scale and temperature error

t=barometer temperature

t_0=standard temperature for height of mercury column, usually 0° C or 32° F

t_1=temperature at which the scale indicates the true height

m=cubical coefficient of thermal expansion of mercury per ° C or ° F as applicable

s=linear coefficient of thermal expansion of the scale per ° C or ° F, as applicable

h=height of the mercury column at t

F=a factor defined in eq (24) and (25).

The basic formula for the temperature correction will be derived for the general case where the reference temperature for both the mercury column and scale is unspecified.

First, to determine the height h of the mercury column at temperature t, it is seen that as the temperature of the scale decreases from t to t_1, the reading on the scale at the meniscus level increases. The height h of the column at t is the original reading R_s plus the contraction of the scale in going from t to t_1, or

$$h=R_s[1+s(t-t_1)]. \tag{18}$$

The contraction of the mercury column from temperature t to t_0 can now be written,

$$h=R_t[1+m(t-t_0)]. \tag{19}$$

If

$$R_t=R_s+C_t, \tag{20}$$

it follows from eq (18) and (19) that

$$C_t=\frac{s(t-t_1)-m(t-t_0)}{1+m(t-t_0)}R_s. \tag{21}$$

Ordinarily the coefficient of expansion s is listed with reference either to 0° C or 32° F; therefore s in eq (18) and (21) differs from the ordinarily defined value if t_1 is not 0° C or 32° F. Let s_1 be the value of s at t_1. Then

$$L_2=L_0[1+s(t-t_1)] \tag{22}$$

$$L_2=L_1[1+s_1(t-t_1)] \tag{22a}$$

where L_0, L_1, and L_2 are the scale lengths at 0° C, t_1, and t, respectively.

It follows that

$$s_1=\frac{L_0}{L_1}\left(\frac{1}{t-t_1}+s\right)-\frac{1}{t-t_1}=\frac{sL_0}{L_1}. \tag{23}$$

Since L_0/L_1 is very nearly unity, the approximation sL_0/L_1 is justified; in fact with usually insignificant error in all but precise manometry, $s=s_1$.

The choice of the form of the above formulas is based upon the premise that it is more convenient to apply a small correction, derived from convenient tables than to make basic computations. A constant value of the thermal expansion of mercury, m, is assumed, which is sufficiently accurate for all but precise manometry. (See sec. 4.1.)

If an electric computer is available, a more fundamental procedure is outlined in section 10.1, eq (45), where the temperature and gravity corrections are made in one operation.

9.2. Fortin Barometers, U-tube Barometers and Manometers

Since pressure in terms of the height of a mercury column is defined in terms of the density of mercury at 0° C (32° F), t_0 in eq (21) is either 0° or 32°, depending upon whether t is in degrees Celsius (Centigrade) or Fahrenheit.

While generally scales are used or specified to have the indicated length at 0° C, exceptions exist. These cases will be discussed in the sections immediately following.

It is assumed that the scales are graduated to indicate a length accurately, that is the scale is not foreshortened, as in the case of cistern instruments. It is also assumed that the scale, or metal the same as the scale material, extends downward to the level of the mercury in the cistern. This assumption is usually violated in Fortin barometers to some degree in that diverse materials are used in the cistern. Thus the coefficient of expansion s may not apply for a short length just above the cistern mercury level. Only the difference from the coefficient of expansion of the scale introduces an error. Neglect of these sources of error does not seriously affect the accuracy if the ambient barometer temperatures do not differ greatly from the temperature at which the barometer was tested. The error in the applied temperature correction is completely absorbed by the applied scale correction when the barometer is at the temperature at which the scale error test was made, and to a major amount at other barometer temperatures.

9.2.1. Scale Accurate at 0° C

When the scale is graduated to be accurate at 0° C, $t_0=t_1$. Equation (21) then becomes, when t is in °C

$$C_t=R_t-R_s=\frac{(s-m)\,tR_s}{1+mt}=FR_s \qquad (24)$$

and when t is in degrees Fahrenheit

$$C_t=\frac{(s-m)\,(t-32)\,R_s}{1+m\,(t-32)}=FR_s \qquad (25)$$

The factor F is identical in value in eq (24) and (25) at the same temperature. It follows therefore that a table of corrections against temperature in either ° C or ° F is equally applicable for all units of pressure, including millibars, millimeters or inches of mercury, if entered with the temperature in the unit for which the table was computed. Note, however, that F is not identical in the two equations if the scales are not accurate at 0° C or 32° F.

When a mechanical computer is available, the following relation is useful, particularly when many readings are taken at the same temperature.

$$R_t=\left[1+\frac{(s-m)\,(t-t_0)}{1+m\,(t-t_0)}\right]R_s=YR_s. \qquad (26)$$

where $Y=1+C_t$.

The value of Y can be obtained from a computed table of Y against temperature t or table 7 as discussed in sec. 9.5.

For portable barometers it is sufficiently accurate to use a constant value of m, the cubical expansion of mercury, over the temperature range normally expected; if more precision is necessary, see sec. 4.1. The accepted value of m is 181.8×10^{-6} per ° C or 101.0×10^{-6} per ° F.

The value of the linear coefficient of expansion varies somewhat for a given scale material, depending upon its exact composition and the degree of cold work. The exact value when required must be determined experimentally. Average values for a number of materials used either for the scale or cistern are given in table 5. The value for brass is taken from ref [512]; the others, from other published data.

Commonly the scales of Fortin and other barometers are made of yellow brass for which the value of s, the coefficient of linear expansion, is generally assumed to be 18.4×10^{-6} per ° C. Using this value of s and 181.8×10^{-6} for m, the cubical expansion of mercury, eq (24) becomes

$$C_t=-\frac{163.4\times10^{-6}tR_s}{1+181.8\times10^{-6}t} \qquad (27)$$

and eq (25) where t is in ° F, becomes

$$C_t=-\frac{90.78\times10^{-6}\,(t-32)\,R_s}{1+101.0\times10^{-6}\,(t-32)}. \qquad (28)$$

In these equations C_t, will be in the same unit of pressure as R_s, and apply equally for scales graduated in any pressure unit. The correction C_t is negative for temperatures above 0° C or 32° F, and the correction is therefore to be subtracted from reading R_s, corrected for scale error.

Correction tables based upon eq (27) are given in table 6 of this report (see sec. 9.5. for discussion), and also in ref [512]. If the barometer temperature is measured in °F, as indicated in eq (28), these tables are equally applicable if they be entered with the equivalent temperature in °C. Tables based upon eq (28) are given in ref [591].

9.2.2. Fortin Barometers, Scale Accurate at 62° F

Fortin barometers graduated in inches of mercury used in meteorology have the scale specified graduated to be accurate at 62° F (16.67° C). In view of the adoption of the millibar as the international standard unit of pressure by the meteorological services, Fortin barometers calibrated in inches of mercury are becoming obsolete; however, some of these are still used in industry. It is advocated that in the future the scales of all

Fortin barometers be calibrated accurate at 0° C, to secure agreement with the calibration practice followed for Fortin barometers calibrated in other pressure units.

For barometer scales graduated to be accurate at 62° F, formula (22) becomes, when t is in °F.

$$C_t=\frac{(t-62)\,s-(t-32)\,m}{1+m\,(t-32)}\,R_s. \qquad (29)$$

Inserting the value of s for a brass scale, 10.2×10^{-6} per °F and m, the volume expansion coefficient of mercury, 101.0×10^{-6} per °F, eq (29) becomes

$$C_t=-\frac{(90.8\,t-2599.6)\,10^{-6}}{1+101\times10^{-6}(t-32)}\,R_s. \qquad (30)$$

Here t is in °F and C_t and R_t are customarily in inches of mercury only.

The temperature correction is zero at all values of R_s at 28.6° F and is negative at all temperature above this value, meaning that the correction is to be subtracted from the barometer reading.

Correction tables based upon eq (30) are available [301, 512, 591].

9.2.3. Scale Accurate at Unknown Temperature

It is necessary to consider the case where the temperature at which the scale is accurate is unknown. It is assumed that the scale is graduated uniformly.

For U-tube instruments and Fortin barometers with a thermometer graduated in °C, eq (22) can be modified to give

$$C_t=\frac{[s\,(t-t_1)-mt]\,R_s}{1+mt}=\frac{(s-m)t\,R_s}{1+mt}-\frac{st_1\,R_s}{1+mt}, \qquad (31)$$

where t_1 is the temperature at which the scale correctly indicates the height of the column.

The last member of the equation contains the factor $1+mt$ which affects the value of the last member only 0.7 percent at $t=40°$ C, and less at lower temperatures and C_t not more than 0.1 percent. Without significant error eq (31) then becomes

$$C_t=\frac{(s-m)t\,R_s}{1+mt}-st_1R_s. \qquad (32)$$

The last term in eq (32) is therefore a constant at a given reading R_s well within the accuracy of barometers of this quality and therefore can be incorporated into the scale correction. To do so may require determining the scale error against reading over the range of indication. In determining the scale error, the temperature correction applied is the same as that for the case when the scale reads correctly at 0° C or 32° F given by eq (24) or (25). The residual error, after applying the usual gravity correction to the reading, is the scale error. Thus, at the calibration temperature, the term $st_1R_s=0$.

If the barometer has a brass scale, table 6 can be used to obtain the temperature correction.

9.2.4. Scale Indicates Pressure, Instrument Temperature Not 0° C

Assume that the scale indicates the height of the mercury column at 0° C when the instrument is at a temperature t_s. This procedure is fairly common for U-tube manometers and barometers but rarely for Fortin barometers. A temperature between 20° to 25° C (68° to 77° F) is commonly selected and it is here assumed that the temperature of the barometer or manometer is not subsequently controlled.

When the ambient temperature, that is the instrument temperature t, differs from t_s, the temperature at which the barometer reads free from temperature error, the temperature correction is (noting the discussion on the value of s in sec. 9.1.):

$$C_t=\frac{(s-m)\,(t-t_s)\,R_s}{1+mt}. \qquad (33)$$

It is seen that table 6 can be used to obtain approximate temperature corrections based upon eq (33), if the scale is of brass, by entering the table with R_s, the reading corrected for scale error and the temperature difference $(t-t_s)$ in degree centigrade. Obviously, the correction is to be subtracted from R_s if $(t-t_s)$ is positive; otherwise, added. In the table the computation is for $1+m\,(t-t_s)$, instead of $1+mt$ given in the equation; the error in the correction is less than 0.3 percent when $t_s=25°$ C and $t-t_s$ does not exceed 10° C.

Some manometers designed for relatively rough measurements have scales graduated as described. With the advent of air conditioning for most laboratories, the need for any temperature correction for manometers of this quality almost disappears. In any event, corrections based upon eq (33) are accurate.

Many manometers and barometers of high quality are installed in a temperature controlled room or in a cabinet the temperature within which is controlled to give readings free from temperature errors. The only temperature error which may need to be applied is that for minor deviations, of the order of 1° C, from the supposedly maintained temperature. Greater temperature deviations indicate improper functioning which should be corrected. The temperature correction can be obtained without significant error from table 6, or computed accurately from eq (33).

9.3. Fixed Cistern Barometers and Manometers

The temperature correction for fixed cistern instruments differs only from that of U-tube instruments in that the differential expansion of the

mercury in the cistern and of the cistern changes the zero position of the mercury surface with reference to the scale zero.

If the zero error of a fixed cistern instrument can be determined at several temperatures, as is the case for many modern designs, it is only necessary to apply the zero correction for the particular barometer temperature. Only the temperature correction as discussed for U-tube instruments needs then to be applied.

9.3.1. Scale Accurate at 0° C

When the zero error can not be determined, the temperature correction of fixed cistern barometers and manometers is difficult to compute accurately because simplifying assumptions must be made as to the construction of the parts affecting the change in reading with temperature, in order to obtain formulas practical to use. In the end it is essential to test each design of fixed cistern barometer at two or more temperatures in order to be able to compute a valid temperature correction.

Assume most simply that the fixed cistern instrument is so designed that the scale extends down to the level of the mercury in the cistern, reads zero at zero pressure and 0° C and is graduated to be accurate at 0° C. Also assume that the cistern is made of materials having the same coefficient of expansion. In this simple case the temperature correction C_t is, neglecting second order terms,

$$C_t=\frac{(s-m)tR_s}{1+mt}+\frac{V_0\ (3s_c-m)\ t}{A_0(1+mt+2s_ct)}. \qquad (34)$$

The terms not previously defined are:

V_0=the volume of mercury at zero pressure and at 0° C

A_0=the effective area of the cistern at 0° C, assumed to be uniform

s_c=the linear coefficient of thermal expansion of the cistern material

t=barometer temperature in ° C.

If the cistern is made of diverse materials, s_c is not a simple constant, but is a function of several constants. For example if the cistern has a steel base and glass walls, $3s_c$ becomes s_g+2s_s and $2s_c$ becomes $2s_s$ where the subscripts g and s refer to glass and steel, respectively.

With obvious modifications the formula applies also if the temperature is measured in degrees Fahrenheit.

The first term of eq (34) is the same as the temperature correction for Fortin barometers; the second term corrects for the rise of level of mercury in the cistern with temperature which introduces an error because the scale, and its zero point, are in a fixed position.

The term V_0/A_0 in eq (34) equals the height of the mercury in the cistern at zero pressure.

More or less approximately, in eq (34)

$$\frac{(s-m)}{1+mt}=\frac{3s_c-m}{1+(m-2s_c)t}, \qquad (35)$$

since in general s_c is much less than s and m. Approximately therefore eq (34) becomes

$$C_t=\frac{(s-m)t}{1+mt}\ (R_s+K), \qquad (36)$$

where K is a constant approximately equal to V_0/A_0 which can be added to the reading corrected for scale error Rs [231]. This simplifies computation and permits using table 6 if the scale is brass, which is entered with $Rs+K$ and the barometer temperature.

In various designs of fixed cistern barometers the computed K will vary from about 35 to 75 mm, with an uncertainty up to 20 percent due to deviations from the simple assumptions made. If K is determined by tests made at two or more temperatures, the uncertainty of course disappears, but some lack of constancy may remain, in the practical case usually negligible. It is a matter of convenience whether this deviation is incorporated in the temperature error or in the scale error; if the latter, the scale error will vary with temperature.

The difficulties in determining the exact temperature correction of fixed cistern barometers is a limitation upon the attainable accuracy. When the accuracy must be better than about ±0.1 mm of mercury (0.004 in.) it is necessary to maintain the barometer at constant temperature, so that the temperature error can be incorporated once for all into the scale error. This remark applies particularly to altitude barometers.

9.3.2. Scale Accurate at Unknown Temperature

In some barometers and manometers of the fixed cistern type of relatively low precision and accuracy, scales, desired to be correct at 0° C, are ruled without care being taken to have them read correctly at precisely 0° C. This case is discussed in some detail for Fortin barometers in section 9.1.2. For fixed cistern instruments the last term of eq (31) or (32) needs to be added to eq (36). Again this approximately constant term can be absorbed into the scale error with negligible error in the practical case.

9.3.3. Scale Indicates Pressure, Instrument Temperature Not 0° C

In this case the barometer or manometer is to be maintained at some constant temperature in the range 25° to 45° C, and the scale is ruled so that the pressure is indicated, that is, no temperature (and no gravity) correction needs to be

applied. For small deviations in temperature from the selected constant temperature, t_s, the temperature correction, is with negligible error,

$$C_t=\frac{(s-m)(t-t_s)}{1+mt}(R_s+K). \qquad (37)$$

This relation is based upon eq (33) and (36) and the assumptions made in their deviation also apply. The equation should only be used if the zero error can not be measured at the two temperatures t and t_s. If it can, the procedure outlined in section 9.3. is preferable and more accurate.

9.3.4. Fixed Cistern Barometers With An Altitude Scale

In calibrating altimeters it is often required that the altimeter be subjected to pressures corresponding to definite pressure altitudes. The barometer is always equipped with a pressure scale and sometimes with an auxiliary scale graduated at 1,000 or 500 ft intervals. Having an altitude scale only is impractical because the graduations are nonuniform, making the use of a vernier impractical.

On the above basis, it follows that accuracy in producing fixed pressure altitudes from an altitude scale is obtainable only when the barometer is maintained at a constant temperature and has no scale error. The altitude scale should be graduated so that allowance is made for the temperature error (and the gravity error at any one location).

If the barometer temperature is allowed to vary with uncontrolled ambient temperature, the most practical procedure is to precompute the barometer reading in pressure units for the desired pressure altitudes. The pressure in the system is then successively brought to correspond with these readings. In precomputing, it must be remembered that the available corrections are to be applied to the readings, not the pressure. Therefore, the temperature (and gravity) corrections (with reversed signs) are first applied to the pressure giving an approximate reading. Repeating the process, using the approximate reading instead of the pressure usually gives a sufficiently accurate reading. The process can be repeated if greater accuracy is warranted. The scale (and zero, if determined,) corrections (with reversed signs) need still to be applied to the reading corrected for temperature (and gravity) to obtain the reading corresponding to the pressure.

Since pressure altitude varies as the logarithm of the pressure, the limiting sensitivity or accuracy in altitude units varies with pressure. Thus, if the accuracy of the barometer in measuring pressure is 0.1 mm of mercury, in pressure altitude units this equals 3.6 ft at 0; 6.8 ft at 20,000 ft; 14.8 ft at 40,000 ft; and 39 ft at 60,000 ft of pressure altitude.

Theoretically it is of interest that the temperature correction c_h of a fixed cistern barometer in pressure altitude units,

$$c_h=\frac{RT}{gP}\frac{(m-s)t}{(1+mt)}(R_s+K) \qquad (38)$$

is almost constant at all values of the pressure, since $(R_s+K)T/P$ is almost constant in value. Here R is the gas constant for air, T and P are respectively the temperature and pressure in the standard atmosphere and g is the acceleration of gravity.

9.4. Method of Test

The method of testing for temperature errors differs only from that for scale error for the various types of instruments described in sec. 8.1. in that control of the temperature of the barometers and manometers is required. The standard instrument is probably best maintained at its usual operating temperature, but it is advantageous to operate working standards at the same temperature as the instrument under test.

Generally U-tube instruments do not require temperature tests. It is ordinarily only necessary to check their scales, or the precision screw if used, at several temperatures in order to determine its thermal coefficient of expansion, or its length at the temperature of use, if the instrument temperature is controlled. The temperature correction can then be accurately computed.

This makes it only necessary to test Fortin and fixed cistern barometers, particularly the latter. The choice of temperature chamber lies between a small one in which manipulation of the sighting means, sighting, and reading are done from the outside and a temperature chamber large enough for personnel to enter to make the adjustments and reading. The large temperature chamber is definitely more advantageous for fixed cistern instruments with airtight cisterns. Only temperature control is needed which offers no primary difficulty.

For Fortin barometers and fixed cistern barometers which measure ambient pressure only, and thus have cisterns which are not gastight, pressure and temperature must both be simultaneously controlled in the temperature chamber. This is more difficult in a large temperature chamber, but the difficulty is balanced by the difficulty of adding means for operation and reading from the outside of a small temperature pressure chamber. It is debatable which of the two sizes of chamber is preferable; experience indicates a preference for the large chamber.

It appears necessary to test instruments at least three temperatures if they will experience large temperature differences in service. For computing, it is the aim to divide the overall error into a scale error constant at any one reading, and into a temperature error linear with the reading corrected for scale error. The temperature error so derived should be reasonably consistent with the applicable equation for temperature correction, after insertion of the values of the constants computed from the test results. Any other test

result gives rise to the suspicion that either the test results are unreliable or the design or construction of the barometer needs improvement.

A procedure is outlined in ref. [591] whereby the temperature and scale errors of cistern barometers can be determined from tests at three temperatures, if the pressure is adjusted so that the cistern barometers have precisely the same readings at each temperature.

9.5. Temperature Correction Tables

As has been stated correction tables are given in table 6, based upon the equation

$$C_t=\frac{(s-m)tR_s}{1+mt}=\frac{163.4\times10^{-6}tR_s}{1-181.8\times10^{-6}t}. \qquad (27)$$

The table covers the temperature range 0° to 50° C and barometer readings (corrected for scale error) from 100 to 1,195 in steps of 5. The table may be entered with the barometer reading in any unit of pressure, ordinarily millibars, inches or millimeters of mercury to obtain a correction in the same unit of pressure.

The table applies only when the scale is graduated to indicate length accurately at 0° C and has a thermal coefficient of expansion of 18.4×10^{-6} per degree Celsius (centigrade) which is closely that of yellow brass. The volume coefficient of expansion of mercury assumed is 181.8×10^{-6} per degree Celsius (centigrade).

All corrections given in table 6 are to be subtracted from the instrument reading, corrected for scale error.

Temperature corrections can be obtained with sufficient accuracy from table 6 for practically all portable barometers which have brass scales. The instruments for which it can be used are listed below, together with a discussion of the limitations.

(a) The table applies to all Fortin barometers and U-tube barometers and manometers which have brass scales graduated to be accurate at 0° C in any pressure unit, particularly millibars, inches, or millimeters of mercury, and when the instrument temperature of which is measured in, or converted to ° C.

(b) The table applies to all Fortin barometers and U-tube barometers and manometers which have brass scales graduated presumably to measure length, or a length proportional to pressure, accurately at 0° C but actually do so at some temperature between about −10 to 25° C. The instrument temperature must be measured, or converted to, degrees Centigrade. Using the table may necessitate applying a scale error determined by test which will vary with the reading as indicated by eq (32). For example, if the scale is accurate at 20° C, the scale error will vary linearly from 0.20 to 0.30 mm at readings varying from 543 to 815 mm.

(c) The table can be used usually with negligible error to obtain the temperature correction of U-tube barometers and manometers the scales of which are graduated to read free from temperature error at a selected temperature other than 0° C, if the temperature of the instrument differs only slightly from the selected temperature. The scale must be brass and the temperature deviation must be in deg Celsius (Centigrade). The table is entered with the deviation in temperature and the instrument reading corrected for scale error. The resulting correction is subtracted if the instrument temperature is greater than the selected temperature, and vice versa.

(d) The table can be used to obtain the temperature corrections of fixed cistern barometers and manometers with brass scales graduated in any pressure unit, particularly millimeters or inches of mercury or millibars and the instrument temperature is known in deg Celsius (Centigrade). The table is entered with the instrument temperature and with the sum of two quantities as indicated in eq (36), the barometer reading corrected for scale error, and the approximate constant K. This K is approximately the height at 0° C of the mercury in the cistern at zero pressure difference in the tube and cistern, but should be determined by testing the instrument at several temperatures. There is somewhat less uncertainty in the computed value of K if the brass scale is graduated to be accurate at 0° C and extends down to the mercury level in the cistern and if the cistern is made of materials having a low value of the thermal coefficient of expansion.

(e) The table can be used usually with negligible error to obtain the temperature corrections of fixed cistern barometers and manometers, the brass scales of which are calibrated to read free from temperature error at a selected barometer temperature other than 0° C, if the instrument temperature differs only slightly from the selected temperature. The table is entered with the deviation of the instrument temperature from the selected temperature, instead of the instrument temperature. With this exception the discussion in (d) above applies. The correction obtained from the table is subtracted from the reading where the instrument temperature is higher than the selected temperature, and vice versa.

It is perhaps unnecessary to add that for highly precise measurements for which correspondingly high quality instrumentation is required, table 6 is not sufficiently accurate. The temperature errors of the scale may need to be determined more precisely and more accurate values of the density of mercury as given in tables 2, 3, or 4 may need to be used.

The temperature correction factor F defined in eq (24) and (25), that is

$$F=\frac{(s-m)t}{1+mt} \qquad (39)$$

is given in table 7 as a function of instrument temperature and of the thermal coefficient of

expansion s of the scale. These are useful for making computations when table 6 does not apply. The values are for a value of the thermal coefficient of the volume expansion of mercury m of 181.8×10^{-6} per deg Centrigrade. Values of Y, eq (26) can be obtained from table 6 by adding 1 to the value of F, if $t_1=t_0=0$ in eq (26).

The factor F given in table 7 can be used for computing the temperature correction with an accuracy sufficient for most portable barometers and manometers having scales of the material indicated. For greater accuracy the precise value of the expansion coefficient s must be known for the scale.

If the corrections for the expansion of the scale and of mercury are determined separately, the value of F in table 7 for invar ($s=o$) applies for the effect of the expansion of mercury.

The factor F given for brass ($s=18.4\times10^{-6}$) was used in computing table 6.

10. Gravity Errors

10.1 Basic Relations

It is necessary to correct the observed height of all mercury columns for the deviation of the acceleration of gravity from the standard value, 980.665 cm/sec² (32.1740 ft/sec²). The standard acceleration of gravity is assumed in the definition of the inch and millimeter of mercury as a unit of pressure and in the graduation of barometer scales in millibars.

The correction, derived from eq (1) is

$$C_g=\frac{g-g_s}{g_s}R_t=F_gR_t \tag{40}$$

$$R_g=R_t+C_g \tag{41}$$

where C_g is the gravity correction; g and g_s, the acceleration of gravity at the location of the instrument and the standard value, respectively; R_t and R_g, the instrument reading corrected for temperature and for gravity, respectively.

If no additional corrections are to be applied, as is often the case with portable instruments, R_g is the pressure in any unit in which the instrument is calibrated.

With equal accuracy

$$C_g=\frac{g-g_s}{g_s}R_s=F_gR_s \tag{42}$$

$$R_{sg}=R_s+C_g. \tag{43}$$

Here R_s is the instrument reading corrected for scale error and R_{sg} is the same corrected for scale and gravity error. The temperature correction is then obtained for R_{sg} and applied to R_{sg} to obtain the reading corrected for both temperature and gravity errors.

It may be preferable in precise measurements to compute the temperature and gravity corrections in a single operation, particularly if corrections are first and separately made for the calibration and temperature errors of the scale. The temperature error of the scale is given by eq (19). From eq (1)

$$\rho_s g_s h_s=\rho gh \tag{44}$$

and

$$h_s=\frac{\rho gh}{\rho_s g_s}. \tag{45}$$

Here ρ_s and ρ are respectively the densities of mercury at 0° C and at the instrument temperature; h is the true height of the mercury column at the instrument temperature and ambient gravity; h_s is the desired true height under standard conditions, that is the pressure, if no other corrections are to be applied; and g and g_s have been defined.

The ratio of the densities of mercury can be obtained from table 2, or computed from table 3 or table 4.

10.2. Value of Gravity at the Instrument Location

It remains to discuss how the acceleration of gravity g may be obtained. The U.S. Coast and Geodetic Survey has determined the acceleration of gravity at many points in the United States and using these values, the U.S. Geological Survey has made determinations at additional locations. At the moment the gravity values are based upon the Potsdam primary determination; later primary determinations indicate that the Postdam value is 0.013 cm/sec² too high. The International Meteorological Organization has adopted the latest primary value; gravity data given in ref. [512] are also based on the latest primary value. If the location of the instrument is reasonably close to a point or points where the value is known, interpolation and application of the elevation correction to be discussed below, may serve to obtain the value of g to sufficient accuracy.

For precise work it is necessary to have the value of gravity measured at the instrument location.

When due to the lack of observed values, interpolation and computation can not be used to determine g, its value may be obtained by entering table 9, discussed later, with the latitude of the instrument location. The value so obtained is for sea level and requires a correction for elevation, as also discussed below. The value of g so obtained

has a relatively low accuracy, particularly in mountainous regions where the elevation correction is approximate and where anomalies in the value of gravity in the United States may amount to 0.110 cm/sec² or 0.011 percent.

For a general discussion of the acceleration of gravity as applied to manometry and for pertinent tables, see ref [512].

10.3. Variation of Gravity With Latitude and Elevation

The value of gravity at sea level varies with latitude as follows, based upon simple assumptions and taking no account of anomalies:

$$g_\phi = 980.616(1 - .0026373 \cos 2\phi + 5.9\times10^{-6}\cos^2 2\phi). \quad (46)$$

Here g_ϕ is the value in cm/sec² at latitude ϕ and 980,616 cm/sec² is the presently accepted value at sea level and 45 deg lat. See ref. [512]. Values of g_ϕ computed from eq (46) are given in table 9.

The empirical relation for the value of gravity g at elevations above sea level is

$$g = g_\phi - 0.0003086h + .0001118\,(h - h') \quad (47)$$

where g_ϕ=the acceleration of gravity at sea level; h=the elevation in meters of the instrument above sea level; and h'=the elevation in meters of the general terrain for a radius of 100 miles. For further details and sample computations, see ref. [591].

It is quite obvious that arriving at an accurate value of h' is difficult in mountainous terrain.

For a relation similar to eq (47) but applying to a station under water, see ref [512].

10.4. Gravity Correction Tables

Gravity corrections are given in two tables, Nos. 8 and 9. They are alike in that the corrections are given for selected values of gravity and of instrument reading. They differ only in that in table 9 the selected values of gravity are associated with latitude.

Correction table 8 was computed from eq (40) for various value of g and R_t. The table is entered with g and R_t to obtain the gravity correction to be applied. The correction is subtracted from R_t if the sign is minus, and added to R_t, if plus.

Table 8 can be entered equally well with R_s, the reading corrected for scale error only. The correction is applied to R_s which gives R_{sg}, the reading corrected for scale and gravity error. Table 5 can be entered with R_{sg} to obtain the temperature error, which must however be applied to R_{sg}. The final result is a reading corrected for both temperatures and gravity errors.

Table 8 can be entered with R_s in any pressure unit, generally millibars, inches or millimeters of mercury, to obtain a correction in the same unit. The correction varies linearly with R_s so that by interpolation or other obvious numerical manipulation of R_s and the corrections, a correction for any reading can be obtained. A table computed for a given location is more convenient, in the preparation of which table 8 may be helpful.

The values of gravity are given in table 8 in cm/sec². If available in ft/sec², multiply by 30.48006 (or 30.48 if the international inch is used) to convert to cm/sec².

Table 8 also includes the value of $(g-g_s)/g_s$ used in making the calculations. This value when algebraically added to unity gives the value of g/g_s, needed if eq (45) is used in computing corrections.

Table 9 differs from table 8 only in that it is entered with latitude instead of g, the acceleration of gravity. The value of gravity, g, and the ratio $(g-g_s)/g_s$ are also given. The correction obtained is applicable only if the instrument is at sea level; further correction for elevation may be necessary using eq (47).

The value of g at a given latitude in table 9 was determined from eq (46). Otherwise, the discussion of table 8 presented above applies.

11. Capillary Errors

The meniscus of mercury in containers, either tubes or cisterns, is drawn down at the line of contact at the container wall. As a result the center of the meniscus is depressed somewhat below the level of an infinite surface of mercury. The amount of the depression tends to vary with the age of the barometer, with the direction of the change in pressure, and with local differences in the condition of the surface of the container. Theoretically, the amount of the depression is a function of the bore of the container, the meniscus height and the value of the surface tension of mercury. Foreign material on the container wall, such as grease, and contamination of the mercury surface, affect the meniscus height.

It has been reported that greater uniformity in the meniscus height may be secured by putting mercurous nitrate at the interface [291] or coating the container surface with a material to stabilize the meniscus height. Neither of these procedures have found serious application in manometry.

A serious difficulty is lack of knowledge of the surface tension of mercury, except in a freshly distilled state under a vacuum. When in contact with air, it is known to be less than 484 dynes/cm at 25° C, the value for freshly distilled mercury in a vacuum. Surface contamination, even apparently trivial, will affect the value of the surface tension. Kistemaker, [451] in a series of careful experiments deduces from measurements of the capillary depression of mercury in a series of clean tubes of various bores up to over 30 mm (1.2 in.)

that the surface tension of mercury in contact with air at about 18° C was 430 ±5 dynes/cm. There is no certainty that this value holds for the mercury in other tubes.

Thus the capillary depression, a function of the surface tension for a given bore of tube and meniscus height, can not be accurately determined. Hopefully, the error in the determination of the capillary depression is estimated to be less than ±20 percent but the error will exceed this amount in many circumstances.

For highest accuracy there is only one safe recourse for avoiding excessive capillary corrections, that is making the areas of the mercury surface large enough so that the capillary depression is negligible. In precision manometry and barometry, if the capillary depression is not negligible, it is always considered desirable to measure the heights of the menisci and to apply the capillary correction.

It is common practice with ordinary barometers and manometers to incorporate the capillary depression into the zero correction (if one is applied). In the case of U-tube instruments it is often neglected on the assumption that the capillary depression is the same within the accuracy expected, for each mercury surface. When and if a correction is applied it is obtained from tables (see sec. 11.3).

11.1. Tube

It is practical only to correct the indicated position of the mercury surface in transparent tubes for the capillary depression. If the correction is to be made, the height of the mercury meniscus must be measured, in effect requiring, in addition to the usual measurements, the measurement of the position of the mercury-glass-gas boundary. This can be done only if the mercury surface is clean. Also tapping of the barometer or manometer is normally required to obtain a continuous, level boundary to measure and to eliminate nonuniform sticking of mercury to the cistern wall. The capillary depression is obtained from tables such as table 10, entered with the tube diameter and the meniscus height.

In view of the lack of inherent accuracy in determining the capillary depression, it seems hardly worthwhile to apply the correction for tubes less than 10 mm in diameter. In fact, the uncertainty in the capillary correction is such that if an accuracy of 0.1 mm of mercury is desired, a tube of not less than 12 to 16 mm in diameter should be used.

Kistemaker [452] describes a procedure for determining the capillary depression in tubes which is of interest, but not often as practical as using tubes of bore so large that the variations in the capillary depression can be neglected. An additional tube of smaller bore is used in parallel with the primary, subjected to the same pressure and of the same kind of glass and degree of cleanliness. The measurements made are: d, difference in heights of the mercury column in the two tubes, which should be of the order of 1 mm, in effect the difference in the capillary depression of the two tubes; m_1 and m_2, the meniscus heights in the primary and secondary tubes, respectively. Entering an accepted table, as described in sec. 11.3, with m_1 and m_2 and the applicable bore of the tubes, the capillary depressions c_1 and c_2 are secured. The difference, $c_2-c_1=d_c$ is compared with d, the measured difference. If the difference, d_c-d, is significant, the values given in the table 10 for the primary tube are adjusted percentage-wise to give $d_c-d=o$, and then used to make the corrections for the capillary corrections for that primary tube. One obvious assumption is made that the condition of the mercury surface in the two tubes is directly comparable and that this relative condition remains stable. It is claimed that, while the method is theoretically an approximation, an accuracy of ±2 percent in determining the capillary correction is obtained.

11.2. Cistern

Corrections for the capillary depression of the mercury in the cistern of manometers and barometers can not be applied because the meniscus height can not be measured as a routine. The cistern is usually, or should be, large enough in diameter so that the depression itself is negligible.

Ordinarily with time the mercury surface in the cistern, and the cistern walls, foul up so that the meniscus height changes. In fixed cistern barometers or manometers where the scale zero is fixed, there are two effects acting to give rise to errors in measuring the pressure. First, the actual height of the mercury column falls by the amount of the capillary depression. Second, a readjustment of the volumes of mercury in the cistern and tube takes place which affects the relation between the zero of the scale and the cistern mercury surface. Due to the elimination of capillary depression, when the meniscus flattens, a slight rise takes place in the mercury level in the cistern; also as the meniscus flattens, the volume of the meniscus decreases, which decrease must result in the lowering of the level of the mercury in both the cistern and the tube. The latter, the volume effect, is predominant so that at constant pressure the barometer reading on the fixed scale falls as the meniscus flattens. The combination of these effects can be reduced somewhat by using cisterns of large diameter. The error occurs at any pressure, and may vary with time, pressure and the manner in which the pressure is changed.

The capillary effects just described also occur in the cistern of Fortin barometers. Since the mercury level in the cistern is adjusted in height to a fixed index, the residual error is only that due to the change in the capillary depresssion. Change in the volume of the meniscus does not affect the reading. In an extreme case of mercury fouling

in the cistern of a Fortin barometer, with a ¼ in. bore tube, the change in reading of a good meniscus to no meniscus, was 0.02 in. (0.5 mm) of mercury.

It is thus necessary to calibrate both Fortin barometers and fixed cistern barometers and manometers more or less frequently.

11.3. Correction Table

The correction table for the capillary depression in table 10 is given by Gould and Vickers [521]; it was computed from a mathematical development described in ref. [401]. It is seen that knowledge of the surface tension of mercury is needed, as well as the meniscus height and bore of the tube, in order to enter the table. Since it is not practical to measure the surface tension of the mercury in the barometer, some value must be assumed.

Kistemaker [452] has computed a table of values for the capillary depression based upon observations made on the depression of the mercury in tubes of various bores and partly on the theory given in ref. [401]. The menisci were in contact with atmospheric air at 75 ±5 percent relative humidity for 24 hr before the tests and the temperature was 19 ±1° C during the tests. These data are compatible with a surface tension of 430 dynes/cm for mercury. On this basis the values of the capillary depression should be about 5 percent less than those given in table 10 for a surface tension of 450 dynes. Actually for a 12 mm tube the values in table 10 are higher, rising from 10 to 20 percent for meniscus heights from 0.2 to 1.8 mm. Again, for a 19 mm tube, the values in the capillary depression are practically identical up to a meniscus height of 1.0 mm; those in table 10 rise to 10 percent higher for meniscus heights from 1.2 to 1.8 mm. In general, the capillary depressions given by Kistemaker are intermediate to those for surface tensions of 400 and 500 dynes/cm given in table 10; however, at high meniscus heights and small bore tubes (10 mm and below), Kistemaker's values are lower than those for 400 dynes/cm.

The capillary depression given in table 10 for a surface tension of 450 dynes/cm are from 5 to 10 percent lower than those of a much used correction table [231], a discrepancy made greater by the fact that the latter table was computed for a surface tension of 432 dynes/cm. Both tables were prepared in the National Physical Laboratory of Great Britian.

Since there is no practical way to know the applicable value of surface tension of the mercury under the various conditions of use, in contact with air or vacuum, and degree of surface cleanliness of the mercury, there is little to gain in choosing one set of tables over another. For the moment, Gould's table (table 10), for 450 dynes/cm seems as applicable as any.

For one important purpose any table is adequate, that is for the selection of a bore of tube sufficiently large so that the variations in the capillary depression will have negligible effect on the required overall accuracy. In this connection note that the percentage variation in the capillary depression with surface tension at all meniscus heights presented in table 10 is greater the larger the bore of the tube. Thus for a change in surface tension from 400 to 500 dynes/cm the capillary depression varies as much as 100 percent.

Note that for Fortin and fixed cistern barometers, the capillary depression given in the table is added to the reading of the mercury barometer. For U-tube barometers and manometers the capillary depression at the upper mercury surface is added to, and at the lower mercury surface subtracted from, the indicated height of the mercury column.

12. Return Head and Elevation Corrections

Usually a differential pressure is measured simply by the height of the mercury column. Actually the differential pressure, measured at the level of the mercury surface on the high pressure side of a mercury manometer, is the difference of the specific weight of the mercury column and of the column of equal height of the gas or liquid on the high pressure side. The specific weight of the latter column is defined as the head correction.

Both differential pressure and absolute pressure measured with any manometer or barometer, liquid or mechanical, applies only to the elevation at which made. In the case of mercury manometers this level is that of the mercury surface of the high pressure side of the barometer. If pressures are desired at any other level above or below, the decrease or increase in absolute pressure with elevation due to the intervening head of gas or liquid in both legs of a manometer must be considered. The elevation correction is defined as the correction which needs to be applied to transfer the pressure measured at an elevation to another elevation.

Elevation corrections discussed in this section are mainly restricted to elevation differences of several hundred feet and pressures of several atmospheres. These are conditions commonly met with in laboratories and industry. Determination of sea level pressure from readings of a barometer installed at elevations well above sea level are outside the scope of this paper; this computation is discussed in the publications of the U.S. Weather Bureau.

12.1. Definition of Symbols

e=base of natural logarithms=δ 2.71828
g=acceleration of gravity. In this section assumed to be the standard reference value, 980.665 cm/sec²
h=vertical height of the gas column (see fig. 4)
h_0=the elevation with reference to the level at zero differential pressure of a barometer or a manometer (see fig. 4)
h_l=the height above or below a mercury surface of a liquid used to transmit the pressure
H=scale height=RT/g
P=absolute pressure
P_0=absolute pressure in a gas column at elevation h_0 (see fig. 4)
P_{00}=absolute reference pressure, measured at some level other than h_0
P_1, P_2=absolute pressures at various levels on the low pressure side of the system (see fig. 4)
P_{10}, P_{11}, P_{12}=absolute pressures at various levels on the high pressure side (see fig. 4)
p=differential pressure measured by the mercury column (see fig. 4)
R=a constant for a gas
T=absolute temperature of the gas at any level; assumed to be constant at all levels of the gas column
ρ=density of the gas at temperature T and pressure P
ρ_l=density of the liquid which is used to transmit pressure

12.2. Change in Gas Pressure with Elevation

The return head correction or the elevation correction involves the computation of the change in gas pressure in going from one level to another. Since a gas compresses under its own weight, its density at a higher elevation is less than at a lower elevation; this necessitates an integration.

The basic relation is

$$\frac{dP}{dh}=-\rho g. \tag{48}$$

Substituting for ρ in eq (48) its value

$$\rho=\frac{P}{RT} \tag{49}$$

there is obtained

$$dP=-\frac{Pgdh}{RT}. \tag{50}$$

Integrating eq (50)

$$P=P_0e^{-\frac{gh}{RT}}=P_0e^{-\frac{h}{H}}. \tag{51}$$

Approximately, with an accuracy within 0.1 mm of mercury for h equal to several hundred feet and P_0 equal to several atmospheres:

$$P=P_0\left(1-\frac{h}{H}\right). \tag{52}$$

Here T is the temperature of the gas at pressure P; and P_0 and P are the absolute pressures of the gas at the reference level $h=0$ and level h, respectively. If the level of P is above the level of P_0, h is plus; if below, h has a minus sign. See section 12.1 for other definitions.

The temperature of the gas column ordinarily can be assumed to be constant. If the gas temperature varies in the gas column an arithmetic average of the temperature based on equal increments of log p or here with sufficient accuracy, of equal increments of elevation, will give the temperature T to use in computing H. The factor H is called "scale height" because it has the dimensions of a length.

Equations (51) or (52) are primary for computing the difference in pressure at two elevations due to a head of gas. In its derivation it has been assumed that the gas law given in eq (49) holds, and of course that the gas does not condense anywhere in the system.

For each gas a table of values of H against temperature will be useful. In computing H the gas constant R, varies with the gas. It equals the universal gas constant, 8.31439×10^7 erg/mole deg, divided by the molecular weight of the gas. Values of R for a few gases are given below [531]. Using these values of R, g in cm/sec² and T in degrees Kelvin, gives H in centimeters which can readily be converted to be in the same unit as the elevation h.

Gas	Constant R cm²/sec² °K	Molecular weight
Air, dry	2.8704×10^6	28.996
Carbon dioxide	2.0800×10^6	44.01
Hydrogen	41.242×10^6	2.016
Helium	38.910×10^6	4.003
Nitrogen	2.9673×10^6	28.02
Oxygen	2.5982×10^6	32.00

From some points of view the method of computation to be presented is preferable, although it is an approximation with about the same accuracy as eq (52). In the absence of a mechanical computer it is definitely less laborious. This method will be used in all of the examples given below; if the use of eq (51) or (52) is preferred, the substitutions to be made are straightforward.

In eq (48), dP/dh is the rate of change of pressure per unit change in elevation. This rate varies directly as the product of the gas density, inde-

pendent of its composition, and the acceleration of gravity. The latter varies less than 0.3 percent over the surface of the earth, and, as will develop, introduces an error of this amount in a small correction term and therefore can be assumed to be a constant.

Thus, if precomputed values of dP/dh are available, changes in pressure with elevation can be computed by the relation

$$P=P_0-\Delta P=P_0-\frac{dP_0}{dh}h. \qquad (53)$$

In order to facilitate computation using eq (53), tables 11 and 12 have been prepared. The value of dP/dh, the rate of change of pressure per unit change in height of the gas column, is presented in table 11 for selected values of the gas density and for five different convenient units of measurement. For convenience the absolute pressure for air only is given for three air temperatures. Three assumptions underly table 11: (a) The value of gravity is 980.665 cm/sec^2; (b) the gas is dry and does not condense in the system; and (c) the air temperature of the gas column is constant, usually the case to a sufficient degree in laboratories. It should be noted that the gas density and the corresponding rates of change of absolute pressure given in table 11 are independent of the composition of the gas, pure or mixtures.

Table 12 is presented as an aid in determining the density of dry air when the air pressure and temperature are known. Air is assumed to have an air density of 0.001293 g/cm^3 at 0° C and a pressure of 760 mm of mercury. The coefficient of expansion of air is assumed to be 1/273; the slight error thus introduced is inconsequential in the practical use of the table.

An example will illustrate the utility of the tables in computing the pressure difference caused by a head of gas. Assume the pressure of air to be 810 mm of mercury and the temperature 21° C, to determine the pressure at a point 11 ft higher in elevation. From table 12, the air density corresponding to 810 mm of mercury and 21° C is, by interpolation, 0.001280 g/cm^3. Entering table 11 with this value, it is found that dP/dh= 0.02861 mm of mercury per foot. The difference in pressure at the two levels is

$$\Delta p=-\frac{dP}{dh}h=-0.0286\times 11=-0.31 \text{ mm } Hg$$

and

$$P=810-0.31=809.69 \text{ mm } Hg.$$

It is seen that variations in gravity up to 0.3 percent affect the pressure decrease of 0.31 in. of mercury to an insignificant degree. Two sources of error should be considered. First the density itself and therefore dP/dh, may be in error. An error in temperature measurement of 1° C, unlikely in practice, introduces roughly an error of 0.3 percent in gas density or in dP/dh. This error is usually insignificant. Second, the value of dP/dh varies with gas density, so that its value is not precisely the same at 810 and 809.69 mm of mercury. The difference here is less than 0.04 percent, obviously insignificant. In this example the method is accurate to at least 0.01 mm of mercury.

In the second case the accuracy is about the same as the ratio of the pressure difference to the reference pressure. If excessive, the error may be reduced approximately one-half by two computations, first determining an approximate pressure difference as outlined above, and finally, determining the pressure by using a value of dP/dh given by the average of two values of dP/dh, one for the density at the measured pressure at $h=0$ and the other for the density determined by the approximate pressure computed for level h.

12.3. Return Head Correction

In many cases the differential pressure at the level of the lowest mercury surface is desired. In figures 4 and 5 this differential pressure is

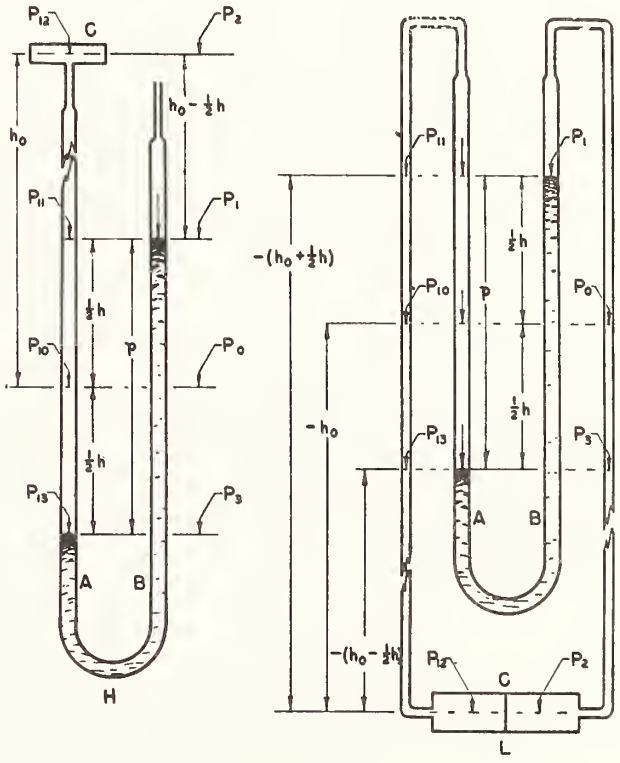

FIGURE 4. *Diagram illustrating computation of gas pressure at two levels from differential pressure measured with U-tube manometer.*

H, system with unknown pressure at high level; *L*, system with unknown level at lower level. *A*, tube connected to system the pressure of which is to be measured; *B*, manometer tube open to the atmosphere or connected to pressure reference; *C*, level at which pressure is desired; P_{10}, P_{11}, P_{13}, absolute pressure in system at various levels; P_0, P_1, P_3, absolute atmospheric or reference pressure at various levels. *p*, the measured differential pressures *h*, h_0, differences in elevation.

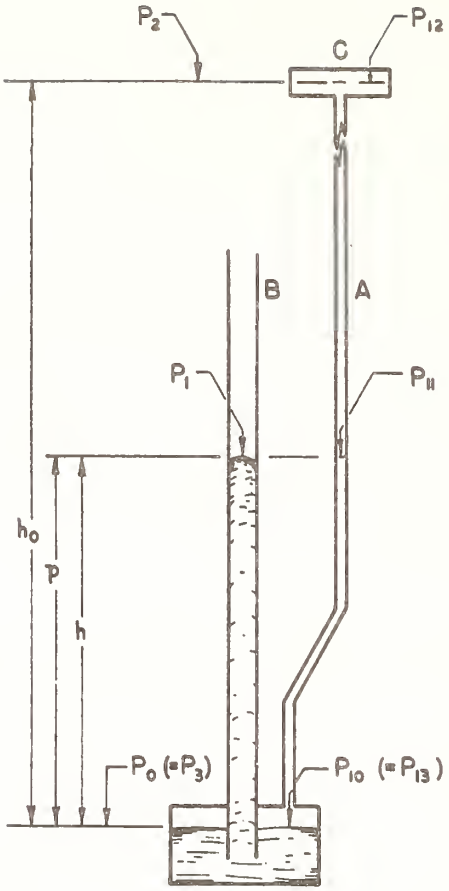

FIGURE 5. *Diagram illustrating computation of gas pressure at two levels from gage pressure measured with cistern manometer.*

See figure 4 for meaning of symbols.

$P_{13}-P_3$. The gas pressure impressed upon the mercury surface at the upper level is P_1, figures 4 and 5, and must be known or obtainable. The problem reduces to the computation of P_3 in terms of P_1. The significant elevation here is h which is also the height of the mercury column.

From eq (53)

$$P_3=P_1+\frac{dP_0}{dh}h. \tag{54}$$

The absolute pressure P_3 is greater than P_1, therefore the correction is additive.

$$P_{13}=P_1+p \tag{55}$$

and

$$P_{13}-P_3=p-\frac{dP_0}{dh}h. \tag{56}$$

Alternatively, based upon eq (51) and (52) or

$$P_{13}-P_3=p+P_1(1-e^{h/H}) \tag{57}$$

$$=p-\frac{h}{H}P_1 \tag{58}$$

The terms $-(dP_0/dh)h$, $P_1(1-e^{h/H})$ and $-h/HP_1$ are nearly equivalent various forms of the return head correction; only the term in eq (57) is strictly rigorous, but the accuracy of the others is usually quite adequate.

For all practical purposes, in eq (56)

$$\frac{dP_0}{dh}=\frac{dP_1}{dh}$$

a fact which often simplified computations.

Equations (56), (57), and (58) give the return head correction for all forms of U-tube manometers and for cistern manometers, with a change in notation as indicated in figure 5.

For mercury barometers of all forms, the return head correction is zero.

All of the above discussion is for the case when the low pressure side of manometer has a gas above the mercury surface. In some applications this space is filled with a liquid, that is for example the line from P_1 to P_2 in figure 4L may be filled with a liquid of density ρ_l. It is unlikely that the differential pressure $P_{13}-P_3$ is of any interest, but if so, it is

$$P_{13}-P_3=p-\rho_l gh \tag{59}$$

where $\rho_l gh$ is the return head correction. Here ρ_l is the density of the liquid at the pressure P_1 and at its temperature. Compression effects can ordinarily be neglected.

If ρ_l is in grams per cubic centimeter, g in centimeters per second squared in h in centimeters, the head correction is in dynes per square centimeter, which can be converted to the units of p with the aid of table 1.

12.4. Elevation Correction, Gas Head

The basic relations for pressure change with elevation enable computation to be made of the absolute pressure at the significant levels in any pressure system. The difference in the absolute pressures at a given level in the two legs of a manometer gives the required gage or differential pressure. For barometers one of the absolute pressures is essentially zero. The computations will be made based only upon eq (53).

Generally, measurements of p, h_0, and h as indicated in figures 4 and 5 need to be available. To compute dP/dh using table 11, it is necessary to enter table 11 with the density of the gases involved. This, most simply requires that measurements be made of the gas temperature and the absolute pressure of the two gas columns at the zero reference level; absolute pressures at other

levels can be substituted without significant error if these levels are within the height of the liquid column.

In making computations a choice must be made of the reference level from which elevations are measured. This zero elevation can be one of the mercury surfaces but this choice has the disadvantage that the zero reference level then varies with pressure. Computations are often more conveniently made if the zero elevation of the gas column is chosen to be the level at which the differential pressure indicated by the barometer or manometer is zero. The height of the gas column is then, as indicated in figure 4, $h_0 \pm h/2$ for U-tube instruments, or $h_0 \pm h$ for cistern instruments.

12.4.1 U-tube Manometers

Consider the pressure system figure 4*H*, where one leg of the manometer is open to the atmosphere and the other leg connected to a chamber at a level above the manometer. It is required to determine the gage pressure $P_{12}-P_2$.

In leg *B* of the manometer the absolute gas pressures are:

$$P_1=P_0-\frac{dP_0}{dh}\frac{h}{2} \tag{60}$$

$$P_2=P_0-\frac{dP_0}{dh}h_0. \tag{61}$$

If the atmospheric pressure is measured at some other elevation h_{00} than at the zero elevation level,

$$P_0=P_{00}-\frac{dP}{dh}h_{00}. \tag{62}$$

If the level of P_0 is below that of P_{00}, the minus sign in eq (62) changes to plus.

In leg *A* of manometer *H*, the significant gas pressures are, based upon eq (53) and (61).

$$P_{13}=p+P_0-\frac{dP_0}{dh}\frac{h}{2} \tag{63}$$

$$\begin{aligned}P_{12}&=P_{13}-\frac{dP_{10}}{dh}\left(h_0+\frac{h}{2}\right)\\&=p+P_0-\frac{dP_0}{dh}\frac{h}{2}-\frac{dP_{10}}{dh}\left(h_0+\frac{h}{2}\right).\end{aligned} \tag{64}$$

The gage pressure at level h_0 is (eq 61 and 64)

$$P_{12}-P_2=p+\frac{dP_0}{dh}\left(h_0-\frac{h}{2}\right)-\frac{dP_{10}}{dh}\left(h_0+\frac{h}{2}\right). \tag{65a}$$

For cases, such as illustrated in figure 4*L*, where the level at which the differential pressure is below the level of P_0, it is only necessary to change the sign of h_0. Equation (65a) becomes

$$P_{12}-P_2=p-\frac{dP_0}{dh}\left(h_0+\frac{h}{2}\right)+\frac{dP_{10}}{dh}\left(h_0-\frac{h}{2}\right). \tag{65b}$$

12.4.2. Cistern Manometers

For cistern manometers, figure 5, the zero reference level is at the mercury surface in the cistern, which ordinarily can be assumed not to vary significantly with pressure. Then for reference absolute pressures in leg *B*,

$$P_1=P_0-\frac{dP_0}{dh}h \tag{66}$$

$$P_2=P_0-\frac{dP_0}{dh}h_0 \tag{67}$$

and for absolute pressures in leg *A*,

$$P_{10}=p+P_1=p+P_0-\frac{dP_0}{dh}h \tag{68}$$

$$P_{12}=P_{10}-\frac{dP_{10}}{dh}h_0=p+P_0-\frac{dP_0}{dh}h-\frac{dP_{10}}{dh}h_0. \tag{69}$$

The differential pressure at level P_{12} is:

$$P_{12}-P_2=p+\frac{dP_0}{dh}(h_0-h)-\frac{dP_{10}}{dh}h_0. \tag{70}$$

Again, if the level of P_2 is below the level of P_0, eq (70) applies if the sign of h_0 is changed, as indicated in eq (65a) and (65b).

12.4.3. Barometers

In all cases the pressures $P_0=P_1=P_2=P_3=0$, since the space above the mercury column is evacuated.

In U-tube barometers the absolute pressure at an elevation differing from that of P_{10} is simply, using the notation in figure 4,

$$P_{12}=P_{10}\pm\frac{dP_{10}}{dh}h_0=P_{13}-\frac{dP_{13}}{dh}\left(\frac{h}{2}\pm h_0\right). \tag{71}$$

In cistern barometers the absolute pressure at an elevation above or below the level of the mercury surface in the cistern, where the pressure is P_{10}, is:

$$P_{12}=P_{10}\pm\frac{dP_{10}}{dh}h_0. \tag{72}$$

12.5. Elevation Correction, Liquid Head

To consider this case, assume in figure 4*L* that the tubing from both mercury surfaces to chamber *C* are filled with the same pressure transmitting liquid of density ρ. Assume that the pressures are low so that compression of the transmitting liquid and of mercury can be neglected. It is then seen in figure 4*L* that

$$P_{10}-P_0=P_{13}-P_3=P_{12}-P_2=p-\rho_l gh. \quad (73)$$

Thus, the differential pressure at any level requires only a correction for the return head, as discussed in connection with eq (59).

To take care of compression of the transmitting liquid it is only necessary to modify the value of the density ρ_l in eq (73).

It is unusual for the transmitting liquids to to differ in the two legs of the manometer, so that this case is not considered here.

13. Vacuum Error of Barometers

The vacuum above the mercury column of barometers is never perfect; mercury vapor and some air, and perhaps other gases are always present. The pressure of the gases in the vacuum space results in an error in the measured pressure, and when known either by computation or measurement must be added to the measured pressure to secure the pressure.

In precise measurements the vacuum is maintained below a value set by the desired precision of measurement by means of a diffusion pump. The vacuum can be checked with a McLeod gage to an accuracy of the order of ± 10 percent. In this procedure however the effect of the mercury vapor is neither eliminated nor measured. If the precision desired warrants, a correction must also be applied for the pressure of the mercury vapor, obtained from tables of observed values, as table 3. The operation schedule of the diffusion pump and temperature conditions must be such that equilibrium values of the mercury vapor pressure exist at the time readings are made.

The precision in measurement desired may be such that a less elaborate procedure than that just described can be followed. The correction to be applied is the sum of the mercury vapor pressure at the barometer temperature and of the pressure measured by the McLeod gage. The diffusion pump is only operated when the vacuum has deteriorated to a value where the uncertainty of the McLeod gage measurement is of the same order as the desired precision in the measured pressure. It should be noted the vacuum correction varies with the height of the mercury column, since the volume of the vacuum space varies and the mass of the gas, except the mercury vapor, is approximately constant.

In portable barometers no correction is ordinarily made, or justified, for the back pressure in the vacuum space above the mercury column. If the barometer tube is equipped with a mercury seal valve, the vacuum can be kept within requirements for precision in pressure measurement by periodic evacuation of the tube through the valve. The frequency of evacuation needed can be determined only by experience; in general evacuation is needed after subjecting the barometer to some definite number of pressure cycles.

If the portable barometer is not equipped with a valve in the top of the tube, a poor vacuum may be detected by tipping the tube with suitable precautions to avoid damage or uncovering the bottom of the tube, so that the gas is subjected to about one-fourth of an atmosphere. If the apparent size of the bubble is greater than about two or three millimeters the vacuum needs improvement. In general barometers in the best of condition will have a bubble upon tipping, of the order of about one millimeter in size. Barometers subjected only to ambient atmospheric pressure have been known to maintain a satisfactory vacuum for years; on the other hand, altitude barometers in frequent use over a large pressure range may maintain a satisfactory vacuum only for periods as short as a month. The vacuum is reestablished either by a complete overhaul job on the barometer, or if the design permits, by removing the gas within satisfactory limits by the procedure described in sec. 6.4.

14. Compression of Mercury

The compression of mercury with pressure affects its density as discussed in sec. 4.4. The standard values of the density of mercury are generally for mercury subjected to 1 atm of pressure. The compression of mercury must be considered particularly in high pressure manometers (sec. 5.6) and only in very precise measurements at relatively low pressures. In barometry and for all portable barometers and manometers the accuracy usually obtainable makes application of any correction for mercury compression insignificant.

Consider a manometer in which mercury surface in the two legs are subjected to pressures P and P_1. Then

$$P-P_1=\rho gh. \quad (48)$$

The mercury at the lower mercury level is compressed by pressure P or $P_1+\rho gh$. Assuming that the compression of mercury is given by $\rho=\rho_0(1+aP)$, eq (11), sec. 4.4

$$\rho=\rho_0[1+a(P_1+\rho gh)]. \quad (74)$$

In a more accurate derivation for the compression effect due to a column of mercury the relation is

$$\rho=\rho_0[1+a\,(P_1+\rho_0 gh)]. \quad (75)$$

Here ρ and ρ_0 are respectively the densities of mercury at pressure $P_1+\rho gh$ and at zero pressure; h is the height of the mercury column; and a is the volume coefficient of compression per unit pressure.

The standard density ρ_s applies to mercury under a pressure of one atmosphere. Therefore, if a_s is the compression coefficient per atmosphere,

$$\rho_s=\rho_0\,(1+a_s). \quad (76)$$

Without significant error eq (75) now becomes

$$\rho=\rho_s\,[1-a_s+a_s\,(P_1+\frac{h}{h_s})]. \quad (77)$$

and eq (48) where in atmospheres $P-P_1=\rho h/\rho_s h_s$

$$P-P_1=\frac{h}{h_s}\,[1-a_s+a_s\,(P_1+\frac{h}{h_s})]. \quad (78)$$

All of the quantities in the right hand side of the equation are either constants or measured. The pressure $P-P_1$ is in atmospheres and h_s is the height of the mercury column at 1 atm of absolute pressure.

Consider the case of the barometer where 1 atm of pressure is defined as a mercury column 760 mm in height subjected to standard gravity with the density of mercury equal to 13.5951 g/cm.[3] This density is the commonly accepted value at 0° C and under a pressure of 1 atm. To consider this case, eq (78) can be written, since $P_1=0$.

$$P=\frac{h}{h_s}\,[1-a_s+a_s\frac{h}{h_s}]. \quad (79)$$

At the bottom of the mercury column where the mercury is subjected to 1 atm of pressure, eq (79) gives P=unity. At the top of the column the term $a_s h/h_s$ is practically zero and $P=h(1-a_s)/h_s$. Two conclusions can be derived. First, an interval of 1 mm will represent a higher pressure at the bottom than at the top of the column, specifically for 1 atm difference in compressing pressure, about 4 parts per million. Second, a pressure of 1 atm is defined as 1,013.250 dynes/cm², which when converted to a mercury column of 760 mm implies a mean density of mercury of 13.5951 g/cm² at 0° C. Thus in a mercury column of 760 mm representing 1 atm of absolute pressure, the density of mercury assumed is 2 parts per million greater than 13.5951 g/cm² at the bottom of the column and the same amount less at the top of the column. Thus the assumed density at 0° C and at 1 atm differs from the presently accepted value by about 2 parts per million. For most purposes the point is academic.

In manometers measuring gage pressure (differential pressure with reference to atmospheric pressure) the situation is the reverse of that for barometers, since the mercury is generally subjected to pressures above atmospheric. A millimeter of column height is equivalent to a pressure greater than 1 mm of mercury under standard conditions, roughly amounting to 4 parts per million per atmosphere of applied pressure.

15. Computation of Corrections

Representative examples of the computation of corrections as outlined in the previous sections may be useful. For many types of portable barometers and manometers the only corrections ordinarily applied are for scale, temperature and gravity errors. Two examples of such cases will be given.

One additional example will be presented where higher accuracy is desired and corrections for the more significant errors will be applied. Some errors will remain uncorrected, such as for the compressibility of mercury, since the accuracy attainable normally makes them insignificant.

The application of the corrections is based upon: (a) adequate primary data; and (b) upon the use of tables such as presented in this paper. It must be emphasized that valid alternative methods of computing the corrections exist and that the methods here used are justified only by their convenience.

15.1. Fortin Barometer

The following readings are taken:

Reading: 1021.15 mb

Barometer temperature: 23.2° C.

Other needed data or information are:

Acceleration of gravity: 979.640 cm/sec²

Scale correction (includes correction for zero, capillary and vacuum errors)+0.35 mb

Brass scale calibrated to be accurate at 0° C.

(a) Scale Correction

Reading $=1021.15$

Scale correction $=+0.35$

R_s $=1021.50$ mb

(b) Temperature Correction.

Table 6 is entered with 1021.50 and 23.2° C to obtain by interpolation −3.86 mb for the temperature error C_t.

$R_s=1021.50$

$C_t=-3.86$

$R_t=1017.64$ mb

R_t is the reading corrected for temperature error.

(c) Gravity Correction.

Table 8 is entered with 1017.64 mb and 979.640 cm/sec² to obtain by interpolation −1.06 mb for the gravity correction C_g.

R_t=1017.64
C_g= −1.06

P=1016.58 mb

The pressure P is then 1016.58 mb at the level of the mercury surface in the cistern.

15.2. Altitude Barometer, Fixed Cistern

This example is included as an illustration of the application of the temperature correction. The following readings are taken:

Reading: 352.7 mm of mercury
Barometer temperature: 23.6° C.

Other needed data or information are:

Acceleration of gravity=979.640 cm/sec²
Constant K to be added to reading to obtain the temperature correction: 65 mm
Scale correction (includes correction for zero, capillary and vacuum errors): −0.5 mm of mercury at the reading.

Brass scale calibrated to be correct at 0° C or if not, error is absorbed in the scale correction.

(a) Scale correction

Reading R=352.7
Scale correction C_s=−0.5

Corrected reading R_s=352.2 mm of mercury

(b) Temperature correction

R_s =352.2
Constant K= 65.0 (see eq (36) sec. 9.3.1.)

R_s+K =417.2 mm of mercury.

Temperature correction table 6 is entered with R_s+K and 23.6° C to obtain −1.6 mm as the temperature correction C_t

R_s=352.2
C_t=−1.6

R_t=350.6 mm of mercury=reading corrected for scale and temperature errors.

(c) Gravity correction

Gravity correction table 8 is entered with the acceleration of gravity 979.640 cm/sec² and R_t, to obtain −0.37 mm as the correction.

R_t=350.6
C_g=−0.4

P=350.2 mm of mercury.

Thus, the pressure at the level of the mercury surface in the cistern is 350.2 mm of mercury.

15.3. Manometer, U-tube

In this example all corrections normally applied will be made based upon an accuracy of 0.01 mm of mercury in a pressure by a U-tube manometer.

The procedure is essentially the same for a U-tube barometer, except for differences, easy to handle, due to the fact that the pressure above one mercury surface is nominally zero in the barometer; this fact may however make a vacuum correction necessary.

The following readings are taken on a manometer illustrated in figure 4L.

Reading on scale:
upper mercury surface 1150.92 mm
lower mercury surface 130.27 mm
Manometer temperature: 23.21° C
Meniscus heights: upper 1.0 mm; lower 1.3 mm

Other needed data or information are:

Bore of tube: 20 mm
Acceleration of gravity: 979.640 cm/sec²
Absolute pressure P_0, figure 4L: 380.22 mm of mercury
Elevation at which differential pressure is desired: 20 ft below the mercury surface at which the differential pressure is zero (h_0 in fig. 4L).

Zero correction: the reading at zero differential pressure averages 0.02 mm higher in tube A, figure 4L (high-pressure side), after applying the capillary correction. While it is questionable if this correction is a constant independent of differential pressure, it will be applied.

Scales and vernier will be assumed to measure column heights accurately at 0° C.

Thermal coefficient of expansion of scale: 17.2×10^{-6} per ° C

Alinement errors are assumed to be zero.

(a) Nominal height of mercury column

R_1= 1150.92
R_2=−130.27

Nominal height= 1020.65

(b) Zero correction

Since the reading tube A reads higher at zero differential pressure, the nominal reading should be increased 0.02 mm and becomes 1020.67 mm.

(c) Capillary correction

From table 10 the correction for a meniscus height of 1.0 mm, tube bore, 20 mm=+0.024 mm; for a meniscus height of 1.3 mm=+0.030 mm. The nominal reading, corrected for capillarity is 1020.67−0.030+0.024=1020.66 mm, which is h_t, the corrected scale reading at 23.21° C.

(d) Actual height of mercury column at 23.21° C

To reduce the nominal height h_t to the actual height h at 23.21° C, a correction must be made for the thermal expansion of the scale. In the absence of tables,

$$h=\frac{h_t}{1+st}=\frac{1020.66}{1+17.2\times23.21\times10^{-6}}=1020.25 \text{ mm}.$$

(e) Temperature and gravity correction

These corrections can be made in one of two ways, both of which will be presented. In the first procedure a correction to be applied to h will be computed. The sum of the temperature correction C_t and the gravity correction C_g is:

$$C_t+C_g=\left(\frac{mt}{1+mt}+\frac{g-g_s}{g_s}\right)h.$$

The term $mt/(1+mt)$ is obtained from table 7,

the column headed invar, since here the thermal expansion of the scale is zero. For 23.21° C, $F=-0.0042018$.

The term $(g-g_s)g_s$ is obtained from table 8 from the column headed "Correction factor". For 979.640 cm/sec² it equals −0.0010452.

Their sum gives

$$C_t+C_g=-0.0052470(1020.25)=-5.35 \text{ mm}.$$

The reading corrected for temperature and gravity errors, the differential pressure p in figure 4L is then

$$p=1020.25-5.35=1014.90 \text{ mm of mercury}.$$

Alternatively, the differential pressure P can be computed directly from

$$p=\frac{\rho g h}{\rho_s g_s}. \tag{45}$$

Here ρ_s, and ρ are the density of mercury respectively at 0° C and 23.21° C, 13.5951 and 13.5380 (from table 3) gs/cm³; and g_s and g are the standard and ambient accelerations of gravity, 980.665 and 979.640 cm/sec², respectively.

Inserting these values, and the value for h in (d) above, in eq (45)

$$p=\frac{13.5380\times 979.640\times 1020.25}{13.5951\times 980.665}$$

$$=1014.90 \text{ mm of mercury}.$$

A slight difference of the order of a few microns (0.001 mm) in the values of p by the two methods of computation can be expected from the fact that m, the volume coefficient of thermal expansion of mercury is an average value. The latter value of p is the more accurate.

(f) Return head correction

If the differential pressure (fig. 4L) $P_{13}-P_3$ is desired:

$$P_{13}-P_3=p-\frac{dP_0}{dh}h. \tag{57}$$

Here $p=1014.90$ mm of mercury and $h=1020.25$ mm (3.347 ft).

For an air pressure $P_0=380.22$ mm of mercury and temperature of 23.21° C, the air density is obtained by interpolation from table 12 to be 595.7×10^{-6}g/cm³. From table 11, dP_0/dh corresponding to this density is found to be 0.0133 mm Hg/ft. Then

$$P_{13}-P_3=1014.25-0.0133\times 3.347$$

$$=1014.21 \text{ mm of mercury}.$$

The return head correction is 0.04 mm of mercury.

(g) Differential pressure at level 20 ft below P_0 level

In this case, referring to figure 4L:

$$P_{12}-P_2=p-\frac{dP_0}{dh}\left(h_0+\frac{h}{2}\right)+\frac{dP_{10}}{dh}\left(h_0-\frac{h}{2}\right). \tag{65b}$$

Here $p=1014.25$ mm of mercury; $dP_0/dh=0.0133$ mm of mercury / ft;

$$h_0+\frac{h}{2}=20+1.673 \text{ ft.; and } h_0-\frac{h}{2}=18.327 \text{ ft}.$$

To compute dP_{10}/dh, P_{10} to sufficient accuracy $=p+P_0=1014.25+380.2=1394.4$ mm of mercury. Following the procedure outlined above under (f) using tables 11 and 12, $dP_{10}/dh=0.0489$ mm of mercury / ft for $p+P_0$ and 23.21° C, therefore

$$P_{12}-P_2=1014.25-0.0133\times 21.7+0.0489\times 18.3$$

$$=1013.64 \text{ mm of mercury}.$$

The elevation correction is +0.61 mm of mercury $(P_{12}-P_2-P_{13}+P_3)$.

16. Testing at the National Bureau of Standards

For testing mercury barometers, the National Bureau of Standards has a standard barometer and barostat installed in a subbasement room the temperature of which is maintained closely at 25° C. See secs. 5.4, 6.1.3, 6.2.2, and 8.2 for details. The accuracy, now 0.02 to 0.03 mm of mercury, is not considered entirely adequate for testing portable barometers with accuracies approaching 0.05 mm of mercury. Continuing effort is made to improve the accuracy.

For testing manometers the Bureau has a mercury manometer with a range of 50 psi (100 in. of mercury). Piston gages of the air type are under development for use as standards in order to improve the accuracy and convenience of operations.

The National Bureau of Standards accepts for test mercury barometers and manometers which are: (a) the reference standard or one working standard of an organization or laboratory; and (b) reference tests when the measurement of pressure is in dispute. The accuracy of the instruments submitted must be at least ±0.1 mm of mercury. See ref. [582] for details regarding the acceptance of instruments for test.

Instruments submitted for test should be sent to "National Bureau of Standards, Attn: Mechanical Instruments Section, Washington 25, D.C."

A purchase order issued to the National Bureau of Standards authorizing the test must be supplied. It is advisable to arrange for the test by correspondence or telephone previous to shipping the instrument. Tests fees are listed in the current NBS Test Fee Schedules which are based on cost.

The experience of the Bureau is available to laboratories and manufacturers on the various problems associated with the precise measurement of pressure. Visits of technical personnel to discuss problems should be arranged in advance.

The authors are grateful to Dr. H. F. Stimson and to L. F. Harrison, of the Weather Bureau for many suggestions and correction.

17. References

The first two digits in each number are the year of publication of the reference.

[011] Comptes rendus des séances de la troisième conférence génerale des poids et mesures, réunie à Paris en 1901. Travaux et memoires de Bureau International des Poids et Mesures.

[121] P. W. Bridgman, Mercury, liquid and solid under pressure, Proc. Am. Acad. Arts Sci. **47**, 347 (1912).

[141] M. H. Stillman, Note on the setting of a mercury surface to a required height, BS Sci. Pap. **10**, 371 (1914) S214.

[191] P. W. Bridgman, The measurement of high hydrostatic pressures; a secondary mercury resistance gauge, Proc. Am. Acad. Arts. Sci. **44**, 221 (1919).

[231] F. A. Gould, Barometers and manometers, Dict. Applied Physics **3**, 140 (Macmillan & Co. London, 1923).

[271] F. G. Keyes and J. Dewey, An experimental study of the piston pressure gage to 500 atmospheres, J. Opt. Soc. Am. **14**, 491 (1927).

[291] K. C. D. Hickman, The mercury meniscus, J. Opt. Soc. and Rev. Sci. Instr. **19**, 190 (1929).

[301] U.S. Weather Bureau, Barometers and the measurement of atmospheric pressure, Circular F, Instrument Division, reprinted (1930).

[311] C. H. Meyers and R. S. Jessup, A multiple manometer and piston gauges for precision measurements, BS J. Research **6**, 1061 (1931) RP324.

[321] A. Michels, The calibration of a pressure balance in absolute units, Proc. Krinkl. Akad. Wetenschap., Amsterdam **35**, 994 (1932).

[331] F. E. Fowle, Smithsonian physical tables, 8th rev. ed., (Smithsonian Inst., 1933).

[332] F. A. Gould and J. C. Evans, A new form of barostat, J. Sci. Instr. **10**, 215 (1933).

[333] J. E. Sears and J. S. Clark, New standard barometer, Proc. Roy. Soc. (A)**139**, 130 (1933).

[341] I. B. Smith and F. G. Keyes, Steam research, III A. Compressibility of liquid mercury from 30° to 300° C, Proc. Am. Acad. Arts Sci. **69**, 313 (1934).

[351] C. Moon, A precision cathetometer, J. Research NBS **14**, 363 (1935) RP774.

[361] E. Schmidt, Measurement of small pressure differences at high pressure, VDI **80**, 635 (1936). (In German).

[371] J. R. Roebuck and W. Cram, A multiple column mercury manometer for pressures to 200 atmospheres, Rev. Sci. Instr. **8**, 215 (1937).

[391] J. Reilly and W. N. Rae, Physico-chemical methods, **1**, (D. Van Nostrand Co., N.Y., 1939).

[401] B. E. Blaisdell, The physical properties of fluid interfaces of large radius of curvature. II. Numerical tables for capillary depressions and meniscus volumes, in moderately large tubes, J. Math. and Phys. **19**, 217 (1940).

[411] J. A. Beattie, B. E. Blaisdell, and J. Kaye, An experimental study of the absolute temperature scale. IX. The determination of the capillary depression and meniscus volume of mercury in a manometer, Proe. Am. Acad. Arts Sci. **74**, 389 (1941).

[412] J. A. Beattie, D. D. Jacobus, J. M. Gaines, Jr., M. Benedict, and B. E. Blaisdell, An experimental study of the absolute temperature scale. VI. The gas thermometer assembly and the experimental method, Proc. Am. Acad. Arts Sci. **74**, 327 (1941).

[413] J. A. Beattie, B. E. Blaisdell, J. Kaye, H. T. Gerry, and C. A. Johnson, An experimental study of the absolute temperature scale. VIII. The thermal expansion and compressibility of vitreous silica and the thermal dilation of mercury, Proc. Am. Acad. Arts Sci. **74**, 370 (1941).

[414] G. W. C. Kaye, and T. H. Laby, Physical and chemical constants (Longman, Green & Co., 1941).

[421] E. Wickers, Pure mercury, Chem. Eng. News **20**, 1111 (1942).

[451] J. Kistemaker, On the volume of mercury meniscus and the surface tension of mercury and deduced from them, Physica **11**, 270 (1945).

[452] J. Kistemaker, The capillary depression of mercury and high precision manometry, Physica **11**, 277 (1945).

[453] D. J. LeRoy, An automatic differential manometer, Ind. Eng. Chem. Anal. Ed. **17**, 652 (1945).

[454] H. F. Stimson, The measurement of some thermal properties of water, J. Wash. Acad. Sci. **35**, 201 (1945).

[461] C. Kemball, On the surface tension of mercury, Trans. Faraday Soc. **42**, 526 (1946).

[471] D. R. Stull, Vapor pressure of pure substances, Ind. Eng. Chem. **39**, 517 (1947). (References and data on vapor pressure of mercury.)

[481] D. P. Johnson, Calibration of altimeters under pressure eonditions simulating dives and climbs, NACA Tech. No. 1562, (1948).

[482] W. G. Bromacher and H. E. Ferguson, Manometer tables, Inst. Soc. Am. RP2.1, 32 pp. (1948).

[483] I. E. Puddington, Sensitive mercury manometer, Rev. Sci. Instr. **19**, 577 (1948).

[491] W. G. Brombacher, Some problems in the precise measurement of pressure, Instruments **22**, 355 (1949).

[492] H. Ebert, Establishment of a pressure scale and experimental realization up to 20,000 atmospheres, Z. angew. Phys. **1**, 331 (1949). (In German.)

[493] H. F. Stimson, The international temperature scale of 1948, J. Research NBS **42**, 209 (1949) RP1962.

[494] R. S. Burden, Surface tension and the spreading of liquids, (Cambridge Univ. Press, 2d ed., 1949).

[495] W. D. Wood, The development and maintenance of calibrating standards by an instrument manufacturer, Instruments **22**, 1004 (1949).

[496] P. W. Bridgman, The physics of high pressure (G. Bell & Sons, London, 1931 ed. with suppl., 1949).

[501] F. P. Price and P. D. Zemany, A simple recording manometer, Rev. Sci. Instr. **21**, 261 (1950).

[511] S. Haynes, Automatic calibration of radiosonde baroswitches, Electronics **24**, 126 (May 1951).

[512] R. G. List, Smithsonian Meteorological Tables 6th Rev. ed. (Smithsonian Instit., 1951).

[513] J. M. Los and J. A. Morrison, A sensitive differential manometer, Rev. Sci. Instr. **22**, 805 (1951).

[514] R. Meaken, Determination of mercury level in steel-tube manometer. J. Sci. Instr. **28**, 372 (1951).

[515] E. C. Hass, Correcting mechanism for mercury column type measuring instruments, U.S. Patent No. 2,542,671 (Feb. 20, 1951).

[516] T. B. Douglas, A. F. Ball, and D. C. Ginnings, Heat capacity of liquid mercury between 0° and 450°C; calculation of certain thermodynamic properties of the saturated liquid and vapor, J. Research NBS 46, 334 (1951) RP2204.

[521] F. A. Gould and T. Vickers, Capillary depression in mercury barometers and manometers, J. Sci. Instr. 29, 85 (1952).

[522] J. B. Lawrence, Mercury, Instruments 25, 310 (1952).

[531] Charles D. Hodgman, ed. Handbook of physics and chemistry (Chemical Publishing Co., 35th ed., 1953–54).

[532] H. J. Svec and D. S. Gibbs, Recording mercurial manometer for pressure range 0–760 mm Hg, Rev. Sci. Instr. 24, 202 (1953).

[533] World Meteorological Organization, Commission for Instruments and Methods of Observation, Abridged final report of the first session, Toronto, 1953. WMO No. 19, RP 9, p. 73, Secretariat of the WMO, Geneva, Switzerland, 1953.

[534] World Meteorological Organization, Fourth session of the Executive Committee, Geneva, 1953. Abridged report with resolutions. WMO No. 20, RC5, p. 86, Secretariat of the WMO, Geneva, Switzerland, 1953.

[535] R. H. Busey and W. F. Giauque, The heat capacity of mercury from 15 to 330°C. Thermodynamic properties of solid, liquid and gas. Heat of fusion and vaporization, J. Am. Chem. Soc. 75, 806 (1953).

[541] K. E. Bett, P. F. Hayes, and D. M. Newitt, The construction, operation and performance of a primary standard mercury column for the measurement of high pressure. Phil. Trans. 247, 59 (1954).

[542] K. E. Bett, K. E. Weale, and D. M. Newitt, The critical evaluation of compression data for liquids and a revision of the isotherms of mercury, Brit. J. Appl. Phys. 5, 243 (1954).

[543] T. F. W. Embleton, A semi-automatic electrical manometer designed to calibrate a Mack-Zehnder interferometer system for the recording of transient pressure changes. Rev. Sci. Instr. 25, 246 (1954).

[544] J. R. Roebuck and H. W. Ibser, Precision multiple-mercury-column-manometer, Rev. Sci. Instr. 25, 46 (1954).

[551] L. V. Judson, Units of weight and measure; definitions and tables of equivalents, NBS Misc. Publ. 214, (1955).

[552] National Physical Laboratories, Teddington, Measurement of pressure with the mercury barometer, Notes on App. Sci. No. 9, (1955).

[553] H. F. Stimson, Precision resistance thermometry and fixed points; Temperature, its measurement and control, Am. Inst. Phys. 2, 141 (1955).

[554] E. T. Levanto, A new normal barometer, Ann. Acad. Sci. Fennicae AI, No. 191, (1955).

[555] Helmut Moser, High temperature gas thermometry. Temperature, its measurement and control, Am. Inst. Phys. 2, 103 (1955).

[556] Second Congress of the World Meteorological Organization, Geneva, 1955. Final report, vol. II, Technical regulations. WMO No. 48, RC10, p. 23, Secretariat of the WMO, Geneva, Switzerland, 1956.

[557] E. C. Halliday and H. J. Richards, The barometer calibrating facilities at the South African National Physical Laboratory. S. African J. Sci. 51, 217 (1955).

[558] F. M. Ernsberger and H. W. Pitman, New absolute manometer for vapor pressures in the micron range, Rev. Sci. Inst. 26, 584 (1955).

[561] N. Fuschillo, Improved method for cleaning mercury, Rev. Sci. Instr. 27, 410 (1956).

[562] M. Ross and E. E. Suckling, Permanent record from a mercury manometer, Rev. Sci. Instr. 27, 409 (1956).

[563] E. C. Halliday, Temperature corrections for commercial barometers. S. African J. Sci. 52, 178 (1956).

[564] World Meteorological Organization Technical Regulations, Secretariat of the WMO, Geneva, Switzerland 1, WMO No. 49, Bd 2 (1956).

[571] A. H. Cook and N. W. B. Stone, Precise measurements of the density of mercury at 20° C. I. Absolute displacement method. Phil. Trans. [A] 250, 279 (1957).

[572] J. Farquharson and H. A. Kermicle, Precise automatic manometer reader, Rev. Sci. Instr. 28, 324 (1957).

[573] K. W. T. Elliot and D. C. Wilson, An optical probe for accurately measuring displacements of a reflecting surface, J. Sci. Instr. 34, 349 (1957).

[574] C. L. Gordon and E. Wichers, Purification of mercury and its physical properties, Ann. N.Y. Acad. Sci. 65, 369 (1957).

[575] H. Moser, J. Otto and W. Thomas, Gasthermometrische Messungen bei hohen Temperaturen, Z. Physik 147, 59 (1957).

[576] J. Gielessen, Ueber ein Normalbarometer neuerer Konstruktion, Z. Instrumentenk 65, 63 (1957).

[581] A. J. Eberlein, Laboratory pressure measurement requirements for evaluating air data computer, Aeronaut. Eng. Rev. 17, 53 (1958).

[582] Test for schedules of the National Bureau of Standards, Mechanics, Reprinted from Federal Register 23, No. 188, (1958).

[591] WBAN Manual of barometry. Published under sponsorship of U.S. Weather Bureau, Dept. of the Air Force, Air Weather Service and Dept. of the Navy, Naval Weather Service Division. Govt. Printing Office 1 (1959). In press.

[592] Jean Terrien, Méthodes optiques pour measurer la hauteur de mercure d'un manomètre; noveau manomètre interferéntiel, Rev. d'Optique 38, 24 (1959).

TABLE 1. *Conversion factors for various pressure units equivalent for unit value in first column*

Pressure unit value	*mb*	*mm mercury 0° C*	*in. mercury 0° C*	*g/cm²*	*lb/in².*	*lb/ft²*	*cm water 20° C*	*in. water 20° C*
1 atm	1013.250	760.000	29.9213	1033.227	14.69595	2116.22	1035.08	407.513
1 mb	1	0.75006	0.029530	1.0197	0.014504	2.0885	1.0215	0.40218
1 mm mercury	1.3332	1	0.03937	1.3595	.019337	2.7845	1.3619	.53620
1 in. mercury	33.864	25.400	1	34.531	.49115	70.726	34.593	13.619
1 g/cm²	0.98067	0.73556	0.028959	1	.014223	2.0482	1.0018	0.39441
1 lb/in.²	68.9476	51.715	2.0360	70.307	1	144	70.433	27.730
1 lb/ft²	0.47880	0.35913	0.014139	0.48824	0.0069444	1	0.48912	0.19257
1 cm water 20° C	.97891	.73424	.028907	.99821	.014198	2.0444	1	.3937
1 in. water 20° C	2.4864	1.8650	.073424	2.5354	.036063	5.1930	2.5400	1

1 atm=10332.3 Kg/m²=1.03323 Kg/cm².
1 bar=1000 mb=10⁶dynes/cm².
1 in.=2.54 cm (old value, 2.54000508 cm; 2 parts per million greater).
1 lb=.45359237 Kg (old value, .45359243 Kg; 2 parts per 15 million greater).
Density of water at 20° C=. 998207 grams/cm².

TABLE 2. *Ratio of the density of mercury at t° to the density at 0° C at 1 atm of pressure*

°C	0	1	2	3	4	5	6	7	8	9
0	1.0000 0000	0.9998 1859	0.9996 3722	0.9994 5591	0.9992 7465	0.9990 9344	0.9989 1229	0.9987 3118	0.9985 5012	0.9983 6911
10	0.9981 8816	.9980 0725	.9978 2639	.9976 4559	.9974 6483	.9972 8412	.9971 0346	.9969 2285	.9967 4228	.9965 6177
20	.9963 8130	.9962 0088	.9960 2051	.9958 4019	.9956 5991	.9954 7968	.9952 9950	.9951 1936	.9949 3927	.9947 5923
30	.9945 7923	.9943 9928	.9942 1938	.9940 3952	.9938 5970	.9936 7993	.9935 0021	.9933 2053	.9931 4089	.9929 6130
40	.9927 8175	.9926 0225	.9924 2279	.9922 4337	.9920 6400	.9918 8467	.9917 0538	.9915 2614	.9913 4694	.9911 6777
50	.9909 8866	.9908 0958	.9906 3054	.9904 5155	.9902 7260	.9900 9369	.9899 1482	.9897 3598	.9895 5719	.9893 7844

TABLE 3A. *Density and vapor pressure of mercury*

The density is based upon the value 13.5951 g/cm³ at 0° C and the ratios of Table 2.

Temperature		Density	Vapor pressure 0.001 mm of mercury	Temperature		Density	Vapor pressure 0.001 mm of mercury
°C	°F	g/cm³		°C	°F	g/cm³	
−20	−4	13.6440	0.024	30	86	13.5214	2.94
−10	14	13.6198	.073	31	87.8	13.5190	----------
0	32	13.5951	.203	32	89.6	13.5165	----------
1	33.8	13.5926	----------	33	91.4	13.5141	----------
2	35.6	13.5902	----------	34	93.2	13.5116	----------
3	37.4	13.5877	----------	35	95	13.5092	4.37
4	39.2	13.5852	----------	36	96.8	13.5067	----------
5	41	13.5828	.330	37	98.6	13.5043	----------
6	42.8	13.5803	----------	38	100.4	13.5018	----------
7	44.0	13.5779	----------	39	102.2	13.4994	----------
8	46.4	13.5754	----------	40	104	13.4970	6.32
9	48.2	13.5729	----------	41	105.8	13.4945	----------
10	50	13.5705	.540	42	107.0	13.4921	----------
11	51.8	13.5680	----------	43	109.4	13.4896	----------
12	53.6	13.5655	----------	44	111.2	13.4872	----------
13	55.4	13.5631	----------	45	113	13.4848	9.20
14	57.2	13.5606	----------	46	114.8	13.4823	----------
15	59	13.5582	.820	47	116.6	13.4799	----------
16	60.8	13.5557	----------	48	118.4	13.4775	----------
17	62.0	13.5533	----------	40	120.2	13.4750	----------
18	64.4	13.5508	1.08	50	122	13.4726	13.26
19	66.2	13.5484	----------	51	123.8	13.4702	----------
20	68	13.5459	1.28	52	125.6	13.4677	----------
21	69.8	13.5435	----------	53	127.4	13.4653	----------
22	71.6	13.5410	1.52	54	129.2	13.4629	----------
23	73.4	13.5385	----------	55	131	13.4604	18.78
24	75.2	13.5361	1.80	56	132.8	13.4580	----------
25	77	13.5336	----------	57	134.6	13.4550	----------
20	78.8	13.5312	2.12	58	136.4	13.4531	----------
27	80.6	13.5287	----------	50	138.2	13.4507	----------
28	82.4	13.5263	2.50	60	140	13.4483	20.32
29	84.2	13.5239	----------	----------	----------	----------	----------

TABLE 3B. *Density of mercury*

The density is based upon the conversion factor: unit g/cm³=0.03612729 lb/in.³ in which 1 in.=2.54 cm and 1 lb=453.59237 g

Temperature	Density	
°F	lb/in.³	g/cm³
0	0.49274	13.6391
10	.49225	13.6253
20	.49175	13.6116
32	.491154	13.5951
40	.49076	13.5841
50	.49026	13.5704
60	.48977	13.5568
70	.48928	13.5431
80	.48878	13.5295
90	.48829	13.5159
100	.48780	13.5023
110	.48731	13.4888
120	.48683	13.4753
130	.48633	13.4617

TABLE 4. *Density of mercury*

Based upon the value of 13.5458 925 g/cm³ at 20° C and the ratios of table 2

Temperature		Density	Temperature		Density
°C	°F	g/cm³	°C	°F	g/cm³
0	32.00	13.5950 889	30	86.00	13.5213 930
1	33.80	13.5926 226	31	87.80	13.5189 466
2	35.60	13.5901 569	32	80.60	13.5165 000
3	37.40	13.5876 019	33	01.40	13.5140 550
4	39.20	13.5852 277	34	93.20	13.5110 110
5	41.00	13.5827 641	35	95.00	13.5001 670
6	42.80	13.5803 014	36	96.80	13.5067 237
7	44.60	13.5778 392	37	98.60	13.5042 809
8	46.40	13.5753 777	38	100.40	13.5018 387
9	48.20	13.5729 168	39	102.20	13.4993 971
10	50.00	13.5704 568	40	104.00	13.4969 561
11	51.80	13.5679 073	41	105.80	13.4945 158
12	53.60	13.5655 385	42	107.60	13.4020 761
13	55.40	13.5630 905	43	109.40	13.4896 368
14	57.20	13.5606 230	44	111.20	13.4871 983
15	59.00	13.5581 663	45	113.00	13.4847 603
16	60.80	13.5557 102	46	114.80	13.4823 228
17	62.60	13.5532 548	47	116.60	13.4798 860
18	64.40	13.5507 999	48	118.40	13.4774 498
19	66.20	13.5483 459	49	120.20	13.4750 139
20	68.00	13.5458 924	50	122.00	13.4725 789
21	69.80	13.5434 395	51	123.80	13.4701 443
22	71.60	13.5409 874	52	125.60	13.4677 103
23	73.40	13.5385 359	53	127.40	13.4652 769
24	75.20	13.5360 850	54	129.20	13.4628 440
25	77.00	13.5336 347	55	131.00	13.4604 117
26	78.80	13.5311 852	56	132.80	13.4579 800
27	80.60	13.5287 362	57	134.60	13.4555 486
28	82.40	13.5262 878	58	136.40	13.4531 180
29	84.20	13.5238 402	59	138.20	13.4506 878

TABLE 5. *Coefficients of linear expansion*

Multiply all values by 10^{-6}

Material	Coefficient	
	per °C	*per* °F
Aluminum	24.5±0.5	13.6
Brass, yellow	18.4±0.8	10.22
Cast iron	8.5±0.5	4.7
Duralumin	23.5±1	13 1
Glass, soda lime	8.5±0.5	4.7
Glass, Pyrex	3.0	1.7
Invar	0 to 5	0 to 3
Monel metal	14 ±0.5	7.8
Stainless steel (18+8)	17 ±1	9.4
Stainless steel, Carpenter No. 8	17 ±0.5	9.4
Steel, low carbon	11.5±0.5	6.4

TABLE 6. *Temperature corrections for Fortin barometer with brass scales*

All corrections are to be subtracted from the reading.

Temperature	Correction factor	Barometer reading, millibars, inches or millimeters of mercury																			
		100	105	110	115	120	125	130	135	140	145	150	155	160	165	170	175	180	185	190	195
°C	%																				
0	0.0	0.00	0.00	0.00	0.00	0.00	0.00	0.00	0.00	0.00	0.00	0.00	0.00	0.00	0.00	0.00	0.00	0.00	0.00	0.00	0.00
5	.081620	.08	.09	.09	.09	.10	.10	.11	.11	.11	.12	.12	.13	.13	.13	.14	.14	.15	.15	.16	.16
10	.16310	.16	.17	.18	.19	.20	.20	.21	.22	.23	.24	.24	.25	.26	.27	.28	.29	.29	.30	.31	.32
11	.17938	.18	.19	.20	.21	.22	.22	.23	.24	.25	.26	.27	.28	.29	.30	.30	.31	.32	.33	.34	.35
12	.19565	.20	.21	.22	.22	.23	.24	.25	.26	.27	.28	.29	.30	.31	.32	.33	.34	.35	.36	.37	.38
13	.21192	.21	.22	.23	.24	.25	.26	.28	.29	.30	.31	.32	.33	.34	.35	.36	.37	.38	.39	.40	.41
14	.22818	.23	.24	.25	.26	.27	.29	.30	.31	.32	.33	.34	.35	.37	.38	.39	.40	.41	.42	.43	.44
15	.24443	.24	.26	.27	.28	.29	.31	.32	.33	.34	.35	.37	.38	.39	.40	.42	.43	.44	.45	.46	.48
16	.26068	.26	.27	.29	.30	.31	.33	.34	.35	.36	.38	.39	.40	.42	.43	.44	.46	.47	.48	.50	.51
17	.27692	.28	.29	.30	.32	.33	.35	.36	.37	.39	.40	.42	.43	.44	.46	.47	.48	.50	.51	.53	.54
18	.29316	.29	.31	.32	.34	.35	.37	.38	.40	.41	.43	.44	.45	.47	.48	.50	.51	.53	.54	.56	.57
19	.30939	.31	.32	.34	.36	.37	.39	.40	.42	.43	.45	.46	.48	.50	.51	.53	.54	.56	.57	.59	.60
20	.32562	.33	.34	.36	.37	.39	.41	.42	.44	.46	.47	.49	.50	.52	.54	.55	.57	.59	.60	.62	.63
21	.34183	.34	.36	.38	.39	.41	.43	.44	.46	.48	.50	.51	.53	.55	.56	.58	.60	.62	.63	.65	.67
22	.35805	.36	.38	.39	.41	.43	.45	.47	.48	.50	.52	.54	.55	.57	.59	.61	.63	.64	.66	.68	.70
23	.37426	.37	.39	.41	.43	.45	.47	.49	.51	.52	.54	.56	.58	.60	.62	.64	.65	.67	.69	.71	.73
24	.39046	.39	.41	.43	.45	.47	.49	.51	.53	.55	.57	.59	.61	.62	.64	.66	.68	.70	.72	.74	.76
25	.40665	.41	.43	.45	.47	.49	.51	.53	.55	.57	.59	.61	.63	.65	.67	.69	.71	.73	.75	.77	.79
26	.42284	.42	.44	.47	.49	.51	.53	.55	.57	.59	.61	.63	.66	.68	.70	.72	.74	.76	.78	.80	.82
27	.43903	.44	.46	.48	.50	.53	.55	.57	.59	.61	.64	.66	.68	.70	.72	.75	.77	.79	.81	.83	.86
28	.45520	.46	.48	.50	.52	.55	.57	.59	.61	.64	.66	.68	.71	.73	.75	.77	.80	.82	.84	.86	.89
29	.47137	.47	.49	.52	.54	.57	.59	.61	.64	.66	.68	.71	.73	.75	.78	.80	.82	.85	.87	.90	.92
30	.48754	.49	.51	.54	.56	.59	.61	.63	.66	.68	.71	.73	.76	.78	.80	.83	.85	.88	.90	.93	.95
31	.50370	.50	.53	.55	.58	.60	.63	.65	.68	.71	.73	.76	.78	.81	.83	.86	.88	.91	.93	.96	.98
32	.51986	.52	.55	.57	.60	.62	.65	.68	.70	.73	.75	.78	.81	.83	.86	.88	.91	.94	.96	.99	1.01
33	.53600	.54	.56	.59	.62	.64	.67	.70	.72	.75	.78	.80	.83	.86	.88	.91	.94	.96	.99	1.02	1.05
34	.55215	.55	.58	.61	.63	.66	.69	.72	.75	.77	.80	.83	.86	.88	.91	.94	.97	.99	1.02	1.05	1.08
35	.56328	.57	.60	.63	.65	.68	.71	.74	.77	.80	.82	.85	.88	.91	.94	.97	.99	1.02	1.05	1.08	1.11
36	.58442	.58	.61	.64	.67	.70	.73	.76	.79	.82	.85	.88	.91	.94	.96	0.99	1.02	1.05	1.08	1.11	1.14
37	.60054	.60	.63	.66	.69	.72	.75	.78	.81	.84	.87	.90	.93	.96	.99	1.02	1.05	1.08	1.11	1.14	1.17
38	.61666	.62	.65	.68	.71	.74	.77	.80	.83	.86	.89	.92	.96	.99	1.02	1.05	1.08	1.11	1.14	1.17	1.20
39	.63277	.63	.66	.70	.73	.76	.79	.82	.85	.89	.92	.95	.98	1.01	1.04	1.08	1.11	1.14	1.17	1.20	1.23
40	.64883	.65	.68	.71	.75	.78	.81	.84	.88	.91	.94	.97	1.01	1.04	1.07	1.10	1.14	1.17	1.20	1.23	1.27
41	.66498	.66	.70	.73	.76	.80	.83	.86	.90	.93	.96	1.00	1.03	1.06	1.10	1.13	1.16	1.20	1.23	1.26	1.30
42	.68108	.68	.72	.75	.78	.82	.85	.89	.92	.95	.99	1.02	1.06	1.09	1.12	1.16	1.19	1.23	1.26	1.29	1.33
43	.69717	.70	.73	.77	.80	.84	.87	.91	.94	.98	1.01	1.05	1.08	1.12	1.15	1.19	1.22	1.25	1.29	1.32	1.36
44	.71325	.71	.75	.78	.82	.86	.89	.93	.96	1.00	1.03	1.07	1.11	1.14	1.18	1.21	1.25	1.28	1.32	1.36	1.39
45	.72933	.73	.77	.80	.84	.88	.91	.95	.98	1.02	1.06	1.09	1.13	1.17	1.20	1.24	1.28	1.31	1.35	1.39	1.42
46	.74541	.75	.78	.82	.86	.89	.93	.97	1.01	1.04	1.08	1.12	1.16	1.19	1.23	1.27	1.30	1.34	1.38	1.42	1.45
47	.76147	.76	.80	.84	.88	.91	.95	.99	1.03	1.07	1.10	1.14	1.18	1.22	1.26	1.29	1.33	1.37	1.41	1.45	1.48
48	.77744	.78	.82	.86	.89	.93	.97	1.01	1.05	1.09	1.13	1.17	1.21	1.24	1.28	1.32	1.36	1.40	1.44	1.48	1.52
49	.79359	.79	.83	.87	.91	.95	.99	1.03	1.07	1.11	1.15	1.19	1.23	1.27	1.31	1.35	1.39	1.43	1.47	1.51	1.55
50	.80964	.81	.85	.89	.93	.97	1.01	1.05	1.09	1.13	1.17	1.21	1.25	1.30	1.34	1.38	1.42	1.46	1.50	1.54	1.58

Temperature	Barometer reading, millibars, inches or millimeters of mercury																			
	200	205	210	215	220	225	230	235	240	245	250	255	260	265	270	275	280	285	290	295
°C																				
0	0.00	0.00	0.00	0.00	0.00	0.00	0.00	0.00	0.00	0.00	0.00	0.00	0.00	0.00	0.00	0.00	0.00	0.00	0.00	0.00
5	.16	.17	.17	.18	.18	.18	.19	.19	.20	.20	.20	.21	.21	.22	.22	.22	.23	.23	.24	.24
10	.33	.33	.34	.35	.36	.37	.38	.38	.39	.40	.41	.42	.42	.43	.44	.45	.46	.46	.47	.48
11	.36	.37	.38	.39	.39	.40	.41	.42	.43	.44	.45	.46	.47	.48	.48	.49	.50	.51	.52	.53
12	.39	.40	.41	.42	.43	.44	.45	.46	.47	.48	.49	.50	.51	.52	.53	.54	.55	.56	.57	.58
13	.42	.43	.45	.46	.47	.48	.49	.50	.51	.52	.53	.54	.55	.56	.57	.58	.59	.60	.61	.63
14	.46	.47	.48	.49	.50	.51	.52	.54	.55	.56	.57	.58	.59	.60	.62	.63	.64	.65	.66	.67
15	.49	.50	.51	.53	.54	.55	.56	.57	.59	.60	.61	.62	.64	.65	.66	.67	.68	.70	.71	.72
16	.52	.53	.55	.56	.57	.59	.60	.61	.63	.64	.65	.66	.68	.69	.70	.72	.73	.74	.76	.77
17	.55	.57	.58	.60	.61	.62	.64	.65	.66	.68	.69	.71	.72	.73	.75	.76	.78	.79	.80	.82
18	.59	.60	.62	.63	.64	.66	.67	.69	.70	.72	.73	.75	.76	.78	.79	.81	.82	.84	.85	.86
19	.62	.63	.65	.67	.68	.70	.71	.73	.74	.76	.77	.79	.80	.82	.84	.85	.87	.88	.90	.91
20	.65	.67	.68	.70	.72	.73	.75	.77	.78	.80	.81	.83	.85	.86	.88	.90	.91	.93	.94	.96
21	.68	.70	.72	.73	.75	.77	.79	.80	.82	.84	.85	.87	.89	.91	.92	.94	.96	.97	.99	1.01
22	.72	.73	.75	.77	.79	.81	.82	.84	.86	.88	.90	.91	.93	.95	.97	.98	1.00	1.02	1.04	1.06
23	.75	.77	.79	.80	.82	.84	.86	.88	.90	.92	.94	.95	.97	.99	1.01	1.03	1.05	1.07	1.09	1.10
24	.78	.80	.82	.84	.86	.88	.90	.92	.94	.96	.98	1.00	1.02	1.03	1.05	1.07	1.09	1.11	1.13	1.15
25	.81	.83	.85	.87	.89	.91	.94	.96	.98	1.00	1.02	1.04	1.06	1.08	1.10	1.12	1.14	1.16	1.18	1.20
26	.85	.87	.89	.91	.93	.95	0.97	.99	1.01	1.04	1.06	1.08	1.10	1.12	1.14	1.16	1.18	1.21	1.23	1.25
27	.88	.90	.92	.94	.97	.99	1.01	1.03	1.05	1.08	1.10	1.12	1.14	1.16	1.19	1.21	1.23	1.25	1.27	1.30
28	.91	.93	.96	.98	1.00	1.02	1.05	1.07	1.09	1.12	1.14	1.16	1.18	1.21	1.23	1.25	1.27	1.30	1.32	1.34
29	.94	.97	.99	1.01	1.04	1.06	1.08	1.11	1.13	1.15	1.18	1.20	1.23	1.25	1.27	1.30	1.32	1.34	1.37	1.39
30	.98	1.00	1.02	1.05	1.07	1.10	1.12	1.15	1.17	1.19	1.22	1.24	1.27	1.29	1.32	1.34	1.37	1.39	1.41	1.44

TABLE 6. *Temperature corrections for Fortin barometer with brass scales*—Continued

All corrections are to be subtracted from the reading.

Temperature	Barometer reading, millibars, inches or millimeters of mercury																			
	200	205	210	215	220	225	230	235	240	245	250	255	260	265	270	275	280	285	290	295
°C																				
31	1.01	1.03	1.06	1.08	1.11	1.13	1.16	1.18	1.21	1.23	1.26	1.28	1.31	1.33	1.36	1.39	1.41	1.44	1.46	1.49
32	1.04	1.07	1.09	1.12	1.14	1.17	1.20	1.22	1.25	1.27	1.30	1.33	1.35	1.38	1.40	1.43	1.46	1.48	1.51	1.53
33	1.07	1.10	1.13	1.15	1.18	1.21	1.23	1.26	1.29	1.31	1.34	1.37	1.39	1.42	1.45	1.47	1.50	1.53	1.55	1.58
34	1.10	1.13	1.16	1.19	1.21	1.24	1.27	1.30	1.33	1.35	1.38	1.41	1.44	1.46	1.49	1.52	1.55	1.57	1.60	1.63
35	1.14	1.16	1.19	1.22	1.25	1.28	1.31	1.34	1.36	1.39	1.42	1.45	1.48	1.51	1.53	1.56	1.59	1.62	1.65	1.68
36	1.17	1.20	1.23	1.26	1.29	1.31	1.34	1.37	1.40	1.43	1.46	1.49	1.52	1.55	1.58	1.61	1.64	1.67	1.69	1.72
37	1.20	1.23	1.26	1.29	1.32	1.35	1.38	1.41	1.44	1.47	1.50	1.53	1.56	1.59	1.62	1.65	1.68	1.71	1.74	1.77
38	1.23	1.26	1.29	1.33	1.36	1.39	1.42	1.45	1.48	1.51	1.54	1.57	1.60	1.63	1.66	1.70	1.73	1.76	1.79	1.82
39	1.27	1.30	1.33	1.36	1.39	1.42	1.46	1.49	1.52	1.55	1.58	1.61	1.65	1.68	1.71	1.74	1.77	1.80	1.84	1.87
40	1.30	1.33	1.36	1.40	1.43	1.46	1.49	1.52	1.56	1.59	1.62	1.65	1.69	1.72	1.75	1.78	1.82	1.85	1.88	1.91
41	1.33	1.36	1.40	1.43	1.46	1.50	1.53	1.56	1.60	1.63	1.66	1.70	1.73	1.76	1.80	1.83	1.86	1.90	1.93	1.96
42	1.36	1.40	1.43	1.46	1.50	1.53	1.57	1.60	1.63	1.67	1.70	1.74	1.77	1.80	1.84	1.87	1.91	1.94	1.98	2.01
43	1.39	1.43	1.46	1.50	1.53	1.57	1.60	1.64	1.67	1.71	1.74	1.78	1.81	1.85	1.88	1.92	1.95	1.99	2.02	2.06
44	1.43	1.46	1.50	1.53	1.57	1.60	1.64	1.68	1.71	1.75	1.78	1.82	1.85	1.89	1.93	1.96	2.00	2.03	2.07	2.10
45	1.46	1.50	1.53	1.57	1.60	1.64	1.68	1.71	1.75	1.79	1.82	1.86	1.90	1.93	1.97	2.01	2.04	2.08	2.12	2.15
46	1.49	1.53	1.57	1.60	1.64	1.68	1.71	1.75	1.70	1.83	1.86	1.90	1.94	1.98	2.01	2.05	2.00	2.12	2.16	2.20
47	1.52	1.56	1.60	1.64	1.68	1.71	1.75	1.79	1.83	1.87	1.90	1.94	1.98	2.02	2.06	2.09	2.13	2.17	2.21	2.25
48	1.56	1.50	1.63	1.67	1.71	1.75	1.70	1.83	1.87	1.90	1.94	1.98	2.02	2.06	2.10	2.14	2.18	2.22	2.25	2.29
49	1.59	1.63	1.67	1.71	1.75	1.79	1.83	1.86	1.90	1.04	1.08	2.02	2.06	2.10	2.14	2.18	2.22	2.26	2.30	2.34
50	1.62	1.66	1.70	1.74	1.78	1.82	1.86	1.90	1.94	1.98	2.02	2.06	2.11	2.15	2.19	2.23	2.27	2.31	2.35	2.30

Temperature	Barometer reading, millibars, inches or millimeters of mercury																			
	300	305	310	315	320	325	330	335	340	345	350	355	360	365	370	375	380	385	390	395
°C																				
0	0.00	0.00	0.00	0.00	0.00	0.00	0.00	0.00	0.00	0.00	0.00	0.00	0.00	0.00	0.00	0.00	0.00	0.00	0.00	0.00
5	.24	.25	.25	.26	.26	.27	.27	.27	.28	.28	.29	.29	.29	.30	.30	.31	.31	.31	.32	.32
10	.49	.50	.51	.51	.52	.53	.54	.55	.55	.56	.57	.58	.59	.60	.60	.61	.62	.63	.64	.64
11	.54	.55	.56	.57	.57	.58	.59	.60	.61	.62	.63	.64	.65	.65	.66	.67	.68	.69	.70	.71
12	.59	.60	.61	.62	.63	.64	.65	.66	.67	.67	.68	.69	.70	.71	.72	.73	.74	.75	.76	.77
13	.64	.65	.60	.67	.68	.69	.70	.71	.72	.73	.74	.75	.76	.77	.78	.79	.81	.82	.83	.84
14	.68	.70	.71	.72	.73	.74	.75	.76	.78	.79	.80	.81	.82	.83	.84	.86	.87	.88	.89	.90
15	.73	.75	.76	.77	.78	.79	.81	.82	.83	.84	.86	.87	.88	.89	.90	.92	.93	.94	.95	.97
16	.78	.80	.81	.82	.83	.85	.86	.87	.89	.90	.91	.93	.94	.95	.96	.98	.99	1.00	1.02	1.03
17	.83	.84	.86	.87	.89	.90	.91	.93	.94	.96	.97	.08	1.00	1.01	1.02	1.04	1.05	1.07	1.08	1.09
18	.88	.89	.91	.92	.94	.95	.97	.98	1.00	1.01	1.03	1.04	1.06	1.07	1.08	1.10	1.11	1.13	1.14	1.16
19	.93	.94	.96	.97	.99	1.01	1.02	1.04	1.05	1.07	1.08	1.10	1.11	1.13	1.14	1.16	1.18	1.10	1.21	1.22
20	.98	.09	1.01	1.03	1.04	1.06	1.07	1.09	1.11	1.12	1.14	1.16	1.17	1.19	1.20	1.22	1.24	1.25	1.27	1.29
21	1.03	1.04	1.06	1.08	1.09	1.11	1.13	1.15	1.16	1.18	1.20	1.21	1.23	1.25	1.26	1.28	1.30	1.32	1.33	1.35
22	1.07	1.09	1.11	1.13	1.15	1.16	1.18	1.20	1.22	1.24	1.25	1.27	1.29	1.31	1.32	1.34	1.36	1.38	1.40	1.41
23	1.12	1.14	1.16	1.18	1.20	1.22	1.24	1.25	1.27	1.29	1.31	1.33	1.35	1.37	1.38	1.40	1.42	1.44	1.46	1.48
24	1.17	1.19	1.21	1.23	1.25	1.27	1.29	1.31	1.33	1.35	1.37	1.30	1.41	1.43	1.44	1.46	1.48	1.50	1.52	1.54
25	1.22	1.24	1.26	1.28	1.30	1.32	1.34	1.36	1.38	1.40	1.42	1.44	1.46	1.48	1.50	1.52	1.55	1.57	1.59	1.61
26	1.27	1.29	1.31	1.33	1.35	1.37	1.40	1.42	1.44	1.46	1.48	1.50	1.52	1.54	1.56	1.59	1.61	1.63	1.65	1.67
27	1.32	1.34	1.36	1.38	1.40	1.43	1.45	1.47	1.49	1.51	1.54	1.56	1.58	1.60	1.62	1.65	1.67	1.69	1.71	1.73
28	1.37	1.39	1.41	1.43	1.46	1.48	1.50	1.52	1.55	1.57	1.59	1.62	1.64	1.66	1.68	1.71	1.73	1.75	1.78	1.80
29	1.41	1.44	1.46	1.48	1.51	1.53	1.56	1.58	1.60	1.63	1.65	1.67	1.70	1.72	1.74	1.77	1.79	1.81	1.84	1.86
30	1.46	1.49	1.51	1.54	1.56	1.58	1.61	1.63	1.66	1.68	1.71	1.73	1.76	1.78	1.80	1.83	1.85	1.88	1.90	1.93
31	1.51	1.54	1.56	1.50	1.61	1.64	1.66	1.69	1.71	1.74	1.76	1.79	1.81	1.84	1.86	1.89	1.91	1.94	1.96	1.99
32	1.56	1.59	1.61	1.64	1.66	1.69	1.72	1.74	1.77	1.79	1.82	1.85	1.87	1.90	1.92	1.95	1.98	2.00	2.03	2.05
33	1.61	1.63	1.66	1.69	1.72	1.74	1.77	1.80	1.82	1.85	1.88	1.90	1.93	1.96	1.98	2.01	2.04	2.06	2.09	2.12
34	1.66	1.68	1.71	1.74	1.77	1.79	1.82	1.85	1.88	1.90	1.93	1.06	1.99	2.02	2.04	2.07	2.10	2.13	2.15	2.18
35	1.70	1.73	1.76	1.79	1.82	1.85	1.88	1.90	1.93	1.96	1.99	2.02	2.05	2.07	2.10	2.13	2.16	2.19	2.22	2.24
36	1.75	1.78	1.81	1.84	1.87	1.90	1.03	1.96	1.99	2.02	2.05	2.07	2.10	2.13	2.16	2.19	2.22	2.25	2.28	2.31
37	1.80	1.83	1.86	1.89	1.92	1.95	1.98	2.01	2.04	2.07	2.10	2.13	2.16	2.10	2.22	2.25	2.28	2.31	2.34	2.37
38	1.85	1.88	1.91	1.94	1.07	2.00	2.03	2.07	2.10	2.13	2.16	2.19	2.22	2.25	2.28	2.31	2.34	2.37	2.40	2.44
39	1.90	1.93	1.06	1.99	2.02	2.06	2.09	2.12	2.15	2.18	2.21	2.25	2.28	2.30	2.34	2.37	2.40	2.44	2.47	2.50
40	1.95	1.98	2.01	2.04	2.08	2.11	2.14	2.17	2.21	2.24	2.27	2.30	2.34	2.37	2.40	2.43	2.47	2.50	2.53	2.56
41	1.99	2.03	2.06	2.09	2.13	2.16	2.19	2.23	2.26	2.29	2.33	2.36	2.39	2.43	2.46	2.49	2.53	2.56	2.59	2.63
42	2.04	2.08	2.11	2.15	2.18	2.21	2.25	2.28	2.32	2.35	2.38	2.42	2 45	2.49	2.52	2.55	2.59	2.62	2 66	2.69
43	2.00	2 13	2.16	2.20	2.23	2.27	2.30	2 34	2.37	2 41	2.44	2.47	2.51	2.54	2 58	2.61	2.65	2 08	2 72	2.75
44	2.14	2.18	2.21	2.25	2.28	2 32	2.35	2 39	2.43	2.46	2.50	2.53	2.57	2.60	2.64	2.67	2.71	2.75	2.78	2.82
45	2.19	2.22	2.26	2.30	2.33	2.37	2.41	2.44	2.48	2.52	2.55	2.50	2.63	2.66	2.70	2.74	2.77	2.81	2.84	2.88
46	2.24	2.27	2.31	2.35	2.39	2.42	2.46	2.50	2.53	2.57	2.61	2.65	2.68	2.72	2 76	2.80	2.83	2.87	2.01	2.94
47	2.28	2.32	2.36	2.40	2.44	2.47	2.51	2.55	2.50	2.63	2 67	2.70	2 74	2.78	2.82	2.86	2.89	2.93	2.97	3.01
48	2.33	2.37	2 41	2.45	2.49	2.53	2.57	2 60	2 64	2 68	2 72	2.76	2 80	2 84	2 88	2 92	2.95	2.99	3.03	3.07
49	2.38	2.42	2 46	2.50	2 54	2.58	2.62	2 66	2.70	2 74	2.78	2 82	2.86	2.90	2.94	2 08	3.02	3 06	3.10	3.13
50	2.43	2.47	2.51	2.55	2 59	2.63	2.67	2.71	2.75	2.79	2.83	2.87	2.91	2.06	3.00	3.04	3.08	3.12	3.16	3.20

TABLE 6. *Temperature corrections for Fortin barometer with brass scales*—Continued

All corrections are to be subtracted from the reading.

Temperature	Barometer reading, millibars, inches or millimeters of mercury																			
	400	405	410	415	420	425	430	435	440	445	450	455	460	465	470	475	480	485	490	495
°C																				
0	0.00	0.00	0.00	0.00	0.00	0.00	0.00	0.00	0.00	0.00	0.00	0.00	0.00	0.00	0.00	0.00	0.00	0.00	0.00	0.00
5	.33	.33	.33	.34	.34	.35	.35	.35	.36	.36	.37	.37	.38	.38	.38	.39	.39	.40	.40	.40
10	.65	.66	.67	.68	.69	.69	.70	.71	.72	.73	.73	.74	.75	.76	.77	.77	.78	.79	.80	.81
11	.72	.73	.74	.74	.75	.76	.77	.78	.79	.80	.81	.82	.83	.83	.84	.85	.86	.87	.88	.89
12	.78	.79	.80	.81	.82	.83	.84	.85	.86	.87	.88	.89	.90	.91	.92	.93	.94	.95	.96	.97
13	.85	.86	.87	.88	.89	.90	.91	.92	.93	.94	.95	.96	.97	.99	1.00	1.01	1.02	1.03	1.04	1.05
14	.91	.92	.94	.95	.96	.97	.98	.99	1.00	1.02	1.03	1.04	1.05	1.06	1.07	1.08	1.10	1.11	1.12	1.13
15	.98	.99	1.00	1.01	1.03	1.04	1.05	1.06	1.08	1.09	1.10	1.11	1.12	1.14	1.15	1.16	1.17	1.19	1.20	1.21
16	1.04	1.06	1.07	1.08	1.09	1.11	1.12	1.13	1.15	1.16	1.17	1.19	1.20	1.21	1.23	1.24	1.25	1.26	1.28	1.29
17	1.11	1.12	1.14	1.15	1.16	1.18	1.19	1.20	1.22	1.23	1.25	1.26	1.27	1.29	1.30	1.32	1.33	1.34	1.36	1.37
18	1.17	1.19	1.20	1.22	1.23	1.25	1.26	1.28	1.29	1.30	1.32	1.33	1.35	1.36	1.38	1.39	1.41	1.42	1.44	1.45
19	1.24	1.25	1.27	1.28	1.30	1.31	1.33	1.35	1.36	1.38	1.39	1.41	1.42	1.44	1.45	1.47	1.49	1.50	1.52	1.53
20	1.30	1.32	1.34	1.35	1.37	1.38	1.40	1.42	1.43	1.45	1.47	1.48	1.50	1.51	1.53	1.55	1.56	1.58	1.60	1.61
21	1.37	1.38	1.40	1.42	1.44	1.45	1.47	1.49	1.50	1.52	1.54	1.56	1.57	1.59	1.61	1.62	1.64	1.66	1.67	1.69
22	1.43	1.45	1.47	1.49	1.50	1.52	1.54	1.56	1.58	1.59	1.61	1.63	1.65	1.66	1.68	1.70	1.72	1.74	1.75	1.77
23	1.50	1.52	1.53	1.55	1.57	1.59	1.61	1.63	1.65	1.67	1.68	1.70	1.72	1.74	1.76	1.78	1.80	1.82	1.83	1.85
24	1.56	1.58	1.60	1.62	1.64	1.66	1.68	1.70	1.72	1.74	1.76	1.78	1.80	1.82	1.84	1.85	1.87	1.89	1.91	1.93
25	1.63	1.65	1.67	1.69	1.71	1.73	1.75	1.77	1.79	1.81	1.83	1.85	1.87	1.89	1.91	1.93	1.95	1.97	1.99	2.01
26	1.69	1.71	1.73	1.75	1.78	1.80	1.82	1.84	1.86	1.88	1.90	1.92	1.95	1.97	1.99	2.01	2.03	2.05	2.07	2.09
27	1.76	1.78	1.80	1.82	1.84	1.87	1.89	1.91	1.93	1.95	1.98	2.00	2.02	2.04	2.06	2.09	2.11	2.13	2.15	2.17
28	1.82	1.84	1.87	1.89	1.91	1.93	1.96	1.98	2.00	2.03	2.05	2.07	2.09	2.12	2.14	2.16	2.18	2.21	2.23	2.25
29	1.89	1.91	1.93	1.96	1.98	2.00	2.03	2.05	2.07	2.10	2.12	2.14	2.17	2.19	2.22	2.24	2.26	2.29	2.31	2.33
30	1.95	1.97	2.00	2.02	2.05	2.07	2.10	2.12	2.15	2.17	2.19	2.22	2.24	2.27	2.29	2.32	2.34	2.36	2.39	2.41
31	2.01	2.04	2.07	2.09	2.12	2.14	2.17	2.19	2.22	2.24	2.27	2.29	2.32	2.34	2.37	2.39	2.42	2.44	2.47	2.49
32	2.08	2.11	2.13	2.16	2.18	2.21	2.24	2.26	2.29	2.31	2.34	2.37	2.39	2.42	2.44	2.47	2.50	2.52	2.55	2.57
33	2.14	2.17	2.20	2.22	2.25	2.28	2.30	2.33	2.36	2.39	2.41	2.44	2.47	2.49	2.52	2.55	2.57	2.60	2.63	2.65
34	2.21	2.24	2.26	2.29	2.32	2.35	2.37	2.40	2.43	2.46	2.48	2.51	2.54	2.57	2.60	2.62	2.65	2.68	2.71	2.73
35	2.27	2.30	2.33	2.36	2.39	2.42	2.44	2.47	2.50	2.53	2.56	2.59	2.61	2.64	2.67	2.70	2.73	2.76	2.78	2.81
36	2.34	2.37	2.40	2.43	2.45	2.48	2.51	2.54	2.57	2.60	2.63	2.66	2.69	2.72	2.75	2.78	2.81	2.83	2.86	2.89
37	2.40	2.43	2.46	2.49	2.52	2.55	2.58	2.61	2.64	2.67	2.70	2.73	2.76	2.79	2.82	2.85	2.88	2.91	2.94	2.97
38	2.47	2.50	2.53	2.56	2.59	2.62	2.65	2.68	2.71	2.74	2.77	2.81	2.84	2.87	2.90	2.93	2.96	2.99	3.02	3.05
39	2.53	2.56	2.59	2.63	2.66	2.69	2.72	2.75	2.78	2.82	2.85	2.88	2.91	2.94	2.97	3.01	3.04	3.07	3.10	3.13
40	2.60	2.63	2.66	2.69	2.73	2.76	2.79	2.82	2.86	2.89	2.92	2.95	2.98	3.02	3.05	3.08	3.11	3.15	3.18	3.21
41	2.66	2.69	2.73	2.76	2.79	2.83	2.86	2.89	2.93	2.96	2.99	3.03	3.06	3.09	3.13	3.16	3.19	3.23	3.26	3.29
42	2.72	2.76	2.79	2.83	2.86	2.89	2.93	2.96	3.00	3.03	3.06	3.10	3.13	3.17	3.20	3.24	3.27	3.30	3.34	3.37
43	2.79	2.82	2.86	2.89	2.93	2.96	3.00	3.03	3.07	3.10	3.14	3.17	3.21	3.24	3.28	3.31	3.35	3.38	3.42	3.45
44	2.85	2.89	2.92	2.96	3.00	3.03	3.07	3.10	3.14	3.17	3.21	3.25	3.28	3.32	3.35	3.39	3.42	3.46	3.49	3.53
45	2.92	2.95	2.99	3.03	3.06	3.10	3.14	3.17	3.21	3.25	3.28	3.32	3.35	3.39	3.43	3.46	3.50	3.54	3.57	3.61
46	2.98	3.02	3.06	3.09	3.13	3.17	3.21	3.24	3.28	3.32	3.35	3.39	3.43	3.47	3.50	3.54	3.58	3.62	3.65	3.69
47	3.05	3.08	3.12	3.16	3.20	3.24	3.27	3.31	3.35	3.39	3.43	3.46	3.50	3.54	3.58	3.62	3.66	3.69	3.73	3.77
48	3.11	3.15	3.19	3.23	3.27	3.30	3.34	3.38	3.42	3.46	3.50	3.54	3.58	3.62	3.65	3.69	3.73	3.77	3.81	3.85
49	3.17	3.21	3.25	3.29	3.33	3.37	3.41	3.45	3.49	3.53	3.57	3.61	3.65	3.69	3.73	3.77	3.81	3.85	3.89	3.93
50	3.24	3.28	3.32	3.36	3.40	3.44	3.48	3.52	3.56	3.60	3.64	3.68	3.72	3.76	3.81	3.85	3.89	3.93	3.97	4.01

Temperature	Barometer reading, millibars, inches or millimeters of mercury																			
	500	505	510	515	520	525	530	535	540	545	550	555	560	565	570	575	580	585	590	595
°C																				
0	0.00	0.00	0.00	0.00	0.00	0.00	0.00	0.00	0.00	0.00	0.00	0.00	0.00	0.00	0.00	0.00	0.00	0.00	0.00	0.00
5	.41	.41	.42	.42	.42	.43	.43	.44	.44	.44	.45	.45	.46	.46	.47	.47	.47	.48	.48	.49
10	.82	.82	.83	.84	.85	.86	.86	.87	.88	.89	.90	.91	.91	.92	.93	.94	.95	.95	.96	.97
11	.90	.91	.91	.92	.93	.94	.95	.96	.97	.98	.99	1.00	1.00	1.01	1.02	1.03	1.04	1.05	1.06	1.07
12	.98	.99	1.00	1.01	1.02	1.03	1.04	1.05	1.06	1.07	1.08	1.09	1.10	1.11	1.12	1.12	1.13	1.14	1.15	1.16
13	1.06	1.07	1.08	1.09	1.10	1.11	1.12	1.13	1.14	1.15	1.17	1.18	1.19	1.20	1.21	1.22	1.23	1.24	1.25	1.26
14	1.14	1.15	1.16	1.18	1.19	1.20	1.21	1.22	1.23	1.24	1.25	1.27	1.28	1.29	1.30	1.31	1.32	1.33	1.35	1.36
15	1.22	1.23	1.25	1.26	1.27	1.28	1.30	1.31	1.32	1.33	1.34	1.36	1.37	1.38	1.39	1.41	1.42	1.43	1.44	1.45
16	1.30	1.32	1.33	1.34	1.36	1.37	1.38	1.39	1.41	1.42	1.43	1.45	1.46	1.47	1.49	1.50	1.51	1.52	1.54	1.55
17	1.38	1.40	1.41	1.43	1.44	1.45	1.47	1.48	1.50	1.51	1.52	1.54	1.55	1.56	1.58	1.59	1.61	1.62	1.63	1.65
18	1.47	1.48	1.50	1.51	1.52	1.54	1.55	1.57	1.58	1.60	1.61	1.63	1.64	1.66	1.67	1.69	1.70	1.71	1.73	1.74
19	1.55	1.56	1.58	1.59	1.61	1.62	1.64	1.66	1.67	1.69	1.70	1.72	1.73	1.75	1.76	1.78	1.79	1.81	1.83	1.84
20	1.63	1.64	1.66	1.68	1.69	1.71	1.73	1.74	1.76	1.77	1.79	1.81	1.82	1.84	1.86	1.87	1.89	1.90	1.92	1.94
21	1.71	1.73	1.74	1.76	1.78	1.79	1.81	1.83	1.85	1.86	1.88	1.90	1.91	1.93	1.95	1.97	1.98	2.00	2.02	2.03
22	1.79	1.81	1.83	1.84	1.86	1.88	1.90	1.92	1.93	1.95	1.97	1.99	2.01	2.02	2.04	2.06	2.08	2.09	2.11	2.13
23	1.87	1.89	1.91	1.93	1.95	1.96	1.98	2.00	2.02	2.04	2.06	2.08	2.10	2.11	2.13	2.15	2.17	2.19	2.21	2.23
24	1.95	1.97	1.99	2.01	2.03	2.05	2.07	2.09	2.11	2.13	2.15	2.17	2.19	2.21	2.23	2.25	2.26	2.28	2.30	2.32
25	2.03	2.05	2.07	2.09	2.11	2.13	2.16	2.18	2.20	2.22	2.24	2.26	2.28	2.30	2.32	2.34	2.36	2.38	2.40	2.42
26	2.11	2.14	2.16	2.18	2.20	2.22	2.24	2.26	2.28	2.30	2.33	2.35	2.37	2.39	2.41	2.43	2.45	2.47	2.49	2.52
27	2.20	2.22	2.24	2.26	2.28	2.30	2.33	2.35	2.37	2.39	2.41	2.44	2.46	2.48	2.50	2.52	2.55	2.57	2.59	2.61
28	2.28	2.30	2.32	2.34	2.37	2.39	2.41	2.44	2.46	2.48	2.50	2.53	2.55	2.57	2.59	2.62	2.64	2.66	2.69	2.71
29	2.36	2.38	2.40	2.43	2.45	2.47	2.50	2.52	2.55	2.57	2.59	2.62	2.64	2.66	2.69	2.71	2.73	2.76	2.78	2.80
30	2.44	2.46	2.49	2.51	2.54	2.56	2.58	2.61	2.63	2.66	2.68	2.71	2.73	2.75	2.78	2.80	2.83	2.85	2.88	2.90

TABLE 6. *Temperature corrections for Fortin barometer with brass scales*—Continued

All corrections are to be subtracted from the reading.

Temperature	Barometer reading, millibars, inches or millimeters of mercury																			
	500	505	510	515	520	525	530	535	540	545	550	555	560	565	570	575	580	585	590	595
°C																				
31	2.52	2.54	2.57	2.59	2.62	2.64	2.67	2.69	2.72	2.75	2.77	2.80	2.82	2.85	2.87	2.90	2.92	2.95	2.97	3.00
32	2.60	2.63	2.65	2.68	2.70	2.73	2.76	2.78	2.81	2.83	2.86	2.89	2.91	2.94	2.96	2.99	3.02	3.04	3.07	3.09
33	2.68	2.71	2.73	2.76	2.79	2.81	2.84	2.87	2.89	2.92	2.95	2.97	3.00	3.03	3.06	3.08	3.11	3.14	3.16	3.19
34	2.76	2.79	2.82	2.84	2.87	2.90	2.93	2.95	2.98	3.01	3.04	3.06	3.09	3.12	3.15	3.17	3.20	3.23	3.26	3.29
35	2.84	2.87	2.90	2.93	2.96	2.98	3.01	3.04	3.07	3.10	3.13	3.15	3.18	3.21	3.24	3.27	3.30	3.32	3.35	3.38
36	2.92	2.95	2.98	3.01	3.04	3.07	3.10	3.13	3.16	3.19	3.21	3.24	3.27	3.30	3.33	3.36	3.39	3.42	3.45	3.48
37	3.00	3.03	3.06	3.09	3.12	3.15	3.18	3.21	3.24	3.27	3.30	3.33	3.36	3.39	3.42	3.45	3.48	3.51	3.54	3.57
38	3.08	3.11	3.14	3.18	3.21	3.24	3.27	3.30	3.33	3.36	3.39	3.42	3.45	3.48	3.51	3.55	3.58	3.61	3.64	3.67
39	3.16	3.20	3.23	3.26	3.29	3.32	3.35	3.39	3.42	3.45	3.48	3.51	3.54	3.58	3.61	3.64	3.67	3.70	3.73	3.76
40	3.24	3.28	3.31	3.34	3.37	3.41	3.44	3.47	3.50	3.54	3.57	3.60	3.63	3.67	3.70	3.73	3.76	3.80	3.83	3.86
41	3.32	3.36	3.39	3.42	3.46	3.49	3.52	3.56	3.59	3.62	3.66	3.69	3.72	3.76	3.79	3.82	3.86	3.89	3.92	3.96
42	3.41	3.44	3.47	3.51	3.54	3.58	3.61	3.64	3.68	3.71	3.75	3.78	3.81	3.85	3.88	3.92	3.95	3.98	4.02	4.05
43	3.49	3.52	3.56	3.59	3.63	3.66	3.70	3.73	3.76	3.80	3.83	3.87	3.90	3.94	3.97	4.01	4.04	4.08	4.11	4.15
44	3.57	3.60	3.64	3.67	3.71	3.74	3.78	3.82	3.85	3.89	3.92	3.96	3.99	4.03	4.07	4.10	4.14	4.17	4.21	4.24
45	3.65	3.68	3.72	3.76	3.79	3.83	3.87	3.90	3.94	3.97	4.01	4.05	4.08	4.12	4.16	4.19	4.23	4.27	4.30	4.34
46	3.73	3.76	3.80	3.84	3.88	3.91	3.95	3.99	4.03	4.06	4.10	4.14	4.17	4.21	4.25	4.29	4.32	4.36	4.40	4.44
47	3.81	3.85	3.88	3.92	3.96	4.00	4.04	4.07	4.11	4.15	4.19	4.23	4.26	4.30	4.34	4.38	4.42	4.45	4.49	4.53
48	3.89	3.93	3.97	4.00	4.04	4.08	4.12	4.16	4.20	4.24	4.28	4.32	4.35	4.39	4.43	4.47	4.51	4.55	4.59	4.63
49	3.97	4.01	4.05	4.09	4.13	4.17	4.21	4.25	4.29	4.33	4.36	4.40	4.44	4.48	4.52	4.56	4.60	4.64	4.68	4.72
50	4.05	4.09	4.13	4.17	4.21	4.25	4.29	4.33	4.37	4.41	4.45	4.49	4.53	4.57	4.61	4.66	4.70	4.74	4.78	4.82

Temperature	Barometer reading, millibars, inches or millimeters of mercury																			
	600	605	610	615	620	625	630	635	640	645	650	655	660	665	670	675	680	685	690	695
°C																				
0	0.00	0.00	0.00	0.00	0.00	0.00	0.00	0.00	0.00	0.00	0.00	0.00	0.00	0.00	0.00	0.00	0.00	0.00	0.00	0.00
5	.49	.49	.50	.50	.51	.51	.51	.52	.52	.53	.53	.53	.54	.54	.55	.55	.56	.56	.56	.57
10	.98	.99	.99	1.00	1.01	1.02	1.03	1.04	1.04	1.05	1.06	1.07	1.08	1.08	1.09	1.10	1.11	1.12	1.13	1.13
11	1.08	1.09	1.09	1.10	1.11	1.12	1.13	1.14	1.15	1.16	1.17	1.17	1.18	1.19	1.20	1.21	1.22	1.23	1.24	1.25
12	1.17	1.18	1.19	1.20	1.21	1.22	1.23	1.24	1.25	1.26	1.27	1.28	1.29	1.30	1.31	1.32	1.33	1.34	1.35	1.36
13	1.27	1.28	1.29	1.30	1.31	1.32	1.34	1.35	1.36	1.37	1.38	1.39	1.40	1.41	1.42	1.43	1.44	1.45	1.46	1.47
14	1.37	1.38	1.39	1.40	1.41	1.43	1.44	1.45	1.46	1.47	1.48	1.49	1.51	1.52	1.53	1.54	1.55	1.56	1.57	1.59
15	1.47	1.48	1.49	1.50	1.52	1.53	1.54	1.55	1.56	1.58	1.59	1.60	1.61	1.63	1.64	1.35	1.66	1.67	1.69	1.70
16	1.56	1.58	1.59	1.60	1.62	1.63	1.64	1.66	1.67	1.68	1.69	1.71	1.72	1.73	1.75	1.76	1.77	1.79	1.80	1.81
17	1.66	1.68	1.69	1.70	1.72	1.73	1.74	1.76	1.77	1.79	1.80	1.81	1.83	1.84	1.86	1.87	1.88	1.90	1.91	1.92
18	1.76	1.77	1.79	1.80	1.82	1.83	1.85	1.86	1.88	1.89	1.91	1.92	1.93	1.95	1.96	1.98	1.99	2.01	2.02	2.04
19	1.86	1.87	1.89	1.90	1.92	1.93	1.95	1.96	1.98	2.00	2.01	2.03	2.04	2.06	2.07	2.09	2.10	2.12	2.13	2.15
20	1.95	1.97	1.99	2.00	2.02	2.04	2.05	2.07	2.08	2.10	2.12	2.13	2.15	2.17	2.18	2.20	2.21	2.23	2.25	2.26
21	2.05	2.07	2.09	2.10	2.12	2.14	2.15	2.17	2.19	2.20	2.22	2.24	2.26	2.27	2.29	2.31	2.32	2.34	2.36	2.38
22	2.15	2.17	2.18	2.20	2.22	2.24	2.26	2.27	2.29	2.31	2.33	2.35	2.36	2.38	2.40	2.42	2.43	2.45	2.47	2.49
23	2.25	2.26	2.28	2.30	2.32	2.34	2.36	2.38	2.40	2.41	2.43	2.45	2.47	2.49	2.51	2.53	2.54	2.56	2.58	2.60
24	2.34	2.36	2.38	2.40	2.42	2.44	2.46	2.48	2.50	2.52	2.54	2.56	2.58	2.60	2.62	2.64	2.66	2.67	2.69	2.71
25	2.44	2.46	2.48	2.50	2.52	2.54	2.56	2.58	2.60	2.62	2.64	2.66	2.68	2.70	2.72	2.74	2.77	2.79	2.81	2.83
26	2.54	2.56	2.58	2.60	2.62	2.64	2.66	2.69	2.71	2.73	2.75	2.77	2.79	2.81	2.83	2.85	2.88	2.90	2.92	2.94
27	2.63	2.66	2.68	2.70	2.72	2.74	2.77	2.79	2.81	2.83	2.85	2.88	2.90	2.92	2.94	2.96	2.99	3.01	3.03	3.05
28	2.73	2.75	2.78	2.80	2.82	2.85	2.87	2.89	2.91	2.94	2.96	2.98	3.00	3.03	3.05	3.07	3.10	3.12	3.14	3.16
29	2.83	2.85	2.88	2.90	2.92	2.95	2.97	2.99	3.02	3.04	3.06	3.09	3.11	3.13	3.16	3.18	3.21	3.23	3.25	3.28
30	2.93	2.95	2.97	3.00	3.02	3.05	3.07	3.10	3.12	3.14	3.17	3.19	3.22	3.24	3.27	3.29	3.32	3.34	3.36	3.39
31	3.02	3.05	3.07	3.10	3.12	3.15	3.17	3.20	3.22	3.25	3.27	3.30	3.32	3.35	3.37	3.40	3.43	3.45	3.48	3.50
32	3.12	3.15	3.17	3.20	3.22	3.25	3.28	3.30	3.33	3.35	3.38	3.41	3.43	3.46	3.48	3.51	3.54	3.56	3.59	3.61
33	3.22	3.24	3.27	3.30	3.32	3.35	3.38	3.40	3.43	3.46	3.48	3.51	3.54	3.56	3.59	3.62	3.64	3.67	3.70	3.73
34	3.31	3.34	3.37	3.40	3.42	3.45	3.48	3.51	3.53	3.56	3.59	3.62	3.64	3.67	3.70	3.73	3.75	3.78	3.81	3.84
35	3.41	3.44	3.47	3.49	3.52	3.55	3.58	3.61	3.64	3.67	3.69	3.72	3.75	3.78	3.81	3.84	3.86	3.89	3.92	3.95
36	3.51	3.54	3.56	3.59	3.62	3.65	3.68	3.71	3.74	3.77	3.80	3.83	3.86	3.89	3.92	3.94	3.97	4.00	4.03	4.06
37	3.60	3.63	3.66	3.69	3.72	3.75	3.78	3.81	3.84	3.87	3.90	3.93	3.96	3.99	4.02	4.05	4.08	4.11	4.14	4.17
38	3.70	3.73	3.76	3.79	3.82	3.85	3.88	3.92	3.95	3.98	4.01	4.04	4.07	4.10	4.13	4.16	4.19	4.22	4.25	4.29
39	3.80	3.83	3.86	3.89	3.92	3.95	3.99	4.02	4.05	4.08	4.11	4.14	4.18	4.21	4.24	4.27	4.30	4.33	4.37	4.40
40	3.89	3.93	3.96	3.99	4.02	4.06	4.09	4.12	4.15	4.19	4.22	4.25	4.28	4.32	4.35	4.38	4.41	4.44	4.48	4.51
41	3.99	4.02	4.06	4.09	4.12	4.16	4.19	4.22	4.26	4.29	4.32	4.36	4.39	4.42	4.46	4.49	4.52	4.56	4.59	4.62
42	4.09	4.12	4.15	4.19	4.22	4.26	4.29	4.32	4.36	4.39	4.43	4.46	4.50	4.53	4.56	4.60	4.63	4.67	4.70	4.73
43	4.18	4.22	4.25	4.29	4.32	4.36	4.39	4.43	4.46	4.50	4.53	4.57	4.60	4.64	4.67	4.71	4.74	4.78	4.81	4.85
44	4.28	4.32	4.35	4.39	4.42	4.46	4.49	4.53	4.56	4.60	4.64	4.67	4.71	4.74	4.78	4.81	4.85	4.89	4.92	4.96
45	4.38	4.41	4.45	4.49	4.52	4.56	4.59	4.63	4.67	4.70	4.74	4.78	4.81	4.85	4.89	4.92	4.96	5.00	5.03	5.07
46	4.47	4.51	4.55	4.58	4.62	4.66	4.70	4.73	4.77	4.81	4.85	4.88	4.92	4.96	4.99	5.03	5.07	5.11	5.14	5.18
47	4.57	4.61	4.64	4.68	4.72	4.76	4.80	4.84	4.87	4.91	4.95	4.99	5.03	5.06	5.10	5.14	5.18	5.22	5.25	5.29
48	4.67	4.70	4.74	4.78	4.82	4.86	4.90	4.94	4.98	5.02	5.05	5.09	5.13	5.17	5.21	5.25	5.29	5.33	5.36	5.40
49	4.76	4.80	4.84	4.88	4.92	4.96	5.00	5.04	5.08	5.12	5.16	5.20	5.24	5.28	5.32	5.36	5.40	5.44	5.48	5.52
50	4.86	4.90	4.94	4.98	5.02	5.06	5.10	5.14	5.18	5.22	5.26	5.30	5.34	5.38	5.42	5.47	5.51	5.55	5.59	5.63

TABLE 6. *Temperature corrections for Fortin barometer with brass scales*—Continued

All corrections are to be subtracted from the reading.

Temperature	Barometer reading, millibars or millimeters of mercury																		
	700	705	710	715	720	725	730	735	740	745	750	755	760	765	770	775	780	785	790	795
°C																				
0	0.00	0.00	0.00	0.00	0.00	0.00	0.00	0.00	0.00	0.00	0.00	0.00	0.00	0.00	0.00	0.00	0.00	0.00	0.00	0.00
5	.57	.58	.58	.58	.59	.59	.60	.60	.60	.61	.61	.62	.62	.62	.63	.63	.64	.64	.64	.65
10	1.14	1.15	1.16	1.17	1.17	1.18	1.19	1.20	1.21	1.22	1.22	1.23	1.24	1.25	1.26	1.26	1.27	1.28	1.29	1.30
11	1.26	1.26	1.27	1.28	1.29	1.30	1.31	1.32	1.33	1.34	1.35	1.35	1.36	1.37	1.38	1.39	1.40	1.41	1.42	1.43
12	1.37	1.38	1.39	1.40	1.41	1.42	1.43	1.44	1.45	1.46	1.47	1.48	1.49	1.50	1.51	1.52	1.53	1.54	1.55	1.56
13	1.48	1.49	1.50	1.52	1.53	1.54	1.55	1.56	1.57	1.58	1.59	1.60	1.61	1.62	1.63	1.64	1.65	1.66	1.67	1.68
14	1.60	1.61	1.62	1.63	1.64	1.65	1.67	1.68	1.69	1.70	1.71	1.72	1.73	1.75	1.76	1.77	1.78	1.79	1.80	1.81
15	1.71	1.72	1.74	1.75	1.76	1.77	1.78	1.80	1.81	1.82	1.83	1.85	1.86	1.87	1.88	1.89	1.91	1.92	1.93	1.94
16	1.82	1.84	1.85	1.86	1.88	1.89	1.90	1.92	1.93	1.94	1.96	1.97	1.98	1.99	2.01	2.02	2.03	2.05	2.06	2.07
17	1.94	1.95	1.97	1.98	1.99	2.01	2.02	2.04	2.05	2.06	2.08	2.09	2.10	2.12	2.13	2.15	2.16	2.17	2.19	2.20
18	2.05	2.07	2.08	2.10	2.11	2.13	2.14	2.15	2.17	2.18	2.20	2.21	2.23	2.24	2.26	2.27	2.29	2.30	2.32	2.33
19	2.17	2.18	2.20	2.21	2.23	2.24	2.26	2.27	2.29	2.30	2.32	2.34	2.35	2.37	2.38	2.40	2.41	2.43	2.44	2.46
20	2.28	2.30	2.31	2.33	2.34	2.36	2.38	2.39	2.41	2.43	2.44	2.46	2.47	2.49	2.51	2.52	2.54	2.56	2.57	2.59
21	2.39	2.41	2.43	2.44	2.46	2.48	2.50	2.51	2.53	2.55	2.56	2.58	2.60	2.62	2.63	2.65	2.67	2.68	2.70	2.72
22	2.51	2.52	2.54	2.56	2.58	2.60	2.61	2.63	2.65	2.67	2.69	2.70	2.72	2.74	2.76	2.77	2.79	2.81	2.83	2.85
23	2.62	2.64	2.66	2.68	2.69	2.71	2.73	2.75	2.77	2.79	2.81	2.83	2.84	2.86	2.88	2.90	2.92	2.94	2.96	2.98
24	2.73	2.75	2.77	2.79	2.81	2.83	2.85	2.87	2.89	2.91	2.93	2.95	2.97	2.99	3.01	3.03	3.05	3.07	3.08	3.10
25	2.85	2.87	2.89	2.91	2.93	2.95	2.97	2.99	3.01	3.03	3.05	3.07	3.09	3.11	3.13	3.15	3.17	3.19	3.21	3.23
26	2.96	2.98	3.00	3.02	3.04	3.07	3.09	3.11	3.13	3.15	3.17	3.19	3.21	3.23	3.26	3.28	3.30	3.32	3.34	3.36
27	3.07	3.10	3.12	3.14	3.16	3.18	3.20	3.23	3.25	3.27	3.29	3.31	3.34	3.36	3.38	3.40	3.42	3.45	3.47	3.49
28	3.19	3.21	3.23	3.25	3.28	3.30	3.32	3.35	3.37	3.39	3.41	3.44	3.46	3.48	3.51	3.53	3.55	3.57	3.60	3.62
29	3.30	3.32	3.35	3.37	3.39	3.42	3.44	3.46	3.49	3.51	3.54	3.56	3.58	3.61	3.63	3.65	3.68	3.70	3.72	3.75
30	3.41	3.44	3.46	3.49	3.51	3.53	3.56	3.58	3.61	3.63	3.06	3.68	3.71	3.73	3.75	3.78	3.80	3.83	3.85	3.88
31	3.53	3.55	3.58	3.60	3.63	3.65	3.68	3.70	3.73	3.75	3.78	3.80	3.83	3.85	3.88	3.90	3.93	3.95	3.98	4.00
32	3.64	3.66	3.69	3.72	3.74	3.77	3.79	3.82	3.85	3.87	3.90	3.92	3.95	3.98	4.00	4.03	4.05	4.08	4.11	4.13
33	3.75	3.78	3.81	3.83	3.86	3.89	3.91	3.94	3.97	3.99	4.02	4.05	4.07	4.10	4.13	4.15	4.18	4.21	4.23	4.26
34	3.87	3.89	3.92	3.95	3.98	4.00	4.03	4.06	4.09	4.11	4.14	4.17	4.20	4.22	4.25	4.28	4.31	4.33	4.36	4.39
35	3.98	4.01	4.03	4.06	4.09	4.12	4.15	4.18	4.21	4.23	4.26	4.29	4.32	4.35	4.38	4.40	4.43	4.46	4.49	4.52
36	4.09	4.12	4.15	4.18	4.21	4.24	4.27	4.30	4.32	4.35	4.38	4.41	4.44	4.47	4.50	4.53	4.56	4.59	4.62	4.65
37	4.20	4.23	4.26	4.29	4.32	4.35	4.38	4.41	4.44	4.47	4.50	4.53	4.56	4.59	4.62	4.65	4.68	4.71	4.74	4.77
38	4.32	4.35	4.38	4.41	4.44	4.47	4.50	4.53	4.56	4.59	4.62	4.66	4.69	4.72	4.75	4.78	4.81	4.84	4.87	4.90
39	4.43	4.46	4.49	4.52	4.56	4.59	4.62	4.65	4.68	4.71	4.75	4.78	4.81	4.84	4.87	4.90	4.94	4.97	5.00	5.03
40	4.54	4.57	4.61	4.64	4.67	4.70	4.74	4.77	4.80	4.83	4.87	4.90	4.93	4.96	5.00	5.03	5.06	5.09	5.13	5.16
41	4.65	4.69	4.72	4.75	4.79	4.82	4.85	4.89	4.92	4.95	4.99	5.02	5.05	5.09	5.12	5.15	5.19	5.22	5.25	5.29
42	4.77	4.80	4.84	4.87	4.90	4.94	4.97	5.01	5.04	5.07	5.11	5.14	5.18	5.21	5.24	5.28	5.31	5.35	5.38	5.41
43	4.88	4.92	4.95	4.98	5.02	5.05	5.09	5.12	5.16	5.19	5.23	5.26	5.30	5.33	5.37	5.40	5.44	5.47	5.51	5.54
44	4.99	5.03	5.06	5.10	5.14	5.17	5.21	5.24	5.28	5.31	5.35	5.39	5.42	5.46	5.49	5.53	5.56	5.60	5.63	5.67
45	5.11	5.14	5.13	5.21	5.25	5.29	5.32	5.36	5.40	5.43	5.47	5.51	5.54	5.58	5.62	5.65	5.69	5.73	5.76	5.80
46	5.22	5.26	5.29	5.33	5.37	5.40	5.44	5.48	5.52	5.55	5.59	5.63	5.67	5.70	5.74	5.78	5.81	5.85	5.89	5.93
47	5.33	5.37	5.41	5.44	5.48	5.52	5.56	5.60	5.63	5.67	5.71	5.75	5.79	5.83	5.86	5.90	5.94	5.98	6.02	6.05
48	5.44	5.48	5.52	5.56	5.60	5.64	5.68	5.71	5.75	5.79	5.83	5.87	5.91	5.95	5.99	6.03	6.06	6.10	6.14	6.18
49	5.56	5.59	5.63	5.67	5.71	5.75	5.79	5.83	5.87	5.91	5.95	5.99	6.03	6.07	6.11	6.15	6.19	6.23	6.27	6.31
50	5.67	5.71	5.75	5.79	5.83	5.87	5.91	5.95	5.99	6.03	6.07	6.11	6.15	6.19	6.23	6.27	6.32	6.36	6.40	6.44

Temperature	Barometer reading, millibars, inches or millimeters of mercury																		
	800	805	810	815	820	825	830	835	840	845	850	855	860	865	870	875	880	885	890	895
°C																				
0	0.00	0.00	0.00	0.00	0.00	0.00	0.00	0.00	0.00	0.00	0.00	0.00	0.00	0.00	0.00	0.00	0.00	0.00	0.00	0.00
5	.65	.66	.66	.67	.67	.67	.68	.68	.69	.69	.69	.70	.70	.71	.71	.71	.72	.72	.73	.73
10	1.30	1.31	1.32	1.33	1.34	1.35	1.35	1.36	1.37	1.38	1.39	1.39	1.40	1.41	1.42	1.43	1.44	1.44	1.45	1.46
11	1.44	1.44	1.45	1.46	1.47	1.48	1.49	1.50	1.51	1.52	1.52	1.53	1.54	1.55	1.56	1.57	1.58	1.59	1.60	1.61
12	1.57	1.57	1.58	1.59	1.60	1.61	1.62	1.63	1.64	1.65	1.66	1.67	1.68	1.69	1.70	1.71	1.72	1.73	1.74	1.75
13	1.70	1.71	1.72	1.73	1.74	1.75	1.76	1.77	1.78	1.79	1.80	1.81	1.82	1.83	1.84	1.85	1.86	1.88	1.89	1.90
14	1.83	1.84	1.85	1.86	1.87	1.88	1.89	1.91	1.92	1.93	1.94	1.95	1.96	1.97	1.99	2.00	2.01	2.02	2.03	2.04
15	1.96	1.97	1.98	1.99	2.00	2.02	2.03	2.04	2.05	2.07	2.08	2.09	2.10	2.11	2.13	2.14	2.15	2.16	2.18	2.19
16	2.09	2.10	2.11	2.12	2.14	2.15	2.16	2.18	2.19	2.20	2.22	2.23	2.24	2.25	2.27	2.28	2.29	2.31	2.32	2.33
17	2.22	2.23	2.24	2.26	2.27	2.28	2.30	2.31	2.33	2.34	2.35	2.37	2.38	2.40	2.41	2.42	2.44	2.45	2.46	2.48
18	2.35	2.36	2.37	2.39	2.40	2.42	2.43	2.45	2.46	2.48	2.49	2.51	2.52	2.54	2.55	2.57	2.58	2.59	2.61	2.62
19	2.48	2.49	2.51	2.52	2.54	2.55	2.57	2.58	2.60	2.61	2.63	2.65	2.66	2.68	2.69	2.71	2.72	2.74	2.75	2.77
20	2.60	2.62	2.64	2.65	2.67	2.69	2.70	2.72	2.74	2.75	2.77	2.78	2.80	2.82	2.83	2.85	2.87	2.88	2.90	2.91
21	2.73	2.75	2.77	2.79	2.80	2.82	2.84	2.85	2.87	2.89	2.91	2.92	2.94	2.96	2.97	2.99	3.01	3.03	3.04	3.06
22	2.86	2.88	2.90	2.92	2.94	2.95	2.97	2.99	3.01	3.03	3.04	3.06	3.08	3.10	3.12	3.13	3.15	3.17	3.19	3.20
23	2.99	3.01	3.03	3.05	3.07	3.09	3.11	3.13	3.14	3.16	3.18	3.20	3.22	3.24	3.26	3.27	3.29	3.31	3.33	3.35
24	3.12	3.14	3.16	3.18	3.20	3.22	3.24	3.26	3.28	3.30	3.32	3.34	3.36	3.38	3.40	3.42	3.44	3.46	3.48	3.49
25	3.25	3.27	3.29	3.31	3.33	3.35	3.38	3.40	3.42	3.44	3.46	3.48	3.50	3.52	3.54	3.56	3.58	3.60	3.62	3.64
26	3.38	3.40	3.43	3.45	3.47	3.49	3.51	3.53	3.55	3.57	3.59	3.62	3.64	3.66	3.68	3.70	3.72	3.74	3.76	3.78
27	3.51	3.53	3.56	3.58	3.60	3.62	3.64	3.67	3.69	3.71	3.73	3.75	3.78	3.80	3.82	3.84	3.86	3.89	3.91	3.93
28	3.64	3.66	3.69	3.71	3.73	3.76	3.78	3.80	3.82	3.85	3.87	3.89	3.91	3.94	3.96	3.98	4.01	4.03	4.05	4.07
29	3.77	3.79	3.82	3.84	3.87	3.89	3.91	3.94	3.96	3.98	4.01	4.03	4.05	4.08	4.10	4.12	4.15	4.17	4.20	4.22
30	3.90	3.92	3.95	3.97	4.00	4.02	4.05	4.07	4.10	4.12	4.14	4.17	4.19	4.22	4.24	4.27	4.29	4.31	4.34	4.36

TABLE 6. *Temperature corrections for Fortin barometer with brass scales*—Continued

All corrections are to be subtracted from the reading.

Temperature	Barometer reading, millibars, inches or millimeter of mercury																			
	800	805	810	815	820	825	830	835	840	845	850	855	860	865	870	875	880	885	890	895
°C																				
31	4.03	4.05	4.08	4.11	4.13	4.16	4.18	4.21	4.23	4.26	4.28	4.31	4.33	4.36	4.38	4.41	4.43	4.46	4.48	4.51
32	4.16	4.18	4.21	4.24	4.26	4.20	4.31	4.34	4.37	4.39	4.42	4.44	4.47	4.50	4.52	4.55	4.57	4.60	4.63	4.65
33	4.29	4.31	4.34	4.37	4.40	4.42	4.45	4.48	4.50	4.53	4.56	4.58	4.61	4.64	4.66	4.69	4.72	4.74	4.77	4.80
34	4.42	4.44	4.47	4.50	4.53	4.56	4.58	4.61	4.64	4.67	4.69	4.72	4.75	4.78	4.80	4.83	4.86	4.89	4.01	4.04
35	4.55	4.57	4.60	4.63	4.66	4.69	4.72	4.75	4.77	4.80	4.83	4.86	4.80	4.02	4.04	4.97	5.00	5.03	5.00	5.09
36	4.68	4.70	4.73	4.76	4.79	4.82	4.85	4.88	4.91	4.94	4.97	5.00	5.03	5.06	5.08	5.11	5.14	5.17	5.20	5.23
37	4.80	4.83	4.86	4.89	4.92	4.95	4.98	5.01	5.04	5.07	5.10	5.13	5.16	5.10	5.22	5.25	5.28	5.31	5.34	5.37
38	4.93	4.96	4.09	5.03	5.06	5.09	5.12	5.15	5.18	5.21	5.24	5.27	5.30	5.33	5.36	5.40	5.43	5.46	5.49	5.52
39	5.06	5.09	5.13	5.16	5.19	5.22	5.25	5.28	5.32	5.35	5.38	5.41	5.44	5.47	5.51	5.54	5.57	5.60	5.63	5.66
40	5.19	5.22	5.26	5.29	5.32	5.35	5.39	5.42	5.45	5.48	5.52	5.55	5.58	5.61	5.65	5.68	5.71	5.74	5.78	5.81
41	5.32	5.35	5.39	5.42	5.45	5.49	5.52	5.55	5.50	5.62	5.65	5.69	5.72	5.75	5.70	5.82	5.85	5.80	5.92	5.95
42	5.45	5.48	5.52	5.55	5.58	5.62	5.65	5.69	5.72	5.76	5.79	5.82	5.86	5.89	5.93	5.96	5.99	6.03	6.06	6.10
43	5.58	5.61	5.65	5.68	5.72	5.75	5.79	5.82	5.86	5.89	5.93	5.96	6.00	6.03	6.07	6.10	6.14	6.17	6.20	6.24
44	5.71	5.74	5.78	5.81	5.85	5.88	5.92	5.96	5.90	6.03	6.06	6.10	6.13	6.17	6.21	6.24	6.28	6.31	6.35	6.38
45	5.83	5.87	5.91	5.94	5.98	0.02	6.05	6.09	6.13	6.16	6.20	6.24	6.27	6.31	6.35	6.38	6.42	6.45	6.40	6.53
46	5.96	6.00	6.04	6.08	6.11	6.15	6.19	6.22	6.26	6.30	6.34	6.37	6.41	6.45	6.40	6.52	6.56	6.60	6.63	6.67
47	6.09	6.13	6.17	6.21	0.24	6.28	6.32	6.36	6.40	6.43	6.47	6.51	6.55	6.59	6.62	6.66	6.70	6.74	6.78	6.82
48	6.22	6.26	6.30	6.34	6.38	6.41	6.45	6.49	6.53	6.57	6.61	6.65	6.69	6.73	6.76	6.80	6.84	6.88	6.92	6.06
49	6.35	6.39	6.43	6.47	6.51	6.55	6.59	6.63	6.67	6.71	6.75	6.79	6.82	6.86	6.90	6.94	6.98	7.02	7.06	7.10
50	6.48	6.52	6.56	6.60	6.64	6.68	6.72	6.76	6.80	6.84	6.88	6.02	0.06	7.00	7.04	7.08	7.12	7.17	7.21	7.25

Temperature	Barometer reading, millibars, inches or millimeters of mercury																			
	900	905	010	015	920	925	030	035	940	045	050	955	960	965	070	975	980	985	090	095
°C																				
0	0.00	0.00	0.00	0.00	0.00	0.00	0.00	0.00	0.00	0.00	0.00	0.00	0.00	0.00	0.00	0.00	0.00	0.00	0.00	0.00
5	.73	.74	.74	.75	.75	.75	.76	.76	.77	.77	.78	.78	.78	.70	.70	.80	.80	.80	.81	.81
10	1.47	1.48	1.48	1.49	1.50	1.51	1.52	1.53	1.53	1.54	1.55	1.50	1.57	1.57	1.58	1.50	1.60	1.61	1.61	1.62
11	1.61	1.62	1.63	1.64	1.65	1.66	1.67	1.68	1.69	1.70	1.70	1.71	1.72	1.73	1.74	1.75	1.76	1.77	1.78	1.78
12	1.76	1.77	1.78	1.79	1.80	1.81	1.82	1.83	1.84	1.85	1.86	1.87	1.88	1.89	1.90	1.91	1.92	1.93	1.94	1.05
13	1.91	1.02	1.93	1.04	1.95	1.96	1.97	1.98	1.99	2.00	2.01	2.02	2.03	2.05	2.06	2.07	2.08	2.09	2.10	2.11
14	2.05	2.07	2.08	2.09	2.10	2.11	2.12	2.13	2.14	2.16	2.17	2.18	2.19	2.20	2.21	2.22	2.24	2.25	2.26	2.27
15	2.20	2.21	2.22	2.24	2.25	2.26	2.27	2.29	2.30	2.31	2.32	2.33	2.35	2.36	2.37	2.38	2.40	2.41	2.42	2.43
16	2.35	2.36	2.37	2.39	2.40	2.41	2.42	2.44	2.45	2.46	2.48	2.49	2.50	2.52	2.53	2.54	2.55	2.57	2.58	2.59
17	2.49	2.51	2.52	2.53	2.55	2.56	2.58	2.59	2.60	2.62	2.63	2.64	2.66	2.67	2.69	2.70	2.71	2.73	2.74	2.76
18	2.64	2.65	2.67	2.68	2.70	2.71	2.73	2.74	2.76	2.77	2.79	2.80	2.81	2.83	2.84	2.86	2.87	2.89	2.90	2.92
19	2.78	2.80	2.82	2.83	2.85	2.86	2.88	2.89	2.01	2.92	2.94	2.95	2.07	2.09	3.00	3.02	3.03	3.05	3.06	3.08
20	2.93	2.05	2.96	2.98	3.00	3.01	3.03	3.04	3.06	3.08	3.09	3.11	3.13	3.14	3.16	3.17	3.19	3.21	3.22	3.24
21	3.08	3.09	3.11	3.13	3.14	3.16	3.18	3.20	3.21	3.23	3.25	3.26	3.28	3.30	3.32	3.33	3.35	3.37	3.38	3.40
22	3.22	3.24	3.26	3.28	3.29	3.31	3.33	3.35	3.37	3.38	3.40	3.42	3.44	3.46	3.47	3.49	3.51	3.53	3.54	3.56
23	3.37	3.39	3.41	3.42	3.44	3.46	3.48	3.50	3.52	3.54	3.56	3.57	3.59	3.61	3.63	3.65	3.67	3.69	3.71	3.72
24	3.51	3.53	3.55	3.57	3.59	3.61	3.63	3.65	3.67	3.69	3.71	3.73	3.75	3.77	3.70	3.81	3.83	3.85	3.87	3.89
25	3.66	3.68	3.70	3.72	3.74	3.76	3.78	3.80	3.82	3.84	3.86	3.88	3.00	3.92	3.94	3.96	3.90	4.01	4.03	4.05
26	3.81	3.83	3.85	3.87	3.89	3.91	3.93	3.95	3.97	4.00	4.02	4.04	4.06	4.08	4.10	4.12	4.14	4.16	4.19	4.21
27	3.95	3.97	4.00	4.02	4.04	4.06	4.08	4.10	4.13	4.15	4.17	4.19	4.21	4.24	4.26	4.28	4.30	4.32	4.35	4.37
28	4.10	4.12	4.14	4.17	4.19	4.21	4.23	4.26	4.28	4.30	4.32	4.35	4.37	4.39	4.42	4.44	4.46	4.48	4.51	4.53
29	4.24	4.27	4.29	4.31	4.34	4.36	4.38	4.41	4.43	4.45	4.48	4.50	4.53	4.55	4.57	4.60	4.62	4.64	4.67	4.69
30	4.39	4.41	4.44	4.46	4.49	4.51	4.53	4.56	4.58	4.61	4.63	4.66	4.68	4.70	4.73	4.75	4.78	4.80	4.83	4.85
31	4.53	4.56	4.58	4.61	4.63	4.66	4.68	4.71	4.73	4.76	4.79	4.81	4.84	4.86	4.89	4.91	4.94	4.96	4.99	5.01
32	4.68	4.70	4.73	4.76	4.78	4.81	4.83	4.86	4.89	4.91	4.94	4.96	4.99	5.02	5.04	5.07	5.09	5.12	5.15	5.17
33	4.82	4.85	4.88	4.90	4.93	4.96	4.98	5.01	5.04	5.07	5.09	5.12	5.15	5.17	5.20	5.23	5.25	5.28	5.31	5.33
34	4.97	5.00	5.02	5.05	5.08	5.11	5.13	5.16	5.19	5.22	5.25	5.27	5.30	5.33	5.36	5.38	5.41	5.44	5.47	5.49
35	5.11	5.14	5.17	5.20	5.23	5.26	5.29	5.31	5.34	5.37	5.40	5.43	5.46	5.48	5.51	5.54	5.57	5.60	5.63	5.65
36	5.26	5.29	5.32	5.35	5.38	5.41	5.44	5.46	5.49	5.52	5.55	5.58	5.61	5.64	5.67	5.70	5.73	5.76	5.79	5.81
37	5.40	5.43	5.46	5.49	5.52	5.55	5.59	5.62	5.65	5.68	5.71	5.74	5.77	5.80	5.83	5.86	5.89	5.92	5.95	5.98
38	5.55	5.58	5.61	5.64	5.67	5.70	5.73	5.77	5.80	5.83	5.86	5.89	5.92	5.95	5.98	6.01	6.04	6.07	6.10	6.14
39	5.69	5.73	5.76	5.79	5.82	5.85	5.88	5.92	5.95	5.98	6.01	6.04	6.07	6.11	6.14	6.17	6.20	6.23	6.26	6.30
40	5.84	5.87	5.90	5.94	5.97	6.00	6.03	6.07	6.10	6.13	6.16	6.20	6.23	6.26	6.29	6.33	6.36	6.39	6.42	6.46
41	5.98	6.02	6.05	6.08	6.12	6.15	6.18	6.22	6.25	6.28	6.32	6.35	6.38	6.42	6.45	6.48	6.52	6.55	6.58	6.62
42	6.13	6.16	6.20	6.23	6.27	6.30	6.33	6.37	6.40	6.44	6.47	6.50	6.54	6.57	6.61	6.64	6.67	6.71	6.74	6.78
43	6.27	6.31	6.34	6.38	6.41	6.45	6.48	6.52	6.55	6.59	6.62	6.66	6.69	6.73	6.76	6.80	6.83	6.87	6.90	6.94
44	6.42	6.45	6.49	6.53	6.56	6.60	6.63	6.67	6.70	6.74	6.78	6.81	6.85	6.88	6.92	6.95	6.99	7.03	7.06	7.10
45	6.56	6.60	6.64	6.67	6.71	6.75	6.78	6.82	6.86	6.89	6.93	6.97	7.00	7.04	7.07	7.11	7.15	7.18	7.22	7.26
46	6.71	6.75	6.78	6.82	6.86	6.90	6.93	6.97	7.01	7.04	7.08	7.12	7.16	7.19	7.23	7.27	7.31	7.34	7.38	7.42
47	6.85	6.89	6.93	6.97	7.01	7.04	7.08	7.12	7.16	7.20	7.23	7.27	7.31	7.35	7.39	7.42	7.46	7.50	7.54	7.58
48	7.00	7.04	7.08	7.11	7.15	7.19	7.23	7.27	7.31	7.35	7.39	7.43	7.46	7.50	7.54	7.58	7.62	7.66	7.70	7.74
49	7.14	7.18	7.22	7.26	7.30	7.34	7.38	7.42	7.46	7.50	7.54	7.58	7.62	7.66	7.70	7.74	7.78	7.82	7.86	7.90
50	7.29	7.33	7.37	7.41	7.45	7.49	7.53	7.57	7.61	7.65	7.69	7.73	7.77	7.81	7.85	7.89	7.93	7.97	8.02	8.06

TABLE 6. *Temperature corrections for Fortin barometer with brass scales*—Continued

All corrections are to be subtracted from the reading.

Temperature	Barometer reading, millibars, inches or millimeters of mercury																			
	1,000	1,005	1,010	1,015	1,020	1,025	1,030	1,035	1,040	1,045	1,050	1,055	1,060	1,065	1,070	1,075	1,080	1,085	1,090	1,095
°C																				
0	0.00	0.00	0.00	0.00	0.00	0.00	0.00	0.00	0.00	0.00	0.00	0.00	0.00	0.00	0.00	0.00	0.00	0.00	0.00	0.00
5	.82	.82	.82	.83	.83	.84	.84	.84	.85	.85	.86	.86	.86	.87	.87	.88	.88	.89	.89	.89
10	1.63	1.64	1.65	1.66	1.66	1.67	1.68	1.69	1.70	1.70	1.71	1.72	1.73	1.74	1.75	1.75	1.76	1.77	1.78	1.79
11	1.79	1.80	1.81	1.82	1.83	1.84	1.85	1.86	1.87	1.87	1.88	1.89	1.90	1.91	1.92	1.93	1.94	1.95	1.96	1.90
12	1.96	1.97	1.98	1.99	2.00	2.01	2.02	2.03	2.03	2.04	2.05	2.06	2.07	2.08	2.09	2.10	2.11	2.12	2.13	2.14
13	2.12	2.13	2.14	2.15	2.16	2.17	2.18	2.19	2.20	2.21	2.23	2.24	2.25	2.26	2.27	2.28	2.29	2.30	2.31	2.82
14	2.28	2.29	2.30	2.32	2.33	2.34	2.35	2.36	2.37	2.38	2.40	2.41	2.42	2.43	2.44	2.45	2.46	2.48	2.49	2.50
15	2.44	2.46	2.47	2.48	2.49	2.51	2.52	2.53	2.54	2.55	2.57	2.58	2.59	2.60	2.62	2.63	2.64	2.65	2.60	2.68
16	2.61	2.62	2.63	2.65	2.66	2.67	2.69	2.70	2.71	2.72	2.74	2.75	2.76	2.78	2.79	2.80	2.82	2.83	2.84	2.85
17	2.77	2.78	2.80	2.81	2.82	2.84	2.85	2.87	2.88	2.80	2.91	2.92	2.94	2.95	2.96	2.98	2.99	3.00	3.92	3.03
18	2.93	2.95	2.96	2.98	2.99	3.00	3.92	3.93	3.05	3.06	3.08	3.99	3.11	3.12	3.14	3.15	3.17	3.18	3.20	3.21
19	3.09	3.11	3.12	3.14	3.10	3.17	3.19	3.20	3.22	3.23	3.25	3.26	3.28	3.30	3.31	3.33	3.34	3.36	3.37	3.39
20	3.26	3.27	3.29	3.31	3.32	3.34	3.35	3.37	3.39	3.49	3.42	3.44	3.45	3.47	3.48	3.50	3.52	3.53	3.55	3.57
21	3.42	3.44	3.45	3.47	3.49	3.59	3.52	3.54	3.56	3.57	3.59	3.61	3.62	3.64	3.60	3.67	3.69	3.71	3.73	3.74
22	3.58	3.60	3.62	3.63	3.65	3.67	3.69	3.71	3.72	3.74	3.76	3.78	3.89	3.81	3.83	3.85	3.87	3.88	3.90	3.92
23	3.74	3.76	3.78	3.80	3.82	3.84	3.85	3.87	3.89	3.91	3.93	3.95	3.97	3.99	4.00	4.92	4.94	4.96	4.98	4.19
24	3.90	3.92	3.94	3.96	3.98	4.00	4.02	4.04	4.06	4.08	4.19	4.12	4.14	4.16	4.18	4.20	4.22	4.24	4.26	4.28
25	4.07	4.09	4.11	4.13	4.15	4.17	4.19	4.21	4.23	4.25	4.27	4.29	4.31	4.33	4.35	4.37	4.39	4.41	4.43	4.45
26	4.23	4.25	4.27	4.29	4.31	4.33	4.36	4.38	4.40	4.42	4.44	4.46	4.48	4.50	4.52	4.55	4.57	4.59	4.61	4.63
27	4.39	4.41	4.43	4.46	4.48	4.50	4.52	4.54	4.57	4.59	4.61	4.63	4.65	4.68	4.70	4.72	4.74	4.76	4.79	4.81
28	4.55	4.57	4.60	4.02	4.64	4.67	4.69	4.71	4.73	4.76	4.78	4.80	4.83	4.85	4.87	4.89	4.92	4.94	4.96	4.98
29	4.71	4.74	4.76	4.78	4.81	4.83	4.86	4.88	4.90	4.93	4.95	4.97	5.00	5.02	5.04	5.07	5.09	5.11	5.14	5.16
30	4.88	4.90	4.92	4.95	4.97	5.00	5.02	5.05	5.07	5.09	5.12	5.14	5.17	5.19	5.22	5.24	5.27	5.29	5.31	5.34
31	5.04	5.06	5.09	5.11	5.14	5.16	5.19	5.21	5.24	5.26	5.29	5.31	5.34	5.36	5.39	5.41	5.44	5.47	5.49	5.52
32	5.20	5.22	5.25	5.28	5.30	5.33	5.35	5.38	5.41	5.43	5.46	5.48	5.51	5.54	5.56	5.59	5.61	5.64	5.67	5.69
33	5.36	5.39	5.41	5.44	5.47	5.49	5.52	5.55	5.57	5.60	5.63	5.65	5.68	5.71	5.74	5.76	5.79	5.82	5.84	5.87
34	5.52	5.55	5.58	5.60	5.63	5.66	5.69	5.71	5.74	5.77	5.80	5.83	5.85	5.88	5.91	5.94	5.96	5.99	6.02	6.05
35	5.68	5.71	5.74	5.77	5.80	5.82	5.85	5.88	5.91	5.94	5.97	0.00	6.02	6.05	6.08	6.11	6.14	6.17	6.19	6.22
30	5.84	5.87	5.90	5.93	5.96	5.99	6.02	6.05	6.08	6.11	6.14	6.17	6.19	6.22	6.25	6.28	6.31	6.34	6.37	6.40
37	6.01	6.04	6.07	6.10	6.13	6.16	6.19	6.22	6.25	6.28	6.31	6.34	6.37	6.40	6.43	6.46	6.49	6.52	6.55	6.58
38	6.17	6.20	6.23	6.26	6.29	6.32	6.35	6.38	6.41	6.44	6.47	6.51	6.54	6.57	6.60	6.63	6.66	6.69	6.72	6.75
39	6.33	6.36	6.39	6.42	6.45	6.49	6.52	6.55	6.58	6.61	6.64	6.68	6.71	6.74	6.77	6.80	6.83	6.87	6.90	6.93
40	6.49	6.52	6.55	6.59	6.62	6.65	6.68	6.72	6.75	6.78	6.81	6.85	6.88	6.91	6.94	6.98	7.01	7.04	7.07	7.11
41	6.65	6.68	6.72	6.75	6.78	6.82	6.85	6.88	6.92	6.95	6.98	7.02	7.05	7.08	7.12	7.15	7.18	7.22	7.25	7.28
42	6.81	6.84	6.88	6.91	6.95	6.98	7.02	7.05	7.08	7.12	7.15	7.19	7.22	7.25	7.29	7.32	7.36	7.39	7.42	7.46
43	6.97	7.01	7.04	7.08	7.11	7.15	7.18	7.22	7.25	7.29	7.32	7.36	7.39	7.42	7.46	7.49	7.53	7.56	7.60	7.63
44	7.13	7.17	7.20	7.24	7.28	7.31	7.35	7.38	7.42	7.45	7.49	7.52	7.56	7.60	7.63	7.67	7.70	7.74	7.77	7.81
45	7.29	7.33	7.37	7.40	7.44	7.48	7.51	7.55	7.59	7.62	7.66	7.69	7.73	7.77	7.80	7.84	7.88	7.91	7.95	7.99
46	7.45	7.49	7.53	7.57	7.60	7.64	7.68	7.71	7.75	7.79	7.83	7.80	7.90	7.94	7.98	8.01	8.05	8.09	8.12	8.10
47	7.61	7.65	7.69	7.73	7.77	7.81	7.84	7.88	7.92	7.96	8.00	8.03	8.07	8.11	8.15	8.19	8.22	8.26	8.30	8.34
48	7.78	7.81	7.85	7.89	7.93	7.97	8.01	8.05	8.09	8.13	8.16	8.20	8.24	8.28	8.32	8.36	8.40	8.44	8.48	8.51
49	7.94	7.98	8.02	8.05	8.09	8.13	8.17	8.21	8.25	8.29	8.33	8.37	8.41	8.45	8.49	8.53	8.57	8.01	8.05	8.09
50	8.10	8.14	8.18	8.22	8.20	8.39	8.34	8.38	8.42	8.40	8.50	8.54	8.58	8.62	8.06	8.70	8.74	8.78	8.83	8.87

Temperature	Barometer reading, millibars, inches or millimeters of mercury																			
	1,100	1,105	1,110	1,115	1,120	1,125	1,130	1,135	1,140	1,145	1,150	1,155	1,160	1,105	1,170	1,175	1,180	1,185	1,190	1,195
°C																				
0	0.00	0.00	0.00	0.00	0.00	0.00	0.00	0.00	0.00	0.00	0.00	0.00	0.00	0.00	0.00	0.00	0.00	0.00	0.00	0.00
5	.90	.90	.91	.91	.91	.92	.92	.93	.93	.93	.94	.94	.95	.95	.95	.96	.96	.97	.97	.98
10	1.79	1.86	1.81	1.82	1.83	1.84	1.84	1.85	1.86	1.87	1.88	1.88	1.89	1.90	1.91	1.92	1.92	1.93	1.94	1.95
11	1.97	1.98	1.99	2.00	2.01	2.02	2.03	2.04	2.04	2.05	2.06	2.07	2.08	2.09	2.10	2.11	2.12	2.13	2.13	2.14
12	2.15	2.16	2.17	2.18	2.19	2.20	2.21	2.22	2.23	2.24	2.25	2.26	2.27	2.28	2.29	2.30	2.31	2.32	2.33	2.34
13	2.33	2.34	2.35	2.36	2.37	2.38	2.39	2.41	2.42	2.43	2.44	2.45	2.46	2.47	2.48	2.49	2.50	2.51	2.52	2.53
14	2.51	2.52	2.53	2.54	2.56	2.57	2.58	2.59	2.60	2.61	2.62	2.64	2.65	2.66	2.07	2.68	2.69	2.70	2.72	2.73
15	2.69	2.70	2.71	2.73	2.74	2.75	2.76	2.77	2.79	2.80	2.81	2.82	2.84	2.85	2.86	2.87	2.88	2.90	2.91	2.92
16	2.87	2.88	2.89	2.91	2.92	2.93	2.95	2.96	2.97	2.98	3.00	3.01	3.02	3.04	3.05	3.06	3.08	3.09	3.10	3.12
17	3.05	3.06	3.07	3.09	3.10	3.12	3.13	3.14	3.16	3.17	3.18	3.20	3.21	3.23	3.24	3.25	3.27	3.28	3.30	3.31
18	3.22	3.24	3.25	3.27	3.18	3.30	3.31	3.33	3.34	3.36	3.37	3.39	3.40	3.42	3.43	3.44	3.46	3.47	3.49	3.50
19	3.40	3.42	3.43	3.45	3.47	3.48	3.50	3.51	3.53	3.54	3.56	3.57	3.59	3.60	3.62	3.64	3.65	3.67	3.68	3.70
20	3.58	3.60	3.61	3.63	3.65	3.66	3.68	3.70	3.71	3.73	3.74	3.76	3.78	3.79	3.81	3.83	3.84	3.80	3.87	3.89
21	3.76	3.78	3.79	3.81	3.83	3.85	3.86	3.88	3.90	3.91	3.93	3.95	3.97	3.98	4.00	4.02	4.03	4.05	4.07	4.08
22	3.94	3.96	3.97	3.99	4.01	4.03	4.05	4.06	4.08	4.10	4.12	4.14	4.15	4.17	4.19	4.21	4.22	4.24	4.26	4.28
23	4.12	4.14	4.15	4.17	4.19	4.21	4.23	4.25	4.27	4.29	4.30	4.32	4.34	4.36	4.38	4.40	4.42	4.43	4.45	4.47
24	4.30	4.31	4.33	4.35	4.37	4.39	4.41	4.43	4.45	4.47	4.49	4.51	4.53	4.55	4.57	4.59	4.61	4.63	4.65	4.67
25	4.47	4.49	4.51	4.53	4.55	4.57	4.60	4.62	4.64	4.66	4.68	4.70	4.72	4.74	4.76	4.78	4.80	4.82	4.84	4.86
26	4.65	4.67	4.69	4.71	4.74	4.76	4.78	4.80	4.82	4.84	4.86	4.88	4.90	4.93	4.95	4.97	4.99	5.01	5.03	5.05
27	4.83	4.85	4.87	4.90	4.92	4.94	4.96	4.98	5.00	5.03	5.05	5.07	5.09	5.11	5.14	5.16	5.18	5.20	5.22	5.25
28	5.01	5.03	5.05	5.08	5.10	5.12	5.14	5.17	5.19	5.21	5.23	5.26	5.28	5.30	5.33	5.35	5.37	5.39	5.42	5.44
29	5.19	5.21	5.23	5.26	5.28	5.30	5.33	5.35	5.37	5.40	5.42	5.44	5.47	5.49	5.52	5.54	5.56	5.59	5.61	5.63
30	5.36	5.39	5.41	5.44	5.46	5.48	5.51	5.53	5.56	5.58	5.61	5.63	5.66	5.68	5.70	5.73	5.75	5.78	5.80	5.83
31	5.54	5.57	5.59	5.62	5.64	5.67	5.69	5.72	5.74	5.77	5.79	5.82	5.84	5.87	5.89	5.92	5.94	5.97	5.99	6.02
32	5.72	5.74	5.77	5.80	5.82	5.85	5.87	5.90	5.93	5.95	5.98	6.00	6.03	6.06	6.08	6.11	6.13	6.16	6.19	6.21
33	5.90	5.92	5.95	5.98	6.00	6.03	6.06	6.08	6.11	6.14	6.16	6.19	6.22	6.24	6.27	6.30	6.32	6.35	6.38	6.41
34	6.07	6.10	6.13	6.16	6.18	6.21	6.24	6.27	6.29	6.32	6.35	6.38	6.40	6.43	6.46	6.49	6.52	6.54	6.57	6.60
35	6.25	6.28	6.31	6.34	6.36	6.39	6.42	6.45	6.48	6.51	6.54	6.56	6.59	6.62	6.65	6.68	6.71	6.73	6.76	6.79

TABLE 6. *Temperature corrections for Fortin barometer with brass scales*—Continued

All corrections are to be subtracted from the reading.

Temperature	Barometer reading, millibars, inches or millimeters of mercury																			
	1,100	1,105	1,110	1,115	1,120	1,125	1,130	1,135	1,140	1,145	1,150	1,155	1,160	1,165	1,170	1,175	1,180	1,185	1,190	1,195
°C																				
36	6.43	6.46	6.49	6.52	6.55	6.57	6.60	6.63	6.66	6.69	6.72	6.75	6.78	6.81	6.84	6.87	6.90	6.93	6.95	6.98
37	6.61	6.64	6.67	6.70	6.73	6.76	6.79	6.82	6.85	6.88	6.91	6.94	6.97	7.00	7.03	7.06	7.09	7.12	7.15	7.18
38	6.78	6.81	6.84	6.88	6.91	6.94	6.97	7.00	7.03	7.06	7.09	7.12	7.15	7.18	7.21	7.25	7.28	7.31	7.34	7.37
39	6.96	6.99	7.02	7.06	7.09	7.12	7.15	7.18	7.21	7.25	7.28	7.31	7.34	7.37	7.40	7.44	7.47	7.50	7.53	7.56
40	7.14	7.17	7.20	7.24	7.27	7.30	7.33	7.36	7.40	7.43	7.46	7.49	7.53	7.56	7.59	7.62	7.66	7.69	7.72	7.75
41	7.31	7.35	7.38	7.41	7.45	7.48	7.51	7.55	7.58	7.61	7.65	7.68	7.71	7.75	7.78	7.81	7.85	7.88	7.91	7.95
42	7.49	7.53	7.56	7.59	7.63	7.66	7.70	7.73	7.76	7.80	7.83	7.87	7.90	7.93	7.97	8.00	8.04	8.07	8.10	8.14
43	7.67	7.70	7.74	7.77	7.81	7.84	7.88	7.91	7.95	7.98	8.02	8.05	8.09	8.12	8.16	8.19	8.23	8.26	8.30	8.33
44	7.85	7.88	7.92	7.95	8.99	8.02	8.06	8.10	8.13	8.17	8.20	8.24	8.27	8.31	8.35	8.38	8.42	8.45	8.49	8.52
45	8.02	8.06	8.10	8.13	8.17	8.20	8.24	8.28	8.31	8.35	8.39	8.42	8.46	8.50	8.53	8.57	8.61	8.64	8.68	8.72
46	8.20	8.24	8.27	8.31	8.35	8.39	8.42	8.46	8.50	8.53	8.57	8.61	8.65	8.68	8.72	8.76	8.80	8.83	8.87	8.91
47	8.38	8.41	8.45	8.49	8.53	8.57	8.60	8.64	8.68	8.72	8.76	8.79	8.83	8.87	8.91	8.95	8.99	9.02	9.06	9.10
48	8.55	8.59	8.63	8.67	8.71	8.75	8.79	8.83	8.86	8.90	8.94	8.98	9.02	9.06	9.10	9.14	9.17	9.21	9.25	9.29
49	8.73	8.77	8.81	8.85	8.89	8.93	8.97	9.01	9.05	9.09	9.13	9.17	9.21	9.25	9.29	9.32	9.36	9.40	9.44	9.48
50	8.91	8.95	8.99	9.03	9.07	9.11	9.15	9.19	9.23	9.27	9.31	9.35	9.39	9.43	9.47	9.51	9.55	9.59	9.63	9.68

TABLE 7. *Temperature Correction factor*

Numbers under scale material are values of expansion coefficient s, all of which must be multiplied by 10^{-4}

$$F=\frac{(s-m)t}{1+mt}$$

Factor F (minus sign omitted) in percent

Temperature		Aluminum 24.5	Brass 18.4	Stainless steel 17	Steel 11.5	Pyrex 3.0	Invar 0
°C	°F						
0	32.0	0	0	0	0	0	0
2	35.6	0.0314	0.03267	0.0329	0.0340	0.0357	0.03635
4	39.2	.0629	.06531	.0659	.0681	.0715	.07267
6	42.8	.0943	.09793	.0988	.1021	.1072	.10896
8	46.4	.1257	.13053	.1316	.1360	.1428	.14523
10	50.0	.1570	.16310	.1645	.1700	.1785	.18147
12	53.6	.1883	.19565	.1973	.2039	.2141	.21768
14	57.2	.2197	.22818	.2301	.2378	.2497	.25387
16	60.8	.2510	.26068	.2629	.2717	.2853	.29004
18	64.4	.2822	.29316	.2955	.3055	.3208	.32617
20	68.0	.3135	.32562	.3284	.3394	.3563	.36228
22	71.6	.3447	.35805	.3611	.3732	.3918	.39837
24	75.2	.3759	.39046	.3938	.4069	.4273	.43442
26	78.8	.4071	.42284	.4265	.4407	.4627	.47046
28	82.4	.4382	.45520	.4591	.4744	.4981	.50646
30	86.0	.4693	.48754	.4917	.5081	.5335	.54244
32	89.6	.5004	.51986	.5243	.5418	.5689	.57840
34	93.2	.5315	.55215	.5569	.5755	.6042	.61432
36	96.8	.5626	.58442	.5894	.6091	.6395	.65022
38	100.4	.5936	.61656	.6219	.6427	.6748	.68610
40	104.0	.6247	.64888	.6544	.6763	.7100	.72195
42	107.6	.6557	.68108	.6869	.7098	.7453	.75778
44	111.2	.6866	.71325	.7194	.7434	.7805	.79357
46	114.8	.7176	.74541	.7518	.7769	.8157	.82934
48	118.4	.7485	.77744	.7842	.8104	.8508	.86509
50	112.0	.7794	.80964	.8166	.8438	.8859	.90081

TABLE 8. *Gravity correction*

$$C_g=\frac{(g-g_s)R_t}{g_s}=F_gR_t \text{ or } F_gR_s$$

Correction for height of mercury column R_s or R_t in any unit of pressure

Gravity	Correction factor F_g	100	200	300	400	500	600	700	800	900	1,000	1,100	1,200	1,300
cm/sec²	%													
978.0	−0.27175	−0.272	−0.544	−0.815	−1.087	−1.359	−1.631	−1.902	−2.174	−2.446	−2.718	−2.989	−3.261	−3.533
.1	.26156	−.262	−.523	−.785	−1.046	−1.308	−1.569	−1.831	−2.092	−2.354	−2.616	−2.877	−3.139	−3.400
.2	.25136	−.251	−.503	−.754	−1.005	−1.257	−1.508	−1.760	−2.011	−2.262	−2.514	−2.765	−3.016	−3.268
.3	.24116	−.241	−.482	−.724	−0.965	−1.206	−1.447	−1.688	−1.929	−2.170	−2.412	−2.653	−2.894	−3.135
.4	.23097	−.231	−.462	−.693	−.924	−1.155	−1.386	−1.617	−1.848	−2.079	−2.310	−2.541	−2.772	−3.003
.5	.22077	−.221	−.442	−.662	−.883	−1.104	−1.325	−1.545	−1.766	−1.987	−2.208	−2.428	−2.649	−2.870
.6	.21057	−.211	−.421	−.632	−.842	−1.053	−1.263	−1.474	−1.685	−1.895	−2.106	−2.316	−2.527	−2.737
.7	.20037	−.200	−.401	−.601	−.801	−1.002	−1.202	−1.403	−1.603	−1.803	−2.004	−2.204	−2.404	−2.605
.8	.19018	−.190	−.380	−.571	−.761	−0.951	−1.141	−1.331	−1.521	−1.712	−1.902	−2.092	−2.282	−2.472
.9	.17998	−.180	−.360	−.540	−.720	−.900	−1.080	−1.260	−1.440	−1.620	−1.800	−1.980	−2.160	−2.340
979.0	.16978	−.170	−.340	−.509	−.679	−.849	−1.019	−1.188	−1.358	−1.528	−1.698	−1.868	−2.037	−2.207
.1	.15959	−.160	−.319	−.479	−.638	−.798	−0.958	−1.117	−1.277	−1.436	−1.596	−1.755	−1.915	−2.075
.2	.14939	−.149	−.299	−.448	−.598	−.747	−.896	−1.046	−1.195	−1.345	−1.494	−1.643	−1.793	−1.942
.3	.13919	−.139	−.278	−.418	−.557	−.696	−.835	−0.974	−1.114	−1.253	−1.392	−1.531	−1.670	−1.809
.4	.12899	−.129	−.258	−.387	−.516	−.645	−.774	−.903	−1.032	−1.161	−1.290	−1.419	−1.548	−1.677
.5	.11880	−.119	−.238	−.356	−.475	−.594	−.713	−.832	−0.950	−1.069	−1.188	−1.307	−1.426	−1.544
.6	.10860	−.109	−.217	−.326	−.434	−.543	−.652	−.760	−.869	−0.977	−1.086	−1.195	−1.303	−1.412
.7	.09840	−.098	−.197	−.295	−.394	−.492	−.590	−.689	−.787	−.886	−0.984	−1.082	−1.181	−1.279
.8	.08821	−.088	−.176	−.265	−.353	−.441	−.529	−.617	−.706	−.794	−.882	−0.970	−1.059	−1.147
.9	.07801	−.078	−.156	−.234	−.312	−.390	−.468	−.546	−.624	−.702	−.780	−.858	−0.936	−1.014
980.0	.06781	−.068	−.136	−.203	−.271	−.339	−.407	−.475	−.542	−.610	−.678	−.746	−.814	−0.882
.1	.05761	−.058	−.115	−.173	−.230	−.288	−.346	−.403	−.461	−.518	−.576	−.634	−.691	−.749
.2	.04742	−.047	−.095	−.142	−.190	−.237	−.285	−.332	−.379	−.427	−.474	−.522	−.569	−.616
.3	.03722	−.037	−.074	−.112	−.149	−.186	−.223	−.261	−.298	−.335	−.372	−.409	−.447	−.484
.4	.02702	−.027	−.054	−.081	−.108	−.135	−.162	−.189	−.216	−.243	−.270	−.297	−.324	−.351
.5	.01682	−.017	−.034	−.050	−.067	−.084	−.101	−.118	−.135	−.151	−.168	−.185	−.202	−.219
.6	.00663	−.007	−.013	−.020	−.027	−.033	−.040	−.046	−.053	−.060	−.066	−.073	−.080	−.086
.665	0	0	0	0	0	0	0	0	0	0	0	0	0	0
.7	+.00357	+.004	+.007	+.011	+.014	+.018	+.021	+.025	+.029	+.032	+.036	+.039	+.043	+.046
.8	.01377	+.014	+.028	+.041	+.055	+.069	+.083	+.096	+.010	+.124	+.138	+.151	+.165	+.179
.9	.02396	+.024	+.048	+.072	+.096	+.120	+.144	+.168	+.192	+.216	+.240	+.264	+.288	+.311
981.0	.03416	+.034	+.068	+.102	+.137	+.171	+.205	+.239	+.273	+.307	+.342	+.376	+.410	+.444
.1	.04436	+.044	+.089	+.133	+.177	+.222	+.266	+.311	+.355	+.399	+.444	+.488	+.532	+.577
.2	.05455	+.055	+.109	+.164	+.218	+.273	+.327	+.382	+.436	+.491	+.546	+.600	+.655	+.709
.3	.06475	+.065	+.130	+.194	+.259	+.324	+.389	+.453	+.518	+.583	+.648	+.712	+.777	+.842
.4	.07495	+.075	+.150	+.225	+.300	+.375	+.450	+.525	+.600	+.675	+.749	+.824	+.899	+.974
.5	.08515	+.085	+.170	+.255	+.341	+.426	+.511	+.596	+.681	+.766	+.851	+.937	+1.022	+1.107
.6	.09534	+.095	+.191	+.286	+.381	+.477	+.572	+.667	+.763	+.858	+.953	+1.049	+1.144	+1.239
.7	.10554	+.106	+.211	+.317	+.422	+.528	+.633	+.739	+.844	+.950	+1.055	+1.161	+1.266	+1.372
.8	.11574	+.116	+.231	+.347	+.463	+.579	+.694	+.810	+.926	+1.042	+1.157	+1.273	+1.389	+1.505
.9	.12593	+.126	+.252	+.378	+.504	+.630	+.756	+.882	+1.007	+1.133	+1.259	+1.385	+1.511	+1.637
982.0	.13613	+.136	+.272	+.408	+.545	+.681	+.817	+.953	+1.089	+1.225	+1.361	+1.497	+1.634	+1.770
.1	.14633	+.146	+.293	+.439	+.585	+.732	+.878	+1.024	+1.171	+1.317	+1.463	+1.610	+1.756	+1.902
.2	.15653	+.157	+.313	+.470	+.626	+.783	+.939	+1.096	+1.252	+1.409	+1.565	+1.722	+1.878	+2.035
.3	.16672	+.167	+.333	+.500	+.667	+.834	+1.000	+1.167	+1.334	+1.500	+1.667	+1.834	+2.001	+2.167
.4	.17692	+.177	+.354	+.531	+.708	+.885	+1.062	+1.238	+1.415	+1.592	+1.769	+1.946	+2.123	+2.300
.5	.18712	+.187	+.374	+.561	+.748	+.936	+1.123	+1.310	+1.497	+1.684	+1.871	+2.058	+2.245	+2.433
.6	.19732	+.197	+.395	+.592	+.789	+.987	+1.184	+1.381	+1.579	+1.776	+1.973	+2.171	+2.368	+2.565
.7	.20751	+.208	+.415	+.623	+.830	+1.038	+1.245	+1.453	+1.660	+1.868	+2.075	+2.283	+2.490	+2.698
.8	.21771	+.218	+.435	+.653	+.871	+1.089	+1.306	+1.524	+1.742	+1.959	+2.177	+2.395	+2.613	+2.830
.9	.22791	+.228	+.456	+.684	+.912	+1.140	+1.367	+1.595	+1.823	+2.051	+2.279	+2.507	+2.735	+2.963
983.0	.23810	+.238	+.476	+.714	+.952	+1.191	+1.429	+1.667	+1.905	+2.143	+2.381	+2.619	+2.857	+3.095
.1	.24830	+.248	+.497	+.745	+.993	+1.242	+1.490	+1.738	+1.986	+2.235	+2.483	+2.731	+2.980	+3.228
.2	.25850	+.258	+.517	+.775	+1.034	+1.292	+1.551	+1.809	+2.068	+2.326	+2.585	+2.843	+3.102	+3.360
.3	.26870	+.269	+.537	+.806	+1.075	+1.343	+1.612	+1.881	+2.150	+2.418	+2.687	+2.956	+3.224	+3.493
.4	.27889	+.279	+.558	+.837	+1.116	+1.394	+1.673	+1.952	+2.231	+2.510	+2.789	+3.068	+3.347	+3.626
.5	.28909	+.289	+.578	+.867	+1.156	+1.445	+1.735	+2.024	+2.313	+2.602	+2.891	+3.180	+3.469	+3.758

425-56

TABLE 9. *Gravity corrections at various latitudes at sea level*

$$\text{Correction} = \frac{g - g_s}{g_s} R_s = F_s R_s \text{ or } F_s R_t$$

Correction for height of mercury column R_s or R_t in any unit of pressure measurement

Latitude	Gravity	Correction factor F_s	100	200	300	400	500	600	700	800	900	1,000	1,100	1,200	1,300
deg	*cm/sec²*	%													
0	978.036	−0.26808	−0.268	−0.536	−0.804	−1.072	−1.340	−1.608	−1.877	−2.145	−2.413	−2.681	−2.949	−3.217	−3.485
2	978.042	.26747	−.267	−.535	−.802	−1.070	−1.337	−1.605	−1.872	−2.140	−2.407	−2.675	−2.942	−3.210	−3.477
4	978.061	.26553	−.266	−.531	−.797	−1.062	−1.328	−1.593	−1.859	−2.124	−2.390	−2.655	−2.921	−3.186	−3.452
6	978.092	.26237	−.262	−.525	−.787	−1.049	−1.312	−1.574	−1.837	−2.099	−2.361	−2.624	−2.886	−3.148	−3.411
8	978.135	.25799	−.258	−.516	−.774	−1.032	−1.290	−1.548	−1.806	−2.064	−2.322	−2.580	−2.838	−3.096	−3.354
10	978.191	.25228	−.252	−.505	−.757	−1.009	−1.261	−1.514	−1.766	−2.018	−2.271	−2.523	−2.775	−3.027	−3.280
12	978.258	.24545	−.245	−.491	−.736	−0.982	−1.227	−1.473	−1.718	−1.964	−2.209	−2.454	−2.700	−2.945	−3.191
14	978.337	.23739	−.237	−.475	−.712	−.950	−1.187	−1.424	−1.662	−1.899	−2.137	−2.374	−2.611	−2.849	−3.086
16	978.427	.22821	−.228	−.456	−.685	−.913	−1.141	−1.369	−1.597	−1.826	−2.054	−2.282	−2.510	−2.739	−2.967
18	978.528	.21791	−.218	−.436	−.654	−.872	−1.090	−1.307	−1.525	−1.743	−1.961	−2.179	−2.397	−2.615	−2.833
20	978.638	.20670	−.207	−.413	−.620	−.827	−1.033	−1.240	−1.447	−1.654	−1.860	−2.067	−2.274	−2.480	−2.687
22	978.759	.19436	−.194	−.389	−.583	−.777	−0.972	−1.166	−1.361	−1.555	−1.749	−1.944	−2.138	−2.332	−2.527
24	978.888	.18120	−.181	−.362	−.544	−.725	−.906	−1.087	−1.268	−1.450	−1.631	−1.812	−1.993	−2.174	−2.356
26	979.026	.16713	−.167	−.334	−.501	−.669	−.836	−1.003	−1.170	−1.337	−1.504	−1.671	−1.838	−2.006	−2.173
28	979.172	.15224	−.152	−.304	−.457	−.609	−.761	−0.913	−1.066	−1.218	−1.370	−1.522	−1.675	−1.827	−1.979
30	979.324	.13674	−.137	−.273	−.410	−.547	−.684	−.820	−0.957	−1.094	−1.231	−1.367	−1.504	−1.641	−1.778
32	979.483	.12053	−.121	−.241	−.362	−.482	−.603	−.723	−.844	−0.964	−1.085	−1.205	−1.326	−1.446	−1.567
34	979.648	.10371	−.104	−.207	−.311	−.415	−.519	−.622	−.726	−.830	−0.933	−1.037	−1.141	−1.244	−1.348
36	979.817	.08647	−.086	−.173	−.259	−.346	−.432	−.519	−.605	−.692	−.778	−0.865	−0.951	−1.038	−1.124
38	979.991	.06873	−.069	−.137	−.206	−.275	−.344	−.412	−.481	−.550	−.619	−.687	−.756	−0.825	−0.893
40	980.167	.05078	−.051	−.102	−.152	−.203	−.254	−.305	−.355	−.406	−.457	−.508	−.559	−.609	−.660
42	980.346	.03253	−.033	−.065	−0.098	−.130	−.163	−.195	−.228	−.260	−.293	−.325	−.358	−.390	−.423
44	980.526	.01417	−.014	−.028	−0.043	−.057	−.071	−.085	−.099	−.113	−.128	−.142	−.156	−.170	−.184
45	980.616	.00500	−.005	−.010	−0.015	−.020	−.025	−.030	−.035	−.040	−.045	−.050	−.055	−.060	−.065
	980.665	0	0	0	0	0	0	0	0	0	0	0	0	0	0
46	980.706	+.00418	+.004	+.008	+.013	+.017	+.021	+.025	+.029	+.033	+.038	+.042	+.046	+.050	+.054
48	980.886	.02254	+.023	+.045	+.068	+.090	+.113	+.135	+.158	+.180	+.203	+.225	+.248	+.270	+.293
50	981.065	.04079	+.041	+.082	+.122	+.163	+.204	+.245	+.286	+.326	+.367	+.408	+.449	+.489	+.530
52	981.242	.05884	+.059	+.118	+.177	+.235	+.294	+0.353	+.412	+.471	+.530	+.588	+.647	+.706	+.765
54	981.416	.06658	+.077	+.153	+.230	+.306	+.383	+0.459	+.536	+.613	+.689	+.766	+.842	+.919	+.996
56	981.586	.09392	+.094	+.188	+.282	+.376	+.470	+0.564	+.657	+.751	+.845	+.939	+1.033	+1.127	+1.221
58	981.751	.11074	+.111	+.221	+.332	+.443	+.544	+0.664	+.775	+.886	+.997	+1.107	+1.218	+1.329	+1.440
60	981.911	.12706	+.127	+.254	+.381	+.508	+.635	+0.762	+.889	+1.016	+1.144	+1.271	+1.398	+1.525	+1.652
62	982.064	.14266	+.143	+.285	+.428	+.571	+.713	+0.856	+.999	+1.141	+1.284	+1.427	+1.569	+1.712	+1.855
64	982.210	.15755	+.158	+.315	+.473	+.630	+.788	+0.945	+1.103	+1.260	+1.418	+1.575	+1.733	+1.891	+2.048
66	982.349	.17172	+.172	+.343	+.515	+.687	+.859	+1.030	+1.202	+1.374	+1.545	+1.717	+1.889	+2.061	+2.232
68	982.479	.18498	+.185	+.370	+.555	+.740	+.925	+1.110	+1.295	+1.480	+1.665	+1.859	+2.035	+2.220	+2.405
70	982.601	.19742	+.197	+.395	+.592	+.790	+.987	+1.185	+1.382	+1.579	+1.777	+1.974	+2.172	+2.369	+2.566
72	982.712	.20874	+.209	+.417	+.626	+.835	+1.044	+1.252	+1.461	+1.670	+1.879	+2.087	+2.296	+2.505	+2.714
74	982.813	.21904	+.219	+.438	+.657	+.876	+1.095	+1.314	+1.533	+1.752	+1.971	+2.190	+2.409	+2.628	+2.848
76	982.904	.22831	+.228	+.457	+.685	+.913	+1.142	+1.370	+1.598	+1.826	+2.055	+2.283	+2.511	+2.740	+2.968
78	982.983	.23637	+.236	+.473	+.709	+.945	+1.182	+1.418	+1.655	+1.891	+2.127	+2.364	+2.600	+2.836	+3.073
80	983.051	.24330	+.243	+.487	+.730	+.973	+1.217	+1.460	+1.703	+1.946	+2.190	+2.433	+2.676	+2.920	+3.163
82	983.107	.24901	+.249	+.498	+.747	+.996	+1.245	+1.494	+1.743	+1.992	+2.241	+2.490	+2.739	+2.988	+3.237
84	983.151	.25350	+.254	+.507	+.761	+1.014	+1.268	+1.521	+1.775	+2.028	+2.282	+2.535	+2.789	+3.042	+3.296
86	983.183	.25676	+.257	+.514	+.770	+1.027	+1.284	+1.541	+1.797	+2.054	+2.311	+2.568	+2.824	+3.081	+3.338
88	983.202	.25870	+.259	+.517	+.776	+1.035	+1.294	+1.552	+1.811	+2.070	+2.328	+2.587	+2.846	+3.104	+3.363
90	983.208	.25931	+.259	+.519	+.778	+1.037	+1.297	+1.556	+1.815	+2.074	+2.334	+2.593	+2.852	+3.112	+3.371

TABLE 10. *Capillary depression of mercury column*

Millimeters of mercury at 20°C and under standard gravity.

Bore of tube	Meniscus height in mm																		
mm	0.1	0.2	0.3	0.4	0.5	0.6	0.7	0.8	0.9	1.0	1.1	1.2	1.3	1.4	1.5	1.6	1.7	1.8	1.9	2.0
	Surface tension, 400 dynes/cm																			
8	0.054	0.108	0.162	0.214	0.265	0.315	0.363	0.409	0.453	0.494	0.533	0.569	0.603	0.633	0.660	0.684	0.705	0.723	0.737	0.749
10	.029	.058	.087	.115	.143	.170	.196	.222	.247	.270	.292	.314	.333	.352	.369	.384	.398	.410	.421	.430
16	.006	.011	.016	.022	.027	.032	.037	.042	.047	.052	.056	.060	.065	.068	.072	.076	.079	.082	.084	.086
22	.001	.002	.003	.004	.005	.006	.008	.009	.010	.010	.011	.012	.013	.014	.014	.015	.016	.016	.017	.018
	Surface tension, 450 dynes/cm																			
6	0.128	0.254	0.379	0.500	0.617	0.729	0.836	0.937	1.03	1.12	1.20	1.27	1.33	1.38	1.43	1.47	1.50	------	------	------
7	.088	.176	.263	.348	.430	.510	.587	.661	0.730	0.794	0.855	0.910	0.961	1.01	1.05	1.08	1.11	1.14	1.16	------
8	.063	.126	.189	.250	.310	.368	.424	.478	.530	.579	.625	.668	.708	0.744	0.777	0.807	0.833	0.855	0.874	0.890
9	.046	.093	.138	.183	.228	.271	.313	.353	.392	.429	.464	.498	.529	.557	.584	.608	.630	.649	.665	.679
10	.035	.069	.103	.137	.170	.202	.234	.264	.294	.322	.349	.375	.399	.422	.443	.462	.480	.495	.509	.522
11	.026	.052	.078	.104	.128	.153	.177	.200	.223	.245	.265	.285	.304	.322	.338	.354	.368	.380	.392	.402
12	.020	.040	.059	.079	.098	.117	.135	.153	.170	.187	.203	.218	.233	.247	.260	.272	.283	.293	.303	.311
13	.015	.030	.045	.060	.075	.089	.104	.117	.131	.144	.156	.168	.180	.190	.200	.210	.219	.227	.234	.241
14	.012	.023	.035	.046	.058	.069	.080	.090	.101	.111	.120	.130	.139	.147	.155	.163	.170	.176	.182	.187
15	.009	.018	.027	.036	.045	.053	.062	.070	.078	.086	.093	.101	.108	.114	.120	.126	.132	.137	.141	.146
16	.007	.014	.021	.028	.035	.041	.048	.054	.060	.067	.072	.078	.083	.089	.093	.098	.102	.106	.110	.113
17	.006	.011	.016	.022	.027	.032	.037	.042	.047	.052	.056	.061	.065	.069	.073	.076	.080	.083	.086	.088
18	.004	.008	.013	.017	.021	.025	.029	.033	.036	.040	.044	.047	.050	.054	.057	.059	.062	.064	.067	.069
19	.003	.006	.010	.013	.016	.019	.022	.026	.028	.031	.034	.037	.039	.042	.044	.046	.048	.050	.052	.054
20	.003	.005	.008	.010	.013	.015	.017	.020	.022	.024	.026	.029	.030	.032	.034	.036	.037	.039	.040	.042
21	.002	.004	.006	.008	.010	.012	.014	.015	.017	.019	.020	.022	.024	.025	.027	.028	.029	.030	.031	.032
22	.002	.003	.005	.006	.008	.009	.011	.012	.013	.015	.016	.017	.018	.020	.021	.022	.023	.024	.024	.025
	Surface tension, 500 dynes/cm																			
8	0.072	0.143	0.215	0.286	0.354	0.421	0.485	0.547	0.607	0.663	0.716	0.766	0.813	0.855	0.894	0.929	0.961	0.989	1.01	1.03
10	.040	.080	.120	.159	.197	.235	.272	.308	.342	.375	.407	.436	.464	.491	.517	.542	.563	.582	.600	.615
16	.009	.017	.026	.034	.043	.051	.059	.067	.075	.082	.090	.097	.104	.110	.116	.122	.128	.133	.138	.142
22	.002	.004	.006	.008	.010	.012	.014	.016	.018	.020	.021	.023	.025	.026	.028	.029	.031	.032	.033	.034

TABLE 11. *Rate of change of absolute pressure with height of a gas column of any composition at various densities*

The rate of pressure change is negative; the absolute pressure increases for levels below, and decreases for levels above, the reference density

Density	Absolute air pressure			Rate of change of absolute pressure, dP/dh				
$g/cm^3 \times 10^6$	20°C mm Hg	25°C mm Hg	30°C mm Hg	mb/ft	mm Hg/ft	in. Hg/ft	psi/ft	mb/m
500	315.6	321.0	326.4	0.01490	0.01118	0.0004400	0.0002012	0.04903
600	378.7	385.2	391.6	.01788	.01341	.0005280	.0002415	.05884
700	441.9	449.4	457.0	.02086	.01565	.0006160	.0002817	.06865
800	505.0	513.6	522.2	.02384	.01788	.0007040	.0003219	.07845
900	568.1	577.8	587.5	.02682	.02012	.0007920	.0003622	.08826
1000	631.2	642.0	652.7	.02980	.02235	.0008800	.0004024	.09807
1100	694.4	706.2	718.1	.03278	.02459	.0009680	.0004427	.1079
1200	757.5	770.4	783.4	.03576	.02682	.001056	.0004829	.1177
1300	820.6	834.6	848.6	.03874	.02906	.001144	.0005231	.1275
1400	883.7	898.8	913.9	.04172	.03129	.001232	.0005634	.1373
1500	946.8	963.0	979.1	.04470	.03353	.001320	.0006036	.1471
1600	1010.0	1027.2	1044.5	.04768	.03576	.001408	.0006439	.1569
1700	1073.1	1091.4	1109.7	.05066	.03800	.001496	.0006841	.1667
1800	1136.2	1155.6	1175.0	.05364	.04023	.001584	.0007243	.1765
1900	1199.3	1219.8	1240.2	.05662	.04247	.001672	.0007646	.1863
2000	1262.5	1284.0	1305.6	.05960	.04470	.001760	.0008048	.1961
2500	1578.1	1605.0	1632.0	.07450	.05588	.002200	.001006	.2452
3000	1893.7	1926.0	1958.3	.08940	.06708	.002640	.001207	.2942
3500	2209.3	2247.0	2284.7	.1043	.07823	.003080	.001408	.3432
4000	2524.9	2568.0	2611.1	.1192	.08941	.003520	.001610	.3923
4500	2840.5	2889.0	2937.5	.1341	.1006	.003960	.001811	.4413
5000	3156.2	3210.1	3263.9	.1490	.1118	.004400	.002012	.4903
5500	3471.8	3531.0	3590.3	.1639	.1229	.004840	.002213	.5394
6000	3787.4	3852.0	3916.7	.1788	.1341	.005280	.002415	.5884

TABLE 12. *Air density at various absolute pressures and temperatures based on air density at 760 mm of Hg and 0° C of 0.001293 g/cm³*

Absolute pressure				Air density, g/cm³×10⁶					
mm Hg	*in. Hg*	*mb*	*psi*	*20° C*	*22° C*	*24° C*	*26° C*	*28° C*	*30° C*
300	11.81	400.0	5.801	475.5	472.3	469.1	465.9	462.8	459.8
350	13.78	466.6	6.768	554.8	551.0	547.2	543.6	540.0	536.4
400	15.75	533.3	7.735	634.0	629.7	625.4	621.3	617.1	613.1
450	17.72	599.9	8.702	713.2	708.4	703.6	698.9	694.2	689.7
500	19.68	666.6	9.668	792.5	787.1	781.8	776.6	771.4	766.3
550	21.65	733.3	10.64	871.8	865.8	860.0	854.2	848.5	842.9
600	23.62	799.9	11.60	951.0	944.5	938.1	931.9	925.7	919.6
650	25.59	866.6	12.57	1030	1023	1016	1010	1003	996.2
700	27.56	933.3	13.54	1110	1102	1094	1087	1080	1073
750	29.53	999.9	14.50	1189	1181	1173	1165	1157	1149
760	29.9213	1013.25	14.696	1204.6	1196.4	1188.3	1180.4	1172.5	1164.8
800	31.50	1067	15.47	1268	1259	1251	1243	1234	1226
850	33.46	1133	16.44	1347	1338	1329	1320	1311	1303
900	35.43	1200	17.40	1426	1417	1407	1398	1388	1379
950	37.40	1267	18.37	1506	1495	1485	1476	1466	1456
1000	39.37	1333	19.34	1585	1574	1564	1553	1543	1533
1050	41.34	1400	20.30	1664	1653	1642	1631	1620	1609
1100	43.31	1467	21.27	1744	1732	1720	1708	1697	1686
1150	45.28	1533	22.24	1823	1810	1798	1786	1774	1763
1200	47.24	1600	23.20	1902	1889	1876	1864	1851	1839
1250	49.21	1667	24.17	1981	1968	1954	1941	1928	1916
1300	51.18	1733	25.14	2060	2046	2033	2019	2006	1992
1350	53.15	1800	26.10	2140	2125	2111	2097	2083	2069
1400	55.12	1866	27.07	2219	2204	2189	2174	2160	2146
1450	57.09	1933	28.04	2298	2283	2267	2252	2237	2222
1500	59.06	2000	29.01	2378	2361	2345	2330	2314	2299
1600	62.99	2133	30.94	2536	2519	2502	2485	2468	2452
1700	66.93	2266	32.87	2694	2676	2658	2640	2623	2605
1800	70.87	2400	34.81	2853	2834	2814	2796	2777	2759
1900	74.80	2533	36.74	3012	2991	2971	2951	2931	2912
2000	78.72	2666	38.67	3170	3148	3127	3106	3086	3065
2100	82.68	2800	40.61	3328	3306	3283	3262	3240	3219
2200	86.60	2933	42.54	3487	3463	3440	3417	3394	3372
2300	90.55	3066	44.48	3646	3621	3596	3572	3548	3525
2400	94.49	3200	46.41	3804	3778	3753	3728	3703	3678
2500	98.42	3333	48.34	3962	3936	3909	3883	3857	3832
2600	102.4	3466	50.28	4121	4093	4065	4038	4011	3985
2700	106.3	3600	52.21	4280	4250	4222	4194	4165	4138
2800	110.2	3733	54.14	4438	4408	4378	4349	4320	4291
2900	114.2	3866	56.08	4596	4565	4534	4504	4474	4445
3000	118.1	4000	58.01	4755	4723	4691	4659	4628	4598
3100	122.0	4133	59.94	4914	4880	4847	4815	4783	4751
3200	126.0	4266	61.88	5072	5037	5003	4970	4937	4904
3300	129.9	4400	63.81	5230	5195	5160	5125	5091	5058
3400	133.9	4533	65.75	5389	5352	5316	5281	5245	5211
3500	137.8	4666	67.68	5548	5510	5472	5436	5400	5364

WASHINGTON, D. C., April 2, 1959.

UNITED STATES DEPARTMENT OF COMMERCE • Luther H. Hodges, *Secretary*

NATIONAL BUREAU OF STANDARDS • A. V. Astin, *Director*

Reduction of Data for Piston Gage Pressure Measurements

J. L. Cross

National Bureau of Standards Monograph 65

Issued June 17, 1963

Reprinted with corrections - August 1964

For sale by the Superintendent of Documents, U.S. Government Printing Office
Washington 25, D.C. - Price 15 cents

Contents

Library of Congress Catalog Card Number: 63–60036

Reduction of Data for Piston Gage Pressure Measurements

J. L. Cross

Pressure measurements made with piston gages are affected by gravity, temperature, pressure, and several other variables. For accurate determinations of pressure the calculations must take these variables into account. A general equation is developed and simplified procedures for calculating pressure are illustrated.

1. Introduction

The dead weight piston gage is one of the few instruments that can be used to measure pressure in terms of the fundamental units, force, and area. Piston gages are known by several names such as "dead weight gage," "dead weight tester," "gage tester," and "pressure balance." The name, "piston manometer," is used in Germany, and, since it aptly describes the instrument, might very well be used more extensively in this country. In principle, it is a piston inserted into a close fitting cylinder. Weights loaded on one end of the piston are supported by fluid pressure applied to the other end. Construction of piston gages varies as to method of loading, methods of rotating or oscillating the piston to reduce friction, and design of the piston and cylinder. Three designs of cylinders are commonly used; the simple cylinder with atmospheric pressure on the outside; the re-entrant cylinder with the test pressure applied to the outside as well as the inside; and the controlled clearance cylinder with an external jacket in which hydraulic pressure can be applied so as to vary the clearance between the piston and cylinder at the will of the operator. In order to use the piston gage for the measurement of pressure, one must take into account a number of parameters of the instrument and its environment.

Error in measurement results from failure to account for the parameters or from the uncertainty of the measured values of them. It is obvious that error results from the uncertainty of the mass of the loading weights and the measurement of the effective area of the piston and cylinder. Other sources of error may not be so easily recognized. Such sources include the air buoyancy on the weights, the fluid buoyancy on the piston, the value of local gravity, the force on the piston due to the surface tension of the fluid, the thermal expansion and elastic deformation of the piston and cylinder, and the fluid heads involved. These effects can be evaluated and corrections applied to reduce the magnitude of overall error of measurement.

Air buoyancy corrections amount to about 0.015 percent of the load. The corrections for the buoyancy of the pressure fluid on the piston have been found to range from zero to nearly 0.5 psi, and could be larger. A brief discussion of gravity error is given by Johnson and Newhall [1],[1] and detailed information can be found in the Smithsonian Meteorological Tables [2]. The values of local gravity differ by over 0.3 percent at different places in the United States. The pressure correction due to surface tension is usually negligible, but may amount to more than 0.003 psi. Thermal expansion of the effective piston area is usually about 0.003 percent per °C and elastic distortion may amount to 0.05 percent at 10,000 psi. Fluid head amounts to about 0.03 psi per inch for lubricating oils.

Other errors resulting from corkscrewing (vertical force caused by a helical scratch on the piston, cylinder, or guide bearing), vertical component of the force used to rotate or oscillate the piston, eccentric loading of the piston, and the force of air currents against the weights, are not readily evaluated. They may be kept small by good design and workmanship and by careful operating technique, but usually no attempt is made to apply corrections for them.

2. Pressure

The pressure in any system may be defined as

$$P=\frac{F}{A} \tag{1}$$

where F=force and A=area over which the force is applied. When a piston gage is in equilibrium with a pressure system, the pressure, p_p, measured at the piston gage is

$$p_p=\frac{F_e}{A_e} \tag{2}$$

where F_e=the force due to the load on the piston, A_e=the effective area of the piston.

[1] Figures in brackets indicate the literature references on page 6.

The pressure p_p, is not necessarily the quantity desired. It is the pressure measured by the piston gage at its reference level, whereas, the pressure that we may wish to measure may be at another level within a system which is connected to the piston gage by a length of tubing filled with a pressure transmitting fluid. The pressure exerted by the head of fluid in the connecting line, from the level within the system to the reference level of the piston gage, must be added to the piston gage pressure. If the total (absolute) pressure is to be determined, the atmospheric pressure at the reference level of the piston gage must also be added to the piston gage pressure, so we have

$$P=p_p+H_{fp}+P_a \tag{3}$$

where P=total pressure at a particular level in the system,
p_p=pressure at the reference level of the piston gage (piston gage pressure),
H_{fp}=pressure exerted by the head of pressure transmitting fluid,
P_a=atmospheric pressure at the reference level of the piston gage.

Usually the quantity to be measured is the difference between the total internal pressure in the system and the atmospheric pressure outside of the system. If the pressure is to be measured at a level in the system (which might be the reference level of another gage) which is different from the reference level of the piston gage, the atmospheric pressure at these levels is different and the equation for the difference between the internal and external pressure or gage pressure, p_g, of the system is

$$p_g=p_p+H_{fp}-H_a \tag{4}$$

where H_a=the difference in the atmospheric pressure between the reference level of the piston gage and the level in the system at which the pressure is to be measured.

3. Force and Fluid Heads

The force, F, due to the gravitational attraction between the earth and a mass, M, is numerically

$$F=kMg_L \tag{5}$$

where g_L is the local acceleration due to gravity, and k is a proportionality factor, the numerical value of which depends upon the units of F, M, and g_L as follows:

$k=1$, for F in dynes, M in grams, and g_L in cm/sec^2,
$k=1$, for F in newtons, M in kilograms, and g_L in meter/sec^2,
$k=1$, for F in poundals, M in pounds mass, and g_L in feet/sec^2,
$k=1$, for F in pounds force, M in slugs, and g_L in feet/sec^2,
$k=\frac{1}{32.174}$, for F in pounds force, M in pounds mass, and g_L in feet/sec^2,
$k=\frac{1}{980.665}$, for F in pounds force, M in pounds mass, and g_L in cm/sec^2,
$k=\frac{1}{980.665}$, for F in kilograms force (in some countries, kiloponds, kp), M in kilograms, and g_L in cm/sec^2.

There are several quantities that must be used in the determination of the force, F_e, (eq (2)) acting upon the effective area of the piston. These include, the mass of the weights, M_m, the mass of the air displaced by the load, M_a; the mass of the pressure fluid contributing to the load, M_f; the local acceleration due to gravity, g_L, and the force due to the surface tension, γ, of the pressure fluid acting upon the circumference of the piston, C, where it emerges from the surface of the fluid. The value for F_e can be determined from the following equation,

$$F_e=(M_m+M_f-M_a)kg_L+\gamma C. \tag{6}$$

3.1. Mass of Weights

The mass of the weights, including the piston and all parts which contribute to the load on the piston when in operation, is determined by comparison with the mass of accurately known standard weights. This is usually done by means of an equal arm balance.

3.2. Mass of Air

The mass of air displaced by the load on the piston is

$$M_a=\rho_a V_m, \tag{7}$$

where ρ_a=the mean density of the air displaced by the load. The volume of the load,

$$V_m=\frac{M_m}{\rho_m}+\frac{M_f}{\rho_f}, \tag{8}$$

where ρ_m=the density of the weights, M_m, and ρ_f=the density of the pressure fluid, M_f. Substituting eq (8) in eq (7) we get

$$M_a=\frac{\rho_a}{\rho_m}M_m+\frac{\rho_a}{\rho_f}M_f. \tag{9}$$

The value, ρ_m, depends upon the way in which the values for the loading weights are reported. When they are reported as true mass, the actual value for the density of the weights should be used. If, however, the apparent mass is given, as determined by comparison with brass standards in air having a density of 0.0012 g/cm^3, the density of the weights should be assumed to have the same density as the brass standards (8.4 g/cm^3). Apparent mass values are usually used when reporting loading weight values.

By substituting eq (9) in eq (6) we obtain the following expression for F_e,

$$F_e=\left[M_m\left(1-\frac{\rho_a}{\rho_m}\right)+M_f\left(1-\frac{\rho_a}{\rho_f}\right)\right]kg_L+\gamma C. \tag{10}$$

Piston gages operating with the piston assembly partially submerged in a liquid are subjected to a force resulting from the surface tension of the liquid acting on the periphery of the piston where it emerges from the surface of the liquid. This force, γC, is added to the force due to the load on the piston.

3.3. Fluid Head

The fluid head pressure, H_{fp}, eq (3) and (4), exerted by the column of pressure fluid between the reference level of the piston gage and the reference level of the pressure system to be measured, may be calculated as follows:

$$H_{fp}=-\rho_{fp}h_{fp}kg_L \tag{11}$$

where ρ_{fp}=the density of the pressure fluid at pressure P,
h_{fp}=the height of the column of fluid of density ρ_{fp}, measured from the reference level of the piston gage. Measurements up from the reference level are positive and down from the reference level are negative.

3.4. Air Head

The air head pressure, H_a, eq (4), exerted by the column of air between the reference level of the piston gage and the reference level of the pressure system to be measured, may be calculated as follows:

$$H_a=-\rho_a h_a kg_L \tag{12}$$

where ρ_a=the density of the air at the ambient atmospheric pressure, and temperature,
h_a=the height of the air column measured from the reference level of the piston gage. Measurements above the reference level have a positive sign and those below have a negative sign.

3.5. Fluid Buoyancy

In certain instances, the pressure fluid in which the piston is immersed contributes to the load on the piston. This effect may be accounted for in two ways. One method is to compute the mass of the fluid, M_f, contributing to the load on the piston and include it in the calculation of the force as shown in eq (6). The other method is to shift the reference level (the level at which the piston gage pressure, p_p, is measured) from the lower end of the piston by an amount equal to the height of a column of oil that will compensate for the mass of the fluid acting on the piston.

In order to determine the contribution of the pressure fluid to the load on the piston, first consider the case of a piston of uniform cross section exactly fitting the cylinder (fig. 1). If the pressure is measured at the level of the lower end of the piston (level R), the fluid exerts no vertical forces other than that against the area of the end of the piston. In this case, therefore, there is no buoyancy correction to be applied.

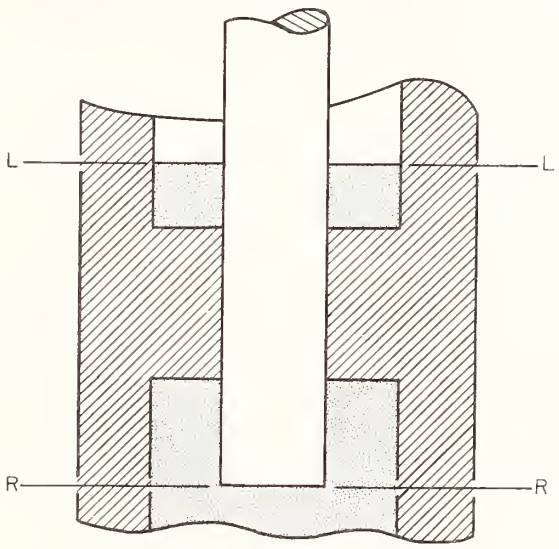

FIGURE 1. *Piston of uniform cross section*

Next consider a piston with grooves or holes machined in it as shown in figure 2. The weight of the fluid contained in the grooves and holes, is part of the load on the piston. That is to say that all of the material included within a cylinder having a cross section equal to the effective area of the piston is included in the load on the piston.

In practice, the effective area of a piston is very nearly equal to the mean of the areas of the piston and the cylinder as shown in figure 3 by the dotted lines C and C′. Any metal extending beyond those bounds displaces a volume of fluid the mass of which must be subtracted from the load on the piston and any fluid within those bounds must be added to the load on the piston.

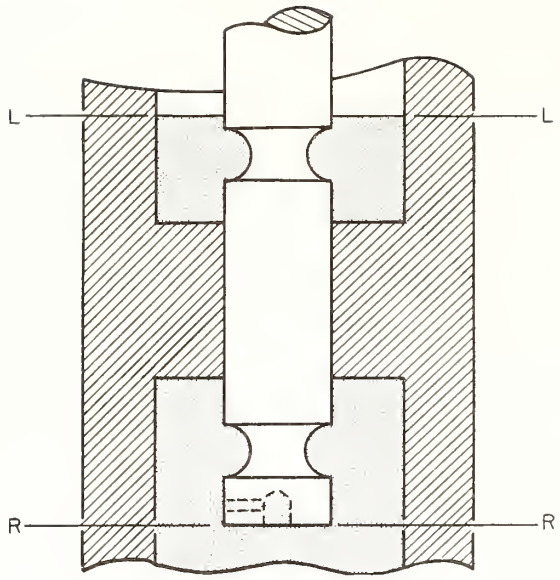

FIGURE 2. *Piston of irregular cross section.*

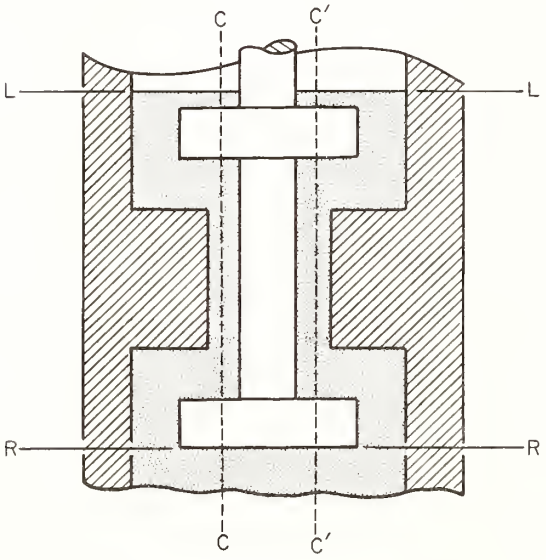

FIGURE 3. *Piston of irregular cross section.*

From these examples we see that the fluid buoyancy correction can be either positive or negative. It can be calculated from the following equation:

$$M_f=(A_e y_f-V_s)\ \rho_f \tag{13}$$

where A_e=the effective area of the piston as before,
y_f=the length of the submerged part of the piston,
V_s=the volume of the submerged part of the piston.

To determine the pressure equivalent, p_f, of the fluid, M_f, the following equation may be used:

$$p_f=\frac{M_f}{A_e}\left(1-\frac{\rho_a}{\rho_f}\right)kg_L \tag{14}$$

Shifting the reference level of the piston gage by an amount, Δh, effectively consists of adding the pressure exerted by a column of fluid of height, Δh, and density, ρ_{fp}, and subtracting the pressure exerted by a column of air of height, Δh, and density, ρ_a. The resulting pressure change,

$$\Delta p=\rho_{fp}\Delta hkg_L-\rho_a\Delta hkg_L. \tag{15}$$

By shifting the reference level an amount sufficient to make the resulting fluid head compensate for the pressure equivalent of the fluid buoyancy [3, 4] $\Delta p=p_f$ we obtain (from eqs 13, 14, and 15),

$$\Delta h=\frac{(A_e y_f-V_s)}{A_e}\frac{(\rho_f-\rho_a)}{(\rho_{fp}-\rho_a)}. \tag{16}$$

When the buoyancy correction is determined as shown in eq (13) the density of the fluid, ρ_f, is included. For the portion of the piston between the cylinder and the surface of the fluid (level L) the value of ρ_f will be the density of the fluid at atmospheric pressure, ρ_{fa}, but for the portion of the piston below the cylinder the value of ρ_f will be the density of the fluid, ρ_{fp}, at pressure, P, and may not be easily determined.

On the other hand, when the buoyancy correction for the lower end of the piston is applied by shifting the reference level, ρ_f in eq (16) is equal to ρ_{fp}, and the ratio $\frac{(\rho_f-\rho_a)}{(\rho_{fp}-\rho_a)}$ is equal to 1, so that the value for ρ_{fp} need not be known.

3.6. Mass of Fluid

By applying the buoyancy correction for the upper portion of the piston as a load correction, eq (13) becomes

$$M_{fa}=(A_e y_{fa}-V_{fa})\rho_{fa} \tag{17}$$

where y_{fa}=the length of the submerged part of the piston above the cylinder,
V_{fa}=the volume of the submerged part of the piston above the cylinder,

and eq (10) becomes

$$F_e=M_m\left[\left(1-\frac{\rho_a}{\rho_m}\right)+M_{fa}\left(1-\frac{\rho_a}{\rho_{fa}}\right)\right]kg_L+\gamma C. \tag{18}$$

3.7. Reference Level

By applying the buoyancy correction for the lower portion of the piston as a reference level change, eq (16) becomes

$$\Delta h = y_{fp} - \frac{V_{fp}}{A_e} \tag{19}$$

where y_{fp}=the length of the piston below the cylinder,
V_{fp}=the volume of the piston below the cylinder.

4. Area

The effective area, A_e, of the piston, can be expressed by the relationship

$$A_e = A_0[1+a(t-t_s)][1+bp_p)][1+d(p_z-p_j)] \tag{20}$$

where A_0=the effective area of the piston at temperature, t_s, and atmospheric pressure,
a=the fractional change in effective area per unit change in temperature,
t=the temperature of the piston and cylinder,
t_s=the reference temperature,
b=the fractional change in effective area per unit change in pressure,
d=the fractional change in effective area per unit change in jacket pressure of a controlled clearance piston gage,
p_z=the jacket pressure required to reduce the piston clearance to zero at pressure p_p,
p_j=the jacket pressure.

4.1. Temperature Coefficient of Area

The fractional change in effective area per unit change in temperature can be determined as follows:

$$a = \alpha_k + \alpha_c \tag{21}$$

where α_k=the temperature coefficient of linear expansion of the piston,
α_c=the temperature coefficient of linear expansion of the cylinder.

The most convenient reference temperature, t_s, is the average temperature of the room in which the instrument is used. In many instances the difference $t-t_s$ may be insignificant.

The temperature, t, of the piston and cylinder is usually assumed to be the same as the temperature of the base of the instrument. The fact is, in practice, the piston and cylinder are usually at a temperature higher than that of the rest of the instrument, although, in a gas lubricated piston gage they may be lower. So many factors affect the temperature that the order of magnitude calculation of the temperature rise may be unreliable. Some of the more important factors are: speed of rotation, clearance, pressure, viscosity, Joule-Thompson coefficient, and thermal conductivity of the pressure fluid. One precaution that can be taken to keep the uncertainty of temperature, t, from being unnecessarily large, is to keep the speed of rotation no greater than is required to maintain hydrodynamic lubrication.

4.2. Effective Area at Atmospheric Pressure

A_0 is very nearly equal to the mean of the area of the piston and the area of the cylinder [3,4] at the reference temperature and can be calculated as follows:

$$A_0 = \frac{A_k + A_c}{2}[1+a(t_s-t_m)] \tag{22}$$

where A_k=the area of the piston,
A_c=the area of the cylinder,
t_m=the temperature at which A_k and A_c are measured.

The value of $\frac{A_k+A_c}{2}$ may be determined from direct measurements of the diameters of the piston and cylinder, or by comparison with a piston gage of known area. In a controlled clearance piston gage, the jacket pressure, applied to the outside of the cylinder, is used to vary the diameter of the cylinder as desired and A_c is assumed to be equal to A_k.

4.3. Pressure Coefficient of Area

The fractional change in area with pressure is most readily obtained by comparing the instrument against a controlled clearance piston gage for which the pressure coefficient, b, can be computed, or by comparison with a piston gage of known characteristic. To the first approximation, for a controlled clearance piston gage,

$$b = \frac{3\mu - 1}{Y} \tag{23}$$

where μ=Poisson's ratio for the piston,
Y=Young's modulus for the piston.

The product, bp_p, is small and therefore an approximate value for p_p is adequate. Deffet and Trappeniers [4], Dadson [6], Bridgman [7], and Ebert [8] give more detailed discussions of the elastic distortion of piston gages.

4.4. Change of Area With Jacket Pressure

The factor $[1+d(p_z-p_j)]$ is used only for controlled clearance piston gages. The fractional change of area with jacket pressure, d, is best obtained experimentally by varying the jacket pressure, p_j, and measuring the change in pressure, p_p. Since the change in pressure will be small, the measuring instrument must be sensitive.

The jacket pressure required to reduce the clearance between the piston and cylinder to zero, at a particular value of p_p, may be determined by two methods. One method is to observe the torque required to turn the piston as the jacket pressure is varied. An abrupt increase of torque is observed when the clearance is reduced to zero. The other method is to measure the fall rate of the piston at several jacket pressures. The cube root of the fall rate is then plotted against jacket pressure, and the curves are extrapolated to zero fall rate to get values of p_z.

5. Piston Gage Pressure

The complete equation for p_p can be obtained from combining eqs (2), (18), and (20);

$$p_p=\frac{\frac{M_m}{A_o}\left(1-\frac{\rho_a}{\rho_m}\right)kg_L+\frac{M_{fa}}{A_o}\left(1-\frac{\rho_a}{\rho_{fa}}\right)kg_L+\frac{\gamma C}{A_o}}{[1+a(t-t_s)](1+bp_p)[1+d(p_z-p_j)]} \tag{24}$$

where the reference level is determined as shown in eq (19).

Equation (24) would be rather formidable if it were necessary to solve it for each pressure measurement. Fortunately the terms can be grouped so that the amount of calculation can be reduced to practical proportions for some instruments, and some terms can be ignored if the accuracy requirements are low. It should be noted that eq (24) is not exact. Some second order terms have been dropped and the coefficients are constant only to a first approximation.

6. Conclusions

The accuracy of pressure measurements depends not only on the performance of the piston gage, but on the application of corrections derived from parameters of the system. These depend upon the construction of the instrument, composition of the pressure fluid, environment, pressure, and physical arrangement of the pressure system. The accuracy to which the values of these parameters are known usually establishes the overall accuracy of the measurements.

7. References

[1] The piston gage as a precise pressure measuring instrument, D. P. Johnson and D. H. Newhall, Trans. ASME **75,** 3, 301 (April 1953).

[2] Smithsonian Meteorological Tables, published by the Smithsonian Institution, Washington, D.C., Sixth Revised Edition (1951).

[3] A multiple manometer and piston gages for precision measurements, C. H. Meyers and R. S. Jessup, BS J. Research **6,** 1061 (June 1931).

[4] Les balance manometriques, L. Deffet and N. Trappeniers, Memorial de l'Artillerie Francaise, 4 fascicule (1954).

[5] Elastic distortion error in the dead weight piston gage, D. P. Johnson, J. L. Cross, J. D. Hill, and H. A. Bowman, Ind. Eng. Chem. **49,** 2046 (Dec. 1957).

[6] A new method for the absolute measurement of high pressure, R. S. Dadson, Nature **176,** 188 (July 30, 1955).

[7] The measurement of hydrostatic pressures up to 20,000 kilograms per square centimeter, P. W. Bridgman, Proc. Am. Acad. Arts and Sci. **47,** 321 (1912).

[8] Aufstellung einer Druckskale und deren experimentelle Erprobung bis 20,000 at., H. Ebert, Z. Angew. Phys. **7,** 331 (March 1949).

8. Appendix A. Computation of Pressure

8.1. Calculation of Correction Factors

To illustrate a method for simplifying the calculations, suppose that a particular piston gage is to be used in Room 131, MTL Bldg. at the National Bureau of Standards in Washington, D.C., to calibrate Bourdon gages. The local value of gravity $g_L=980.10$ gals, ρ_a will be assumed to have the value of the average density of air at this location, so $\rho_a=0.00117$ g/cm³. The fluid being used in the instrument is aviation instrument oil for which the density, $\rho_{fa}=0.862$ g/cm³ or 0.0321 lb/in.³ and the surface tension, $\gamma=0.00017$ lbf/in., at atmospheric pressure and 25 °C.

The piston gage is not a controlled clearance piston gage, therefore the factor $1+d(p_z-p_j)$ will be omitted. From direct measurements on the instrument, we find that $C=1.964$ in., $y_{fa}=2.5$ in., $V_{fa}=1.525$ in.³, $y_{fp}=1.625$ in., and $V_{fp}=0.2778$ in.³.

From a previous calibration against a controlled clearance piston gage, we have: $A_0=0.13024$ in.² (at $t_s=25$ °C) and $b=1.48\times10^{-7}$ in.²/in.² psi. We also know that the piston is steel with the temperature coefficient, $\alpha_k=12\times10^{-6}$ in./in. deg C at 25 °C and the cylinder is brass with the temperature coefficient $\alpha_c=18.4\times10^{-6}$ in./in. degree C at 25 °C.

The masses of the loading weights have been determined and have been reported in tabular form as shown in columns 1 and 2 of table 1. The value given in column 2 is the apparent mass and therefore the density, ρ_m, is assumed to be 8.4 g/cm³.

All of the quantities thus determined can be listed as illustrated in table 2 and from these values the factors and terms of the numerator of eq (24) and the reference level, Δh, can be computed as shown in table 2.

The importance of the various factors and terms of the numerator can now be evaluated. In the first term $\frac{M_m}{A_0}$ is the dominant factor, while the factor kg_L accounts for about 0.06 percent and the factor $\left(1-\frac{\rho_a}{\rho_m}\right)$ accounts for about 0.014 percent. The contribution of the second term is −0.295 psi with the factor $\left(1-\frac{\rho_a}{\rho_{fa}}\right)$ having an effect amounting to about 0.0004 psi. In this case the third term amounts to 0.0027 psi. The importance of each factor and term depends upon the design of the instrument, the environment, and the application, and none should be neglected without first evaluating it to determine its significance.

8.2. Machine Computation

The temperature and pressure factors, $1+a(t-t_s)$ and $(1+bp_p)$, in the denominator of eq (24) can be combined in a double entry table to give values of

$$\frac{1}{[1+a(t-t_s)](1+bp_p)}$$

for values of t and p_p as illustrated in table 3.

To further facilitate computations the weight table, table 1, has been extended to give values of M_m times the factor 7.6726 (from table 2) for each weight as shown in column (3) and the value of

$$M_{fa}\left(1-\frac{\rho_a}{\rho_{fa}}\right)\frac{kg_L}{A_0}+\frac{\gamma C}{A_0}=-0.292$$

is added to the value of 7.6726 M_m for the piston. Accumulative totals, for frequently used combinations of weights, are given in column (4). Computation of pressure p_p is now simplified to the process of multiplying the sum of values from column (3) or a value from column (4) by the appropriate value from table 3. Greater simplification to suit the requirements of specific applications will be left to the ingenuity of the user.

8.3. Slide Rule Computation

The method just described can be modified slightly for use with a slide rule. Using the same values as were used in the preceding illustration, eq (24) for p_p may be written in the form

$$p_p=(M_m 7.6726-0.292)+(M_m 7.6726-0.292)\times\left(\frac{1}{[1+a(t-t_s)](1+bp_p)}-1\right). \quad (25)$$

TABLE 1. *List of weights and appropriate values for weight set and piston gage No. 1357 used at Washington, D.C., with aviation instrument oil*

Piston gage No. 1357 with weight set No. 1357
Location—NBS, Washington, D.C.
Fluid—Aviation instrument oil

(1) Weight No.	(2) Mass (M_m)	(3) $M_m\times7.6726$	(4) Accumulative Total
	lb	*psi*	*psi*
piston	1.3024	9.993−0.292*=9.701	9.701
1	2.6042	19.981	29.682
2	2.6045	19.983	49.665
3	6.5123	49.966	99.631
4	26.0473	199.85	299.48
5	26.0454	199.84	499.32
6	65.1095	499.56	998.88
7	65.1190	499.63	1498.51
8	65.1065	499.54	1998.0
9	65.1165	499.61	2497.7

*Fluid buoyancy and surface tension correction,

$$M_{fa}\left(1-\frac{\rho_a}{\rho_{fa}}\right)\frac{kg_L}{A_0}+\frac{\gamma C}{A_0}=-0.292 \text{ psi.}$$

TABLE 2. *Tabulated values of parameters for piston gage No. 1357 used at Washington, D.C., with aviation instrument oil*

Values for Piston Gage No. 1357

A_0=0.13024 in².
y_{fa}=2.5 in.
V_{fa}=1.525 in³.
C=1.964 in.
$a=\alpha_k+\alpha_c=(12+18.4)\times10^{-6}=30.4\times10^{-6}$in²./in². °C
t_s=25 °C
b=1.48×10⁻⁷ in²./in².psi
y_{fp}=1.625 in.
V_{fp}=0.2778 in³.

Values for Weight Set No. 1357

ρ_m=8.4 g/cm³

Values for Room 131, MTL Bldg., NBS, Washington, D.C.

ρ_a=0.00117 g/cm³ or 0.0000423 lb/in³.
g_L=980.10 cm/sec²

Values for Aviation Instrument Oil

ρ_{fa}=0.0321 lb/in³.
γ=0.00018 lbf/in.

Computations

kg_L=0.99942

$\frac{kg_L}{A_0}$=7.6737/in².

$\left(1-\frac{\rho_a}{\rho_m}\right)$=0.99986

$M_m\left(1-\frac{\rho_a}{\rho_m}\right)\frac{kg_L}{A_0}=M_m\times7.6726$ psi

$M_{fa}=(A_e y_{fa}-V_{fa})\rho_{fa}=-0.0385$ lb (17)

$\left(1-\frac{\rho_a}{\rho_{fa}}\right)=-0.9987$

$M_{fa}\left(1-\frac{\rho_a}{\rho_{fa}}\right)\frac{kg_L}{A_0}=-0.295$ psi

$\frac{\gamma C}{A_0}$=0.0027 psi

$p_p=(M_m\times7.6726-0.292)\frac{1}{[1+a(t-t_s)](1+bp_p)}$ (25)

$\Delta h=y_{fp}-\frac{V_{fp}}{A_e}=-0.508$ in. (19)

TABLE 3. *Temperature and pressure correction factors for piston gage No. 1357, for calculation of pressure, in psi*

Values of $\frac{1}{[1+a(t-t_s)](1+bp_p)}$ for piston gage No. 1357

Pressure, p_p	Temperature, t, °C				
	23	24	25	26	27
psi					
2500	0.99969	0.99966	0.99963	0.99960	0.99957
2000	.99976	.99973	.99970	.99967	.99964
1500	.99984	.99981	.99978	.99975	.99972
1000	.99991	.99988	.99985	.99982	.99979
500	.99999	.99996	.99993	.99990	.99987
0	1.00006	1.00003	1.00000	.99997	.99994

TABLE 4. *Temperature and pressure correction factors for piston gage No. 1357, for calculation of corrections, in psi*

Values of $\frac{1}{[1+a(t-t_s)](1+bp_p)}-1$ for piston gage No. 1357

Pressure, p_p	Temperature, t, °C				
	23	24	25	26	27
psi					
2500	−0.00031	−0.00034	−0.00037	−0.00040	−0.00043
2000	−.00024	−.00027	−.00030	−.00033	−.00036
1500	−.00016	−.00019	−.00022	−.00025	−.00028
1000	−.00009	−.00012	−.00015	−.00018	−.00021
500	−.00001	−.00004	−.00007	−.00010	−.00013
0	+.00006	+.00003	.00000	−.00003	−.00006

A double entry table for values of

$$\frac{1}{[1+a(t-t_s)](1+bp_p)}-1$$

for various values of t and p_p can be prepared as illustrated in table 4. A slide rule can be used to multiply the appropriate value from this table by the sum of values from column (3) or a value from column (4) of table 1 to obtain a correction to be added to the value from table 1 to give pressure p_p.

TABLE 5. *Temperature and pressure corrections in psi, for piston gage No. 1357*

Values of $p_p\left[\frac{1}{[1+a(t-t_s)](1+bp_p)}-1\right]$ for piston gage No. 1357

Pressure, p_p	Temperature, t, ° c				
	23	24	25	26	27
	Corrections, psi				
psi					
2500	−0.8	−0.8	−0.9	−1.0	−1.1
2000	−.5	−.5	−.6	−.7	−.7
1500	−.24	−.28	−.33	−.38	−.42
1000	−.09	−.12	−.15	−.18	−.21
500	.00	−.02	−.04	−.05	−.06
0	.00	.00	.00	.00	.00

8.4. Correction Table Computation

A correction table may be preferred in many instances. Again using the same values as before to illustrate, a double entry table of values of

$$p_p\left(\frac{1}{[1+a(t-t_s)](1+bp_p)}-1\right)$$

for various values of p_p and t is prepared as illustrated by table 5. Appropriate corrections from the table are added to values of M_m 7.6726 − 0.292 obtained from table 1 to obtain pressure p_p.

8.5. Conclusions

By construction of tables a procedure similar to one of those illustrated can be established to suit the particular needs and application of the user. The computation of pressure from piston gage data is thereby reduced to a simple, fast operation.

9. Appendix B. Working Equations

The equations that may be required for the computation of the absolute or the gage pressure in a system, from measurements made with a piston gage, are listed below:

$$P=p_p+H_{fp}+P_a \tag{3}$$

$$p_g=p_p+H_{fp}-H_a \tag{4}$$

$$H_{fp}=-\rho_{fp}h_{fp}kg_L \tag{11}$$

$$H_a=-\rho_a h_a kg_L \tag{12}$$

$$A_0=\frac{A_k+A_c}{2}[1+a(t_s-t_m)] \tag{22}$$

$$a=\alpha_k+\alpha_c \tag{21}$$

$$b=\frac{3\mu-1}{Y} \tag{23}$$

$$M_{fa}=(A_e y_{fa}-V_{fa})\rho_{fa} \tag{17}$$

$$\Delta h=y_{fp}-\frac{V_{fp}}{A_e} \tag{19}$$

$$p_p=\frac{\frac{M_m}{A_0}\left(1-\frac{\rho_a}{\rho_m}\right)kg_L+\frac{M_{fa}}{A_0}\left(1-\frac{\rho_a}{\rho_{fa}}\right)kg_L+\frac{\gamma C}{A_0}}{[1+a(t-t_s)](1+bp_p)[1+d(p_z-p_j)]} \tag{24}$$

Definitions of the Symbols Used in the Above Equations

A_c Cylinder area.
A_e Effective area of piston.
A_k Piston area.
A_0 Effective area of the piston at atmospheric pressure and temperature t_s.
C Circumference of the piston at the surface of the pressure fluid.
H_a Pressure difference in the atmosphere between the reference level of the piston gage and the reference level of the system to be measured.
H_{fp} Pressure head of the column of pressure transmitting fluid between the reference level of the piston gage and the reference level of the system to be measured.
M_{fa} Mass of the pressure fluid at atmospheric pressure contributing to the load on the piston.
M_m Mass of the loading weights, including the piston assembly.
P Absolute (total) pressure.
P_a Atmospheric pressure at the reference level of the piston gage.
V_{fa} Volume of the submerged part of the piston above the cylinder.
V_{fp} Volume of the part of the piston below the cylinder.
Y Young's modulus.
a Fractional change in effective area with unit change in temperature.
b Fractional change in effective area with unit change in pressure.
d Fractional change in area with unit change in jacket pressure.
g_L Local acceleration due to gravity.
h_a Height of the air column measured from the reference level of the piston gage to the reference level of the system. Measurements up from the piston gage reference level are positive.
h_{fp} Height of the column of pressure fluid measured from the reference level of the piston gage to the reference level of the system. Measurements up from the piston gage reference level are positive.
Δh Height of the reference level of the piston gage with respect to the bottom of the piston. Measurements up from the bottom of the piston are positive.
k Proportionality factor relating force, mass and gravity.
p_g Gage pressure.
p_j Jacket pressure.
p_p Pressure measured by piston gage at the reference level of the piston gage.
P_z Jacket pressure required to reduce the piston-cylinder clearance to zero.
t Temperature of the piston gage.
t_m Temperature at which piston and cylinder are measured.
t_s Reference temperature (usually the nominal room temperature).
y_{fa} Length of the submerged part of the piston above the cylinder.
y_{fp} Length of the part of the piston below the cylinder.
α_c Temperature coefficient of linear expansion of the cylinder.
α_k Temperature coefficient of linear expansion of the piston.
γ Surface tension of the pressure fluid.
μ Poisson's ratio for the piston.
ρ_a Mean density of the air displaced by the load.
ρ_{fa} Density of the pressure fluid at atmospheric pressure.
ρ_{fp} Density of the pressure fluid at pressure P.
ρ_m Density of the weights.

10. Appendix C. Examples of Calculations

Fluid—Aviation instrument oil
Piston gage No. 1357, Washington, D.C.

Machine Calculation:

a. Weights: Piston, 1, 2, 3, 4, 5, 6, 7, 8
Accumulative total: 1998.0 psi (from table 1, column (4))
Temperature: 26 °C
Correction factor: 0.99967 (from table 3)
$p_p = 1998.0 \times 0.99967 = 1997.3$ psi

b. Weight No. $M_m \times 7.6726$ (from table 1, column (3))

Piston	9.701	
1	19.981	99.631 accumulative total from column (4)
2	19.983	
3	49.966	
6	499.56	
7	499.63	
8	499.54	
	1598.361 psi	

Temperature: 26 °C
Correction factor: 0.99975 (from table 3)
$p_p = 1598.36 \times 0.99975 = 1598.0$ psi

Slide Rule Calculation:

a. Weights: Piston, 1, 2, 3, 4, 5, 6, 7, 8
Accumulative total: 1998.0 psi (from table 1, column (4))
Temperature: 26 °C
Correction factor: −0.00033 (from table 4)
Correction $= -0.00033 \times 1998.0 = -0.7$ psi
$p_p = 1998.0 - 0.7 = 1997.3$ psi

Correction Table Calculation:

a. Weights: Piston, 1, 2, 3, 4, 5, 6, 7, 8
Accumulative total: 1998.0 (from table 1, column (4))
Temperature: 26 °C
Correction = −0.7 psi (from table 5)
$p_p = 1998.0 - 0.7 = 1997.3$ psi

The Bi I–II Transition Pressure Measured with a Dead-Weight Piston Gauge

Peter L. M. Heydemann

National Bureau of Standards, Gaithersburg, Maryland

(Received 10 October 1966; in final form 19 January 1967)

A dead-weight piston gauge was used to determine the bismuth I–II transition pressure and the volume change at the transition. The transition pressure at 25°C for one sample, believed to contain less than 0.001% impurities, was found to be 25 306 bar, with an estimated uncertainty of 60 bar. With another sample, of substantially less purity and of larger grain size, a transition pressure of 25 500±60 bar was measured. The average relative volume change was 0.035. See erratum sheet.

I. INTRODUCTION

The importance of the Bi I–II transition—also called the α, β transition—as a fixed point on the pressure scale is amply demonstrated by the many references made to this point in literature and by the number of recent attempts to determine the transformation pressure more accurately[1] (summarized in Ref. 2). These determinations have been made with simple piston-cylinder equipment. The bismuth sample may thus be subjected to a stress field with strong nonhydrostatic components. The transition is usually detected by the accompanying volume change. Internal as well as external friction produces an hysteresis loop in compression and decompression, the size of which can be reduced but not easily eliminated. The mean between critical pressures observed in compression and decompression is usually assumed to be close to the thermodynamic transition pressure. The width of the hysteresis loop adds to the over-all uncertainty of the measurement.

II. 26-kbar PISTON GAUGE

In the investigation reported here, a dead-weight piston gauge with a freely rotating piston (and load) was used for the first time in an attempt to determine the Bi I–II transition pressure with samples subjected to hydrostatic pressure. The idea for this piston gauge was conceived by Johnson, Hutton, and Newhall. It was designed and constructed by Newhall of Harwood Engineering. Since the gauge will be described elsewhere in detail, only a short explanation of the apparatus is given here.

Figure 1 shows a cross section through the gauge. The tungsten carbide gauge piston P and the tapered cylinder C with jacket J are shown in the center of the apparatus. Jacket pressure is applied at the port JP. Samples are placed in the cylinder and the rest of the space is filled with amyl alcohol as a confining liquid. Pressure is built up by advancing the ram R with the mushroom head seal S into the cylinder. Endload is applied to the cylinder through the ram E. Pressure produced on the tapered surface of the cylinder by means of the endload supports the cylinder and controls the clearance between gauge piston and cylinder. Also the jacket pressure affects the clearance.

The gauge piston pushes against a pivot carrying the weight hanger and an oil pan. In operation piston, weight hanger, weights and oil pan rotate as one unit to relieve friction between piston and cylinder. Oil pumped into or withdrawn from the oil pan serves to change the load, and hence the pressure in the cylinder, continuously at rates between about 2 and 14 bar/min [1 bar $=10^5$ N/m^2] over a range of up to 1% of the internal pressure.

In operation the gauge piston was kept floating at about constant level while the ram R was continuously advanced to make up for leakage and compression of oil and sample. The leakage around the mushroom seal is believed to be negligible. The position of the ram is read from a sight column connected to the volume above the large ram piston, giving an almost two-hundredfold magnification. The change of the sight column reading is proportional to the change of volume in the cylinder as caused by compression, transition and leakage. Another sight column indicates the amount of oil pumped into or withdrawn from the oil pan. Both sight columns are read at 1-min intervals.

III. SAMPLES

Two different samples were used. Sample A was cast from granules supplied by Allied Chemical and Dye Corporation, General Chemical Division. It was claimed to be 99.8% pure with the following maximum impurities:

As	0.0001%
Sb	0.01%
Fe	0.002%
Cu	0.002%.

Sample B was cast from granules supplied by the American Smelting and Refining Company. The stated purity was 99.999%. Both samples were machined to cylinders of about 0.9 cm diameter, 0.9 cm long. The volume of sample A was 0.556 cm^3, that of B 0.607 cm^3. Before use in the piston gauge, sample B was exposed to several runs through the I–II and II–III transitions in a simple piston and cylinder assembly. This resulted in an average grain size of about 0.03 cm as compared

[1] G. C. Kennedy and P. N. Lamori, *Progress in Very High Pressure Research* (J. Wiley & Sons, New York, 1961), p. 304.

[2] G. C. Kennedy, and P. N. Lamori, J. Geophys. Res. 67, 851 (1962).

to about 0.15 cm in sample A. Care was taken to avoid contamination of the samples.

IV. EXPERIMENTAL RESULTS

A typical curve obtained from a successful run on 11–16–65 is shown in Fig. 2. The ram sight column reading is plotted versus the applied mass. At a given rate of change of load the slope of the straight lines is determined by the leak rate; their vertical separation gives the volume change of the sample. For very small load rates the transition would appear as an almost vertical straight line connecting the two inclined lines. At higher rates the effect of latent heat and, possibly, a finite transition rate and inhomogeneities in the sample cause the transition to be spread out over a certain range of pressure as shown in Fig. 2. The effect of the latent heat of transition is treated in greater detail in Sec. VI of this report.

Eight such curves were obtained from successful runs. They permit determination of the following significant information: (a) the apparent transition pressure P_a; (b) the transition pressure P_{th} corrected for the effect of latent heat; and (c) the volume change at the transition ΔV.

V. THE APPARENT TRANSITION PRESSURE P_a

The apparent transition pressure is defined as that pressure at which the beginning of the transition is first observed. At this point, due to the limited sensitivity of the apparatus, a small amount of material has already been converted and the actual transition

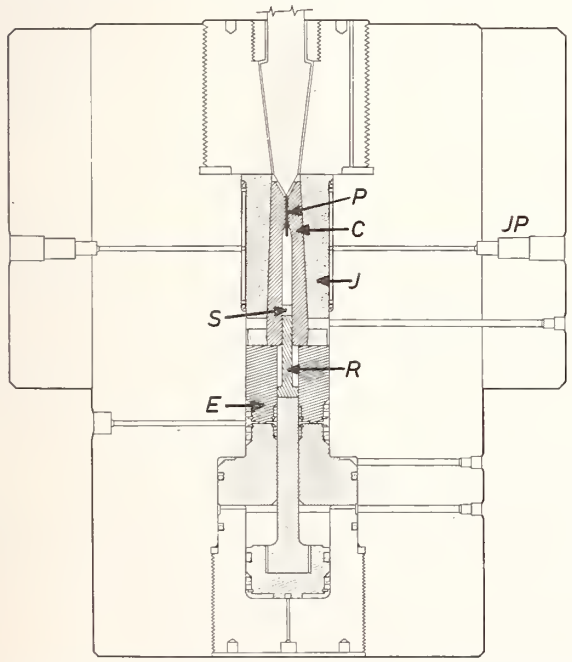

FIG. 1. 26-kbar piston gauge, schematic: P, carboloy gauge piston; C, cylinder, J, jacket; JP, connection for jacket pressure; S, seal; R, pressure generator ram; E, end load ram.

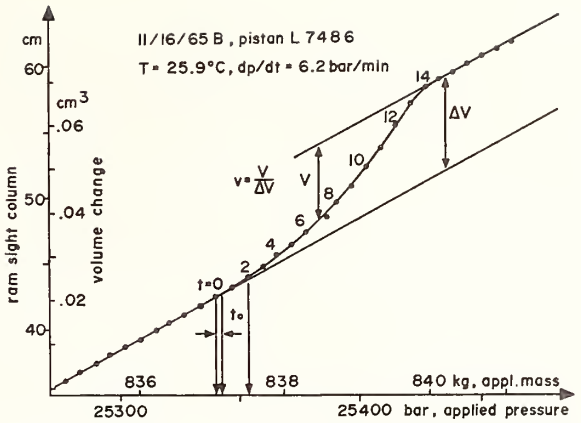

FIG. 2. Ram position as indicated by sight column vs applied load (uncorrected) and applied pressure. t(min) is a time scale with arbitrary starting point assigned to the run.

pressure is slightly lower or higher, depending on the direction from which the transition is approached. In Fig. 2 this point ($t=2$) is marked. The data from this and the other runs are collected in Table I and apparent transition pressures P_a are calculated.

The piston diameters (row 2, Table I) were obtained from calibration by the NBS Engineering Metrology Section prior to their use. Except for run 12–6–65 all successful runs were preceded by one or more runs causing wear of the piston. The uncertainty connected with this is probably very small compared to the uncertainty ascribed to the clearance. The same holds for taper of the pistons. Since the clearance can not be reset to a predetermined value, the jacket pressure-clearance relation can not be determined and the clearance can only be estimated (row 4). An upper limit for the clearance is obtained by extrapolating low pressure data to the present conditions. The lower limit is set by zero clearance. The uncertainty then is half the difference between the two limiting values. This extrapolation was made for the lowest fall rate (dh/dt). Clearance values C for larger fall rates were then computed from $C=\text{constant}\times(dh/dt)^{1/3}$. The fall rates (row 19) are determined from the leak rates (row 18) assuming that there is no leak around the mushroom seal. A correction factor of 0.999278 is applied to the piston diameter for elastic distortion.[3] The elastic constants for the cemented carbide were determined by ultrasonic measurements at atmospheric pressure.

The mass of the stainless steel weights on the weight hanger (row 10) was obtained from calibrations by the NBS Mass Section. The mass of the weight hanger of 173.841 kg was determined in substitution weighing on a hydraulic load cell. The mass of oil in the load pan (row 9) was obtained from sight column readings on the oil reservoirs. The density of the oil is well-

[3] D. P. Johnson *et al.*, Ind. Eng. Chem. 49, 2046 (1957).

TABLE I. Computation of transition pressure.

1. Run and sample	5/7-A	I 5/14-A	II 5/14-A	III 5/14-A	11/15-B	11/16-B	12/6-B	12/7-B	Estimated uncertainty
2. Piston diameter (cm)	0.202758		0.202758		0.202758		0.202778		6×10^{-5}
3. Calibration rep.			*L* 7342		*L* 7486		*L* 7485		
4. Estimated clearance (μm)	2.00	2.09	2.03	2.03	2.06	1.91	1.53	1.63	±2 μm
5. Effective area (cm^2)	0.032305	0.032308	0.032306	0.032306	0.032307	0.032303	0.032297	0.032300	$\pm2\times10^{-3}$
6. Temperature (°C)	24.3	25.0	25.0	25.0	26.8	26.9	26.7	26.4	±0.1°C
7. Change of res. level (cm)	103.5	46.0	45.0	49.5 decomp	19.5	129.0	60.0	48.0 decomp	±0.1 cm
8. Corrected oil density (g/cm^3)	0.8777	0.8772	0.8772	0.8772	0.8759	0.8768	0.8763	0.8763	
9. Mass of oil[a] (kg)	9.289	4.126	4.037	4.441	1.750	11.567	5.377	4.307	±10 g
10. Constant mass[b] (kg)	831.557	836.093	836.093	836.093	836.088	827.016	831.552	831.552	
11. Total applied mass[c] (kg)	840.846	840.219	840.130	840.534	837.838	838.583	836.929	835.859	$\pm10^{-4}$
12. Pressure at onset of observable transition P_a (kbar)	25.510	25.489	25.488	25.500	25.417	25.443	25.398	25.363	
* 13. Pressure red. to 25°C[d] (kbar)	25.548	25.489	25.488	25.500	25.318	25.340	25.305	25.287	
* 14. Pressure corrected for latent heat effect.	25.523	25.490	25.486	25.501	25.318	25.341	25.305	25.291	
* 15. Transition pressure P_{tr} (kbar)			25.500				25.306		±0.06 kbar
16. Load rate (kg/min)	0.460	0.224	0.158	−0.24	0.123	0.206	0.089	−0.215	
17. Rate of change of pressure (bar/min)	13.9	6.8	4.77	7.26	3.72	6.23	2.71	−6.50	
18. Leak rate (cm^3/min)	0.00217	0.00251	0.00227	0.00227	0.00244	0.00193	0.00098	0.00118	
19. Fall rate (cm/min)	0.069	0.080	0.072	0.072	0.078	0.062	0.031	0.038	

[a] Air buoyancy correction for oil 0.99867. [b] Air buoyancy correction for steel 0.99986. [c] g=980.10 cm/sec.^{2} [d] −54.5 bar/°C.

* See erratum sheet, last page.

known; a temperature correction was applied. Air buoyancy correction was applied to all parts of the load. A temperature correction of −54.5 bar/°C was applied to the apparent transition pressures. The apparent transition pressures reduced to 25°C are entered in row 13 of Table I. Row 14 contains the transition pressures corrected for the latent heat effect discussed in the next paragraph. The mean values for the samples A and B respectively are given in row 15.

The last column of Table I contains the estimated uncertainties for the data going into the computation.

Whether the difference of the transition pressures for samples A and B is due to difference in purity, grain size, etc., can only be decided on the basis of more experiments. The difference is beyond the estimated range of uncertainty.

VI. CORRECTION FOR THERMAL EFFECTS

The transition of bismuth I to II and vice versa is accompanied by absorption and release of heat. According to Butuzov's[4] recent measurement the latent heat Q for this transition is −1.78 cal/g. This causes a change of sample temperature at the interface between the rare and the dense phases, which due to the negative slope of the phase boundary in the phase diagram has a retarding effect on the transition. To estimate the magnitude of the time constants involved, first the time constant for heat flow from the sample into the surrounding apparatus is calculated.

The thermal conductivity of the sample and the surrounding steel cylinder are assumed to be very large compared to that of the confining fluid.

Let the sample be surrounded by a cylindrical layer of amyl alcohol with d_o and d_i being the outer and inner diameter, L its length. The flow of heat through this cylinder is

$$\frac{dE}{dt} = -\frac{2\pi L\lambda(T_0 - T_i)}{\ln d_o/d_i}, \tag{1}$$

with λ thermal conductivity, T_0 temperature of the steel vessel, and T_i temperature of the sample.

The temperature difference is determined by the thermal energy released or absorbed during the transformation, and the heat capacity of the sample. The maximum value for $T_0 - T_i$ follows for instant release of the heat of transformation Q

$$T_0 - T_i = Q/c = -60°\text{C}, \tag{2}$$

where c is the specific heat of the sample.

Whence, with $E = Qm$,

$$E^{-1}\frac{dE}{dt} = -\frac{2\pi L\lambda}{mc\ \ln d_o/d_i} \tag{3}$$

and

$$E = \exp -\frac{2\pi L\lambda t}{mc\ \ln d_o/d_i}. \tag{4}$$

Heat is removed from the sample with the time constant

$$\tau = \frac{mc\ \ln d_o/d_i}{2\pi L\lambda} = -mc/\sigma = 5\text{ sec}, \tag{5}$$

where $m = 5.9$ g; $c = 0.0295$ cal/g·deg; $d_o = 0.94$ cm; $d_i = 0.88$ cm; $\lambda = 0.0235$ cal/cm·min·deg; $L = 0.9$ cm. σ in Eq. (5) is the heat flow in cal/min·deg.

According to equations developed by D. P. Johnson in connection with the determination of the freezing point of mercury the relative amount v of bismuth I decreases as the pressure is increased as

$$v = 1 - \frac{dp}{dt}\left[\left(\frac{\alpha V p_0}{Q} + \frac{c}{QB}\right)t + \frac{\sigma}{2QBm}t^2\right], \tag{6}$$

where α compressibility of bismuth at the transition pressure p_{tr}; V specific volume of bismuth I at p_{tr}; p_0 reference pressure close to p_{tr}; B slope of the phase boundary = −54.5 bar/°C.

In order to determine the time $(t - t_0)$ at which during a measurement the transition pressure was reached, the experimental data for v up to about 0.5 were fitted to curves of the type

$$v - 1 = a(t - t_0) + b(t - t_0)^2. \tag{7}$$

The best fit in the least-squares sense then determines a, b, and t_0. The load at t_0 is used to compute the transition pressure corrected for the effect of latent heat. This pressure is generally found to be a few bars below the apparent transition pressure. The corrected pressure is entered in row 14 of Table I.

The constant b, as determined from the curve-fitting operation, is in fair agreement with calculated values. The term at cannot satisfactorily be determined from the experimental data since it is rather small compared to bt^2. The mean value of the corrected pressures obtained from compression runs with sample A does not differ from the pressure obtained from the decompression run. With sample B this difference is 34 bar. This indicates a very small zone of indifference; probably less than our uncertainty of 60 bar and also less than the value of 60 bar reported by Bridgman as an upper limit.[5] Butuzov's value of 1000 bar is much in contrast to our own observation.

VII. VOLUME CHANGE ΔV AT THE TRANSITION

The experiment is not designed for a precise determination of ΔV. However, in four runs the leak rate was sufficiently constant to permit the determination of the volume change at the transition. Table II

[4] V. P. Butuzov *et al.*, Kristallografia VI (A56), 572 (1956).

[5] P. W. Bridgman, Proc. Am. Acad. Arts Sci. **74**, 1 (1940).

TABLE II. Volume change at the Bi I–II transition.

	5-7-65	I 5-14-65	II 5-14-65	11-16-65
ΔV	0.021	0.020	0.018	0.021 cm³
V_0	0.556	0.556	0.556	0.607 cm³
M	5.421	5.421	5.421	5.915 g
$\Delta V/M$	0.0039	0.0037	0.0033	0.0035 cm³/g
$\Delta V/V_0$	0.038	0.036	0.032	0.035
	$\Delta V/V_0$ average: 0.035			

lists the results for these runs. The average relative volume change of 0.035 with an estimated uncertainty of ± 0.01 is less than Bridgman's value of 0.046 (7) or Butuzov's value of 0.055.

VIII. CONCLUSIONS

The present study demonstrated the feasibility of dead-weight piston gages for the generation of precisely known pressures up to at least 25 kbar. The piston gage may be used to determine transition pressures for polymorphic phase transitions accompanied by volume changes with an estimated uncertainty of about ± 60 bars at 25 kbar.

Because of leakage of the pressure transmitting fluid past the gauge piston, volume transitions cannot be observed at constant pressure. Rather the pressure has to be increased or decreased continuously. The latent heat of transformation absorbed or released during the transformation causes the transition to be spread out over a certain pressure range. A simplified thermodynamic treatment adequately describes the shape of the experimental transition curve and permits the determination of the transition pressure. A value of 25 306 bar with an uncertainty of 60 bar is ascribed to the transition pressure of a bismuth sample of high purity (99.999%) at 25°C.

One of the earliest determinations of this pressure under hydrostatic conditions was made by Bridgman[6] in 1937 using the change of the electrical resistance as an indicator for the transition. Bridgman's value, extrapolated to 25°C, was 24.5 kbar. If, as we in fact assume, detection of the transition by electrical resistance measurements is equivalent to volumetric methods, this value now appears rather low. Another determination is that by Butuzov,[4] using differential thermal analysis. His data extrapolate to 25 350 bar at 25°C. Butuzov's value is within our range of uncertainty.

Bridgman determined the bismuth transition pressure also under nonhydrostatic conditions. With a piston cylinder device[7] using volumetric methods of detecting the transition, his results give 25 150 bar (extrapolated to 25°C) and with electrical resistance measurements in anvils[8] he obtained the same value.

None of the quoted reports gives a detailed analysis of the uncertainty of the end result. The major source of uncertainty in all these cases is the width of the hysteresis loop, which in the case of Bridgman's work of 1940 was 1500 bar.

Using their oscillating piston and cylinder device, Kennedy and Lamori[1] reported the reduction of the hysteresis loop (or friction band) to about 200 bars. When a temperature correction of 55 bar/°C—a mean value of the coefficients quoted in Refs. 7 and 9—is applied to Kennedy's data, his mean value becomes 25 400 bar. This compares very favorably with our value and the close agreement might be an indication that the presence of the high shear stresses in Kennedy's apparatus does not greatly affect the transition pressure.

Kennedy's paper, however, does not contain a statement of the uncertainties systematic to the measurement. We will therefore have to assume that the estimated uncertainty of a measurement with Kennedy's apparatus is the same as with our own piston and cylinder assembly of the same type. Such an assembly has been used in this laboratory for a variety of transition pressure measurements, but the results are as yet unpublished. In this work the estimated uncertainty includes the mean value for half the friction and hysteresis (about 100 bar), the uncertainty in ram pressure (25 bar), the uncertainty in the computation of the cylinder distortion (50 bar) and a number of other, smaller effects. Our total uncertainty of a measurement in a piston and cylinder assembly of this type then exceeds 175 bar.

[6] P. W. Bridgman, Proc. Am. Acad. Arts Sci. **72**, 157 (1937).

[7] P. W. Bridgman, Phys. Rev. **48**, 893 (1935).

[8] P. W. Bridgman, Proc. Am. Acad. Arts Sci. **81**, 165 (1952).

[9] F. P. Bundy, Phys. Rev. **110**, 314 (1958).

Reprinted from JOURNAL OF APPLIED PHYSICS, Vol. 38, No. 6, 2640–2644, May 1967

Reprinted from JOURNAL OF APPLIED PHYSICS, Vol. 38, No. 8,
3424, July 1967

Erratum: The Bi I–II Transition Pressure Measured with a Dead-Weight Piston Gauge

[38, 2640 (1967)]

PETER L. M. HEYDEMANN
National Bureau of Standards, Gaithersburg, Maryland

Due to an arithmetical mistake rows 13 to 15 in Table I are partly in error. They should read:

row 13
25.472 25.489 25.488 25.500 25.515 25.547 25.491 25.439
row 14
25.447 25.490 25.486 25.501 25.515 25.548 25.491 25.443
row 15
25.481 25.499

The pressures given in lines 3 and 5 of the abstract should read 25499 bar and 25481 bar, respectively. The pressure given in line 18 of Sec. VIII should read 25499 bar.

MEASUREMENTS IN THE HIGH PRESSURE ENVIRONMENT

Excerpt[1]

The following excerpt summarizes the consensus on the initial development of a pressure scale, analogous to the International Practical Temperature Scale for temperature, reached at the final session of the 1968 Symposium on Characterization of the High Pressure Environment.[2]

Key Words: Ba I-II transition, Bi I-II and III-V transition, Fixed points, High pressure, Mercury freezing points, Phase transformations as fixed points, Pressure coefficients of thermocouples, Pressure scale, Sodium chloride pressure scale, Thallium I-II transition.

[1]From "Measurements in the High Pressure Environment", Beckett, C. W., Boyd, E. C., and Lloyd, E. C., Science 164, No. 3881, 860-861 (May 16, 1969).

[2]The Symposium on Characterization of the High Pressure Environment was held at the National Bureau of Standards on October 14-18, 1968. The sponsors were the National Bureau of Standards and the Geophysical Laboratory of the Carnegie Institution of Washington. Expenses were covered by a grant from the National Science Foundation. The papers presented, together with the discussion from the floor will be published as a special publication of the National Bureau of Standards.

It was recommended [by an informal committee on fixed point standards] that these five phase transitions and accompanying pressures be used as pressure fixed points:

Transition	Fixed-Point pressure kilobars	Present estimated uncertainty kilobars
Mercury freezing point at 0 °C	7.569	0.002
Bismuth I to II transition at 25 °C	25.50	0.06
Thallium I to II transition at 25 °C	36.7	0.3
Barium I-II transition at 25 °C	55	2
Bismuth III to V transition at 25 °C	77	3

The fixed points recommended represent equilibrium values.

Users are to consider the fixed points as exact. The values of "present estimated uncertainty" are given only to indicate the range within which a value may be expected to shift as a result of improved measurements in the future. The reproducibility of pressures based on these phase changes may be better or poorer than these uncertainties, and is dependent strongly on technique in any given case. It is the responsibility of the experimenter to establish reproducibility and hysteresis for his own apparatus and technique, and the relationship between his experimental values and the above equilibrium values.

In addition to the five points listed above, covering the pressure scale up to 77 kilobars, a consensus was reached that the cesium II to III and III to IV transitions on <u>increasing pressure</u> be taken as 42.5 kilobars and 43.0 kilobars respectively, with a present estimated uncertainty of 1 kilobar, and that the tin I to II transition be tentatively used as a fixed point with an equilibrium transition value of 100 kilobars and a present estimated uncertainty of 6 kilobars.

In addition to the fixed point of 7.569 kilobars at the freezing pressure of mercury at 0 °C, the committee favored use of the mercury melting curve to establish other reference pressures up to 15 kilobars, corresponding to the freezing pressure of mercury at about 36.8 °C. It recommended that such reference pressures be based on the Simon equation, adjusted to agree with the value 7.569 kilobars at 0 °C as follows:

$$P = 38227\left[\left(\frac{T}{234.29}\right)^{1.1772} - 1\right]$$

where T is the temperature in K on the International Practical Temperature Scale (1948), and P is the pressure in bars. Small adjustments in this equation will be needed when the new temperature scale, IPTS 1968, is used.

Several pressure scales derived from equations of state of cubic solids were proposed at the meeting. Both metallic and nonmetallic substances such as the cesium halides were considered. Sodium can be treated most accurately from the theoretical viewpoint, but its high chemical reactivity is inconvenient. Aluminum can be treated by quantum mechanical methods if parameters are adjusted to fit some of the observed properties. Both aluminum and copper have been investigated experimentally as standards in shock wave measurements. These metals also could be used as standards in x-ray measurements.

The new data on copper and aluminum shock standards have been used to reevaluate the equation of state of several other metals that have been used in determination of pressure based on x-ray measurements of lattice constants.

Sodium chloride has been used most often as a reference material in recent applications of x-ray methods for estimating pressure. An informal committee on equation of state standards considered requirements in this application such as high compressibility, low yield strength, chemical stability, availability of accurate data over a wide range of pressure, and other properties. The committee selected sodium chloride first with copper and aluminum as alternates.

Four evaluations of data relevant to the sodium chloride scale now are available, including two which were presented at this meeting. In these evaluations differences in reported pressures are less than the combined errors (about four percent) at pressures from 25 to 300 kilobars. When these NaCl scales are combined with x-ray data on sodium chloride media in which transitions of bismuth and barium have been studied, the computed transition pressures lie within the uncertainties indicated in the table above for Ba and for Bi III - V.

The committee recommended that a single sodium chloride scale be adopted and that it be adjusted to give values of pressure as close as possible to those selected for the fixed points. An average of the two most recent sodium chloride scales would very nearly fulfill these requirements. An exact fit of selected fixed points appears unlikely without arbitrary adjustments in the equation of state. Nevertheless, a provisional sodium chloride scale consistent to within experimental error with the fixed points selected for the region below 100 kilobars is attainable and if accepted could be very useful.

A SURVEY OF MICROMANOMETERS[1]

By W. G. Brombacher

Abstract

This survey is concerned with instrumentation for measuring pressures from about 0.001 to 50 mm of mercury (0.13 to 6650 Nm^{-2}), described in publications during the years 1900-1968. U-tube micromanometers and diaphragm-capacitance gages are treated in considerable detail. Other instrumentation described includes gas column manometers; elastic element micromanometers with optical, inductance, resistance wire, strain gage, and vacuum tube transducers; piston gages; vane gages; and centrifugal micromanometers. The measurement of dynamic pressure, atmospheric pressure oscillations, low vapor pressure and calibration techniques are discussed. Only technical periodicals, books and government or university laboratory serials were used as sources of information. Details of electrical measurement circuits, amplifiers and recorders have been omitted. Schematic diagrams of approximately 70 instruments are included. References to the sources of information and available performance data are given.

Key Words: Calibration techniques, Capacitance pressure gages, Gas column manometers, Manometers, Meteorographs, Micromanometers, Piston gages, Pressure measurement, Vane gages, Vapor pressure measurement.

---

[1] To be published as an NBS Monograph.

7. Strain

CHARACTERISTICS OF THE TUCKERMAN STRAIN GAGE

By Bruce L. Wilson[1]

Synopsis

By means of an interferometric calibration device used at the National Bureau of Standards for calibrating gages and autocollimators, experimental results are secured which indicate the variations of the calibration factor with different conditions of use. The results indicate that (1) the change in autocollimator reading is accurately proportional to the change in length of the gage length of the strain gage, (2) the calibration factor is not greatly influenced by the material of the specimen provided the gage is properly attached, (3) the calibration factor is practically independent of the position of the gage in space, and (4) the calibration factor is almost independent of the temperature within the range 70 to 100 F. Provided the gage is properly attached, the change in calibration factor due to position of the gage and variations in material of the specimen does not exceed 0.1 per cent. Variations in mounting force from 1 oz. to 20 lb. reduced the calibration factor by as much as 0.9 per cent for celluloid and by less than 0.3 per cent for duralumin. By standardizing the mounting force during calibration and use, errors due to variations in mounting force can be eliminated. Results indicate that for nonvibrating specimens it is desirable to attach the gages by means of low spring-constant springs deflected to push the lozenge against the specimen with a force not exceeding 1 lb.

Because of the sensitivity, the small size, and the light weight of the Tuckerman strain gage, it is well adapted to measuring deformations of specimens and structures over short gage lengths. It is now being applied in the laboratories of the National Bureau of Standards and elsewhere to a large variety of problems, many of which involve the testing of specimens or structures made of thin sheet materials. It is customary to calibrate the gages with their lozenge axes and gage axes horizontal and with the gages held in place during calibration with a force of a few ounces in addition to the weights of the gages. They are actually used in many different positions, with different mounting forces and on materials of widely varying mechanical properties. Since it has been shown by Vose[2] that the conditions of use may alter the calibration factors of Huggenberger tensometers by as much as 5 per cent, the question naturally arises as to the magnitude of the variation of the calibration factor of a Tuckerman strain gage under various conditions of use.

To determine the variation of the calibration factors of a typical gage of

[1] Associate Physicist, National Bureau of Standards, Washington, D. C.

[2] R. W. Vose, "Characteristics of the Huggenberger Tensometer," *Proceedings*, Am. Soc. Testing Mats., Vol. 34, Part II, p. 862 (1934).

current design when subjected to widely different conditions of use, the gage was and on a variety of materials having Vickers numbers from about 10 to 800.

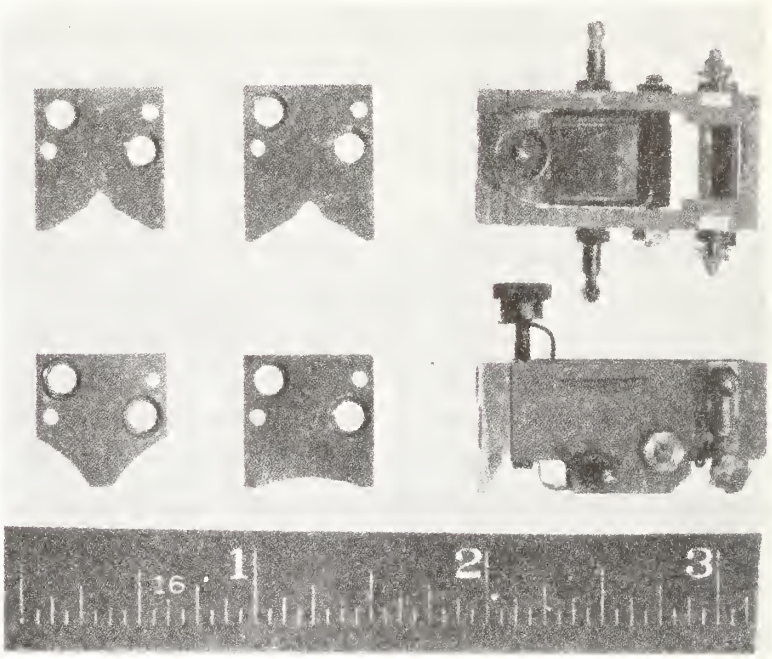

FIG. 1.—Tuckerman Strain Gages, Gage Length 1 in., Lozenge Diagonal 0.2 in., with Knife-edges for Use on All Shapes of Specimens.

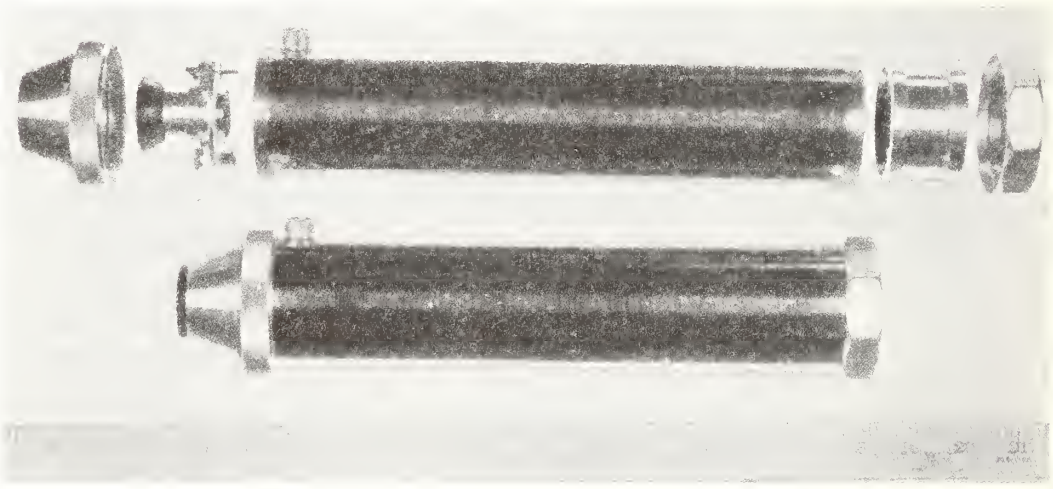

FIG. 2.—Tuckerman Autocollimator for Use with Optical Strain Gages.

calibrated by means of an interferometric calibration device for five different positions, at two different temperatures, for mounting forces varying from the weight of the gage (about 1 oz.) to 20 lb.,

DESCRIPTION OF AUTOCOLLIMATOR AND STRAIN GAGE

Two 1-in. gage length Tuckerman strain gages having 0.2-in. lozenges, and the four different types of knife-edges

required to adapt the gage to various-shaped specimens, are shown in Fig. 1. Two autocollimators, one disassembled to show the Ramsden eyepiece and lamp assembly and the objective lens cell, are shown in Fig. 2.

When the device is in use, the gage is attached to the specimen or structure, and the autocollimator is separately supported or held in the hand. A 1-in. gage weighs about 1 oz., the autocollimator weighs about 2 lb. The gages are about $1\frac{1}{4}$ in. wide, project about 1 in. above the surfaces to which they are attached, and are only slightly longer than their gage lengths.

A complete description of the Tuckerman autocollimator and the combination double and triple mirror system used in the strain gage has been given by Tuckerman.[3] Many improvements in the details of the design of the autocollimator and gages have been made since 1923, but the basic principles of the design have not been altered. For this reason only a brief description of the instruments is given here.

A diagrammatic sketch of the autocollimator and gage is shown in Fig. 3. The autocollimator consists of a highly corrected two-component objective lens having a focal length of about 250 mm., a reticule having a uniformly graduated scale, a fiduciary line and vernier accurately positioned to lie in the focal plane of the objective lens, a lamp for illuminating the fiduciary line and vernier, and a Ramsden type eyepiece. Reticules, which are produced photographically on glass, are mounted in cells which bear against definitely positioned stops in the autocollimator tube so that they can be removed and replaced without changing the calibration of the instrument. Likewise the objective lens is mounted in a cell which bears against a stop in the tube and it may be removed for cleaning and replaced without changing the calibration of the instrument.

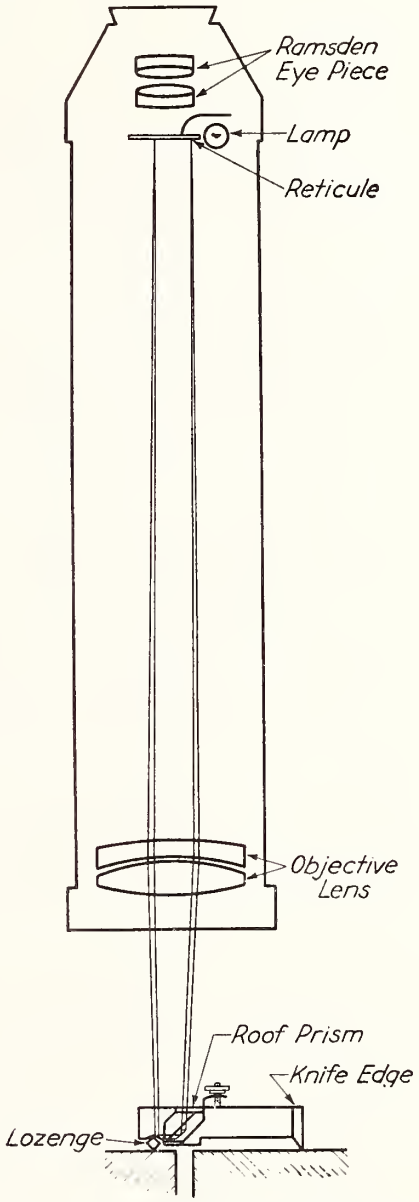

FIG. 3.—Diagrammatic Sketch of the Tuckerman Autocollimator and Strain Gage.

The gage consists of a steel or aluminum body to which is attached a knife-edge and the parts of the mirror system, which consists of the lozenge and the roof prism. The movable mirror is one

[3] L. B. Tuckerman, "Optical Strain Gages and Extensometers," *Proceedings*, Am. Soc. Testing Mats., Vol. 23, Part II, p. 602 (1923).

surface of the lozenge, which rests in seats formed by hardened steel plates attached to the gage body, and rotates about an axis perpendicular to the axis of the gage. The two fixed, mutually perpendicular mirrors of the three-mirror system are the roofs of a prism mounted in a housing which can be rotated by means of a knurled nut to reset the gage. The prism rotates about an axis perpendicular to the plane which bisects the dihedral angle formed by the roof surfaces. As the specimen deforms, the lozenge rotates about an axis perpendicular to this plane.

The roof prism contains a third reflecting surface, known as the flash surface, which, together with the lozenge, forms the two-mirror system. This surface is parallel to the line of intersection of the two roof surfaces and perpendicular to the plane which bisects the dihedral angle formed by the roof surfaces. When the instrument is read, it is necessary to have the image reflected from the flash surface in the field of view, to avoid the introduction of a cosine error.

Light from the fiduciary line and vernier scale is rendered parallel in passing through the objective lens of the autocollimator and falls upon both the lozenge and the roof prism. Only the light which falls upon the roof prism is shown in Fig. 3. This light is reflected by the two roof surfaces of the prism and by the surface of the lozenge, back into the objective lens to form an image on the scale of the reticule. Deformation of the surface upon which the gage rests will result in a rotation of the lozenge and will move the image along the scale.

The image shown in Fig. 3 is called the compression image. A tension image, not shown in Fig. 3, is formed by the light which falls first upon the lozenge. This image would not be visible through the eyepiece because it would lie as far to the right of the fiduciary line as the compression image shown lies to the left.

As the lozenge is rotated to move the compression image toward the fiduciary line (toward 0 on the visible scale) both the visible compression image and the invisible tension image will approach the fiduciary line. If the rotation is continued, the compression image will disappear from view after passing the 0 scale line and the tension image will appear and move up the scale. Since the distance from the fiduciary line to the 0 scale line is equivalent to 5 numbered divisions, neither image is visible for a rotation of the lozenge corresponding to 10 numbered divisions. If the incident and reflected light from the gage are parallel, the image of the fiduciary line lies on the line itself and is, therefore, masked from the field of view.

The scale of the reticule, which is about $\frac{1}{2}$ in. in length, is graduated into 25 numbered divisions, each of which is subdivided into 5 divisions, making a total of 125 divisions. Tenths of a division may be read from the vernier. By "splitting" a vernier division twentieths of a division may be estimated. Each numbered division corresponds to 0.001 radians rotation of the lozenge. An image is obtainable from a gage provided the angle between the incident and reflected light lies within the range 0.005 to 0.030 radians.

For the gages shown in Fig. 1, having 0.2-in. lozenges, one numbered division corresponds to a deformation of 2×10^{-4} in., and one vernier division corresponds to a deformation of 4×10^{-6} in. During calibration the autocollimator is read to one-half vernier division, which corresponds to a deformation of 2×10^{-6} in.

The Calibration Device

The device used to calibrate Tuckerman strain gages at the National Bureau of Standards is shown in Fig. 4. It con-

sists of a rigid frame to which one fixture for supporting the strain gage is attached, and a movable piece, supported by two flexure plates, to which the other fixture for supporting the gage is attached. The movable fixture is moved relative to the frame by means of a screw actuated by a worm gear. Provision is made for attaching plates of different materials to the fixed and movable fixtures to permit the calibration of gages on different materials. The pitch of the screw and the reduction of the worm gear are such that no difficulty is experienced in making adjustments to less than one-millionth of an inch.

The change in length of the gage length of the instrument being calibrated is measured by means of an interference method originated by Fizeau[4] and described by Tuckerman.[3] Light from a helium lamp is reflected from two interferometer plates attached to the frame and the movable piece of the cali-

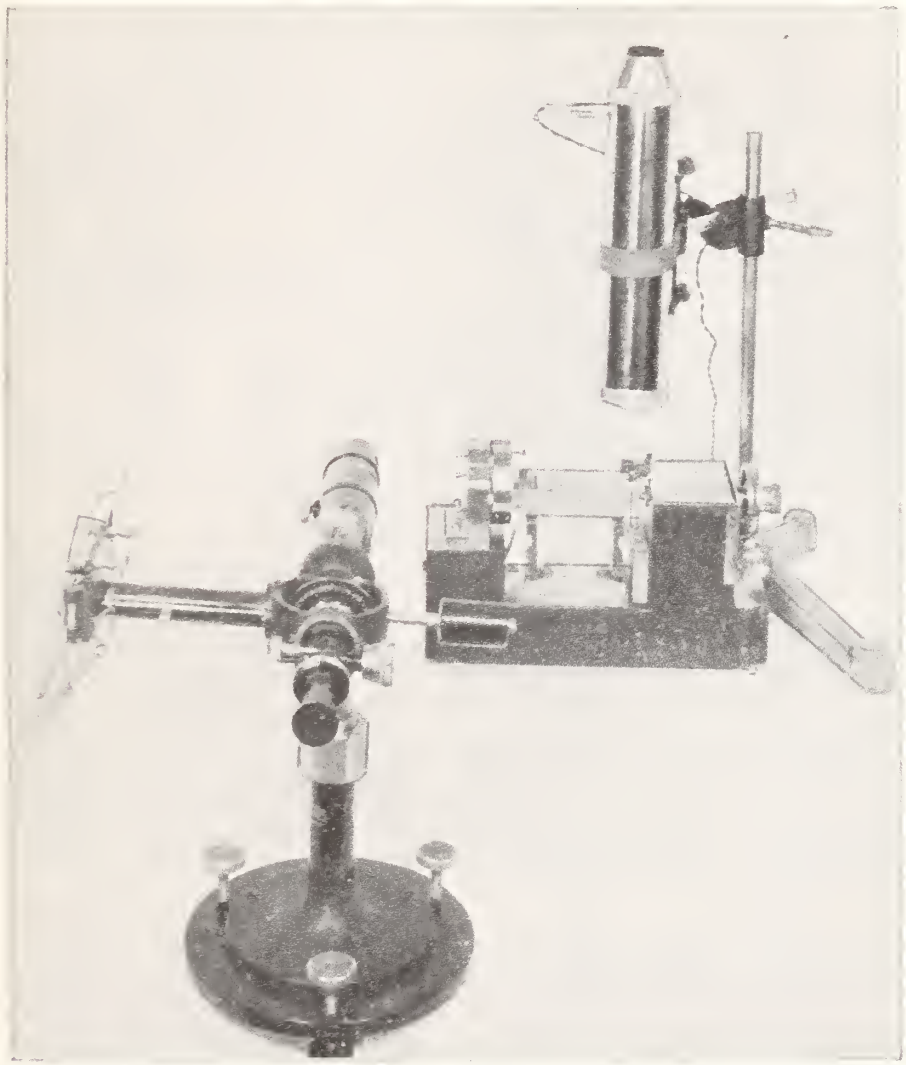

FIG. 4.—Interferometric Calibration Device for Calibrating Tuckerman Strain Gages.

[4] L. Fizeau, *Ann. Physik*, Vol. 128, p. 564 (1866).

bration device, respectively. The interference bands are viewed through a Pulfrich spectral system and the reading consists of counting the bands which pass the fiduciary mark (double cross hairs). One band corresponds to a displacement of the movable piece relative to the frame of one-half wave length of the line used, 0.00001156615 in.

Over the usable range of the calibration device, the distance between bands remains relatively constant and rotation of the bands with respect to the fiduciary mark is negligible. These are positive indications that the motion of the movable piece is practically a pure translation.

The calibration device is usually used in the position shown, with the surfaces to which the gages are attached horizontal. It may, however, be used satisfactorily in other positions to determine the calibration factors of gages in different positions.

The gage shown on the calibration device is held in place by a weight of 1 lb. supported equally by the two side bars which project from the gage body. This method is used for the routine calibration of gages. The calibration device functions satisfactorily with as much as 20 lb. applied to the gage. Forces greater than 1 lb. are applied by means of a lever and weights.

Behavior of the Gage

Linear Relationship:

The calibration results for one complete run on a typical gage are given in Table I. The gage length of the gage was being shortened during the run. During the first five readings the tension image was in view, between the fifth and sixth readings the tension image disappeared from view and the compression image appeared. During the last five readings the compression image was in view. In calculating the change in observed autocollimator reading, the 10.00 divisions corresponding to a change in reading from 0.00 with the tension image to 0.00 with the compression image (twice the distance from the fiduciary line to the 0 scale line) were added to the results calculated from the readings of the compression image. The equation of the least squares line calculated from the results given in columns 1 and 3, assuming that only the autocollimator readings were subject to error, is given in footnote *c* and the values calculated from this equation are given in column 4. The differences between the observed and calculated autocollimator readings, given in column 5, represent the departure of the readings from a truly linear relationship, The maximum difference is 0.017 divisions, which is less than one vernier division (0.02 division).

TABLE I.—CALIBRATION DATA FOR A TYPICAL TUCKERMAN STRAIN GAGE.

Gage length 1 in., lozenge diagonal 0.2 in.

Number of Bands[a]	Autocollimator Reading, divisions[b]	Change In Autocollimator Reading, divisions		Difference Between Observed and Calculated Changes in Autocollimator Readings, divisions
		Observed	Calculated[c]	
0.....	21.48	0	−0.011	0.011
50.....	18.58	2.90	2.897	0.003
150.....	12.78	8.70	8.712	−0.012
250.....	6.96	14.52	14.528	−0.008
350.....	1.12	20.36	20.343	0.017
550.....	0.48	31.96	31.973	−0.013
650.....	6.30	37.78	37.788	−0.008
750.....	12.12	43.60	43.604	−0.004
850.....	17.94	49.42	49.419	0.001
900.....	20.86	52.34	52.326	0.014

[a] One band equivalent to a change in length of 0.00001156615 in.

[b] One division corresponds to 0.001 radians rotation of the lozenge, equivalent to strain of 0.0002 with a 0.2 in. lozenge over a 1-in. gage length.

[c] Calculated changes in autocollimator reading computed from the least squares line:
Autocollimator reading = $-0.0105 + 0.0581522 \times$ no. of bands

Table I. The gage length of the gage was being shortened during the run. During the first five readings the tension image was in view, between the fifth and sixth readings the tension image disappeared from view and the compression image appeared. During the last five readings the compression image was in view. In calculating the change in observed autocollimator reading, the 10.00 divisions corresponding to a change in reading from 0.00 with the tension image to 0.00 with the compression image (twice the distance from the fiduciary line to the 0 scale line) were added to the results calculated from the readings of the compression image. The equation of the least squares line calculated from the results given in columns 1 and 3, assuming that only the autocollimator readings were subject to error, is given in footnote *c* and the values calculated from this equation are given in column 4. The differences between the observed and calculated autocollimator readings, given in column 5, represent the departure of the readings from a truly linear relationship, The maximum difference is 0.017 divisions, which is less than one vernier division (0.02 division).

It is customary to take several sets of readings such as those given in Table I in calibrating a gage. Readings are taken for both increasing and decreasing

gage lengths. For each run the calibration factor of the gage and autocollimator is calculated by dividing the change in length corresponding to one band, 0.00001156615 in., by the product of the gage length and the slope of the least squares line. The results of six runs on the same gage are given in Table II. The maximum percentage deviation from the average factor is 0.08 per cent. The maximum difference between observed and calculated changes in autocollimator readings is 0.024 division.

TABLE II.—REPRODUCIBILITY OF RESULTS FOR A TYPICAL TUCKERMAN STRAIN GAGE.
Gage length 1 in., lozenge diagonal 0.2 in.

Run	Gage Length	Calibration Factor	Deviation From Average Calibration Factor	Percentage Deviation From Average Factor	Maximum Difference Between Observed and Calculated Changes in Autocollimator Readings, divisions[a]
No. 1...	Lengthened	1.9884	−0.00025	−0.01	0.012
No. 2...	Shortened	1.9884	−0.00025	−0.01	0.016
No. 3...	Lengthened	1.9889	0.00025	0.01	0.017
No. 4...	Shortened	1.9902	0.00155	0.08	0.024
No. 5...	Lengthened	1.9886	−0.00005	0.00	0.018
No. 6...	Shortened	1.9874	−0.00125	−0.06	0.014

Average calibration factor = 1.98865

[a] Calculated changes in autocollimator readings computed from equations for least squares lines for each run. One vernier division is equal to 0.02 autocollimator divisions which is equivalent to a strain of 0.000004 in. per inch for a 0.2 in. lozenge over a 1-in. gage length.

For five of the six runs the maximum difference between observed and calculated readings is less than one vernier division (0.02 division).

Experience in calibrating a large number of gages indicates that the maximum departure of the readings from linearity when calibrated over this range seldom exceeds 0.025 divisions. When the calibration range is reduced to about 22 autocollimator divisions (one scale length), the maximum departure from linearity seldom exceeds 0.015 divisions.

The range of calibration used in determining the effects on the calibration factor of variations in mounting force, material, position, and temperature was about 20 autocollimator divisions (350 interference bands). For each run eight autocollimator readings were taken corresponding to eight equally spaced settings of the calibration device. The calibration factor for each run was computed from the slope of the least squares line.

Effect of Seating of the Lozenge:

During the calibration of a Tuckerman strain gage the lozenge may be turned through an angle greater than the range of calibration in an effort to seat it without disturbing the alignment of the gage on the calibration device. In attaching the gage to a specimen or structure it is difficult to seat the lozenge by this method. To determine the variation in calibration factor with the seating of the lozenge, a gage having a gage length of 1 in. and a 0.2-in. lozenge was calibrated on 9 different materials having Vickers numbers ranging from about 10 to 800. The maximum difference between the calibration factor for the initial rotation of the lozenge and the calibration factor for the twentieth rotation of the lozenge was 0.05 per cent for metals and 0.1 per cent for plastic materials for a mounting force of 1 lb. These values are very much less than the variations of 1 to 5 per cent reported by Vose[2] for the Huggenberger tensometer. This is probably due, as was pointed out by Tuckerman in his discussion of Vose's paper, to the greater stiffness of the lozenge and the greater included angle at its edge.

Effect of Mounting Force:

The variation of the calibration factor of a gage with mounting force was deter-

mined by calibrating the gage on various materials with mounting forces varying from the weight of the gage (1 oz.) to 20 lb. The results for two materials, celluloid and duralumin, are given in Fig. 5. The deviation of the observed factor from the average factor for a number of materials having Vickers numbers from about 10 to 800 for a mounting force of 1 lb. is plotted as the ordinate.

The slight increase in factor shown for a mounting force of only the weight of the gage over the factor for a mounting force of 1 lb. may be attributed to slight slipping of the gage. More consistent results were obtained with a mounting force of 1 lb. than for any other force used. For static tests there is no necessity to use mounting forces in excess of about 1 lb. It is unlikely, however, that excesssive force would actually be used

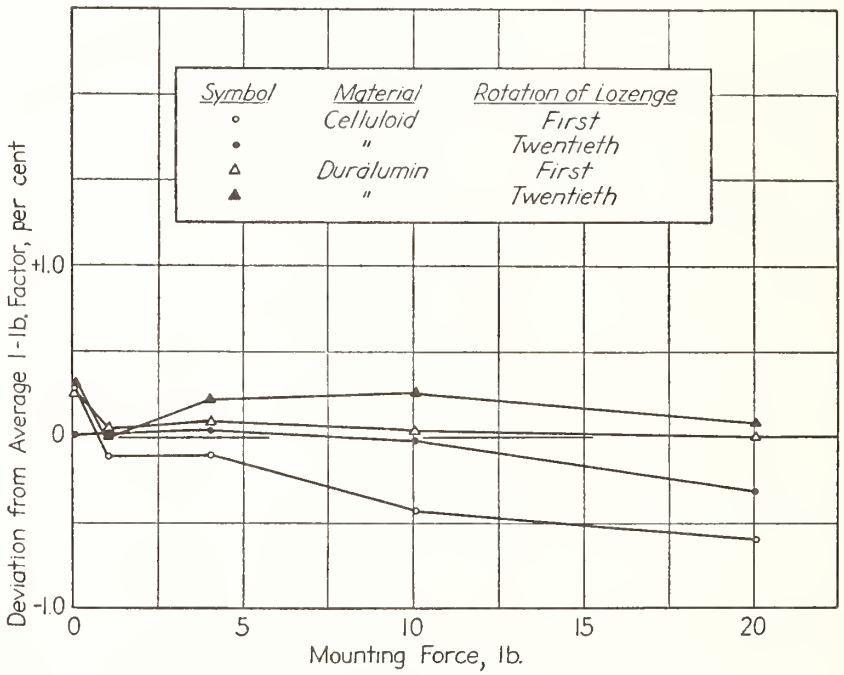

FIG. 5.—Variation of Calibration Factor with Mounting Force.

The maximum variation of calibration factor with mounting force (0.6 per cent) was obtained on celluloid. For celluloid the calibration factor with mounting forces greater than 4 lb. is less than the factor for 1 lb. while for duralumin the factor is greater than the factor for 1 lb. In addition to the results shown in Fig. 5, tests were made on spring steel (Vickers number 545) with both 1- and 2-in. gage length gages having 0.2-inch lozenges. The maximum difference between the factor for 1 lb. and the factor for 20 lb. was 0.25 per cent.

in testing materials such as celluloid since so large an amount of creep is observed after the application of forces of 10 and 20 lb. that no reliable readings can be obtained until sufficient time has elapsed for the rate of creep to become negligible.

It is desirable that the mounting force be applied by means of low spring constant springs so that the force will not vary greatly during a test, since the reading of the gage varies with the mounting force because of deformation of the gage body and knife-edge.

Effect of Material:

The variation of the calibration factor with material of the specimen for a 1-lb. mounting force is shown in Fig. 6. The maximum deviation of an individual factor from the average factor is less than 0.14 per cent for an organic plastic material. The maximum deviation for metallic specimens is 0.12 per cent. The Vickers number of the Stellite of which the lozenge is made is somewhat less than 777.

Effect of Position:

The calibration factors of a typical 1-in. gage for five different positions are given in Table III. In each position the gage was attached to steel spindles (Vickers number 187) with a spring force of approximately 1 lb. The maximum percentage deviation from the average is 0.06 per cent. This difference is not believed to be significant since variations as great as this are observed in repeated calibrations of a given gage in the same position.

Effect of Temperature:

A 1-in. gage was calibrated at constant temperatures of 70 F. and 100 F. to determine the variation of the calibration factor with temperature. Eight runs were taken at each temperature. The average factor for 100 F. was 0.05 per cent greater than the average factor for 70 F. This value is not believed to be significant.

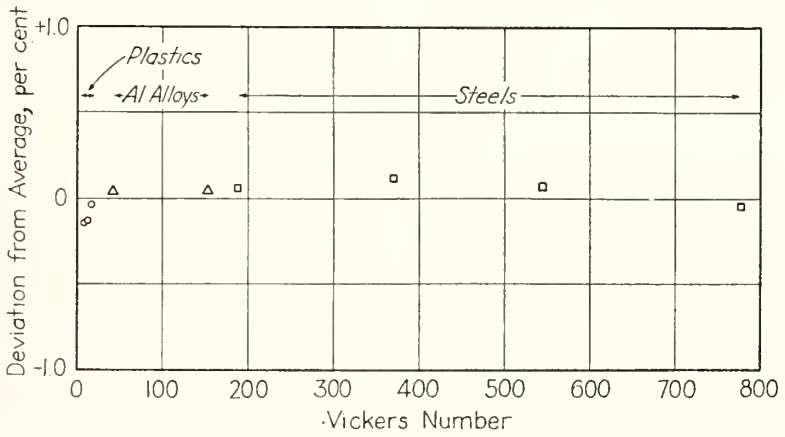

FIG. 6.—Variation of Calibration Factor with the Material of the Specimen for a Mounting Force of 1 lb.

TABLE III.—VARIATION OF CALIBRATION FACTOR WITH POSITION OF GAGE.

Gage Axis	Lozenge Axis		Calibration Factor	Deviation from Average Calibration Factor	Percentage Deviation from Average Factor
Horizontal	Horizontal	Gage above spindles	1.9874	0.0001	0.01
Horizontal	Horizontal	Gage below spindles	1.9884	0.0011	0.06
Horizontal	Vertical		1.9862	−0.0011	−0.06
Vertical	Horizontal	Lozenge up	1.9877	0.0004	0.02
Vertical	Horizontal	Lozenge down	1.9866	−0.0007	−0.04
Average.....			1.9873		

Accuracy and Sensitivity:

Calibration results reported indicate that the calibration factor for an individual run may differ from the average calibration factor for a number of runs by almost 0.1 per cent. These deviations are probably due to variations in the seating of the lozenge which result in different effective lengths of the lozenge diagonal. Since the modulus of

elasticity is inversely proportional to the calibration factor used in computing the indicated strain, variations as great as 0.1 per cent are to be expected in determinations of the modulus of elasticity.

The results reported indicate that the readings of the autocollimator are proportional to the change in length of the gage length of the gage to about one vernier division (4×10^{-6} in.) for a range of calibration of 0.010 in. For the 1-in. gage length gage used in the tests reported, for a range of calibration of 0.004 in., less than 3 per cent of more than 750 readings differed from the least squares lines by more than $\frac{1}{2}$ vernier division (2×10^{-6} in.). More than 60 per cent of the readings differed by less than $\frac{1}{4}$ vernier division (1×10^{-6} in.). The maximum variation was 1.4 vernier divisions.

All the results reported were obtained in a temperature-controlled room. For variable temperatures the readings of the autocollimator will change because of unequal expansion of the specimen and the body of the gage. Even if the coefficients of linear thermal expansion of the specimen and gage bodies are equal, in general the cross-sectional areas are unequal, and there is a differential rate of expansion or contraction which results in a shift of reading due to temperature. To avoid this source of error it is necessary to wait until temperature equilibrium is established after the gages and specimen are handled, and then to maintain the specimen and gages at a constant temperature during tests. Unfavorable temperature conditions may introduce errors much greater than any of the variations reported.

Conclusions

The readings of a Tuckerman strain gage are proportional to the change in length of the gage length to about 1 vernier division.

Mounting forces of 20 lb. produced changes in calibration factor as great as 0.6 per cent. For non-vibrating tests most satisfactory results were obtained on all materials with a mounting force of about 1 lb. This should be applied with low spring constant springs to minimize changes in mounting forces during a test.

If a mounting force of about 1 lb. is used, probably the most satisfactory material for the spindles of the calibration device would be a metallic material having a Vickers number in the neighborhood of 150 to 200.

The position of the gage in space has no significant effect on the calibration factor.

For constant temperatures within the range 70 to 100 F. the calibration factor is independent of temperature.

Authorized Reprint from the Copyrighted Proceedings of the
American Society for Testing Materials
Philadelphia, Pa.
Volume 44, 1944

A Method for Measuring the Instability of Resistance Strain Gages at Elevated Temperatures*

R. L. BLOSS†
and
J. T. TRUMBO‡
National Bureau of Standards
Washington, D.C.

▶ The usefulness of resistance strain gages at elevated temperatures is frequently limited by the instability of gage resistance with time. Methods and equipment that have been developed to measure this effect are described.

INTRODUCTION

A FEW YEARS ago mechanical testing of structures was revolutionized by the advent of the reliable, inexpensive resistance strain gage. Instrumentation for use with these gages has become very highly developed, and it is not unusual for strains to be determined for hundreds or even thousands of positions on a structure during a single test. Data may be automatically recorded and reduced by high-speed computers.

In recent years the operational requirements for high-performance aircraft, missiles, spacecraft, nuclear reactors, and other items have placed the additional demand of operation at elevated temperatures upon structural components. Laboratory and field testing of these structures under simulated and actual operating conditions require the use of strain gages capable of giving reliable results under these conditions. Resistance-type strain gages have been called upon to meet these larger demands.

As the operating temperature level increases, the problems associated with the use of these gages also increase. One of the factors that may limit the usefulness of a gage at elevated temperatures is the lack of stability of its resistance with time even though the temperature and strain are not changed. Since the instrumentation will interpret any uncompensated change of gage resistance as strain, a knowledge of the resistance instability is necessary so that appropriate corrections can be made to the data if justified, the data derated if necessary, and the use of unsuitable gages avoided.

The resistance instability, or drift, of the gages is recognized to be a complex combination of effects that will depend upon the material of the strain-sensitive element, the adhesive used to attach the gage to the specimen, the temperature to which the gage is exposed, other environmental conditions, and the history of the gage. Other factors not presently recognized may also have considerable influence. Since the drift is dependent upon so many factors, a theoretical prediction of its value is not practical. It would also be very difficult, if not impossible, for one testing facility to furnish enough information to permit corrections to be made to data obtained from gages used under all test conditions. However, sufficient experimental information should be made available to permit the selection of a gage type most likely to give reliable results, and to minimize the amount of testing that the user must do prior to gage use. Of course, other gage characteristics would need to be considered in selecting the proper type of gage.

A few publications that include considerations of some aspects of gage instability are listed in the bibliography.

*Presented at the Annual Conference, Los Angeles, California, September 11–15, 1961.
†Senior Member—ISA Washington Section.
‡Physicists, National Bureau of Standards, Washington, D.C.

METHOD

The methods which have been used to determine the resistance instability of the gages at elevated temperatures involve bringing a gage installation to a predetermined temperature and maintaining it at this temperature for an extended period of time while the change of gage resistance, or apparent strain indicated by the circuit, is measured. Differences in the methods are in methods of heating, heating rates, "soaking" time before readings are taken, time intervals between readings, duration of tests, and instrumentation used to obtain readings. It seemed that a nearly ideal method would (a) use the heating method most commonly used in tests where the gages are used, (b) provide as rapid a temperature change as possible without significant overshoot, (c) minimize the time after reaching temperature before readings are started, (d) provide continuous recording of the change of gage resistance as a function of time, (e) use instrumentation having sufficient sensitivity, accuracy, and stability to provide the desired information, and (f) continue for sufficient time to establish the trend of the gage behavior. An idealized temperature–time program for such tests would be a stairstep function.

After considering known user needs, experience that had been gained at the National Bureau of Standards, and information that was available from other investigators, the current method was conceived. With this method, a small metal test strip and its attached gage are heated with radiant heaters at a rate of about 10 F per second. A record of the change of gage resistance with time is started one minute after the test temperature is reached and continues for at least thirty minutes. Changes of gage resistance are indicated by the output voltage of a bridge circuit as recorded on a recorder having a maximum sensitivity of 0.5 mv/in.

In an actual test, a small test strip with a gage installed in the normal manner is suspended within the furnace so as to be free of restraints. The gage is connected as one arm of a bridge circuit with the input terminals connected to a constant voltage power supply and the output to one axis of the recorder. The input voltage and recorder sensitivity are adjusted to appropriate values and the recorder chart marked in terms of relative change of gage resistance. Power is then supplied to the heaters. The actual temperature and time values used would depend upon the characteristics of the gage being tested and the base material upon which it is mounted. This information would normally be obtained from the manufacturer's literature, known properties of materials, and preliminary tests. Figure 1 shows part of an actual temperature program to which a stainless steel test strip was subjected.

The circuit used for determining the change of gage resistance is the familiar bridge circuit shown in Figure 2, where R_g represents the gage being tested, R_b and R_c are fixed resistors, R_a is a resistor that can be adjusted to balance the bridge circuit, E_i is the input voltage, and E_o is the output voltage signal from the bridge circuit.

One method of using this circuit to measure the resistance of R_g is to adjust R_a until $E_o = 0$. The value

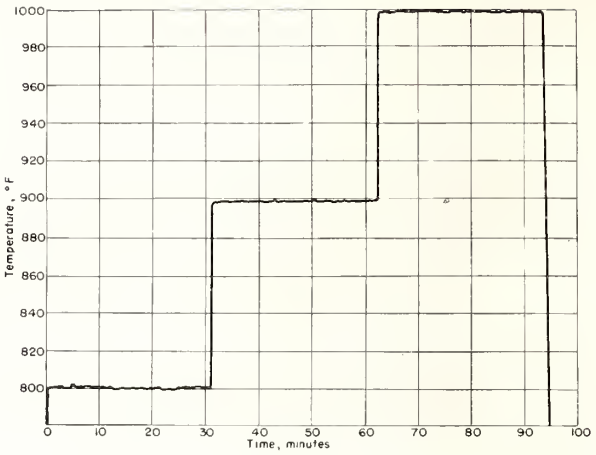

Figure 1. Test strip temperature during a portion of a simulated test.

of R_g is then computed from the usual relationship required for bridge balance. This method is capable of sufficient sensitivity and accuracy but it is not well adapted to continuous recording of the change of gage resistance. There is, however, a convenient relationship between the output voltage, E_o, of an unbalanced bridge circuit and the difference between the gage resistance and the resistance value required to balance the circuit. For simplification, justified by actual operating conditions, the assumptions are made that (a) $R_g = R_a$, (b) $R_b = R_c$, (c) $I_o \ll I_1$ or I_2, and (d) instantaneous gage resistance $= R_g + r$, where r is the difference between the gage resistance and the resistance value required to balance the circuit.

If the circuit is adjusted to satisfy assumptions (a) and (b) when balanced and if assumption (c) is valid, the potential difference across the gage is

$$V_g = \frac{E_i(R_g + r)}{2R_g + r} \tag{1}$$

and the potential difference across R_b is

$$V_b = \frac{E_i}{2} \tag{2}$$

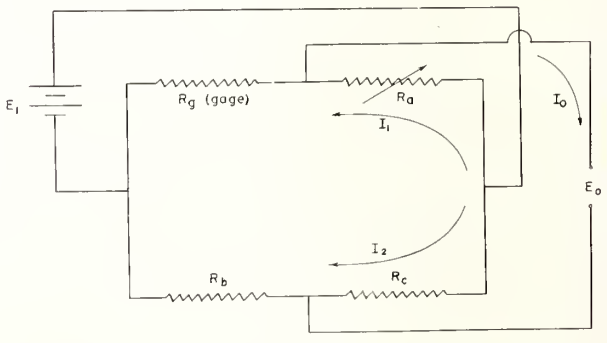

Figure 2. Circuit for measuring change of gage resistance.

The output voltage E_o then is given by

$$E_o = V_g - V_b = E_i\left[\frac{r/R_g}{4 + 2r/R_g}\right] \tag{3}$$

This equation may be written in terms of apparent strain by noting that $r/R_g = K\epsilon$, where K is the gage factor of the gage and ϵ is apparent strain. This substitution gives

$$E_o = E_i\left[\frac{K\epsilon}{4 + 2K\epsilon}\right] \tag{4}$$

Therefore it is seen that, by using a high-impedance recorder to satisfy assumption (c), the change of gage resistance can be conveniently determined by recording the output voltage of the circuit as a function of the independent variable, in this case time. Assumption (c) is justified since the recorder used requires 7×10^{-6} ampere for full scale deflection and the gage current is of the order of 2×10^{-2} ampere.

In order to find the relative change of gage resistance from measured output voltages, equation (3) is rearranged into

$$r/R_g = \frac{4E_o}{E_i - 2E_o} \tag{5}$$

From this form of the equation it can readily be seen that the accuracy of the measurement depends upon the accuracy with which output voltage, E_o, is measured, the accuracy with which the input voltage, E_i, is known, and the validity of assumptions (a), (b), and (c). However, no absolute measurements have to be made if one of the arms of the bridge circuit, preferably R_c, can be varied in accurately known increments. If the arms of the bridge are of nearly the same value, the output voltage produced by a change of R_c will be the same as would be produced by the same percentage change of R_g. The system can therefore be calibrated just prior to use by changing R_c in known increments and noting the recorder deflection. The resulting accuracy is then dependent upon the stability and sensitivity of the recording instrument, the ability to hold the input voltage constant, and the accuracy of the calibrating arm, R_c. Such a system with overall errors not exceeding $\frac{1}{2}\%$ of the full scale of the recorder is practical.

EQUIPMENT

The equipment that has been developed and assembled for conducting these tests is shown schematically in Figure 3. A suitable test strip with a gage installed on it is suspended in the furnace so as to be free of restraints. A compensating lead wire configuration is used to connect the gage into its electrical circuit. Two thermocouples attached to the test strip are used to control and monitor the temperature. Commercial units are used for temperature control, power supply to the gage circuit, recording, and temperature monitoring. The input voltage is kept constant by comparing it,

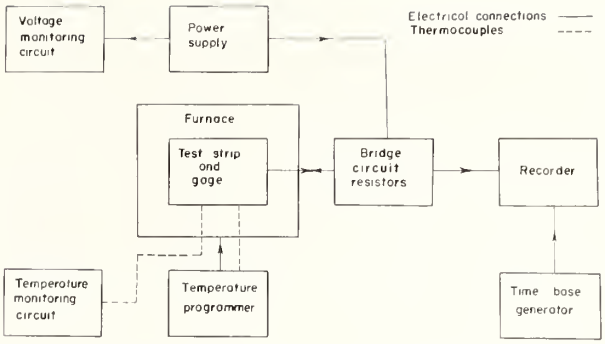

Figure 3. Method of measuring strain gage instability.

by means of a voltage divider circuit, to the potential of a mercury cell. Any power supply change is indicated by a deflection of the galvanometer and appropriate adjustment of the input voltage is made. The time base generator is a voltage divider circuit made from a precision potentiometer, stable resistors, and a mercury cell. The potentiometer shaft is driven by a synchronous motor and gear chain, and the resulting varying voltage between the potentiometer terminals is connected to the recorder. Power to the heating units is supplied from a commercial temperature controller that varies the voltage to the heaters in accordance with the difference between a thermocouple voltage and a signal generated within the controller. The power voltage is varied by adjusting the firing angle of thyratron power tubes. This unit provides a fast acting and sensitive system of control, capable of heating a stainless steel test strip $1 \times 6 \times 0.050$ in., painted with a heat-resisting black paint to provide a high, uniform emissivity, at rates of at least 10°F per second to temperatures between 600° and 1500°F with an overshoot not exceeding 5°F. After initial stabilization, a temperature constant to within ± 2°F can be held for extended periods of time. The input voltage power supply is a well regulated and filtered unit having a voltage range of 5 to 12 v determined by the position of a ten-turn potentiometer. The temperature-monitoring unit is a standard thermocouple potentiometer with an electronic null indicator as a galvanometer. Recording is by means of an X-Y recorder having sensitivities of 0.5 mv/in. to 50 v/in. on each axis and the ability to record accurately at rates as great as 2 in./sec.

The construction and use of the furnace are shown in Figures 4 and 5. Radiant heaters, each having a rating of 1000 w at 240 v, are used because their fast response and low thermal inertia permit the use of fairly high heating rates without a large temperature overshoot. Eight of these heaters are mounted on a 4-in.-diameter circle and are contained within a cylindrical reflector of polished aluminum 8 in. in diameter and 10 in. long. The reflector has a wall thickness of $\frac{1}{8}$ in. The heater and reflector are held in position by holes and grooves in cement-asbestos board. Additional pieces of cement-asbestos board are used to prevent contact with the electrical terminals of the heaters. Threaded rods and spacers are used to assemble the pieces. In order to

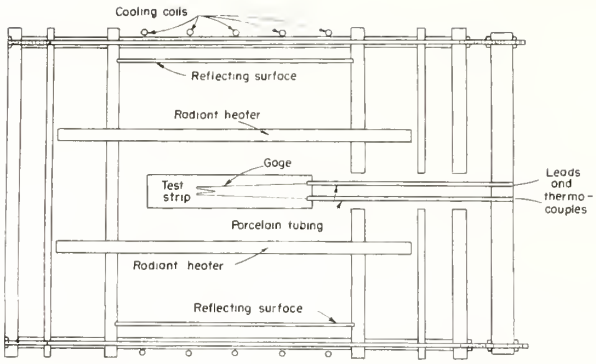

Figure 4. Radiant heating furnace.

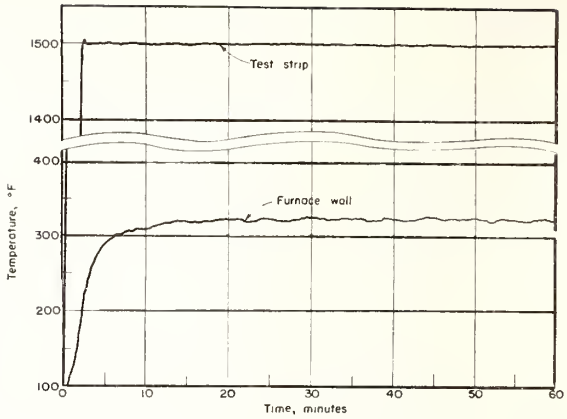

Figure 6. Effectiveness of air flow for cooling furnace wall.

prevent the aluminum cylinder from overheating, air is blown onto the surface through small holes in the inner surface of rings of copper tubing that encircle the cylinder. The rings are connected into a larger-diameter chamber in order to provide equal air distribution over the length of the cylinder. The distribution chamber is connected to a compressed air supply. This furnace unit has a low thermal inertia, thus permitting a rapid heating rate without excessive temperature overshoot.

The ability of the air flow over the aluminum cylinder to keep the reflector at a safe operating temperature is shown in Figure 6. During a test period of one hour, a test strip was brought to 1500°F at 10°F per second and held at that temperature for the remainder of the test. The temperature of the aluminum cylinder, as measured by a thermocouple imbedded in the cylinder wall, did not exceed 330°F during this time. Care was taken to avoid direct impingement of an air stream upon the thermocouple.

RESULTS OF TESTS

The type of information obtained is shown in Figure 7, which gives the results obtained from one gage. It is not implied that these results are typical of any gage type for it is possible that the behavior of a gage would vary considerably depending upon the gage history, the test conditions to which it is subjected, and other factors. However, it is interesting to note the variation of the magnitude of drifts at various temperatures; the possibility of positive and negative drifts; the effect of history on the gage instability; and that, in at least this case, the drift during the second test series at 900°F was greater than during the first series even though the gage had been at 1000°, 1100°, and 1200°F for 30 minutes each during the first test series. The irregularities in the recorded curves are caused by temperature fluctuations of about ±2°F. The magnitude of drift shown by this gage could have contributed errors as great as 3500 μin./in. during a 30-minute test, assuming a gage factor of 2, if the possible behavior of the gage were not known.

CONCLUDING REMARKS

When resistance strain gages are to be used at elevated temperatures, their characteristics must be examined closely to preclude the possibility of very large errors. The instability of gage resistance with time is one of the characteristics that may become very important. The

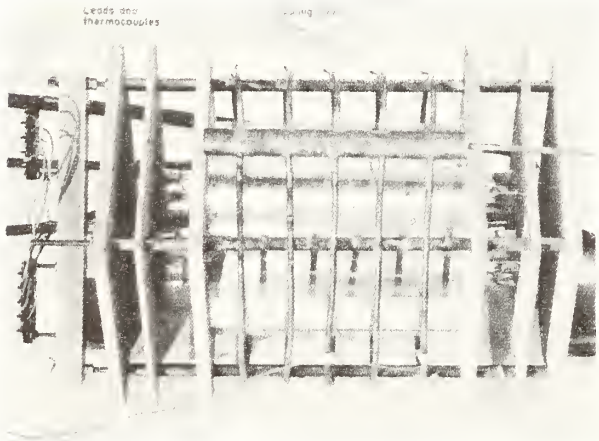

Figure 5. Radiant heating furnace.

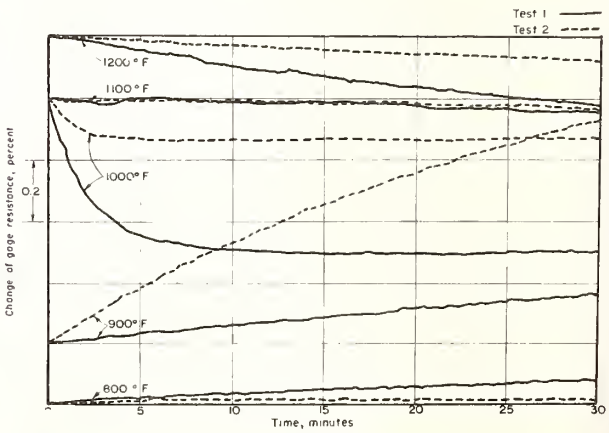

Figure 7. Instability of one gage at elevated temperatures.

amount of resistance drift to be expected from a gage can be estimated from tests carried out using an easily constructed furnace and standard commercial instruments. The equipment that has been described might also be used to subject other small objects to well-defined temperature programs.

BIBLIOGRAPHY

1. *Symposium on Elevated Temperature Strain Gages*, Am. Soc. Testing Mats. Spec. Tech. Pub. No. 230, 1958.
2. Bloss, R. L., The Evaluation of Resistance Strain Gages at Elevated Temperatures, *Materials Research and Standards* **1**, No. 1, 9, 1961.
3. Bloss, R. L., *Characteristics of Resistance Strain Gages, in* Mills Dean III and R. D. Douglas (eds.) *Semiconductor and Conventional Strain Gages*, Academic Press, 1962, pp. 123-142.
4. Pitts, J. W., and Moore, D. G., *Development of High Temperature Strain Gages*, Natl. Bur. Standards Monograph 26, 1961.
5. *Strain Gages, Bonded Resistance*, National Aircraft Standard 942, Aerospace Industries Association of America, Inc., 1960.

Four Methods of Determining Temperature Sensitivity of Strain Gages at High Temperatures

C. H. Melton
R. L. Bloss
National Bureau of Standards
Washington, D.C.

Reprinted from ISA Journal

Test results compare four techniques for determining temperature sensitivity of bonded resistance strain gages at temperatures to 1,000 deg F.

Theory

For a strain gage bonded to an unrestrained base material, the relative change of resistance due to a temperature change[1] is

$$(\Delta R/R)_T = \Delta T\,[(a_b - a_g)K + c_g] \qquad (1)$$

where

ΔR = change in gage resistance
R = initial gage resistance at room temperature or at a reference temperature
ΔT = temperature change
a_b = temperature coefficient of expansion of base material
a_g = temperature coefficient of expansion of gage sensing element
K = gage factor of the gage element, and
c_g = temperature coefficient of resistance of gage element

The gage factor is defined as

$$K = \frac{(\Delta R/R)_L}{\Delta L/L} \qquad (2)$$

where

ΔR = change in gage resistance,
R = initial gage resistance when the base material is unrestrained or at a reference strain,
Subscript L indicates the change is due to a change of length, and
$\Delta L/L$ = unit change of length to which the gage is subjected.

Generally the combined effects in Eq. 1 are measured over a small temperature increment or while changing the temperature of a given base material to which a gage is bonded.

It must also be recognized that the gage resistance will change, or appear to change, due to effects that are not shown in Eq. 1. Probably the two most significant effects are drift (a change of resistance that will occur with time at a constant temperature) and the leakage resistance between the gage and the test strip.

Measurements of drift are made by holding a gage installation at a constant temperature and measuring the change of gage resistance as a function of time.

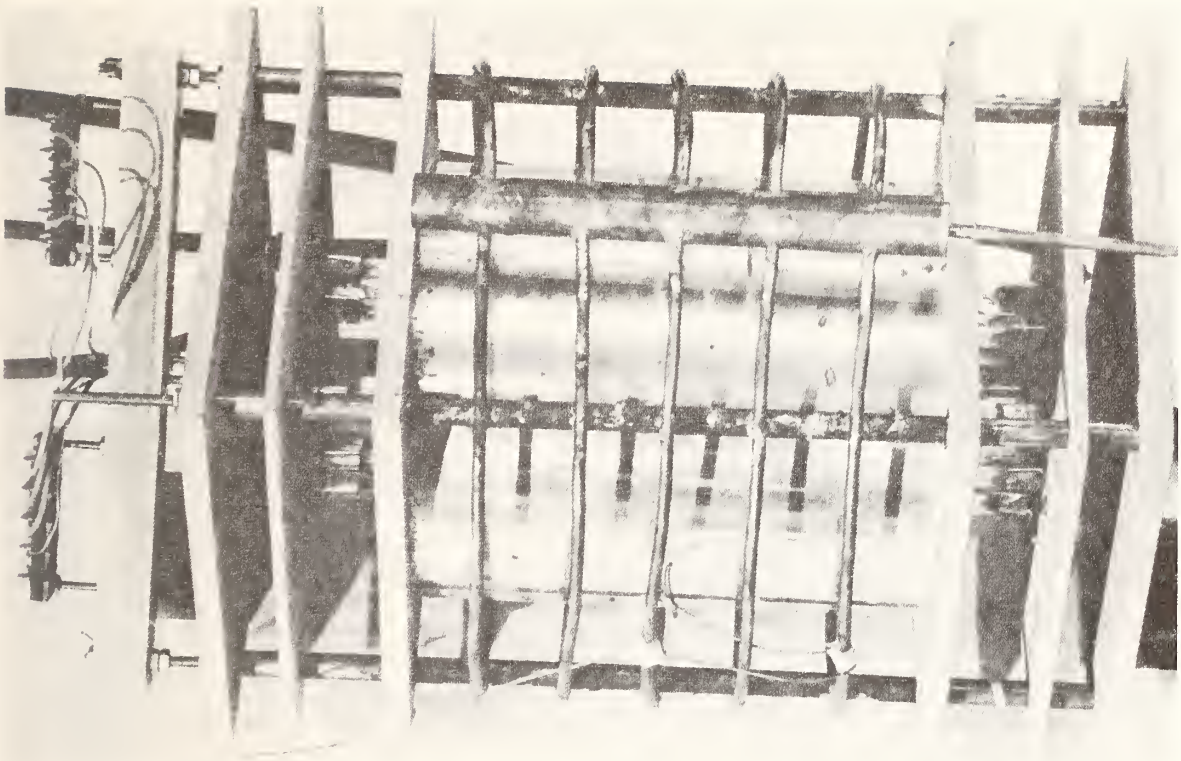

Fig. 1. Radiant heating furnace.

However, drift is undoubtedly present even under transient heating conditions at high rates. Under such conditions, the total relative change of gage resistance would be given as

$$\Delta R/R = (\Delta R/R)_T + (\Delta R/R)_D \qquad (3)$$

where the subscripts T and D indicate that the changes are due to temperature change and drift respectively. If the drift rate is known, it is possible to apply a correction to the observed data in order to obtain a better value of temperature sensitivity. If the total relative change of gage resistance is recorded as a function of temperature, the drift term of Eq. 3 would be given by

$$(\Delta R/R)_D = \beta/H \qquad (4)$$

where

β = drift rate, and
H = heating rate.

The leakage resistance would appear as a distributive shunt resistance across the gage. It is quite possible that it would not be uniformly distributed along the gage element. If this leakage resistance remains high, e.g. greater than ten megohms, the effect is small and can be ignored. Since the value and distribution of the leakage resistance are not usually known, data correction is not generally possible. However, this effect should be recognized as possibly contributing to erratic or erroneous data.

Another possible source of error in temperature sensitivity determinations using d-c instrumentation is an uncompensated thermal emf generated within the gage circuit. Junctions of dissimilar materials should be avoided if possible, especially within the high temperature region. Care should also be taken during the gage installation and hook up to have junctions in pairs and in close proximity so that an emf generated at one junction will be compensated for by an equal emf from the other junction.

Equipment

The furnace, described previously[2] and shown in Fig. 1, consists of eight quartz tube radiant heaters enclosed by a reflecting cylinder of aluminum and asbestos-cement plates. The aluminum cylinder is cooled by air forced onto it from small holes in the surrounding tubing. Electric power to the furnace is supplied by a voltage-proportioning temperature controller. Voltage to the heaters is varied to adjust the temperature of the test strip to match an internally generated signal. The test strip temperature is measured with a thermocouple. The internal signal may be chosen to increase linearly with time. Heating rates from zero (constant temperature) to greater than 100 deg F per second are available. Because of fast response of the controller and low thermal inertia of the gage strip and furnace, the temperature of the gage strip can be changed at 10 deg F per second to a selected temperature with no significant overshoot and then held constant, usually within ± 0.5 deg F for several minutes.

Two types of instrumentation were used. Diagrams of these are shown in Figs. 2 and 3. In Fig. 2 the gage and three stable resistors form a Wheatstone bridge circuit that is connected to a constant-voltage d-c power supply. The output terminals of the bridge circuit are connected to the Y-axis of an X-Y recorder. The X-axis of the recorder is connected to a thermocouple that is spotwelded to the

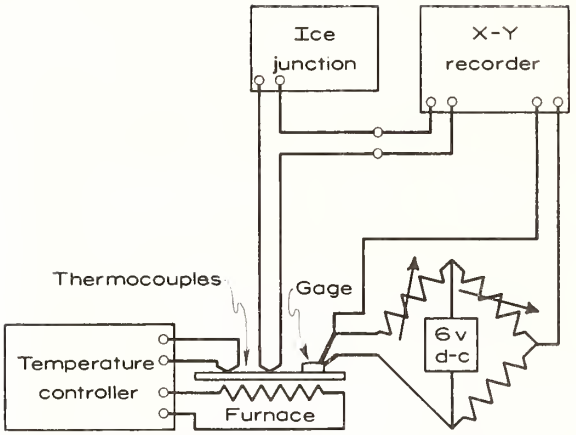

Fig. 2. Instrumentation for the fast slope and slow slope methods.

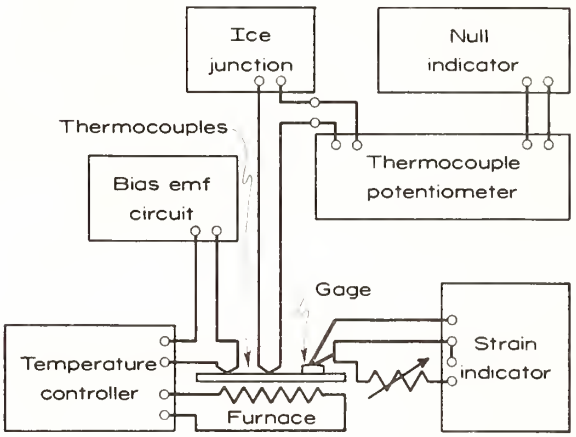

Fig. 3. Instrumentation for the simultaneous equations and graph methods.

test strip. The entire resistance measuring system can be calibrated readily by varying the resistor opposite the gage in known increments.

In Fig. 3, gage response is measured by a strain indicator and the temperature of the gage strip by a thermocouple and potentiometer. This temperature may be changed a given small amount by placing a small bias voltage in series with another thermocouple which is connected to the temperature controller. This bias voltage was obtained from a mercury cell and voltage divider circuit.

Test Methods

For identification purposes, the four methods that were compared are referred to as the *fast slope, slow slope, simultaneous equations,* and *graph methods.*

Equipment for the *fast slope method*[3] is shown in Fig. 2. The temperature controller is set to heat the gage strip at 10 deg F per second. As the strip is heated, the X-Y recorder makes a graph of the relative change of gage resistance as a function of the test strip temperature. Then, for any temperature selected, the temperature sensitivity is found by determining the slope of a line drawn tangent to the curve at that temperature.

The *slow slope method* also uses the equipment shown in Fig. 2 and employs the same procedure as the *fast slope method* except that the test strip is heated at a rate of 0.4 deg F per sec. This slower heating rate was chosen because it is called for in the specifications of the Aerospace Industries Association of America, Inc. (NAS 942).[4] Although there are some differences between the *slow slope method* and the test procedure and equipment outlined in NAS 942, it is believed that the results obtained by the two methods should be comparable.

For the *simultaneous equations method*[5] the equipment is shown in Fig. 3. The temperature of the gage strip is increased at the rate of 10 deg F per sec until the test temperature is reached. After this temperature is reached, a period of 5 minutes is allowed for the temperature to be stabilized within 1 deg F of the desired temperature as indicated by the thermocouple potentiometer, for the thermal gradients to minimize, and for the drift rate to become more nearly constant. At the end of this period, readings are taken simultaneously from the strain indicator and the potentiometer. The bias voltage is immediately introduced into the controller thermocouple circuit causing the temperature to decrease about 5 deg F. At this lower temperature readings are again taken one minute after the first readings. The bias voltage is removed, the temperature rises to the initial value, and readings are again taken two minutes after the initial readings. This procedure is repeated for each of the other temperatures for which a determination of temperature sensitivity is to be made. After the testing, the data taken at each test temperature is used to form simultaneous equations,

$$\alpha\Delta T_1 + \beta\Delta t_1 = \Delta S_1 \qquad (5)$$

$$\alpha\Delta T_2 + \beta\Delta t_2 = \Delta S_2 \qquad (6)$$

where

α = temperature sensitivity of the gage and test strip combination,

ΔT_1 and ΔT_2 = the temperature changes between readings 1 and 2 and readings 2 and 3 respectively,

β = drift rate (assumed to be constant over the time and temperature intervals involved),

Δt_1 and Δt_2 = time intervals of one minute each, corresponding to the temperature changes, and

ΔS_1 and ΔS_2 = changes in indicated strain at the gage corresponding to the temperature changes and time intervals.

The temperature sensitivity, a, is determined by eliminating the drift rate, b, from the equations.

Instrumentation for the *graph method* is the same as that shown in Fig. 3. The temperature of the gage strip is increased at the rate of 10 deg F per sec until the test temperature is reached. After this temperature is reached, one minute is allowed for the temperature to be stabilized to within 1 deg F of the desired temperature and for temperature gradients to minimize. Five sets of strain and temperature readings are taken one minute apart. After the last set of readings is taken, the temperature is decreased about 10 deg F by placing the bias voltage into the temperature controller thermocouple circuit. Starting one minute after the last set of readings is taken, another group of five sets of strain and temperature readings are taken at one minute intervals. The temperature is then raised to approxi-

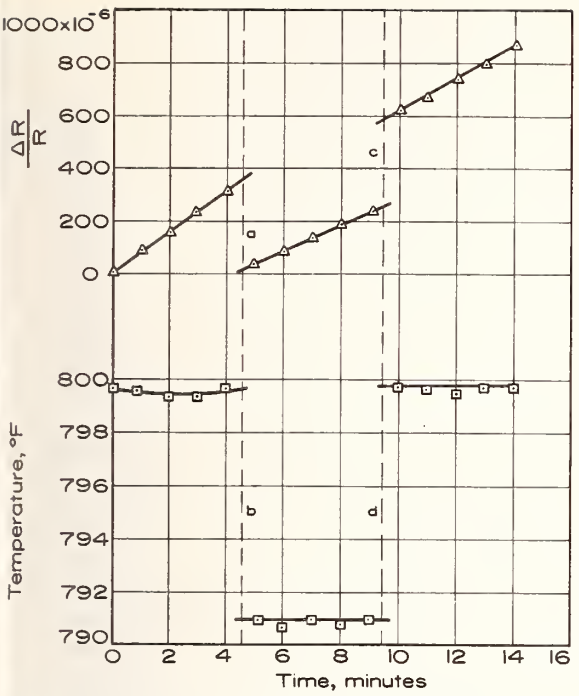

Fig. 4 Typical graph method results at 800 deg F.

Table I — Testing Schedule*

Test method	Test cycle number Gage 1	Gage 2	Gage 3	Gage 4
Fast Slope	1,2.3.7,7a**	6,10	5,9	4,8
Slow Slope	4,8	1,2,3,7	6,10	5,9
Simultaneous Equations	5,9	4,8	1,2,3,7	6,10
Graph	6,10	5,9	4,8	1,2,3,7

*The temperature sensitivities at all test temperatures were determined during a test cycle.
**No power to the gage circuit during this test cycle.

mately the first value by removing the bias voltage. Starting one minute after the last set of readings, another group of five sets is taken. This procedure is repeated for each of the other temperatures for which a determination of temperature sensitivity is to be made. After the testing, the strain and temperature data are graphed against time for each test temperature region. Figure 4 shows a typical graph of test results. Smooth curves are fitted to the plotted points. The curves are extrapolated so that they overlap on the time scale. At the mid-points of the time intervals during which the temperature was changing, vertical lines are constructed to intersect the strain and temperature curves as shown in Fig. 4. The temperature sensitivity is the ratio of the magnitudes of the line segments "a" to "b" or the ratio of "c" to "d." The average value of these two ratios is reported.

Testing and Results

For comparing the methods of measuring temperature sensitivity, four Nichrome V foil gages were bonded with a ceramic cement to small test strips of type 302 stainless steel. These gages were of the same type and lot number and were installed in the

Table II — Temperature Sensitivity Values

Test cycle No.	Temperature sensitivity, microhms/ohm deg F: 400° F Fast Slope	400° F Slow Slope	400° F Simultaneous Equations	400° F Graph	600° F Fast Slope	600° F Slow Slope	600° F Simultaneous Equations	600° F Graph	800° F Fast Slope	800° F Slow Slope	800° F Simultaneous Equations	800° F Graph	1000° F Fast Slope	1000° F Slow Slope	1000° F Simultaneous Equations	1000° F Graph
1	59.9	57.6	58.2	57.6	59.7	59.0	65.4	57.2	76.0	138.3	56.5	50.7	187.8	135.9	—19.6	27.5
2	47.9	44.1	42.2	42.5	47.7	42.6	41.3	41.3	46.2	46.7	40.7	39.3	65.3	—18.7	—12.2	14.4
3	46.3	44.1	44.7	43.2	46.3	43.5	39.6	41.2	45.0	47.9	40.7	39.8	53.8	0.0	—10.7	0.4
4	43.4	52.4	44.2	42.7	41.7	49.4	43.1	41.1	41.4	49.0	40.0	41.2	34.8	—8.2	—7.7	6.9
5	44.1	44.3	44.8	43.2	42.1	41.9	42.6	42.1	41.4	44.0	†	40.8	36.7	—31.9	—4.5	10.5
6	44.3	44.7	45.4	42.7	42.4	42.4	43.2	40.7	41.2	45.5	42.0	39.0	33.9	—43.7	—9.7	—0.9
7	44.3	44.3	47.8	43.4	41.7	42.1	43.8	41.8	42.4	44.5	41.0	40.6	37.9	—35.5	—6.9	11.9
8	44.7	44.3*	44.7	44.8	42.6	41.9*	41.9	41.3	42.1	45.0*	39.4	40.8	35.5	—37.5*	—10.5	—3.2
9	46.5	45.0	46.1*	44.0	43.1	43.8	44.9*	42.4	42.9	46.4	40.3*	40.5	36.5	—13.2	—8.6*	3.3
10	45.6	44.5	45.4	44.4*	42.4	44.0	42.8	42.5*	42.4	46.7	40.0	41.1*	37.2	—41.5	—4.3	16.3*
Average (cycles 2-10)	45.2	45.3	45.0	43.4	43.3	43.5	42.6	41.6	42.8	46.2	40.5	40.3	41.3	—25.6	—8.3	6.6
Standard deviation** (cycles 2-10)	1.44	2.68	1.50	0.81	2.15	2.35	1.52	0.62	1.72	1.62	0.79	0.79	10.81	15.89	2.75	7.07

*The gage from which these values were obtained received an extra cycle at the Fast Slope heating rate between the scheduled cycles 7 and 8.

** $\sigma = \left[\frac{\sum_{i=1}^{n}(x_i - x)^2}{n - t}\right]^{1/2}$

†Reading missing

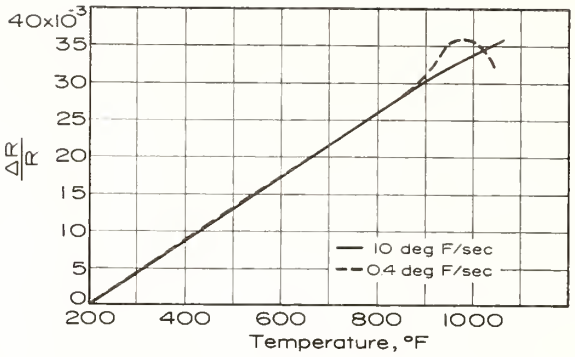

Fig. 5. Typical gage response at two heating rates.

same way on the same day by the same person. This number of gages was chosen so that each test method could start with an untested gage. The testing schedule is shown in Table 1. By using this schedule, the first three test cycles of a gage were carried out using the same test method and each gage was tested at least twice by each of the methods. Using four gages permitted each method to be used for each test cycle 1 through 10. The exceptions were with gage 1. This gage was heated to 1000 deg F at 10 deg F per sec (*fast slope method*) between cycles 7 and 8. There was no voltage to the gage circuit during this time. This heating cycle is noted in Table I as cycle 7a. During test cycle 5 (*simultaneous equations method*), a reading was missed at 800 deg F and a temperature sensitivity value could not be obtained.

The results of the tests are shown in Table II. Temperature sensitivity values are expressed as the change of resistance in parts-per-million per deg F. The values obtained for the first test cycles are considerably different from values obtained from subsequent tests. Therefore, an average value for each method for cycles 2 through 10 and the standard deviation of these nine values were computed. These values are shown in Table II.

Discussion

Table II shows that the maximum differences between average temperature sensitivity values found by the various methods are less than five per cent at 400 deg and 600 deg F after the first test cycle. The first cycle values at these temperatures are also in similar agreement except the *simultaneous equations method* at 600 deg F which is about twelve per cent above the other values. At 800 deg F the first cycle values vary widely, but subsequent values are in agreement except the *slow slope method* which gives a value about eight per cent higher than the average of the other values. At 1000 deg F the values differ widely for the various methods and even between test cycles for the same method. The most consistent data at this temperature were obtained for test cycles 4 through 10 with the *fast slope method*. The average of these seven values is 36.1 with a standard deviation of 1.41. This standard deviation compares favorably with values obtained at the lower temperatures. It is also interesting to note that, excluding the first cycle, two of the methods gave positive values and two methods gave negative values.

The differences between temperature sensitivity values obtained by the different methods and variations between cycles for one method might be due to several factors. The most probable of these are:

1. A temperature sensitivity that is varying rapidly with temperature, and
2. A drift rate that varies over a wide range.

At 1000 deg F it is quite possible that both of these conditions exist.

Figure 5 shows representative curves obtained during tests using the *fast slope* and *slow slope methods*. The change of slope of the curve for the *slow slope method* indicates that the temperature sensitivity changes from positive to negative just below 1000 deg F. The curve for the *fast slope method* does not show this change. Since the gage element is completely covered with cement, the insulating and thermal emission properties of the cement in conjunction with the different heating rates used could cause the gage elements to be at considerably different temperatures for the same test strip temperature. It is also quite possible, under radiant heating conditions, that in neither case is the gage element at the same temperature as the test strip. Since the temperature sensitivity depends upon the temperature of both the gage and the test strip (Eq. 1), errors due to a temperature differential are possible.

The curve, Fig. 5, for the *slow slope method* might also represent the conditions for the *simultaneous equations* and the *graph methods*. The temperature sensitivity values for these two methods were determined as the slope of a chord over a temperature increment of 5 deg and 10 deg F, respectively. It is possible that considerably different values, even differing in sign, could be obtained near the knee of the curve depending upon the temperature increment used.

Drift rate values, computed from the data for the *simultaneous equations method*, are shown in Table III. The high drift rate at 800 deg F and the erratic values obtained at 1000 deg F could affect the temperature sensitivity values. The *simultaneous equations* and *graph methods* are designed to eliminate this effect by algebraic and graphical means respectively. The values obtained by the slope methods may be corrected for drift as shown in Eq. 4 if the drift rate is known. Using the average of the drift rate values of Table III for cycles 2 through 10 to apply corrections to data of the *fast slope* and *slow slope methods* at 800 deg F average temperature sensitivity values of 42.7 and 43.1 respectively are obtained. If these corrected values are accepted, the maximum difference between average values for all methods at 800 deg F is less than seven per cent. The maximum difference with the uncorrected values is nearly fifteen per cent. The erratic drift

Table III — Drift Rates Computed from Simultaneous Equations Method Data

Test cycle No.	Drift rate, microhms/ohm • minute			
	400° F	600° F	800° F	1000° F
1	0.2	22.8	729.4	269.4
2	—1.0	3.6	65.8	11.2
3	4.0	8.2	75.6	1.6
4	3.0	2.2	82.8	67.6
5	4.2	2.0	—	47.8
6	3.0	1.6	73.6	59.4
7	—3.2	3.2	82.2	—11.0
8	4.0	2.6	75.6	41.4
9	0.0	0.2	77.4	36.6
10	3.0	7.4	71.6	59.6

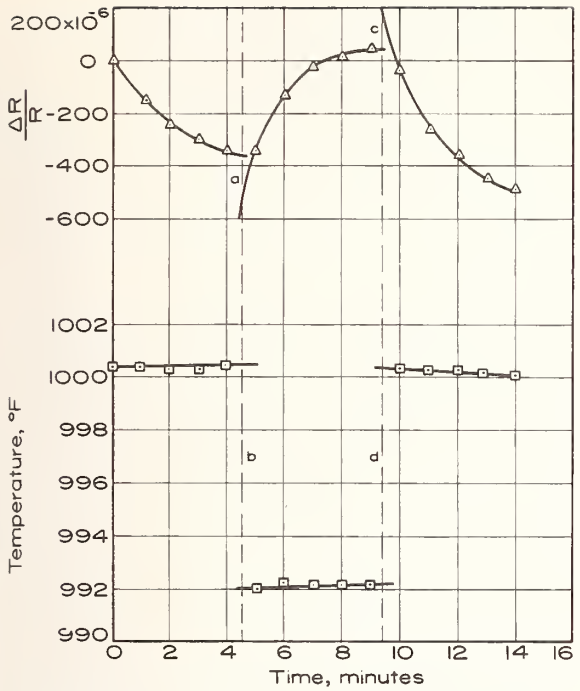

Fig. 6. Graph method results at 1000 deg F showing variable gage response with time and temperature.

rates shown in Table III for 1000 deg F are indicative of the problems that might be encountered. Large variations of drift rate with time and with small temperature changes are also possible as shown in Fig. 6.

Any test made using d-c instrumentation is subject to error due to thermal emf. To avoid such errors care had been taken to use ribbon and wire leads of the same material as the gage element. Success in avoiding any uncompensated emf was verified by making a test by the *fast slope method* with no input voltage to the gage circuit. There was no output signal from the bridge circuit detected during this test. Temperature differences that would cause an uncompensated thermal emf would be most likely to occur in this test method. It was therefore assumed that the error due to thermal emf was negligible during any test.

Although not technical in nature, an important consideration in any test program is the number of man-hours required. It should be recognized that this may vary considerably depending upon the personnel involved, the familiarity with a particular test method, and even the policies of the organization doing the work. To provide some comparison of the methods, Table IV has been compiled from information gathered during the comparison tests. The time for laboratory work includes installing the test strip in the holder, connecting gage leads, preparing necessary data sheets, actual test time, and cooling between test cycles. The time required to install the gages on test specimens is not included. Two people were used during the actual test and cooling periods. The time allowed for data reduction includes calculations by a desk calculating machine and plotting necessary graphs to obtain numerical values of temperature sensitivity. As indicated by the title of the table, the times shown are based on

Table IV — Estimated Time for Determining Temperature Sensitivity Values for One Gage at Ten Temperatures up to 1000 F during Five Heating Cycles

Test method	Laboratory work	Data reduction	Total
	man-hours	man-hours	man-hours
Fast Slope	10	5	15
Slow Slope	15	5	20
Simulataneous Equations	20	5	25
Graph	35	30	65

five test cycles for one gage with ten temperature sensitivity values determined for each cycle.

Conclusions

The results of the comparison tests show that the four methods give values of temperature sensitivity that are in reasonable agreement when the gage resistance is a nearly linear function of temperature and the drift rate is low. Under these conditions the method to be used might be determined by the availability of equipment, familiarity with the method, economics, or other non-technical factors. The "slope" methods are also attractive because they provide a complete record of the gage resistance as a function of temperature while the *simultaneous equations* and *graph methods* give temperature sensitivity values at selected temperatures only. However, the uncertainty in the experimental results, as indicated by the standard deviation, is slightly greater for the "slope" methods.

When a high, constant drift rate is present, the *simultaneous equations* and *graph methods*, which correct for drift, give values that are in close agreement. Values obtained by the *fast slope method*, which should be quite insensitive to drift, agree fairly well with these values. However, values obtained by the *slow slope method* are significantly different unless the data are corrected for the drift.

At temperatures where a variable drift rate and temperature sensitivity are present, the best method would be the one most nearly simulating the conditions of anticipated use. Since the "right" method is the one that predicts what the gage will do under field conditions, it would be presumptuous to say that any of the methods described are "right."

Acknowledgment

The authors gratefully acknowledge the support of the Bureau of Naval Weapons and the Air Force Flight Dynamics Laboratory.

References

1. DeMichele, D. J., Problems in Thermal Stress Measurements, Symposium on Elevated Temperature Strain Gages, American Society for Testing and Materials, Special Technical Publication No. 230, 1958.

2. Bloss, R. L., and Trumbo, J. T., A Method for Measuring the Instability of Resistance Strain Gages at Elevated Temperatures, *ISA Transactions*, Vol. 2, No. 2, 1963.

3. Bloss, R. L., Evaluation of Resistance Strain Gages at Elevated Temperatures, Materials Research and Standards, Vol. 1, No. 1, American Society for Testing and Materials, 1961.

4. Strain-Gages, Bonded Resistance, National Aerospace Standard 942, Aerospace Industries Association of America, Inc., 1963.

5. Bloss, R. L., A Facility for the Evaluation of Resistance Strain Gages at Elevated Temperatures, Symposium on Elevated Temperature Strain Gages, American Society for Testing and Materials Special Technical Publication No. 230, 1958.

8. Vacuum

Micrometer U-Tube Manometers for Medium-Vacuum Measurements

Allan M. Thomas and James L. Cross

National Bureau of Standards, Washington, D. C.
(Received 28 July 1966)

A family of U-tube manometers, suitable for use as standard instruments, has been designed and constructed at the National Bureau of Standards to cover the range of pressures from 100 to 1×10^{-2} Torr. In these instruments the levels of the two liquid surfaces are measured by adjusting micrometers with conical points ground on the ends of the spindles. One hundred-millimeter and 50-mm range mercury manometers, with spindles approaching the liquid surface from above, are used for differential or absolute pressure measurements up to 100 Torr. Pressures less than 3.5 Torr are measured with oil manometers, in which the micrometer spindles approach the surfaces from below. Measurements made with the mercury manometer have an uncertainty of about 4×10^{-3} Torr plus 8 parts in 10^5 of the reading. Measurements made with the oil manometer have an uncertainty of about 4×10^{-4} Torr plus 1 part in 10^4 of the reading.

I. Introduction

There is a need for more accurate pressure measurements in the medium and high vacuum ranges. To fill this need, instruments are required which can be calibrated directly in terms of basic quantities, and which are more suitable than the McLeod gauge over its range. Efforts have been made in our laboratory to extend the useful range of U-tube manometers for this purpose.

The instruments described in this paper were designed for the medium vacuum range. Micrometer-driven index points are employed for the measurement of the liquid column heights. Mercury is used for the range 0.1 to 100 Torr while silicone oil (DC704) serves for pressures below 3.5 Torr. Measurements made with the mercury manometers have an uncertainty in the order of 4×10^{-3} Torr plus 8 parts in 10^5 of the reading. Measurements made with the oil manometer have an uncertainty in the order of 4×10^{-4} Torr plus 1 part in 10^4 of the reading.

These instruments are used to measure differences of pressure, and in the application to vacuum measurements the reference pressure is small compared to the pressure being measured. Some restriction is necessary in the use of the oil manometer because subsequent reduction in pressure after use in the differential mode at high pressures can lead to excessive outgassing. Dissolved gas is not a problem with water as the fluid, but the high vapor pressure limits its use to differential measurements at pressures well above 24 Torr. The advantage of the water manometer, when applicable, is that the value of the density is so accurately known.

The U-tube type instrument was chosen in preference to the fixed-cistern type of manometer, i.e., one in which the height of only one liquid surface is measured, because of lower attainable accuracy with the fixed-cistern instrument. The zero point of a fixed-cistern manometer is affected by the volume of the liquid, the volumes of the liquid menisci, the amount of liquid sticking on the walls as the column is lowered, and the temperature of the manometer. The zero point of the fixed-cistern type is also pressure-dependent because of the change in volume, with change in pressure, of gas trapped beneath the surface in scratches, crevices, and corners. These sources of error are greatly reduced or do not exist in the U-tube instrument (one in which the height of both liquid surfaces is measured).

The principles upon which the design of these instruments is based are not new. Index points and micrometers have been used many times in the last 200 years for locating and measuring the heights of liquid surfaces.[1, 2] However, we feel that the potential performance of this type of instrument has not been fully realized, and we have attempted to obtain improved performance by careful design, by adherence to basic principles of manometry, and by improved measurements through a detailed study of the uncertainties involved.

II. Design Factors

For high accuracy, those factors which are particularly relevant are capillarity fluctuations, uncertainties in the measurement of the column lengths, sine errors

[1] C. F Muendel, Z. Physik. Chem. (Frankfurt) 85, 435 (1913).
[2] M. H. Stillman, Bur. Stds. Sci. Paper. 10, 371 (1914).

associated with changes in level, and uncertainties in the liquid density.

A. Capillarity

Fluctuation in capillary depression, or rise, due to variations in surface tension of the liquid–gas interface and variations in contact angle of the liquid–gas interface with the tube wall are made small by using tubes of large diameter.

B. Column Length

The position of the liquid surface is detected by the formation of a dimple caused by the contact of the index point with the surface. The detection is facilitated by placing a card with a sharply defined boundary between light and dark areas so that the boundary image distorts when the dimple is formed. The setting of an index point on a mercury surface is reproducible to better than 0.001 mm². Such precision can be retained with oil and water as the fluids if the index point is made to approach the liquid–gas interface from below, as in the hook gauge, and the dimple is viewed from below.

C. Leveling

Deviation of the micrometer axes from the vertical introduces a second order (cosine) error in the measurement of column height. Error in this vertical length measurement will be negligible if moderate care is taken to insure that the micrometer axes are vertical.

Of more concern is the uncertainty introduced by a change in the level of the instrument in the plane of the micrometer axes during time of measurement, i.e., between the times of the "zero" and "pressure" settings. This introduces a sine error independent of manometer reading and equal to the product of the distance between the micrometer axes and the sine of the angle corresponding to the change in level.

The effect is reduced by keeping the distance between micrometer axes small and by precise level control.

D. Liquid Density

The fluid densities are affected to varying degrees by pressure, temperature, and the amount of dissolved gases. The value of the density and its dependence upon these factors is well known for both water and mercury. This was not the case for the oil, and such factors had, therefore, to be determined.

To determine density differences in the oil due to differences in the amount of absorbed gases the twin pycnometer method was used.[3] The method consists of filling two similar pycnometers with fluids of two different densities, weighing, switching the fluids, and then weighing again. The difference in density can then be calculated to a high degree of accuracy.

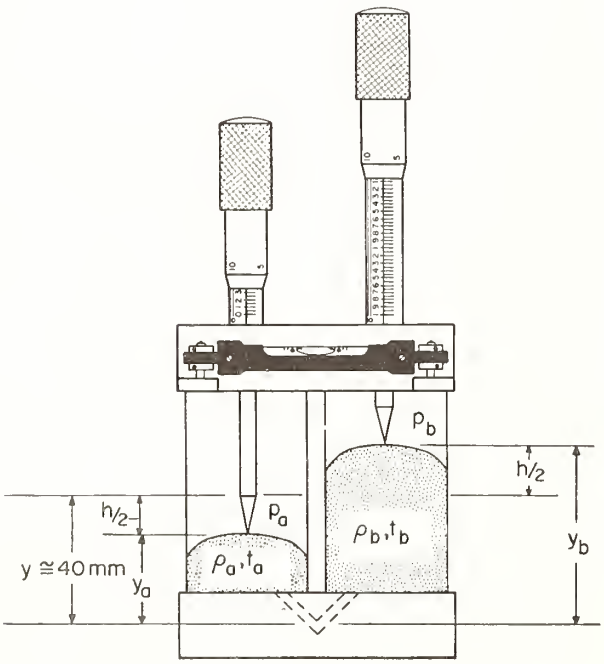

FIGURE 1. Schematic of 2-in. micrometer manometer.

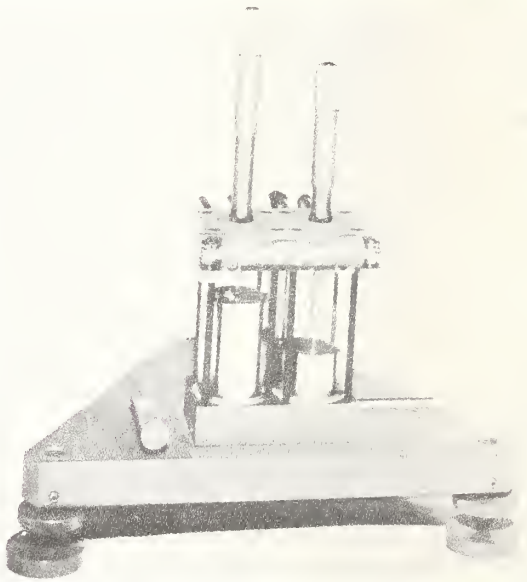

FIGURE 2. Mercury manometer showing four pressure connections from rear of top plate and a dimple formed on the mercury surface.

[3] E. R. Smith and M. Wojciechowski, *The Differential Method of Measuring Differences in Density by Means of Twin Pycnometers.* Committee of Physico-Chemical Data, International Union of Chemistry.

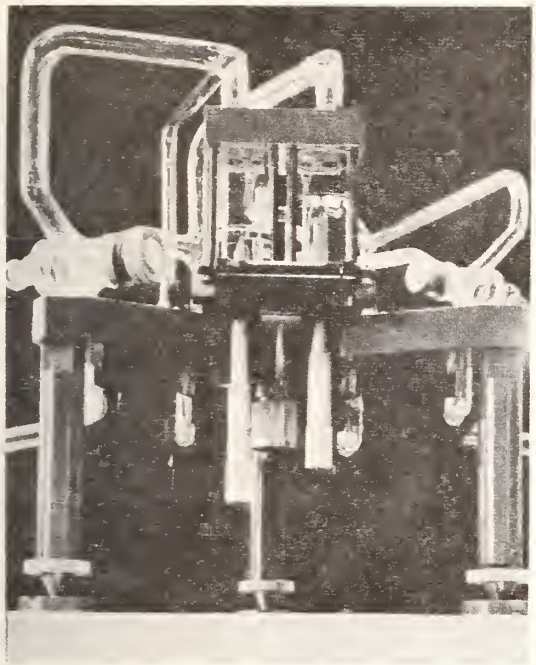

FIGURE 3. Oil manometer with index points approaching the liquid surface from below.

III. Description

A schematic of the mercury manometer is given in Fig. 1. Photographs of the mercury manometer and the oil manometer are given in Figs. 2 and 3, respectively.

In each version, large-diameter (1½ in.) precision-bore glass tubes are clamped between rigid stainless steel end plates and sealed with flat Teflon gaskets. Liquid connection between the tubes is provided by holes drilled in the bottom plate. Vacuum ports are provided in the top plate.

Micrometer-driven index points are mounted in the top plate of the mercury manometer and in the bottom plate of the oil (and water) manometer. Index points, ground on the ends of the micrometer spindles, have a radius of approximately 0.01 mm.

A sensitive level is mounted on the front of that end plate which bears the micrometers. A smaller, less sensitive level is mounted on the base plate perpendicular to the first level. A horizontal hole extending through the length of the lower end plate serves as a thermometer well with good thermal connection to the fluid. Viton O-rings seal the micrometer spindles, which are carefully polished to produce acceptable moving seals.

IV. Error Analysis

The uncertainties associated with these instruments are summarized in Table I. Micrometer calibration is assumed. Note, that the uncertainties independent of reading for the three fluids are proportional to the fluid densities except for capillarity and density errors.

A. Capillarity

With the numerical solutions of Blaisdell,[4] appropriate values for fluid density and surface tension, and contact angle (angle between the liquid surface and the wall) of 0°, the resulting capillarity corresponds to 5×10^{-4} Torr for mercury, 5×10^{-5} Torr for oil, and 1.2×10^{-3} Torr for water. Densities used are 13.5 g/cc for mercury, 1.06 for oil, and 0.997 for water. Surface tension values are 460 dyn/cm for mercury, 38 for oil, and 72 for water.

Since oil and water wet clean glass, it seems unlikely that the difference in the capillary rise in the two tubes would exceed 20% of the capillarity itself, giving an estimate of maximum error of 1×10^{-5} Torr for oil and $\sim 2 \times 10^{-4}$ Torr for water.

The capillarity of mercury is much more variable, but by avoiding readings when the meniscus is nearly flat, the difference in capillary depression in the two tubes will probably be less than 3×10^{-4} Torr.

TABLE I. Summary of analysis of errors.

	Oil	*Water*	*Mercury*
I. Errors not proportional to reading (Estimated bounds of error)		Error (E) in microns of mercury	
1. Level change	0.06	0.05	0.74
2. Capillarity	0.01	0.2	0.3
3. Setting and reading	0.16	0.15	2.0
4. Density	~~0.32~~ 0.44	0.15	1.5
5. Micrometer temperature	0.20	0.19	2.6
Total theoretical ($\sum E^2$)$^{\frac{1}{2}}$	~~0.41~~ 0.51	0.35	3.7
Observed 3 S. D.	0.3		
II. Errors proportional to reading		Error in parts per 10 000 of the reading	
1. Density	~~1.0~~ 1.4	0.5	0.4
2. Micrometer temperature	0.2	0.2	0.2
Total estimated	~~1.2~~ 1.6	0.7	0.6
III. Total of I and II for full scale		Error in microns of mercury	
	0.83	0.60	6.7

[4] B. E. Blaisdell, J. Math. Phys. 19, 217 (1940).

B. Column Length

1. *Micrometer Setting and Reading*

The micrometers used have a vernier reading directly to 0.0001 in. (0.00254 mm). After some experience in detection of the dimple formed by contact of the index point with the surface of the liquid, the surface-height readings by different observers can be reproduced to less than half a vernier division. Our experience indicates that an upper limit of uncertainty for careful setting and reading for two calibrated micrometers of the type used can be taken as about 0.002 mm.

2. *Temperature Effects on Micrometers*

Uncertainties exist because of temperature differences in the micrometer parts and in temperature drift during the time of measurements, particularly due to manipulation. To determine the magnitude of uncertainty, assume that the mounting level shown in Fig. 4 remains constant. The length of the barrel is L_B as shown. The length of spindle below the top of the barrel is L_S at the time of the first setting and $(L_S + L_R)$ after resetting to a new height.

The distance from the mounting level to the point after the first setting is: $D' = L'_S - L'_B$. Correcting for temperature variations from the calibration temperature t_0 to the actual temperatures t'_S and t'_B with temperature coefficients α_S and α_B for the spindle and barrel, respectively, gives

$$D' = L^o_S[1 + \alpha_S(t'_S - t_0)] - L^o_B[1 + \alpha_B(t'_B - t_0)].$$

The zero superscripts indicate that the given lengths are true at temperature t_0. After resetting the micrometer to a new height, the distance D, corrected for new temperatures t''_S and t''_B, is

$$D'' = (L^o_S + L^o_R)[1 + \alpha_S(t''_S - t_0)] - L^o_B[1 + \alpha_B(t''_B - t_0)].$$

The difference in micrometer readings $(R'' - R')$ is

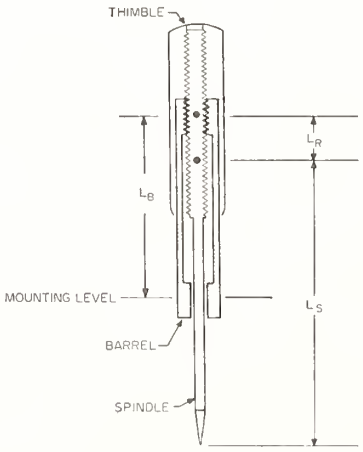

FIGURE 4. Schematic of one micrometer.

L^o_R. Since the temperature of the components is close to the manometer temperature t_m, let $\delta t = t''_S - t_m$. Also, setting $t''_S - t'_S = \delta t_S$, and $t''_B - t'_B = \delta t_B$, the difference in height of the point at the two settings is

$$h = D'' - D' = (R'' - R')[1 + \alpha_S(t_m - t_0)] + (R'' - R')\alpha_S\,\delta t + (L^o_S\alpha_S\,\delta t_S - L^o_B\alpha_B\,\delta t_B).$$

The last two terms represent uncertainties due to the temperature uncertainties δt, δt_S, and δt_B.

Measurements made on the parts of the micrometers during manipulation showed temperature increases in the barrel of as much as $\frac{1}{2}$°C and in the spindle of as much as $1\frac{1}{2}$°C. The temperature increase can be expressed as a variation about an average so that, in the difference between two readings, the average drops out. Normally, several zero readings are taken and averaged so that variations are effectively eliminated in the zero reading.

The temperature increases, δt_B and δt_S, may therefore be expressed as temperature variations of ± 0.25°C and ± 0.75°C, respectively. The barrel length is ~75 mm and the spindle length to the middle of the micrometer range is ~125 mm. The estimated uncertainty of the length measurement from two micrometers, based on an expansion coefficient of 11.5×10^{-6}/°C, is 2 parts in 10^5 of the reading plus 2.6×10^{-3} mm.

C. Leveling

The distance between micrometer axes is 47.6 mm. The level parallel to the plane of the axes has a sensitivity of 16 sec of arc/div. As the manometers can be leveled to within one-fifth of a division, the sine error is not greater than 47.6 sin (0.2×16), or 0.00074 mm.

D. Density

The densities of mercury and water are well-documented. Measurements of the density of DC 704 in our laboratory gave a value of 1.0610 g/cc for oil at 25°C saturated with air at 1 atm.

1. *Compressibility*

This is a negligible effect as the compressibility of oil[5] and water are about 50 ppm for a pressure change of 1 atm, and that of mercury[6] is ~4 ppm.

2. *Temperature*

The pressure balance at the liquid-connecting port of the two manometer tubes, as shown in Fig. 1, is simply

$$p_a + y_a\rho_a g = p_b + y_b\rho_b g,$$

where p, y, and ρ are the pressure, column height, and

[5] ASME Research Publication, Pressure-Viscosity Report (1953).

[6] W. G. Brombacher *et al., Mercury Barometers and Manometers*, NBS Monograph 8 (1960).

density for the particular limb. The density varies with temperature as

$$\rho = \rho_r/[1 + m(t - t_r)],$$

where ρ_r, t_r are reference values, and m is the volume expansion coefficient. Thus,

$$(p_a - p_b)/\rho_r g = \{y_b/[1 + m(t_b - t_r)]\} - \{y_a/[1 + m(t_a - t_r)]\}.$$

The factors are readily separated by referencing column heights to the average value (essentially the heights at zero differential pressure) and temperatures to the thermometer value (manometer temperature, t_m); i.e., let

$$y_a = y - h/2 \quad \text{and} \quad y_b = y + h/2$$
$$t_a = t_m + \delta t_a \qquad t_b = t_m + \delta t_b,$$

where h is the pressure head. Then, to first-order approximation,

$$(p_a - p_b)/\rho_r g = h - hm(t_m - t_r) + ym(\delta t_a - \delta t_b) - (hm/2)(\delta t_a + \delta t_b).$$

The second term is a correction. The third is an uncertainty independent of reading while the fourth represents an uncertainty proportional to the reading.

The length of the columns at zero pressure differential is about 40 mm. The expansion coefficient for mercury is 182×10^{-6}/°C and, for water, 250×10^{-6}/°C. The value for DC 704 was determined in our laboratory and is 70×10^{-5}/°C. Temperature variations of the liquid in each tube from the manometer temperature reached 0.2°C in a room with temperature fluctuations of several degrees. The resulting uncertainties are shown in Table I.

3. *Gas Absorption*

Measurement of the density difference between degassed oil and oil saturated with air at 1 atm, using the twin pycnometer method,[3] showed that for DC 704 and 705 the differences were less than 1 part in 10^4 of the density.

V. Observation of Zero Reproducibility

To determine the performance of a U-tube type manometer, the most significant test is the agreement of observations taken at zero pressure difference. In such a test the observations are affected by all random effects which are not proportional to the pressure.

In the present case, repeated zero readings for the oil manometer, extending over a period of weeks, resulted in a standard deviation of approximately 1×10^{-4} Torr for more than 30 readings. The value of three standard deviations (3σ) is about the same as the estimated 4.1×10^{-4} Torr given in Table I. A check of the standard deviation of zero readings for the mercury manometer resulted in a similar fair agreement with the estimated error.

VI. Remarks

The practical potentiality of this type of manometer is believed to be somewhat better than reported here. The uncertainties associated with the micrometer measurements can certainly be decreased. The technique of pressure reversal, i.e., applying the unknown pressure first to one leg and then to the other, can effectively reduce the level error, not the least of those to be considered.

Based on the foregoing analysis of errors we believe that the uncertainty associated with the oil manometer can be reduced to about 1×10^{-4} Torr plus about 5 parts in 10^5 of the pressure being measured.

Calibration to High Precision in the Medium Vacuum Range with Stable Environments and Micromanometer*

Stanley Ruthberg

National Bureau of Standards, Washington, D. C.

(Received 22 July 1968)

Ultrastable vacuum environments are combined with a micrometer-point contact manometer to obtain a calibration uncertainty of 1.2×10^{-4} Torr + 6 parts in 10^5 of the reading for the range 1×10^{-4} Torr to several Torr. The stable pressures are generated with a dynamic vacuum system and a servo control loop which employs cascaded error signals from a capacitance-diaphragm gauge to obtain pressure stabilities of better than ±1 part in 10^5 at 1 Torr. Precise evaluation of systems and procedures is given. Operational factors that affect accuracy were studied, for example, sorption in the manometer fluid, pressure distribution in the test chamber, time constants of the micromanometer, and thermal response of the control loop.

Introduction

Absolute pressure measurements of increased accuracy are needed in the medium vacuum range for calibration activities and for direct application to a number of scientific problems. Furthermore, such improvement can also lead to increased measurements confidence at yet lower pressures. These measurement techniques would serve as a base against which to compare other reference instruments, such as the McLeod gauge, which are intended for use in a lower pressure range, and could be applied to the upstream stages of the various pressure dividers used for calibration at even lower pressures.

The attainment of high accuracy requires the combination of a suitable reference standard along with a vacuum environment so stable as to cause little degradation in performance. Calibration activities would further be facilitated by a relatively rapid and reproducible generation of test point pressures.

The first requirement for an "absolute" reference instrument was met with one of a family of U-tube micrometer-point contact manometers previously evolved at this laboratory for the purpose. Analysis of instrument design and experimental observation of zero point behavior established that a measurement uncertainty of less than 5×10^{-4} Torr[1] plus 1.6 parts in 10^4 of the reading should be obtainable with silicone pump fluid as the manometric medium. It was predicted that a limiting uncertainty would be about 1×10^{-4} Torr plus 5 parts in 10^5 of the reading.[2] However, the use of the micromanometer as a reference standard required thorough evaluation of and appropriate compensation for those operational factors which could degrade over-all measurement accuracy. Examples are sorption effects in the manometer fluid, time constants due to oil drainage on the U-tube walls, mechanical stability, and the effects of temperature variations.

Ultrastable pressures, the second requirement, were generated by a dynamic vacuum system and an electrical servo-control loop with cascaded error signals from a capacitance-diaphragm gauge. Stabilities were obtained of better than ± 1 part in 10^5 at 1 Torr. Given values of pressure were generated at will and reproducible to within the measurements uncertainty.

The overall calibration uncertainty obtained (three standard deviations) was about 1.2×10^{-4} Torr plus 6 parts in 10^5 of the reading from 1×10^{-4} Torr to several Torr. This accomplishment is not so much dependent on the actual equipment that is used as on a careful evaluation of the factors involved and the development of operational procedures, which are appropriate to any laboratory. Systems, vacuum and electronic, were essentially assembled from commercially available components, and the micromanometer is of relatively simple construction.[3]

The following text describes and gives precise evaluation of the systems, procedures, and factors involved in generating such stable, reproducible pressures and for obtaining so small a measurement uncertainty. The dynamic systems and control loop for generating the stable environments are presented in Sec. I. Procedures for further reducing the uncertainty with the micrometer manometer toward that of the predicted level

[1] 1 Torr = 1.33322 millibar = 133.322 newtons/m^2.

[2] A. M. Thomas and J. L. Cross, J. Vac. Sci. Technol. 4, 1 (1967).

[3] A. M. Thomas and J. L. Cross, NBS Tech. Note 420 (1967).

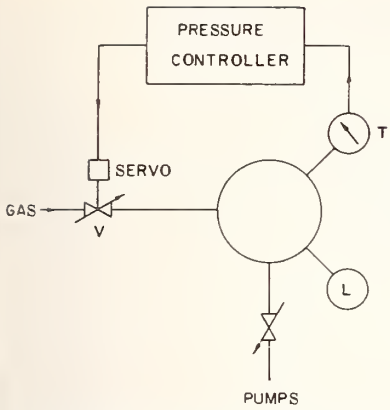

FIGURE 1. Schematic for pressure regulation with a servo loop and dynamically operated vacuum system.

are detailed in Sec. II. Operational factors affecting accuracy are covered in Sec. III.

I. Generation of Stable Pressures

A. Operational Concepts

It is a familiar procedure to regulate the pressure in a vacuum chamber by use of a servo-controlled valve. With an arrangement as in Fig. 1 the pressure control unit accepts an electrical output signal from a suitable vacuum gauge T attached to the chamber, compares this signal against a reference voltage, and amplifies the difference signal to actuate a motor-driven valve V in a correcting mode to reduce the difference signal to zero. In practice, both the gain and the frequency response of the controller must be adjusted for optimal effect, which obviously is a function of the integrated characteristics of both the electronic and vacuum elements of the control loop. That is, as a feedback problem, control depends upon the sensitivity, stability, and frequency response of the vacuum gauge, upon the stability of the reference voltage, on the servo amplifier and motor drive characteristics, on the conductance vs. position dependency of the leak valve, on the gas supply pressure and its stability, on the time constants of the vacuum manifold, and on the behavior of the pumping array. Therefore, increased pressure stability depends upon upgrading the performance of the controls, upon reduction of base pressure fluctuations, and upon achieving favorable time constants.

Commercially available pressure controllers have maximum sensitivities of approximately one part in 1000 of full-scale with an actual control capability of somewhat less than this. Pressure stabilities of about 1% are normally obtained. Our procedure for increased control capability is to insert an extra differential stage between the commercial pressure controller (Figs. 1, 2) and the stable pressure transducer T. In principle, this stage takes the output signal from the transducer and compares it against a very stable reference voltage. The difference signal so obtained is amplified and then applied to the pressure controller. Thus, this affects a cascading of error signals which shifts the burden of stability and sensitivity from the pressure controller to the transducer and differential stage. In practice, the stable transducer and differential stage are available as incorporated into certain commercially supplied capacitance-diaphragm gauges.

Extreme pressure stability is now achieved through the sensitivity of the transducer in conjunction with stable gas pressures of suitable magnitudes upstream

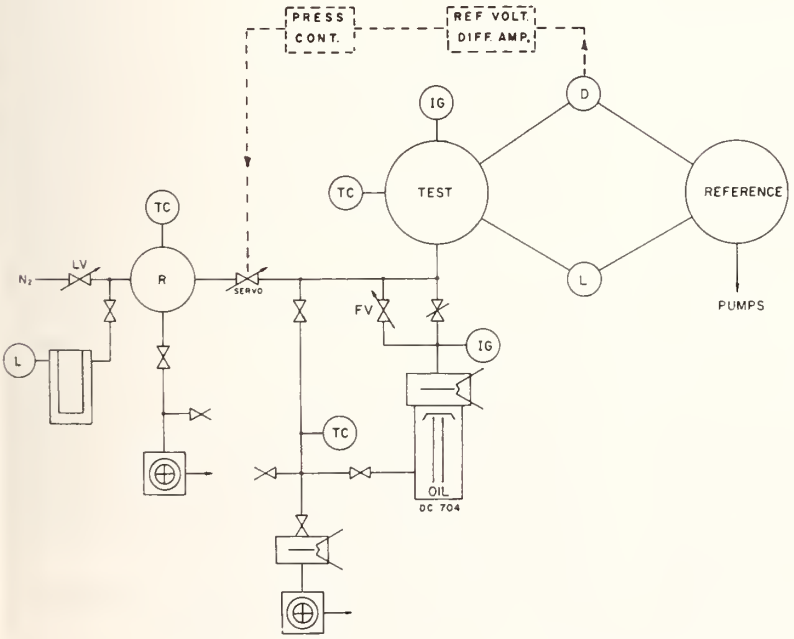

FIGURE 2. Operational vacuum system circuit diagram with pressure generator in detail. Reference system was essentially identical to test system.

to the leak valve, clean vacuum systems, the throttling of the vacuum pumps to appropriate speeds, the selection of servo characteristics for proper gain-time constants, and close temperature control.

B. Vacuum Systems

1. *General Circuit Description*

Two vacuum systems are needed, one for the reference vacuum and a second for the pressure generator. The two used here were identical except for the features added to the pressure generator for increased stabilization. Figure 2 is the vacuum circuit diagram for the overall systems with the pressure generator shown in detail.[4] The features that are additional to the basic circuit are the servo-operated leak valve and the stable gas source. This source comprises chamber R, mechanical pump, leak valve LV, and gauges L and TC. As erratic behavior of the vacuum system had to be minimized, clean and stable manifold wall conditions were necessary. Bakeout was not used, but the materials, components, and operating procedures used conformed to those common to ultrahigh vacuum practice. All fixtures in the high vacuum region were stainless steel except for the manometer glassware. The joints were inert gas fusion welded, or flanged and metal gasketed with aluminum foil seals.[5] The valves were bellows sealed. The only elastomers present were in the valve disks, in the manometer, and in the capacitance-diaphragm gauge head. The pump fluid was the same as the manometer fluid, DC 704 silicone oil, and the baffles over the diffusion pumps were mechanically refrigerated to $-25°$ C. Pumping speeds at the chambers were estimated as about 30 liters/sec. Ultimate chamber pressures with the manometer and capacitance-diaphragm gauge connected were routinely $< 2 \times 10^{-7}$ Torr.

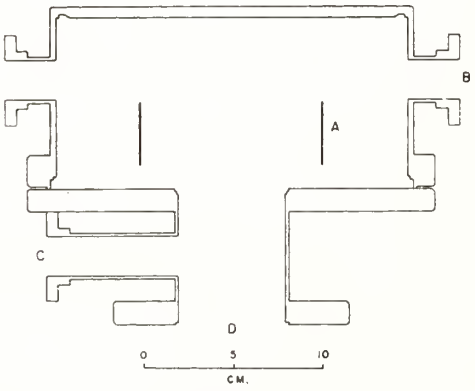

FIGURE 3. Schematic of cylindrical test chamber geometry with internal baffle for low pressure symmetry. A—baffle, B—test port, C—gas inlet, D—pump lead.

2. *Vacuum Chamber*

In order to minimize pressure gradients within the test chamber, the gas inlet and outlet (Fig. 2) were placed below the chamber so that the net gas exchange in the test chamber was essentially zero at steady state. As the inlet line was asymmetrical about the chamber axis, an internal baffle was further incorporated to insure a symmetrical pressure distribution at the ports for conditions of long molecular mean free path. The chamber geometry and the baffle location used here are given in the sketch of Fig. 3. The cylindrical baffle is of such a length and location as to optically block the ports from the inlet line.

3. *Pump Stability*

Since the servo loop becomes very sensitive and limited in response time at these precisions, it becomes necessary to minimize abrupt pressure fluctuations in the test chamber. Diffusion pumps are a source of such disturbance. But, this effect is readily attenuated by adjusting the throughput by use of the throttling valve between the chamber and the pump to lower the pump pressure. Adjustment is made until the fluctuation of base pressure over the pump and, hence, that reflected into the chamber is within the control band of the servo, and small compared to the manometer uncertainty. The servo-controlled leak valve automatically repositions to hold pressure constant. However, its position, hence response, is a factor in control characteristics, and the pump speed determines allowable throughput.

The pumps used here were of standard metal, fractionating design with a rated speed of greater than 150 liters/sec. Observation of base pressure showed fluctuations of up to 8% of the operating pressure. Pressures as indicated at the ionization gauge between the baffle (Fig. 2) and the test chamber of 4×10^{-4} Torr were found adequate for chamber pressure of $\geq 1 \times 10^{-1}$ Torr and ranged downward to 6×10^{-7} Torr for chamber pressure of 1×10^{-4} Torr. Throughputs ranged from the order of 1×10^{-5} Torr liters/sec. at the low pressure to 1×10^{-2} Torr liters/sec at the high end.

4. *Gas Supply*

The gas supply can also be a source of pressure fluctuations. In addition, the pressure of the gas supply is a parameter that affects the time constants of the servo loop. Thus, a quiescent gas supply was obtained with an isolating reservoir R adjusted to the desired pressure.

In our operation, the reservoir R of 4-liter volume

[4] AVS Standard (tentative) 7.1-1966. (See, J. Vac. Sci. Technol. 4, 139 (1967).

[5] S. Ruthberg and J. E. Creedon, Rev. Sci. Instr. 26, 1208 (1955).

was initially roughed to $\sim 10^{-2}$ Torr and filled to the desired pressure; between 50 Torr and 1 atm. The leak valve *LV* was then set to allow a small flow of gas into *R* which was just sufficient to maintain the pressure to within a few Torr.

Use of such a quiescent gas supply of chosen pressure gave a 30-fold improvement in stability over the use of a gas bottle with a normal pressure reducer.

C. Control Function

1. *Control Gauge*

The procedure requires a gauge (D, Fig. 2) whose sensitivity is greater than that of the micrometer-point contact manometer in the range of operation. Linearity of response is not essential, only that the pressure response be 1-to-1 and continuous throughout the range. Hysteresis and repeatability are not basic factors in this operation, but stability is. Commercially available capacitance-diaphragm gauges are capable of obtaining a smaller minimum detectable signal and evidence greater sensitivity than the micrometer-point contact manometer. These gauges can also be equipped to operate in a balanced or differential mode with an adjustable reference value and with various ranges of differential signal amplification.

The characteristic response of such an instrument equipped for 1 Torr full range is shown in Fig. 4 as compared against both an ionization gauge and the micrometer-point contact manometer. The data for pressures greater than 1×10^{-5} Torr represent the control mode; that is, these data were obtained with pressures stabilized by the described procedures and with the apparatus under discussion.

2. *Pressure Controller*

The automatic pressure controller comprised a control unit and a servo motor-driven ultrahigh vacuum valve. Maximum sensitivity was 0.2% of full scale. Reference, gain, and damping functions were incorporated. An input range selector was also provided in the form of an attenuator.

3. *Servo Loop Operation*

Initially the servo-controlled leak valve is closed and the chamber pumped to low pressure (Fig. 2). The reservoir *R* is filled and leak valve *LV* is adjusted. The fine valve *FV* between the chamber and the pump is set and the main valve closed. The reference value for the desired pressure is set on the capacitance-diaphragm gauge and a large differential scale is selected. The reference value on the controller is set to zero. The motor drive is actuated, controller gain is activated, and the pressure allowed to stabilize. A smaller range differential scale is then selected and

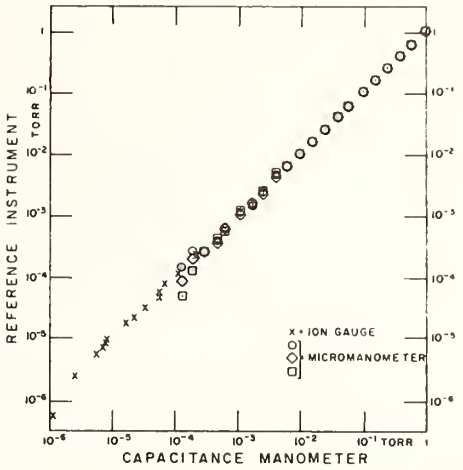

FIGURE 4. Gauge characteristic for the capacitance-diaphragm instrument used in the servo loop. Three independent runs are indicated with the micromanometer as reference.

the pressure allowed to restabilize. However, one cannot simply continue to increase the initial amplification by proceeding to smaller and smaller differential scales for corresponding improvement in stability, for such cascading technique is soon limited in application by the gain-time constant characteristics of the control loop itself, i.e., pressure gauge—pressure control unit—servo-driven leak valve—vacuum manifold—gas inlet supply—pumping speed.

In practice, the gain and damping functions of the pressure controller are optimized for minimum pressure excursion for any given input signal. A variable attenuator is also used at the input to the controller to modify the difference signal from the pressure gauge for further adjustment of gain-time constants and sensitivity. This function can be performed by the input range selector of the controller itself. If the gauge sensitivity is then increased by stepping to smaller differential scale, the gain-damping settings on the controller will have to be changed accordingly. Usually controller gain is reduced and damping increased until with successive steps regulation is lost. Greater sensitivity then depends upon change in the time constants and further reduction in system noise. In the present case noise reduction was achieved with stabilized gas supply, throttled pumps, clean systems, and use of constant voltage sources for the electronics. Time constants were modified by the pressure in the gas supply reservoir and by pumping speeds.

We found that our most stable and best control conditions were obtained for a less than critically damped system, i.e., with the loop gain almost large enough to hold the system in a steady oscillatory state. Once locked in, the pressures can be held constant for extended periods. Such a situation is evidenced in Fig. 5 which shows initial lock-in and response of

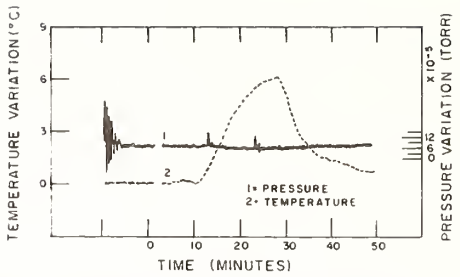

FIGURE 5. Servo control characteristic: Initial lock-in and response to a large temperature pulse at an operating pressure of 1 Torr.

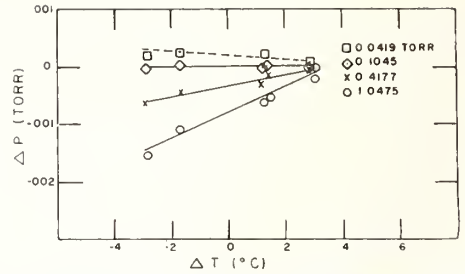

FIGURE 7. Change in controlled operating pressure due to change in temperature on the control gauge head for various pressure control settings, a measure of temperature coefficient.

indicated pressure to a large ambient temperature change. As indicated, pressure fluctuation was about 1.5×10^{-5} Torr peak-to-peak at a pressure of 1 Torr. Stabilities of 2.6×10^{-6} Torr peak-to-peak have been obtained.

Determination of the control settings for given chamber pressures is a time consuming, painstaking operation. Once these are determined, however, the very same pressures and stabilities can be quickly reestablished. It is easier to find and repeat the control settings if the orderly procedure is used of starting at the lowest pressure and working upward, since the gain-time constant factors vary progressively with pressure.

4. *Zero Drift and Temperature Coefficient*

The pressure in the chamber is automatically adjusted by the servo control loop to obtain a constant electrical output from the pressure gauge. The true pressure can deviate from the electrical indication of the pressure gauge because of gauge drift and because of thermal transpiration resulting from the rise in operating temperature of the gauge head. Ambient temperature effects on the capacitance-diaphragm gauge head were examined by use of a thermal enclosure with forced air circulation in which temperature could be held constant to within 0.1°C.

Transient drift, as evidenced in the change of gauge zero, was evaluated with the vacuum chamber at system ultimate pressure and servo control inoperative. When the enclosure was held at a constant tempera-

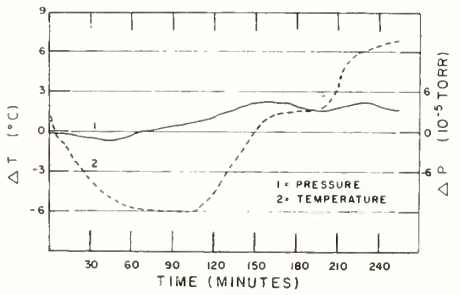

FIGURE 6. Zero drift of the controlling capacitance-diaphragm gauge with change in ambient temperature.

ture equal to average room ambient and with the room ambient temperature variation of not more than ± 0.5°C, zero drift was found to be $< 3 \times 10^{-6}$ Torr for 8-h periods. Slow temperature changes within the enclosure, however, caused initial zero shift in the same direction as the temperature change followed by some recovery. This behavior is indicated in Fig. 6. A negative temperature excursion roughly trapezoidal in profile with a range of about 7°C and of a 3-h duration caused variation of the indicated pressure of $\sim 5.4 \times 10^{-5}$ Torr peak-to-peak or a zero drift of $\sim 0.8 \times 10^{-5}$ Torr/°C.

The temperature coefficient was determined with the control loop in a stabilized mode of operation. A given temperature was established in the enclosure, and a sequence of stable pressures was generated. Each was measured with the micrometer-point contact manometer. This procedure was repeated for a number of temperatures above and below the normal operating ambient temperature ($\sim$ 23° C) with the identical servo control settings used for each pressure sequence. The resultant data, including the effect of gauge repeatability, are indicated in Fig. 7 where, for the purpose of display, the pressure differences are referenced to the pressures measured at $\Delta T = 2.9$°C. The measured operational temperature coefficient (per degree Celsius) amounts to $\sim$ 2.5 parts in 10^4 of the pressure at the higher pressures, becomes zero at $\sim$ 0.1 Torr, and appears to be reversed in sign at $\sim$ 0.04 Torr.

The temperature coefficient found here, due to closer coupling in the thermal enclosure, is somewhat larger than would be obtained with normal ambient variations. The behavior shown in Fig. 8 indicates a factor of $\sim$ 0.8; therefore, the temperature coefficient for operational environment is $\sim$2 parts in 10^4/°C at higher system pressures. It is also clear from Fig. 8 and from Fig. 11 that temperature fluctuations of short duration receive greater attenuation than those of long duration and are thence of less concern.

Stability requirements of the order of 1 part in 10^5 at 1 Torr thus set a limit on the variation in average ambient temperature of < 0.1°C at the transducer, with appropriate relaxation in requirement for lower

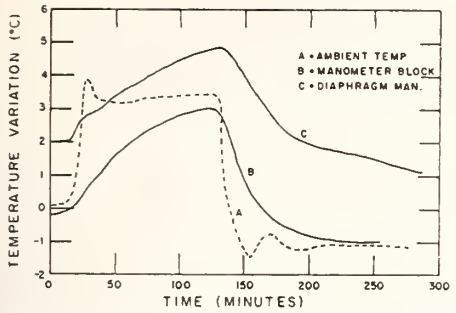

FIGURE 8. Thermal response of the housing of the control gauge head and of an end plate of the micrometer-point contact manometer for a square temperature wave. Housing operated ~ 2°C above ambient under normal conditions.

pressures. Comparison of data for slightly different ambient temperatures can be done by incorporating corrections derived from the temperature coefficients.

Presumably, the negative slope of the 0.04 Torr characteristic in Fig. 7 is due to thermal transpiration. As the pressure decreases, the magnitude of the instrument's temperature effect diminishes and that of transpiration increases to a maximum value in the molecular flow range of $P_1/P_2 = (a/b)\ (T_1/T_2)^{1/2}$, where a and b are related to the transition probabilities of the vacuum lines connecting gauge and manometer to the chamber, and P_1 and P_2 are the values at the gauge and micromanometer.[6] The two effects are in the opposite sense. The transpiration effect between the micromanometer at ambient temperature and the gauge head increases with the head temperature; thus, the system pressure will adjust to lower values at the micromanometer as the gauge head gets warmer, since the controlled pressure at the head is essentially constant. Specifically, in terms of the data of Fig. 7 for an estimated internal temperature of the head of 30°C for normal conditions, a ΔT of 6°C from −3 to +3°C in the head leads to values of $(T_1/T_2)^{1/2}$ for T_2 at 23°C of 1.0067 and 1.0168 resulting in a 1% change of apparent pressure. While the instrumental temperature effect would be a $+ 6 \times 10^{-5}$ Torr at 0.04 Torr for the 6°C change, a maximum transpiration effect would be -4×10^{-4} Torr. Therefore, the net effect should be a shift of not greater than $\sim -3 \times 10^{-4}$ Torr with actual value determined by proximity to the transition region of pressures. The observed change in pressure of $\sim 1.5 \times 10^{-4}$ Torr was just within the precision of our manometer.

D. Thermometry

Measurement of relative temperatures and temperature variations at various parts of the equipment and of the atmospheric air were obtained with sensitive thermocouple procedures. Thermocouple junctions were inserted into small aluminum disks, which were then clamped to a given part or suspended in the ambient air. All thermocouple leads were connected to a master thermocouple switch bearing a common reference junction at the ice point. Thermocouple output was compared against a stable millivolt source to generate a difference signal which was amplified by a dc microvoltmeter and recorded with a strip chart recorder for a sensitivity of ~0.01°C. Initial calibration of relative response was determined by clamping all units within a small area on an end plate of the micromanometer when exposed to ambient air.

Precision mercury thermometers calibrated to 0.1° C were used to measure the ambient atmosphere and manometer temperatures.

II. Uncertainties in Micrometer Manometer Measurements

A. Description and Mounting of the Micromanometer

The micrometer point contact manometer is a U-tube instrument of large bore (1½ in.) in which the fluid surfaces are located from below by micrometer-driven index points. Sensitive levels are mounted to monitor sine and cosine errors. The manometer temperature is determined with a precision thermometer set into a lower end plate and closely coupled to the DC 704 fluid. Complete description is given in Ref. 2.

The arrangement used in these studies to allow for various interconnections of the micromanometer, capacitance-diaphragm gauge and vacuum systems is given schematically in Fig. 9. The setting of valves for normal operation is shown. It was possible to reverse each gauge or to interconnect them in order to evaluate performance as discussed below. The instrument was mounted on a solid pier with mechanical isolation from the vacuum systems obtained by the use of long metal bellows in each connection. The vacuum systems and the mechanical pumps were each in turn set on vibration dampeners. Actual setup is shown in the photograph of Fig. 10.

The relationship of the pressure to the measured manometric height and to the various uncertainties is as derived from Ref. 2 and used here:

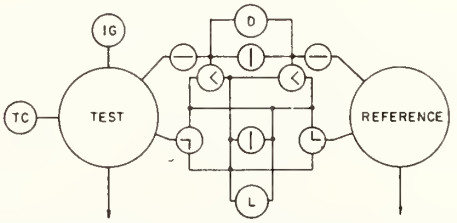

FIGURE 9. Manometer manifold. Arrangement of valves and lines for the control gauge and micromanometer. Valve settings correspond to normal operation.

[6] T. Edmonds and J. P. Hobson, J. Vac. Sci. Technol. 2, 182 (1965).

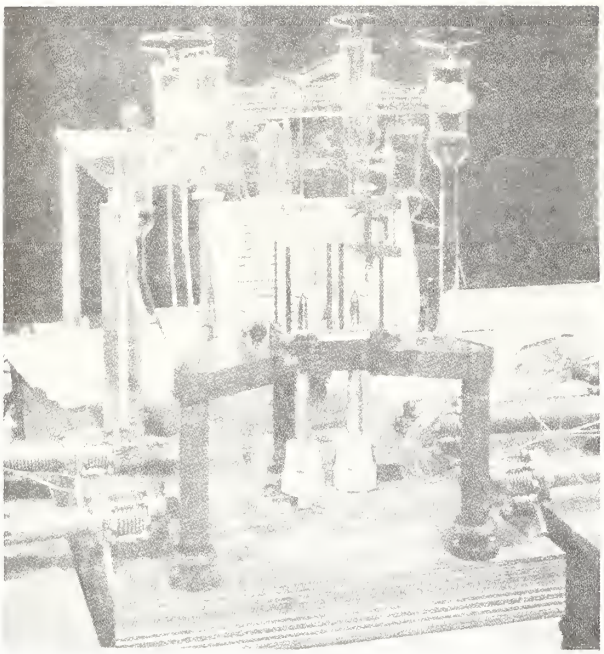

FIGURE 10. Mounting and details of the micrometer-point contact manometer.

$$\frac{P_a - P_b}{\rho_r g} = H[1 - m(t_m - t_r)] + H(m/2)\,(\delta t_a + \delta t_b) + ym(\delta t_a - \delta t_b). \quad (1)$$

For which

$$H = [(R_h'' - R_l'') - (R_h' - R_l')][1 + \alpha_s(t_m - t_0)] + [(R_h'' - R_l'') - (R_h' - R_l')]\alpha_s\,\delta t + 2[L_s^0\alpha_s\,\delta t_s - L_\beta^0\alpha_\beta\,\delta t_\beta], \quad (2)$$

where:

P_a, P_b = pressures over each arm of manometer, Torr;
R_h'', R_l'' = micrometer readings for high and low column levels;
R_h', R_l' = zero point readings;
ρ_r, t_r = reference density and temperature for fluid (1.0610 g/cm^3, 25°C);
m, α_s, α_β = expansion coefficients for fluid, micrometer spindles and barrels (70 × 10^{-5}/°C, 11.5 × 10^{-6}/°C, respectively);
L_s^0, L_β^0 = spindle and barrel lengths;
t_m = manometer temperature, °C;
t_0 = reference temperature for micrometer calibration (20°C);
y = average length of columns;
δt_a, δt_b, δt_s, δt_β = uncertainties in temperature of manometer columns and micrometer parts and,
δt = difference in temperature between micrometer spindles and manometer.

TABLE I. Summary of analysis of errors.

I. Errors not proportional to reading: (Estimated bounds of error)	Previous error (E) in millitorr	Present
(1) Level change	0.06	0.03
(2) Capillarity	0.01	0.01
(3) Setting and reading	0.16	0.10
(4) Density	0.44	0.06
(5) Micrometer temperature	0.20	0.02
(6) Pressure stability	...	0.01
Total theoretical $(\Sigma E^2)^{\frac{1}{2}}$	0.51	0.12
Observed 3 S. D.	0.3	0.07 to 0.13
II. Errors proportional to reading:	**Error in parts per 10 000 of the reading**	
(1) Density	1.4	0.4
(2) Micrometer temperature	0.2	0
(3) Manometer temperature	...	0.2
	1.6	0.6
Total of I and II for 1 Torr	6.7×10^{-4}	1.8×10^{-4}

These uncertainties as previously evaluated[2] and the present improved values are listed in Table I.

B. Leveling

Any change in the level of the instrument in the plane of the micrometer axes that occurs between measurements of the liquid surfaces introduces a sine error. This is independent of manometer reading and equals the product of the distance between the axes and the sine of the angle of change.

The valving arrangement indicated in Fig. 9 allowed testing of pressure reversal as a possible procedure to reduce leveling errors. Its application depends upon retention of identical levels during the reversal; whereas, implementation requires operation of valves, pump down, and reestablishment of the identical test pressure in that arm which was the reference arm previously. This proved to be somewhat awkward in practice.

Rather than using that procedure, uncertainty was reduced by increased mechanical stability and by greater precision in the use of the level. Optical magnification of the level's scale and bubble along with the positioning of one end of the bubble at a fiducial mark allowed sensing to 0.1 scale divisions. The mechanical stability was such that the bubble remained in this position for long periods. Its position was monitored and occasional level adjustment made

to hold the identical position. Any change in level thus corresponded to less than 0.1 divisions of the level scale or to less than 3×10^{-5} Torr, which is $\frac{1}{2}$ the previous estimate of uncertainty.

C. Micrometer Setting and Reading

A dimple is formed in the liquid surface on contact with an index point. It is observed by the distortion of a geometrical pattern, reflected in the liquid surface as viewed from below with a magnifying lens. The micrometer is adjusted for minimum detectable dimple with final micrometer motion always in the same direction. The micrometers used for the present effort had verniers reading directly to 0.0001 in. (0.00254 mm). With experience and the aid of optical magnification, it was found possible to read these to $\frac{1}{5} \pm \frac{1}{10}$ of a vernier division by comparing the index marks bounding an interval on the vernier scale to their counterparts on the thimble scale; that is, it is possible to distinguish fractions of a vernier division of 0.2 from 0.4 from 0.6, etc. Thus, we believe our uncertainty for reading of the micrometers was $\pm$ 0.1 vernier divisions or $\pm 1 \times 10^{-5}$ in.

The estimated uncertainty for setting and reading is derived in the following way: Experience shows that detection of the surface can be accomplished at least as precisely as the micrometers can be read. We, therefore, choose the uncertainty for setting and reading of a single surface as twice that of a reading and, thence, quadruple for both surfaces, as a conservative estimate. We consider this value, 4×10^{-5} in., as a minimum uncertainty. At the other extreme, many observations have indicated a maximum spread in a series of fixed surface readings to be 6×10^{-5} in. or $\pm 3 \times 10^{-5}$ in.; therefore, for two surfaces we choose a variation of $\pm 6 \times 10^{-5}$ in. as a maximum value, where these data include setting, reading, short term leveling and temperature effects. The estimated uncertainty for setting and reading is then taken as the mean value of 5×10^{-5} in. (1.27μm) which is equivalent to $\sim 1 \times 10^{-4}$ Torr.

D. Temperature Effects on Micrometers

Three uncertainties are evidenced in Eq. (2) as arising from micrometer use. One is in the average micrometer temperature (t_m), and two are due to differences in the temperatures of the micrometer components caused primarily by manipulation. Of the latter, the major contribution is independent of reading. These uncertainties were reduced and determined by the following.

Thermocouples were firmly taped to the parts of a micrometer while in position in the manometer end plate. Temperatures were monitored with the sensitive procedures given in I.D. The micrometer temperatures were recorded initially with ambient temperature under close regulation. Sufficient insulation was then placed over the thimble, as can be seen in Fig. 10, until no change in temperature was indicated upon long time manipulation. Any change in temperature was < 0.05°C. A cork layer $\frac{1}{4}$ in. thick over the sides and end of the thimble was necessary.

Thermal uncertainties proportional to the reading are by the second term of Eq. (2) < 1 part in 10^6. With spindle length of 125 mm and barrel length of 75 mm, the fixed uncertainty by the last term of Eq. (2) with δt's of ~ 0.05°C is equivalent to $\sim 2 \times 10^{-5}$ Torr.

Consideration of local errors in the micrometer screws was not included, since the uncertainties arising are a function of the particular micrometer calibration itself and do not bear on the present investigation. Such micrometer uncertainties would be added for absolute measurement.

E. Density and Column Length

The magnitude of the effect of temperature variations on the density of the oil columns makes the measurement and control of temperature critical. Each tenth degree of uncertainty in the last two terms of Eq. (1) leads to an uncertainty of 2.2×10^{-4} Torr plus 0.7 parts in 10^4 of the reading for 40-mm-length oil columns. From the first term of Eq. (1) each tenth degree of error in the manometer temperature causes an error of 0.7 parts in 10^4 of the reading. The difficulty is not so much with short time ambient fluctuations as Figs. 8 and 11 show, for these higher frequencies are attenuated in the manometer itself. The problem is with low frequency cycling and drift where the manometer temperature responds closely to such variations.

Ambient temperature was regulated to remain within a bandwidth of $<\frac{1}{4}$°C. The variation in average temperature was $<\pm$ 0.1°C as shown in Fig. 12. The manometer thermometer (t_m) could be read with a precision of $\pm$ 0.02°C for a resultant uncertainty in pressure, then, of <2 parts in 10^5 of the reading. With

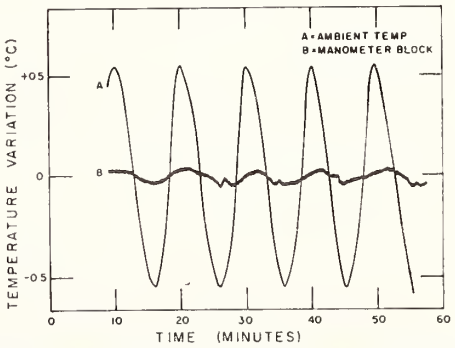

FIGURE 11. Thermal response of a micrometer-point contact manometer end plate to a periodic temperature variation of short period.

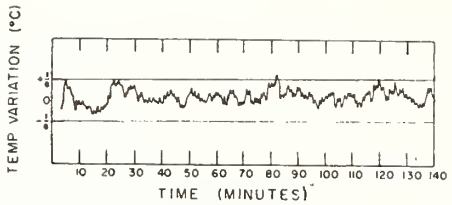

FIGURE 12. Typical ambient temperature profile under controlled conditions.

ambient temperature constant, it is found that operator presence causes a shift in manometer temperature of several tenths of a degree Celsius.

An evaluation was made of the deviation in temperature of the oil columns from that of the manometer block due to slow ambient temperature variations. The change in length of the oil columns was compared with the change in temperature of the manometer block, where the change in the sum of the lengths is a sensitive measure of the change in their average temperature independent of level changes. As the change in length is itself a measure, the uncertainty of setting and reading of the micrometers is taken as the minimum value stated in IIC. This is $\pm$ 2 $\times$ 10^{-5} in. for each surface or $\pm$ 4 $\times$ 10^{-5} in. for the sum of the two surface heights. Hence, the change between two observations of total column length has a maximum uncertainty of $\pm$ 8 $\times$ 10^{-5} in., which corresponds to a maximum uncertainty for change in column temperature of $\sim$ 0.04°C for a total length of 80 mm. The change in the manometer block temperature is determined from the change in position of the thermometer column, which gives the same uncertainty as a single reading or $\pm$ 0.02°C.

Data for equivalent column temperature changes are shown in Fig. 13 for two zero points and for 1 Torr chamber pressure. These zero point data show an initial temperature rise on appearance of the operator

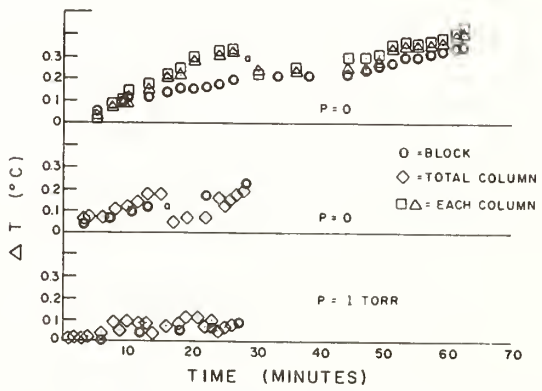

FIGURE 13. Temperature drift of the manometer oil columns from that of the manometer end plate and from each other. The equivalent temperature change is given for each oil column in the first zero run and for the total column length in the last two runs. The regions marked (a) indicate behavior resulting from blurping at a micrometer O-ring seal.

of $\sim$ 0.3°C. Column temperatures deviated 0.1°C from the block temperature but remained within 0.03°C of each other. The data at 1 Torr represent behavior after long operator presence for a manometer drift of $\sim$ 0.08°C and a column deviation from the block of $\leq$ 0.06°C. The uncertainty in comparison of the block and column temperatures has a maximum value of 0.06°C or a probable value (two standard deviations) of $\sim$ 0.03°C in consideration of the consistency of the data. Similarly, column temperatures can be compared to within 0.08°C max or to within a probable value of slightly greater than 0.03°C. A reasonable value for $\delta t_a = \delta t_b$ is then 0.1°C for the initial rise and half this thereafter. All in all, a reasonable value for $\delta t_a - \delta t_b$ for the stabilized case is 0.03°C. These values introduce an uncertainty of about four parts in 10^5 of the reading plus about 6 $\times$ 10^{-5} torr after stabilization.

F. Drainage and Capillarity

After extended operation, droplets of manometer fluid collect along the glass walls above the oil surfaces. With change in pressure, individual columns can initially gain or lose fluid. Subsequent stabilization in column heights is a function of drainage and transfer of liquid between the columns. These effects were examined by measuring the pressure and observing the sum of the column lengths as a function of time after level changes. An interval of about 5 min is required for pressure restabilization after a small pressure change. Larger pressure changes require longer times. After such delays no significant effect has been observed.

No change was made in estimates on capillarity.

G. Observed Reproducibility

Statistical information has been derived for the operation of the micrometer manometer at stabilized pressures over the range to 1 Torr. Resultant data for two separate runs involving 25 determinations at each pressure are given in Fig. 14 and Table II. Figure 14 shows the histogram, position of average value, and 6 standard deviation range for each pressure point. Table II lists the pressure, average value, and 3 standard deviation value corresponding to each histogram. Zero points are listed in original form as the difference in indicated column heights in inches. Equivalent 3 S.D. in Torr is approximately twice the value in inches [as derived from Eqs. (1) and (2)].

III. Factors Affecting Accuracy

A. Sorption and Leakage

A potential major source of distrust in the use of the oil manometer is the effect of gas sorption by the fluid. Leakage through the seals is also a factor. In our mode

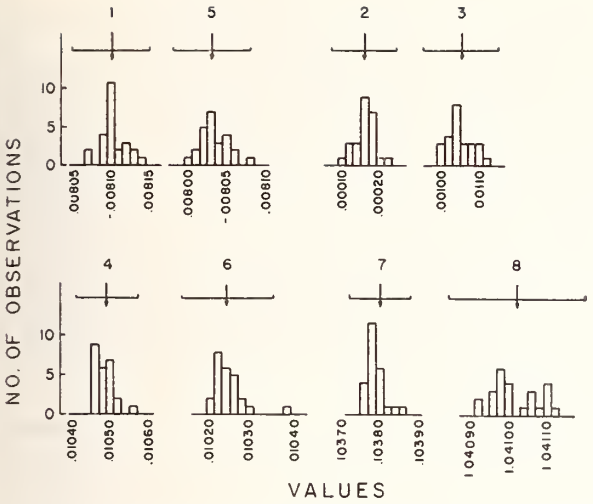

FIGURE 14. Observed reproducibility. Histograms, average values, and expected distribution (6 S.D.) for 25 determinations at each stabilized pressure. Expected range (6 S.D.) is indicated by horizontal lines above the histograms, average value by arrow through center of range.

of operation the net effect would be a pressure gradient in connecting tubulation due to gas flow. This can be diminished by use of relatively high conductance tubulation.

The leakage and sorption effects were measured *in situ* by cycling the manometer between 0 and 1 Torr. After long exposure of the manometer to ultimate pressures, the test arm was isolated by closing the connecting valve and the manometer pressure measured over a period of time. Next, with the chamber at 1 Torr the test arm was briefly reconnected, then reisolated, and the pressure again measured over a period of time. Finally, after remaining at 1 Torr for over an hour the test arm was again reconnected to and isolated from the vacuum chamber at blank-off pressure and the pressure measured in time. Behavior is indicated in Fig. 15. The data for the runs at ultimate pressure and at 1 Torr show initial perturbations due to pressure bursts from operation of the connecting stopcock, but the concern here is with gross effects. The upper, linear portions of the curves indicate a typical leak rate for this instrument of $\sim 4 \times 10^{-7}$ Torr-liters/sec, where the volume of the test arm and associated lines is $\sim$ 150 cm.³ The absorption and leakage rates balanced out in the early part of the 1 Torr characteristic to give an upper value for absorption rate of $\sim 2 \times 10^{-7}$ Torr-liters/sec for the first 20 min. The largest effect is for the combined outgassing and leakage on return to zero pressure. The initial net gas increase is $\sim 1 \times 10^{-6}$ Torr-liters/sec for an initial outgassing rate of $\sim 7 \times 10^{-7}$ and an average outgassing of $\sim 2 \times 10^{-7}$ over the first 20 min.

With connecting line conductance of about 1 liter /sec our worst effect is thus a pressure difference between the manometer and the chamber of $\sim 1 \times 10^{-6}$ Torr. Operation in the direction of increasing pressures reduces this.

B. Chamber Temperature and Thermal Transpiration

For the arrangement as in Fig. 1 and in the molecular flow range of pressure, differences in temperatures between the control gauge, manometer, and chamber will give rise to thermal transpiration effects of the form mentioned earlier (I.C.4). However, in control or comparison modes, only the temperature at the gauge and manometer are of consequence. If these were static procedures in the viscous flow region, the chamber temperature would indeed affect the pressures at the gauges as dependent upon the ratio of volumes and temperatures, but for dynamic control operation the system pressure is determined only by the condition at the control gauge and the time constants of the system. That is, as long as the temperature at the control gauge remains within a range compatible with its temperature sensitivity and as long as throughput is large enough to effect control, the pressure in the system should remain constant in the viscous flow range independent of the chamber and micrometer manometer temperatures.

Experimentally, a heat exchanger was clamped to the test chamber and thermal insulation appropriately applied. Temperature regulated fluid was passed through the exchanger to hold the chamber walls at a given temperature difference compared to am-

TABLE II. Observed reproducibility for 25 determinations at each stabilized pressure.

No.	1	2	3	4	5	6	7	8
Pressure range (Torr)	0 $R_h'-R_l'$	1.6×10^{-4}	1×10^{-3}	1×10^{-2}	0 $R_h'-R_l'$	1×10^{-2}	1×10^{-1}	1
Average in. Torr	−0.00810 ···	0.00016	.00105	.01049	−0.00803 ···	0.01024	0.10380	1.04102
3 S. D. in. Torr	0.5×10^{-4} 1.0×10^{-4}	0.9×10^{-4}	1.0×10^{-4}	0.8×10^{-4}	0.5×10^{-4} 1.0×10^{-4}	1.1×10^{-4}	0.7×10^{-4}	1.8×10^{-4}

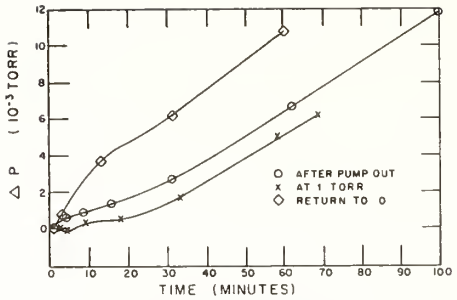

FIGURE 15. Change in pressure of the sealed-off test arm of the micrometer due to sorption and leakage. A measure of the outgassing, pumping, and leakage effects.

bient. Ambient temperature was held within a bandwidth of $<\frac{1}{4}$°C. A sequence of pressures was generated with the test chamber at +4.4°C and at −4.2°C with respect to ambient (~23°C) with the identical control settings for both sequences. The data are listed in columns 1–3 of Table III. We see that there is no distinguishable difference, that both sets of data fall within the expected distributions associated with the listed uncertainty.

C. Line Effects

The valving and vacuum line arrangement (Fig. 9) allowed the control gauge and micromanometer to be connected directly to each other to share a common vacuum line to the chamber, rather than to utilize separate lines and ports. This provided an alternate procedure for examination of the net effects of pressure gradients in the lines due to gas flow, variation in pressure within the test chamber between two adjacent ports, and thermal transpiration. It did, however, affect the servo loop operation and gave some deterioration in stability.

Several runs were first made with each instrument independently coupled to the test chamber. Then two runs were made with the instruments on the common line. Each run consisted of 5–10 measurements for zero point determination and a sequence of pressures of 5 per decade from 1×10^{-4} to 1 Torr. Each run used the identical pressure settings on the control loop. Ambient temperatures were held constant for each run with all run temperatures within a $\frac{3}{4}$°C band. Small corrections were applied to bring data to a common temperature base $\pm$ 0.1°C as derived from the temperature coefficients.

Columns 4–8 of Table III list the data for the runs with individual lines along with the average values and maximum differences from average. Columns 9–12 are the corresponding data for use of common line along with combined values and differences from the previous average.

No significant deviations were found.

D. Pressure Distribution in the Test Chamber

With the capacitance-diaphragm gauge independently connected to the test chamber, the micrometer manometer connection was moved to other chamber ports, one at 180° and one at 120° from initial position. In each case an identical run was made as described in the previous Sec. III. C. Resultant data are listed in columns 13–16 of Table III for each run along with differences from the average values of column 7, which averages represent the initial position. Again no significant deviations were indicated.

Table III. Repeated pressure sequences, torr.

1	2	3	4	5	6	7	8	9	10	11	12	13	14	15	16
Heated Chamber			Separate connections - Ambient					Common Connection				Different Ports			
+4.4°	−4.2°	Δ	Run 1	2	3	Av	Max Diff	Run 1	2	Combined	Deviation 7-11	180°	Deviation 7-13	120°	Deviation 7-15
0.00013	.00014	+.00001	.00015	.00009	.00006	.00010	.00005	.00022	.00013	.00017	-.00007	.00015	-.00005	.00013	-.00003
.00023	.00020	-.00003	.00027	.00021	.00013	.00020	.00007	.00044	.00027	.00035	-.00015	.00019	+.00001	.00023	-.00003
.00031	.00030	-.00001	.00029	.00029	.00029	.00029	0	.00048	.00019	.00033	-.00004	.00025	+.00004	.00029	0 0
.00041	.00043	+.00002	.00037	.00047	.00035	.00040	.00007	.00054	.00035	.00044	-.00004	.00043	-.00003	.00035	+.00005
.00057	.00065	+.00008	.00061	.00053	.00057	.00057	.00004	.00078	.00063	.00070	-.00013	.00067	-.00010	.00059	-.00002
.00098	.00095	-.00003	.00106	.00114	.00105	.00108	.00006	.00119	.00100	.00109	-.00001	.00105	+.00003	.00101	+.00007
.00160	.00162	+.00002	.00156	.00178	.00182	.00172	.00016	.00169	.00182	.00175	-.00003	.00170	+.00002	.00162	+.00010
.00253	.00242	-.00011	.00271	.00279	.00257	.00269	.00012	.00260	.00259	.00260	+.00009	.00269	0 0	.00271	-.00002
.00406	.00410	+.00004	.00422	.00428	.00406	.00412	.00016	.00419	.00408	.00412	0 0	.00428	-.00016	.00414	-.00002
.00612	.00611	-.00001	.00642	.00654	.00628	.00641	.00013	.00643	.00628	.00635	+.00007	.00630	+.00011	.00634	+.00007
.01034	.01031	-.00003	.01047	.01070	.01039	.01052	.00018	.01054	.01045	.01049	+.00003	.01057	-.00005	.01053	-.00001
.01651	.01654	+.00003	.01687	.01697	.01692	.01692	.00005	.01693	.01721	.01707	-.00015	.01682	+.00010	.01681	+.00011
.02599	.02594	-.00005	.02628	.02640	.02624	.02631	.00009	.02633	.02626	.02629	+.00003	.02640	-.00009	.02639	-.00008
.04167	.04158	-.00009	.04213	.04225	.04223	.04220	.00007	.04208	.04199	.04204	+.00016	.04209	+.00011	.04206	+.00014
.06265	.06242	-.00023	.06310	.06324	.06312	.06312	.00009	.06306	.06316	.06311	+.00004	.06317	-.00002	.06318	-.00003
.10410	.10389	-.00021	.10464	.10467	.10465	.10465	.00003	.10456	.10465	.10461	+.00004	.10471	-.00006	.10460	+.00005
.16658	.16641	-.00017	.16758	.16758	.16746	.16754	.00008	.16766	.16774	.16770	-.00016	.16760	-.00006	.16749	+.00005
.25973	.25969	-.00004	.26154	.26146	.26130	.26143	.00013	.26144		.26144	-.00001	.26150	-.00007	.26140	+.00003
.41512	.41505	-.00007	.41764	.41774	.41757	.41765	.00009	.41764		.41764	+.00001	.41755	+.00010	.41757	+.00008
.62272	.62259	-.00013	.62643	.62650	.62637	.62643	.00007	.62636		.62636	+.00007	.62660	-.00017	.62627	+.00016
1.04130	1.04108	-.00022	1.04732	1.04731	1.04724	1.04729	.00005	1.04703		1.04703	+.00025	1.04725	+.00004	1.04713	+.00016

IV. Concluding Remarks

A major factor in the precision of vacuum measurements is, of course, the stability of the environment itself. Instrumentation and procedures have been presented here to provide measurements and calibration accuracies of 1.2×10^{-4} Torr plus 6 parts in 10^5 of the reading, from 1×10^{-4} Torr to several Torr. However, the procedures for highly stable pressure generation are straightforward and applicable to lower pressures where other gauges can be used, such as the ionization gauge, provided null balance, differential readout, and stable reference voltages are used.

The uncertainty with the micromanometer is now limited by the setting and reading of the fluid surfaces. At present the reading uncertainty is probably the larger of the two effects. This could presumably be reduced somewhat further to bring calibration uncertainties of $\leq 1 \times 10^{-4}$ Torr.

Acknowledgments

Thanks are particularly due to W. A. Cullins for both fabrication of many of the components and assembly of the apparatus. Acknowledgment is also given to E. I. Klein for the glasswork and to R. L. Raybold for assistance in operation.

reprinted from the journal of vacuum science and technology vol. 6 no. 3

9. Vibration

9. Vibration—Continued

Journal of Research of the National Bureau of Standards Vol. 57, No. 4, October 1956 Research Paper 2714

Calibration of Vibration Pickups by the Reciprocity Method

Samuel Levy and Raymond R. Bouche

The reciprocity theory for the relationship between mechanical force and velocity and electric current and voltage is presented for a linear electrodynamic vibration-pickup calibrator having a driving coil, a velocity-sensing coil, and a mounting table. The theory takes account of flexibility in the calibrator structure and in the coils, electric coupling between different parts of the same coil and between parts of one coil and parts of the other, and flexibility in the magnet structure. The theory shows what measurements are required in using a linear electrodynamic calibrator for the absolute calibration of vibration pickups.

A description is given of the mechanical arrangement and electric circuitry used at the National Bureau of Standards in calibrating calibrators by the reciprocity method. A typical velocity-sensing-coil calibration curve is presented showing the effect of pickup mass on the calibration factor. Typical examples of measurement of calibration factor and mechanical impedance of pickups are also presented.

Practical limitations of the reciprocity method due to nonlinearity resulting from lack of tightness of mechanical joints, resonance effects, amplitude effects, etc., are discussed.

1. Introduction

An early application of the reciprocity method to the measurement of mechanical quantities was that by R. K. Cook [1] [1] in 1940. He applied the method to the absolute calibration of microphones. This was followed in 1948 with papers by H. M. Trent [2] and A. London [3], who showed how the reciprocity method could be used for the absolute calibration of vibration pickups. The reciprocity method was applied to the calibration of electrodynamic transducers in 1948 by S. P. Thompson [4] and to the calibration of piezoelectric accelerometers in 1952 by M. Harrison, A. O. Sykes, and P. G. Marcotte [5].

Commercially available calibrators for vibration pickups have a mounting table that is connected by a relatively rigid internal structure to a driving coil and to a velocity-sensing coil. This internal structure is supported from the frame by flexure springs or guide wires. John C. Camm, formerly of NBS, in 1953 showed how the reciprocity method could be applied to the calibration of the velocity-sensing coil of such a calibrator in connection with work for the Office of Naval Research. In 1955 the authors of the present report, in connection with work for the Diamond Ordnance Fuze Laboratories, extended Camm's theory to take account of pickup mass and flexibility in the internal structure for the frequently occurring case where the driving coil, sensing coil, and mounting table are mechanically joined at a point.

The present report gives a broader basis for the application of the reciprocity method to the calibration of the velocity-sensing coil of calibrators, by considering both the internal structure and the magnet to be flexible and by taking account of electric-coupling effects. It also shows how the calibrator, once its velocity-sensing coil has been calibrated by the reciprocity method, can be used to determine the calibration factor and to measure the mechanical impedance of vibration pickups.

2. Reciprocity Theory for Flexible Vibration-Pickup Calibrators

In the appendix the general reciprocity theory for a calibrator is presented. This theory is applicable to a calibrator operating in any frequency or amplitude range in which it can be considered to be a linear system. Neither the internal structure nor the magnet structure need be considered rigid. The theory is applicable, for example, not only at low frequencies and at frequencies near certain resonances, but also at frequencies above axial resonance where

[1] Figures in brackets indicate the literature references at the end of this paper.

the driving coil and mounting table move in opposite directions. The theory is also applicable where there is electric coupling between different parts of the same coil and between parts of one coil and parts of the other.

The positive terminals of the driving and sensing coils are designated as those having positive voltages when the mounting table is moving inward. Conversely, positive current in the coils produces outward velocity at the mounting table.

When the calibrator is energized with current in the driving coil at any particular frequency, the calibration factor, F, is defined as the ratio of the voltage in volts in the velocity-sensing coil to the velocity in inches per second at the surface of the mounting table. It is shown in the appendix that

$$F=a+bY_p \tag{1}$$

where Y_p is the pickup mechanical impedance (lb-sec/in.), and all the symbols represent complex numbers in the manner commonly used for alternating-current electrical theory. The calibrator constants, a and b, are determined by the following two experiments and computational procedure.

Experiment 1: The equipment is shown in figure 1 (a). Attach weights to the mounting table and measure for each weight the transfer admittance in amperes per volt, G, between the driving and sensing coils:

$$G=\frac{I_o^D}{E_o^{OS}} \tag{2}$$

where

I_o^D= current in driving coil.

E_o^{OS}= voltage generated in open-circuited sensing coil. (It is permissible to leave a voltmeter permanently connected to the sensing coil. If this is done, the open-circuit condition is obtained when no other connection is made to the sensing coil.)

Experiment 2: The equipment is shown in figure 1 (b). Couple a second vibration exciter to the calibrator being calibrated at the mounting table, and measure the ratio, R, of open-circuited voltages generated in the sensing and driving coils:

$$R=E_o^{OS}/E_o^D. \tag{3}$$

Computational Procedure: Determine the ordinate intercept, J, and the slope, Q, of the function $W/(G-G_o)$ when plotted against the weight, W, attached to the mounting table in experiment 1, where G_o is the value of G when $W=0$. Constants a and b in eq (1) are then given by

$$a=0.01711\sqrt{j\omega JR}, \qquad b=6.601Q\sqrt{R/(j\omega J)}, \tag{4}$$

where ω is the frequency in radians per second, and j is the unit imaginary vector.

It is shown in the appendix that the vibration-pickup calibrator calibrated by the reciprocity method can be used to determine the mechanical impedance, Y_p, of a pickup by measuring the admittance, G_p, eq (2), with the pickup attached to the mounting table, and the admittance, G_o, when nothing is attached to the table, by use of the relationship

$$Y_p=j\left(\frac{\omega}{386}\right)\left(\frac{J(G_p-G_o)}{1-Q(G_p-G_o)}\right). \tag{5}$$

To carry out the calibration of a pickup the following procedure is used: The driving coil of the calibrator is energized at the desired frequency and the value of Y_p is determined. The

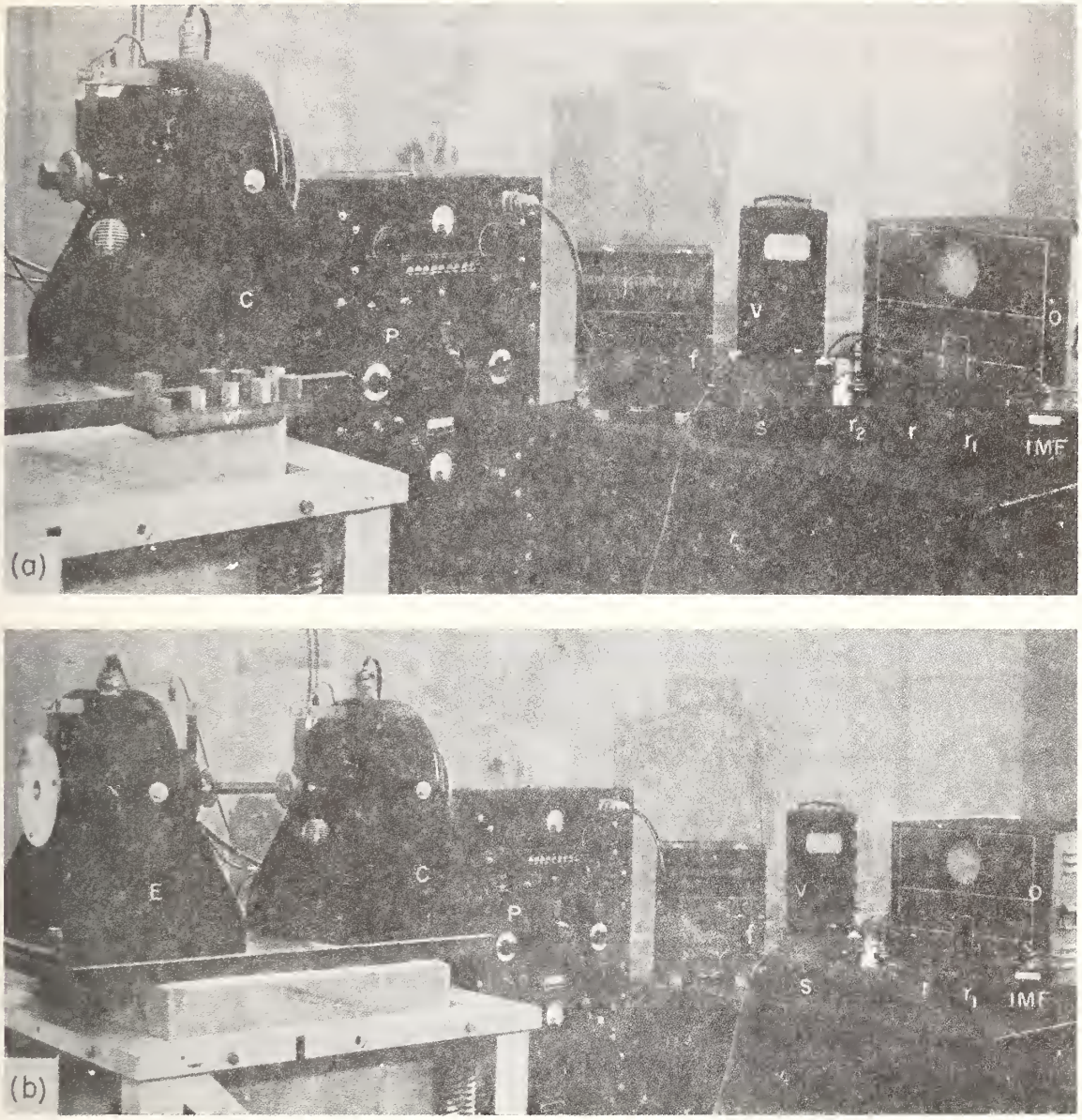

FIGURE 1. *Measurement of constants of vibration-pickup calibrator.*

(a) Weights, *W*, are attached to mounting table of calibrator, *C*, in experiment 1. (b) External vibration exciter, *E*, is required to provide sinusoidal motion to calibrator, *C*, in experiment 2.

calibrator is then driven at the desired amplitude as indicated by the voltage, E_o^s, in the sensing coil, and then the velocity is given by

$$v = E_o^s / F, \tag{6}$$

where F is obtained by substituting Y_p in eq (1). The output of the pickup corresponding to this excitation is then measured. Ordinarily the term bY_p in eq (1) for F is negligibly small, except at frequencies high enough to cause relative displacements between the mounting table and the sensing coil. Where it is known that bY_p is negligibly small, the determination of Y_p may be omitted from the calibration procedure.

3. Measurement of Constants

3.1. Accuracy of Weights

The weights attached to the table in carrying out experiment 1 at the Bureau are shown at W in figure 1 (a). The weights increase in 0.1-lb steps from 0 to 1 lb. They vary less than 0.1 percent from their rated values. Their attachment surface has a stud that engages the mounting table and a contacting ring, ⅛ in. wide, which provides a connection of high rigidity. A film of oil is wiped on this ring before engagement to eliminate air in the contact surface.

3.2. Accuracy of Frequency Measurements

The frequency was measured with a calibrated electronic frequency meter. The indicated audio oscillator frequency did not differ from the measured frequency by more than 0.2 percent.

3.3. Measurement of Transfer Admittance

The circuit shown in figure 2 (a) is used to measure the transfer admittance. With the switch in the "up" position, the values of r and r_1 are adjusted until the voltage drops $|E_{12}|$ across terminals 1 and 2, and $|E_{13}|$ across terminals 1 and 3, are equal as measured on a high-impedance voltmeter. The magnitude of G is then given by

$$|G|=\frac{r+r_1+r_2}{rr_2}. \tag{7}$$

The accuracy of $|G|$ determined in this manner depends only on the accuracy of the circuit elements and the repeatability of the voltmeter reading, but not on the accuracy of the voltmeter. Values of the resistances are chosen to load the amplifier suitably. Typical values for this calibrator are r_2, equal to 10 ohms, and $r+r_1$, approximately 1,000 times greater than r_2.

Voltage $|E_{23}|$ across terminals 2 and 3 is then read from the voltmeter. The switch is lowered to the "down" position. The value of r_1 is adjusted until $|E_{14}|$ equals $|E_{13}|$, and voltages $|E_{13}|$ and $|E_{43}|$ are read on the voltmeter. The phase angle, ϕ_G, of the transfer admittance, G, is the phase angle of I_o^D with respect to E_o^S. Because the currents in r, r_1, and r_2 are in phase with I_o^D, phase angle ϕ_G can be determined from a construction of a polygon of voltages as

$$\phi_G=\cos^{-1}\left(1-\frac{1}{2}\frac{|E_{23}^2|}{|E_{13}^2|}\right). \tag{8}$$

A suitable value of r_2 is used so that $r_1\omega 10^{-6}$ is greater than 100; then the approximate value of

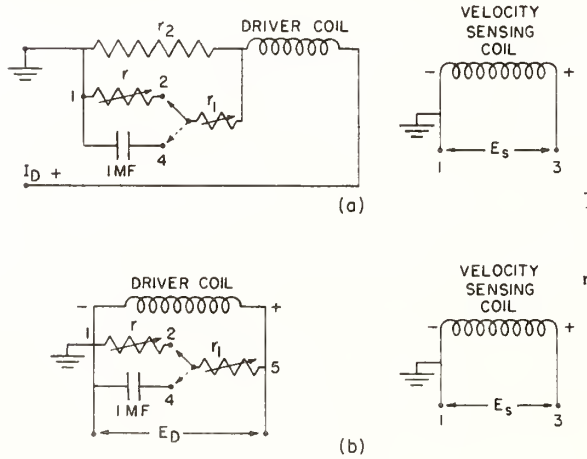

FIGURE 2. *Circuits used in the measurement of constants of vibration-pickup calibrator.*

(a) Measurement of transfer admittance. (b) Measurement of voltage ratio.

ϕ_G can be determined from

$$(\phi_G)\ \text{approx}=90°-\cos^{-1}\left(1-\frac{1}{2}\frac{|E_{34}^2|}{|E_{13}^2|}\right). \tag{9}$$

The use of both eq (8) and (9) determines the magnitude and quadrant for ϕ_G. It happens, though, except near certain resonances, that ϕ_G is near $\pm 90°$. Small errors in $|E_{43}|$ or $|E_{13}|$ result in large changes in the angle

$$\cos^{-1}\left(1-\frac{1}{2}\frac{|E_{43}^2|}{|E_{13}^2|}\right)$$

when ϕ_G is near $-90°$. Difficulty in measuring the small value of $|E_{43}|$ results in error when ϕ_G is near 90°. Therefore, eq (8) is used to determine the magnitude of ϕ_G and (9) its quadrant.

3.4. Measurement of Voltage Ratio

The circuit shown in figure 2(b) is used to measure the ratio of the open-circuit voltages of the driving and sensing coils when the calibrator being calibrated is driven by an external vibration exciter. With the switch in the "up" position and with r_1 set at 10,000 ohms, resistor r is adjusted until the voltages across terminals 1 and 2 and terminals 1 and 3 are equal. The magnitude of the voltage ratio, R, is then given by

$$|R|=\frac{r}{10{,}000+r}. \tag{10}$$

(In the case of a calibrator for which 10,000 ohms is not effectively an infinite impedance across the driving coil, r_1 in figure 2(b) should be increased to an adequate value and eq (10) correspondingly modified.)

To determine the phase angle of R, $|E_{13}|$ and $|E_{23}|$ are measured. The switch is then put in the "down" position, r_1 is adjusted until $|E_{14}|$ equals $|E_{13}|$, and $|E_{43}|$ is measured. Then from a construction of a polygon of voltages

$$\phi_R=\cos^{-1}\left(1-\frac{1}{2}\frac{|E_{23}^2|}{|E_{13}^2|}\right), \tag{11}$$

and

$$\phi_R=\cos^{-1}\left(1-\frac{1}{2}\frac{|E_{43}^2|}{|E_{13}^2|}\right)-\cos^{-1}(|R|). \tag{12}$$

It happens that ϕ_R is near either 0° or 180°. Equation (11) is insensitive for these angles, either because $|E_{23}|$ is very small for ϕ_R near 0° or because the cosine is insensitive to small changes in $|E_{23}|$ near 180°. Therefore, eq (12) is used to determine the magnitude of ϕ_R and eq (11) only its quadrant.

4. Typical Results

4.1. Calibration of Sensing Coil

Results obtained in the calibration of the sensing coil of a typical calibrator having a nominal 50-lb driving-force rating are now presented. All measurements were made after thermal equilibrium was approached. The positive terminals of the driving and sensing coils were determined as those having positive voltage when the mounting table had inward velocity. Positive velocity is then outward.

First, the transfer admittance, G, experiment 1, was measured for a sequence of weights, W, on the mounting table at each frequency for which a calibration was desired. Typical results at frequencies of 900 and 5,000 cps are presented in figure 3. In figure 4 are the corresponding plots of $W/(G-G_o)$ against W. The data were fitted by a weighted least-squares procedure for a straight line. The weighting as determined by a consideration of the expected error in $1/(G-G_o)$ was 1, 2, 3, . . ., 10 for W=0.1, 0.2, 0.3, . . ., 1.0 lb. Intercepts J and

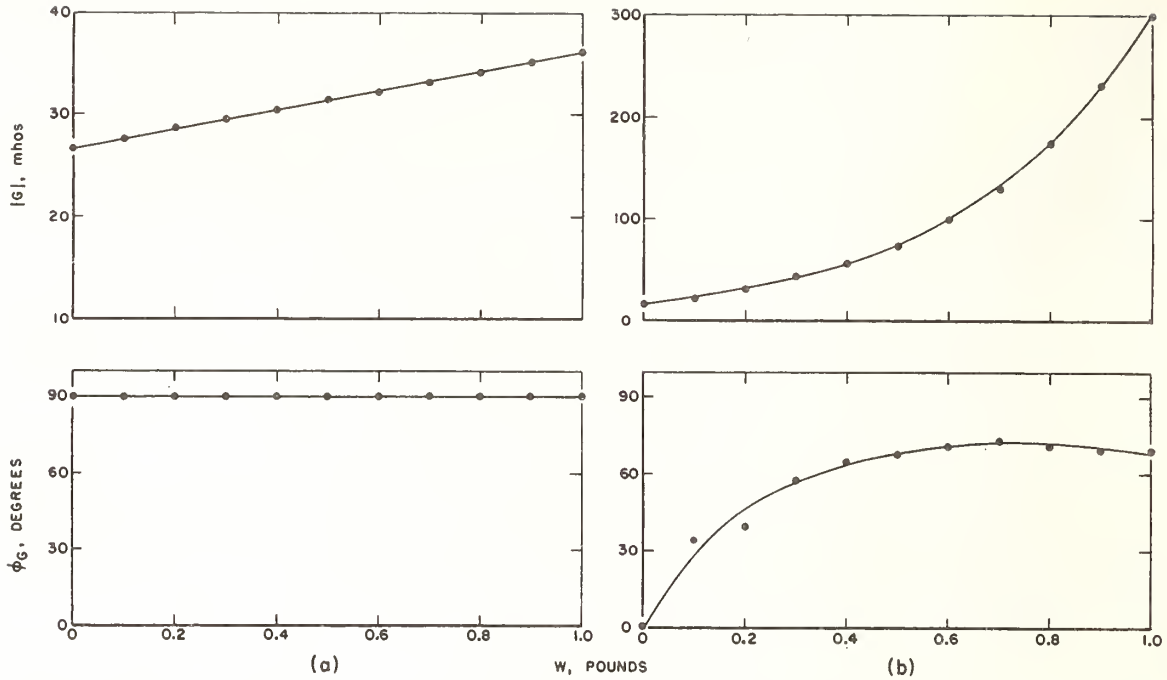

FIGURE 3. *Variation of transfer admittance, G, with weight, W, on the mounting table for a typical vibration pickup calibrator at frequencies of (a) 900 cps and (b) 5,000 cps.*

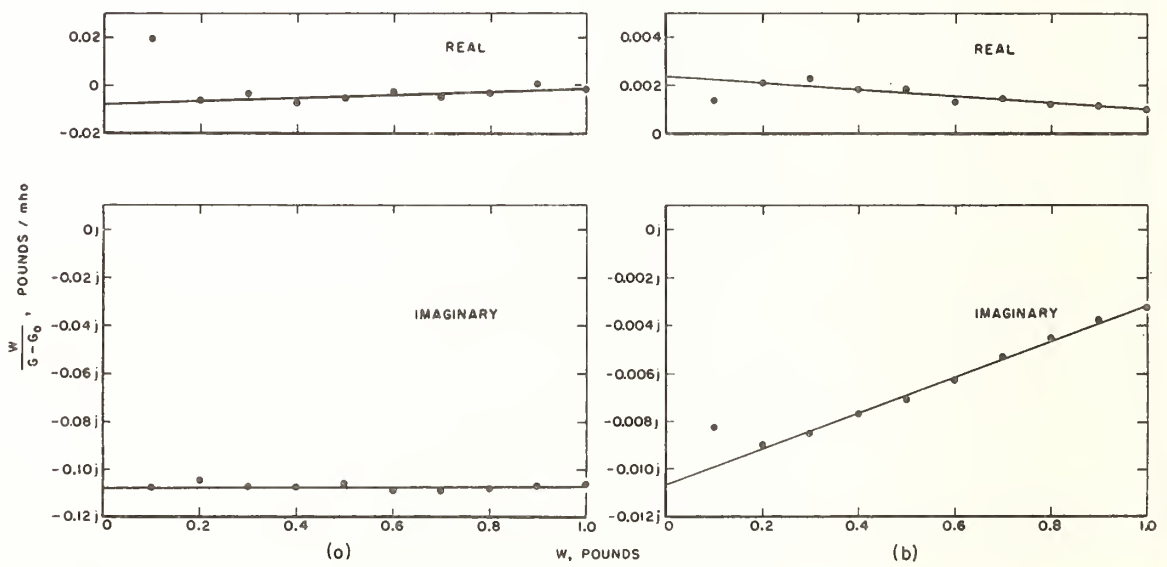

FIGURE 4. *Plot of $W/(G-G_o)$ as a function of W for a typical vibration pickup calibrator at frequencies of (a) 900 cps and (b) 5,000 cps.*

slopes Q, determined by this procedure, are at 900 cps $J=0.1089/\underline{-94.2°}$ lb-ohm, and $Q=0.00767/\underline{11.8°}$ ohm, and at 5,000 cps, $J=0.01094/\underline{-77.4°}$ lb-ohm, and $Q=0.00765/\underline{100.4°}$ ohm.

The voltage ratio, R, when driven by an external vibration exciter, experiment 2, was then determined as $R=0.1090/\underline{-2.6°}$ at 900 cps and $R=0.2495/\underline{-2.0°}$ at 5,000 cps. Next the constants a and b in eq (4) were computed. Substituting their values in eq (1) gave calibration factors of the sensing coil with a pickup of mechanical impedance Y_p on the mounting table,

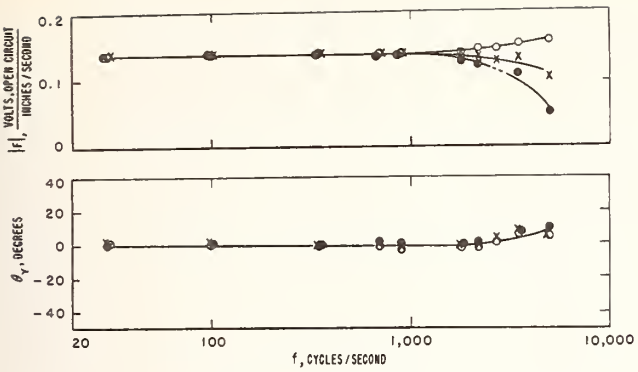

FIGURE 5. *Variation of calibration factor of velocity-sensing coil with frequency and pickup weight for a typical vibration pickup calibrator.*

○=0 lb, ×=½ lb, ●=1 lb.

at 900 cps, $F=0.1402/\underline{-3.4°}+0.000674/\underline{12.6°}\ Y_p$ v-sec/in., and at 5,000 cps, $F=0.1584/\underline{5.5°}+0.001360/\underline{93.1°}\ Y_p$ v-sec/in.

In figure 5 are shown the magnitude and phase angle of the calibration factor of the velocity-sensing coil of this typical vibration-pickup calibrator as a function of frequency for pickups having a mechanical impedance Y_p corresponding to weights W of 0, 0.5, and 1.0 lb ($Y_p=j\omega W/386$). It is evident that, for this particular vibration-pickup calibrator, the calibration factor of the velocity-sensing coil is nearly independent of frequency and pickup weight up to 900 cps. The curve for 1 lb is dotted in the vicinity of 2,700 cps because the plot similar to that shown in figure 4 was not linear beyond 0.5 lb. The source of this nonlinearity could not be localized. This nonlinearity has not been found in other calibrators of the same make and model number calibrated at the same frequency.

4.2. Calibration of a Variable-Resistance-Type Accelerometer and a Piezoelectric-Type Accelerometer

Results obtained in the calibration of a variable-resistance-type accelerometer and piezoelectric-type accelerometer are now presented. In these calibrations the circuit shown in figure 2 (a) was used with the pickup terminals designated 6 and 7, in place of velocity-sensing-coil terminals 1 and 3. The method given in section 3.3 was then used for the measurement of G_p, the value of G with the pickup attached to the mounting table.

For the piezoelectric pickup, the value of G_p obtained at 900 cps was $G_p=I_o^D/E_o^S=28.51/\underline{91.8°}$ mhos, and at 5,000 cps, $G_p=37.9/\underline{43.6°}$ mhos. With terminal 6 grounded and terminal 7 replacing terminal 3, the same procedure gave, at 900 cps, $I_o^D/E_p=16.35/\underline{2.5°}$ mhos, and at 5,000 cps, $I_o^D/E_p=3.201/\underline{-44.6°}$ mhos, where E_p is the output voltage of the pickup. From eq (5), the mechanical impedance, Y_p, of the pickup was computed by using, at 900 cps, $G_o=26.81/\underline{92.0°}$ mhos, and at 5,000 cps, $G_o=16.51/\underline{18.1°}$ mhos, and the values of J and Q obtained in section 4.1. This gave, at 900 cps, $Y_p=2.712/\underline{83.3°}$ lb-sec/in. and at 5,000 cps, $Y_p=18.23/\underline{70.5°}$ lb-sec/in. Using these values of Y_p in eq (1), the velocity sensing-coil calibration factors at 900 cps and 5,000 cps, respectively, are $F=0.1399/\underline{-2.7°}$ v-sec/in. and $F=0.1357/\underline{9.2°}$ v-sec/in. The pickup acceleration calibration factor, F_p, is

$$F_p=\frac{(I_o^D/E_o^S)}{(I_o^D/E_p)}\frac{Fg}{j\omega} \tag{13}$$

where $Fg/(j\omega)$ is the acceleration calibration factor of the sensing coil. Using this equation, at 900 cps, $F_p=0.0166/\underline{-3.4°}$ v/g, and at 5,000 cps, $F_p=0.0197/\underline{6.5°}$ v/g. Figure 6 shows the complete calibration of the piezoelectric-type accelerometer.

The calibration of the variable-resistance-type accelerometer, which was performed in a similar manner, is shown in figure 7. To compute the results on the variable-resistance

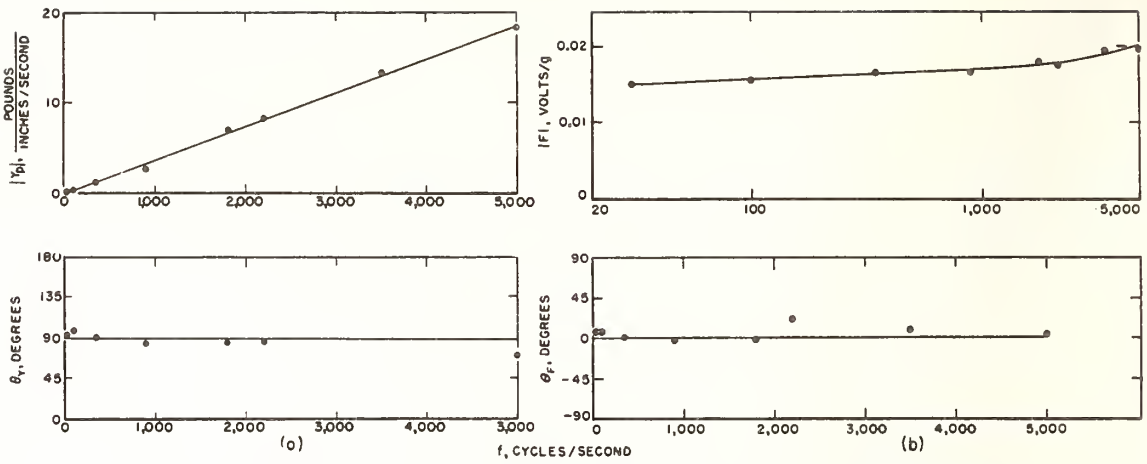

FIGURE 6. *Calibration of piezoelectric-type accelerometer at a nominal acceleration level of 2 g.*

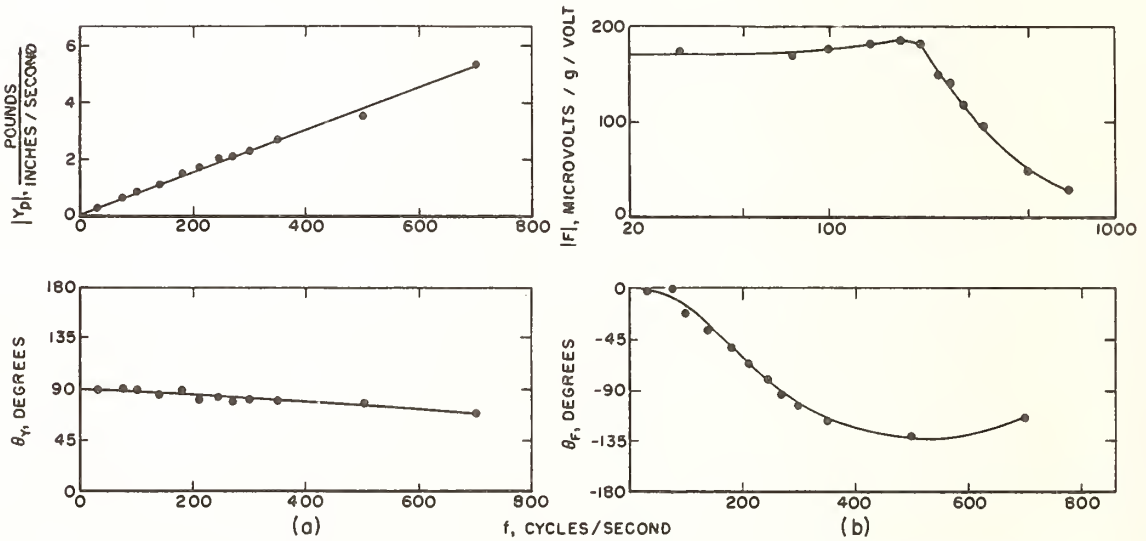

FIGURE 7. *Calibration of variable-resistance-type accelerometer at a nominal acceleration level of 2 g.*

pickup at frequencies other than those at which the vibration-pickup calibrator was calibrated, it was necessary to interpolate suitably for a, b, R, and Q, and compute J from eq 4. This interpolation was only used at frequencies below 900 cps. In this frequency range, such interpolation results in no appreciable error for this calibrator when the resonant frequencies of the flexures are avoided. The frequencies used for the pickup calibration were not those at which flexure resonance was present.

5. Effects of Calibrator Construction on Accuracy

Inaccuracy in the reciprocity method, exclusive of electrical measurements, arises primarily from deviations from true linearity in the calibrator performance. The more important forms of nonlinearity are discussed below.

5.1. Resonance Effects

Resonance accentuates inaccuracy due to nonlinearity because relatively small changes in the calibrator constants, which are caused by very small changes in the structure of the calibrator and small changes in the exciting frequency, can cause large changes in the amplitude of vibration. Even when such changes do not occur, the large amplitudes associated with resonance may exceed the linear range. The resonance of the driving coil relative to the velocity-sensing coil reduces the accuracy of the reciprocity calibration over a small frequency range because $|R|$ is very small and therefore difficult to measure, and because the large amplitude of the driver coil may exceed its linear range. Operation of the calibrator near resonance frequencies should therefore be avoided. Some common resonance conditions in their usual order of appearance with increasing frequency follow:

a. Resonance of mounting table and coils as a rigid body on the guiding flexures.
b. Local resonance in the flexures.
c. Transverse vibration of the shaft connecting mounting table and driving coil.
d. Longitudinal resonance of shaft connecting mounting table and driving coil.
e. Local resonance in table or coils.

5.2. Transverse Motion

Transverse motion from any source invalidates the reciprocity method, which requires the mounting table to have uniaxial motion. Transverse motion occurs at the resonance frequencies of the flexures and at the transverse resonance frequencies of the shaft on which the moving parts are mounted. At resonance, the amplitude will vary substantially for small changes in frequency and the resonance may occur at a frequency that is a harmonic of the driving frequency. Flexures can be detuned by attaching small weights to them.

5.3. Tightness of Mechanical Joints

The tightness of the mechanical joints in a calibrator will have little effect on its performance at low frequencies, where the moving assembly of mounting table and coils acts as a "rigid body." At frequencies approaching those for internal resonance in the assembly, looseness in the joints can affect behavior by, for example, changing the structural stiffness or by introducing coulomb friction. At very high frequencies, joints normally thought to be tight may be a source of erratic behavior, which is difficult to eliminate as tightness will ordinarily vary with temperature and time. Coating all joints with oil improves their rigidity.

5.4. Amplitude Effects

The nonuniformity of the magnetic fields surrounding the coils is a primary source of nonlinearity. This effect tends to be greatest at low frequencies, where the displacement amplitude is large for a given acceleration. At high frequencies, the displacement amplitude is relatively small, and this effect is negligible. The change in equilibrium position of the moving assembly of a calibrator, when its orientation is changed, may cause a change in calibration factor due to change in the effective field strength.

The structure of a calibrator will ordinarily experience small deformations in its linear range at permissible current intensities. At resonance, the deformations are larger. Little is known about the linearity of structural damping for a structure as complicated as a calibrator; however, so long as the damping is small, its possible lack of linearity would affect only the resonant response.

5.5. Temperature Effects

Changes in temperature cause moderate changes in elastic constants and in the tightness of joints, and in this way can affect the calibrator performance near resonance. Changes in temperature may also affect the field flux density, and thus the electrical characteristics of the driving coil, but should not ordinarily affect the calibration factor of the velocity-sensing coil.

5.6. Purity of Electric-Power Sources

If the magnets are excited by direct current containing an alternating-current ripple, this ripple may appear in the velocity output of the calibrator owing to currents included in the driving coil by transformer action from the field. Such a disturbance can readily be detected by exciting the field and observing the velocity of the mounting table with the driving coil short-circuited.

Any harmonic content in the power supply to the driving coil will excite the calibrator at the harmonic frequencies, as well as at the primary frequency. The techniques described in this paper are applicable only for excitation at a single frequency.

6. Conclusions

It is concluded that the reciprocity methods described can be used for the accurate calibration of vibration pickups and calibrators having linear response. The accuracy is limited primarily by the accuracy of electrical measurement, by deviations from true linearity in construction, and by impurities in power supplies to the field and driving coils. The frequency range is limited theoretically only to frequencies for which the mechanical impedance of the weights attached to the mounting table can be computed. Ordinarily this limits the range to that at which the weights act as though they were rigid bodies. Practically, the calibrator used as an example in this report is most suited for use at frequencies of 900 cps and below, where its calibration factor is not affected by the mechanical impedance of most vibration pickups that would be attached to its mounting table. The calibrator is suited for use above 900 cps, however, with some loss in precision primarily due to the electromechanical properties of the calibrator being less constant with respect to field-coil temperature than they are at lower frequencies. The upper acceleration range of most calibrators, when resonance is avoided, is below 50 g. This would be the limit for calibrating by the reciprocity method.

7. Appendix. General Reciprocity Theory

7.1. Reciprocity for Electric Circuit

If a complicated electric circuit is considered to be made up of a number of meshes, the almost trivial fact that the common impedance between meshes i and k, for example, is the same as that between k and i is the basis for the proof of the reciprocity theorem. This proof is elegantly presented by Guillemin on page 152 of reference [6]. Guillemin states on page 276 that the reciprocity theorem can be proved for both transient and steady-state performance. This means, for example, that if we impress a voltage in mesh 5 of a given network and measure the current, say in mesh 2, and then place the voltage in mesh 2 instead of in mesh 5 and measure the current in mesh 5, we will find the current exactly the same in the two cases, both in magnitude and phase.

7.2. Reciprocity for Mechanical System

If a complicated mechanical system can be replaced by an equivalent system having discrete mass-points joined by springs and dashpots, the fact that the spring and dashpot connecting points i and k is the same as that connecting points k and i makes possible a proof of the reciprocity theorem for mechanical systems completely analogous with that for electric circuits. (Reference [7] gives a proof of this theorem for conservative systems.) In other words, this reciprocity theorem states, for example, that if we impress a force on point 5 of a given system and measure the velocity, say at point 2, we will find the same velocity in magnitude and phase when we place the force at point 2 instead of at point 5 and measure the velocity at point 5. It should be mentioned that it is possible to have a mechanical system consisting of discrete elements that is not reciprocal, for example, if it contains gyroscopic elements.

7.3. Reciprocity for Combined System

In developing the reciprocity theorem for the combined electric-mechanical system of a calibrator, we will use matrix notation. This will permit us to consider the coils as flexible bodies and take account of electric coupling between coils, as well as deformation in the field and movable structure. The notation and theorems given by Frazer, Duncan, and Collar [8] will be used.

Currents and voltages in the velocity-sensing coil will be indicated by S and in the driving coil by D. We will consider the coils subdivided into a sufficient number of segments so each moves as a rigid body and number them consecutively in the two coils. The subscript o will indicate terminal values. Complex notation used in alternating-current electrical theory will be used throughout. All symbols represent vector quantities, unless otherwise noted. An English system of units (inches, pounds, and seconds) will be used.

Current I_o^S at the terminals of the sensing coil is given by

$$I_o^S = \frac{E_o^S}{z_{oo}^{SS}} + \frac{E_o^D}{z_{oo}^{SD}} + [z^S]\{E\}, \tag{A1}$$

where

E_o^S = voltage at terminals of coil S.

E_o^D = voltage at terminals of coil D.

z_{oo}^{SS} = impedance at terminals of coil S.

z_{oo}^{SD} = transfer impedance from terminals of coil S to terminals of coil D.

$[z^S] = \left[\frac{1}{z_{o1}^S} \frac{1}{z_{o2}^S} \cdots \frac{1}{z_{on}^S}\right]$, where z_{on}^S is the transfer impedance from segment n to the terminals of coil S.

$$\{E\} = \begin{bmatrix} E_1 \\ E_2 \\ \cdot \\ \cdot \\ \cdot \\ E_n \end{bmatrix}, \quad E_n \text{ is the voltage generated in segment } n.$$

A similar expression can be written for I_o^D. Both of these expressions can be expressed as

$$\{I_o\} = [z_o]\{E_o\} + [z]\{E\}, \tag{A1a}$$

where

$$\{I_o\} = \begin{bmatrix} I_o^S \\ I_o^D \end{bmatrix}; \quad \{E_o\} = \begin{bmatrix} E_o^S \\ E_o^D \end{bmatrix}$$

$$[z_o] = \begin{bmatrix} \frac{1}{z_{oo}^{SS}} & \frac{1}{z_{oo}^{SD}} \\ \frac{1}{z_{oo}^{DS}} & \frac{1}{z_{oo}^{DD}} \end{bmatrix}$$

$$[z] = \begin{bmatrix} \frac{1}{z_{o1}^S} & \frac{1}{z_{o2}^S} & \cdots & \frac{1}{z_{on}^S} \\ \frac{1}{z_{o1}^D} & \frac{1}{z_{o2}^D} & \cdots & \frac{1}{z_{on}^D} \end{bmatrix}.$$

The current in any segment is given by

$$\{I\}=[z]'\{E_o\}+[Z]\{E\}, \tag{A2}$$

where

$\{I\}=\begin{bmatrix} I_1 \\ I_2 \\ . \\ . \\ . \\ I_n \end{bmatrix}$, I_n is the current in segment n,

$[Z]=\begin{bmatrix} \frac{1}{z_{11}} & \frac{1}{z_{12}} & \cdots & \frac{1}{z_{1n}} \\ \frac{1}{z_{21}} & \frac{1}{z_{22}} & \cdots & \frac{1}{z_{2n}} \\ . & . & & . \\ . & . & & . \\ . & . & & . \\ \frac{1}{z_{m1}} & \frac{1}{z_{m2}} & \cdots & \frac{1}{z_{mn}} \end{bmatrix}$, z_{mn} is the transfer impedance from segment m to segment n,

$[z]'$=transpose of $[z]$.

Velocity v_o at the mounting table, taken positive outward is given by

$$v_o=\frac{F_o}{Y_{oo}}+L_1[y][k]\{I\}, \tag{A3}$$

where

F_o=the force at the mounting table.

Y_{oo}=the mechanical impedance at the mounting table.

$L_1=2.249\times10^{-7}$, a conversion factor.

$[y]=\begin{bmatrix} \frac{1}{y_{o1}} & \frac{1}{y_{o2}} & \cdots & \frac{1}{y_{on}} \end{bmatrix}$, where y_{on} is the transfer mechanical impedance from the mounting table to segment n.

$[k]=\begin{bmatrix} B_1l_1 & 0 & 0 & \cdots & 0 \\ 0 & B_2l_2 & 0 & \cdots & 0 \\ 0 & 0 & B_3l_3 & \cdots & 0 \\ . & . & . & & . \\ . & . & . & & . \\ . & . & . & & . \\ 0 & 0 & 0 & \cdots & B_nl_n \end{bmatrix}$, where B_n is the flux density, and l_n is the length for segment n.

In eq (A3), the product $L_1 B_n l_n I_n$ gives the force, in pounds, at segment n when I_n is the current, in amperes. The velocity of the various segments is given by

$$\{v\}=[y]'F_o+L_1[Y][k]\{I\}, \tag{A4}$$

where

$\{v\}=\begin{bmatrix} v_1 \\ v_2 \\ . \\ . \\ . \\ v_n \end{bmatrix}$, v_n is the velocity of segment n.

$[y]'$ = transpose of $[y]$.

$[Y]=\begin{bmatrix} \frac{1}{y_{11}} & \frac{1}{y_{12}} & \cdots & \frac{1}{y_{1n}} \\ \frac{1}{y_{21}} & \frac{1}{y_{22}} & \cdots & \frac{1}{y_{2n}} \\ . & . & & . \\ . & . & & . \\ . & . & & . \\ \frac{1}{y_{m1}} & \frac{1}{y_{m2}} & \cdots & \frac{1}{y_{mn}} \end{bmatrix}$, y_{mn} is the transfer mechanical impedance from segment m to segment n.

The corresponding velocity in the magnetic field at the various segments is given by

$$\{v^M\}=L_1[Y^M][k]\{I\}+[y^M]'F_o, \tag{A4a}$$

where

$\{v^M\}=\begin{bmatrix} v_1^M \\ v_2^M \\ . \\ . \\ . \\ v_n^M \end{bmatrix}$, v_n^M is the velocity of the magnetic field at segment n.

$[Y^M]=\begin{bmatrix} \frac{1}{y_{11}^M} & \frac{1}{y_{12}^M} & \cdots & \frac{1}{y_{1n}^M} \\ \frac{1}{y_{21}^M} & \frac{1}{y_{22}^M} & \cdots & \frac{1}{y_{2n}^M} \\ . & . & & . \\ . & . & & . \\ . & . & & . \\ \frac{1}{y_{m1}^M} & \frac{1}{y_{m2}^M} & \cdots & \frac{1}{y_{mn}^M} \end{bmatrix}$, y_{mn}^M is the transfer mechanical impedance from the location of segment m to that of segment n in the magnetic field.

$$[y^M]' = \begin{bmatrix} \frac{1}{y^M_{o1}} \\ \\ \frac{1}{y^M_{o2}} \\ \\ \cdot \\ \cdot \\ \cdot \\ \\ \frac{1}{y^M_{on}} \end{bmatrix},$$ y^M_{on} is the transfer mechanical impedance from the mounting table to the magnetic structure opposite segment n.

The voltage generated in each segment is

$$\{E\} = -L_2[k]\{v\} + L_2[k]\{v^M\}, \tag{A5}$$

where $L_2 = 2.540 \times 10^{-8}$, a conversion factor. In eq (A5), $-L_2 B_n l_n (v_n - v_n^M)$ is the electromotive force generated in segment n, in volts, when the relative velocity between segment n and the magnetic field, in inches per second, is $(v_n - v_n^M)$. Substituting (A2) into (A4) and (A4a), and substituting the results into (A5) gives

$$\{E\} = -F_o L_2[k][y - y^M]' - L_1 L_2[K][z]'\{E_o\} - L_1 L_2[K][Z]\{E\}, \tag{A6}$$

where

$$[K] = [k][Y][k] - [k][Y^M][k]. \tag{A7}$$

Letting

$$[V^{-1}] = [1] + L_1 L_2[K][Z], \tag{A8}$$

where

$$[1] = \begin{bmatrix} 1 & 0 & 0 & \cdot & \cdot & \cdot & 0 \\ 0 & 1 & 0 & \cdot & \cdot & \cdot & 0 \\ 0 & 0 & 1 & \cdot & \cdot & \cdot & 0 \\ \cdot & \cdot & \cdot & & & & \cdot \\ \cdot & \cdot & \cdot & & & & \cdot \\ \cdot & \cdot & \cdot & & & & \cdot \\ 0 & 0 & 0 & \cdot & \cdot & \cdot & 1 \end{bmatrix}, \text{ the unit matrix,}$$

$[V^{-1}]$ = inverse of $[V]$.

$$\{E\} = -F_o L_2[V][k][y - y^M]' - L_1 L_2[V][K][z]'\{E_o\}. \tag{A9}$$

Substituting (A9) into (A1a),

$$\{I_o\} = [z_o]\{E_o\} - F_o L_2[z][V][k][y - y^M]' - L_1 L_2[z][V][K][z]'\{E_o\}. \tag{A10}$$

Substituting (A9) in (A2) and the result in (A3) gives

$$v_o = \frac{F_o}{Y_{oo}} - L_1 L_2 F_o[y - y^M][k][Z][V][k][y - y^M]' + L_1[y - y^M][k][V]'[z]'\{E_o\}, \tag{A11}$$

using

$$[V]' = [1] - L_1 L_2[Z][V][K]. \tag{A12}$$

The proof of eq (A12) is obtained as follows: By using (A8),

$$\begin{aligned}[1]-L_1L_2[Z][V][K]&=[K^{-1}]([K]-L_1L_2[K][Z][V][K])\\&=[K^{-1}]([K]+(1-[V^{-1}])[V][K])\\&=[K^{-1}][V][K].\end{aligned}\tag{A13}$$

Also, premultiplying both sides of (A8) by $[K^{-1}]$,

$$[K^{-1}][V^{-1}]=[K^{-1}]+L_1L_2[Z].\tag{A14}$$

As $[K]$ is symmetric, $[K^{-1}]$ is symmetric. As $[Z]$ is also symmetric, $[K^{-1}][V^{-1}]$ is symmetric. Its inverse $[V][K]$ is therefore also symmetric. The transpose of a symmetric matrix is itself or

$$[V][K]=[K]'[V]'=[K][V]'.\tag{A15}$$

Substituting (A15) in (A13) gives (A12).

The current in the velocity-sensing coil is always zero,

$$I_o^S=[1\ 0]\{I_o\}=0.\tag{A16}$$

Substituting (A10) into (A16) and solving for E_o^S gives

$$E_o^S=\frac{F_oL_2z_{oo}^{SS}[z^S][V][k][y-y^M]'-E_o^D\left(\frac{z_{oo}^{SS}}{z_{oo}^{SD}}-L_1L_2z_{oo}^{SS}[z^S][V][K][z^D]'\right)}{1-L_1L_2z_{oo}^{SS}[z^S][V][K][z^S]'}.\tag{A17}$$

The current in the driving coil is

$$I_o^D=[0\ 1]\{I_o\}.\tag{A18}$$

Substituting (A17) into (A10) and the result into (A18) gives

$$\begin{aligned}I_o^D=F_oL_2&\frac{\left(\frac{z_{oo}^{SS}}{z_{oo}^{SD}}[z^S][V][k][y-y^M]'-[z^D][V][k][y-y^M]'\right.}{1-L_1L_2z_{oo}^{SS}[z^S][V][K][z^S]'}\\&\frac{\left.+L_1L_2z_{oo}^{SS}[z^S][V][K][z^S]'[z^D][V][k][y-y^M]'-L_1L_2z_{oo}^{SS}[z^S][V][K][z^D]'[z^S][V][k][y-y^M]'\right)}{1-L_1L_2z_{oo}^{SS}[z^S][V][K][z^S]'}\\+E_o^D&\frac{\left(\frac{1}{z_{oo}^{DD}}-\frac{z_{oo}^{SS}}{(z_{oo}^{SD})^2}-L_1L_2\frac{z_{oo}^{SS}}{z_{oo}^{DD}}[z^S][V][K][z^S]'+2L_1L_2\frac{z_{oo}^{SS}}{z_{oo}^{SD}}[z^S][V][K][z^D]'-L_1L_2[z^D][V][K][z^D]'\right.}{1-L_1L_2z_{oo}^{SS}[z^S][V][K][z^S]'}\\&\frac{\left.+L_1^2L_2^2z_{oo}^{SS}[z^S][V][K]([z^S]'[z^D]-[z^D]'[z^S])[V][K][z^D]'\right)}{1-L_1L_2z_{oo}^{SS}[z^S][V][K][z^S]'}.\end{aligned}\tag{A19}$$

Substituting (A17) into (A11) gives

$$\begin{aligned}v_o=F_o&\frac{\left(\frac{1}{Y_{oo}}-L_1L_2[y-y^M][k][Z][V][k][y-y^M]'-L_1L_2\frac{z_{oo}^{SS}}{Y_{oo}}[z^S][V][K][z^S]'\right.}{1-L_1L_2z_{oo}^{SS}[z^S][V][K][z^S]'}\\&\frac{+L_1^2L_2^2z_{oo}^{SS}[z^S][V][K][z^S]'[y-y^M][k][Z][V][k][y-y^M]'}{1-L_1L_2z_{oo}^{SS}[z^S][V][K][z^S]'}\\&\frac{\left.+L_1L_2z_{oo}^{SS}[z^S][V][k][y-y^M]'[z^S][V][k][y-y^M]'\right)}{1-L_1L_2z_{oo}^{SS}[z^S][V][K][z^S]'}\\-L_1E_o^D&\frac{\left(\frac{z_{oo}^{SS}}{z_{oo}^{SD}}[z^S][V][k][y-y^M]'-[z^D][V][k][y-y^M]'\right.}{1-L_1L_2z_{oo}^{SS}[z^S][V][K][z^S]'}\\&\frac{\left.+L_1L_2z_{oo}^{SS}[z^S][V][K][z^S]'[z^D][V][k][y-y^M]'-L_1L_2z_{oo}^{SS}[z^S][V][K][z^D]'[z^S][V][k][y-y^M]'\right)}{1-L_1L_2z_{oo}^{SS}[z^S][V][K][z^S]'}.\end{aligned}\tag{A20}$$

The coefficient of L_2F_o in equation (A19) equals the coefficient of $-L_1E_o^D$ in (A20). Equations (A19) and (A20) are subjected first to the condition $v_o=0$ and then to the condition $I_o^D=0$. Eliminating E_o^D in (A19), when $v_o=0$, and F_o in (A20), when $I_o^D=0$, we obtain

$$\frac{F_o}{L_1 I_o^D}\bigg|_{v_o=0} = -\frac{E_o^D}{L_2 v_o}\bigg|_{I_o^D=0} \tag{A21}$$

This is the reciprocity relation that exists in the combined electromechanical system.

Equations (A20), (A19), and (A17) can be written for brevity as

$$v_o = CF_o + AL_1E_o^D \tag{A22}$$

$$I_o^D = -AL_2F_o + BL_1E_o^D \tag{A23}$$

$$E_o^S = HF_o + NL_1E_o^D, \tag{A24}$$

where the constants A, B, C, H, and N depend only on the calibrator construction.

In eq (1) a relationship is given for the calibration factor, defined as $F=E_o^S/v_o$, as a function of the mechanical impedance, Y_p, of the object on the mounting table. We will determine this equation in terms of the calibrator constants A, B, C, H, and N of eq (A22) to (A24). If the force, F_o, is only the reaction to driving a mechanical impedance Y at a velocity v_o,

$$v_o = -F_o/Y. \tag{A25}$$

Substituting (A25) in (A22) and solving for F_o,

$$F_o = -E_o^D \frac{AL_1}{C+1/Y}. \tag{A26}$$

Substituting (A26) into (A24) and (A25) and forming the ratio E_o^S/v_o,

$$F = \frac{E_o^S}{v_o} = \frac{N}{A} + \left(\frac{NC}{A} - H\right)Y. \tag{A27}$$

We see that N/A in eq (A27) is a in eq (1) and $(NC/A)-H$ in eq (A27) is b in eq (1) when Y is Y_p.

$$a = N/A, \qquad b = (NC/A) - H. \tag{A28}$$

In experiment 1, section 2, the transfer admittance $G=I_o^D/E_o^S$ is determined for a series of weights, W, attached to the mounting table. Substituting (A26) into (A23) and (A24) and forming the ratio G,

$$G = \frac{I_o^D}{E_o^S} = \frac{B+(BC+A^2L_2)Y}{N+(NC-AH)Y}. \tag{A29}$$

In experiment 1, Y is the mechanical impedance $j\omega W/g$, where W is the weight on the mounting table, ω the frequency in radians per second, and g the acceleration of gravity, 386 in./sec^2. Making this substitution in (A29) and forming $W/(G-G_o)$, where G_o is the value of G when $Y=0$, we find

$$\frac{W}{G-G_o} = \frac{386}{j\omega}\frac{N^2}{A^2NL_2+ABH} + \frac{N^2C-AHN}{A^2NL_2+ABH}W. \tag{A30}$$

We see that the intercept J and slope Q found in determining $W(G-G_o)$ experimentally are

$$J=\frac{386}{j\omega}\frac{N^2}{A^2NL_2+ABH} \tag{A31}$$

$$Q=\frac{N^2C-AHN}{A^2NL_2+ABH}. \tag{A32}$$

In experiment 2, section 2, the voltage ratio, $R=E_o^s/E_o^p$, is determined when I_o^p is zero. Eliminating F_o between (A23) and (A24) and setting $I_o^p=0$, we see that

$$R=E_o^s/E_o^p=\frac{HBL_1+ANL_1L_2}{AL_2}. \tag{A33}$$

Equation (4) is obtained when eq (A31) through (A33) are substituted into (A28) and L_1 and L_2 have the values given previously.

From eq (A29), $G_o=B/N$, when Y is zero, that is, G_o is the value of G when nothing is attached to the mounting table of the calibrator. If G_p is the value of eq (A29) when $Y=Y_p$, where Y_p is the mechanical impedance of a pickup to be determined, we find that

$$Y_p=\frac{N^2(G_p-G_o)}{(A^2L_2N+AHB)-(N^2C-AHN)(G_p-G_o)}. \tag{A34}$$

The substitution of eq (A31) and (A32) into (A34) gives eq (5) for determining the mechanical impedance of a pickup attached to the mounting table of the calibrator.

We are indebted to L. R. Sweetman for guidance in setting up the laboratory equipment, and to Richard Harwell, Jr., for the careful machining of the masses and the various fixtures used. Ruth Woolley performed the least-squares calculations and Carol Waldron prepared the figures.

8. References

[1] Richard K. Cook, Absolute pressure calibrations of microphones, J. Research NBS **25**, 489–505 (1940) RP1341.

[2] Horace M. Trent, The absolute calibration of electromechanical pickups, J. Appl. Mechanics **15**, 49–52 (1948).

[3] Albert London, The absolute calibration of vibration pickups, NBS Tech. News Bul. **32**, 8–10 (1948).

[4] Sanford P. Thompson, Reciprocity calibration of primary vibration standards, Naval Research Laboratory Rept. F–3337, 8 p. (August 16, 1948).

[5] M. Harrison, A. O. Sykes, and P. G. Marcotte, The reciprocity calibration of piezoelectric accelerometers, David Taylor Model Basin Rept. 811, 14 p. (March 1952).

[6] Ernst A. Guillemin, Communication networks (John Wiley & Sons, Inc., New York, N. Y., 1931).

[7] Horace Lamb, On reciprocal theorems in dynamics, Proc. London Math. Soc. **19**, 144–151 (1889).

[8] R. A. Frazer, W. J. Duncan, and A. R. Collar, Elementary matrices (MacMillan Co., New York, N. Y. 1947).

Washington, March 12, 1956.

Modulated Photoelectric Measurement of Vibration

V. A. Schmidt,* S. Edelman, E. R. Smith, and E. T. Pierce
National Bureau of Standards, Washington 25, D. C.
(Received November 27, 1961)

This paper describes an improvement in the method of setting vibration amplitudes for calibrating vibration pickups by the disappearance of an interferometric fringe pattern. In the usual method, one plate of an interferometer is stationary, the other vibrates with the pickup, and the fringe pattern disappears at zeros of the Bessel function $J_0[(4\pi\xi)/\lambda]$, where ξ is the amplitude of vibration and λ is the wavelength of light used. In the improved method, the fringes are observed by a photomultiplier, the previously stationary plate is vibrated at a modulating frequency much lower than the calibrating frequency applied to the pickup, and the signal from the photomultiplier, filtered at the modulating frequency, has minima at the zeros of $J_0[(4\pi\xi)/\lambda]$. Observation of the nulls on a meter allows faster calibration with greater precision and less observer fatigue.

I. INTRODUCTION

THE method of setting amplitudes by the use of visually observed fringe disappearance has long been used for the precise calibration of vibration pickups. In this method, a Newton's rings pattern is formed between the two nearly parallel plates of a Fizeau interferometer and visually observed through a microscope. The upper plate of the interferometer is fixed while the lower plate is firmly attached to the vibrating shake table holding the accelerometer to be calibrated. Due to the integrating action of the eye, the fringe pattern disappears at a set of discrete amplitudes located at the nulls of the function $J_0(4\pi\xi/\lambda)$, where J_0 is the zero-order Bessel function, ξ is the vibration amplitude, and λ the wavelength of light used to illuminate the interferometer.[1] The first null of this function corresponds to an amplitude of 1045 A at any frequency, using the 5461 A green mercury line.

Though the method basically enjoys that precision associated with optical measurements, the visual determination of the disappearance introduces considerable subjective uncertainties. The present method is an extension of work previously reported[2] and eliminates these subjective errors by displaying the null electrically. Fringe disappearance measurements with shakers whose shake tables are supported compliantly (in particular, with electromagnetic shakers) have been unsatisfactory because of jitter of the fringe pattern. Visually this makes it difficult to determine exactly when disappearance occurs with resulting large errors and observer fatigue. The modulated-frequency photometric interferometer described here is not an integrating device, however, and functions reliably with both compliant and stiff vibration exciters.

In the current method, one of the plates of a Fizeau interferometer is attached to the vibrating surface and the other plate is held by a support that may be vibrated independently from the shaker. The accelerometer and lower interferometer plate are vibrated at the driving frequency f with amplitude ξ by the shaker. The upper plate is driven at the modulating frequency f_1 with a constant amplitude ξ_1 of about 800 A. Good null detection requires that $f \geqq 5f_1$. A photomultiplier looks at the center spot of the Newton's rings pattern formed by the interferometer. The photocurrent is amplified and sent through a narrow bandpass filter tuned to the modulating frequency f_1. The filtered photocurrent is found to have the functional dependence $J_0(4\pi\xi/\lambda)$. A vacuum-tube voltmeter is used to determine the nulls of the function and thus to determine the amplitude of vibration in terms of the wavelength of light used to illuminate the interferometer.

II. THEORY OF OPERATION

In a Fizeau interferometer normal illumination is allowed to fall on two nearly parallel plates of clean, uncoated glass. The reflected beams from the two adjacent surfaces are very nearly equally bright and combine to form an interference fringe pattern. Consider the effect of allowing a small portion of the fringe pattern to fall on a photomultiplier. The photocurrent is given by

$$I = A + B\cos k\delta, \quad k = 2\pi/\lambda, \tag{1}$$

where δ is the optical path difference between the two interfering rays and λ is the wavelength of the incident light. This path difference is twice the separation d of the two surfaces plus the difference in phase change at reflection from the two surfaces.

If, now, the lower plate is vibrated with angular frequency ω and amplitude ξ, and the upper plate is vibrated with angular frequency ω_1 and amplitude ξ_1,

$$d = d_0 + \xi\cos\omega t + \xi_1\cos\omega_1 t, \tag{2}$$

and the optical path difference is given by

$$\begin{aligned} \delta &= \delta_0 + 2(\xi\cos\omega t + \xi_1\cos\omega_1 t), \\ \delta_0 &= 2d_0 + \tfrac{1}{2}\lambda, \end{aligned} \tag{3}$$

where $\frac{1}{2}\lambda$ is due to a phase reversal at only one of the surfaces. The photocurrent then takes the form

$$I = A + B\cos k[\delta_0 + 2(\xi\cos\omega t + \xi_1\cos\omega_1 t)]. \tag{4}$$

---

* Present Address: Carnegie Institute of Technology, Pittsburgh, Pennsylvania.

[1] D. H. Smith, Proc. Phys. Soc. (London) **57**, 534 (1945).

[2] V. A. Schmidt, S. Edelman, E. R. Smith, and E. Jones, J. Acoust. Soc. Am. **33**, 748 (1961).

With algebraic manipulation, this may be rewritten in the form

$$I=A+B\{\cos k\delta_0[\cos(2k\xi\cos\omega t)\cos(2k\xi_1\cos\omega_1 t)-\sin(2k\xi\cos\omega t)\sin(2k\xi_1\cos\omega_1 t)]-\sin k\delta_0[\sin(2k\xi\cos\omega t)\cos(2k\xi_1\cos\omega_1 t)+\cos(2k\xi\cos\omega t)\sin(2k\xi_1\cos\omega_1 t)]\}. \quad (5)$$

We now make use of the Fourier expansion of the two terms[3] in Bessel functions

$$\cos(2k\xi\cos\omega t)=J_0(2k\xi)-2J_2(2k\xi)\cos 2\omega t+\cdots, \quad (6)$$

$$\sin(2k\xi\cos\omega t)=2J_1(2k\xi)\cos\omega t-2J_3(2k\xi)\cos 3\omega t+\cdots,$$

in order to rewrite Eq. (4) in the form

$$I=A+B\cos k\delta_0\{[J_0(2k\xi)-2J_2(2k\xi)\cos 2\omega t+\cdots]\times[J_0(2k\xi_1)-2J_2(2k\xi_1)\cos 2\omega_1 t+\cdots]-[2J_1(2k\xi)\cos\omega t-2J_3(2k\xi)\cos 3\omega t+\cdots]\times[2J_1(2k\xi_1\cos\omega_1 t-2J_3(2k\xi_1)\cos 3\omega_1 t+\cdots)]\}-B\sin k\delta_0\{[2J_1(2k\xi)\cos\omega t-2J_3(2k\xi)\cos 3\omega t+\cdots]\times[J_0(2k\xi_1)-2J_2(2k\xi_1)\cos 2\omega_1 t+\cdots]+[J_0(2k\xi)-2J_2(2k\xi)\cos 2\omega t+\cdots]\times[2J_1(2k\xi_1)\cos\omega_1 t-2J_3(2k\xi_1)\cos 3\omega_1 t+\cdots]\}. \quad (7)$$

If the photocurrent is now sent through a bandpass filter tuned to angular frequency ω_1, terms whose time dependent part is anything other than $\cos\omega_1 t$ alone will drop out, leaving only

$$I=|2B\sin k\delta_0 J_1(2k\xi_1)J_0(2k\xi)|\cos\omega_1 t.$$

The absolute value of the coefficient is used since the light intensity is never negative. We now see that the motions of the two interferometer plates are nicely separated. The $\sin k\xi_0$ and $J_1(2k\xi_1)$ terms will be held constant at their maximum values by adjusting the mean mirror separation and the amplitude of the upper plate, respectively. The dependence of the output on the amplitude of the shaker is then simply $|J_0(4\pi\xi/\lambda)|$ as shown in Fig. (1).

Even though several of the cross terms in Eq. (7) may happen to have Fourier components very close to ω_1, it is easily shown that these terms also drop out provided the condition is met that $\omega\geqslant 5\omega_1$. Cross terms of the form $\cos n\omega_1 t\cos\omega t$, where n is an integer, will pass the filter only if $n\omega_1-\omega\approx\omega_1$. The $\cos n\omega_1 t$ term, however, carries with it the coefficient $J_n(2k\xi_1)$ in each case. In practice, ξ_1 will be adjusted to bring $J_1(2k\xi_1)$ in Eq. (8) to its first maximum. For this value of ξ_1, the coefficients $J_n(2k\xi_1)$ will all be negligibly small for $n\geqslant 5$. This relationship between the Bessel functions of different orders is beautifully illustrated in Fig. 67 of Jahnke and Emde.[4]

It has been shown[2] that the effect of allowing the phototube to see a finite and hence nonuniform portion of the fringe pattern alters Eq. (8) only by a constant. As a result, we may allow the photomultiplier to examine a large portion of the center spot of the Newton's rings pattern, making the signal-to-noise ratio as large as possible.

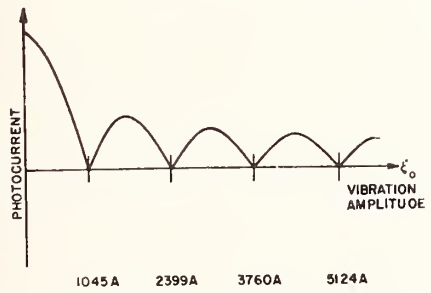

FIG. 1. Dependence of filtered photomultiplier output on vibration amplitude of shake table. Measurements are made at the zeros of the curve.

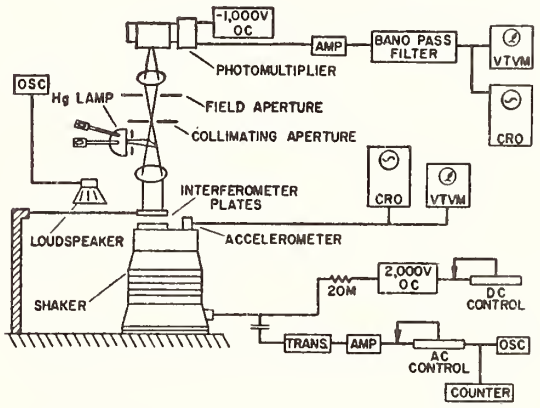

FIG. 2. Block diagram of modulated-frequency calibrator.

III. INSTRUMENTATION AND OPERATION

Figure 2 shows the essential details of the modulated-frequency interferometer. A small, plane, unsilvered mirror is attached to the shake table immediately beside the accelerometer to be calibrated. The upper plate, a 0.012 diopter plano-convex lens, is mounted just above the plane mirror. The support for this lens was found to have structural resonances between 100 and 200 cps. In order to induce the low modulating frequency of vibration in the upper plate, a small loudspeaker rests on the lens support and is driven at one of the structural resonances.

Light falling on the interferometer plates is collimated by a standard microscope vertical illuminator and a collimating pinhole inside the microscope barrel. As previously reported,[2] collimation is critical and deviations from normally incident illumination were held to less than 0.7° in this apparatus. A field aperture is placed at the focal plane of the fringe pattern so that

[3] H. B. Dwight, *Tables of Integrals and other Mathematical Data* (The Macmillan Company, New York, 1951), p. 184.

[4] E. Jahnke and F. Emde, *Tables of Functions* (Dover Publications, Inc., New York, 1951), p. 126.

the photomultiplier will see only the center spot of the Newton's rings pattern. The photomultiplier signal is amplified and sent through a narrow bandpass filter tuned to the modulating frequency of the upper plate before being measured by a vacuum-tube voltmeter.

In operation, the shaker is first left at rest and the modulating frequency is induced in the upper plate by the loudspeaker. The amplitude of the modulating vibration is adjusted to bring the metered output to its first maximum, corresponding to the first maximum of $J_1(4\pi\xi_1/\lambda)$. The mean mirror separation is then adjusted to further maximize the output, corresponding to a maximum of $\sin k\delta_0$. These two terms are now left constant, though the mean mirror separation may have to be readjusted periodically because of mechanical drift. Control of the mean mirror separation was achieved for the case of piezoelectric stack shakers by superimposing a dc bias on the ac driving signal to the shaker (see Fig. 2). Electromagnetic shakers were mounted on top of a low, squat piezoelectric shaker that was fed by an adjustable dc signal only.

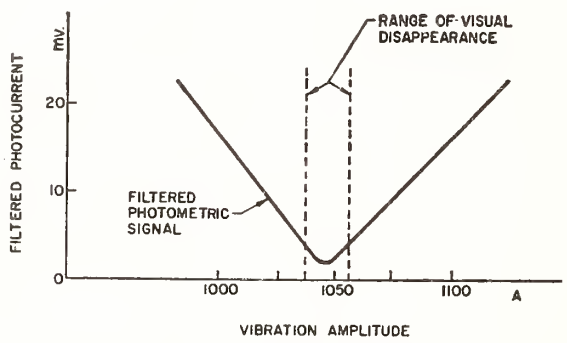

FIG. 3. Modulated-frequency and visual calibration sensitivities.

The shaker on which the accelerometer is mounted is now driven to first disappearance amplitude, at which time the filtered photocurrent drops to a very distinct null, the first zero of $J_0(4\pi\xi/\lambda)$ in Eq. (8). If the mercury green line is being used as the standard, the amplitude of vibration ξ has the value 1045 A. The output of the accelerometer can now be measured, constituting one calibration point. As with the visual method, calibration may be carried out at higher orders of disappearance as well.

Using a GE H 100-A4 mercury vapor lamp in a water-cooled jacket, a signal-to-noise ratio of the filtered photocurrent in excess of 50 db was not difficult to obtain.

IV. CONCLUSIONS

A comparison of the sensitivities of the visual disappearance and modulated photometric methods is given in Fig. 3. The shape of the filtered photocurrent curve demonstrates the sharpness of the null, while the area between the dashed lines indicates the range over which

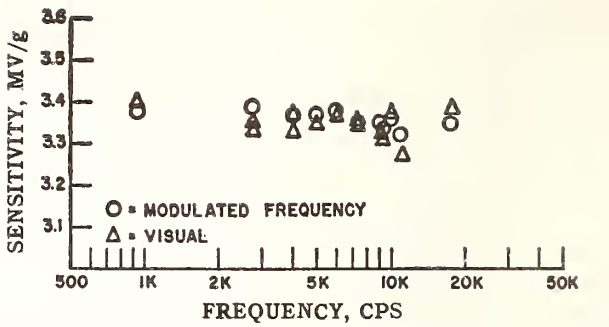

FIG. 4. Pickup calibration by modulated-frequency and visual methods. Calibration of small piezoelectric accelerometer NBS Z-54. Two separate piezoelectric shakers were used for this calibration. The frequency range shown does not reflect the range of the modulated-frequency interferometer but rather covers only the range where uniaxial motion was obtainable with the particular shakers employed. Circles show measurements taken with the modulated interferometer; triangles show points taken using visual fringe disappearance.

visual fringe disappearance is complete under the best conditions. The human eye cannot distinguish any change in contrast within this region.

Figure 4 shows the results of a calibration of a small vibration pickup using both visual disappearance and the modulated-frequency interferometer. In general the points for the modulated-frequency interferometer represent fewer measurements than the visual points; this was due to the smaller spread of photometric data. The agreement is within the known precision of the visual method. In general, the total range of scatter in the modulated-frequency photometric data was on the order of 0.7%. The accuracy of calibration, however, depends primarily on the absence of relative motion between the lower interferometer plate and the accelerometer. Only if perfectly uniaxial (piston-like) motion is maintained can the accuracy of this method be fully exploited. With existing piezoelectric shakers, the effects of transverse vibration on the calibration can be held to $\pm 2\%$ with careful monitoring. The data in Fig. 3 reflect this situation.

Since the modulated-frequency interferometer does not duplicate the integrating effect of the human eye, several undesirable features of the visual disappearance method are eliminated. Very compliant shakers tend to introduce a considerable amount of jitter into the fringe pattern due to building-borne vibrations or acoustic pickup. This jitter tends to wash out the visually observed null and generally precludes satisfactory calibration by the visual fringe disappearance method. It is interesting to note that the null obtained with the modulated-frequency interferometer is as complete with a jittery signal as with a clean one, and only slightly more difficult to locate provided the jitter is not so large as to bring about a disappearance itself. If necessary, then, this method may be used in a noisy environment where even the use of a vibration isolation system is not sufficient to allow use of the visual method.

With the elimination of visual observation and the

need for taking many measurements to ensure reproducibility, observer fatigue is greatly reduced.

With the present apparatus, a modulating frequency of 100 cps was obtainable, allowing a range of calibration from 500 cps to about 30 kc, beyond which sufficient uniaxial motion for disappearance is difficult to obtain.

An attempt was made to extend the lower frequency limit by reversing the roles of the two interferometer plates, driving the top plate at a higher modulating frequency f_1 and driving the shaker at a very low frequency f such that $f \ll f_1$, with the filter tuned to f_1. This was unsuccessful due to the presence in Eq. (8) of a $\cos\omega t \cos\omega_1 t$ term, whose sum and difference components were too close to the modulating frequency f_1 to be rejected by the filter. It was concluded that with the present apparatus the modulating frequency must always meet the requirement $f > 5f_1$ for the method to be reliable.

The loudspeaker drive for the upper plate is admittedly crude, and the inclusion of a means for directly driving it from a controlled source should make much lower frequencies accessable to the instrument.

ACKNOWLEDGMENTS

This work was sponsored by the Special Projects Office, Department of the Navy.

Reprinted from The Journal of the Acoustical Society of America

Vol. 34, No. 4, 455–458, April, 1962

Calibration of Vibration Pickups at Large Amplitudes

E. Jones, S. Edelman, and K. S. Sizemore
National Bureau of Standards, Washington, D. C.
(Received July 18, 1961)

Axial resonances of long rods and tubes were used to generate motion for accurate calibration of vibration pickups over the frequency range from below 1 to above 20 kc at acceleration levels up to 12 000g. The resonators were driven by an electromagnetic shaker at low frequencies and by a piezoelectric ceramic stack shaker at high frequencies. Vibration amplitude was measured optically by means of a microscope using stroboscopic light and by means of the interference fringe disappearance technique. Adequate overlap between the two methods was achieved by going up to the 60th disappearance of the fringes. A simple, direct measurement of the phase angle between the pickup signal and the motion is described. Construction details of a small, light pickup which is unaffected by the high acceleration levels are given.

INTRODUCTION

A PROGRAM of vibration pickup calibration at high levels of sinusoidal acceleration arose from a need to determine if the pickup sensitivity is linear over a large range of amplitude and the extent to which a pickup can undergo sustained large acceleration forces without structural damage or change of sensitivity. Pickups which are unaffected by large accelerations are suitable for studies of mechanical fatigue and failure, studies of the vibrations of high speed rotating machinery and of projectiles, accelerated life and environmental tests, and studies of the effectiveness of vibration isolators and mounts. Their use for measurements in which the effects of sinusoidal excitation are compared with the effects of shock are more informative if the phase lag between the mechanical vibration and the output signal from the pickup is known. One measurement of phase lag is reported here to show how it can be made, but phase information was not required for our calibrations.

VIBRATION GENERATORS

The accelerations for most of the tests in the paper were generated by piezoelectric ceramic shakers constructed in our laboratory. Each consists of a driver element cemented between a heavy base of brass or steel and a top, usually steel, or sometimes aluminum. The driving element is a number of lead-zirconium-titanate discs cemented together with a conducting epoxy resin which acts both as cement and electrode. The behavior and construction details of these shakers will be described in a later paper.

Motion for a few of the lower frequencies was generated by a modification of an electromagnetic shaker which was described in a previous paper.[1]

A major factor limiting the accuracy of pickup calibration is the problem of generating uniaxial, undistorted sinusoidal motion. Much of the unwanted noise, distortion, and transverse motion of the shake table can be minimized through the insertion of a mechanical filter between the shaker and the pickup it drives.

In most of the calibrations for this study such a filter was formed by a slender rod or tube driven at one of its longitudinal resonances. The amplification of the motion by the resonant rod allowed a given amplitude to be reached with a reduction in the noise and distortion generated by the shaker and associated driving circuits. The amplification derived from the mechanical resonant system also reduced the brute force required from the power amplifiers.

A brief survey of possible resonant system types led to our selection of tubes and rods in longitudinal resonance for use in these studies. Although usable results have been reported,[2,3] our study showed that with any type of bending system it is difficult to generate large vibration amplitudes precisely along any preferred axis except at low frequencies. Modes above the fundamental are useless because, unlike longitudinal systems, bending systems have twisting and rotating effects difficult to control that increase with mode order. The problem of off-axis motion is less severe with longitudinal systems.[4–8] First, the bending modes in the frequency range of any longitudinal resonance, fundamental included, of a slender rod are of high order and attenuated. Second, there is seldom coincidence between the two mode types either with respect to frequency or node location. Therefore, a small transverse damping constraint at a longitudinal node usually suffices to eliminate transverse motion with little effect on longitudinal motion.

The shorter rods and tubes were usually attached upright to a solidly supported ceramic shaker and

[1] S. Edelman, E. Jones, and E. R. Smith, J. Acoust. Soc. E. R. Am. 27, 728–734 (1955).

[2] F. G. Tyzzer and H. C. Hardy, J. Acoust. Soc. Am. 22, 454 (1950).

[3] T. A. Perls and C. W. Kissinger, "High range accelerometer calibrations," Natl. Bureau Standards Rept. No. 3299, June, 1954.

[4] W. P. Mason and R. F. Wick, J. Acoust. Soc. Am. 23, 209 (1951).

[5] R. O. Belsheim, "Delayed yield time effect in mild steel under oscillatory axial loads," NRL Rept. 4312, March 22, 1954.

[6] J. N. Brennan, J. Acoust. Soc. Am. 25, 610 (1953).

[7] J. S. Nisbet, J. N. Brennan, and H. I. Tarpley, J. Acoust. Soc. Am. 32, 71 (1960).

[8] Ivan E. Walenta and Benjamin V. Connor, "A sinusoidal vibrator for generating high acceleration of high frequencies," Technical Report No. 32-13, Jet Propulsion Laboratory, California Institute of Technology, January, 15, 1960.

viewed in vertical vibration. Considerable care was required to suspend the rather flexible, longer units so that the rod was held with its axis unchanging and with longitudinal motion unhampered. Our choice was to orient shaker and rod horizontally, the shaker resting on a fixed support. About midway of the rod a rigid upright support held a horizontal beam over the rod free to pivot about a horizontal axis normal to the rod. At each end of the horizontal beam two smaller beams were attached, each also free to pivot about a horizontal axis normal to the rod. From the four ends of the smaller beams flexible cords dropped to support the rod. This method provided equally distributed support to four points along the rod. Attachment of the cords to points which were as near as possible to longitudinal nodes and transverse antinodes served further to constrain transverse motion. One of the smaller beams can be seen in upper left of Fig. 1.

Important considerations in choosing rods and tubes for resonators are uniformity of cross section and lack of curvature. In order to calibrate over a wide frequency range a set of resonators is necessary, although it is not required to have a separate resonant element for each test frequency. A given resonator can be used at many of its higher order harmonics. Tubes have lower resonant frequencies than rods of the same length and mechanical load and are used at the lower frequencies where space becomes important.

The rods were selected from hex aluminum alloy stock either $\frac{5}{8}$ or $\frac{1}{2}$ in. in diameter, one end machined for attachment to a shaker and the other machined flat for pickup attachment. The tubes were constructed from sections of stock aluminum alloy tubing 1 in. o.d., $\frac{1}{32}$ in. wall thickness having a shaker adapter on one end, and a pickup adapter with area enough to mount a small mirror for interferometric measurements next to the pickup on the other. The adapters were about 1 in. long cut from 1 in. hex aluminum and cemented to the squared-off tube with epoxy cement.

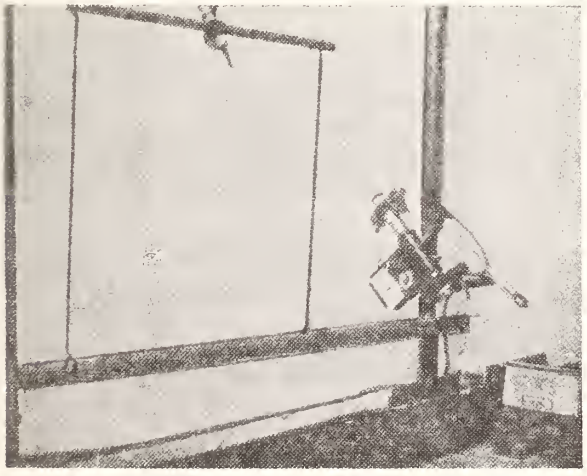

Fig. 1. Stroboscopic microscope measurement on horizontally supported resonator.

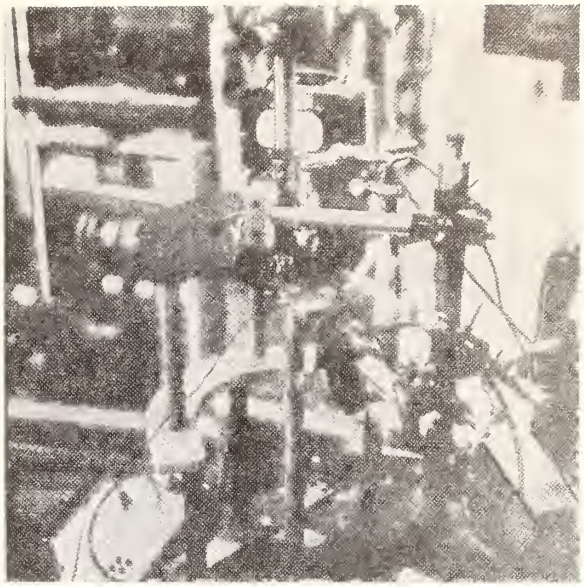

Fig. 2. Simultaneous interferometric and stroboscopic measurements on vertical resonator.

A number of tubes and rods were prepared with different lengths to constitute a set of resonators for calibrating at many points over a wide frequency range.

The power amplifiers used to drive the shakers are standard heavy duty hi-fi amplifiers. Since these amplifiers are designed to power low impedance loads, we use audio output transformers as step-up transformers to drive piezoelectric shakers. The shakers are essentially capacitors and become low impedance loads at the higher frequencies. Inductors of a value to present the amplifier an electrically tuned circuit at a given frequency are connected in parallel across the shaker terminals. In addition to permitting maximum driving voltage for a particular frequency, tuning serves to filter out distortion in the driving signal.

PICKUP ATTACHMENT

For high acceleration-level calibration considerable care is required in attaching test pickups. Failure to seat the pickup base firmly against the driving surface can result in chatter or loosening of the pickup under sustained vibration. Some pickups have screw mounting studs large enough for adequate torquing. Pickups with flat bottoms can be cemented to the driving surface. This seems to provide the best attachment.

PROCEDURE

In all our calibrations the sinusoidal acceleration level was determined by measuring the displacement amplitude of vibration. The frequency of vibration was determined from Lissajou comparisons with NBS standard frequencies or by electronic frequency counters. Acceleration amplitudes were computed from frequency and displacement.

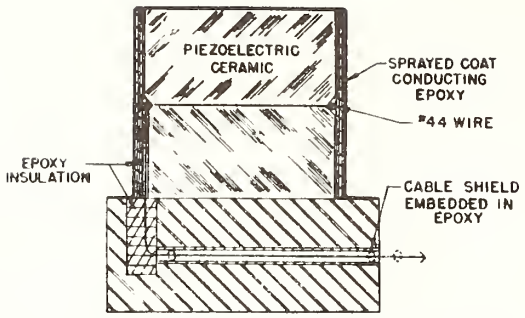

FIG. 3. Construction of pickup designed to withstand high acceleration levels.

Most displacement measurements were made by means of a microscope, with a micrometer eyepiece viewing a spot on the base of the pickup under stroboscopic illumination as it vibrated at constant amplitude. A description of this method, shown in Fig. 1, has been published.[1] For large vibration displacements the method of measuring motion directly with a microscope is well suited for the accurate determination of amplitudes. Also, it serves the equally useful function of determining precisely the direction of shaker motion. With a distortion check of the output waveform this method affords a complete description of large amplitude sinusoidal vibration.

The interference-fringe-disappearance method was used to measure the smaller displacements. A description of this method has also been given.[1] An overlap between the two calibration methods was secured by making an interferometer calibration past the 40th disappearance which corresponds to a displacement that the microscope method can measure accurately. To keep the setup physically small enough for interferometer use at a frequency low enough to measure displacements corresponding to 1g, a tube resonator was used. The interferometer microscope was focused on the fringe pattern formed above the small mirror cemented to the surface carrying the test pickup. The direct view strobe microscope was focused to measure the motion of a spot on the base of the pickup. Figure 2 shows how a simultaneous calibration was made. On a few occasions interferometric calibrations have been made up to the 60th disappearance. Due to the tediousness of calibrating at large orders of disappearance, the simultaneous check on sensitivity was not made at all frequencies after it was found that the two methods agreed.

PICKUPS CALIBRATED

High g calibrations have been made on commercial-type accelerometers and on pickups constructed in our laboratory. A homemade piezoelectric pickup was selected for most of this work since we were certain of its ability to stand up under a long series of high accelerations. This pickup is a cemented type similar in construction to our ceramic shakers.

Figure 3 is a diagram of the pickup which is 0.250 in. in diameter, 0.300 in. in height, and weighs 1.5 g. Its unmounted resonant frequency is about 150 kc. The capacitance of the pickup and 5 in. of permanently attached connector cable is 120 $\mu\mu f$. Sensitivity is about 3.5 mv/g. It consists of a circular cemented piezoelectric-ceramic sandwich cemented to a stainless steel base. The adhesive is conducting epoxy. The pickup cable passes through the base to which the shield is both electrically and mechanically anchored. The center conductor connects through a shallow groove in the lower disc to the conducting interface of the sandwich. A coating of plain epoxy insulates the center lead at all other points. The unit is shielded with a sprayed-on coating of conducting epoxy. No inertial mass other than the ceramic is used in this design.

TABLE I. Phase angle between pickup CB-1 signal and displacement.

Frequency (cps)	Phase angle by which signal lags displacement (deg)
2500	5-8
3000	10
3250	15
3500	40
3750	60
Resonant frequency—3900 cps	

PHASE MEASUREMENT

Information on phase lag between pickup output and motion was not needed in this study but might be required in other applications. Two sets of phase lag measurements were made during these experiments. One set was made on the pickup which was used for most of the high acceleration level calibrations and showed no measurable lag in the frequency range of calibration. The other set of phase lag measurements was made on a larger pickup of the cemented ceramic type which had a large mass and weaker equivalent spring. The latter pickup was designed to have a comparatively low resonant frequency so that significant values of phase lag could be found at audio frequencies. These measurements are given in Table I.

The phase measurements were made during a strobe microscope calibration. Using the circuit shown in Fig. 4, strobe flashes, triggered by the signal used for

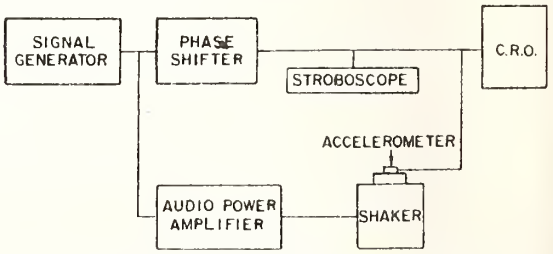

FIG. 4. Electronic circuit for stroboscopic measurement of displacement amplitude and phase.

TABLE II. Maximum acceleration level and resonator at a number of frequencies.

Calibration frequency	Maximum acceleration level peak g		Resonator Shape	Material alum alloy	Length
830	2000	C	Round tubing 1 in. o.d. $\frac{1}{32}$ in. wall	2024-T3	52 in.
1400	5000	E	$\frac{3}{8}$-in. hex rod	2017-T4	35-in.
2600	6000	H	$\frac{3}{8}$-in. hex rod	2017-T4	18 in.
4300	8000	E	$\frac{3}{8}$-in. hex rod	2017-T4	35 in.
10 000	6000	E	$\frac{3}{8}$-in. hex rod	2017-T4	35 in.
13 000	6000	E	$\frac{3}{8}$-in. hex rod	2017-T4	35 in.
19 000	11 000	F	$\frac{3}{8}$-in. hex rod	2017-T4	18 in.
20 000	10 000	B	$\frac{1}{2}$-in. hex rod	2017-T4	20 in.
22 000	12 000	G	$\frac{3}{8}$-in. hex rod	2017-T4	27 in.

driving the shaker, were phased to illuminate the pickup at a displacement extreme as viewed by the microscope. Signals from these pulses were superimposed on the pickup output signal and displayed on an oscilloscope as in Fig. 5. The phase lag was the adjustment on the calibrated phase shifter in Fig. 4 required to place the strobe pips at the peaks of the pickup sine wave signal. Similar phase measurements have been made at higher frequencies and smaller amplitudes. The apparent motion of interference fringes formed by stroboscopic light was used to detect the extremes of displacement instead of the apparent motion of the pickup.

These measurements indicate that over the frequency range for which its response is reasonably flat, phase lag considerations are negligible for a piezoelectric-ceramic vibration pickup.

RESULTS

Figure 6 shows the range of accelerations through which a pickup was calibrated at one frequency. The pickup was mounted on a resonant tube in a way to permit the two types of measurements shown in Fig. 2.

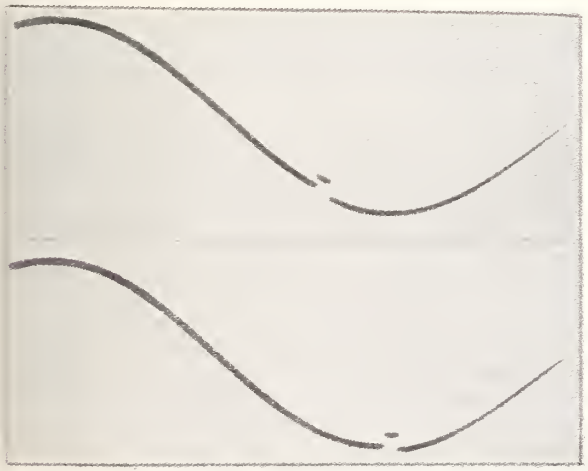

FIG. 5. Oscilloscope trace, strobe pulse superimposed on accelerometer output signal. Upper trace shows pip on pickup signal at time of extreme displacement of pickup. Lower trace shows pip shifted to extreme value of signal by calibrated phase shifter. The phase angle introduced by the phase shifter to move pip from position in upper trace to position in lower trace is phase lag of signal behind motion.

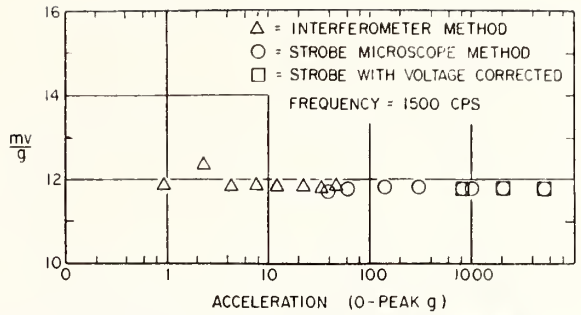

Fig. 6. Sensitivity vs acceleration of 2-9 accelerometer.

The higher acceleration points are labeled "corrected" because the pickup signal was too high for the meter circuit cathode follower, and signal attenuation was required ahead of the cathode follower. Table II shows the high acceleration levels obtained over the frequency range 800 to 20 000 cps.

In general, rods are used for higher frequencies and tubes at lower frequencies. It is to be noted that a given resonator is often usable at several of its harmonics, as well as in its fundamental mode.

SIDELIGHTS

It may be in order to mention a few sidelights of our experience in high g level calibrating. Sometimes a transverse resonance is mistaken for or lies close enough to be excited along with a longitudinal mode. The mistaken identity is usually detected acoustically in short order. In place of pure sine tones there is a build up of loud noises, and the slender rods whip about in a violent manner.

Sometimes attempts to raise the amplitude of a particular longitudinal resonance sets off a transverse mode many octaves below the driving frequency. The low frequency mode gradually builds up and takes over sufficiently to damp the longitudinal mode to a level where it no longer excites the low frequency mode, and the latter diminishes. The longitudinal resonance again builds up, and the whole sequence repeats every few seconds, as in the textbook description of coupled modes.

We have noticed that if the driving signal is ultrasonic and everything else is quiet, sliding the hand over antinodes produces mouse-like squeaks. The antinodes have a warm silky touch as though coated with oil.

The standing wave pattern of a rod tends to force contacting objects towards its nodes. If a wheel is moved along the rod from node to node, it will spin rapidly first in one direction and then another, always toward a node.

CONCLUSIONS

We have found it possible and convenient to calibrate vibration pickups at thousand g levels over a wide

frequency range. It is also possible to establish amplitude linearity checks over a range of nearly 10.[4]

Many people, using other methods, have attained larger amplitudes of vibration than those reported here. Levels up to 100 kg were reported for the equipment described in reference 8 and similar equipment made by the Sandia Corporation, Livermore, California.[9] When amplitudes greater than those reported here were reached on our resonators we found that the motion was no longer undistorted and uniaxial. Some of the departure from good motion was due to the effect of the pickup and its mounting aided by the unbalancing effect of the cable. Some was caused by incipient nonlinearity in the rod and in the power amplifier. Thus the acceleration levels reported here are the highest our present equipment allows with proper regard for accuracy and precise control.

For any of our points the errors are estimated to be no greater than 2%. A program is presently underway to improve this figure. Many pickups are described as not being affected by high acceleration levels applied as shocks. We have found that some are damaged by lower levels applied as sustained vibration.

[9] H. J. Jensen, (Acoustical Society of America, 61st Meeting, Paper N5, May 12, 1961).

ACKNOWLEDGMENT

This work was sponsored by the Special Projects Office, Department of the Navy.

Reprinted from The Journal of the Acoustical Society of America, Vol. 33, No. 11, pp. 1462–1466, November, 1961

JOURNAL OF RESEARCH of the National Bureau of Standards—C. Engineering and Instrumentation
Vol. 66D, No. 4, October–December 1962

A Dual Centrifuge for Generating Low-Frequency Sinusoidal Accelerations

R. O. Smith, E. A. Willis, and J. S. Hilten

(July 10, 1962)

This paper describes an experimental "dual centrifuge" in which an accelerometer being calibrated is carried around a circular path in a horizontal plane. If the instrument is constrained to have nonrotational motion, such as is provided by a parallel link device, sinusoidal excitation along its sensitive (horizontal) axis is obtained. The excitation obtainable is equivalent to linear excitation but at unusually low frequency and large displacement. For example, a machine has been built which has a frequency range from 0.5 to 30 cycles per second, a displacement (zero to peak) up to 12 inches, and develops an acceleration amplitude, useful for calibration, up to 100 gravity at 10 cycles per second and above.

1. Introduction

Because of the wide use of low-frequency accelerometers there is a need for a calibration system tailored to the requirements of these instruments. This necessity has led to the consideration of several methods of generating the required low-frequency accelerations. At low frequencies most systems suffer from one or more limitations, such as poor waveform, restricted amplitude, or excessive superimposed vibration.

The several systems for obtaining low-frequency sinusoidal calibration have been reviewed, which may be classified as (1) electrodynamic, (2) transient, or (3) mechanical shakers.

The electrodynamic shaker is undoubtedly the most useful calibrator for laboratory use. However, it usually suffers from insufficient amplitude at low frequencies. A typical example of a low-frequency electrodynamic shaker has a frequency range of 0.35 to 500 c/s but provides a maximum displacement of only 2 in. (double amplitude), whereas about 20 in. displacement is required to develop 1 g at 1 c/s.

Transient shakers usually take the form of a cantilever spring upon whose free end the instrument under test is fixed. They suffer from the fact that the excitation is transient, so that it is difficult to correlate excitation amplitude with response. In addition each shaker is usually restricted to a single frequency and several shakers are required to cover any appreciable range.

The mechanical shakers reviewed may be subdivided into three classifications: (1) four-bar linkages, (2) inertial shakers, and (3) rotary calibrators. Four-bar linkages, e.g., scotch yokes and slider-crank mechanisms, cannot generate a truly sinusoidal test motion because of the varying effective moment of inertia. In order to get the requisite stiffness in the reciprocating parts it is required that a relatively large mass be subjected to the test motion so that the sinusoidally varying inertial forces are necessarily large. If the test motion is to be nearly sinusoidal it is required that the angular velocities of the rotating parts be nearly uniform and it will therefore be required that the rotating members have a high moment of inertia, and a bulky, massive device results.

An inertial shaker suitable for calibration purposes has been designed by the Engineering Mechanics Section of the Bureau [1] [1] which consists of a spring-mass driven by an eccentric weight. Its frequency range is 20 to 110 c/s. Inertial shakers of lower frequency are rarely used for calibration because of poor waveform.

A rotary dynamic calibrator which uses the earth's field for excitation has been devised by Wildhack and Smith [2]. This device is limited in acceleration amplitude to a maximum of 1 g at all frequencies. It is presently in use by the Mechanical Instruments Section of the Bureau over the frequency range 1 to 30 c/s.

The dual centrifuge, which uses its own centrifugal field for excitation, was described by Woolard in 1939 [3]. It consists essentially of a small turntable mounted on a large one, each turning in a horizontal plane. The instrument under test is mounted on the small table. When the turntables have constant angular velocities the seismic mass of the accelerometer responds to a sinusoidally varying component of the centrifugal force field generated by the rotation of the large table. Woolard published an equation showing the acceleration amplitude in terms of angular velocities, original displacement, and relative displacement of the seismic mass, but did not publish a complete mathematical analysis of the response. However, he did point out that when the small table turns backwards so that it has zero absolute rotation, the accelerometer is submitted to sinusoidal acceleration which may be of large amplitude. This is the practically important feature of the dual centrifuge and one that has been generally overlooked.

The following discussion, which describes a mechanical configuration similar to Woolard's design, and develops the equation of motion of the seismic mass, shows the dual centrifuge to be a useful tool for dynamic calibration, particularly when a large amplitude is required at low frequencies.

[1] Figures in brackets indicate the literature references at the end of this paper.

2. Analysis of the Response of a Linear 1-Degree of Freedom Seismic Accelerometer to General Plane Motion Excitation

Although the conclusion of this paper is that the useful form of the dual centrifuge is that one in which the small table has zero absolute rotation, a general analysis of the motion without this limitation is instructive.

In the general case, the housing of the instrument under test will have motion of 3 degrees of freedom, i.e., two of translation and one of rotation. The physical situation is shown in figure 1. The large turntable turns with an absolute angular velocity ω_0 about its center 0. The small table rotates about point p with constant absolute angular velocity ω_p, and an angular velocity $\Omega=\omega_p-\omega_0$ relative to the large table. The point 0 is chosen as the origin of a plane nonrotating coordinate system, with positive directions chosen according to usual convention. Let the radius from 0 to p be R_0. In general, the test position p' of the seismic mass m will not coincide with p. If a-b represents the direction of the sensitive axis, then p' is located an amount d from p, perpendicular to a-b, and an amount e parallel to a-b. Response of the instrument consists of displacement S along a-b and the equation of motion is therefore in terms of S.

The following assumptions apply to the analysis:

(1) Plane horizontal motion,
(2) Point 0 is fixed,
(3) R_0, ω_0, and ω_p are constant,
(4) The instrument has no transverse response,
(5) The instrument is a linear 1-degree of freedom system,
(6) Accelerometer damping is viscous.

Referring to figure 1, it will be seen that if the seismic mass m is constrained to motion along the axis a-b the motion of the mass may be described by the following coordinate equations in which s, s, and $\ddot{s}$ are relative to the instrument case:

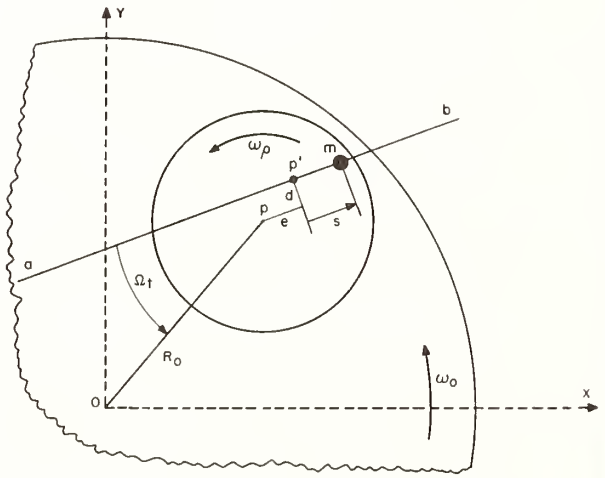

FIGURE 1. *Schematic diagram of the dual centrifuge.*

$$x=R_0\cos\omega_0 t-d\sin\omega_p t+(e+s)\cos\omega_p t \tag{1}$$

$$y=R_0\sin\omega_0 t+d\cos\omega_p t+(e+s)\sin\omega_p t. \tag{2}$$

Double differentiation shows that the coordinate equations which describe the acceleration of m are:

$$\ddot{x}=-R_0\omega_0^2\cos\omega_0 t+d\omega_p^2\sin\omega_p t-(e+s)\omega_p^2\cos\omega_p t -2\dot{s}\omega_p\sin\omega_p t+\ddot{s}\cos\omega_p t \tag{3}$$

$$\ddot{y}=-R_0\omega_0^2\sin\omega_0 t-d\omega_p^2\cos\omega_p t-(e+s)\omega_p^2\sin\omega_p t +2\dot{s}\omega_p\cos\omega_p t+\ddot{s}\sin\omega_p t. \tag{4}$$

The acceleration along the axis a-b to which the mass m is subjected is the sum of the projections of these coordinate components along a-b, i.e., acceleration $=\ddot{x}\cos\omega_p t+\ddot{y}\sin\omega_p t$ or acceleration $=\ddot{s}-(e+s)\omega_p^2-R_0\omega_0^2\cos\Omega t$.

So that the equation of motion may be derived:

$$m\ddot{s}+c\dot{s}+ks=mR_0\omega_0^2\cos\Omega t+m(e+s)\omega_p^2. \tag{5}$$

If $\omega_n=\sqrt{\dfrac{k}{m}}$ and $p=c/c$ critical when c critical $=2\sqrt{mk}$, this equation can be reduced to:

$$\ddot{s}+2p\omega_n\dot{s}+(\omega_n^2-\omega_p^2)s=R_0\omega_0^2\cos\Omega t+e\omega_p^2. \tag{6}$$

The solution of eq (6) is:

$$s=Ae^{-\omega_n t\left(p+\sqrt{p^2-1+\frac{\omega_p^2}{\omega_n^2}}\right)}+Be^{-\omega_n t\left(p-\sqrt{p^2-1+\frac{\omega_p^2}{\omega_n^2}}\right)} +\frac{R_0\omega_0^2[(\omega_n^2-\Omega^2-\omega_p^2)\cos\Omega t+2p\omega_n\Omega\sin\Omega t]}{(\omega_n^2-\omega p^2-\Omega^2)^2+4p^2\omega_n^2\Omega^2}+\frac{e\omega_p^2}{\omega_n^2-\omega_p^2}. \tag{7}$$

The steady state portion of eq (7) reduces to:

$$s=\frac{R_0\omega_0^2\cos(\Omega t-\phi)}{[(\omega_n^2-\omega_p^2-\Omega^2)^2+4p^2\omega_n^2\Omega^2]^{1/2}}+\frac{e\omega_p^2}{\omega_n^2-\omega_p^2} \tag{8}$$

in which

$$\tan\phi=\frac{2p\omega_n\Omega}{\omega_n^2-\omega_p^2-\Omega^2}.$$

It should be noted that in the form of the dual centrifuge in which $\omega_p=0$, i.e., $\Omega=-\omega_0$, eq (7) takes a form almost identical with the familiar equation for a spring-mass accelerometer subject to sinusoidal linear motion

$$s=Ae^{-\omega_n t(p+\sqrt{p^2-1})}+Be^{-\omega_n t(p-\sqrt{p^2-1})} +\frac{R_0\omega_0^2[(\omega_n^2-\Omega^2)\cos\Omega t+2p\omega_n\Omega\sin\Omega t]}{(\omega_n^2-\Omega^2)^2+4p^2\omega_n^2\Omega^2} \tag{9}$$

In which $\Omega\equiv-\omega_0$.

The steady state portion may be written:

$$s=\frac{-R_0\omega_0^2\cos(\omega_0 t-\phi)}{\sqrt{(\omega_n^2-\omega_0^2)^2+4p^2\omega_n^2\omega_0^2}} \tag{10}$$

From the foregoing it is evident that for the special case in which the instrument has only translational motion, the motion of m is simple sinusoidal and hence may be directly compared with data using an electrodynamic shaker. In fact, for a given instrument, data from the double centrifuge and the electrodynamic shaker may be used together to construct a single response curve (see figs. 7, 8, and 9).

3. Limitations of the Dual Centrifuge

Consideration of the response of a linear, single degree of freedom system to the general case of the dual centrifuge in which the angular velocity of the little table is independent of that of the large table indicates that this form of the equipment is not attractive for accurate calibration. Examination of the response equation (7) shows that the magnitude of the transient at any instant depends upon ω_p as well as upon the instrument natural frequency ω_n and the instrument damping p. When $p^2+\frac{\omega p^2}{\omega_n^2}<1$, the transient is oscillatory. At $p^2+\frac{\omega p^2}{\omega_n^2}=1$, the transient is critically damped and when $p^2+\frac{\omega p^2}{\omega_n^2}>1$, it is over-damped. This latter suggests that at very large values of the ratio $\frac{\omega_p}{\omega_n}$ the decay of the transient may be so slow as to prevent the practical attainment of the steady state condition. Moreover, examination of the steady bias portion of eq (8) shows that, even after steady state conditions have been attained, there is a range of ω_p over which the seismic mass will be frozen against the instrument stops, the frequency range over which this condition will exist depending on the magnitude of the offset e in figure 1.

Without further evaluation of either of the above conditions, a decisive consideration is found by examination of the periodic portion of eq (8) which discloses that the condition of resonance will be realized whenever $\omega_p^2+\Omega^2=\omega_n^2$, so that a frequency-response curve of the instrument can be drawn only if the condition $\omega_p=$constant, i.e., $\omega_0+\Omega=$constant, can be maintained. Since the frequency-response curve is the objective of sinusoidal input testing, this limitation appears to make use of the general case of the dual centrifuge unprofitable. Accordingly the test machine which will be described in the next section was made to operate with $\omega_p=0$ so that eq (10) is applicable.

It is to be noted that, since a transverse axis undergoes the same motion as the sensitive axis, the instrument under test is subjected to a sinosoidal transverse excitation of the same amplitude and frequency as the excitation along the sensitive axis. If the transverse response of the instrument is linear and independent of the principal (axial) response, the transverse response will be sinusoidal and will lag, or lead, the axial response by 90°. Under this circumstance the error in calibration can easily be estimated by assuming the electrical output of the instrument to be proportional to the vector sum of the axial and transverse responses. At a transverse response of 5 percent of the axial response, the error is thus found to be about 0.12 percent. In some instruments, however, the response along one transverse axis is dependent on the axial response, increasing with the axial response. For this case the error is not easily computed as the phase between the axial and transverse responses will depend upon this rate of increase of transverse response. Moreover, in this case, the transverse response is most likely to be nonsinusoidal. However, it appears that instruments with an appreciable dependence of transverse on axial response along more than one transverse axis are rare.

4. Description of the Dual Centrifuge

In view of the obvious advantage in having available for instrument test purposes the large acceleration amplitude at low frequency that can be generated with the dual centrifuge and in view of the great simplicity of the dual centrifuge when it operates with $\omega_p=0$, a dual centrifuge of this type has been built.

A pilot model was first designed, constructed, and tested in order to investigate the potential performance of this type of apparatus. This was subsequently replaced with an improved version suitable for continuous laboratory use. The pilot model dual centrifuge shown in figures 2 and 3 consists essentially of a small turntable (2) mounted on a large turntable (1) by means of a roller bearing cartridge (6) and a radius arm (4). The instrument (3) is mounted on the small turntable (2). Its leads are brought to the overhead arm (15), no slip rings being required. Since the pulleys which drive the small table are all the same size, the absolute angular velocity of the small turntable is controlled only by the coaxial control pulley (14). In this case the control pulley was fixed and hence the small turntable has zero absolute angular velocity. Motion is transmitted through a system of open timing belts and pulleys (7, 8). The main table is turned by a motor (11) which is a shunt wound d-c motor with armature rheostat speed control. Power is transmitted via belt drive (12). The roller bearing cartridge of the countershaft (5) serves to center radius arm (4). The radius arm assembly is made symmetrical by the addition of a small balance weight (9). Thus the effective radius from the center of the large turntable to the center of the small turntable may be varied without altering the dynamic balance of the machine. Counterweight (10) serves to balance the combined effect of the radius arm assembly and the countershaft assembly. In

FIGURE 2. *Experimental dual centrifuge.*

preparation for a calibration, the accelerometer is balanced by adding an equal weight to the small counterbalance (9) and twice that to the large counterbalance (10). The whole assembly is supported by the machine frame (13).

The machine shown in figure 4 conforms with the basic design illustrated in figures 2 and 3, but has an extended amplitude and frequency range. It has a frequency range from 0.5 to 30 c/s, a displacement amplitude range up to 12 in., and an acceleration amplitude range up to 100 g at 10 c/s and higher suitable for calibration purposes. The zero to peak amplitude of the displacement is measured to within ± 0.02 in. by means of two measurements of the distance from a fiducial line on the frame to the edge of the small table. The angular velocity $\omega_0 \equiv -\Omega$ is measured by counting on an electronic events per unit time meter the number of pulses from a small generator driven by the main shaft which develops 600 pulses for each revolution. If the count is over a period of 10 sec the accuracy with which the average velocity can be determined is ± 1 part in 6,000 at 1 rps and with better accuracies at higher velocities. Errors in velocity measurement due to a progressive change in velocity can be minimized by observing the velocity over a period of time both before and after as well as during the calibration. Errors in calibration due to wow and to flutter at any frequency other than the frequency of test can be

FIGURE 3. *Experimental dual centrifuge.*
View of lower control pulleys

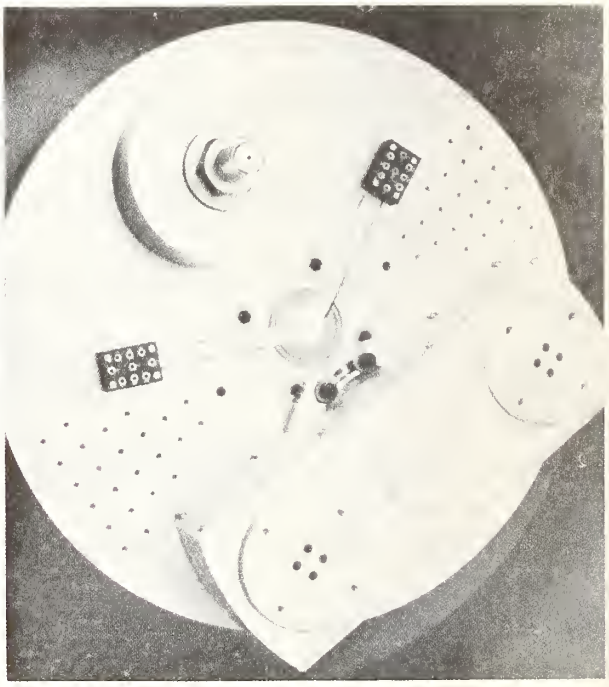

FIGURE 4. *Dual centrifuge.*

detected as a deviation from sinusoidal wave shape of the response of the instrument under test. It is estimated that in practice the total error in velocity measurement does not exceed ± 0.02 percent of the velocity at any velocity above 1 rps.

An additional source of error is found in the fact that even the best rotating devices are not in perfect dynamic balance. The machine pictured in figure 4 has a critical speed around 22 rps, varying with the load, near which no calibrations have been made. There is some unwanted sinusoidal vibration due to dynamic unbalance at any frequency of test, but an independent measurement of it can be made with a piezo-electric accelerometer, which has no zero

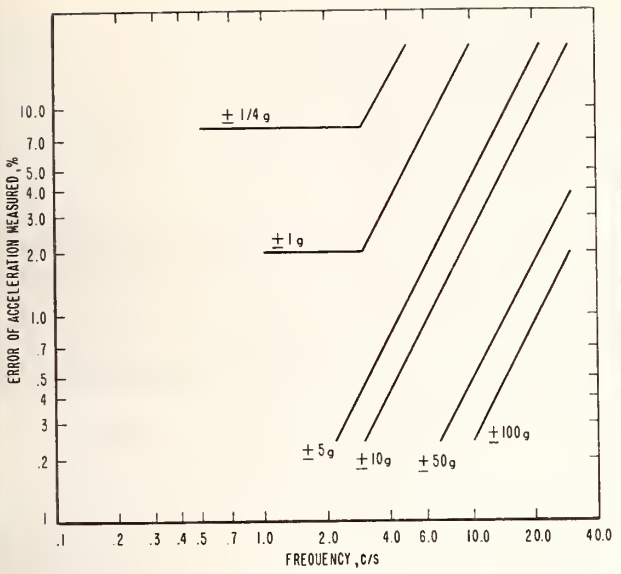

FIGURE 5. *Dual centrifuge calibration accuracy of sinusoidal linear accelerations.*

frequency response, mounted to the big table with its axis along a radius. The response of this instrument is then a measure of the unwanted vibration. Its phase relation to the response of the instrument under test is unknown, so that it can only be said that the sum of the error due to this vibration plus any other periodic errors due to either vibration, flutter or wow, or similar source does not exceed the response of the monitoring piezo-electric instrument to within the accuracy of the monitoring instrument. In the case of the machine pictured in figure 4 no such error greater than ± 0.02 *g* has been observed during any test.

The estimated calibration accuracy attained with this device over the acceleration range $\pm 1/4$ to ± 100 *g* and the frequency range 0.5 to 30 c/s is shown graphically on figure 5.

The phase of the response can be measured to within an estimated $\pm 5°$ by recording the output of a photocell excited by a fixed light and a mirror attached to the large table on a dual trace oscillograph with the response of the instrument under test.

5. Experimental Results

Figures 6, 7, 8, and 9 show the results of calibrations on the dual centrifuge. They appear to be typical frequency-response curves. Figure 6 shows

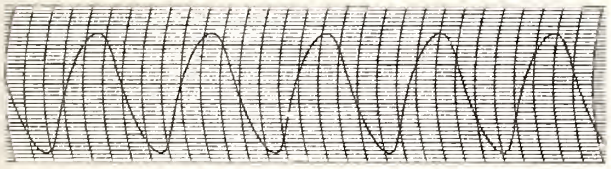

FIGURE 6. *Output of potentiometer-type accelerometer under dual centrifuge excitation at 0.86 c/s and 0.5 g (zero peak).*

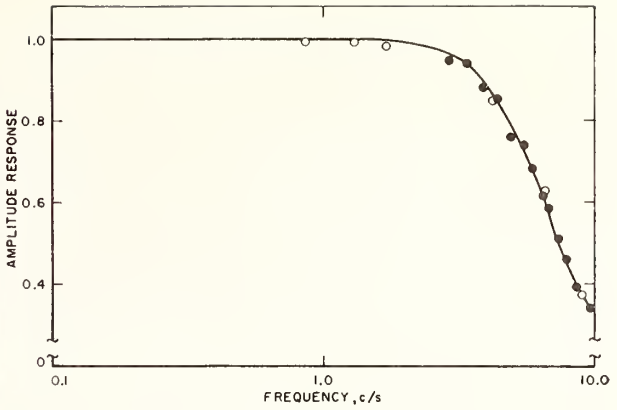

FIGURE 7. *Frequency response of potentiometer-type accelerometer.*

Theoretical curve for a linear system of one degree of freedom witb a damping ratio of 0.75 and a natural frequency of 6.0 c/s.
●, excitation by electromagnetic shaker
○, excitation by dual centrifuge

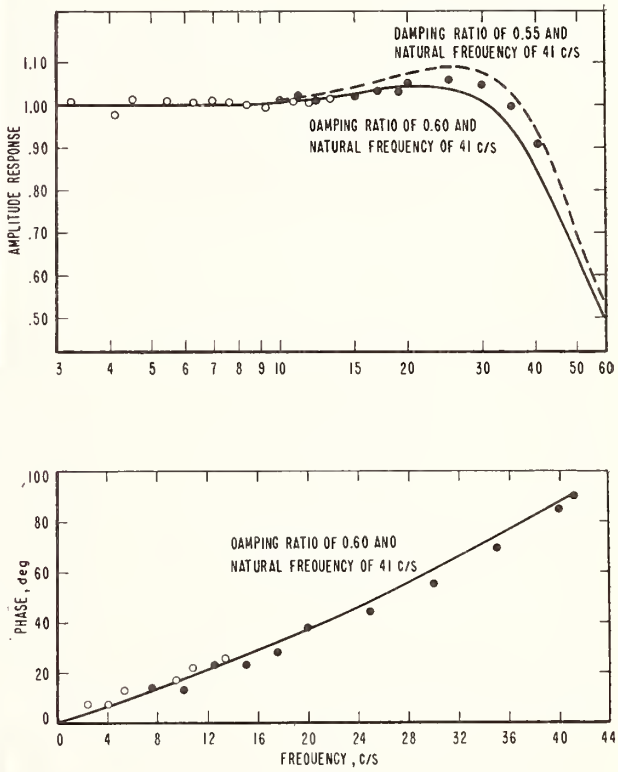

FIGURE 8. *Frequency response of bonded strain-gage type accelerometer.*

●, excitation by electromagnetic shaker
○, excitation by dual centrifuge

the response of a potentiometer type acceleration transducer when tested on the experimental equipment pictured in figures 2 and 3, as recorded by a pen writing oscillograph. Figure 7 shows the amplitude

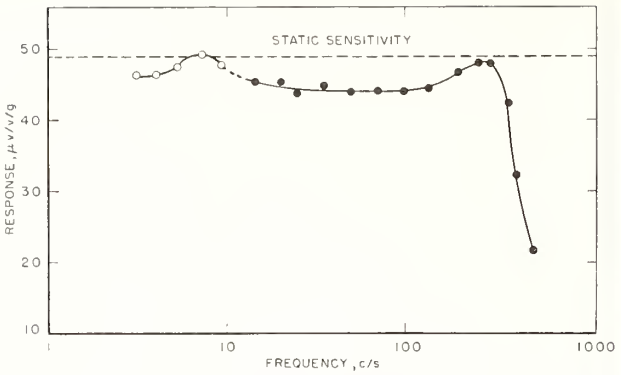

FIGURE 9. *Frequency response of unbonded strain-gage type accelerometer.*

●, excitation by electromagnetic shaker
○, excitation by dual centrifuge

response of the same instrument obtained by calibrations on the experimental equipment compared with the results of calibrations on an electromagnetic shaker. Figure 8 shows the frequency response, both amplitude and phase, of a bonded strain gage accelerometer determined by calibrations on the equipment pictured in figure 4 and by calibrations on an electromagnetic shaker.

Figure 9 shows the amplitude response of an unbonded strain gage accelerometer from calibrations on the equipment pictured on figure 2 and on an electromagnetic shaker.

6. References

[1] S. Levy, A. E. McPherson, and E. V. Hobbs, J. Research NBS **41,** 359 (1948).
[2] W. A. Wildhack and R. O. Smith, ISA Paper No. 54–40–3.
[3] A. W. Woolard, Instruments **12,** 322 (Dec. 1939).

(Paper 66C4–111)

Electrodynamic Vibration Standard with a Ceramic Moving Element

T. Dimoff

National Bureau of Standards, Washington, D. C. 20234

This paper describes a new rectilinear vibration exciter specifically developed for accurate calibration of piezoelectric accelerometers. It is an electrodynamic shaker, using a permanet magnet with a ceramic moving element guided by an air-bearing system. The moving element has a simple circular cross section and the driving coil is wound directly onto it. Its first axial resonance is near 25 000 Hz. The working range of the shaker extends from 5000 to less than 5 Hz. The moving element includes a means of mounting an internal accelerometer that can be used as a secondary standard. Alternatively, the moving element/accelerometer assembly can be calibrated by a reciprocity method and used as an absolute standard. The results of measurements of transverse motion and harmonic distortion are presented, as well as an exmple of pickup calibration.

INTRODUCTION

As described in a previous paper,[1] the modification made in a commercial electrodynamic exciter, in which the flexural plates were replaced with air bearings, eliminates or reduces many of the transverse motions. The moving element—consisting of table, connecting shaft, and driving coil—was not significantly changed. In this moving element, Fig. 1(a), there are several materials with different moduli of elasticity. Troublesome resonances are present not only in the long aluminum shaft but also in the other parts: the velocity coil wound on thin Bakelite, and the driving coil wound on four studs and held together with coil varnish and a large supporting ring. It is unlikely that the transverse motions of this exciter can be reduced more or the useful range of frequency increased without changing the geometry of the moving element.

Exciters of this type have been calibrated by a reciprocity method and used for calibration of vibration pickups at the National Bureau of Standards.[2] The output of the pickup mounted on the table for calibration is compared with the output of the velocity coil. The range of calibration is between 10–2000 Hz, but many frequencies in this range have to be avoided because of the distorted motion of the vibration table caused by the shortcomings described above. More-detailed discussions of the principles of operation and limitations of the electrodynamic vibration standard are given in the first three Refs. 1–3.

The present paper describes a new electrodynamic exciter developed at the National Bureau of Standards for calibration of small piezoelectric vibration pickups. The moving element has a simple uniform cross section and maximum axial and transverse stiffness. The characteristics of the exciter are listed in Table III.

I. CONSTRUCTION

Considering the moving element as two masses connected by a spring, where one mass represents the table, the second mass the driving coil, and the spring the material between, the fundamental axial resonance

[1] T. Dimoff and B. F. Payne, "Application of Air Bearings to an Electrodynamic Vibration Standard,." J. Res. Natl. Bur. Std. (U. S.) **67c**, 327–333 (1963).

[2] S. Levy and R. R. Bouche, "Calibration of Vibtation Pickups by the Reciprocity Method,." J. Res. Natl. Bur. Std. (U. S.) **57**, 227–243 (1956).

[3] Anon., "Calibration of Shock and Vibration Pickups," ASA S2.2-1959 (Feb. 1959).

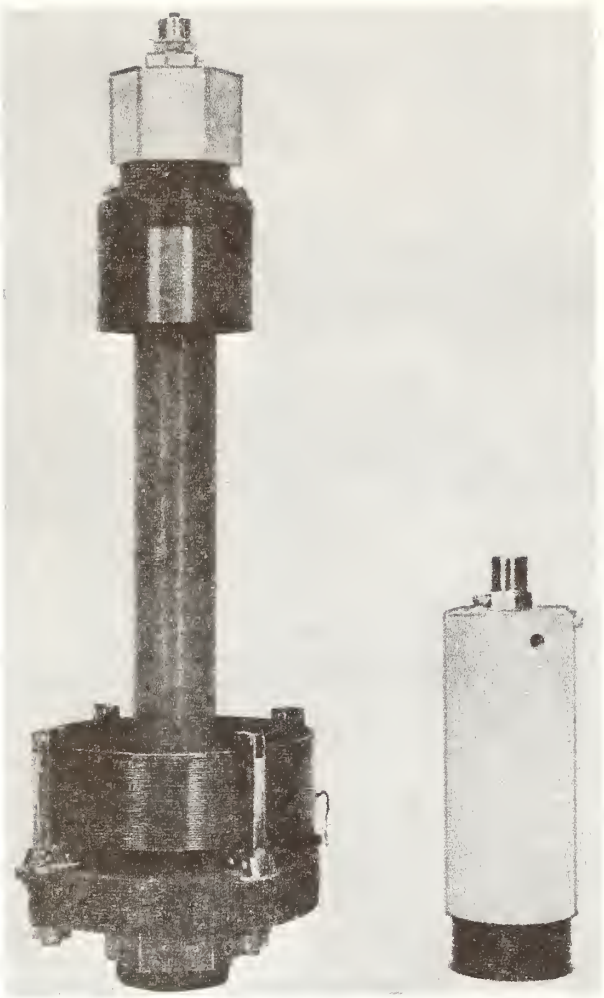

(a) (b)

FIG. 1. (a) Moving element with velocity coil. (b) Ceramic moving element.

frequency of this system is given by

$$f=\frac{1}{2\pi}[K(M_1+M_2)/M_1M_2]^{\frac{1}{2}}, \qquad (1)$$

where K is the spring constant, and M_1 and M_2 are the two masses. It can be seen from this equation that, to obtain a high resonance frequency, the spring constant should be as large as possible and the masses as small as possible. In addition to the resonances of the mass–spring system of the moving element, we have the resonances of the suspension system and the magnet assembly. In order to have each of these major resonances at the highest possible frequency within the limitation of size and form of the moving element, sintered aluminum oxide [alumina (Al_2O_3)] was selected as the material for the moving element.[4]

[4] E. Jones, "Use of High-Strength Ceramics in Vibration Transducers," J. Acoust. Soc. Am. 36, 1615–1616 (1964).

TABLE I. Some physical properties of alumina ceramic contrasted with those of steel and aluminum.

Material	Modulus of elasticity (psi)	Specific gravity	Thermal expansion (in./in. °C)
Alumina (Al_2O_3)	54×10^6	3.7	7.8×10^{-6}
Steel	30×10^6	7–8	18×10^{-6}
Aluminum	10×10^6	2.5–2.8	24×10^{-6}

The relevant properties of this material are contrasted with those of steel and aluminum in Table I. In addition, alumina is an excellent electrical insulator.

For the magnetic field, a permanent magnet was selected instead of the usual electromagnet. The magnetic field in an exciter with an electromagnet is produced by a field coil that generates unwanted heat, complicates the mechanical structure, and presents some danger of an ac ripple in the dc field current. Such perturbations cannot be tolerated if calibrations of high accuracy are to be attained. The new types of permanent magnets are stable and provide enough magnetic-field strength to produce the necessary force output.

To minimize transverse motion due to the suspension system of the moving element, the moving element was supported in the lateral direction and guided by air bearings. The air bearing permits free axial motion and prevents or reduces lateral motions.

A. Ceramic Moving Element

The vibration exciter with the ceramic moving element and the airbearing suspension is shown in Figs. 2 and 3. The moving element is a $5\frac{1}{4}$-in.-long tube of alumina ceramic with an integral closure at one end. The outside diameter is 1.8770 in. and the inside diameter is 1.4920 in. The closed end is the mounting table. It is $\frac{3}{4}$ in. thick and has a center hole with a 10–32 thread. The standard pickup and the pickup to be calibrated are mounted along the center axis of the moving element on opposite sides of the $\frac{3}{4}$-in.-thick mounting table, as shown in Fig. 2; the table surfaces are flat and parallel. The standard builtin pickup, in conjunction with the driving coil,[5] can be calibrated absolutely by the reciprocity method or as a secondary standard by comparison. The hole at one side of the mounting table is for the lead of the builtin pickup. The three threaded radial holes are for an auxiliary radial suspension, which consists of three pieces of rubber tubing $\frac{1}{4}$ in. in diameter. It provides an elastic vertical support for the moving element and it can be adjusted to maintain the position of the driving coil with respect to the permanent magnet. These pieces of rubber tubing are attached to the bearing by Teflon® studs. The

[5] R. R. Bouche and L. C. Ensor, "Use of Reciprocity Calibrated Accelerometer Standards for Performing Routine Laboratory Comparison Calibration," Shock & Vibration Bull. 34, No 4 (Dec. 1964).

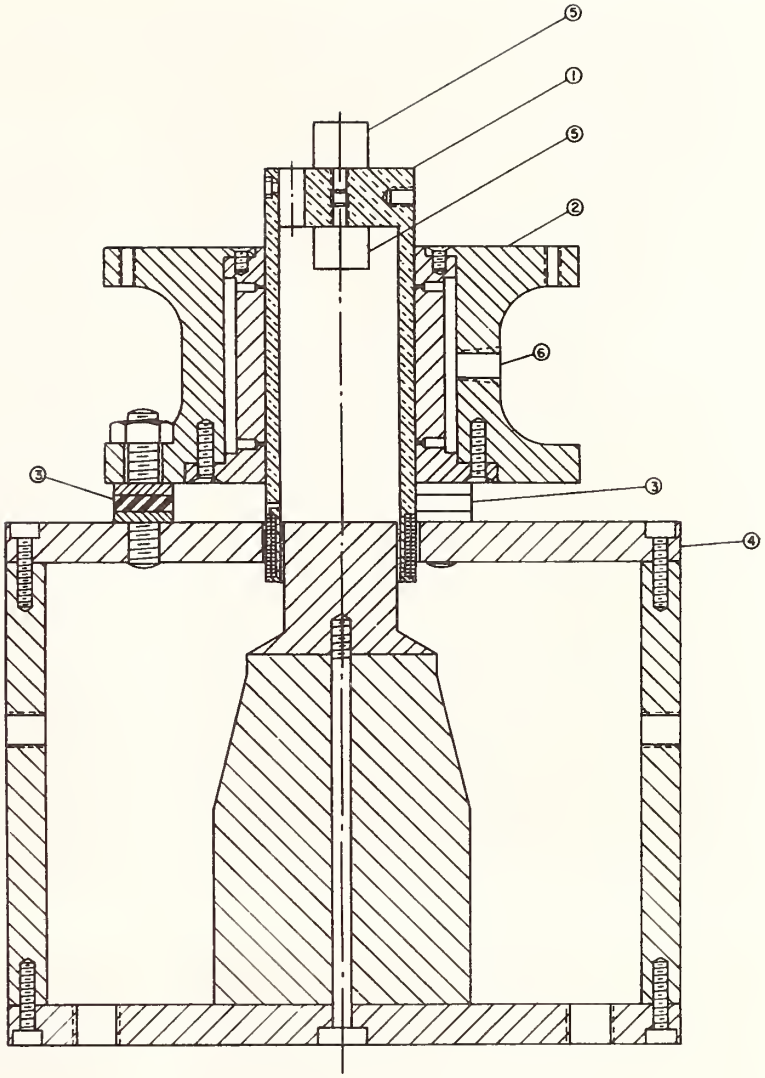

FIG. 2. Electrodynamic vibration exciter equipped with ceramic moving element 1 and air bearing 2, vibration absorber 3, permanent magnet 4, vibration pickup 5, and air inlet 6.

vertical suspension stiffness can be adjusted easily by tensioning the rubber tubing (Fig. 4). The vertical suspension can be accomplished also by passing a dc current through the coil simultaneously with the ac current and the rubber tubing can be eliminated completely.[6]

The driving coil is wound on the reduced-diameter portion of the moving element, directly on the ceramic. Thus, as shown on Fig. 1(b), a separate housing for the coil is eliminated. Each layer of copper wire is impregnated with high-strength epoxy cement. The constant flow of cool air (60°F) keeps the mounting table cool. Having the lead of the driving coil coming to the top of the shaft permits the moving element to be easily removable (Fig. 5). Armatures with different configurations or different standard pickups can be inserted and removed conveniently when required.

[6] B. Reznek, "Elimination of Static Shaker Deflection by D. C. Armature Biasing," Proc. Inst. Environ. Sci. 1963, 425–432 (1963).

B. Air Bearing

The air bearing, shown in Figs. 2 and 3, is of the external pressure or hydrostatic type. It is 1.8772 in. in diameter and 3 in. long. The material is 303 stainless steel. There are two rows of six orifices each, 2 in. apart. The orifices of 0.02 in. diam are drilled through the inner sleeve. The surface of the bearing and the journal have a surface finish of approximately 8 μin. and this permits a bearing–journal radial clearance of 0.0001 in.

The compressed air used is the building supply, filtered twice. The air is transmitted to the bearing by means of flexible tubing with an inside diameter of $\frac{1}{8}$ in. The pressure is kept at 50 psi, and no oscillatory effect due to the air flow is observed.

C. Magnet

The permanent magnet, shown in Figs. 2 and 3, consists of a soft steel outer part, a center piece of

Alnico® 7 magnet, and a Permandur® pole piece. The air gap is $\frac{1}{4}$ in. and the magnetic-field strength in this gap is 8000 G (8×10^7 T). The magnetic stray field on the table top is 13 G (13×10^4 T).

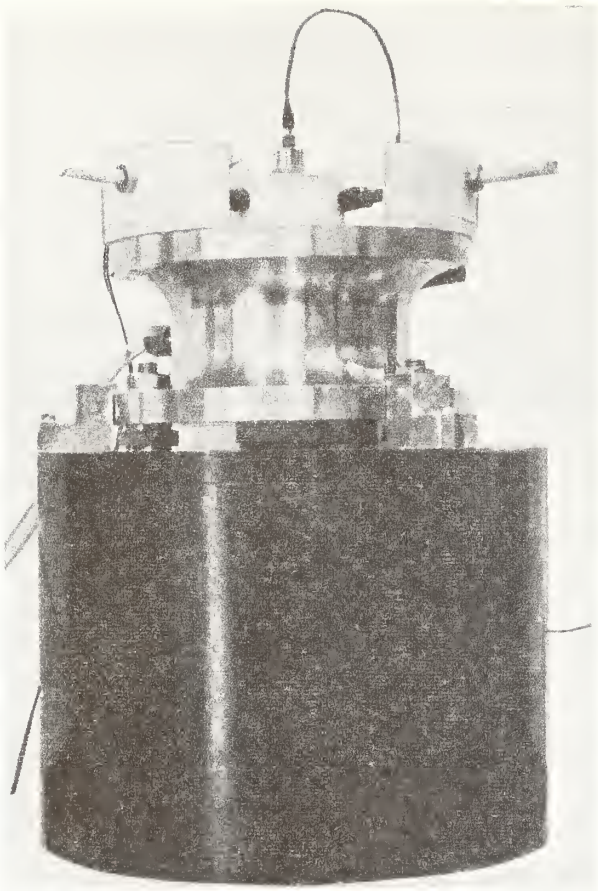

FIG. 3. Electrodynamic vibration exciter equipped with air bearing and ceramic moving element.

FIG. 5. Removable moving element.

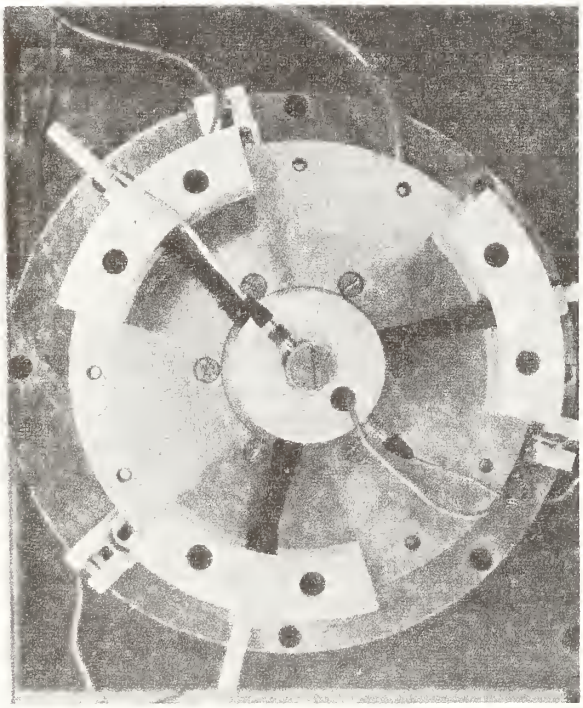

FIG. 4. Setup for calibration of a piezoelectric accelerometer.

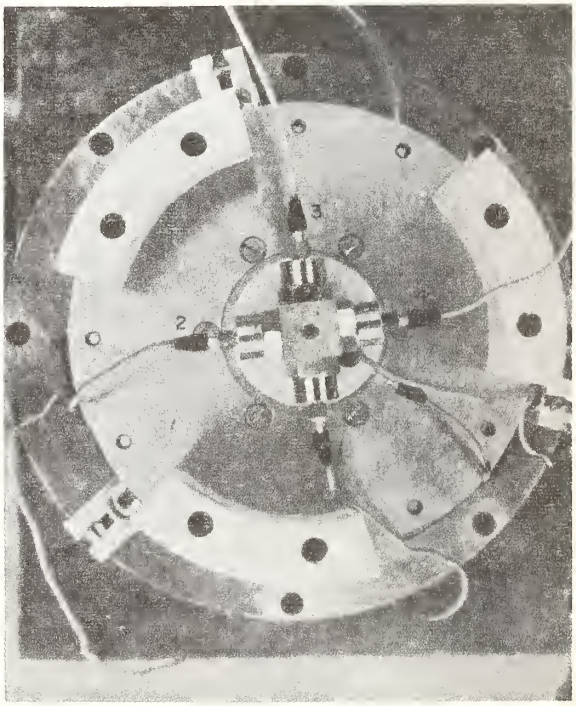

FIG. 6. Setup for measuring transverse accelerations.

If the bearing-table assembly were mounted rigidly to the permanent magnet, many of the resonances generated at the permanent magnet would be transmitted to the bearing, and, consequently, to the mounting table. This would cause undersirable transverse motions superimposed on the required sinusoidal axial motion of the moving element. By mounting the bearing-table assembly, as shown in Figs. 2 and 3, on three rubber vibration isolators, the troublesome resonances are isolated from the mounting table.

II. TRANSVERSE-MOTION MEASUREMENTS

The ideal vibration exciter–calibrator should produce pure sinusoidal motion without any transverse motions. Transverse motions or accelerations of the mounting table were measured using two piezoelectric accelerometers mounted with their principal axes mutually perpendicular to each other and to the direction of motion. As shown in Fig. 6, the accelerometers were mounted in pairs to provide a symmetrical inertial load on the moving element. No significant difference was observed between measurements made with individual members of any pair. Axial acceleration was measured with the builtin accelerometer. The equipment used for the measurements is listed in Table III.

Figure 7 shows the transverse acceleration of the exciter in percent of the axial acceleration. The transverse motions indicated by these devices should not be attributed entirely to the exciter, since no correction was made for the transverse sensitivity of these pickups.

According to the manufacturer's specification, they have 0.5% transverse sensitivity at low frequencies. The manufacturers' determination of the transverse sensitivity of an accelerometer is usually performed at a single low frequency. Thus, the indicated transverse acceleration at high frequencies in Fig. 7 may be owing to transverse response of the accelerometers or to transverse motion of the exciter or both. However, a number of different determinations provide assurance that the transverse acceleration is no worse than the $1\frac{1}{2}\%$ in Fig. 7.

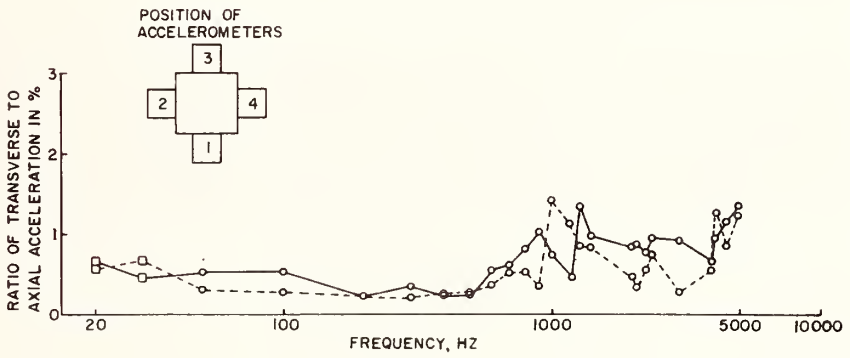

FIG. 7. Measured transverse accelerations due to transverse motions. —○: Horizontal No. 2. – – –○: Vertical No. 1. ○: 10 g. □: 5 g.

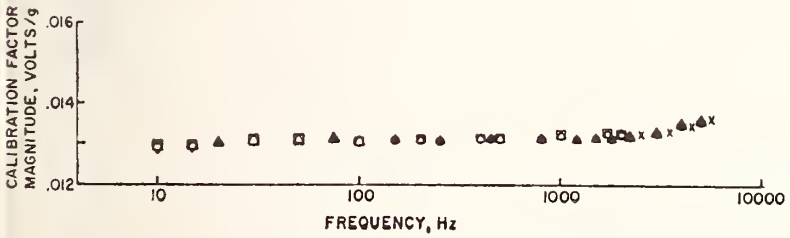

FIG. 8. Calibration factors of a piezoelectric acceleration pickup. *Air-bearing exciter*—●: 10 g. ▲: 5 g. ■: 2 g. *Vibration Standard*—○: 10 g. □: 5 g. △: 2 g. ▽: 1 g. *Piezoelectric exciter*—×: 4 μ in.

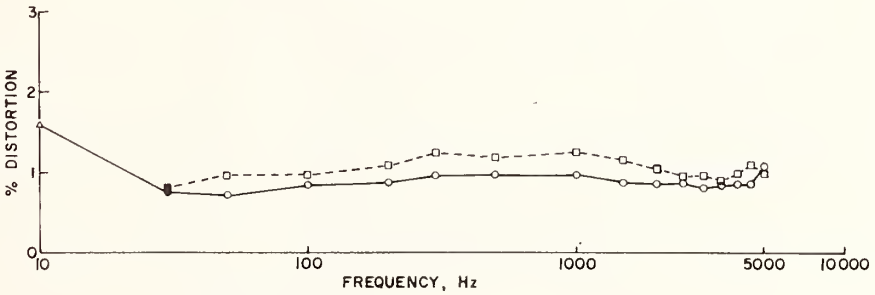

FIG. 9. Indicated distortion vs frequency. —○: 0.06-lb payload. – – –□: 0.285-lb payload. ○: 10 g. □: 10 g. ●: 5 g. ■: 5 g. △: 2 g.

TABLE II. Performance data for air-bearing exciter.

Weight of moving element	1 lb
Force rating	15 lb
Maximum table excursion	0.7 in.
Frequency of major resonance	25 000 Hz
Driver-coil resistance	3.3 Ω
Stray magnetic field at table level	13 G (13×10^4 T)

TABLE III. Equipment used.[a]

1. Standard built in accelerometer, Kistler, model 808Kl.
2. Accelerometers for measurements of transverse motions, Endevco, model 2224C.
3. Oscillator, Hewlett–Packard, model 202CR.
4. Amplifier, optimation model P. A. 250.
5. Distortion analyzer, Hewlett–Packard, model 331A.

[a] Certain commercial materials and equipment are identified in this paper in order to specify adequately the experimental procedure. In no case does such identification imply recommendation or endorsement by the National Bureau of Standards, nor does it imply that the material or equipment identified is necessarily the best available for the purpose.

III. CALIBRATION OF PICKUP

The setup for calibration of a piezoelectric accelerometer is shown in Fig. 4. Figure 8 shows the calibration factors of a piezoelectric accelerometer obtained by 3 independent calibrations.

The first set of symbols represents the results of calibration by the comparison method using the air bearing exciter. The second set of symbols represents the results of calibration using a vibration standard of the conventional design that has a velocity-sensing coil calibrated by the reciprocity method. The third set of symbols represents the results obtained by measuring the amplitude of vibration by photometric interferometry on a piezoelectric exciter.

IV. DISCUSSION

The tests performed on the new exciter indicate that the goal for which it was designed has been attained. The performance data of the exciter are given in Table I. In the frequency range below 5000 Hz, the exciter meets present requirements for accurate calibration of piezoelectric accelerometers weighing less than 0.5 lb. For such loads, a level of 10 g can be generated throughout the frequency range with transverse acceleration due to transverse motion everywhere less than $1\frac{1}{2}\%$ and with distortion less than 1% (see Fig. 9).

If care is taken to avoid a few narrow frequency ranges, good motion can be obtained at frequencies up to 20 kHz.

ACKNOWLEDGMENTS

The objectives of this project as shown by the performance described in the body of this paper depended on the skilled work of G. E. Crowther and R. H. Harwell, in machining the bearing and supporting assembly.

This work was made possible by the financial support and technical cooperation of the HQ2802d Inertial Guidance and Calibration Group (USAFLC), Newark Air Force Station, Newark, Ohio.

Reprinted from

THE JOURNAL
OF THE
ACOUSTICAL SOCIETY OF AMERICA

Volume 40 Number 3

SEPTEMBER 1966

Improved Transfer Standard for Vibration Pickups

E. Jones, D. Lee, and S. Edelman

Mechanics Division, National Bureau of Standards, Washington, D. C. 20234

This paper describes a vibration transfer standard designed to provide comparison calibrations of pickups with minimum degradation. Features of the design are the use of a ceramic housing of a stiff, light, lossy material; provision of a means for evaluating the quality of the motion by the use of three integral accelerometers oriented parallel to the nominal direction of motion; and design of the geometry to minimize differences in motion between the pickup being calibrated and the standard. The useful frequency range is 10–10 000 Hz.

INTRODUCTION

In most vibration laboratories, calibration of a vibration pickup consists of comparing its output with that of a transfer standard when both are subjected to the same motion. A transfer standard is a standard pickup that can be used to calibrate other pickups conveniently with the accuracy required. Usually the comparison is performed on a calibrator that can be mounted on a shake table with provision for mounting the pickup to be calibrated (the test pickup) on the calibrator. The active portion of the calibrator may be a separate pickup mounted near the test pickup, or it may be an integral part of the fixture. The accuracy of a comparison calibration depends on the characteristics of the standard and of the motion. The various features of an improved experimental calibrator and their influence on the factors that determine the quality of a calibration are described below. The characteristics of the motion applied to the test pickup and the standard depend on a number of factors in addition to the design of the transfer standard. The improved design provides a means for detecting "bad" motion that would cause inaccuracy.

Fig. 1. Assembled standard.

I. DESIGN OF IMPROVED TRANSFER STANDARD

The improved calibrator is pictured in Fig. 1 and shown schematically in Fig. 2. Its principal parameters are given in Table I.

Experience in calibrating vibration pickups by many different techniques at the National Bureau of Standards indicates that defects in the motion cause most of the inaccuracies in a calibration. Among the more serious of such defects are differences in the motion applied to the two pickups, as well as nonaxial and nonsinusoidal motion, all of which are likely to have different effects on the standard and test pickups. The new

Table I. Characteristics of improved transfer standard.

Mass	0.110 kg
Height	2.54 cm
Diameter of mounting surface for pickup	3.17 cm
Diameter of calibrator mounting surface	3.81 cm
Typical resonant frequency (mounted)	65 kHz
Typical calibration factor	25 mV (peak)/g (peak)
Material of housing	Sintered aluminum oxide (AD99)
Piezoelectric element	PZT-5
Inertial mass	Carboloy 999
Material of coating for electrical shielding (mounting surfaces not coated)	Moly-manganese
Thickness of Al_2O_3 between test pickup and standard	1.14 cm

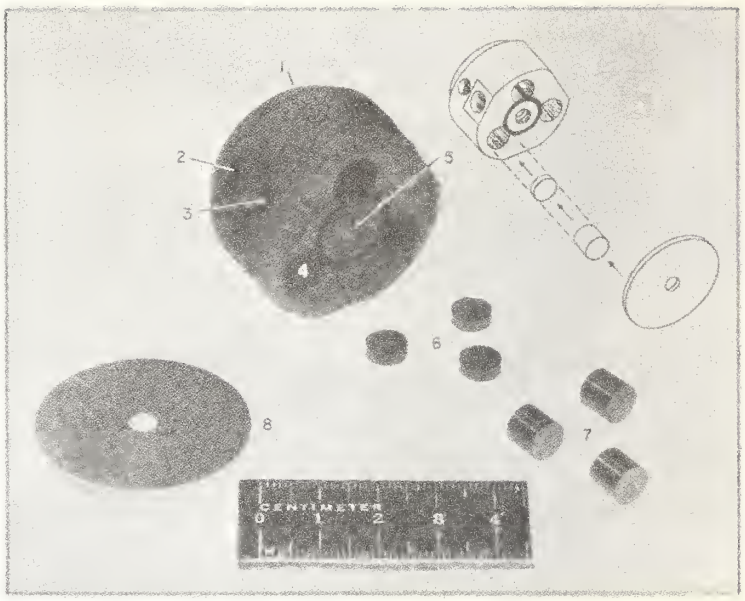

FIG. 2. Parts of standard. 1. Ceramic housing with moly-manganese coating. 2. Hole for spanner wrench. 3. Mounting hole for pickup lead. 4. Recess for pickup elements. 5. Center hole with 10–32 thread. 6. Piezoelectric elements for pickups. 7. Inertial masses for pickups. 8. Ceramic cover plate and bottom mounting surface.

transfer standard is designed to minimize the harmful consequences of such defects in the motion.

The size, shape, and mass of a calibrator directly affect the motion applied to the two pickups. The modes of vibration of the shaker affect the motion of the calibrator and vice versa, while the combination of the two has still another set of resonances. Extremely long, thin shapes tend to promote flexural modes of the shaker–calibrator system and magnify the nonaxial motion at the location of the test pickup. A wide, thin disk is an undesirable shape because it has little resistance to nonuniform surface motion of the shake table at higher modes of vibration and, at some frequencies, may even *promote* such nonuniform motion. The calibrator should be light, compact, and stiff so that its resonances and its effect on the resonances of the shaker will be out of the frequency range of interest as much as possible. The shape shown in Figs. 1 and 2 represents the best compromise we have found between these requirements and the needs for mounting space.

The choice of sintered aluminum oxide for the housing is one of the most important features of the design. It has been found to have considerable advantages over more usual materials for shake tables and pickups.[1] Its properties are compared with those of other materials used for vibration fixtures in Table II.

Because of the low density, the calibrator loads this shaker less than it does one of a similar size and shape made of more usual materials. Because of the combination of low density and high Young's modulus together with considerable damping for such a stiff material, the frequency at which wave motion becomes signficant is well above the frequency range of interest. Hence, inaccuracies due to different motion of the test pickup and the standard are minimized, whether the differences are caused by different deformations, by each pickup, of the mounting surfaces or by a mode of vibration of the mounting surface that provides more motion at one location than at another.

In this calibrator, the standard consists of the combination of three small pickups mounted in wells on the underside of the surface on which the test pickup is mounted. The use of the same pickups to determine when the motion is free of defects that might cause inaccuracy is described in a later section. Each of the small pickups built into the calibrator consists of an active element of lead zirconate–titanate piezoelectric ceramic and an inertial mass of tungsten carbide. The parts of the pickup are cemented together with a silver-filled epoxy, which is also used to cement the pickup to the calibrator. The construction is adapted from a technique described previously,[2,3] which is one of a number of techniques developed at NBS to provide vibration pickups for special applications for which suitable commercial instruments were not available.[4–7] With this background to draw on, we are reasonably sure that the type of construction used will produce as good stability of the calibration factor over long periods of time as the type of piezoelectric material allows.

Since the sintered aluminum oxide is an electrical insulator (see Table II), the pickups are isolated from

[1] E. Jones, J. Acoust. Soc. Am. 36, 1215–1216 (1964).

[2] E. Jones, S. Edelman, and K. S. Sizemore, J. Acoust. Soc. Am. 33, 1462–1466 (1961).

[3] E. Jones, S. Edelman, and E. R. Smith, 23rd Shock and Vibration Bulletin (1956).

[4] L. T. Fleming, J. Instr. Soc. Am. 24, 968–972 (1951).

[5] T. A. Perls and C. W. Kissinger, Rev. Sci. Instr. 25, 983–988 (1954).

[6] S. Edelman, E. Jones, and E. R. Smith, J. Acoust. Soc. Am. 27, 728–734 (1955).

[7] J. E. McKinney, S. Edelman, and R. S. Marvin, J. Appl. Phys. 27, 425–430 (1956).

TABLE II. Properties of materials used for vibration fixtures (typical values).[a]

Material	Modulus of elasticity (psi)	Specific gravity	Thermal coefficient of expansion (in./in.·°C)	Electrical resistivity ($\mu\Omega$·cm)
Alumina (Al_2O_3)	54×10^6	3.7	7.8×10^{-6}	10^{21}
Steel	30×10^6	7–8	18×10^{-6}	15–20
Aluminum	10×10^6	2.5–2.8	24×10^{-6}	6
Tungsten carbide	105×10^6	15.25	4.0×10^{-6}	17
Tungsten	59×10^6	19.4	4.0×10^{-6}	6

[a] Adapted from T. Dimoff, J. Acoust. Soc. Am. 40, 671–677 (1966).

each other and from ground except where connections are deliberately introduced. Electrical shielding is provided by a coating of moly-manganese electrolytically deposited on the surfaces indicated in Fig. 2. The top and bottom mounting surfaces are left uncoated so that they are electrically insulating.

The high value for the mounted resonant frequency of the pickups helps minimize the inaccuracy caused by harmonic distortion in the motion. If a calibration is performed to 10 kHz, the response of the standard to distortion even as high as the third harmonic will not be too much different from its response to the fundamental. However, inaccuracy in the calibration may occur if the response of the test pickup to the third harmonic is much different from its response to the fundamental; but such inaccuracy will depend on the characteristics of the test pickup rather than on the characteristics of the standard.

II. BEHAVIOR AS STANDARD PICKUP

The frequency response of a typical transfer standard is given in Table III. Transfer Standard No. 109 was calibrated on the NBS vibration standards by the methods used in routine calibrations. The output terminals of the three sensing elements were connected in parallel into a cathode follower. The transfer standard was attached to the shake table with a stud that permitted the base of the standard to be in direct contact with the mounting surface. The contacting surfaces were coated with medium petroleum lubricating oil. A solid, cylindrical 28-g stainless-steel mass, 1.59 cm in diam, was mounted on top of the standard to simulate the effect of a pickup. The standard and the weight were tightened with a torque of 18 lb-in. The results are shown in Table III. The calibration factor is the ratio of the open circuit output of the cathode follower in millivolts (peak) to the acceleration in g (peak). The effect of other masses is being studied.

III. USE TO EVALUATE QUALITY OF MOTION

As noted above, most errors in calibration are caused by bad motion. Nonsinusoidal motion can be detected by analyzing the pickup output with a distortion analyzer. There is no similarly simple way to detect other kinds of bad motion. For example, at the frequencies of flexural resonances of the shake table and at the resonant frequencies of higher-order modes of vibration of fixtures, large-amplitude nonaxial motion can occur. Such motion may generate unusually clean sinusoidal signals from the pickups. The sensitivity of the pickup for such excitation usually is much different from its sensitivity when the motion is axial.

TABLE III. Results of calibration of NBS transfer standard No. 109.

Frequency (Hz)	Calibration factor (mV/g)	Gain of cathode follower
10	24.7	0.9667
15	24.7	0.9707
30	24.8	...
50	24.8	0.9744
100	24.8	0.9746
200	24.8	0.9748
500	24.7	0.9747
900	24.8	...
1700	24.6	0.9747
2000	24.7	...
2500	24.7	...
3000	24.8	...
3500	24.6	...
4000	24.9	...
4500	25.1	...
5000	25.0	0.9747
5500	25.0	...
6000	25.0	...
6500	25.2	...
7000	25.2	...
7500	25.2	...
8000	25.3	...
8500	25.3	...
9000	25.3	...
9500	25.3	...
10 000	25.4	0.9746

The three pickups in the transfer standard provide a sensitive means for detecting nonaxial motion of the pickup being calibrated. The outputs of each of the three internal pickups and the output of the pickup being calibrated are used in pairs to form Lissajous figures. The three Lissajous figures formed by the internal pickups and one or more formed by combining the output of one of the internal pickups with the pickup being calibrated are exhibited on an oscilloscope. At a low frequency where the motion is good, the gains of the various amplifiers are adjusted so that each figure is a straight line at 45° to the vertical. As the frequency of vibration is changed, bad motion shows as changes in one or more of the lines. Rotation of the surface of the shake table about any axis through the table, or breakup of the surface motion into higher modes, causes one or more of the figures generated by the internal pickups to become an ellipse. Rotation about an axis outside the table is shown by rotation of one or more of the traces away from the 45° position. Motion of the central portion of the table out of phase with the motion

of the periphery shows as opening of the figure that uses the signal from the pickup being calibrated. Various combinations of the different modes may occur.

Purely transverse components of the motion of the shake table are not detected by this calibrator. However, we assume that the transverse components of the motion of a shake table are always accompanied by other undesirable components which are detected by this calibrator. This conclusion is supported by the results of many experiments under various conditions and with many different shakers.

The interpretation of signals from the internal pickups to determine when the motion of the shaker is suitable for accurate calibration requires much experience and study. The motion is obviously unsuitable if the oscilloscope traces show ellipses or lines far from 45°. However, with experience, one can detect much less obvious bad motion by small changes in the Lissajous figures as the frequency is changed. A correlation has been noted between bad motion detected by the calibrator and erratic results of the calibration. Data are being gathered now to demonstrate the connection quantitatively. Enough work has been performed to make it possible to say with assurance that the results of a calibration in the useful frequency and amplitude ranges of a pickup will be reproducible when the calibrator indicates that the motion is good. When the results given in Table III are used to calibrate a pickup by comparison with this transfer standard, we estimate that the over-all uncertainty is less than 2% when used in a temperature-controlled laboratory.

IV. CONCLUSION

For most vibration laboratories, we believe that a device of the type described in this paper will be useful principally as a transfer standard, that is, a standard pickup that can be used to calibrate other pickups conveniently with the accuracy needed. For the few laboratories concerned with calibrations of the best attainable accuracy, the principal usefulness of the device will be to monitor the motion during calibration.

ACKNOWLEDGMENT

This work was supported by the Sandia Corporation, as prime contractor for the U. S. Atomic Energy Commission.

Reprinted from

THE JOURNAL
OF THE
ACOUSTICAL SOCIETY OF AMERICA

Volume 41 Number 2

FEBRUARY 1967

ABSOLUTE CALIBRATION OF VIBRATION GENERATORS WITH TIME-SHARING COMPUTER AS INTEGRAL PART OF SYSTEM

B. F. Payne
National Bureau of Standards
Washington, D.C.

Improved shakers with a simplified ceramic moving element and a reference accelerometer now permit reciprocity calibration over a frequency range from 10 to 5000 Hz. This paper describes the present NBS shaker calibration procedure in which magnitude and phase lag measurements are made. Calibrations to 10 kHz are planned.

A teletypewriter gives access to a central time-sharing computer which can accept commands and data from punched paper tape or from the keyboard. The data may be recorded from digital measuring instruments by a special coupling system. Data reduction is rapid and permits errors to be corrected quickly. The combined use of the computer and the digital data recording system cuts the calibration time to about one-fourth that required by previous methods. Monitoring the quality of motion of the shaker by the computer makes possible improved accuracy of the calibration process. Calibration of one of the improved shakers is described.

B. F. Payne

INTRODUCTION

In calibration of vibration standards, accuracy is affected by many mechanical and electrical factors, and exact reproduction of conditions is extremely difficult. Accordingly, it is particularly important to know the results of measurements while the experimental setup is still in place. It is useful to know almost immediately if data are changing uniformly or randomly, and to assess the effects of varying the parameters to obtain optimum performance.

This paper describes a system for data collection and reduction with a time-sharing computer as an integral part of a calibration system. Data from digital instruments such as voltmeters and frequency counters are transmitted to a teletypewriter either automatically or manually. The teletypewriter prints a copy of the data and also punches a paper tape. Data from the tape can be fed into the computer through the teletypewriter, and the computed results are recorded in return by the teletypewriter. Various combinations of data sources can be read into the recording system by a switch located on the interface equipment.

Most of this paper is devoted to the application of this technique to the known reciprocity calibration of vibration exciters. The ratio circuitry is presented in a general form and other applications for the circuitry are suggested in the Appendix.

The data analysis techniques follow current practice which has been found to be useful. Additional experience with the calibration system may lead to alternative criteria for the screening of data due to bad motion and other

causes. Other aspects of data analysis techniques are also being investigated.

FEATURES OF TIME-SHARING COMPUTER SERVICE

A time-sharing computer gives the user a connection between the computer and his laboratory and permits him to communicate with the computer by some suitable means — usually a typewriter. By typing in or reading in taped data and commands, the user can receive answers in a matter of seconds or minutes.

The time-sharing system here is a commercial system using the BASIC language. There are other systems available which in addition to BASIC can be programmed in ALGOL and a special version of FORTRAN. The computer used in this system has a 16 K word storage and a 6-μsec memory cycle.

Changes in the program are easily made by retyping a statement number and statement for each correction since a program is recompiled on each run. New statements can be inserted between existing ones. Each user is allocated a certain amount of space in which he can store his programs and recall them later by typing out the name of the desired program. Storing the most commonly used programs provides a rapid means of access to a large amount of information. Some of the systems also have libraries of commonly used programs, called system programs, available to each user. If a laboratory has a number of instruments which are used as reference standards, a detailed calibration or performance characteristic chart can be compiled in the form of a program for each instrument. The users of the instruments use the computer efficiently by naming the program for that instrument when the calibration information is desired for a comparison test.

The remote consoles are commercial teletypewriters connected to the central computer by telephone lines. The computer time is sold to customers by the terminal hour each month; usually 25 or 50 hr is the minimum. The teletypewriter can be rented or purchased.

BASIC is a user-oriented language. It is similar in structure to FORTRAN, but does not take as much training and time to learn. The average person can learn the essentials of BASIC in 2 hr using an instruction book. For more sophisticated programming, FORTRAN and ALGOL are available.

One of the attractive features of this system is that one can program, edit, debug, store, and update at the typewriter console with only a small delay between commands. The editing commands have a higher priority than the run command, thus making it possible to debug a program very rapidly. Programs in the user's storage can be combined to form still other programs. Large segments of a program can be deleted from the current program in the working area of the computer without affecting the "saved" program in the memory area. This residual program can then be combined with another program, using the "merge" or "weave" commands, thus creating a new program which, if desired, can be renamed and saved for future use. In all this, the two original programs are unchanged and are still available for use. An application of this technique is in transferring data from one program to another, eliminating the need for re-reading in the data for the second program.

DESIGN OF IMPROVED SHAKER

For a number of years the reference in the National Bureau of Standards calibration service for vibration pickups has been a velocity sensing coil calibrated by a reciprocity method. The coil was part of the shaker used to provide motion for the pickups being calibrated. The large size and complicated structure of the shaker caused resonances and cross-axis motions which limited the accuracy which could be achieved and the frequencies at which satisfactory calibrations could be performed. Modifications of the flexures of the shaker reduced cross-axis motion but provided little significant improvement because the basic design remained unchanged. A much smaller, simpler shaker has been built specifically for calibration and has been found suitable to 5 kHz [1]. The new shaker uses an accelerometer in place of a velocity coil. This change was necessary because at the higher frequencies the velocity coil signal was lost in the noise level. Also, since most of the pickups calibrated are accelerometers, it was convenient to have a standard that was linear with acceleration instead of velocity.

The shaker is shown schematically in Fig. 1. The moving element is made from a single casting of alumina (Al_2O_3) which is ground to fit the stainless steel bearing. The driver coil is wound on and epoxied in place to make the whole moving element rigid. Pickups can be mounted on this by a 10-32 screw.

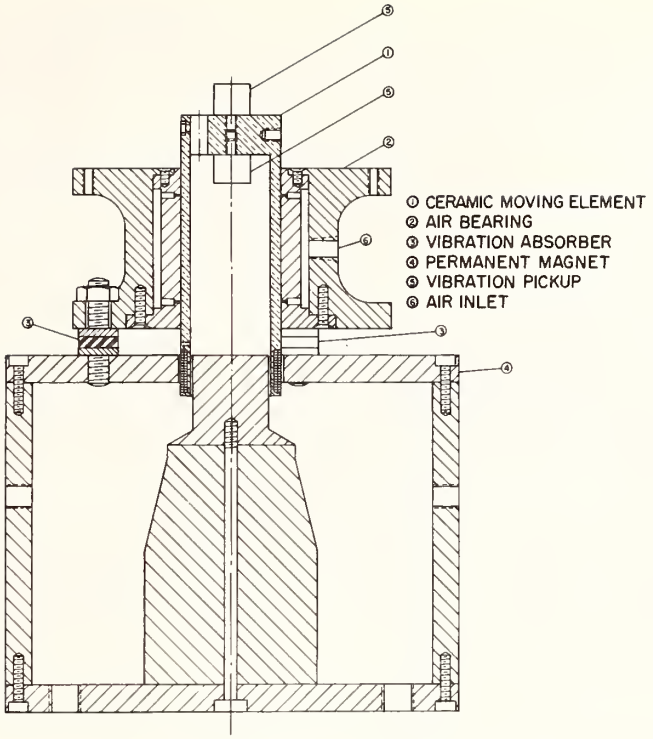

Fig. 1 - Electrodynamic vibration exciter equipped with air bearing and ceramic moving element

RECIPROCITY CALIBRATION

By the reciprocity technique, a shaker equipped with a velocity coil or transducer is calibrated. This shaker can then be used to calibrate other transducers. The reciprocity calibration is called "absolute" because it is independent of arbitrary standards. It is based on measurements of voltage ratio, resistance, frequency, and mass, and is not a technique of comparison of secondary standards. The accuracy attained reflects the accuracy with which one makes the measurements and the character of the physical motion of the exciter, for example, whether the motion is purely sinusoidal or distorted and whether or not one is operating near a resonance.

Until recently the reciprocity calibration of shakers was limited in frequency range to 10 to 2000 Hz. In large part, this limitation was due to the complicated structure of the shakers. With the advent of the new shakers described earlier, it has been possible to extend the range to 5000 Hz.

The reciprocity calibration technique used was an adaptation of the one given in Refs. 2 and 3. A brief outline of the measurements necessary for a reciprocity calibration follows.

Experiment 1

With the shaker being driven by an oscillator and amplifier and the circuit as shown in Fig. 2, the first set of measurements consists of the transfer admittance given by

$$\bar{Y} = \frac{\bar{I}\ (\text{driver coil})}{\bar{E}\ (\text{standard accelerometer})} ,$$

where a bar above the symbol for the variable denotes a complex number. This ratio can be measured by computing the current I from the known drop in voltage across a 10-ohm resistor in series with the driver coil and amplifier. The quantity measured is

$$\bar{R} = \frac{\bar{E}\ (\text{10-ohm resistor})}{\bar{E}\ (\text{standard accelerometer})} .$$

Therefore,

$$\bar{Y} = \frac{\bar{R}}{10}\ \text{mho} .$$

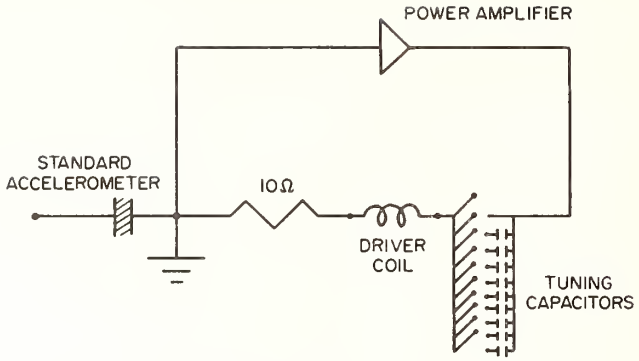

Fig. 2 - Schematic for transfer admittance measurements and use as calibrator

A block diagram of the electrical circuit for the ratio measurements is given in Fig. 3. This shows a general circuit used for voltage ratio measurements. In the case of experiment 1, the reference signal is the voltage drop across the 10-ohm resistor and signal 2 is the voltage generated by the standard accelerometer. Both switches are in position 1. A series of such readings is taken for each frequency and consists of readings taken with incremental weights attached to the mounting table one at a time; the increments ranged from 0.1 to 0.5 lb in this calibration. Zero load readings are taken after each load. Also, the phase angle for each point is needed. In all, 22 data points for each frequency are required for a calibration.

Having measured the transfer admittance for a series of loads at a given frequency, we now plot graphs of the real and imaginary components of the ratio $W/(\bar{Y}_W - \bar{Y}_0)$ vs W, where W is the value of mass attached to the table and $\bar{Y}_W$ and $\bar{Y}_0$ are the transfer admittance for the various loads and zero load, respectively. The zero intercepts of these plots and their slopes are computed by the weighted least square method of Bouche [4], who has shown that the error in $W/(\bar{Y}_W - \bar{Y}_0)$ is inversely proportional to W.

The values of $\bar{Y}_0$ used in the calculations are obtained by averaging the values of the $\bar{Y}_0$ measurements before and after each measurement of $\bar{Y}_W$. The computed values of intercept $\bar{J}$ and slope $\bar{Q}$ are used in determining the sensitivity of the standard. Figure 4 shows the shaker and readout instruments used for these measurements.

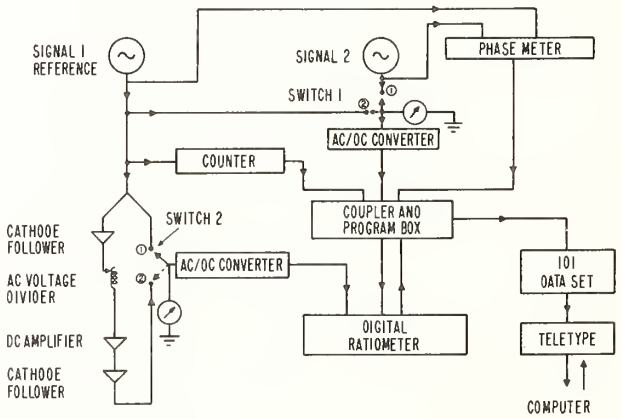

Fig. 3 - Block diagram for phase angle and/or voltage ratio measurements for two ac signals

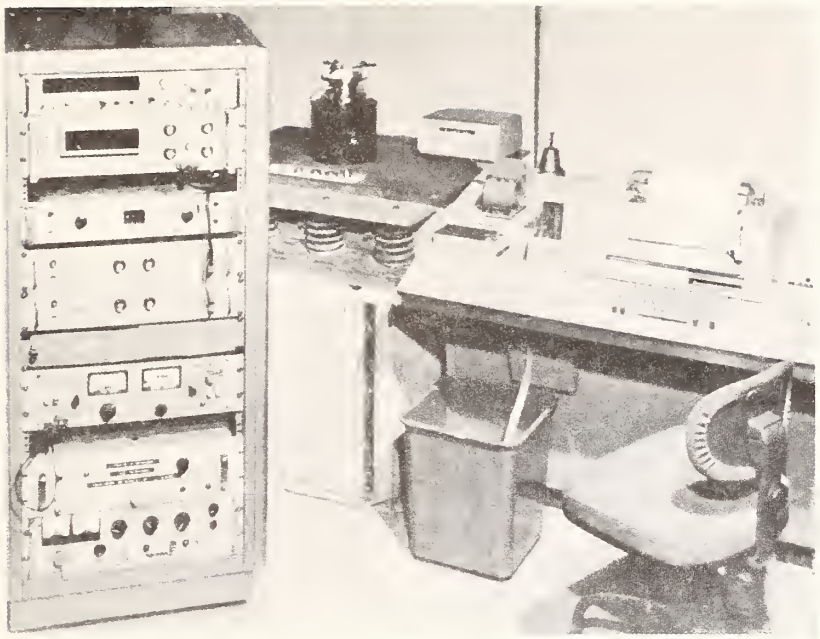

Fig. 4 - Experimental setup for obtaining transfer admittance data

Experiment 2

In this experiment, the open circuit voltage ratio of the standard accelerometer to the driver coil is measured when the shaker is driven with a second shaker. The moving element of the second shaker is connected to the mounting table of the shaker being calibrated. The ratio circuit is again given by Fig. 3. This time the reference is the voltage generated by the driver coil as it moves in the magnetic field of the shaker. Signal 2 is the voltage generated by the standard accelerometer. In such a case, where both signals fall below 2 v, the reference is amplified before being fed into the reference channel of the ratiometer. Measurements are usually taken every 50 Hz throughout the calibration frequency range. Three sets of data are usually taken and are used to compute the final value used. Phase angles are also taken here for each ratio data point. For the frequency range of 10 to 2000 Hz, a Goodman's V47 shaker was used to drive the standard shaker. For the frequency range of 2000 to 5000 Hz, a piezoelectric shaker was used. While driving with the piezoelectric shaker, a matching transformer and a network of step inductors in parallel with the driver coil was found to be necessary to minimize the distortion in the motion. By a careful adjustment of the inductor bank, the distortion was kept at approximately 1 percent. Data from these two experiments are sufficient to determine the sensitivity of the mounting table of the shaker in volts output of the standard accelerometer per g (acceleration of gravity) of table acceleration.

DRIVING ELECTRONICS

The oscillator provided a signal with no more than 0.05 percent distortion and fluctuations in amplitude after one hour warmup of no more than ± 10 μv for a 0.5-v signal level, as measured by a differential voltmeter.

The potentiometer which controlled the amplitude of the signal to the power amplifier had the equivalent of 10 turn resolution.

The power amplifier provided 250 watts with less than 0.1 percent distortion. The combined harmonic distortion of the oscillator and amplifier was checked periodically at less than 0.1 percent.

A matching network of capacitors, varying from 0.1 to about 150 μf, was used to tune the amplifier and shaker for best efficiency. Paper or mylar-paper capacitors were used, since they are the least noisy for this purpose.

MEASURING SYSTEM

The principal measurements in reciprocity calibration are ac/ac ratios. The instruments available to measure such ratios have improved greatly in the last few years. Systems used earlier are described in Refs. 2, 5 and 6.

The system used for the work described here consists of the following components: (a) two ac/dc voltage converters effective to frequencies as low as 1 Hz, (b) frequency counter, (c) phase meter with dc voltage output to feed into a digital voltmeter, (d) dual trace oscilloscope, (e) coupler program box, (f) digital ratiometer-voltmeter, (g) Model 101 data set, (h) Model 35 teletypewriter, (i) two high-input impedance cathode followers, (j) dc amplifier, (k) two voltmeters (3 percent) for setting levels, and (ℓ) ac voltage divider.

The digital ratiometer used consists of two ac/dc converters and a dc/dc ratiometer. It measures ac voltages over the frequency range from 10 to 10,000 Hz with an accuracy of approximately 0.5 percent for voltage signals from 10 mv to 10 volts. Ratios of ac/ac can be measured with greater accuracy by keeping the reference voltage (denominator) at 3 v or more. Over the frequency range from 10 to 10,000 Hz, the accuracy of the ratio will be about 0.2 percent if the numerator signal is as low as 5 mv, and it improves to about 0.1 percent if the numerator signal is above 10 mv. If the reference signal is less than 3 v, a good dc amplifier can be used in the reference branch of the ratiometer. The gain of the amplifier can be measured so accurately that the overall accuracy of the ratio is not appreciably impaired.

In using the dc amplifier in the reference branch of the circuit, we found we needed to buffer it on the ratiometer side by a cathode follower of high-input impedance (1000 megohms). A cathode follower was also used on the signal side of the dc amplifier to buffer the signal feeding into the voltage divider (Fig. 3). These cathode followers prevent loading effects which otherwise would introduce appreciable errors. For signals whose reference signal is greater than 2 v, both switches 1 and 2 are in position 1 and the ratiometer reads the ratio directly.

The procedure for obtaining voltage ratio measurements for signals whose reference drops below 2 v is as follows:

1. Set the dc amplifier to some convenient gain (usually × 30) and adjust the voltage divider to give a reference signal of 5 to 10 v.

2. With switch 1 in position 1 and switch 2 in position 2, record a voltage ratio R 1.

3. With switch 1 in position 2 and switch 2 in position 2, record a second voltage ratio R 2.

4. Program the computer to calculate the ratio R = R 1/R 2.

An alternate method for signals with low reference voltage is to measure the combined gain of the dc amplifier and cathode followers for the various frequencies of the calibration and then program the computer to make the gain corrections.

The system described above can reflect changes in ratio very quickly (5/sec in tracking mode), has an overall accuracy of at least 0.2 percent, has provision for printer output, and will feed a paper tape punch and typewriter.

INTERFACE BETWEEN MEASURING INSTRUMENTS AND COMPUTER

In Fig. 3 the interface equipment is denoted by the coupler and program box and the data set. The coupler accepts information from the digital ratiometer, frequency counter, and phase meter. It operates on this information by coding, formatting, and transmitting it to the teletype. The data set, a standard piece of telephone hardware, permits the user to use the teletype as a device to record data, both as hard copy and on paper tape. The coupler can work with many different printout devices, including magnetic tape producing units as well as the teletypewriter. The teletypewriter, however, is an economical printer-tape punch as well as a computer outlet.

The choice of data is made by providing various format options of all the possible types of data sequences likely to be needed for a particular application. A switch on the front panel of the coupler is used to choose the format option. Each position of the switch provides a particular sequence of data to be collected and the various positions comprise all possible sequences likely to be needed for a given application. The data collection is done while the teletypewriter is disconnected from the telephone line to the computer. This is accomplished by a switch located on the teletype which either connects the telephone line or the coupler to the teletype. For data recording, the teletype is connected to the coupler.

The coupler has two modes of operation, manual and automatic. In the manual mode, one data logging cycle is executed when the command button is depressed; in the automatic mode, the coupler continues to log data one cycle after another until switched out of the automatic position. The coupler also formats the data for use on the computer. The coupler has a number of features for data formatting. Extra characters can be inserted, such as commas and decimal points. A manual data entry panel provides for manual data entries, such as run numbers or time. After the coupler logs the data, it automatically advances the statement number.

After the data are collected on the paper tape, the teletype is connected to the telephone line and the data on the paper tape are read into the computer by the tape reader located on the teletype. The results of the computer program are printed on the teletype and can also be put on tape for future use.

FROM DATA TO RESULTS—USE OF TIME-SHARED COMPUTER SYSTEM

In practice the voltage ratio experiment is performed first. Usually, three sets of ratios covering the frequency range are taken. The data, collected on tape and teletypewriter as described above, consist of frequency, voltage ratio, and phase angle. The phase angle can be recorded at the same time as the ratio, or it can be recorded in a separate run.

To measure the phase angle, a digital phase meter is used which utilizes the digital dc voltmeter part of the ratiometer. By a remote command feature, the ratiometer can be electronically switched from voltage to ratio and the input can be switched to the signal from the phase meter, so that the coupler will present to the teletypewriter voltage ratio, phase angle, and frequency.

In the voltage ratio experiment, the computer is asked to read in the ratio, phase, and frequency data points, normalize the ratio by dividing by $2F\pi \times 10^{-6}$ (F = frequency), and give a second-degree polynomial fit for the normalized data vs frequency. Using the constants for this fitted equation, the computer calculates and prints out the fitted voltage ratio for integral frequencies (every 50 Hz). Thus, even though the original data were taken at only approximate frequency intervals, in its final form results are for exact intervals.

After the voltage ratio is taken (experiment 2), the calibration measurements are completed by obtaining the transfer admittance (experiment 1). Figure 4 shows the shaker and equipment setup for obtaining the transfer admittance readings. First, we establish the frequency at which we wish to calibrate. In this experiment we take voltage ratio and phase with a sequence of masses attached one at a time to the shake table. After obtaining the necessary 22 data points, plus the frequency and voltage ratio from experiment 2, the data are entered into the computer to obtain the final results. The results are illustrated by an actual run given in Fig. 5. At the top of the page is the frequency, value of the standard resistor used in experiment 1, and magnitude and phase (radians) of the voltage ratio of experiment 2. Next is a printout of the data, consisting of the load attached to the table, ratio and phase angle as given for experiment 1, and the computed transfer admittance. In the following columns are the average of the zero load transfer admittances (YEO-AVE), the difference in these and the loaded transfer admittances (Y-YEOAVE), and the real and imaginary components YMR and YMI using the recorded phase angles. The YM's are the components of the quantity

$$W/[(YM) - (YEO\text{-}AVE)] .$$

In the next step, the computer develops a weighted least squares fit for each of the real and imaginary components YMR and YMI, respectively, vs the masses W. The J's and Q's are the intercepts and slopes, respectively, of these plots. Next the experimental and calculated YMR and YMI and the deviation (DEV) and percent deviation (YMI-DP and YMR-DEV-PC) for these data are printed out. The index is a measure of how well the data fit a straight line. It is an average weighted deviation given by

$$\text{Index} = \frac{\sum_{n=1}^{N} n\,|\Delta m|}{N} ,$$

where n is the loading factor which varies directly as the mass (that is, 0.1 lb is counted once, 0.5 lb is counted 5 times); m is the percentage deviation of the YMR (since YMR contributes much more to the final answer than YMI, we are more interested in how YMR behaves); and N is the number of masses used in the sequence (in this case, five).

Next there is a second pass made; that is, the computer decides which points, if any, should be eliminated based on how far the point

```
F= 1500          R2= 10.215      VR= 1.31067     VR-PH= 1.52193

LOAD             RATIO           PHASE           YM

 0                .006881         2.25            14.2269
 .1               .006219         2.5             15.7413
 0                .00688          2.33            14.229
 .2               .005679         2.7             17.2381
 0                .006881         2.33            14.2269
 .3               .005222         2.79            18.7467
 0                .006882         2.33            14.2248
 .4               .004831         2.92            20.264
 0                .006882         2.33            14.2248
 .5               .004492         2.95            21.7932
 0                .006885         2.33            14.2186


YEO-AVE          Y-YEOAVE        YMR             YMI
 14.2279          .128041         6.57791 E-2     5.58006 E-3
 14.2279          .233591         6.62036 E-2     5.15001 E-3
 14.2259          .334152         6.61502 E-2     4.90075 E-3
 14.2248          .453969         6.60196 E-2     4.97474 E-3
 14.2217          .543394         6.58459 E-2     4.73635 E-3

J1= 5.43901 E-3                  J2= .066392
Q1=-1.37130 E-3                  Q2=-1.02902 E-3


LOAD             YMI-EX          YMI-CAL         YMI-DEV         YMI-DP
 .1               5.58006 E-3     5.30188 E-3     2.78176 E-4     4.98517
 .2               5.15001 E-3     5.16475 E-3    -1.47426 E-5    -.286263
 .3               4.90075 E-3     5.02762 E-3    -1.26876 E-4    -2.58892
 .4               4.97474 E-3     4.89050 E-3     8.42489 E-5     1.69353
 .5               4.73635 E-3     4.75337 E-3    -1.70121 E-5    -.359181

LOAD             YMR-EX          YMR-CAL         YMR-DEV         YMR-DEV-PC
 .1               6.57791 E-2     6.62891 E-2    -5.09980 E-4    -.775292
 .2               6.62036 E-2     6.61862 E-2     1.73568 E-5     2.62174 E-2
 .3               6.61502 E-2     6.60833 E-2     6.68957 E-5     .101127
 .4               6.60196 E-2     6.59804 E-2     3.92104 E-5     5.93921 E-2
 .5               6.58459 E-2     6.58775 E-2    -3.15631 E-5    -4.79348 E-2
INDEX= .107223

XXXXXXXXXXXXXXXX    SECOND PASS    XXXXXXXXXXXXXXXXXXXXXXX

LOADING FACTOR PC DEV

 1               -.775292
 2                2.62173 E-2
 3                .101127
 4                .059392
 5               -4.79349 E-2
INDEX= .107223


SUMMARY FOR 1500    HZ
                 IMAGINARY       REAL            MAGNITUDE       PHASE
J                -5.43901 E-3     .066392         6.66144 E-2    -8.17401 E-2
Q                 1.37130 E-3    -1.02902 E-3     1.71445 E-3     2.21455
BYP                                               .258693         2.23099

SEN- 0 LOAD                                       20.1028        -3.74164
SEN- 1/2 LB                                       19.9321        -3.18528
```

Fig. 5 - Calibration data sheet for typical frequency calibration point

deviates from the straight line. The limit for selection is programmed into the computer beforehand; usually it is 2 percent. The limit of 2 percent is tentatively selected as a working rule based on experience to date. With cumulation of additional data, this figure may be adjusted upwards or downwards. Other reasonable rules for the screening or editing of data are also being investigated. A new index is then computed and is printed with the loading factor used. In this sample run, no points were omitted on the second pass.

The components of the new $\bar{J}$'s and $\bar{Q}$'s are combined to get magnitudes and phases of J and Q which, together with the voltage ratio from experiment 2, provide all the information for obtaining the sensitivity. The computer now substitutes these quantities into the equation

$$S = 2634.95 \left[\frac{\bar{R}\,\bar{J}}{\bar{j}\,F}\right]^{1/2} \left[1 + \frac{W\bar{Q}}{\bar{J}}\right] \text{mv/g},$$

where

j = unit imaginary vector,

W = weight attached to exciter table (lb), and

F = frequency (Hz).

Using the usual rules of complex numbers, the computer then computes sensitivities for W as zero and 1/2-lb loads from this equation.

The final summary at the bottom of the data sheet (Fig. 5) gives the pertinent information for the intercepts, slope, and sensitivities for zero and 1/2-lb loads. The sensitivities here are in millivolts per g and degrees.

The computer then fits two second-degree polynomials to each of the two sensitivity-frequency curves by the method of least squares. The interpolation formula for sensitivity for other weights is given by

$$S_W = S_0 - \frac{W}{0.5}\,(S_0 - S_{1/2}),$$

where S_0 are the values given by the zero load second-degree equation and $S_{1/2}$ are the values given by the 1/2-lb load second-degree equation.

This sensitivity is tabulated by the computer for incremental loads which might be attached to the mounting table, usually every 0.05 lb from 0.0 to 0.5 lb for the various frequencies which are ordinarily used in a pickup calibration. These tables provide a convenient calibration listing for any load up to 1/2 lb throughout the calibration frequency range. Having established the calibration of the primary standard in millivolts output per g of acceleration, we can use the same ratio circuit to establish by comparison techniques the sensitivities of secondary standards.

Before the computer was used, not only was the calibration slower, but also some of the data handling could not have been done. For example, computing deviations and quality indexes would not have been considered practicable.

The reciprocity technique is independent of other calibration methods and a calibration resulting from the procedures described above can be considered as equal in accuracy and resolution to a calibration derived by any other means. However, vibration measurements are subject to so many sources of error that check measurements are desirable to minimize chances of systematic error. The calibration described in this paper was checked in a number of ways, since both the shaker and the computer routine were fairly new.

The accelerometer used as the calibration standard was calibrated by the usual NBS routine: from 10 to 2000 Hz on two electrodynamic shakers using velocity sensing coils, and from 1.5 to 10 kHz by the modulated frequency interferometric technique [7]. These results were compared with the manufacturer's calibration. After the new shaker was calibrated as described above, it was used to calibrate a number of accelerometers maintained at NBS which are known to produce repeatable results on the current standard shakers. A good check at 10, 15, and 30 Hz was obtained by using the new shaker to calibrate a servo accelerometer which had been calibrated statically on a tilt table. A further check over the frequency range below 2000 Hz was obtained by using a strobe light synchronized with the motion, and a microscope with a filar micrometer eyepiece. The discrepancies between the reciprocity calibration and the check measurements were well within the estimated uncertainties of the measurements.

USE OF RECIPROCITY TECHNIQUE TO EVALUATE DESIGN

The reciprocity experiments combined with the computer can be used to evaluate design features of shakers under development. This can be seen from the data collected on the new shaker shown in Fig. 2. Figure 6 shows the frequency response for the voltage ratio experiment 2. The smoothness of the curve indicates undistorted uniaxial motion of the shaker. If distortion occurs or local resonances affect the motion, it will be reflected in these data. On the older shaker, these data would show breaks in the curve indicating bad motion.

The transfer admittance data also reflect the quality and uniformity of the motion. The scatter indices described above, taken on three

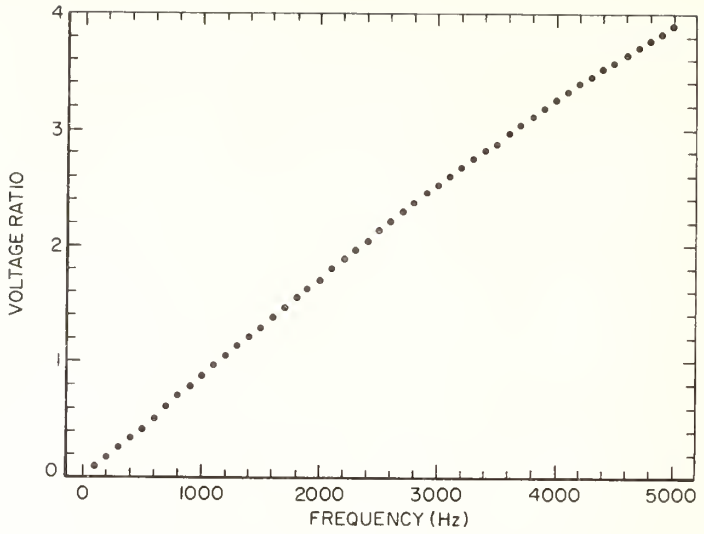

Fig. 6 - Voltage ratio vs frequency for experiment 2

shakers calibrated with the readout system described here, are given in Table 1. Shakers 619 and 676 are an older modified commercial type, and the indices reflect their scatter on the first pass through the computer. On the shaker AF II, very few points were rejected by the computer with a cutoff limit of 2 percent. These data indicate that the new design of the ceramic shaker reduced the scatter by a factor of about three. Figure 7 shows the frequency response of the shaker calibrated by reciprocity using an accelerometer as the standard.

TABLE 1

Shaker	Average Scatter Index	
	1st Pass	2nd Pass
No. 619	0.886	0.415
No. 676	1.00	0.420
AF II	0.327	0.259

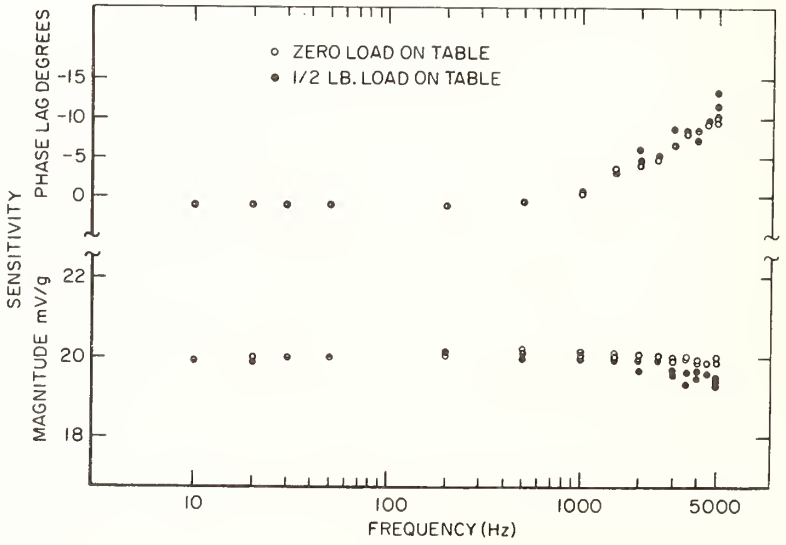

Fig. 7 - Sensitivity vs frequency for Shaker AF II

REFERENCES

1. T. Dimoff, "Electrodynamic Vibration Standard with a Ceramic Moving Element," J. Acoust. Soc. Am., Vol. 40, No. 3, pp. 671-676, Sept. 1966

2. Samuel Levy and Raymond R. Bouche, "Calibration of Vibration Pickups by the Reciprocity Method," J. Res. NBS, Vol. 57, No. 4, pp. 227-243 (1956)

3. R. R. Bouche and L. C. Ensor, "Use of Reciprocity Calibrated Accelerometer Standards for Performing Routine Laboratory Comparison Calibrations," Shock and Vibration Bull. No. 34, Part 4, pp. 21-29, Feb. 1965

4. R. R. Bouche, "Development of Standards for the Measurement of Vibratory Motion," Ph.D. thesis, Dept. of Mech. Eng., Univ. of Maryland, Dec. 1958

5. "American Standard Methods for the Calibration of Shock and Vibration Pickups," Am. Standards Assoc., S2.2, 1959

6. J. R. Houghton, NBS Tech. Note 266, Govt. Print. Off., Dec. 1965

7. V. A. Schmidt, S. Edelman, E. R. Smith, and E. T. Pierce, "Modulated Photoelectric Measurement of Vibration," J. Acoust. Soc. of Am., Vol. 34, No. 4, pp. 455-458, April 1962

Appendix

The circuit given in Fig. 3 can also be used for the calibration of pickups by comparison with the reciprocity calibrated shaker using the standard accelerometer. The sensitivity of an unknown pickup mounted on the exciter table is given by

$$S_{unknown} = \left[\frac{E_{unknown}}{E_{standard}\, G}\right] \times S_{standard},$$

where G is the gain of the dc amplifier and $S_{standard}$ is the sensitivity of the standard accelerometer. The quantity in brackets is that measured by the ratiometer. Our standard accelerometer has a sensitivity of approximately 20 mv/g. By setting the dc amplifier gain on approximately 50 and using the voltage divider to correct for small variations in the sensitivity of the standard and the gain of the amplifier and cathode followers, the meter will read the sensitivity of the unknown pickup directly.

This leads to a simple means of setting the system for direct reading of sensitivity:

1. Feed the output from an oscillator into both inputs of Fig. 3. That is to say, use position 2 on both switches 1 and 2. Let the amplitude level be approximately what the output of the standard pickup would be at 5 g.

2. Pick a gain setting on the dc amplifier so that its reciprocal will be approximately the $S_{standard}$ in the above equation (in volts per g). In our case 1/G should be 0.02.

3. Adjust the voltage divider so that the exact calibration factor of the standard accelerometer appears on the ratiometer when switch 2 is in position 2. Note this voltage divider setting.

4. Repeat step 4 for the various frequencies taken in the calibration range, noting the voltage divider setting for each frequency.

To calibrate pickups, the standard accelerometer output will be fed into channel 1 (reference); the unknown to be calibrated will be fed into channel 2. Switch 1 will be in position 1 and switch 2 in position 2. If the voltage divider is now set for the appropriate frequency, the ratiometer will read the sensitivity of the unknown directly in volts per g.

At the two lowest frequencies, 15 and 10 Hz, the reference in the system drops below 1.5 v at the lower acceleration levels if the dc amplifier is held at the same gain. Therefore, at these two frequencies, the system must be calibrated for the separate levels of acceleration. In our case this is 5, 2, 1 for 15 Hz and 2, 1, 0.5 at 10 Hz. This is especially convenient when using the coupler and teletype to record the data. Activating the command button provides a direct printout of the sensitivity.

Mr. Ames (Frankford Arsenal): What method is used to support the moving element in the vertical axis?

Mr. Payne: At the present time we use two methods: a flexible rubber tube or by a dc voltage imposed on the driving coil. The rubber tube works a little better than the dc suspension.

Mr. Jackman (General Dynamics/Pomona): What is the cross-axis sensitivity in your calibrations?

Mr. Payne: It runs under 2 percent over the calibration range, with some points below 1 percent.

Mr. Jackman: Is that 2 percent more or less uniform, or do you have resonances pulling up to the 2 percent?

Mr. Payne: Throughout the calibration range from 10 to 5000 Hz, we do not have any evidence of resonances. The cross-axis motion seems to have a more or less random pattern. A paper in the Journal of the Acoustical Society of America, September 1966, gives the actual experimental data on this.

* * *

A Publication of
THE SHOCK AND VIBRATION
INFORMATION CENTER
Naval Research Laboratory, Washington, D.C.

February 1967

Bulletin 36, Part 6 (of 7 Parts)

JOURNAL OF RESEARCH of the National Bureau of Standards—C. Engineering and Instrumentation
Vol. 73C, Nos. 3 & 4, July–September 1969

Optical FM System for Measuring Mechanical Shock

L. D. Ballard and W. S. Epstein,

Institute for Basic Standards, National Bureau of Standards, Washington, D.C. 20234

E. R. Smith,

Harry Diamond Laboratories, U.S. Army Materiel Command, Washington, D.C., 20438

and

S. Edelman

Institute for Materials Research, National Bureau of Standards, Washington, D.C. 20234

(August 13, 1969)

A technique is described for calibrating shock accelerometers by measuring the Doppler shift in light frequency produced by the change in velocity of a target. The system employs a quadrature laser interferometer and a single-sideband carrier insertion circuit to distinguish between positive and negative velocities.

Key words: Accelerometer; calibration; Doppler; interferometer; laser; shock measuring; single-sideband.

1. Introduction

Shock loading may be one of the most destructive or most beneficial environments encountered by mechanical systems. The damage to structures by sudden loads, such as produced by the collision of objects, is familiar. The forming of materials into desired shapes by forging or explosive forming techniques are examples of desirable effects of controlled impact, or shock loading.

There is a demonstrated need to measure shock loads accurately over a wide range of amplitudes and wave forms. The design of structures to withstand such loads and the efficient use of energy for forming materials are only two of the more obvious benefits of a knowledge of shock loadings and their effects.

One of the problems in measureing mechanical shock has been the inability to calibrate shock measuring systems absolutely except by subjecting them to intense, steady state, sinusoidal motion at a few discrete frequencies. Such calibrations are inherently suspect because they are not characteristic of the environment to be measured, and transducers are frequently damaged during such tests. Sinusoidal calibrations of this nature offer the added difficulty that the tests are very time consuming and expensive.

Shock measuring transducers can also be calibrated by measuring lumped response integrated over the total energy spectrum with no attempt to determine response as a function of frequency. An example of this type of calibration is a peak value calibration where the transducer is subjected to a shock input and calibrated as to the peak reading obtained. The calibration comes from either a reference transducer or computed accelerations via measuring velocity changes over finite time intervals. There is a need for a fast, accurate and absolute method for calibrating shock measuring systems under conditions closely simulating those encountered in actual use [1–7].[1]

2. Shock Measuring System

An interferometer system has been devised to provide an absolute calibration facility for measuring shock induced motion. This system produces an electrical signal that is directly proportional to the velocity of the moving element being studied. This signal can be processed, analyzed and compared to the signal from a transducer that is subjected to the same motion. The system has the following advantages: (1) it is a system completely independent of the transducer, (2) it is based on the Doppler shift of light frequency detected by a moving interferometric fringe pattern, a phenomenon that is known to be linear with velocities

[1] Figures in brackets indicate the literature references at the end of this paper.

in the range of the mechanical shock spectrum, (3) it is capable of measuring actual shock motion having a wide range of amplitudes and rich in frequency content, and (4) the resulting signal can be rapidly and accurately analyzed by known methods and techniques [8].

2.1. Theory

The moving reflector of an optical interferometer is attached to the object whose motion is to be measured. A narrow section of the fringe pattern is viewed by a photodetector; if the interferometer plates are uncoated the photodetector output is [9].

$$E_1 = A + E_0 \sin [k(\delta + 2\xi)] \tag{1}$$

E_1 = output voltage

E_0 = signal out, dependent upon light intensity

A = d-c term

$k = 2\pi/\lambda$

λ = wavelength of monochromatic light

δ = average optical separation between interfering light beams

ξ = displacement of reflector

If we had, instead of eq (1)

$$E_2 = A + E_0 \sin [\omega t + k(\delta + 2\xi)] \tag{2}$$

ω = carrier frequency

which is a frequency modulated wave [10], the velocity of the reflector could be obtained by demodulation. The output of a demodulator is proportional to the instantaneous frequency deviation and the instantaneous frequency in eq (2) is

$$f_1 = \frac{1}{2\pi}\frac{d}{dt}[\omega t + k\delta + 2k\xi] = \frac{\omega}{2\pi} + \frac{2\dot{\xi}}{\lambda} \tag{3}$$

Therefore, the instantaneous frequency will define what the instantaneous velocity is. Equation (3) could have been obtained by direct application of doppler shift equation [11].

If E_1 in eq (1) were demodulated directly, or even after up-conversion of the frequencies, the sign of the output would be ambiguous. The problem is therefore to insert a carrier into E_1 of eq (1) and convert it to E_2 of eq (2).

2.2. Description

The interferometer used in the present work is a commercial model shown schematically in figure 1. It is a modified Michelson type, illuminated by a single-frequency He-Ne laser so that long path differences are possible. The moving retroreflector is a corner cube for the usual reasons. The interfering beams are circularly polarized so that by use of a beam splitter and analyzers, followed by two photodetectors, two electrical outputs in phase quadrature are obtained. The original purpose of this arrangement is for fringe counting [12]. The instrument has internal preamplifiers of bandwidth DC to 500 kHz; for higher velocity external preamplifiers of bandwidth 20 Hz to 60 MHz were used.

If one output is described by eq (1), which we rewrite, dropping the constant A and replacing $k(\delta+2\xi)$

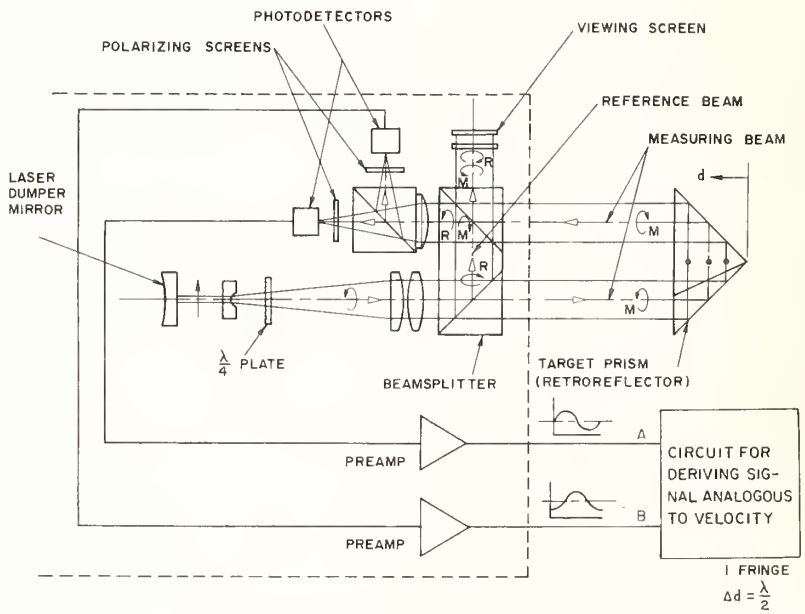

FIGURE 1. *Schematic, laser interferometer.*

by x, as

$$E_A = C \sin x$$

then the other is

$$E_B = C \cos x.$$

The signal E_B is multiplied, in a balanced mixer by the output $D \sin \omega t$ of a local oscillator, giving

$$CD \sin \omega t \cos x, \tag{4}$$

and E_A is multiplied, in another balanced mixer, by $D \cos \omega t$, giving,

$$CD \cos \omega t \sin kt \tag{5}$$

the outputs (4) and (5) are added in a suitable circuit to give

$$CD \sin (\omega t + x) = CD \sin [\omega t + k(\delta + 2\xi)] \tag{6}$$

which is the frequency-modulated wave of eq (2). As already explained, demodulation of this wave yields an output proportional to the velocity of the reflector.

The above method is similar to the phase-shift method of single-sideband generation [13] with the distinct difference that the signal phase shift is produced optically.

The single-sideband circuit was assembled from off-the-shelf hardware of balanced mixers, quadrature hybrid, FM demodulator and carrier oscillator. The carrier used in this case is 60 MHz. The signal is demodulated by a conventional FM discriminator, and the resulting signal can be analyzed by either digital or analog techniques.

The system can be readily calibrated by subjecting the moving element to steady state sinusoidal motion. One technique that has been used involves counting interference fringes over a known time interval. Average and peak velocities can then be computed for the frequency of vibration. Other methods for calibrating the system, such as the Crosby method for determining peak FM swing, could also be used. [14, 15, 16] Inherent in the system is a possible means of checking the calibration factor during the course of each experiment. The calibration factor can be determined by comparison of the average velocity over a known time interval, during which there are no velocity reversals, with the average discriminator output over the same interval. The former is the displacement, determined from a fringe count, divided by the time interval.

3. Performance

To obtain data an accelerometer was attached directly to the face of a corner cube retroreflector. The accelerometer was small enough to fit in a quadrant of the corner cube so as not to interfere with the laser beams. The moving corner cube of the interferometer was mounted on the table of an electrodynamic shaker. The input signal to the shaker was a single sine pulse (301 Hz) repeated at a rate of 75.3 Hz. Qualitative comparisons of signals obtained from various subsystems can be made from figures 2a, b, and c. Figure 2a shows the signals from the discriminator of the interferometer system and from the accelerometer. Figure 2a shows the signals from

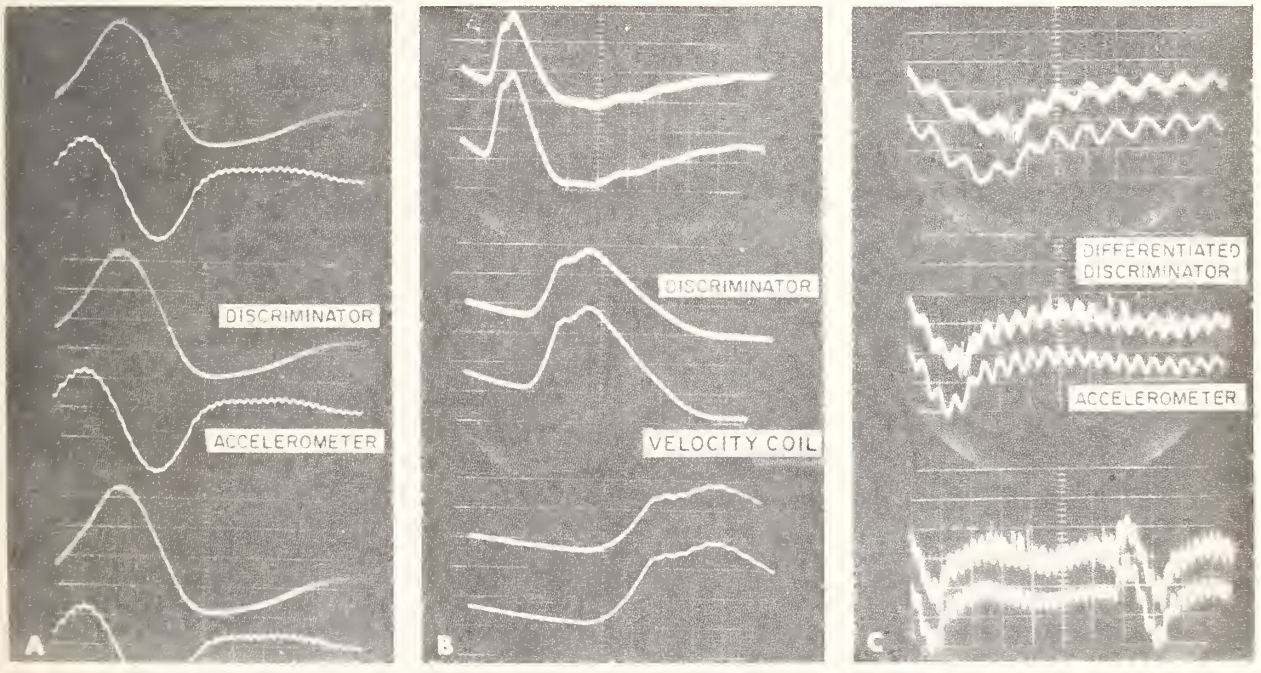

FIGURE 2. *Simultaneous signals from shock motion measuring system.*
a. Discriminator versus accelerometer, b. discriminator versus velocity coil, c. differentiated discriminator versus accelerometer.

the discriminator of the interferometer system and from the accelerometer. Figure 2b shows the signals from the discriminator and from the velocity coil of the shaker. Figure 2c shows the differentiated output of the discriminator and the output of the accelerometer. The two outputs shown in figure 2c were fed to a frequency analyzer and the results plotted on an X-Y plotter. The measured peaks of response are shown in table 1. The calibration factors were arbitrary and the results are only meaningful when compared to each other as shown in the percent deviation column. The differences in harmonic relationships of the frequencies are due to errors in determining the frequency at a point in a logarithmic sweep.

TABLE 1. *Comparison between accelerometer and differentiated discriminator output spectrum due to repetitive sine pulse*

Frequency	Differentiated discriminator[b]	Accelerometer[b]	Accelerometer output deviation from discriminator output[a]
Hz	*Units*	*Units*	*Percent*
76.5	4.50	4.63	+3.6
151	8.23	8.18	0.0
225	7.76	7.75	+.5
301	7.41	7.45	+1.2
376	6.46	6.72	+4.6
2104	6.02	5.75	−3.8

[a] Normalized to maximum discriminator amplitude recoreed at 151 Hz.
[b] Amplitude as measured on a X-Y plotter.

4. Other Applications

The development of this system was oriented towards motion with large velocities and displacements. If the emphasis is changed from detecting frequency to detecting phase modulation, it is feasible to measure fractional parts of a fringe displacement. [17] This approach is not limited to a laser as an electromagnetic radiation source; any coherent source will do, such as radar.

5. Summary

A system has been described that is capable of sensing mechanical shock induced motion and providing a signal that is proportional to the velocity of the motion. The system makes use of the Doppler shift in light frequency, a phenomenon that is known to be linear with amplitude and frequency of motion. The information output is a variable frequency thereby minimizing the linearity requirements for electronic components other than the discriminator. The system can be readily calibrated by use of steady state sinusoidal motion. The information is available in a form that can be analyzed by known methods and techniques.

The authors wish to express their appreciation for the financial support received from:

U.S. Atomic Energy Commission
Sandia Corporation
Albuquerque, New Mexico AL–67–421,

U.S. Army Missile Command
U.S. Army Metrology and Calibration Center
Redstone Arsenal, Alabama YP–369,

Naval Ordnance System Command
Naval Plant Representative
Metrology Engineering Center
Pomona, California 4355/N1(N69–35).

6. References

[1] Conrad, R. W., and Vigness, Irwin, Calibration of accelerometers by impact techniques, Proc. Inst. Soc. Am. **8**, 166 (1953).
[2] Bouche, R. R., The absolute calibration of pickups on a drop-ball shock machine of the ballistic type, Proc. Inst. Environmental Sci., 115 (1961).
[3] Ramboz, J. D., and Blanchard, C. A., Report No. ESEE08, Endevco 2965 Shock Calibrator, Metrology Engineering Center Naval Plant Representative, Pomona, California; Private Communication.
[4] Burke, R. G., Improved velocity measurement techniques for the shock calibration of accelerometers, Proc. Inst. of Environmental Sci. (1963).
[5] Kelley, R. W., Calibration of shock accelerometers, Proc. 22nd ISA Conf., M18–2–MESTIND–67, Inst. Soc. Am. (1967).
[6] Levy, S., and Kroll, W. D., Response of accelerometers to transient accelerations, J. Res. Nat. Bur. Stand. (U.S.) **45**, No. 4, 303 (1950) RP2138.
[7] Bundy, D. E., The calibration of transducers for use in high intensity shock measurement, Technical Note W.C. 56, Royal Aircraft Establishment, Ministry of Aviation, London W.C. 2, England, March 1964, AD–449463.
[8] IEEE Transactions on Audio and Electroacoustics, **AU–15** No. 2, June 1967, Special Issue on Fast Fourier Transform and Its Application to Digital Filtering and Spectral Analysis.
[9] Schmidt, V. A., Edelman, S., Smith, E. R., and Jones, E., Optical calibration of vibration pickups at small amplitudes, J. Acous. Soc. Am. **33**, 748 (1961).
[10] Hund, A., in the book Frequency Modulation, Eq. 10, p. 16, McGraw-Hill Book Co., New York (1942).
[11] T. P. Gill, in the book The Doppler Effect, Chapter 5 (Academic Press, New York, 1965).
[12] Rowley, W. R. C., Some aspects of fringe counting in laser interferometers, IEEE, Transactions on Instrumentation and Measurement, **Im–15**, No. 4, 146 (1966).
[13] Norgaard, D. E., The Phase-Shift Method of Single-Sideband Signal Generation, Proceedings of the IEEE, **44**, No. 12, 1718 (1956).
[14] Hund, A., ibid., p. 86.
[15] Smith, D. H., Method for Obtaining Small Mechanical Vibrations of Known Amplitude, Proc. Phy. Soc. (London) **57**, 534 (1945).
[16] Ziegler, C. A., Electromechanical Pickup Calibration by the Interferometer Method, J. Acous. Soc. Am. **25**, 135 (1953).
[17] von Willisen, F. K., Time resolved photoelectric interferometry of very high phase resolution, Oral Presentation at 1968 Spring Meeting Optical Soc. Am.

(Paper 73C3&4–291)

10. Viscosity

CALIBRATION OF VISCOMETERS

Robert S. Marvin
Rheology Section
National Bureau of Standards

INTRODUCTION

Detailed descriptions of and directions for the use of viscometers, particularly those intended for measurements on liquids, are available in a number of publications. In most cases, however, the physical principles and basic problems associated with this measurement are not discussed, but must be sought in references on hydrodynamics or rheology.

This paper is intended to present to those charged with the calibration of viscometers or routine measurement of viscosity a concise summary of the principles underlying such measurements. It is addressed to those who need a general understanding of the principles and problems associated with the measurement of viscosity and not primarily to those developing new methods of measurement or interpreting the rheological properties of materials.

DEFINITION OF VISCOSITY; UNITS

Viscosity is a material property involved in the relationship between the internal forces in a moving fluid and the kinematical quantities describing the motion. Our qualitative ideas about viscosity are based on the analysis of a Newtonian fluid, one in which the stress is proportional to the rate of strain. This is a hypothesis about material behavior which has been found adequate to describe the behavior of many real fluids under a wide range of conditions. It leads to a definition of two coefficients of viscosity exactly analogous to the shear and bulk moduli of classical elasticity theory: the shear viscosity (referred to commonly as viscosity) and the bulk viscosity. These two material properties are constants in the sense that they do not depend on kinematic quantities, that is, they are functions of the material and not of the type of flow. They are, of course, functions of pressure and temperature.

Stress, being defined in terms of forces acting across imaginary planes in a material, cannot be measured directly. It must be inferred from measurements made at a surface of the material, and its calculation implies some assumptions about the rheological properties of the material studied. These are expressed in what is termed a constitutive equation, the simplest of which (except for an inviscid fluid) is the Newtonian hypothesis mentioned above. This, or any other constitutive equation, is properly speaking an abstraction or a model. When we refer to a real liquid as a "Newtonian liquid" we mean its flow behavior is consistent with that of a hypothetical Newtonian liquid.

Most low molecular weight, homogeneous liquids do behave in this fashion, at least in the flows normally studied. Many other liquids show marked deviations from such behavior, and their properties must be described by more complicated constitutive equations. In such liquids the stress associated with a steady flow is not proportional to the velocity gradient and, indeed, will not even be oriented in the same direction. Nonetheless, it is frequently possible to define a viscosity for such liquids as the ratio of shear stress to rate of shear as measured in a simple shear flow after a sufficiently long time of shearing. The viscosity so defined is, of course, a function of the rate of shear.

In most viscometers the rate of shear varies throughout the sample. If measurements on a non-Newtonian liquid whose viscosity varies with the rate of shear are analyzed as though the liquid were Newtonian, the result will be an apparent viscosity which will depend on the particular instrument employed as well as on the properties of the liquid and a rate of shear. The non-Newtonian viscosity defined as shear stress divided by rate of shear, however, is a material property, defined without reference to any particular instrument.

The stress associated with a flow in which the motion is sufficiently small or the velocity sufficiently low will be (at least within the precision of ordinary meas-

urements) proportional to the magnitude of the velocity gradient, but time effects will normally still be observed in a non-Newtonian fluid. In this limit one may describe the material properties in terms of a (complex) dynamic viscosity (and dynamic bulk viscosity), a function of frequency, which can be measured directly employing motions with a sinusoidal time dependence. At one time the term dynamic viscosity was used for the quantity here called viscosity. Though still occasionally used in this sense, dynamic viscosity now generally denotes a frequency dependent quantity.

For some non-Newtonian liquids it has been found that the steady-flow viscosity is, approximately and over a limited range, the same function of the rate of shear as the (amplitude independent) dynamic viscosity is of frequency or of a quantity proportional to frequency. This is a property of the particular constitutive equation which describes such liquids, but such observations have at times been presented in a manner which seems to confuse rate of shear and frequency.

The cgs unit of viscosity is the poise (dyne s cm^{-2} or g cm^{-1} s^{-1}). The SI unit, N s m^{-2}, is equal to ten poise, i.e., the viscosity of water is approximately 10^{-2} poise or 10^{-3} SI units. No coined name has been adopted for viscosity in the SI system, and it is still customarily expressed in poise. η or μ are the symbols commonly employed for viscosity. The ratio of viscosity to density (η/ρ), termed kinematic viscosity, is the quantity measured directly in many instruments, and is often tabulated in lieu of viscosity. Its cgs unit is the stokes (cm^2 s^{-1}). The SI unit, again with no coined name, equals 10^4 stokes, i.e., the kinematic viscosity of water is approximately 10^{-2} stokes or 10^{-6} m^2 s^{-1} (SI units).

MEASUREMENT OF VISCOSITY

The substitution of the Newtonian constitutive equation into the equations of motion yields the Navier-Stokes equation on which most of hydrodynamics is based. The solution of this nonlinear differential equation (the differential equation is nonlinear even though the Newtonian constitutive equation used is linear), subject to the equation of continuity, an energy equation, and boundary conditions, cannot be carried out exactly for most types of flow. The equations solved for most viscometer flows are simplified by assuming that the fluid is incompressible, or more precisely by assuming that density and viscosity are functions of temperature alone and ignoring viscous heating [1]*. The resulting equations are still nonlinear so that, with few exceptions, the exact solutions obtained are for geometries in which the accelerations either vanish, such as Poiseuille or pipe flow, or can be balanced by a pressure gradient, such as Couette flow between concentric cylinders [1,2].

Poiseuille flow has been employed for most of the few absolute measurements of viscosity. By assuming a Newtonian, incompressible fluid, constant temperature, zero velocity of the fluid at the boundaries, and a steady velocity directed along the axis of the pipe (no radial flow), the pressure gradient along the pipe, P_z, can be related to the volume rate of flow through the pipe, Q, by:

$$P_z/Q = B\,\eta/A^2$$

where A is the cross-sectional area of the pipe and B is a constant depending only on the geometry of the cross-section. For a circular pipe of radius R, $B = 8\pi$, yielding the familiar Poiseuille equation:

$$P_z/Q = 8\,\eta/\pi R^4.$$

B can be calculated for a uniform pipe of any given cross-section, with perhaps some purely computational difficulty.

To insure the laminar flow assumed in the above solution with a pressure difference large enough to be measured accurately and at the same time a pipe length small enough to be thermostatted accurately, diameters from a few tenths of a mm to a few mm, depending on the viscosity of the liquid, must be employed. It is not possible to obtain capillaries of this size with diameters uniform to better than the order of one percent. This limitation raises the possibility of systematic error because the effective radius is not known accurately and also because a non-uniformity of the capillary will cause radial flow.

Another possible source of systematic error in such determinations has to do with the measurement of the effective pressure gradient, P_z, in the equation above. The quantity required is the constant pressure gradient existing in the pipe in the region of steady flow. In most absolute measurements the pressure difference between two reservoirs connected by the capillary is

* Figures in brackets indicate the literature references at the end of this paper.

measured. The change from essentially zero velocity in the reservoirs to a constant velocity profile (parabolic for circular cross section) in the region of steady flow within the pipe requires a pressure drop which cannot be calculated exactly. The usual corrections for end effects are based on several assumptions which are not strictly correct and the available experimental checks leave some doubt as to their adequacy, particularly for capillaries with square cut ends.

Most of these difficulties and uncertainties can be avoided by the use of relative viscometers which require calibration with a liquid of known viscosity. It is comparatively simple to design an instrument which will measure relative viscosities to 0.1 percent (at least in the range from 10^{-2} to 1 poise), and most measurements of viscosity are made with relative instruments which are calibrated using water, or liquids whose viscosity has been measured relative to water at some central laboratory.

Various absolute measurements of the viscosity of water, most with a precision of about ±0.1 percent, have yielded results which differ by as much as 0.8 percent [3]. The value now accepted in this country and throughout most of the world is that obtained by Swindells, Coe, and Godfrey [4], 0.01002 poise at 20°C and one atmosphere. Though the reproducibility of their (capillary) measurements and the uncertainties connected with measurements of pressure, rate of flow, etc., yielded an estimated uncertainty of ±0.03 percent, this figure does not include the effects of possible systematic errors of the type discussed above. In an effort to place limits on this uncertainty, we have compared the results obtained using two new absolute measurement techniques, each with a precision of slightly better than 0.1 percent. They differ by about 0.4 percent, by chance bracketting the value of Swindells, et al. The continued use of 0.01002 poise for the viscosity of water at 20°C permits the comparability of values so determined in different laboratories with an uncertainty of ±0.1 percent. However, it should be recognized that all values of viscosity measured on this basis may contain a common systematic error of as much as 0.2 percent.

VISCOMETERS AND THEIR CALIBRATION

The most widely used relative viscometers are based on Poiseuille flow through a circular pipe or Couette flow between concentric cylinders, parallel plates, or coaxial cones. Various types of rotating or oscillating members immersed in a fluid and cylinders or balls falling or sliding through a fluid are also employed. Some of these instruments are quite similar to those which have been (or could be) used for an absolute measurement, but even in such cases calibration with a liquid of known viscosity is generally much simpler than calculation of the appropriate instrument constant from the dimensions. Other instruments depend on a flow pattern much too complicated to analyze; in some cases a number with no simple relationship to viscosity is measured.* Such instruments are often adopted for convenience or because of long established practice in a certain industry. Misleading results can easily follow their use for liquids differing significantly from those for which accepted empirical correlations have been established.

A number of commercial instruments of various types are described by Van Wazer, Lyons, Kim, and Colwell [5], in ASTM Standards, Part 17 [6], as well as in the literature of the various manufacturers and supply houses. Some, particularly the rotational instruments, are sold as rather elaborate units including thermostatic controls and automatic recorders. Others, including most of the capillary instruments, are comparatively simple and inexpensive but require auxiliary equipment for temperature control and measurement of flow times.

Some instruments are supplied calibrated by the manufacturer. Such calibrations should certainly be checked by the user whenever accurate measurements are required. In any event, a calibration provides a valuable check of the user's technique and of any auxiliary equipment employed.

Capillary instruments are usually employed when the highest precision is required. In several designs a capillary connects two reservoirs in a U-tube type of construction with the driving pressure provided by the difference in the levels of the reservoirs. In this type the total volume of sample used must be constant. This requires a special correction when the temperatures of filling and measurement differ [7]. The kinematic viscosity of the sample is equal to an instrument constant times the time of flow minus a second instrument constant divided by the time of flow. This second term, the kinetic energy correction, will always be much smaller than the first in a well-designed instrument, and often may

* For example, the Saybolt viscosity.

be ignored when long flow times (200 seconds or more) are involved. The entrance and exit regions of the capillaries are designed to minimize some of the complications discussed above, but since the correction term accounts for effects which depend on the rate of flow and hence the viscosity of the liquid being measured, it is not unambiguously established. The use of a correction term proportional to t^{-2} rather than t^{-1} has been advocated [8], and is the form now specified in ASTM D-2515. For the most reliable results, the flow times should be so long that the correction term is negligible.

Rotational viscometers can be designed to cover a much greater range of viscosities than capillary instruments, and are particularly useful in the study of non-Newtonian liquids since the rate of shear can be varied easily. Though they are convenient and versatile, it is more difficult to maintain close temperature control in rotational than in capillary instruments. Adequate temperature control is often the factor limiting the precision attainable in the measurement of viscosity. The temperature coefficient of viscosity (percentage change per degree) of liquids increases with viscosity, typically from something like 2 percent per degree C at 10^{-2} poise to 10 percent per degree C at a few hundred poise. Temperature control to ±0.01°C or better is normally necessary for accurate viscosity measurements, and this is most easily attained with a viscometer which, like a capillary type, can be completely immersed in a thermostat.

Many of the other types of commercial viscometers available offer features important for certain specific uses. Some are particularly quick and convenient to use, ordinarily at some sacrifice in the precision of measurement. Some require only a small amount of sample. Most are designed as relative, rather than absolute instruments.

CALIBRATING LIQUIDS

The need thus generated for calibrating liquids of known viscosity cannot be met by tabulation of viscosities of pure compounds. Those compounds that can be purified without elaborate equipment have viscosities of the same order of magnitude as water, while a set of liquids with viscosities ranging up to a few hundred poise is needed for calibration of the various instruments commonly used.

In the United States, ASTM Committee D-2 has undertaken to supply viscometer calibrating liquids through contract with the Cannon Instrument Company. A series of liquids with the approximate kinematic viscosities shown in Table 1 are prepared in lots for each of which the viscosity, kinematic viscosity, and

Viscosity	Approximate Kinematic Viscosity in Centistokes, at -							
Standard	-53.89°C	-40°C	20°C	25°C	30°C	37.78°C	50°C	98.89°C
	-65°F*	-40°F*	68°F	77°F	86°F	100°F	122°F	210°F
S-3	300	80	4.6	4.0	-----	3.0	-----	1.2
S-6	---	--	10	9.0	-----	6.0	-----	1.8
S-20	---	--	44	35	-----	20	-----	3.9
S-60	---	--	160	120	-----	60	-----	7.7
S-200	---	--	700	480	-----	200	-----	16
S-600	---	--	2500	1600	-----	600	280	32
S-2000	---	--	9000	5700	-----	2000	-----	76
S-8000	---	--	38000	22000	-----	8000	-----	----
S-30000	---	--	-------	-------	50000	27000	11000	----

Table 1. Samples, with the measured values of viscosity, kinematic viscosity, and density at the temperatures shown (* Only kinematic viscosity is given at -53.89° and -40°C), can be obtained for $15 per pint ($25 per pint for S-8000 and S-30000) from Cannon Instrument Co., P. O. Box 16, State College, Pennsylvania 16801. Telephone: (814) 466-6232.

density are measured by Cannon at the temperatures shown. These measurements are carried out in relative capillary instruments calibrated by a step-up procedure. After calibrating one instrument with water, a more viscous liquid is measured in that instrument; this liquid is then used to calibrate the next viscometer in the series, and thus through a series of eight instruments. Each lot is checked independently by at least three other laboratories. Other series of calibrating liquids are available from different sources, but none are measured with the degree of precision and control of the ASTM series. One available series uses silicone liquids. These are very stable chemically, but they are difficult to remove from some viscometers.

The ASTM series uses various white oils and Pennsylvania bright stocks, plus three polybutene liquids for the most viscous liquids. Experience has indicated that the viscosity of standards S-3 through S-60 should be reliable to ±0.1 percent for at least a year, if stored at room temperature without exposure to light and in the original closed containers. A series of tests at the National Bureau of Standards on standards of this type showed no appreciable change in some lots over a period of several years, but not enough systematic evidence has been accumulated to justify recommendation of use after storage for more than one year. The standards with viscosities greater than one poise generally show a distinct (though small, and quite irregular) increase in viscosity with age. These should not be used after storage for more than six months--no more than two months for the two most viscous oils. The viscosity values over one poise should be assigned an uncertainty of ±0.3 percent, because of the limited stability of these standards and the uncertainty of calibration of the instruments used in this range (several steps away from the initial instrument calibrated with water).

Calibrating liquids with viscosities above the range of the present ASTM series would be useful, but several problems impose increasingly severe limitations on the reliability of standards as the viscosity increases. One is that the step-up procedure required to relate their viscosity to that of water involves more steps and thus an increasing uncertainty in the values assigned. Another is that characteristics which limit the usefulness of such standards (non-Newtonian behavior, limited stability, high temperature coefficient of viscosity) become more prominent with increasing viscosity. In addition, the need for material standards in this range appears less critical than it is in the range covered by the present series. The acceptable and attainable precision becomes poorer as the viscosity increases, and is seldom as good as one percent for viscosities above this range. Inertial effects generally become less important relative to viscous effects as the viscosity increases. Thus, the accuracy of the measurement of high viscosities is likely to be limited by the reproducibility of measurement rather than by the type of systematic error important in the lower viscosity range.

Key Words: Measurement of viscosity, relative measurements, systematic errors, viscometer calibrating liquids (material standards for viscosity), viscosity.

REFERENCES

[1] W. E. Langlois, Slow Viscous Flow, (Macmillan, New York, 1964), p. 56.

[2] G. Barr, A Monograph of Viscometry, (Oxford, London, 1931); A. C. Merrington, Viscometry, (Edward Arnold & Co., London, 1949).

[3] E. C. Bingham, Journal of Rheology 2, 403 (1931).

[4] J. F. Swindells, J. R. Coe, Jr., and T. B. Godfrey, J. Res. NBS 48, 1 (1952); RP-2279.

[5] J. R. Van Wazer, J. W. Lyons, K. Y. Kim, and R. E. Colwell, Viscosity and Flow Measurement, (Interscience, New York, 1963).

[6] 1967 Book of ASTM Standards, Part 17, (American Society for Testing and Materials, Philadelphia, 1967).

[7] R. C. Hardy, NBS Monograph 55 (1962).

[8] M. R. Cannon, R. E. Manning, and J. D. Bell, Anal. Chem. 32, 355 (1960).

Author Index[1]

[1] The letter "A" following the paper number indicates an abstract only.

Subject Index

[1] The first "boldface" number in this index identifies the section in which the paper appears: 1. Acoustics 2. Fluid 3. Force 4. Gravity 5. Humidity 6. Pressure 7. Strain 8. Vacuum 9. Vibration 10. Viscosity

G

H

I

[1] The first "boldface" number in this index identifies the section in which the paper appears: **1.** Acoustics **2.** Fluid **3.** Force **4.** Gravity **5.** Humidity **6.** Pressure **7.** Strain **8.** Vacuum **9.** Vibration **10.** Viscosity

L

M

N

O

P

Subject Index — Continued

[1] The first "boldface" number in this index identifies the section in which the paper appears: 1. Acoustics 2. Fluid 3. Force 4. Gravity 5. Humidity 6. Pressure 7. Strain 8. Vacuum 9. Vibration 10. Viscosity

☆ U. S. GOVERNMENT PRINTING OFFICE : 1971 O - 450-124

Announcement of New Volumes in the NBS Special Publication 300 Series Precision Measurement and Calibration

Superintendent of Documents,
Government Printing Office,
Washington, D. C. 20402

Dear Sir:

Please add my name to the announcement list of new volumes to be issued in the series: National Bureau of Standards Special Publication 300, Precision Measurement and Calibration.

(cut here)

Name _____

Company _____

Address _____

City _____ State _____ Zip Code _____

(Notification key N-353)

Official SI Unit Names and Symbols

For a complete statement of NBS practice, see NBS Tech. News Bull. Vol. 55, No. 1, Jan. 1971, 30¢.*
See also NBS Special Publication 330, The International System of Units SI, Jan. 1971, 15¢*.
*Available by purchase from the Supt. of Documents, Government Printing Office, Washington, D. C. 20402

Name	Symbol	Name	Symbol
meter	m	newton	N
kilogram	kg	joule	J
second	s	watt	W
ampere	A	coulomb	C
kelvin [1]	K	volt	V
candela	cd	ohm	Ω
radian	rad	farad	F
steradian	sr	weber	Wb
hertz	Hz	henry	H
lumen	lm	tesla	T
lux	lx		

Additional Names and Symbols approved for NBS use

curie [2]	Ci	mole	mol
degree Celsius [3]	°C	siemens [4]	S
gram	g		

[1] The same name and symbol are used for thermodynamic temperature and temperature interval. (Adopted by the 13th General Conference on Weights & Measures, 1967).
[2] Accepted by the General Conference on Weights & Measures for use with the SI, but to be eventually abandoned.
[3] For expressing "Celsius temperature"; may also be used for a temperature interval.
[4] Adopted by IEC and ISO.

Table for Converting U.S. Customary Units to Those of the International System (SI)[5]

To relate various units customarily used in the United States to those of the International System, the National Bureau of Standards uses the conversion factors listed in the "ASTM Metric Practice Guide", designation:E 380–70. These are based on international agreements effective July 1, 1959, between the national standards laboratories of Australia, Canada, New Zealand, South Africa, the United Kingdom, and the United States.

To convert from:

(1) inches to meters, multiply by 0.0254 exactly.
(2) feet to meters, multiply by 0.3048 exactly.
(3) feet (U.S. survey) to meters, multiply by 1200/3937 exactly.
(4) yards to meters, multiply by 0.9144 exactly.
(5) miles (U.S. statute) to meters, multiply by 1609.344 exactly.
(6) miles (international nautical) to meters, multiply by 1852 exactly.
(7) grains (1/7000 lbm avoirdupois) to grams, multiply by 0.064 798 91 exactly.
(8) troy or apothecary ounces mass to grams, multiply by 31.103 48 . . .
(9) pounds-force (lbf avoirdupois) to newtons, multiply by 4.448 222 . . .
(10) pounds-mass (lbm avoirdupois) to kilograms, multiply by 0.453 592 . . .
(11) fluid ounces (U.S.) to cubic centimeters, multiply by 29.57 . . .
(12) gallons (U.S. liquid) to cubic meters, multiply by 0.003 785 . . .
(13) torr(mm Hg at O °C) to newtons per square meter, multiply by 133.322 exactly.
(14) millibars to newtons per square meter, multiply by 100 exactly.
(15) psi to newtons per square meter, multiply by 6894.757 . . .
(16) poise to newton-seconds per square meter, multiply by 0.1 exactly.
(17) stokes to square meters per second, multiply by 0.0001 exactly.
(18) degrees Fahrenheit to kelvins, use the relation $T_{68}=(t_F+459.67)/1.8$.
(19) degrees Fahrenheit to degrees Celsius, use the relation $T_{68}=(t_F-32)/1.8$.
(20) curies to disintegrations per second, multiply by 3.7×10^{10} exactly
(21) roentgens to coulombs per kilogram, multiply by $2.579\ 760\times10^{-4}$ exactly.

[5] Systeme International d'Unites (designated SI in all languages).